ISBN 978-3-902842-49-7

International Commission on Illumination
Commission Internationale de l'Eclairage
Internationale Beleuchtungskommission

PROCEEDINGS of CIE 2014 „Lighting Quality and Energy Efficiency"

23 – 26 April 2014

Hotel Istana

Kuala Lumpur, Malaysia

CIE x039:2014

UDC: 628.9 Descriptor: Lighting. Illuminating engineering

THE INTERNATIONAL COMMISSION ON ILLUMINATION

The International Commission on Illumination (CIE) is an organization devoted to international co-operation and exchange of information among its member countries on all matters relating to the art and science of lighting. Its membership consists of the National Committees in about 40 countries.

The objectives of the CIE are:

1. To provide an international forum for the discussion of all matters relating to the science, technology and art in the fields of light and lighting and for the interchange of information in these fields between countries.
2. To develop basic standards and procedures of metrology in the fields of light and lighting.
3. To provide guidance in the application of principles and procedures in the development of international and national standards in the fields of light and lighting.
4. To prepare and publish standards, reports and other publications concerned with all matters relating to the science, technology and art in the fields of light and lighting.
5. To maintain liaison and technical interaction with other international organizations concerned with matters related to the science, technology, standardization and art in the fields of light and lighting.

The work of the CIE is carried on by seven Divisions each with about 20 Technical Committees. This work covers subjects ranging from fundamental matters to all types of lighting applications. The standards and technical reports developed by these international Divisions of the CIE are accepted throughout the world.

A plenary session is held every four years at which the work of the Divisions and Technical Committees is reported and reviewed, and plans are made for the future. The CIE is recognized as the authority on all aspects of light and lighting. As such it occupies an important position among international organizations.

LA COMMISSION INTERNATIONALE DE L'ECLAIRAGE

La Commission Internationale de l'Eclairage (CIE) est une organisation qui se donne pour but la coopération internationale et l'échange d'informations entre les Pays membres sur toutes les questions relatives à l'art et à la science de l'éclairage. Elle est composée de Comités Nationaux représentant environ 40 pays.

Les objectifs de la CIE sont :

1. De constituer un centre d'étude international pour toute matière relevant de la science, de la technologie et de l'art de la lumière et de l'éclairage et pour l'échange entre pays d'informations dans ces domaines.
2. D'élaborer des normes et des méthodes de base pour la métrologie dans les domaines de la lumière et de l'éclairage.
3. De donner des directives pour l'application des principes et des méthodes d'élaboration de normes internationales et nationales dans les domaines de la lumière et de l'éclairage.
4. De préparer et publier des normes, rapports et autres textes, concernant toutes matières relatives à la science, la technologie et l'art dans les domaines de la lumière et de l'éclairage.
5. De maintenir une liaison et une collaboration technique avec les autres organisations internationales concernées par des sujets relatifs à la science, la technologie, la normalisation et l'art dans les domaines de la lumière et de l'éclairage.

Les travaux de la CIE sont effectués par 7 Divisions, ayant chacune environ 20 Comités Techniques. Les sujets d'études s'étendent des questions fondamentales, à tous les types d'applications de l'éclairage. Les normes et les rapports techniques élaborés par ces Divisions Internationales de la CIE sont reconnus dans le monde entier.

Tous les quatre ans, une Session plénière passe en revue le travail des Divisions et des Comités Techniques, en fait rapport et établit les projets de travaux pour l'avenir. La CIE est reconnue comme la plus haute autorité en ce qui concerne tous les aspects de la lumière et de l'éclairage. Elle occupe comme telle une position importante parmi les organisations internationales.

DIE INTERNATIONALE BELEUCHTUNGSKOMMISSION

Die Internationale Beleuchtungskommission (CIE) ist eine Organisation, die sich der internationalen Zusammenarbeit und dem Austausch von Informationen zwischen ihren Mitgliedsländern bezüglich der Kunst und Wissenschaft der Lichttechnik widmet. Die Mitgliedschaft besteht aus den Nationalen Komitees in rund 40 Ländern.

Die Ziele der CIE sind :

1. Ein internationales Forum für Diskussionen aller Fragen auf dem Gebiet der Wissenschaft, Technik und Kunst der Lichttechnik und für den Informationsaustausch auf diesen Gebieten zwischen den einzelnen Ländern zu sein.
2. Grundnormen und Verfahren der Messtechnik auf dem Gebiet der Lichttechnik zu entwickeln.
3. Richtlinien für die Anwendung von Prinzipien und Vorgängen in der Entwicklung internationaler und nationaler Normen auf dem Gebiet der Lichttechnik zu erstellen.
4. Normen, Berichte und andere Publikationen zu erstellen und zu veröffentlichen, die alle Fragen auf dem Gebiet der Wissenschaft, Technik und Kunst der Lichttechnik betreffen.
5. Liaison und technische Zusammenarbeit mit anderen internationalen Organisationen zu unterhalten, die mit Fragen der Wissenschaft, Technik, Normung und Kunst auf dem Gebiet der Lichttechnik zu tun haben.

Die Arbeit der CIE wird in 7 Divisionen, jede mit etwa 20 Technischen Komitees, geleistet. Diese Arbeit betrifft Gebiete mit grundlegendem Inhalt bis zu allen Arten der Lichtanwendung. Die Normen und Technischen Berichte, die von diesen international zusammengesetzten Divisionen ausgearbeitet werden, sind auf der ganzen Welt anerkannt.

Alle vier Jahre findet eine Session statt, in der die Arbeiten der Divisionen berichtet und überprüft werden, sowie neue Pläne für die Zukunft ausgearbeitet werden. Die CIE wird als höchste Autorität für alle Aspekte des Lichtes und der Beleuchtung angesehen. Auf diese Weise unterhält sie eine bedeutende Stellung unter den internationalen Organisationen.

Published by the

COMMISSION INTERNATIONALE DE L'ECLAIRAGE
CIE Central Bureau
Babenbergerstrasse 9, A-1010 Vienna, AUSTRIA
Tel: +43(1)714 31 87
e-mail: ciecb@cie.co.at
www.cie.co.at

ISBN 978-3-902842-49-7

International Commission on Illumination
Commission Internationale de l'Eclairage
Internationale Beleuchtungskommission

PROCEEDINGS of CIE 2014 „Lighting Quality and Energy Efficiency”

23 – 26 April 2014

Hotel Istana

Kuala Lumpur, Malaysia

CIE x039:2014

UDC: 628.9 Descriptor: Lighting. Illuminating engineering

Lighting Quality
& Energy Efficiency
April 23 - 26, 2014
Kuala Lumpur, Malaysia

MyCIE MALAYSIA
International Commission on Illumination

International Scientific Committee

Ohno, Yoshi (Chair)	US	CIE Vice-President Technical
Blattner, Peter	CH	CIE Director Division 2
Faidz, A.R.	MY	MyCIE
Gerloff, Thorsten	DE	CIE Division 2
Gibbons, Ron	US	CIE Associate Director Division 4
Goodman, Teresa	GB	CIE Vice-President Publications
Horak, Werner	DE	CIE Division 6
Lin, Yandan	CN	CIE Associate Director Division 4
Luo, Ronnier	GB	CIE Director Division 1
Morovic, Jan	GB	CIE Director Division 8
Nakamura, Yoshiki	JP	CIE Division 3, CIE Vice-President
O'Hagan, John	GB	CIE Director Division 6
Rengasamy, Narendren	MY	MyCIE
Schwarcz, Peter	HU	CIE Director Division 5
Tan, Ching Seong	MY	MyCIE
Zwick, Peter	AT	CIE Central Bureau Technical Manager

International Organizing Committee

Webb, Ann (Chair)	GB	CIE President
Siew, C.T. (Chair)	MY	MyCIE
Goodman, Teresa	GB	CIE Vice-President Publications
Ohno, Yoshi	US	CIE Vice-President Technical
Paul, Martina	AT	CIE General Secretary
Whitehead, Lorne	CA	CIE Treasurer

Lighting Quality & Energy Efficiency
April 23 - 26, 2014
Kuala Lumpur, Malaysia

MyCIE MALAYSIA International Commission on Illumination

The following table provides an overview of the oral presentations and posters presented at the conference. The papers are published in the proccedings in consecutive order of presentation. Papers that have not been submitted are marked as such ("n.s.").

The authors are responsible for the contents of their papers.

Please note: For direct access of a paper click on the respective page number.

IT03

LIGHTING QUALITY FOR AUTOMOTIVE LIGHTING

Tran Quoc Khanh[1]
[1] Technische Universität Darmstadt, Darmstadt, GERMANY
khanh@lichttechnik.tu-darmstadt.de

Abstract

Automotive lighting has three tasks: 1.Enabling good visual conditions for all traffic participants (drivers, pedestrians, cyclists); 2. Creation of suitable technical possibilities for the improvement of comfort, well-being and concentration for the drivers at night; and 3. energy saving and contribution to worldwide environmental protection. In this paper, recent achievements of improving lighting quality for automotive lighting are summarized in the following three main application areas: 1. Headlamps and signal lamps of front lighting for the illumination of the field in front of the car; 2. rear lamps (e.g. brake lamp); and interior lighting (with LED devices).

Keywords: lighting quality, automotive lighting, AFS, marking light, matrix beam

1 Introduction

In 1886, automotive industry started its history with the invention of Carl Benz for the internal combustion engine and, in 1908, the first electrical light sources found their way to car technology. Since this time, automotive industry and its technology have been the symbol of a dynamic innovation and mobility of a dynamic society in the process of industrial revolution and telecommunication. In this context, automotive lighting has overtaken a central place in car philosophy since 1990 and has been the driving force for the whole car innovation since 2006 with the introduction of LED technology.

Generally, automotive lighting has three tasks:

- Enabling good visual conditions for all traffic participants (drivers, pedestrians, cyclists);
- Creation of suitable technical possibilities for the improvement of comfort, well-being and concentration for the drivers at night;
- Energy saving and contribution to worldwide environmental protection.

Lighting quality for automotive lighting has three main application areas:

a) Headlamps and signal lamps of front lighting for the illumination of the field in front of the car (low beam, high beam, bending light, cornering beam) and signalling aims (daytime running light, position light);
b) Rear lamps (brake lamp); and
c) Interior lighting (with LED devices).

2 Interior lighting technology

In the next future or even currently in case of high-class vehicles, interior lighting technology shall introduce some fundamental developments with LED components in order to

a) improve viewing conditions inside the car depending upon weather, clock time and traffic situation (traffic density, driving in a city with city light or driving on a dark country road;
b) improve relaxation and concentration of the drivers by adjusting the lighting set-up to “relaxing mode” for driving after the working hours and to “sport mode” with rather bluish white light.

The philosophy of lighting quality is related to the aspect and question of how can concentration be improved and stress be reduced to support car drivers?

3 Rear lamp technology

Rear lamp technology was the first LED based lighting unit of the car due to its fast pulse time i.e. rise and fall time of the LED pulses in order to make a faster signal appearance for other traffic participants possible while braking. Besides signalling tasks, rear lamps with LEDs do have high potentials for styling and improving the value of the vehicles. From the scientific point of view, the maximal and minimal luminous intensity of the rear lamps has to be reconsidered. All luminous intensity requirements for rear lamps have not taken the change of weather, day time, ambient luminance and distance between the cars into account.

In the last 8 years, research on rear lamp technology has focused on flickering and stroboscopic effects because rear lamps LEDs are operated with pulse width modulation (see Figure 1). In order to minimize this effect which can lead to the distraction of visual attention of normal drivers and to serious health impairing reactions for photo-sensitive drivers, the frequency must be increased and has to be adjusted to at least 400 Hz if the detection rate of flicker or the stroboscopic effect should be lower than 5% (see Figure 2).

Figure 1 – Illustration of the beads effect or bead string artefact. Image source: Technische Universität Darmstadt

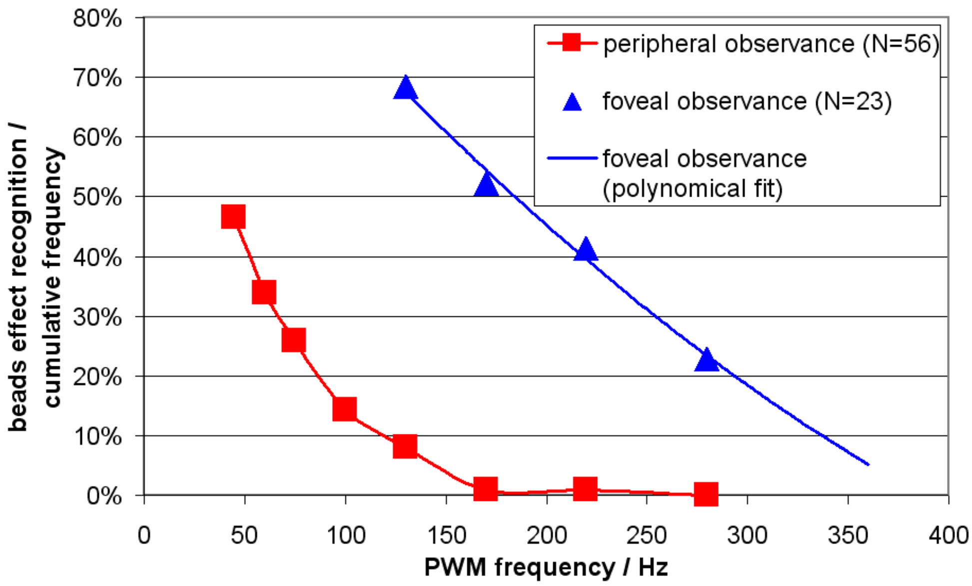

Figure 2 – Beads effect or bead string artefact (see Figure 1) recognition rate under two observing conditions [1]

4 Front lighting technology

On the front lighting side, lighting quality of automotive lighting has been influenced by three developments and innovations:

- the development of new light sources (Halogen tungsten lamp, Xenon lamp 35 W in 1990 and 25 W in 2011, LED front lighting in 2007 and laser beam in the next time in 2014);
- the concept of adaptive front lighting (AFS, AFL); and
- the concept of lighting situation based front lighting.

4.1 New light sources

Table 1 summarizes current lamp types for automotive front lighting.

Table 1 – Current lamp technologies in automotive front lighting

Lamp type	**Luminous flux**	**Max. luminance**	**Luminous efficacy**	**CCT**
Halogen tungsten lamp(H7)	~ 1500 lm	~ 30 Mcd/m²	25 lm/W	3200 K
Xenon lamp (D2S)	~ 3200 lm	~ 90 Mcd/m²	90 lm/W	4200 K
LED (cold white)	~ 150-1500 lm	~ 20 Mcd/m²	65 lm/W	4000 K - 6000 K

With a Xenon lamp with 3200 lm and with a typical optical efficiency of 35%, a luminous flux of the Xenon low beam (passing beam) of 1100 lm is achievable. In comparison, the luminous flux of a halogen tungsten lamp low beam is maximal 500 lm. In recent research studies at the Technische Universität Darmstadt for automotive industry the following visibility distances of low beam headlamps were determined (see Table 2). With a luminous flux of the best current LED low beam of higher class vehicles of 900 lm, the visibility distance of LED and Xenon lamp low beam is nearly comparable.

Table 2 – Visibility distances under 0° and 20° viewing directions

Low beam with	Visibility distance [2]	Visibility distance under 0° [3]	Visibility distance under 20° [3]
Halogen tungsten lamp	70 m	63 m	18,3 m
Xenon lamp D2S	85 m	80 m	25,8m

4.2 Adaptive Front Lighting (AFS)

Since 1998, until 2010 the concepts of AFS (adaptive front lighting systems) were developed and realized in many vehicle products (see Figure 3).

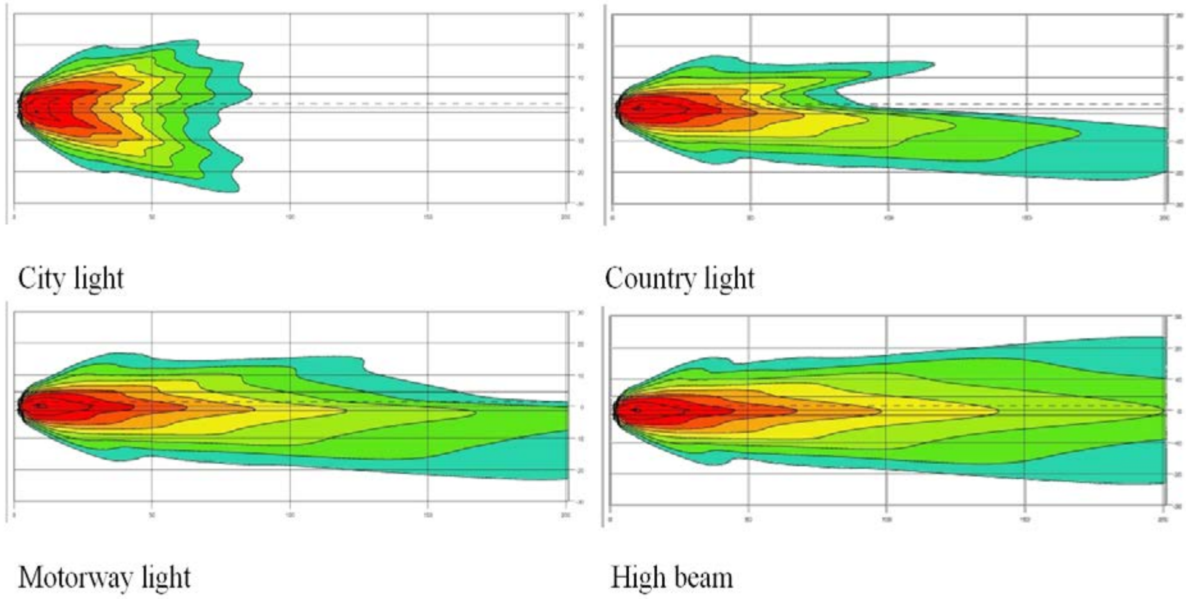

Figure 3 – Adaptive Front Lighting (AFS) functions

As can be seen from Figure 3, standard low beam is changed if the car is driven in a city to have a broader light distribution but not with a longer visibility distance because street lights also illuminate the road. Depending on the speed of the car when driving on the highway, the low beam distribution can be adjusted from -0.57° to -0.23° to the horizontal line so that the visibility distance can be increased from about 80 m (low beam) to 110 nm (motorway light). The AFS functions and high beam assistance can be controlled by cameras, sensors and a data processor (see Figure 4).

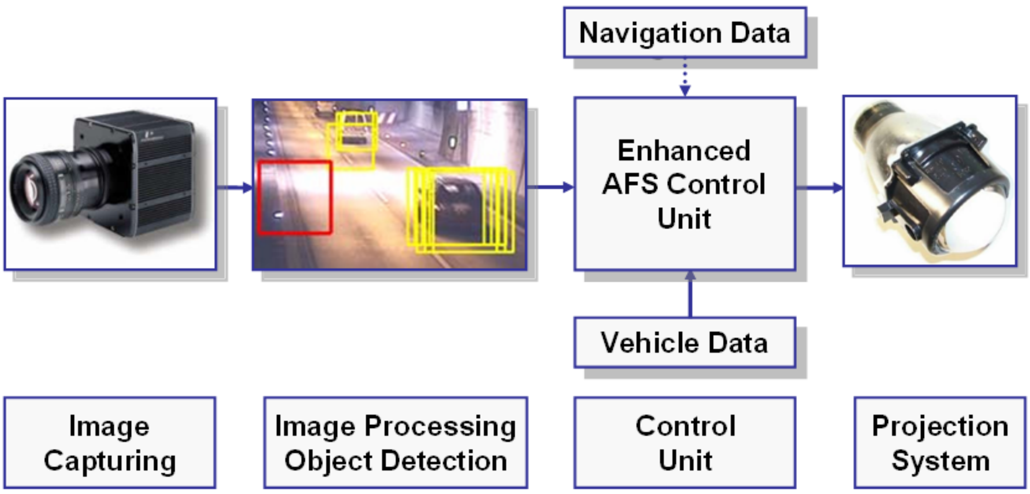

Figure 4 – Data and image processing unit inside the car [4]

Because the low beam has a maximal visibility distance of 85 m and highway light has about 110 m, the idea was to increase the number of occasions when high beam is used. Until 2005, high beam could be set manually and the error rate has been very high. With high beam assistance and with its camera detecting when other traffic participants appear on the road, the high beam can be activated automatically. It enables a visibility distance of up to 140 m.

4.3 Lighting situation based headlamp technologies

However, AFS functions also have some disadvantages. They are only used depending on the topology of the road (bend, city, high way, country road) and the real dynamic road situation cannot be taken into account. Therefore, lighting situation based headlamp concepts have been developed since 2009 including:

- Marking light: illumination of animals and other objects on and beside the road with a marking spot light (Figure 5);
- Vertical dynamic cut-off line (Figure 6);
- Glare free high beam (Figure 7).

Figure 5 – Marking light principle (image source: Company Hella/Lippstadt, [5])

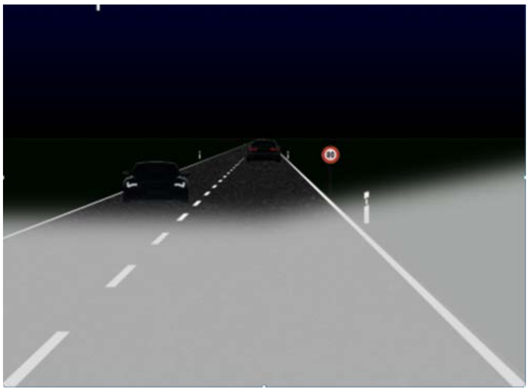

Figure 6 – Vertical dynamic cut-off line [6]

Figure 7 – Glare free high beam, matrix beam [7]

In a study of the Technische Universität Darmstadt for the international automotive headlamp suppliers in 2013, Zydek et al. investigated visibility distances of different headlamp technologies. Results are illustrated in Figure 8. The discomfort glare of the tested glare free high beam with HID Xenon lamp was equal 7 (mean value) on the De Boer scale.

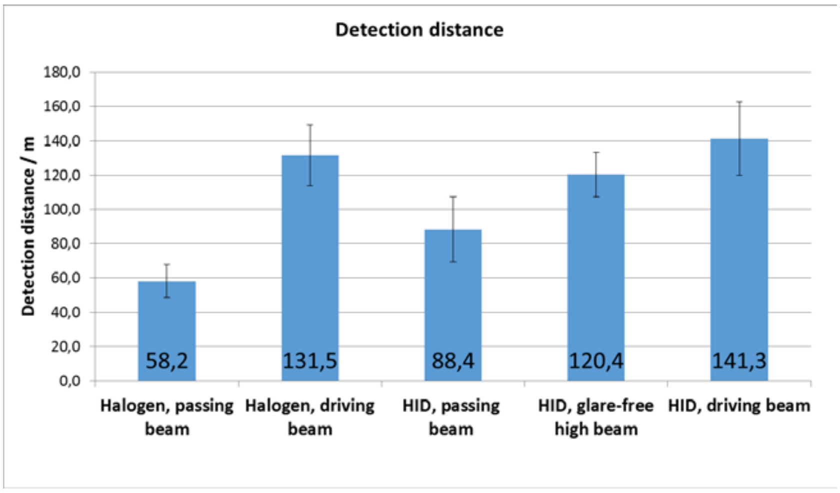

Figure 8 – Detection (visibility) distance of different headlamp technologies

References

[1] S. Brückner, T. Q. Khanh, A field experiment on the perception of automotive rear lights using pulsed LEDs with different frequencies, Proceedings of the 7th International Symposium of Automotive Lighting, ISAL 2007, Darmstadt, 2007.

[2] E.-O. Rosenhahn, M. Hamm, Motorway Light in Adaptive Lighting Systems, in: Progress in Automobile Lighting (PAL), Technische Universität Darmstadt, Utz Verlag, München, S. 868-882, 2003.

[3] C. Schiller, Lichttechnische Tests an derzeitigen Xenon- und Halogenlampenscheinwerfern, Technische Universität Darmstadt, interner Bericht des Fachgebiets Lichttechnik, 2007.

[4] J. H. Sprute, T. Q. Khanh, Approval Requirements for a Front-Lighting-System with Variable Cut-Off Line in Europe, in: International Symposium on Automotive Lighting (ISAL), Technische Universität Darmstadt, Utz Verlag, München, S. 31-37, 2007.

[5] M. Kleinkes, K. Eichhorn, N. Schiermeister, LED technology in headlamps - extend lighting functions and new styling possibilities, in: International Symposium on Automotive Lighting (ISAL), Technische Universität Darmstadt, Utz Verlag, München, S.55-63, 2007.

[6] F.-J. Kalze, C. Schmidt, Dynamic Cut-Off-Line geometry as the next step in forward lighting beyond AFS, in: International Symposium on Automotive Lighting (ISAL), Technische Universität Darmstadt, Utz Verlag, München, S. 346-354, 2007

[7] A. Totzauer, Kalibrierung und Wahrnehmung von blendfreiem LED-Fernlicht, Technische Universität, Darmstadt, PhD thesis, 2013.

[8] Zydek et al., Quantifying Detection Distance and Glare of Headlamp Systems with Adaptive Vertical Cut-Off Lines, ISAL conference, Darmstadt, 2013.

IT04

EXPLORING THE POWER OF LIGHT: FROM PHOTONS TO HUMAN HEALTH

George C. Brainard and John P. Hanifin
Thomas Jefferson University, Department of Neurology, Philadelphia, Pennsylvania, USA
george.brainard@jefferson.edu, john.hanifin@jefferson.edu

Abstract

Light is a potent stimulus for regulating circadian, neuroendocrine and neurobehavioural responses in humans. Further, light therapy is effective for treating select affective, circadian and sleep disorders. Over the past decade, discoveries show that these biological and behavioural effects of light are mediated by a newly discovered photoreceptor in the eye that is distinct from the classical rods and cones for vision. These findings are providing a basis for major changes in lighting of advanced habitats for space exploration, as well as everyday buildings on Earth.

Keywords: action spectra, circadian, light, light therapy, melanopsin, melatonin, neurobehavioral, neuroendocrine, photoreceptor, pineal gland

1 Introduction

Four traditional objectives of architectural lighting have been to provide light that: 1) is optimum for visual performance; 2) is visually comfortable; 3) permits aesthetic appreciation of the space; and 4) conserves energy. During the past three decades, scientific evidence has led to a growing understanding that, relatively separate from vision and visual reflexes, light perceived by the eye can be a potent biological, behavioural, and therapeutic stimulus in humans [Wetterberg, 1993; Lam, 1998; CIE, 2004a b; IESNA, 2008**]**. Over the past decade, there has been an upheaval in the understanding of photoreceptive input to the circadian and neuroendocrine systems of humans. A study on healthy human subjects confirmed that the three-cone system that mediates human photopic vision is not the primary photoreceptor system that transduces light stimuli for acute melatonin suppression [Brainard, 2001a]. That discovery was rapidly followed by the elucidation of two action spectra in healthy human subjects that identified 446 nm to 477 nm as the most potent wavelength region for melatonin suppression [Brainard, 2001b; Thapan, 2001]. Those data suggested that a novel photosensory system in humans, distinct from the visual rods and cones, is primarily responsible for regulating melatonin, a hormone secreted by the pineal gland.

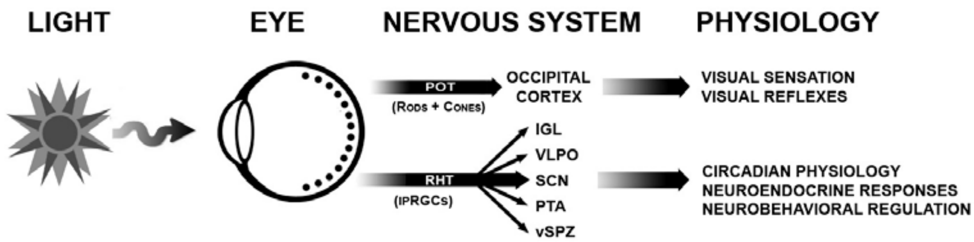

Figure 1 – The diagram above provides a simplified schematic of the neuroanatomy responsible for mediating both the sensory capacity of the visual system and the non-visual regulation of circadian, neuroendocrine and neurobehavioural functions.
Abbreviations: POT - primary optic tract; RHT - retinohypothalamic tract; ipRGCs - intrinsically photosensitive retinal ganglion cells; IGL - intergeniculate leaflets; VLPO -ventrolateral preoptic nuclei; SCN - suprachiasmatic nuclei; PTA -pretectal areas; vSPZ -ventral subparaventricular zones. This figure is from [Brainard, 2006] and is reprinted with permission by the Commission Internationale de l'Eclairage (CIE).

Studies using both animal and human models are clarifying the neuroanatomy and neurophysiology of the photosensory system that provides input for circadian, neuroendocrine, and neurobehavioural regulation. A recently discovered photopigment, named melanopsin, has been localized both in the retinas of rodents and humans [Provencio, 2000]. More specifically, melanopsin is found in a subtype of intrinsically photoreceptive retinal ganglion cells (ipRGCs). These seminal discoveries and further clarification of the biochemistry, anatomy, and physiology of melanopsin and the ipRGCs have been a crowning achievement of neuroscience [Provencio, 1998, 2000, 2002; Gooley, 2001; Berson, 2002; Hattar, 2002]. Figure 1 provides a simplification of the neural anatomy that support vision and circadian, neuroendocrine and neurobehavioural responses [Brainard, 2006].

The professional communities of lighting manufacturers, designers and architectural engineers have opened the door to understanding this emergent physiology. Together, they are fostering the development of appropriate applications that might emerge from these discoveries [JCIE 2004; CIE, 2004a, 2004b, 2006; IESNA, 2008, DIN 2009]. Ultimately, lighting based on the classical design objectives will need to accommodate the recent discoveries about the role of light in human health and well-being.

2 Circadian, Neuroendocrine, and Neurobehavioural Action Spectra

An action spectrum is one of the principal tools for identifying the photopigment that initiates a light-induced response. A photopigment's pattern of wavelength sensitivity, or its absorbance spectrum, is like a fingerprint – it is unique to that molecule. Photobiologists define an action spectrum as the relative response of an organism to different wavelengths of visible and near-visible electromagnetic radiation. Over the years, a set of approaches for determining action spectra that are applicable to all light responsive organisms has been refined [Horspool, 1994; Coohill, 1999].

In the photobiological literature, there are two basic types of action spectra: polychromatic and analytical [Coohill, 1999]. Generally investigators begin exploring light sensitive biological reactions by determining polychromatic action spectra. Such action spectra are developed by employing broader bandwidth light stimuli that either have half-peak bandwidths greater than 15 nm to 20 nm or by emphasizing particular wavelengths against backgrounds of "white" artificial or natural light. Polychromatic action spectra are useful for: 1) identifying interactions of biological responses to multiple wavelengths; 2) clarifying how organisms respond to light in more natural settings; and 3) guiding the development of the more sophisticated analytical action spectra. Polychromatic action spectra, however, have limited utility for identifying the specific photopigments that initiate light-sensitive responses [Coohill, 1999]. As in other fields of photobiology, the earliest action spectrum studies on neuroendocrine and circadian responses to light utilized polychromatic stimuli. From 1972 through 2004, a set of published polychromatic action spectra developed in both rodents and humans consistently indicated that the spectral region between 450 nm and 550 nm provided the strongest stimulation of circadian and neuroendocrine responses [Brainard, 2005, for review].

Concurrent with the remarkable discovery of melanopsin and ipRGCs, ten recent analytical action spectra have demonstrated the wavelength sensitivity of some of the physiological responses mediated by these newly characterized sensory cells. Those action spectra are presented in Table 1. It is significant that each of the studies in Table 1 indicate a λ_{max} ranging from 459 nm to 483 nm in the short wavelength portion (blue) of the visible spectrum [Brainard, 2001b; Thapan, 2001; Berson, 2002; Yoshimura, 1996; Lucas, 2001; Hankins, 2002; Hattar, 2003; Dacey, 2005; Gamlin, 2007; Zaidi, 2007]. Given the differences in laboratories, experimental models, physiological endpoints and specific investigative techniques, this consistent identification of peak responses across the blue portion of the spectrum is remarkable. It is also notable that the data from each of the action spectra in Table 1 were fit to single opsin nomograms with relatively high coefficients of correlation. Although full analytical action spectra have yet to be developed, a set of studies have confirmed that shorter wavelength monochromatic light is more potent than equal photon densities of longer wavelength light for evoking circadian phase shifts, suppressing melatonin, enhancing subjective and objective correlates of alertness, increasing heart rate, increasing body temperature, inducing expression of the circadian clock gene *Per2* and fMRI brain responses in humans [Lockley, 2003; Warman, 2003; Cajochen, 2005, 2006; Revell, 2005a; Lockley, 2006; Vandewalle, 2007a, 2007b, 2010; Zaidi, 2007; Gooley 2010; Ruger, 2013; Rahman, 2014]. Together, the full analytical action spectra and selected wavelength testing indicate that a novel photoreceptor system is primarily involved in circadian, neuroendocrine, and neurobehavioural responses mediated by the eyes of humans and other mammals.

Table 1 - Each of the below action spectra is based on fluence response curves of 6 to 10 wavelengths. Each λ max is derived from a best fit opsin nomogram.

Analytical Action Spectra Studies Showing Peak Sensitivity to Blue Light for Circadian, Neuroendocrine and Neurobehavioural Responses

Peak (λ Max)	**Species**	**Response**	**Citation**
480	Mouse *rd/rd*	Circadian Phase Shifting	Yoshimura and Ebihara., 1996
464	Human	Melatonin Suppression	Brainard *et al*., 2001
459	Human	Melatonin Suppression	Thapan *et al*., 2001
479	Mouse *rd/rd*	Pupillary Light Reflex	Lucas *et al.,* 2001
483	Human	Cone Cell ERG Wave	Hankins and Lucas, 2002
483	Rat	Ganglion Cell Depolarization	Berson *et al*., 2002
481	Mouse *rd/rd cl*	Circadian Phase Shifting	Hattar *et al*., 2003
482	Monkey	Ganglion Cell Depolarization	Dacey *et al*., 2005
482	Monkey Human	Pupillary Light Reflex	Gamlin *et al.,* 2007
480	Human	Pupillary Light Reflex	Zaidi *et al.,* 2007

It is important to note that not all analytical action spectra identify a λ_{max} in the blue part of the spectrum. Analytical action spectra with wildtype mice and hamsters showed peaks in the 500 to 511 nm range for phase shifting locomotor activity and pupillary constriction [Yoshimura, 1996; Lucas, 2001,Takahashi, 1984; Provencio, 1995]. It may be that the intact rodent retina combines input from ipRGCs and classical visual photoreceptors for circadian phase shifting and pupillary responses. In contrast, when mice do not have functioning visual photoreceptors (such as in the *rd/rd* and *rd/rd cl* models), their retinal responses appear to shift sensitivity to the shorter wavelengths for circadian and pupillary responses [Yoshimura, 1996; Lucas, 2001].

3 Rods and Cones Interact with Ganglion Cell Photoreceptors

Abundant evidence shows that the melanopsin containing ipRGCs provide primary input for circadian, neuroendocrine, and neurobehavioral regulation. It has also been demonstrated, however, that rod and cone photoreceptors still play a role in this physiology. Studies with genetically altered mice show that the classical rod and cone photoreceptors can compensate for the loss of melanopsin and, at least partially mediate, light-induced circadian, neuroendocrine and neurobehavioural responses [Panda, 2002; Lucas, 2003; Dkhissi-Benyahya, 2007; Altimus, 2010; Lall, 2010]. In contrast, when both melanopsin is knocked out and the classical visual photoreceptors are compromised, animals lose all visual and nonvisual photoreceptive functions of the eye [Hattar, 2003; Panda, 2003]. Further, cellular recording studies from nonhuman primate retinas have demonstrated that rod and cone cells can directly activate ipRGCs [Dacey, 2005]. Data from human studies also suggest that the visual rods and cones provide input to the SCN [Herbert, 2002; Lockley, 2003; Figueiro, 2004; Jasser, 2006; Revell, 2007; Gooley, 2010]. Importantly, despite rapid experimental progress on ipRGC physiology, it is currently unknown precisely how these newly discovered photoreceptors work with the classical visual photoreceptors in transducing light in the dynamic, complex polychromatic environments where humans carry out their daily activities [Lucas, 2014].

4 Lamp Colour Temperature and the Biological Effects of Light

Independent of the research done with monochromatic wavelengths, studies have investigated a variety of circadian, neuroendocrine and neurobehavioural changes relative to correlated colour temperature (CCT) of broad spectrum polychromatic fluorescent lights [Hanifin, 2007, for review]. In general, higher colour temperature lamps emit more energy in the short wavelength part of the visible spectrum than lower colour temperature lamps. Lamps emitting higher CCT light were found to evoke stronger melatonin suppression in healthy human subjects compared to lamps with lower CCT light [Morita, 1998; Sato, 2005; Figueiro, 2004; Kozaki, 2008; Hanifin, 2011; Chellappa, 2011]. Additionally, fluorescent light with a higher colour temperature was observed to have a more potent effect on core body temperature than low colour temperature light [Yasukouchi, 2000; Sato, 2005]. Furthermore, blood pressure and EEG frequency have been shown to increase with exposure to high CCT light as compared to lower CCT light [Noguchi, 1999; Yasukouchi, 2000]. When examining the effects of illumination prior to sleep, deep sleep was reduced after exposure to high CCT light compared to low CCT light during the first half of sleep [Kozaki, 2005]. Finally, compared to lower CCT light, higher CCT light enhanced subjective alertness and led to faster reaction times in cognitive tasks associated with sustained attention [Chellappa, 2011]. In addition, one group recently explored nighttime exposures of 3 000 K fluorescent light attenuated in the short wavelengths with a yellow filter. That study showed that although the short wavelength attenuated light elicited very little suppression of melatonin, some performance tests results were similar to brighter, non-attenuated light [van de Werken, 2013]. Together, this literature is generally consistent in demonstrating that higher correlated colour temperature lamps induce stronger <u>acute</u> neurophysiological and neurobehavioural effects than lower correlated colour temperature lamps in healthy subjects. Those findings are reasonably coherent with the analytical action spectra shown in Table 1. Based on this emergent literature, some investigators are beginning to field test high CCT lamps in the work place for potential influence of this lamplight on employee alertness, performance, and well-being [Geerdinck, 2006; Mills, 2007; Viola, 2008].

It should be noted, however, that colour temperature may not always be a predictor of lamp potency for biological and behavioural effects [Rea, 2006]. For example, two studies compared equivalent bright, possibly saturating exposures of cool white fluorescent light (4 100 K) versus blue-enriched fluorescent light (17 000 K) for phase-shifting the circadian system. In each study, both types of light elicited strong phase-shifts with no significant difference between groups [Smith, 2009a; 2009b). A lower intensity comparison of these same lamplights revealed a greater, albeit non-significant, phase-delay shift of the 17 000 K exposure [Hanifin, 2009]. Taken together, the literature indicates that short wavelength enriched light has enhanced potency for eliciting acute biological and behavioral responses, but longer term effects like circadian phase-shifting may not reflect that same sensitivity. More work is needed to clarify the differences between the effects of polychromatic light on short versus long term effects.

5 From Basic Science to Applications of Light Therapy

Following the discovery that bright white light exposure at 2 500 lux suppressed melatonin secretion in healthy humans, researchers quickly determined that light could be used therapeutically to treat Seasonal Affective Disorder (SAD or winter depression) and to phase shift human circadian rhythms [Lewy, 1980; Rosenthal, 1984; Czeisler, 1986; Lewy, 1987]. Since then, light therapy has proven to be an effective therapeutic intervention for SAD patients and its subclinical variant, sSAD [Wetterberg, 1993; Lam, 1998; Lam, 1999; Golden, 2005]. A variety of light treatment devices have been tested for treating these affective disorders, including light boxes, dawn simulators, and head mounted delivery systems (e.g. light visors). The current standard practice is for patients to undergo a trial of 10 000 lux white fluorescent light for 30-60 minutes in the morning upon awakening [Lam, 1999; Golden, 2005]. As with the treatment of many medical disorders, patients vary in their responsiveness to light therapy. Although a majority of clinical trials employing light therapy have been concerned with the treatment of SAD, additional clinical applications have been explored including light treatment of non-seasonal depression, various sleep disorders, menstrual cycle- related problems, bulimia nervosa, and problems associated with senile dementia [Wetterberg, 1993; Lam, 1998; Tuunainen, 2004; Parry, 1997; Riemersma van der lek, 2008; Lieverse, 2011]. In addition, the utility of light therapy for resolving circadian disruption associated with intercontinental jet travel and shift work has been studied [Wetterberg, 1993; Boulos, 1995; 2002; Lam, 1998; Eastman, 1995; Revell, 2005b]. Similarly, light has been tested as a potential countermeasure for disruption of circadian rhythms and sleep-wake patterns in astronauts. Disturbed circadian rhythms and sleep-wake cycles are major risk factors for the health and safety of astronauts [NASA, 2013]. Studies of astronauts and ground crews have shown light treatment to be an effective tool for supporting circadian entrainment [Czeisler, 1991; Stewart, 1995; Dijk, 2001; Barger, 2012]. Ground-based studies continue to investigate the optimization of light as a countermeasure for circadian and sleep disruption in space flight missions [Wright, 2001; Fucci, 2005; Basner, 2013; Brainard, 2013]. The aerospace community is evaluating how lighting can be engineered properly for supporting vision, circadian regulation, and alertness of astronauts in advanced human environments such as the International Space Station as well as future space vehicles and habitats [NASA, 2013]. Such work is likely to be relevant to general architectural lighting design on Earth for civilians with specific clinical disorders as well as problems associated with shift work and jet lag. Indeed, preliminary methods are being developed to analyse the circadian efficacy of daylight in architectural designs [Andersen, 2012], and active discussions between biomedical researchers and lighting design professionals are beginning to foster a synthesis between these disparate fields [CIE, 2004a, 2004b, 2006; Brainard, 2007; IESNA 2008].

How does the seminal discovery of a novel photosensory system in the human eye with a high sensitivity to blue light intersect with the further development of therapeutic and architectural lighting applications? One recent thrust has been to test shorter wavelength (blue) light treatment for improved efficacy to evoke circadian phase-shifts and enhance acute alertness in healthy individuals [Lockley, 2003; Warman, 2003; Cajochen, 2005; Revell, 2005; Lockley, 2006; Revell, 2006; Cajochen, 2006, Ruger, 2013; Rahman, 2014]. Similarly, a Phase I clinical study tested prototype light panels with arrays of light emitting diodes (LEDs) for clinical efficacy in treating SAD [Glickman, 2006]. In that study, the panels emitted either brighter narrow-band blue light (468 nm, at 607 μW/cm^2 or about 400 lux) or dimmer narrow-band red light panels (an intended placebo light of 652 nm, at 34 μW/cm^2 or about 25 lux). Study results showed that symptom improvement was significantly better in the group treated with the blue LED light compared to those treated with the red LED light. Further, the remission rates of the patients treated with the blue LED panel were comparable to the remission rates typically reported in patients utilizing current standard bright light treatment, even though the blue light panel was at a much lower intensity [Lam, 1999; Glickman, 2006]. Additional studies on light therapy for SAD have shown that narrowbandwidth blue light or blue-enriched white light is potent for treating this disorder [Anderson, 2009; Strong, 2009;

Meesters, 2011]. Although these data illustrate the importance of wavelength in light therapy for SAD, additional larger scale studies are needed with other lighting comparison conditions.

In addition to treating SAD, studies have explored using light from LEDs to treat jet lag, shift human circadian rhythms, and evoke acute alertness [Boulos, 2002; Wright, 2004; Figueiro, 2007]. The rapid development of solid state lighting technologies is bound to have an increasing impact on light used for biological, behavioural and therapeutic applications. More work must be done, however, before there is any certainty about the optimum blend of wavelengths for these types of applications. Furthermore, as new lighting devices are developed, caution must be exercised in assuring both the efficacy and the ocular safety of such technologies [ICNIRP, 1997; ANSI, 2006; ACGIH, 2010].

6 Conclusions

Exploring the physics of light and the physiology of vision has been a passion for philosophers and scientists for at least two millennia [Zajonc, 1993]. In sharp contrast, the empirical study of the circadian, neuroendocrine, neurobehavioural, and therapeutic effects of light is relatively recent - spanning only a few decades. Despite its relative youth, this field of study is critically important in understanding how to optimize lighting in places where people live and work. The discovery and characterization of a new photosensory system in the human eye opens the door to significant challenges and innovation in the field of architectural lighting. These advancements create opportunities for pioneering new lighting technologies and design strategies that optimize illumination for vision, well-being and health.

Acknowledgements

The authors gratefully acknowledge the dedicated support of Benjamin Warfield, Michael Jablonski, and Kat West for development of Figure 1, editorial review, formatting, and referencing. With permission from the CIE, Figure 1 and portions of this manuscript were adapted and updated from an earlier publication [Brainard, 2006]. The work was supported, in part, by grants from NSBRI under NASA Cooperative Agreement NCC 9-58, NIH RO1NS36590, NIMH1R43, Apollo Health, Philips Healthcare, NSF EEC-0812056, The Institute for Integrative Health, and Philadelphia Section of the Illuminating Engineering Society.

References

ALTIMUS, C. M., GULER, A. D., ALAM, N. M., ARMAN, A. C., PRUSKY, G. T., SAMPATH, A. P. & HATTAR, S. (2010) Rod photoreceptors drive circadian photoentrainment across a wide range of light intensities. *Nature Neuroscience,* 13, 1107-1112.

AMERICAN CONFERENCE OF GOVERNMENTAL INDUSTRIAL HYGIENISTS (2010) *Nonionizing radiation and fields. Documentation of the Threshold Limit Values and Biological Exposure Indices*, Cincinnati, Ohio.

AMERICAN NATIONAL STANDARDS INSTITUTE AND ILLUMINATING ENGINEERING SOCIETY OF NORTH AMERICA (2005) *Recommended Practice for Photobiological Safety for Lamps and Lamp Systems- General Requirements, RP 27.1-05* New York, American National Standards Institute and Illuminating Engineering Society of North America.

ANDERSEN, M., MARDALJEVIC, J. & LOCKLEY, S. W. (2012) A framework for predicting the non-visual effects of daylight - Part I: photobiology-based model. *Lighting Research and Technology,* 44, 37-53.

ANDERSON, J. L., GLOD, C. A., DAI, J., CAO, Y. & LOCKLEY, S. W. (2009) Lux vs. wavelength in light treatment of Seasonal Affective Disorder. *Acta Physiologica Scandinavica,* 120**,** 203-212.

BARGER, L. K., SULLIVAN, J. P., VINCENT, A. S., FIEDLER, E. R., MCKENNA, L. M., FLYNN-EVANS, E. E., GILLILAND, K., SIPES, W. E., SMITH, P. H., BRAINARD, G. C. & LOCKLEY, S. W. (2012) Learning to live on a Mars day: fatigue countermeasures during the Phoenix Mars Lander mission. *Sleep,* 35**,** 1423-1435.

BASNER, M., DINGES, D. F., MOLLICONE, D., ECKER, A., JONES, C. W., HYDER, E. C., DI ANTONIO, A., SAVELEV, I., KAN, K., GOEL, N., MORUKOV, B. V. & SUTTON, J. P. (2013) Mars 520-d mission simulation reveals protracted crew hypokinesis and alterations of sleep duration and timing. *Proceedings of the National Academy of Sciences of the United States of America,* 110**,** 2635-2640.

BERSON, D. M., DUNN, F. A. & TAKAO, M. (2002) Phototransduction by retinal ganglion cells that set the circadian clock. *Science,* 295**,** 1070-1073.

BOULOS, Z., CAMPBELL, S. S., LEWY, A. J., TERMAN, M., DIJK, D.-J. & EASTMAN, C. I. (1995) Light treatment for sleep disorders: consensus report. VII. jet lag. *Journal of Biological Rhythms,* 10**,** 167-176.

BOULOS, Z., MACCHI, M. M., STÜRCHLER, M. P., STEWART, K. T., BRAINARD, G. C., SUHNER, A., WALLACE, G. & STEFFEN, R. (2002) Light visor treatment for jet lag after westward travel across six time zones. *Aviation Space and Environmental Medicine,* 73**,** 953-963.

BRAINARD, G. C., HANIFIN, J. P., ROLLAG, M. D., GREESON, J., BYRNE, B., GLICKMAN, G., GERNER, E. & SANFORD, B. (2001a) Human melatonin regulation is not mediated by the three cone photopic visual system. *Journal of Clinical Endocrinology and Metabolism,* 86**,** 433-436.

BRAINARD, G. C., HANIFIN, J. P., GREESON, J. M., BYRNE, B., GLICKMAN, G., GERNER, E. & ROLLAG, M. D. (2001b) Action spectrum for melatonin regulation in humans: evidence for a novel circadian photoreceptor. *Journal of Neuroscience,* 21**,** 6405-6412.

BRAINARD, G. C. & HANIFIN, J. P. (2005) Photons, clocks and consciousness. *Journal of Biological Rhythms,* 20**,** 314-325.

BRAINARD, G. C. & PROVENCIO, I. (2006) Photoreception for the neurobehavioral effects of light in humans. *Proceedings of the 2nd CIE Expert Symposium on Light and Health. CIE x031:2006* Vienna, CIE.

BRAINARD, G. C. & VEITCH, J. A. (2007) Lighting and health workshop - final report. *Proceedings of the 26th Session of the CIE. 178:2007* Vienna, CIE.

BRAINARD, G. C., COYLE, W., AYERS, M., KEMP, J., WARFIELD, B., MAIDA, J., BOWEN, C., BERNECKER, C., LOCKLEY, S. W. & HANIFIN, J. P. (2013) Solid-state lighting for the International Space Station: tests of visual performance and melatonin regulation. *Acta Astronautica,* 92**,** 21-28.

CAJOCHEN, C., MUNCH, M., KOBIALKA, S., KRAUCHI, K., STEINER, R., OELHAFEN, P., ORGUL, S. & WIRZ-JUSTICE, A. (2005) High sensitivity of human melatonin, alertness, thermoregulation, and heart rate to short wavelength light. *Journal of Clinical Endocrinology and Metabolism,* 90**,** 1311-1316.

CAJOCHEN, C., JUD, C., MUNCH, M., KOBIALKA, S., WIRZ-JUSTICE, A. & ALBRECHT, U. (2006) Evening exposure to blue light stimulates the expression of the clock gene PER2 in humans. *European Journal of Neuroscience,* 23**,** 1082-1086.

CHELLAPPA, S. L., STEINER, R., BLATTNER, P., OELHAFEN, P., GOTZ, T. & CAJOCHEN, C. (2011) Non-visual effects of light on melatonin, alertness and cognitive performance: can blue-enriched light keep us alert? *PLoS ONE,* 6**,** e16429.

COMMISSION INTERNATIONALE DE L'ECLAIRAGE (2004a) *Ocular Lighting Effects on Human Physiology and Behaviour, Technical Report 158,* Vienna, CIE.

COMMISSION INTERNATIONALE DE L'ECLAIRAGE (2004b) *Proceedings of the CIE Symposium on Light and Health: Non-Visual Effect. CIE x027:2004,* Vienna, CIE.

COMMISSION INTERNATIONALE DE L'ECLAIRAGE (2006) *Proceedings of the 2nd CIE Expert Symposium on Light and Health. CIE x031:2006* Vienna, CIE.

COOHILL, T. P. (1999) Photobiological action spectra- what do they mean? IN MATTHES, R., SLINEY, D., DIDOMENICO, S., MURRAY, P., PHILLIPS, R. & WENGRAITIS, S. (Eds.) *Measurements of Optical Radiation Hazards.* Munchen, Germany, ICNIRP.

CZEISLER, C. A., ALLAN, J. S., STROGATZ, S. H., RONDA, J. M., SANCHEZ, R., RIOS, C. D., FREITAG, W. O., RICHARDSON, G. S. & KRONAUER, R. E. (1986) Bright light resets the human circadian pacemaker independent of the timing of the sleep-wake cycle. *Science,* 233**,** 667-671.

CZEISLER, C. A., CHIASERA, A. J. & DUFFY, J. F. (1991) Research on sleep, circadian rhythms and aging: applications to manned spaceflight. *Experimental Gerontology,* 26**,** 217-232.

DACEY, D. M., LIAO, H.-W., PETERSON, B. B., ROBINSON, F. R., SMITH, V. C., POKORNY, J., YAU, K.-W. & GAMLIN, P. D. (2005) Melanopsin-expressing ganglion cells in primate retina signal colour and irradiance and project to the LGN. *Nature,* 433**,** 749-754.

DEUTSCHES INSTITUT FUR NORMUNG (2009) Optical radiation physics and illuminating engineering - Part 100: Non-visual effects of ocular light on human beings - Quantities, symbols and action spectra. Berlin.

DIJK, D. J., NERI, D. F., WYATT, J. K., RONDA, J. M., RIEL, E., A., R.-D., HUGHES, R. J., ELLIOTT, A. R., PRISK, G. K., WEST, J. B. & CZEISLER, C. A. (2001) Sleep, performance, circadian rhythms, and light-dark cycles during two space shuttle flights. *American Journal of Physiology,* 281**,** R1647-R1664.

DKHISSI-BENYAHYA, O., GRONFIER, C., DE VANSSAY, W., FLAMANT, F. & COOPER, H. M. (2007) Modeling the role of mid-wavelength cones in circadian responses to light. *Neuron,* 53**,** 677-687.

EASTMAN, C. I., BOULOS, Z., TERMAN, M., CAMPBELL, S. S., DIJK, D.-J. & LEWY, A. J. (1995) Light treatment for sleep disorders: consensus report. VI. shift work. *Journal of Biological Rhythms,* 10**,** 157-164.

FIGUEIRO, M. G., BULLOUGH, J. D., PARSONS, R. H. & REA, M. S. (2004) Preliminary evidence for spectral opponency in the suppression of melatonin by light in humans. *Neuroreport,* 15**,** 313-316.

FIGUEIRO, M. G., REA, M. S. & BULLOUGH, J. D. (2006) Circadian effectiveness of two polychromatic lights in suppressing human nocturnal melatonin. *Neuroscience Letters,* 406**,** 293-297.

FIGUEIRO, M. G., BULLOUGH, J. D., BIERMAN, A., FAY, C. R. & REA, M. S. (2007) On light as an alerting stimulus at night. *Acta Neurobiologiae Experimentalis,* 67**,** 171-178.

FUCCI, R. L., GARDNER, J., HANIFIN, J. P., JASSER, S., BYRNE, B., GERNER, E., ROLLAG, M. & BRAINARD, G. C. (2005) Toward optimizing lighting as a countermeasure to sleep and circadian disruption in space flight. *Acta Astronautica,* 56**,** 1017-1024.

GAMLIN, P. D. R., MCDOUGAL, D. H., POKORNY, J., SMITH, V. C., YAU, K.-W. & DACEY, D. M. (2007) Human and macaque pupil responses driven by melanopsin-containing retinal gangion cells. *Vision Research,* 47**,** 946-954.

GEERDINCK, L. M. & SCHLANGEN, L. J. (2006) Well-being effects of high color temperature lighting in office and industry. *Proceedings of the 2nd CIE Expert Symposium on Light and Health. CIE x031:2006.*Vienna, CIE.

GLICKMAN, G., BYRNE, B., PINEDA, C., HAUCK, W. W. & BRAINARD, G. C. (2006) Light therapy for Seasonal Affective Disorder with blue narrow-band light-emitting diodes (LED). *Biological Psychiatry,* 59**,** 502-507.

GOLDEN, R. N., GAYNES, B. N., EKSTROM, R. D., HAMER, R. M., JACOBSEN, F. M., SUPPES, T., WISNER, K. L. & NEMEROFF, C. B. (2005) The efficacy of light therapy in the treatment of mood disorders: a review and meta-analysis of the evidence. *American Journal of Psychiatry,* 162**,** 656-662.

GOOLEY, J. J., LU, J., CHOU, T. C., SCAMMELL, T. E. & SAPER, C. B. (2001) Melanopsin in cell of origin of the retinohypothalamic tract. *Nature Neuroscience,* 4**,** 1165.

GOOLEY, J. J., RAJARATNAM, S. M., BRAINARD, G. C., KRONAUER, R. E., CZEISLER, C. A. & LOCKLEY, S. W. (2010) Spectral responses of the human circadian system depend on the irradiance and duration of exposure to light. *Science Translational Medicine,* 2**,** 31ra33.

HANIFIN, J. P. & BRAINARD, G. C. (2007) Photoreception for circadian, neuroendocrine and neurobehavioral regulation. *Journal of Physiological Anthropology and Applied Human Science,* 26**,** 87-94.

HANIFIN, J., LOCKLEY, S., CECIL, K., WEST, K., JABLONSKI, M., WARFIELD, B., JAMES, M., THIESSEN, M., BYRNE, B., GERNER, E., ROLLAG, M. & BRAINARD, G. (2009) Polychromatic blue-enriched fluorescent light for melatonin suppression and circadian phase resetting. Berlin, Germany, June 24-27, 21st Annual Meeting of the Society for Light Treatment and Biological Rhythms.

HANIFIN, J., KEMP, J., DOWNES, M., WARFIELD, B., AYERS, M., CECIL, K., GERNER, E., NOGUCHI, H., SHIMIZU, M. & BRAINARD, G. (2011) Effects of fluorescent light correlated color temperature on melatonin regulation in healthy humans. Montreal, Canada, July 10-13, 23rd Annual Meeting of the Society for Light Treatment and Biological Rhythms.

HANKINS, M. W. & LUCAS, R. J. (2002) The primary visual pathway in humans is regulated according to long-term light exposure through the action of a nonclassical photopigment. *Current Biology,* 12**,** 191-198.

HATTAR, S., LIAO, H.-W., TAKAO, M., BERSON, D. M. & YAU, K.-W. (2002) Melanopsin-containing retinal ganglion cells: architecture, projections, and intrinsic photosensitivity. *Science,* 295**,** 1065-1070.

HATTAR, S., LUCAS, R. J., MROSOVSKY, N., THOMPSON, S., DOUGLAS, R. H., HANKINS, M. W., LEM, J., BIEL, M., HOFMANN, F., FOSTER, R. G. & YAU, K.-W. (2003) Melanopsin and rod-cone photoreceptive systems account for all major accessory visual functions in mice. *Nature,* 424**,** 76-81.

HEBERT, M., MARTIN, S. K., LEE, C. & EASTMAN, C. I. (2002) The effects of prior light history on the suppression of melatonin by light in humans. *Journal of Pineal Research,* 33**,** 198-203.

HORSPOOL, W. M. & SONG, P.-S. (Eds.) (1994) *Organic Photochemistry and Photobiology,* New York, CRC Press.

ILLUMINATING ENGINEERING SOCIETY OF NORTH AMERICA (2008) *Light and Human Health: An Overview of the Impact of Optical Radiation on Visual, Circadian, Neuroendocrine, and Neurobehavioral Responses, IES TM-18-08,* New York, Illuminating Engineering Society of North America.

INTERNATIONAL COMMISSION ON NON-IONIZING RADIATION PROTECTION (1997) Guidelines on limits of exposure to broad-band incoherent optical radiation (0.38 to 3 microM). *Health Physics,* 73**,** 539-554.

JAPANESE COMMISSION ON ILLUMINATION (2004) Bio-safety standardization WG report of the LED light source. Tokyo, Japan.

JASSER, S. A., HANIFIN, J. P., ROLLAG, M. D. & BRAINARD, G. C. (2006) Dim light adaptation attenuates acute melatonin suppression in humans. *Journal of Biological Rhythms,* 21**,** 394-404.

KOZAKI, T., KITAMURA, S., HIGASHIHARA, Y., ISHIBASHI, K., NOGUCHI, H. & YASUKOUCHI, A. (2005) Effect of color temperature of light sources on slow-wave sleep. *Journal of Physiological Anthropology and Applied Human Science,* 24**,** 183-186.

KOZAKI, T., KOGA, S., TODA, N., NOGUCHI, H. & YASUKOUCHI, A. (2008) Effects of short wavelength control in polychromatic light sources on nocturnal melatonin secretion. *Neuroscience Letters,* 439**,** 256-259.

LALL, G. S., REVELL, V. L., MOMIJI, H., AL ENEZI, J., ALTIMUS, C. M., GULER, A. D., AGUILAR, C., CAMERON, M. A., ALLENDER, S., HANKINS, M. W. & LUCAS, R. L. (2010) Distinct contributions of rod, cone, and melanopsin photoreceptors to encoding irradiance. *Neuron,* 66**,** 417-428.

LAM, R. W. (Ed.) (1998) *Seasonal Affective Disorder and Beyond: Light Treatment for SAD and Non-SAD Disorders,* Washington, D.C., American Psychiatric Press.

LAM, R. W. & LEVITT, A. J. (Eds.) (1999) *Canadian Consensus Guidelines for the Treatment of Seasonal Affective Disorder,* Vancouver, British Columbia, Clinical and Academic Publishing.

LEWY, A. J., WEHR, T. A., GOODWIN, F. K., NEWSOME, D. A. & MARKEY, S. P. (1980) Light suppresses melatonin secretion in humans. *Science,* 210**,** 1267-1269.

LEWY, A. J., SACK, R. L., MILLER, L. S. & HOBAN, T. M. (1987) Antidepressant and circadian phase-shifting effects of light. *Science,* 235**,** 352-354.

LIEVERSE, R., VAN SOMEREN, E. J., NIELEN, M. M., UITDEHAAG, B. M., SMIT, J. H. & HOOGENDIJK, W. J. (2011) Bright light treatment in elderly patients with nonseasonal major depressive disorder: a randomized placebo-controlled trial. *Archives of General Psychiatry,* 68**,** 61-70.

LOCKLEY, S. W., BRAINARD, G. C. & CZEISLER, C. A. (2003) High sensitivity of the human circadian melatonin rhythm to resetting by short wavelength light. *Journal of Clinical Endocrinology and Metabolism,* 88**,** 4502-4505.

LOCKLEY, S. W., EVANS, E. E., SCHEER, F. A., BRAINARD, G. C., CZEISLER, C. A. & AESCHBACH, D. (2006) Short-wavelength sensitivity for the direct effects of light on alertness, vigilance, and the waking electroencephalogram in humans. *Sleep,* 29**,** 161-168.

LUCAS, R. J., DOUGLAS, R. H. & FOSTER, R. G. (2001) Characterization of an ocular photopigment capable of driving pupillary constriction in mice. *Nature Neuroscience,* 4**,** 621-626.

LUCAS, R. J., HATTAR, S., TAKAO, M., BERSON, D. M., FOSTER, R. G. & YAU, K. W. (2003) Diminished pupillary light reflex at high irradiances in melanopsin-knockout mice. *Science,* 299**,** 245-247.

LUCAS, R. J., PEIRSON, S. N., BERSON, D. M., BROWN, T. M., COOPER, H. M., CZEISLER, C. A., FIGUEIRO, M. G., GAMLIN, P. D., LOCKLEY, S. W., O'HAGAN, J. B., PRICE, L. L. A., PROVENCIO, I., SKENE, D. J. & BRAINARD, G. C. (2014) Measuring and using light in the melanopsin age. *Trends in Neurosciences,* 37**,** 1-9.

MEESTERS, Y., DEKKER, V., SCHLANGEN, L. J. M., BOS, E. H. & RUITER, M. J. (2011) Low-intensity blue-enriched white light (750 lux) and standard bright light (10,000 lux) are equally effective in treating SAD. A randomized controlled study. *BMC Psychiatry,* 11**,** 17. doi: 10.1186/1471-244X/11/17.

MILLS, P. M., TOMKINS, S. C. & SCHLANGEN, L. J. M. (2007) The effect of high correlated colour temperature office lighting on employee wellbeing and work performance. *Journal of Circadian Rhythms,* 5**,** 2-10.

MORITA, T. & TOKURA, H. (1998) The influence of different wavelengths of light on human biological rhythms. *Applied Human Science,* 17**,** 91-96.

NATIONAL AERONAUTICS AND SPACE ADMINISTRATION (2013) *Human Research Program Requirements Document, Revision F, February 2013, HRP-47052,* Houston, Texas, Johnson Space Center.

NOGUCHI, H. & SAKAGUCHI, T. (1999) Effect of illuminance and color temperature on lowering of physiological activity. *Applied Human Science,* 18**,** 117-123.

PANDA, S., SATO, T. K., CASTRUCCI, A. M., ROLLAG, M. D., DEGRIP, W. J., HOGENSCH, J. B., PROVENCIO, I. & KAY, S. A. (2002) Melanopsin (Opn4) requirement for normal light-induced circadian phase-shifting. *Science,* 298**,** 2213-2216.

PANDA, S., PROVENCIO, I., TU, D. C., PIRES, S. S., ROLLAG, M. D., CASTRUCCI, A. M., PLETCHER, M. T., SATO, T. K., WILTSHIRE, T., ANDAHAZY, M., KAY, S. A., VAN GELDER, R. N. & HOGENSCH, J. B. (2003) Melanopsin is required for non-image-forming photic responses in blind mice. *Science,* 301**,** 525-527.

PARRY, B. L., BERGA, S. L., MOSTOFI, N., KLAUBER, M. R. & RESNICK, A. (1997) Plasma melatonin circadian rhythms during the menstrual cycle and after light therapy in premenstrual dysphoric disorder and normal control subjects. *Journal of Biological Rhythms,* 12**,** 47-64.

PROVENCIO, I. & FOSTER, R. G. (1995) Circadian rhythms in mice can be regulated by photoreceptors with cone-like characteristics. *Brain Research,* 694**,** 183-190.

PROVENCIO, I., JIANG, G., DE GRIP, W. J., HAYES, W. P. & ROLLAG, M. D. (1998) Melanopsin: an opsin in melanophores, brain, and eye. *Proceedings of the National Academy of Sciences of the United States of America,* 95**,** 340-345.

PROVENCIO, I., RODRIGUEZ, I. R., JIANG, G., HAYES, W. P., MOREIRA, E. F. & ROLLAG, M. D. (2000) A novel human opsin in the inner retina. *Journal of Neuroscience,* 20**,** 600-605.

PROVENCIO, I., ROLLAG, M. D. & CASTRUCCI, A. M. (2002) Photoreceptive net in the mammalian retina. *Nature,* 415**,** 493.

RAHMAN, S. A., FLYNN-EVANS, E. E., AESCHBACH, D., BRAINARD, G. C., CZEISLER, C. A. & LOCKLEY, S. W. (2014) Diurnal spectral sensitivity of the acute alerting effects of light. *Sleep,* 37**,** 271-281.

REA, M. S., BULLOUGH, J. D., BIERMAN, A., FIGUEIRO, M. G. (2006) Implications for white light sources of different colour temperatures. *Proceedings of the 2nd CIE Expert Symposium on Light and Health. CIE x031:2006.*Vienna, CIE.

REVELL, V. L., ARENDT, J., TERMAN, M. & SKENE, D. J. (2005a) Short-wavelength sensitivity of the human circadian system to phase-advancing light. *Journal of Biological Rhythms,* 20**,** 270-272.

REVELL, V. L. & EASTMAN, C. I. (2005b) How to trick mother nature into letting you fly around or stay up all night. *Journal of Biological Rhythms,* 20**,** 353-365.

REVELL, V. L., ARENDT, J., FOGG, L. F. & SKENE, D. J. (2006) Alerting effects of light are sensitive to very short wavelengths. *Neuroscience Letters,* 399**,** 96-100.

REVELL, V. L. & SKENE, D. J. (2007) Light-induced melatonin suppression in humans with polychromatic and monochromatic light. *Chronobiology International,* 24**,** 1125-1137.

RIEMERSMA-VAN DER LEK, R. F., SWAAB, D. F., TWISK, J., HOL, E. M., HOOGENDIJK, W. J. & VAN SOMEREN, E. J. (2008) Effect of bright light and melatonin on cognitive and noncognitive function in elderly residents of group care facilities: a randomized controlled trial. *JAMA,* 299**,** 2642-2655.

ROSENTHAL, N. E., SACK, D. A., GILLIN, J. C., LEWY, A. J., GOODWIN, F. K., DAVENPORT, Y., MUELLER, P. S., NEWSOME, D. A. & WEHR, T. A. (1984) Seasonal affective disorder. A description of the syndrome and preliminary findings with light therapy. *Archives of General Psychiatry,* 41**,** 72-80.

RUGER, M., ST. HILAIRE, M. A., BRAINARD, G. C., KHALSA, S. B., KRONAUER, R. E., CZEISLER, C. A. & LOCKLEY, S. W. (2013) Human phase response curve to a single 6.5h light pulse of short-wavelength light. *Journal of Physiology,* 591**,** 353-363.

SATO, M., SAKAGUCHI, T. & MORITA, T. (2005) The effects of exposure in the morning to light of different color temperatures on the behavior of core temperature and melatonin secretion in humans. *Biological Rhythm Research,* 36**,** 278-292.

SMITH, M. R. & EASTMAN, C. I. (2009a) Phase delaying the human circadian clock with blue-enriched polychromatic light. *Chronobiology International,* 26, 709-725.

SMITH, M. R., REVELL, V. L. & EASTMAN, C. I. (2009b) Phase advancing the human circadian clock with blue-enriched polychromatic light. *Sleep Medicine,* 10, 287-294.

STEWART, K. T. & EASTMAN, C. I. (1995) The light stuff: shiftwork, circadian rhythms, and manned spaceflight. *Photodermatology, Photoimmunology and Photomedicine,* 11, 83.

STRONG, R. E., MARCHANT, B. K., REIMHERR, F. W., WILLIAMS, E., SONI, P. & MESTAS, R. (2009) Narrow-band blue-light treatment of seasonal affective disorder in adults and the influence of additional nonseasonal symptoms. *Depression and Anxiety,* 26, 273-278.

TAKAHASHI, J. S., DECOURSEY, P. J., BAUMAN, L. & MENAKER, M. (1984) Spectral sensitivity of a novel photoreceptive system mediating entrainment of mammalian circadian rhythms. *Nature,* 308, 186-188.

THAPAN, K., ARENDT, J. & SKENE, D. J. (2001) An action spectrum for melatonin suppression: evidence for a novel non-rod, non-cone photoreceptor system in humans. *Journal of Physiology,* 535, 261-267.

TUUNAINEN, A., KRIPKE, D. F. & ENDO, T. (2004) Light therapy for non-seasonal depression. *The Cochrane Database of Systemic Reviews,* 2, 1-83.

VANDEWALLE, G., GAIS, S., SCHABUS, M., BALTEAU, E., CARRIER, J., DARSAUD, A., STERPENICH, V., ALBOUY, G., DIJK, D. J. & MAQUET, P. (2007a) Wavelength-dependent modulation of brain responses to a working memory task by daytime light exposure. *Cerebral Cortex,* 17, 2788-2795.

VANDEWALLE, G., SCHMIDT, C., ALBOUY, G., STERPENICH, V., DARSAUD, A., RAUCHS, G., BERKEN, P. Y., BALTEAU, E., DEGUELDRE, C., LUXEN, A., MAQUET, P. & DIJK, D. J. (2007b) Brain responses to violet, blue, and green monochromatic light exposures in humans: prominent role of blue light and the brainstem. *PLoS ONE,* 207, 11.

VANDEWALLE, G., SCHWARTZ, S., GRANDJEAN, D., WUILLAUME, C., BALTEAU, E., DEGUELDRE, C., SCHABUS, M., PHILLIPS, C., LUXEN, A., DIJK, D. J. & MAQUET, P. (2010) Spectral quality of light modulates emotional brain responses in humans. *Proceedings of the National Academy of Sciences of the United States of America,* 107, 19549-19554.

VAN DE WERKEN, M., GIMENEZ, M. C., DE VRIES, B., BEERSMA, D. G. M. & GORDIJN, M. C. M. (2013) Short-wavelength attenuated polychromatic white light during work at night: limited melatonin suppression without substantial decline of alertness. *Chronobiology International,* 30, 843-854.

VIOLA, A. U., L.M., J., SCHLANGEN, L. J. M. & DIJK, D. J. (2008) Blue-enriched white light in the workplace improves self-reported alertness, performance and sleep quality. *Scandinavian Journal of Work, Environment and Health,* 34, 297-306.

WARMAN, V. L., DIJK, D.-J., WARMAN, G. R., ARENDT, J. & SKENE, D. J. (2003) Phase advancing human circadian rhythms with short wavelength light. *Neuroscience Letters,* 342, 37-40.

WETTERBERG, L. (Ed.) (1993) *Light and Biological Rhythms in Man,* Stockholm, Pergamon Press.

WRIGHT, H. R., LACK, L. C. & KENNAWAY, D. J. (2004) Differential effects of light wavelength in phase advancing the melatonin rhythm. *Journal of Pineal Research,* 36, 140-144.

WRIGHT, K. P., HUGHES, R. J., KRONAUER, R. E., DIJK, D.-J. & CZEISLER, C. A. (2001) Intrinsic near-24-h pacemaker period determines limits of circadian entrainment to a weak synchronizer in humans. *Proceedings of the National Academy of Sciences of the United States of America,* 98, 14027-14032.

YASUKOUCHI, A., YASUKOUCHI, Y. & ISHIBASHI, K. (2000) Effects of color temperature of fluorescent lamps on body temperature regulation in a moderately cold environment. *Journal of Physiological Anthropology and Applied Human Science,* 19**,** 125-134.

YASUKOUCHI, A. & ISHIBASHI, K. (2005) Non-visual effects of the color temperature of fluorescent lamps on physiological aspects in humans. *Journal of Physiological Anthropology and Applied Human Science,* 24**,** 41-43.

YOSHIMURA, T. & EBIHARA, S. (1996) Spectral sensitivity of photoreceptors mediating phase-shifts of circadian rhythms in retinally degenerate CBA/J (rd/rd) and normal CBA/N (+/+) mice. *Journal of Comparative Physiology [A],* 178**,** 797-802.

ZAIDI, F. H., HULL, J. T., PEIRSON, S. N., WULFF, K., AESCHBACH, D., GOOLEY, J. J., BRAINARD, G. C., GREGORY-EVANS, K., RIZZO, J. F., CZEISLER, C. A., FOSTER, R. G., MOSELEY, M. J. & LOCKLEY, S. W. (2007) Short-wavelength light sensitivity of circadian, pupillary, and visual awareness in humans lacking an outer retina. *Current Biology,* 17**,** 2122-2128.

ZAJONC, A. (1993) *Catching the Light: the Entwined History of Light and Mind,* New York, Oxford University Press.

IT05

HOMOGENEITY AND LIFETIME OF OLEDS FOR LIGHTING

Thorsten Vehoff[1], Martina Ascher[2], Siegmund Staggl[2], Wilfried Pohl[2], Markus Canazei[2], Thorsten Gerloff[3], Karsten Diekmann[1]

[1]Osram Opto Semiconductors GmbH, Regensburg, GERMANY,
[2]Bartenbach GmbH, Aldrans, AUSTRIA
[3]Physikalisch-Technische Bundesanstalt, Braunschweig, GERMANY
thorsten.vehoff@osram-os.com

Abstract

OLEDs are on the verge of revolutionizing the lighting market as extremely thin area light sources. As such there are many new challenges posed on the way various lighting applications. Two of these are addressed here. First, the definition of homogeneity for an OLED light source is evaluated based on a perception study. The standard display definitions for homogeneity are not sufficient to capture the actual visual perception and thus new homogeneity formulas are evaluated. Second, the lifetime of large area OLEDs is predicted based on small area test devices aged under accelerated conditions. Influence of temperature and current on the aging behaviour of OLEDs is analyzed focusing on the effect of homogeneity and self-heating for increasingly large OLEDs.

1 Brightness homogeneity

To ensure the broad acceptance of OLEDs for general lighting applications, a homogeneous appearance of the OLED lighting tiles is very important. Much more so than for displays, since the latter rarely show the same colour with every pixel nor do they display the same picture for a long time. At present the most common formulas in use to calculate the homogeneity of luminance distributions on surfaces take into account only the maximum and the minimum luminance of a panel (VESA):

$$H_1 = 1 - \frac{L_{max} - L_{min}}{L_{max} + L_{min}} \tag{1}$$

where

H is the homogeneity,

L_{max} and L_{min} are the minimum and maximum luminance levels of the panel.

However, perception studies (OLED100.EU) have shown that the appearance of homogeneity depends greatly on the luminance pattern. For example a luminance distribution showing a gradient from the lower left to the upper right corner of a rectangular device does not appear as inhomogeneous as an OLED with a centered distribution, where there is a gradient between a dark stripe in the center and bright edges (so-called “bathtub” pattern). An intensive perception study performed within the OLED100.EU project funded by the European Union has indicated that the gradient of a luminance distribution might be a more appropriate measure (Ashdown, 1996). Two new homogeneity formulas were proposed as the result:

$$H_2 = 1 - max\left\{\frac{|L_i - L_j|}{d_{ij}}\right\} / \frac{L_{av}}{max\{d_{ij}\}} \tag{2}$$

$$H_3 = 1 - \sum \frac{|L_i - L_j|}{d_{ij}} / \sum \frac{L_{av}}{\{d_{ij}\}} \tag{3}$$

where

L_i and L_j are the luminance at points i and j within the lighting area and

d_{ij} is the Euclidean distance between the points.

Eqn. (2) emphasizes the maximum gradient, eqn. (3) the average gradient, normalized by the average luminance divided by the maximum distance or the sum of distances, respectively. Clearly in this case for a rectangular OLED the two formulas would give lower values for a gradient stretching from the lower left to the upper right corner than for a distribution from a dark center to a bright edge, assuming the maximum and minimum luminance values are identical and thus eqn. (1) yields identical results for both lighting tiles.

1.1 An advanced homogeneity perception study

Despite many interesting insights on the perception of OLED lighting tiles, the OLED100.EU study also had two main drawbacks. Firstly, the mean luminance of the artificially created OLEDs was less than 1000 cd/m² and thus way below that of OLEDs to be used for lighting (≥ 2000 cd/m²). Secondly, the patterns analyzed were idealized patterns such as the “bathtub” that do not necessarily show up in actual OLED lighting tiles. Both topics were addressed in this study, which was conducted in cooperation with Bartenbach in Austria. To artificially create OLEDs of different brightness and homogeneity, a high brightness display screen capable of reaching a maximum luminance of 5000 cd/m² was used. To obtain realistic homogeneity patterns, a finite element model of OLEDs was used to simulate the homogeneity of a square OLED based on different contacting methods and various conductivities of anode and cathode. The resulting patterns chosen for the study are shown in figure 1.

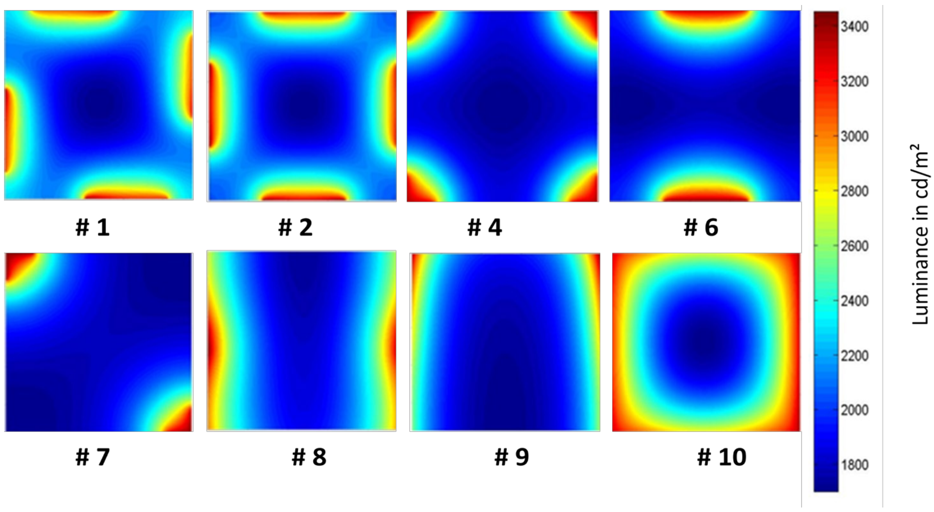

Figure 1 – The eight different brightness patterns used in the study.

The study was divided into three parts. In two parts, two OLEDs were shown next to each other. In the first, one of the two OLED was perfectly homogeneous while the other was inhomogeneous. Observers were asked to identify the inhomogeneous OLED. In the second, both OLEDs were inhomogeneous. Observers were asked to determine which of the OLEDs was more inhomogeneous. In the third part, an OLED cluster of three by two OLEDs all with the same type of homogeneity pattern was shown. The observer was asked to rate how strongly he noticed the inhomogeneity and whether the OLED cluster was considered disturbing or attractive in appearance, both on a 6-point Likert scale from zero to five. The correlated color temperature of the surrounding room and the display background was adjusted to 4300 K. The ambient luminance was set to 50 cd/m² in all studies and additionally to 200 cd/m² in the third study as well. The mean luminance and color temperature of the OLEDs were chosen to be either 1520 cd/m² at 3000K or 2135 cd/m² at 5000K, in part due to the color limitations of the display. For each pattern, the relation between minimum and maximum brightness was varied to yield values of H_1 (see eqn. 1) between 60 and 100%. The study was carried out with 40 people, aged between 20 and 59 years - with an average of 32.6 years.

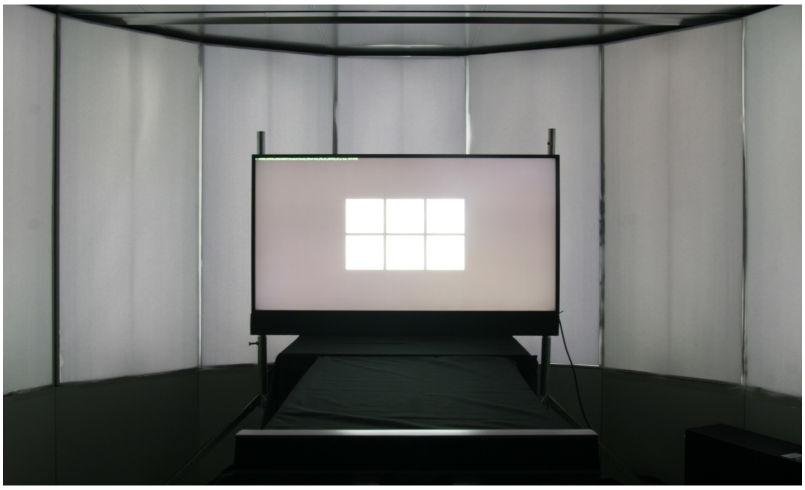

Figure 2 – Simulated OLED-cluster as used within part 3 of the study.

1.2 Results

We began the study with four hypotheses to be tested:

1. The brighter the OLED, the harder it is to recognize inhomogeneities.
2. The color temperature does not influence the perception of inhomogeneities.
3. The perception threshold depends on the homogeneity pattern.
4. Inhomogeneities in a cluster of OLEDs are more disturbing than for single OLEDs.

Surprisingly, in part 1 (comparison of two OLEDs, one perfectly homogeneous) no dependence on brightness was found. In part 3 (cluster of 2 by 3 OLEDs), however, it was indeed more difficult for the observers to recognize inhomogeneities at higher luminance of the OLEDs. Regarding color temperature part 1 showed that it has no influence on perception. But for the OLED cluster observers found inhomogeneities more easily recognizable and more disturbing at higher correlated color temperatures.

The perception threshold was indeed shown to depend on the homogeneity pattern. As shown in figure 3 for the patterns number 7, 8 and 9 the correct recognition of inhomogeneity is harder, i.e. less people correctly identified this OLED as the inhomogeneous one in part 1 of the study. In other words at the same display uniformity (H_1), these distributions appear more homogeneous than the others.

Figure 3 – Dependence of perception threshold on homogeneity pattern.

Finally, the fourth hypotheses was shown to be true. The more inhomogeneous an OLED is, the more disturbing the resulting OLED cluster appears. For none of the available homogeneity patterns was an inhomogeneous OLED cluster considered to be more attractive than a homogeneous one. Moreover, in a cluster OLEDs were more easily perceived as inhomogeneous, i.e. the perception threshold is lowered compared to a single OLED. This makes the production of homogeneous OLEDs even more important, since any OLED luminaire will most certainly consist of a cluster of OLEDs.

Equations (2) and (3) were used to calculate the homogeneity of the different OLED patterns at varying H_1 values. However, they did not show a clear preference of patterns 7, 8 and 9 as illustrated by figure 3. Taking a closer look at the patterns, it appears that in patterns 7, 8 and 9 there might be less really bright or dark areas than in the other patterns. Thus we decided to use a formula based on a frequency mapping of bright and dark areas in a pattern with respect to the average luminance of the panel to calculate the homogeneity $\boldsymbol{H_4}$.

$$H_4 = \frac{1}{N}\left[N - \sum_{i=1}^{N}\left(\Theta_{L_{av}-L_i-s} + \Theta_{L_i-L_{av}-s}\right)\right]\frac{L_{av}-s}{L_{av}} \qquad (4)$$

where

N is the number of pixels, where the luminance is evaluated,

L_i is the luminance evaluated pixel number i,

L_{av} is the average luminance,

s is the empirical standard deviation of the luminance and

$\Theta_x = 1$ for $x > 0$ and $\Theta_x = 0$ for $x < 0$, x is a place holder for the terms in eqn. 4.

The ability of this formula or combinations thereof with eqn. (1) to (3) to correctly describe the perception threshold are still under investigation and will be published elsewhere in the future. In addition the eye movement of the observers was tracked by an SMI red-eyetracker. An analysis of the way people observe homogeneity patterns is expected to give insights for an appropriate mathematical model for homogeneity as well.

2 Lifetime of large area OLEDs for lighting

One of the main challenges with long living light-sources such as LEDs and OLEDs is to predict their substantial lifetime after a finite test time. LEDs have the grand advantage of having seen plenty of use in the field over the last years, while OLEDs are still a niche product with lifetime predictions relying heavily on modelling and aging at accelerated conditions. To speed up the development of long-lived devices and keep the material bill for testing as low as possible, operating lifetime is preferably tested on small scale devices of a few mm² or cm². In addition one cannot afford to wait several thousand hours for devices to age at rated current and ambient temperature. Thus aging at accelerated conditions is used in order to implement improvements quickly. For OLEDs the two main acceleration parameters are driving current and temperature. The ultimate goal is two-fold: to predict the lifetime of large area products based on accelerated measurements on research-sized OLEDs and to provide acceleration conditions for the customer to test the lifetime of products as swiftly as possible. The operating lifetime is defined as the time when the light output of the OLED – measured in lumens or more conveniently in candelas per square meter in 0° direction – drops to a certain percentage of its initial value. In this work we will always refer the time when the initial luminance has dropped to 70%, i.e. LT70. Note that spontaneous failures are not included in these considerations. The approach to predict the lifetime consists of two complementing methods. The most straight-forward is to extrapolate a short lifetime measurement until end of life. The obvious draw-back is that one needs to know the aging behaviour beforehand to be reasonably sure of an extrapolation and even the uncertainty of the forecast is unacceptably high based on measurements having lasted only 20% or less of the total lifetime. Another approach is to use accelerated conditions. This allows aging of devices up to their end of life condition without spending too much time. However, one needs to find a reliable way to predict the lifetime under normal conditions based on these measurements. This requires tests at multiple acceleration conditions and comparison to data obtained under normal conditions. An additional challenge not previously addressed in literature is the prediction of the lifetime of large area devices based on the aging of small devices. This is complicated by the decreasing homogeneity and increased self-heating with size.

2.1 Scaling experiments

OLEDs of five different sizes shown in figure 4 were used to predict the scaling behaviour under operating conditions. To obtain a large array of acceleration conditions, experiments were carried out at four different temperatures (25, 40, 60 and 75°C) and multiple different current densities ranging from the 2.56 mA/cm² (rated current) up to 20 mA/cm². The high current densities were only applied to small devices (1.68 and 0.04 cm²), because the homogeneity drops dramatically for large devices at such currents. Thus 7.5 mA/cm² was used as maximum acceleration for large OLEDs.

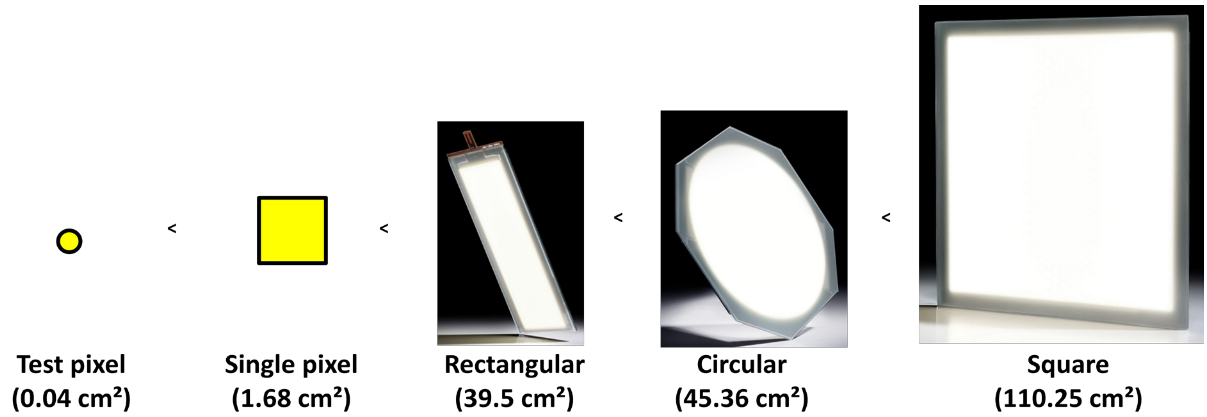

Figure 4 – OLEDs of different sizes used for scaling experiments

For the sake of simplicity, we will focus on a comparison of the small test pixel with the large square OLED throughout. For development, the goal is to predict the lifetime of a large OLED based on highly accelerated measurements with test pixels. In the ideal case, an acceleration factor should be found between a 4 mm² pixel aged at 75°C at 20 mA/cm² and an OLED of any given size at normal operating conditions, i.e. 25°C at rated current. In this study we will judge the quality of the acceleration factor between a pixel at 75°C at 20 mA/cm^2 and a square OLED with 110.25 cm² lighting area aged at 25°C at 2.56 mA/cm².

2.2 Extrapolation of lifetime

To obtain the operating lifetime of an OLED under certain conditions without waiting for the luminance to drop to 70% of its initial value, it is easiest to extrapolate the data as soon as possible. Since lifetimes of OLEDs already exceed ten thousand hours under normal operating conditions, i.e. ambient temperature and rated current, extrapolation is necessary to predict the lifetime based on measurements at operating or weakly accelerated conditions. Nonetheless, it is important to wait long enough to ensure the initial behaviour often characterized by an abrupt drop has passed and the long term behaviour has been reached. For simplicity and to negate minor differences between devices with the same stack, the normalized luminance $L(t)/L_0$ is used for lifetime prediction. Multiple different models are available for extrapolation (Buckley, 2013):

1. Linear extrapolation (after the initial drop)

   $L(t)/L_0 = b\text{-}a\boldsymbol{t}$

2. Power law (generalize root)

   $L(t)/L_0 = 1\text{-}a\boldsymbol{t}^b$

3. Power law with additive constant (generalized root (loose))

   $L(t)/L_0 = c\text{-}a\boldsymbol{t}^b$

4. Stretched exponential function

   $L(t)/L_0 = c\text{-}exp\{(-\boldsymbol{t}/a)^b\}$

5. Model free extrapolation

Here a, b, and c are fitting parameters.

$L(t)$ is the luminance at a certain time $\boldsymbol{t}$ and L_0 is the initial luminance at t=0 hours. Model free extrapolation uses the lifetime behaviour of a highly accelerated condition and stretches the time axis until the resulting curve matches that of the condition of interest. This is extremely helpful for small devices at the same temperature differing only in current density. As soon as the temperature changes, however, the curve shape is also found to change too much for this method to work. Since we expect self-heating in larger devices, this method will not be treated here. For past stack architectures, the stretched exponential function has seen much successful use in the prediction of OLED lifetimes, for current device architectures this approach turned out to be inappropriate, however. Instead, the linear fit (1) as well as the generalized root fit with an additional additive constant (3) yield the best results as shown in figure 5.

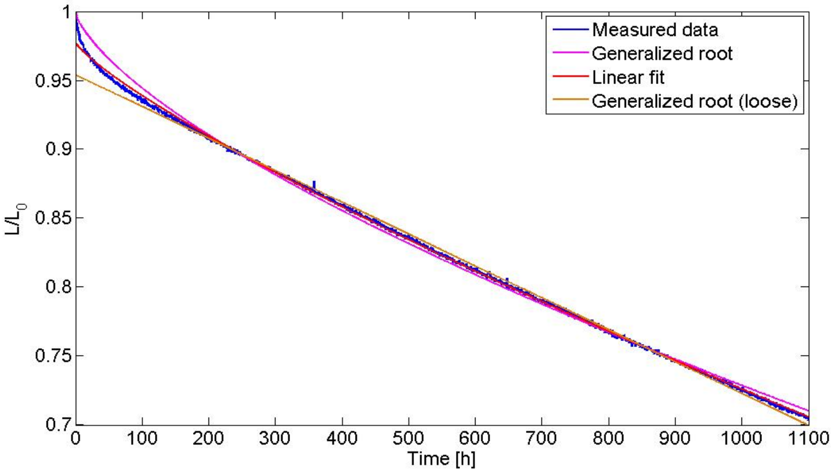

Figure 5 – Extrapolation of OLED lifetime (40°C, twice rated current) using different models

While very helpful to predict the lifetime under accelerated conditions, the uncertainty is very high when predicting the lifetime at normal operating conditions after less than a few thousand operating hours, since even with a known aging behavior it is risky to predict the appropriate parameters based on less than 10% of the expected lifetime. Thus it is important, to compute the lifetime at normal conditions based on the known lifetime under accelerated conditions.

2.3 Conversion from accelerated to standard conditions

The two main parameters used for accelerating the lifetime behavior are current and temperature. At high temperatures it is assumed that the organic molecules responsible for light emission can decay or denature at a given probability or rate. This rate is controlled by an activation energy, $\boldsymbol{E_A}$, for example the energy of the weakest molecular bond. Mathematically this leads to an Arrhenius equation $\boldsymbol{LT} \sim \exp\{\boldsymbol{E_A}/(\boldsymbol{k_B T})\}$, where $\boldsymbol{LT}$ is the lifetime, $\boldsymbol{T}$ the temperature and $\boldsymbol{k_B}$ the Boltzmann constant (Giebink, 2008). The resulting lifetime of an OLED is then proportional to the inverse of the decay rate. The aging due to current or current density is described by an inverse power law $\boldsymbol{LT \sim J^{-n}}$, where $\boldsymbol{J}$ is the current density (Zhang, 2013). On the one hand this is a well-know equation to describe aging processes on the other hand n=1 is known to correspond to electronic processes, while n=2 describes excitonic two-electron processes. A value of 1<n<2 corresponding to a mix of electronic and excitonic processes is thus expected for OLEDs. Model 1 for the aging of OLEDs is thus given by (Buckley, 2013):

1. $LT = a * e^{E_A/k_B T} * J^{-n}$

In model 2 the current density term is considered to be temperature dependent and the exponent $\boldsymbol{n}$ is replaced by $\boldsymbol{n'/(k_B T)}$. The third model attempts to treat self-heating due to high currents. Thus the thermal energy $\boldsymbol{k_B T}$ is replaced by $\boldsymbol{k_B T+bJ}$, where $\boldsymbol{b}$ is a new parameter. The fourth model replaces this term by $\boldsymbol{k_B T+bJ^2}$, since heating in ohmic resistances is proportional to the current squared. For OLEDs, as for idealized diodes in general, the current increases exponentially with voltage (Shockley equation). Since the self-heating $\boldsymbol{dT}$ of OLED is proportional to the electrical input power density $\boldsymbol{UJ}$, where $\boldsymbol{U}$ is the voltage and $\boldsymbol{J}$ the current density. Since the current rises strongly with voltage, it seems appropriate to approximate the voltage as constant for the currents relevant for general lighting and hide all effects other than current density in the constant $\boldsymbol{b}$, thereby approximating the temperature rise due to self-heating by $\boldsymbol{dT \sim bJ}$. In addition, while increasing current leads to self-heating, it is unclear whether increasing temperature has a positive or negative effect on the aging due to the current density. Thus the fifth and final model considered here is identical to model 3, but neglects any temperature effects on the current density term. Thus all advanced models considered are:

2. $LT = a * e^{E_A/(k_B T)} * J^{-n'/(k_B T)}$
3. $LT = a * e^{E_A/(k_B T + bJ)} * J^{-n'/(k_B T + bJ)}$
4. $LT = a * e^{E_A/(k_B T + bJ^2)} * J^{-n'/(k_B T + bJ^2)}$
5. $LT = a * e^{E_A/(k_B T + bJ^2)} * J^{-n}$

Model 1 has shown excellent agreement with lifetime measurements for 4 mm² pixels. Presumably this is due to the negligible self-heating observed even at very high current densities. As shown in figure 6 all models give extremely similar predictions for the lifetime behavior. The activation energy in all cases lies between 0.39 and 0.45 eV. The ***b*** parameter for models 3 to 5 is below 9e-5 in all cases, thus illustrating that self-heating indeed has no effect on devices of this size.

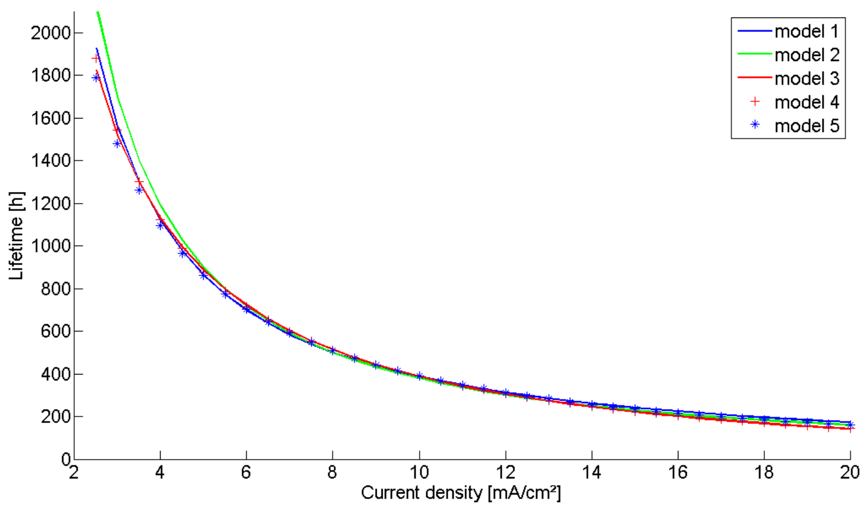

Figure 6 – OLED lifetime predicted at 40°C based on 4 mm² devices

2.4 Effects of scaling

For large area devices, homogeneity and self-heating might no longer be negligible. It is well-known that at higher currents the homogeneity of an OLED decreases. This is easily explained by the potential drop from the contacts to the centre of the lighting area. With increasing voltage the current-voltage dependence becomes stronger. Due to an almost linear behaviour of luminance with respect to current this leads to the OLED's brightness increasing more strongly near the contacts than far away from them. To improve the homogeneity of large area devices, busbars are often used, which reduce the voltage drop toward the centre of the device. This is also the case for the 110.25 cm² square device used in this study.

Self-heating is due to the fact that the main part of the energy flowing into the device is not converted to light, but to heat. The temperature increase ***dT*** due to heating may be approximated by

$$dT = JU(1 - WPE)FF/C \quad (5)$$

J is the current density [A/m²], U is the applied voltage [V],

WPE is the wall-plug-efficiency, FF is the fill factor and

C is an approximate value for the cooling [W/(m²K)].

The wall plug efficiency is the ratio of the power of the emitted light output and the electrical input power. The fill factor is the ratio between lighting area and total device area. *C* is a cooling term for the OLED taking into account convection and emission. By comparison to experiments a value of C = 20 W/(m²K) has proven to yield good approximations for ***dT***. The resulting heat distribution in the OLED is an interplay between cooling, which is stronger at the edge of the lighting area as well as at the edge of the device, and heating due to current, which is highest, where the most current flows. As long as self-heating is low, the temperature maximum is in the centre of the device, despite most current flowing near the contacts. As soon as self-heating becomes a dominant effect, the rising temperature leads to an exponential rise in current which leads to a complex reorganization of the heat and current distribution. To prevent this and the resulting sequential aging, heat spreaders are commonly used to ensure an evenly distributed temperature across the lighting area. Heat spreaders designed to be larger than the lighting area additionally enhance the cooling. For the large square OLED a graphite-based heat-spreader is used. A comparison of the operating lifetime of a 110 cm² OLED heated to 40°C by electrical transistors on the back and an OLED with a heat spreader, where temperature is measured in the centre of the heat spreader, shows that, once self-heating reaches approximately 40°C, the aging behaviour is also very similar (see figure 7). This proves that up to the maximum self-heating considered in this study, the heat spreader successfully homogenizes the temperature across the device.

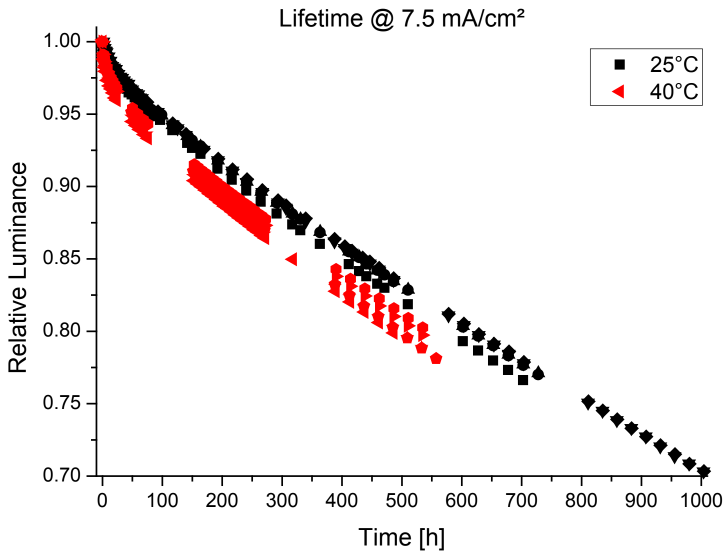

Figure 7 – Luminance decrease of OLED at 7.5 mA/cm². One device is heated to 40°C by electrical transistors, while the other is operated at room temperature. Due to the high current, the device operated at room temperature heats up to 39.6°C on average.

The temperature increase due to self-heating is 4.7 K at 2.56 mA/cm², 9.6 K at 4.2 mA/cm² and 16.4 K at 7 mA/cm² for devices operated in vertical orientation. Application of the five different models for lifetime prediction thus yield quite contrary results as shown in figure 8.

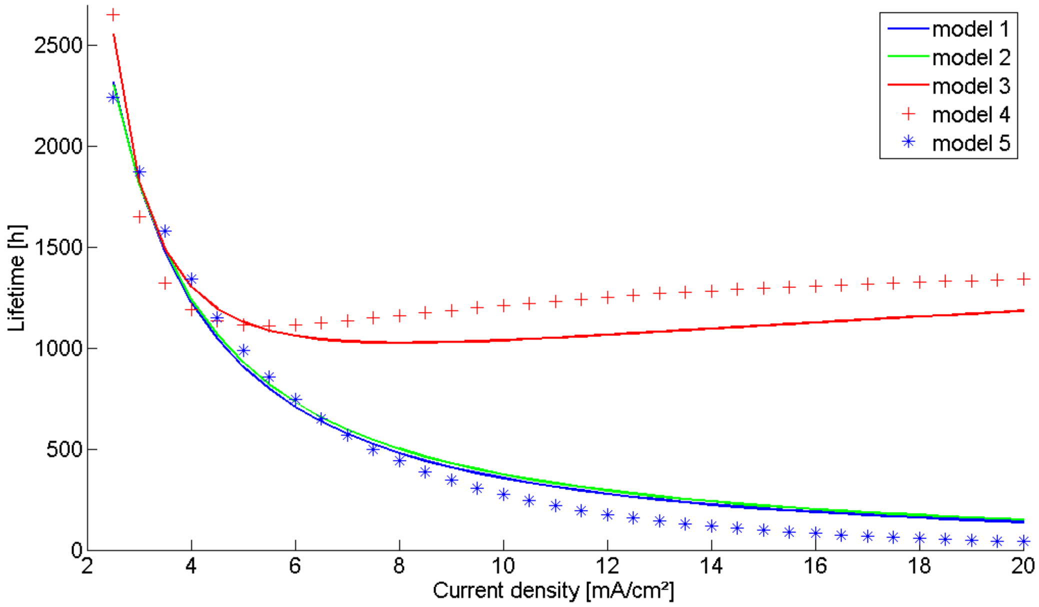

Figure 8 – OLED lifetime predicted at 40°C based on 110.25 cm² devices

As can clearly be seen, models 3 and 4 completely fail to describe the aging behavior. This is due to the fact that the self-heating actually has a positive effect in the aging term related to current. The models neglecting self-heating (1, 2) as well as model 5 yield reasonable descriptions of the data. They begin to significantly deviate only at currents above 7 mA/cm², which were not measured in this study. At 20 mA/cm², which is the acceleration condition used for the small test pixels, the lifetime predictions vary by a factor of two between the models.

Conditions	**Model 1**	**Model 2**	**Model 3**	**Model 4**	**Model 5**
25°C, 2.6 mA/cm², 4 mm²	3850	4590	3910	4200	3603
25°C, 2.6 mA/cm², 110 cm²	4010	4050	2430	2470	4034
75°C, 20 mA/cm², 4 mm²	41	42	40	30	40
75°C, 20 mA/cm², 110 cm²	44	60	1180	1340	21

The actual experimental lifetime of 110 cm² devices at 2.56 mA/cm² and 25°C was measured to be 4050 hours. The low lifetime is due to a two-year old state-of-the-art of the OLEDs used for this study chosen for comparability with OLED100.EU results. The lifetime of 4 mm² devices at 20 mA/cm² and 75°C was measured to be 40 hours. Thus the prediction from small devices at high acceleration to large devices at normal operating conditions is perfectly valid with an error of approximately 5% due to the fact that self-heating at normal operating conditions is negligible and the homogeneity is very high (~90%). Predicting accelerated lifetime conditions of large area devices based on small devices is highly dangerous, however. Due to self-heating deviations between large and small devices may go up to a factor of two at 20 mA/cm².

3 Conclusions

In the first part, it has been shown that the homogeneity of an OLED is an essential requirement to create an attractive appearance. It has also been shown, that inhomogeneities are more easily perceived for OLED clusters than for single OLEDs. For the homogeneity patterns there were also substantial differences in perception, which couldn't be described by any existing homogeneity equation at present. However, new considerations are still under testing.

The study has also shown that the prediction of lifetime for general lighting OLEDs with heat spreader and busbars based on small 4 mm² devices at highly accelerated conditions is indeed possible with less than 5% expected error. This is solely due to the fact that at normal operating conditions the homogeneity is excellent and self-heating is low. Note that this is not the case for transparent OLEDs, where neither heat spreaders nor busbars can be used to ensure a good homogeneity.

Acknowledgements

We would like to acknowledge the financial support given by the German ministry for research and education (BMBF) in the framework of the OLYMP project.

References

Ashdown, I 1996, *Luminance gradients: photometric analysis and perceptual reproduction,* JIES 25 (1):69-82 (Winter)

BUCKELY, A. 2013. *Organic Light-Emitting Diodes (OLEDs)*, 1st edition, Woodhead Publishing, 601-634

GIEBINK, N.C. et al. 2008, *Intrinsic luminance loss in phosphorescent small-molecule organic light emitting devices due to bimolecular annihilation reactions,* Journal of Applied Physics, 103, 044509

OLED100.EU, http://www.oled100.eu/homepage.asp

ZHANG, J.-P. et al. 2013. Lifetime prediction *of white OLED based on MLE under lognormal distribution*. Journal of Testing and Evaluation, Vol. 41, No, 3, 398-402.

VIDEO ELECTRONICS STANDARDS ASSOCIATION (VESA) 2005, Flat Panel Display Interface Committee, Flat Panel Display Measurements Standard Working Group, *Flat Panel Dipslay Measurements Standard FPDM Version 2*, www.vesa.org

IT06

LIGHTING QUALITY WITH LEDS

Martine Knoop[1]
[1] Technische Universität Berlin, Berlin, GERMANY
martine.knoop@tu-berlin.de

Abstract

CIE Technical Committee 3-50 *Lighting Quality Measures for Interior Lighting with LED Lighting Systems* looked into available research results that underlines the suitability or discard the applicability of existing measures to evaluate lighting quality of interior lighting with LED lighting systems. The work has been summarized in the CIE report 205:2013 "Review of lighting quality measures for interior lighting with LED lighting systems". The document gives recommendations in the use of quality measures for LED lighting solutions, including background information, research results and literature references, as well as an indication of the relevant parameters to look into. To that, it gives an indication of needed research to ensure quality lighting in all situations with LED systems.

This paper will focus on two reviewed quality criteria. A summary of the conclusions by CIE TC 3-50 as well as recent research activities with respect to these quality metrics are presented.

Keywords: LED, Lighting Quality, Indoor Applications, Interior Lighting, Review

1 Introduction

Light Emitting Diodes (LEDs) have shown a rapid evolution in the last few years and replacing conventional light sources in luminaires for general, functional, lighting in indoor applications. Even though the application of LED replacement lamps and LED luminaires will likely increase energy efficiency, the resulting lighting conditions are not always rated positively by the users. A reason for this might be that quality measures are applied, which are derived from research with and referring to the use of diffuse fluorescent lighting. As LEDs have different characteristics, such as a small size, a relatively high brightness and a different spectral power distribution, it seemed to be required to validate the applicability of the existing quality measures in situations with LED lighting solutions. CIE TC 3-50 *Lighting Quality Measures for Interior Lighting with LED Lighting Systems* looked into available research results that underline the suitability or discard the applicability of existing measures to evaluate lighting quality of interior lighting with LED lighting systems. The work has been summarized in the report "Review of lighting quality measures for interior lighting with LED lighting systems" (CIE 2013).

2 Review of Quality Measures

The quality measures included in the review conducted by CIE TC 3-50 were derived from a number of relevant publications, such as CIE conference proceedings and reports, European and US handbooks, guidelines and standards (e.g. CIE 1998, CIE 2002a, CIE 2002b, CEN 2011, IESNA 2000, IESNA 2004, IESNA 2008, McGowan 2009 2009).

A distinction has been made between quality criteria and recommendations. Quality criteria focus on visual performance and avoiding visual discomfort, to ensure performance and safety. Recommendations go beyond task performance and safety aspects and generally aim at a higher lighting quality.

The following quality criteria were considered:

- Task visibility: uniformity of task illumination, reflected glare, veiling reflections and shadows
- Visual comfort: discomfort glare, overhead glare, luminance ratios, visual fatigue and eyestrain
- Flicker and stroboscopic effects

To that, the following recommended measures for quality of interior lighting were reviewed:

- Modelling of faces and objects
- Colour rendering, light colour preference, object colour appearance
- Appearance of spaces: room surface brightness, distribution of light on surfaces
- Consistency of colour and luminous flux over time and space

Literature on research looking into these quality measures was studied to identify the gaps and weaknesses in existing measures to assess the quality of interior lighting with LED lighting systems. This paper will address two quality aspects: discomfort glare and flicker, relevant to secure visual performance and avoid visual discomfort. The complete review can be found in the report of CIE TC 3-50 (CIE 2013).

3 Lighting Quality: Discomfort Glare

The Technical Committee identified that the appearance of the LED lighting solution is one of the major topics that affects the applicability of existing quality measures. Whereas style, size, integration into architecture and appropriateness of appearance is as relevant as it was for conventional lighting solutions, a non-uniform luminance distribution or patterns of bright spots within the luminaire`s exit window can induce a feeling of restlessness, which might impact well-being, visual fatigue and performance. The author is not aware of research dealing with this topic up until today. Yet, a larger number of studies looked into the effect of non-uniformity on perceived discomfort glare, which are described in the report of CIE TC 3-50 (CIE 2013).

The review of research* on discomfort glare from non-uniform stimuli indicates that LED lighting solutions with a non-uniform luminance distribution cannot be evaluated with the Unified Glare Rating (CIE 1995) or the Visual Comfort Probability (IESNA 2000), typically employed to assess discomfort glare from conventional indoor lighting solutions. In general, the non-uniform stimuli induce more glare than conventional, fluorescent lighting solutions of the same size, with the same average luminance. Based on the available research on metrics to asses discomfort glare from LED lighting solutions, CIE TC 3-50 concluded that the UGR and VCP should not be used for non-uniform light sources.

Recently, Xia et al. (2011) and Hara and Hasegawa (2012) indicated that the UGR can be modified to address discomfort glare from non-uniform light sources. Geerdinck et al. (2013) stated that this seems to be suitable for luminance contrasts within the exit window up to 1:10, but the UGR does not correlate well with the subjective assessments of luminaires with a more non-uniform luminance distribution. Geerdinck et al. (2013) indicate that peak luminance, luminance contrasts and spatial luminance distribution play an important role in the glare assessment and need to be considered in the construction of a new glare index. To that, the LED spacing and arrangement seem to be of importance (review in CIE 2013).

Division 3 of the CIE has set up a new Technical Committee addressing discomfort glare by luminaires with a non-uniform source luminance. The TC will identify the non-uniformity parameters that influence the glare rating, define the limits to the validity of UGR and propose a preliminary correction to the UGR that takes into account non-uniformity of glare sources.

* published until Fall 2012

4 Lighting Quality: Flicker and Stroboscopic Effects

Looking into quality of interior lighting with LED lighting systems, photometric flicker is a relevant quality parameter; a large variety of photometric flicker is observed in LED products (Paget 2011; Poplawski and Miller 2013) and flicker affects performance and well-being (IEEE 2010). In this context, flicker is defined as “the rapid variation in light source intensity” (IESNA 2000) and reflected in the modulation of luminous flux and the detection of stroboscopic effects.

Drivers of LEDs can produce photometric flicker, and dimming of LEDs can reinforce light modulation. A minimum driver output frequency of 100 or 120 Hz to avoid perceptible flicker seems to be insufficient to ensure lighting quality (review in Poplawski and Miller 2013). Based on the available research on metrics to asses flicker from LED lighting solutions, CIE TC 3-50 concludes that flicker and stroboscopic effects are not addressed appropriately by current quality criteria, such as flicker frequency and flicker percentage.

Bullough et al. (2012; Alliance for Solid-State Illumination Systems and Technologies (ASSIST) 2012) propose a function of flicker frequency and percent flicker to predict the detection and acceptability of stroboscopic effects, based on experiments under worst-case conditions. Further research is required to assess the applicability of this approach in typical applications. Minimum recommendations for flicker criteria as well as guidelines for applications in which flicker is a relevant quality criteria can be found in Poplawski and Miller 2013). CIE TC 1-83 *Visual Aspects of Time-Modulated Lighting Systems* and the IEEE PAR1789 committee are also investigating stroboscopic effects.

5 Outlook and Future Research

The small size of LEDs offers design freedom. It is to be expected that LEDs are not only used in conventional luminaires, but will be, for example, embedded in furniture or room surfaces. This can result in an atypical positioning of the light source, which in return can affect visual comfort in a room. Discomfort glare from a source at the line of sight is typically greater than from the same source positioned above the line of sight, especially when dealing with non-uniform stimuli. Research looking into discomfort glare from non-uniform vertical artificial light sources (e.g. Takahashi et al. 2007, Kasahara et al. 2006) or larger vertical artificial light sources (e.g. Osterhaus 1996, Sendrup 2001) is available, but the research is inconclusive. Further studies are necessarily.

The LED features directional light, small size and high brightness, in their combination uncharacteristic for interior lighting, led to the review of existing quality measures by CIE TC 3-50. Considering the development of larger and commercial OLEDs, it seems to be appropriate to review the quality measures with respect to OLED applications as well. OLEDs have light emitting surfaces with a more uniform luminance distribution, realizing a very diffuse lighting contribution to the room. This lighting condition is deviating from the one realised by conventional, fluorescent lighting as well. The use of OLEDs will affect room appearance. Research indicates that an increase of room surfaces’ luminance positively affects room appearance (e.g. Loe et al. 1994, Houser et al. 2002, Veitch and Newsham 2006). At the same time, too diffuse lighting can cause a low degree of modelling, resulting a in a monotonous visual environment (e.g. Newsham et al. 2004, Fostervold and Nersveen 2008). Direction of light, modeling and shadows are important aspects of lighting quality, which all need further research to define an appropriate metric and determine minimum, as well as maximum requirements (CIE 2013, Knoop 2014).

6 Summary

The work of TC 3-50 has been summarized in the report “Review of lighting quality measures for interior lighting with LED lighting systems”. The document gives recommendations in the use of quality measures for LED lighting solutions, including background information, research results and literature references, as well as an indication of the relevant parameters to look into. It gives an indication of needed research to ensure quality lighting in all situations with LED systems. Focussing on two quality measures in this paper, discomfort glare and flicker, research continued and is expected to lead to suitable metrics in the near future. Quality aspects related to future applications of LEDs and OLEDs need to be considered. Available research needs to be reviewed and new research activities need to be started up, to provide the lighting community with additional recommendations on the use of criteria to evaluate lighting quality of interior lighting using new technologies.

7 Acknowledgements

The author would like to thank all authors and advisors of TC 3-50 "Lighting Quality Measures for Interior Lighting with LED Lighting Systems" for their contribution in the preparation of the Technical Report.

References

Alliance for Solid-State Illumination Systems and Technologies (ASSIST) 2012. ASSIST recommends … Flicker Parameters for Reducing Stroboscopic Effects from Solid-State Lighting Systems. Troy, NY.

Bullough, J.; Hickcox, K. S.; Klein, T.; Lok, A.; Narendran, N. 2012. Detection and acceptability of stroboscopic effects from flicker. Lighting Research and Technology. 44. pp. 477–483.

CEN 2011. EN 12464-1:2011 Light and lighting - Lighting of work places - Part 1: Indoor work places.

CIE 1995. CIE 17 - 1995 Discomfort glare in interior lighting. Vienna. Commission Internationale de l'Eclairage.

CIE 1998. CIE 15 - 1998 Proceedings of the First CIE Symposium on Lighting Quality. Vienna. Commission Internationale de l'Eclairage.

CIE 2002a. CIE 147-2002 Glare from small, large and complex sources. Vienna. Commission Internationale de l'Eclairage.

CIE 2002b. IES 008/ISO 8995-1:2002 Lighting of Work Places Part 1: Indoor. Vienna. Commission Internationale de l'Eclairage.

CIE 2013. CIE 205-2013 Review of Lighting Quality Measures for Interior Lighting with LED Lighting Systems. Vienna. Commission Internationale de l'Eclairage.

Fostervold, K. I.; Nersveen, J. 2008. Proportions of direct and indirect indoor lighting—The effect on health, well-being and cognitive performance of office workers. Lighting Research and Technology. 40. pp. 175–200.

Geerdinck, L. M.; van Gheluwe, J. R.; Vissenberg, M. C. J. M. 2013. Discomfort glare perception of non-uniform light sources in an office setting. Manuscript submitted for publication.

Hara, N.; Hasegawa, S. 2012. Study on discomfort glare rating of the luminaire with LED array. Journal of the Illuminating Engineering Institute of Japan. 96. pp. 81–88.

Houser, K. W.; Tiller, D. K.; Bernecker, C. A.; Mistrick, R. G. 2002. The subjective response to linear fluorescent direct/indirect lighting systems. Lighting Research and Technology. 34. pp. 243–260.

IEEE 2010. PAR 1789 - Recommended Practices of Modulating Current in High Brightness LEDs for Mitigating Health Risks to Viewers.

IESNA 2000. The IESNA lighting handbook. New York, NY. Illuminating Engineering Society of North America.

IESNA 2004. American National Standard Practice for Office Lighting. New York, NY. Illuminating Engineering Society of North America.

IESNA 2008. IES DG-18: Light + Design A Guide to Designing Quality Lighting for People and Buildings. New York, NY.

Kasahara, T.; Aizawa, D.; Irikura, T.; Moriyama, T.; Toda, M.; Iwamoto, M. 2006. Discomfort Glare Caused by White LED Light Sources. Journal of Light & Visual Environment. 30. pp. 95–103.

Knoop, M. 2014. Lighting quality measures for interior lighting with LEDs: A review and outlook. In: Proceeding of the 14th International Symposium on the Science and Technology of Lighting (to be published). Proceedings of the LS 14. Como, Italy, June 22 - 27, 2014.

Loe, L.; Mansfield, K. P.; Rowlands, E. 1994. Appearance of lit environment and its relevance in lighting design: Experimental study. Lighting Research and Technology. 26. pp. 119–133.

McGowan, T. 2009. R3-24 Overhead Glare. Report to CIE Division 3.

Newsham, G. R.; Marchand, R. G.; Veitch, J. A. 2004. Preferred surface luminances in offices, by evolution. Journal of the Illuminating Engineering Society. 33. pp. 14–29.

Osterhaus, W. 1996. Discomfort glare from large area glare sources at computer workstations. In: Proceedings of the 1996 International Daylight Workshop: Building with Daylight: Energy Efficient Design. pp. 103–110.

Paget, M. 2011. CALIPER Round 11 Testing. http://apps1.eere.energy.gov/buildings/publications/pdfs/ssl/ns/caliper-round-11-webcast.pdf.

Poplawski, M. E.; Miller, N. M. 2013. Flicker in Solid-State Lighting: Measurement Techniques, and Proposed Reporting and Application Criteria. In: Proceedings of CIE Centenary Conference "Towards a New Century of Light". Paris, France, April 15/16, 2013.

Sendrup, P. 2001. Generalization of the unified glare rating method: a proposal and laboratory test. Lighting Research and Technology. 33. pp. 243–257.

Takahashi, H.; Irikura, T.; Mariyama, T.; Toda, M.; Iwamoto, M. 2007. Discomfort glare and annoyance caused by LED lamp (D1-80). In: Proceedings of the 26th Session of the CIE. Beijing, China, 4 July - 11 July 2007.

Veitch, J. A.; Newsham, G. R. 2006. Quantifying Lighting Quality Based on Experimental Investigations of End User Performance and Preference. Report: NRCC-38940, National Research Council Canada,[Online], Available: http://www. nrc-cnrc. gc. ca/obj/irc/doc/pubs/nrcc38940. php.

Xia, L.; Tu, Y.; Liu, L.; Wang, Y.; Peng, S.; Knoop, M.; Heynderickx, I. 2011. A study on overhead glare in office lighting conditions. Journal of the Society for Information Display. 19. pp. 888.

IT08

WHAT IS COLOUR FIDELITY IN MUSEUM LIGHTING?

Schanda J.
University of Pannonia, Veszprém, HUNGARY
Schanda@vision.vein.hu

Abstract

Best colour fidelity can be obtained if the spectrum of illumination of the painting is the same as under which the painter created his painting. For paintings older than hundred years this is daylight.

Thus one could consider that lighting with best colour fidelity should be artificial daylight. But one knows that daylight has too much harmful radiation (short wavelength visible and UV radiation) and museum curators usually protest against light sources with correlated colour temperatures as high as 6500 K.

Based on the request of museum curators to use light with a correlated colour temperature not higher than 3500 K, a method has been elaborated to find the light spectrum that will provide the smallest colour distortions between the colours seen under daylight and under the light in the museum for a given LED light source combination. This will not be the light with the highest colour rendering index.

Keywords: e.g. Colour Rendering, colour fidelity, colour preference

1 Introduction

Museum lighting is undergoing a major revolution. With the introduction of LED lighting illuminating engineers got the freedom of selecting light source spectra almost at their will. The present paper will discuss the question by concentrating on picture galleries, as the colour and colour rendering of the light source is probably most demanding in this section of museum lighting, where at the same time also the possible artefact damaging by optical radiation is critical. CIE published two reports on the question of avoiding deterioration of exhibited objects by optical radiation (CIE 1991, CIE 2004). These reports were published still before the widespread application of LEDs in indoor lighting, and the publications do not dealt with LED lighting in detail. The question has been discussed in the paper by Szabó et al (Szabó 2012), but still did not went into detail of best light source spectrum for art gallery lighting. A recent report by Druzik and Michalski discusses the selection of solid state lighting in museums in more detail (Druzik and Michalski 2012).

A number of recent publications reported on refurbishing the lighting system in museums. If one tries to enumerate the requirements for museum lighting one certainly has to distinguish between the task of the museums. There are smaller museums where only a few artefacts are shown, as e.g. museums introducing the heritage of an artist, or a traditional peasant art (e.g. an old wind-mill). In such cases the educational character is the most important, and good visibility, pleasant visual atmosphere is an important element. There are many medium size museums that serve as educational facilities, where the artefacts have to be presented in an eye-catching form, it is important that the visitor should feel himself at home in the museum, that he/she is guided by light from artefact to artefact. The task for the lighting designer and the museum curator can be compared to the role of the conductor of an orchestra, where they have to re-interpret the masterpiece of the past, so that it should be interesting to the modern audience/observers. Naturally also in these cases the art preservation is of paramount importance.

But there is a third category of museums, where the most prestigious artefacts of mankind are preserved, where – according to the viewpoint of the author – it is mandatory to present the artefacts in a form as they were conceived, as the artist who prepared them intended to show them to the public. In the following a few examples of this type of museums should be presented, as also the main subject of the paper, the new lighting of the Sistine Chapel falls into this category.

Without going into details, just a few highlights from European museums might show current trends. In the Louvre Museum, Paris, Leonardo's Mona Lisa got its first LED illumination, based on 7 different LEDs, in 2005. Although this lighting scheme was absolutely up-to-date at that time, in 2013 the designers of the illumination decided to modernize it further, using 34 LEDs (Fontoynont 2013). The final adjustment of LED spectra was based on the judgement of the curators.

At the National Gallery, London, a project for „Improving our Environment" was conducted in 2013, refurbishing the lighting in several parts of the Gallery (Padfield 2013). 100 W 2800 K incandescent lamps have been replaced by 14 W LEDs of 3200 K correlated colour temperature (CCT). Interestingly the relatively small increase in CCT was found by curators to "correspond more closely with filtered natural light" and "that the light produces a notable increase in the sense of space in many paintings". The illuminance was at the same time reduced from 150 lx to 130 lx.

The lighting of the Rijksmuseum in Amsterdam has been refurbished using LED lighting by Philips, the Lenbachhaus in Munich and recently the Sixtus Chapel in the Vatican are works of OSRAM, where new LED lighting had been introduced. Up to this very last example, in all cases the lighting engineer could prepare only the framework of the lighting, and the final word was that of the museum curator. Just for the Sixtus Chapel we try to prepare a lighting scheme based on a new paradigm: the artificial lighting of relatively low correlated colour temperature – as requested by the curators – should show the frescos as far as possible in colours that correspond to those as seen by the contemporary first observers of the masterpieces.

2 Museum lighting requirements

The two partially contradictory requirements are the art conservation and the presentation for the visitors. In this paper the art conservation issues will not be discussed in detail, many papers have been published on this subject; see e.g. (Feller 1964, Aídinli 1990, CIE 1991, CIE 2004). Based on these one can just state that UV and IR irradiation should be avoided, and light levels should be as low as still acceptable for good colour vision.

In refurbishing he museum lighting in buildings that were built, when electrical lighting was still not available, or its quality was low, lighting engineers tried to retain the natural overhead lighting, but have built in complicated automatic shielding apparatuses and some supplementary lighting, see Figure 1.

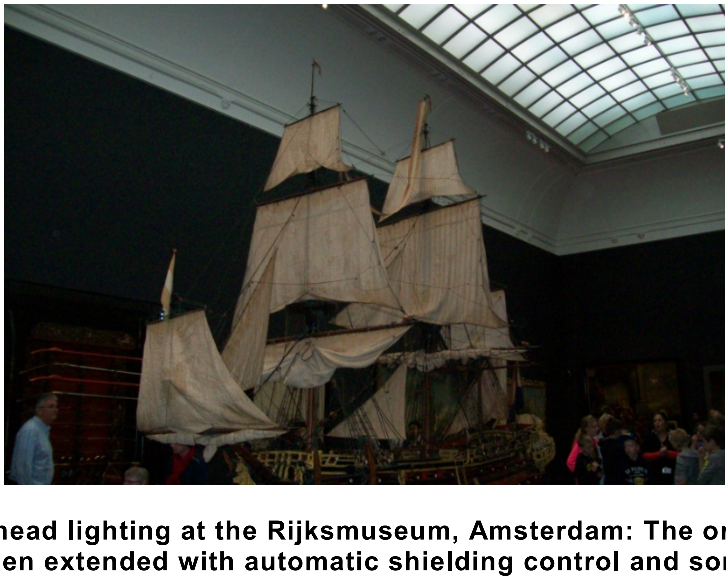

Figure 1. Overhead lighting at the Rijksmuseum, Amsterdam: The original daylight lighting has been extended with automatic shielding control and some fluorescent lighting.

While the requirement for UV and IR radiation-free illumination is more easily fulfilled with LED lighting, curators usually require also so little blue light as possible, as the photon energy of blue light is not much lower than that of the adjacent UV radiation. This means relatively low correlated colour temperature (CCT). During the days of incandescent lighting this was not an issue, as CCTs much above 3000 K with reasonable life time were not available. With LEDs the situation is different, and again harmonization between two demands has to be fulfilled: colours of pictures painted in open air or in a studio lit by daylight will certainly look natural under relatively high CCT and high illumination, but the museum lighting has to harmonize in different parts of the building, thus if other departments are illuminated with sources of lower CCT and 200 lx to 300 lx illumination, an abrupt change in CCT will produce difficulties of re-adaptation. Our experience was – and this is in line with the findings of other investigators – that museum curators will opt for CCTs not higher than 3500 K.

Loe and co-workers (Loe 1982) performed investigations in a mock-up art gallery mustering real oil and watercolour paintings under different illuminants, and concluded that 200 lx is an acceptable level of illumination. Scuello and co-workers (Scuello 2004) performed visual investigations in a simulated museum environment with postcard reproductions of paintings and came to the conclusion that 3600 K CCT is an optimum value for a 200 lx illumination.

3 Designing the LED spectrum

3.1 The question of the test samples

Detailed experiments were conducted already at the time of developing the CIE colour rendering calculation method to select the test samples now in use (Nickerson 1962). Experiments have shown that for the light sources that were available in the mid 1950th the eight test samples were enough to properly characterize the colour rendering of a light source.

Already with the introduction of the three band fluorescent lamps discrepancies between calculated and visually perceived were observed. These became even more apparent when RGB-LEDs and p-LEDs (blue LED with colour conversion yellowish phosphor) were compared. Several reflectance data-sets have been calculated and incorporated into different light source colour quality metrics (Davis 2005, Smet 2011, etc.), and Prof. Khanh and co-workers have shown that if the CIE test sample set was changed to art-paint samples, considerable discrepancies are observed in the colour rendering indices (Pepler 2013).

For the Sistine Chapel project – to determine the LED spectra to illuminate the frescos – first the reflectance spectra of the different pigments used to create the masterpieces were determined (see Szabó et al 2014). The spectrum of more than 200 samples has been measured and from these a set of non-redundant samples has been selected, see Figure 2 (for further details see next section).

3.2 Classifying the test samples

Colorimetric characteristics of the test samples differ from sample to sample. Important characteristics of pigments are their light-fastness, hiding power, etc. If one wishes to view an image under a light source the spectrum of which differs from the spectrum under which the image was created, an important characteristic of the pigment is its colour constancy, i.e. how different the colour appearance of the pigment's colour will be under the second light source compared to its colour appearance under the first light source, taking chromatic adaptation into consideration. If the pigments of an image are colour constant, the visual impression of the picture will be very similar under the two light sources. Naturally the spectrum of the two sources is also critical in the determination of colour constancy. Due to practical reasons most colour constancy calculations use daylight as one of the light sources and either Illuminant A, or an often used fluorescent lamp spectrum (e.g. F11) as the other light source (with the more widespread application of LED illumination this might change in the future).

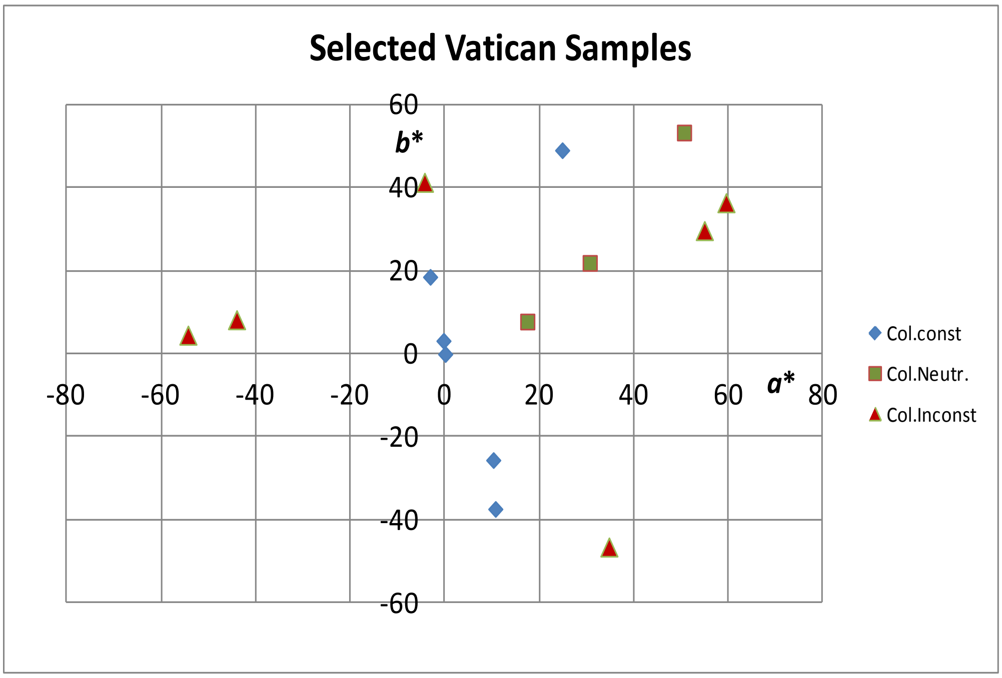

Figure 2. a*,b* co-ordinates of selected samples.

In the following calculations the CIE standard illuminant A and D65 spectral power distributions (SPD) were used as test and reference SPD. This is in line with the general assumption that the frescos were painted under Daylight and should be illuminated by low colour temperature general lighting, not too different from current incandescent lamp lighting. Rumours that Michelangelo painted parts of the Last Judgement under candle light are hard to believe: he might have done some brush work under candle light, but selecting the proper hue and shade would have been too difficult at the low light levels of candle light – and the images were produced to be seen in daylight.

The Luo et al method of calculating the colour inconsistency index, with Illuminant A and D65 as sources was used (Luo at al. 2003.). The CIECAM02 colour appearance model, with its built in chromatic adaptation calculation to get the test sample colour co-ordinates transformed (CIE 2004), and the UCS colour space to calculate the colour differences (Luo et Li 2007) were used.

The fifteen pigment spectra, selected from the Sistine Chapel measurements were grouped into three categories, where the inconstancy index (the CIECAM02-UCS colour difference) was beyond 3, these samples we called colour constant, between 3 and 6, they have been termed colour neutral, and samples with a higher ΔE as 6, these are the colour inconstant samples. The next figures show the reflectance spectra of the samples falling into the three categories.

As can be seen, the colour constant samples have smooth curves, the neutral ones show slightly more curvatures, while the colour inconstant ones have narrower peaks and/or steep rising portions. If such a steep rising portion of the reflectance spectrum coincides with parts of the two emission spectra, where their characteristic are very different, this will manifest itself in a high colour inconstantness.

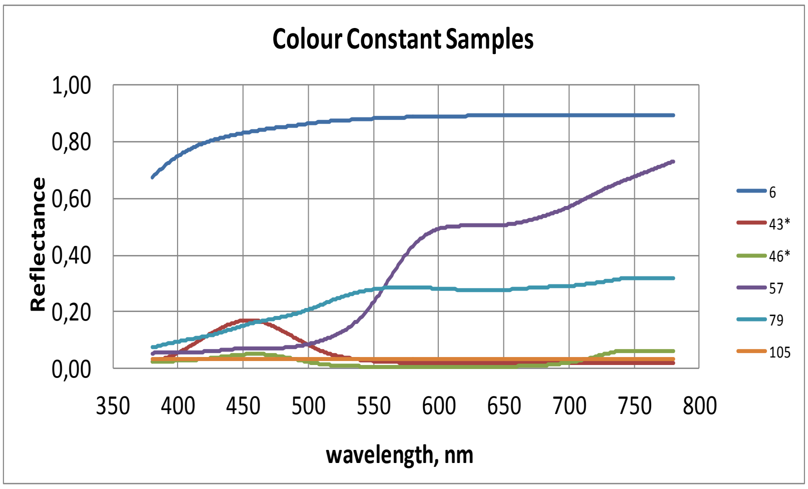

Figure 3. Spectra of the six colour constant samples

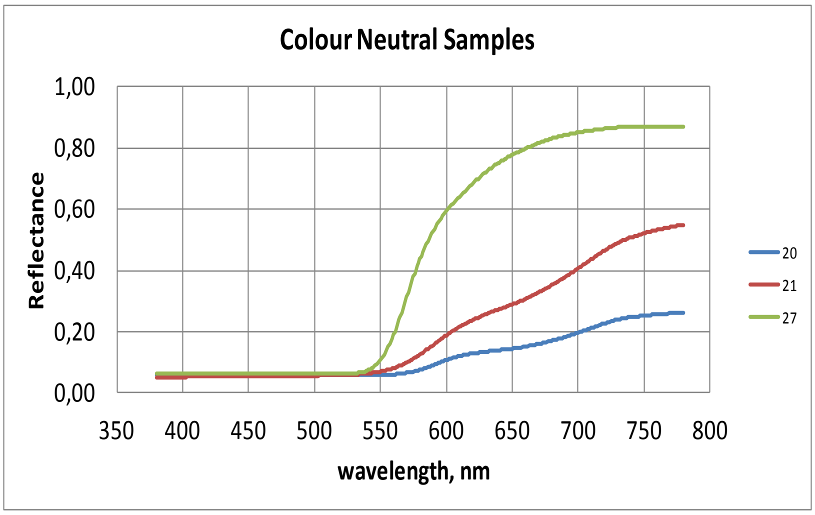

Figure 4. Spectra of the three colour neutral samples.

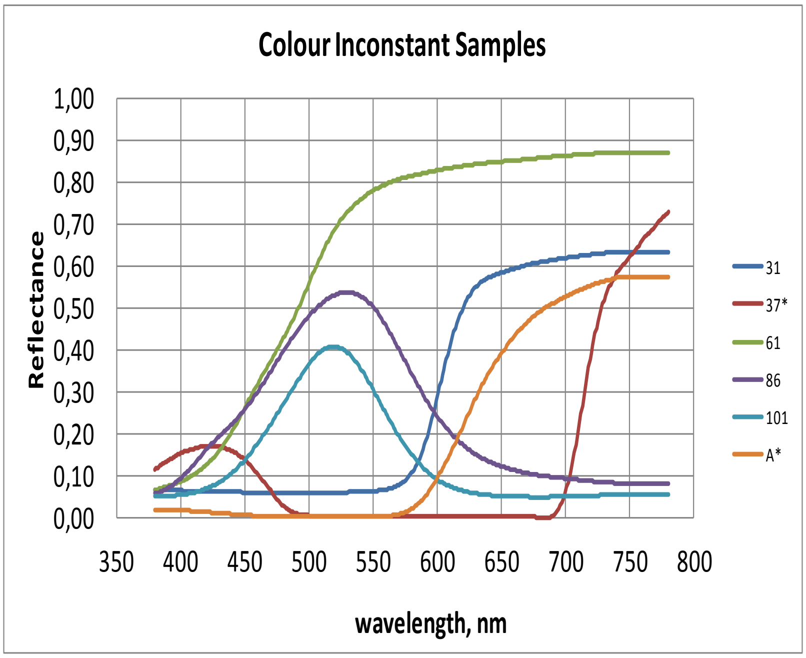

Figure 5. Spectra of the six colour inconsistent samples.

Doing these studies it has been realized that the artificial samples of the CRI2012 model (Smet 2013) resemble quite well the spectral shapes of the colour inconstant samples (see the CRI2012 theoretical test sample spectra in Figure 6.). Thus – as a first test – the CRI2012 theoretical samples were used to optimise the LED spectra intended for the Sistine Chapel illumination.

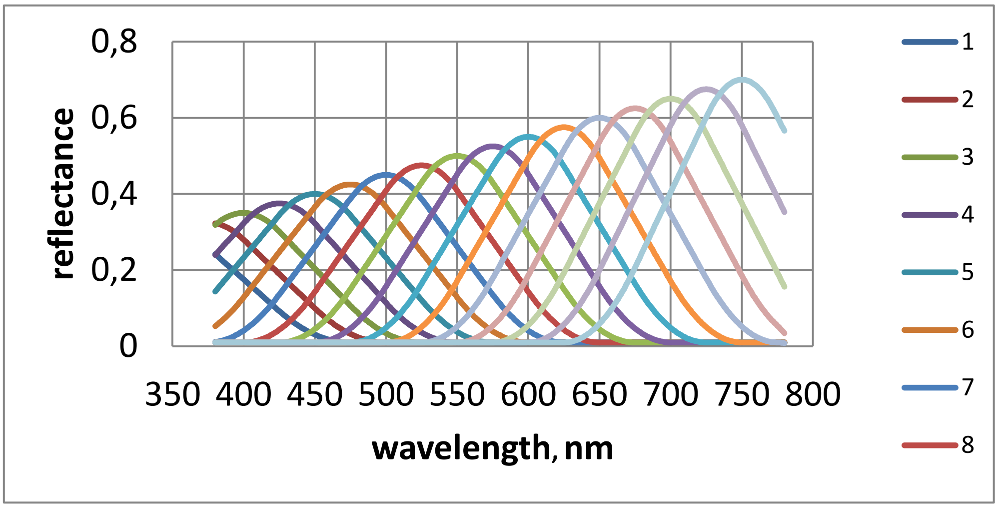

Figure 6. Theoretical test samples of the CRI2012 colour rendering model.

3.3 Selection and optimisation of the LED spectra to be used in the Sistine Chapel

For illuminating single pictures specially designed multi channel LED projectors can be used, as e.g. done for the Mona Lisa at the Louvre (Fontoynont 2013). The entire Sistine Chapel had to be illuminated with LEDs of the same spectra. Thus one had to construct the lighting from a smaller number of LEDs of different SPD. A white LED and red, green, blue LEDs had been selected, that enabled an easy tuning of the CCT and gave a reasonable freedom to optimise for best colour appearance, i.e. to have the smallest colour difference between the corresponding colours of the selected pigments under daylight and the selected warm white colour in the museum.

The spectra of the four LED types are shown in Figure 7.

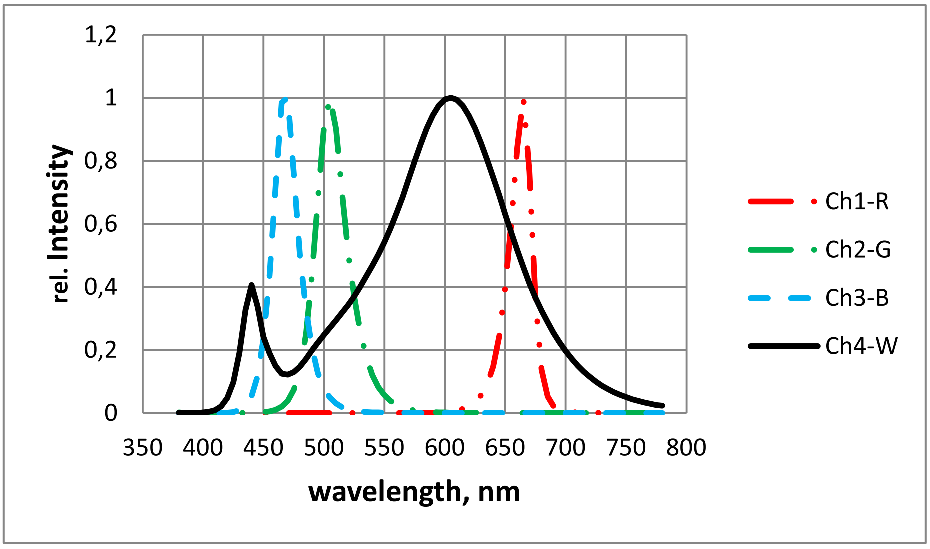

Figure 7. SPD of the four selected LEDs.

Optimization was performed for the additive mixture of the light of the four LEDs and the 17 theoretical reflectance spectra. Results are seen in the following two figures, comparing the colour distortions if a 3500 K Planck source would be used (slightly filtered incandescent lamp) and the optimized four LED combination. Also for the CRI2012 samples they were grouped into three groups according to their colour inconstancy.

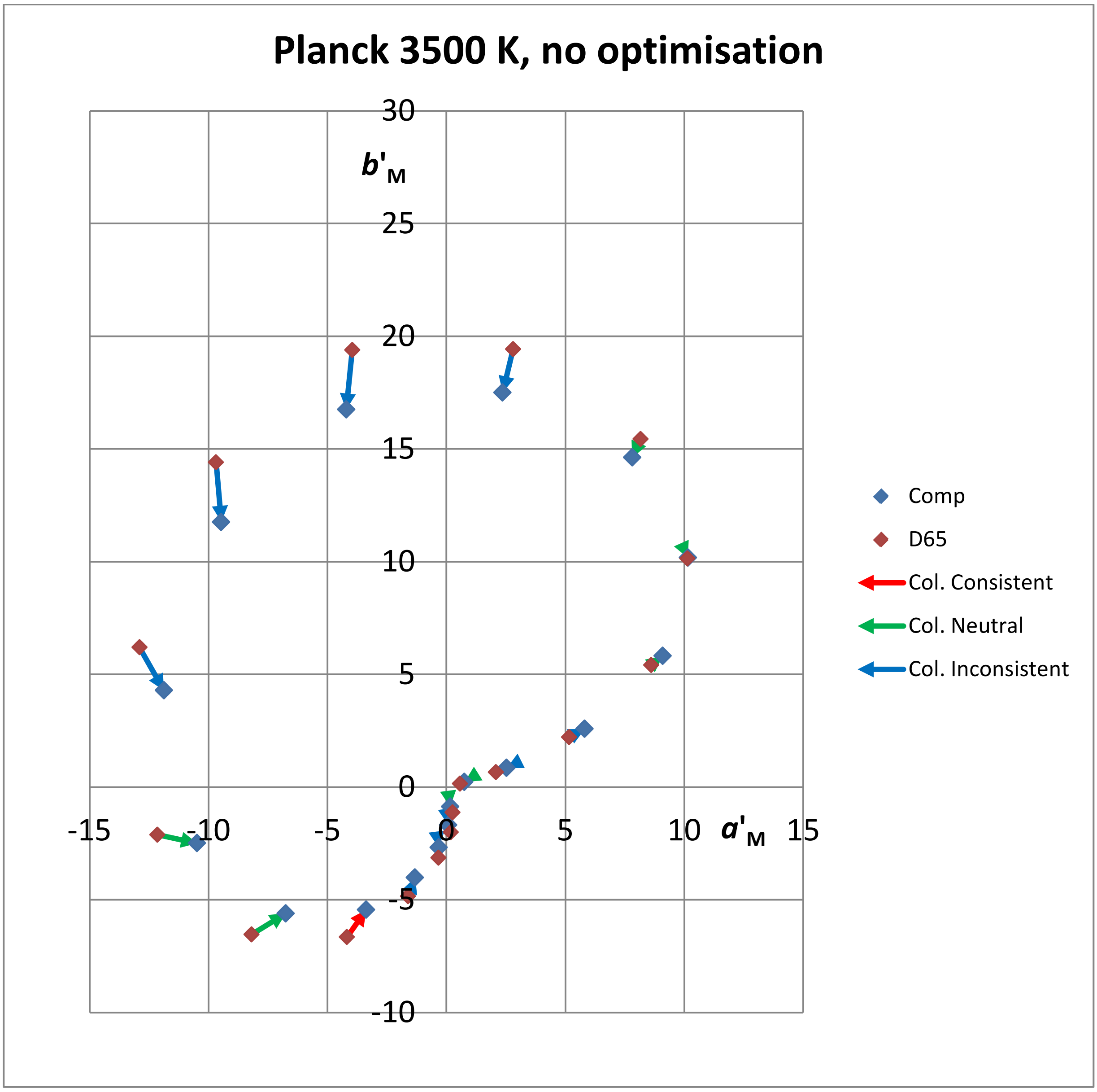

Figure 8. ***a*'$_M$, *b*'$_M$ co-ordinates of the test samples under D65 illumination and the corresponding colours for Planck 3500 K illumination.**

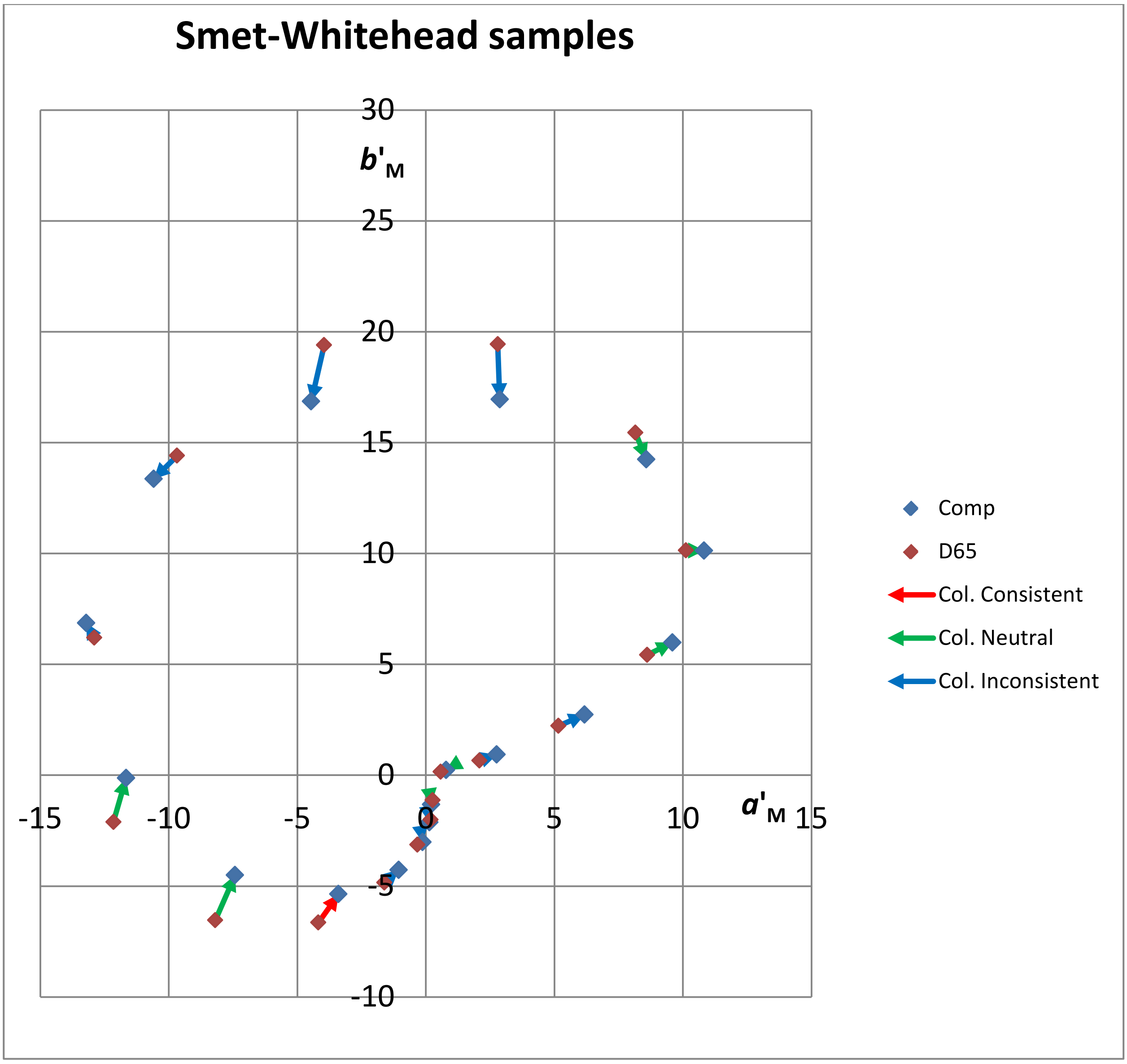

Figure 9. a'_M, b'_M co-ordinates of the test samples under D65 illumination and the corresponding colours for optimized 3500 K LED illumination.

4 Summary and Conclusions

The illumination of museum objects is under a dramatic change. Due to energy saving requirements many museums consider the use of LED lighting. In the USA one could observe a trend to change halogen spotlights to LED retrofit lamps (Miller 2012, Miller and Druzik 2012). In Europe one can observe the trend that lamp companies produce new luminaires directly for exhibition lighting using LED sources (Padfield 2013).

Despite the fact that some recent investigations show that most pleasing lighting for illuminating paintings is at 550 K to 5700 K (Nascimento 2014), most museum curators opt for warm-white lighting with a CCT not higher than 3500 K.

As most paintings produced up the end of the 19th Century were painted under natural daylight, a new paradigm has been introduced: the light should show the colours of the paintings as closely as possible to their original appearance. This means the spectral distribution of the 3500 K CCT light source should be optimized in such a form that the corresponding colours of the different pigments should be as close as possible to the colours of the pigments seen under 6500 K (naturally other starting and viewing CCTs are equally possible). A further requirement – that can be fulfilled using the CIECAM02 model to establish the corresponding colours – is that the lower level of the illumination should also be considered.

On the example of pigments used by Michelangelo and the other Renaissance painters in the Sistine Chapel it has been shown that using this paradigm one can come nearer to the original appearance of the paintings using a LED lighting of 3500 K CCT.

Acknowledgement

This research was supported by EU ICT-PSP-2010-5 project (grant number: 297262) entitled High Quality and Energy Efficient LED Lighting for Art (LED4ART).

References

AYDINLI, S., BECKER, B., HILBERT G., KROCHMANN E., KROCHMANN J. 1990 Museumsbeleuchtung, Farbänderungen von museumstypischen Materialien durch optische Strahlung. *Licht* TAB 11/90:861-866.

CIE 2004. CIE 159:2004. A Colour Appearance Model for Colour Management Systems: CIECAM02. Vienna :CIE.

CIE 1991. CIE 89-1991. On the deterioration of exhibited museum objects by optical radiation, in *CIE Technical Collection 1990*. Vienna: CIE.

CIE 2004. CIE 157:2004. Control of damage to museum objects by optical radiation. Vienna: CIE.

DAVIS W., OHNO, Y. 2005. Toward an improved color rendering metric. *Proc. SPIE 5941* 59411G1-G8.

DRUZIK, J. R., MICHALSKI, W. 2012. Guidelines for Selecting Solid-State Lighting for Museums. Canadian Conservation Institute, www.cci-ge.ca; The Getty Conservation Institute, www.getty.edu/conservation.

FELLER, R. L. 1964 Control of deteriorating effects of light upon museum objects. *Museum* **XVII**, No 2, 1964.

FONTOYNONT, M., MIRAS, J.P., ANGELINI, M., CHANUSSOT, J., MARTY, C., DUCHÊNE, G., NOVAKOVSKI, L., MAKITA, K., MORIYAMA, T. 2013. Lighting Mona Lisa with LEDs: details concerning innovating techniques (TOSHIBA Lamp – 2013). http://www.fraensrl.com/monalisa.html.

LOE, D. L., ROWLANDS, E., WATSON, N.F. 1982 Preferred lighting conditions for the display of oil and watercolour paintings. *Lighting Res. & Technol*. **14**:173-192.

LUO, M. R., LI, C. 2007. COLOUR APPEARANCE MODELS AND ASSOCIATED COLOUR SPACES in. Colorimetry: Understanding the CIE system, ed. J. Schanda, Wiley-Interscience 2007.

LUO, M.R., LI, C.J., HUNT, R.W.G, RIGG, B., SMITH, K.J. 2003. CMC 2002 colour inconsistency index: CMCCON02. *Color. Technol.* **119**:280-285.

MILLER, N. J. 2012. Demonstration of LED retrofit lamps at the Smithonian American Art Museum, Washington, DC. US Department of Energy Report PNNL-21476.

MILLER, N. J., DRUZIK, J. R. 2012. Demonstration of LED retrofit lamps at an exhibit of 19th Century photography at the Gety Museum. Final report in support of the DOE Solid-State Lighting Technology Demonstration GATEWAY Program. PNNL-21225.

NASCIMENTO, S. M., MASUDA, O. 2014. Best lighting for visual appreciation of artistic paintings—experiments with real paintings and real illumination. *JOSA A* **31**:A214-219.

NICKERSON, D., KELLEY, E.F. 1962 Interim method of measuring and specifying color rendering of light sources. Report, 27 p., *Illuminating Engineering* 1962, July, p. 471-495

PADFIELD, J., VANDYKE, S. AND CARR D. 2013 'Improving our Environment', http://www.nationalgallery.org.uk/paintings/research/improving-our-environment.

PEPLER, W, KHANH, T.Q. 2013. Museumsbeleuchtung - Lichtquellen, reflexionsspektren, optische Objektschädigung, Teil1. *Licht* 1-21.

SCUELLO,M., ABRAMOV, I., GORDON, J., WEINTRAUB, S. 2004 Museum lighting: Optimizing the illuminant. *COLOR Res. & Appl*. **29**:121-127.

SMET, K., WHIETHEAD, L. 2011. Meta-Standards for Color Rendering Metrics and Implications for Sample Spectral Sets. *CIC Conf*. 2011.

SMET, K.A.G., SCHANDA, J., WHITHEAD, L., LUO, R. M. 2013. CRI2012: A proposal for updating the CIE colour rendering index. *Lighting Res. & Technol*. **45**:689-709.

SZABÓ, F. and SCHANDA J. 2012. Solid State Light Sources in Museum Lighting – Lighting Reconstruction of the Sistine Chapel in the Vatican. In: *CIE 2012 Lighting Quality and Energy Efficiency conference,* Hangzhou. CIE **x037**:2012, 256-263.

SZABÓ, F., CSUTI, P., SCHANDA, J. 2014. Museum lighting with LEDs: LED lighting for the Sistine Chapel. Present Conference.

IT09

ALMOST ALL LAMPS ARE SAFE, BUT SAFETY OF NEW LAMPS IS QUESTIONED

David H. Sliney, Ph.D,
Department of Environmental Health Sciences
Johns Hopkins Bloomberg School of Public Health, Baltimore, MD, USA
david.sliney@att.net

Abstract

Human exposure limits for ultraviolet visible and infrared radiation based upon clinical experience and biomedical research were the basis of Emission Limits for lamp product risk groups. Photobiological safety standards for lamps have been published by the CIE (S009:2002) based upon ANSI/IESNA RP27.1-3 and the CIE Standard was also adopted by the International Electrotechnical Commission as IEC 62471:2006. Primary optical safety concerns relate to actinic ultraviolet radiation and blue light. Although IARC classifies sunlight as a Group I (known) carcinogen, it is nearly impossible to protect against the UV in sunlight to currently recommended ACGIH/ICNIRP exposure guidelines for the skin during summer months, and emissions from fluorescent lamps are trace amounts compared to sunlight. Unlike laser exposures, which are rare, one is continuously exposed to artificial light sources. Studies of the biological effects of light on human health is a very active current area of biomedical research, and we do not understand all effects as well as we would like, particularly with respect to the effects of visible light upon newly discovered retinal photoreceptors—the photosensitive retinal ganglion cells. Although the biological effects of ultraviolet radiation has been studied for decades, there continues to be a debate with regard to obtaining an optimum balance of preventing excessive exposure that increases risks of delayed effects upon the skin and eye, while at the same time having the benefits of low-level UV. Realistic time-weighted exposure conditions are essential for risk-group assessment. This applies to compact-fluorescent lamps and LED sources. More application-specific optical-safety standards are needed.

Keywords: e.g. lamp technology, Photobiology, Lamp Safety

1 Introduction

During the past 50 years a wide body of biomedical research has been conducted to understand the factors which influence injury from optical radiation—particularly with respect to the eye. Human exposure limits for ultraviolet visible and infrared radiation from the American Conference of Governmental Industrial Hygienists (ACGIH) and the International Commission on Non-Ionizing Radiation Protection (ICNIRP) were the basis of Emission Limits for lamp product risk groups (ACGIH, 2014; ICNIRP, 2013). Exposure limits are freely available from the ICNIRP website (http://www.icnirp.org). Photobiological safety standards for lamps were first published by the CIE (S009:2002) in 2002, based largely upon ANSI/IESNA RP27.1-3 recommended practice documents; and the CIE Standard was also adopted by the International Electrotechnical Commission as IEC 62471:2006. These guidelines and standards address the principle optical safety concerns of actinic ultraviolet radiation and blue light from conventional lamps. Although the International Agency for Research on Cancer (IARC, 1992) classifies sunlight as a "Group I carcinogen," i.e., a known human carcinogen, it is nearly impossible to protect against the UV in sunlight to currently recommended ACGIH/ICNIRP exposure guidelines for skin exposure during summer months; whereas, the emissions from fluorescent lamps are only trace amounts compared to sunlight (Lytle, 1993; Sliney, 1980). IARC classified fluorescent lighting as Group 3, i.e., "*not classifiable as to its carcinogenicity to humans.*" Nevertheless, these trace emissions of UV from fluorescent lamps have been measured to assess potential risk (Bickford, 1974; Levin, 1977; Lytle, 1993). It is from an understanding of outdoor, solar UV exposure, that lamp safety standards could emerge. Unlike laser exposures, which are rare, one is continuously exposed to artificial light sources (CIE, 2002).

Studies of the biological effects of light on human health is a very active current area of biomedical research, and we do not understand all effects as well as we would like, particularly with respect to the effects of visible light upon newly discovered retinal photoreceptors—the photosensitive retinal ganglion cells. Beneficial uses of light in phototherapy to correct circadian disorders or mood disorders must be balanced by a careful review of potential side-effects and actual retinal hazards. Although the biological effects of ultraviolet radiation have been studied for decades, there continues to be a debate with regard to obtaining an optimum balance of preventing excessive exposure that increases risks of delayed effects upon the skin and eye, while at the same time having the benefits of low-level UV in producing Vitamin D and possibly obtaining other positive effects for the immune system.

In addition to potential UV hazards from lamps, the lamp safety standards (IEC/CIE, 2006) consider several other potential optical hazards, such as infrared effects on the eye and theoretical thermal hazards, but besides UV, the only other hazard that may significantly affect risk group classification is the "blue-light hazard." The blue-light hazard refers to the potential risk of photomaculopathy, or Photoretinitis, a retinal injury which can occur if one overcomes their natural aversion response to bright light and stares at e.g., the sun, a welding arc or an arc lamp (CIE, 1998; Okuno, 2002; Sliney, 1980). Only very bright light sources such as a xenon-arc searchlight pose such a risk under any reasonably foreseeable viewing conditions (Figure 1). However, even a bright quartz-halogen lamp used to illuminate the eye during ophthalmic surgery can produce a photomaculopathy, resulting in vision loss (Byrnes, 1996).

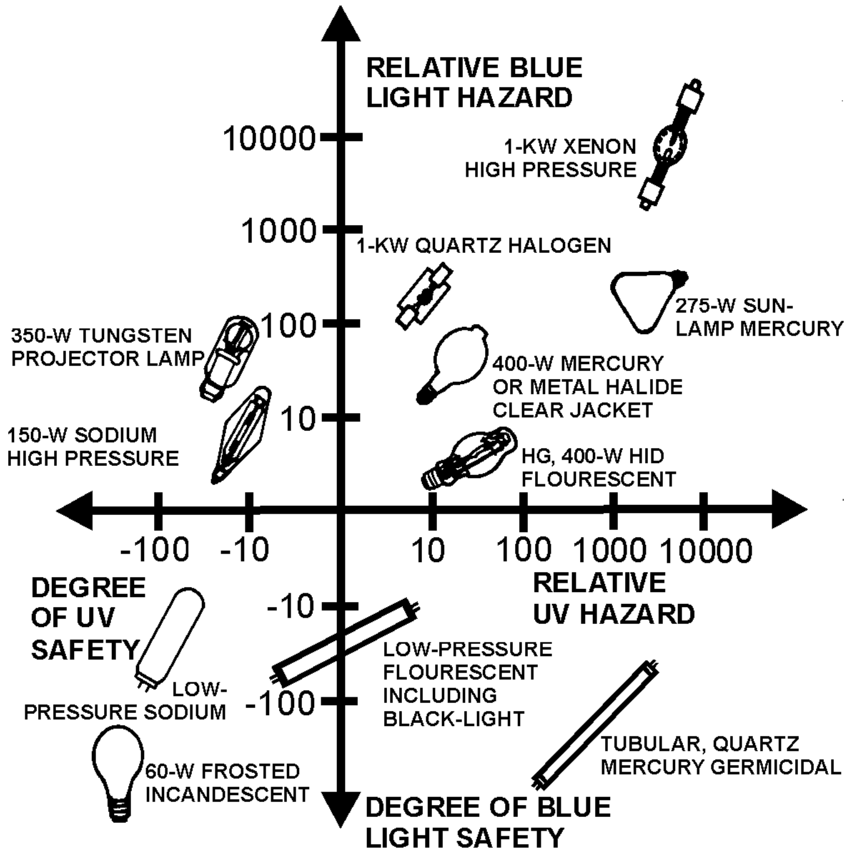

Figure 1 – Relative Ultraviolet and „Blue-Light" Risks of conventional Lamps (adapted from Sliney and Wolbarsht, 1980). White LEDs would fall left of the vertical axis.

In drafting photobiological (optical) safety standards for lamps, expert committees have been challenged to balance the potential, theoretical risks of exposure to real exposure conditions. The Committee on Photobiology of the Illuminating Engineering Society of North America (IESNA) struggled for 20 years to develop lamp-safety risk groups (RG-0, RG-1, RG-2 and RG3) before the first recommended-practice (RP) documents were published in 1993 (Sliney, 2013). Lamps are considered generally safe, and only under the most unusual exposure conditions have retinal injuries (as during eye surgery) occurred. Certainly, lamps used for general light service (GLS) are not hazardous under CIE S009 and the IESNA RPs when properly assessed. Unfortunately, some assessments of LEDs and special-purpose lamps using CIE S009 emission limits have placed lamps in a higher risk group than would be consistent with the rationale and true photobiological risks. Revisions are now being proposed for the current photobiological safety standards to provide more realistic time-weighted exposure conditions for risk-group assessment. This applies to compact-fluorescent lamps and LED sources. For example, no one is exposed with a lamp in their face at 20 cm for 8 hours/day, as some have interpreted the current standards and guidelines. Much of the problem stems from assuming that a proximal measurement distance of 20 cm (needed to obtain a measureable UV spectroradiometric signal from fluorescent lamps) was somehow related to an expected exposure condition! More application-specific optical-safety standards are needed. Figure 1 illustrates the relative risks for a fixed exposure distance.

2 Solid-State-Lighting Optical Safety Questions

As with the introduction of any new technology, solid-state lighting (SSL) has – not surprisingly – raised new safety concerns. Although “white” LEDs emit no significant UV, because the earliest white LEDs were frequently rich in the blue part of the spectrum, some scientists, governmental agencies and journalists began to raise the issue of the “blue-light hazard.” Indeed, some media and Internet posts have occasionally contained warnings of potentially adverse health effects from solid-state lighting (SSL). Most of these media reports or Internet postings referring to “the blue-light hazard” are lacking in a realistic risk assessment of retinal exposure (Prevent Blindness, 2013; Roberts, 2011; Wikipedia entry, 2013). Some of these reports are generally exaggerated and have been considered to paint an unfair picture of SSL, and even prompted the Building Technology Office of the US Department of Energy to issue a fact sheet on the optical safety of LEDs (USDOE, 2013). Other media reports also consider that human circadian effects are more possible from blue-rich light emitted by high CCT lamps (ABC News, 2011; Haim, 2011; Harvard Health Letter, 2012). This only briefly summarizes why some concerns have been raised, but we should ask why some scientific studies have led to such concerns and statements to avoid SSL use. What are the scientific bases of these reports? Can there be any validity in the concerns raised? These are valid questions to address.

Concerns based upon the stronger influence of blue or blue-rich white LEDs with circadian, neuroendocrine system and neurobehavioural responses (e.g., melatonin regulation), arise because of the blue-light sensitivity of the intrinsically photosensitive retinal ganglion cells (Berson, 2001; IESNA, 2008; West, 2011). It is therefore important to understand the available scientific evidence that raised these questions in the first place. Can differing spectra alone be cause for concern? Are there any realistic exposure conditions where there would be potential photobiological effects? For those concerned about the potential health and safety impact of a future, blue-rich, artificially illuminated environment by LEDs, it is well to note that current solid-state lamp offerings have a lower correlated colour temperature (CCT).

2.1 Age-Related Macular Degeneration

For several decades there has been a growing concern about the potential role of light in the etiology (cause) or promotion of age-related macular degeneration (AMD). Although the scientific evidence for this link has remained controversial, questions have arisen with regard to new lighting technologies. Probably unwarranted, in the past few years there has been growing concern that light from new light sources (luminaires) employing light emitting diodes (LEDs), or even compact-fluorescent lamps (CFLs) may pose a special risk. The reason for the concern appears to have arisen from the fact that most early “white-light” LEDs had a very strong emission in the blue end (450-470 nm) of the visual spectrum compared to existing light sources, and LEDs are small and bright. Compact fluorescent lamps (CFLs) also tend to be sold with higher CCT values than the previous, ubiquitous incandescent lamps most frequently installed in domestic lighting.

But what do we really know about the etiology of AMD? The possible link of sunlight exposure with AMD has been fostered by animal studies with bright (particularly short-wavelength) light (Rozanowska, 2005; Sparrow, 2005; Sykes, 1981; Wielgus, 2010) and some suggestive epidemiological evidence (Delcourt, 2001; Mitchell, 1998; Taylor, 1990). All of the animal studies were for relatively short periods of some days, and many of the animals were nocturnal rodents without cone photoreceptors. The applicability of the findings of the large number of studies of daily exposure of nocturnal rodents with fluorescent lamps has led to the criticism that the results have little relevance to the human species. At least one study, however, employed non-human primates (Sykes, 1981) to show the light damage from constant viewing of white fluorescent lamps; however, to obtain the results, the primate had to have pupils medically dilated. Current guidelines for human exposure to bright light sources take into account the uncertainties in extrapolating animal experimental data to the human condition (ACGIH, 2014; ICNIRP, 2005, 2013). One criticism of the current exposure guidelines has been that the limits appear to be solely based upon acute (minutes to days in duration) exposures and those chronic, life-long exposures are not really possible in experimental settings (Behar-Cohen, 2010, 2011). Most of the animal studies that exposed rodents to direct cool-white fluorescent lamps for days at close range produced in retinal irradiances of the order of summer sunlight over snow or even higher – retinal irradiances almost never experienced by humans, and certainly not for many hours each day. Because of the ratio of pupils size, to ocular focal length, rodents exposed to bright fluorescent lamps experience a significantly higher retinal irradiance than would humans observing the same lamp (Sliney, 1984), Retinal pigment epithelial cell culture biochemical studies as well as rodent studies show retinal changes that have been suggestive of some changes believed to be precursors of AMD (Algvere, 2006; Arnault, 2013; Remé, 2004; Rozanowska, 2005; Sparrow, 2004; Magrain, 2004; Organisciak, 1994; Waxler, 1986; Wielgus, 2010; Winkler, 1999; Zhou, 2011). The action spectrum for light damage has been questioned, but most rodent studies clearly show the greatest sensitivity in the blue-end of the visible spectrum (Ham, 1976: van Norren, 2011). The connection between light exposure and AMD is best made by the laboratory studies, but the majority of epidemiological studies in human exposure to sunlight do not show a statistically significant relationship (Delcourt, 2001; Cruickshanks, 1993; Mainster, 2010). Epidemiological studies of lifetime human retinal exposures are fraught with difficulties, since there are significant differences (~2X) in pupil size outdoors for different people viewing the same scene and behavioural avoidance of bright light differs among different individuals (Sliney, 1999, 2005). Recall bias is also a large issue with epidemiological studies. We are therefore presented with strongly suggestive evidence for a relationship of light exposure and AMD from laboratory studies, but few epidemiological studies supporting this hypothesis. It may be that a link exists for a sub-population of persons with a genetic pre-disposition for AMD and chronic light exposure that has not yet come out of the epidemiological studies to date because of our current knowledge. Only further research will finally answer that question. Because of this potential link, some experts have cautioned against interior lighting at unusually high CCT values in domestic settings, although high CCT values of daylight may be justified in a workplace setting to increase alertness (CIE 2004, 2006).

2.2 Circadian Effects

Blue-rich white LEDs and high CCT fluorescent lamps have been linked to circadian, neuroendocrine system and neurobehavioural responses (e.g., melatonin regulation), because of the blue-light sensitivity of the intrinsically photosensitive retinal ganglion cells (Berson, 2001; CIE, 2004, 2006; IESNA, 2008; Rahman, 2014; West, 2011). Studies linking night-time indoor illumination to breast cancer in night-shift workers are based upon both animal studies and epidemiological studies (Blask, 2011; Stephens, 2014; Wren, 2014). However, the interpretation of these findings remains rather controversial. Indeed, like the AMD studies, the findings of the basic science investigations can be interpreted either to be a cause for real concern and the impetus for further research, or the findings can be largely dismissed as either irrelevant to realistic human exposure condition, confounding factors, or that exposure doses required are not experienced in the normal household lighting levels or from street lighting.

The current photobiological safety standards with risk group classification were based upon the understanding of human photobiological thresholds known in the 1970s and 1980s. At that time the enhanced circadian effects of blue light were not known. However, the criticism that human exposure limits and risk group emission limits (ACGIH, 2014; CIE, 1998; ICNIRP, 2005, 2013; Sliney, 2013) were based largely upon acute effects and ignored chronic exposure are unjustified. Certainly the UV limits were based upon human exposure studies, skin-cancer studies over a lifetime as well as acute erythema thresholds. The blue-light hazard radiance limits are based upon an acute effect (photomaculopathy) which only clearly applies to staring at the sun, a welding arc or an arc lamp, or ophthalmic surgery exposures (ISO, 2007), and upon experimental threshold exposures data ranging from 10 to 1,000 s. These limits are *not* based upon the rodent studies under fluorescent lamps, as such exposures were considered unrealistic for human viewing of lamps (Sliney, 2013), but outdoor viewing of bright environments was taken into account. At present there is clearly insufficient biomedical data upon which to suggest safety criteria to protect against only hypothesised neuroendocrine effects. But lighting designers should consider the spectral content of lighting recommended for domesting and nursing-home settings.

2.3 Realistic Time-Weighted Averaged Viewing Conditions

The greatest challenge encountered in the development of the lamp safety standards and recommended risk-group classifications has been agreement on what constitute realistic exposure conditions. The measurement conditions needed to detect trace emissions of UV led to a 20-cm default measurement distance. But this had nothing to do with human exposure distances, that have to be based upon a time-weighted average (TWA) of direct viewing for the eye and direct and indirect exposure of the skin (Sliney, 2013). See Figure 2.

A. “Lamp-in-the-Face Ocular Exposures	B. Ocular Exposure from Indirect Lighting

Figure 2 – Staring directly into a bright lamp is not a realistic exposure condition; the natrual aversion response to bright light results in strong squinting reaction or lid closure as shown in (A). Using task lighting or overhead lighting is the chronic exposure condition for the eyes under artificial illumination, and reflected exposure of the eye is far more comfortable (B).

Risk groups were based upon probabilistic risk analysis of reasonably foreseeable human exposure and ocular viewing conditions (Sliney, 1999; Sliney, 2013; ??). Unfortunately, the vertical (application-specific) recommended practice documents originally envisioned by IESNA, were not completed, but such documents on UV lamp applications, Infrared lamp applications, and projection lamp systems are being drafted. Hopefully the CIE effort to update CIE S009 will also consider more realistic application conditions and not consider emission limits, which are based upon exposure limits under TWA as equivalent (Figure 4).

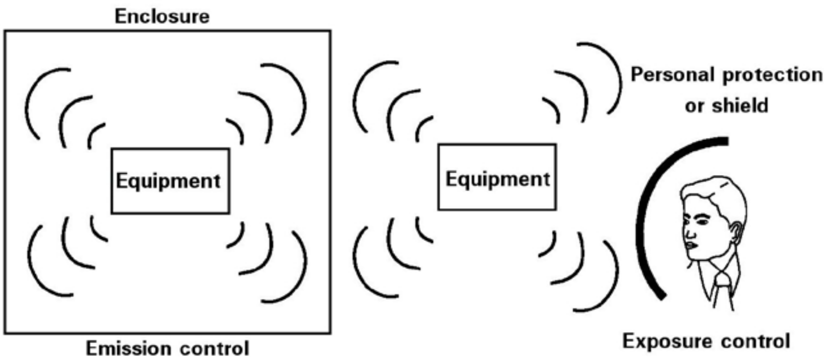

Figure 4 – Emission limits developed in product-safety (manufacturer) standards are based upon risk assessment of time-weighted average (TWA) exposure conditions. Exposure limits are used in occupational (workplace) and public/environmental health safety standards by trained specialists examining specific, on-site exposures and risks.

Momentary direct viewing of a lamp at 20 cm viewing distance or even at greater distances will be limited by glare. Direct lighting is positioned to minimize glare under normal use (Figure 2). The maximum TWA of 300 or 1000 s used in higher risk groups also had to be based upo realistic exposure distances. The 500-lux criterion for GLS lamps was based upon many studies of use conditions and lighting design (Bickford, 1974; Levin, 1977; Lytle, 1993; Sliney, 2000, 2013). Extensive research has led to the conclusion that the UV-B component in fluorescent, or tungsten-halogen lighting at very high levels was the conservative equivalent to 500 lx measured from the bare lamp. This was not to say that exposures were only at 500 lx, but that was a test condition. RG-1 was really intended for fluorescent lamp products, where ultraviolet skin exposure could be based upon the equivalent dose from 2.8 h (10,000 s) daily exposure at the reference measurement position corresponding to the temporal-spatial, worst-case exposure conditions, as opposed to 8-h, or continuous exposures, and would not have to consider unusually photosensitive skin.

Finally, the measurement conditions now provided in current standards and guidelines (CIE S009; IESNA, 2000) need to be approached with common sense. It would be very rare that all criteria apply as illustrated in Figure 4 and 5.

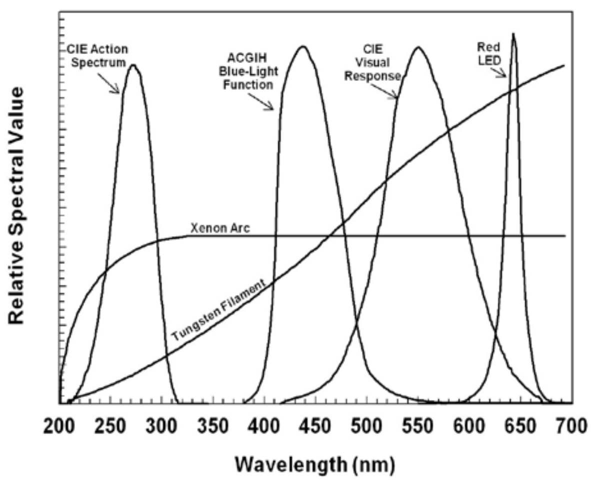

Figure 4. Spectral weighting of the UV S(λ) function and the Blue-Light-Hazard function B(λ) are only required if the lamp emits in the spectral region of interest.

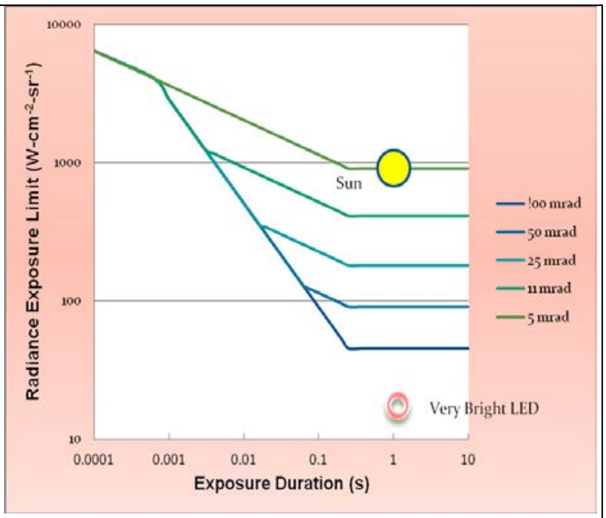

Figure 5 - Retinal thermal hazard limits are rarely required for a risk-group classification except for large arc lamps.

3 Conclusions

Current photobiological safety standards simply do not apply to circadian effects and lighting guidelines are appropriate (IESNA, 2008). Use of low CCT SSL should avoid any concerns (whether warranted or unwarranted) of indoor lighting significantly contributing to AMD compared to sunlight. Current LEDs (without UV pumping) do not pose any concerns about UV and UV measurements would be absurd. Two major conclusions relate to “time-weighted averaging” of exposures and to the meaning of the exposure distances. The primary health and safety concern built into current standards relate to ultraviolet and blue-light photobiological hazards and lengthy exposures (both photochemical mechanisms). For these exposures, a risk can only materialize from very lengthy exposures, and time-weighting of different irradiances experienced at different distances were considered in the development of lamp risk groups. Extensive research led to the conclusion that the UV-B component in fluorescent or tungsten-halogen lighting at very high levels was the conservative equivalent to 500 lx measured from the bare lamp. This was not to say that exposures were only at 500 lx, but that is the relevant test condition. Although the 500-lx criterion was based principally on UV, it applies as well to blue-light retinal hazards because of behavioral avoidance of glare.

4 References

ABC News. 2011. Do LEDs Disrupt our Biological Clocks? www report at: http://abcnews.go.com/Technology/daylight-savings-time-2011-white-light-emitting-diodes/story?id=14838491

ACGIH (American Conference of Governmental Industrial Hygienists). 2014. *TLV's, Threshold Limit Values and Biological Exposure Indices for 2014*, American Conference of Governmental Industrial Hygienists, Cincinnati, OH.

ALGVERE P.V., MARSHALL J, SEREGARD S. 2006. Age-related maculopathy and the impact of blue light hazard. *Acta Ophthalmol Scand*. 84(1):4-15.

ARNAULT E, BARRAU C, NANTEAU C, GONDOUIN P, BIGOT K, VIÉNOT F, GUTMAN E, FONTAINE V, VILLETTE T, COHEN-TANNOUDJI D, SAHEL JA, PICAUD S. 2013. Phototoxic action spectrum on a retinal pigment epithelium model of age-related macular degeneration exposed to sunlight normalized conditions. *PLoS One.* 2013. 8(8):e71398.

BEHAR-COHEN, F. ATTIA, D., A. BARLIER-SALS, A., CESARINI, J.-P., ENOUF O, GARCIA, M., MARTINSON C., MERCKEL, O., PICAUD, S., VIENNOT F., ZISSIS, G. 2010. *Light-Emitting Diodes: Potential Hazards*. A report of an expert group for the French Agency for Environmental and Occupational Health Safety (AFSSET), Paris.

BEHAR-COHEN F, MARTINSONS C, VIÉNOT F, ZISSIS G, BARLIER-SALSI A, CESARINI JP, ENOUF O, GARCIA M, PICAUD S, ATTIA D. 2011. Light-emitting diodes (LED) for domestic lighting: any risks for the eye? *Prog Retin Eye Res*. 30(4):239-57.

BICKFORD, E.D., CLARK, G.W., & SPEARS, G.R. 1974. Measurement of ultraviolet irradiance from illuminants in terms of proposed public health standards,J. /num. *Eng. Soc.* **4:**43-48 & 5(4):234-236.

BLASK DE, HILL SM, DAUCHY RT, XIANG S, YUAN L, DUPLESSIS T, MAO L, DAUCHY E, SAUER LA. 2011. Circadian regulation of molecular, dietary, and metabolic signaling mechanisms of human breast cancer growth by the nocturnal melatonin signal and the consequences of its disruption by light at night. *J Pineal Res.* 51(3):259-69.

BYRNES GA, MAZUR DO, MILLER SA. 1996. Retinal light damage and eye surgery, *Ophthalmology* 103(4):546-547.

CIE (Commission International de l'Eclairage, the International Commission on Illumination). 2002. CIE Standard S-009E-2002, *Photobiological Safety of Lamps and Lamp Systems*, Vienna, CIE. Joint-logo standard with IEC as: IEC64271-2006.

CIE. 1998. CIE x016-1998: *Measurement of Optical Radiation Hazards,* Vienna, CIE.

CIE. 2004. CIE x027:2004: *Proceedings of the CIE Symposium 2004 on Light and Health: Non-Visual Effects, 30 Sep. - 2 Oct. 2004, Vienna, Austria*, Vienna, CIE.

CIE. 2006. CIE x031:2006: *Proceedings of the 2nd CIE Expert Symposium "Lighting and Health", 7-8 September 2006, Ottawa, Ontario, Canada*. Vienna, CIE.

CRUICKSHANKS, K.J., KLEIN, R., KLEIN, B.E.K., 1993. Sunlight and age related macular degeneration — the Beaver Dam Eye Study. *Arch. Ophthalmol*. 111, 514–518.

DELCOURT C, CARRIÈRE I, PONTON-SANCHEZ A, et al. 2001. Light exposure and the risk of age related macular degeneration: the Pathologies Oculaires Liées à l'Age (POLA) study. *Arch Ophthalmol*. 119:1463–8.

FALCHI F, CINZANO, P., ELVIDGE C.D., KEITH D.M., HAIM A. 2011. Limiting the impact of light pollution on human health, environment and stellar visibility. *J. Environ. Mgmnt*. 2011; 92 (10): 2714.

HAIM, A. 2011. Exposure to 'white' light LEDs appears to suppress body's production of melatonin more than certain other lights, research suggests, *Science Daily*, see web report at: http://www.sciencedaily.com/releases/2011/09/110912092554.htm.

HAM, W.T., JR., MUELLER H.S., SLINEY, D.H. 1976. Retinal sensitivity to damage by short-wavelength light. *Nature*, 260(5547):153-155.

HARVARD HEALTH LETTER. 2012. Blue light has a dark side. *Harvard Health Letter,* Boston, Harvard Medical School, see website: http://www.health.harvard.edu/newsletters/Harvard_Health_Letter/2012/May/blue-light-has-a-dark-side/.

ICNIRP (International Commission on Non Ionizing Radiation Protection). 2013. ICNIRP guidelines on limits of exposure to incoherent visible and infrared radiation, *Health Phys*, 105(1):74-91

IESNA (Illuminating Engineering Society of North America). 2008. *Light and Human Health—An Overview of the Impact of Light on Visual, Circadian, Neuroendocrine and Neurobehavioral Responses.* TM-18-08, New York, IESNA.

IESNA. 2005. *Photobiological Safety of Lamps and Lighting Systems, RP27. 1,* New York, American National Standards Institute/Illuminating Engineering Society of North America.

IESNA. 2000. Photobiological Safety for Lamps & Lamp Systems - Measurement Systems, RP27.2-00, New York, American National Standards Institute/Illuminating Engineering Society of North America.

IESNA. 2006. *Photobiological Safety of Lamps and Lighting Systems, RP27.3*, New York, American National Standards Institute/Illuminating Engineering Society of North America.

INTERNATIONAL COMMISSION ON NON-IONIZING RADIATION PROTECTION (ICNIRP). 2004. Guidelines on limits of exposure to ultraviolet radiation of wavelengths between 180nm and 400nm (incoherent optical radiation). *Health Phys.* 87: 171–186.

INTERNATIONAL STANDARDS ORGANIZATION (ISO), IS0 15004-2:2006. International Standards Organization (ISO). 2007. International Standard, ISO 15004-2:2007, *Ophthalmic Instruments—Fundamental requirements and test methods—Part 2: Light hazard protection,* Geneva, ISO.

LEVIN, R.E., CLARK, G.W., SPEARS, G.R., & BICKFORD, E.D. 1977. Ultraviolet radiation - considerations in interior lighting design - part 1, *J. Illum. Eng. Soc.* **7:**80-89.

LYTLE, CD; CYR, WH; BEER, JZ; MILLER, SA; JAMES, RH; LANDRY, RJ; JACOBS, ME; KACZMAREK, RG; SHARKNESS, CM; GAYLOR, D; et al (1993). An estimation of squamous cell carcinoma risk from ultraviolet radiation emitted by fluorescent lamps. *Photodermatol Photoimmunol Photomed*, 9(6): 268-74.

MITCHELL, P., SMITH, W., WANG J.J. 1998. Iris color, skin sun sensitivity, and age-related maculopathy. The Blue Mountains eye study. *Ophthalmology* 105(8): 1359-1363.

O'HAGAN, J.B., KHAZOVA M., JONES C.W. 2011. Ultra-violet emissions from HMI daylight luminaires, *Lighting Res. Technol.* 43(2): 249-258

TAYLOR, H.R., MUNOZ, B. WEST, S., BRESSLER, N.M., et al. 1990. Visible light and risk of age-related macular degeneration. *Trans Am Ophthalmol Soc* 88: 163-173; with discussion 173-178.

WAXLER, M. AND HITCHENS, V. (eds), *Optical Radiation and Visual Health*, Boca Raton: CRC Press (1986).

OKUNO T., SAITO H., OJIMA J. 2002. Evaluation of blue-light hazards from various light sources. *Dev Ophthalmol.* 35:104-12.

ORGANISCIAK, D.T., WINKLER, B.S., 1994. Retinal light damage: practical and theoretical considerations. Prog. *Ret. Eye Res.* 13, 1–29.

ROBERTS, D. 2011. Artificial Lighting and the Blue Light Hazard, *Living Well with Low Vision,* Prevent Blindness, http://lowvision.preventblindness.org/daily-living-2/artificial-lighting-and-the-blue-light-hazard.

WIKIPEDIA ENTRY. 2013. High-Energy Visible Light, http://en.wikipedia.org/wiki/High-energy_visible_light.

PREVENT BLINDNESS AMERICA. 2013.http://lowvision.preventblindness.org/daily-living-2/artificial-lighting-and-the-blue-light-hazard.

ESSILOR. 2013. Blue light hazard: New Knowledge, New approaches to Maintaining Ocular Health, report of a roundtable, March 16, 2013, New York City. Essilor Blue Light Roundtable, http://www.crizalusa.com/SiteCollectionDocuments/Crizal-Literature/Blue%20Light%20Roundtable_White%20Paper.pdf.

LYTLE, CD; CYR, WH; BEER, JZ; MILLER, SA; JAMES, RH; LANDRY, RJ; JACOBS, ME; KACZMAREK, RG; SHARKNESS, CM; GAYLOR, D; et al (1993). An estimation of squamous cell carcinoma risk from ultraviolet radiation emitted by fluorescent lamps. *Photodermatol Photoimmunol Photomed,* 9(6): 268-74.

MAINSTER M.A., TURNER P.L. 2010. Blue-blocking IOLs decrease photoreception without providing significant photoprotection. Surv Ophthalmol 55:272–289.

MARGRAIN T.H., BOULTON M., MARSHALL J., D.H. SLINEY D.H. 2004, Do blue light filters confer protection against age-related macular degeneration? *Progr. Ret. Eye Res.* 23: 523–531.

RAHMAN S.A., FLYNN-EVANS E.E., AESCHBACH D., BRAINARD G.C., CZEISLER C.A., LOCKLEY S.W. 2014. Diurnal spectral sensitivity of the acute alerting effects of light. *Sleep*. 37(2):271-81.

REMÉ, C. 2005. The dark side of light: rhodopsin and the silent death of vision, The Proctor Lecture. *Invest. Ophthalmol. Vis. Sci.*, 46(8):2672-2682

RÓZANOWSKA M, SARNA T. 2005. Light-induced damage to the retina: role of rhodopsin chromophore revisited. *Photochem Photobiol*. 81(6):1305-30.

SPARROW J.R., BOULTON, M. 2005. RPE lipofuscin and its role in retinal pathobiology. *Exp Eye Res.* 80(5):595-606.

SLINEY, D.H., AND WOLBARSHT, M.L., 1980 *Safety with Lasers and Other Optical Sources, A Comprehensive Handbook*, New York, Plenum Publishing Corp., 1000 pp.

SLINEY, D.H. 1984. Quantifying retinal irradiance levels in light damage experiments, *Curr. Eye Res*. 3(1):175-179.

SLINEY D.H. 2005. Exposure geometry and spectral environment determine photobiological effects on the human eye. *Photochem Photobiol*. 81(3):483-9.

SLINEY, D.H. 1999. Geometrical assessment of ocular exposure to environmental UV radiation--implications for ophthalmic epidemiology. *J Epidemiol*. 1999; 9(6 Suppl):S22-32.

STEVENS R.G., BRAINARD G.C., BLASK D.E., LOCKLEY S.W., MOTTA M.E. 2014. Breast cancer and circadian disruption from electric lighting in the modern world. *CA Cancer J Clin.* 64:[in press; e-pub ahead of print, Dec 2013].

SYKES, S. M., ROBINSON, W. G., WAXLER, M., KUWARBARA, T., Damage to the monkey retina by broad spectrum fluorescent light, *Invest Ophthal Vis Sci*, 20(4):425-434 (1981).

US DEPARTMENT OF ENERGY (USDOE), BUILDING TECHNOLOGIES OFFICE. 2013. *Optical Safety of LEDs.* Fact Sheet PNNL-SA-96340, USDOE, Pacific Northwest National Laboratory.

VAN NORREN D., GORGELS T.G. 2011. The action spectrum of photochemical damage to the retina: a review of monochromatic threshold data. *Photochem Photobiol.* 87(4):747-53.

WEST KE, JABLONSKI MR, WARFIELD B, CECIL KS, JAMES M, AYERS MA, MAIDA J, BOWEN C, SLINEY DH, ROLLAG MD, HANIFIN JP, BRAINARD GC. 2011. Blue light from light-emitting diodes elicits a dose-dependent suppression of melatonin in humans. *J Appl Physiol*. 110(3):619-26.

WIELGUS, A.R., COLLIER, R.J., MARTIN E., LIH, F.B., TOMER, K.B., CHIGNELL, C.F., ROBERTS, J.E. 2010. Blue light induced A2E oxidation in rat eyes--experimental animal model of dry AMD. *Photochem Photobiol Sci.* 9(11):1505-12.

WINKLER B.S., BOULTON M.E., GOTTSCH J.D., STERNBERG P. 1999. Oxidative damage and age-related macular degeneration. *Mol Vis.* 3(5):32.

WREN MA, DAUCHY RT, HANIFIN JP, JABLONSKI MR, WARFIELD B, BRAINARD GC, BLASK DE, HILL SM, OOMS TG, BOHM RP JR. 2014. Effect of different spectral transmittances through tinted animal cages on circadian metabolism and physiology in Sprague-Dawley rats. *J Am Assoc Lab Anim Sci.* 53(1):44-51.

WORLD HEALTH ORGANIZATION, INTERNATIONAL AGENCY FOR RESEARCH ON CANCER (IARC). *Solar and Ultraviolet Radiation*, Volume 55, IARC Monographs on the Evaluation of the Carcinogenic Risks to Humans, IARC, Lyon.

ZHOU J., SPARROW J.R. 2011 Light filtering in a retinal pigment epithelial cell culture model. *Optom Vis Sci* 88: 759-765.

OP01

DO OLEDS AND LEDS ILLUMINATIONS GIVE THE SAME IMPRESSIONS ON SPACE? − INTERNATIONAL SURVEY –

Yamauchi, Y.[1], Yokoyama, R.[1], Hirasawa, M.[1], Kawashima, Y.[1], Nagai, T.[1] and Ishida, T.[2]
[1] Graduate School of Science and Engineering, Yamagata University, Yonezawa, JAPAN,
[2] Graduate School of Engineering, Kyoto University, Kyoto, JAPAN
yamauchi@yz.yamagata-u.ac.jp

Abstract

Organic electroluminescent lighting (OLED) is expected to become one of the next generation lighting devices. In this research, we investigated the impression of a furnitured miniature room illuminated by either flat type LED lighting panels or OLED panels with Japanese subjects and European subjects. The chromaticities and illuminance of the room was the same for those two illuminations. We found that the room gave significant difference in impression for some adjective items. The scores of “calm”, “warm” and “gentle” were significantly higher for OLED. From the results of factor analysis, three factors were extracted: “amenity”, “activeness”, and “personality”. Moreover, the impressions obtained from both groups of subjects were almost the same regardless of the nationality.

Keywords: OLEDs, LEDs, spatial impression, subjective evaluation, factor analysis

1 Introduction

In recent years, Organic Electro-Luminescence (OLED) lighting has been attracted attention as a next-generation lighting. This lighting has various features: its wide range of illumination, thickness, flexibility etc. OLED lighting is expected to replace conventional lighting devices in near future. The researches dealing OLED in practical use, however, has just started, and it is essential to explore various aspects of OLEDs before it comes into market.

One of the biggest differences of OLED from other lighting device is that OLED is a surface-emitting light source, while LED is a point light source. As a result, when LEDs are installed to appear as a pseudo surface light source, the residual differences coming from the light source itself produces different impressions for the space illuminated when compared against a real surface light source. In CIE2012, we showed that the room illuminated with OLED gave subjects an impression of gentle and warm compared with those illuminated with LED [1]. However, the experimental conditions such as the chromaticities and illuminances of the room were not fully controlled.

The purpose of this research is to test if our findings are still true under the identical chromaticities and illuminances (Experiment 1), and then to test subjects from different countries to compare their results (Experiment 2). As Experiment 2, we conducted the same experiments in Japan and in Germany to record impressions of miniature rooms illuminated by either LEDs or OLEDs with the same procedure. In the experiments conducted in Japan, we repeated our previous conditions[1].

2 Methods

The experiment was conducted with a 300 x 350 x 320 mm box that imitated a room. In order to mimic a habitation space, some miniature furniture were placed inside the box: a dining set composed of a table and four chairs was arranged in the center, a sofa and a television were arranged at the left and the right back, respectively (Figure 1). Four light source panels, either OLED or LED, were installed as ceiling lights. Two combinations of light sources were used. In the first condition, commercially available OLED panels (Lumiotec) and colour tuneable LED light boxes of our own making were used. In the second condition, commercially available LED panels (Epoch Lighting) and also commercially available colour tuneable OLED panels (Pioneer) were used. As one of the light sources in both combinations was colour tuneable, we could match the chromaticities and illuminance of the room in both combinations. The chromaticities used in the experiment are shown in Figure 2.

Figure 1 – Appearance of a miniature room

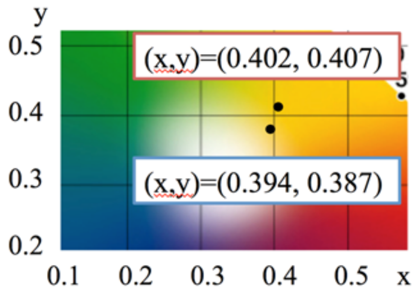

Figure 2 – Chromaticities of the illuminants Colour 1 (0.402, 0.407) & Colour 2 (0.394, 0.387)

The area of the illuminations was varied in the experiment 1 in Japan: 10%, 50%, and 100%. Four panels were set at the configuration of 2 x 2. The slit was used to restrict the area. The illuminances of the center of the room, measured at the top of the table, were kept at 480 lx for all the conditions.

The position of the box was adjusted so the height of the furniture figures and eyes were in the same level. The distance between a box and a subject was set to be approximately 50 cm, although the head position of the subject was not fixed. Subjects were asked to evaluate the impression of the room for 20 adjective items in five steps, while observing the imitated habitation space (Figure 3). Table 1 shows all the adjectives used in the experiment. We picked up these adjectives based on the previous reports [2,3]. In the Experiment 1 and Experiment 2 conducted in Japan, the adjectives were given to the subjects written in Japanese, while the adjectives were shown in English in Experiment 2 conducted in Germany. In the real experiment, we built two identical miniature rooms, one is illuminated with OLED, and the other with LED.

Table 1 – Adjectives used in the experiments

・calm	・large
・relaxing	・interesting
・natural	・uniform
・warm	・premium
・relief	・gentle
・soft	・unique
・tasteful	・spacious
・cheerful	・vivid
・bright	・showy
・lively	・dazzling

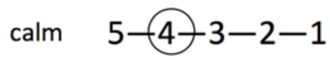

Figure 3 – example of the evaluation

Before starting the experiment, the subject observed the room for three minutes. This was long enough for adaptation. Five male students were served as subjects in Japan, while 13 paid persons participated in the experiments in Germany. As four among 13 subjects were from Europe, we show their results in this paper.

3 Results and Discussions

3.1 Experiment 1: Effects of area

The results obtained from 5 subjects in Colour 1 condition are shown in Figure 4. The x-axis indicates the area of the illumination, changing from 10% to 100%, and the y-axis indicates the evaluated values. The solid symbols (black line) and open symbols (gray line) denote the results obtained from OLED, and LED, respectively. As most of the subject showed the same trends, we averaged all the values, and the standard error are shown as error bars in each symbol. As the results obtained from Colour 2 showed the similar trends, we only show the results of condition Colour 1 here.

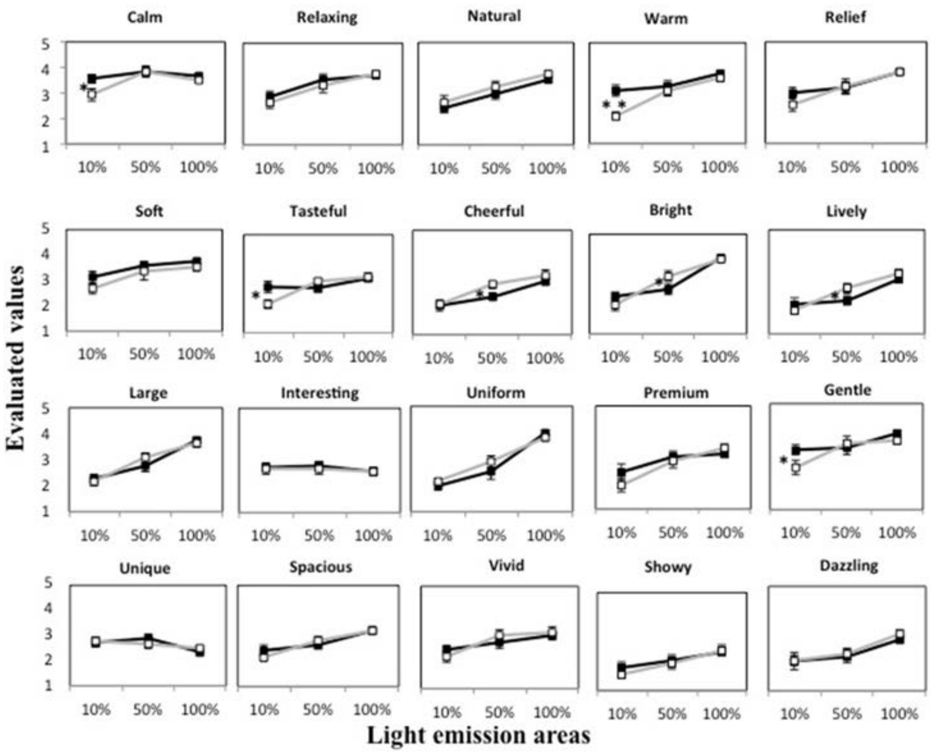

Figure 4 – Evaluated values across the light emission area (Colour 1)

As clearly shown in the figure, the values increased as the area of the illumination increased in most of the adjectives except the adjective “interesting”. Some data show statistically difference between the results obtained from OLED and LED, which are shown with asterisks (*: <0.05 and **: <0.01). The impression of “warm” in area 10% condition showed the biggest difference, and OLED was superior in this point.

Factor analysis was performed. The factor extraction method of maximum-likelihood estimation method was used. Factors for three high ranks were adopted. The rotation of factor axes using the Varimax method made it easier to extract factors. Table 2 shows the factor loading after rotation. Cumulative contribution ratio of first and second factors is 45.3%.

Table 2 – Factor loading (after rotation)

	Factor 1	Factor 2	Factor 3
bright	0.822	0.287	0.158
cheerful	0.764	0.134	0.034
large	0.741	0.329	0.065
uniform	0.723	0.385	0.002
lively	0.706	0.103	0.487
spacious	0.63	0.336	0.087
dazzling	0.612	−0.105	0.251
soft	0.074	0.81	−0.007
gentle	0.168	0.809	0.058
relaxing	0.286	0.759	0.077
warm	0.229	0.743	0.233
relief	0.419	0.701	0.058
calm	0.004	0.65	0.142
natural	0.469	0.516	−0.059
showy	0.367	0.092	0.709
vivid	0.304	0.1	0.689
interesting	−0.03	0.013	0.674
unique	−0.202	−0.036	0.644
tasteful	0.386	0.322	0.588
premium	0.311	0.393	0.561
contribution ratio	23.39%	21.95%	14.68%
cumulative contribution ratio	23.39%	45.34%	60.02%

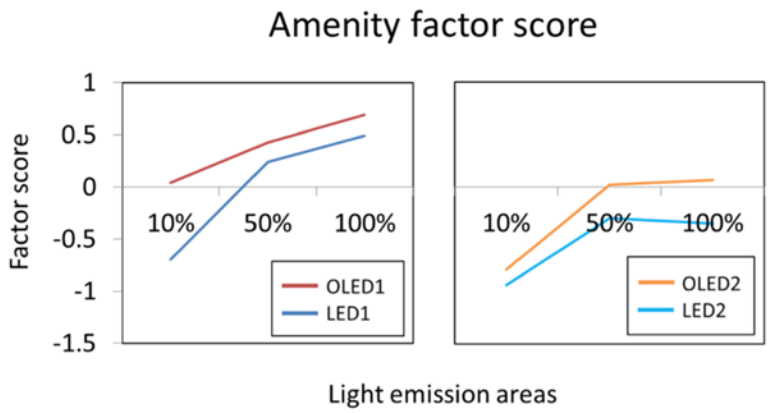

Figure 4 – The effects of the area on the impressions of the illuminated room

We named the first factor as “activeness”, derived from the factor loadings such as “lively” and “bright”. The second factor was named as “amenity”, derived from the factor loadings such as “warm”, “gentle” and “relaxing”. Naming of these factors was referring to the studies of a number of semantic differential scale method [4]. Further, we calculate the factor score coefficient matrix, and derived factor score by multiplying the evaluated values. The factor scores of amenity are shown in Figure 4. Panel (a) denotes the results obtained from Colour 1, while (b) obtained from Colour 2. Red and orange lines indicate the scores of OLEDs, while blue lines indicate those of LEDs.

Both panels show the same trends: the scores of OLEDs were superior to those of LEDs in all the area conditions. These results are consistent with our previous results. In this experiment, the chromaticities of OLED and LED were the same, and the same results were obtained from two different chromaticities.

3.2 Experiment 2: Comparison between Japanese and European People

Due to the time constraint, the experiment in Germany was conducted only in 100% conditions in two chromaticities: Colour 1 and Colour 2.

The results of Colour 1 condition obtained from European subjects are shown in Figure 5 (a). Red and orange symbols and lines indicate the results with OLED while blue lined indicate those with LED. Expect some adjectives such as “bright”, “vivid”, “uniform”, the rated values showed the similar trends. In order to compare the results from Japanese, we show them in Figure 5 (b) (Colour 1). These values were extracted from Experiment 1 (100% condition). No adjectives were significantly different among Japanese subjects, while “bright” and “vivid” showed significant differences ($p<0.05$) among European subjects.

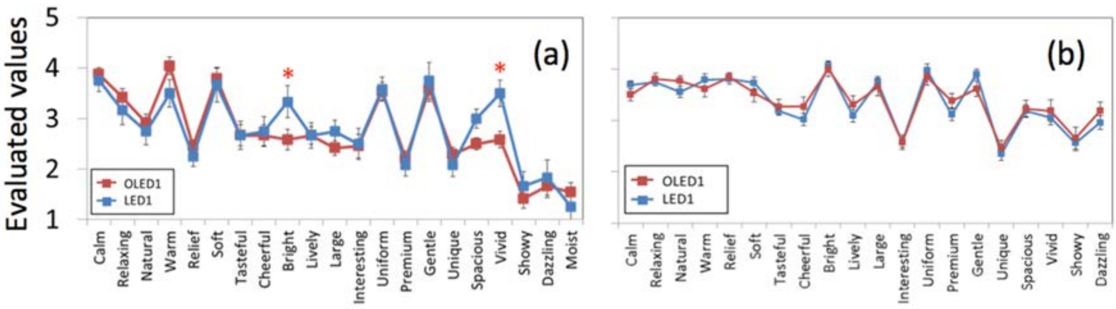

Figure 5 – Evaluated values from (a) European (b) Japanese subjects for all adjectives

Factor analysis was conducted to the results obtained from European subjects. The same procedure was adopted to derive factors. Table 3 shows the factor loading after rotation. Several factors were extracted. “Personality”, “amenity”, “activeness” were the first three factors.

Table 3 – Factor Loading of European subjects

	Factor			
	1	2	3	4
tasteful	0.879	−0.089	−0.158	−0.088
interesting	0.747	−0.15	0.03	0.001
premium	0.733	−0.099	−0.059	0.162
cheerful	0.717	0.15	0.12	−0.069
lively	0.592	0.224	0.386	0.093
natural	0.557	0.239	0.111	−0.059
relief	0.535	0.169	0.217	0.072
unique	0.481	0.258	0.058	−0.081
soft	0.144	0.798	−0.181	−0.285
gentle	0.184	0.786	−0.097	−0.236
warm	0.176	0.775	−0.283	−0.031
relaxing	0.247	0.739	−0.049	0.16
calm	−0.205	0.614	0.209	−0.092
spacious	−0.114	0.003	0.877	0.025
large	0.063	−0.393	0.683	0.005
bright	0.312	−0.58	0.633	0.024
vivid	0.217	−0.009	0.609	0.014
uniform	0.044	0.004	0.295	0.098
dazzling	0.175	−0.281	0.216	0.821
showy	−0.159	−0.359	0.467	0.549
moist	−0.304	0.188	−0.29	0.338
contribution ratio	19.34%	17.99%	13.64%	6.36%
cumulative contribution ratio	19.34%	37.33%	50.97%	57.33%

Table 4– Factor Loading of all the subjects

	Factor			
	1	2	3	4
soft	0.858	−0.072	0.191	0.039
gentle	0.797	0.025	0.217	0.071
warm	0.727	0.256	0.147	−0.070
calm	0.667	0.001	−0.129	0.174
relaxing	0.649	0.131	0.430	0.089
dazzling	−0.534	0.246	0.314	0.195
interesting	0.041	0.694	0.117	−0.078
lively	−0.053	0.688	0.272	0.226
unique	0.185	0.669	0.014	0.020
vivid	−0.020	0.642	−0.088	0.199
tasteful	0.011	0.631	0.487	−0.158
premium	0.090	0.578	0.401	0.062
showy	−0.288	0.560	0.076	0.326
relief	0.213	0.130	0.687	0.191
natural	0.266	0.031	0.601	0.160
cheerful	−0.015	0.169	0.490	0.185
spacious	0.119	0.106	0.150	0.791
large	−0.161	0.072	0.475	0.670
uniform	0.196	0.037	0.074	0.539
bright	−0.352	0.241	0.407	0.504
contribution ratio	17.50%	15.67%	11.99%	10.18%
cumulative contribution ratio	17.50%	33.16%	45.15%	55.33%

To find the common factors among European and Japanese subjects, we tried to run factor analysis on all the data. Table 4 shows the factor loading after rotation. As the contributions of top three factors do not have significant difference, the term “amenity” was extracted as the first factor, based on the adjectives “soft”, “gentle”, “warm”. We can set “personality” as the second factor.

Again, we calculate the factor score coefficient matrix, and derived factor score by multiplying the evaluated values. The factor scores of amenity and personality are shown in Figure 6. Red and orange bars indicate scores of OLEDs, and blue bars those of LEDs. Colour 1 and Colour 2 are indicated in the legend with 1 and 2, respectively.In both colour conditions, the amenity factors of OLEDs were higher than those of LEDs, which showed the same trends as the Experiment 1. On the other hand, we could not see any clear trends in personality factor score.

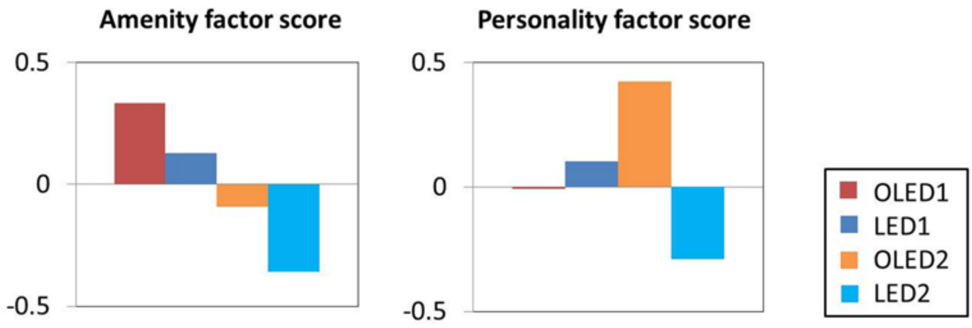

Figure 6 – Factor scores of amenity and personality from all the subjects

In order to find if there could be any region dependent factor, we calculated the amenity factor score from European and Japanese subjects separately. The scores are shown in Figure 7. Solid bars indicate the scores calculated from Japanese subjects, while the hatched bars indicate those from European subjects. Colours of the bars are the same with those of Figure 6.

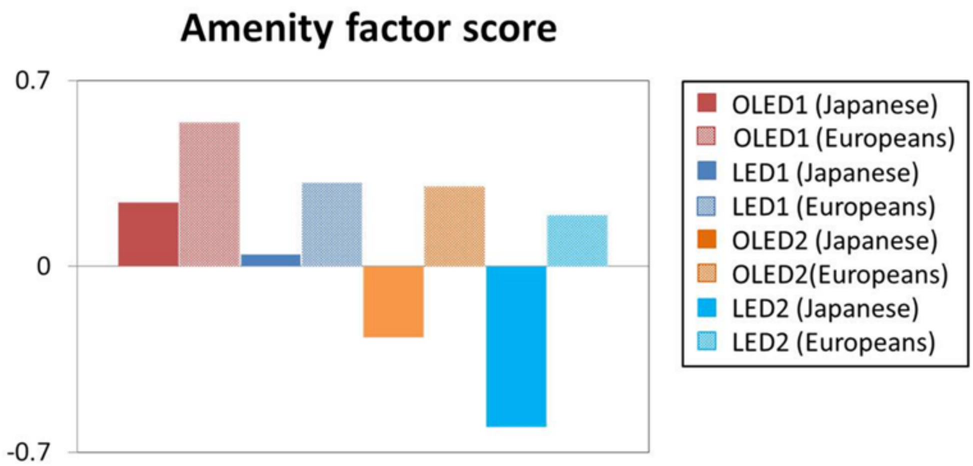

Figure 7 – Factor scores of amenity from Japanese and European subjects

From Figure 7, it is shown that both Japanese and Europeans show the same trends, even though the score of each illumination are different.

To explain these results, we assume that the spectral distribution and the color of the furnitures installed in the miniature room affected for some impressions. When we measured the chromaticities of some furnitures, the chromaticities obtained from OLEDs shifted towards reddish direction. Reddish appearance of the room could give impression of warm, soft higher, which led the amenity score of OLEDs higher.

4 Conclusions

Some significant differences in impression of the miniature room illuminated with OLED and LED were observed in common among all the subjects, regardless of their nationality. We expect that continued investigations will reveal further advantages of the OLED, and also the factors which controls the impression of the room. Also we need to conduct the experiment in the real environment.

Acknowledgement

We would like to thank Mr. Alexander Isphording for his great assistance for conducting our experiments in Aachen, Germany.

References

[1] Yokoyama, R., Yamauchi, Y. and Ishida, T. 2012. The effects of the luminescence area of lighting on the impression of space, CIE2012, 741-747

[2] Wake, T., Kikuchi, T., Takeichi, K., Kasama, M. and Kamisasa, H. 1977. The effects of illuminance, color temperature and color rendering index of light sources upon comfortable visual environments –in the case of office-, J. Light & Vis, Env.,1, No.2, 31-39

[3] Nakayama, K. Sato, M. and Inui, M. 2000. Study on affluent lighting in a Japanese living room: meanings of affluent lighting and elements concerned, J. Light & Vis. Env., 1, No.1, 59-65

[4] Osgood, C., Suci. G. and Tannenbaum,P.1957. The Measurement of Meaning. University of Illinois Press

OP02

SCALING APPEARANCE IN A ROOM ILLUMINATED BY LED SOURCES

Li. H.[1], Luo, M.R.[1,2*], Liu, X.Y.[1,3]
[1]State Key Laboratory of Modern Optical Instrumentation, Zhejiang University, Hangzhou, CHINA
[2] School of Design, University of Leeds, UK
3School of Science, Harbin Engineering University, Harbin, CHINA
*M.R.Luo@leeds.ac.uk

Abstract

This study investigated the whiteness of white lights close to the blackbody locus, and the appearance of a living room. Thirty observers took part in the experiment under 20 lighting conditions. A questionnaire was designed for observers to answer different questions in each condition. The present results confirm Rea and Freyssinier's finding, i.e. the whiter whites are located above and below the blackbody locus for above and below 4000K, respectively. For scaling the whiteness in a room, different assessment methods gave similar results. For scaling the appearance in a room, a brighter room will make the room to be less colourful, and more uniform. A cooler room will make the room to be brighter, but less colourful. However, it will make the objects in the room to appear more colourful.

Keywords: Room appearance, Category judgement method, Whiteness, Brightness, Colourfulness, Uniformity, Hue composition.

1 Introduction

The perception of white lights is a quality indicator of LED illumination. American standard, ANSI.377-2008 (2008) defined LED white sources in x y chromaticity coordinates. Figure 1 shows the region representing white sources. It is consisted of eight quadrangles corresponding to CCTs ranging from 2700K to 6500K. The blackbody locus goes through the quadrangles. In industry, people assume that the whitest whites are all located on the blackbody locus.

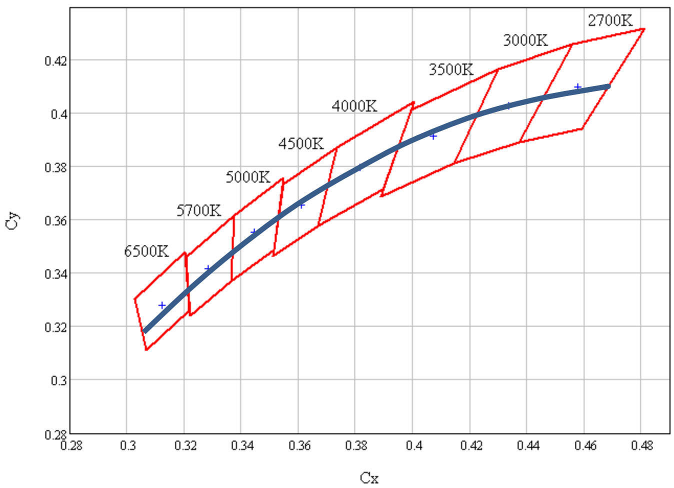

Figure 1 – The basic ANSI.377-2008 quadrangles (red) with centers. The blackbody locus (blue) goes through the centers of quadrangles.

However, Rea and Freyssinier (2013) showed that the whitest lights located above the blackbody locus when CCT>4000K, and located below the blackbody locus when CCT<4000K. Their results disagreed with the general perception that the points located on the blackbody locus were whiter than those depart from the locus. Figure 2 shows the lights used in their experiment in x y chromaticity diagram. Six groups of lights with different CCTs were selected: 2700K, 3000K, 3500K, 4100K, 5000K and 6500K. In each group, there were seven sources having different spectral power distributions (SPD). The seven SPDs distributed uniformly in the iso-colour temperature line in x y chromaticity diagram. Twenty Observers participated in the experiment. Observers were asked to judge the amount of hue in different white lights. Note that a pure white light should not be perceived any hue. The whitest lights in each of the six groups are connected as a locus of whites as shown in Figure 2. There are 4 loci obtained from different scaling methods. However, all of them agreed with each other well. The loci showed that when CCT>4000K, the whitest lights located above the blackbody locus, and when CCT<4000K the whitest lights located below the blackbody locus. Recently, they also built a visual model to predict the perceived tint in white lights (Rea, M. S., 2013).The results disagreed with the general perception that the blackbody locus represented the whitest lights. However, their experiment was conducted in a viewing box, which might not provide complete adaptation. Therefore, an experiment was designed and conducted in a real room to verify Rea and Freyssinier's finding.

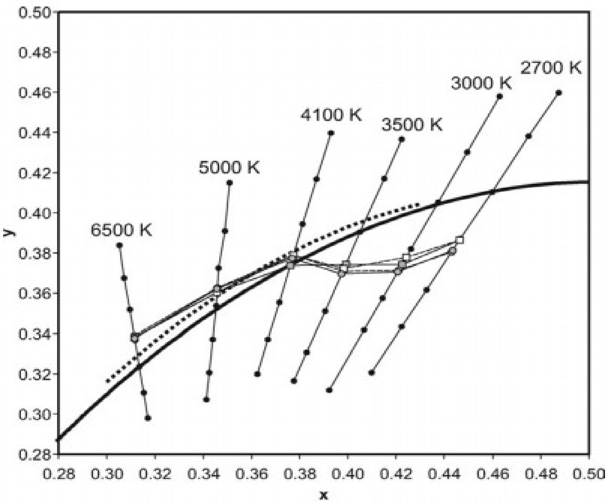

Figure 2 – The experimental lights in x y chromaticity diagram in Rea and Freyssinier's research. The smooth solid curve represents the blackbody locus. The smooth dotted curve represents the daylight. The curve connected with six points represents the whitest lights.

Colour appearance model such as CIECAM02 (CIE 159:2004) have been developed to predict the colour appearance correlates including brightness, lightness, colourfulness, chroma, saturation and hue. However, they can only predict colour patches under well defined viewing conditions such as illuminant, luminance of the adaption field, types of surround, luminance factor of the background. In lighting design, a colour appearance model for predicting room appearance is required. The typical correlates predicted should be spatial brightness, colourfulness, hue and uniformity. The present study will provide the experimental data in scaling the appearance of a real room and of some colour patches inside the room.

Overall, there are two goals in this study: one is to verify Rea and Freyssinier's results of white locus and the other is to assess colour appearance of a real room and colour patches.

2 Experimental

2.1 Observers

Thirty observers (23 males and 7 females) participated in the experiment. All had normal colour vision as confirmed by the Ishihara test. The mean age for all observers was 23 ranged from 18 to 33.

2.2 Experimental setup

The experiment was conducted in a room with a physical size of 5.4m (L) by 4.7m (W) by 2.7m (H) as shown in Figure 3. It was decorated as a living room with typical furniture such as sofa, tea table, TV and plants. The room was illuminated by a LED panel (3m by 1.5m) consisting about 1800 LEDs in 11 colours. By adjusting the proportions of 11 LEDs, the panel could produce lights with different chromaticity coordinates and SPDs.

Figure 3 – The experimental situation

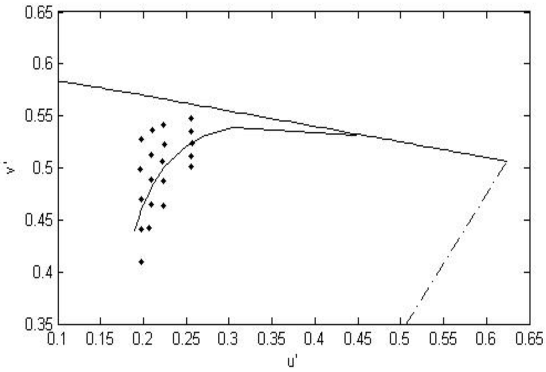

Figure – 4 the experimental lights in u' v' chromaticity diagram

2.3 Light settings

Four groups of test sources were generated by the LED panel and each group had 5 sources. Figure 4 shows the distribution of the light sources in u' v' chromaticity diagram. Lights in the same group had the same u' value but different v' values. Two adjacent lights had an equal interval in v' direction. The middle light source in each group is always close to the blackbody locus. All the lights had a luminance about 85 cd/m^2, when measure a reference white paper on top of the tea table in Figure 3. The height of the tea table was 45 cm. Most of the sources had a CRI value around 80 ranged from 75 to 90. Table 1 shows the lighting parameters for all lights. Figure 5 shows SPD of all the lights used in the present study.

Table 1 – the parameters of experimental lights

		x	Y	u'	v'	Y	CCT	CRI
Group1	1	0.3746	0.4449	0.2058	0.5261	87.39	4512	82.8
	2	0.3406	0.3848	0.2041	0.4971	86.55	5240	77.8
	3	0.3127	0.3319	0.202	0.4684	86.6	6475	82
	4	0.2903	0.2875	0.1984	0.4421	86.5.	9002	83.8
	5	0.2689	0.2474	0.1968	0.4129	86.45	---	83
Group2	1	0.4049	0.4596	0.215	0.5377	86.05	3961	82.4
	2	0.3729	0.407	0.2121	0.514	85.79	4385	83.8
	3	0.3467	0.3606	0.2156	0.4868	86.61	4970	81.4
	4	0.3234	0.3194	0.2136	0.4629	85.5	5969	84.6
	5	0.302	0.2858	0.2077	0.4423	85.68	7924	80.5
Group3	1	0.4283	0.4614	0.227	0.5418	85.82	3557	75
	2	0.4044	0.4195	0.2301	0.521	85.97	3733	84
	3	0.3807	0.3862	0.2257	0.5046	85.82	4059	82.3
	4	0.3626	0.3518	0.2303	0.4839	84.66	4365	77.6
	5	0.3398	0.3138	0.2279	0.4613	84.53	5096	82.2
Group4	1	0.4823	0.4597	0.2572	0 .5497	85.91	2760	66.6
	2	0.4634	0.431	0.2586	0.5357	86.39	2804	78.8
	3	0.4479	0.4058	0.2622	0.5219	86.62	2838	89
	4	0.4299	0.3821	0.2622	0.5081	86.09	2934	87
	5	0.416	0.3634	0.2547	0.5012	85.56	3024	74.7

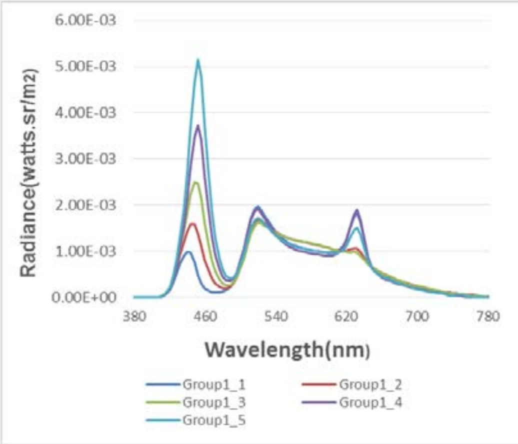

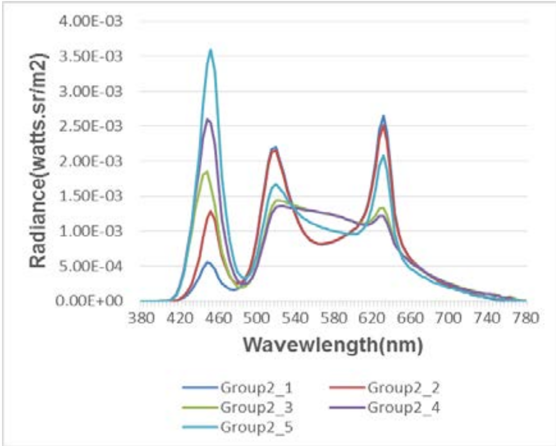

(a) **(b)**

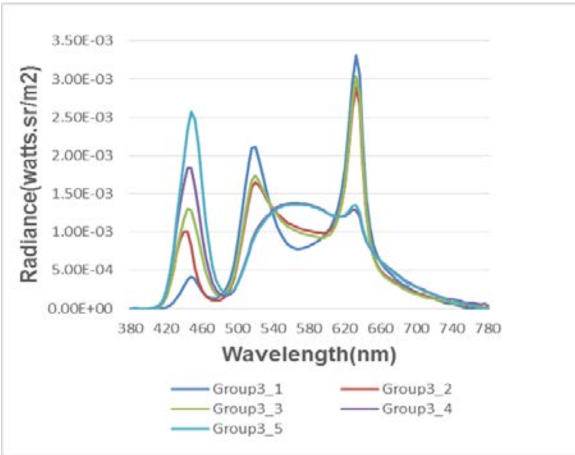

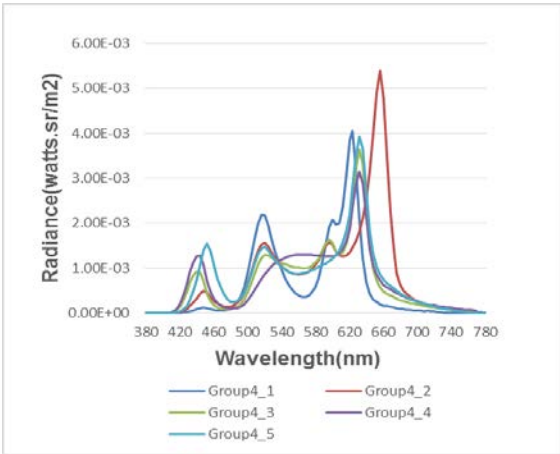

(c) **(d)**

Figure 5 – Spectral power distributions of the experimental lights of (a) Group1 (b) Group2 (c) Group3 (d) Group4.

2.4 Questionnaire

A questionnaire was designed to study the perception of white lights, the appearance of the room and the appearance of colour patches. For the appearance of the room, observers were asked to observe the whole room. For the appearance of colour patches, observers were asked to sit in the sofa and observe two colour charts on the tea table in 0/45 geometry (see Figure 6). For the perception of white lights, observers were asked to observe the white patch in the top right corner of the colour chart on the right as shown in Figure 6. Table 3 shows the questionnaire. The brightness, colourfulness and uniformity of the room and the brightness and colourfulness of the colour patches were evaluated. Four questions were designed to evaluate the whiteness of the white patch. They were ‘not white - white’, ‘white percentage’, ‘not prefer - prefer’ and hue composition. For the white percentage, 100 represents a pure white and 0 represents a chromatic colour with no trace of white. For the hue composition, observers were asked to select two of the unitary hues (red, green, yellow, and blue) and then estimated the proportion of the two. For example, orange is constituted by 50% red and 50% yellow. For other questions, the score were between ‘-3’ and ‘+3’, the extreme positive and negative scores respectively. Table 4 gives an example of all the categories for scaling ‘dark - bright’.

Figure 6 – The colour patches used in the experiment

Table 3 – The experiment questionnaire

(1) The perception of white lights	
1	not white - white
2	white percentage (0 -100)
3	not prefer - prefer (dislike-like)
4	hue composition
(2) The appearance of the room	
5	dark - bright
6	not colourful - colourful
7	not uniform - uniform
(3) The appearance of colour patches	
8	dark - bright
9	not colourful - colourful

Table 4– The relationship between the number and the feelings

-3	-2	-1	1	2	3
very dark	dark	a little dark	a little bright	bright	very bright

2.5 Procedure

A typical procedure for visual assessment is given below. Observers first read an instruction. Then all the sources were shown to make observers to have an overall understanding of experimental lights. It took thirty seconds to have an adaptation after changing lights. To avoid the influence of the white paper on the judgement, observers orally answered questions instead of filling the questionnaire. All the questions followed a random sequence. Observers could sit down or walked around freely when observe the whole room, but when assessing the colour patches, they must sit on the sofa with a 0/45 viewing geometry.

2.6 Summary

In summary, thirty observers participated in the experiment. Under each light, observers estimated 9 scales of the perception of white lights, the appearance of the room and the appearance of colour patches. Hence, the total estimation was 20 lights × 30 observers × 9 scales. It took about five minutes to evaluate all the questions under each light. And the total experiment remained two hours and was divided as two one-hour sessions.

3 Results and Discussion

The inter-observer variability was calculated using the correlation of variation (CV). For a perfect agreement, CV should be zero. A value of 20 means 20% disagreement. It had a mean value of 26% ranging from the most consistent observer (21%) to the least consistent observer 35%.

3.1 The perception of white lights

In the part of the perception of white lighting, the mean of the white amount of the white patch was calculated. The lights having high mean value were considered to be whiter. Figure 7 shows the results in a bubble chart in u'v' diagram. The size of bubble is related to the amount of white. A whiter white will have a larger bubble than a darker white. Its location corresponds to the u'v' coordinates of experimental lights.

The results showed that for the first three groups, the whitest lights are located close to the blackbody locus. But for the last group (2800K), the whitest one is located far away below the blackbody locus. In other words, when CCT>4000K, the whitest lights are above the blackbody locus and when CCT<4000K, the whitest lights locates below the blackbody locus. It can be seen that the present locus agrees well with that found by Rea and Freyssinier.

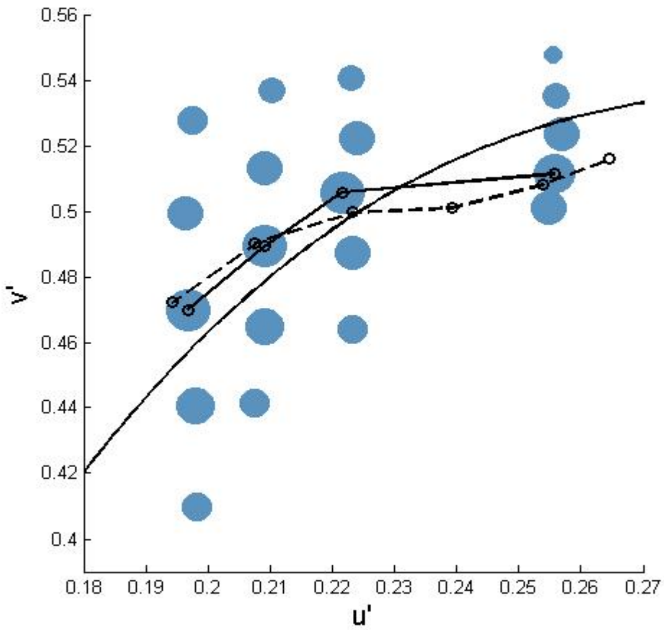

Figure 7 -The bubble chart plotted in u' v' chromaticity diagram. The solid and dotted loci represent the white locus in this study and in Rea and Freyssinier's study.

Another assessment task was to scale the preference of the white illumination. The correlation of determination (r-square) between the results of white amount and white preference was calculated. The high value of r-square, 0.83, illustrates that people prefer to like the whiter whites. Figure 7 shows the scatter plots of white amount and white preference. It can be seen that all points are located around the best fitted line with very small scattering of the data. This implies that a purer white will be more preferred by observers.

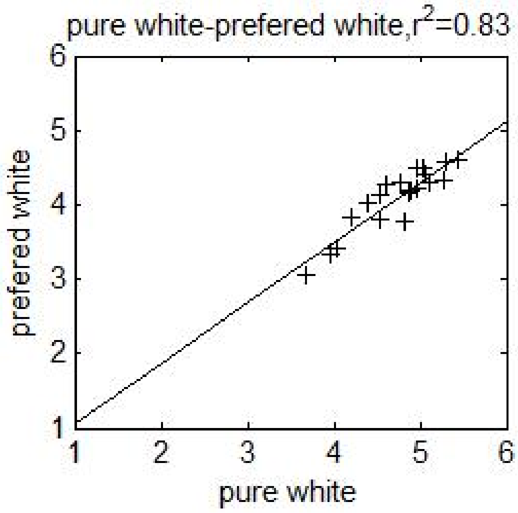

Figure 8 - The scatter plot of the visual results between white amount and white preference.

3.2 The Visual Effects

In order to understand the visual effect between visual attributes, the scatter diagrams were drawn, and the correlation of determination were also calculated. The results will be discussed in the following sessions.

3.2.1 The effect of the brightness of the room on the other attributes

Figure 9(a) shows the visual results of the dim-bright scale plotted against those of the cool–warm scale. It can be seen that people tend to feel cooler in a bright room. The two attributes are highly correlated with a r-square value of 0.65. Figure 9(b) shows the scatter plots of visual results between the dim-bright scale and the cool–warm scale. It can be seen that although all lights were produced by the same LED panel, people tend to feel more uniform in a brighter room.

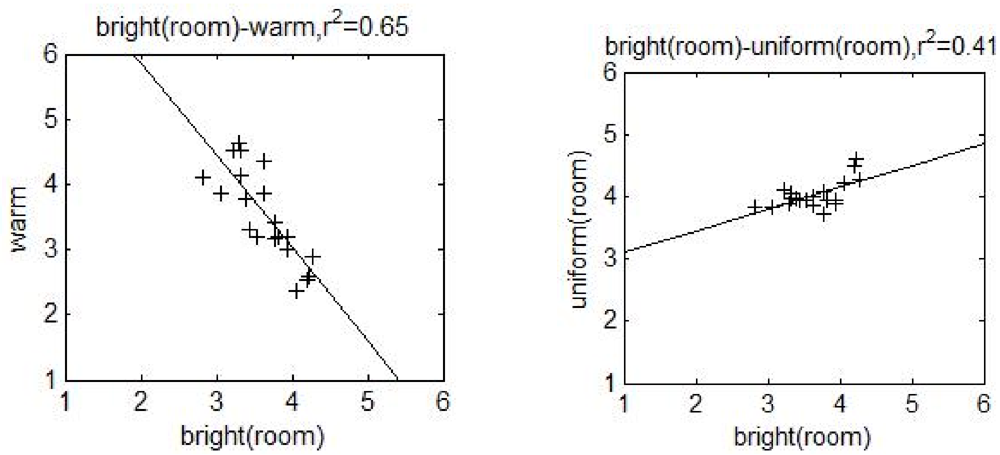

(a) (b)

Figure 9 - The plots of the visual results (a) between brightness of the room and 'warm-cool' (b) between brightness and uniformity in the room.

Figures 10a and 10b show the room brightness results plotted against the brightness and colourfulness of the colour patches on the charts, respectively. The results showed that an increase of room brightness will make colour patches appear brighter and more colourful. The high correlation of determination values (0.87 and 0.75) demonstrate that the brightness and colourfulness of the colour patches are closely correlated to the brightness of the room.

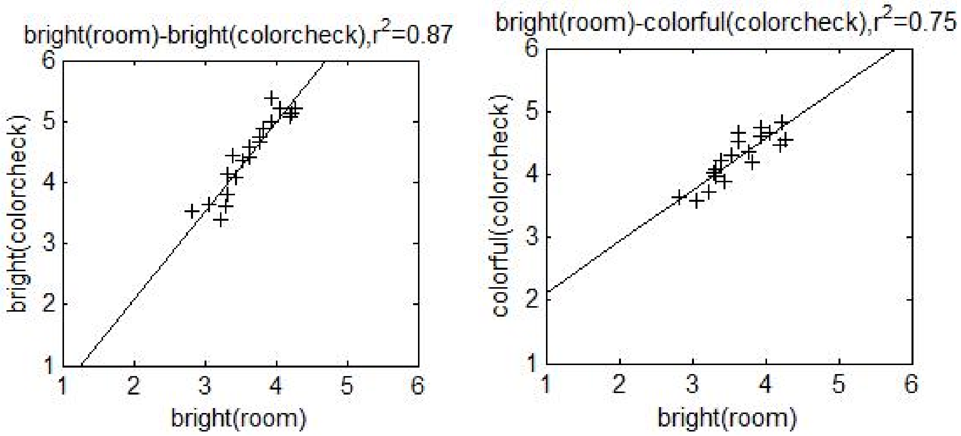

(a) (b)

Figure 10 - The plots of the visual results between brightness of the room and (a) brightness of the colour patches, and (b) colourfulness of the colour patches.

Figures 11a and 11b show the room brightness results plotted against the colourfulness results of the room and colour patches, respectively. It can be seen that the colourfulness results of the room and colour patches had an opposite effect, i.e. a brighter room would make the room less colourful and make the colour patches more colourful. For colour patches, this is well understood as the Hunt effect (Hunt., R. W. G., 1952), an increase of luminance to make sample more colourful. However, this led to a reduction of room colourfulness. This suggests that brighter lights would appear less tinted so that the room looks less colourful.

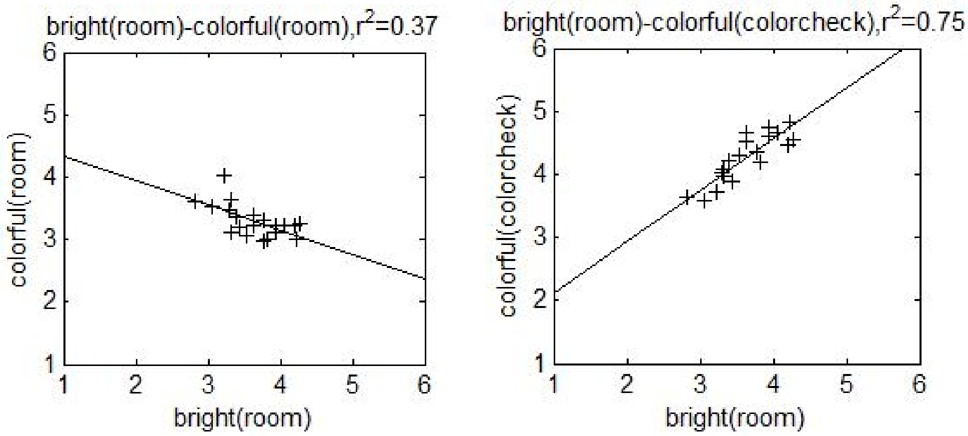

(a) (b)

Figure 11 - The scatter plots of the visual results between the room brightness and (a) room colourfulness, and (b) colourfulness of colour patches.

Figure 12 plots the visual results of room brightness and pure white of colour patch. The results showed a strong positive relationship. This implies that in a brighter room, the white patch becomes less tinted and appears whiter than in a darker room.

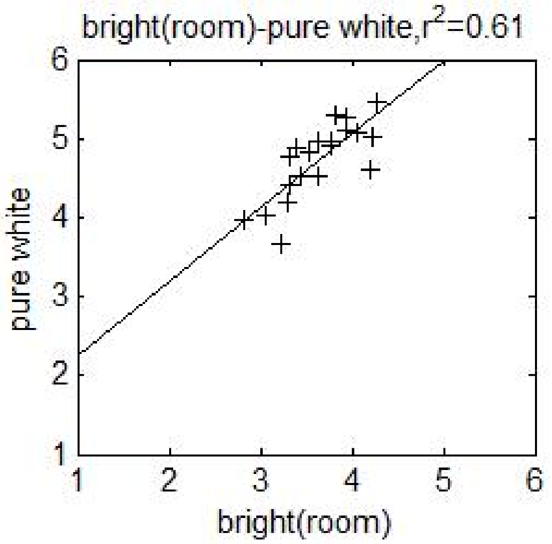

Figure 12 - The scatter plot of the visual results between the room brightness results and the white amount of the white patch.

3.2.2 The effect of the hue composition of lights on the appearance of the room

Each observer was also asked to scale the hue composition of each light. If it is a pure white light, there will be no trace of hue. Otherwise, each light will be scaled using the concept of unitary hues: red, yellow, green, and blue. The raw data of hue composition was first transformed to the values corresponding to 0, 100, 200 and 300, respectively. For example, a yellow-green colour has 40% of yellow and 60% of green. Then the result will be calculated as 40%*100+60%*200=160. The final results were analysed by calculating correlation of determination values with the other attributes of the appearance in the room. The correlation of determination values between hue composition and the warm extent, brightness, and colourfulness were 0.8,0.55 and 0.24, respectively. Figures 13a, 13b and 13c show the scatter plots of the hue results from 0 to 400. We can see that the lights having reddish hue (left of the diagrams) will make the room to appear warmer, darker, and slightly more colourful than the lights having bluish hue (right of the diagram).

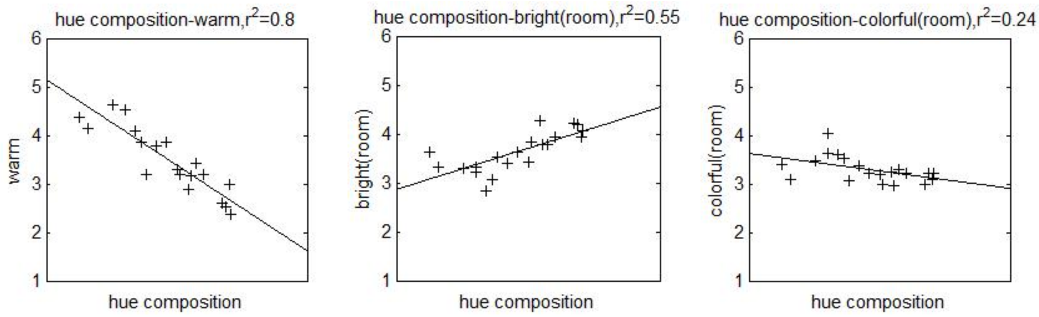

(a) (b) (c)

Figure 13 - The scatter plots of visual results between the hue composition of the light and a) the warm amount of the room, (b) the brightness of the room, and (c) the colourfulness of the room.

4 Conclusion

The line representing the perception of white lights locates above the locus when CCT>4000K and locates below the locus when CCT<4000K. The results verified Mark's conclusion.

People prefer the whiter lights to the tinted ones.

A brighter room seems to be cooler and more uniform, and make the colour patches to appear brighter, and the white patch to be whiter. On the contrary, a darker room looks warmer and less uniform, and make the colour patches to looks darker and the white patch to be more tinted.

A brighter room appears less colourful, but make colour patches to be more colourful.

The lights having reddish hue make the room to appear warmer, darker, and more colourful, and those with bluish hue will lead to opposite effects, making the room cooler, brighter, and less colourful.

References

ANSI. 2008. ANSI C78.377:2008. Specifications for the chromaticity of solid state lighting products.

Rea, M. S. and Freyssinier, J. P. 2013. White lighting, Colour Research and Application, 38(2), 82-92.

Rea, M. S. and Freyssinier, J. P. 2013. White lighting: A provisional model for predicting perceived tint in “white” illumination, Colour Research and Application, 0(0), 1-14.

CIE. 2004. CIE 159:2004. A colour appearance model for colour management systems: CIECAM02, Vienna.

Hunt., R. W. G. 1952. Light and Dark Adaptation and the Perception of Color, Optical Society of America, 42(3),190-192.

OP03

THE IMPACT OF THE LUMINANCE LEVELS AND COLOUR TEMPERATURE ON VIEWING FINE ART UNDER LED LIGHTING

Zhai, Q.Y.[1], Luo, M.R.[1,2*], Liu, X.Y.[1,3]
[1]State Key Laboratory of Modern Optical Instrumentation, Zhejiang University, Hangzhou, CHINA
[2]School of Design, University of Leeds, Leeds, UK
[3]School of Science, Harbin Engineering University, Harbin, CHINA
*M.R.Luo@leeds.ac.uk

Abstract

The aims of this study are to investigate suitable LED lighting conditions in viewing fine art paintings in museum environment and to verify the Kruithof's rule to define the pleasant zone in terms of the correlated colour temperature (CCT) and illuminance. The experiment was conducted in a room to simulate the exhibition of real paintings in museums. Twenty four observers of different genders and of different education backgrounds were invited to evaluate oil and gouache paintings under different illumination conditions. Each painting was assessed via 14 word pairs using the categorical judgment method. The results showed that illuminance had a larger impact than CCT on visual perception, and three factors dominate visual perceptions: Comfort, Vividness and Definition. The present results only partially agreed with the Kruithof's rule.

Keywords: Museum lighting, LED lighting, CCT, Illuminance, The Kruithof's rule

1 Introduction

The main missions for museums are presentation, conservation and education. The former two are in general competing with each other (Berns, 2011). For example, to achieve a high quality presentation requires a high visibility perception by applying higher luminance lighting. This could contain higher UV and IR components to damage the artefacts (Cuttle, 1996). So, a successful design of museum lighting should consider appearance, conservation and energy saving. LED lighting is perfectly suited for museum lighting because of its unique features, no UV and IR, and low energy consumption. Also, it is capable of adjusting its spectral power distribution (SPD), to enhance the aesthetics and atmosphere perception for viewing the artefacts. There have recently been large efforts to improve the colour rendering and visual performance on LED lighting. However, not much work has been done to investigate the optimal condition of the colour temperature and luminance levels in museums under modern lightings.

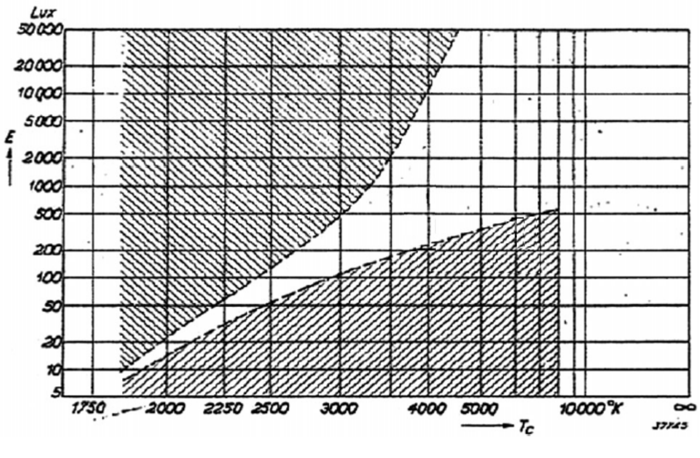

Figure 1 – Pleasing Area Figured by Kruithof (unshaded area).

Figure 1 shows the Kruithof's (1941) pleasing area between the two defined curves (see the unshaded area) by investigating incandescent lamps, daylight and luminescence. It clearly indicates the pleasing area to be a higher CCT illumination at a higher illuminance and a lower CCT illumination at a lower illuminance for general application. However, the zone has limited pleasing area below 200 lux as the maximum illuminance for museum lighting defined by the CIE (CIE 157:2004). Viénot et al (2009) conducted experiments using LED illuminations to verify the Kruithof's rule and they concluded that a higher CCT at a lower illuminance is unpleasant, but it is inconclusive that a higher CCT source will be judged as more pleasant than a lower CCT source at higher illuminance levels as suggested by Kruithof. Yoshizawa et al (2013) studied LED illumination according to the change of CCT, colour rendering index (CRI), and illuminances (up to 400lux) in two similar experiments. One was in a Mock-up room using reproductions of artworks and the other was in Morohashi Museum using original oil paintings. Their results showed that two factors driving visual perceptions for viewing oil paintings, visibility and texture. The parameter of CCT had a negative correlation with texture while illuminance had a positive correlation with both factors. Luo, H. et al (2013) also performed the experiment using engineering and art students to evaluate three types of art paintings under LED lightings. The results showed that all the 11 scales studied can be reduced to two factors, Visibility and Warmth.

This paper describes an experiment carrying out in the viewing environment close to real museums to study the impact of CCT and luminance on visual perception and to verify the Kruithof's rule.

2 Experimental

2.1 Overview

The experiment was conducted in a room refurbished close to the viewing conditions in museums. There were 12 phases of viewing conditions including 4 CCTs, 3 illuminance levels and 6 paintings. In total, 24 observers participated in the experiment. Fourteen scales were used to assess each painting associated with appearance and atmosphere perceptions.

2.2 Illuminations

Figure 2 shows the experimental situation for visual assessment against a white wall to simulate visual effect of an exhibition of paintings in a gallery. The viewing geometry of observer was carefully controlled by considering the size of painting to ensure a constant viewing angle.

Figure 2 – Experimental Situation

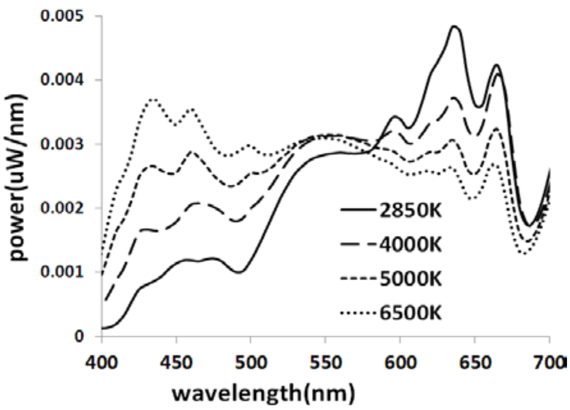

Figure 3 – SPDs of the Illuminations at 800lux

A Telelumen Light Replicator ® from Telelumen Limited Liability Company with 16-channel LEDs was used to illuminate the paintings. Table 1 shows the measured parameters of the 12 lighting conditions in the experiment. Each was defined at 4 CCTs (2850K, 4000K, 5000K and 6500K) and 3-level of illuminances (50lux, 200lux and 800lux). The lowest and highest CCTs match CIE standard illuminant A and D65 well. The lowest and highest illuminances corresponded to the upper limitation for the artefacts in a museum as defined byCIE 157 standard (2004). All sources had high CIE colour rendering index values (Ra>93) due to good match of SPD to the reference illuminants using the 16 LEDs. Figure 3 shows the SPDs of 800lux in experiment at 4 CCTs. The SPDs at 50lux and 200lux of the same CCT had difference only in the intensity of power and similar in the shape of SPD. So, they are not plotted here.

Table 1 – Parameters of the 12 Illuminations as Viewing Conditions

Target CCT (K)	Target illuminance (lux)	Measured CCT (K)	Measured illuminance (lux)	x	y	du'v'	CIE-Ra
2850	50	2860.3	49.3	0.4476	0.4039	0.0013	96.7
	200	2856.1	201.3	0.4457	0.4047	0.0008	93.5
	800	2836.5	803.8	0.4379	0.4092	0.0020	95.5
4000	50	3896.4	49.6	0.3838	0.3750	0.0018	93.6
	200	3958.6	200.9	0.3807	0.3728	0.0020	94.2
	800	3984.6	804.4	0.3824	0.3819	0.0018	95.4
5000	50	4992.5	48.9	0.3446	0.3466	0.0056	95.5
	200	5029.8	200.0	0.3437	0.3461	0.0055	95.9
	800	5099.7	803.8	0.3424	0.3501	0.0029	95.3
6500	50	6538.8	50.6	0.3131	0.3188	0.0055	96.9
	200	6498.7	202.9	0.3139	0.3195	0.0056	97.3
	800	6514.6	802.0	0.3135	0.3213	0.0044	96.4

2.3 Paintings and Observers

Table 2 shows the paintings used in the experiment including 4 oil paintings (1-4) and 2 gouache paintings (5-6) drawn by the art students from China Academy of Art. The smallest one is Painting 3 with a size of 300mm × 400mm while the largest one is Painting 6 with a size of 765mm × 523mm.

Table 2 – Paintings Used in the Experiment

		
1 Portrait of Woman	2 Portrait of Man	3 Wetland Scenery
		
4 Cold-tone Still-life	5 Cold-tone Still-life	6 Warm-tone Still-life

Twenty four Chinese observers aged 21 to 24 participated in the experiment. They all passed the Ishihara test as normal colour vision and are divided equally into two groups named

Scientists (students major in science or engineering) and Designers (students major in design or art) according to their education background. Also, in each group, there were 6 male and 6 female observers.

2.4 Scale

Fourteen word pairs in Chinese were used for evaluating each painting under different illumination conditions. Six of them were associated with appearance of the paintings (High-Contrast/Low-Contrast, Warm/Cool, Bright/Dark, Clear/Unclear, Colourful/Dull, Natural/Artificial), and the others were associated with atmosphere (High-Quality/Low-Quality, Active/Negative, Relaxed/Tense, Soft/Hard, Artistic/Business, Lively/Boring, Comfortable/Uncomfortable, Pleasant/Unpleasant). Most of them were chosen from the former researches by Viénot (2009), Yoshizawa (2013) and Vogels (2008). The latter scales were mainly design used to scale atmosphere. Each scale was evaluated using an 8-point categorical scale. Scores 1 to 4 stand for the extent of the perception. The positive word was recorded as a positive number while the negative word as a negative number. For example, Bright/Dark scale is judged from extremely bright (+4) to extremely dark (-4).

2.5 Arrangements

The categorical judgment was carried out by oral questioning and answering but not by hand writing questionnaires. This is to avoid the visual impact on chromatic adaption of staring at data sheet given on white paper. The experiment was designed for each observer to evaluate 5 of the 6 paintings respectively under 12 illuminations, while ensured all 6 observers in one subgroup (male scientist，male designer，female scientist，female designer) to evaluate each painting 5 times. In total, there were 20160 evaluation results. Each observer participated three sessions, about one hour each (three hours in total).

In the experiment, each observer was first tested for their colour vision by the Ishihara test and then listened to the instruction. In each session, observers went through four phases of illuminations. After 1-minute adaptation, they estimated each painting one by one using the 14 word pairs. They then proceeded into the next illumination with adaptation until the completion of all 12 phases in 3 sessions. The sequences of illuminations for each observer, of the paintings in each phase, and of the scales for each painting were all randomised in each session.

3 Results and Discussion

3.1 Inter Observer Variation

Inter- observer variability was investigated in terms of standard deviation. The experimental result had a mean standard deviation of 1.6 with the highest consistency for Relaxed/Tense while Artistic/Business the worst. The results of correlation coefficient between different gender and different education background showed that Artistic/Business and Natural/Artificial led to the most marked difference while some physical judgments such as Warm/Cool and Bright/Dark reach good consistency between different groups.

3.2 Impact of Illuminance and CCT

Figure 4 shows the impact of CCT on the visual results for most of the word pairs, while Figure 5 shows the illuminance affecting visual results. Only the positive word was used to represent a word pair in Figures 4 and 5. The higher the number is, the stronger the perception to the positive word. For most of the word pairs, score decreases when CCT increases while score increases when illuminance increases. When CCT increases to 5000K, Relaxed, Warm, Soft and Artistic perception reduce sharply and then reduce slowly to reach 5000K. However, the tendency of High Contrast, Bright and Clear perception appear a peak at 5000K indicating that CCT have no monotonic relationship with them. When illuminance increases, most scales increase sharply to 200lux and then increase slowly or flatten out while Soft and Artistic perceptions decrease. It is said that positive evaluations most come from appropriately brighter illumination, but too bright illumination make paintings lose softness and artistic value.

The score range in Figure 5 is obviously larger than Figure 4. It indicates that illuminance should have a larger impact than that of CCT. Illuminance shows a positive correlation to most scales and this influence obviously weakens when illuminance increases, especially higher than 200lux, while CCT shows negative correlation to most evaluation scales. The present result implies that a moderate illuminance level and low CCT could help build positive evaluation result in majority of indexes.

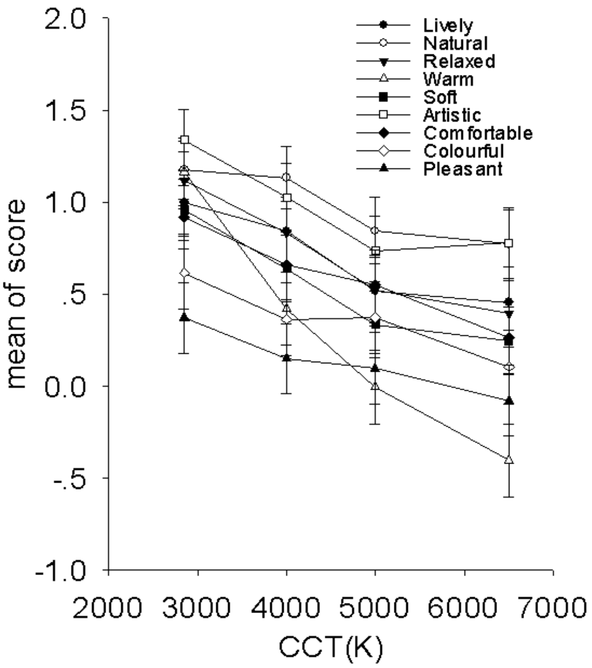

Figure 4 – Impact of CCT on the Word Pairs to Have Negative Effect

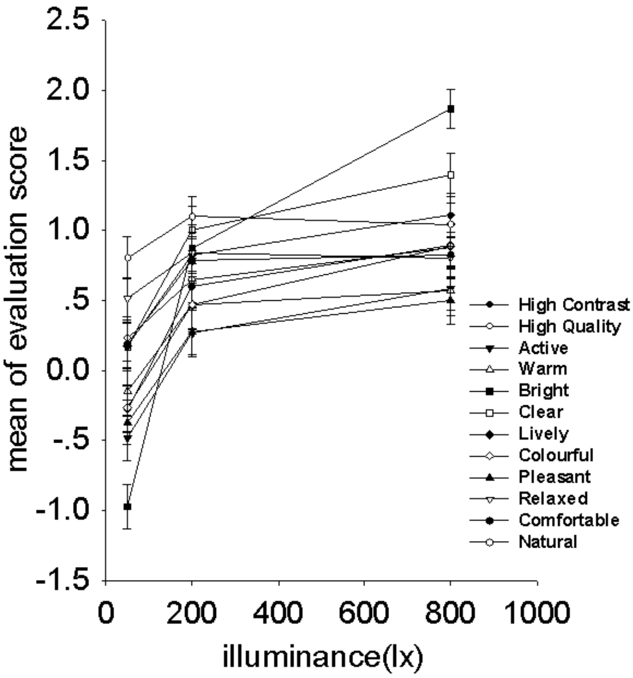

Figure 5 – Impact of Illuminance on the Word Pairs to Have Positive Effect

3.3 Factor Analysis and ANOVA

The goal of factor analysis is to reduce the large number of word pairs into fewer underlying dimensions. Principal component analysis and orthogonal rotation were the methods used in the factor analysis. Table 3 shows the result of factor analysis with total variance explained in brackets. The impressions of each factor are based on the members of words pairs in the raw data. Three main factors were found and they are named Comfort, Vividness and Definition. They explained about 60% of variance.

Table 3 – Rotated Component Matrix of Factor Analysis

Factor (68.292%)	1 (28.309%)	2 (17.731%)	3 (13.385%)
Meaning	Comfort	Vividness	Definition
Comfortable	.819	.213	.170
Natural	.775	-.045	.193
Pleasant	.772	.346	.101
Relaxed	.743	.118	-.084
Active	.684	.411	.098
Lively	.651	.383	.204
Soft	.469	.247	-.443
Colourful	.325	.771	.077
High Contrast	.069	.690	.423
Warm	.255	.668	-.142
Bright	.185	.593	.481
Clear	.110	.155	.837
High Quality	.455	.177	.633
Artistic	.046	-.031	.077

The Comfort factor includes half of the word pairs studied and represents the atmosphere perception of museum lighting, while Vividness and Definition are more related to appearance. Vividness is an important factor about contrast information of a painting such as higher colourful, higher contrast, brighter. Definition is associated with the word of visibility in a sense such as clearer and higher image quality. Another factor was Artistic and was on its own having a low rotation sum (8%).

The ANOVA result shows that illuminance had a large impact to all 14 word pairs and the 3 factors in Table 3, while CCT had a large impact to the 3 factors and most word pairs except High Contrast, High Quality, Bright and Clear. The ANOVA result testified that the illuminance had a larger impact than CCT on this viewing condition. Figure 6 and Figure 7 show the impact of CCT and illuminance respectively on the 3 factors. Each factor was independently affected by CCT and illuminance. It may be interpreted as that all the 3 factors increase when illuminance increases but Comfort perception would not increase when lighting is brighter than a critical level. When CCT increases, the perceptions of Comfort and Vividness decrease while Definition increases.

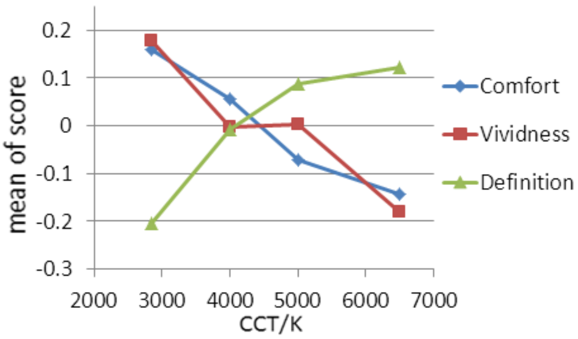

Figure 6 – Impact of CCT on the 3 Factors

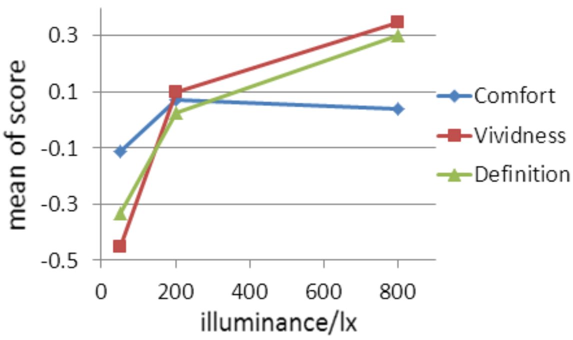

Figure 7 – Impact of Illuminance on the 3 Factors

3.4 About the Kruithof’s rule

Figure 8 shows the score of Pleasant/Unpleasant of different illuminance levels plotted against CCT. It can be seen that there is a reasonable agreement between two curves for 200lux and 800lux. They are much higher than the curve of 50lux. Scores decrease slightly when CCT is increased. This suggests that a lower CCT and appropriately a higher illuminance will be perceived as more comfortable. The comparison with the Kruithof’s rule (1941) led to a similar conclusion to Viénot’s statement (2013) that a higher CCT at a lower illuminance is unpleasant, and a higher CCT source will not be more pleasant than a lower CCT source at higher illuminance levels.

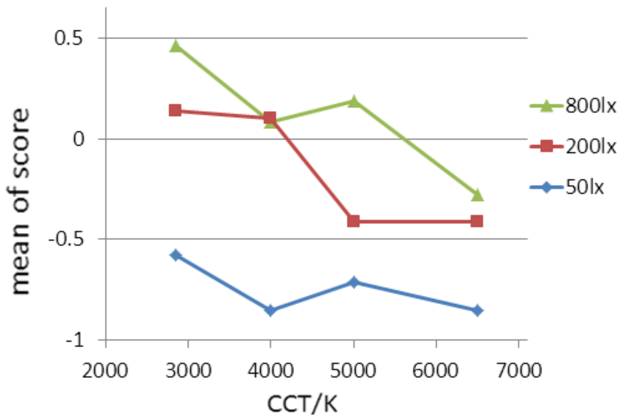

Figure 8 – Score of Pleasant/Unpleasant

Figure 9 shows the contours (solid curve) representing different degrees of Comfort perception from top left (most comfortable) towards the right (the less comfort) of Comfort factor. The Kruithof’s pleasing area is expressed between the two dotted curves. The squared dots in Figure 9 are the conditions studied in the present experiment.

The rectangular area in Figure 9 encompassed by 2850K-4000K and 200lux-800lux is considered to be a comfortable or pleasing zone for LED museum lighting both in the Kruithof’s and present results. However, the area of high illuminance and high CCT judged to be pleasing by Kruithof had very low scores on the contours in Figure 9. This implies that present results do not totally in accordance with the Kruithof’s rule. The Kruithof’s rule may not be suitable for LED museum lighting.

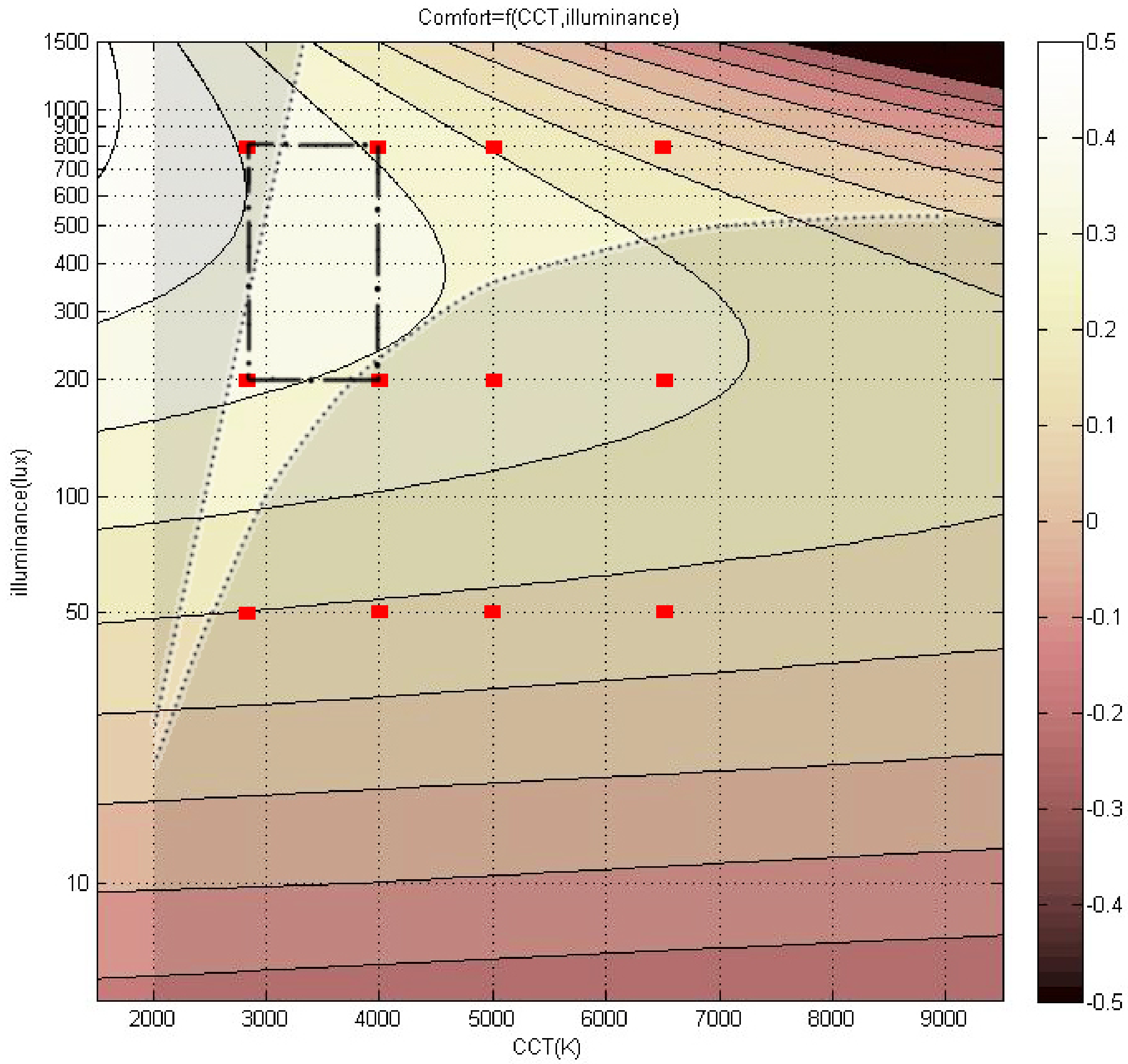

Figure 9 – The Contour Line (solid curve) of Factor Comfort Overlapping with Kruithof's Area (in dotted curve). Square dots are the condition of this experiment.

4 Conclusions

An experiment was carried out to investigate the impact of LED lighting parameters of CCT and illuminance on visual perceptions when viewing fine art paintings.

It was found that the illuminance had a larger overall impact than CCT on viewing museum paintings. An increase of illuminance will sharply raise the score for most of the scales from 50lux to 200 lux and tend to slow down when reach 800 lux except for Soft/Hard and Artistic/Business perception. CCT had a negative correlation to all the scales except contrast, brightness and clearness perceptions.

Factor analysis revealed that there are three dominating visual factors: Comfort (including scales of comfortable, natural, pleasant, relaxed, active, lively, soft), Vividness (colourful, high-contrast, warm, bright), and Definition (clear, high-quality). The three determine the quality of LED lighting for observing fine art paintings.

In consideration of the experimental conditions, illuminations with the CCT range of 2850K-4000K and a moderately illuminance range of 200lux-800lux is considered to be a comfortable or pleasing on museum LED lighting for paintings. The present results also had some disagreements with the Kruithof's rule.

References

Berns, R. S. 2011. Designing white-light LED lighting for the display of art: A feasibility study. Color Research & Application, 36(5), 324-334.

Cuttle, C. 1996. Damage to museum objects due to light exposure. Lighting Research and Technology, 28(1), 1-9.

Ezrati, J. J. 2013. Back on hundred year of technological development in the service of the museum lighting. CIE x038:2013, 16-22.

Szabó, F., Schanda, J. 2012. Solid state light sources in museum lighting - lighting reconstruction of the Sistine chapel in the Vatican. CIE x037:2012, 256-263.

Mou, X., Berns R. 2013 Design of LED for museum lighting application. CIE x038:2013, 758-766.

Thorseth, A., Corell, D.D Behrensdorff Poulsen, P., Dam-Hansen, C., Petersen, P.M. 2013. Dynamic miniature lighting system with low correlated colour temperature and high colour rendering index for museum lighting of fragile artefacts. CIE x038:2013, 777-782.

Kruithof, A. A. 1941. Tubular luminescence lamps for general illumination. Philips Technical Review.

CIE 2004. CIE 157:2004. Control of damage to museum objects by optical radiation. Vienna: CIE Central Bureau.

Viénot, F., Durand, M. L., & Mahler, E. 2009. Kruithof's rule revisited using LED illumination. Journal of Modern Optics, 56(13), 1433-1446.

Yoshizawa, N., Fujiwara, T., Miyashita, T. 2013. A Study on the appearance of paintings in the museum under violet and blue LED. CIE x038:2013, 374-381.

Luo, H. et al. 2013. Using LED technology to build up museum lighting environment, AIC Colour 2013, 8-12 July, 2013, Newcastle upon Tyne, UK, Volume 4. 1757-1760.

Vogels, I. 2008. Atmosphere metrics. In Probing Experience (pp.25-41). Springer Netherlands.

OP04

THE RELATION BETWEEN COMFORTABLE LIGHTING AND PERCEIVED GLARE

Zhang Jihuang[1], Tu Yan[*1], Lu Fan[1],Liu Lu[1], Wang Lili[1], Peng Sheng[2]
[1] Dong Fei R&D Centre, School of Electronic Science and Engineering, Southeast University,Nanjing, P.R. CHINA
[2] Philips Research China – Shanghai, P.R. CHINA
tuyan@seu.edu.cn

Abstract

In office lighting conditions, glare was considered as a vital issue for the comfort of lighting, but not the unique. In this paper, we describe an experiment that investigates the relation between perceived glare and comfortable lighting. The comfort of lighting and the perceived glare were evaluated at various luminance levels with subjective evaluation methodologies. The results indicate a significant influence of luminance level on perceived glare. The perceived glare increases with the logarithm of the luminance and the vertical illuminance at eye. There is a quadratic relation between rating on comfort and vertical illuminance at eye. A vertical illuminance at the eye in the range of 130lx to 340lx is considered comfortable for more than 70% of the people.

Keywords: perceived glare, comfort of lighting, vertical illuminance at eye, BCD (the border between comfort and discomfort).

1 Introduction

A comfortable lighting design is a comprehensive consideration of, a.o., perceived brightness, glare and light distribution. Within the lighting community, glare has been widely studied and it was considered as a vital issue for lighting design in offices. However, glare is just one factor of perceived comfort of lighting. There is more than only glare that determines comfortable lighting in e.g. offices, and to what extent glare that is not considered uncomfortable determines comfortable lighting is still unclear.

The Illuminating Engineering Society of North America (IESNA) defines glare as “the sensation produced by luminance within the visual field that is sufficiently greater than the luminance to which the eyes are adapted to cause annoyance, discomfort or loss in visual performance and visibility.”[1]. The CIE makes a distinction between Disability Glare, defined as “glare that impairs the vision of objects without necessarily causing discomfort”, and Discomfort Glare, defined as “glare that causes discomfort without necessarily impairing the vision of objects” [2]. This study mainly focuses on discomfort glare.

In this paper, we describe an experiment to investigate the relation between perceived glare and comfortable lighting, and try to understand that to what extent glare that is not considered uncomfortable determines comfortable lighting.

2 Experimental set-up

2.1 Experimental equipment

The experiment room was furnished as an office which is an 11.8m by 6.3m rectangular space with a 3.2m ceiling. The walls and ceiling of the room were painted white, and the floor was

* Address of the corresponding author: Yan Tu, School of Electronic Science and Engineering,Display R&D center, Southeast University, Nanjing, 210096, P.R.China; Email address: tuyan@seu.edu.cn; fax 86-25-83363222

covered with gray carpet to avoid reflections of the light. The windows in the south wall were sealed with opaque shades of a cream color. Fifteen LED luminaires were installed in the ceiling (see Fig.1).

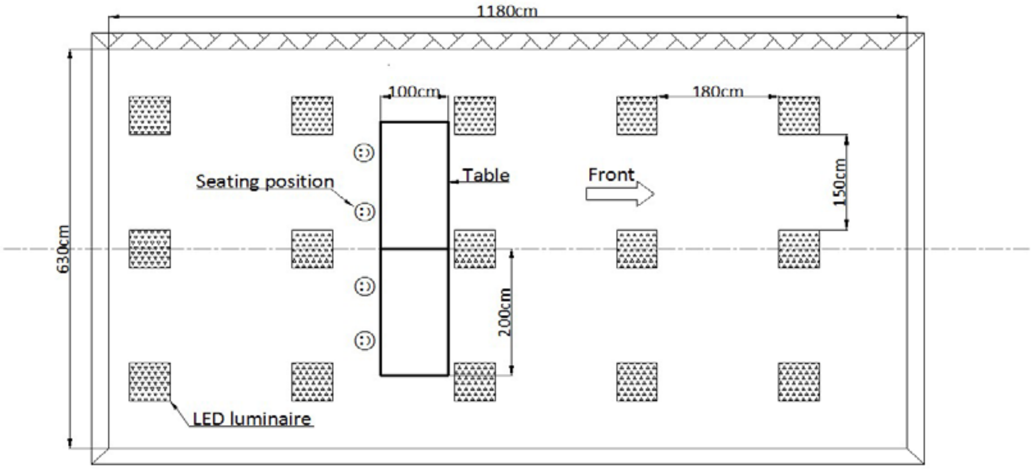

Figure 1 – Schematic overview of the experimental room showing the location of the luminaires and the subjects

The LED luminaire specifically built for the experiment by Philips Lighting consisted of 49 small LED source (each with a size of about 1 mm2 for the lighting area and a peak luminance as high as 560000 cd/m2 as measured with CS-200 Luminance & Color Meter). The LED sources were arranged in a 7 by 7 matrix configuration, with a pitch of 7 cm in both horizontal and vertical direction. The total luminaire area covered 60x60 cm2. The area of its exit window (red contour in Fig.2a) was 43×43 cm2. Further, a diffuser was used, see Fig.2b. The average luminance of the exit window of the LED luminaire was controlled by a DALI (Digital Addressable Lighting Interface) controller from 968cd/m2 to 3397cd/m2. The normalized luminance distribution over the exit window is shown in Fig.2c.

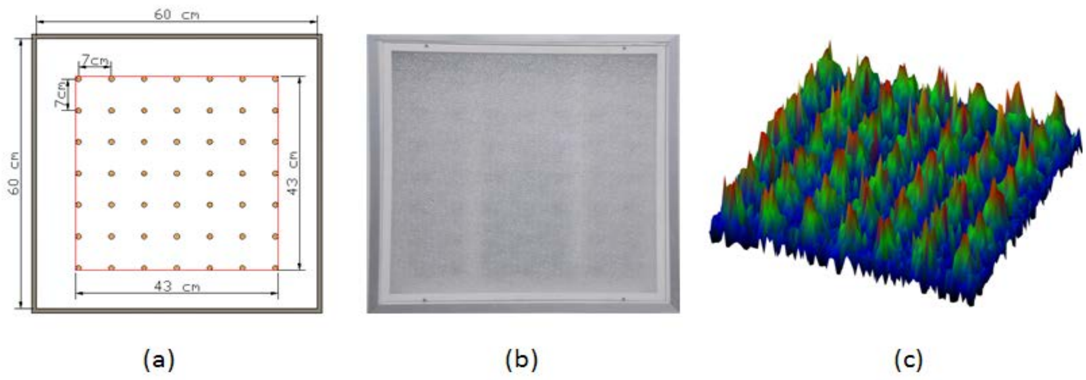

Figure 2 – Illustration of the tested LED luminaire; (a) diagram showing actual dimensions, (b) picture of the actual luminaire (c) normalized luminance distribution over the exit window

2.2 Experimental design and procedure

In order to evaluate the comfort of lighting and the perceived glare, we performed a between-subject experiment with the comfort of lighting and the perceived glare as the dependent variables, and the luminance level (i.e., five levels) as the independent variable.The experiment included two sessions depending on the two evaluation objects, i.e., the comfort of lighting and glare perception. In each session, the fifteen LED luminaires were switched on and five different luminance levels of the exit window were used: 2.99, 3.19, 3.33, 3.43 and 3.52

log10cd/m2, corresponding to 977cd/m2, 1548cd/m2, 2138cd/m2, 2691 cd/m2 and 3311 cd/m2 respectively. The exit window luminance of the luminaire was measured at the height of 1.15m under the tested luminaires with a LMK mobile CCD camera.

In each session, the subjects experienced all five luminance levels of the LED luminaires. Once a particular luminance level was selected, the subjects were asked to watch a short cartoon (1 minute) on the screen of the laptop in front of them so that they were forced to look in front of them and could experience the comfort of lighting and the perceived glare for a sufficient amount of time. The short cartoon shown on the screen had no sound and the viewing distance is 60cm, positioned such that the horizontal line of the sight of the participant was around the center of the screen. In addition, the subjects were explicitly requested to continue focusing on the screen in front of them without looking directly at the light source or the rest of the room when they scored perceived glare and the comfort of lighting. The evaluation forms were shown on the screen and the evaluations were performed with the keyboard. In the comfort of lighting evaluation session, subjects evaluated the comfort of the lighting with two different methodologies: once on a five-point rating scale (see Table 1), and once by indicating whether the lighting condition was comfortable or not. In the perceived glare evaluation session, subjects were asked to evaluate perceived glare also with two different methodologies: once on a seven-point rating scale which was the same as the scale used in the research of Boyce and Ngai [3, 4] (see Table 2), and once by indicating whether the perceived glare was comfortable or not. Both sessions of the experiment were performed by four groups of four subjects. The four subjects were seated by two large tables placed symmetrically in the experimental room.Each session contained five lighting conditions and lasted about 8 minutes.

Table 1 – Comfort of the lighting rating scale in the experiment

Category	Name
1	Comfortable
2	Hardly uncomfortable
3	Slightly uncomfortable
4	Uncomfortable
5	Extremely uncomfortable

Table 2 – Glare rating scale in the experiment

Category	Name
1	Imperceptible
2	Just perceptible
3	Noticeable
4	Just uncomfortable
5	Uncomfortable
6	Just intolerable
7	Intolerable

2.3 Participants

Thirty two paid subjects were recruited in the experiment, including 18 males and 14 females. They were divided into two equal groups for two sessions. The participants were mostly students of Southeast University in Nanjing (China). Their age varied between 21 and 25 years, with average age of 23 years.

3 Results

An analysis of variance (ANOVA) (with the software package SPSS version 16) was performed with the ratings on perceived glare as dependent variable, luminance level (5 levels) as fixed factors, and the subjects as a random factor. The result of the analysis is shown in Table 3. It illustrates a statistically significant influence of luminance ($p<0.001$) and subject ($p=0.022$) on perceived glare.

Table 3 – Result of the ANOVA on the perceived glare ratings; df refers to the the degree of freedom, F to the F-value, and Sig. to the significance level.

Factor	df	F	Sig.
Luminance	4	7.794	<0.001
Subject	15	2.155	0.022

Fig.3 shows the mean rating on perceived glare including the 95% confidence interval for every luminance level. It illustrates a linear increase in perceived glare with the logarithm of the luminance, as already reported in literature for direct glare [5, 6]. In addition, there is also a linear relation between perceived glare and vertical illuminance at eye; and the higher the vertical illuminance at eye is, the more the glare is perceived (see Fig.4).

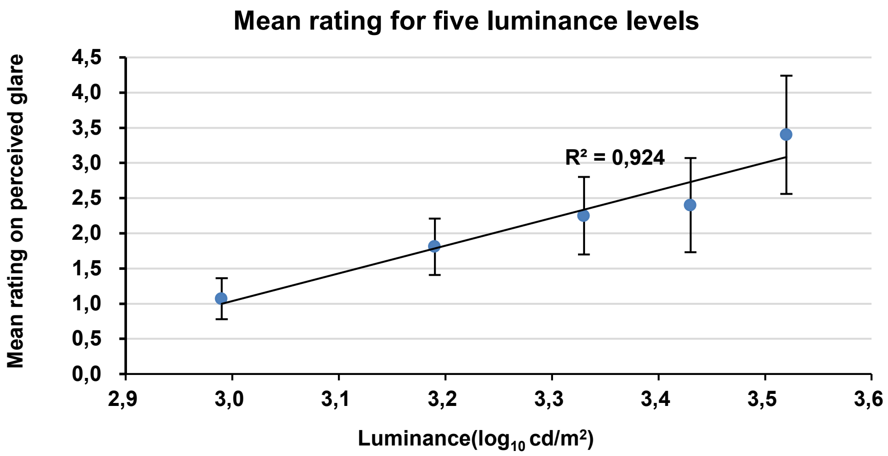

Figure 3 – Mean rating (on the seven-point scale) for five luminance levels; the error bars represent the 95% confidence interval of the mean.

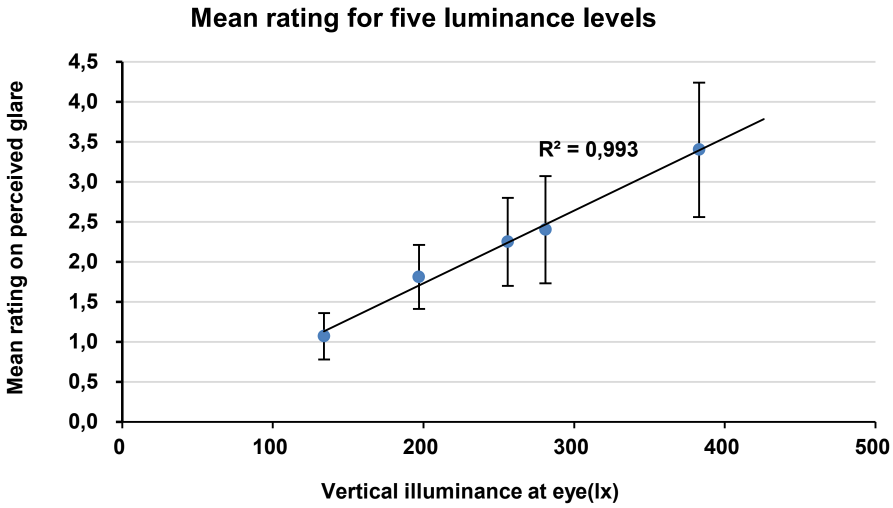

Figure 4 – Mean rating (on the seven-point scale) for five vertical illuminance levels at eye; the error bars represent the 95% confidence interval of the mean.

Fig.5 shows the percentage of people who responded “comfortable” to perceived glare in a given light setting plotted against the mean rating on perceived glare of that light setting. The five data points are separated for the five luminance levels used in the experiment. The negative slope of the fitted lines indicates that the percentage of subjects considering perceived glare comfortable decreases with an increase in mean rating on perceived glare, as expected. More specifically, the border of comfort-discomfort (BCD) defined as the glare level that 50% of the subjects experienced as uncomfortable corresponded to a glare rating of about 3 (on the seven-point scale). Hence, the BCD corresponded to the point where perceived glare became “noticeable”. This is consistent with our findings in a previous study [7].

Combining the BCD value with the linear relation between rating on perceived glare and vertical illuminance at the eye resulted in the conclusion that the border of discomfort glare occurs for a vertical illuminance at the eye higher than about 340lx.

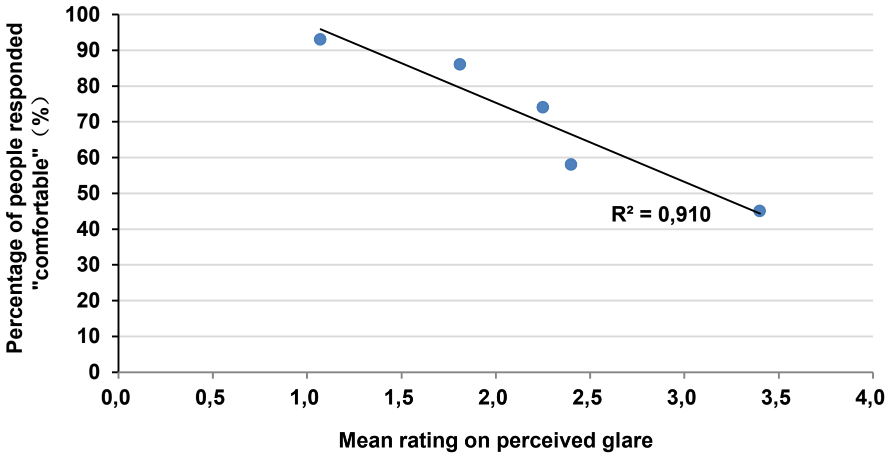

Figure 5 – Percentage of people saying that perceived glare is comfortable plotted against the mean rating on the seven-point scale.

Fig. 6 shows the relation between mean rating on comfort of lighting(left), percentage of people saying that light is comfortable(right) and the vertical illuminance at eye. It shows that there was a quadratic relation between rating on comfort and vertical illiminance at eye. At low illuminance levels lighting becomes more comfortable with increasing vertical illuminance at the eye, while above about 240lx vertical illuminance at the eye a decrease in the comfort of the light with increasing illuminance was found. Obviously, the increase in comfort with increasing vertical illuminance at eye is a consequence of improving visibility, whereas the decrease at higher illuminance is a consequence of perceived glare. In addition, there was also a quadratic relation between percentage of people that found the light comfortable and vertical illuminance at eye. By comparing the two quadratic relations, scores on the comfort scale referring to “comfort” and “hardly uncomfortable” at least 70% of the people indicated to find the light comfortable. So, the range of levels in vertical illuminance at the eye found to be comfortable (in the quadratic relation) was between 130 and 340 lux.

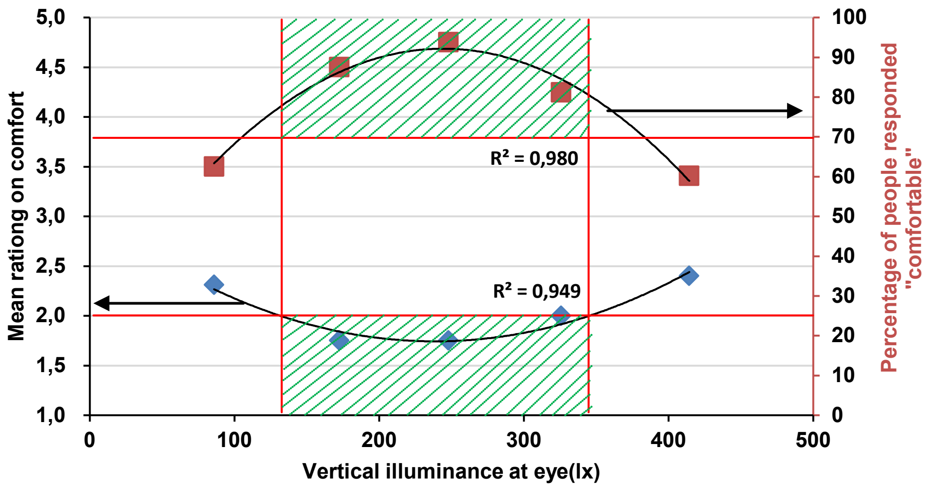

Figure 6 – Mean rating on comfort and percentage of people saying that light is comfortable plotted against the mean rating on the seven-point scale.

4 Conclusions

In this paper, a subjective experiment was performed to investigate the relation between perceived glare and comfortable lighting. The results of perceived glare evaluation indicate a significant influence of luminance level on perceived glare, furthermore, perceived glare increases with the logarithm of the luminance and the vertical illuminance at eye. The results of comfort of lighting illustrate that there is a quadratic relation between rating on comfort and vertical illuminance at eye, and a vertical illuminance at the eye in the range of 130lx to 340lx is considered comfortable for more than 70% of the people.

It should be noted that in this study, horizontal illuminance at the work plane and vertical illuminance at the eye were directly related. Further research needs to focus on different ratios between horizontal illuminance at the work plane and vertical illuminance at the eye and on possible other parameters affecting perceived glare and comfortable lighting.

Acknowledgements

The authors would like to thank Prof. Ingrid Heynderickx from Eindhoven Technical University for her valuable suggestions and discussions related to our work. Finally, we are grateful to the volunteers for participating in the subjective experiments.

References

1. IESNA Committee on Recommendations of Quality and Quantity of Illumination Report No.2 1972, Outline of a standard procedure for computing visual comfort ratings for interior lighting, J.IES 2, No. 3,328-344.
2. CIE 1987. International Lighting Vocabulary, Bureau Central de la Commission Electrotechnique International, J.CIE publication No. 17, 4.
3. NGAI, P. and BOYCE, P. 2000. The Effect of Overhead Glare on Visual Discomfort. Illuminating Eng. Soc., 29-38.
4. BOYCE, P.R., HUMTER, C.M., INCAN, C. 2003. Overhead Glare and Visual Discomfort. Illuminating Eng. Soc., 73-87.
5. Zhu X. et al. 2012. Perception Study of Discomfort Glare from LED Road Lighting. Proceedings of CIE 2012, “Lighting Quality and Energy Efficiency”, CIE x037:2012, OP38, 297-303.
6. Lee, Chang-Mo et al. 2007. A Study on the Estimation of Discomfort Glare for LED Luminaires. CIE 26th. D3 33-36.
7. Ling X. et al.2011. A study on overhead glare in office lighting conditions. Journal of SID. 888-898.

OP05

SOLID STATE LIGHTING IN OFFICES: IMPACT ON LIGHTING QUALITY AND ROOM APPEARANCE

Kirsch, R., Völker, S.
Berlin Institute of Technology, Department of Lighting Technology, Berlin, GERMANY
raphael.kirsch@tu-berlin.de

Abstract

This paper investigates minimum recommendations of EN 12464-1:2011 for office lighting and their validity for solid-state lighting. In a subject experiment the influence of different photometric criteria on visual appearance is examined. Results show that surrounding area illuminance is not an effective way to enhance visual lightness and room attractiveness. Effects of decreased work plane illuminances can be compensated by increased wall and ceiling illuminance. In accordance with other research, a luminance in a 40° horizontal band in the order of ~40 cd/m2 was found to correspond to a point where a space appears generally bright and attractive.

Keywords: Office Lighting, Lighting Quality, Standardisation, Visual Appearance, Background Luminance, Ambient Lighting

1 Introduction

International lighting standardisation for offices provides the lighting designer with illuminance values for different surfaces and areas in the space to support the occupants' work performance. Recent amendments of the European standard EN 12464-1 (2011) have included illuminance recommendations for vertical non-task areas for the first time. This marked an important step in the inclusion of lighting quality criteria affecting visual appearance of work places. However, as described in (Kirsch & Völker 2013a), new office-lighting installations based on LEDs enable lighting designs in a detailed way previously hardly achievable with conventional light sources. Driven by an increasing demand for energy savings designers often strive to meet standard recommendations as accurately as possible and - due to available LED-light sources - have the possibility to do so. Bearing a high potential to reduce energy consumption, it is highly important that lighting designers consider lighting quality criteria that go beyond a mere compliance with lighting standards.

Lighting quality criteria involve many different factors such as assistance with task performance, avoidance of visual fatigue and biological effects of light on humans. In the present study, recommendations derived from EN 12464-1 (2011) are examined regarding their impact on visual appearance.

2 Photometric Criteria Influencing Visual Appearance

Factors to determine visual appearance and lighting quality in office spaces have been investigated extensively over the last decades. Quality criteria include spectral aspects of lighting such as colour rendering and spectral power distribution as well as physiological and biological effects. In this work, two factors influencing the appearance of a space based on the distribution of light are examined:

- Ambient lighting
- Luminances in the visual field

Table 1 shows requirements for horizontal and vertical illuminances in a standard cell office according to EN 12464-1:2011.

Table 1 – Lighting requirements

	Task area	Surrounding area	Walls	Ceiling
Illuminance	500 lux	300 lux	75 lux	50 lux

2.1 Task area illuminance

A task area illuminance of 500 lux is recommended by most current standards such as IESNA RP-1 (2004) and EN 12464-1 (2011). Osterhaus (1993) states a decrease of task area illuminance recommendations by about 50% since 1973. General lighting levels, especially for computer visual display units, “will most likely be reduced further in exchange for a more efficient design […]” (Osterhaus 1993, p.10). This indicates that an illuminance level of 500 lux in the task area is generally accepted and thus, will be kept constant throughout this study.

2.2 Ambient Lighting and Surrounding Area Illuminance

There are several different definitions for ambient lighting. In North America and Asia ambient lighting usually refers to a general illumination of a space including illuminances on the work plane and the background. A similar quantity often used in Europe is the surrounding area illuminance, which is restricted to horizontal illuminances on the work plane. Lighting standardisation distinguishes between immediate surroundings of the task and a horizontal background area covering the rest of the space. In lighting design practice these two areas are often treated as one. Especially in Germany, other regulations for workplaces take precedence over EN 12464-1:2011. The surrounding are according to the ‘decree for workplaces’ covers a “spatial area adjacent to one or more task areas that is bounded by walls or circulation areas” (BAuA 2011, p.3). This area is to be lit with an average illuminance of 300 lux if task area illuminance is 500 lux. In lighting design practice, this area is usually reduced by a 0.5 m boundary along the walls. Thus, in this study surrounding area illuminaces restricted to the workplane less the task area and a 0.5 m boundary area along the walls are investigated.

According to EN 12464-1 the illuminance in the surrounding areas must be related to the task area illuminance to “provide adequate adaptation luminance” and “provide a well-balanced luminance distribution in the visual field”. Increasing the illuminance in the surrounding area will to some extend indeed result in higher luminances in the visual field. However, the visual effectiveness of illuminance on the work plane and floor is probably low due to low floor-lining reflectance of typically 20 %.

Research on preferred and accepted surrounding area illuminances is inconsistent to some degree. It is commonly agreed that the preferred surrounding area illuminance levels depend on the overall illuminance of the workplane including the task area (e.g. (Slater et al. 1993), (Tabuchi et al. 1995) or (Inoue 2010)). Thus, task to surrounding illuminance ratios are often reported rather than absolute values. Preferred ratios are usually in the area of 1:1 (e.g. (Bean & Hopkins 1980), (Tabuchi et al. 1995)). However, ratios can be much higher and still accepted. For a task area illuminance of 500 lux, surrounding area illuminance as low as 85 lux (task to surrounding illuminance ratio ≈ 6:1) can still be acceptable for a high percentage of office workers (Inoue 2010). Additionally, research by Flynn (1977), Loe (1991) and Houser (2002) indicates a lower correlation of apparent floor brightness with the overall brightness perception of a space than for other surfaces.

Since most research mentioned here does not clearly distinguish between horizontal and vertical illuminances it can be questioned if surrounding area illuminance as defined in this study was the only influencing variable. In some of the studies a change in work plane illuminance resulted in a change of wall illuminance (and therefore luminance), which may well have a greater effect on acceptance and preference than the specified illuminances.

Research question 1:

Does a reduction of surrounding area illuminance levels derived from office lighting standards (300 lux) have a negative effect on visual appearance?

2.3 Luminances in the Visual Field

Reflectances of room surfaces often used in lighting calculations are 70/50/20% for ceiling/walls/floor. Diffuse paint or wallpapers can be approximated by lambertian reflectance where luminances can be calculated from illuminances according to (1).

$$L = \rho \cdot \frac{E}{\pi} \tag{1}$$

where L is the luminance of a surface; E is the illuminance on this surface and ρ is the reflectance of this surface. Recommendations of 12464-1:2011 (table 1) will result in wall and ceiling luminances of about 11 to 12 cd/m^2.

Current research indicates that luminances three to four times higher than the recommendations lead to a enhanced visual appearance of the office space. Loe et al. (1994) identified a luminance of 30 cd/m^2 in a 40° horizontal band as the point where the appearance of an office changes from generally dim to generally bright. In a later study (Loe et al. 2000) this value was found to be more around 40 cd/m^2. These findings are in accordance with other research (e.g. (van Ooyen et al. 1987), (Veitch & Newsham 2000), (Newsham et al. 2005) and others). Many different researchers have investigated the strong effect of vertical luminances on room appearance. Davis and Ginthner (1990), Baron et al, (1992) and McCloughan et al. (1999) are examples of research where wall and ceiling luminances affected the apparent brightness of a space. Research by Marsden (1972), Fischer (1973) and Houser et al. (Houser et al. 2002) also indicates effects on the pleasantness and attractiveness of a space.

Thus it can be assumed that room surface illuminances recommended in EN 12464-1:2011 cannot always ensure sufficient lighting quality regarding the appearance of a space.

Research question 2:

How is room appearance affected by different background luminances when all other lighting parameters are held constant?

Research question 3:

Can a decreased surrounding area illuminance be compensated by increased background luminances?

3 Hypotheses:

To quantify the influence of different photometric criteria on visual appearance and to find answers to the research questions the following hypotheses are tested:

- Surrounding area illuminance has an effect on visual lightness, not on room attractiveness
- Background luminance has an effect on both, visual lightness and room attractiveness
- Background luminance is a more effective way to enhance visual appearance than illuminance based quantities

4 Methodology

4.1 Experimental set-up

The experiments are conducted in the office lighting simulator at the Department of Lighting Technology of the Technical University Berlin. Dimensions of the space are 5 m x 4 m x 2,8 m (LxWxH). Walls and ceiling are equipped with acrylic glass plains backlit by LED-panels to create the desired wall and ceiling luminances. Six projectors inside the ceiling provide work plane illuminance. The setup allows for a strict separation of illumination on vertical and horizontal surfaces. A more detailed description of the simulator can be found in (Kirsch & Völker 2013a) and (Kirsch & Völker 2013b).

4.2 Experimental Design and Independent Variables

The experiment was arranged as a 3x4 repeated measures design where all participants rated all scenes acting as their own control group. Within subject variables were three levels of surrounding area illuminance and four levels of wall/ceiling luminance..

Table 2 – Independent variables

Within Subject Factor	Range
Surrounding Area Illuminance	100 lux, 200 lux, 300 lux
Walls/Ceiling Luminance	11 cd/m^2, 30 cd/m^2, 50 cd/m^2, 75 cd/m^2

The range of the factors was determined using current research findings with respect to acceptable energy usage. Values for the surrounding area illuminance started at 100 lux representing findings of Inoue (2010) and corresponding to an accepted recommendation for circulation areas. 300 lux were suggested by Tabuchi et al. (1995) among others and are also the current standard recommendation for offices (e.g. CEN 2011).

11 cd/m2 were calculated from wall and ceiling illuminances recommended in (CEN 2011) according to formula (1). 75 cd/m2 represent a luminance that, due to energy consumption concerns, cannot realistically be exceeded in a real office.

4.3 Experimental Procedure

To avoid experimental biases influencing the participants' judgement, a number of countermeasures exemplary described in (Poulton 1989) were included in the experiment (e.g. anchor stimuli at the beginning of each session, randomised order of experiments, distraction scenes between rated scenes, continuous scales without digits).

Each scene was presented for a time period of five minutes before the questionnaire could be filled out. In this way, judgements based solely on first impressions are partly replaced by a 'sensory image' (CIE 2006). During the five-minute-period participants performed a simple office task including writing and reading.

4.4 Dependent Measures

The dependent measure was a short version of the room appearance judgement introduced by Veitch and Newsham (1998) consisting of eight of eight sematic differential scales. Using principal component analysis (PCA), the set of observations was converted into two components that were named 'visual lightness' and 'room attractiveness'.

4.5 Sample

64 naïve participants (age: 20-47 years, mean 26.47 years, median 26 years, sex: 46 % male, 54 % female) rated all scenes.

5 Results

A multivariate analysis of variance (MANOVA) was conducted to test for an overall difference of outcomes.

There was a significant main effect of surrounding area illuminance. Orthogonal planned comparisons revealed a significant effect of surrounding area illuminance on visual lightness but not on room attractiveness.

There was also a significant main effect of walls/ceiling luminance. Planned comparisons indicated an influence on both, visual lightness and room attractiveness. Effect sizes between luminance levels decreased with higher luminances.

There was no significant effect of the surrounding area illuminance*background luminance interaction.

The participants' subjective responses were examined further using boxplots (Figure 1 and Figure 2).

As can be seen clearly, changes in subjective responses due to changes in surrounding area illuminance, although existent, were by far smaller than for changes in wall and ceiling luminance. For all cases an increase in luminance by one factor level affected attractiveness and brightness appraisal in a way that the effect of decreased surrounding area illuminance was outbalanced.

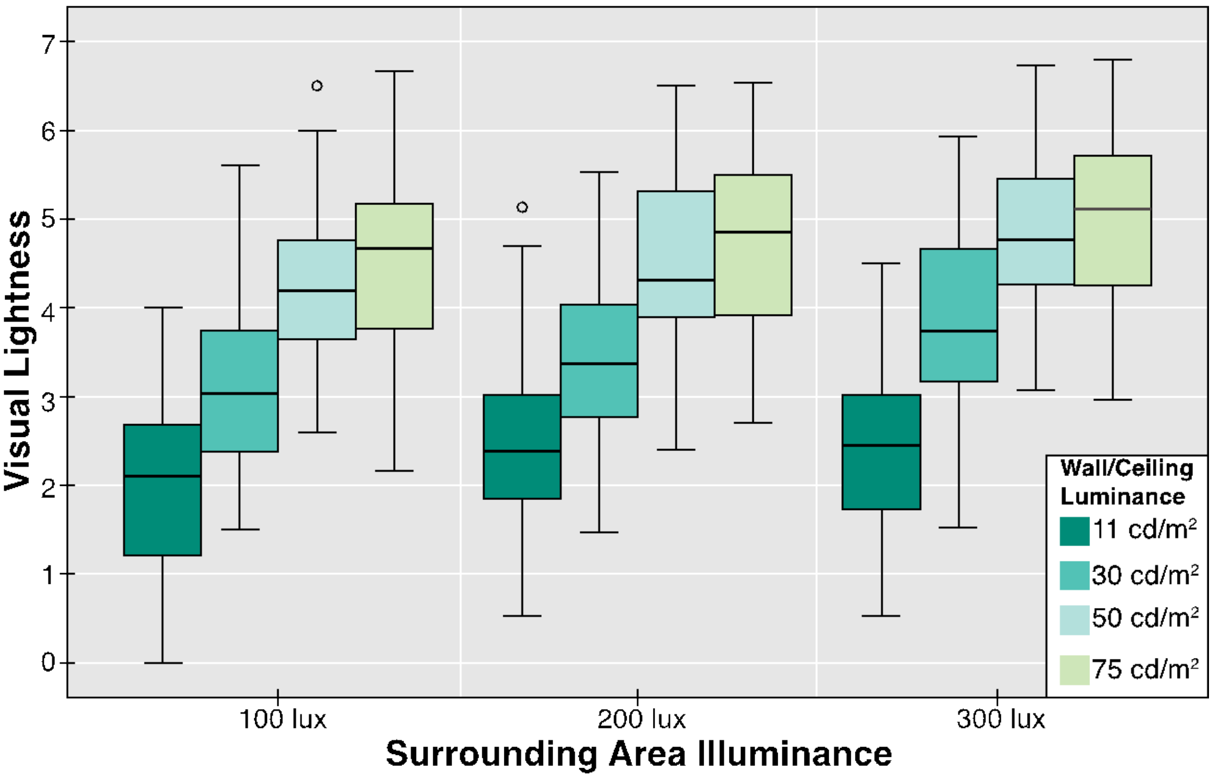

Figure 1 – Boxplot of 'visual lightness'

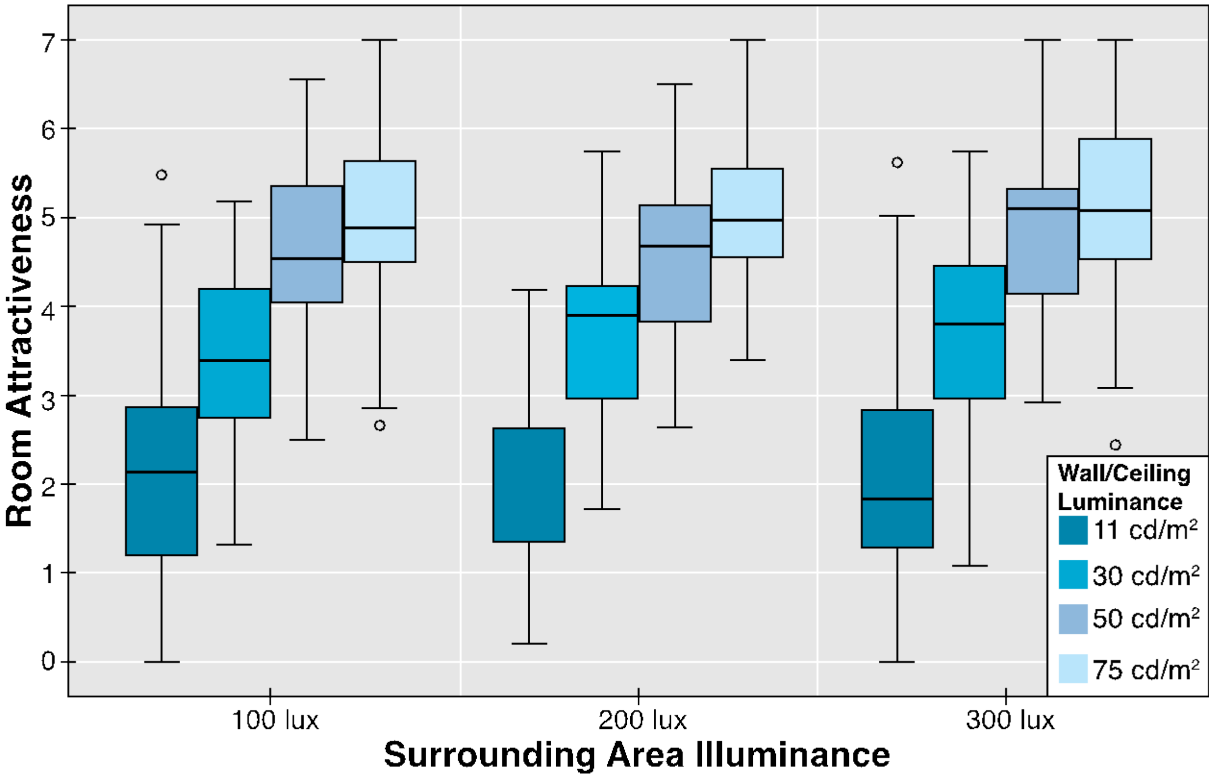

Figure 2 – Boxplot of 'visual attractiveness'

Mean subjective responses of visual lightness and room attractiveness showed a very good correlation with the average luminance in a 40° horizontal band first described by Loe (1994). Trends were estimated by regression with a power function, with $R^2 > 0.7$ for both components.

Although the semantic differential scales do not have a defined centre-point, they are often assumed to have an arbitrary zero-point that can be regarded as the point where general subjective responses change from one of the bipolar adjectives to the other ((van Ooyen et al. 1987), (Loe et al. 1994), (Völker 2006)). Thus, in this work around the zero point of the visual lightness scale subjective responses are assumed to change from generally dim to generally bright and for the room attractiveness scale from generally unattractive to generally attractive respectively.

The luminance value in the 40° horizontal band corresponding to the middle of the visual lightness scale was found to approximately 38.4 cd/m^2, for the room attractiveness scale to 38.8 cd/m^2. Thus, it can be assumed that for a room to appear generally bright and attractive, the average luminance in the 40° horizontal band should be in this order of magnitude.

6 Discussion and Conclusion

Results indicate a low visual effectiveness of surrounding area illuminance on visual appearance of the space. The pleasantness of the test laboratory was not affected withing the range of the independent variables used in this work. Visual lightness as a measure of brightness perception was affected significantly when increasing surrounding area illuminance from 300 lux to 100 lux. However, graphical evaluation showed only small changes of about ΔMedian≈0.3 rating units.

Changes in wall and ceiling luminance on the other hand led to significant enhancements of room appearance judgement. An increase from 11 cd/m2 to 30 cd/m2 alone more than counterbalanced the effect of decreased surrounding area illuminance.

For the space to appear generally attractive and bright, the derived luminance values in the order of ~40 cd/m2 are in good accordance with previous research (e.g. (van Ooyen et al. 1987), (Loe et al. 2000), (Veitch & Newsham 2000) and others).

The results show that regarding visual appearance the inclusion of wall and ceiling illuminances in current standards such as EN 12464-1 is a step in the right direction. The illumination of vertical surfaces has a great impact on perceived lighting quality and makes an office space appear brighter and more attractive. However, illuminance recommendations are not an adequate design approach since the characteristics of the observed surface are not included. The unproblematic applicability of illuminance values in lighting calculations is undisputed. Still, appropriate recommendations are minimum quantities of luminances since this is the measure actually seen and appraised by occupants. Moreover, the recommended values of 50 lux for the ceiling and 75 lux for the walls are to low regardless of the actual surface reflectance. If one assumes reflectances of 70%/50%/20% for ceiling/walls/floor, illuminance values should be in the order of 180 lux for the ceiling and 250 lux for the walls to achieve luminances of about 40 cd/m2 according to formula (1). This appears to lead to a major increase in energy consumption. However, if recommendations for the illuminance in surroundings can be decreased to 100 lux, the impact on energy consumption can be optimised. If energy efficiency can be re-defined as lighting quality per connected load, a lighting installation with brighter walls and lower surrounding area illuminance is more energy-efficient than an installation exactly meeting lighting standard recommendations.

References

Baron, R.A., Rea, M.S. & Daniels, S.G., 1992. Effects of indoor lighting (illuminance and spectral distribution) on the performance of cognitive tasks and interpersonal behaviors: The potential mediating role of positive affect. *Motivation and Emotion*, 16(1), pp.1–33.

BAuA, 2011. *ASR A3.4 Technische Regeln für Arbeitsstätten*,

Bean, A.R. & Hopkins, A.G., 1980. Task and background lighting. *Lighting Research and Technology*, 12(3), pp.135–139.

CEN, 2011. *EN 12464-1:2011: Lighting of work places — Part 1: Indoor work places*, Berlin, Germany: Beuth Verlag GmbH.

CIE, 2006. *CIE 175:2006: A FrameworkK for the Measurement of visual appearance*, Vienna, Austria.

Davis, R.G. & Ginthner, D.N., 1990. Correlated color temperature, illuminance level, and the Kruithof curve. *Journal of the Illuminating Engineering Society*, 19(1), pp.27–38.

Fischer, D., 1973. Comparison of some European interior lighting recommendations. *Lighting Research and Technology*, 5(4), pp.186–190.

Flynn, J.E., 1977. A study of the subjective responses to low energy and non-uniform lighting systems. *Lighting Design and Application*, 7, pp.167–179.

Houser, K.W. et al., 2002. The subjective response to linear fluorescent direct/indirect lighting systems. *Lighting Research and Technology*, 34(3), pp.243–260.

IESNA, 2004. *ANSI/IESNA RP-1-04: American National Standard Practice for Office Lighting*, New York, USA: Illuminating Engineering Society of North America.

Inoue, Y., 2010. Study on Illuminance Balance between Working Area and Ambient - Consideration of initial Lighting Condition, Visual Task performance and Impression of Lighting. In *Proceedings of the CIE 2010 Lighting Quality and Energy Efficiency, Vienna*. Vienna: CIE, pp. 776–782.

Kirsch, R. & Völker, S., 2013a. Lighting quality versus energy efficiency. In *Proceedings of CIE Centenary Conference „Towards a New Century of Light“*. Paris: CIE, pp. 895–902.

Kirsch, R. & Völker, S., 2013b. Neukonzipierter Lichtsimulator im Fachgebeit Lichttechnik an der Technischen Universität Berlin. *Licht*, 4, pp.68–70.

Loe, D.L., Mansfield, K.P. & Rowlands, E., 2000. A step in quantifying the appearance of a lit scene. *Lighting Research and Technology*, 32(4), pp.213–222.

Loe, D.L., Mansfield, K.P. & Rowlands, E., 1994. Appearance of lit environment and its relevance in lighting design: Experimental study. *Lighting Research and Technology*, 26(3), pp.119–133.

Loe, D.L., Mansfield, K.P. & Rowlands, E., 1991. Light patterns and their relevance to spatial appearance and the quality of the lit environment. In *Proceedings CIE 22nd session, Melbourne*. Vienna, Austria: CIE, pp. 41–44.

Marsden, A.M., 1972. What do we want from our lighting? *Lighting Research and Technology*, 4(3), pp.139–150.

McCloughan, C.L.B., Aspinall, P.A. & Webb, R.S., 1999. The impact of lighting on mood. *Lighting Research and Technology*, 31(3), pp.81–88.

Newsham, G.R. et al., 2005. Task lighting effects on office worker satisfaction and performance, and energy efficiency. *LEUKOS - Journal of Illuminating Engineering Society of North America*, 1(4), pp.7–26.

Van Ooyen, M.H.F., van de Weijgert, J.A.C. & Begemann, S.H.A., 1987. Preferred Luminances in Offices. *Journal of the Illuminating Engineering Society*, Summer, pp.152–156.

Osterhaus, W.K.E., 1993. Office lighting: a review of 80 years of standards and recommendations. In *Proceedings of the 1993 IEEE Industry Applications Society Annual Meeting,Toronto*. New York: IEEE, pp. 2365–2374.

Poulton, E.C., 1989. *Bias in quantifying judgements*, Lawrence Erlbaum Associates.

Slater, A.I., Perry, M.J. & Carter, D.J., 1993. Illuminance differences between desks: Limits of acceptability. *Lighting Research and Technology*, 25(2), pp.91–103.

Tabuchi, Y., Matsushima, K. & Nakamura, H., 1995. Preferred Illuminances on Surrounding Surfaces in Relation to Task Illuminance in Office Room Using Task-ambient Lighting. *Journal of Light & Visual Environment*, 19(1), pp.28–39.

Veitch, J.A. & Newsham, G.R., 1998. Lighting quality and energy-efficiency effects on task performance, mood, health, satisfaction and comfort. *Journal of the Illuminating Engineering Society*, 27(1), pp.107–129.

Veitch, J.A. & Newsham, G.R., 2000. Preferred luminous conditions in open-plan offices: research and practice recommendations. *Lighting Research and Technology*, 32(4), pp.199–212.

Völker, S., 2006. *Hell- und Kontrastempfindung - ein Beitrag zur Entwicklung von Zielfunktionen für die Auslegung von Kraftfahrzeug-Scheinwerfern*. University of Paderborn.

OP06

THE PREFERENCE OF COLOUR TEMPERATURE DEPENDING ON DAYLIGHT AND WEATHER

1st Tralau, B. [1], 2nd Schierz, C.
[1] Zumtobel Lighting GmbH, Dornbirn, AUSTRIA, [2] Technical University of Ilmenau, GERMANY
birthe.tralau@zumtobelgroup.com

Abstract

This paper focuses on the effect of colour temperature on humans depending on various parameters such as the time of day, the colour temperature of daylight or the weather. Therefore a field study in a school in Innsbruck was set up. The lighting was variable in colour temperature. Six different lighting scenarios following different automatisms have been evaluated from 36 pupils.

The study in general has shown that the choice of constant artificial light's colour temperature is a very individual choice and that there is no clear preference. For a dynamic variation of the colour temperature within the classroom, the direction of variation was the main important factor. A variation of the colour temperature of artificial light against the direction of colour temperature of daylight was not accepted at all.

Keywords: Colour Temperature, Daylight, Weather

1 Motivation

The increasing demand for energy efficiency represents a challenge for the development of lighting systems and lighting design. Besides increasing efficiency of luminaires and lamps, lighting control more often becomes used as to save additional energy. The biggest saving potential is the use of daylight. Therefore currently a lot of systems are used which measure daylight entry into the interior and add artificial light in order to get a constant light level is achieved.

But daylight has more advantages. From many studies which where conducted at office workplaces, we know that there is a strong preference for workplace illumination with daylight. On the one hand this involves the view out of a window and on the other hand the daylight usage itself. In addition to the continuous daylight spectrum, the continuing change in light colour, light direction and intensity ends up with very special characteristics.

Light, especially daylight, also fulfils a non-visual function. It acts as a Zeigeber for the human circadian rhythm. Responsible for that are receptors in the retina of the human eye, which react primarily on shorter wavelengths of the visual light spectrum. Many recent studies focus on the effect of light colour on well-being and performance of humans - and on long-term effects. As a result dynamic lighting controls for artificial light have been developed. The dynamics are often based on typical variations of natural daylight or on the human daily performance curve.

2 Problem

Both approaches for the use of lighting control of artificial light over time have different goals: the reduction of energy consumption on the one hand and the support of the human circadian rhythm on the other hand. Both have disadvantages from a user point of view and are rarely accepted by inhabitants.

One main reason for this rejection is usually the light colour.

Different colour combinations of artificial lighting with daylight, which vary depending on daytime or weather are the result of automated lighting control systems. Depending on room shape, window openings and seating position different colour adaptation states are the result, influencing the evaluation of light colour and light colour combinations. Changes in habitual lighting conditions affect the user perception of the current lighting situation.

The aim of this thesis is to investigate the effect of light colour and light colour combinations in terms of user acceptance, lighting quality and energy efficiency - and to implement the results in recommendations on control strategies for artificial light.

3 Theoretical Framework

Previous knowledge about the effect of light colour and light colour combination goes back to the '40s, when the fluorescent lamps were introduced. Starting with this new technology it was possible to choose light colours in interior rooms.

The question of how different colour temperatures should be used in practice was first investigated by Kruithof. He found that colour temperature - depending on illumination level - must be within certain limits, otherwise it will be felt unpleasant. Moreover, according to Kruithof a low illumination level goes hand in hand with a low colour temperature and a high illumination level with a high colour temperature. Until today the work of Kruithof is highly accepted among lighting designer.

But Kruithof's results are also subject to scientific criticism. For example Davis, Bodmann, Newsman, Cockram, Boyce and others could later present results that contradict the simple context of the "Kruithof curve". They revealed that for the preference of an illumination in the interior the lighting level is a more important factor than the light colour itself. Every lighting situation, but especially the light colour, is judged individually highly differentiated and emotionally.

In the project "Harmonious light" Fleischer investigated the effect of light condition changes on the human emotional state. In addition the study observed the effect of external factors such as weather, activity or the circadian rhythm corresponding to the daytime or the sky situation. Therefore the artificial light was varied in terms of direction (direct/indirect) as well as in terms of light colour. The findings suggest that dynamic lighting systems have a positive effect on people’s mood. Moreover, Aldworth and Bridges could proof that variable lighting options are usually preferred over static situations.

Essential requirements for control strategies of dynamic lighting systems have been formulated by Bieske. She conducted studies on the variation of light colour and its appropriate rate of change.

A study in flight cabins analyzed the relation between the colour temperature of light and the felt room temperature. They found out that the room temperature feels two degree less, for lighting with cooler colour temperatures and two degree more with warmwhite colour temperatures.

In the context of this work, fundamental studies on the effect of light colour and light colour variation can be expanded - to provide evidence of the effect of local light colour combinations depending on various parameters such as time of day, daylight and weather.

4 Method

This paper presents a field study which was set up in a school in Innsbruck (Austria).

In two different classrooms a new lighting system was installed (see table 1). The reference classroom has got a modern direct lighting with a static colour temperature of 4000K and a micro-prism optic (MPO) to reduce glare.

The second classroom has got a direct lighting, variable in colour temperature from 3000K to 6500K. In both classrooms the illuminance was controlled to 300lux to guarantee the same amount of light in both classrooms in order to focus the investigation on colour temperature.

Analysing the results from previous studies on light colour it can be expected that artificial light with colour temperature equally to the colour temperature of daylight will have the highest acceptance. Additionally the hypothesis was investigated that the preferred colour temperature of artificial light will change depending on the weather due to the feeling of room temperature, which is correlated to the colour temperature - e.g. for good (warm) weather situation a cold light colour is preferred and for bad (cold) weather situation a warm light colour is preferred.

Table 1 – Two classrooms in comparison

Classroom Standard Reference	Classroom LED Experimental
• Direct lighting with MPO optic • 4000K (fluorescent) • Illuminance constant (300lx) controlled depending on daylight	• Direct lighting with MPO optic • 3000K-6500K (LED) • Illuminance constant (300lx) controlled depending on daylight • Colour temperature following different automatisms (see investigation scenarios)

To proof the hypothesis six different lighting scenarios are examined within a field study (see table 2). The first three scenarios had a static colour temperature of 3000K, 4000K and 6500K (see figure 1). In another scenario the colour temperature of the artificial light followed exactly the colour temperature of the daylight measured on the roof top and in the room. The last two scenarios changed the colour temperature depending on the weather situation. For example in lighting scenario five: When the weather was good and a clear blue sky was present the colour temperature was 6500K. Scenario six was the inverse scenario to scenario five.

Table 2 – Lighting Scenarios of Classroom LED Experimental

nr	name	description
1	baseline	300lux, 4000K
2	warm white	300lux, 3000K
3	daylight white	300lux, 5800K
4	daylight	300lux, CCT daylight = CCT artificial light
5	weather	300lux, (sunny) = 6500K; (overcast) = 4000K; (rain) = 3000K
6	weather invers	300lux, (sunny) = 3000K; (overcast) = 4000K; (rain) = 6500K

For the automatism of the colour temperature within the experimental classroom, an algorithm was used which was developed by Tridonic for another scientific project (Austrian FFG-project K-Licht, subproject P01). Data from the daylight sensor on the roof was used. As a result of the sky illuminance and a shadiness vs. direct sun comparison the colour temperature could be calculated and used for the automatism of the lighting.

Within the field study six different lighting scenarios have been examined in dependence on the parameters day time, weather and daylight. Each scenario was presented for two weeks to the pupils and has been repeated. The order of the scenarios was randomised.

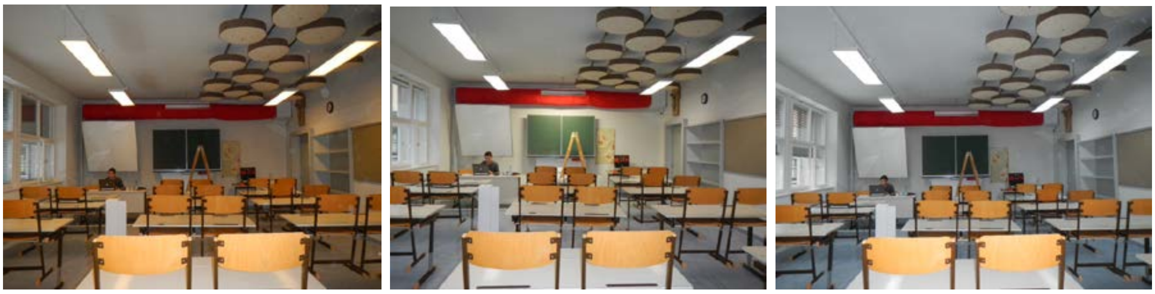

Figure 1 – Classroom with different colour temperatures (3000K, 4000K, 6500K)

The lighting scenarios were evaluated by two teachers and 36 pupils (18 pupils per classroom) aged between 12 and 14 years of both classrooms in particularly with regard to user acceptance and light.

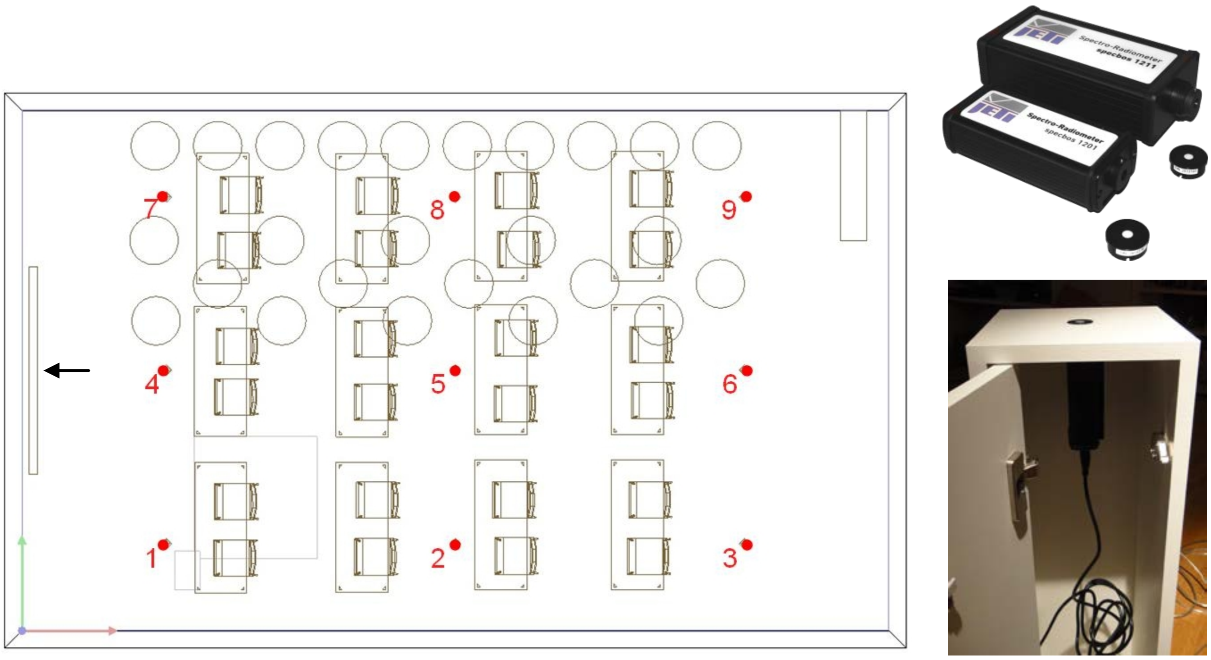

Figure 2 – Measurement equipment for horizontal and vertical illuminance, colour temperature and spectral distribution with a fixed installation of a JETI Specbos; 9 reference points

In order to come to a clear conclusion about the user acceptance subjective assessments of users were recorded and their behaviour was observed. For the subjective assessment an interactive voting system was used which guides the pupils playfully through the questionnaire. The survey was executed every second week on Wednesday. Additionally, the pupils had to fill out a mini diary every morning and afternoon, asking for their actual opinion and feeling.

The investigation started at the beginning of January 2013 and ended mid of July.

Next to the evaluation of lighting scenarios, the colour temperature, spectral distribution and the illuminance level was measured continuously (see figure 2).

Even so studies in schools are very difficult and the reliability of results is often questionable, an interesting result could be found within the investigation.

4. Results

For most of the scenarios and questions no significant difference could be found. The spread of the individual preferences and evaluations of lighting quality was very wide. This leads to the conclusion that the colour temperature of the artificial light in general is a very individual decision. And even if the light colour in the interior is not the preferred one, it is not distracting or disturbing the visual task and the situation can be accepted.

However, surprisingly there was one scenario which was not accepted at all (see figure 3). Due to the feeling of room temperature which is correlated to the colour temperature the expectation was that pupils would prefer cooler colour temperatures when the weather is good outside and the other way around. Contradictory to this hypothesis the scenario was refused from the subjects with statistical significance.

Additionally, most of the subjects have perceived the change of light colour and evaluated the change as disturbing. Also after the repetition of the scenario some weeks later, pupils refused the weather dependency. Since the other two dynamic lighting scenarios where evaluated more or less equally as the static once, the dynamic change of colour temperature itself cannot be the reason for the disapproval.

MEDIAN

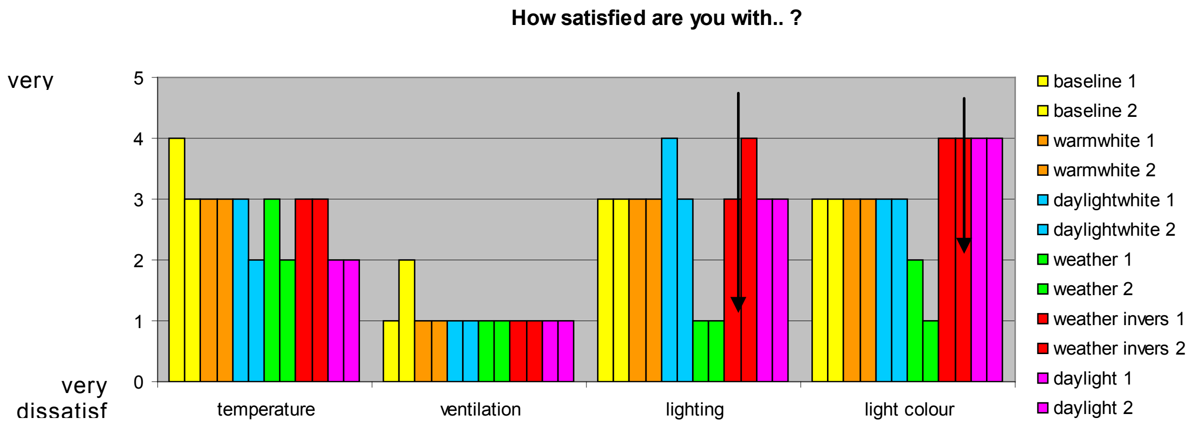

Figure 3 – "How satisfied are you with..?" (Median)

Comparing the change of colour temperature over the day measured in the room with the measurements of daylight on the roof, it can be concluded that for the weather depending scenario the direction of variation of colour temperature of both components is inverse (see figure 4).

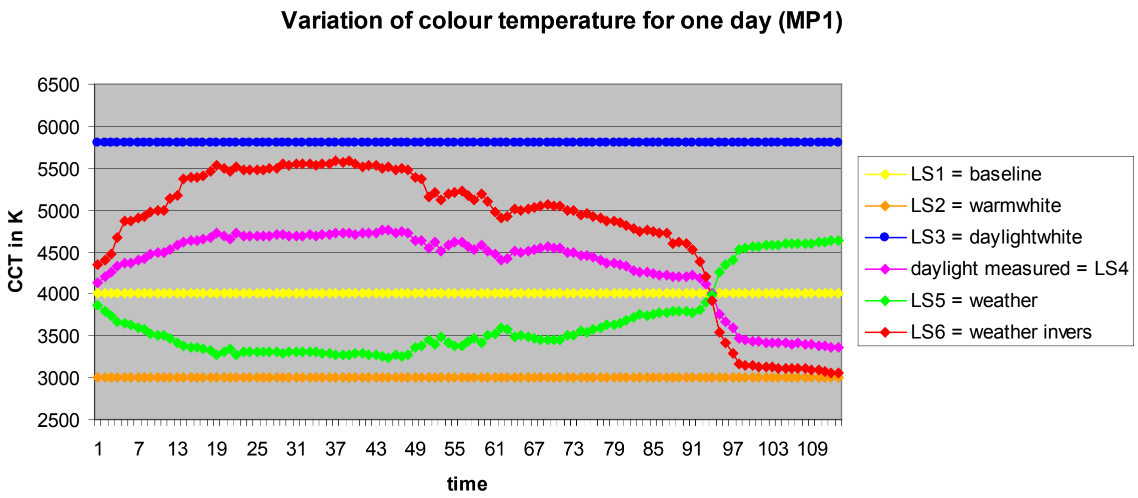

Figure 4 – Example for the variation of colour temperatures of lighting scenarios for one day at measurement point 1 in the room

This leads to the conclusion that when a dynamic colour temperature in the interior as well as a good daylight situation is present, the direction of the colour temperature's change of the artificial light is important. It is accepted to change the colour temperature in the same direction as the daylight. It doesn't matter if there is a difference of colour temperatures. It is not accepted to change the colour temperature against the colour temperature of daylight.

5 Outlook

The study has provided some insights for the use of different colour temperatures in combination with daylight. The next step will be to evaluate the effects of the change direction of the colour temperature in a laboratory.

References

Aldworth, R.C., Bridges, D.J. 1971: *Design for variety in lighting*. Light. Res. Technol. 3 (1), 8-23

Bieske, K 2009.: *Über die Wahrnehmung von Lichtfarbenänderungen zur Entwicklung dynamischer Beleuchtungssysteme*, Dissertation, Ilmenau: Technische Universität Ilmenau

Bodmann, H.W., Söllner, G., Voit,E. 1963: *Bewertung von Beleuchtungsniveaus bei verschiedenen Lichtarten*, CIE Compte Rendu, Quinzieme session, Wien, 502-509

Boyce, P. 2003: *Human Factors in Lighting*, Second Edition, CRC

Boyce, P.; Veitch, J.; Newsham, G.; CC, J.; Heerwagen, J.; Myer, M. & Hunter, C. 2006: *Lighting quality and office work: two field simulation experiments.* Lighting Research Technology, 38,3, 191-223

Boyce, P.R., Hunter, C.M., Carter, C.B. 2002: *Perception of full- spectrum, polarized lighting*, Journal of the Illuminating Engineering Society, 31, 119-135

Brainard, G. C. & Hanifin, J. P. 2004: *The effects of light on human health and behavior: Relevance to architectural lighting*. Light and Health: non-visual effects

Cockram, A.H., Collins, J.B., Langdon, F.J.: *A study of user preference for fluorescent lamp colours for daytime and night- time lighting*, Light. Res. Technol., 2, 249-256

Davis, R.G., Ginthner, D. 1990: *Correlated Colour Temperature, Illuminance level and Kruithof curve*, Journal of the Illuminating Engineering Society

Fleischer, S. 2001: *Die psychologische Wirkung veränderlicher Kunstlichtsituationen auf den Menschen*. Dissertation. Zürich: Eidgenössische Technische Hochschule Zürich, 125ff.

Fleischer, S., Krueger, H., Schierz, Ch.: *Effect of brightness distribution and light colours on office staff. Results of the "Lighting Harmony" project*. Proceedings of Lux Europa 2001, the 19th European Lighting Conference (18.-20. June 2001) Reykjavik, Island, P76-80.

Knoop, M.; Tenner, A. & Schriek, M. 2008: *Energieeffizienz und erhöhte Akzeptanz von Lichtlösungen mit nichtvisueller Wirkung*. Tagungsband Licht2008, 512-518

Kruithof, A.A. 1941: *Röhrenlampen mit Leuchtstoffe für allgemeine Beleuchtungszwecke*, Philips Technische Rundschaus Nr.3, 65-73

Lam, W.M.C. 1992: *Perception & Lighting as Formgivers for Architecture*

Lang, D. & Fassian, M. 2007: *Planungsempfehlungen für biologisch effiziente Beleuchtung*. Licht und Lebensqualität

Marggraf-Micheel, C., Winzen, J., Albers, F. 2011: Klimaempfinden und Komfort in der Flugzeugkabine moderiert durch farbiges Licht?! – Ergebnisse einer Studie aus dem Projekt Likab, DGLR 20122

Newsham G., Veitch J. 2001: *Lighting quality recommendations for VDT offices: a new method of derivation*, Light. Res. Technol., 33, 97-116

Pickelein, A. Polle, D.: *Beeinflussung des Wohlbefindens am Büroarbeitsplatz durch Variation von Lichtfarb- und Leuchtdichteverteilung.* DIAL

Rea, M. S.; Bullough, J. D.; Bierman, A. & Figueiro, M. G. 2006: *Implications for white light sources of different colour temperatures.* 2nd CIE Expert Symposium on „Lighting and Health“

Thapan, K.; Arendt, J. & Skene, D. J. 2001: *An action spectrum for melatonin suppression: evidence for a novel non-rod, non-cone photoreceptor system in humans.* Journal of Physiology, 535.1, 261-267

van Bommel, W. 2006: *Dynamic Lighting at work - Both in level and colour*. 2nd CIE Expert Symposium on „Lighting and Health“

Veitch, J.; Newsham, G.; PR, B. & Jones, C. 2008: *Lighting appraisal, wellbeing and performance in open-plan offices: A linked mechanism approach.* Lighting Research Technology, 40, 133-151

Wald, A. 1953:*Praktische Untersuchung der Wirkung von Leuchtdichte und Lichtfarbe auf den Menschen*, Lichttechnik Nr.6, 183-186

OP07

ATRAPALUZ: DAYLIGHT SYSTEM TO INTERVENE SPACES AND PERCEPTION

Wolff, C. [1]**,** Silva, R. [1], Letelier, S. [1], Oteiza, P. [2]
[1] Universidad de Chile, Santiago, CHILE, [2] UPM, ETSAM, Madrid, SPAIN
momwolff@uchile.cl, bekysilva@uchile.cl

Abstract

Atrapaluz is proposed as a sustainable natural lighting system to induce patrimonial buildings reuse, looking for their better environmental, social and economic performance. However, it can be useful in any blind or dark area of human habitat, for perceptual, aesthetic and ergonomic improvement. It was tested as a prototype system (patented in Chile) and it is in process for an international copyright. Like many daylight devices, Atrapaluz consists of three parts: capture, transport and emission of light, but it is considered an innovation because it doesn't depend on a singular shape, but on an adaptable combination of two optical principles: a mirror reflection in the transport zone and a total internal reflection in the emission zone. Here we present and evaluate its performing in a dark residential building considered a modern heritage architecture.

Keywords: Sustainable Architecture, refurbishment, daylighting, lighting technology.

1 Foreword

The vestiges of the architectural Patrimony in Chile, very little for seismic, technological and historical reasons, are non-monumental, in general, but valuable as a Chilean patrimonial identity. Its recovery at the central urban zones requires public policies of incentives and promotion. But by their antiquity, these buildings show inadequate luminance comfort and energetic deficiency, increasing its maintenance costs. These factors make them aesthetically unattractive for young peopleATRAPALUZ proposal, a 'non-invasive, minimum and adaptable device', could allow to transform perception of dark intermediate enclosures spaces, taking natural light into them for its comfortable use during day time, with consistent results, contemporary sensitivity and sustainable philosophy, taking advantage of the optical characteristics of materials available on the market.

Thus, natural light –free and with a known trajectory, regularity and intensity- can be the factor that raise 'sustainable improvement' of aged buildings in our city. solar light can be the material of perceptual revitalization, and keep the favorable physiological effect related to the light activation of circadian cycle and its derived hormonal effects. So, as long as possible, during the day, natural light should not be replaced with artificial light.

ATRAPALUZ, an innovative version of the '*lumiduct*' category, is an adaptable device, that captures and transmit solar light with several options for the reflector/distributor components, and that re locates light by a diffuser of variable form. In its prototype version it included: a receiver with an inverted pyramidal trunk form, a straight tubular transmitter - both with superficial reflection properties-, and a diffusing PMMA block with the property of 'total internal reflection', in addition to the necessary elements of protection, fixation and connection between conduits and block.

2 Objectives

The project aim was to offer an instrument that could improve conditions of old built spaces, enhancing people perception and comfort by creating a flexible and adaptable light interface. It could allow designers and architects to handle natural light, and its unique qualities related to benefits in biological, psychological and social welfare,allowing awareness of 'time passing' for those who enjoy space with a contemporary aesthetic sensibility. With this purpose, we have considered the inhabitant to be a perceptually active and reactive receptor in front of light effects (Noe, 2004), involving his biological cycles during year and daytime (Rea, 2007) and his cognitive/emotional behaviour (Maturana, 1984). An ergonomic approach (Norman, 2004) was also used to qualify and quantify factors associated with the lighting criteria as a condition of spatial comprehensibility, sense of ownership and wellbeing. So, our our installed devices were developed under an anthropologist heritage approach (Chanfón 1996, UNESCO 1982), trying to give an adequate answer to real contemporary requirements of natural light.

3 A method for the unknown

When dealing with a problem that requires solutions from designers, architects or creative professionals, they usually know the effect to look for but not exactly how or where it will take place. For that reason in these fields the methodologies are commonly of 'rough estimate and iteration' (Letelier, 2000) or, at least, controlled ways to reduce the uncertainty of the problem, simplifying it to appreciate it better. Being the appreciation one of the most complex human processes, a problem of illumination leaves us habitually with an ideal that seems to be a non-real challenge. For that reason, the methodologies that serve better in our disciplines are those of multiple and successive approaches, while do not lose focus of perceptual intention. This intention could be promoted with anything we have by hand, accepting the associations that such stimuli suggest at diverse moments, and allowing us to calibrate without prejudice, all the possibilities.

We proceeded to define the conditions for the technical feasibility of the projects through study models in 1:10 scale, knowing that experimentations in architecture can hardly intervene real spaces and that light is indifferent to scale (its appearance in a reduced model is identical in form and intensity than what will be in real dimension) (Pattini, 2009).

The quality and quantity of light in the models was instrumentally measured in various alternatives, which threw sufficient data and criteria (in technical, spatial and perceptual aspects) to decide the solution to be developed into a prototype 1:1 scale, the **Atrapaluz**. This allowed us to verify the real lighting efficiency, the ergonomic improvements and its feasibility of installation. After creating the prototype, a modified version of its shape was applied to a real case (in an experimental model) that maintained physical principles used in the Atrapaluz prototype.

To evaluate the results of all proposals we used ergonomic criteria considering that optimization of comfort and effectiveness of tasks is fundamental in designing for any human activity, based on the triad of usability: effectiveness, efficiency and satisfaction (ISO 9241-11, 1998). Thus, during the process, the product was transformed while transforming its architectural intervention possibilities: the architectural intervention became indistinguishable from the design product, being part in the evaluation, installation and use. The limits of architectural perception and practical design merge in the transformation of places when you are looking for a new user experience. Space modification implies loss of the limits between design and architecture, while the product becomes 'with and in' architectural intervention.

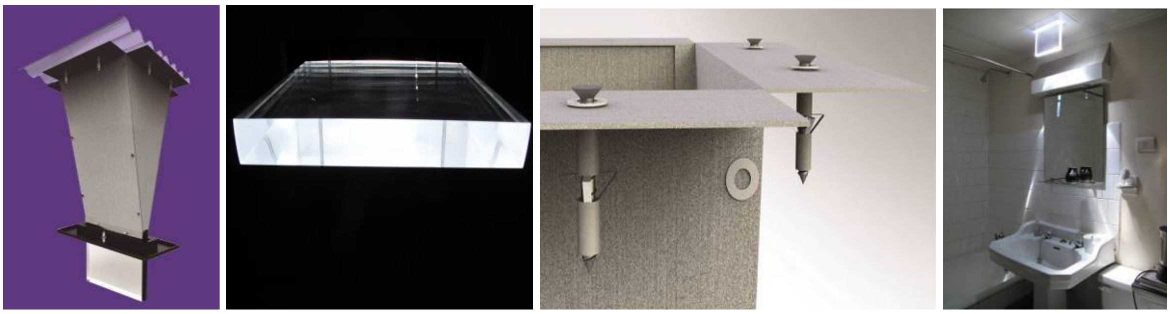

Figure 1 – Atrapaluz prototipe

4 The UVP case

UVP is a complex of middle class apartment blocks, built in the fifties that have 70m long and with four levels each. We choose this case to work in because it is considered a Modernist Heritage, a new and interesting case of Patrimony. We worked in the central corridor of the second floor, which is 32m long from the central stairway. During the day it has serious problems of darkness and glare because of an only source of natural light (a window) placed at the end of the corridor. Inhabitants are forced to use electrical lighting during 24hrs every day of the year in order to eliminate darkness and minimize glare that impede a good visibility in the corridor.

The visible effects in the models were evaluated by experimental subjects (inhabitants of the building) that emit their perceptual appreciation on a conventional punctuated range. In the other hand, it was also evaluated by the research team, whose judgment considered various aspects: the type of optical phenomenon of the light (simple reflection, diffusion, refraction, total internal reflection, etc.), shadows, spots of light; disintegrating effects of the materials, etc.

4.1. Actual perception at UVP

Current daylighting sources: hall 32m long, 2.5m tall with 6 opaque doors of apartments, 3 on each side. The central hall gives some indirect light from the outside. The picture shows the only source of direct natural light at its end (north), through a window that occupies the entire wall. This situation causes a strong glare because the rest of the corridor remains in almost total darkness.

Effect of the quality of surfaces: the walls are semi gloss and white and they produce diffuse reflected light from the background window, increasing a little the illuminance in the hallway. The floor is black, shiny and polished and produces reflection of the window, but doesn’t contribute to increase the overall illuminance. The glare effect increases with the distance from the window. At 24 m doors hardly differ during the day.

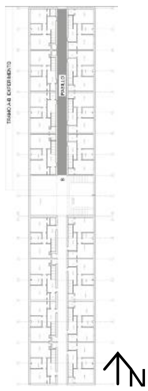

Figure 2 – A. The UVP. B. UVP corridor. C. Floor plan

4.1.1 Spatial perception

a. Understanding the shape of the place: while the spot light is farthest, the hallway exposes better its rectangular section, but never its true length. The huge power of window light and its luminance at the end of the corridor do not allow comprehending the shape and boundaries of the place during the day. Its powerful brightness makes it look as a cylinder box as we approach to the focus.

b. Comprising depth. The doors are arranged at irregular distances that prevent to infer modules to estimate length and amount. The bright end seems to be closer, thus perceptual distance is shorter. Hiding their true length can be positive in an excessive long hallway.

c. Constitutive peculiarities of architectural space: darkness level in this place, obscure architectural details (cornices and baseboards) reinforcing the notion as tunnel space. An aesthetic intention in rhythmic accents of the doors is not understood.

d. Pragmatic key for habitability: There is a tract of the hallway where the doors details are unnoticed, neither their numbers nor their locks. People are seen as silhouettes and their faces are not recognizable, suggesting insecurity.

5 Alternatives Proposals for UVP Corridor

Two proposals were developed for this case: a **Reflective Slatted Shutters** and an **Anidolic System**. The optical principles developed for the Atrapaluz system were tested in both cases. Knowing that light is not affected by scale (Pattini, op.cit.), we conducted quantitative evaluations of proposals in two scale models each (1:25 and 1:10). For qualitative evaluation we assessed them in-situ using projection of photomontage techniques for opposed stages: current and projected state. The experimental work is now completed for the Anidolic System for the UVP building, while the analyses for Reflective Slatted Shutters for the same corridor are in progress. Nevertheless, we present here a description of both perceptual effects.

5.1. Reflective Slatted Shutters

In the first proposal, for the capture zone we used a reflective and movable set of slatted shutters (ideally associated to an heliostat-system), whose light beams converged at 10 m from the light capture point. This point is the new beginning of the reflective false ceiling. Thus, in the first part of the corridor, light trajectory does not have intermediate reflections so it can reach the end of the space with a shorter reflective box: this produces few rebounds and fewer losses. The final emission was done only at the darkest corridor zone, also with PMMA transparent plates.

Daylighting sources: This alternative proposes to use the entire surface of the window as a source of natural light, but directing and converging the incident rays to a distant point where the ceiling begins. From this point the light travels through the ceiling (as a *lumiduct*) and emits its light in PMMA prisms arranged in the corridor. The shutter can be controlled by a heliostat system.

Effect of the quality of surfaces: While most of the rays are able to concentrate during the day to illuminate the interior of the hall, closer to the window it creates an interesting effect by the reflection promoted in the satiny walls. In the *lumiduct* ceiling we have installed many pmma boards to diffuse and give off light, increasing the illuminance in the corridor.

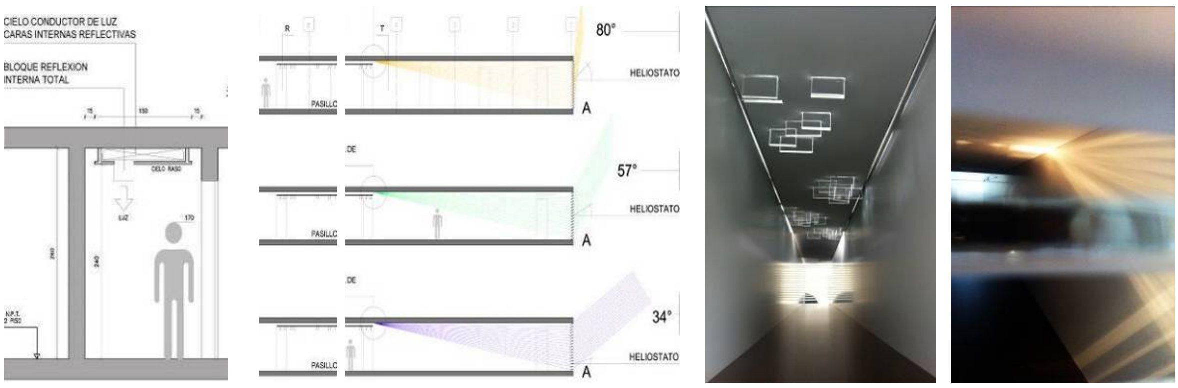

Figure 3 – A. UVP corridor seccion. B. Converging sunrays scheme. C. Interior images

5.1.1 Spatial perception

a. Understanding the shape of the place: In this alternative, when the sightless allowed to enter a low light, the 'space box' seems to expand and promotes misleading by the reflections and multiplication of light in the walls. The most interesting effect is that the horizontal banding of the slatted shutters also produces an increase in its height (by Helmholz illusion).

b. Comprising depth. When the background (window) is very luminous, it surpasses every other focus of attention, so perception is dizzying to that point, shortening the distance perception, turning off any other detail. Instead, when the background is dark and the glare disappears, the light plates that come down from the ceiling appears and illuminate the hallway.

c. Constitutive peculiarities of architectural space: The side walls, as limits, are not very important with the shutter open because reflections are low. The floor and ceiling, however, become important in perception. When the background is dark, the ceiling takes importance with its lighting plates and walls are enhanced with powerful light spots. In that scenario the floor and the sightless almost disappear.

d. Pragmatic solution for habitability: This alternative provides a high degree of illumination in the two situations, half open and closed, allowing a good habitability.

5.2 Lighting with Anidolic System at UVP

In the second proposal, the capture zone was performed using an anidolic system; the distribution zone was worked in a reflective box over all the ceiling and emission part was achieved with transparent PMMA plates hanging along the ceiling, until 32 meters away.

Daylighting sources: A screen is placed at the background (window) to prevent glare and which is part of the collector. The incident rays on the façade are redirected to the reflective lumiduct ceiling. The ceiling plates are longitudinally arranged PMMA, not parallel to the corridor, which transmit light by total internal reflection.

Effect of the quality of surfaces: The visible surface of the lumiduct ceiling is smooth and semi glossy. The zigzag light fold where plates are inserted as a keel, so reflections and glare are not monotonic but discontinuous breaks that avoid monotony. Each light stretch is replicated on the polished floor. The white walls are now along all the way

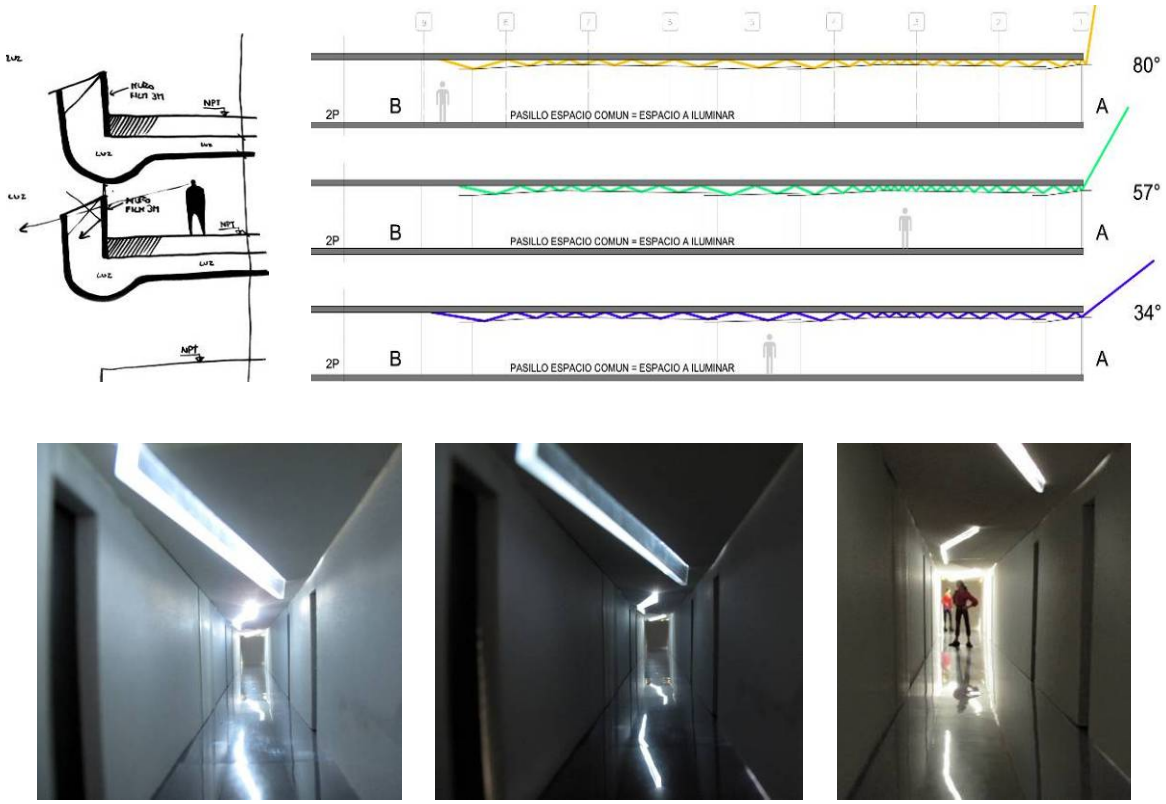

Figure 4 – A. Idea schemes. B. Interior images of path sunlight.

5.2.1 Spatial perception

a. Understanding the shape of the place: Tunnel feeling is gone, replaced by a space with a central, dynamic and unpredictable axis. Its shape produces inflections and inquiries, promoting visual interest. Walls definition and its boundaries are clear.

b. Comprising depth. With only three non-parallel linear features, the hall seems shortened by two reasons: the length of the beam lines tends to generate a *gestalt* compressed zigzag.

c. Constitutive peculiarities of architectural space: Light lines that allow seeing the silhouette of the window gives a better sensation to the space perception. Ground floor are easily distinguishable from the walls and accidents.

d. Pragmatic solution for habitability: Glare disappearance and increased brightness (though slight) make doors distinguishable, including its location, numbers and locks. People are also more easily identifiable in all the way.

6 Evaluation and results

The alternative with Anidolic System was quantitatively evaluated with a luxometer to measure illuminance levels every meter along the corridor, at different dates, seasons and times of the day, keeping the study model towards the precise real orientation because we worked without a heliodon.

Qualitative evaluation compared the actual situation of corridor and the proposed one with Atrapaluz, in its aesthetic and functional effects, and also dimensional aspects perceived with and without light intervention. An exploratory tool was developed by a Psychologist, consisting in a questionary to compare a set of 24 opposite pairs of relevant items that were presented to a sample of 19 inhabitants of the building. They were exposed to scenes with and without the Atrapaluz intervention, so they could compare the effects *in situ* and answer the questionary. Analyses were divided into three stages: i) Analysis of perceived attributes and accidents perception in current conditions, ii) Analysis of perceived attributes and accidents with the Atrapaluz intervention and iii) Compare results to distinguish differences in perception and preferences between the two scenes.

6.1. Qualitative study

An exploratory research of aesthetics conditions of spatial perceptions was performed. It aims to identify and to associate the corridors in the UVP studied case. The study employed a qualitative approach, using a survey and data visualization in a monitor computer.

People included in the survey were at least 19 years old and they were currently living in the building. 38 surveys were applied but just 19 were collected. Each dimension was required to be measured in scale of 1 to 7.

6.2. Application procedures

Meetings were set previously with the management committee of the UVP complex in order to introduce them material and application procedures. The survey was applied using images displayed on screen visualization data display.

The case was presented to each person so they were able to observe *in situ* the corridor with the proposed Atrapaluz. The implementation was performed in two consecutive steps; the first was to use the survey regarding the current perception of the corridor, the second with with the section on the project perception.

With Atrapaluz

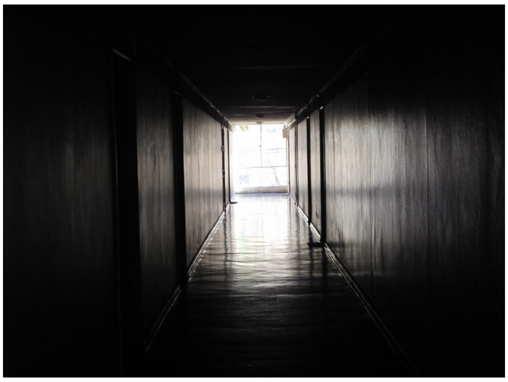

Without Atrapaluz

Figure 5 – Images shown in the application of the survey.

6.3. Results analysis

The analysis of results was divided into three stages. The first one refers to the perception analysis of the corridor attribute in the current conditions, it means without the Atrapaluz device. Subsequently, results of attributes perceived with Atrapaluz intervention were analyzed. Finally, results of previous steps were compared to determine if there was a modification of perception and any preference (with or without the Atrapaluz proposal) for the corridor.

Step 1 (Perception without Atrapaluz intervention): according to the interpretation of responses, the results obtained suggest that initially the corridor was categorized as heavy, sad , dark , nasty, boring, useless, uncomfortable, expulsive , locked , gray. It was also classified as cold , simple , spacious , quiet , tall and big. Moreover, regarding perception of the corridor lights, on average, subjects felt that there were three lights in the corridor. Additionally, according to the presented categorization, it was possible to establish that people consider lighting unpleasant and inadequate, even when they did not find anything good or bad about their location. Finally, from this data, it was possible to conclude that people consider the color of walls, floor and sky of the corridor as diffuse, the end of the corridor as clear, and they thought that it makes difficult to clearly see clothing or faces.

Concerning the luminaries, the data were obtained shown that on average only one subject considers there are 3 lighting in the corridor. Furthermore, using the scale mapping criteria previously described, it is posible to state that people considered lighting unpleasant and insufficient, but do not find anything good or bad about their location.

Step 2 (Perception with intervention Atrapaluz): Results allowed to conclude that the corridor was qualified as safe , bright, cheerful, clear , simple, nice, interesting , quiet , useful , comfortable, cozy and colorful. Moreover, regarding perception of the corridor lights, again, on average, subjects felt that there were approximately three lights in the corridor and according to the categorization previously presented,it was possible to state that people perceive the corridor as properly illuminated, nice and well-located after intervention. Finally, it was possible to conclude that people considered color of the walls, floor and ceiling clear. They also estimated that it is easy to see clothes, but they don’t distinguish as easy or difficult to see clearly people’s faces in the corridor.

Concerning the luminaries, the data were obtained shown that on average subjects considers there are 3.2 lighting in the corridor. Furthermore, using the scale mapping criteria previously described, it is posible to state that people considered lighting as sufficient, nice and well placed after the intervention. No group differences were found regarding these distributions.

Step 3 (perception comparison with / without Atrapaluz intervention) : Regarding the corridor and its equipment, as previously stated, definitions performed by the subjects did change after the proposed enhancement. So far, most of the studied dimensions of analysis related to perception were differentially evaluated by the subjects after the simulation with Atrapaluz

was presented.. That means it was possible to change the perception of the responders regarding the attributes of the corridor as an object of study.
In this sense , there were changes in all features except complexity, length, noise, symmetry, closure, height and size . All of these characteristics are associated with the dimensional space rather than to attribute from the "Atrapaluz" itself as spatial aesthetic perception contribution to the residents of UVP neighborhood.

As previously stated, regarding the corridor and its equipment, the definition that those subjects performed during the study changed. Below it is shown a curve that contains perceptions before and after (with and without the Atrapaluz intervention).

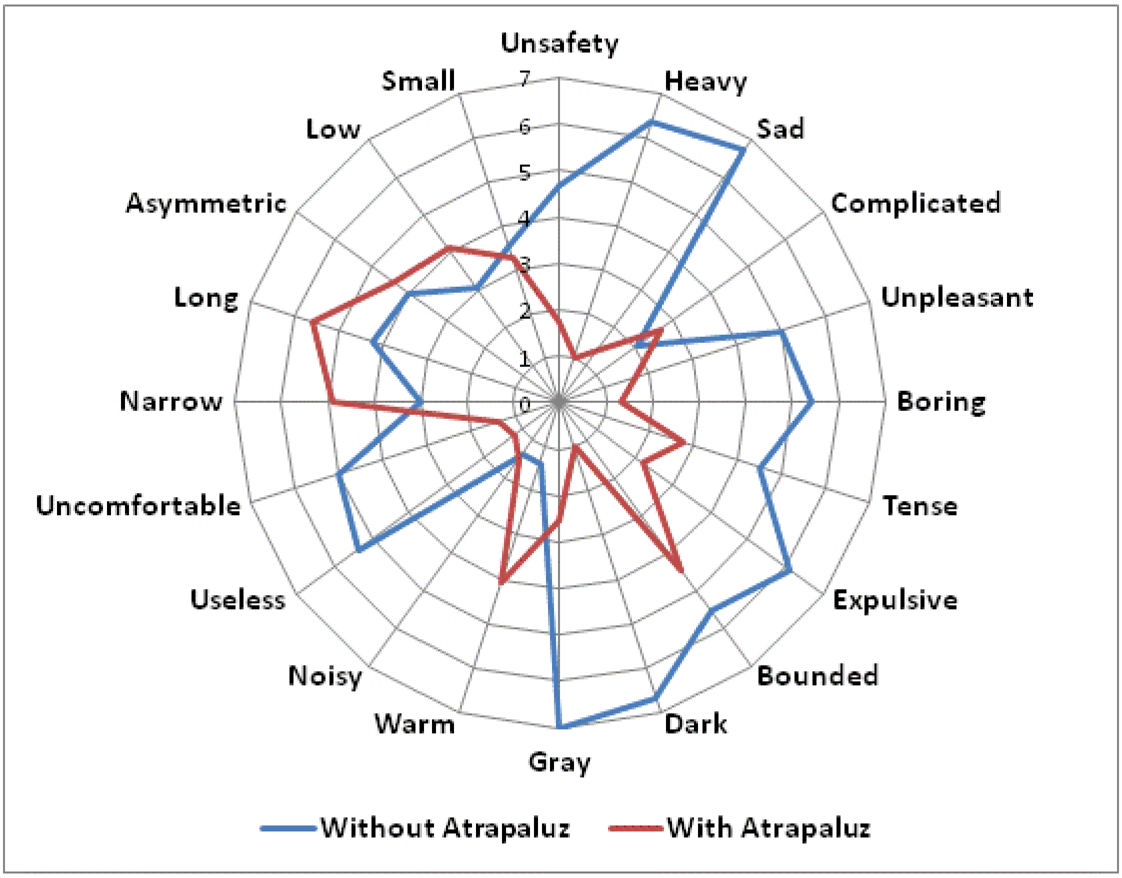

Figure 6 – Graphic results of comparison perception with and without the Atrapaluz (measured in scale of 1 to 7).

For each dimension, averages were subtracted from each other to highlight variations due to Atrapaluz effect and the results are shown in the following figure.

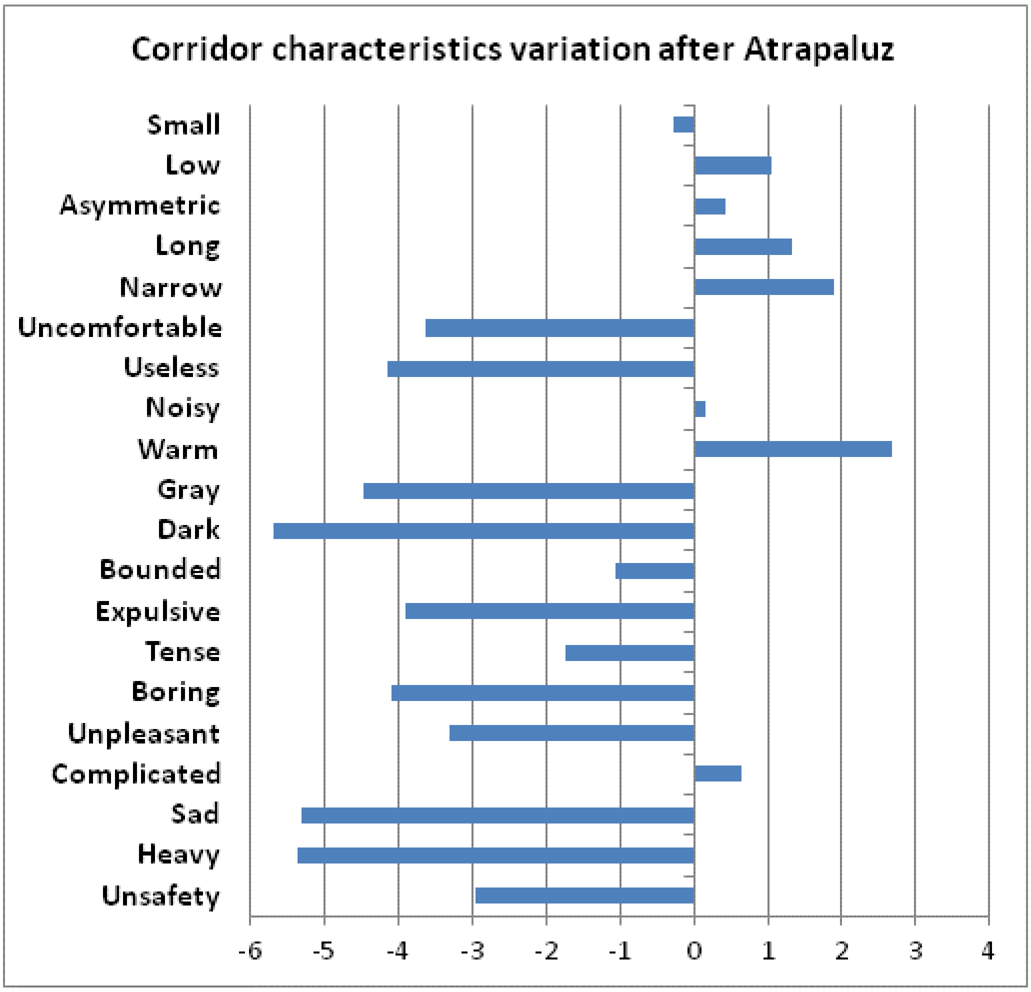

Figure 7 – Graphic of variation after Atrapaluz.

7 Conclusions

Quantitative results show that despite the device did not achieve minimum illuminance levels for a public space (100 lx), there was a significant glare decrease, which improves the performance in scotopic vision.

Qualitative results show that in 18 of the 24 comparative questions (75%) there were positive perception changes in the inhabitant sample. Results of comparison between these two situations lead to conclude that there were positive perceptual changes in most of the dimensional space aspects without significant changes in illuminance levels. That means it was possible to change perception of responders regarding the attributes of the corridor as an object of study.

From a cognitive ergonomics perspective, the intervention Atrapaluz in the UVP case makes it more accessible because it increases the ability to receive information of the corridor by increasing its lighting level and reducing uncertainty of people (Cañas, 2001). Therefore, it increases both the perception of security and the ability to perform decisions during the act of walking the corridor.

The achievement of perceptual changes and habitability improvements is perhaps the main concern for architects and designers. In all operated cases, a better presence of real space, its architectural and functional accidents are evident. On the other handand most importantly, the alternative use of the appliance at different times of day, provide new insights - formal and dimensional – of an stimulating space, always providing interest and attention of the inhabitants.

So, it could be argued that design lighting solutions should be considered early in the design process to promote accessibility of daylighting systems to the people, providing further visual comfort experiences for human living.

To finish, effectively Atrapaluz intervention improves perception of space by inhabitants, which means that it becomes more comfortable with the use of natural light and its dynamic changes, the final goal of this work.

Acknowledgements

We´d like to thanks to Victor Nadal for his assist to development the prototypes. Also to Carlos Díaz Canepa, for his help in the analysis of the survey and their results. Finally to Betzabe Ortiz for her effort during the application of the surveys.

References

CAÑAS, J.J., AND WAERN, Y., 2001. *Ergonomía Cognitiva*. Editorial Médica Panamericana, Madrid.

CHANFÓN, C., 1984. *Fundamentos teóricos de la Restauración*. UNAM, México D.F.

ISO 9241-11. *Ergonomic requirements for office work with visual display terminals (VDTs) Part 11: Guidance on usability*, 1998.

LETELIER, S. 2000. *Caleidoscopio de la creatividad*. Editorial Universitaria, Santiago.

MATURANA, H; MPODOZIS J., 1987. Percepción: *Configuración conductual del objeto*. Arch. Biol. Med. Exp. 20: 319-328

NOE, A., 2004. *Action in Perception*. MIT Press. Boston

NORMAN, Donald A., 2004. *El Diseño Emocional*. Editorial Paidos, Barcelona

PATTINI, A., 2009. *La Luz Natural en las Escuelas*. Ed. Dunken, Buenos Aires

REA, M., 2007. *More than vision*. Editorial Domus, Milán

UNESCO. World Conference on Cultural Policies, Mexico DF, July 26 - August 6, 1982

OP08

NATURAL EXPERIMENT ON THE EFFECT OF ARTIFICIAL LIGHTING AND DAYLIGHT

Favero, F.[1], Lowden, A.[2], Ejhed, J. [1]
[1] Lighting Laboratory, KTH STH, Royal Institute of Technology, Stockholm – SWEDEN
[2] Stress Research Institute, Stockholm University, Stockholm – SWEDEN
Email address: ffavero@kth.se

Abstract

In this case study we investigated the effect of the exposure to daylight and artificial light indoor during Scandinavian winter. Twenty-one subjects experienced two radically different lighting solutions for three days in a row, eight hours each day: one group (n=12) was exposed only to daylight, one (n=9) only to artificial electric lighting (>500lx average on work plane, 3000K). We observed an effect between light conditions on mood, which was elevated in the daylight room. Mean levels of alertness and perceived energy ratings were higher in the daylight condition. An effect of the lighting condition was found for activity levels as measured by the actigraphs, especially in the morning. Due to the experimental design it is at present difficult to tease out if observed effects were due to the lighting exposure or to other environmental factors, e.g. architectural layout, timing or intensity of the exposure, therefore future further studies would be needed to examine different combinations of factors.

Keywords: office environment, school environment, sleepiness, mood, space perception

1 Introduction

Today in industrialised societies, lifestyle and working conditions changed the patterns of exposure to natural light and darkness compared to few generation before ours. Indeed a difference in timing and intensity of exposure between workers working indoor and outdoor was reported (Dumont et al., 2010), as well as the effects of lack of natural exposure on workers' wellbeing, especially on sleep disturbances (Leger et al., 2011).

This paper would like to contribute to the understanding of the user's experience of lighting conditions indoor in an everyday setting; we were specifically interested in investigating whether a day-lit scenario could provide beneficial effects on subjective and objective parameters in comparison with an artificial lighting condition. We were interested to observe differences in perceived qualitative aspects, such as parameters of lighting, and quantitative aspects, illuminance, activity levels and sleep timing. One scenario presented exposure to static artificial lighting with warm colour temperature, a typical configuration for office lighting in Scandinavian countries, and no daylight contribution. The other scenario was only day-lit, with no contribution of artificial lighting; therefore subjects were exposed to natural variation of spectrum and intensity during a whole working day.

Bright-light exposure reduced the intensity of depressive symptoms and improved vitality, indicating that exposure to bright light did have a beneficial effect on mood in healthy adults (Partonen & Lönnqvist, 2000). Results of a field investigation, showed that persons who were exposed to short durations of bright light experienced higher feelings of vitality shortly after (Smolders et al., 2013). Hubalek et al. (2010) reported that the amount of light entering the eye appeared to have an impact on sleep quality during the following night.

Daylight has three main characteristics: it continuously varies in intensity, colour and distribution. In cloudy conditions, continuous and (relatively) unpredictable variation of illuminance values is a strong feature of daylight (Tregenza & Wilson, 2011). Veitch (2011) suggested that psychological and physiological effects of light are mediated through three processes by which skylights and windows affect health and well-being: dose of light and darkness, view and architectural aesthetics. Indeed the complexity of daylight distribution in a room makes it difficult to identify one single parameter that might have more relevance than the others.

High intensity and a spectrum rich in the short wavelengths, characteristics of natural outdoor conditions, were proved in previous literature to be effective for circadian regulation and improvement of alertness and mood. Therefore it can be expected that daylight exposure cause different outcomes regarding direct and long-term effects on the human body compared to a static light of warm colour temperature.

2 Method and design

The controlled observation took place at KTH – Royal Institute of Technology, in Sweden (N 59° 10', E 18° 8'), in February 2012. Two rooms with radically different lighting conditions were used: one only exposed to an artificial electrical lighting system – the Artificial Lighting Condition (ALC); and one with only access to daylight and no electrical light – the Day-Light Condition (DLC). The experiment was performed from 8:30 to 16:30 h with an hour break during lunch, at 12 o'clock, which was not controlled, see figure 1.

A total of 23 students took part, randomly assigned to each room on the first experimental day. Two male subjects from the ALC didn't complete the test, therefore 21 subjects were considered in the analysis. Average age was 29.3 (SD = 4.4) in the ALC, 29.2 (SD = 5.4) in the daylight condition. The subjects reported their chronotype on a diurnal scale type questionnaire (Torsvall & Åkerstedt, 1980). Both groups scored between evening and intermediate type – *ALC was 2.0 (SD = 0.5), DLC 2.0 (SD = 0.4).*

The lighting in the artificial room provided a standard illumination at the workplace (>500lx; 3000 K) with a combination of direct and indirect distribution. Total installed power, considering ballast consumption, was 0.529 KW (8.3 W/m2).

Figure 1 – Timing of the experiment and exposure conditions in the two rooms. The blue line with variable thickness illustrates daylight exposure during experimental days. The inner orange line with continuous thickness illustrates artificial light. In the daylight room (right in figure) subjects were exposed to a varying stimulus. Subjects in the artificial room (left in figure) were instead exposed to a constant lighting. The experimental conditions were not controlled during lunch break (12-13:00 h).

The daylight room was equipped with one window (80% of wall area) and a tilted skylight over a light-shaft. The daylight factor as calculated by software (ReluxPro, Relux Informatik AG, Basel Switzerland) was 7. Weather was characterized by overcast conditions, illuminance registered by actiwatch varied with a similar temporal distribution during the three days, see figure 2.

A wake diary which included sleepiness – KSS, Karolinska Sleepiness Scale (Åkerstedt and Gillberg, 1990), perceived energy level and subjective mood evaluation, was filled in every hour by the subjects. The subjects wore an actigraph (Actiwatch Spectrum, Philips Healthcare, Best – The Netherlands) for four days including one day before the study. Subjective ratings of the lighting conditions (Liljefors, 1999; Ejhed, 1991) were registered every day at 15:00.

The participants were studying during the experiment. Use of personal laptops was allowed but students were requested to lower the screen brightness as much as possible. We followed the ethical procedure of the Institute and participants signed written consent. Data was processed with SPSS and STATA analysis software. Significant effects are reported here and in Favero et al., (2014), in review.

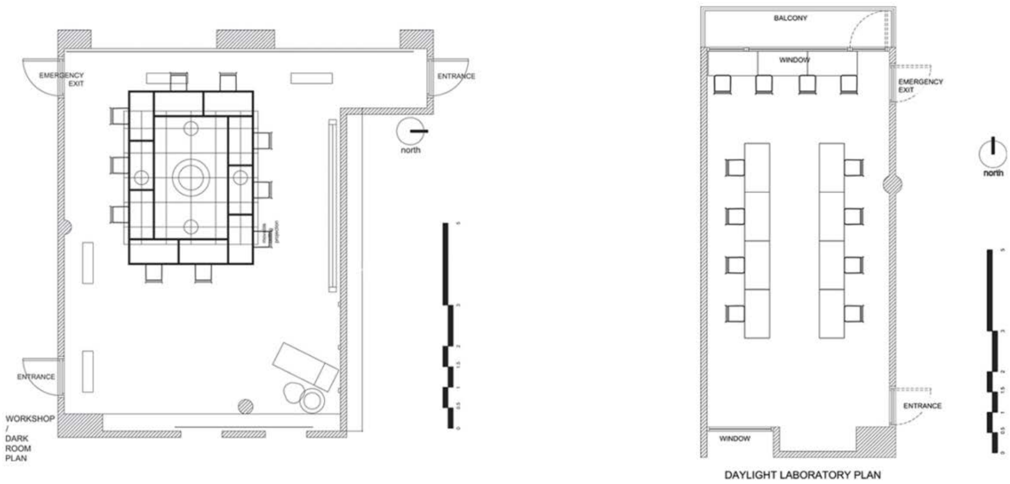

Figure 2 Pictures and plans of experimental rooms. The seating plan was set up in a similar layout in the two rooms, as in the plan on the left. Subjects in the daylight room (right in figure) changed the layout in the afternoon of day 1 to the configuration shown, with three tables facing the window.

3 Results and discussion

From the analysis of the subjects' chronotype and sleep pattern on the night preceding the first day the groups appeared to enter into the experiment with a similar sleep history. There was no significant difference between groups also in the two following nights analysed: the artificial condition subjects' sleep duration were 6:09 h (SD = 0:44) and 6:23 h (SD = 1:07) the nights preceding day 2 and day 3; daylight condition subjects' sleep duration was 6:02 h (SD = 0:57) and 5:52 h (SD = 1:07). Furthermore no significant difference in terms of waking up time or bed time was registered. Therefore the lighting conditions in the experiment did not cause an effect on sleep, in opposite direction of previous studies where the amount of light (Hubalek, 2010) or the spectral composition of light (Figueiro et al., 2010) received in the day did have an impact on sleep the following night. It is likely that sleep patterns were more influenced by social factors and uniform work hours.

Nevertheless the daylight room generated more activity, especially in the morning and in the early afternoon; see figure 3. From informal observations, in the daylight room there was also a higher level of social interactions compared to the artificial room, where subjects seemed more focused on personal work. These findings are in line with what was observed in a previous investigation: in day-lit rooms researchers observed higher levels of sociability, while in windowless environments children showed better concentration (Küller and Lindsten, 1992).

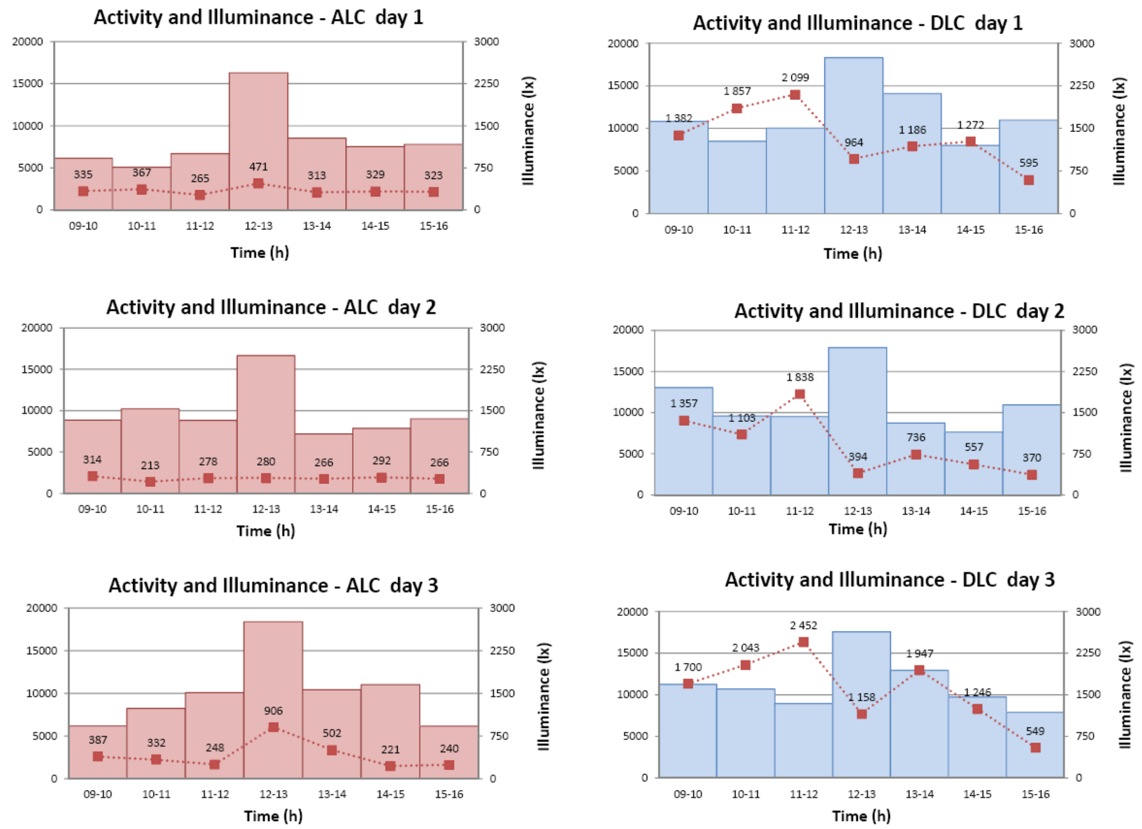

Figure 3 Actigraph derived activity levels and illuminance at the wrist, day by day in the Artificial Lighting Condition (ALC), on the left and the DayLight Condition (DLC), right. The actigraphy data was reported minute by minute; we summed this one minute epochs into hour measurements, then averages per each hour per room were produced and analysed. The chart also shows the average illuminance levels measured by the actigraphs at the wrist; they are an indication of the trend in temporal distribution of illuminance.

The subjects reported as expected a significant difference between qualitative characteristics of the lighting condition, see table 1 and 2. Interestingly, the perceived level of light and its evaluation in the two rooms were similar, despite the fact that average measured illuminance levels are in a scale of 2.5 up to 3 times higher in the daylight room and that, when evaluation was performed, the illuminance values were similar on the second day only. Visual adaptation mechanisms could explain the similarity in observations related to brightness. Another interesting finding is that, although the subjects did report a difference in colour of light, the ALC being warmer and the DLC colder, the two conditions were not evaluated differently.

Opposite consideration can be done for the light distribution which according to the subjects was similarly evaluated but the evaluation of light distribution was significantly different, the DLC showing better evaluation. The other lighting parameters were very differently appreciated: the evaluation of shadows, appearance of surface colour and glare were significantly worse in the artificial room. In this specific study, light level did not seem to be a critical factor to differentiate the two rooms. Instead shadows, colour of light and glare were identified as strong differences in the two conditions; distribution, shadows, surface colour and glare were critical factors in the evaluation of the lighting conditions.

The character of the room, investigated through a series of associations, was very distinct, the artificial condition being more frequently associated to enclosed environments and the daylight condition to more open, public spaces.

Table 1 – Lighting parameters, mean values and standard deviation of the seven parameters. The values indicate the rating of the seven basic parameters describing light in a room that help to identify the quality of light and the character of a space. * = p<0.05 ** = p<0.001 effect between conditions.

			ALC	DLC
Level of light	1=very dark	5=very bright	3.5 ±0.73	3.6 ±0.87
Light distribution	1=uniform	5=very dramatic	2.6 ±0.77	2.2 ±1.01
Shadows **	1=very vague	5=very marked	2.7 ±0.69	2.0 ±0.89
Reflections *	1=none	5=very marked	2.9 ±1.08	2.4 ±1.09
Colour of light **	1=cool/cold	5=warm	3.5 ±0.88	2.8 ±1.21
Surface Colour	1=natural	5=deteriorated	2.8 ±0.85	2.4 ±1.05
Glare **	1=none	5=intolerable	2.4 ±0.88	1.9 ±0.92

Table 2 – Lighting parameters evaluation, mean values and standard deviation. The values indicate the user's assesment of the seven lighting parameters, from good to poor. Averages for three days observation. * = p<0.05 ** = p<0.001 effect between conditions.

			ALC	DLC
Ev. Level of light	1=good	5=poor	2.7 ±0.92	2.4 ±1.07
Ev. Light distribution **	1=good	5=poor	2.9 ±0.82	2.0 ±1.05
Ev. Shadows *	1=good	5=poor	3.0 ±0.94	2.5 ±1.15
Ev. Reflections	1=good	5=poor	2.6 ±1.09	2.3 ±1.08
Ev. Colour of light	1=good	5=poor	2.9 ±0.97	2.7 ±1.10
Ev. Surface colour *	1=good	5=poor	2.8 ±0.80	2.3 ±1.04
Ev. Glare *	1=good	5=poor	2.6 ±0.97	2.1 ±1.05

Subjects entered the experiment each morning with similar evaluations of sleepiness and energy levels. On day 1 mean sleepiness and energy level were rather stable during the day, with an increase in sleepiness after lunch in the ALC but not in the DLC. On day 2 a significant increase in the levels of sleepiness was registered among the subjects in the ALC, the DLC showing a stable level throughout the day. In the third day, the levels were similar at the start and the end of the session, with a decrease of sleepiness in the morning in both rooms and an increase in the afternoon.

Results from the analysis of self-reported mood showed a significant difference between the two conditions from the beginning of the study. Mean values for mood decreased day by day in the DLC, i.e. mood seemed to improve in the DLC, although no statistical significance was registered; mood in the ALC was rather stable after the three days.

3.1 Limitations

The study was based on a limited target group being exposed for a relatively short duration of time; there is a potential to replicate it in different seasons.

We did not control subjects' lighting exposure at lunch break; actigraphs measure light levels at the wrist, therefore we did not trust illuminance measurement from the devices, especially during breaks when subjects might have worn a jacket. For practical and economical reasons we did not include lunch in the design of the experiment but this should be better controlled in a repeat study.

The study made an attempt to use a combination of subjective and objective methods in order to evaluate lighting conditions. Measurement of biological markers could have been collected in order to gauge circadian patterns although previous laboratory studies didn't report significant effects of lighting conditions on cortisol and melatonin is naturally very low during the day.

4 Conclusions and future thoughts

The results from this experiment indicate that sleepiness was reduced, mood was elevated and perception of energy levels was higher in daylight conditions compared to an artificial lighting condition. These states were also associated with elevated activity counts based on actigraph measures. The results corresponded to subjective evaluations of the lighting conditions, suggesting that daylight may provide beneficial effects in every day spaces. Despite earlier literature providing support for the use of daylight in buildings we were not sure whether we would have found any difference in the current study during winter at Northern latitudes. We could indeed observe that at this latitude it is possible to reach high light levels indoor with daylight, even during wintertime, and register an effect of this condition on subjects. Therefore we would strongly promote use of daylight for future research alongside artificial dynamic lighting.

The research layout presented several factors that likely could have confounded the results, therefore it was not possible in the current study to determine whether the differences could be attributed exclusively to the lighting conditions employed. The complexity of everyday setting in terms of temporal and spatial elements (intensity, variation, timing, duration, distribution, colour of light and view) makes it difficult to identify single mechanisms of action. The experience of the space might be modulated through this complexity, therefore it is a challenge for further studies to isolate and capture the critical factors among them. Advances in technology allow for smart characterization of artificial lighting patterns, which could contribute to create a natural relation between users and the artificially lit environment (Favero, 2011); research and application would certainly benefit by exploring the behaviour and the effect of natural light (and dark) patterns on humans in order to build this relation.

References

Dumont, M., Beaulieu, C. (2007). Light exposure in the natural environment: Relevance to mood and sleep disorders. Sleep medicine, 8, 557-65

Ejhed, J. (1991). Lighting and environmental design. Proceedings of the 22nd session of the CIE, Melbourne, Australia.

Favero, (2011). Natural light: Lighting qualities for the design of future spaces. Development of a methodology. Proceedings of the 27th session of the CIE, Sun City, South Africa.

Favero, F., Lowden, A., Ejhed, J. (2014). Natural experiment on the effect of artificial lighting and daylight on subjective and objective parameters. Journal of Environmental Psychology, in review.

Hubalek, S., Brink, M., Schierz, C. (2010). Office worker's daily exposure to light and its influence on sleep quality and mood. Lighting Research and Technology, 42, 33-50

Kuller, R., Lindsten, C. (1992). Health and behaviour of children in classrooms with and without windows. Journal of Environmental Psychology, 12, 305-17

Leger, D., Bayon, V., Elbaz, M., Philip, P., Choudat, D. (2011). Underexposure to light at work and its association to insomnia and sleepiness. J. Psychosomatic research 70, 29-36

Liljefors, A. (1999). Lighting - Visually and physically. Stockholm: School of Architecture, Royal Institute of Technology

Partonen, T., Lönnqvist, J. (2000). Bright light improves vitality and alleviates distress in healthy people. Journal of Affective Disorders, 57(1-3), 55-61

Rea MS, Figueiro MG, Bullough JD, Bierman A. (2005). A model of phototransduction by the human circadian system. Brain Research Reviews, 50(2), 213-28.

Smolders, K.C.H.J., de Kort, Y.A.W, van den Berg, S.M. (2013). Daytime light exposure and feelings of vitality: results of a field study during regular weekdays. Journal of Environmental Psychology 36, 270-9

Tregenza P.R., Wilson, M. (2011).Daylighting Architecture and Lighting Design. London and New York: Routledge Taylor and Francis Group

Veitch, J. (2011). The Physiological and psychological effects of windows, daylight, and view at home. Ottawa: National Research Council of Canada.

Åkerstedt, T., Gillberg, M. (1990). Subjective and objective sleepiness in the active individual. International Journal of Neuroscience, 52, 29-37

OP09

EVALUATION ON VISUAL ENVIRONMENT IN A FAST FOOD RESTAURANT EQUIPPED WITH DAYLIGHT DUCT SYSTEM

Iwata, T.[1], Hirai, T [2], Shinohara, N.[3] , Kaiho, K.[3], Nakao, R.[3]
[1]Tokai University, Hiratsuka, JAPAN, [2]Toda Corporation, Tokyo, JAPAN, [3]Nikken Sekkei, Tokyo JAPAN
Iwata@keyaki.cc.u-tokai.ac.jp

Abstract

A type of light tube, which has a rectangular- section duct is called a “light duct”. Besides the ducts themselves, daylight duct systems contain a light-collecting unit and light-emitting unit. In order to identify the effect of the daylight duct system on the visual environment, a performance measurement, investigation of customer behaviour and a subjective experiment were carried out in a fast food restaurant with the daylight duct system. The measurement and calculation showed that the light-emitting unit reduced efficiency. The SPD of daylight was maintained through the light duct systems due to the materials employed in the fabrication of the duct system. On a sunny day, the customers prefer the tables illuminated by the duct system to the tables illuminated only by the electric lighting. The subjects at the tables illuminated by the duct system feel space more comfortable and preferable.

Keywords: Daylight, Light Tube, Field Measurement, Customer Behaviour, Subjective Experiment

1 Introduction

Generally light tubes, also called light pipes, are used to transport daylight to another location. A tube uses highly reflective material or plastic optical fibre to direct the light rays. A type of light tube, which has a rectangular- section duct lined with highly reflective material is called a “daylight duct”. Apart from the tubes which function as light-transferring units, light duct systems also comprise a light-collecting unit and light-emitting unit. For each unit, different functions are required. Light-collecting unit and light-transmitting unit should collect and transmit daylight (sunlight and skylight (diffused light)) efficiently. On the other hand, light-emitting unit should avoid a strange appearance such as an extreme irregular distribution of luminance or of colour, as well as discomfort glare. There are previous studies which showed methods to calculate transmission of rectangular-section mirror light pipes (Swift et al. 2008, Edmonds. 2010） and results of field survey in office buildings and schools equipped with tubular daylight guidance (Mawaee and Carter. 2006).

Depending on the space usage, it is important to maintain not only the quantity (luminous flux) of daylight, but also quality (the spectral power distribution (SPD)) of daylight. Recently a new reflective material, which can reflect light with short wavelength (400 to 500 nm) as well as middle or long wavelengths, has been developed. A daylight duct system using this material was installed in a fast food restaurant where the visual environment including colour rendering is important. In order to identify the effect of the daylight duct system on the luminous environment and the visual environment in the restaurant, a three-part investigation was carried out. First, an empirical performance measurement of the daylight duct system was performed followed by an observation and analysis of customer behaviour in the restaurant. Finally, an *in-situ* subjective experiment was carried out in cooperation with the management of the restaurant.

2 Performance Measurements of the daylight duct system

2.1 Methods

The fast food restaurant with the daylight duct system is located in a residential area of Tokyo. Performances of light–collecting unit, light-transmitting unit (duct part) and light-emitting unit were evaluated.

2.1.1 Outline of the duct system

The daylight duct system has two openings (internal dimensions: 600mm × 840mm) on the roof of the building, functioning as the passive light-collecting unit. The plane of the opening is tilted 45 degrees from the horizontal plane to face south. Two vertical ducts, which transmit daylight, are connected to one horizontal duct (light-emitting unit) which has translucent part distributing the light into the room. The daylight duct system was combined with LED lighting installed inside of the light-emitting unit. Usually the LED lighting is turned on at 3 p.m. when the daylight is insufficient.

Figure 1 – Light-collecting unit

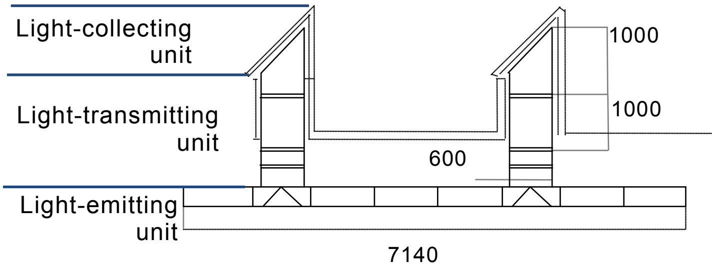

Figure 2 – Sectional view of duct

2.1.2 Measurements

Table 1 shows evaluated performance and measured values. In order to evaluate performances of light–collecting unit, light-transmitting unit and light-emitting unit independently, calculation and measurement were combined.

Table 1 – Evaluated performance and measured values

Evaluated Performance	Calculation parameters	Measurement position	Measured value	time	Measurement equipment
Collecting light	Sky factor	Light-collecting unit	Configuration factor		
	Possible sunshine duration	light-emitting unit	Obstruction on sun path		Nikon D40 X with fish-eye
Maintaining luminous flux	Incident luminous flux	Light-collecting unit	Illuinance [lx]	Every 2 minutes	Illuminance meterT-10 Konicaminolta
	Luminous flux emitted	light-emitting unit	Luminance [cd m^{-2}]	Every 30 minutes	Nikon D40 X with fish-eye
Maintaining SPD	SPD of incident light	Light-collecting unit	SPD	Every 2 hours	Illuminance Spectrophotometer CL-500A Konicaminolta
	SPD of light emitted	Light-emitting unit			

2.2 Results

2.2.1 Collecting Light

In order to measure sky factor, the image taken with fish eye of equisolid angle projection was converted to an image of orthographic projection as shown Figure 3. The sky factor was 82%.

To calculate sunshine duration, sun path diagram was drawn on equisolid angle projection image as shown in Figure 4.The ratio of the possible sunshine duration to the theoretical possible sunshine duration was 60 % on summer solstice and 55% on winter solstice.

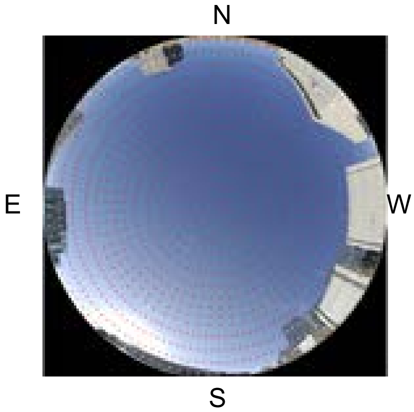

Figure 3 – Orthographic projection image calculating sky factor

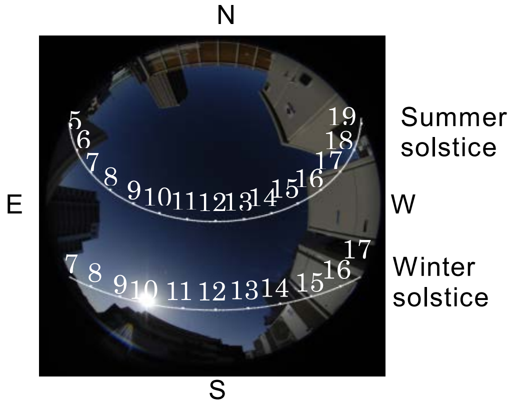

Figure 4 – Sunpath diagram and surronding buildings

2.2.2 Maintaining luminous flux

Luminance distribution image of light-emitting surface was taken as shown in Figure 5 to measure luminous flux. Images taken from different position showed that the surface of the light emitting area could be considered as Lambertian surface. Luminous flux from the light-emitting surface is calculated as follows,

$$F_o = \int L_o \, \pi \, \mathrm{d}S_o \tag{1}$$

where

- F_o is luminous flux from light emitting surface;
- L_o is luminance of light-emitting surface;
- S_o is area of light-emitting surface.

Figure 6 shows luminous flux at the exit of the light-transmitting unit, which is calculated from outdoor illuminance, by using the method shown in previous studies (Swift et al. 2008, AIJ 2010) and measured luminous flux at the exit of the light-emitting unit. The efficiency of the light emitting-unit (the ratio of luminous flux at the exit of the light emitting unit to that at the exit of the light-transmitting unit) was constantly 0,4. 3. We also found that the light emitting unit of the daylight duct system reduced luminous flux enough to provide natural luminance while avoiding discomfort glare.

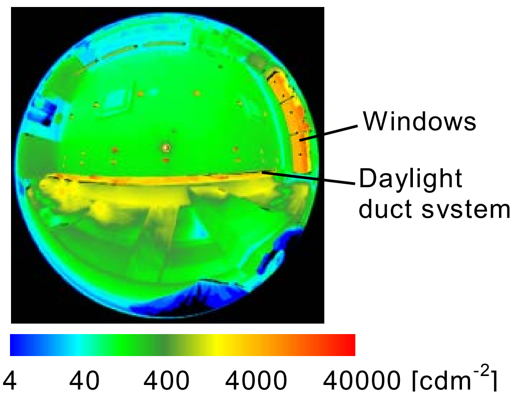

Figure 5 –Luminance distribution of ceiling (13:40)

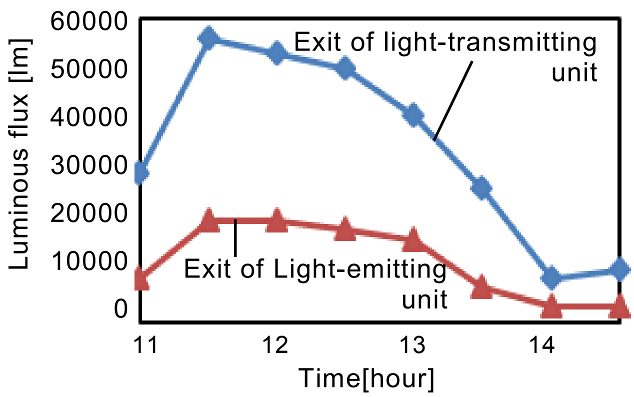

Figure 6 –Lumimous flux at exit of light-transmitting unit and at exit of light-emitting unit

2.2.3 Maintaining SPD

A preliminary experiment using scale model of duct (75mm×75mm×1000mm) was carried out. Three different mirror materials, aluminium, silver coated reflective aluminium and multilayer specular film were used. By using parallel light generated by a slide projector and Fresnel lens, spectral distributions of the reflectance of the three materials were measured. Figure 7 shows the results. It was shown that the reflectance of the multilayer film was even within the wavelength of visible range. That means the colour of light from the light-emitting unit is similar to daylight as show in Figure 8.

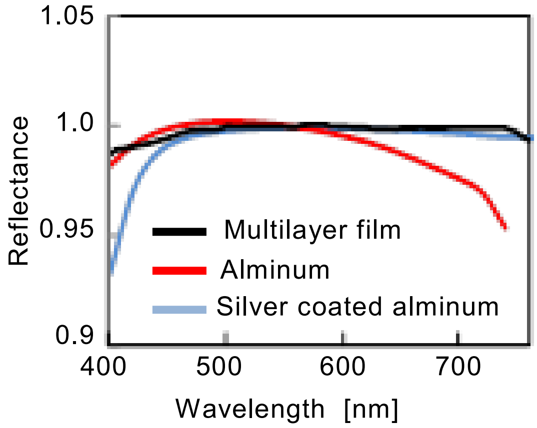

Figure 7– Spectral distribution of reflectance

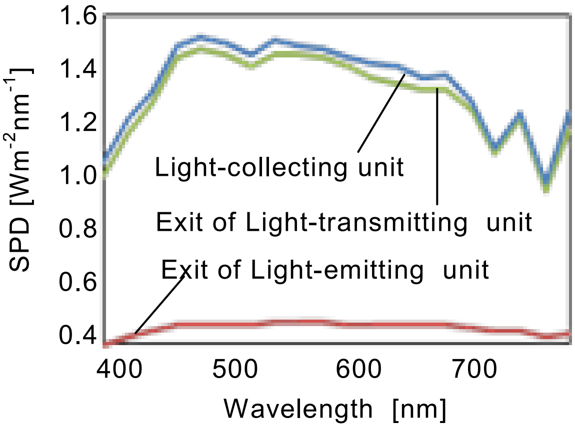

Figure 8– SPD at the exit of light-emitting unit

3 Investigation of customer behaviour

3.1 Methods

Customer behaviour was observed in the fast food restaurant on weekdays between June 27 to July 6 of 2012. Figure 9 shows a plan and a cross section of the eating and drinking area of the restaurant. Figure 9 shows a measurement point where horizontal illuminance, CCT, air temperature and relative humidity were measured every 10 minutes. Positions of luminaires and light–emitting unit of the daylight duct and window are also shown in Figure 9. The outline of luminaires is show in Table 2. The space was divided into 3 areas; area illuminated only by the electric lighting (I)(Figure 4), area illuminated by the daylight duct system (II) and area near the window (III).

Three cases were tested. Two were sunny days, one with the duct system and one without duct system. In the latter, the light-collecting unit of the system was covered by a blackout curtain. The third was a cloudy day with the duct system.

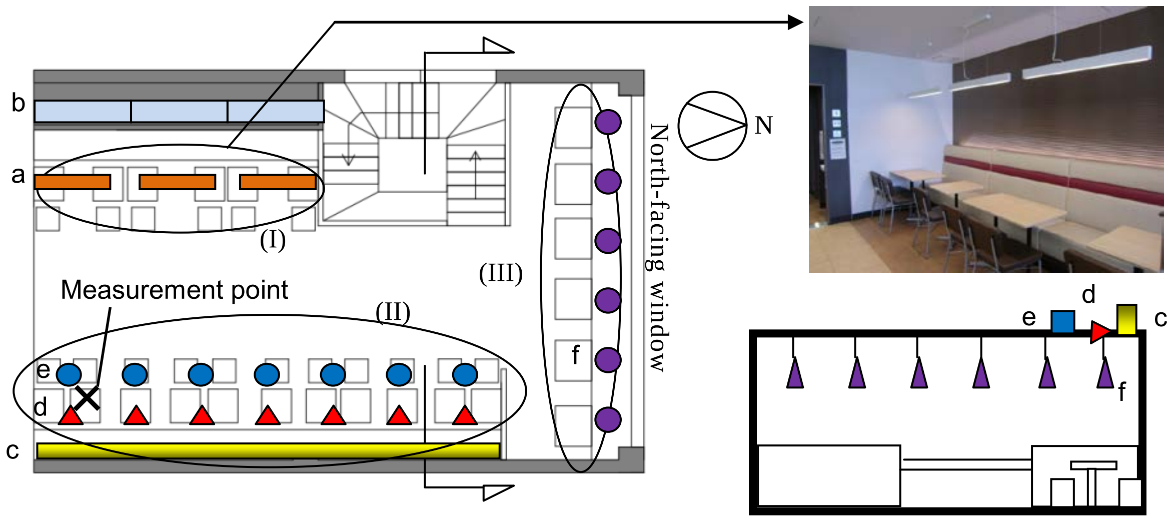

Figure 9 – Plan, Section and photo

Customer behaviour (seat choice, stay duration etc.) was observed and recorded every 10 minutes by an observer. In order to visually observe the customer behaviour without drawing attention to the observer; the observer sat down as a customer.

Table 2 – Kinds of luminaires

Symbol in Figure	Luminaire	lamp	*CCT*
a	Indirect pendant light	LED line unit 26W×1	3000K
b	Cornice light	LED14W×1	3000K
c	Daylight duct		
d	Spotlight	LED14W×1	3000K
e	Down light	LED14W×1	3000K
f	Pendant light	LED23W×1	3500K

3.2 Results

The numbers of customers are 106 on the sunny days with the duct system, 111 on the sunny days without the duct system and 121 on the cloudy days. Figure 10 shows the type of the customer. This restaurant has more female customers than male customer because it is located in a residential region in Tokyo.

Figure 11 shows the change in air temperature and relative humidity on a sunny day and on a cloudy day. Average air temperature was 25 degrees C (standard deviation =2 degrees) while average relative humidity was 65% (s.d.=10%).

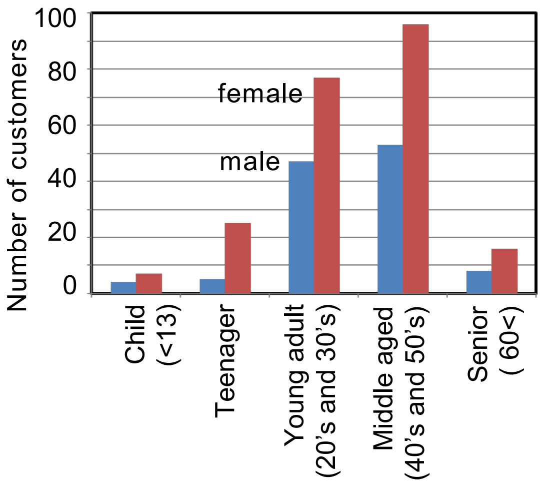

Figure 10 – Type of customers

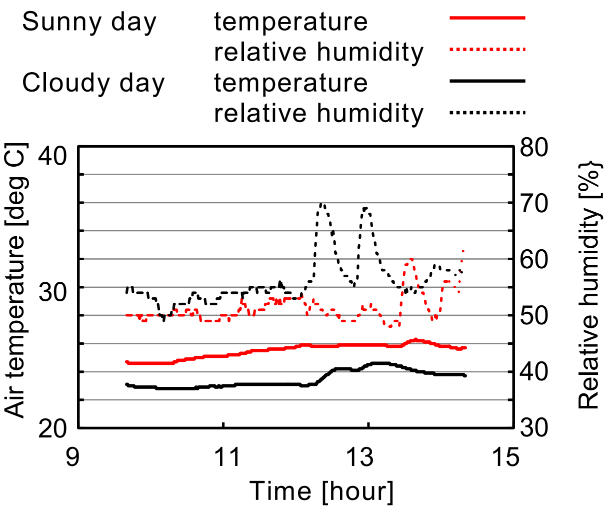

Figure 11 – Air temperature and relative humidity

Figures 12 and 13 show the change in illuminance and *CCT* at measurement point respectively. At 3 p.m. LED lighting installed inside of the light-emitting unit of the duct system is turned on. Light from the daylight duct system increased *CCT* as well as illuminance.

The average number of customers per a table n_{ave} and the percentage of occupied table time P_{occu} are defined as follows,

$$n_{ave} = \frac{\sum_{i=1}^{N} n_i}{N} \quad (2)$$

$$P_{occu} = \frac{\sum_{i=1}^{N} t_i}{N t_{observ}} \tag{3}$$

where

n_{ave} is the average number of customers per a table;
n_i is the number of customers at each table;
N is the number of tables;
P_{occu} is the percentage of occupied table time;
t_i is the occupied table time at each table;
t_{observ} is observation time.

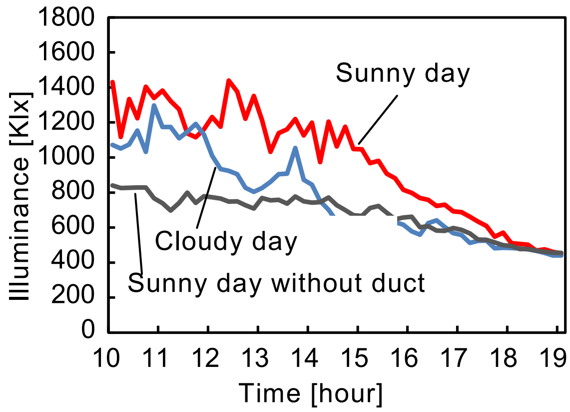

Figure 12 – Illuminance

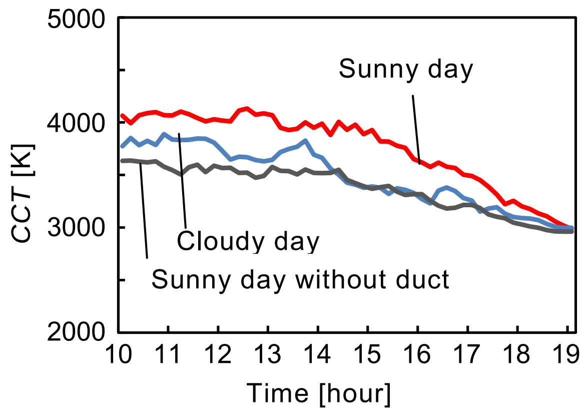

Figure 13 – *CCT*

Figures 14 and 15 show the average number of customers per a table n_{ave} and the percentage of occupied table time, respectively. The area illuminated by the daylight duct system showed a higher value of the average number of customers per a table, and a higher value of the percentage of occupied table time, on sunny days with the duct system. The area illuminated only by the electric lighting shows the highest value of both indices on cloudy days with daylight duct, while area near the window shows the higher value of both indices on sunny days without the daylight duct system.

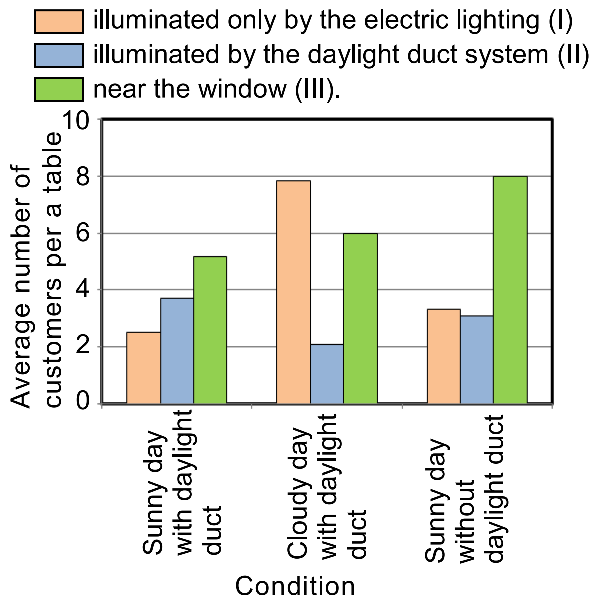

Figure 14 – Number of customer per a table

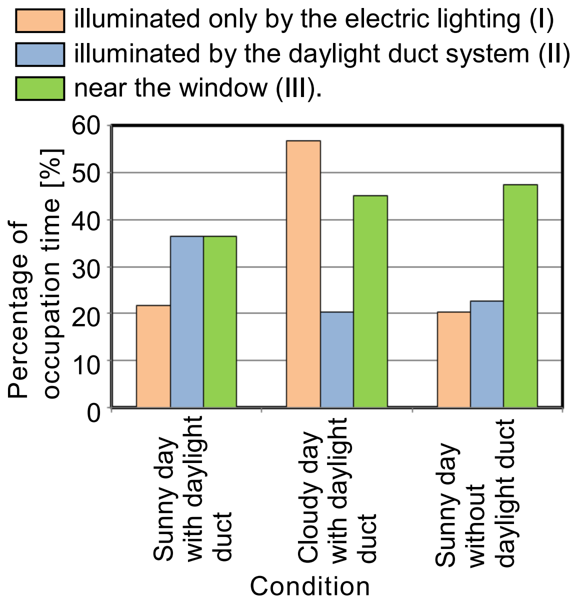

Figure 15 – Percentage of occupied table time

4 Subjective experiment

4.1 Methods

The experiment was carried out from 9 to 11 a.m. on October 9th, 10th and 11th, 2012.Twenty-four students (5 males and 19 females) participated as subjects. Figure x shows positions of the evaluation. There are four seat rows (Row (1)to (4)).

Semantic differential 7-point scale was used. As shown in Table 4 rating scales ask to evaluate the appearance of the food while 8 rating scales ask to evaluate atmosphere of the space. Four experimental conditions were tested: spotlight with daylight duct, spotlight without daylight duct, no spotlight with daylight duct, and no spotlight without daylight duct. A subject conducts the evaluation from all rows. Figure 17 shows subjects evaluating at the Row (2). Between changing condition, subjects were asked to leave the restaurant and re-enter.

.

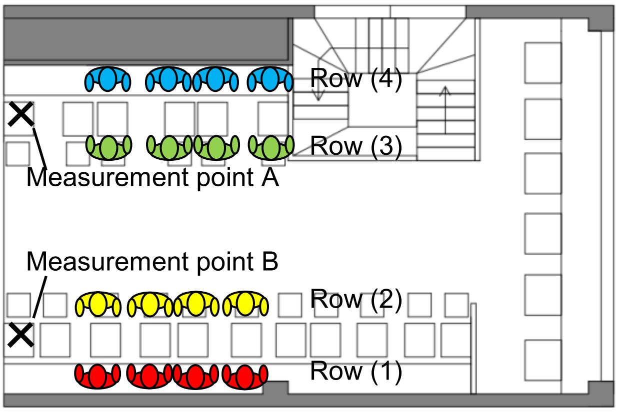

Figure 16 – Positions of subjects

Figure 17 – Subjects in Row (2)

Table 3 – Rating scale

Object evaluated	Question number	Semantic Differential Ratings	
Appearance of food	Q1	Colour looks natural	Colour looks unnatural
	Q2	Attractive	Unattractive
	Q3	Warm	Cold
	Q4	Glossy	Not Glossy
Atmosphere of space	Q5	Comfortable	Uncomfortable
	Q6	Like	Dislike
	Q7	Bright	Dark
	Q8	Open	Closed
	Q9	Cosy	Not cosy
	Q10	Glaring	Not glaring
	Q11	Relaxed	Not relaxed
	Q12	Warm space	Cool space

4.2 Results

Table 4 shows average illuminance and CCT during experiment. Average air temperature was 22 degrees C (s.d.=1 degrees) while average relative humidity was 50% (s.d.=5%).

Table 4 – Illuminance and *CCT* during Experiment

Conditions		Point A		Point B	
		Illuminance[lx]	CCT[K]	Illuminance [lx]	CCT[K]
Spot light turned on	With daylight duct system	577.8	3110	733.2	3782
	Without daylight duct system	536.9	3026	461.8	3395
Spot light turned off	With daylight duct system	528.6	2966	778.1	3546
	Without daylight duct system	519.1	2946	554.1	3217

Figures18 and 19 show the results of the SD rating (average and standard deviation) at Rows (1) and (2).When the spotlight was turned on, no significant difference in the ratings was found between with the daylight duct system and without the daylight duct, either at Row(1) or at Row(2).

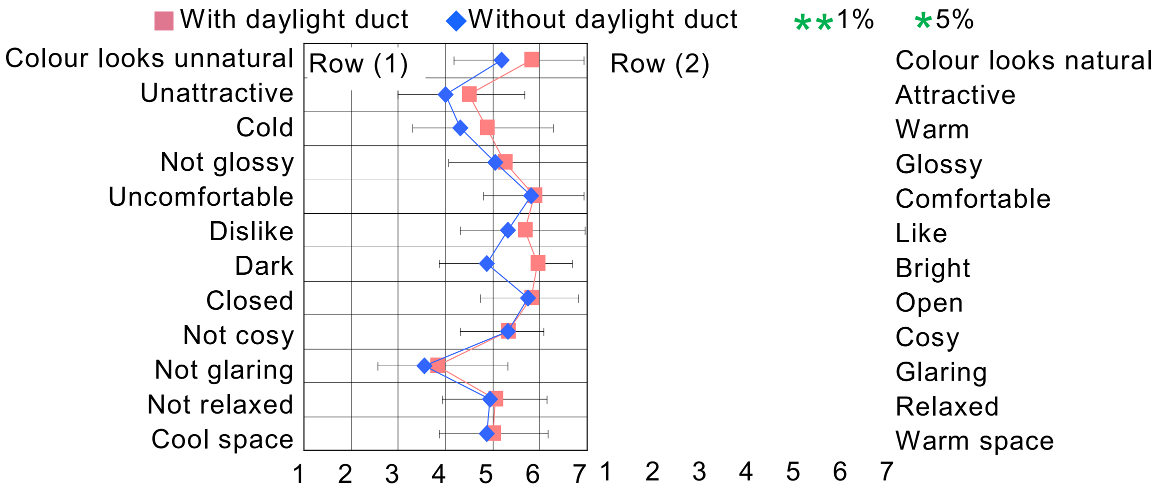

Figure 18– The result of SD ratings (when the spotlight was turned on)

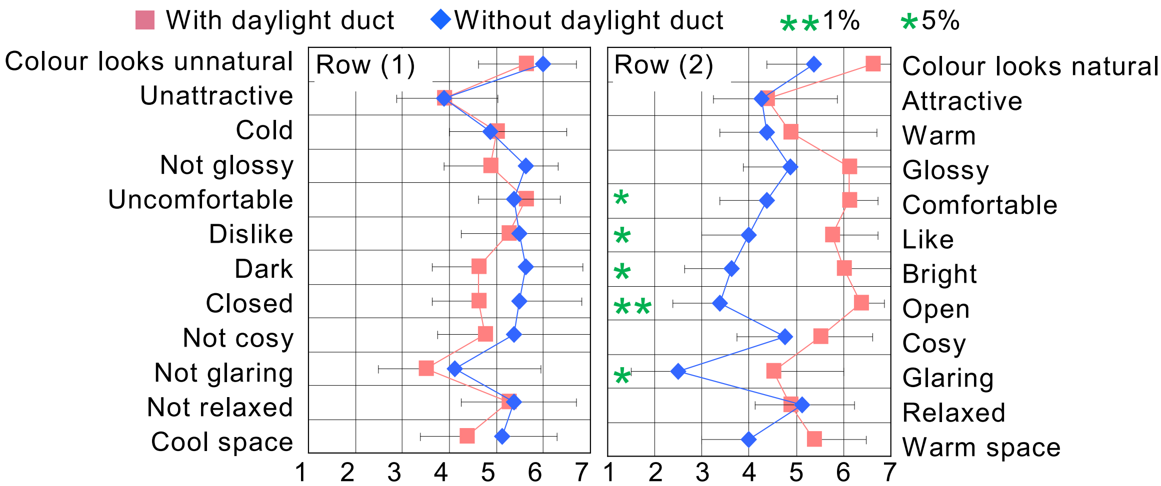

Figure 19 – The result of SD ratings (when the spotlight was turned off)

At the Row (2), when the spotlight was turned off, significant difference was found in some of the ratings between with the daylight duct system and without the daylight duct system, as shown in Figure 19.However at the Rows (1) (3) and (4), no significant difference was found between with and without the daylight duct system. The subjects at Row (2), who saw daylight from the daylight duct system, feel the space more open, brighter, more comfortable and preferable.

Table 5 shows the result of the factor analysis. Figure 20 shows biplot indicating scores of Factor 1 and Factor 2. For the subjects at the Row (2), where the subject feel the most uncomfortable, the space becomes more comfortable and the food becomes glossier when the space has daylight duct.

Table 5 – The result of Factor Analysis (Rotation:Varimax)

Semantic differential ratings	Factor 1	Factor 2	Factor 3
Like - dislike	**0.866**	0.132	0.141
Cozy- not cozy	**0.852**	0.017	0.051
Comfortable-uncomfortable	**0.827**	0.129	0.145
Open - closed	**0.710**	0.000	0.266
Relaxed – not relaxed	**0.700**	0.116	-0.236
Warm space – cool space	**0.512**	0.281	0.184
Colour looks natural – colour looks unnatural	**0.448**	0.360	0.100
Glossy – not glossy (food)	0.052	**0.786**	0.069
Warm – cold (food)	0.163	**0.728**	0.063
Attractive –Unattractive (food)	0.069	**0.690**	0.174
Bright - dark	0.471	0.058	**0.745**
Glaring – not glaring	-0.023	0.197	**0.522**
Contribution	32.29%	16.02%	9.00%
Accumulated contribution	32.29%	48.31%	57.31%

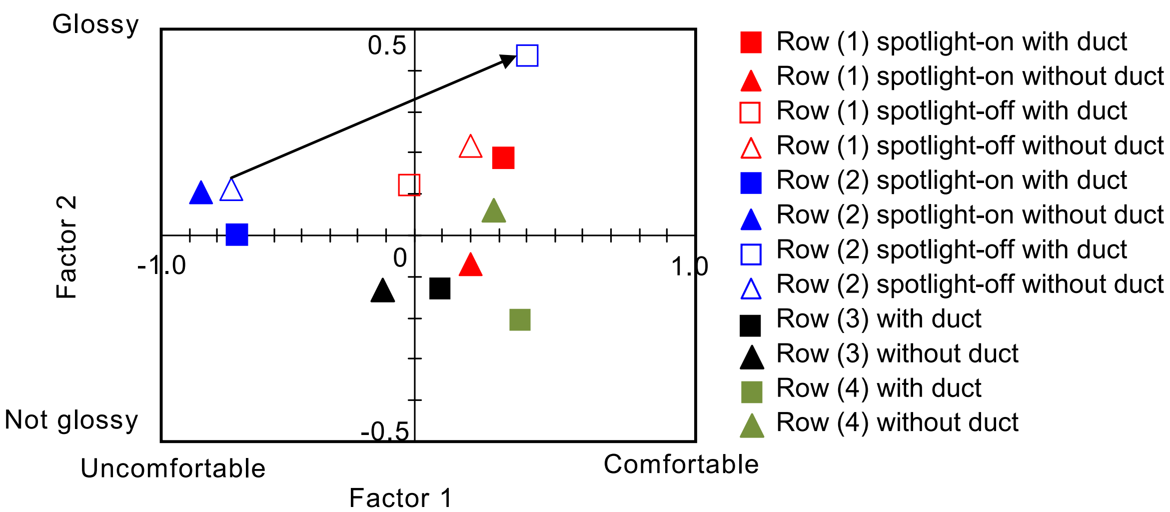

Figure 20 – Factor score of each condition

5 CONCLUSION

In order to identify the effect of the daylight duct system on the visual environment, performance measurements of the daylight duct system, an investigation of customer behaviour and an *in-situ* subjective experiment was carried out in the fast food restaurant with the daylight duct system. The following conclusions were obtained:

1. The measurement and calculation showed that only 40% of the luminous flux that passes through the light-collecting and light transfer units is ultimately emitted from the light emitting unit.

2. Due to the materials employed in the fabrication of the duct system, the spectral power distribution of daylight was not affected.

3. On a sunny day, customers preferred tables that were illuminated by the daylight duct system over tables illuminated by electric lighting only.

4. Subjects seated in the row, which is directly opposite the areas illuminated by the daylight duct system, found the space much more preferable with the electric lighting off and the daylight duct system in place.

Acknowledgement

We would like to express our thanks to Mr.A.Noro and Mr. A. Hirasa (Sumitomo 3M) and Mr. Y. Takekoshi (KFC Japan)for their collaborations.

References

MAWAEE, M. AI., CARTER, D. J. 2006. A Field Study of Tubular Daylight Guidance Installations Model for Calculation. Lighting Res. Technol., 38.3, 241-258.

SWIFT, P. D., LAWLOR, R., SMITH, G. B. GENTLE, A. 2008. Rectangular-Section Mirror Light Pipes. Solar Energy Materials & Solar Cells.,92, 969-975.

EDMONDS, I. 2010. Transmission of Mirror Light Pipes with Triangular, Rectangular, Rhombic and Hexagonal Cross Section. Solar Energy. 94, 928-938.

ARCHITECTURAL INSTITUTE OF JAPAN (AIJ) 2011. *Seeing, Using and Learning Environment-conscious Architecture*, Chapter 5.3. Tokyo. Ohmsha (in Japanese)

OP10

ANALYSIS OF SPATIALLY RESOLVED MEASUREMENT APPROACHES TO ASSESS SPECTRAL CHARACTERISTICS OF SKY PATCHES

Martine Knoop[1]
[1] Technische Universität Berlin, Berlin, GERMANY
martine.knoop@tu-berlin.de

Abstract

In order to properly evaluate the impact of daylight on human beings, materials, room appearance and energy conservation, it is required to generate data sets of long term spatially resolved spectral power distribution measurements of daylight. At the Technical University of Berlin, different measurement approaches were analysed and used to select a sky scanner that will be operational on site from summer 2014 onwards. The acquired, long term, measurements on orientation-depending daylighting conditions will be used to create data sets for research, lighting design and product development. Additionally to that, the collected information allows for further develop of equipment to obtain spectral characteristics of sky patches.

Keywords: Daylight, Orientation, Sky Patches, Spectral Sky Measurements, Sky Scanner

1 Introduction

Information about the spectral distribution of daylight is very relevant in the evaluation of the impact of daylight on human beings, materials, room appearance and energy conservation, for example to allow performance assessments of new technologies such as spectral selective fenestration materials or to determine the resulting non-visual effects of daylight in indoor and outdoor premises. To date, the typical attributes to describe the colorimetric characteristics of daylight are correlated colour temperature and spectral power distribution. In 2013, a project started at Berlin University of Technology to look into long term spectral power distribution measurements of sky patches, to create data sets with spatially and spectrally resolved daylight conditions. These data will offer the possibility to consider orientation-depending daylighting conditions in research, lighting design and product development. This paper analyses the different approaches to perform spatially and spectrally resolved measurements and motivates the chosen implementation at Berlin University of Technology.

1.1 Daylight spectral power distributions

In 1964, Judd et al. looked into typical daylight spectral power distributions based on 622 spectral measurements of skylight with and without sunlight conducted in Rochester (US), Enfield (UK) and Ottawa (CA). They indicated that the chromaticities of daylight lay on a curve more or less parallel to the Planckian curve in the CIE x,y chromaticity diagram. Judd et al. proposed a method for reconstruction of daylight spectral power distributions between 300 – 830 nm by means of three functions and two factors based on the chromaticity coordinates of the daylighting condition, which was adopted by the CIE to represent the spectral characteristics of outdoor daylighting conditions (CIE 1967, CIE 2004). Research showed that the linear model of the CIE with three dimensions gives a good estimate, especially between 330 and 700 nm (e.g. in Hernández-Andrés et al. 1998). To achieve higher accuracy and include UV or near IR a minimum of seven dimensions is required (e.g. Hernández-Andrés et al. 2001).

In 2004, Chain compared measured (1°, spot meter) and calculated spectral power distributions (380 - 780 nm) of sky patches with correlated colour temperatures in the range of 4 000 and 50 000 K. The results confirmed that the CIE method to construct spectral power distributions for daylight phases based on chromaticities is reliable for sky patches as well, and only slightly inaccurate for both ends of the visual spectrum (395 nm and > 650 nm).

Judd et al. (1964) found a variation in the above mentioned subsets of spectral measurements within the range of 330 – 400 nm and concluded that the ultraviolet content of daylight is poorly correlated with correlated colour temperature. By lack of available measurements, the authors extended the spectral distribution between 300 and 330 nm and beyond 700 nm based on Moon's data for spectral absorbance of the earth's atmosphere. CIE (2004) stated that variations in the daylight spectral power distribution related to season and geographic location are found, especially for the ultraviolet spectral region (e.g. by Kok et al. 1978, Kok et al. 1979, Dixon 1978). As the short wavelength contribution is of specific interest for the non-visual effects of lighting and the degradation of materials, the reconstitution of spectral power distribution as adopted by the CIE (1967) needs to be verified and extended. CIE (1994) recommends to consider to extend spectral measurements with the range between 280 and 380 nm (UV-B and UV-A).

The available daylight spectral power distributions are partly based on measurements combining diffuse (skylight) and direct light (sunlight) (e.g. the data set of Condit and Grum (1964) used in Judd et al. (1964) and already discussed in Hernandez-Andres et al. (2004)). Yet, the correlated colour temperature and the resulting spectral characteristics differ:

- skylight including sunlight: typically between 6 000 and 7 000 K (e.g. CIE 2013, based on work by Taylor and Kerr; Collins 1965),
- daylight from an overcast (north) sky: between 4 600 and 8 500 K (e.g. Henderson and Hodgkiss 1963; Nayatani and Wyszecki 1963)
- skylight from a clear (north) sky: between 5 000 and 25 000 K (CIE 2013), 40 000 K (Henderson and Hodgkiss 1963) up to 100 000 K (Nayatani and Wyszecki 1963)

Hernández-Andrés et al. (2003) indicated that the sky's luminance and spectral distribution is asymmetric and total differences of ΔE up to 160 can be found. Within the ultraviolet range, spatial variations in the spectral power distribution are found as well (e.g. Cordero et al. 2013; Blumthaler et al. 1996).

Resulting, the colorimetric characteristics of a specific region of the sky are of interest, when considering the wavelength dependent daylight contribution on a tilted plane or in a room.

1.2 Need for spatially and spectrally resolved daylight measurements

To get a better insight into the non-visual effects of daylighting, the degradation of materials or the functionality of spectral selective fenestration materials it is required to evaluate the (indoor) daylighting conditions with the appropriate lighting properties, representative for the prevailing sky conditions. For indoor applications, the indoor daylight illuminants as formulated in CIE (2009) are inadequate for this purpose, being derived for D50 and D65 only, with an average angle of incidence, an average thickness of glass and average spectral transmission factor.

Next to the (integrated) daylight and solar radiation measurements already typically monitored by daylight measuring stations, such as the International Daylight Measurements Program (IDMP) stations, orientation depending information is required. In order to consider different spectral weighting functions for non-visual effects of lighting (Lucas et al. 2014) or spectral selective transmission functions for fenestration materials, the actual daylight spectral power distribution is desired to describe the outdoor illuminant more accurately and to address requests from the lighting community looking into research, design and technology development.

2 Review of existing approaches

A literature review identified different approaches to conduct spatially and spectrally resolved measurements. The presented approaches are representative for the bandwidth of available solutions. The solutions look into characteristics of patches of the sky hemisphere: spectral power distribution (SPD), sky radiance (L_e) or the contribution of specified wavelengths. All reviewed solutions can conduct a complete measurement series within 10 minutes. In some cases the spectral approach can be separated from the spatial approach and could be cross-linked with others. Spatially resolved solutions optimized for a specific weighting function are not included in the review. Global and orientation dependent measurements as addressed in the introduction of this paper are also not included.

2.1 Sky radiance $L_{e,200\text{-}1100\ nm}$

As a measuring instrument for solar radiation dependent applications, such as daylight control and harvesting systems, the University of Paderborn developed a 'Solar Igel' (solar hedgehog) to monitor sky radiance, L_e, distribution (Bendfeld et al. 2000). The measuring instrument has 135 fixed sensors with an aperture angle of 14,5°, which allows a high coverage of the sky, with some overlap in sky patches (see Ineichen 2007). Irradiance, as well as global and diffuse irradiance on the horizontal plane, is measured every second, and one-minute average values are saved. Irradiance is measured within 200 and 1100 nm. The advantage of this solution is the scan time as well as the robustness of having no moving parts. On the other hand, a large number of sensors is needed and calibration is time consuming, as each sensor has to be calibrated individually. The installation needs to be monitored on pollution. At this stage, only integral measurements are conducted, and spectral measurements would require a large number of more expensive sensors.

2.2 $SPD_{290\text{-}550nm}$ and specified wavelengths

Spatially resolved sky radiance measurements within the short wavelength range have been performed by a number of researchers. Two recent examples can be found in Cordero et al. (2013) and Sandmann and Stick (2014). In both cases, a double monochromator spectroradiometer was used, placed in a temperature controlled box, with a fiber optic and a (collimator) tube realizing an opening angle of 4,5° (4,84 x 10^{-3} sr) and 5° (5,98 x 10_{-3} sr) respectively. In both cases the input optic was automatically pointed to the positions to be measured, using a scanner or a two axis positioner.

Cordero et al. (2013) measured 79 points (including at the zenith) in a single-wavelength scan (e.g. 320 and 400 nm). A complete single-wavelength scan of the sky hemisphere took approximately 4 minutes. In the second type of scan, in which the spectral irradiance was measured within a bandwidth of 290 – 550 nm at 1 nm intervals for two points on horizon height (land and sea) and at the zenith. A spectral irradiance scan took approximately 5 minutes.

Sandmann and Stick (2014) included 107 predetermined positions on the sky hemisphere, as well as the actual position of the sun in the measurements. Each measurement took approximately 5 seconds, resulting in a total of 9 minutes per sky scan. Radiance was measured at 307, 350 and 550 nm, spatial radiance distributions of the sky hemisphere were derived by inverse distance weighted (IDW) interpolation method.

(Double) monochromator measurements are highly accurate, but time-consuming when scans of the complete sky hemisphere are required.

2.3 Reconstruction of $SPD_{380\text{-}780nm}$

Research by Hernandez-Andres et al. (2004), based on work by Min and Harrison (1998) has shown that the input of three specified Gaussian sensors is sufficient to reconstruct daylight and skylight spectral power distributions within a spectral range of 380 – 780 nm. This is used by the authors to develop a trichromatic CCD camera with a fish-eye lens (e.g. López-Álvarez et al. 2008), allowing a sky scan within a time frame smaller than 1 second. A comparison of measurements with a spectroradiometer in many different situations and those obtained with the CCD camera show that the CCD measurements are, according to the author, reliable enough to obtain normalized spectral power distributions, but cannot be used for absolute radiometric information.

Tohsing et al. (2014) also used a compact camera with a fish eye lens (field of view 183°) and three channels, red, green and blue, with a maximum response at 602, 527 and 441 nm respectively, to reconstruct spectral power distribution and to derive spectral sky radiance. The results were compared with measurements of 113 sky patches collected with a CCD array spectroradiometer system. A deviation of less than 20% was found for the spectral sky radiance and (reconstructed) spectral power distributions between 380 and 760 nm under all sky conditions. The authors conclude that the RGB system provides reasonable accurate and reliable information.

Cameras have a short scan time and high robustness due to the fixed position of the system, without moving parts. The accuracy of reconstructed spectral power distributions is not acceptable for all applications.

2.4 Specified wavelengths

Spectral and spatial radiance measurements within the visible spectral range were already proposed and performed by Dehne in 1971. In his research, Dehne used a sky scanner equipped with a light-beam oscilloscope using a flexible optical conductor with an aperture angle of 2 x 4,9° to obtain radiance measurements for 409, 561 and 620 nm. Model measurements were conducted, but no long term monitoring has been published in literature.

2.5 Reconstruction of $SPD_{380\text{-}780nm}$ with sky luminance

Chain (2004) conducted a large number of manual measurements with a spectroradiometer with an aperture angle of 1° in 77 measuring points at the sky hemisphere. Cloud coverage was determined through pictures made before and after the series of measurements, the sky luminance in 145 sky patches according to Tregenza (1987) was derived at the nearby IDMP station. To that, Chain included one year measurements for an aperture angle of 20° in 4 orientations and pointed to the zenith, each 10 minutes.

From these measurements, Chain proposed a novel approach for implementation of spectral and directional characteristics of daylight in lighting design (described in Chain et al. 2003, Chain 2004). In this approach a LCF factor (luminance to correlated colour temperature) was introduced, depending on sun height (linear), and sky type, brightness and clearness according to Perez (logarithmic). The resulting correlated colour temperature is used to reconstruct the spectral power distribution (Chain et al. 1999). This approach was validated within the research of Chain (2004). The author concludes that it provides reasonable accurate information, and spectral characteristics could be derived from sky luminance measurements.

Luminance sky scanners are already in place in daylight measuring stations, and researchers as well as the community working with high-end daylighting simulations tools are experienced in using acquired luminance data sets. The approach to reconstruct spectral power distributions from these luminance data, combined with information on sky type and clearness is not implemented in daylighting simulation tools up till now. Further validation of this approach seems to be necessary.

2.6 $SPD_{250 \text{ and } 874 \text{ nm}}$

Kómar et al. (2013) constructed a portable sky scanner to obtain measurements that are used to determine relative indicatrix functions and relative gradation of sky luminances to compute diffuse irradiance on arbitrary inclined surfaces. The sky scanner, with an aperture angle of 11°, is equipped with an array spectroradiometer with a spectral range of 250 to 874 nm, realized by using neutral density filters. A complete scan of 145 sky patches of the hemisphere takes about 5 minutes. The authors estimate a maximum measurement uncertainty of 11%, due to measurement uncertainties in the spectroradiometer's calibration and the determination of the filters' transmittance and stray light, as well as the effect of using the entire measuring system on a tripod. Detailed spectral information is not available for the public up till now.

A similar set up was used by Leers et al. (2011); a sky scanner with a spectrometer to obtain spectral measurements within an aperture angle of 5° in 61 positions distributed over the sky hemisphere.

The sky scanners use an array spectroradiometer, allowing fast sky scans with an appropriate accuracy in the visible spectral range. A scan scanner has moveable parts and can be expected to be less robust.

2.7 Summary

In principle, different levels of spatially and spectrally resolved solutions can be found in the literature. One can distinguish by the used

- mechanics: a moving construction (sky scanner, two axis positioner) or a fixed construction (CCD camera, Solar Igel), and
- measuring equipment: RGB sensors, a (double) monochromator or an array spectro-radiometer.

Typically, the spectral power distribution between 380 and 780 nm is determined by actual measurements of the complete range or through reconstruction. Spatially resolved measurements in the short wavelength range are typically focusing on a few wavelengths.

3 Spatially and spectrally resolved daylight measurements at TUB daylighting measuring station

From summer 2014 onwards, spatially and spectrally resolved data for daylight will be collected at the lighting measuring station at the Berlin University of Technology (TUB). The collected data will be used for the following projects:

1) Characterization of spatially and spectrally resolved daylight conditions to create data sets that can be used in simulations tools, to
2) support healthy lighting design and development of spectral selective products.
3) Further development of measuring equipment to assess the required spatially and spectrally resolved characteristics of daylight.

The following requirements were drawn up for the measuring equipment to be installed at the daylighting measuring station at the TUB.

Spatially resolved – In line with recommended practice for luminance measurements (CIE 1994), bidirectional measurements of complex fenestration systems (e.g. Boer 2006; Aydinli and Kaase 1999) and the use of sky models in software tools such as Radiance (e.g. Ward et al. 2011; Mardaljevic 2000), a subdivision of the sky hemisphere in 145 sky patches according to Tregenza (1987; CIE 1994) is adopted for this purpose. CIE (1994) suggests a field of view of 11°, and indicates that smaller aperture angles can be used as differences in mean values are expected to be very small.

Spectrally resolved – The majority of projects at the TUB require a spectral range of 320 – 830 nm, essential to determine indoor daylighting conditions, the non-visual response to light as well as the performance of spectral selective products. As stated before, the CIE (1994) recommends to include measurements up to 280 nm. This project will consider the actual daylight spectral power distribution within the range of 280 – 830 nm to describe the outdoor illuminant more accurately.

As stated before, Hernandez-Andres et al. (2004) found that the input of three specified (optimum spectral position and bandwidth) Gaussian sensors is sufficient to reconstruct daylight and skylight spectral power distributions within a spectral range of 380 – 780 nm with a linear recovery algorithm.

With respect to the short wavelength spectral range, a number of approaches can be found. Min and Harrison (1998) looked into reconstruction of spectral power distributions from a multifilter narrowband, addressing accuracy and uncertainty due to measurement and calibration errors. Davis et al. (2005) and Wang et al. (2006) report of reconstruction of the UV spectral power distributions based on irradiance measurements for seven specific wavelengths (300, 305, 311, 317, 325, 332,and 368 nm) with a Multiple Filter Rotating Shadow band Radiometer (UV MFRSR). With an advanced neural network-based model, Feister et al. (2005) derived solar spectral irradiance from five narrowband irradiance measurements collected with a UV spectroradiometer on a filter model basis (UV-SPRAFIMO).

Resulting, three different approaches could be applied to determine the spectral distribution of daylight within 280 and 830 nm, using:

1) spectral irradiance or radiance measurements over the complete bandwidth,
2) daylight chromaticities or measurements with three specified sensors to reconstitute the spectral power distribution between 380 – 780 nm, combined with high precision spectral measurements within a bandwidth of 280 and 380 nm.
3) a total of up to 10 specified measurements for the reconstruction of both ranges; three for the visible spectral range combined with five to seven narrow band measurements

To allow for radiometric, photometric, and colorimetric evaluation, spectral irradiance or radiance measurements are preferred at this moment over the reconstitution of daylight spectral power distribution. The spectral irradiance, $E_{e\lambda,11°}$, is to be measured within a maximum solid angle of 0,0289 steradian (11° aperture angle), for a bandwidth of at least 320 – 830 nm, with a possible extension to 280 nm, which will provide the spectral radiance $L_{e\lambda}$ of 145 pre-defined sky patches.

For the daylighting measuring station at the TUB, the following of the above mentioned approaches were considered:

- the Solar Igel mechanics, because of its robustness. Increasing the number of sensors up to 145 and reducing the aperture angle, results in an appropriate spatial resolution of measurements. Requiring 145 measuring units to assess the spatially and spectrally resolved power distribution, a cost effective sensor or a combination of cost effective sensors to reconstruct spectral power distributions needs to be looked into.
- the reconstruction of spectral power distributions from sky luminance measurements as proposed by Chain. A luminance sky scanner is already in place at the measuring station of the TUB.
- the sky scanner as already used extensively for sky luminance measurements, and adopted for spectral measurements by Kómar et al.. Only one single sensor or sensor head is required, which can be more costly, to achieve high quality or to use a sensor tailor made to the specifications of the project. Depending on the used measuring equipment, fast sky scans can be performed.

The first two solutions need further validation or development, and seem to be suitable for spectral analysis within the visual spectral range only. Therefore, the sky scanner solution is preferred at the moment. Detailed measurements acquired with this measuring equipment will give further insight into the development of the Solar Igel approach as well as the Chain reconstruction based on luminance measurements. This will allow the development of more robust and / or faster measuring equipment.

The sky scanner solution, which will collect data for 145 sky patches, will be provided with measuring equipment fulfilling the specifications within the project. Typically, spectral measurements including the short wavelength spectral range are conducted with a (double) monochromator to achieve high precision, with a considerable measuring time. Alternatives are broadband instruments, multi-channel filter instruments and array spectroradiometers. Broadband instruments do not provide spectrally resolved measurements, and multi-channel filter instruments require the reconstruction of spectral power distributions as discussed before. Array spectroradiometers allow fast measurements and have therefore been discussed in recent literature as an alternative for the monochromator solution. Array spectroradiometers suffer from stray light from the longer wavelength regions which especially affects the measurements in the short wavelength range (typically < 300 nm according to Seckmeyer et al. 2010). Blumthaler et al. (2013) give guidelines relevant for the application of array spectroradiometers for this purpose, including measurements that should be repeated on a regular basis, such as measurements for stray light over the whole spectral range and the spectral structure of the dark signal.

To allow the possibility to combine measurements of a luminance sky scanner available at the measuring site of TUB, the recommended time frame for luminance distribution measurements according to CIE (1994) was adopted. Spectral measurements should be made (at least) every 30 minutes centred at 15 and 45 minutes after the hour. The duration of the complete sky scan should be as short as possible, for luminance measurements CIE recommends an upper limit of 2,5 minutes. Within this time frame, a sky scan of 145 patches for a spectral range from 320 – 830 nm with wavelength intervals from 2 nm to 5 nm is not feasible with a (double) monochromator. Therefore it was decided to use a single array spectroradiometer in the set up.

3.1 Description of the spectral sky scanner

The spectral measurements will be performed with an array spectroradiometer (Zeiss Multi-Channel-Spectrometer MCS CCD with a Hamamatsu back-thinned CCD) using a maximum step size of 5 nm between 280 and 980 nm. The input optic has an aperture angle of 10° (0.0239 steradian). The spectroradiometer measures the spectral irradiance, $E_{e\lambda,10°}$, which will provide the spectral radiance $L_{e\lambda}$. To operate the device under stable temperature conditions, it is placed in a temperature-controlled box.

A sky scanner based on a two axis goniometer was chosen for this project. The sky scanner (by Czibula & Grundmann) is functionally identical to the PRC Krochmann sky scanner for luminance measurements already available at the daylighting measuring station (see Figure 1). This is allows for comparison between measurements. The axial range of rotation is 180° vertically and ± 90° horizontally, realized through vertical rotation of the optic housing and horizontal movements of the spectroradiometer. 145 sky patches according to Tregenza are covered within one scan across the sky hemisphere, which takes about one minute, with a longer duration for twilight. Sky patches in the vicinity of the sun will not be taken into consideration to prevent inaccuracy due to scattered light within the instrument, as well as to protect the photocell.

Figure 1 – sky scanner at the daylighting measuring station, Berlin University of Technology

4 Discussion and Outlook

The chosen measuring equipment has also drawbacks. At this stage, the majority of projects at the TUB require a spectral range of 320 – 780 nm, but an extension of the spectral to 280 – 830 nm is considered to describe the outdoor illuminant more accurately. As stated before, array spectroradiometer can be inaccurate in the short wavelengths range. Given guidelines for the use of array spectroradiometers (e.g. Blumthaler et al. 2013) will be taken into consideration. In order to validate these measurements, a monochromator equipped with a fiber optic and a tube with apertures realizing an opening angle of 10° will be used to measure the spectral irradiance, $E_{e\lambda,10°}$. The monochromator will be fixed and pointed to a pre-defined sky patch in the upper part of the sky hemisphere, as the radiance at the zenith tends to be higher than at the horizon for shorter wavelengths (Cordero et al. 2013). The measurement sequences of the monochromator, the spectral sky scanner as well as the luminance sky scanner will be aligned in time, to ensure data sets that can be combined and compared.

In comparison to the monochromator and luminance sky scanner, the array spectrometer has a higher detection threshold. This needs to be taken into consideration for measurements during twilight. Threshold irradiance values to obtain accurate measurements will be determined in a laboratory setting. Integral irradiance measurements derived with the existing luminance sky scanner will be used to get insight in these threshold values, their frequency, and the impact as well as relevance for running and future projects at TUB.

The measurements obtained from summer 2014 onwards will be used to provide data sets for research, lighting design and product development. Next to that, the measurements will provide information for further development of measuring equipment to assess the required spatially and spectrally resolved characteristics of daylight. Firstly, equipment with reduced complexity will be looked at. In this, the previously mentioned luminance approach of Chain, the Solar Igel of the University of Paderborn, as well as the possibilities of using a simplified sensor head that allows reconstruction of a wide spectral range with a total of up to 10 specified measurements, will be considered. The latter could be considered for the second approach in development of measuring equipment for this purpose, focusing on a broader spectral range, an increased accuracy and a higher sensitivity to also address twilight conditions. In the near future, this project will provide reliable and detailed data sets for a large variety of applications, to evaluate the orientation-depending impact of daylight on human beings, materials, room appearance and energy conservation.

Acknowledgements

The presented work is part of the project “Environmental and ergonomic optimization of new lighting solutions for retrofitting and new construction of buildings” (03ET1148B) funded by the Federal Ministry of Economics and Technology (BMWi).

References

Aydinli, S.; Kaase, H. 1999. Measurement of Luminous Characteristics of Daylighting Materials. http://task21.iea-shc.org/data/sites/1/publications/report.pdf.

Bendfeld, J.; Gruffke, M.; Ortjohann, E.; Voß, J. 2000. Der Solar-Igel Neue Möglichkeiten der Steuerung solarstrahlungsabhängiger Anlagen und Geräte. Bundes Bau Blatt. 3.

Blumthaler, M.; Gröbner, J.; Egli, L.; Nevas, S. 2013. A guide to measuring solar UV spectra using array spectroradiometers. In: Radiation Processes in the Atmosphere and Ocean (IRS2012). Proceedings of the International Radiation Symposium (IRC/IAMAS). Dahlem Cube, Free University, Berlin, 6–10 August 2012. pp. 805–808.

Blumthaler, M.; Gröbner, J.; Huber, M.; Ambach, W. 1996. Measuring spectral and spatial variations of UVA and UVB sky radiance. Geophysical Research Letters. 23. pp. 547–550.

Boer, J. d. 2006. Modelling indoor illumination by complex fenestration systems based on bidirectional photometric data. Energy and Buildings. 38. pp. 849–868.

Chain, C. 2004. Caractérisation spectrale et directionnelle de la Lumière naturelle : Application à l Éclairage des Bâtiments. Thesis of ENTPE, Laborataire des Sciences de l'Habitat, Département Génie Civil et Bâtiment.

Chain, C.; Dumortier, D.; Fontoynont, M. 1999. A comprehensive model of luminance, correlated colour temperature and spectral distribution of skylight: Comparison with experimental data. Solar Energy. 65. pp. 285–295.

Chain, C.; Dumortier, D.; Fontoynont, M. 2003. Lighting simulation using spectral and directional characteristics of daylight and glazing. In: CIE 152-2003 Proceedings of the 25th session of the CIE.

CIE 1967. CIE 14-1967 Recommendations on standard illuminants for colorimetry. In: CIE Washington Session. pp. 95–97.

CIE 1994. CIE 108-1994 Guide to recommended practice of daylight measurement. Vienna. CIE Central Bureau.

CIE 2004. CIE 15-2004 Colorimetry. Vienna. CIE Central Bureau.

CIE 2009. CIE 184-2009 Indoor daylight illuminants. Vienna. CIE Central Bureau.

CIE 2013. CIE 204-2013 Methods for Re-defining CIE D Illuminants. Vienna. CIE Central Bureau.

Collins, J. F. 1965. The colour temperature of daylight. British Journal of Applied Physics. 16. pp. 527–532.

Condit, H. R.; Grum, F. 1964. Spectral Energy Distribution of Daylight. Journal of the Optical Society of America. 54. pp. 937–944.

Cordero, R. R.; Damiani, A.; Da Silva, L.; Laroze, D.; Labbe, F. 2013. Spectral UV radiance measured at a coastal site: a case study. Photochemical & Photobiological Sciences. 12. pp. 1193.

Davis, J. M.; Slusser, J. R.; Bernhard, G.; Herman, J. R.; Gao, W. 2005. In: Optics & Photonics 2005. San Diego, CA, 31 July 2005. pp. 58860B.

Dehne, K. 1971. Die Entwicklung eines Sky-scanners zur kurzzeitigen Bestimmung der Verteilung der spektralen Strahldichte über das Himmelsgewölbe in drei sichtbaren Spektralbereichen. Thesis of Fachbereich Physik, Universität Hamburg. Hamburg.

Dixon, E. R. 1978. Spectral distribution of Australian daylight. Journal of the Optical Society of America. 68. pp. 437.

Feister, U.; Kaifel, A.; Grewe, R. D.; Kaptur, J.; Gericke, K.; Reutter, O.; Wohlfart, M. 2005. Fast measurements of solar spectral UV irradiance—first performance results of two novel spectroradiometers. Optical Engineering. 44. pp. 41007.

Henderson, S. T.; Hodgkiss, D. 1963. The spectral energy distribution of daylight. British Journal of Applied Physics. 14. pp. 125–131.

Hernandez-Andres, J.; Nieves, J. L.; Valero, E. M.; Romero, J. 2004. Spectral-daylight recovery by use of only a few sensors. Journal of the Optical Society of America A. 21. pp. 13.

Hernández-Andrés, J.; Lee, R. L.; Romero, J. 2003. Color and Luminance Asymmetries in the Clear Sky. Applied Optics. 42. pp. 458.

Hernández-Andrés, J.; Romero, J.; García-Beltrán, A.; Nieves, J. L. 1998. Testing Linear Models on Spectral Daylight Measurements. Applied Optics. 37. pp. 971.

Hernández-Andrés, J.; Romero, J.; Nieves, J. L.; Lee, Jr., R. L. 2001. Color and spectral analysis of daylight in southern Europe. Journal of the Optical Society of America A. 18. pp. 1325.

Ineichen, P. 2007. Sky luminance/radiance distribution Quality control.

Judd, D. B.; MacAdam, D. L.; Wyszecki, G.; Budde, H. W.; Condit, H. R.; Henderson, S. T.; Simonds, J. L. 1964. Spectral Distribution of Typical Daylight as a Function of Correlated Color Temperature. Journal of the Optical Society of America. 54. pp. 1031.

Kok, C. J.; Chalmers, A. N.; Hengstberger, F. 1978. Measurement of the middle ultraviolet at Durban. Atmospheric Environment (1967). 12. pp. 1119–1123.

Kok, C. J.; Chalmers, A. N.; Turner, R. 1979. Spectroradiometry of daylight at sea level in the Southern Hempsphere: Durban. S.-Afr. Tydskr. . 2. pp. 47–53.

Kómar, L.; Rusnák, A.; Dubnička, R. 2013. Analysis of diffuse irradiance from two parts of sky vault divided by solar meridian using portable spectral sky-scanner. Solar Energy. 96. pp. 1–9.

Leers, M.; Preiss, A.; Ferretti, N.; Krauter, S. 2011. Measurement of spectral-spatial distribution of global irradiance. In: The most inspiring platform for the global PV solar sector ; CCH Congress Centre and International Fair. Hamburg, Germany, 5 - 9 September 2011. pp. 3378–3382.

López-Álvarez, M. A.; Hernández-Andrés, J.; Romero, J.; Olmo, F. J.; Cazorla, A.; Alados-Arboledas, L. 2008. Using a trichromatic CCD camera for spectral skylight estimation. Applied Optics. 47. pp. H31.

Lucas, R. J.; Peirson, S. N.; Berson, D. M.; Brown, T. M.; Cooper, H. M.; Czeisler, C. A.; Figueiro, M. G.; Gamlin, P. D.; Lockley, S. W.; O'Hagan, J. B.; Price, L. L.; Provencio, I.; Skene, D. J.; Brainard, G. C. 2014. Measuring and using light in the melanopsin age. Trends in Neurosciences. 37. pp. 1–9.

Mardaljevic, J. 2000. Daylight Simulation: Validation, Sky Models and Daylight Coefficients. Thesis of Institute of Energy and Sustainable Development, De Montfort University.

Min, Q.; Harrison, L. C. 1998. Synthetic spectra for terrestrial ultraviolet from discrete measurements. Journal of Geophysical Research. 103. pp. 17033.

Nayatani, Y.; Wyszecki, G. 1963. Color of Daylight from North Sky. Journal of the Optical Society of America. 53. pp. 626.

Sandmann, H.; Stick, C. 2014. Spectral and Spatial UV Sky Radiance Measurements at a Seaside Resort Under Clear Sky and Slightly Overcast Conditions. Photochemistry and Photobiology. 90. pp. 225–232.

Seckmeyer, G.; Bais, A.; Bernhard, G.; Blumthaler, M.; Drüke, S.; Kiedron, P.; Lantz, K.; McKenzie, R. L.; Riechelmann, S.; Kouremeti, N. 2010. Instruments to measure solar ultraviolet radiation, part 4: array spectroradiometers.
http://www.wmo.int/pages/prog/arep/gaw/documents/GAW191_TD_No_1538_web.pdf.

Tohsing, K.; Schrempf, M.; Riechelmann, S.; Seckmeyer, G. 2014. Validation of spectral sky radiance derived from all-sky camera images – a case study. Atmospheric Measurement Techniques Discussions. 7. pp. 69–97.

Tregenza, P. 1987. Subdivision of the sky hemisphere for luminance measurements. Lighting Research and Technology. 19. pp. 13–14.

Wang, X.; Gao, W.; Slusser, J. R.; Davis, J.; Gao, Z.; Scott, G.; Olson, B.; Krotkov, N.; Xu, M.; Liang, X.-Z.; Ustin, S. L. 2006. In: Optics & Photonics. San Diego, CA, 13 August 2006. pp. 62980L.

Ward, G.; Mistrick, R.; Lee, E. S.; McNeil, A.; Jonsson, J. 2011. Simulating the Daylight Performance of Complex Fenestration Systems Using Bidirectional Scattering Distribution Functions within Radiance. Leukos, Journal of the Illuminating Engineering Society of North America. 7.

OP12

WHITENESS METRIC FOR LIGHT SOURCES

Aurélien DAVID[1], Michael R. KRAMES[1], Minchen WEI[2] and Kevin W. HOUSER[2]
[1]Soraa Inc., Fremont CA, USA
[2]Dept. of Architectural Engineering, Pennsylvania State University, University Park PA, USA
adavid@soraa.com

Abstract

We discuss the impact of a light source's spectral power distribution (SPD) on the rendering of white objects containing fluorescent whitening agents. We put forth a formula to quantify the whiteness of an object under sources of arbitrary correlated colour temperature (CCT). We show that standard white LEDs don't render enhanced whiteness, but that violet-pumped white LEDs can. Finally, we argue for the necessity of a source whiteness metric and discuss some of the aspects of such a metric.

Keywords: Whiteness rendering, Optical Brightening Agents, Fluorescent Whitening agents, Colour fidelity, Light-emitting Diodes, Quality of light.

1 Whiteness enhancement and fluorescent whitening agents

The strive to obtain ever-purer white materials is centuries-old. The first step to obtain a bright white colour is to remove any absorption in the material, for instance by a bleaching process. However, it was realized early on that slight chromatic shifts could further enhance the *perception* of whiteness: an object with a slight bluish tint usually appears whiter to an observer than a material with a similar reflectance but no tint. For this reason, small amounts of yellow-absorbing dyes have been added to some white materials.

The ability to manufacture white materials leapfrogged in the middle of the last century, when Fluorescent Whitening Agents (FWAs, also called Optical Brightening Agents) were discovered [KRAIS29]. FWAs are fluorescent particles which absorb short-wavelength radiation (SWR) in the ultra-violet and violet range (λ<430nm), and emit blue light around 440-480nm. A white object containing OBAs can thus absorb the short-wavelength radiation emitted by natural sources and undergo a chromatic shift towards the blue (together with a slight luminance increase) which results in a pronounced perception of whiteness. Fig. 1 qualitatively illustrates this effect, which we will call "enhanced whiteness".

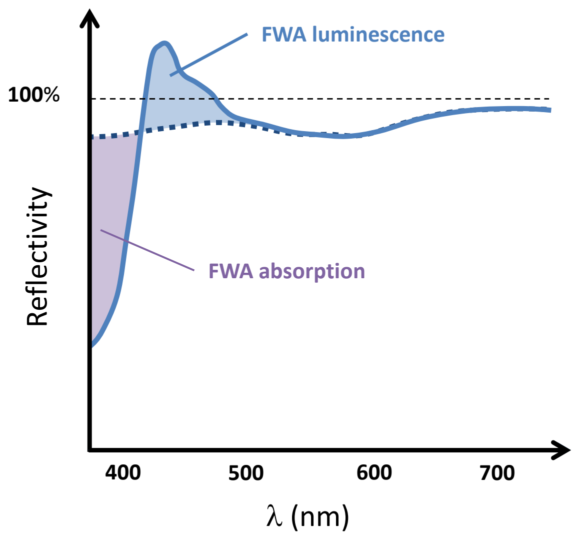

Figure 1 – Sketch of reflectance for a non-fluorescent white material (dotted line) and of total radiance factor for a FWA-containing white material (solid line).

Because enhanced whiteness produces such a strong visual effect, there has been a vigorous effort from various manufacturing industries to integrate and optimize FWAs in white objects. They are now common in papers, plastics, fabrics, laundry detergents…

To quantify enhanced whiteness, manufacturers were in need of a metric. A research effort in the past century led to the derivation of various formulas [GANZ79, GRIESSER94]. Perhaps the best-known metric today is the CIE Whiteness formula [CIE04]:

$$W_{10} = Y_{10} + 800(x_{n,10} - x_{10}) + 1700(y_{n,10} - y_{10}) \tag{1}$$

Where:

$W10$ is the whiteness;

$Y10$ is the Y-tristimulus value of the object under standard illuminant D65;

$x\text{-}y_{n,10}$ are the chromaticity coordinates of D65;

$x\text{-}y_{10}$ are the chromaticity of the object under consideration illuminated by D65.

The subscript 10 indicates that all quantities are computed with the 1964 10^{o} colour-matching functions (CMFs). The use of D65 as the light source is in part due to the fact that many whiteness perception experiments were undertaken in daylight settings. Intuitively, this formula measures a chromaticity shift away from D65 and towards the blue direction; larger shifts correspond to higher whiteness.

The amount of FWA incorporated in white materials is used to modulate the perceived whiteness – from FWA-free objects with a somewhat 'cream' white to heavily FWA-loaded objects with a very strong enhanced whiteness; in fact, an excessive amount of FWA leads to a perceived blue tint, thus limiting how far enhanced whiteness can be harnessed. For instance, FWA-free papers can reach W_{10}~90 while FWA-loaded papers can reach W_{10}~140-150.

2 Impact of the source spectrum on whiteness

FWAs are activated by SWR. Therefore, for a given FWA loading, the whiteness enhancement is governed by the amount of SWR)in the source's SPD. As discussed in [ZWINKELS11, DAVID13], and as we will show below, this is an important effect: sources with no SWR are unable to render whiteness enhancement.

2.1 D65 and similar sources

The original CIE Whiteness metric was developed for outdoor daylight (approximated by standard illuminant D65). However, it was soon realized that D65 was poorly representative of indoor conditions. The amount of SWR indoors is lower, for instance due to absorption by glazing. Therefore, a second Whiteness metric (Indoors Whiteness) was developed using standard illuminant C instead of D65 [CIE10]. Because the chromaticities of both illuminants are similar, the coefficients of the whiteness equation were unchanged – in other words, the same chromatic shift is relevant for both illuminants.

More generally, one may consider a series of sources metameric with D65. For these, it is natural to expect that the amount of short-wavelength radiation modulates the whiteness enhancement, and use of the CIE whiteness formula (using the new SPD instead of D65) is intuitively straightforward.

2.2 Whiteness at other CCTs

For sources at a different CCT however, the CIE whiteness formula can't be trivially applied and requires some adaptation. In [DAVID13] we proposed such an approach which we briefly summarize below.

First, we recall that CIE Whiteness has an underlying geometric interpretation [GRIESSER94]: the formula follows the general form:

$$W = Y - \omega \cdot \cos(\eta + \varphi) / \cos(\varphi) \cdot (x - x_0) - \omega \cdot \sin(\eta + \varphi) / \cos(\varphi) \cdot (y - y_0) \tag{2}$$

Where:

- W is the whiteness;
- Y is the Y-tristimulus value of the object under the source;
- ω, φ are coefficients chosen to fit experimental data;
- η is the direction of whiteness enhancement (e.g. toward 470nm on the spectrum locus);
- $x\text{-}y_0$ are the chromaticity coordinates of the source;
- $x\text{-}y$ are the chromaticity of the object under consideration illuminated by the source.

In essence, the formula measures a chromatic shift toward the blue and rewards it with proper coefficients. Thus, pending some assumptions (namely that ω and φ are CCT-independent), it is possible to repeat this geometric construction at other CCTs and produce new coefficients for the whiteness formula. Fig. 2 illustrates this ‘geometric translation’ of the whiteness formula. This adapted formula is expected to predict the whiteness perception of an object under a light source of arbitrary CCT (and SPD).

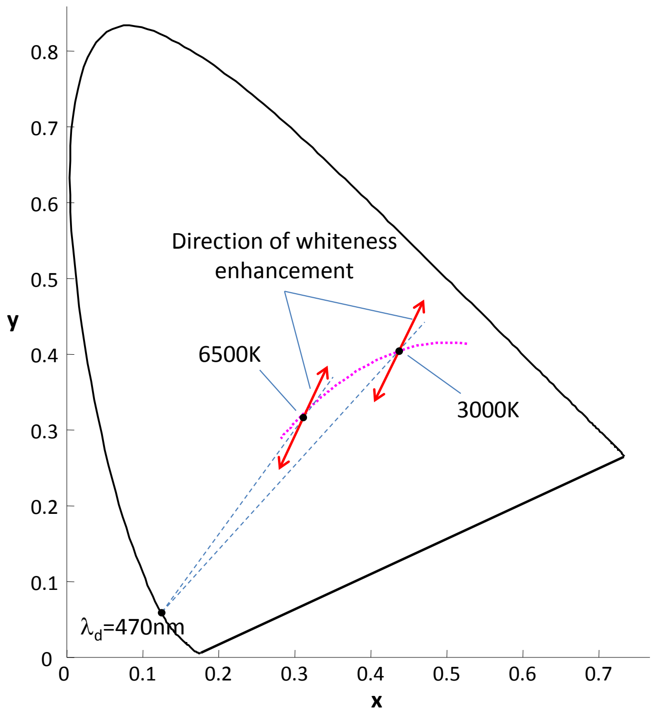

Figure 2 – Illustration of the geometric nature of the CIE Whiteness formula, and of its generalization to other CCTs.

We note that Eq. (2) makes no prescription regarding which CMFs should be used. However, as will be discussed further, additional work points toward the use of 10° CMFs for good agreement with experimental data [HOUSER14].

As an illustration of the formula, we consider a specific white object: a whiteness standard manufactured by Avian Technologies having W_{10}=140. We characterize this object by bispectral reflectance [ZWINKELS08], so that we can compute its luminance under any source [DAVID13]. Using our formula, we can then compute the whiteness of this object under blackbody (BB) radiators of various CCTs. The result is shown on Fig. 3.

We see that for low CCT<2000K, the whiteness saturates at a value of about 90 – this is simply the Y-tristimulus value of the object in the absence of fluorescence, since low-CCT BBs contain very little SWR and cannot excite FWAs substantially. At higher CCT however, the amount of SWR increases and fluorescence is induced, thus increasing whiteness. At 5000K whiteness reaches 150 (this is higher than the CIE whiteness of the object, because a 5000K BB has more UV radiation than D65). (Incidentally, we note that the predictions of Fig.

3 are not fully accurate for the highest CCTs since our bispectral reflectance characterization stops at 360nm, whereas high-CCT BBs have radiation at shorter wavelength).

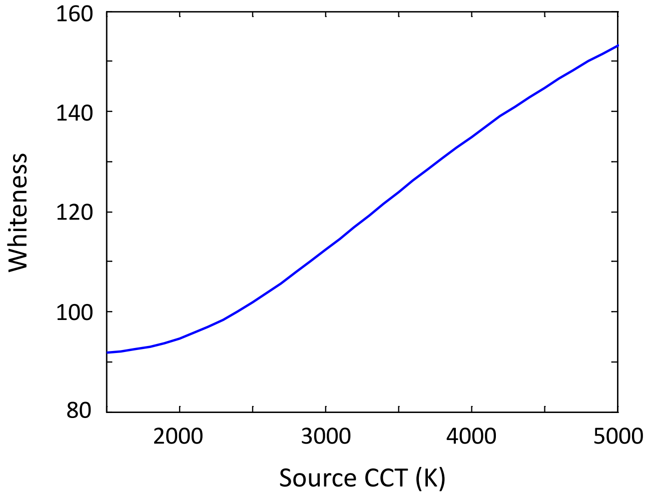

Figure 3 – Predicted whiteness of a whiteness standard (W_{10}=140) under blackbody radiators of various CCTs

2.3 The issue of white LEDs

Therefore, as a general trend, natural sources of higher CCT induce more enhanced whiteness. This effect is already sizeable for warm-white sources of CCT 2700-3000K, as seen on Fig. 3. In other words, standard incandescent and halogen lamps are expected to induce a noticeable whiteness enhancement.

However, the same is not necessarily true for other light sources of similar SPD. Specifically, let us consider a typical blue-pumped white LED (BLED) made of a blue-emitting die and two down-converting phosphors. The SPD of such a source is shown on Fig. 4: it hardly contains any SWR below 430nm, and therefore can't excite FWAs. This is in contrast to a BB of the same CCT. This issue was first described in [ZWINKELS11], and discussed in detail in [DAVID13]. We argue that this issue is substantial: the science and engineering of FWAs has been refined for decades to obtain white objects with preferred rendering which are ubiquitous in our everyday life; it is clearly problematic to introduce light sources which significantly distort this rendering. As shown in [DAVID13], the corresponding colour error is indeed substantial: up to 8*Du'v'* points between a halogen lamp and a BLED at 3000K!

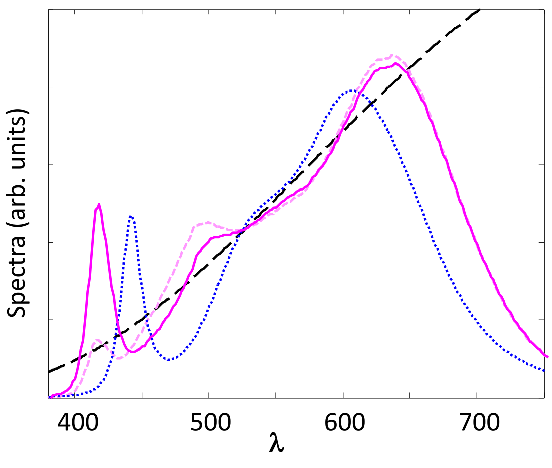

Figure 4 – SPDs of 3000K sources, all scaled for equal lumens. Dashed: blackbody. Dotted: BLED. Solid: VLED.

Fig. 4 also shows our proposed solution to this issue: the use of violet-pumped white LEDs (VLEDs) with a redesigned SPD whose violet emission (λ~415nm) can excite FWAs.

We can use our proposed whiteness formula (Eq. (2)) to check that VLEDs can be designed to render enhanced whiteness. To do so, we once again consider the whiteness standard of Section 2.2 and compute its perceived whiteness for various VLEDs where the violet content is varied. We define the violet emission as the fraction of the SPD in the range 400-430nm. As shown on Fig. 5-a), the chromaticity of the whiteness standard is shifted towards the blue direction as violet emission increases. The corresponding whiteness is shown on Fig. 5-b): as expected, whiteness increases with violet emission. For about 8% violet emission, the whiteness of a 3000K BB is approximately matched.

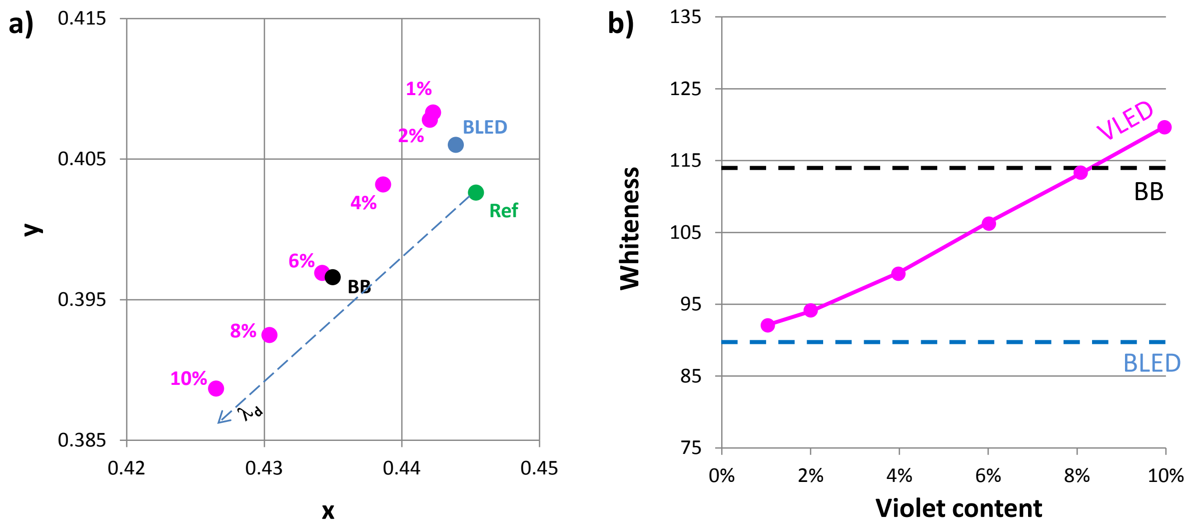

Figure 5 – a) Chromaticity of the whiteness standard under various 3000K sources. Ref: chromaticity of a 3000K blackbody. BB: chromaticity of the standard under BB illumination. BLED: chromaticity of the standard under BLED illumination. x%: chromaticity of the standard under illumination by a VLED with x% violet emission. b) Corresponding whiteness according to Eq. (2). For VLEDs, whiteness increases with violet emission.

Therefore, we see that a proper design of the SPD of an LED source enables rendering of enhanced whiteness, and even a rendering similar to a standard halogen lamp.

3 Whiteness perception – experimental results

The above discussion is based on theoretical arguments. To assess their validity, a psychophysical experiment was performed in the Lighting Laboratory of the Department of Architectural Engineering at Penn State University. The results are presented in details in [HOUSER14]; we offer a partial summary here.

3.1 Experimental protocol

Thirty-nine participants within the range 19-25 years and normal colour vision were recruited for the experiment: 20 Caucasians, 17 Asians, and 2 Hispanics; 21 males and 18 females. Most of them were university students but none of them were studying lighting.

Two identical booths with dimension of 0.53m x 0.53m x 0.78m were built adjacent to each other for the three tasks included in the experiment: forced choice, selection, and sorting. Here, we only discuss the sorting task – the other experiments can be found in [HOUSER14].

In this task, five lamp types with a nominal CCT of 3000K were used to provide five light settings: a filtered halogen lamp, a typical BLED, and three VLEDs with 2.5%, 5% and 6.5% violet emission. Due to the use of a diffuser to homogenize luminance distribution in the booths, the UV radiation of the halogen lamp was reduced, thus decreasing its ability to excite FWAs by a factor 2-3 (hence the label 'filtered' halogen).

The independent variable was the spectrum of the light setting, which had five levels with one for each lamp type. Six whiteness standards were placed in random order in one booth under a light setting (Fig. 6). These are analogous to the standard previously discussed, but they have various levels of CIE whiteness. We label them as W82, W102, W108, W115, W128 and W141 according to their CIE Whiteness.

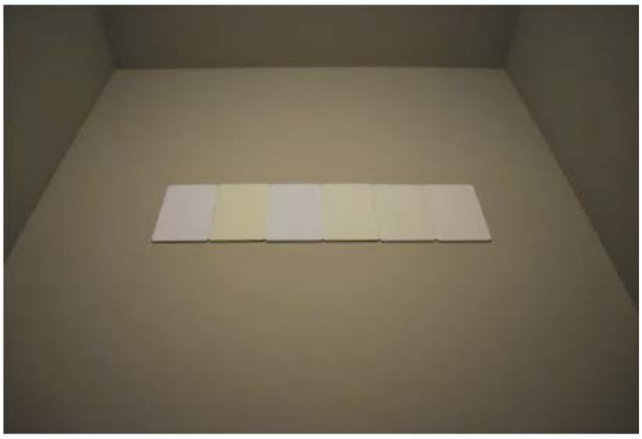

Figure 6 – Picture of a booth with six whiteness standards, illuminated by the 6.5%VLED

Each participant was asked to arrange these six targets based on their whiteness appearance under each of the five lamp types with a horizontal illuminance at 300 lux. Under each light setting, the participant was required to observe these targets for 30 seconds before making arrangement, so that they were chromatically adapted to the illumination. There was a three-minute washout period between two light settings, during which the participant sat outside the experiment room and the experimenter recorded the arrangements made by the participant under the previous light setting, rearranged them in random order, and changed the light setting to the next. In order to counter a possible positional bias associated with the side-by-side booths, 20 participants finished the sorting task under five light settings in the left booth; the other 19 finished that in the right booth. The dependent variable was the rank of each standard arranged by participants.

3.2 Results

The order of the six targets arranged by each participant under each light setting was recorded from 1 to 6, with 6 as the whitest. The summary of the average ranks of the targets arranged under each setting in each booth is provided in Fig. 7. No significant difference existed between the results obtained in the two booths, as tested by Wilcoxon Signed Rank test.

Under illumination by the filtered halogen lamp, the sorting agrees with the CIE whiteness rating of the samples: enough fluorescence is induced to render the whiteness in the expected order. The sorting is identical under the 5% and 6.5%-VLEDs: here again, the violet emission is sufficient to induce significant fluorescence. Under the 2.5%-VLED, the sorting order is mostly the same except for an inversion of samples W115 and W128: the difference in FWA content is moderate between the two samples, and the slight difference in tint between the samples is enough to override it. Finally, under the BLED the order is not respected at all. Interestingly however, the ranking is highly consistent between participants. Indeed, in the absence of fluorescence, the only difference between samples is a slight change in reflectivity and therefore in perceived tint. Participants rank the samples according to this residual tint, regardless of the FWA content.

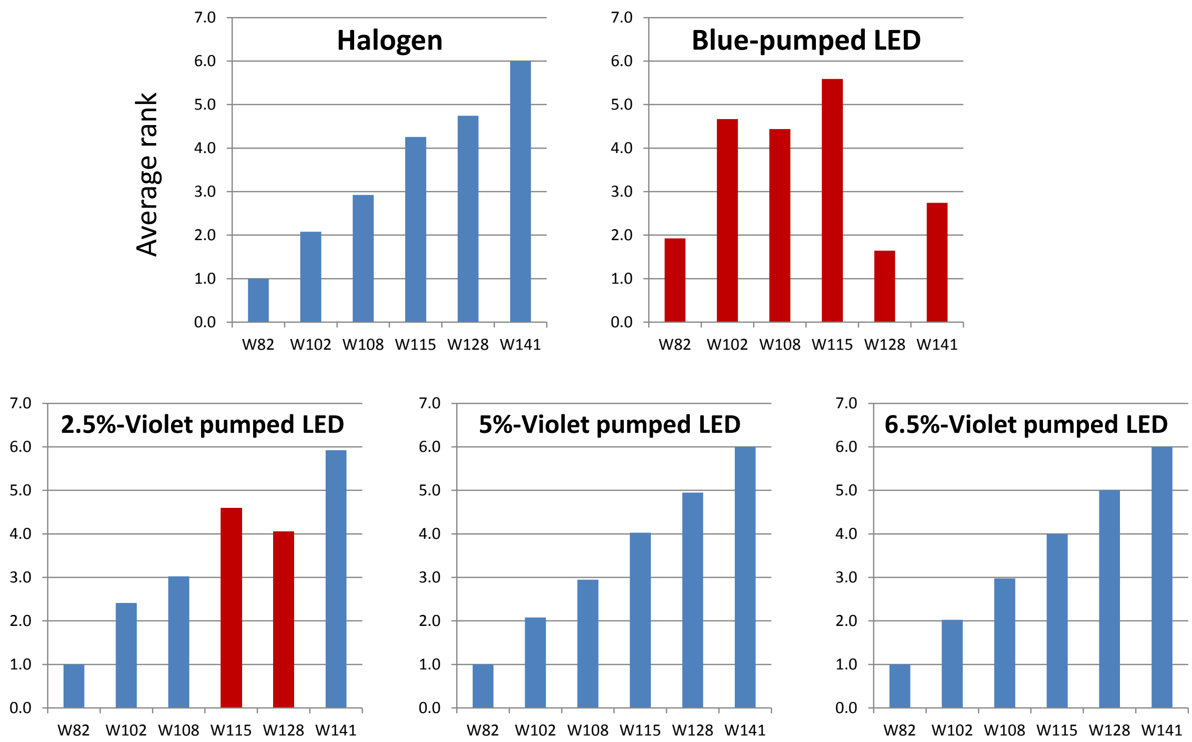

Figure 7 – Results of the sorting experiment. The mis-ordered samples are indicated as red bars. Ordering is accurate under the halogen lamp and the 5% and 6.5%-VLEDs, while it is completely inaccurate under the BLED.

These results are in good qualitative agreement with the expectations from our previous discussion: the BLED is unable to excite FWAs and to increase whiteness; for the other sources whiteness increases with the amount of SWR, enabling a sorting of the whiteness standards according to their FWA content.

Further experiments described in [HOUSER14] show that this agreement is also quantitative. When the whiteness formula of Eq. (2) is adapted to employ the recent colour-matching functions proposed by TC1-36 [CIE13, CVRL13], its predictions are in full agreement with participants' observations, both in the forced-choice and selection tasks.

4 Towards a Source Whiteness metric

4.1 Source whiteness: a fidelity metric

It is apparent that the ability of a light source to render enhanced whites is strongly dependent on the short-wavelength content of its SPD. Although our previous discussion has been focused on LEDs, one may wonder how other lighting technologies fare in this respect. As discussed in [WEI14] there is a very large variability in whiteness rendering across different sources, even for a given CCT. Unsurprisingly, LEDs have very little to no rendering; metal halides have very high whiteness rendering (usually more than a reference illuminant at the same CCT); fluorescents have some whiteness rendering, with a lot of variation.

This large variability and the lack of general awareness about it are quite surprising. In part, this may be due to the lack of a metric to describe the whiteness rendering of a source – in contrast, other aspects of colour quality which are described by well-known metrics (such as CCT and CRI) are usually well understood. Therefore, we suggest that a source whiteness rendering metric should be developed to quantify this issue and help its understanding.

One must be mindful of the distinction between existing *object* whiteness metrics (such as CIE Whiteness) and a potential *source* whiteness metric; the former describe the perceived whiteness of objects under a reference illuminant, whereas the latter would describe the (average) ability of a light source at inducing enhanced whiteness.

Without going as far as proposing such a metric, we discuss here some of its possible aspects and some questions it raises; we focus our thoughts in indoor light sources.

We argue that the question of whiteness rendering is essentially a matter of colour fidelity, applied to FWA-containing materials. For standard reflecting objects, fidelity answers the following questions: does the test source render the colour of the object like a reference source? In colour fidelity metrics, the reference source is usually a blackbody illuminant or a phase of sunlight (depending on the CCT). The fidelity score decreases as the colour error between the test and source increases.

Likewise, a whiteness metric should indicate how a source renders the (near-white) colour of FWA-containing white objects. For a given CCT, it is reasonable to consider a standard illuminant as a baseline for whiteness rendering and compare it to the whiteness rendering of the test source (however the metric should differentiate between *less* and *more* whiteness than the reference illuminant, as discussed below).

For the sake of illustration, Fig. 8 depicts a simplified workflow of such a source whiteness metric.

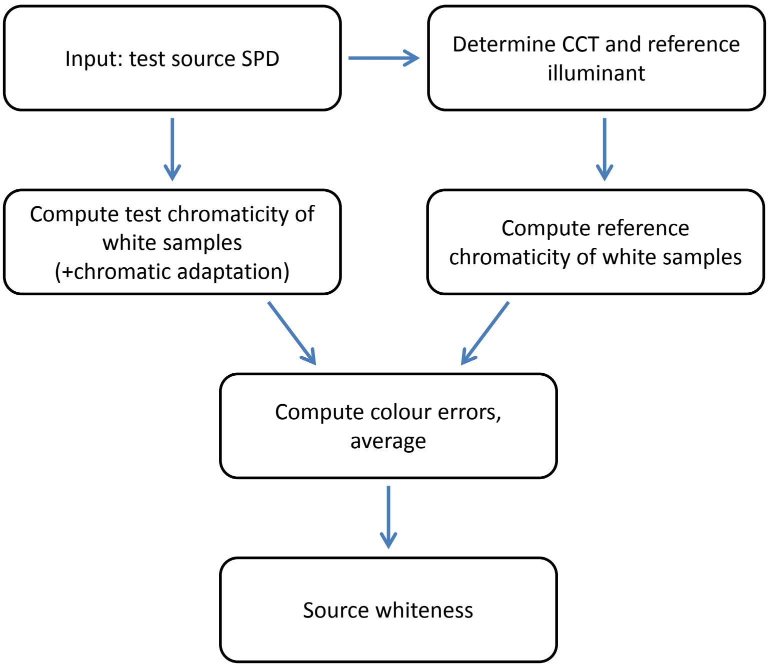

Figure 8 – Computation flow of a source whiteness fidelity metric.

4.2 Open questions

Several points need to be considered when developing a source whiteness metric. We mention some key questions below and, without providing complete answers, we offer some thoughts:

- Which test white samples (TWS) should be used? The choice of test samples has been, and still is, the object of debate for colour fidelity metrics [DAVIS10, SMET13,DAVID14]. It appears to us that the choice should be more straightforward for a whiteness metric: a few FWAs are used in the vast majority of practical applications [PUEBLA14]. Therefore, a set of objects containing these FWAs would constitute a natural choice of test samples. Like for colour fidelity, an average of the white samples' individual scores could be performed, while individual scores would still be of value for applications where a particular test sample is most relevant to the lighting application. These TWS would still need to be thoroughly characterized by bispectral reflectance, but once this is performed their chromaticities under any light source can be accurately predicted from computations (as illustrated in [DAVID13]).

- What standard illuminants should be used? For the CRI, the illuminants switch from blackbody to daylight at 5000K. This has minimal effect on the CRI because a 5000K Blackbody and D50 render colours quite similarly. However this is not true for whiteness, since their SWR content is markedly different. More generally, the proper reference illuminant for indoor sources of arbitrary CCT is a rather open question (both blackbody sources and Dxx phases of daylight contain more SWR than natural daylight filtered by glazing, as illustrated by the use of illuminant C for the indoor Whiteness formula [CIE10]). Fortunately, for warm-white sources at least, the use of blackbody references appears non-controversial.

- How should colour difference be evaluated? First, a modern colour error formula should be used. Second, and more importantly, “positive” and “negative” errors should be differentiated. Standard colour fidelity metrics have a maximum value (e.g. 100) when the test and reference colours are exactly identical: any colour difference lowers fidelity, whether it comes from a decrease or increase in chroma/hue. However in the case of whiteness, various sources induce more whiteness than standard illuminants (for instance, this is the case of warm-white metal halides as shown in [WEI14b]), and this is not necessarily a bad thing (in some applications a lot of whiteness may be desired, for instance in retail). Therefore, a good whiteness metric should differentiate between low whiteness (score <100 and as low as 0) and high whiteness (score >100), with a value of 100 being a match to the reference illuminant.

- What colour space is suitable? Our proposed formula uses the CIE 1931 (xy) colour space. However, one may consider operating in a more modern space (such as CIELAB or CIECAM), where chromatic adaptation is intrinsically incorporated. Besides, colour-appearance spaces taking into account background and surround colours (such as CIECAM) may be especially relevant since enhanced whiteness relies on a differential chromaticity effect.

- What CMFs should be used? As we showed in [HOUSER14], good agreement between chromaticity calculations and experimental data is contingent upon the selection of proper CMFs. We concluded that the 10^{o} CMFs tentatively proposed by TC1-36 gave the best results, but further data would be helpful. For instance, the 1964 10^{o} CMFs are very similar to the TC1-36 CMFs, and it is unclear if one yields better results than the other.

- What wavelength range should be used? Some FWAs have absorption deep in the ultra-violet (including in the UV-B). Likewise, some high-CCT illuminants emit a lot of UV radiation. Realistically, in indoor settings, only UV-A will be present and in moderate amount. Still data will be needed below the usual range (380nm for colour fidelity). Besides, the extrapolation scheme for missing short-wavelength data may have a strong impact and should be considered with care, as shown in [ZWINKELS11].

5 Conclusions

The use of fluorescent whitening agents in white materials produces a strong effect of enhanced whiteness, which is commonly observed in our environment. We discussed the impact of the light source’s spectral power distribution (SPD) on this effect. We proposed a formula for predicting whiteness enhancement for sources of arbitrary CCT. We showed that, although whiteness enhancement is significant under conventional sources such as halogen lamps, it is non-existent for standard white LEDs – a significant problem in terms of colour fidelity for these white materials. We illustrated how violet-pumped white LEDs could be designed to accurately render whiteness, and confirmed these predictions with psychophysical experiments on whiteness perception. Finally, we argued that a metric is needed to describe the ability of a light source at rendering enhanced whiteness, and we discussed some of the key points which should be addressed to derive such a metric.

References

CIE 2004. Paper and board - determination of CIE whiteness, D65/10^{o} (outdoor daylight), ISO norm 11475:2004

CIE 2010. Paper and board - determination of CIE whiteness, C/2^{o} (indoor illumination conditions), ISO norm 11476:2010.

CIE. 2013. TC1-36: Fundamental chromaticity diagram with physiologically significant axes. January 2013 Report (Personal communication, 2013).

CVRL. 2013. http://www.cvrl.org/ (Accessed Jun 14, 2013).

DAVID, A. 2013. Whiteness metric for light sources of arbitrary color temperatures: proposal and application to light-emitting-diodes. *Opt. Expr.* 21, 16702-16715.

DAVID, A. 2014. Color Fidelity of Light Sources Evaluated over Large Sets of Reflectance Samples. *Leukos* 10(2), 59-75.

DAVIS, W. 2010. Color Quality Scale. *Optical Engineering* 49(3), 033602.

GANZ, E. 1979. Whiteness formulas - a selection, *Appl. Opt.* 18, 1073–1078.

GRIESSER, R. 1994. Assessment of whiteness and tint of fluorescent substrates with good interinstrument correlation, *Col. Res. Appl.* 19, 446–460.

HOUSER, KW. 2014. Whiteness Perception under LED Illumination, *Leukos*, 10(3), 165-181.

KRAIS, P. 1929. On a new black and a new white, *Melliand Textileber* 10, 468.

PUEBLA, C. 2014. Personal communication.

SMET, K. 2013. CRI2012: A proposal for updating the CIE colour rendering index. *Lighting Res. Technol.*, 45, 689-709.

WEI, M. 2014. Blue-pumped LEDs fail to render whiteness. CIE Conference on Lighting Quality and Energy Efficiency, Kuala Lumpur.

ZWINKELS, J. 2008. Surface fluorescence: the only standardized method of measuring luminescence, in “Standardization and Quality Assurance in Fluorescence Measurements I,” Springer Berlin Heidelberg, pp. 163–192

ZWINKELS, J. 2011. CIE whiteness assessment of papers: impact of LED illumination, “27th Session of the CIE,” (Sun City, South Africa, 2011).

OP13

BLUE-PUMPED WHITE LEDS FAIL TO RENDER WHITENESS

Wei, M.,[1] Houser, K.W.[1], David, A.,[2] Krames, M.R.[2]
[1] Department of Architectural Engineering, The Pennsylvania State University, University Park, PA, USA, [2] Soraa, Inc., Fremont, CA, USA
khouser@engr.psu.edu

Abstract

Measures of whiteness for six calibrated whiteness standards containing varying amount of fluorescent whitening agents (FWAs) were computed under 406 illuminants using the formula proposed by David et al (2013) and adapted by Houser et al (2014). The computational results indicate that typical blue-pumped LED sources are deficient at rendering the whiteness of these standards. The lack of violet or UV optical radiation makes them fail to excite the FWAs contained in the calibrated standards. Thus, the blue-shift and whiteness enhancement associated with FWAs does not occur. Appropriate spectral engineering that provides proper violet emission is necessary for LED sources to render whiteness with the desired effect.

Keywords: Whiteness, Spectral Power Distribution (SPD), Light-emitting Diode (LED), Blue-pumped, Violet-emission

1 Introduction

Fluorescent whitening agents (FWAs), which were initially discovered in 1929 (Krais, 1929), are contained in many manmade objects that are engineered to appear white. FWAs absorb ultraviolet (UV) and violet optical radiation and re-emit blue light, creating a blue tint and increasing lightness (Choudury, 2006; Katayama and Fairchild, 2010). In order to create a desired degree of whiteness, manufacturers modulate the amount of FWAs. FWAs are also found in some natural materials, such as human teeth (Hartles and Leaver, 1953; Hall et al, 1970).

Formulae characterizing perceived whiteness were first proposed in the 1930s (Judd, 1935; MacAdam, 1934); various modifications have been proposed over the years (Ganz, 1979; Griesser, 1994; Griesser, 1996). The CIE whiteness formula, which was recommended by CIE in 1986, characterizes whiteness under CIE Illuminant D65. The general geometry is illustrated in Figure 1 (ISO, 2004). The formula works well to characterize whiteness perception under a reference illuminant (Jordan and O'Neill, 1991), but it is not suitable for other light sources (ISO, 2004; ISO, 2010). A whiteness formula, characterizing whiteness perception under light sources with arbitrary colour temperatures (CCTs), proposed by David et al (2013a) and adapted by Houser et al (2014) agreed well with results of psychophysical experiments (David et al, 2013b; Houser et al, 2014).

In this paper, we compare computed measures of whiteness for six calibrated whiteness standards under 406 SPDs that represent various illuminants, including light-emitting diode (LED), fluorescent, high-intensity discharge (HID), blackbody radiation, CIE D-illuminants, and theoretical models. The measures of whiteness were computed using the formula proposed by David et al (2013) and adapted by Houser et al (2014). The computed measures reveal the failure of blue-pumped LEDs to render whiteness for the calibrated whiteness standards, a result that is expected to generalize to other white materials that contain FWAs.

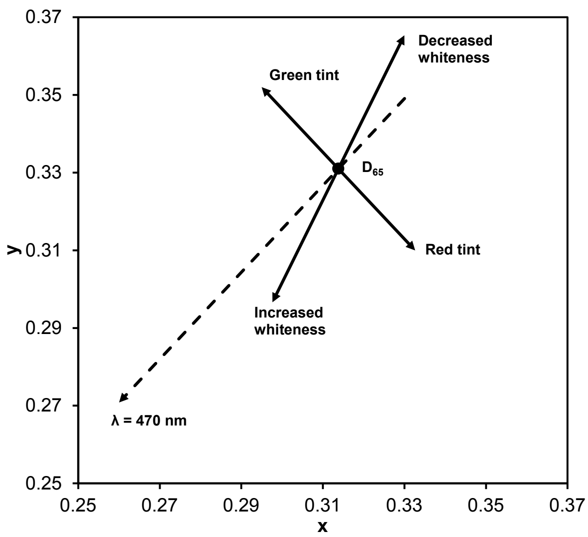

Figure 1 – Graphical representation of the CIE whiteness formula, illustrated in CIE 1964 10° chromaticity diagram (CIE, 2004a). The black dot locates the chromaticity coordinates of the reference illuminant—CIE Illuminant D65. The main direction for CIE whiteness is along the dotted line connecting the chromaticity of the reference illuminant and the spectrum locus at a dominant wavelength at 470 nm. Shifts parallel to this direction, but with a small angle, correspond to changes in whiteness; shifts perpendicular to this direction correspond to changes in tint (ISO, 2004).

2 Methods

2.1 Whiteness Standards

Six calibrated whiteness standards were purchased from Avian Technologies. These standards are representative of commercial papers with varying amounts of FWAs, resulting in different CIE whiteness values between 80 and 140 as measured by the manufacturer. We label these as W××, where the subscript represents the CIE whiteness value. One whiteness standard, W_{82}, did not contain any FWAs; the other five samples—W_{102}, W_{108}, W_{116}, W_{128}, and W_{140}—contain greater amount of FWAs with increasing whiteness values.

The optical properties of a whiteness standard are a combination of spectral reflectance and bispectral luminescence properties. When a whiteness standard is illuminated by a monochromatic light at certain wavelength λ with a unit power, the spectral radiance of the light reflected by the standard can be written as:

$$E(\lambda, \lambda') = R(\lambda) + L(\lambda, \lambda') \qquad (1)$$

where:

$E(\lambda, \lambda')$	is the spectral radiance of the light reflected by the standard measured at the wavelength of λ‘, when illuminated by a monochromatic light at the wavelength of λ;
$R(\lambda)$	is the spectral reflectance of the standard at the wavelength of λ;
$L(\lambda, \lambda')$	is the luminance of the standard due to FWAs at the wavelength of λ’, when illuminated by a monochromatic light at the wavelength of λ.

If E(λ, λ’) is measured with a variety of λ, the optical properties of a standard can be characterized by a two-dimensional matrix M (the Donaldson matrix), whose diagonal is the reflectance of the standard. The double-monochromator method as described in CIE (2007) and Zwinkels (2008) were employed to measure E at various λ.

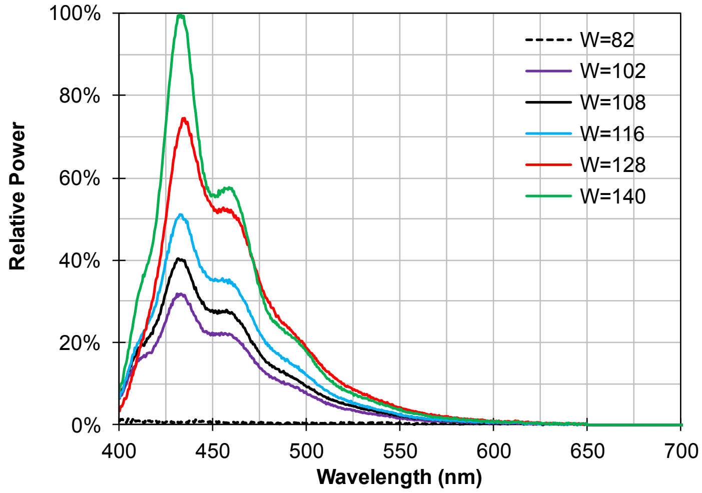

Figure 2 – Spectral emission of six whiteness standards containing different amounts of fluorescent whitening agents (FWAs) under a monochromatic illumination of 390 nm. The curves are scaled to the highest emission intensity among the six curves. The standards with greater amount of FWAs have higher values of whiteness, W. The whiteness standard labelled as W = 82, which exhibits almost no emission, does not contain FWAs (Houser et al, 2014).

2.2 SPDs

Table 1 summarizes the 406 SPDs employed in this study, comprised of 401 SPDs from an existing dataset (Houser et al, 2013) and 5 SPDs from a recent study (Houser et al, 2014). All computations performed here were based on SPDs from 380 – 780 nm with an interval of 5 nm.

Table 1 – Summary of the SPDs included in this study

Type of Illuminant		Counts and Abbreviations			
		Real Illuminants		Theoretical Models	
		Counts	Abbr.	Counts	Abbr.
LED	LED Phosphor	134	LP-R	29	LP-T
	LED Mixed	17	LM-R	51	LM-T
FL	Fluorescent Broadband	30	FB-R	45	FL-T[a]
	Fluorescent Narrowband	31	FN-R		
High-Intensity Discharge		31	HI-R	-	
Tungsten Filament		18	TF-R	-	
Blackbody Radiation		-		8	BB-T
D-Series Illuminants		-		6	DS-T
Other[b]		-		6	OT-T

[a] Fluorescent models include broadband and narrowband

[b] e.g., Equal-Energy, Clipped Incandescent, Ideal Prime Color

2.3 Numerical Computation

The spectrum of the light reflected from a whiteness standard under an illuminant can be computed as the product of the matrix M characterizing the optical properties of the standard and SPD of the illuminant. The accuracy of this computational method was validated by comparing the spectra computed to those measured directly from the standard under various real light sources; Figure 3 shows an example of the comparison for a typical blue-pumped LED.

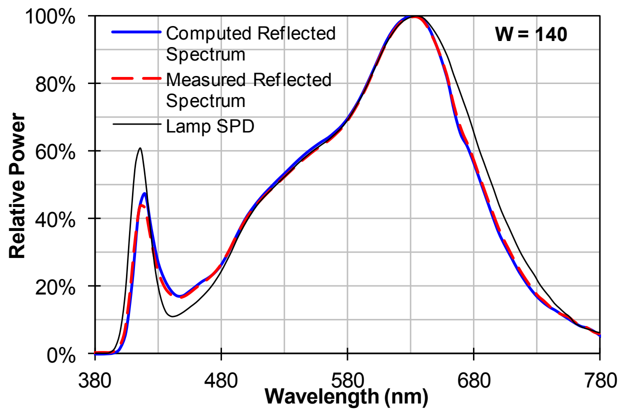

Figure 3 – The SPD of a violet-pumped LED, and the reflected spectrum from a whiteness standard, W_{140}, derived from numerical computation and real measurement.

The whiteness of these standards under each illuminant was computed using the adapted whiteness formula (Houser et al, 2014), employing the 10° colour matching functions (CMFs) that have been tentatively recommended by CIE TC1-36 (CIE, 2013).

Because our data starts at 380 nm the computations are not fully accurate for illuminants that contain a great deal of UV radiation. This is not the case for most illuminants, especially LEDs, but the accuracy of the calculation is limited for some higher-CCT illuminants, as we will discuss.

3 Results

3.1 Chromaticity Shift

Manufacturers modulate the amount of FWAs to provide the desired degree of whiteness rendering. White objects containing more FWAs are expected to have larger chromaticity shift in the direction of increased whiteness (i.e., toward λ_d = 470 nm, as illustrated in Figure 1).Figure 4 illustrates the chromaticity shifts of the six standards under six illuminants. It can be observed that four of the illuminants plotted create a chromaticity shift, while others do not.

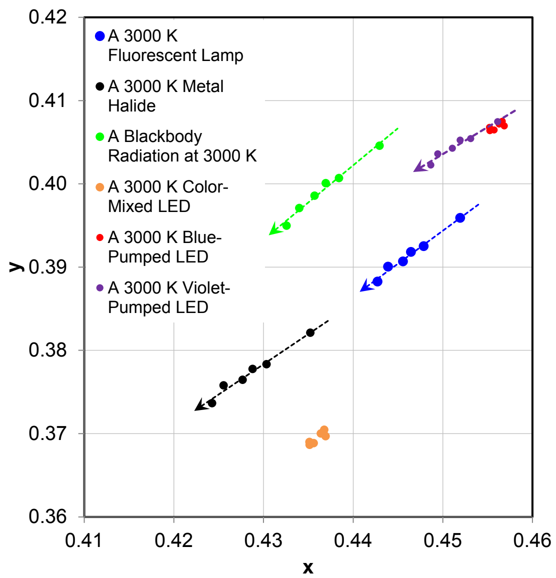

Figure 4 – The chromaticity coordinates of the six standards under six illuminants with similar CCT using the TC 1-36 10° CMFs.

The magnitude of the chromaticity shift from the standard without FWAs, W_{82}, to each standard containing FWAs under each illuminant in CIE u'v' diagram was computed (i.e., five $D_{u'v'}$ differences were computed: $D_{u'v'(82\text{-}102)}$, $D_{u'v'(82\text{-}108)}$, $D_{u'v'(82\text{-}116)}$, $D_{u'v'(82\text{-}128)}$, and $D_{u'v'(82\text{-}140)}$). Large variation of these five values of $D_{u'v'}$ differences would indicate the effectiveness of the illuminant at eliciting different degrees of whiteness for standards containing different amount of FWAs. The standard deviation of these five $D_{u'v'}$ differences, $\sigma(D_{u'v'})$, is employed to characterize the variation for each illuminant, allowing comparison of the ability to excite FWAs between illuminants. As summarized in Figures 5 and 6, most LED products have a small chromaticity shift difference between whiteness standards.

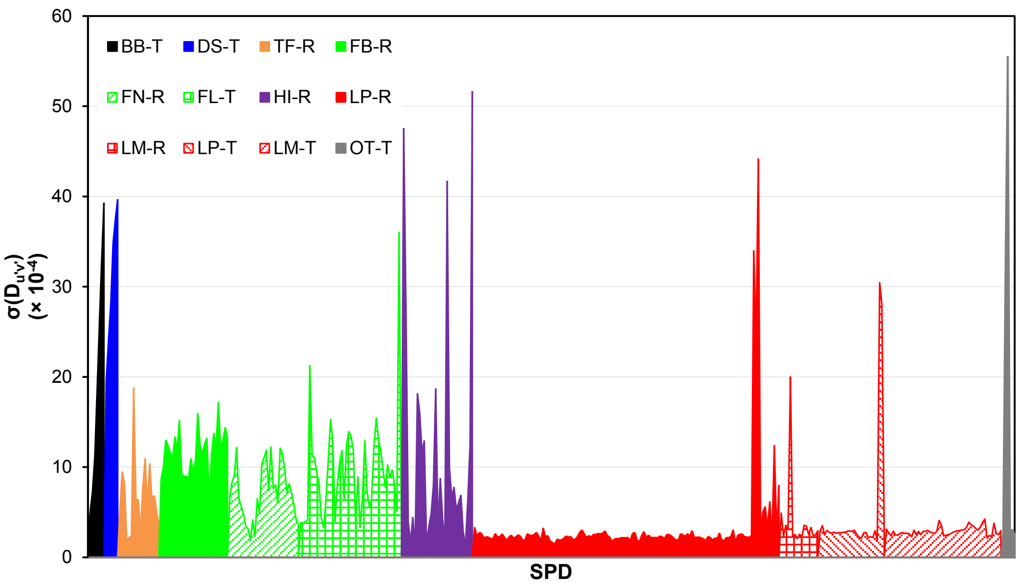

Figure 5 – The standard deviation, $\sigma(D_{u'v'})$, of the five $D_{u'v'}$ (i.e., $D_{u'v'(82\text{-}102)}$, $D_{u'v'(82\text{-}108)}$, $D_{u'v'(82\text{-}116)}$, $D_{u'v'(82\text{-}128)}$, and $D_{u'v'(82\text{-}140)}$) under each illuminant. These five $D_{u'v'}$ values characterize the chromaticity shift from the standard without FWAs, W_{82}, to each standard containing FWAs under each illuminant in CIE u'v' digram.

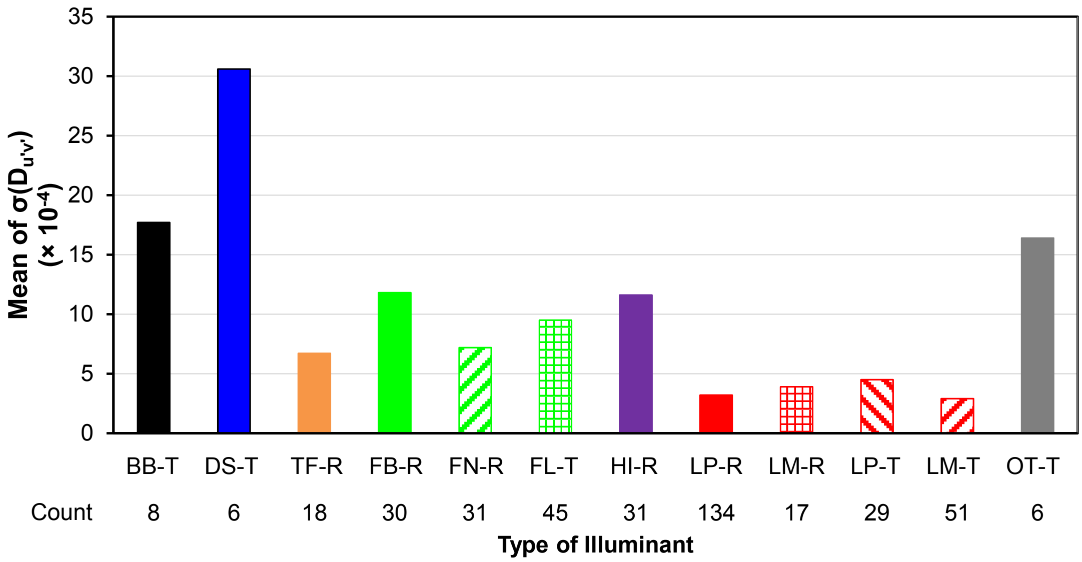

Figure 6 – The mean of $\sigma(D_{u'v'})$ as summarized in Figure 5 for each illuminant type.

3.2 Whiteness Value

The whiteness value of these six whiteness standards was computed for each of the 406 illuminants using our adapted whiteness formula (Houser et al, 2014), as shown in Figure 7.

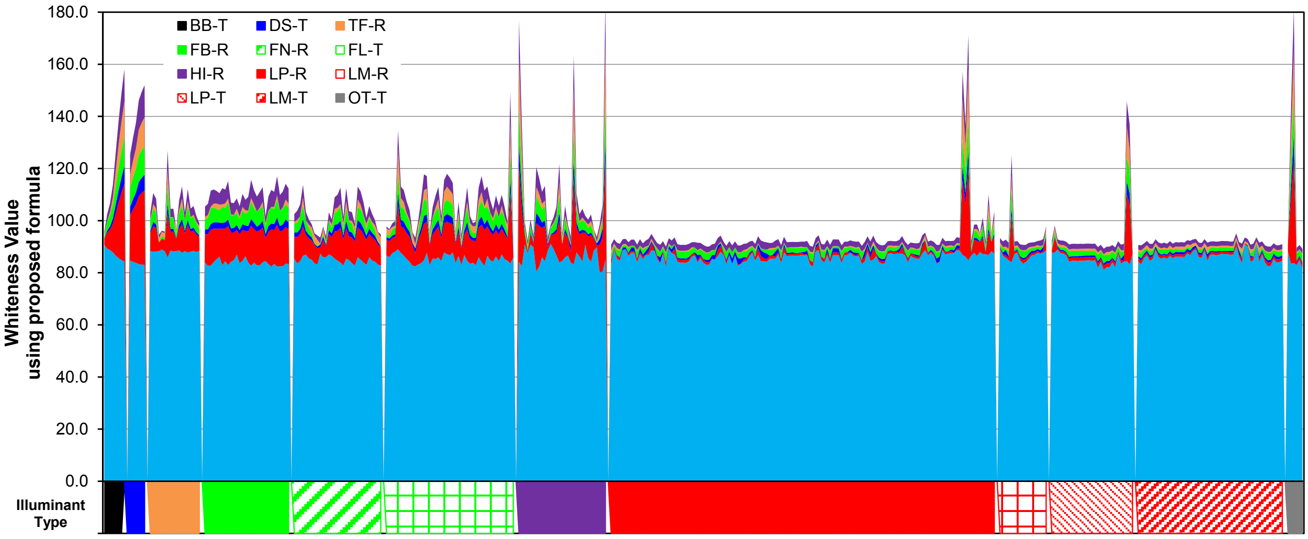

Figure 7 – The whiteness value of each whiteness standards using the proposed formula by Houser et al (2014) under each illuminant.

In order to numerically compare how whiteness rendition of these six whiteness standards is different under each illuminant, two statistical measures are employed: 1) The difference between the highest and the lowest whiteness value of the six standards, ΔW. The larger ΔW, the more effective the illuminant is at activating FWAs. 2) The standard deviation of the whiteness values of the six standards, σ(W). The larger σ(W), the more effective the illuminant is at eliciting differences between whiteness standards containing different amount of FWAs.

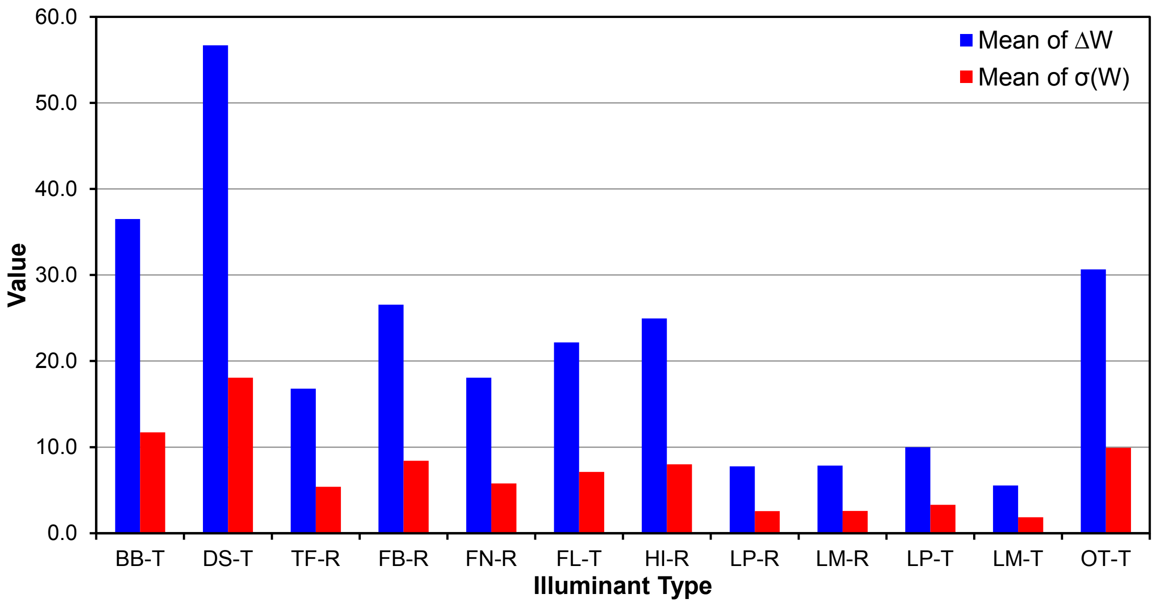

Figure 8 – The mean of ΔW and σ(W) of the six standards under each illuminant for each illuminant type.

Figure 8 summarizes the mean of ΔW (labelled as $\overline{\Delta W}$) and σ(W) (labelled as $\overline{\sigma(W)}$) for each illuminant type. The two quantities are fairly well correlated, suggesting that they measure FWAs excitation in a similar way. Figures 7 and 8 illustrate that most LED illuminants, whether phosphor-converted or colour-mixed, fail to render the whiteness differences intrinsic to these calibrated whiteness standards.

3.3 Violet-emission Level

The amount of UV and violet optical radiation emitted by an illuminant governs FWAs excitation and whiteness rendering. UV radiation is generally undesirable in sources for general illumination because it is damaging to objects (CIE, 2004); it is more prudent to engineer the violet region of the spectrum. Violet emission, defined here as the percentage of optical radiation between 380 and 430 nm to that between 380 to 780 nm, is employed to characterize the relative amount of violet optical radiation contained in an illuminant. As shown in Figure 9, there is modest correlation between violet emission and ΔW, and between violet emission and σ(W).

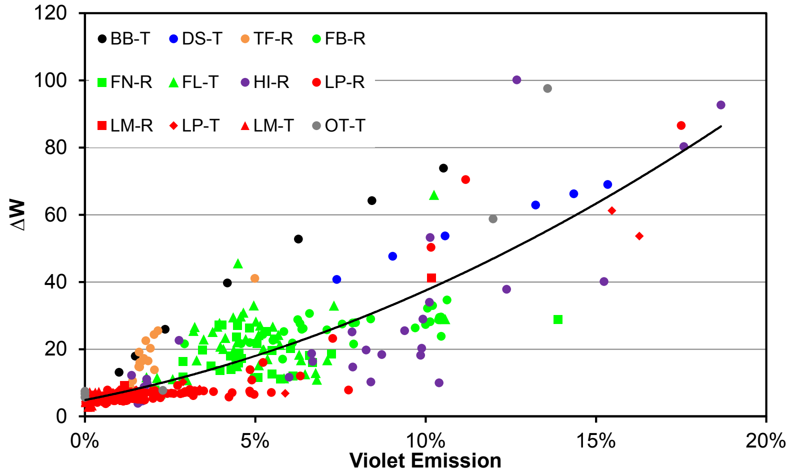

(a)

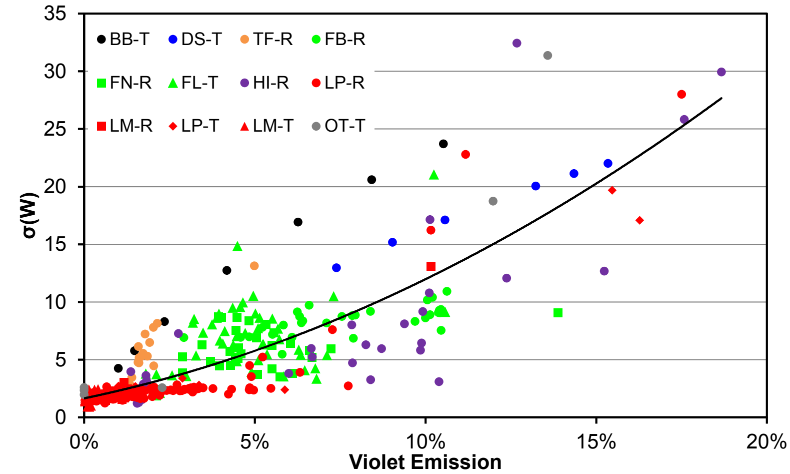

(b)

Figure 9 – The violet emission of each illuminant versus ΔW and σ(W) of the six whiteness standards under each illuminant.

Most LED illuminants have a violet emission of less than 5% and typically 1-2%, which is lower than other illuminants. Most phosphor-converted LEDs considered here employ a blue LED with a blue-pumped phosphor, which is a dominant technique to produce white light using LEDs (Wei and Houser, 2012). Blue-pumped LEDs have very low violet emission, resulting in poor performance to render whiteness of the white objects containing FWAs.

4 Discussion

It might be rational to postulate that an illuminant with higher CCT will yield better whiteness rendering, since an illuminant with higher violet radiation tends to have higher CCT. This is certainly true for standard illuminants (i.e., blackbody radiations and daylight illuminants). Figure 10, however, illustrates that there is not a strong correlation between CCT and either ΔW or $\sigma(W)$ for artificial sources. These computations suggest that higher CCT is not a guarantee to achieve FWAs excitation and appropriate whiteness rendering; this is because, despite their high CCT, many artificial light sources have very little violet emission. Illuminants with any CCT can render white objects with FWAs, but only by purposeful engineering of the source's spectrum.

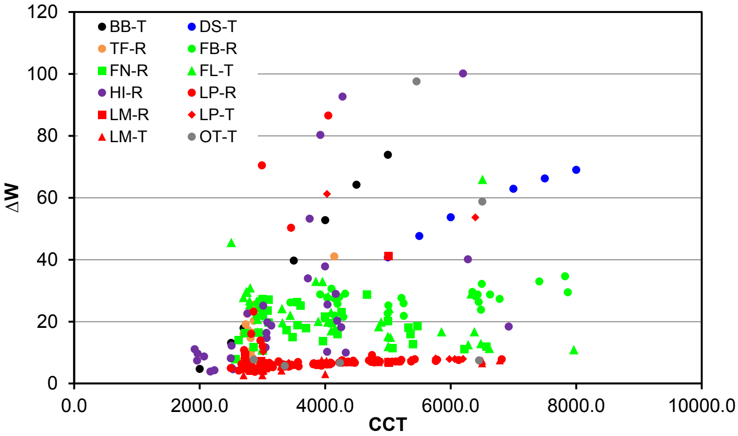

(a)

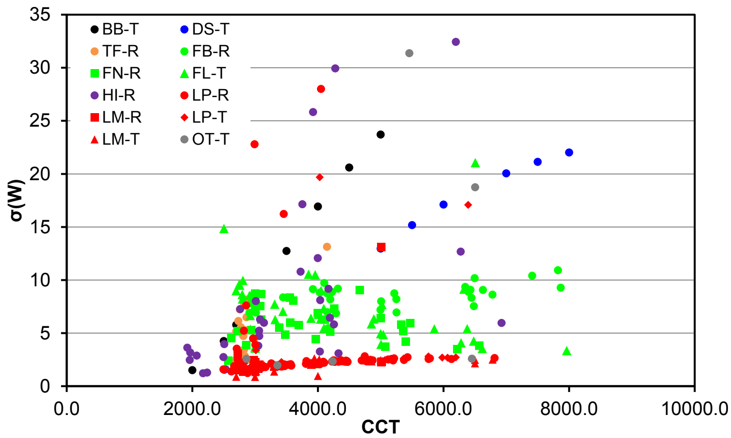

(b)

Figure 10 – CCT of each illuminant versus ΔW and $\sigma(W)$ of the whiteness standards under each illuminant.

We stress again that the present computation may somewhat underestimate the whiteness rendering under the illuminants with high CCT because UV radiation is not accounted for, and illuminants with high CCT usually have some UV radiation. On the other hand, LEDs are accurately characterized here as they typically do not have UV emission.

Nevertheless, illuminants with excessively high violet emission may not render whiteness in a desired way. Figure 11 summarizes the whiteness values of the standards under six phosphor-converted LED real illuminants having various violet emission level with similar CCT (2900 ± 100 K), and whiteness values under a 3000 K blackbody radiator. All these illuminants are violet-pumped LEDs. Although the illuminant with 11.2% violet emission can activate FWAs, it achieves a very high degree of whiteness which may be undesirable or unnatural. A source with 6-8% violet emission is expected to induce whiteness rendering comparable to a 3000K blackbody radiator (David et al, 2013b). Thus, the mere presence of violet optical radiation is not sufficient and desirable; rendering of white objects containing FWAs can only be achieved by appropriate engineering of the source's spectrum.

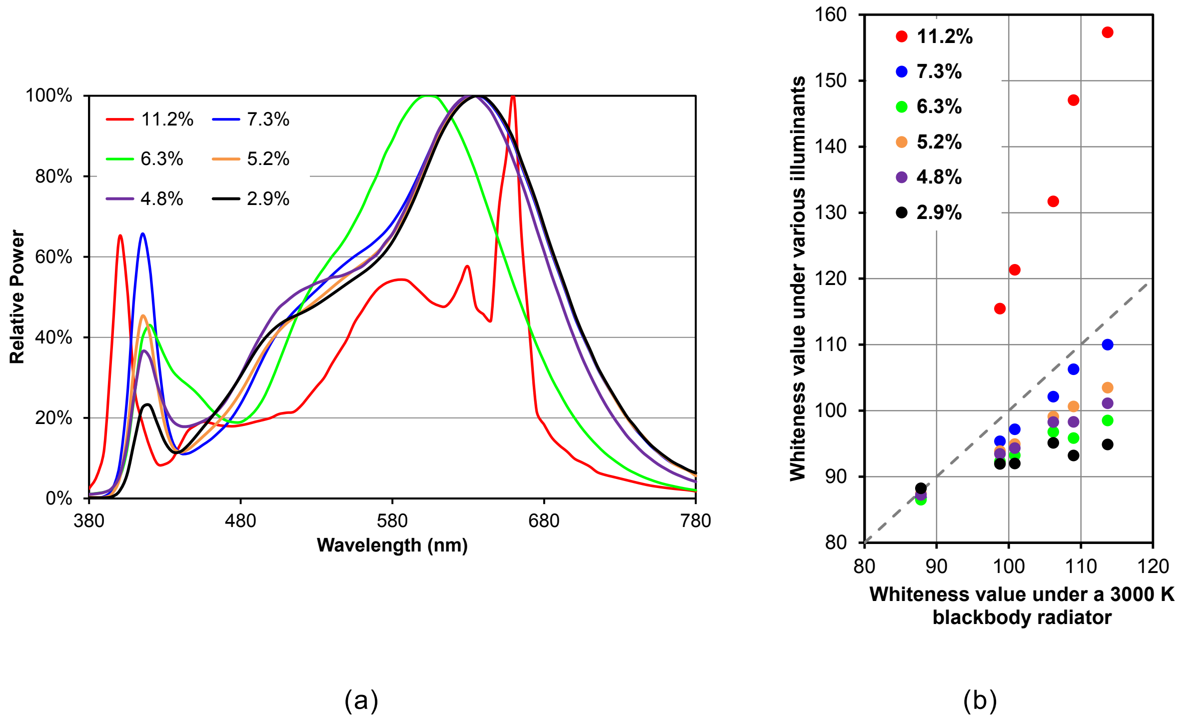

Figure 11 – (a) The SPD of six illuminants with similar CCT but various violet emission; (b) The whiteness value of the six whiteness standards under each of the six illuminants versus those under a 3000 K blackbody radiator.

5 Conclusions

The whiteness value of six calibrated whiteness standards containing varying amount of fluorescent whitening agents (FWAs) was computed under 406 illuminants using an adapted whiteness formula. We conclude that blue-pumped LED sources fail to render whiteness due to the lack of UV and violet emission. Most conventional sources are able to excite FWAs to some extent, although there is great variation even for a given CCT due to the lack of control of the short-wavelength radiation. Violet emission is found to be well correlated with whiteness rendition. Appropriate engineering of the spectral content of LED sources, providing proper violet emission, is necessary to control the degree of whiteness rendition for FWA-containing materials.

References

Choudhury AKR. 2006. Textile preparation and dyeing. Enfield (NH): Science Publishers. 834 p.

CIE. 2004a. CIE 15-2004. Colorimetry. 3rd ed.

CIE. 2004b. CIE 157-2004. Control of damage to museum objects by optical radiation.

CIE. 2007. CIE 182-2007. Calibration methods and photoluminescent standards for total radiance factor measurements.

CIE. 2013. TC1-36: Fundamental chromaticity diagram with physiologically significant axes. Januray 2013 Report (personal communication, 2013).

David A, Krames MR, Houser KW. 2013a. Whiteness metric for light sources of arbitrary color temperatures: proposal and application to light-emitting-diodes. Opt Express. 21(14). 16702-16715.

David A, Krames MR, Wei M, Houser KW. 2013b. Whiteness enhancement by LED sources. IES Annual Conference 2013. Oct 26-29, 2013. Huntington Beach (CA), USA.

[ISO]. International Organization for Standardization. 2004. ISO 11475:2004 Paper and board— - determination of CIE whiteness, D65/10o (outdoor daylight). 12 p.

[ISO]. International Organization for Stadardization. 2010. ISO 11476:2010 Paper and board— - determination of CIE whiteness, C/2o (indor illumination conditions). 13 p.

Ganz E. 1979. Whiteness formulas—A selection. Appl Opt. 18(7). 1073-1078.

Griesser R. 1994. Assessment of whiteness and tint of fluorescent substrates with good interinstrument correlation. Color Res Appl. 19(6). 446-460.

Griesser R. 1996. CIE whiteness and tint: Possible improvements. APPITA J. 49(2). 105-112.

Hall JB, Hefferren JJ, Olsen NH. 1970. Study of fluorescent characterstics of extracted human teeth by use of a clinical fluorometer. J Dent Res. 49(6):1431-1436.

Hartles RL, Leaver AG. 1953. The fluorescence of teeth under ultraviolet irradiation. Biochem J. 52(2). 632-638.

Houser KW, Wei M, David A, Krames MR, Shen XS. 2013. Review of measures for light-source colour rendition and considerations for a two-measure system for characterizing color rendition. Opt Express. 21(8). 10393-10411.

Houser KW, Wei M, David A, Krames MR. 2014. Perceived whiteness under LED illumination. (Accepted for publication in Leukos).

Jordan BD, O'Neill MA. 1991. The whiteness of paper-colorimetry and visual ranking. Tappi J. 74(5). 93-101.

Judd DB. 1935. A method for determining whiteness of paper. Paper trade journal. 100(21). 40-42.

Katayama I, Fairchild MD. 2010. Quantitative evaluation of perceived whiteness based on a color vision model. Color Res Appl. 35(6). 410-418.

Krais P. 1929. On a new black and a new white. Melliand Textil Inteber. 10:468.

MacAdam DL. 1934. Specification of whiteness. J Opt Soc Am. 24. 188-191.

Wei M, Houser KW. 2012. Status of solid-state lighting based on entries to the 2010 US DOE Next Generation Luminaire competition. Leukos. 8(4). 237-259.

Zwinkels J. 2008. “Surface fluorescence: the only standardized method of measuring luminescence” in “Standardization and quality assurance in fluorescence measurements I”, Vol. 5 of Springer Series on Fluorescence, U. Resch-Genger Editor (Springer Berlin Heidelberg). 163-192.

OP14

SPECIFICATIONS FOR THE CHROMATICITY OF WHITE LIGHT SOURCES

LUO, M.R.[1,3*], CUI, G.H.[2], GEORGOULA, M.[3]
[1] State Key Laboratory of Modern Optical Instrumentation, Zhejiang University, Hangzhou, CHINA
[2]Scool of Physics & Electronics Information Engineering, Wenzhou University, Wenzhou, CHINA
[3]School of Design, University of Leeds, LEEDS, UK
*m.r.luo@leeds.ac.uk

Abstract

The present study investigates the colour difference discrimination for light source colours with six colour centres along the blackbody locus. The experiment was carried out on a display to simulate light sources. Each centre includes 20 pairs, which were assessed by 20 observers using the ratio method. The results were used to test various models including xy, u'v' chromaticity diagrams, CIELUV, CIELAB and CAM02-UCS uniform colour spaces and CIEDE2000 colour difference formula. The results showed that those models developed fromthe aperture mode colours such as u'v' and CIELUV predicted the results much more accurately than those developed from the surface mode colours such as CIEDE2000 and CAM02-UCS.

The present results strongly indicate that the current ANSI standard for the specification for the chromaticity of SSL products, based on u'v' chromaticity diagram, is reliable.

Keywords: Aperture mode colours, surface mode colours, MacAdam ellipses, uniform colour space, chromaticity diagram, xy, u'v', CIELUV, CIELAB, CIEDE2000, CAM02-UCS.

1 Introduction

In the lighting industry, the white sources are specified in terms of chromaticity coordinates. American standards, ANSI C78.376(ANSI, 2001) and C78.377(ANSI, 2008) were published for the specification of chromaticity of fluorescent lamps and Solid State Lighting Products for indoor lightings, respectively. The former specifies the colour tolerance of white at 6 correlated colour temperature (CCT): 2700K, 3000K (Warm white), 3500K (White), 4100K (Cool white), 5000K and 6500K (Daylight). The latter adds 2 nominal CCTs (4500K and 5700K) plus flexible CCTs ranged from 2700K to 6500K at 100K intervals. The tolerance were specified in terms of 0.006 $\Delta u'v'$ (CIE 13.3, 2004) units corresponding to the just noticeable difference (JND), defined as 7 units of the MacAdam ellipses [4]. In the Annex of C78.377-2011, it also gives the specification of tolerance, defined as 4 corners of a quadrangle. Its shape makes no gap between the standard sources and its size corresponds to the 7 units of the MacAdam ellipses. Figure 1 shows the specifications for the 8 ANSI white sources in terms of quadrangles in CIE 1931 xy chromaticity diagram. The MacAdam ellipses are also plotted in Figure 1 (those in red colours).

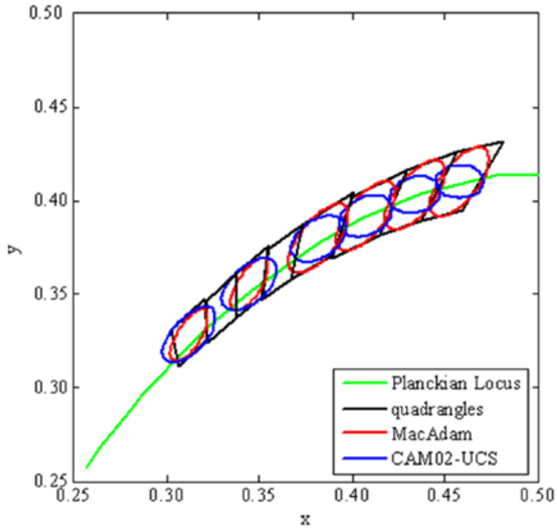

Figure 1 – The quadrangles, MacAdam ellipses and CAM02-UCS ellipses corresponding to the eight ANSI C78.377-2011 whites plotted in CIE 1931 xy chromaticity diagram. The ellipses are plotted in solid and dashed contours respectively.

More recently, new colour difference equations and uniform colour spaces have been developed such as CIEDE2000 (Luo et al, 2001; CIE, 2013) and CAM02-UCS (Luo et al, 2006) respectively, to fit the colour discrimination data based on surface colours (Luo et al, 2001). Although the spaces are for the surface colours, they can still be used to evaluate white lights by illuminating them on a white paper. The chromaticity ellipses corresponding to CAM02-UCS are also plotted in Figure 1 (see blue ellipses). Note that if xy chromaticity diagram is a uniform colour space, all ellipses should be equal sized circles and all quadrangles should be equal sized squares. The results in Figure 1 show that this is not the case. However, it can be seen that large discrepancy between two sets of ellipses. This is particularly marked for those whites in lower CCTs, i.e. all ellipses are long and thin, but blue ellipses are much smaller and have a lower angle. The reason for this could be due to the mode of colours [illuminant (aperture) vs. surface (object)], i.e. the MacAdam data were generated based on aperture colours produced by a visual colorimeter by only a single observer. This study is designed to provide fresh experimental results on perceived colour differences in different whites defined by CCTs using aperture colours.

2 Experimental

Six colour centres were selected in the experiment corresponding to white lights at 2700K, 3000K, 3500K, 4000K, 5000K and 6500K. The experiment was carried out on a wide gamut Eizo CG220 22 inch display with a resolution of 1920 by 1200 pixels, to simulate the light stimuli presented in aperture mode.

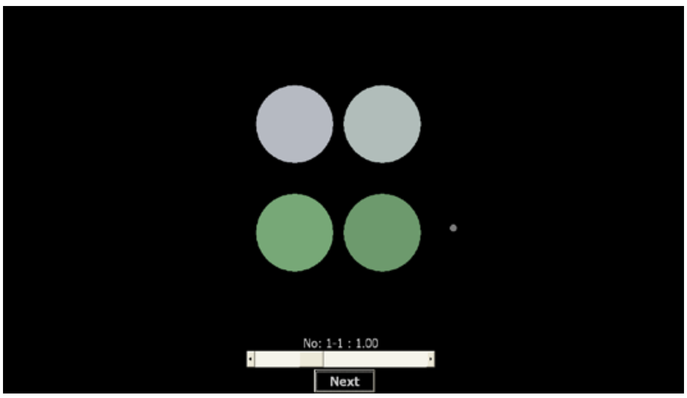

Figure 2 – The sample arrangements in the experiment

Two pairs of lights were presented at one time in a dark room. The sample and reference pairs are shown in the top and bottom in Figure 2. Each colour had a visual field of 4o subtended to observer's eyes. The reference pair green colour had a fixed ∆u'v'[6] colour difference of 0.007 units. Twenty-two normal colour vision observers participated in the experiment using the ratio method, i.e. each observer judged the colour difference of a sample pair against the reference pair having a visual difference of 1.0. If the sample pair having a larger colour difference than that of the reference pair, the result will be larger than one. Otherwise, it will be less than one. Twenty testing pairs were generated from the u'v' chromaticity diagram to have ∆u'v' of 0.007 in a circle from 0 to 360o at 18o intervals. The sequence of the stimuli presented was random for each observer and the locations of the samples in the sample and reference pairs were interchanged. Each observer made two repeated judgments. Overall, the results of 5280 assessments were accumulated, i.e. 20x6x22x2.

3 Results and Discussions

3.1 Observer uncertainty

The results were first analyzed to determine observer uncertainty, which typically includes inter- and intra- observer repeatability. The STRESS factor (Garcia, 2007) was used to express its performance ranged from 0 the best to 100 the worst. These were 15 and 9 STRESS units for the inter- and intra- observer variability, respectively. It was also found that similar STRESS values across all white sources. This means that there is no difference of observer uncertainty between the colour centres studied.

3.2 Testing Colour Models' Performance

Finally, the mean results for each pair were used to test various uniform colour spaces and colour difference formulae such as CIELAB (CIE, 2004), CIELUV (CIE, 2004), CIEDE2000, CAM02-UCS and chromaticity diagrams such as xy and u'v' together with the MacAdam ellipses formula. Their performances are summarized in Table 1 in terms of STRESS unit.

Table 1 –Performance of different colour models in STRESS unit

Center	xy	u'v'	CIELAB	CIELUV	CIEDE2000	CAM02-UCS	MacAdam
STRESS	29.3	10.7	32.4	10.3	28.7	27.4	19.0

Table 1 results showed that u'v' diagram and CIELUV space performed the best (about 11 STRESS units). These two models were mainly developed to fit the aperture mode colours (coloured lights). They will then be followed by the MacAdam ellipses (19 units), and then CAM02-UCS (27 units) and CIEDE2000 (29 units) and finally CIELAB performed the worst (32 units). All the formulae developed based on the surface colours do not perform well, CAM02-UCS, CIEDE2000 and CIELAB.

Figure 3 shows the experimental ellipses in red, u'v' circles in blue and ANSI quadrangles corresponding to the eight centers plotted in CIE 1964 u'v' chromaticity diagram. It can be seen that the u'v' constant sized circles fit well to the experimental ellipses. This concludes that the ANSI standard adopting ∆u'v' measure is reliable to quantify the colour tolerance of light sources.

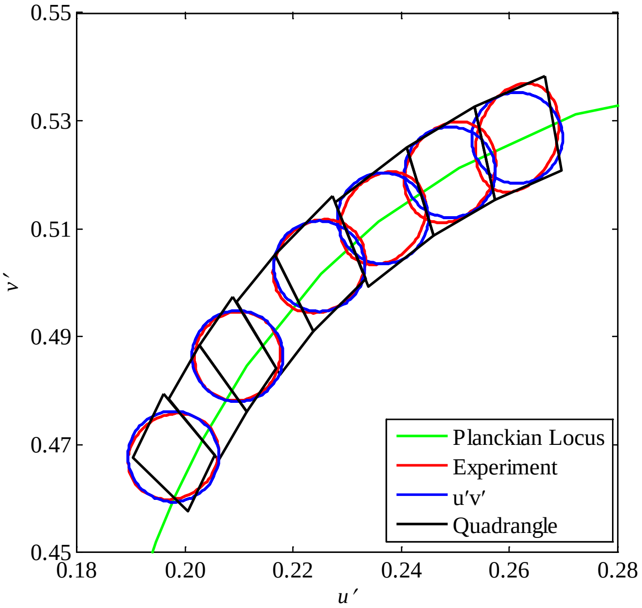

Figure 3 – The experimental ellipses, u'v' circles and ANSI quadrangles corresponding to the eight centers plotted in CIE 1964 u'v' chromaticity diagram. The former two are plotted in red and blue colours respectively.

4 Conclusion

An experiment was carried out to investigate the colour difference discrimination for 6 white sources along the blackbody locus. The results showed that the u'v' and CIELUV based metrics outperformed CIELAB ones. This confirms that the current ANSI standards for defining the colour tolerance of chromaticity are reliable.

It also implies that the condition for viewing the light directly from the source differs from that for viewing illuminated paper from the source. This could mean that there is a need for a colour space for coloured sources such as LED. New experiments have been carried out to perform visual assessments for the majority of the MacAdam data.

References

ANSI C78.376-2001, Specifications for the chromaticity of fluorescent lamps.

ANSI C78.377-2008, Specifications for the chromaticity of solid state lighting products.

CIE13.3:2004 Colorimetry, Central Bureau of the CIE, Vienna, 2004.

MACADAM, D. L. 1942. Visual sensitivities to colour differences in daylight, J. Opt. Soc. Am. 32 247-274.

CIE S 014-6/E: 2013 Colorimetry – Part 6: CIEDE2000 Colour-Difference Formula, Vienna, 2013.

LUO, M. R., CUI, G. and RIGG, B. 2001.The development of the CIE 2000 colour difference formula, Color Res. Appl. 26 340-350.

LUO, M. R. CUI, G. LI, C. 2006 Uniform Colour Spaces Based on CIECAM02 Colour Appearance Model, Color Res. Appl31, 320-330.

GARCIA, P. A. HUERTAS, R. MELGOSA, M. and CUI, G. 2007 Measurement of the relationship between perceived and computed colour difference. J. Opt. Soc. Am. A 24, 823–1829.

OP16

LIGHTING FOR PEDESTRIANS: WHAT ARE THE CRITICAL VISUAL TASKS?

Fotios, S., Uttley, J., Yang, B
School of Architecture, The University of Sheffield, UK
steve.fotios@sheffield.ac.uk

Abstract

Eye tracking was carried out at daytime and after-dark in an outdoor setting, using a dual-task to identify pedestrians' critical visual fixations. The results suggest that fixations determined using the dual task provide a good estimate of the important fixations by helping to ignore the less-critical fixations. Critical fixations also appear to be robust against their frequency of occurrence in a natural setting. It was concluded that the near path (<4 m) and distant people (>4 m) are critical visual fixations for pedestrians.

Keywords: Eye tracking, road lighting, pedestrians, visual tasks

1 Introduction

Recommended illuminance levels for road lighting in the UK are given in BS EN13201-2:2003 [BSI, 2003]. The target average illuminance levels for subsidiary roads (which includes residential roads) range between 2 lux and 15 lux in six classes, chosen according to environmental zone and traffic flow [BSI, 2012]. However, these illuminance levels appear to be based on inappropriate empirical and are in need of review [Fotios and Goodman, 2012]. One approach to identifying optimum illuminances is to investigate how changes in illuminance affects those tasks considered to be important for pedestrians.

There is a tendency to assume that when lighting for pedestrians the critical visual tasks are perceived safety, obstacle detection, recognition of the intent and/or identity of other road users, and these with lighting of an acceptable appearance, following the work of Caminada & van Bommel [1980]. What is not yet known is whether these tasks are indeed appropriate for setting the design characteristics of lighting, whether there are other essential visual tasks that need to be considered, and the relative importance of each task. This article presents the conclusions drawn from a study of pedestrians' visual fixations using eye-tracking carried out to explore the critical visual tasks.

2 Eye tracking

The eye-tracking system used in this experiment was the iView X HED made by SensoMotoric Instruments (Figure 1). Two cameras are mounted on a cycle helmet worn by the participant. One camera records the scene facing the participant, the other camera captures an image of the right eye. A calibration procedure was used to create a reliable track of the participants' gaze position. The eye-tracking helmet was connected to a laptop carried in a rucksack by the participant. The eye-tracking system provides a video output showing the gaze position as a cursor overlay on the video of the scene facing the participant. In addition a data file is created with details of the eye-tracking samples recorded by the system, including coordinates of the gaze position. This can be used to detect fixations, saccades and blinks using software provided with the system. Gaze position accuracy is reported by the manufacturer to be typically between 0.5° - 1.0°.

Participants were asked to walk a short route circumnavigating the University of Sheffield campus whilst wearing the eye-tracking equipment and carrying out a dual task by pressing response button after frequent but random auditory stimuli (see section 3). The route was approximately 900m in length and was split into four sections (Figures 2 and 3), with each section chosen to provide different characteristics, such as road crossings or uneven terrain:

A Pedestrianised area on University campus. Generally busy with a high number of people. Flat, uniform pathway surface, few obstacles and bright road lighting.

B Mainly side streets close to University hub, mixed levels of traffic volumes. Irregular pathway surface, high number of obstacles. Includes steps and a road crossing. Generally high number of people, road lighting of medium brightness.

C Short section with uniform pathway surface. Adjacent to busy road. Generally some other people present but not high volumes. Bright road lighting.

D Residential estate that participants were generally unfamiliar with (as confirmed in debrief interviews). Residential roads with low traffic volumes. Pathway surface generally good but included changing gradients. Low numbers of other people. Some areas without road lighting, other areas with dim road lighting.

Figure 1 – SMI iView X HED mobile eye tracking system (left) and screenshot from recorded video (right). The red cursor shows current gaze location (amplified for this image).

On attending the first trial participants completed a Landolt ring acuity test and an Ishihara colour perception test under normal office lighting conditions. They were then set up with the eye-tracking equipment, taken outside to complete the eye-tracking calibration procedure, and then taken to the start of the route. At the beginning of each route section participants were given a description of where to walk for that section and were shown a schematic map of the route. A researcher followed the participant a short distance behind (approximately 5 m) as they walked each section. The same procedure (but without the initial vision tests) was carried out for the second session. The order of the light condition (daylight or after dark) and route direction (clockwise or anti-clockwise) was counterbalanced.

Forty participants took part in the experiment (53% male; 58% in the 18-29 age group, 35% in the 30-49 age group and 7% in the 50+ age group). Participants were screened for having normal or corrected-to-normal vision using a Landolt ring acuity test and the Ishihara colour perception test. 40% of participants wore glasses or contact lenses for viewing short- or long-distance objects. All participants reported having normal or good hearing. Each participant carried out the walk twice, once during hours of daylight and once during hours of darkness. Trials during hours of daylight occurred between 08:00 and 16:00, whilst after-dark trials occurred between 17:00 and 20:00.

The aim of this experiment was to identify the items fixated by participants and for this eight categories of fixation attention were created, chosen in part following the categories used in past work (Table 1). A ninth ‘unknown’ category was also used to collate instances when the critical fixation could not be determined due to poor eye-tracking quality or if the gaze location was off screen.

Figure 2 – Photographs of the four route sections. Clockwise from top-left: route section A, B, C and D.

Figure 3 – Map of route followed by test participants. Start and end of clockwise route shown: these were reversed for anti-clockwise route.

Table 1 – Description of groups used to categorise fixation targets

Object category	Description	Object category	Description
Person	*Other pedestrians*	Vehicle	*Stationary or moving vehicle, or moving bicycle*
Path	*Pathway in direction of travel*	Trip hazard	*Small object or pathway irregularity that could cause pedestrian to trip*
Latent threat	*Hazards not visible until last moment or that not materialised yet*	Large objects	*Larger object in pathway that pedestrian has to navigate around, e.g. street furniture or lamp post*
Goal	*Target destination or waypoint towards destination*	General environment	*Areas of environment not fitting into other categories*

Frame-by-frame coding of visual fixations is a demanding task, which is perhaps one reason why past studies [e.g. Foulsham et al, 2011] have examined only discrete sections of their video records. Hence, this first analysis of all-fixations used data from only ten (25%) of the forty test participants and 120 s segments from three of the four route sections (A, B and D). These ten test participants were those having high eye-tracking validity (few missing fixation data) and were balanced across trial order (daytime or after dark being the first trial) and route direction. Of the ten participants selected, six were male; five were aged under 30, three were aged 30-49, and two were aged over 50 years old. Three participants wore their normal corrective lenses.

Figure 4 shows the proportions of fixations on the different categories of object for the daytime and after dark trials. Person, path and goal are the most frequently fixated objects, in both daytime and after dark trials. The differences between daytime and after-dark appear to be small other than for the path category where there appears to be a large increase in fixations after-dark than during daytime.

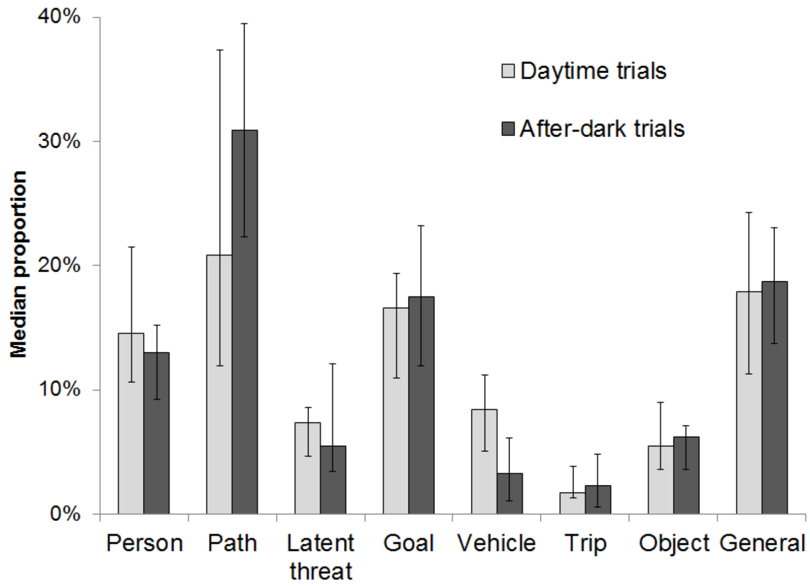

Figure 4 – Proportions of fixations upon the eight fixation categories. These data were determined from trials carried out by 10 test participants and for 120 seconds each from three route sections. Error bars show interquartile range.

These results are compared with those from past studies carried out in real outdoor environments in Table 2. Foulsham et al [2011] recorded visual fixations during a 5-10 minute walk to a café and found that 21% of fixation time was directed towards people, 37% towards the path, and 37% towards other objects. A second study carried out in a real environment is that of Davoudian and Raynham [2012] who found that 41-51% of fixations were directed towards the path but only 3% towards other people. There is a relatively low proportion of fixations on people, suggesting that fixation on people is not a critical task. The large differences in proportion of fixations on people in the Davoudian and Raynham study (3%) and the Foulsham et al study (21%) may arise because only few people were encountered in the Davoudian and Raynham study: these data may not be generalizable to other situations.

Table 2 – Comparison of proportions of fixations on person, path and objects/environment categories between current study, Foulsham et al [2011] and Davoudian and Raynham [2012]

Category of object		Current Results (N=10)		Foulsham et al (2011)	Davoudian & Raynham (2012)	
		Day	After dark	Day	Day	After dark
Person	Near	3%	4%	7%	3%	3%
	Far	16%	8%	14%		
Path	Near	16%	26%	29%	51%	41%
	Far	10%	8%	8%		
Objects / environment		55%	55%	37%	46%	56%

NOTE: Path for the current study includes both Path and Trip hazard categories from earlier analyses. Mean rather than median proportions for current study are shown for comparability with other two studies. Near and far distance distinction is shown for comparison with Foulsham et al (see Section 4 for further details), Davoudian and Raynham did not use near and far distinction; Foulsham et al did not use after dark condition.

Counting the proportion of time for which different categories of object are fixated (all-fixations), a common approach to interpretation of eye-tracking data, suffers two limitations when searching to identify the critical tasks. First, apparent fixation on an object does not imply that fixation on the object is critical to safe walking, and similarly, it does not imply that cognitive attention was being devoted to that obstacle – the observer may have been daydreaming. Walking along a street is not a cognitively taxing task and it is unlikely that all of a pedestrian’s fixations relate to this task. Second, it does not account for the frequency by which an object was encountered during the trial, this likely to be random in outdoor trials in natural settings. For example, if only one person was encountered during a trial the proportion of fixations on other people would necessarily be low, but this would be a function of the number of other people encountered.

3 Dual task

An attempt to better identify critical fixations was made using a dual task, a secondary cognitive task running concurrently with the task of walking, requiring that test participants responded quickly to an acoustic signal by pressing a button: delayed response to this task was used to isolate moments where cognitive attention was distracted toward a critical visual task (critical-fixations). Task instructions have been shown to focus attention allocation in a dual task setting [Kelly et al, 2010], and participants were instructed to respond to the acoustic signal as quickly as possible, so that instances of mind-wandering were reduced.

An Arduino microcontroller connected with a mini-speaker and response button was used to provide the concurrent dual task. The speaker was attached to the underside of the eye-tracking helmet, close to the left ear. The speaker emitted an audible beep at random intervals between 1 s and 3 s. The timing of each beep and each press on the response button was recorded. During trials test participants were instructed to press the button in response to every beep as quickly as possible, and were given an opportunity to practice this response prior to the start.

A delayed response to the dual task was defined as being two standard deviations greater than the participant's mean reaction time for that session. Failure to respond to an auditory stimulus was also classed as a critical time. At an instant suggested to be critical the experimenter inspected the video record to establish the object of visual fixation at that instant. This judgement was made by observing a two-second period of the eye-tracking video starting 1 s before the critical time, and the categorisation was based on what the researcher judged to be the most significant thing being observed at the time.

Figure 5 shows the proportions of fixations on the different categories of object as determined using the critical-fixations and all-fixations methods for the daytime and after-dark trials respectively, and these are for the same 10 test participants as Figure 4. In daytime and after-dark trials, critical-fixations indicate a higher proportion of fixations on people and vehicles than do all-fixations.

A conclusion drawn from the all-fixations data (Figure 4) is that "path" is the most important category of object as it has the highest proportion of fixations: observing other people appears less important. The critical-fixations approach reveals higher proportions of fixations on people and vehicles than did all-fixations, although these differences did not reach statistical significance. This increase in apparent importance reflects the increase in visual attention expected for objects of whose behaviours are less predictable than typically static items such as path, objects and goals. Jovancevic-Misic and Hayhoe [2009] found that pedestrians walking in an unpredictable way were more likely to be fixated, and fixated for a longer duration, than pedestrians who were predictable in their movements. Other research has shown an unpredictable feature of an environment produces greater fixation durations [Cinelli, Patla and Allard, 2009], and more frequent fixations [Droll and Hayhoe, 2007] than a predictable feature. Thus we suggest that the dual task provides an improved approach to identifying the critical fixations from amongst the complete set of fixations. A more complete analysis of critical fixations was therefore carried out using the larger sample size.

Of the 40 test participants recruited for this study, some had relatively high numbers of critical observations in the unknown category due to poor eye-tracking quality. Therefore participants were only included in the analysis if they had a total of at least five critical observations in categories other than unknown in both the daytime trial and after-dark trials. This criterion resulted in 12 participants being excluded. Figure 6 shows the proportion of critical observations in each category during the day and after-dark trials for the remaining 28 participants.

Figure 6 suggests that person and path are the most frequent critical fixation categories, with path more frequently fixated after-dark and people during daytime. Possible differences between day and after-dark are suggested and a series of Wilcoxon signed-rank tests were used to test the significance of these apparent differences. For the person and path categories, the Wilcoxon test suggested day and after-dark differences to be significant at levels of $p=0.034$ and $p=0.067$ respectively, hinting at a difference, a greater proportion of path fixations and a smaller proportion of person fixations after dark than during daytime. This may reflect behaviour to fixate less frequently on people after dark, but it may also reflect that fewer people were present after dark. For the other six categories the differences were not close to significance (p values of 0.143 to 0.849), suggesting a clear difference between the path and person groups and the other groups.

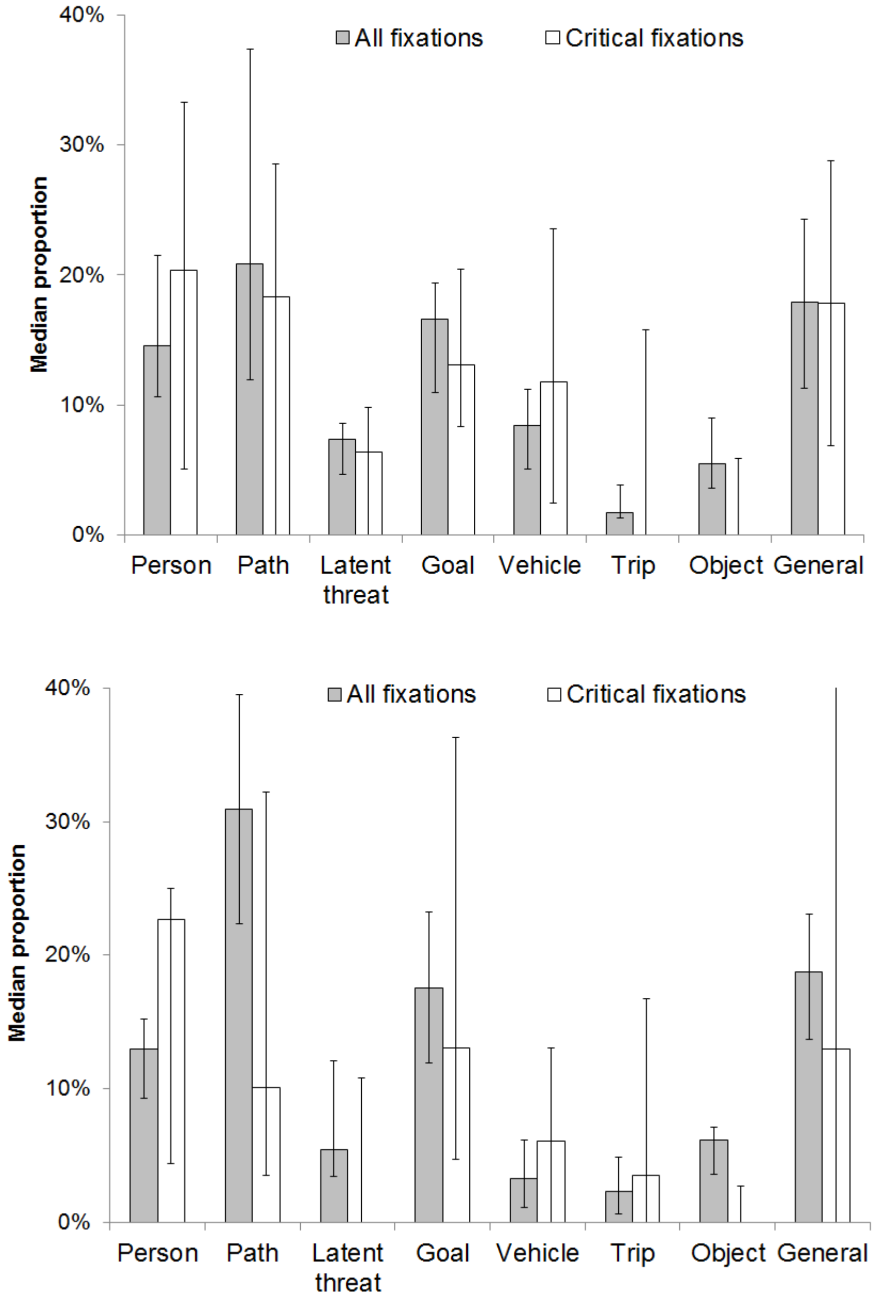

Figure 5 – Median proportions of all-fixations and critical-fixations per category during daytime (top) and after-dark (bottom) test sessions with 10 test participants. Error bars represent interquartile range.

4 Frequency of occurrence: fixation on pedestrians

A limitation of studying fixations when walking in an uncontrolled outdoor setting is that each test participant has a different experience, encountering different samples of pedestrians, vehicles and other discrete items. Hence one possible reason why Davoudian and Raynham report a smaller fixation on people (3%) than did Foulsham et al (21%) is that fewer people were encountered during their trials. An alternative approach to interpretations of eye-tracking data is to examine the probability that a pedestrian appearing in the field of view is fixated at least once. A greater probability of fixation may reflect greater importance as it increasingly demonstrates that visual information about that object is required.

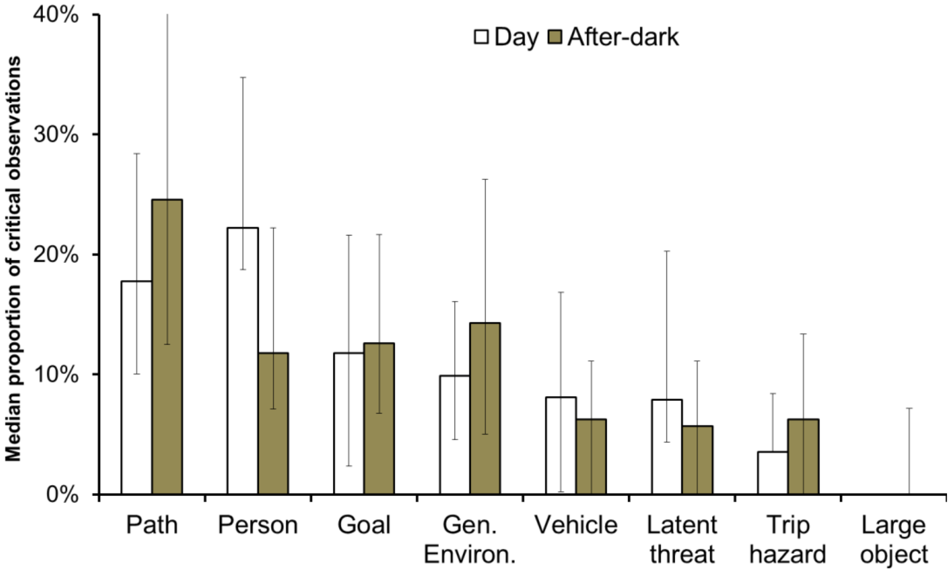

Figure 6 – Median proportion of critical observations in each category by day and after-dark conditions. Error bars show interquartile range. Median value = 0% for Large object day and after-dark conditions. Note: data from 28 test participants

Thus a third procedure was used to interpret the eye-tracking data: probability was determined by counting the number of pedestrians appearing in the field of view, and from these the number who were fixated at least once. One limitation of a probability approach is that only certain types of objects may be meaningfully analysed, i.e. discrete events such as people and vehicles, but not items such as pavements which are likely to be continually present in the field of view. Averaged across the ten test participants (as analysed for the all-fixations approach above) median fixation probability was 0.87 in daytime, 0.86 after dark, and 0.86 overall. These data are of a similar order to that reported by Foulsham et al [2011] (0.83).

Figure 7 shows regression of pedestrian fixation (determined using all-fixations, critical-fixations, or probability of fixation approaches) against the number of pedestrians encountered. These data show the day and after-dark trials for the ten test participants. Fixation proportion, fixation probability and number of pedestrians encountered are different kinds of measures and one way to compare these is to transform the data to z-scores [Rubin, 2013; Konar et al, 2010]. Analysis of the z-score distributions suggested that they are drawn from normally distributed populations except for the all-fixations data.

With the all-fixations data, the fixation proportion increases as the number of pedestrians encountered increases, confirming expectation that this approach suffers from stimulus bias. Spearman's test suggests this correlation to be significant ($r=0.58$, $p<0.01$). With the probability approach there is a negative relationship, in that there is a decrease in the probability of fixation as the number of people encountered increases, and the degree of correlation here is close to significant ($r=-0.40$, $p=0.08$) according to Pearson's test. This may be because with larger numbers of people it is not possible to fixate on all of them or alternatively deemed not necessary to fixate on all others. The horizontal line for critical-fixations shown in Figure 7 indicates that this approach does not have a relationship with the number of people encountered, and the Pearson's test does not suggest correlation to be significant ($r=-0.04$, $p=0.87$).

Thus the critical fixations established using the dual task leads to a more robust measure of the importance of fixating on other people as it is less affected by the number of other people encountered during trials in a natural setting.

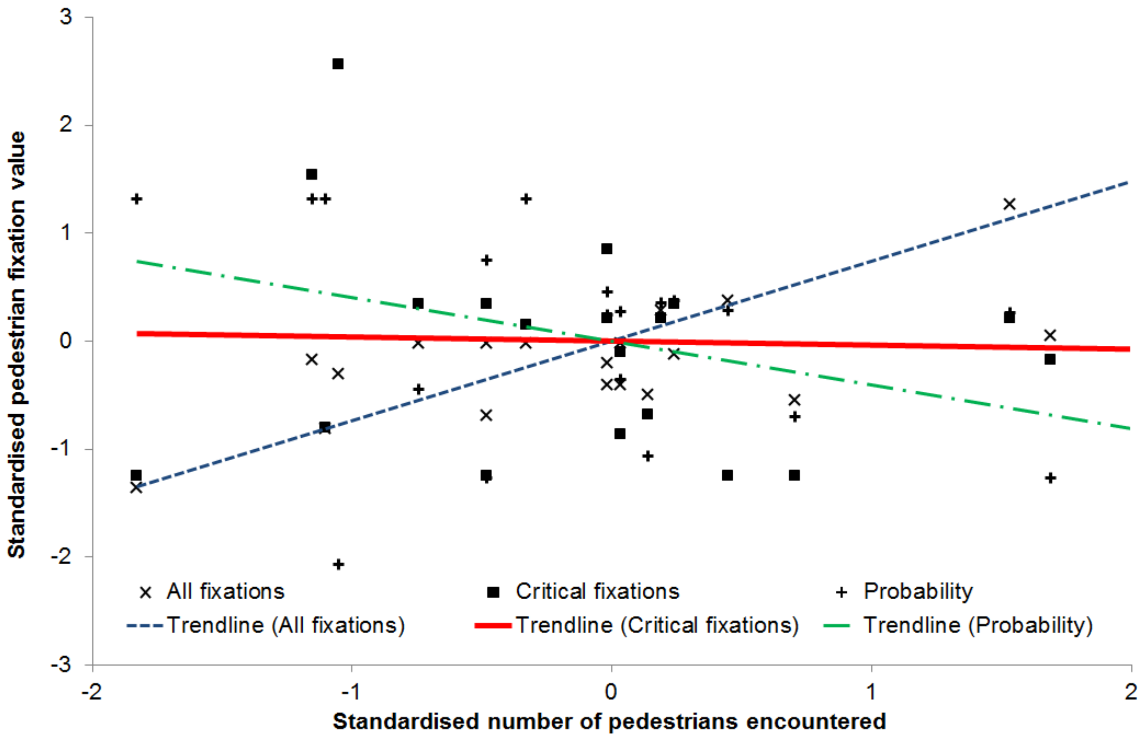

Figure 7 – Regression of measures of pedestrian fixation against the number of pedestrians encountered. This shows data for daytime and after-dark trials

The Path and Person categories have the highest proportions of critical observations (Figure 6). This suggests people and the path are important things for pedestrians to look at. Further analysis was carried out on these categories, examining whether critical observations were performed at a near or far distance, as has been done in past work [Foulsham et al, 2011]. Near items were those judged to be fixated within 4 m of the participant. Accurate physical measurements were not possible however, and the coder was instructed to make their own judgement, following the approach taken in previous research [Foulsham et al, 2011]. For this analysis the Trip hazard category has been included in the Path category, since trip hazards were located on the path. As with the previous analyses, the 12 participants who had less than 5 critical observations in categories other than Unknown, in either trial, were excluded. The remaining 28 participants were included.

A higher proportion of observations appear to be made at the near path compared with the far path and there is a tendency to look at other pedestrians when far away than when they are near. A Wilcoxon signed-rank test suggested the proportion of observations made at the near path was significantly higher than at the far path, when day and after-dark trials were combined (near median = 19.5%, far median = 6.3%, $T = 8$, $p < 0.001$). The proportion of observations at far people was also significantly higher than at near people (far median = 12.1%, near median = 6.6%, $T = 14.1$, $p = .04$).

5 Conclusion

The aim of this article is to use the results of an eye-tracking study to identify those objects of visual fixation that are critical to pedestrians. A dual task (response to an audio stimulus) was used concurrently with the eye-tracking. We conclude that this provides a better indication of which of the fixations are critical, and is less affected by the frequency of occurrence during trials in a natural setting. The data suggest that the path and people are the most important objects of visual fixation as they were more frequently fixated at critical moments than other categories of object. Further interpretation of the data suggest that these may be refined as the near path (<4m) and distant people (>4m). Further details of this work are available elsewhere [Fotios et al, in press a,b].

Acknowledgement: This work was carried out through support from EPSRC (EP/H050817) as part of the MERLIN project, and the EPSRC-funded E-Futures Doctoral Training Centre for Interdisciplinary Energy Research, University of Sheffield.

References

BSI. 2003. BS EN 13201-2:2003. *Road lighting - Part 2: Performance requirements*. London: British Standards Institution (BSI).

BSI. 2012. BS 5489-1:2013. *Code of practice for the design of road lighting Part 1: Lighting of roads and public amenity areas*. London: British Standards Institution (BSI).

CAMINADA, J.F., VAN BOMMEL, W. 1980. New lighting considerations for residential areas. *International Lighting Review*, 3, 69-75.

CINELLI, M.E, PATLA, A.E. & ALLARD, F. 2009. Behaviour and gaze analyses during a goal-directed locomotor task. *The Quarterly Journal of Experimental Psychology*, 62(3), 483-499.

DAVOUDIAN, N., RAYNHAM, P. 2012. What do pedestrians look at at night? *Lighting Research and Technology*, 44(4), 438-448.

DROLL, J.A. & HAYHOE, M.M. 2007. Trade-offs between gaze and working memory use. *Journal of Experimental Psychology*, 33(6),1352-1365.

FOTIOS, S., GOODMAN, T. 2012. Proposed UK guidance for lighting in residential roads. *Lighting Research and Technology*, 44(1), 69-83.

FOTIOS, S., YANG B., CHEAL C.2013. Effects of Outdoor Lighting on Judgements of Emotion and Gaze Direction. *Lighting Research & Technology*, first published on November 11, 2013 as doi:10.1177/1477153513510311

FOTIOS, S., UTTLEY, J., CHEAL, C., HARA, N. (In press (a)). Using Eye-Tracking To Identify Pedestrians' Critical Visual Tasks. Part 1. Dual Task Approach. *Lighting Research & Technology*.

FOTIOS, S., UTTLEY, J., YANG, B. (In press (b)). Using Eye-Tracking To Identify Pedestrians' Critical Visual Tasks. Part 2. Fixation on pedestrians. *Lighting Research & Technology*

FOULSHAM, T., WALKER, E., KINGSTONE, A. 2011. The where, what and when of gaze allocation in the lab and the natural environment. *Vision Research,* 51(17), 1920-1931.

HALL, E. 1969. *The Hidden Dimension*. New York: Anchor Books.

JOVANCEVIC-MISIC J., HAYHOE M. 2009. Adaptive gaze control in natural environments. *The Journal of Neuroscience*, 29(19), 6234-6238.

KELLY, V.E., JANKE, A.A., SHUMWAY-COOK, A. S. 2010. Effects of instructed focus and task difficulty on concurrent walking and cognitive task performance in healthy young adults. *Experimental Brain Research*, 207(1-2), 65-73.

KONAR Y., BENNETT P.J., SEKULER A.B. 2010. Holistic Processing Is Not Correlated With Face-Identification Accuracy. *Psychological Science*, 21(1), 38-43.

PATLA, AE. 1997. Understanding the roles of vision in the control of human locomotion. *Gait and Posture,* 5, 54-69.

ROTHKOPF, CA., BALLARD, DH., HAYHOE, MM. 2007. Task and context determine where you look. *Journal of Vision* 2007; 7(14), 1-20.

RUBIN A. 2013. *Statistics for Evidence-Based Practice and Evaluation*. 3rd Edition. Belmont, California: Brooks/Cole.

OP17

RELATIONSHIP BETWEEN UNIFORMITY AND DISCOMFORT FOR TUNNEL INTERIOR LIGHTING

Hagio,T.[1], Ito,H.[2], Mori,T.[3] Aoki,H.[4]
[1] Nippon Expressway Research Institute Co.Ltd., Tokyo, JAPAN,
[2] Panasonic Corporation, Osaka, JAPAN,
[3] Panasonic Corporation, Hokkaido, JAPAN,
[4] Nexco-East Engineering Co.Ltd., Tokyo, JAPAN,
t.hagio.aa@ri-nexco.co.jp

Abstract

In order to secure a comfort level equal to that of ordinary road lighting, the longitudinal uniformity of road surface luminance (U_l) of tunnel interior lighting needs to be determined according to S/H: ratio of spacing(S) to mounting height of luminaire (H). When S/H is in the range of 1,0 to 4,0, the lower limit of U_l is 0,7 to 0,9. However, the apparent driving speed and road surface luminance have no significant influence on the lower limit of U_l. Also, S/H should be less than 2,0 based on the measurement result of U_l in the tunnels in Japan where opposite luminaire arrangement is adopted, and the lower limit described above. On the other hand, because staggered luminaire arrangement cannot easily exceed the lower limit of U_l for comfort, staggered luminaire arrangement should be avoided for tunnel interior lighting.

Keywords: Uniformity, Tunnel interior lighting, Opposite arrangement, Staggered arrangement

1 Introduction

CIE recommends a minimum longitudinal uniformity of road surface luminance U_l (the ratio of the minimum luminance to the maximum luminance on the center line) of 0,6 in order to reduce discomfort caused by poor uniformity of luminance on the road surface. A same minimum U_l is defined for designing tunnel interior lighting in Japan. However, regarding the minimum U_l, there have been researches on road lighting based on various properties, but no research has been found on the relationship between U_l and comfort of the on tunnel interior lighting, which has shorter spacing, lower mounting height of luminaire than road lighting, and different characteristics of luminous intensity distribution. It is assumed that differences between road lighting and tunnel interior lighting are due to the difference in the luminance slope even with the same U_l, and it causes a difference in discomfort level due to uniformity of luminance on the road surface, resulting in a difference in the minimum U_l between them.

Therefore, experiments were conducted in a dark room by changing tunnel interior lighting properties to determine the lower limit of U_l with a view to reducing discomfort due to poor uniformity of road surface luminance. Then, the relationship between the actual U_l in the tunnel and the lower limit determined by the experiments were discussed.

2 Observation

2.1 Experimental installation

Figure 1 shows the overview of the experimental apparatus installation: in a dark room, the state of the visual field of a driver who is driving in a tunnel can be simulated by using computer graphics (CG) image. As Figure 2 shows, CG image simulate perspective image of the inner tunnel viewed from the center of the driving lane (left-side) in a perspective way. Three projectors projected the CG images on three 100-inch screens that were laterally aligned. The luminance on the road surfaces, walls and ceiling were adjusted by the process computer. The distance between an observer and the screen was 2,5 m. The visual angle of the screens from observation position had the ranges of 18 degrees in the vertical direction and 34 degrees in the horizontal direction of the screen. The luminance of the areas around the screen was almost zero. Assuming the front view of a driver can be partially blocked by the hood of a car, a shield plate was placed between the screens and the observer.

Figure 1 – Experimental apparatus installation

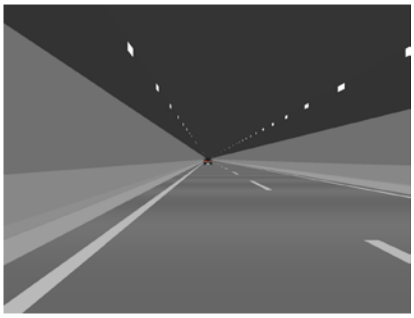

Figure 2 – Example of CG image

2.2 Experiment method

A “constant method” was used for the experiment in which images with specified factors being changed were randomly shown to each observer, and the observer was asked to compare and decide which image looked more comfortable. By identifying the test image (i.e., values of specified factors) with which 50 % of observers answered that it looked more comfortable than the reference image, the conditions of the test image, which has the same comfort level as the reference image, were able to be known. As for the reference image, illumination properties shown in Table 1 recommended by CIE based on the previous researches were used. *S*/*H* refers to ratio of spacing (*S*) to mounting height of luminaire (*H*).Figure 3 shows the CG image of reference image used for the experiment.

Table 1 – Conditions of the reference image

Average road surface luminance	1,0 cd/m^2
U_l	0,7
Spacing	35 m
Mounting height of luminaire	10 m
S/*H*	3,5
Apparent driving speed	100 km/h

Figure 3 – CG image of the reference image

2.3 Experiment conditions

Three levels of apparent driving speed, 60 km/h, 80 km/h and 100 km/h, were used for the test images. Considering the required road surface luminance according to the design speed in Japan, we used three levels of road surface luminance, 2,3 cd/m^2, 4,5 cd/m^2 and 9,0 cd/m^2, for the test images. However, in the conditions where the road surface luminance of a test image with 4,5 cd/m^2 or more, it looked about 2 to 9 times as bright as that of the reference image (1,0 cd/m^2), and this would cause variation in the adaptation levels of the observers, and as a result, the evaluation would be affected. Therefore, experiments with three different combinations of test images and reference images as shown in Table 2 were conducted so that the road surface luminance of a test image became less than 2 times as bright as that of a reference image.

Table 2 – Conditions of the reference image

	Image	Lighting type	Road surface luminance (cd/m²)	U_l
Experiment 1	Reference	Road lighting	1,0	0,7 (Recommended by CIE)
	Test	Tunnel interior lighting	2,3	----
Experiment 2	Reference		2,3	Lower limit determined by Experiment 1
	Test		4,5	----
Experiment 3	Reference		4,5	Lower limit determined by Experiment 2
	Test		9,0	----

Considering the examples in Japan, four levels of *S*/*H*, 1,0, 2,0, 3,0 and 4,0, were set. And considering the preliminary experiment results, five levels of U_l of test images, 0,70, 0,80, 0,85, 0,90 and 0,95, were set for *S*/*H* of 1,0 and 2,0, and five levels of U_l of the test images of 0,60, 0,65, 0,70, 0,75 and 0,80 were set for *S*/*H* of 3,0 and 4,0. For the three types of experiments above, conditions shown in Table 3 were used for the reference images. In addition, the CG image that reproduced the visual environment with a white light source was used, because the influence of light colour on the relation between U_l and comfort level has not been specifically indicated in previous researches on ordinary road lighting.

The observers consist of 15 people (males and females) aged from 24 to 62.

Table 3 – Reference image conditions

	Experiment 1	Experiment 2	Experiment 3
Lighting type	Road lighting	Tunnel interior lighting	
Road surface luminance (cd/m²)	1,0	2,3	4,5
U_l	0,7*1	0,8*2	
Spacing (m)	35	15	
Mounting height of luminaire	10 m	5 m	
S/*H*	3,5	3,0	
Apparent driving speed	100 km/h		

*1 Based on the road lighting recommended by CIE

*2 U_l of Experiment 2 is based on the result of Experiment 1, U_l of Experiment 3 is based on the result of Experiment 2.

3 Measuring lighting characteristic

3.1 Lighting installation

Measurements were taken in 20 tunnels(*S*/*H* ranging 0,48 to 2,6) in Japan in order to obtain the actual U_l of tunnel interior lighting. Table 4 shows the attributes of those tunnels.

Table 4 – Attributes of tunnels where measurements were taken

Pavement type	Luminaire arrangement	Light source	Lighting system	The number of tunnels
Porous asphalt	Opposite	Fluorescence lamp	Symmetrical	11
Cement-concrete				1
		Low-pressure sodium lamp		1
		LED		1
Porous asphalt	Staggered	Fluorescence lamp		4
		high-pressure sodium lamp		1
Cement-concrete		Low-pressure sodium lamp		1

3.2 Measuring lighting characteristic

In order to determine U_l of each tunnel, measurements were taken at five points along the center line in one interval of tunnel lights as shown in Figure 4. Figure 5 shows examples of conditions of tunnels where we measured road surface luminance.

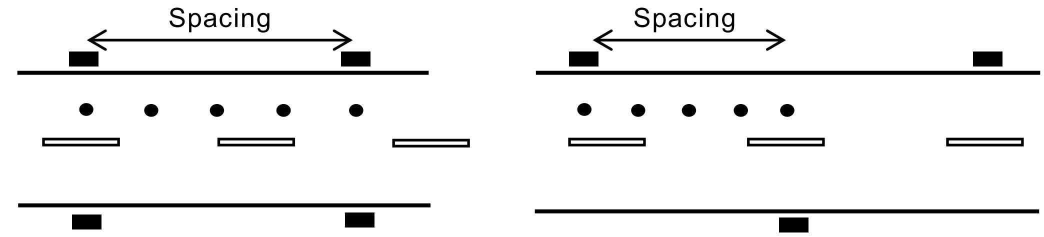

(a) Opposite luminaire arrangement (b) Staggered luminaire arrangement

●: Measured points, ■: luminaire

Figure 4 – Measuring points of road surface luminance (plane view)

Light source: fluorescence lamp
Lightings installed: opposite, Spacing: 12,4 m, *S*/*H*: 2,5
(a) Tunnel A : Pavement: porous asphalt

Light source: fluorescence lamp
Lightings installed: opposite, Spacing: 6,2 m, *S*/*H*: 1,3
(b) Tunnel B :Pavement: porous asphalt

Light source: low-pressure sodium lamp
Lightings installed: opposite, Spacing: 9,4 m, *S*/*H*: 2,0
(c) Tunnel C :Pavement: cement-concrete

Light source: fluorescence lamp
Lightings installed: staggered, Spacing: 6,5 m, *S*/*H*: 1,4
(d) Tunnel D :Pavement: porous asphalt

Light source: low-pressure sodium lamp
Lightings installed: ataggered, Spacing: 7,4 m, *S*/*H*:1,5
(e) Tunnel E : Pavement: cement-concrete

Figure 5 – Examples of measured tunnels

4 Considerations

4.1 Lower limit of U_l

U_l with a comfort level equal to the reference image (hereafter referred as “minimum permissible U_l: MPU_l”) was determined by identifying the test image that 50 % of the observers answered looked more comfortable than the reference image. Figure 6 shows examples of MPU_l for two observers with the road surface luminance of 4,5 cd/m^2. Figure 6(a) and Figure 6(c) show a general tendency that MPU_l became lower as S/H became larger. However, at the same time, as Figure 6(b) shows, the correlation between spacing and MPU_l was minor, and in some cases, the difference among observers exceeded 0,1 point and minimum permissible value tended to significantly depend on an individual observer.

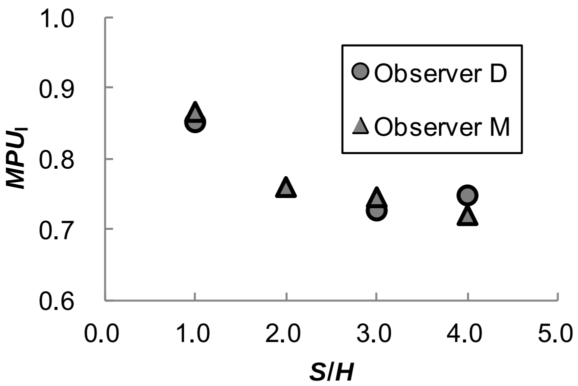

(a) Apparent driving speed: 60 km/h

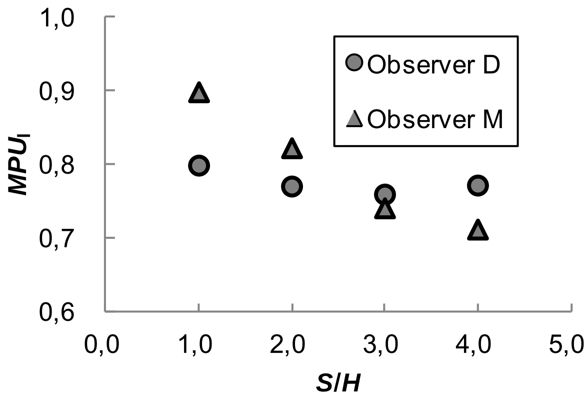

(b) Apparent driving speed: 80 km/h

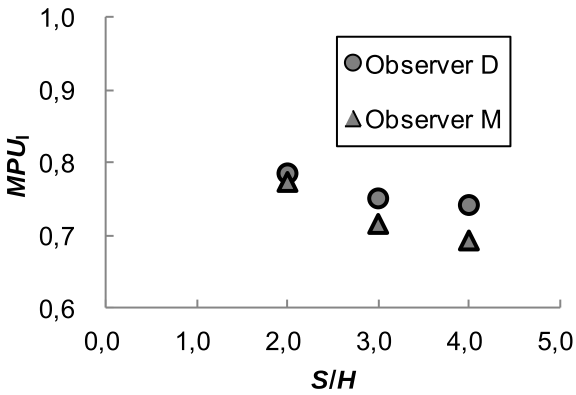

(c) Apparent driving speed: 100 km/h

Figure 6 – Relationship between S/H and MPU_l

Then, MPU_l that 50 % of the observers could accept (hereafter referred to as the “lower limit of U_l: LLU_l”) was determined. Figure 7 shows LLU_l didn’t significantly vary depending on apparent driving speed or road surface luminance, and the regression curve obtained by using LLU_l for every apparent driving speed also showed a relatively high correlation coefficient.

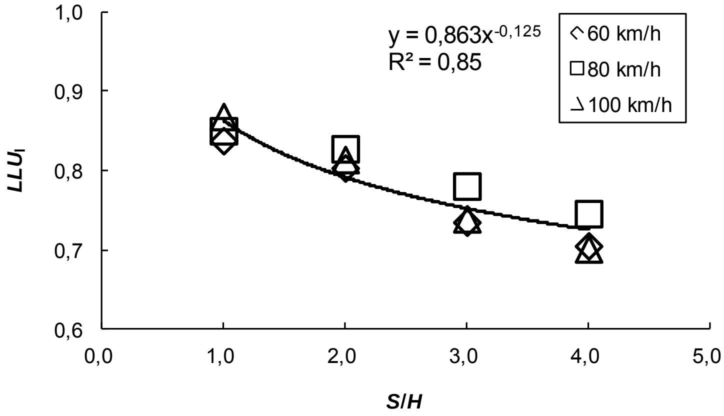

Reference image conditions: Road surface luminance 1,0 cd/m^2, *S*/*H* 3,5 , U_l 0,7
(a) Road surface luminance of the test image: 2,3 cd/m^2,

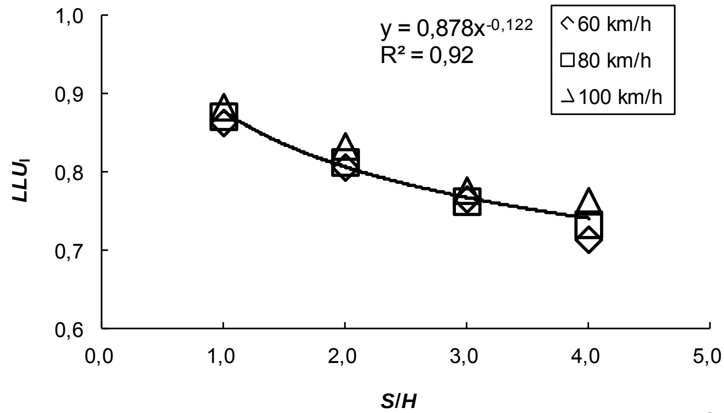

Reference image conditions: Road surface luminance 2,3 cd/m^2, *S*/*H* 1,5 , U_l 0,8
(b) Road surface luminance of the test image: 4,5 cd/m^2

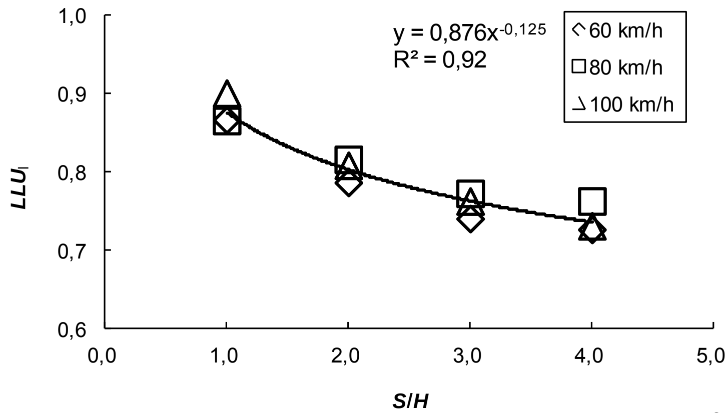

Reference image conditions: Road surface luminance 4,5 cd/m^2, *S*/*H* 1.5 , U_l 0,8
(c) Road surface luminance of the test image: 9,0 cd/m^2

Figure 7 – Relationship between *S*/*H* and LLU_l

Figure 8 shows LLU_l at S/H of 1,0 , 2,0 , 3,0 and 4,0 , which were calculated from the regression formula of the relationship between S/H and LLU_l shown in Figure 7, and shows no significant difference in U_l in relation to road surface luminance.

As mentioned above, CIE sets the tolerant U_l as 0,6 : however, in terms of comfort, it is presumed that a sufficient visual environment cannot be secured if S/H of 2,0 or smaller.

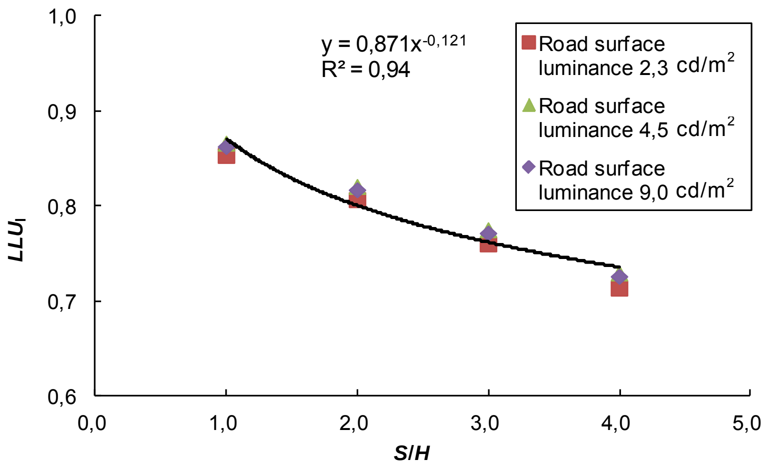

0229

Figure 8 – Relationship between S/H and LLU_l

4.2 Comparison between U_l at site and its lower limit

Figure 9 shows the relationship between U_l determined by actual point-by-point luminance measurements in the tunnels and the regression curve LLU_l determined by the experiments in the dark room. U_l of Tunnel A to Tunnel B in Figure 9 correspond to values measured in them in Figure 5.

Note that U_l in the tunnels was well over 0,6, recommended by CIE. However, in case of the tunnels with opposite luminaire arrangement, when S/H was 2,0 or larger, U_l tended to be smaller than the lower limit determined by the experiments.

On the other hand, all six tunnels with staggered luminaire arrangement and the S/H of about 1,4 to 2,0 had a lower U_l than LLU_l.

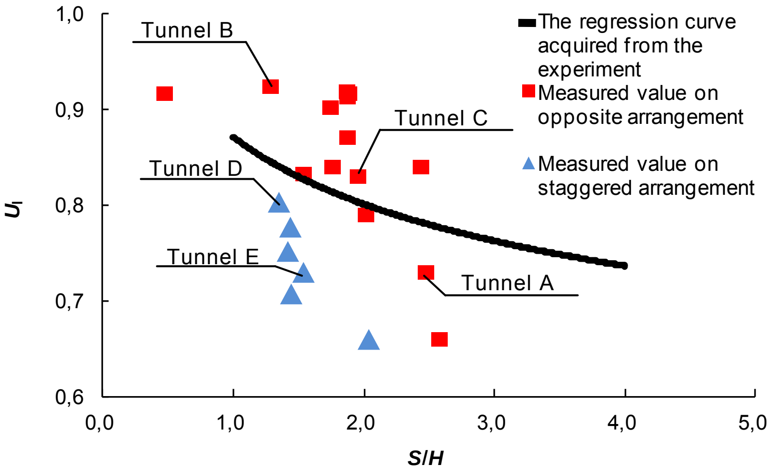

Tunnel A to Tunnel E in Figure 9 correspond to them in Figure 5.

Figure 9 – Ratio of spacing to height

5 Conclusion

Currently, for U_l of basic tunnel interior lighting, 0,6 has been adopted as a recommended value regardless of actual conditions. However, when comfort is considered, U_l has to be designed based on S/H. As S/H becomes smaller, higher U_l is required. In case the opposite luminaire arrangement with Symmetrical lighting distribution is adopted, it is preferable that S/H becomes 2,0 or smaller.

Conventionally, because the conventional light source types for lamp fittings in the tunnel were limited, there have been some cases that staggered luminaire arrangement of lamp fittings is adopted even under the conditions of relatively smaller road surface luminance. However, that makes difficult to secure appropriate U_l. Therefore, staggered luminaire arrangement should be avoided for tunnel interior lighting. Because LEDs have been increasingly adopted as the basic light source for tunnel interior lighting and it is easier to set the luminous flux compared with conventional light sources including fluorescence lamp and Low-pressure sodium lamp, it is preferable to set the luminous flux in opposite to make the lamp fitting interval with S/H 2,0 or smaller.

Acknowledgements

We would like to thank members of the technical committee of The Express Highway Research Foundation of Japan who advised us on about this study.

References

CIE 2004. CIE 88:2004. *Guide for the lighting of road tunnels and underpasses.* Vienna: CIE.

DE BOER J.B., KNUDESEN, B.1964. THE PATTERN OF ROAD LUMINANCE IN PUBLIC LIGHTING, *Proceedings of the CIE 15 the Session of the CIE*, pp.569-577.

OP18

THE FIRST INTERNATIONAL WORKSHOP ON CIRCADIAN AND NEUROPHYSIOLOGICAL PHOTORECEPTION, 2013: A PHYSICIST'S PERSPECTIVE ON THE CONSTRUCTION OF STANDARD UNITS

Price, L.L.A.[1], and Peirson, S.N.[2]
[1] Public Health England, Centre for Radiation, Chemical and Environmental Hazards, Public Health England, Didcot, OX11 0RQ, UK, [2] Nuffield Department of Clinical Neurosciences (Nuffield Laboratory of Ophthalmology), Levels 5-6 West Wing, University of Oxford, John Radcliffe Hospital, Oxford, OXON, UK
Luke.Price@phe.gov.uk

Abstract

An international workshop on the non-visual effects of light held in 2013 has published recommendations for five new measurement units (Lucas, 2014). The model used to define these units and the choice of scale adopted are examined in detail.

Keywords: IWCNP, non-visual, photoreception, melanopic, circadian, equivalent lux, pre-receptoral filtering, normalisation, standards, opinion.

1 Introduction

In January 2013 researchers from several centres involved in the study of circadian and neurophysiological responses to light met for an international workshop aiming to find a consensus on the action spectrum for non-visual responses to light. The consensus that emerged was not exactly as expected.

The Workshop proposed five new measurement units for the characterisation of light exposures – one each for the five known functional photopigments in the human retina. Additional work was still required before these recommended units could be realised in a form that might be appropriate to carry the 'lux' branding. Some of this work was anticipated, whilst other parts had to be introduced to meet the needs of the researchers wishing to follow the Workshop's recommendations.

It is this additional work that will be described in detail. This work determined how these five lux-like quantities should be calculated, how the spectral efficiency functions are normalised and paired with a common spectral efficacy constant, and how intuitive comparisons to lux, the photopic sensitivity curve $V(\lambda)$ and the spectral luminous efficacy constant are made possible by the development of an integrated model of reflectance, transmittance and absorptance for pre-receptoral filtering and detection of light entering the human eye.

2 Action spectra construction

The spectral sensitivity functions were constructed of two main elements:

- A pigment template (Govardovskii, 2000) combined with the best available data concerning the peak absorption wavelengths $\lambda_{\max}$ for the human opsins
- A model for the absolute transmittance of the human eye to allow for pre-receptoral filtering

2.1 Normalisation and Dimensionality

More esoteric elements of the functions included:

- Conversion of the action spectrum to a radiometric basis
- Normalisation of the action spectra with an equi-energy reference illuminant (Standard Illuminant E) against the photopic units

The new α-opic equivalent illuminance quantities E_α can be calculated from spectral irradiance $E_{\mathrm{e},\lambda}(\lambda)$ as follows (Lucas, 2014; CIE, 2014 in press):

$$E_\alpha = K_\mathrm{N} \int E_{\mathrm{e},\lambda}(\lambda) N_\alpha(\lambda) \mathrm{d}\lambda \qquad (1)$$

where

K_N is the spectral efficacy constant $K_\mathrm{N} = 683 \int V(\lambda)\mathrm{d}\lambda = 73\ 000$; and

$N_\alpha(\lambda)$ is the action spectrum normalised to unit area when integrated over wavelength in nanometres.

Normalisation deliberately did not follow the recommendations of SI (BIPM, 2006). These units therefore cannot be expected to be recommended by CIE in the foreseeable future in the form produced by the Workshop. The record of the Workshop (CIE, 2014 in press) includes an opinion concerning difficulties with the SI approach and action spectra dimensionality.

2.2 Pre-receptoral filtering and the standard human observer

There were also several important innovations in the pre-receptoral filtering model adopted, some of which are not present in previous studies:

- Allowance for the self-screening effect due to the non-negligible optical pigment density of the photoreceptive organelles (with the exception of the melanopsin function)
- Standard functions such as cone fundamentals were not used, as the non-visual functions relate to photoreception in the peripheral retina. Importantly the macular pigment is not found in this region.

    A well-tested age-related lens model was adopted (Pokorny, 1997), with a number of modifications:

    The suggested reinstatement of prior data for 400 nm to 420 nm (Wyszecki, 1982)

    Visual extrapolation of the optical density functions using a semi-logarithmic chart down to 380 nm

    On the same chart a line was fitted to the data between 560 nm and 650 nm and extrapolated to 780 nm

- Some visual smoothing was applied to the function between 400 nm and 470 nm
- The outer surface of the eye was recognised to be the tear film rather than the cornea (which is commonly reported); Fresnel reflectance at this surface was approximated with a spectrally neutral optical density and reflection was considered absent or negligible at other surfaces within the eye.
- The non-visual photoreceptive geometry was considered to be represented approximately by a cosine response in a plane parallel to the plane of the pupils (Note that in other species the pupils do not necessarily face in similar directions; personal addition).

The original review of the data forming the basis of the photopic units (Gibson, 1923) was consulted in the construction of a standard human observer (age 32, undilated pupil). This helped to ensure consistency between photopic units and the α-opic equivalent lux units recommended (but not by CIE). The final pre-receptoral filtering (without self-screening) was also compared to a number of studies of human lens transmittance and pre-receptoral filtering.

3 Discussion

A key advantage of the use of combining absolute transmittance data with the pigment template is that this approach creates a systematic method by which other photoreceptive action spectra can be created and improved routinely with further research data. For example, it may be possible and advantageous in a future revision to replace the pre-receptoral filtering data with a highly formularised model whilst retaining consistency with the standard human observer. If accomplished, this would create a genuinely continuous action spectrum model.

Moreover, with this approach to normalisation, the units can be compared intuitively by biological researchers and lighting professionals alike. To illustrate the last point, the table below shows some typical values for familiar and standard illuminants (data from the “Toolbox” in Lucas, 2014):

Table 1 – Log_{10} α-opic equivalent lux values relating to measurements of illuminants producing 100 lux in the same plane (i.e. 2 $\log_{10}$ lux). ipRGC = intrinsically photosensitive retinal ganglion cells.

Pigment	Photopic illuminance	Cyanopic	Melanopic	Rhodopic	Chloropic	Erythropic
Receptor		Short cone	ipRGC	Rods	Med. cone	Long cone
Illuminant	Illuminants in Toolbox (Lucas, 2014)					
Equi-energy, E	2	2	2	2	2	2
Incandescent, A	2	1.5	1.7	1.8	1.9	2.0
Daylight, D65	2	2.0	2.0	2.0	2.0	2.0
Fluorescent, F11	2	1.8	1.8	1.9	1.9	2.0
LED (“~4,730 K”)	2	1.8	1.9	1.9	2.0	2.0
Peak	Narrowband (“monochromatic”) illuminants, FWHM 40 nm					
440 nm	2	3,7	3,2	3,1	2,7	2,4
480 nm	2	2,6	2,8	2,7	2,4	2,1
520 nm	2	0,8	2,1	2,1	2,1	1,9
560 nm	2	-0,9	1,3	1,7	1,9	1,9
600 nm	2	-2,3	0,4	1,1	1,8	2,0
640 nm	2	-3,2	-0,5	0,3	1,5	2,1
T_C	Blackbody radiation with colour temperature, T_C					
2000 K	2	1,1	1,5	1,6	1,9	2,0
3000 K	2	1,5	1,8	1,8	1,9	2,0
5000 K	2	1,9	2,0	2,0	2,0	2,0
7000 K	2	2,1	2,1	2,0	2,0	2,0
10 000 K	2	2,2	2,1	2,1	2,0	2,0
15 000 K	2	2,3	2,2	2,1	2,1	2,0

Even with logarithmic values it is easy to see that across the photoreceptors none of the illuminants considered is as subtly different from equal energy as the daylight standard D65. Narrowband illuminants are highly selective and changes in wavelength produce large changes in stimuli. Blackbody illuminants with colour temperatures over 5000 K to 7000 K add little stimulation with increasing colour temperature. It is also noticeable that the erythropic opsin in the long wavelength cones behaves very differently (relative to photopic lux) than the other opsins, as it has a peak wavelength to environmental irradiance above 555 nm, as well as having a broader action spectrum at the short wavelength end.

4 Conclusion

The Workshop’s approach has been compared to notable previous proposals (Enezi, 2011; Rea, 2005 and 2010; Gall, 2004). Importantly, the Workshop has concluded that no one action spectrum describes the sensitivity for any non-visual response in all circumstances (Lucas, 2014; CIE, 2014 in press). This means that the Workshop has not provided industry with a prediction for the effects of light on parameters relating to health or wellbeing.

When considering applications, scenario modelling of the implications of the different action spectra (e.g. Schulmeister, 2002; Price, 2012) is still possible, but in future action spectra scenarios will need to be drawn from dynamic theories combining the five basis functions underlying the composite spectral sensitivity of the non-visual photoreceptive pathway.

References

BIPM 2006: The International System of Units (SI), 8th Edition. Paris, BIPM.

CIE 2014. CIE TN 003:2014. On The 1st International Workshop on Circadian and Neurophysiological Photometry, 2013. Vienna: CIE. [In press]

ENEZI, J., REVELL, V., BROWN, T., WYNNE, J., SCHLANGEN, L., LUCAS, R.J. 2011. A "melanopic" spectral efficiency function predicts the sensitivity of melanopsin photoreceptors to polychromatic lights. J Biol Rhythm. 26(4):314-323.

GALL, D., BEISKE, K. 2004. Definition and measurement of circadian radiometric quantities. CIE Symposium on Light and Health - non-visual effects 129-132.

GIBSON, K.S., TYNDALL, E.P.T. 1923. Visibility of radiant energy. Bur Stand (US) Sci Paper No. 475, 19:131-191.

GOVARDOVSKII, V.I., FYHRQUIST, N., REUTER, T., KUZMIN, D.G., DONNER, K. 2000. In search of the visual pigment template. Visual Neurosci. 17(4):509-528.

LUCAS, R.J., PEIRSON, S.N., BERSON, D.M., BROWN, T.M., COOPER, H.M., CZEISLER, C.A., FIGUEIRO, M.G., GAMLIN, P.D., LOCKLEY, S.W., O'HAGAN, J.B., PRICE, L.L.A., PROVENCIO, I., SKENE, D.J., BRAINARD, G.C. 2014. Measuring and using light in the melanopsin age. 37(1):1-9.

POKORNY, J., SMITH, V.C. 1997. The Verriest Lecture: How much light reaches the retina? Colour Vision Deficiencies XIII, Springer Netherlands. 491-511.

PRICE L.L.A. 2012. Efficacy and protection ratios for bright light therapy lamps. 6th DIN-Expert-Panel on The effect of light on human beings. Berlin.

REA, M.S., FIGUEIRO, M.G., BIERMAN, A., BULLOUGH, J.D. 2010. Circadian light. J Circadian Rhythms. 8: 2.

REA, M.S., FIGUEIRO, M.G., BULLOUGH, J.D., BIERMAN, A. 2005. A model of phototransduction by the human circadian system. Brain Res Brain Res Rev. 50: 213-228.

SCHULMEISTER, K., WEBER, M., BOGNER, W., SCHERNHAMMER, E. 2002. Application of melatonin suppression action spectra on practical lighting issues. International Symposium on Light and Human Health.

WYSZECKI, G., STILES, W.S. 1982. Color Science: Concepts and Methods, Quantitative Data and Formulae. Wiley Classics Library edition 2000 (from 2nd edition 1982). New York: Wiley.

OP19

EVALUATION OF SPECTRORADIOMETER PERFORMANCE FOR APPLICATION OF PHOTOBIOLOGICAL SAFETY ASSESSMENT OF LIGHTING PRODUCTS

Tongsheng Mou[1], Liling Cheng[2], Yongjun Luo[1], Junkai Li[1]
1. SENSING Instruments Co., Ltd, Hangzhou, CHINA.
2. Zhejiang Entry-Exit Inspection and Quarantine Bureau, Hangzhou, Zhejiang, CHINA.

Abstract

The actinic UV hazard, near UV hazard and retinal blue light hazard are three considerable risks for general lighting sources. Five typical lighting sources are selected to evaluate the performances of the spectroradiometers. The results show that the actinic UV weighted irradiance is very sensitive to stray light, and the monochromator spectroradiometer equipped with visible blind PMT can provide the solution of the assessment of photobiological safety.

Keywords: photobiological safety; spectroradiometer; actinic UV weighted irradiance; stray light

1 Background

Currently, tungsten filament lamps, gas-discharge lamps, and LED light sources are typically applied in general lighting. Besides the visible light, these sources may emit a small quantity of ultraviolet and infrared radiation. The optical radiation safety has been considered in these products. The emission limits and classification for the safety assessment are in IEC 62471/CIE S009[1]. However, the infrared radiation levels in common use lighting sources are generally low and not notable to cause optical radiation hazard. Therefore, actinic UV hazard, near UV hazard and blue light hazard should be considered as potential photobiological effects relating to the optical radiation safety of lighting sources. For the assessment of optical radiation hazards of above products, actinic UV weighted irradiance, near UV irradiance and retinal blue light weighted radiance need to be measured, but It is difficult for broadband detectors to match well with the spectral response as action functions of photobiological effects. Optical radiation for the safety classification of lighting sources is measured via many types of spectroradiometers including scanning monochromator spectroradiometers and CCD array spectroradiometers[2][3][4].

Because of a large difference of the characteristics in current commercial spectroradiometers, such as low cost CCD spectrometers, well-designed array spectroradiometers, single or double monochromator spectroradiometers, it is difficult to select in compare of the performance and cost in the practical applications for correct safety classification.

2 Evaluation conditions

The scanning monochromator spectroradiometer can positively provide broad spectral range, various slit bandwidth and good linearity. It is still widely used in many applications nowadays. With the improvement of CCD array detectors and multi-chromators, the CCD array spectroradiometer is more and more suitable in various applications.

In the spectral irradiance and radiance measurements, the width of both the entrance slit and the exit slit should be the same so that the spectral response function of the spectroradiometer has a isosceles triangle function, which is very important for gas discharge lamps with narrow spectral lines. Double monochromator spectroradiometer possess very low stray light that is excellent in the UV spectrum for the measurement of lighting sources.

In compact array spectroradiometers, the spectrum diffracted by concave holographic grating focuses on an array detector, and the elimination of high order spectrum and stray light are a practical bugbear in the measurement for photobiological safety. The entrance slit width of the array spectroradiometer shall be between the sensitivity and wavelength resolution.

For evaluating the effects on photobiological safety assessment of lighting sources from the spectroradiometer performance, the five lighting sources of above three types which include HID (MH), FL, cool white LED, warm white LED and quartz tungsten lamps are as shown in Figure 1. However, it is mainly considered for the effects in the measurements of actinic UV weighted irradiance, near UV irradiance and retinal blue light weighted radiance.

The risk group of the photobiological safety might be changed under the different application conditions (i.e. viewing conditions) for a certain lighting source. According to the specifications in IEC62471 for GLS sources, the risk should be evaluated at the position where produces 500lx illumination. Therefore, here actinic UV weighted irradiance and near UV irradiance will be in this condition, and the retinal blue light weighted radiance will be under the condition of 10000cd/m2.

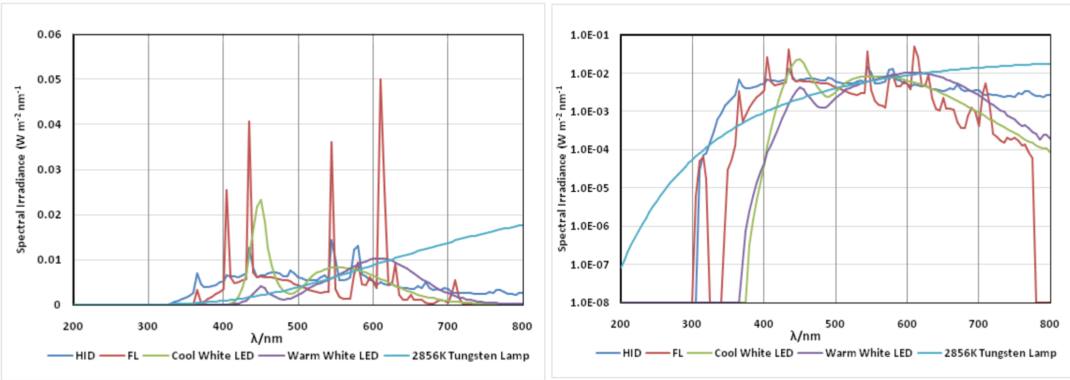

Figure 1. Spectral irradiance distributions of typical lighting sources

3 Effects of the main performances

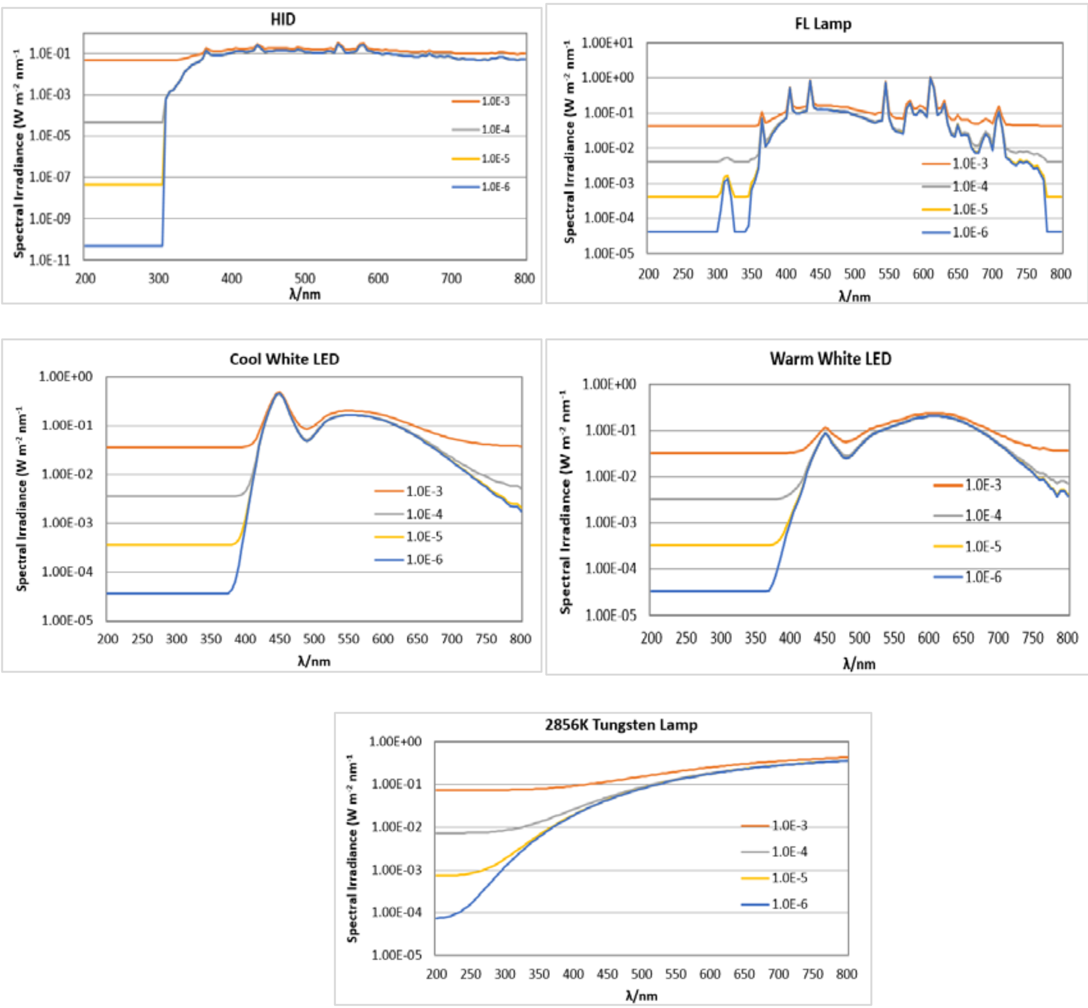

Figure 2. Spectral irradiance distribution including stray light

Stray light, wavelength accuracy and photoelectrical linearity are three main factors in the spectroradiometer performance. The stray light of scanning double monochromators can be better than 10^{-6}; whereas the stray light of small CCD spectroradiometer with short focus length only reaches to 10^{-3} to 10^{-4}. Therefore, the levels of stray light between 10^{-6} and 10^{-5} are to evaluate the effects on the measurement of these photobiological quantities. In Figure 2, it shows the spectral data of the light source with different levels of stray light; the corresponding photobiological quantities are in Table 1, in which the UV actinic weighted irradiance is very sensitive with stray light. If the stray light magnitude of the spectroradiometer were more than 10^{-4}, it would cause the RG0 to be assigned to RG1. Therefore, for the light source with some UV radiation like the 2856K tungsten lamp in Table1, the stray light should be requested to be not more than 10^{-6}. However, for the measurement of the retinal blue light hazard radiance, the stray light needs to be less than 10^{-4} for the quantity change of 5%.

Table 1. The impacts of the stray light

E_{UV}					
Stray Light	HID	FL	Cool White LED	Warm White LED	2856k
0	2.64E-05	1.18E-05	1.03E-08	1.62E-08	8.30E-04
1.0E-6	2.64E-05	1.08E-04	8.35E-05	7.41E-05	9.98E-04
1.0E-5	2.65E-05	9.73E-04	8.34E-04	7.41E-04	2.52E-03
1.0E-4	1.34E-04	9.62E-03	8.34E-03	7.41E-03	1.77E-02
1.0E-3	1.07E-01	9.61E-02	8.34E-02	7.41E-02	1.69E-01
E_{UVA}					
Stray Light	HID	FL	Cool White LED	Warm White LED	2856k
0	2.43E-01	8.48E-02	3.20E-04	1.61E-03	3.75E-02
1.0E-6	2.43E-01	8.44E-02	4.74E-04	5.77E-04	3.79E-02
1.0E-5	2.43E-01	8.61E-02	1.94E-03	1.88E-03	4.08E-02
1.0E-4	2.43E-01	1.03E-01	1.67E-02	1.49E-02	7.06E-02
1.0E-3	4.53E-01	2.72E-01	1.64E-01	1.46E-01	3.68E-01
L_B					
Stray Light	HID	FL	Cool White LED	Warm White LED	2856k
0	9.80	11.77	12.81	2.61	2.96
1.0E-6	9.80	11.77	12.82	2.61	2.97
1.0E-5	9.80	11.80	12.84	2.63	3.01
1.0E-4	9.80	12.06	13.07	2.83	3.47
1.0E-3	13.02	14.65	15.32	4.83	8.02

For general lighting service, the light sources emit radiation mainly in the visible range, and very little in UV range, which is mostly less than 1%. Therefore, the stray light from visible radiation to be spread on UV range should be considered seriously. An alternative method to eliminate the effects of stray light can be used by the combination of a visible blind PMT detector whose response is active only in the $S_{UV}(\lambda)$ effective range of 200nm~320nm and another visible sensitive PMT. In Table 2, it shows that the stray light effect on UV actinic weighted irradiance is reduced significantly after using the visible blind PMT. In Figure 3, its results (dash line) are with common (solid line) spectroradiometer. E_{uv}(th) is the emission limit of the UV actinic hazard irradiance relating to RG0. Here, the safety classification of these five typical lighting sources would not be affected.

Table 2. Stray light effects to UV actinic weighted irradiance(with visible blind PMT)

Stray Light	HID	FL	Cool White LED	Warm White LED	2856K
0	2.64E-05	1.18E-05	1.03E-08	1.62E-08	8.30E-04
1.0E-6	2.64E-05	1.69E-05	3.54E-08	3.85E-08	8.30E-04
1.0E-5	2.64E-05	1.71E-05	2.62E-07	2.39E-07	8.30E-04
1.0E-4	2.65E-05	1.97E-05	2.52E-06	2.25E-06	8.35E-04
1.0E-3	5.87E-05	3.40E-05	2.51E-05	2.23E-05	8.81E-04

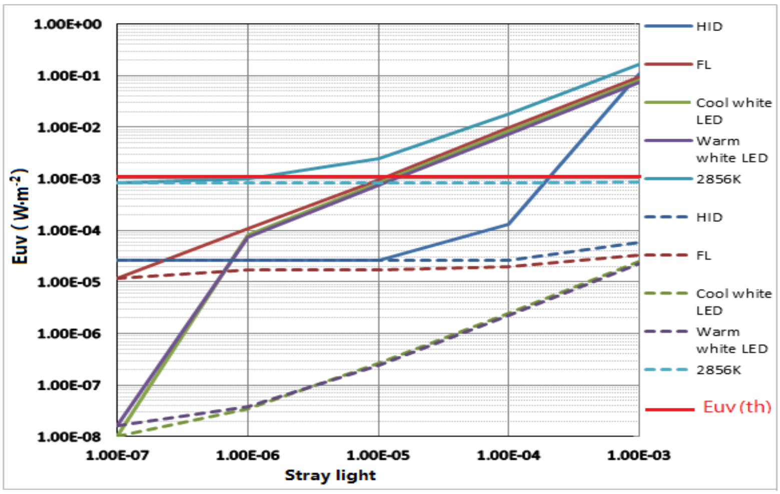

Figure 3. Compare of UV actinic weighted irradiance variations

Table 3 shows the effects of wavelength shifts in spectroradiometers to the quantities for the radiation safety classification. Since the weighting function $S_{UV}(\lambda)$ changes rapidly in the range of 300nm~320nm, which varies 300 times in 20nm range, the effect on UV actinic weighted irradiance of FL is greatest because of the sensitive wavelength at 313nm for FL radiation spectrum. If less than 10% uncertainty is, the wavelength shift should be no more than 0.2nm, and for the light sources with a continuous spectrum should be no more than 0.3nm. Considering the effects of retinal blue light radiance from wavelength shift, the weighting function variation shall be twice as much at each 5nm in sensitive wavelength ranges of 390nm to 415nm and 480nm to 500nm. Therefore, the wavelength accuracy should be better than 0.5nm.

Table 3. Effects of wavelength shifts in the spectroradiometer

E_{uv}					
Wavelength shift	HID	FL	Cool White LED	Warm White LED	2856K
0	2.64E-05	1.18E-05	1.03E-08	1.62E-08	8.30E-04
-0.1	2.68E-05	1.24E-05	1.07E-08	1.79E-08	8.34E-04
-0.2	2.71E-05	1.29E-05	1.11E-08	1.82E-08	8.38E-04
-0.3	2.75E-05	1.35E-05	1.15E-08	1.85E-08	8.43E-04
-0.5	2.82E-05	1.46E-05	1.23E-08	1.92E-08	8.51E-04
+0.1	2.64E-05	1.18E-05	1.03E-08	1.75E-08	8.30E-04
+0.2	2.63E-05	1.17E-05	1.02E-08	1.74E-08	8.26E-04
+0.3	2.61E-05	1.16E-05	1E-08	1.72E-08	8.23E-04
+0.5	2.60E-05	1.14E-05	9.9E-09	1.7E-08	8.19E-04
L_B					
Wavelength shift	HID	FL	Cool White LED	Warm White LED	2856K
0	9.80	11.77	12.81	2.61	2.96
-0.1	9.80	11.77	12.81	2.61	2.96
-0.2	9.80	11.78	12.80	2.61	2.96
-0.3	9.80	11.79	12.78	2.60	2.95
-0.5	9.80	11.79	12.77	2.60	2.95
+0.1	9.80	11.77	12.83	2.61	2.97
+0.2	9.80	11.76	12.84	2.62	2.97
+0.3	9.80	11.76	12.85	2.62	2.97
+0.5	9.81	11.75	12.87	2.63	2.98

4 Conclusion

In photobiological safety assessment, the spectroradiometer is key equipment. Its performance will directly affect the classification of the safety. The results show that stray light of the spectroradiometer will obviously affect the measurement of UV actinic weighted irradiance by considering five typical lighting sources. Double-monochromators system and the single monochromator system with visible blind PMT can be well applied in the classification of the UV risk of general lighting sources. Besides, the wavelength accuracy of the spectroradiometer should be required within 0.2nm in UV range and 0.5nm in the visible range.

References

[1] IEC 62471-2006/CIE S009 Photobiological Safety of Lamps and Lamp Systems Photobiological Safety of Lamps and Lamp Systems.

[2] TONGSHENG, M, 2010.The measurement of weighted LED radiance related to photobiological safety based on the spectroradiometry and imaging methods,CIE Tutorial and Expert Symposium ”Spectral and Imaging Methods for Photometry and Radiometry”, 30- 31 August 2010, Bern, Switzerland.

[3] Stolyarevskaya, R.I.,Bartsev, Methodology of luminaire blue-light hazard measurements, CIE Conference on Lighting quality & energy efficiency, September 19-21, Hangzhou

[4] Tongsheng Mou ; Zhenjian Peng, 2013, Measurement and standardization of eye safety for optical radiation of LED products, Proc. SPIE 8769, Singapore, April 09, 2013.

OP21

VISION EXPERIMENT ON ACCEPTABLE AND PREFERRED WHITE LIGHT CHROMATICITY FOR LIGHTING

Yoshi Ohno[1] and Mira Fein[2]
[1] National Institute of Standards and Technology, Gaithersburg, MD USA
[2] Psychology Department, Oberlin College, Oberlin, Ohio, USA.
ohno@nist.gov

Abstract

Standards on white light chromaticity of fluorescent lamps have been available for more than three decades, but the specifications in these standards have not been based on human vision perception data. Anecdotally, lights with chromaticities below the Planckian locus are expected to provide more preferred lighting for interior. A series of vision experiments have been conducted with 18 subjects on their response to Duv (distance from the Planckian locus on CIE 1960 (*u, v*) coordinates) using the NIST Spectrally Tunable Lighting Facility, with 18 subjects for 6 Duv points (-0.03, -0.02, -0.01, 0, 0.01, 0.02) at four correlated color temperatures (2700 K, 3500 K, 4500 K and 6500 K). The results show that Duv of around -0.015 (below Planckian locus) on average is perceived as the most natural. This Duv level is outside the ranges specified by existing standards. This indicates that new lighting products having more preferred chromaticity than the current products may be possible.

Keywords: chromaticity, lighting, light sources, white light, Duv, visual perception, Planckian locus

1 Introduction

The chromaticity coordinates of light sources for lighting have been designed to be around the Planckian locus for decades since fluorescent lamps were developed. Standards for chromaticity of fluorescent lamps are available (IEC, 1997, ANSI, 2001) and recently for solid state lighting products (ANSI, 2011). In these standards, the center points of the chromaticity ranges are mostly on or slightly above the Planckian locus. In this paper, shifts away from the Planckian locus (yellowish/pinkish shift) is expressed by *Duv* (Symbol: D_{uv}), which is defined as the shortest distance from the chromaticity of the source to the Planckian locus on the CIE (u', $2/3v'$)[1] coordinates, with plus sign for above and minus sign below the Planckian locus (ANSI, 2011), and also discussed in a recent article (Ohno, 2013).

These white light center points for light sources have been widely accepted for many years. However, it is often questioned whether the lights at Planckian locus are really the most natural or preferred white light for indoor lighting, and it is anecdotally said that white points below Planckian locus on chromaticity diagrams is preferred. As evidence, neodymium incandescent lamps, popular in the USA and some other countries for a long time, have slightly pinkish shift with $D_{uv} \approx -0.005$. There have been some researches available on white perception (e.g., Hurvich, 1951) but these are not applicable to judgment of light sources for lighting, and there have been very few researches available on white chromaticities for lighting. CIE (CIE, 2004) specifies the range of (*u, v*) chromaticity to be ±0.05 for calculation of correlated color temperature (CCT), but it is not a definition of white light and not based on visual perception.

A recent report on a vision experiment (Rea, 2013) shows that perceived neutral white points are at $D_{uv} \approx -0.01$ at 2700 K to 3500 K, $D_{uv} \approx 0.00$ at 4000 K, and $D_{uv} \approx 0.005$ at 6500 K (though the report did not use Duv). These results vary with CCT, and no good explanation is given. This experiment was done with a lighting booth with white inner walls and no objects

[1] Equal to CIE 1960 (*u, v*) diagram now obsolete.

inside. It is considered that, due to chromatic adaptation conditions used in this experiment, the results may have been affected by the different ranges of chromaticity points used for different CCTs.

To study perception of white light for lighting, it is considered that that the experiments should be conducted by observing illuminated scenes of real objects including human skin tone. Further, chromatic adaptation needs to be strictly controlled, as perception of color is strongly affected by chromatic adaptation state. Considering these, a series of vision experiments has been conducted at the National Institute of Standards and Technology, using the NIST Spectrally Tunable Lighting Facility (STLF) (Miller et al, 2009), to investigate perceived naturalness of different Duv levels of illumination for simulated interior lighting environment, with full chromatic adaptation conditions. Experiments were conducted using broadband spectra at four Correlated Color Temperatures (CCTs) from 2700 K to 6500 K and at 6 different Duv levels at each CCT.

2 Experimental settings with NIST STLF

The NIST Spectrally Tunable Lighting Facility (STLF) (Miller et al, 2009), as shown in Fig. 1, was used, which has 25 channels of LED spectra (from 405 nm to 650 nm peak) and can control spectral distribution, CCT, Duv, and illuminance, independently, illuminating a real-room size cubicle (2.5 m x 2.5 m x 2.4 m). There are two cubicles side by side, independently controlled, and the walls of different colors and textures can be replaced easily. The facility can produce up to about 300 lx to 800 lx of illumination of white light illumination on the table depending on the spectrum of light.

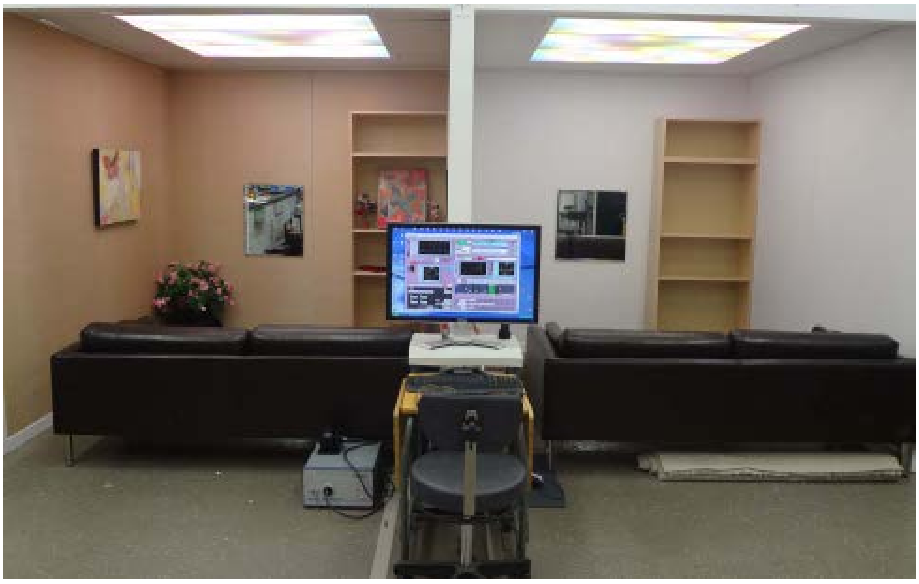

Figure 1. View of the two cubicles of NIST Spectrally Tunable Lighting Facility.

The light source unit of the STLF has very large heat sinks which are cooled by forced air and the temperature of the heat sink is only about 27 °C when these spectra at ~300 lx are produced, while the room temperature is kept to 25 °C ±1 °C. The STLF needs only about 15 minutes to stabilize, after which the chromaticity is stable to within ± 0.0005 in (*u', v'*) for four hours, and reproduces the set chromaticity to within ± 0.001 in (*u', v'*) over one month.

The experiments were conducted mainly using the right side cubicle in Fig.1 with off-white (achromatic) walls, and in addition, experiments with a limited number of subjects were conducted at the left side cubicle with brownish walls.

The experiments were conducted at six different Duv levels (-0.03, -0.02, -0.01, 0, 0.01, 0.02) at four different CCTs (2700 K, 3500 K, 4500 K, 6500 K), except for 2700 K where D_{uv}=0.02 was removed as it is too close to the spectrum locus and perceived as yellow light, and acceptable color rendering could not be achieved. Therefore, a total of 23 points were set up as experimental chromaticity points.

In addition, the Duv levels at ± 0.005 from the six Duv points at each CCT were also needed in the experimental procedures (see section 3). The chromaticities of these points were initially adjusted to be within ±0.0003 from the intended point and were maintained within ±0.0006 throughout the experiment. With these points added, lights at total 50 chromaticity points as shown in Fig. 2 were prepared on the STLF. The Duv ranges were originally set symmetrically from -0.02 to 0.02, but preliminary experiments clearly showed that -0.02 was not sufficient, thus, lower limit was set to D_{uv} = -0.03 in the official experiments. The upper limit of D_{uv} =0.02 was judged sufficient in the preliminary experiments.

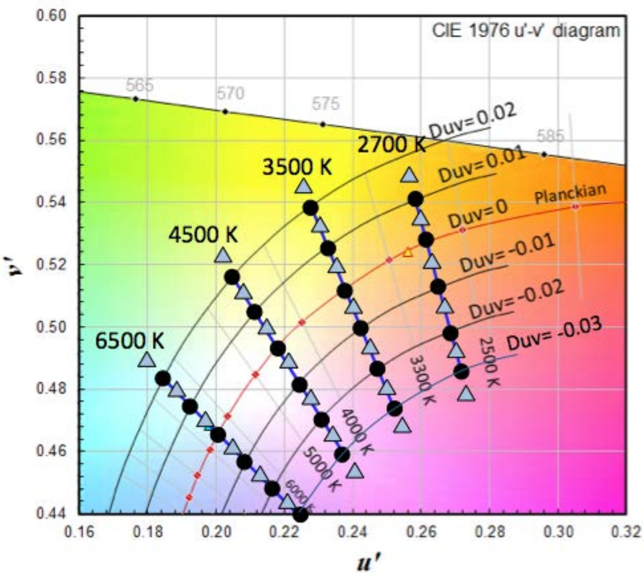

Figure 2 The 50 chromaticity points on STLF prepared for the experiments.

The color quantities of the lights were measured on the center of the table in the cubicle, using an array type spectroradiometer with a small integrating sphere input for cosine response, calibrated with a NIST spectral irradiance standard scale (NIST, 2011). The spectroradiometer measured spectra and illuminance on the table from the 2π solid angle including light from the entire room including reflections from the walls and other objects as well as from the light source itself. The estimated expanded uncertainties (*k*=2) of measurements varied depending on spectra, but in all cases, they were within 0.0012 in *u'*, 0.0011 in v', 0.0009 in Duv, 24 K in CCT at 2700 K and 92 K at 6500 K. The repeatability of the spectroradiometer was 0.0002 in u' and v'. Also, when the spectrum is changed on STLF, the spectrum and color are switched instantly and stable immediately so that sequential comparison of lights is possible.

Broadband spectra with high color fidelity were used in this experiment to avoid possible effects of narrow-band spectra. The measured light spectra for the 50 chromaticity points used for the experiments are shown in Fig. 3. The spectral distributions at D_{uv}=0.000 were first set for the highest CRI R_a or CQS (Davis and Ohno 2010) Q_a value achieved at each CCT at about 300 lx, then lights at other Duv levels were set. The R_a values were 98, 98, 97, 97 and Q_a values were 97, 96, 96, 95 at 2700 K, 3500 K, 4500 K and 6500 K, respectively, at D_{uv}=0. Then the spectra at different Duv levels were prepared. The STLF automatically maintains constant CCT and illuminance when Duv level is changed, only with very small variations due to the system imperfection. The variations of CCT at different Duv points were within ±13 K from the average at 2700 K and ± 40 K from the average at 6500 K, and illuminance was kept within 1 % from an average value for all Duv levels at each CCT.

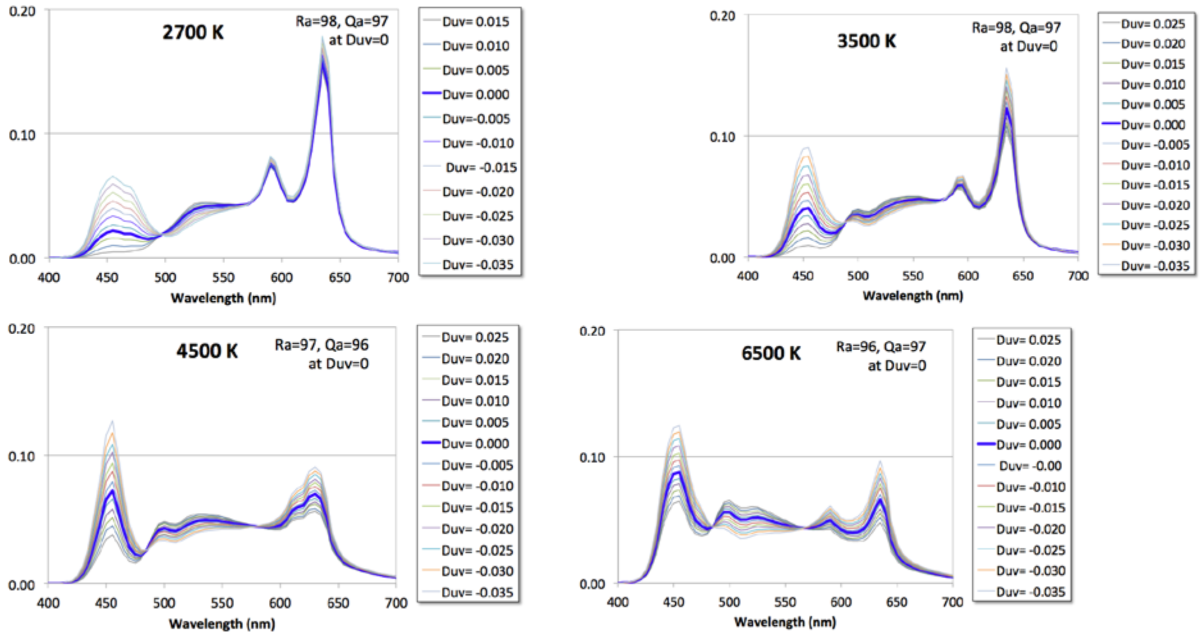

Fig. 2 Spectral power distributions of the lights in STLF used in the experiments at each CCT condition. The thick curves (blue line) are at D_{uv}=0.

The spatial uniformity of color in the room was also evaluated. The uniformity of chromaticity over the tabletop was with ±0.001 in (*u', v'*). The uniformity of chromaticity on the table and on the wall up to 1.5 m high from the floor (measured on a vertical plane) was within ±0.003 in (*u', v'*). The chromaticity on the position of the mirror was within 0.001 in (*u', v'*) from the table top. These values are similar with all lights used in the experiment.

The CCT, Duv, and illuminance (at 4 CCTs at D_{uv}=0) were measured and recorded each day before and after each experimental session, with special attention to the stability of Duv. The Duv values were reproduced to within ±0.0002 each morning in most cases, and to 0.0005 at largest difference from the initial day. Even if there is a small shift in Duv, the same shift appeared in all Duv levels so that the intervals between different Duv points were always kept constant (to within 0.0004).

Fig. 3 shows the experimental settings for the subjects. The subject sat on a coach placed at the open side of the cubicle so that he/she viewed the entire room, and was completely immersed in the lighting environment and his/her full view was adapted to the illumination. For the subjects to be able to judge naturalness and preference, we selected common real objects often seen in daily life. In the cubicle, two dishes of real fruits and vegetables (red apple, yellowish apple, orange, green pepper, lettuce, tomato, banana, strawberries, and grapes) were placed on a table. The fruits and vegetables were replaced at one to several days' intervals depending on the item to keep them fresh. Items with as similar color and shape as much as possible were obtained each time the items were replaced. There was a mirror in front of the subject, and he/she could look at their face skin tone in the mirror, as well as their hands skin tone. Along the wall of the cubicle, there was a bookshelf with some books, artificial flowers, and two paintings hung on the sidewalls (as shown in Fig. 3 left), simulating a small living room.

Eighteen subjects having normal color vision were used in the experiments. They were 11 males and 7 females with their ages from 19 to 70. The subjects were workers at NIST, who are not experts on color, including seven summer students (ages 19 to 22).

The experiments were conducted in June to July 2013. The CCT, Duv, and illuminance were recorded before and after each experimental session for a subject, and they were measured at the center of the table.

Figure 3. The experimental settings for subjects – the room setting (left) and fruits and vegetables on the table (right).

3 Experimental Procedures

At each CCT, the subject was first adapted to the illumination at one end of Duv (e.g., D_{uv}= 0.02) for five minutes, then after adaptation, the subject was asked whether this light is acceptable or not. Then, a pair of lights, ± 0.005 from the adapted light (so, in this case D_{uv} =0.025 and 0.015) was presented and asked which light looked more natural. The subject was instructed to see the fruits, skin tone, the entire room, as they liked, and made overall judgment. The pair of lights was flipped at 3 seconds interval with a computer sound, and the subject clicked the mouse when the light that appeared more natural was presented. If the negative shift was chosen, the adapted light was judged to be too yellowish (greenish) to the observer or vice versa.

Then, next Duv is presented (e.g., 0.015) and the subject was adapted to the illumination for one minute, then the same trial with a pair of lights (± 0.005 shifts) was made.

This was repeated for the six levels of Duv, which completes one run of one CCT. Then, the same run of experiment was made at different CCT. Then another run at the first CCT in reverse order of Duv (start from D_{uv} = –0.03 and ends at D_{uv} = 0.02) was conducted. A run for each direction at each CCT was repeated twice, so there were total four runs for each CCT. The order of CCT and forward/reverse directions were pre-determined and the same combination was used for all subjects.

Special attention was paid to the adaptation time, as the experimental results would depend on the state of chromatic adaptation. Our experiment was intended for the condition of full chromatic adaptation. Previous studies (Hunt, 1950 and Fairchild et al, 1995) indicate that about two minutes would be sufficient for full chromatic adaptation. Due to overall time limitation, we chose one minute adaptation time at each experimental point after the very first point (given 5 min), expecting that adaptation time may be shorter for the very small color changes, but one minute may not be sufficient. Taking this into consideration, the experimental runs were made in both forward and reverse directions and results averaged so that any remaining effects due to incomplete chromatic adaptation would be cancelled.

Each run typically took 12 to 15 minutes, about 1 hour for one CCT (with four runs), and total about 4 hours for each subject. Experiments were typically done in two sessions of 2 hours each. Ishihara color deficiency test was done for each subject. In addition to the experiments using the off-white wall, six of the 18 subjects repeated similar set of experiments in the cubicle with brownish walls, to check whether there is any effect of the color of the walls. The whole experiment with all subjects took over one month.

4 Results

Table 1 and Fig. 4 show an example of results of one subject at one CCT. Table 1 shows the responses of the subject at each Duv point at each CCT run. “0” means the subject chose the higher Duv light (shift in yellowish direction) in the pair as more natural, and “1” means he/she chose the lower Duv light (shift in pinkish direction) in the pair. In this example, the subject always selected higher Duv of the pair at D_{uv}= -0.03 and always lower Duv of the pair at D_{uv}=0.02, which is a typical case. The arrows show the direction of experimental run. Some effects due to the direction are also observed in this example. These results for the four runs of the subject were averaged in the bottom row in Table 1. These average values in percentage are plotted in Fig. 4. From the plotted curve, the Duv value at 50 % crossover point is read. This point is considered to be the light perceived as most natural for this condition.

Table 1. An example of raw results of one subject at one CCT.

Duv=	-0.03	-0.02	-0.01	0.00	0.01	0.02
4500K backward	0	1	1	1	1	1
4500K forward	0	0	0	1	1	1
4500K backward	0	1	1	1	1	1
4500K forward	0	0	0	1	1	1
Average	0	0.5	0.5	1	1	1

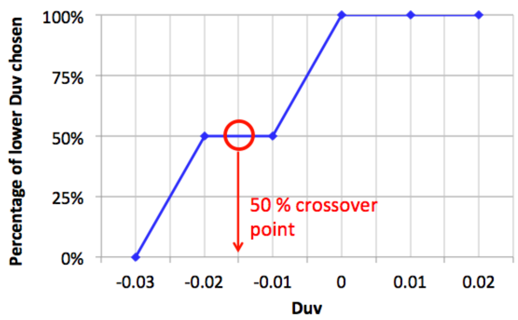

Figure 4. An example of data of one subject - Percentage of the lower Duv in each pair

The data of all the subjects were analyzed as described above, and the 50 % crossover points of Duv for all subjects at all CCTs are presented in Fig. 5. Note that the four lines at the bottom are flat lines at -0.03. The positions of these lines are shifted slightly to show that there are multiple lines here. This also indicated that these subjects may have chosen Duv even lower than -0.03 but it was the limit in this experiment. Also, data of one subject was removed as the result curves did not follow the typical slope and difficult to find crossover points, so data of total 17 subjects are used. The averages and standard deviations of all 17 points for each CCT are shown in Table 2.

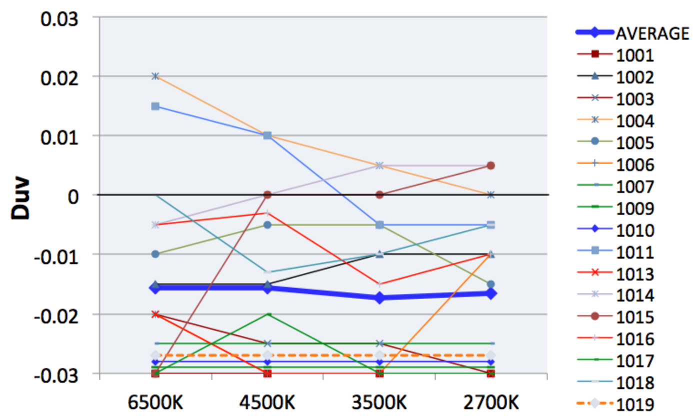

Table 2. Duv values at 50 % crossover points and standard deviation.

CCT	Duv at 50 % crossover	St.dev
2700K	-0.016	0.013
3500K	-0.017	0.014
4500K	-0.016	0.015
6500K	-0.016	0.016

Figure 5. Duv at 50 % cross-over points for all subjects at all CCTs.

These Duv points are far below the Planckian locus and outside the current chromaticity specification for LED lighting products in the USA (ANSI 2011). In Fig. 6, the results of this experiment are plotted over the chromaticity quadrangles in ANSI C78.377. The average crossover points at all four CCTs are at similar Duv levels, in comparison to the results by the other study (Rea, 2013), which showed different results at higher CCTs.

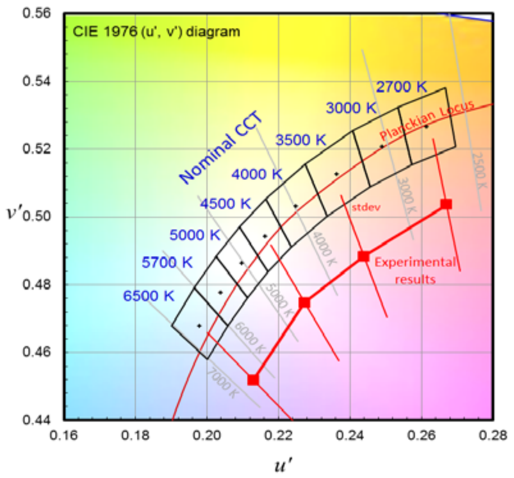

Figure 6. The results of the experiment plotted on ANSI C78.377 chromaticity specifications for SSL products.

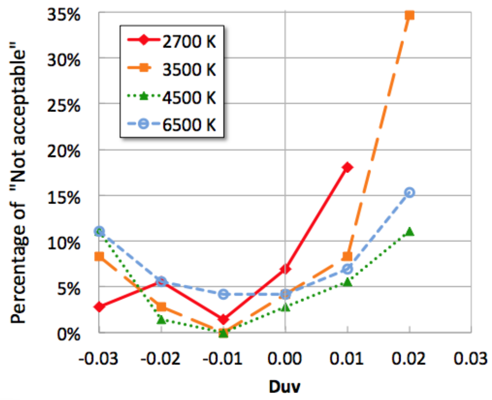

Figure 7. The percentages of subjects' response of "Not acceptable" for lights with different Duv levels.

Figure 7 shows the plots of percentages of subjects who responded "Not acceptable" for presented light after adaptation. The curves are much steeper for positive Duv at low CCTs, and broader at higher CCT, which means that positive Duv is more disliked at low CCTs than at high CCTs. This may be explained by the fact that the Planckian locus at 2700 K is much closer to the spectrum locus (pure yellow) than at other CCTs and thus the effects of positive Duv at 2700 K is much pronounced. Also, the curves generally have a minimum at around Duv =-0.01, which is fairly consistent with the main experimental results.

The experiments with different wall colors were also conducted by five subjects among the 17 subjects. Due to time limitation, only two runs at each CCT were made, and results were compared between the white wall room and the brownish wall room. From these limited data, on the average, no notable differences between the two rooms were observed.

Conclusions

A series of vision experiments were conducted on acceptable or preferred ranges of Duv of white light for indoor illumination under full chromatic adaptation conditions. The results indicate that the chromaticities of lighting sources below the Planckian locus (around $D_{uv} \approx -0.015$) are well preferred for natural appearance of objects in typical indoor lighting environment in the CCT range from 2700 K to 6500 K, and that chromaticities above the Planckian locus are less acceptable or preferred. This indicates that new lighting products having more preferred chromaticity than the current products may be possible. The experimental conditions in this study, however, were limited; e.g., transient effects (when a person comes from outdoor into a room with negative Duv) have not been investigated. Further studies are desired to verify applicability of these results in various real application conditions.

Acknowledgement

This work was supported by U.S. Department of Energy. Authors thank Jim Brodrick for DOE's support of this research. This research was conducted when Mira Fein stayed as a guest researcher at NIST under NIST-NSF Summer Undergraduate Research Fellowship Program.

References

ANSI 2001. C78.376 Specifications for the Chromaticity of Fluorescent Lamps.

ANSI 2011, ANSI_NEMA_ANSLG, C78.377-2008 Specifications for the Chromaticity of Solid State Lighting Products.

CIE, 2004. CIE 15:2004 Colorimetry, 3rd edition.

Davis W. and Ohno, Y., 2010, Color Quality Scale," Optical Engineering, Optical Engineering 033602-1 March 2010/Vol. 49-3.

IEC, 1997, IEC 60081, Double-capped fluorescent lamps – Performance specifications, Annex D.

Fairchild, M.D. and Reniff, L., 1995, Time course of chromatic adaptation for color-appearance judgments, J. Opt. Soc. Am. A/ Vol. 12, No. 5.

Hurvich, L. and Jameson, D. 1951, A psychophysical study of white. III. Adaptation as variant, J Opt Soc Am, **41**:787–800.

Hunt, R.W.G., The Effects of Daylight and Tungsten Light-Adaptation on Color Perception, 1950, J. Opt. Soc. Am. Vol. 40, No. 6.

Miller, C., Ohno, Y., Davis, W., Zong, Y., and Dowling, K. 2009, "NIST spectrally tunable lighting facility for color rendering and lighting experiments," in Proc. CIE 2009: Light and Lighting Conference. 5 pages (2009).

NIST 2011, NIST Special Publicaion 250-89 Spectral Irradiance Calibration

Ohno, Y., Practical Use and Calculation of CCT and Duv, LEUKOS, 10:1, 47-55, DOI: 10.1080/15502724.2014.839020 (2013)

Rea, M. S. and Freyssinier, J. P., 2013, White Lighting, Color Research and Application, **38**- 2

OP22

INVESTIGATING OBSERVER VARIABILITY FOR ASSESSING MEMORY COLOURS

Liu, X.Y.[1,2], Luo, M.R.[1,3*], Lou, D.[4] and Bian, J.[4]
[1] State Key Laboratory of Modern Optical Instrumentation, Zhejiang University, Hangzhou, CHINA
[2] School of Science, Harbin Engineering University, Harbin, CHINA
[3] School of Design, University of Leeds, Leeds, UK
[4] R&D, Opple Lighting Co., Ltd., Shanghai, CHINA
*m.r.luo@leeds.ac.uk

Abstract

This paper investigated the colour preference and colour naturalness of some familiar objects. Two groups (experienced and inexperienced) of native Chinese normal colour vision observers participated in the psychophysical experiment. They assessed twenty objects shown on a calibrated display with regard to their memory colours. For each object, 24 new images were rendered from the original image according to CIELAB a*b* coordinates. Each image was assessed by all observers. CIELAB colour difference was used to analyse the data. The results showed that the assessments of preference and naturalness were very similar and they were significantly influenced by hue angle, while the influence of chroma on the assessments was depending on the objects. Furthermore, it was found that there might be a culture difference in the assessments, even for the familiar objects.

Keywords: Colour appearance, Psychophysical experiment, Memory colour, Colour Preference, Colour naturalness.

1 Introduction

Memory colours consider the appearance associated with the memory of familiar objects such as skin, sky blue, grass, orange, banana, etc. They have been intensively studied by various researchers (SIPLE & SPRINGER,1983; BODROGI & TARCZALI, 2001; SMET et al, 2011). The results were defined as colour regions of memory colours, which were always used as an internal reference to assess such as image quality on colour reproduction or lighting quality on colour rendering. If a light does not render the memory colours correctly, it will be judged as poor quality. However, memory colours could be culture dependent. The International Commission on Illumination (CIE) is developing a colour rendering index suitable to evaluate the colour rendering ability in relation to colour preference of sources (DAVIS & OHNO, 2005; NARENDRAN & DENG, 2002; VALBERG et al. 1979).

Smet et al (2011) proposed a method, named memory colour rendering index (MCRI), based on memory colour to access the colour rendering of lighting. The method adopts nine test objects having hues distributed around the hue circle of mainly food materials. This paper describes work for scaling memory colours on a display. It is aimed to know the inter-observer variability for assessing memory colour, to find out the difference between the most preferred and natural results, and to reveal culture difference between the western and Chinese. 20 familiar objects for Chinese people were investigated including 7 objects (green apple, banana, orange, lavender, sliced cucumber, cauliflower, and hand skin) studied by Smet et al (2011).The other 2 objects (smurf and strawberry yoghurt) were not studied because they were not so familiar to Chinese.

2 Experimental setup

A wide-gamut Eizo Colour Edge CG243W 24 inch display was adopted in the experiment. The peak white of the monitor was set at 6500K with a luminance at 100 cd/m^2. All colours were measured by a Specbos 1211 (Jeti) telespectrophotometer. The monitor was calibrated to an sRGB monitor, so the sRGB model was used to convert between XYZ and RGB values.

2.1 Selected food

Sixteen kinds of familiar food were selected (grass carp, crab, pork, beef, cauliflower, carrot, cucumber, sliced cucumber, eggplant, purple cabbage, orange, blueberry, lemon, grape, green apple, and banana). Considering that seldom familiar natural food has bluish colour, four extra objects were added in (sky, skin, lavender, and pepsi tin can), i.e. total twenty objects were adopted in this experiment, to make them distributed more uniformly in CIE LAB space. Figure 1 shows the distributions of the selected food's colours in CIE a*b* coordinates.

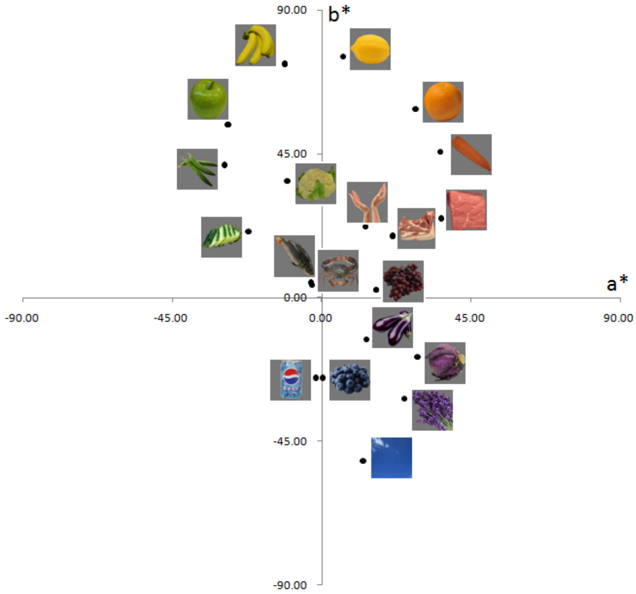

Figure 1 – Distributions of the selected food in CIE a*b* coordinates

2.2 Image preparation

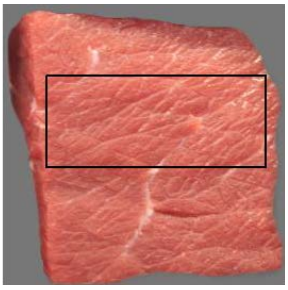

Figure 2 – Crop show for the image of beef

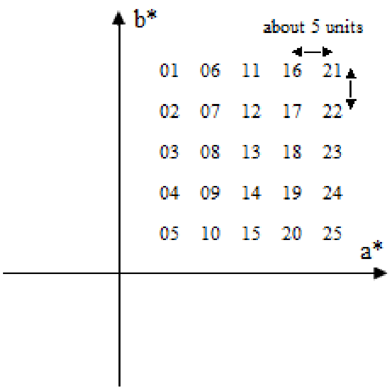

Figure 3 – Distributions of the 25 images' colours in CIE a*b* coordinates

Images were taken for each object in a market. The suitable ones were chosen as the original images as shown in Figure 1. For each original image, a typical area was selected to represent the colour of the image. For example, Figure 2 shows the cropped area for the image of beef. Then, each of the original images was rendered to produce 24 new images at about 5 units (depends on the objects) in Δa^* and Δb^* directions between two neighbouring images. Thus, for each object, there are total 25 images. Figure 3 shows the distributions of the 25 images' colour in the CIE a*b* coordinates. All the images were arranged against a grey background having an L* value of 50.

2.3 Observers

Two groups of native Chinese normal colour vision observers participated in the experiment. Group 1 included 21 experienced observers (6 males and 15 females), aged from 33 to 76, with a mean age of 45. They had worked or were working at supermarket. They are very familiar with the experiment objects. Group 2 included 10 inexperienced observers (5 males and 5 females), aged from 22 to 25, with a mean age of 23. They were all university students.

3 Experiment Procedure

Twenty five images of a particular object were presented on the screen randomly one at a time. Figure 4 shows the experimental environment. The sample was subtended about 5 degree of viewing field. Each observer was asked to scale 'preference', then 'naturalness', in different sessions, using a 6-point category scale from 'extremely dislike/unnatural', 'very dislike/unnatural', 'dislike/unnatural', 'like/natural', 'very like/natural' to 'extremely like/natural'. There was a 1s period between two consecutive images, and a 2s period between the images of two objects. The grey background (L* =50) was shown on the screen in the intervals.

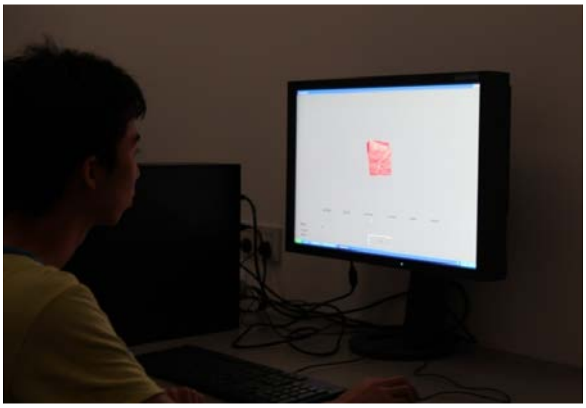

Figure 4 – Experimental enviroment

To test the repeatability, four objects (pork, grape, green apple, and banana) were assessed twice by each observer for investigating the observer repeatability. Therefore, 1200 images in total (25*(20+4)*2) were judged by each observer. Each observer attended four sessions, two for preference and the other two for naturalness. Each session took about half an hour.

4 Results and discussions

For each image, the representative area was cropped. Its RGB value of each pixel was transformed to XYZ via the SRGB model, and then the mean XYZ values of the cropped area were calculated. The XYZ values of 25 images for each object were weighted by the evaluation scores to access the XYZ values of the preferred and the memory colour for each observer for each object. Then the values were transformed to CIELAB values. The agreements between two repeated phases were 0.1 ΔE^*_{ab} units for preference, and 0.09 for naturalness, respectively. This means the method for assessing memory colours are highly repeatable.

ΔE^*_{ab} is also used as a measure of the between-groups variability. The mean ΔE^*_{ab} value between the two groups is 0.42 for colour preference (ranged from 0.19 to 0.72) and 0.39 for colour naturalness (ranged from 0.13 to 0.67), respectively.

The inter-observer variability was evaluated using the mean ΔE^*_{ab} for all the differences between the mean and individual data of an object. The MCDM value was found about 0.83 ΔE^*_{ab} for the observers (ranged from 0.50 to 1.16 for preference and 0.42 to 1.06 for naturalness).

Meanwhile all the observers' preferred and natural colours for each of object were plotted in CIELAB a*b* plane. It can be seen from the most of the plots that all observers' data agreed with each other very well, and all the data distributed around and close to the original image's colour. The example of beef was used to show the typical distributions of the results (see Figures 5(a) and (c)). Figures 5(b) and (d) show the data distributions of banana, from which one can see that the observers' preferred or natural colours of banana were diverse with different hue angles. But the mean preference and the mean naturalness for all the observers were still in the similar hue to the original image. And the chroma of the preferred and the natural colours were lower than that of the original image. A few other objects (orange, lemon, green apple) showed the similar trend as banana.

The colorimetric results between the mean preferred and the mean naturalness agreed well with each other, having a mean of 0.34 (ranged from 0.07 to 0.56 depends on the object) ΔE^*_{ab} units. This means that for familiar objects, preferred colour and natural colour agees very well with each other. These results are clearly shown in Figure 5(c) and (d).

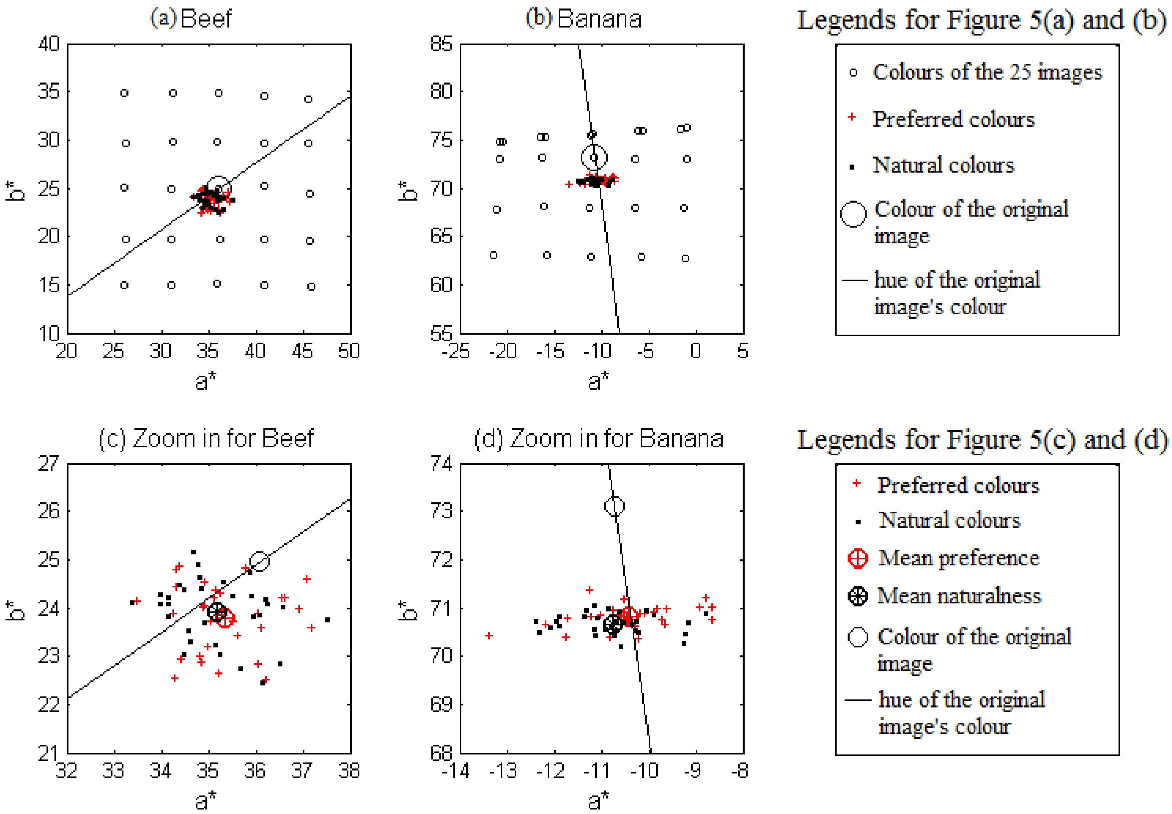

Figure 5 – Distributions of the individual's colour assessment result for (a) beef and (b) banana

To investigate the influence of chroma and hue angle on the observers' assessments for each object, the chroma and hue angle value for each image are plotted against the visual naturalness and preference results as shown in Figure 6. It can be seen that the influence of chroma depends on the objects. For some objects (e.g. beef), the visual perceptions would become lower when choma is increased (see Figure 6(a)). For some objects (e.g. purple cabbage), the perceptions would be higher with increased chroma (see Figure 6(b)). For some other objects ((e.g. banana), the perceptions would have little influenced by chroma (see Figure 6(c)). While for the influence of hue, the results were very consistent. Pork and sliced cucumber were taken as examples to represent all objects to illustrate the influence of the hue angle (.see Figures 6(d) and (e)). It from Figures 6(d) and (e) can be seen that each object had a peak for preference or naturalness perceptions. If an object's colour had a hue deviating from the value, the object will not appear nature or be preferred. These results imply that it is essential to obtain the right hue angle for colour rendering and adjustment of the chroma should depend on the objects.

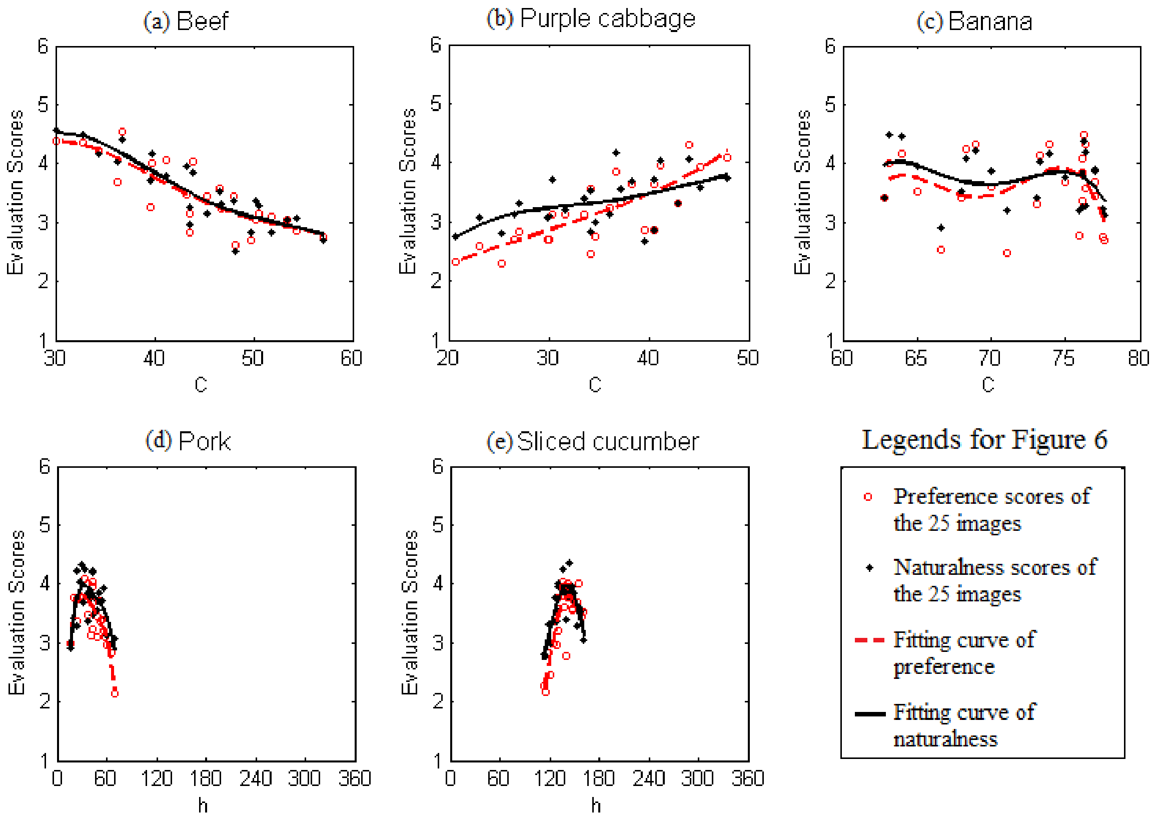

Figure 6 – Evaluations versus (a) chroma for beef; (b) chroma for beef; (c) chroma for purple cabbage; (d) hue angle (in degree) for pork; (e) hue angle (in degree) for sliced cucumber

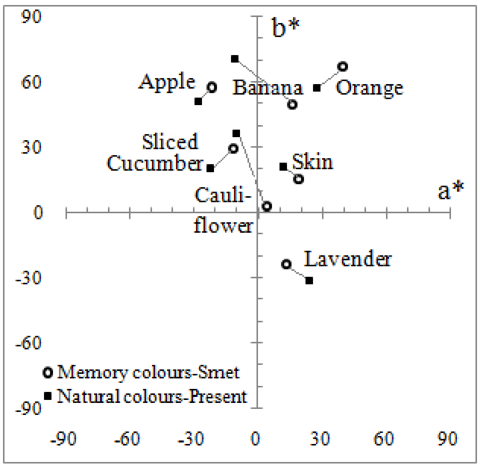

Figure 7 – Comparison of the present results and the data from Smet et al (2011)

Finally, the present memory colours (naturalness) were compared with those obtained by Smet et al (2011). Nine objects were included for predicting memory colour rendering index (MCRI) (SMET, 2011). Seven of them were studied in both experiments (green apple, banana, orange, lavender, sliced cucumber, cauliflower, and hand skin). The other two objects (smurf and strawberry yogurt) were not used in the present study because of their unfamiliarity for Chinese observers. It was found that there are some differences between the present and MCRI data, i.e. with an average of 18 ΔE^*_{ab} units. Figure 7 shows the results of the memory colours obtained by Smet et al (2011) and the natural colours in this study. It can be seen from Figure 7 that there are large differences (especially for the banana and cauliflower) between the results from the observers with different culture backgrounds. Taking the banana as the example, the results showed that the Europeans preferred reddish bananas while the Chinese preferred greenish ones. These differences could also be caused by both culture difference and media difference (between real objects and monitor colours).

5 Results and discussions

This study aimed to investigate the observers' variability for assessing the memory colours, to reveal the differences between the different groups such as experience and race, and finally, to find the impact of the change of chroma and hue angle on visual preference and naturalness assessment.

The results showed that the observers' assessments were very stable. All the data distributed close to the original image except for the objects of orange, lemon, green apple, and banana.

Comparing the two groups of observers' (experienced and inexperienced) results showed that they had good agreements in general. This implies that for familiar objects, experience has no obvious effect on the assessment of colour preference and naturalness.

Comparing the mean preferred colour and mean natural colour, it can be found that the preference and naturalness almost have no difference for all the familiar objects adopted in the experiment.

The results also showed that for all the objects and for both of the preference and naturalness, the assessments were influenced by hue angle significantly, i.e, the visual preference and naturalness assessment was very hue sensitivity. Each object has a unique hue angle corresponding to the highest assessments for both preference and naturalness perceptions. If the object's hue angle deviated from the value, the evaluations of the object would become low. But the influence of chroma depended on the objects. The visual preference and naturalness assessment would not always become higher with the increased chroma.

Furthermore, the comparisons between the results from different culture backgrounds showed that there might be a culture difference in assessing the colour preference and colour naturalness, even for the familiar objects.

References

SIPLE P and SPRINGER R M. 1983. Memory and preference for the colors of objects. Percept Psychophys, 34, 363-370.

BODROGI P and TARCZALI T. 2001. Colour memory for various sky, skin, and plant colors: Effect of the image context. Color Res Appl., 26, 278-289.

SMET K, RYCKAERT W R, and POINTER M R. 2011. Geert Deconinck, Peter Hanselaer. Colour Appearance Rating of Familiar Real Objects Color Res Appl., 36(3), 192-200.

DAVIS W and OHNO Y. 2005. Toward an improved color rendering metric in Fifth International Conference on Solid State Lighting, In: Ferguson IT, Carrano JC, Taguchi T, Ashdown IE, editors. Proc of SPIE 5941. Bellingham, WA: SPIE, G1-G8.

NARENDRAN N and DENG L. 2002. Color rendering properties of LED light sources. Solid state lighting II. Proceedings of SPIE.

VALBERG A, SEIM T, and Sa¨llstro¨m P. 1979. Colour rendering and the three-band fluorescent lamp. Meeting of the CIE 1979, Kyoto, Japan.

OP23

EVALUATION OF LED LIGHTING QUALITY BASED ON COLOUR DISCRIMINATON ASSESSED BY 100-HUE TESTS

Yoko Mizokami[1], Dan Tagawa[1], Hirohisa Yaguchi[1]
[1] Graduate School of Advanced Integration Science, Chiba University, Chiba, JAPAN
mizokami@faculty.chiba-u.jp

Abstract

We investigate whether it is possible to propose a lighting evaluation method for lighting quality based on colour discrimination assessed by 100-hue test. We compared discrimination performances for two types of 100-hue test (ND-100 and FM-100) under LED and conventional lightings to examine the influence of test samples on the evaluation of colour discrimination. The error scores of ND-100 with low saturation and FM-100 with high saturation showed similar trend. Error scores under LED lighting were slightly different from those of conventional light sources in some colours. The score tended to be higher under a daylight type LED lighting, whereas it tended to be lower under an incandescent type LED lighting compared to conventional lightings. It was suggested that colour difference between adjacent colour samples and error score were related, which means the possibility to establish the evaluation of lighting quality based on colour discrimination assessed by 100-hue test.

Keywords: e.g. Lighting quality, colour discrimination, 100-hue test, LED lighting

1 Introduction

As light-emitting diodes (LEDs) lighting has become popular, it is necessary to evaluate the colour qualities of lighting including LED lighting property. There are many criteria for evaluation depending on its purpose, such as fidelity, memory colour, colour category, and so on. One of the important aspects of lighting quality would be colour discrimination, especially for situations that small colour difference is critical, such as museums, the colour management of products, stores and so on.

There are many studies on colour discrimination task under various lightings and multiple indices have been proposed (Houser et al, 2013). Some of them also examined LED lightings (Szabó et al., 2007; Rea and Feyssinir-Nova, 2008; Mahler et al., 2009; Royer et al., 2012). However, they have not reached the consensus of a method to evaluate lighting quality based on colour discrimination. In addition, the systematic or extensive evaluation of LED lighting based on colour discrimination has not been carried out.

100-hue test is one of colour vision tests for measuring colour discrimination and testing colour vision deficiency. It contains various colour samples with constant value and chroma that cover all hues in the Munsell colour system. Observers sort those colour samples in order of hue. Farnsworth-Munsell 100-hue test (FM-100) developed by Farnsworth (FARNSWORTH, 1943) is widely used. The other type of 100-hue test, ND-100 is also available mainly in Japan. The main difference of two types of 100-hue test is their chroma and the number of samples. FM-100 consists of 85 samples with rather high chroma, and ND-100 consists of 100 samples with lower chroma compared to FM-100. They are commercially available and could be useful assessment tools for lighting quality based on colour discrimination. We performed those 100-hue tests under different lightings and found that those error scores were partially influenced by the types of lighting (Tagawa et al., 2013). However, we have not examined whether they could be used as assessment tools.

In this study, we investigate whether it is possible to propose a lighting evaluation method for lighting quality based on colour discrimination assessed by 100-hue test. We compared discrimination performances for two types of 100-hue test under LED and conventional lightings to examine the influence of test samples on the evaluation of colour discrimination.

2 Experiment

2.1 Environment

A viewing box covered with medium grey (approximately equal to Munsell N6.5) matt paper was used for the experiment. Its size was 60 cm (length) × 89 cm (wide) × 40 cm (height). It was illuminated by one of test lamps and a 100-hue test was placed on the centre of its bottom. Horizontal illuminance at the position of the 100-hue test was set to approximately 1000 lx (±10 %).

2.2 Light sources

Conventional lamps with high colour rendering properties and LED lamps were compared. We tested lamps with three illumination colours: daylight, neutral white, and incandescent colour type. Figure 1 shows their relative spectral power distributions. We compared the combination of fluorescent lamps simulating illuminant D65 (correlated colour temperature approx. 6200 K, Ra 98) and daylight type LED (6500 K, Ra 70), neutral white fluorescent lamp (4700 K, Ra 97), and neutral white type LED (5000 K, Ra 68), incandescent lamp (2800 K, Ra 99) and incandescent colour type LED (3000 K, Ra 84). In our previous research on colour fidelity assessed by corresponding colour, we used the same set of lamps and found that there were small differences in colour appearance between the conventional lamps and the LED lamps (Yaguchi et al., 2012).

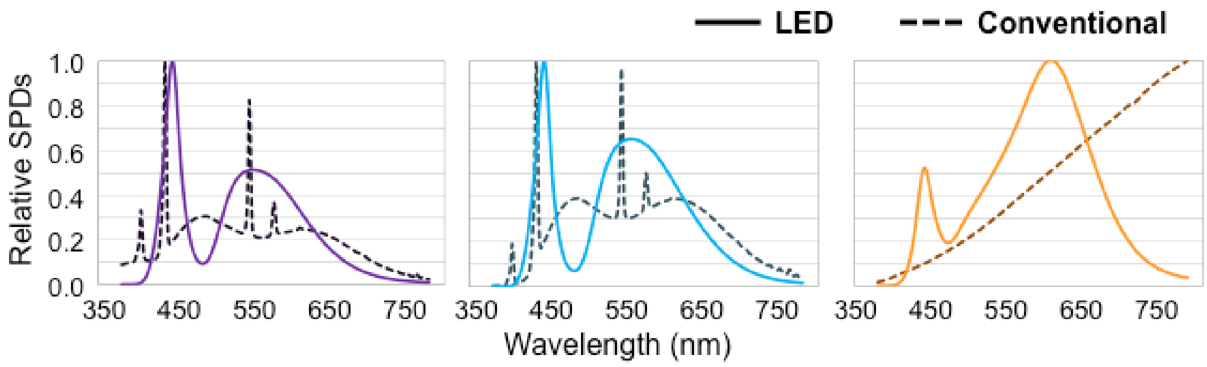

(a) Daylight **(b) Neutral white** **(c) Incandescent colour**

Figure 1 – Relative spectral power Distribution (SPDs) of the light sources

2.3 100-hue tests

We used two types of 100-hue test for discrimination task. One was ND-100 (Japan Colour Research Institute) consisted of 100 colour disc samples with low saturation, and the other was Farnsworth-Munsell 100-Hue Test (FM-100, X-rite) consisted of 85 colour disc samples with high saturation. Average chroma and average colour difference between neighbouring samples *are* C^*_{ab} = 13.4 and ΔE^*_{ab} = 0.97 for ND-100, and C^*_{ab} = 25.7 and ΔE^*_{ab} = 2.27 for FM-100. We examined the capabilities of colour discrimination for colours with both low and high saturation, using those two types of 100-hue test. Figure 2 shows the picture of 100-hue tests used for our experiment and the chromaticity coordinates on the CIELAB (a*, b*) diagram. Those in CIECAM02-UCS (Luo et al., 2006) are also shown in Figure 3 to compare the colour difference between LED and conventional lamps with different colour.

The chromaticity coordinates of colour samples in 100-hue tests on the CAM02-UCS colour diagram showed that the shape of colour distribution was different under LED and conventional lightings. Under LED lighting, yellowish and bluish colours tend to have higher chroma, whereas reddish and greenish colours tend to have lower chroma compared to conventional lightings. These trends were common in all colour types of lamps, but difference in incandescent colour type lamp was small.

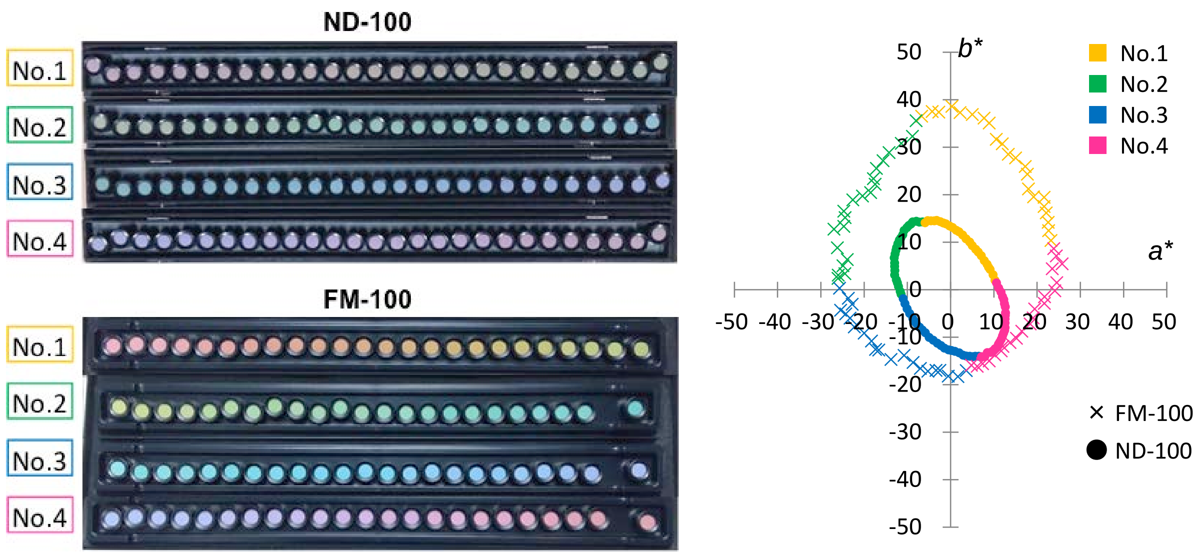

(a) Picture of tests used for experiments (b) a* b* chromaticity coordinates

Figure 2 – ND-100 and FM-100 100 hue test

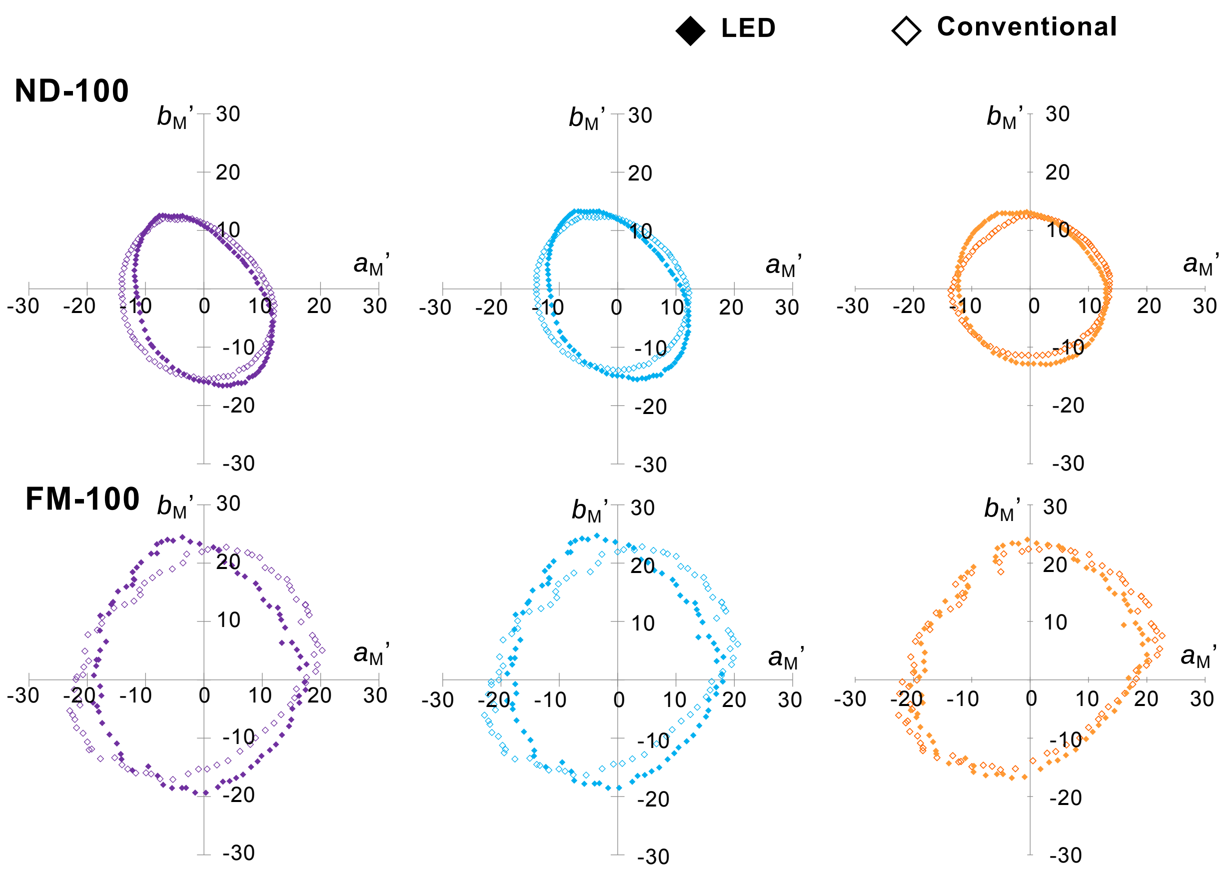

(a) Daylight (b) Neutral white (c) Incandescent colour

Figure 3 – Chromaticity coordinates of ND-100 and FM-100 on the CIECAM02-UCS

Each 100-hue test consists of four trays No.1-4. A discrimination task was carried out for each tray separately. A sample number indicating correct order is printed in the back of each colour sample. We calculated error scores from the results of the task for each tray. The calculation of error score *ES* is based on the differences of neighbouring sample's numbers as shown equation 1.

$$ES_n = |N_{n-1} - N_n| + |N_n - N_{n+1}| - 2 \tag{1}$$

where

n is the order of sample which observer arranged;

N_n is the sample number of *n*th sample;

With increase of the degree or the frequency of misarrangement, the error score also increases. We used equation 1 for calculating error scores of both 100-hue tests.

2.4 Procedure

After adaptation to a light for three minutes, Observers started a discrimination task. They arranged colour samples of 100-hue test in consecutive colour order. Time for the task was limited to two minutes for each tray. They repeated the same task for all 4 trays in successive. Each observer performed the two types of 100-hue test under all test lights, one time for each condition. Six observers (average age 22.3 years old) with normal colour vision participated.

3 Results and discussion

Figure 4 shows the sum of error scores for each tray (No.1-4) and the sum of error scores for all trays (Total) under each combination of LED and conventional lighting. Error bars show the standard deviations of six observers and asterisks show the significance level of the Student's t-test (N = 6; p < .05). The error scores of ND-100 and FM-100 showed similar trend. They tended to be high in tray No. 2 which contains greenish colour samples. It is interesting that the error scores of ND-100 and FM-100 do not show clear differences even if the chroma of FM-100 is higher than that of ND-100, indicating both tests had a similar level of difficulties in the task arranging samples. The error scores for incandescent colour type lamps are generally higher than daylight and neutral white colour lamps, suggesting that the discrimination task was more difficult under coloured light.

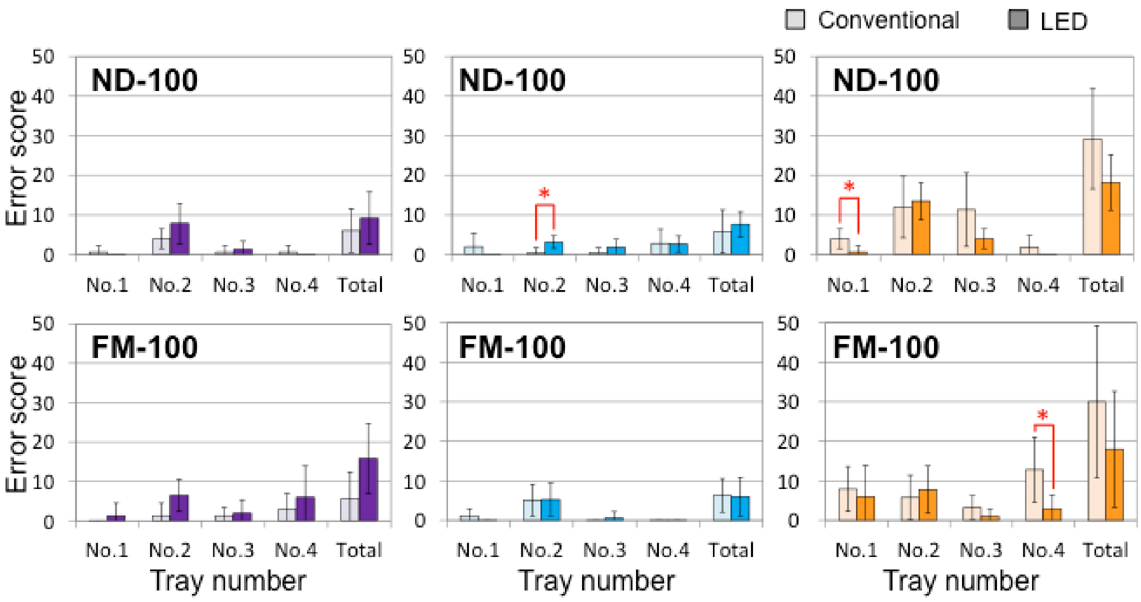

(a) Daylight **(b) Neutral white** **(c) Incandescent colour**

Figure 4 – Error scores of 100-hue tests for each tray and total under all lighting conditions

Although the difference of error score under LED and conventional lighting was small, those of some colour samples under LED lighting were a little higher compared to conventional light sources for daylight and natural white lamps. In the case of incandescent colour type lamp, the error scores under LED lighting were a little lower compared to conventional light sources in general. These suggest that 100-hue tests could be used for evaluating the difference of lighting quality.

We took the adjacent colour differences of samples next to each other for each 100-hue test and examined relationship with the error scores as shown in Figure 5. Colour difference Δ*E*' indicates the average of all adjacent colour differences in CIECAM02-UCS colour space under each condition. Regression lines and the coefficient of determination R^2 are also shown in the figure. ND-100 showed a trend that the average error score was higher when the average of adjacent colour differences was small. It is just as we expected since the colour discrimination is normally harder as colour difference is smaller. It suggests that colour difference between adjacent colour samples and error score are related, and there is a possibility that the quality of lighting based on colour discrimination can be evaluated by the colorimetric data of ND-100 test under an illuminant.

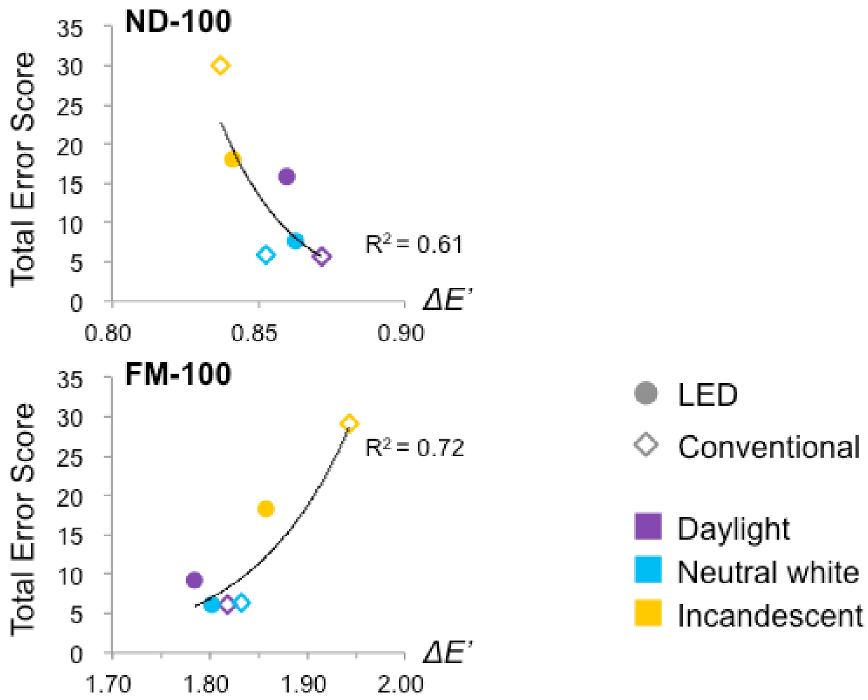

Figure 5 – Relation between the colour differences of adjacent samples and error scores

However, FM-100 did not show similar trend. It could be because FM-100 consists of more saturated colour and the number of samples is smaller compered to ND-100. Variance in the colour of adjacent samples was larger in FM-100, and it might make the colour arrangement task harder. Moreover, there were variances in the colour of samples not only in hue but also in chroma direction. Figure 6 shows relation between error scores and the standard deviation (SD) of the colour difference Δ*E*' (a), hue angle difference Δ*h* (b), and colourfulness differences Δ*M*' (c) of adjacent samples. In the case of FM-100, the SDs are larger and all have positive correlation with error scores. The task of 100-hue test is not solely discriminating two colours, but sorting multiple samples. The large variance of chroma may be the cause of the higher error score and positive correlation between colour difference and error score in FM-100. It would be easy to sort colours if difference is only in hue with constant interval, but the task would become harder with irregular hue and chroma because those randomness would work as some kind of noise or disturbance.

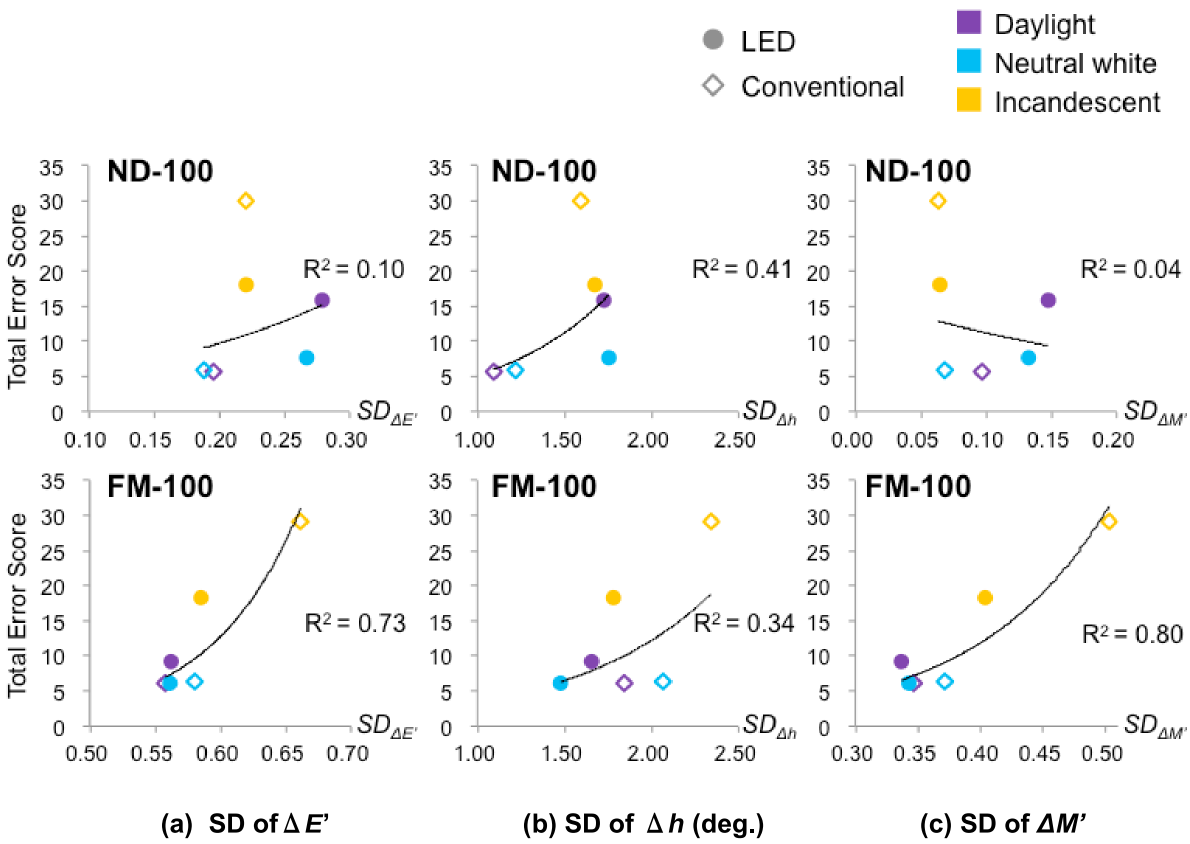

Figure 6 – Relation between SD of the adjacent colour differences of samples and error scores

It was shown that the measurement data of colour difference was related to the error score of ND-100, suggesting the possibility to propose a lighting evaluation method based on the adjacent colour difference of 100-hue test samples. However, the result of FM-100 suggests that the variance of chroma is also needs to be taken into account. Further examination is needed to clarify how the saturation and variance of test samples influences to error score. It should be noted that the higher error score for incandescent type lamps implys that the colour of lighting also needs to be taken into account.

The difference of error score between conventional and LED lamps was not large in present result. We need to further examine experimental conditions to obtain more significant and reliable data to establish a practical method for the evaluation of lighting quality, such as low illuminance level, limited time of sorting task, and so on. It should be also investigated the selection of smaller number of samples since the assessment of 100 samples would be too much work in practice. There are some issues to be determined such as what colours and how many samples are enough.

4 Conclusion

We tested the two types of 100-hue test for evaluating discrimination performance under LED and conventional light sources. Error scores under LED lighting were slightly different from those of conventional light sources in some colours. It was suggested that colour difference between adjacent colour samples and error score were related. Although the effects of various factors such as illuminant colour, the saturation and the colour variance of samples on discrimination performance need to be further investigated, it would be possible to establish the evaluation method of lighting quality based on colour discrimination assessed by 100-hue test.

Acknowledgement

This research project has been supported by NEDO, New Energy Industrial Technology Development Organization of Japanese Government.

References

FARNSWORTH, D. 1943. The Farnsworth-Munsell 100-Hue and Dichotomous Tests for Color Vision. *Journal of the Optical Society of America*, 33(10), 568-574.

HOUSER, K. W., WEI, M., DAVID, A., KRAMES, M. R., and SHEN, X. S. 2013. Review of measures for light-source color rendition and considerations for a two-measure system for characterizing color rendition. *Optics Express*, 21(8), 10393-10411.

LUO, M. R., CUI, G., and LI, C. 2006. Uniform colour spaces based on CIECAM02 colour appearance model. *Color Research & Application*, 31(4), 320-330.

MAHLER, E., EZRATI, J.-J., and VIÉNOT, F. 2009. Testing LED lighting for colour discrimination and colour rendering, *Color Research & Application*, 34(1), 8-17.

REA, M. S., FREYSSINIR-NOVA, and J. P. 2008. Color Rendering: A Tale of Two Metrics. *Color Research & Application*, 33(3), 192-202.

ROYER, M. P., HOUSER, K. W., and WILKERSON, A. M. 2012. Color discrimination capability under highly structured spectra. *Color Research & Application*, 37(6), 441-449.

SZABÓ, F., SCHANDA, J., BODROGI, P., and RADKOV, E. 2007. A Comparative Study of New Solid State Light Sources. *Proc. of the 26th session of the CIE 2007, Beijing*, D18-21.

TAGAWA, D., KOMATSUBARA, H., KOBAYASHI, S., NASUNO, N., MIZOKAMI, and Y., YAGUCHI, H. 2013. Evaluation of color discrimination under LED lighting by two types of 100-Hue test. T*he 1st Asia Color Association Conference, Proc.*, 48-51.

YAGUCHI, H., MIZOKAMI, Y., TOBE, K., KOMATSUBARA, H., KOBAYASHI, S., and NASUNO, N. 2012. Testing of uniform colour space using corresponding colours under different illuminants. *CIE 2012 "Lighting Quality & Energy Efficiency", CIE x037:2012*, 137-141.

OP24

COLOUR FIDELITY EVALUATED OVER LARGE REFLECTANCE DATASETS

Aurélien David
Soraa Inc., Fremont CA, USA
adavid@soraa.com

Abstract

We discuss the use of large reflectance sample sets to assess the colour fidelity of light sources. We introduce three such sets and show how to use these to derive fidelity maps across the whole colour space. We show that fidelity predictions are strongly influenced by the sample set, and that predictions using small and large sets do not agree well.

Keywords: Colour Rendering, Colour fidelity, Light-emitting Diodes

1 Colour fidelity and test samples

The choice of a proper set of test samples for colour fidelity calculations has been the subject of various discussions in recent years. It is generally argued that the eight Munsell Test Colour Samples (TCS) of the Colour Rendering Index (CRI) are an imperfect choice because of their relatively pastel colours and smooth spectral variations. Amongst proposed improvements are the use of more saturated Munsell chips [Davis2010] and the use of specially designed samples which preclude spectral gaming [Smet2013]. In both cases, the number of samples has been maintained below 20 for convenience. However, it has also been suggested that a larger set of samples would be useful to improve accuracy [Vanderburgt2010, Zukauskas2010, Smet2013].

This contribution discusses the use of large sample sets to estimate colour fidelity. We introduce three sets which cover a large fraction of the colour space. We propose a calculation procedure to derive colour fidelity maps, and an associated colour fidelity index. Finally, we compare the predictions of small and large sample sets.

2 Large sample sets

2.1 Real (r) set

Our first set is a large collection of real reflectance spectra, obtained by merging several experimental databases. The details of the r set are discussed in more details in [David2014]. It includes about 60.000 samples of various origins: natural objects, flowers, paints, skins, prints, photos, fabrics. Its gamut covers about 40% of the total volume of the CIELAB space. Our r set has similar properties to another recently introduced large real-objects set, the so-called Leeds set [Smet2013] – although the latter contains even more objects.

2.2 Singular Value Decomposition (SVD) set

The SVD set is a synthetic set aiming at extending the gamut of the real set, while retaining its realistic spectral features. The procedure is described in details in [David14]. In short, we perform a singular value decomposition on the r set to determine its basis vectors. We analyse the statistical correlations between the coefficients of these vectors with a copula method, and generate new random combinations of basis vectors which reproduce these correlations. The resulting reflectance spectra are therefore highly similar to those of the r set, but extend to a wider gamut. For this work, we generated 1E6 such spectra.

2.3 Monte-Carlo (MC) Set

Finally, the MC set is another synthetic set proposed in [Whitehead2010] which covers a large fraction of the colour gamut. It is based on a model of absorbers with realistic widths and uniform spectral distribution. The various spectra are obtained from random number generation, hence the name of this set. For this work, we generated 1E6 such spectra.

Figure 1 shows the respective gamuts of our three sets and other sets in CIELAB space. As can be seen, our three sets cover a substantially larger fraction of the whole space.

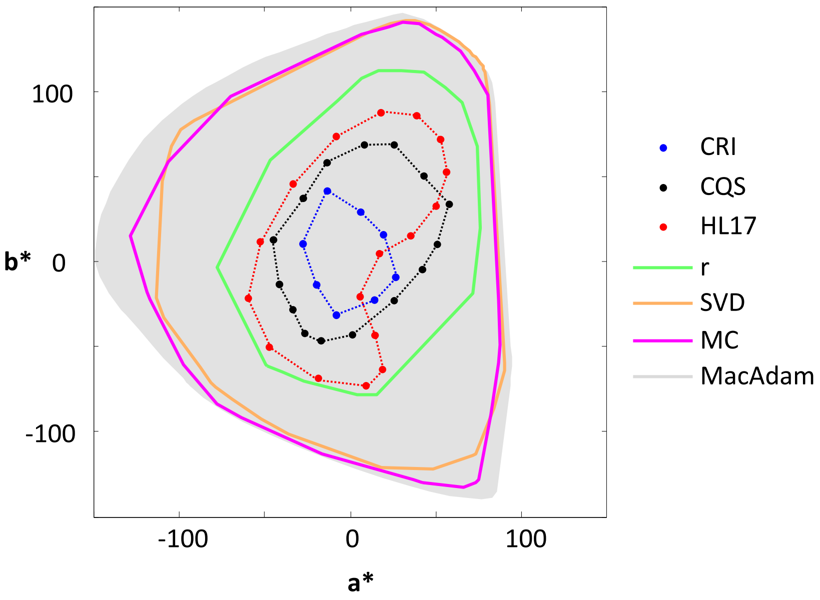

Figure 1 – Gamut of various test samples in CIELAB, projected in the (a*b*) plane. The MacAdam boundary represents the limit of CIELAB. The MC and SVD sets have the largest gamuts, followed by the r set. All of these sets contain many samples within the gamut boundary whereas the CRI, CQS and HL17 samples only consist of a few samples tracing a path in colour space.

3 Colour fidelity maps

For a given test sample set and a Spectral Power Distribution (SPD), we must determine how to compute colour fidelity. This is not trivial because the sample sets are very non-uniform in colour space. For the r set, this is due to the choice of measured samples (for instance there are about 8.500 skin spectra); for the SVD and MC sets this is a consequence of the generating algorithms. Therefore, a “uniformisation” procedure must be applied.

We use the CIELAB colour space and proceed as follows. For each test sample (i) we compute the (L_i, a_i*, b_i*) coordinates and the colour error $dE00_i$ between the SPD and the corresponding reference illuminant. We divide CIELAB into square pixels of lateral size δ=5 and bin the test samples inside each pixel. Some pixels may contain many samples (whereas the pixels outside the sample set’s gamut are empty, of course). For each pixel, we then compute the geometric average of $dE00_i$ over all test samples inside the pixel. Thus, we obtain a pixelated colour error map dE00(La*b*).

As discussed in [David14], the resulting maps are well-behaved: they vary smoothly across colour space, confirming that the average colour error is a well-defined local metric for a given set (in other words, the averaging over nearly-metameric samples is legitimate). Fig. 2 shows an example of such an error map for a typical white LED with a CCT of 3000K and CRI of 80.

Interestingly, the error maps derived from all three large sample sets are quite similar in the regions where they overlap (however the r set has a smaller gamut than the two synthetic sets, and therefore has no data for the most saturated colours – which also correspond to the largest colour errors). This rather good agreement suggests that, to first order, the error map is characteristic of the SPD rather than of the sample set.

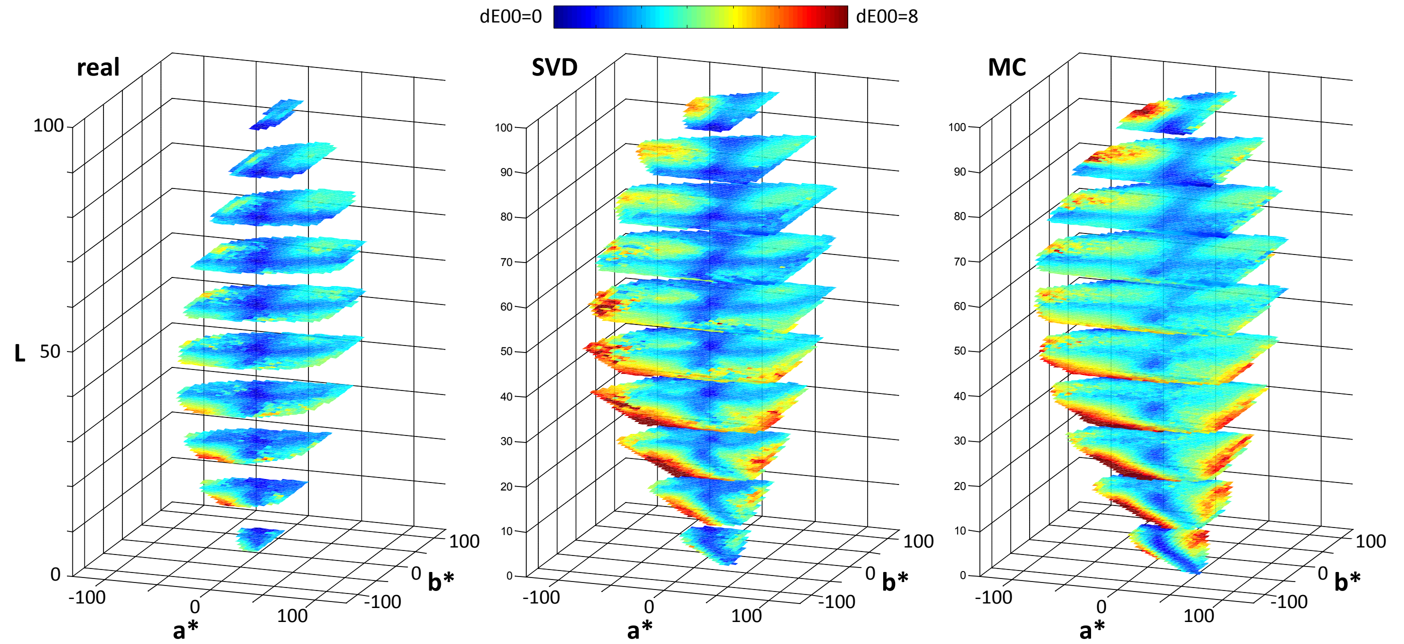

Figure 2 – Color error maps dE00(La*b*) for a white LED light source and the large sample sets. In regions where the sets overlap, they are in good agreement.

It is instructive to compare maps for various SPDs. Fig. 3 compares maps for four 3000K LED sources with a CRI of 95 evaluated over the MC set. The four SPDs are very different and show increasing degrees of structuration (from smooth to very spikey, the last SPD being composed of four laser lines). Fig. 3 reveals that despite their common high-CRI value, the colour error maps are very different: the smoothest spectrum shows very little error across space and more spectral structuration is associated with more colour error.

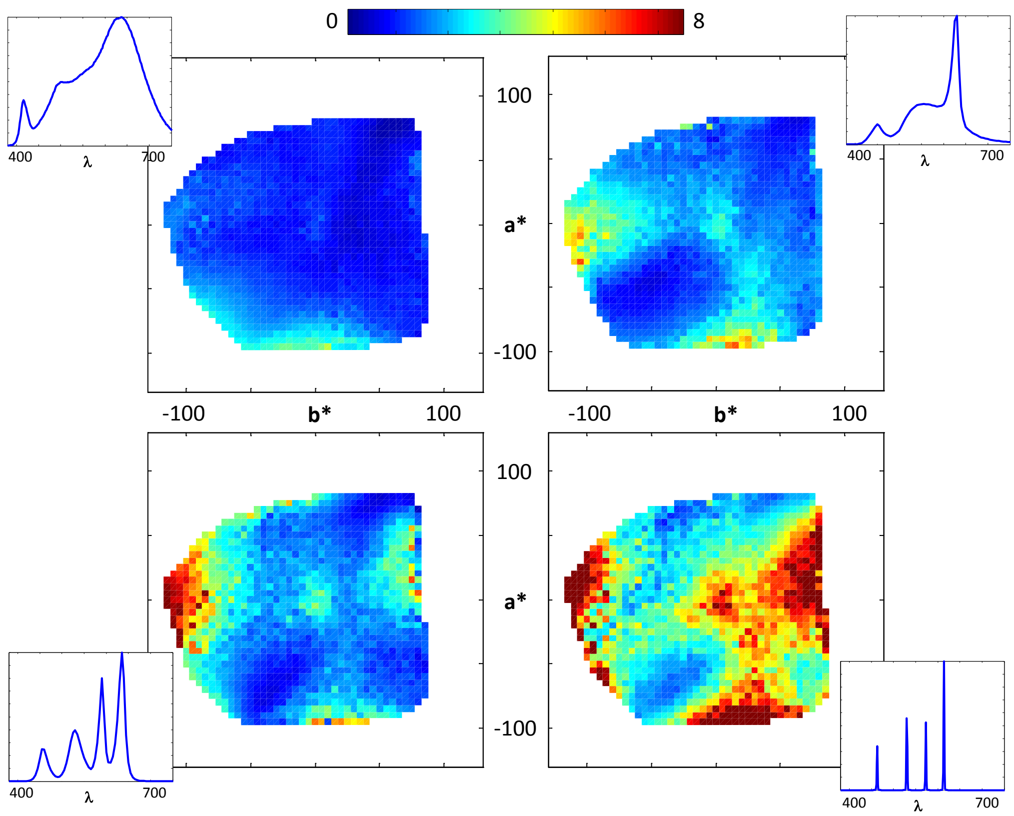

Figure 3 – Colour error maps (cross-section at L=50) for four high-CRI SPDs evaluated over the MC set.

This is a direct illustration of a shortcoming of the CRI TCS. They sample only a small region of the colour space, a colour errors happening outside this region are not accounted for. By using sample sets with a more thorough coverage, these errors are revealed.

In order to summarize the error maps into a single index, we compute the geometric average <dE00> of dE00(La*b*) over the whole CIELAB space. We can then define a fidelity metric Qf=100-k<dE00> where k is a scaling factor set by a customary procedure [Davis2010]. Fig. 4 shows how this fidelity index varies when different sample sets are used.

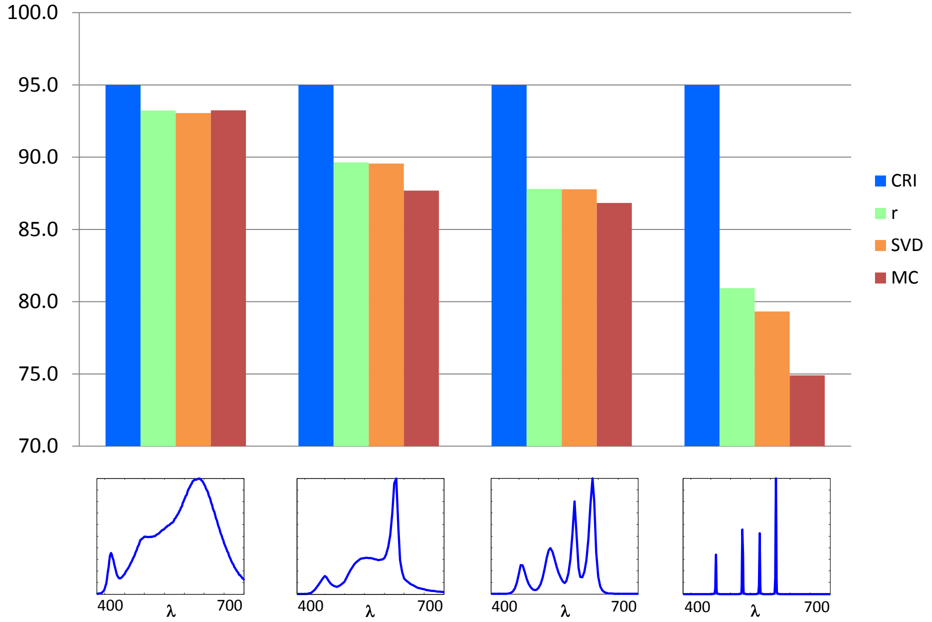

Figure 4 – Colour fidelity of four sources with a CRI of 95. More structured SPDs obtain worse fidelity for larger sample sets.

Different sets predict different fidelity values: smooth SPDs are not very sensitive to the sample set, but structured SPDs are punished by larger sample sets, which probe their colour error more thoroughly. In this example, it is clear that these four CRI-95 sources should not be assigned the same high fidelity value. Interestingly, only the first SPD with very smooth features obtains the same fidelity score with the CRI and large sample sets. This is expected: smooth SPDs are rather well-behaved and only a few test samples are sufficient to characterize them. On the other hand, SPDs with a lot of variation require more and more samples. Given the current interest in the industry for highly structured SPDs, the motivation to improve upon the CRI thus appears well-justified.

4 Correlation between sample sets

The TCS do not correlate well with our large sample sets for the few SPDs considered so far. However the broader question is: given a large library of SPDs, can we find two sample sets which correlate well (i.e. predict the same relative ordering of fidelity across the SPDs)?

To answer this, we consider a library of 401 SPDs recently reported [Houser2013]. This library consists of a variety of source (most real, some computed) from different technologies (natural, incandescent, fluorescent, metal halides, LEDs). For a given sample set, we can compute the average colour error for the SPDs in the library. We can then assess the agreement between two sample sets by studying the statistical correlation of the colour error prediction. As an example, Fig. 5 shows the correlation cloud between the real set and two other sets: TCS and SVDr (described below).

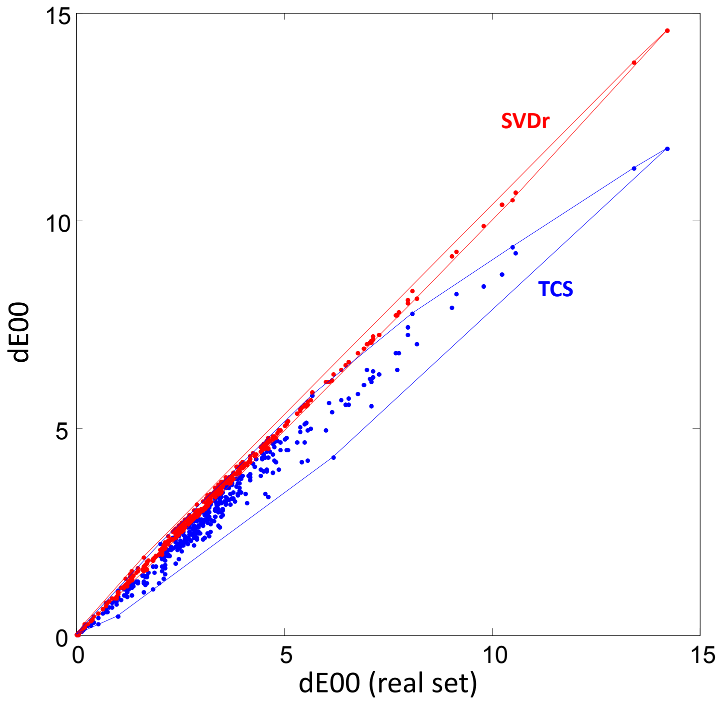

Figure 5 – dE00 statistical correlation between sample sets. Each point is an SPD. Blue: correlation between the r and TCS sample sets; red: correlation between the r and SVDr sets.

It is apparent that the correlation between the r and TCS sets is very poor: there is significant re-ordering of the rank between the SPDs. If we make the reasonable hypothesis that the r set is a good starting point for a sample set, this suggests that the TCS samples are a poor choice. On the other hand, the SVDr set is well correlated to the r set.

To quantify this statistical correlation, we compute the Spearman rank error **E**=1-ρ_Spearman. A small value of **E** indicates that two sample sets are in excellent agreements, e.g. they produce the same fidelity calculations for the SPDs in our library.

We compute **E** for a variety of combinations of sets:

- the three large sets already introduced: r, SVD, MC
- “restricted” versions of the SVD and MC sets, where only samples within the gamut of the real set ate kept; these are denoted as SVDr and MCr
- the 8 CRI TCS
- the 15 CQS samples [Davis2010] and their extension to 32 samples CQS32 [Ohno2014]
- the CRI2012 samples HL17, HL210 and HL1000 [Smet2013]

The rationale for considering the restricted sets SVDr and MCr is as follows. As we have shown, SVD and MC contain many samples with higher saturation than the r set. While these samples are physically plausible, such saturated colours have not been observed in the real-world, and one may thus argue that they should be discarded. By restricting these synthetic sets to the gamut of the r set, we ensure that only samples within a ‘reasonable’ gamut are considered.

Fig. 6 shows the correlation matrix of **E** between all pairs of sets. Most correlations are poor or very poor – this can be checked by converting the dE00 values into Qf fidelity scores: a value of E~10E-3 corresponds to about 8-10 points of ‘noise’ in fidelity, which is clearly not a good correlation. For instance two SPDs with the same Qf=80 according to the real set may have respectively Qf=73 and 87 according to the TCS, a significant discrepancy.

	CQS	CQS32	r	SVD	SVDr	HL17	HL210	HL1000	MC	MCr
TCS	11.4	9.8	13.6	37.5	13.1	94.5	63.2	77.5	83.7	86.7
CQS		1.1	9.2	41.6	11.1	99.9	62.6	72.9	83.5	77.9
CQS32			10.3	38.8	10.8	96.5	58.9	71.4	80.8	77.9
r				21.1	1.6	72.2	41.6	49.1	55.6	53.2
SVD					16.0	40.1	11.9	23.2	17.6	31.6
SVDr						62.7	34.9	42.8	48.5	48.0
HL17							31.4	13.1	22.8	19.4
HL210								18.2	15.1	27.3
HL1000									6.5	3.4
MC										10.5

Figure 6 – Spearman error matrix between all pairs of sample sets (in units of 1E-3). Low values indicate good correlations. The colour code of the cells indicates the goodness of the correlation (a value of one to a few points is desirable)

Only few pairs of sets correlate well. This includes CQS/CQS32 (which are very similar), r/SVDr and MCr/HL1000.

We suggest that the r set is a reasonable 'starting point' for a fidelity metric, because it contains many real objects which have been deemed worthy of measurement and covers a large fraction of the colour space. Below we discuss the correlation of various sets with the r set.

The SVD set does not correlate well with r; this is due to its much larger gamut: some SPDs are only penalized by the most saturated samples of SVD, which are absent from r. On the other hand SVDr (the restriction of SVD to the gamut of r) yields excellent correlation to r. This warrants our construction of the SVD set, which aimed at producing synthetic spectra with realistic features. However the SVDr set contains many more samples than the r set, so it is not a more practical alternative.

Interestingly, the same is not true of MC: even after it is restricted to the gamut of r, there is poor correlation between r and MCr. This suggests that the spectra of the MC set, while they are derived from a physically plausible model, do not actually represent real-world samples well enough.

The lack of correlations between r and small sets (CQS, TCS, HL17...) is not surprising if we consider the amount of variation across the error maps of Figs. 2-3. These small sets only sample a few points in colour space and are unable to characterize the colour error of an SPD thoroughly.

The lack of correlation between HL1000 and r is less easily explained: HL1000 has a gamut quite similar to r and has many samples within this gamut; therefore the two sets sample the colour space in a comparable way. The lack of correlation must therefore be ascribed to the spectral features of the HL1000 samples: these were assembled by 'stitching' of real spectra (see [Smet2013]) in order to reduce spectral gaming. We tentatively suggest that this procedure yields unrealistic spectra. It is worth noting that MCr and HL1000 are in rather good agreement; this is most likely not coincidental: both sets cover a similar gamut and share the same property of 'spectral flatness'; unfortunately it appears that this property was obtained at the expense of realistic features.

In conclusion, no sample set currently proposed in a fidelity metric achieves good correlation with the r set. One may thus consider using the r set to improve the accuracy of fidelity predictions. Certainly, there is a trade-off between accuracy and sample size and some believe that a set of 60.000 samples is impractical. In the view of the author, the size of the r set is in fact quite tractable (see comments on calculation speed in [David2014]); however it would be ideal to obtain a smaller set with good correlation to the full r set. We leave this as a question for further research.

5 Conclusions

We introduced three reflectance sample sets with large gamuts. By using these, we showed that colour fidelity is a smoothly varying function across colour space, which can be characterized by colour maps. In contrast, most currently proposed sample sets are small and only probe the fidelity map at a few points; they are therefore unable to thoroughly characterize fidelity. Accordingly, sample sets agree poorly with each other in terms of fidelity predictions. We suggest that our real sample set is a reasonable starting point for fidelity calculations. Currently, no smaller set correlates well with this set. It would be desirable to obtain a set with high correlation to the real set and the smallest possible size.

References

DAVID, A. 2014. Color Fidelity of Light Sources Evaluated over Large Sets of Reflectance Samples. *Opt. Expr.* 10, 59-75.

DAVIS, W. 2010. Color Quality Scale. *Optical Engineering* 49(3), 033602.

HOUSER, K. 2013. Review of measures for light-source color rendition and considerations for a two-measure system for characterizing color rendition. *Opt. Expr.* 21, 10393-10411.

OHNO, Y. 2014. Private communication with the author.

SMET, K. 2013. CRI2012: A proposal for updating the CIE colour rendering index. *Lighting Res. Technol.*, 45, 689-709.

VAN DER BURGT, P. 2010. About Color Rendition of Light Sources: The Balance Between Simplicity and Accuracy. *Col. Res. Appl.* 35, 85-93.

WHITEHEAD, L. 2010. A Monte Carlo Method for Assessing Color Rendering Quality With Possible Application to Color Rendering Standards. *Col. Res. Appl.* 37, 13-22.

ZUKAUSKAS, A. 2010. Colour-rendition properties of solid-state lamps. *J. Phys D: Appl. Phys.* 43, 354006.

OP25

INFLUENCE OF LIGHT SOURCE LUMINANCE ON DISCOMFORT GLARE FROM LED ROAD LUMINAIRES

Daisy Lai[1], Xiaoyan Zhu[1], Longshi Wang[1], Haldun Dermirdes[1], Ingrid Heynderickx[2,3]
[1] Philips Research China, Shanghai, CHINA
[2] Philips Research Laboratories, Eindhoven, THE NETHERLANDS
[3] Eindhoven University of Technology, Eindhoven, THE NETHERLANDS
Daisy.lai@philips.com

Abstract

Due to their small size and high lumen output, the luminance of the emitting surface of high power LEDs is very high (up to 1×10^7 cd/m^2), and so, when directly visible, may cause severe discomfort glare to road users, such as car or bike drivers and pedestrians. In general, eye illuminance is considered the dominant factor influencing perceived discomfort glare, and obviously eye illuminance increases with the luminance output of the LEDs. In this paper, however, we investigated the effect of light source luminance itself on discomfort glare, while keeping the eye illuminance constant. Our results show that the luminance of the light source has a significant effect on perceived discomfort glare when a person looks directly into the light source, even when the eye illuminance is constant. The perceived discomfort glare decreases with a decrease in luminance level, and people are more sensitive to luminance induced differences in discomfort glare at low than at high luminance.

Keywords: discomfort glare, light source luminance, LED road lighting

1 Introduction

Discomfort glare of road lighting has been studied by various groups in the past using luminaires with traditional light sources. In recent years, LEDs, being a new energy-efficient light source, are introduced in road lighting at a high pace in China, as a consequence of strong governmental support. There is, however, also a rising concern that LED-based road luminaires may cause discomfort glare to road users, including vehicle drivers and pedestrians. To better understand the factors influencing discomfort glare generated by LED sources in a road lighting application, a series of perception experiment has been carried out at Philips Research Lab in Shanghai.

Various factors have been identified as key parameters influencing the sensation of discomfort glare resulting from LED-based road lighting. As with traditional light sources, research of Liu et al (Liu, 2013) has shown the impact of light source luminance and the angle of the light source in the field of view on perceived discomfort glare. In addition, Zhu et al (Zhu, 2012) have shown that the tint of the white light, as characterized by the CCT, also has an impact on perceived discomfort glare; perceived glare is reduced for lower CCT. Also the light beam shape affects perceived discomfort glare (Zhu, 2013), since the light beam shape determines the eye adaptation luminance from multiple luminaires in the field of view and the dynamic change in eye illuminance. Apart from these known effects, the luminance distribution in the emitting area of the light source has received limited attention with respect to discomfort glare. For traditional light sources, this factor was not important as usually the light emitting area was relatively large. For LED-based luminaires, however, the light emitting area may be small, and hence, the impact of luminance and luminance distribution on perceived discomfort glare deserves further research.

Currently, most LED-based road luminaires use an array of high-power spot LEDs. The average luminance of each LED source in the array is about 1×10^7 cd/m^2. With further developments in LED chip technology, the efficiency of the LEDs is expected to continuously increase. Consequently, the lumen output as well as the luminance of the LED light source will further increase as well. This trend raises the concern that the extremely high luminance may cause severe discomfort glare. As mentioned above, discomfort glare is known to increase with light source luminance, but in most of these studies the light conditions were not matched for the amount of illuminance at the eye and used much lower luminance levels. In a first study, Bullough et al (Bullough, 2008) found that the rating of discomfort glare was mainly determined by the illuminance of the light source at the eye, and was not affected by the size and luminance of the (array of) light source(s). Later research, however, showed first evidence that the luminance of the light source may also influence discomfort glare, even for the same illuminance at the eye. The latter was found mainly when the glare source was viewed from a relatively close distance (Bullough, 2011).

To further evaluate the impact of luminance and luminance distribution on perceived discomfort glare (for a fixed illuminance at the eye), we designed a laboratory setup using light source dimensions and a viewing distance proportionally reduced to mimic a road lighting scenario. Light sources with different luminance, luminance distribution and light emitting area, but with matched vertical illuminance level at the eye were evaluated in this setup. Participants were allowed to compare these light sources to a reference light source, and they were asked to rate the perceived discomfort glare of each of the light sources, including the reference one.

2 Experimental method

2.1 Experimental setup

The experiment was conducted in the lab of Philips Research China, where typical road lighting conditions were simulated in a dark room. Subjects were seated at 2m distance from the projection screen with their head fixed by a headrest (as can be seen Figure 1 at the left side). The projection screen (of size 146 x 120 mm^2) could render either a uniform or a non-uniform luminance distribution at different luminance levels, representing various scenes on the road. For the actual experiment described here, the projection screen was illuminated in two parts (as shown in Figure 1 at the right side): the upper part was black with an average luminance of 0.2 cd/m^2 to simulate the dark sky, while the lower part was brighter with an average luminance of 1.5 cd/m^2 to simulate the road surface under road lighting. The reference and test light source were mounted in the upper part of the screen at same height of the subjects' eyes. During the experiment, subjects were asked to look directly into the light source (so, with a viewing angle of 0^o).

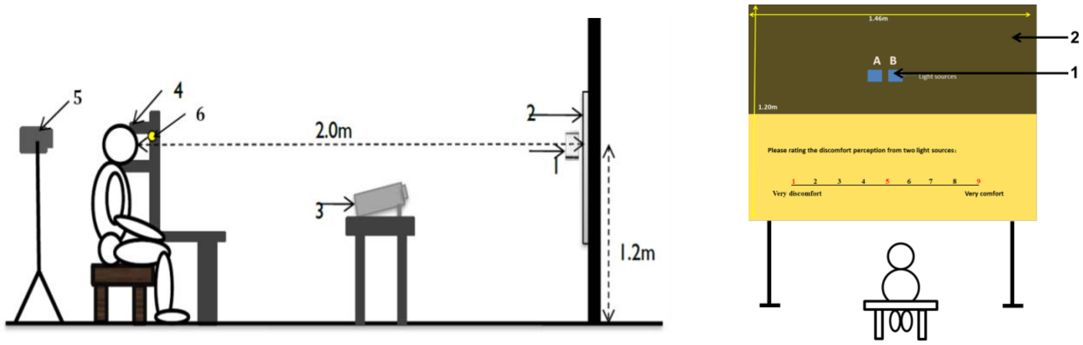

Figure 1 Schematic overview of the experimental setup in a dark room. The figure at the left shows the different components of the experimental setup: 1. Glare source, 2. Projection screen, 3.Projector, 4.Headrest, 5.Luminance meter, and 6.Illuminance meter. The figure at the right shows the projection screen with the two light sources and the scoring scale

2.2 Light sources

The experiment consisted of three parts, each comparing a different situation, as summarized in Table 1. The first part compared two single LEDs at 7 different luminance levels, where the LED with the highest luminance level was used as reference. The second part compared two sources consisting of a 2x2 LED array at 5 different luminance levels, and also here the array with the highest luminance was used as reference. Finally, the third part compared a uniform source with a 2x2 LED array. The luminance of the latter was varied at 5 different levels, while the uniform source at a fixed luminance was considered as the reference. Note that for all three parts of the experiment the vertical illuminance at the eye was matched to a fixed value between the conditions, but this fixed value was different between the different parts, as shown in Table 1. In addition, it should be noted that all light sources used had a CCT of 3000K.

Table 1 Overview of the parameters describing the three parts of the experiment

Parameters	Variables	single vs single	array vs array	uniform vs array
Fixed parameters	Reference light source and luminance (cd/m²)	Single spot / $1,2\times10^7$	Spot array / $7,8\times10^6$	Uniform / 7×10^4
	Eye adaptation time (min)	20		
	Surrounding light	Provide 0,47 lx eye illuminance while luminance on wall is 0,5 cd/m²		
	Eye illuminance provided by glare source (lx)	1	3	3
Independent variable	Test light source	Single spot	Spot array	Spot array
	Luminance of test light source ($\times10^4$ cd/m²)	460/70/45/28/12/7	180/50/30/19	670/163/40/26/15
Dependent variable	Subjective rating			

2.3 Experimental procedure

For the experiment, we recruited 10 subjects with good visual acuity and no colour blindness. Half of the participants were male and the age of all participants varied between 25 and 40 years. Before the actual start of the experiment, each subject was seated in the room for 20 minutes in order to adapt to the dark environment. During this period, he/she was informed on the experimental procedure, instructed on how to use the subjective rating scale, and finally practised some trials to get acquainted with the procedure.

During the experiment each subject assessed all lighting conditions one by one, in a random order, the latter being different for each subject. For each light condition, the two light sources (reference and test) were presented to the subject one by one, and switched on and off repeatedly for 3 times. The on-period for both reference and test light source in this repetition was 3 seconds. After this repetition, the subject was asked to give a rating for the perceived discomfort glare of each light source. We used a 9-points scoring scale (as shown on the projection screen on the right side of Figure 1), with a score of 1 referring to "very discomfortable" and a score of 9 to "very comfortable". Between two light conditions, the subjects got enough time to relax their eyes in order to avoid eye fatigue.

3 Experiment results

3.1 Luminance effect from single spot light source

In this part of the experiment, the influence of the luminance of a single spot light source on discomfort glare was studied, while keeping the eye illuminance constant. The spot light source with a high luminance of $1,2\times10^7$ cd/m^2 was used as reference. Figure 2 shows the mean value of the subjective rating on discomfort glare for the various luminance levels of the single spot light source. It clearly illustrates a decrease in comfort rating (making the light source less comfortable) at higher light source luminance.

To further analyse these results, we performed an Analysis of Variance (ANOVA) with the subjective rating as dependent variable and the luminance of the light source as independent variable. The results showed a significant effect of luminance of the light source on perceived discomfort glare ($F=63,650$, $df=6$, $p<0,001$). To compare the luminance values mutually we used the Bonferroni method (to correct for overall chance), and the results are shown in Table

2. Perceived discomfort glare is significantly reduced as compared to the reference (with a luminance level of $1,2×10^7$ cd/m^2) when the luminance of the glare source is reduced to below $4,5×10^5$ cd/m^2. This corresponds to a reduction ratio of about 27. In addition, subjects reported significantly less discomfort glare when the luminance of the glare source was reduced from $2,8×10^5$ cd/m^2 to $1,2×10^5$ cd/m^2, which corresponds to a luminance ratio of only 2,3.

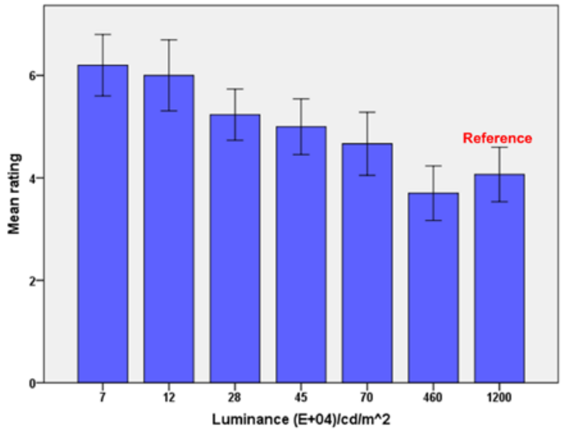

Figure 2 Mean value of subjective rating on discomfort glare from a single spot light source at different luminance (Error bar: 95% CI)

Table 2 Mutual comparisons of light source luminance levels. **indicates a statistically significant difference as measured with the Bonferroni method

P	7	12	28	45	70	460	1200
7	-	1	**0.000	**0.000	**0.000	**0,000	**0,000
12	1	-	**0.009	**0.000	**0.000	**0,000	**0,000
28	**0,000	**0,009	-	1	0.125	**0,000	**0,000
45	**0,000	**0,000	1	-	0.570	**0.000	**0.001
70	**0,000	**0,000	0.125	0.570	-	**0.007	0.294
460	**0.000	**0.000	**0.000	**0.000	**0.007	-	0.066
1200	**0.000	**0.000	**0.000	**0.001	0.294	0.066	-

3.2 Luminance effect from array light source

Most LED road luminaires currently designed are based on an array of LED light sources. Therefore, we here evaluated the effect of light source luminance for a 2x2 LED array. The light source array with the highest luminance of $7,8×10^6$ cd/m^2 was used as reference. Figure 3 shows the mean value of subjective rating on discomfort glare of the array light source at different luminance levels. Obviously, also here the discomfort rating decreases (and so, the perceived discomfort increases) at higher luminance of the light source.

A similar ANOVA, as described above, showed a significant effect of luminance of the light source on perceived discomfort glare ($F=25,515$, $df=4$, $p<0,001$). The results of the comparisons between luminance levels with the Bonferroni method are shown in Table 3. Perceived discomfort glare was significant reduced when the luminance of the array was reduced from its highest value of $7,8×10^6$ cd/m^2 to $5,0×10^5$ cd/m^2, which corresponds to a luminance ratio of about 16. Starting from the lowest luminance of the array light source, being $1,9×10^5$ cd/m^2, subjects perceived significantly more glare for a luminance higher than $5,0×10^5$ cd/m^2, which corresponds to a luminance ratio of about 2,6.

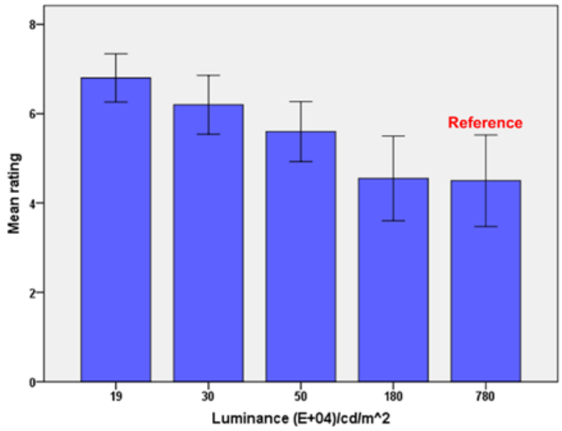

Figure 3 Mean value of subjective rating on discomfort glare from an array of LEDs at different luminance (Error bar: 95% CI)

Table 3 Mutual comparisons of light source luminance levels. **indicates a statistically significant difference as measured with the Bonferroni method

P	19	30	50	180	780
19	-	0.735	**0.001	**0.000	**0.001
30	0.735	-	0.584	**0.009	*0.020
50	**0,001	0.584	-	**0.004	*0.015
180	**0,000	**0,009	**0.004	-	1
780	**0,001	*0,020	*0.015	1	-

3.3 Comparison between uniform and array light source

In this part of the experiment, we wanted to compare discomfort glare between a uniform light source and a 2x2 LED-based array light source, where the latter varied at different luminance levels, while again keeping the eye illuminance constant. The uniform light source with the lowest luminance of 7,0 $\times 10^4$ cd/m^2 was used as reference. Figure 4 shows the mean value of the subjective rating on discomfort glare of the uniform (reference) light source and of the array light source at different luminance. Comparing only the effect of luminance of the array light source, we again see a clear reduction in discomfort rating (and so, an increase in perceived discomfort) with luminance. The first couple of bars in the graph also illustrate that the perceived discomfort of the array light source is comparable to the uniform light source at sufficiently low luminance.

We again used a similar ANOVA to further analyse the results, and this analysis showed a significant effect of luminance of the light source on perceived discomfort glare ($F=20{,}701$, $df=5$, $p<0{,}001$). The results of mutually comparing the luminance levels with the Bonferroni method are shown in Table 4. There is no significant difference in perceived discomfort glare between a uniform light source of 7,0 $\times 10^4$ cd/m^2 and an array light source, as long as the luminance of the latter is lower than 2,6$\times 10^5$ cd/m^2. These luminance levels correspond to a ratio of 3,7. When starting from the array light source with the highest luminance of 6,7$\times 10^6$ cd/m^2, perceived discomfort glare was significant reduced when the luminance was reduced to lower than 4,0$\times 10^5$ cd/m^2, which corresponds to a ratio of about 17.

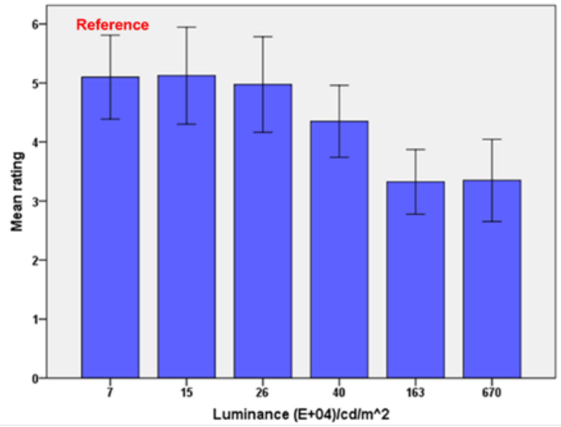

Figure 4 Mean value of subjective rating on discomfort glare from uniform (reference) and array light sources with different luminance (Error bar: 95% CI)

Table 4 Mutual comparisons of light source luminance levels. **indicates a statistically significant difference as measured with the Bonferroni method

P	7	15	26	40	163	670
7	-	1	1	*0.045	**0.000	**0.001
15	1	-	1	0.467	**0.005	*0.034
26	1	1	-	0.224	**0.000	**0.010
40	*0,045	0.467	0.224	-	*0.014	**0.010
163	**0,000	*0,005	**0.000	*0.014	-	1
670	**0.001	*0.034	**0.010	**0.010	1	-

4 Discussion

4.1 Luminance influence on discomfort glare

As shown above, all 3 parts of the experiment resulted in a consistent conclusion, namely that when people look directly into the light source, the light source luminance has a significant influence on perceived discomfort glare, even when the illuminance at the eye was kept constant. For the same eye illuminance, the subjective rating of discomfort glare decreased (implying more discomfort glare) with increasing light source luminance, independent on whether the light source was a single spot or an array of 2x2 LEDs. The difference between minimum and maximum perceived discomfort was 2 steps on the 9-point scale we used.

From each part of the experiment, we deduced two typical luminance levels:

- The lower luminance level that was just significantly different in perceived discomfort glare with the highest luminance level.
- The higher luminance level that was just significantly different in perceived discomfort glare with the lowest luminance level.

These two types of luminance levels are summarized in Table 5. It shows that the luminance ratio that subjects perceive as significantly different in terms of discomfort glare is much lower at low luminance level (R_l) than at high luminance level (R_h). This observation indicates that human eyes are more sensitive to luminance induced differences in perceived glare at low luminance level than at high luminance level. The luminance ratio that subjects perceive as significantly different in discomfort glare at high luminance level is about 27 for a single spot light source and is about 16 for an array light source. As shown in Table 2 for the single spot light source, there is no significant difference in perceived discomfort glare between a light source with a luminance of $1,2\times10^7$ cd/m^2 and a light source with a luminance of $7,0\times10^5$ cd/m^2, yielding a luminance ratio of 17. Hence, this suggests that people are more sensitive to luminance induced glare differences for an array light source than for a single spot light source at high luminance level. On the other hand, when we compare the luminance induced glare differences at the lowest luminance level, we found a luminance ratio of 3,7 between the uniform light source and the array light source, which is considerably higher than the luminance ratios we found for both the single spot light source and the array light source (i.e., 2,3 and 2,6 respectively). The latter suggests that human eyes are more tolerant to luminance induced differences in discomfort glare for the distributed light source than for the uniform light source, at least at a low luminance level.

Table 5 Luminance ratio that subjects just perceive as significantly different in discomfort glare at high and low luminance level.

Experiment	Highest luminance (L_h)/cd/m^2	Significant difference with L_h /cd/m^2	Luminance ratio (R_h)	Lowest luminance (L_l)/cd/m^2	Significant difference with L_l /cd/m^2	Luminance ratio (R_l)
Single vs Single	$1,2\times10^7$	$4,5\times10^5$	27	$1,2\times10^5$	$2,8\times10^5$	2,3
Array vs Array	$7,8\times10^6$	$5,0\times10^5$	16	$1,9\times10^5$	$5,0\times10^5$	2,6
Uniform vs Array	$6,7\times10^6$	$4,0\times10^5$	17	$7,0\times10^4$	$2,6\times10^5$	3,7

4.2 Field verification

The experiment discussed so far was conducted in an indoor lab environment, which may be considered remarkably different from a real road condition in terms of light source size and viewing distance. To verify our results obtained in the lab with a real road condition, a field verification test was performed. For this test, we used a reference light source, existing of high power LEDs with a luminance of $6,6\times10^6$ cd/m^2. This reference light source was compared to 3 COB (chip on board) test light sources with a luminance of $2,8\times10^5$ cd/m^2, $1,7\times10^5$ cd/m^2 and $1,2\times10^5$ cd/m^2, respectively, each providing nonetheless the same illuminance at observer's eye position. Each test light source had the same array structure than the reference light source, consisting of 2x8 LEDs with a distance between 2 LED chips of 33mm. Subjects were asked to observe these light sources directly from 3 different distances (i.e., 10m, 15m and 20m) and to give a rating on perceived discomfort glare using the same 9-point scale as was used in the lab experiment. An ANOVA performed on the results showed that all 3 test luminance levels were significantly less uncomfortable than the reference luminance level. The luminance ratio that described the first significant difference between the reference light source and a test light source was about 23, which is consistent with the conclusions from the lab experiment.

When, however, we increased the viewing distance to 30m or larger, subjects didn't perceive differences in discomfort glare between the reference light source with a luminance of $6,6\times10^6$ cd/m^2 and any of the test light sources, even not with the test light source with the lowest luminance of $1,2\times10^5$ cd/m^2. In the last case, the luminance ratio would be 55, which is much higher than what we found in the lab experiment. Most probably at this viewing distance people cannot resolve the detailed structure of the light source, which was also confirmed by accidental remarks of the participants during the experiment. As a consequence, the halo around the light source made all light sources look similar.

It should be noted that the luminance ratios (as shown in Table 5) is based on lab experiment condition with direct observation. The spacing between LEDs (for array light sources) is fixed, and subjects can distinguish the array structure in all experiment conditions. The effect of spacing between LEDs on discomfort glare perception need further investigated. The absolute value of luminance ratio is not applicable for road luminaire design.

From the results of both the lab test and the field test, we may conclude that luminance, even for the same illuminance at the eye, has an impact on discomfort glare for LED-based road luminaires, especially when people look directly into the light source. The relevance of this finding for car drivers, however, is limited. Indeed, a typical installation of on a major road in China has a mounting height of 12 m and a spacing between luminaires of 35m. Taking into account the cut-off of the visual field due to the car roof, the distance between the driver and the closest luminaire that is perceived is about 30m. As shown above, at this far distance luminance has no impact on perceived discomfort glare. The situation is, however, different for pedestrians in urban or residential areas, where the typical mounting height of a luminaire is 4 to 6 m, and the luminaires are also more closely spaced. In addition, the luminance of the light source used in this application area is much lower than the luminance of luminaires installed in major roads, making - as mentioned before - humans more sensitive to luminance induced differences in discomfort glare. As a consequence, designers of luminaires for urban areas should take luminance of the luminaire into consideration.

5 Conclusions

With the fast development of LED technology, the efficacy of LEDs, and so, their lumen package output increase substantially. Our results have shown that even at constant illuminance at the eye, the actual luminance value itself may also affect perceived discomfort glare, especially when people look directly in the light source from a distance up to 20m. A well-controlled lab experiment showed that people are more sensitive to luminance induced glare differences at low luminance than at high luminance. In addition, we confirmed the main conclusion from our miniaturized lab experiment with a field test on a real road.

References

BULLOUGH, J. D. 2011. Luminance versus luminous intensity as a metric for discomfort glare. *SAE international*, 5.

BULLOUGH, J. D., ET AL 2008. Predicting discomfort glare from outdoor lighting installations. *Lighting reseach and technology,* 40, 17.

LIU, Y. E. A. A study on estimating the discomfort glare caused by LED road lights. ChinaSSL, 2013 Beijing.

ZHU, X. E. A. 2012. Perception study of discomfort glare from LED road lighting. *2012 CIE Lighting Quality & Energy Efficiency Conference.* Hangzhou.

ZHU, X. E. A. 2013. The luminaire beam shape influence on discomfort glare for LED road lighting. *2013 CIE Lighting Quality & Energy Efficiency Conference.* Paris.

OP26

DOMINANT CONTRAST AND VERTICAL ILLUMINANCE FOR PEDESTRIAN ILLUMINATION

Riad Saraiji[1]

[1] United Arab Emirates University, Al Ain, UNITED ARAB EMIRATES

P.O.BOX 15551, corresponding author r.saraiji@uaeu.ac.ae

Abstract

Characterizing the night time visibility of pedestrians is a complex matter. Whereas most studies found in the literature relate visibility to contrast, street lighting design standards use vertical illuminance 1.5 m above ground as a design target. The objective of this manuscript is to examine dominant contrast and vertical illuminance as metrics for pedestrian illumination. A computer simulation was made to find whether vertical illuminance values at various heights correlate with dominant contrast. A procedure to find dominant contrast experimentally as well as using computer simulation is shown. A mathematical model to find dominant contrast index (DCI) is proposed.

Keywords: Pedestrians, Contrast, night time visibility, streetlighting

1 Introduction

Visibility indices found in the literature rely primarily on the target contrast (Adrian 1989, Rea et al. 1991, Ising 2008). In addition to the contrast, the density and pattern of the light in the background relative to the target, can have an effect on how objects stand out (Davoudian 2011). Street lighting design standards such as CIE 115 (CIE 2010) and ANSI/IESNA RP-8-00 (2005), use vertical illuminance at 1.5 m above ground as a design target. Both semi-cylindrical illuminance and vertical illuminance have been studied to compare driver's detection distance or reaction time to the presence of pedestrians (Gibbons et al. 2008). Despite the common use of vertical illuminance as a design target for pedestrians, Saraiji (2009a, 2009b) found vertical illuminance to have minimal values in significant portions of the street that satisfies the IESNA (2005) horizontal illuminance requirement.

One question is whether drivers need to see the upper part of a pedestrian (from which the 1.5 m high design target is based) to recognize his or her presence. Or, can a driver realize the presence of a pedestrian by recognizing any part of a pedestrian's shape.

Pedestrians are three dimensional and their illuminance profile changes from top to bottom and from left to right. Furthermore, the background luminance may also be different from the upper to the bottom part of a pedestrian. Saraiji and Oommen (2013) studied various pedestrian contrast profiles and found that contrast was not constant along the height of the pedestrian or on either side of the pedestrian. Saraiji and Oommen (2013) proposed a new concept called dominant contrast (DC), which was defined as the contrast of any part of the pedestrian that would provide the highest pedestrian visibility. More elaborate discussion of Dominant Contrast as a metric for pedestrian illumination can be found in (Saraiji and Oommen 2014). The studies by Bullough et al (2012) and Ising (2008) further reinforce the need to have a metric that considers the highest contrast area on the target.

The objective of this work is to compare dominant contrast to vertical illuminance and to explore how dominant contrast can be further developed as a metric for pedestrian illumination.

2 Methodology to Characterize Pedestrian Contrast

Dominant contrast and vertical Illuminance at various heights above ground were examined in a street lit by street lights and a car headlights. The intensity distribution of the car headlights was obtained from (Schotelle et al 2004). A Dialux computer simulation was made. Five 3-D pedestrians were placed along the lateral direction of the street (Figure 1). The pedestrians were labeled based on their position relative to an approaching car as follows: Left (L), Left Centre (LC), Centre (C) , Right Centre (RC) and Right pedestrian (R). The street was illuminated with poles that are 10 meters high and 50 meters apart using LED streetlights that have spill control optics. Along the longitudinal direction of the street, we placed 12 pedestrian grids. Each grid was at a particular distance from pole A. For example Grid 12.5 is 12.5 m away from pole A and has five pedestrians along the lateral direction of the street as shown in Figure 1. Vertical illuminance levels were found at various longitudinal and lateral points along the street at 3 different heights: 0.5 m, 1 m, and 1.5 m above ground. An average value along those three points was also found.

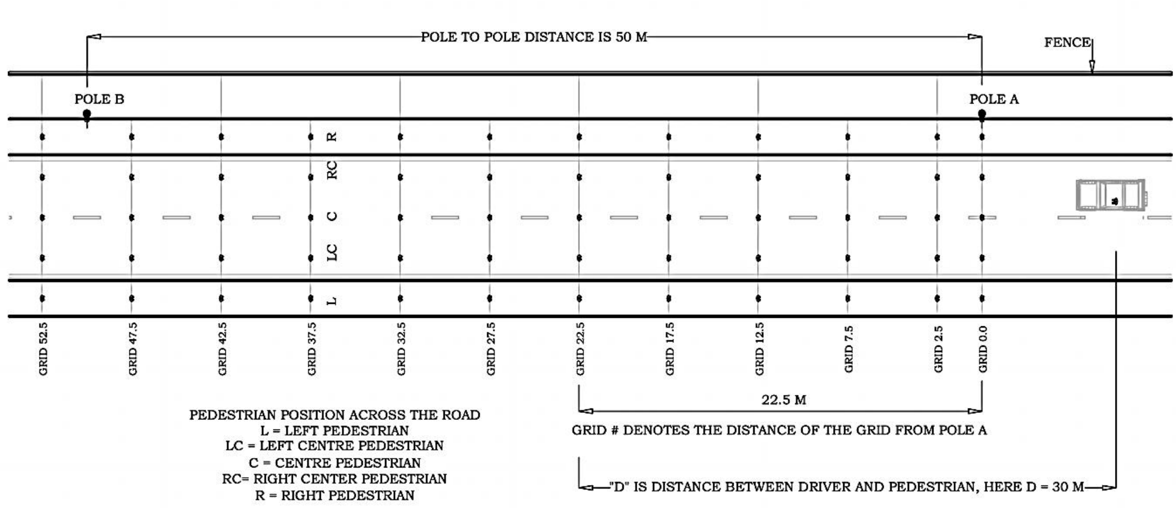

Figure 1 Top view of the street under consideration. Pedestrian locations L,LC,C,RC,R positions are as seen by driver.

To find the pedestrian contrast profile, the luminance values of 12 points along the height of the right side of the pedestrian were obtained with 12 points on the right background. Similarly, the luminance values of 12 points along the height of the left side of the pedestrian with 12 points of the background on the left side were also found. This resulted in two contrast profiles one for the left side and one for the right side of the pedestrian as shown in Figure 2. The contrast (*C*) of each point (*i*) was then obtained by using two equations:

$$Ci = \frac{L_{Ti} - L_{Bi}}{L_{Bi}} \tag{1}$$

Or

$$\mathrm{Ci}' = \frac{\mathrm{L_{Ti}} - \mathrm{L_{Bi}}}{\mathrm{L_{Gi}}} \tag{2}$$

Whereby, L_{Ti} is the pedestrian luminance at point *i*, L_{Bi} is the background luminance at point *i* and L_{Gi} is the greater value of the two luminances (L_{Ti} and L_{Bi}) at point *i*. when the background is the night sky, a luminance of 0.001 cd/m^2 was assigned to the background. This luminance prevents the contrast being ∞. This value was considered reasonable based on the values published by the Dark Sky Association (IDA 1994). The association reports the luminance of the darkest sky ever observed to be 0.0002 cd/m^2 versus a luminance of 0.03 for a sky with full moon. An example of the contrast profiles obtained is shown in Figure 2.

Figure 2: Example where contrast profile changes from top to bottom.

3 Results and Discussion

The vertical illuminance values for the centre pedestrian at grid G12.5 were found and are shown in Figure 3. The vertical illuminance was obtained using street lights and car headlights (Ev cl+sl) When the distance between the driver and the pedestrian grid (D) is larger than 40 m, the illuminance values at different heights converge and the average vertical illuminance at 0.5, 1 and 1.5 m high resembles the values at 1 m high. At short D, the contribution of the car headlights is more significant than the streetlights, especially at lower heights, as can be seen in Figure 3. The relative contribution of the streetlights compared to the car headlights is shown in Figure 4. The figure shows the ratio of the vertical illuminance due to car headlights combined with street lights (Ev cl+sl) relative to the vertical illuminance due to only car headlights (Ev cl). From that figure, we can see that at D<20 m the car headlights do not have any significant contribution on the vertical illuminance at 1.5 m high. As D becomes larger than 40 m, the Ev (cl+sl) becomes greater than 3 times the vertical illuminance due to car headlights Ev (cl). In light of the fact that vertical illuminance (1.5 m high) can be minimal at significant part of the area between two street lighting poles (Saraiji 2009), we have examined Grid 42.5 which has low vertical illuminance levels compared to grid 12.5. Whereas we did examine many grids, this manuscript focuses on two grids only. Figure 5 shows the vertical illuminance at various heights along the centre pedestrian (C) of Grid 42.5. Similar to the results found for grid 12.5, at D < 40 m, we see larger contribution from car headlights than from streetlight, especially at 0.5 m high. The vertical illuminance at 1.5 m high shows little dependence on D. Also, similar to the results found for G12.5, the average values of the vertical illuminance at different heights more closely resembles the values obtained at 1 m high. The contribution of streetlights on grid 42.5 relative to car headlights (Figure 6) is not as much affected by D as was the case in G12.5. This shows that the vertical illuminance due to streetlight is significantly dependent on the location of pedestrian along the longitudinal direction of the street.

The correlation between DC and Ev was studied. Figures 7 through 9 show the results at various pedestrian locations. As the figures imply, a correlation between the DC values and Ev values could not be found. This finding reinforces the fact that contrast and vertical illuminance are not necessarily correlated. Therefore, visibility studies that involve human factors should rely on contrast rather than vertical illuminance.

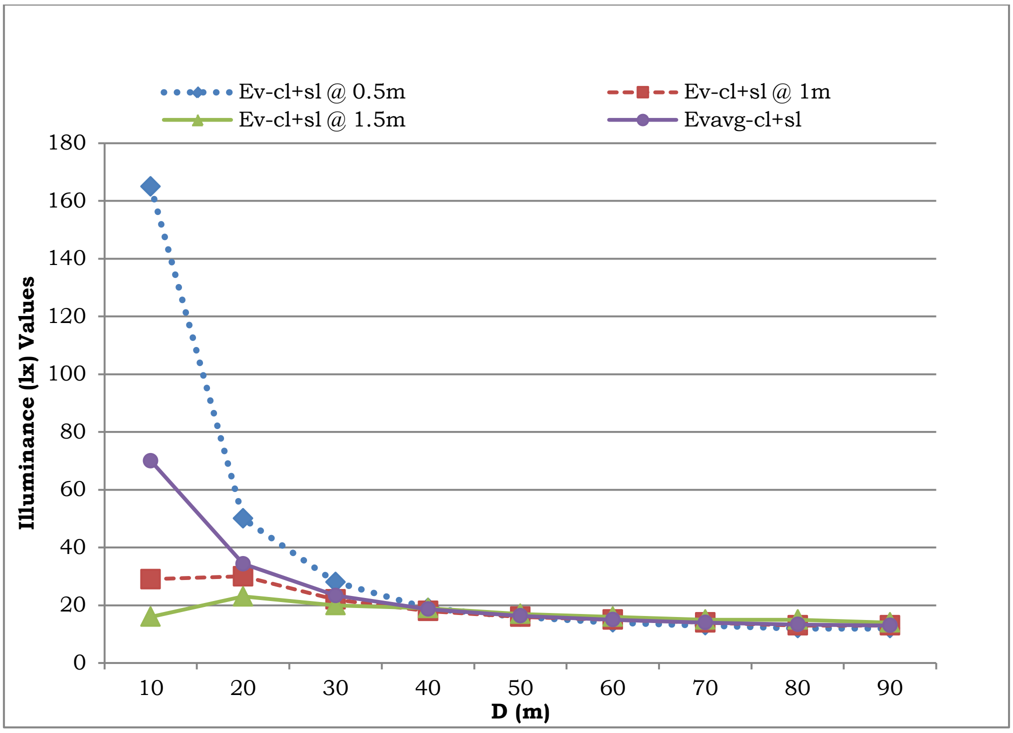

Figure 3: Vertical Illuminance vs. distance with both streetlight and car light for pedestrian grid G12.5. Centre Pedestrian.

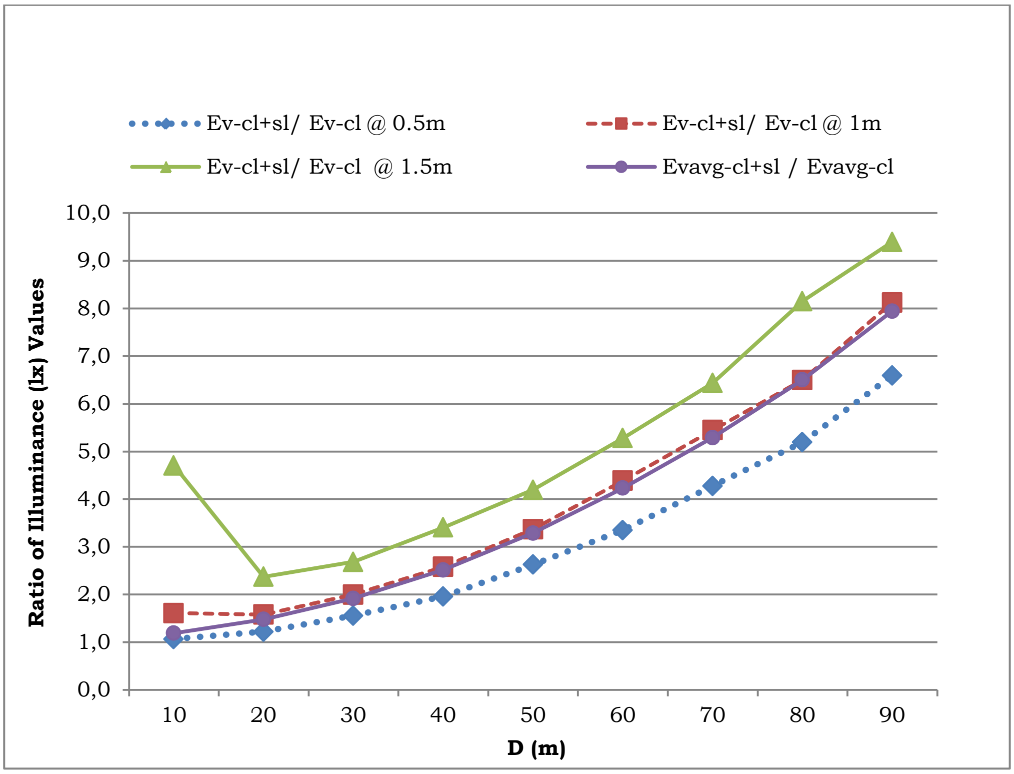

Figure 4: Ratio of vertical illuminance levels between (Car and Street light) and (only Car light) for pedestrian grid G12.5. Centre Pedestrian.

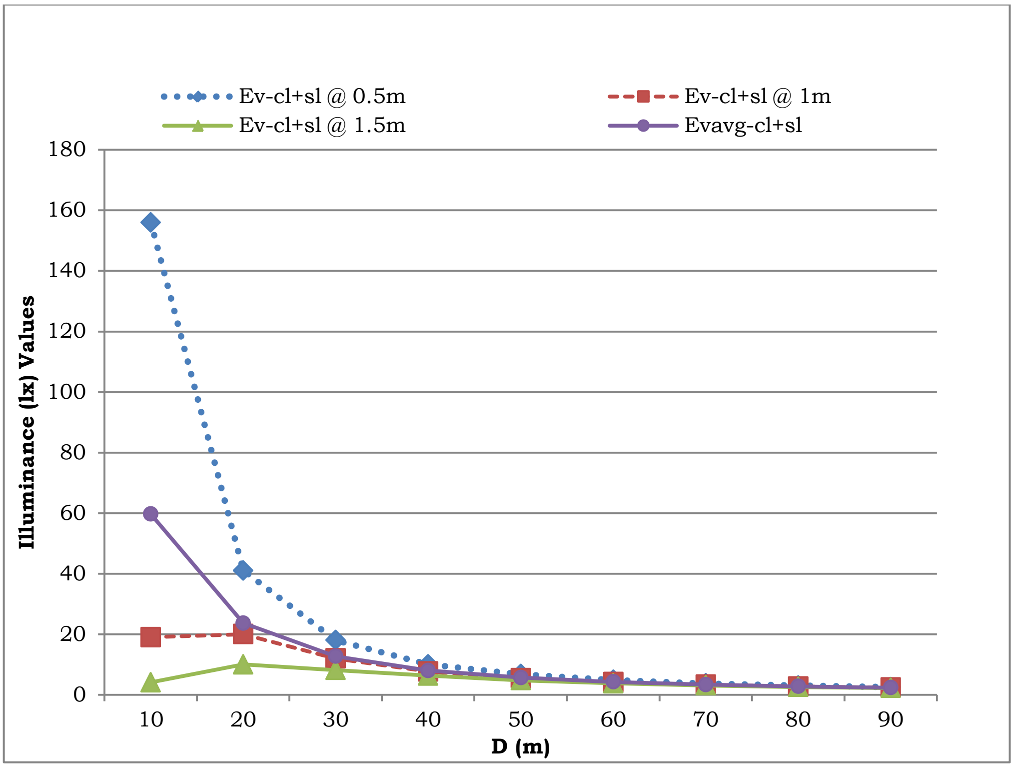

Figure 5: Vertical illuminance vs. distance with both streetlight and car light for pedestrian grid G42.5. Centre Pedestrian.

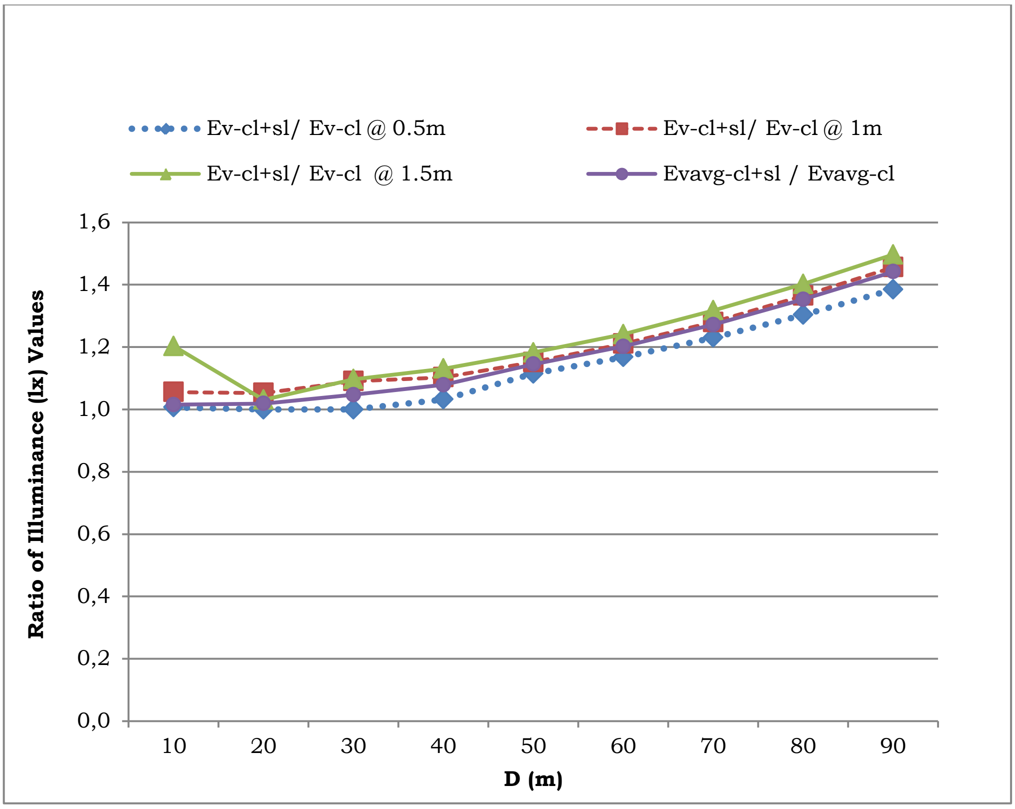

Figure 6: Ratio of vertical illuminance levels between (Car and Street light) and (only Car light) for pedestrian grid G42.5. Centre Pedestrian.

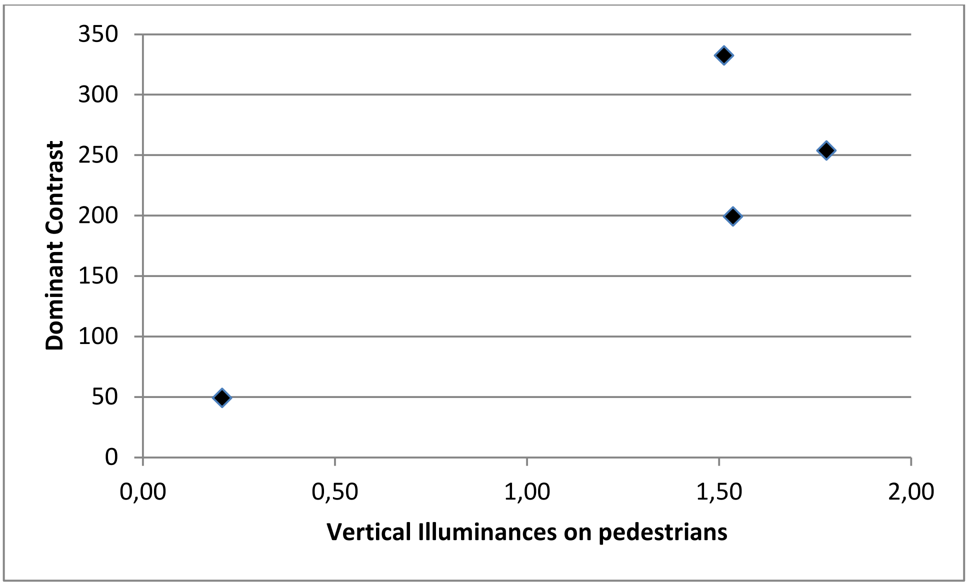

Figure 7: Correlation between Dominant Contrast and vertical illuminance. Left pedestrian Grid 12.5.

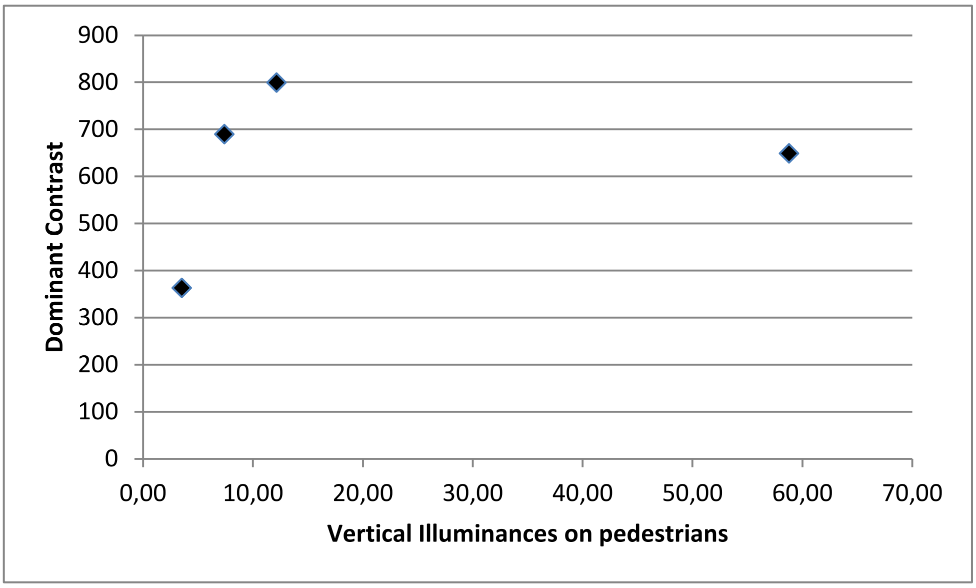

Figure 8: Correlation between Dominant Contrast and vertical illuminance. Centre Pedestrian Grid 12.5.

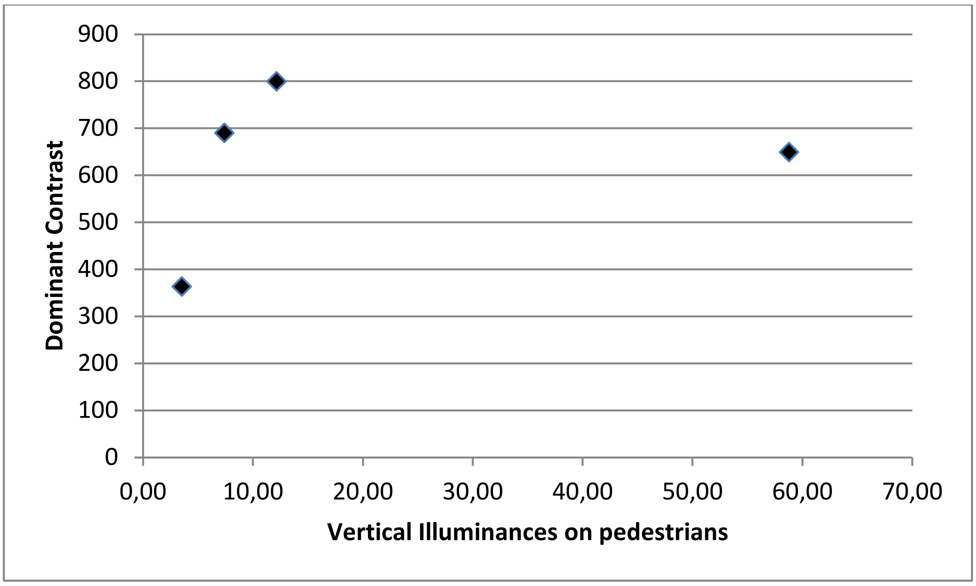

Figure 9: Correlation between Dominant Contrast and vertical illuminance. Right pedestrian. Grid 12.5.

4 Finding Dominant Contrast Experimentally

Dominant contrast can be found experimentally. In Figure 10, a pedestrian is 40 meters away from a driver with car headlights on (streetlights were off), a CCD Camera was used to capture the luminance values. The figure clearly shows that the dominant contrast is at the lower part of the pedestrian and a dominant contrast value can be captured.

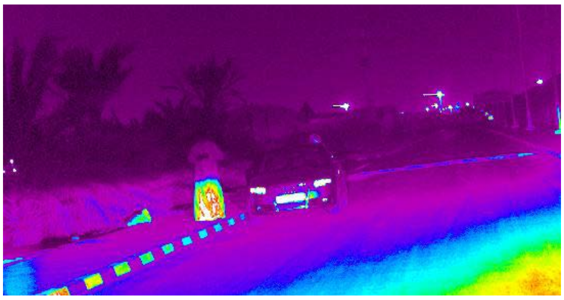

Figure 10 Luminance values of the scene as viewed by a driver when the car is 40 meter away from the pedestrian. Pedestrian wearing white clothing and streetlights were off.

5 Dominant Contrast Index (DCI)

The Dominant contrast index (DCI) gives an overall picture of the pedestrian contrast throughout a particular street segment. To calculate DCI, a street segment is divided into grids. The grids have equal spacing along the longitudinal direction of the street. Then, five pedestrians are placed along the lateral direction of the grid. That makes a total of *n* points to be examined with each point representing a pedestrian as shown in Figure 1. The DC is found for every point by finding the contrast of three parts (upper, middle, lower) of a pedestrian and using the maximum contrast of those points. To find the contrast, the luminance of the target and its background need to be found. The luminance of the upper part of the target (pedestrian in this case) can be calculated using semi-cylindrical illuminance per the following equation

$$L_u = E_{scu}(\rho_u/\pi) \qquad (3)$$

Where L_u is the luminance of the upper part of the pedestrian, ρ_u is the reflectance of the upper part of the target and, E_{scu} is the semi-cylindrical illuminance of the upper part of the pedestrian. The L of the middle and lower part of the pedestrian can be found in a similar way.

The DC at point i (DC_i) is calculated using the following equation.

$$DC_i = Max\left(\left(\frac{E_{sc}\left(\frac{\rho}{\pi}\right)-L_b}{L_b}\right)up, \left(\frac{E_{sc}\left(\frac{\rho}{\pi}\right)-L_b}{L_b}\right)md\,, \left(\frac{E_{sc}\left(\frac{\rho}{\pi}\right)-L_b}{L_b}\right)lo\right) \qquad (4)$$

Whereby, $up,\ md,\ lo$ stand for the upper part, middle part and lower part of the pedestrian respectively. Subsequently, the DC Index for the street segment (with a total number of n points) can be calculated as:

$$DCI = \frac{\sum_{i=1}^{n} DC_i}{n} \qquad (5)$$

6 Summary and Conclusion

The vertical illuminance along the pedestrian can change significantly from the upper part of the pedestrian to the lower part. The vertical illuminance at 1.5 m high is more affected by streetlights than by car headlights. On the other hand, the vertical illuminance at 0.5 m is significantly affected by car headlights and therefore is a function of the distance between the vehicle and the pedestrian. The author believes that car headlights should be included in street lighting design and that the height specified by CIE 115 and IESNA RP 8.00 of 1.5 m should be re-examined. The missing element when car headlights are ignored is that the reach of the headlamps is often larger towards the right side of the street and therefore, the left pedestrian (L) is not covered as well, by car headlights, as the right pedestrian (R). This is especially true as the distance between the vehicle and the pedestrian becomes shorter. This gap should be filled by street lighting. A pole arrangement that is primarily on one side of the street may not be as effective in addressing this issue, as a staggered pole arrangement. A street lighting design that has a one sided pole arrangement could very well miss important sides of the street that are otherwise not well lit by car headlights.

We found that Dominant Contrast and vertical illuminance are not correlated. Therefore, visibility studies that involve human factors should rely on contrast rather than vertical illuminance as a variable. Dominant contrast can be calculated and can be measured. A procedure to find the dominant contrast using computer simulation was shown. Dominant contrast can also be found experimentally using the luminance map from a CCD camera or an HDR image. A method for the calculation of a Dominant Contrast Index (DCI) for a street segment was proposed.

Further research is needed to find target DCI levels and further development of the mathematical model proposed in this manuscript is also needed so that DCI can be incorporated into commercially available street lighting design software.

Acknowledgement

This work was made possible through UAE University grant RTTSRC-1-2013

References

ADRIAN, W. 1989. Visibility of Targets: Model for Calculation. *Lighting Res. Technol.*, 21, 181-188.

ANSI/IESNA 2005. ANSI/IESNA RP-8.00:2005, *Roadway Lighting*, IESNA: New York.

BULLOUGH JD, REA MS, ZHANG X. 2012. Evaluation of visual performance from pedestrian crosswalk lighting: *Proceedings of the Transportation Research Board Annual Meeting*, Transportation Research Board.

CIE 2010. CIE 115. *Recommendations for the Lighting of Roads for Motor and Pedestrian Traffic*. Vienna: CIE.

DAVOUDIAN, N. 2011. Visual Saliency of Urban Objects at Night: The Impact of the Density of Background Light Patterns. *Leukos*, 8(2):137-152.

GIBBONS, R. B., Edwards, C., Williams, B., & Andersen, C. 2008. *Informational report on Lighting Design for Midblock Crosswalks, FHWA-HRT-08-053.* Federal Highway Administration.

IDA 1994, Information Sheet #99, *Terminology and units in Lighting and Astronomy*. International Dark Sky Association, Tucson, Arizona.

ISING, KW. 2008. Threshold Visibility Levels Required for Night time Pedestrian Detection in a Modified Adrian/CIE Visibility Model. *Leukos*, 5 (1): 63-75.

REA, MS. OUELLETTE, M.J. 1991. Relative Visual Performance: A basis for application. *Lighting Research and Technology*. 23(3):135.

SARAIJI, R. 2009. A Methodology for Locating the Maximum Vertical Illuminance in Street Lighting, *Leukos*, *the Journal of the Illuminating Engineering Society of North America*, Vol 6, No. 2, pp. 139-153.

SARAIJI, R. 2009, Vertical Illuminance Based Cross Walk Illumination, *Leukos*, *the Journal of the Illuminating Engineering Society of North America*, Vol 6, No. 2, pp. 153-167

SARAIJI, R. OOMMEN, M.S. 2013. Pedestrian Contrast Profile, *Proceedings of CIE Centenary Conference*, Paris, France.pp. 241-247.

SARAIJI, R. OOMMEN, M.S. 2014. Dominant Contrast as a Metric for Lighting of Pedestrians, accepted for publication in *Lighting Research and Technology*.

SCHOETTLE, B. Sivak, M, FLANNAGAN, M.J., and KOSMATKA, W.J. 2004. A market-weighted description of low-beam headlighting patterns in the U.S: 2004 (Technical Report No. UMTRI-2004-23). Ann Arbor: The University of Michigan Transportation Research Institute.

SULLIVAN, J. M., and FLANNAGAN, M, 2007. Determining the potential safety benefit of improved lighting in three pedestrain crash scenarios. *Accident Analysis and Prevention* 39, 638-647.

TYRRELL, R. A. JOANNE, M, and CARBERRY, T, 2004. On-road measures of pedestrians' estimates of their own nighttime conspicuity. *Safety Research* Vol. 35, pp. 483-490.

OP27

MEASUREMENT OF THE THRESHOLD INCREMENT (TI) IN ROAD LIGHTING BASED ON USING ILMD

Porsch, T.[1], Walkling, A.[2], Schmidt, F.[1], Schierz, C.[2]
[1]TechnoTeam Bildverarbeitung GmbH, Werner-von-Siemens-Straße 5, 98693 Ilmenau, GERMANY, tobias.porsch@technoteam.de
[2]Technical University of Ilmenau, Department of Lighting Technology, Prof.-Schmidt-Straße 26, 98693 Ilmenau, GERMANY, andreas.walkling@tu-ilmenau.de

Abstract

Imaging luminance measuring devices (ILMD) are widely used in different fields of lighting application.

The assessment of glare caused by daylight or artificial lighting installations in outdoor and indoor applications has meanwhile become reality. Furthermore, the measurement of the threshold increment will become a requirement of future standards.

The aim of this study was to develop a simple and an easy-to-use software tool to fulfil lighting requirements by using the ILMD.

This study also includes a comparison of existing calculation methods for the threshold increment regarding their technical requirements to be met by the ILMD and also the validation of new ideas and methods for analysis and evaluation.

Keywords: Imaging luminance measuring device (ILMD), luminance image, outdoor measurement, uniformity, disability glare, veiling luminance, threshold increment (TI)

1 Motivation

ILMD is widely used in different fields of application. The first step in using the ILMD is to analyse luminances “as seen” in the image (ILMD type I). The next step is not only to use luminance but also the position of the measured luminance values in order to extract any relevant information (ILMD type II). From this, it can be stated that the glare assessment of values of TI or any other relevant parameters is feasible.

Based on this starting point, the determination of the disability glare of road lighting installations has been attracting attention.

Another purpose of establishing the measurement of threshold increment based on ILMD is to be able to assess the agreement between measured and calculated values according to CIE and EN standards [6].

2 Threshold increment of road lighting installations

The percentage increment of the detection threshold caused by disability glare in road lighting is quantified by using the value of threshold increment (TI). It can be calculated based on the equivalent veiling luminance L_{veil} and the average road luminance L_{road} [4].

The disability glare describes the effect of stray light generation within the human eye. This leads to a contrast reduction and it is described as an equivalent veiling luminance. Thus, it is mainly a function of the vertical illuminance E_{vert} at the eye and the observer’s position related to the glare source [3]. So the viewing direction of the observer is a further important parameter when analysing luminance images for glare assessment (ILMD type II).

3 Advantages of ILMD and its practical implementation

- Individual perspective measuring grid for photometry adaption to grid points
- Possible variation of the observer viewing direction
- Different automated detection and manual glare source determination
- Simplified comparison of different parameters and equations for disability glare [2, 3]

When using the new software tool it is easy to change the observers viewing direction and thus the glare angle within the acquired luminance image. To do so, one needs to place a cross-hair at the desired position within the image (refer to 4.2.1). The placement depends on the ILMD's field of view measuring cone and direction respectively.

As a second step, the average road luminance is determined and is used as the so-called adaptation luminance. The location of grid points is calculated automatically based on a measuring grid region placed in the perspective view. Therefore, the lighting requirements of paragraph 4.1 are to be fulfilled. The luminance image can be the same as used for the determination of the equivalent veiling luminance or another one (refer to 4.2.2).

If both values are calculated, the tool will show results of TI as integral and individual values (each glare source) as defined in the first step (see figure 1).

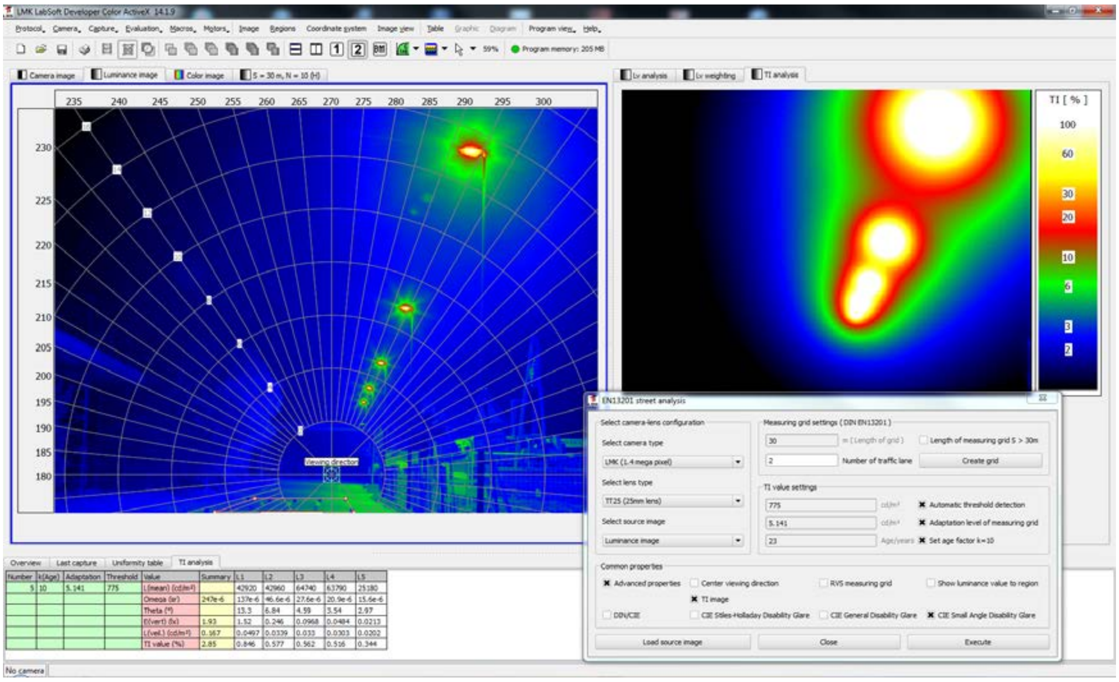

Figure 1 – Luminance image of road lighting installation and presentation of result of the glare assessment

4 Realisation of an ILMD setup and analysis in compliance with the EN 13201

4.1 Setup of ILMD for the photometry of EN 13201-4:2003

Measurement and calculation of relevant values are in line with the grid of measurement points as specified in EN 13201-3.

According to EN 13201-3, the luminance meter shall use a restricted total angle of the measurement cone to at least 0,03° in the vertical plane and at least 0,3° in the horizontal plane. If the ILMD determines the luminance for each grid point by averaging the reading of adjacent pixels, the mentioned limit angles shall not be exceeded [2].

Moreover, the measured vertical illuminance is a summation performed for any glare sources on a plane normal to the line of sight and at the height of the observer's eye (1,5 m above ground level). Any glare source above a screening plane which is inclined at 20° to the horizontal, and which passes through the observer's eye, and which intersects the road in a transverse direction, shall be excluded from the calculation [4].

If using the ILMD with e.g. an imaging resolution of 1400 x 1000 pixel, the values as given in table 1 for several lens types can be derived.

Table 1 – Overview of available measuring cones (1400 x 1000 pixel sensor resolution)

Lens type (focal length)	Measuring cone of the luminance image	Measuring cone of one squared pixel (average values)	Averaging cone adjacent pixel (3(H) x 3(V))	Measuring average road luminance	Measuring vertical illuminance
8 mm	63°(H) x 45°(V)	0,0452°/px	0,1356°	-	x
12 mm	43°(H) x 31°(V)	0,0313°/px	0,0939°	-	x
16 mm	32°(H) x 23°(V)	0,0232°/px	0,0696°	?	?
25 mm	20°(H) x 14°(V)	0,0148°/px	0,0444°	?	?
50 mm	10°(H) x 7,4°(V)	0,0074°/px	0,0222°	x	-

NOTE Available question marks does remark possible configuration under investigation. E. g. the averaging cone for the 25 mm focal length could also be 10(H) x 2(V) adjacent pixel and would now meet the requirements. Furthermore, the setup of the ILMD and the virtual placement of the observers viewing direction in the acquired image for measuring vertical illuminance by 16 mm and 25 mm focal length lens are worth to investigate.

The uncertainty of these parameters is strongly related to the optical properties of the ILMD sensor type and the lens configuration and shall be given besides the measured results.

ILMD's with a larger measurement cone can be used at a closer distance and at a proportional lower height. The angle of view of the meter shall be at (89 ± 0,5)° to the normal of the road surface. The measurement area on the road shall not be more than 0,5 m in transversal and 2,5 m in longitudinal direction.

4.2 Measurement and calculation of average road luminance

The average road luminance $L_{adapt(roadsurface)}$ can be measured with using the same image as used for measuring the equivalent veiling luminance, or by re-considering the results of any other luminance image. It can be done under the perspective view of the ILMD's positioning, specified by the standard requirements.

The assignment of the grid points matching the standard with the perspective pixelwise luminance information of the image is done by the software tool. It requires more information on the length of the road surface as well as the number of driving lanes. The software also uses the information of a perspective measurement grid. It rectifies the perspective image in an ortho-view image, presenting the standard grid points (see figure 2).

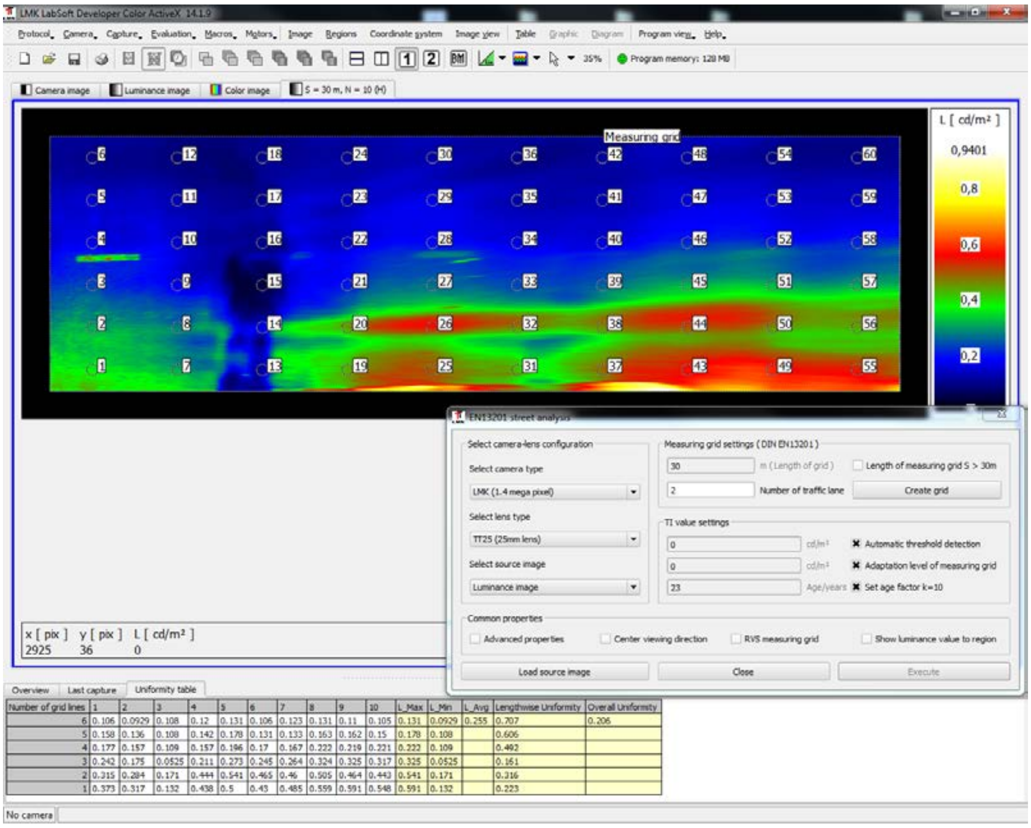

Figure 2 – Ortho-view image of road luminance after processing a rectification algorithm

4.3 Aspects of programming the TI calculation tool considering EN 13201-3:2003

The CIE Stiles-Holladay equation is used to describe the veiling luminance. Glare angles lower than 2° or higher than 30° are seldom in practice [5]:

$$L_{veil.} = k \cdot \frac{E_{vert.(source)}}{\vartheta^2_{source}} \tag{1}$$

where:

L_{veil}	is the equivalent veiling luminance (cd/m^2);
E_{vert}	is the illuminance on a vertical plane of the observer's eye (lx);
ϑ_{source}	is the glare angle (degree);
k	is the age of the observer and equals to constant 10 [2, 3].

Programming equation 1 as image processing function leads to an image. One changeable parameter of this formula is the glare angle ϑ_{source}. Inside the range of the ILMD's viewing angle (i. e. the measuring cone of the image), it is possible to change the applied viewing direction (see figure 3). The software algorithm considers them in a new image formula as shown in figure 4.

When using an ILMD, the vertical illuminance E_{vert} produced by a luminaire (glare source) can be obtained from the measured luminance L_{source} and the approximated glare angle ϑ_{source}. The calculation can be done pixelwise or by averaging both values for the relevant pixel.

$$E_{vert} = \sum_{i,j} L_{(i;j)} \cdot \Delta\Omega_{(i;j)} \cdot \cos\vartheta_{(i;j)} \quad , for \ \forall(i;j) \in source \tag{2}$$

where:

E_{vert}	is the illuminance on a vertical plane of the observer's eye (lx);
$L_{(i;j)}$	is the pixelwise luminance of parts of the glare source (cd/m^2);
$\Omega_{(i;j)}$	is the pixelwise solid angle of the glare source (sr);
ϑ_{source}	is the glare angle (degree).

A simplified model is based on the pixelwise angular approximation of the glare angle ϑ_{source} and the solid angle Ω_{source} of a glare source. This does not depend on the positioning of the origin for the angular coordinates (as employed in the image). Thus, it is possible to obtain the glare angle ϑ_{source} from different perspective analysis on the source image. And so to investigate any possible changes to the observer's viewing directions.

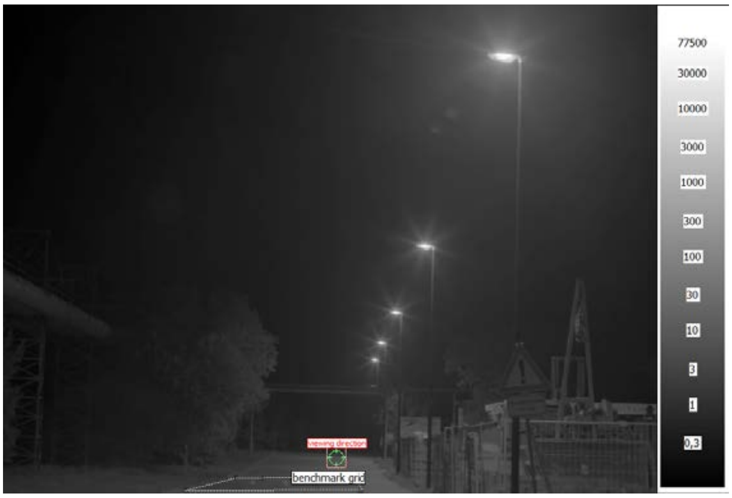

Figure 3 – Luminance image of road lighting installation showing a new defined viewing direction

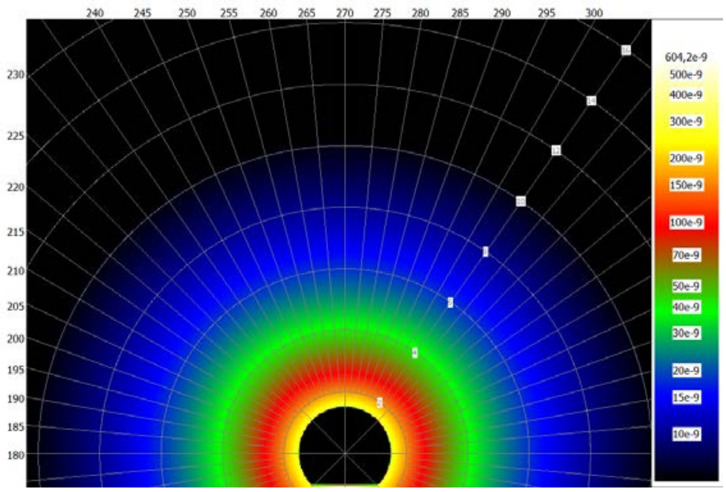

Figure 4 – Image formula for age-weighted Stiles-Holladay relation according to viewing conditions of fig. 3

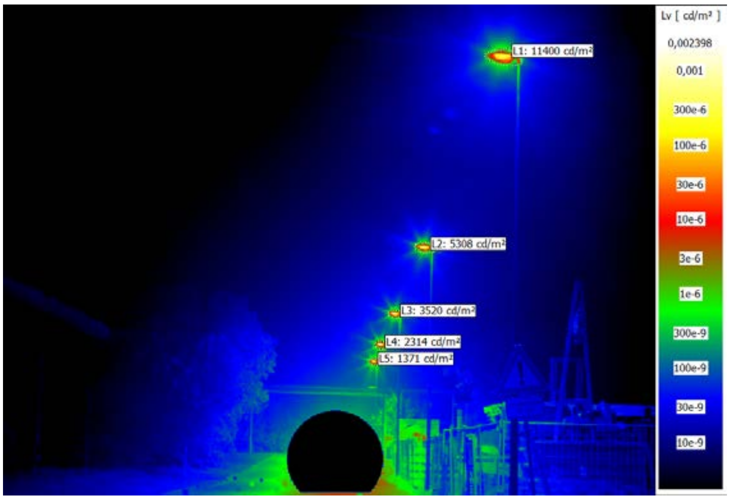

Figure 5 – Image of $L_{veil.}$ distribution (5 x log. scale) and average luminances of the detected glare sources

The result of equation 1 is presented in a product image that shows the L_{veil} pixelwise. For the integration of L_{veil} it is possible to apply the standard statistic to all pixels if classified as part of the glare source (see figure 5).

As a final step, the veiling luminance forms the equation for calculating the loss of visibility due to glare effects of road lighting installations [4]:

$$TI = \frac{65}{(L_{adapt.(roadsurface)})^{0,8}} \cdot L_{veil.} \tag{3}$$

where:

TI	is the relative threshold increment (%);
L_{veil}	is the equivalent veiling luminance (cd/m^2);
$L_{adapt(roadsurface)}$	is the average road luminance (cd/m²).

The result of equation 3 can be one integral value of TI or individual value for each glare source. If performing equation 3 as a pixelwise algorithm (each pixel presents one viewing direction), the result is a value of TI regarding the total image (see figure 6). This type of presentation gives an overview of the measurement of TI from a moving viewing direction.

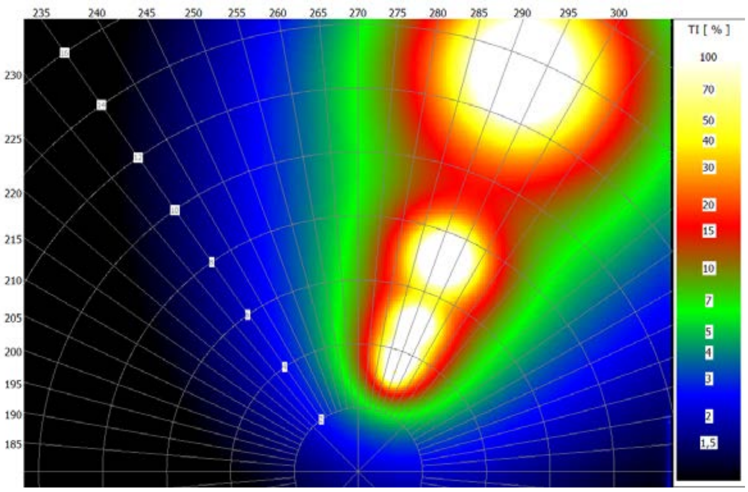

Figure 6 – Image of TI distribution (2 x log. scale)

5 Summary

It can be stated that the ILMD gives an efficient way of measuring TI and of validating any calculated glare data. Owing to the simple image processing methods, there are only a few limitations for integrating complex physiological equations into synthetic images. More advantages are for example: high aspect ratio of local contrast, highly perceptible non-uniformity, and high luminance gradient combined with its solid angle of the luminaire.

The measurement of the threshold increment can offer new opportunities for the development of glare free luminaires and can be used for the realisation of glare control road lighting installations according to relevant CIE and EN standards [6].

References

[1] CEN EN 13201-3:2003: Calculation of performance. German version. Berlin: DIN, 2003

[2] CEN EN 13201-4:2003: Methods of measuring lighting performance. German version. Berlin: DIN, 2003

[3] CIE 146:2002 (TC 1-50 report): CIE equations for disability glare. Vienna: CIE, 2002

[4] CIE xxx:2013 (Draft 2.0, Div. 2, TC 2-59): Characterization of Imaging Luminance Measurement Devices (ILMD). Vienna: CIE, 2013

[5] Narisada, K., Schreuder, D.: Light Pollution Handbook. ASSL Band 322, Dordrecht: Springer, 2004

[6] Walkling, A., Schierz, C.: Is it appropriate to launch additional light distributions in road lighting for wet conditions? LiTG conference „Town and outdoor lighting“, Weimar, 2014

OP29

KEY ASPECTS FOR PHOTOBIOLOGICAL SAFETY MEASUREMENT

Pan, J., Jin, S., Li, Q., Chen, C.
EVERFINE INSTITUTE OF OPTOELECTRONICS
everfine@everfine.net

Abstract

Photobiological safety for lamps and lamp systems has attracted much attention. The assessing conditions and measurement methods for photobiological safety are always complained to be too complex and ambiguous in practice in industry labs. In order to simplify the measurement method, the emission levels of the photobiological hazards for several typical types of general lighting service lamps and general heating service radiation sources are investigated. The measurement method and the required measurement equipment are discussed for different types of radiation sources.

Keywords: Photobiological Safety Measurement, Acceptable Measurement Uncertainty, Emission Limits

1 Introduction

Recently, photobiological safety for lamps and lamp systems has attracted much attention. A series of standards and technical reports[1,2,3] has been published. However, the assessing conditions and measurement methods for photobiological safety are always complained to be too complex and ambiguous in practice in industry laboratories.

In this paper, the hazard emission levels for several typical general lighting service (GLS) lamps and general heating service (GHS) radiation sources are listed according to the publications. The measurement method and the required measurement equipment are discussed for different types of lamps. For the source types whose emission levels can be higher than the emission limits of exempt group (RG0), the risk group could not be determined due to the measurement uncertainty when the emission levels are very close to the corresponding emission limits. In order to guarantee the source is allocated to the RG0 with a high credence (>95%), the safe emission levels assessed by the weighted irradiance or radiance for the hazard is suggested based on the typical testing capability. For the light sources whose emission levels are much below the RG0 limits, the acceptable measurement uncertainty (AMU) is calculated by the conformity assessment method.[4] Base on the calculated emission levels and AMUs, the assessment method and equipment could be simplified. Meanwhile, the paper discusses measurement equipment for the hazard assessment of the GLS lamps and GHS radiation sources. The hazard assessing conditions and measurement methods within the wavelength range of 2500 nm~3000 nm are specially concerned for the lack of spectral irradiance standards for national metrology institutes (NMIs) all over the world. A blackbody based method is introduced in this paper. The paper try to provide more evidences and clues for the right assessing conditions and measurement methods for photobiological safety classification for the lamps and lamp systems.

2 The hazard emission levels and AMU for the typical GLS and GHS sources

The quantities used to assess the emission levels, such as the effective hazard weighted irradiance and radiance are simulated for several types of typical GLS lamps and GHS radiation sources with different relative spectral distributions, including white-LED, halogen and incandescent lamp, gas-discharge lamp (GDL) and the GHS radiation sources. Hereinafter, the emission levels for each kind of light sources are denoted by a unique symbol as listed in Table1.

The relative spectrum of white-LED is simulated by a narrow Gauss blue light peak around 450 nm and a wide excited fluorescent powder Gauss peak around 570 nm. Halogen and incandescent lamps (HIL) can be approximately considered as graybody, therefore, their relative spectrum is calculated by the Planck equation. For the GDL, including high pressure mercury lamp (HPML) and sodium lamp (HPSL) as well as the metal halide lamp (MHL) and fluorescent lamp (FL), the representative experimental relative spectrum is measured by monochromator-based spectroradiometer, meanwhile, theoretical spectral curves are simulated by the characteristic peaks of the corresponding excited filling gas or metallic vapour in the lamp.

Table1 – The symbols used to denote the GLS lamps and GHS radiation sources

Category	Symbol	Light source
LED	●	White light-emitting diode
HIL	△	Halogen and incandescent lamp
GDL	▽	High pressure mercury lamp (HPML)
	●	High pressure sodium lamp (HPSL)
	★	Metal halide lamp (MHL)
	□	Fluorescent lamp (FL)
	◆	Xenon lamp
GHS	—□—	General heating service light sources such as quartz tube heater

2.1 Emission levels of GLS and GHS sources for each type of hazard

2.1.1 Emission levels of the UV hazard and UV-A hazard for the eye

The UV hazard and UV-A eye hazard emission levels of the considered light sources which are illustrated in Figure 1, are calculated by equation (1) and (2), where $S_{UV}(\lambda)$ is the ultraviolet hazard spectral weighting function.

$$E_s = \sum_{200}^{400} E(\lambda) S_{UV}(\lambda) \Delta\lambda \tag{1}$$

$$E_{UVA} = \sum_{315}^{400} E(\lambda) \Delta\lambda \tag{2}$$

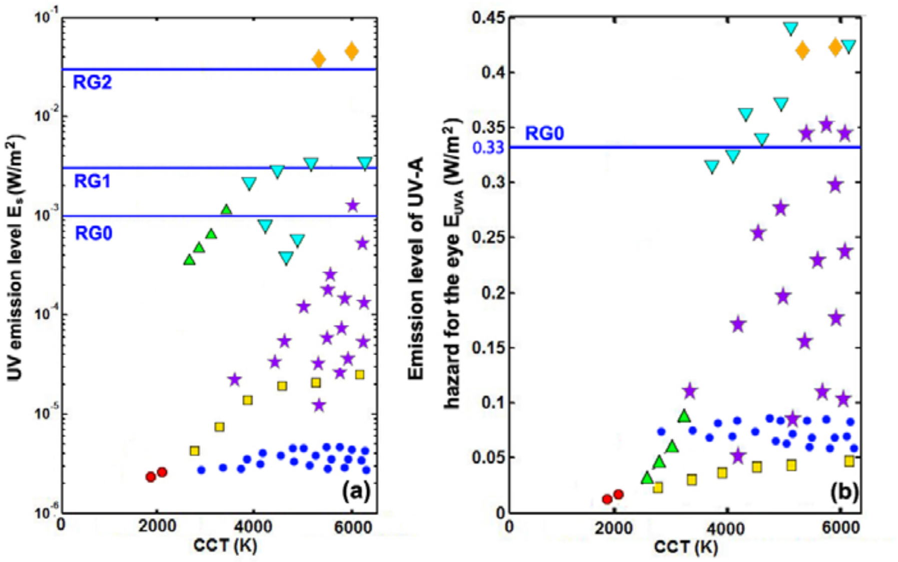

Figure1 –Emission level distribution of GLS and GHS sources for (a) the UV hazard and (b) the UV-A hazard for the eye

For the FL used in GLS, UV radiation below 300 nm which is generated by the excited mercury vapour is used to excite the fluorescent powder to emit visible light. Therefore, the FL has low UV hazard emission levels. According to Figure1 (a), the HPS, FL used in GLS have low emission levels of UV hazard, which are far below the emission limit of RG0, but the HIL, HPM and MHL have UV hazard emission levels near the RG0 emission limit. For HPM and MHL, the UV radiation absorption of the glass bulb has a great influence on the emission level assessment. The xenon lamp has strong UV emission, therefore, the emission level is beyond the emission limit of the risk group 2 (RG2).

For the UV-A hazard, special care should be taken for the MHL and HPM, since the emission level might be higher than the RG0 emission limit. The HPS, FL, HIL have low emission levels of UV-A hazard for the eye as shown in Figure1 (b).

2.1.2 Emission levels of the blue light hazard

Blue light hazard is the key issue for white-LED, by changing the position, intensity as well as the width of these two peaks, thousands of white-LED with different relative spectrum are investigated, the chromaticity coordinate distribution of the simulated white-LED covers most of the white region on the chromaticity diagram.

The emission levels are assessed at a distance where the source produces an illuminance of 500 lx but not less than 200 mm. [1] If the angular subtense α of the light source is larger than the angle of acceptance γ_B, the emission levels of the blue light hazard should be assessed by the radiance. Since the illuminance is fixed to 500 lx, the measured radiance will change with the size of the light source. In order to maximize the measured radiance, the light source size is set to the value that the angular subtense of the light source is equal to the angle of acceptance, the measured average radiance reaches the maximum of E_e/Ω, where E_e is the total irradiance at the measuring distance, Ω is the solid angle of acceptance. Figure 3(a) shows emission level of the blue light hazard for typical light sources with the correlated colour temperature (CCT) lower than 6500 K, which is assessed by the effective blue light weighted radiance:

$$L_B = \sum_{300}^{700} L(\lambda)B(\lambda)\Delta\lambda \,, \tag{3}$$

where $L(\lambda)$ is the spectral radiance that is averaged over the angle of acceptance, $B(\lambda)$ is the blue light hazard spectral weighting function. The emission level distribution of the white-LED is illustrated by blue dot in Figure3, which increases with the CCT. When the CCT is higher than 4450 K, the emission level might touch or cross the emission limit of RG0. For small light sources as shown in Figure 3(b), the emission level of the blue light hazard is assessed by the effective blue light weighted irradiance:

$$E_B = \sum_{300}^{700} E(\lambda)B(\lambda)\Delta\lambda \,, \tag{4}$$

where $E(\lambda)$ is the spectral irradiance determined with an angle of acceptance that is at least as large as γ_B. The emission level might touch or cross the emission limit of RG0 when the CCT is higher than 4400 K. Regardless of the white-LED, the emission level of other GLS lamps with CCT below 6500 K is all below the RG0 emission limit of the blue light hazard.

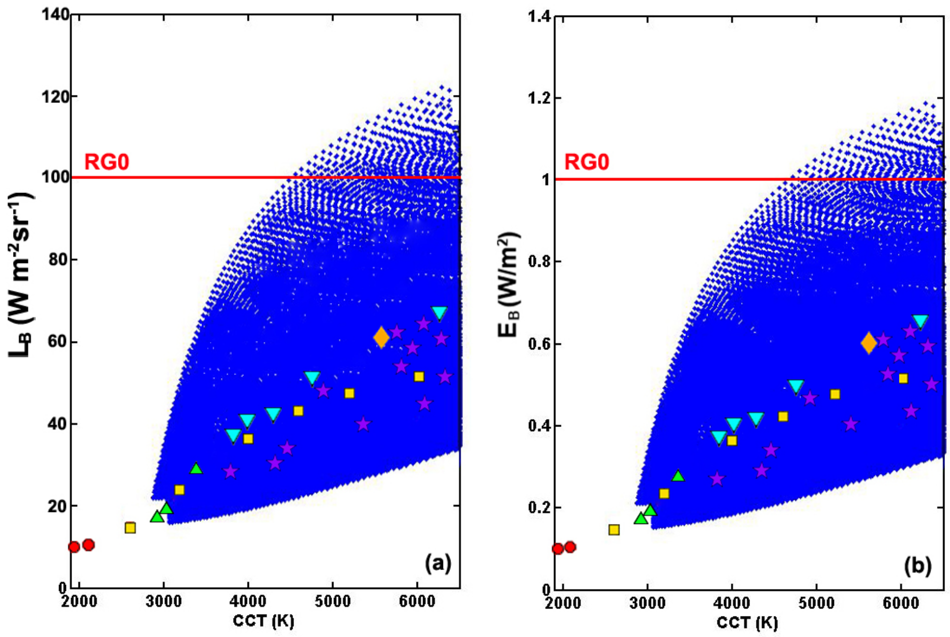

Figure 3 – Emission level of the blue light hazard for typical light sources assessed by (a) the weighted radiance L_B and (b) the weighted irradiance E_B

2.1.3 Emission levels of the retinal thermal hazard and weak visual stimulus

The retinal thermal hazard and the weak visual stimulus are assessed by the effective radiance L_R and L_{IR}, which are calculated by equation (5) and (6), respectively.

$$L_R = \sum_{300}^{1400} L(\lambda)R(\lambda)\Delta\lambda \tag{5}$$

$$L_{IR} = \sum_{780}^{1400} L(\lambda)R(\lambda)\Delta\lambda \,, \tag{6}$$

The emission limits of retinal thermal and weak visual stimulus hazard are inversely proportional to the angular subtense α, [1] which has a minimal value of 0.011 rad but does not exceed 0.1 rad. The lowest and the highest emission limits are calculated using the maximal and minimal α, respectively, as indicated by the red lines in Figure 4. Since the illuminance of the light source is fixed to 500 lx, in order to obtain the highest emission level for the light source, the spectral radiance $L(\lambda)$ is calculated by assuming the light source has the minimal angular subtense α.

Figure 4 (a) shows the maximal emission levels of the considered typical light sources for the retinal thermal hazard. All the considered light sources have low emission levels, which are one order of magnitude below the corresponding emission limits.

The weak visual stimulus is assessed only for the lamps emitting optical radiation in the infrared (780 nm~1400 nm) and whose maximum luminance averaged over a circular field-of-view subtending 0.011 rad is less than 10 cd/m^2. The radiation sources considered in the simulation which can get such a low luminance is only the blackbody with temperature below 1060 K. The luminance L and the weighted radiance L_{IR} of the blackbody versus the temperature is plot in Figure 4(b). When the temperature of the blackbody is 1059.5 K, the luminance equals to 10 cd/m^2, the weighted radiance L_{IR} is only 19.043 W·m^{-2}·sr^{-1}. The lowest emission limit of the weak visual stimulus calculated by the maximal α is 6×10^4 W/m^2. Even for the lowest emission limit, the calculated emission levels of the retinal thermal hazard and weak visual stimulus for all the GLS lamps considered in the simulation are far below the RG0 emission limits, which means the retinal thermal hazard and weak visual stimulus assessment does not have special requirement for the equipment for GLS lamps with the CCT below 6500 K and the GHS radiation sources.

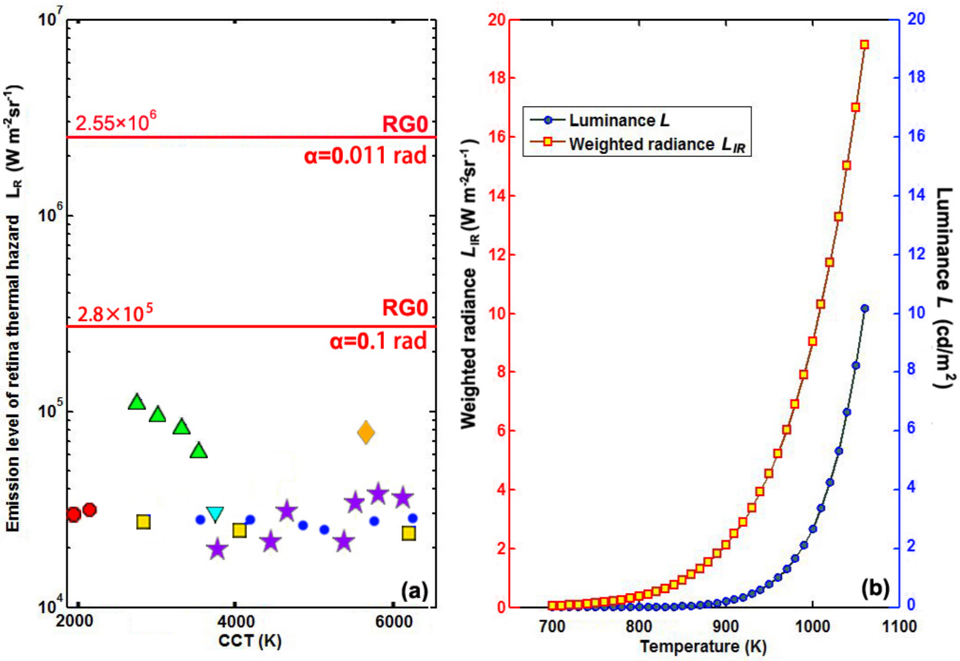

Figure 4 – The emission levels of the typical (a) GLS sources for the retinal thermal hazard and (b) GHS sources for weak visual stimulus

2.1.4 Emission levels of the infrared radiation hazard for the eye

The infrared radiation hazard for the eye is mainly caused by the GHS radiation source, which can be simulated by the low temperature blackbody. The radiance of the blackbody is only determined by the temperature; therefore, the integrated spectral irradiance used to assess the infrared radiation for the eye varies with the emission size of the blackbody. Figure 5 illustrates the emission level of the infrared radiation hazard for the eye, the blackbody considered in the simulation supposes to have square shape with side length 200 mm and 300 mm, respectively, the radiation temperature varies from 700 K to 1000 K. The emission level of the blackbody changes rapidly with the temperature since the radiation power of the blackbody is proportional to the fourth power of the temperature. By changing the size and temperature of the blackbody, the emission level can be higher than the RG0 and RG1 emission limits.

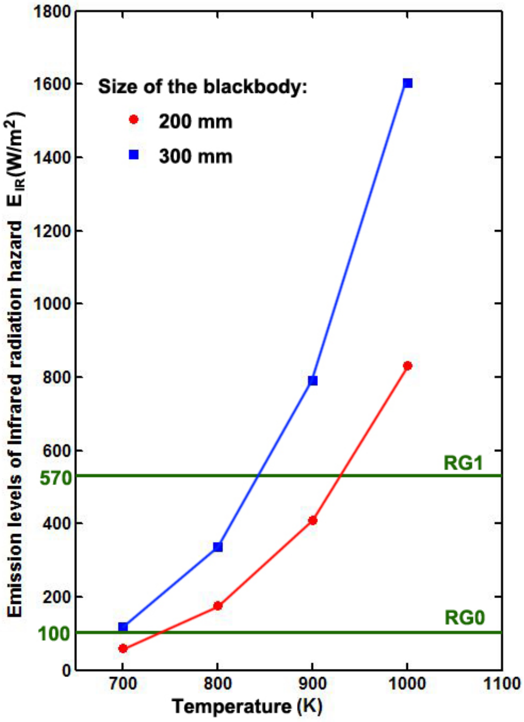

Figure 5 – The low temperature blackbody emission level of the infrared radiation hazard for the eye, which supposes to have square shape with side length 200 mm and 300 mm, respectively.

2.2 AMU for the GLS lamps for each type of hazard

According to the emission level of the GLS lamps and GHS radiation sources, we concluded that the hazard which should be carefully assessed is the UV hazard for HILs, HPMs and Xenon lamps, UV-A eye hazard for the MHLs and HPMs, the blue light hazard for the white-LEDs with the CCT higher than 4000 K and the eye hazard of the infrared radiation for the GHS radiation sources.

For the light source types with emission levels below the corresponding hazard emission limits of RG0, the AMUs for each kind of hazard is calculated by the conformity assessment based on the distances between highest emission levels and the corresponding emission limits, the guarded band is set to be $U=2u$. Assuming the measured emission level has a normal distribution around the calculated average value, the probability density function is a Gaussian function. When the absolute uncertainty u is less than half of the distance between the emission levels and the emission limits, the risk group can be determined by a conformance probability of 95%, which is considered as the AMU.

Table 2 lists the AMU of the light sources for different hazards, the symbol "×" denotes the corresponding hazard need not to assess for the light source; the AMU over 100% implies the emission level of the hazard is far below the RG0 emission limits, as a result, the hazard assessment does not have special requirement for the equipment.

Table 2 – the AMU of the light sources for different hazards

Light sources		AMU for each kind of hazard (k=2)					
		UV	UV-A	Blue light	Retinal thermal	Weak visual stimulus	Infrared radiation
LED	●	>100%	>100%	16% (CCT<4000K)	>100%	×	>100%
HIL	▲	-	>100%	>100%	>100%	×	>100%
GDL	▽	-	-	33%	>100%	×	>100%
	●	>100%	>100%	>100%	>100%	×	>100%
	★	-	-	53%	>100%	×	>100%
	□	>100%	>100%	80%	>100%	×	>100%
	◆	25%	22%	67%	>100%	×	>100%
GHL	—□—	>100%	>100%	>100%	>100%	>100%	-

The symbol "-" denotes there is no AMU for the corresponding hazard of the GLS or GHS source because the emission level can be very close to the RG0 emission limit. For this case, the emission levels should be assessed in high accuracy. The safe emission levels are proposed based on the measurement uncertainty of the typical testing capability and conformity assessment method for the high accuracy assessment. The GLS and GHS sources with the emission levels below the corresponding safe emission level is allocated to the exempt group with a high credence (>95%).

Table 3 lists the typical measurement uncertainty and the calculated safe emission levels assessed by the weighted irradiance or radiance for each kind of hazard in Table 3. The typical uncertainty is evaluated by the measurement system calibrated by the standard lamp of spectral irradiance which could be traceable to the national institute of standards and technology (NIST).

Table 3 – The typical measurement uncertainty and the safe emission levels

	UV	UV-A	Blue light		Infrared radiation
Band range (nm)	200~400	315~400	300~700		780~3000
Measured quantity	E_S	E_{UV}	L_B	E_B	E_{IR}
Typical uncertainty (k=2)	2.60%	1.92%	1.50%	1.38%	2.24%
Safe emission level L ($W \cdot m^{-2} \cdot sr^{-1}$) E (W/m^2)	9.74×10^{-4}	0.324	98.50	0.986	97.76

3 Instrument requirements and calibration

According to the emission level calculation in the previous section, some of the emission levels of a particular hazard for a specified GLS or GHS source is far below the corresponding emission limits, such as the retinal thermal hazard for all the GLS lamps and the UV hazard for the white-LED. But for the hazards of the GLS and GHS sources whose emission levels could be very close to the corresponding emission limits as indicated by "-" in Table 2, in order to determine the risk group of the source, the emission levels should be assessed in high accuracy.

3.1 Influence of the stray light

In order to determine the stray light influence on the photobiological safety measurement, we add stray light in the relative spectrum of light sources, and then calculate the emission levels for each kind of hazard. The stray light is simulated by adding a small background value to the relative spectrum. The stray light ratio is defined to be small background value which is considered as the stray light intensity over the peak value of the relative spectrum. The emission level change rate is calculated by equation (7).

$$R = \frac{\sum Q_{stray}(\lambda)W(\lambda)\Delta\lambda}{\sum Q(\lambda)W(\lambda)\Delta\lambda} \quad , \tag{7}$$

where $Q(\lambda)$ is the measured spectral quantity (radiance or irradiance of the light source), $Q_{stray}(\lambda)$ is the corresponding stray light intensity and $W(\lambda)$ is the spectral weighting function for a specified hazard.

The UV hazard assessment has a strict requirement for the stray light elimination due to the low emission limit (0.001 W/m^2). 0.01% stray light will enhance the emission level of UV hazard by over 10%, which significantly influence the risk group determination. For the visible and infrared band, the change rate of the emission levels caused by 0.1% stray light is less than 0.6% for all the considered GLS lamps.

3.2 Influence of the wavelength accuracy

The wavelength accuracy of the instrument used to determine the relative spectrum of a light source has a significant impact on the effective integrated spectral irradiance of the UV emission level due to the extreme change rate of the UV hazard weighting function $S_{UV}(\lambda)$. The influence of the wavelength accuracy in the photobiological safety measurement is studied by moving the relative spectrum of the light sources from origin by 0.5 nm. Table 4 lists the change rates of the emission levels for all kinds of hazard induced by the wavelength deviation. A 0.5 nm deviation can result in over 10% change rate for the UV hazard emission level, so wavelength accuracy plays an important role in the UV spectral band, 0.1 nm accuracy is recommended.

Table 4 – Change rates of the emission levels induced by 0.5 nm wavelength deviation

Light Source	UV	UV-A	Blue light	Retinal thermal	Infrared
LED	2.8%	1.4%	0.8%	0.01%	0.9%
HIL	3.7%	0.7%	0.3%	0.1%	0.3%
FL	9.4%	3.6%	0.3%	0.4%	0.8%
HPSL	7.8%	0.6%	0.01%	0.6%	0.9%
MHL	14.8%	1.6%	0.07%	0.04%	0.1%
HPM	11.7%	1.2%	0.5%	0.3%	0.4%

For other hazards in visible and infrared band range, the maximal change rate of the emission limits which is caused by 0.5 nm deviation is less than 1.0%.

According to the calculation results, the assessment of UV hazard sensitively depends on the stray light and wavelength accuracy due to the low emission limit value and sharp weighting function $S_{UV}(\lambda)$. It is necessary to use double-monochromator-based spectroradiometers or high accuracy array spectrometers to reduce the influence of stray light and wavelength accuracy. In most other measurement, monochromator-based spectroradiometers or array spectroradiometers are enough to ensure the validity of the assessment results. White LEDs do not emit UV and infrared radiation, the array spectroradiometers or monochromator-based spectroradiometers can work well for the assessment of photobiological safety.

For the light sources with AMU of the hazard greater than 100% as listed in Table 2, it will be very easy to judge the hazard level of the lamps and lamp systems. The measurement can be very much simplified. A common array spectroradiometer with reasonable accuracy is enough for such kinds assessment.

3.3 Detector calibration in spectral range of 2500 nm~3000 nm

The calibration service for the spectral range of 200 nm~2500 nm is usually available in the NMIs. For the spectral range of 2500 nm~3000 nm, the detector calibration is difficult due to the lack of spectral irradiance standards for NMIs all over the world. A calibration method for the detector in 2500 nm~3000 nm is proposed base on blackbody. As shown in Figure 6, the blackbody is used as a standard.

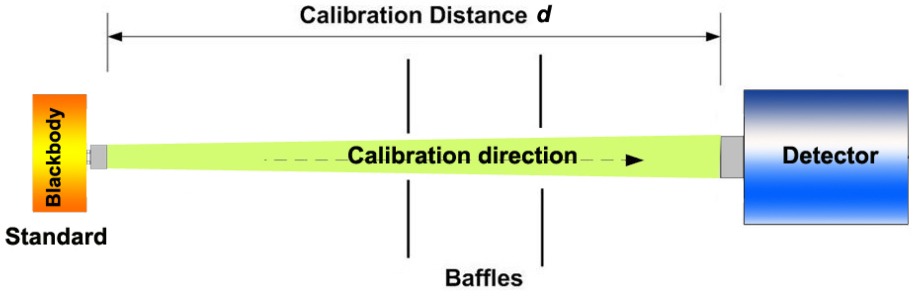

Figure 6 – The schematic diagram of calibration geometry

4 Conclusion

The hazard emission levels for several typical kinds of GLS and GHS sources are calculated and the acceptable measurement uncertainty is discussed. The simulation results indicate that UV and UV-A hazard of HIL, HPM and MHL, blue light hazard of white-LED with CCT higher than 4000 K and the infrared radiation hazard for the GHS radiation sources should be assessed in a high accuracy measurement condition. The safe emission levels for such hazards are suggested according to the typical testing capability. The AMU is calculated for the hazards whose emission levels are below the emission limits according to the conformity assessment .

Based on the calculation results of the emission levels and AMUs, the influence of stray light and wavelength accuracy is investigated. Because of the low emission limit value and sharp weighting function of the UV hazard, low stray light ratio and high wavelength accuracy are required; therefore, double-monochromator-based spectroradiometers or high accuracy array spectrometers are suggested in the assessment. For hazards with large AMU values, the measurement can be much simplified.

References

[1] 62471/CIE S009, Photobiological Safety of Lamps and Lamp Systems. Geneva: IEC.

[2] IEC/TR 62778, Application of IEC 62471 for the assessment of blue light hazard to light sources and luminaires. Geneva: IEC.

[3] ANSI/IESNA RP-27.2-00, Photobiological Safety for lamps and lamp systems- measurement systems. New York: IESNA.

[4] JCGM 106, Evaluation of measurement data – The role of measurement uncertainty in conformity assessment.

OP31

EXPERIMENTS ON HEALTHY LIGHTING AND THE TENTATIVE APPLICATION OF LEDS AT CHINESE ANTARCTIC STATIONS*

Luoxi Hao[1], Lin Yi[1], Zhe Cui[1], Junli Xu[1], Yaodong Chen[1], Kun Zeng[1]
[1] College of Architecture and Urban Planning Tongji University /Luminous Environment Lab,shanghai, CHINA
971558522@qq.com

Abstract

The Antarctica has significant scientific value in geology, oceanography, biology and many other fields. This has attracted the interest of the Chinese government's Antarctic expeditions. The health of the Antarctic expedition team is affected physically and mentally by the climate, the harsh environment and the special phenomena of polar day and night. Cooperating with the Polar Research Institute of China, this research on healthy lighting in Antarctica was carried out in the living quarters of the Great Wall Station, based on preliminary experiments conducted in Shanghai, which aimed at finding suitable LED spectral power distributions (SPDs) that may reduce negative emotions improve sleep quality and create a human-responsive environment. Some of the living quarter's luminaires were replaced with LEDs whose colour temperature and illumination are changeable. The research examined the non-visual biological effects of light, particularly on circadian rhythms. LED luminaires, suitable for polar conditions, were developed to improve sleep quality, regulate emotions and adjust psychology, so that work efficiency might be enhanced. Subjective questionnaires were used to assess the sleep quality of the station's staff. Saliva and urine samples were collected to determine melatonin levels, while activity cycles were monitored by actigraphy.

The conclusions of the research are: coloured light is indispensable in influencing emotion, mood and wellbeing in Antarctica, especially for the wintering team; and LED luminaires with changeable colour temperature and illumination are effective in the periods of polar day and night. Further research on the influence of light on melatonin is still in progress.

Keywords: Healthy Lighting, LEDs, Antarctica.

1 Introduction

Antarctica is the earth's southernmost and highest continent, situated in the Antarctic region of the southern hemisphere and is surrounded by the Southern Ocean. Antarctica is also the coldest and driest continent with, on average, about 98% ice cover. Its unique geographical, climate and ecological environment makes it a reproducible experimental site, of great scientific value. China has built four scientific stations in Antarctica (see Figure 1). The Great Wall Station is located at the southern tip of Fildes Peninsula of King George Island in the Shetland Islands of West Antarctica at 62˚12′59″S, 58˚57′52″W. It was the first Chinese Antarctic research station, opened in 1985, and is composed of 10

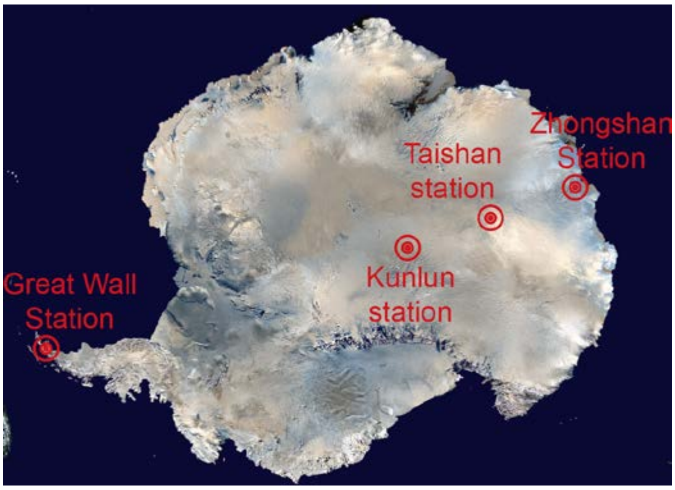

Fig1– Chinese Antarctic Research Stations

* Supported by National High Technology Research an
Supported by National Natural Science Foundation of China, Grant No.: 51178320

permanent buildings, including the Living

Table 1 –Average monthly Solar Duration at the Great Wall Station (1985﹣1994)

Month	Jan	Feb	Mar	Apr	May	Jun	Jul	Aug	Sep	Oct	Nov	Dec
Solar Duration(H)	74	64	38	23	17	5	14	20	49	61	60	74

Quarters and the Scientific Research, Weather, Recreation & Sports, Electric Power and Food buildings. In summer, it can support about 60 people conducting research with about 20 people during the winter.

With regard to Great Wall Station’s climate, the solar duration is changes dramatically through a year. As shown in Table 1, in January, the mid-summer month, the average solar duration is 74h/month but in mid-winter’s June, the average solar duration is only 5h/moth. This special light environment affects expedition teams physically and mentally, especially the wintering teams.

As Chinese Antarctic research work has increased, the harmful health effects of the harsh polar climate have gradually attracted the attention of the scientific community. Illnesses such as, “Winter Syndrome”, ”Antarctic T3 Syndrome” and "Seasonal Affective Disorder” plague expeditions’ staff. Stevens (2009) showed that these conditions have a certain correlation with circadian rhythm disorder, caused by the polar light environment (polar day and night). In 2010, Luoxi Hao’s team from Tongji University researched “Polar Station Semiconductor Lighting Application And Optical Health”, with the support of National High Technology Research and Development Program of China (863 projects). The team carried out a series of experimental studies on healthy lighting and non-visual biological effects at the Great Wall Station, for the very first time in China. This study had two stages: 1) The preliminary theoretical study conducted in Shanghai aimed at finding the suitable LED SPDs; and 2) The experimental study and the tentative application of LEDs at the Great Wall Station.

After the preliminary study, the following conclusions were drawn: 1) Figure 2 shows the Inhibition rate of the melatonin level under the stimulation of coloured light with different wavelengths. The 485nm blue light showed the highest inhibition rate. 2) Figure 3 shows that the melatonin inhibition rate for white light of different colour temperatures and illuminances. The white light with highest colour temperature and illuminance produced the highest inhibition. Based on these conclusions and some useful experiences from the preliminary study, Professor Hao went to Antarctica, as a member of the China 29th Antarctic expedition team, to complete Stage 2 and as the person in charge of the 863 projects. Stage 2 aimed at exploring healthy lighting strategies suitable for the polar environment using LEDs and which could reduce negative emotions, improve sleep quality and release the expedition staff from the physical and mental diseases caused by polar light environment.

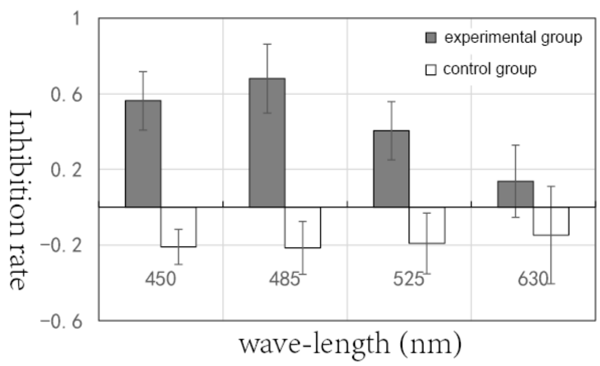

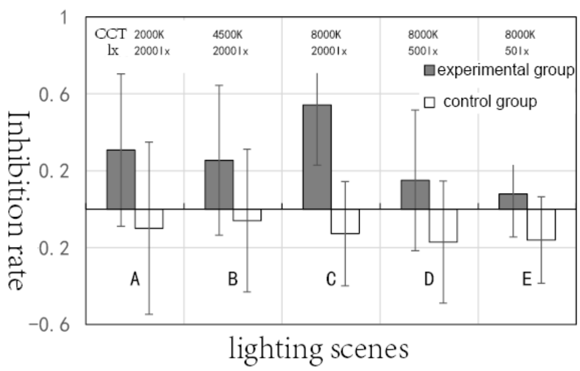

Figure 2–Inhibition rate of coloured light.

Figure 3–Inhibition rate of white light.

Figure 4–Outdoor luminances.

Figure 5–Indoor luminances.

Figure 6–Photographs of some of the living quarter's rooms.

2 Survey

2.1 Light environment survey

This survey collected outdoor and indoor luminances at the Great Wall Station. Figure 4 shows that the outdoor luminances are very high, with the sky reaching 6490cd/m2. The glare is not only high but there is high uv content in both the direct and reflected skylight. Figure 5 shows the surface luminances in a typical dorm room. The window luminance of 8750 cd/m2 is 200 times that of the peripheral walls, producing dramatic brightness contrast and low visual comfort for the occupants. Figure 6 shows a dorm room, meeting room, corridor and restaurant; most of the electric lighting is cool white from compact or linear fluorescent lamps, some of which have no optical control for minimising glare.

2.2 Subjective survey

Twenty male expedition members (age: 25-55) completed a questionnaire, seeking their subjective feelings regarding the living quarters' existing lighting environment. Figure 7 shows the results of the data analysis. Regarding preferred colour temperature, 42.86% of the subjects chose warm white light, 42.86% chose warm yellow light with only 4.76% choosing cold white light. Figure 8 is the pie chart of the subjects, feelings towards the dorm room's lighting environment. Except for the subjects who chose "no comments", all the others thought the lighting was too cold. Figure 9 shows subjects' satisfaction with the living quarters' lighting. Most of the subjects who responded were dissatisfied with the lighting.

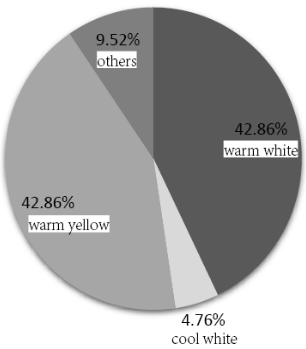

Figure 7–Preferred colour appearance.

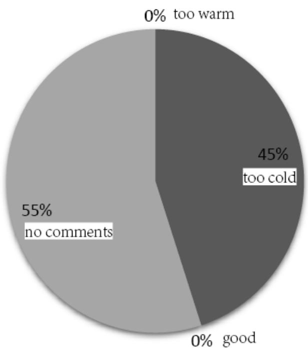

Figure 8–Subjective colour appearance.

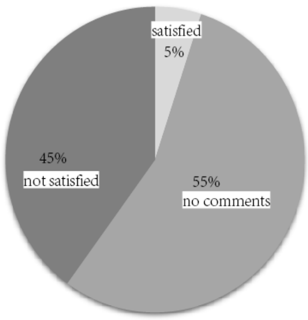

Figure 9–Lighting satisfaction.

Fig10–Photos of The Experimental Lamp

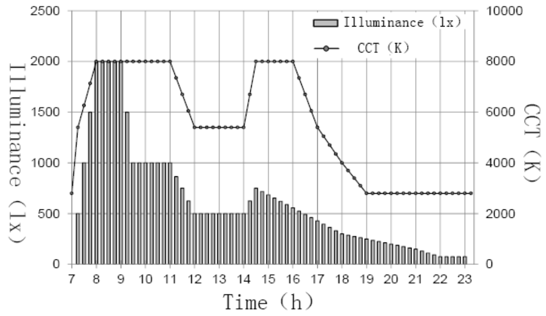

Fig11–Change Curve Of CCT and Illuminance

3 Great Wall Station Experiment

As mentioned above, an experimental luminaire was developed in Shanghai for testing at the Station. The existing luminaires in the experimental rooms were replaced with these luminaires. Saliva and urine samples were collected, activity cycles were monitored using actigraphy and questionnaires were used to examine the non-visual biological effects of lighting.

3.1 Subjects selection

This experiment selected six healthy male subjects from the Antarctic expedition team, with an average age 41±10 years, and occupations including economics, clinical medicine, land management and vehicle maintenance.

3.2 Experimental luminaires

The experimental LED luminaires (Figure 10) allow in colour temperature and illumination to be varied. Figure 11 shows how these are varied over a day, simulating the 24 hours change of sunlight. The experimental luminaires are ceiling-mounted, 520mm in diameter and 48mm deep. They produce about 5000lm. Desk-top lluminances range from 500lx to 2000lx, and colour temperature ranges from 2800K to 8000K.

3.3 Experimental set-up

The six subjects' three dormitory rooms were fitted with the new luminaires and became the experimental sites. Table 2 shows the other rooms in the living quarters that had LED lamps retrofitted into existing luminaires.

Table 2 - Replacement luminaires and retrofitted lamps

Rooms	Existing Light Source	Experimental Light Source
Dorm Rooms	TL-D/36W/765 YZ36RR26/36WW	20W TLED 1200lm T8 4000K
Restaurant	ES-14W/220V.WW/E27 YPZ220/15W-3U /E27 YZ30RR25/30W	My Vision 9.5W-60W Bulb, 2700K A55 Master LED 12W-60W Prince 2700K A60
Kitchen	18W/CFL 45W/CFL	17W- 75W Prince Bulb, 2700K
Meeting Room	40W/Fluorescent	20W TLED 1200lm T8 4000K
Corridor	18W/CFL	My Vision 9.5W-60W Bulb, 2700K A55 Master LED 12W-60W Prince 2700K A60
Toilet	ES-11W/220V.CDL/E27 YPZ220/15-3U-RR-D/E27	My Vision 9.5W-60W Bulb, 2700K A55 Master LED 12W-60W Prince 2700K A60W
Lobby	40W/Fluorescent	20W TLED 1200lm T8 6500K

3.4 Experimental procedure

The experiment was divided into two phases. The first phase, lasting two weeks, was the period before the luminaire replacement and was used evaluate of the existing lighting conditions. The experimental procedure was:

1) for the first 10 days, distribute sleep diaries at 7:00 am (activity logs at 22:30) and collect the previous day's sleep diaries (activity logs);

2) for days 11-14, in addition to the distribution and collection of sleep diaries and activity logs, urine samples were collected at 6:30 and saliva samples at 6:30, 12:00, 16:00, 20:00, 21:00, and 22:00; and

3) on the 14th day, the subjects completed a questionnaire, evaluating the lighting environment of their dorm rooms.

The second phase of the experiment occurred after the luminaire replacement. The experimental lighting condition was evaluated over a two-week period using the same procedure as that of the first phase.

4 Discussion

This experiment collected the following data:

Firstly, the subjects' activity cycles were monitored using actigraphy, however, due to the strong polar magnetic field, the batteries of the six actigraphs flattened after only one week's use, resulting in interrupted data collection. Figure 12 shows the only complete actigraph and it gives a clue that experimental lighting condition improved the sleep quality of the subjects; because the sample was only one, it is not possible to make a stronger inference.

Secondly, the subjects' melatonin levels will be determined from the saliva and urine samples that, at the time of writing, are still at the Great Wall Station, due to the complicated procedure for sending goods back to China. It is expected that the samples will be sent back with the 30th expedition team at the end of 2014.

Lastly, the questionnaires and sleep diaries were used to assess the sleep quality of the station's staff. Both showed that the subjects had positive psychological feelings during the second phase of the experiment.

Based on the results of this experiment and those of the preliminary study, the conclusions of this research are: coloured light is indispensable in influencing emotion, mood and wellbeing in Antarctica, especially for the wintering team; and that LED luminaires with changeable colour temperature and luminance are effective in the periods of polar day and night. Further research on the influence of light on melatonin levels is still in progress.

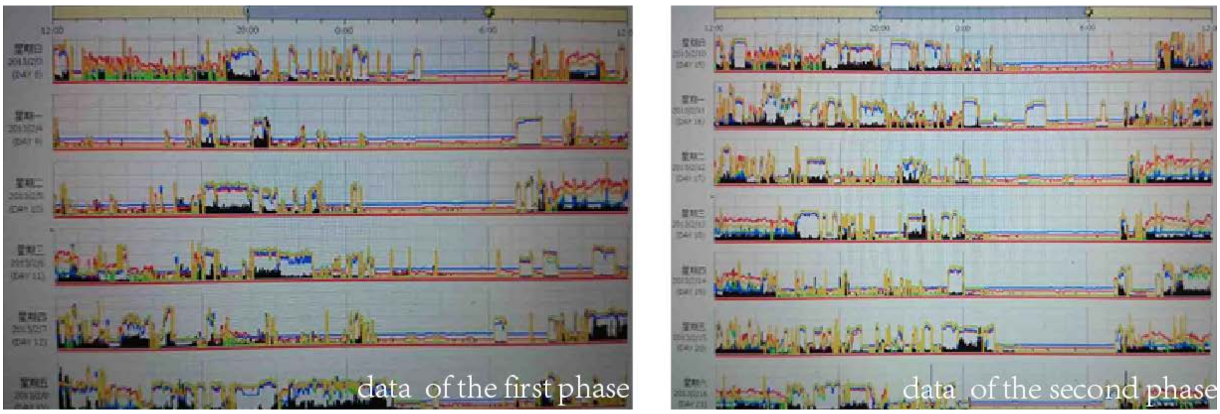

Figure 12– Photo of Actigraphy Data

References

Bian Lingen,Lu Longhua,Lu Changgui, Xue Zhengfu,Jia Penqun,Wang Yong.1998. A Study of Rad Lative Features at the Greatwall and Zhongshan Stations of Antarctica. Quarterly Journal of Applied IED Meteorology. Vol. 9, No. 2, 160-168.

Stevens,R.G. 2009.Light-at-night,Circadian disruption and breast cancer: Assessment of existing evidence. Int.J.Epidemiol.

I.M.McIntyre,T.R.Norman,G.D.Burrows,S.M.Armstrong. 1989. Human melatonin response to light at different times of the night,Psychoneuroendocrinology,14(3),187-193.

Czeisler, C.A., Duffy, J.F., Shanahan, T.L., Brown, E.N., Mitchell, J.F., Rimmer, D.W., Ronda, J.M., Silva, E.J., Allan, J.S., Emens, J.S., Dijk, D.J., Kronauer, R.E. 1999. Stability, precision and near-24-hour period of the human circadian pacemaker. Science, 284(5423), 2177-2181.

郝洛西、崔哲.2014.《昼夜节律生理机制及最新国际研究动态综述》

戸田直宏, 野口公喜.2011.実生活を想定した光暴露条件による夜間メラトニン分泌抑制効果, 日本生理人類学会誌, Vol.16, No.1, pp.39-42.

杉田義郎 1984.睡眠相前進および睡眠相後退症候群. 日本睡眠学会（編）, 生体リズムの発見機構, 理工学社, pp107-118.

日本睡眠学会(编).2009.睡眠学, 朝倉書店, pp165.

OP32

ECO LIGHTING DESIGN PROCESS

Säter, M.
Chalmers Technical University
Department of Architecture Gothenburg SWEDEN

Abstract

This paper is concerned the eco lighting design process (ECO-LDP) developed within a post doc project and aimed for the non urban outdoor environment. The goal for the use of the ECO-LDP is to design applications that handle both direct and indirect negative effects of the use of outdoor lighting in an environmental friendly way. Friendly not only by the limited consumption of electricity for the lighting but also because of the use of well chosen luminaries, an appropriate spectral profile of the light source, by the restricted time when the luminaries are lit and because of the use of low levels of light. An increased number of articles are written about disturbances seen in nature and related to the use of artificially emitted photon flows. Humans need lighting to experience quality of life and to be efficient and secure in the outdoor environment. But we are not alone on the planet. For animals, plants and ecosystems that need the dark night is the use of outdoor lighting a burden and can be a threat. The contradicting needs of a lit environment for humans and a dark night for humans, animals, plants and ecosystem need to be balanced together and a secure use of outdoor lighting be pointed out. Methods used for the development of the ECO-LDP is a combination of literature review and an analyze of the process of lighting design performed in a Thesis [Säter 2012] and within a post doc. project (Säter 2014). The use of the ECO-LDP have the possibility to contribute to a protection of humans, animals, plants and ecosystems from direct and indirect negative effects from the use of artificially emitted photon flows spread in nature.

Keywords: Eco lighting design process; Environmentally friendly lighting

1 Introduction

In the post doc study was the energy saving lighting design process (E-LDP) and the eco lighting design process (ECO-LDP) developed during the beginning of the project. Based on E-LDP was a lighting application installed and followed during a year. Data were analyzed and combined with the result from a literature review. When data from the study was evaluated, the result was compared to other models for lighting design. The models were used theoretically in the same daylight as measured during the year. Energy use for the year was theoretically calculated. It was evaluated if goals about a pleasant space, support for the user psychologically, physiologically and visually (PPV) and energy efficiency where fulfilled or not. The E-LDP was intended for the indoor environment and the urban outdoor environment. The ECO-LDP where developed to be used in the non urban environment.

1.1 The importance of electromagnetic radiation

We live in the great photon flow from the sun. This gives (among many other things) support for visual orientation, for diurnal rhythm and produces through plants oxygen and food. An increasing use of outdoor lighting can be seen all over the planet. The emitted man made photon flow differs from the one that can be seen in daylight when it comes to spectral composition, light distribution and level of light. The by humans used complementary lighting are seldom designed in a way that follows to the rhythm of daylight. The more the manmade and the natural emitted photon flow diverge, the more the use of outdoor lighting will be a threat to nature and by that to us. The need for light-related quality of life and a safe visual orientation for humans in the outdoor environment need to be balanced towards the need of humans, animals, plants and ecosystems for darkness at night. If the need for light at night and at the same time for darkness in nature is met through a well functioning lighting application designed in a way that when used creates low risk for negative effects, this will be light- related quality of life for humans in the long run.

1.2 The climate crisis

The climate crisis is a point of no return. Once and for all need outdoor lighting be designed in

the non urban areas of the world, in a way that gives little harm to nature. Urbanized areas need in the same way be more environmental friendly and outdoor lightning in both non urban and urban areas be more carefully designed and be more restricted in use.

2 Methods

2.1 The development of the project

Phase 1.The development of the process of lighting design for energy efficiency (E-LDP) and the eco lighting design process (ECO-LDP).

Phase 2. Literature review.

Phase 3.The development of the lighting application.

Phase 4. The analysis of the way the daylight appeared during the year. The evaluation of when and where, use the three part system of the installed lighting application. Measurement of the ambient light for 23 occasions in-between 8.00 a.m. - 19.00 p.m. during the year.

Phase 5. Analyse of data from the study.

Phase 6. Criteria´s for the control of the lighting application where developed.

Phase 7. The future more advanced application was described. E-LDP and ECO-LDP was further developed.

Phase 8. The way the lighting was used was analyzed and values (relation between outdoor and indoor level of light) for when to lit and when to switch off the lighting were developed,

Phase 9. The impact from the use of the lighting design process for energy efficient lighting in reduction in energy use where estimated nationally and on a European level. (This will be published in a future article).

2.2 Methods used

The method used were a literature review about methods of lighting design and reported disturbances in nature connected to the use of artificially emitted photon flows for lighting purposes.

3 Literature review

The literature review shows that the use of artificially emitted photon flows in nature is an increasing problem and a source of disturbance in nature.

“Ecologists have long studied the critical role of natural light in regulating species interactions, but, with

limited exceptions, have not investigated the consequences of artificial night lighting. In the past century,

the extent and intensity of artificial night lighting has increased such that it has substantial effects on the biology and ecology of species in the wild.”[Longcore & Rich 2004]

“Humans have now so altered the natural patterns of light and dark that these new conditions must be afforded amore central role in research on species and ecosystems beyond the instances that leave carcasses on the ground” [Longcore & Rich 2004]

"The first global assessment of amphibians provides new context for the well-publicized phenomenon of amphibian declines. Amphibians are more threatened and are declining more rapidly than either birds or mammals." [Stuart et al. 2004]

"As many other manmade changes in the environment are light pollution a risk for the biological diversity" [Holmstrand 2012].

The disturbances induced by emitted photon flows from the use of outdoor lighting that can be seen described in literature, is severe. The problems indicates that methods for lighting design need to be developed that in a careful way design lighting applications with reduced negative impact.

3.1 The basic lighting design process (LDP) developed at the JTH

Common knowledge in lighting design: During 12 years of education at Jonkoping University in Sweden was the basic lighting design process developed and used in every type of project. The basic process with 4 steps concerning the space, the user, the design of daylight and the complementary electrical lighting and the technical part of the lighting application, can be used in general for all types of applications. The basic LDP can be optimized with the ambition to fulfill goals of different kinds. By research in the process of lighting design can important goals be identified and the working moments be identified that need to be performed in order to fulfil the specified goals. The identified process can be used in order to in a better way fulfill goals set out on lighting in society. Ecological lighting is one of these important goals.

3.2 Goals for the ECO-LDP concerning direct effects

- Limited disturbance of humans living in the specific area
- Limited disturbance of animals living in the specific area
- Low impact on the growth of plants in the area
- Limited light-related attraction of animals from light sources and luminaries.

3.2.1 Goals for the ECO-LDP concerning indirect effects

- Limited use of energy and by that limited negative effects on nature

3.3 The ECO-LDP

ECO-LDP for non urban areas

ECO-LDP Introduction to the design. Theory as a start into the process: If animals, plants and ecosystems in the area nearby the lighting application are threatened and declining in number is controlled. If animals or plants have developed known sensitivity to specific wavelengths in daylight is investigated. Examples of how to avoid direct and indirect negative effects of the use of outdoor lighting.

ECOLDP Step 1, the space

- Evaluation at the specific space about in what way daylight and darkness appears, on a yearly basis.

ECOLDP Step 2, the user

- What are the needs in level of light, timing and duration, for a complementary electrical lighting for humans at the specific place?
- What are the needs of daylight and darkness for animals, plants and ecosystems?
- What kind of sensitivity or super sensitivity is developed among animals and plants in the area?
- In what way can the outdoor lighting be designed to decrease light-related attraction of animals?

- In what way can the needs for lighting and darkness be balanced together in order to give a secure visual orientation for humans when needed and as much as possible dark night for animals and plants?

ECOLDP Step 3 the design of the synchronization of daylight and the complementary electrical lighting

- Design the emitted photon flow in a way that mimic daylight in spectral composition during the part of the day when in use.
- Design the emitted photon flow in a way that mimic daylight in rhythm
- Design the emitted photon flow in a way that mimics daylight in appearance at evening and night.
- Design of level of light close to moon light level as much as possible increase level when needed.
- Design the lighting in only a restricted part of the area to give a minimum of attraction to animals.
- Design a minimum of attraction from the light source and luminaries.

ECOLDP Step 4 the design of the lighting application

- Design the emitted photon flow according to the investigation done in step 1, 2 and 3.
- Design the practical application based on the information collected in step 1, 2 and 3.
- Use a light source that does not emit critical specific wavelengths that will disturb animals and plants in the area based on theory in to the project and information from the investigation in step 2.
- Use a control system that can dim the light emitted from the application to moon level and slowly increase when needed and then go back to moon level again and adapt close to the changes in lighting conditions during the year.
- Use luminaries that in a limited way attract animals.
- Use as little energy as possible.

Evaluation if goals are fulfilled or not, goals:

Direct effects

- Safe visual orientation when needed for humans
- Limited disturbance of humans living in the specific area
- Limited disturbance of animals living in the specific area
- Low impact on the growth of plants in the specific area
- Limited light-related attraction of animals from light sources and luminaries.

Indirect effects

- Limited use of energy and by that limited negative effects on nature

Evaluation ECO-LDP step 1

- Updated theory is used in the work with the process in step 1.
- The lighting application fit into the daylight and dark conditions at the space in a way that gives limited disturbances.

Evaluation ECOLDP step 2

- Updated theory is used in the work with the process in step 2.
- The humans using the area have when needed, a safe (lower than pleasant) visual orientation.

- Animals and plants have a limited disturbance of the dark night.

Evaluation ECOLDP step 3

- Updated theory is used in the work with the process in step 3.
- The design of the complementary lighting is done in a way that gives visual orientation to the humans but with a limited disturbance of animals and plants in the area.

Evaluation ECO LDP step 4

- Updated theory is used in the work with the process in step 4.
- The light source and additional equipment is used in order to design the emitted photon flow in a way that mimics daylight in spectral composition during the part of the day when in use.
- The light source and equipment is used in order to design the emitted photon flow in a way that mimics daylight in rhythm during the part of the day when in use.
- The light source and additional equipment is used in order to design the emitted photon flow in a way that mimics daylight in appearance at evening and night.
- The light source and additional equipment is used in order to design a level of light close to moon light level as much as possible and to increase the level of light when needed.
- The light source and additional equipment is used in a way that gives a minimum of light attraction to animals.
- The luminaries are chosen in a way that gives a minimum of light attraction.
- The system is energy efficient and has low direct negative effects on humans, animals and plants and low indirect negative effects on nature.

4 Discussion

4.1 Discussion of methods and results

4.1.1 Methods

When knowledge from the literature review in the post doc were put together, the need for a specific method for lighting design for non urban area was obvious. There are an increasing number of reports about disturbances caused by the use of outdoor lighting. This need to be handled in a positive and constructive way by lighting designers all over the world. Both direct and indirect effects need to be reduced. Contradictory needs of a pleasant lit space and the dark night for humans, animals, plants and ecosystems motivates a more careful lighting design. This careful lighting design have the possibility to reduce direct and indirect negative effects initiated by indoor and outdoor lighting and is a matter of a future more environmental friendly lighting. With this background is the work with a specific model for outdoor lighting in non urban areas, well motivated.

4.1.2 Measurements

Research in lighting science is often seen focused on detailed measurements of emitted photon flows. The researcher in lighting design needs to put this type of non visual and “frozen” data in an ever changing visual scenario. The interaction factors need to be described and the connections between them be evaluated . From this data can the way interaction factors can be put together in order to design an interaction that when used can be experienced as well- functioning. When using the ECO-LDP the world represent the interaction and the interaction factors differ from one part of the world to another. The interaction can be described and evaluated although in a rough and limited way, due to the large perspective.

4.2 Connect problems in a constructive way

The research in the project connects in a constructive way problems and methods to each other. Methods that if used can fulfill goals set out in society and by that decrease problems.

4.3 Discussion of results

Lighting Design and the work of the Lighting Designer is still in a high extent unknown in society today. The development of the ECO-LDP is only a matter of writing down common knowledge in lighting design. When theory into the process, the 4 steps of the process and the fulfillment of the goals set out for the process, is described, they can be better understood. This makes it easier for decision-takers in society to understand the problem according to outdoor lighting and to in the same way understand the potential of Lighting Design as a tool for a decrease of the problem.

5 Conclusion

5.1 A careful lighting design

A careful lighting design that reduces direct and indirect effects of the use of lighting is of a high importance. The development of the ECO-LDP put words on the work needed to get a reduction of the negative effects caused by the use of outdoor lighting.

5.2 Contradictory needs

Contradictory needs are common in the lighting designer’s everyday´s practice. When updated theory about the topic is used in the work with the lighting design, the complexity in the different needs of light and darkness will be better known. When examples of balancing these problems in a successful way are written down and added in to the initial theoretical part of the process, this will be useful for the work with lighting.

The ECO-LDP focuses in the first hand on the direct negative effects of the use of artificially emitted photon flows in nature. The process, if used, can decrease the problem with the conflict between human’s needs of safe visual orientation and the animals and plants need for a dark night outdoors. The use of ECO-LDP can at the same time reduce the indirect negative effects on nature from the production of energy used for outdoor lighting. The reduction will be achieved by fewer luminaries in use, when possible, a lower level of light and luminaries used for a shorter time. The ECO-LDP is a tool for a future better balance between humans need for outdoor lighting and of human’s animals and plants need for a dark night.

5.3 Future work

There is a need to go from an atomistic to a holistic approach to the use of outdoor lighting. When the visual approach to lighting design is increased to be visual and physiological approach criteria for lighting will be better functioning. If the user is seen not only as the human but the animal and the plants too, lighting will become more environmental friendly.

References

AUBRECHT, C., ELVIDG, C.D., ZISKIN, D., RODRIGUES, P., GIL. A. (2010). Observing stress of artificial night lighting on marine ecosystems - a remote sensing application study. ISPRS TC VII Symposium 38: 41-46.

BERSON, D.M., DUNN, E.A. ,TAKAO, M. 2001. Phototransduction by ganglion cells innervating the circadian pacemaker. *Invest Ophtalmol Vis Sci*, 42: S1 13. P. 1070-1073.

BUCHANAN, B.W. 2006. Observed and potential effects of artificial night lighting on anuran amphibians. I: Rich C, Longcore T (red). Ecological consequences of artificial night lighting, ss. 192-220. Island Press, Washington.

CHANG, A.M., SCHEER, F.A., CZEISLER, C.A. 2011. The human circadian system adapts to prior photic history 2011. Published online before print January10, 2011 doi: 10.1113/jphysiol.2010.201194 March 1,2011. The Journal of Physiology, 589,1095-1102.

KRISKA, G., MALIK, P. 2009. Polarized light pollution: a new kind of ecological photopollution. Frontiers in Ecology and the Environment 7: 317-325.

LONGCORE, T, RICH, C. 2004. Ecological light pollution. Frontiers in Ecology and the Environment 2:191-198LORNE, J.K., SALMON, M. 2007. Effects of exposure to artificial lighting on orientation of hatchling sea turtles on the beach and in the ocean. Endangered species research 3: 23-30

MOORE, MV, PIERCE, SM, WALSH, HM, KVALVIK, SK, LIM JD. (2000). Urban light pollution alters the dielvertical migration of Daphnia. Verh Internat Verein Limnol 27: 779-82.

OGDEN LE. 1996. Collision course: the hazards of lighted structures and windows to migrating birds. WWW-dokument 1996-09-01: http://digitalcommons.unl.edu/flap/3/.

PAULEY, S.M. 2004. Lighting for the circadian clock: resent research indicates that lighting has become a public health issue. Medical Hypotheses 63, 4 (2004)

PERRY, G, BUSCHANAN, BW, FISHER, R.N., SALMON, M. (2008). Effects of artificial night lighting on amphibians and reptiles in urban environments. I: Mitchell JC, Jung Brown RE,

RUTHERFORD, A. 2008. Mimicking photosynthesis, but just the best bits Nature [0028-0836] yr: 2008 vol: 453 iss: 7194 pg: 449 -449

SÄTER, M. 2012. Equilibrium. User Centred Lighting Design. Towards the development of a lighting design that is individually psychologically, physiologically and visually supportive. Department of Architecture. Chalmers University of Technology.

SÄTER, M. 2014. Model to an optimized energy efficiency in lighting applications offices and open-plan offices. Post doc project. Chalmers Publication Library (in Swedish)

TORINGTON, L., PARASCANDOLA,L., CUNNINGHAM,L. 1971. Visual and biologic aspects of an artificial sunlight illuminant. Journal of IES/October 1971.

VAN LANGEVELDE, F, ETTEA, J, DONNERS, M, Wallis DE VRIES, M.F., GROENENDIJK, D. (2011). Effect of spectral composition of artificial light on the attraction of moths. Biological Conservation 144:2274-2281.

OP33

COLOUR APPEARANCE OF MESOPIC RELATED COLOURS AT 0.3, 1, 3 AND 10 CD/M²: VISUAL MAGNITUDE ESTIMATION AND MODELLING

Peter Bodrogi[1], Diana Carella[1], Tran Quoc Khanh[1]
[1] Technische Universität Darmstadt, Darmstadt, GERMANY
bodrogi@lichttechnik.tu-darmstadt.de

Abstract

The aim of this paper is to describe a new experimental and modelling method to quantify colour appearance in the mesopic range. The experimental method uses binocular viewing and direct magnitude estimation with an absolute visual colourfulness scale recalled from memory. Modelling is based on a modification of CIECAM02 including rod signals to account for the decrease of colourfulness and lightness with decreasing luminance level and for hue changes. The transition point between the photopic range and the mesopic range where the unmodified CIECAM02 model is no more appropriate seems to occur (depending on hue) between 1 cd/m^2 and 10 cd/m^2. The refinement of mathematical modelling and a validation experiment with a chromatic visual lightness scale are currently underway.

Keywords: e.g. Colour Appearance, Mesopic, Related Colours, Modelling

1 Introduction

The quantification of colour appearance in the mesopic range has several important applications like the prediction of the visibility of weak signal lights, coloured object visibility and conspicuity in night-time city and traffic scenes, design of colour schemes of control room monitors and colour appearance optimization of HDTVs, home cinemas and 2D/3D cinema theatres. Several visual experiments were carried out in the past. Models predicting mesopic colour appearance were also built and analysed (FU et al, 2012; HUNT 1991, 1998; SHIN et al, 2004).

The present paper concentrates on the specific viewing condition of mesopic image or video presentations in dark rooms, e.g. digital home cinemas or cinema theatres. This viewing condition is specific in the sense that the mesopic colour stimuli appear as related colours perceived in the environment of many other colour stimuli and all stimuli are viewed with normal binocular viewing. Experiments found in literature, however, used either a haploscopic viewing technique or dealt with unrelated colours. Therefore, to meet the viewing condition of the above mentioned important application, a new experimental method with normal binocular viewing is presented in this paper. The method represents a combination of colour appearance magnitude estimation and scaling with an absolute colourfulness scale recalled from memory.

2 Method

Five colour stimuli were displayed on a very stable high-end LCD monitor on a grey background which provided the visual lightness anchor (lightness=60). This background took place inside a *peak white* frame which provided the luminance level. Observers had to assess only one stimulus, the one in the middle. The other four colour stimuli were intended as a relation to other colours to be somewhat similar to a typical image or video presentation. The monitor was in a completely dark room. Figure 1 illustrates the stimulus.

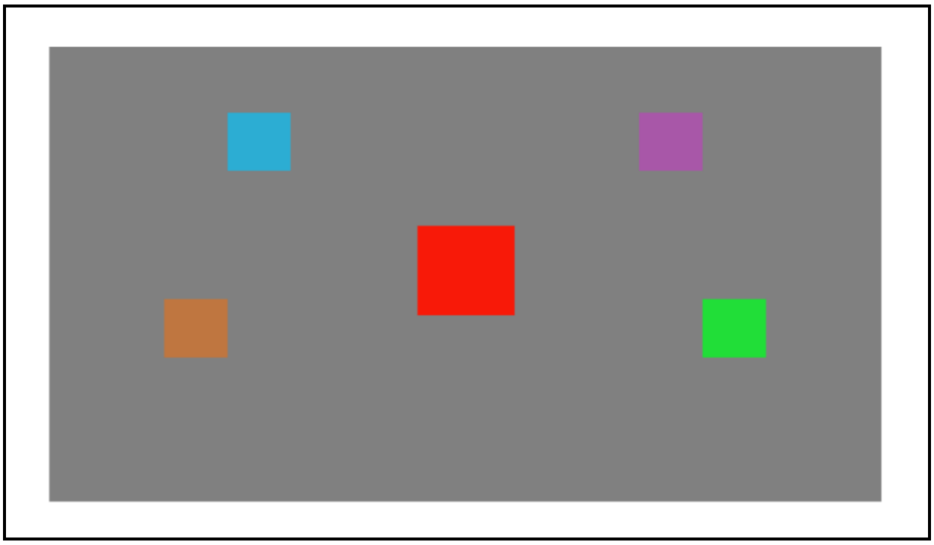

Figure 1 – Stimulus configuration of the experiment. Observers had to evaluate only the colour appearance of the middle colour patch subtending 4° (horizontal) and viewed from 60 cm

Observers had to estimate the magnitude of lightness i.e. its brightness related to the white or greyish-looking frame, between 0 and 100. Observers also had to assess the magnitude of colourfulness and hue composition (e.g. 10% red and 90% yellow) of the observed and visually scaled stimulus in the middle. 28 such colour stimuli appeared at the position of the middle colour patch in Figure 1, at 3 saturation levels and different lightnesses as well as white, grey and black patches as a control condition for scaling, see Figure 2. These 28 colour stimuli were scaled by 12 colour-normal observers (10 male, 2 female subjects) at a photopic luminance level and also at four different mesopic luminance levels.

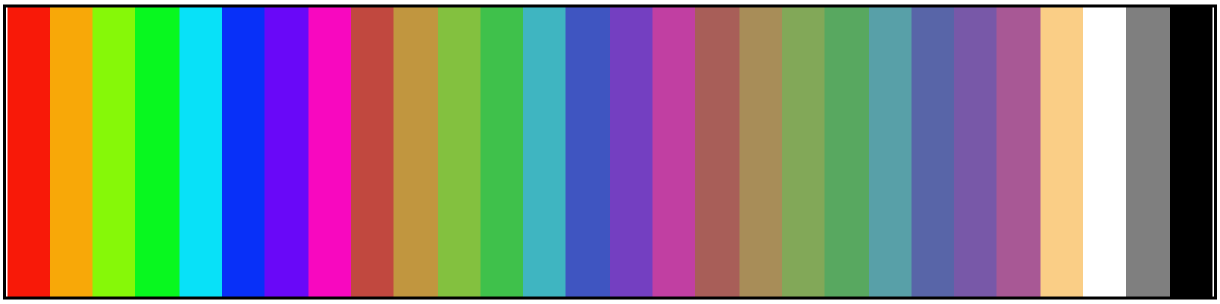

Figure 2 – Illustration of the 28 colour stimuli used as the colour stimulus of the middle colour patch (see Figure 1)

First, a photopic (270 cd/m^2) level was viewed. Observers were trained at this level until they gave stable scaling results and could establish their absolute internal colourfulness scale. Then the levels 0.3 cd/m^2, 1.0 cd/m^2, 3.0 cd/m^2, 10 cd/m^2 and 270 cd/m^2 were observed in a randomized order. The concepts of hue composition, lightness and colourfulness and the differences between saturation, chroma and colourfulness were explained and trained before the experiment to every subject carefully. Every observer judged every colour three times. Figure 3 illustrates all 5 stimulus configurations at a time.

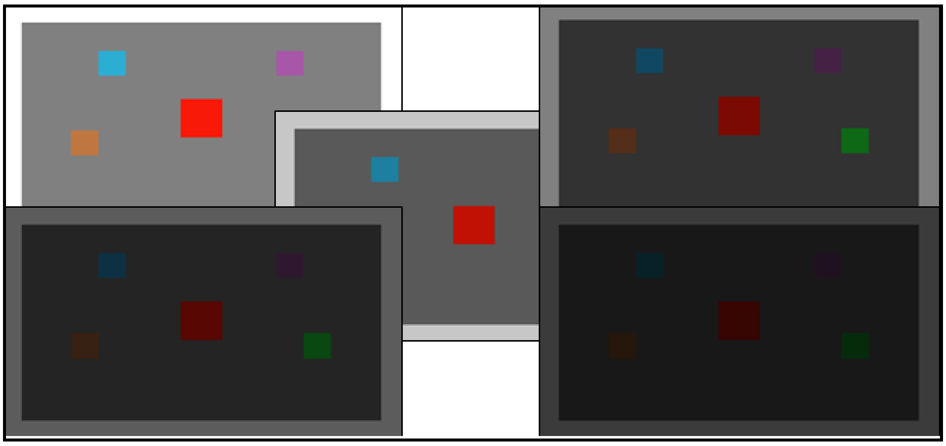

Figure 3 – Illustration of what observers saw and assessed at the 5 mesopic luminance levels. Note that 1. Only one luminance level (0.3 cd/m^2, 1.0 cd/m^2, 3.0 cd/m^2, 10 cd/m^2 or 270 cd/m^2) was observed at a time with binocular observation; 2. Every observer used his own absolute colourfulness scale (well established during the training sessions) across all luminance levels; 3. The "peak white" frame appeared grey at lower levels; 4. Neutral density (ND) filters were placed in front of the monitor to obtain the four non-photopic levels

Every observer had to adapt 20 minutes before testing. Neutral density filters were used in front of the monitor to go down to mesopic levels, see Figure 3. Hue, lightness and colourfulness were scaled by direct magnitude estimation with natural binocular viewing. There was no side-by-side comparison between different luminance levels. There was no haploscopic viewing with bipartite fields. At every mesopic level, the subject used his or her own absolute subjective colourfulness scale established in the photopic training phase: this is the memory scaling aspect of the present magnitude estimation method. There was no chromatic colourfulness reference stimulus but it was communicated that an achromatic colour has zero colourfulness. Every colour stimulus (5 levels x 28 stimuli) was measured spectrally in-situ by using a high-end newly calibrated spectroradiometer (CS2000A) which is reliable at lower luminance levels.

3 Result and discussion

In this paper, the answers of five subjects (1 female, 4 male) will be analysed at four levels, 0.3 cd/m^2, 1.0 cd/m^2, 10 cd/m^2 and 270 cd/m^2. These 5 subjects gave constant answers at all luminance levels. Their interpersonal variability was typically +-5% for scaled hue composition, +-10 for colourfulness and +-5 for scaled lightness. The visual colourfulness scales of these observers ranged typically between 0 and 100-140. Every individual colourfulness scale was rescaled to get an equal value to the CIECAM02 *M* value in average for all test colours at the photopic level. Then this rescaled visual colourfulness value was used for all luminance levels. Mean visually scaled hue composition results are depicted in Figure 4.

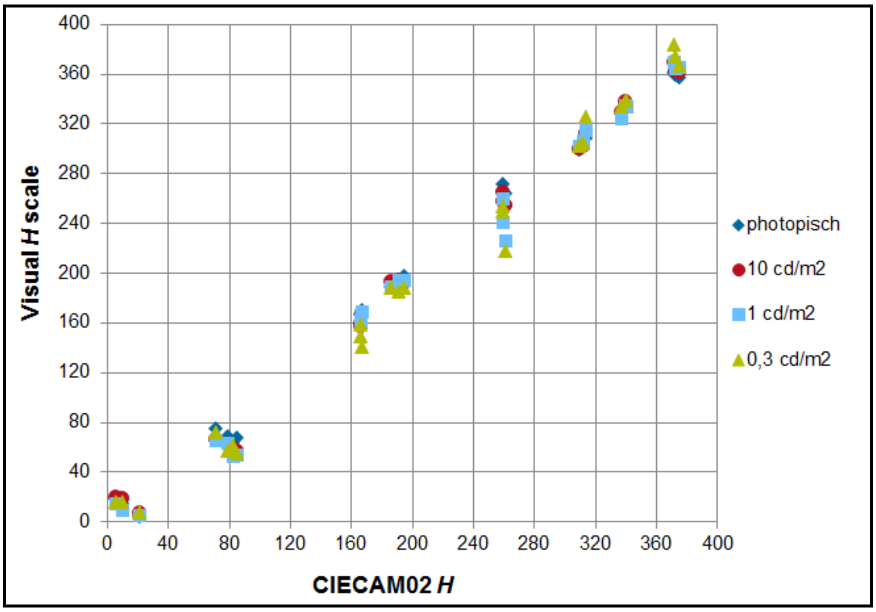

Figure 4 – Mean visually scaled hue composition results (5 observers x 3 repetitions) as a function of CIECAM02 *H* computed from in-situ measured spectral power distributions using the "dark" CIECAM02 condition and the L_A value corresponding to each level

As can be seen from Figure 4, compared to the photopic level, scaled hue composition revealed a significant change at 0.3 cd/m^2 and 1.0 cd/m^2 for bluish stimuli and for 0.3 cd/m^2 for greenish stimuli. Rescaled visual colourfulness is depicted in Figure 5.

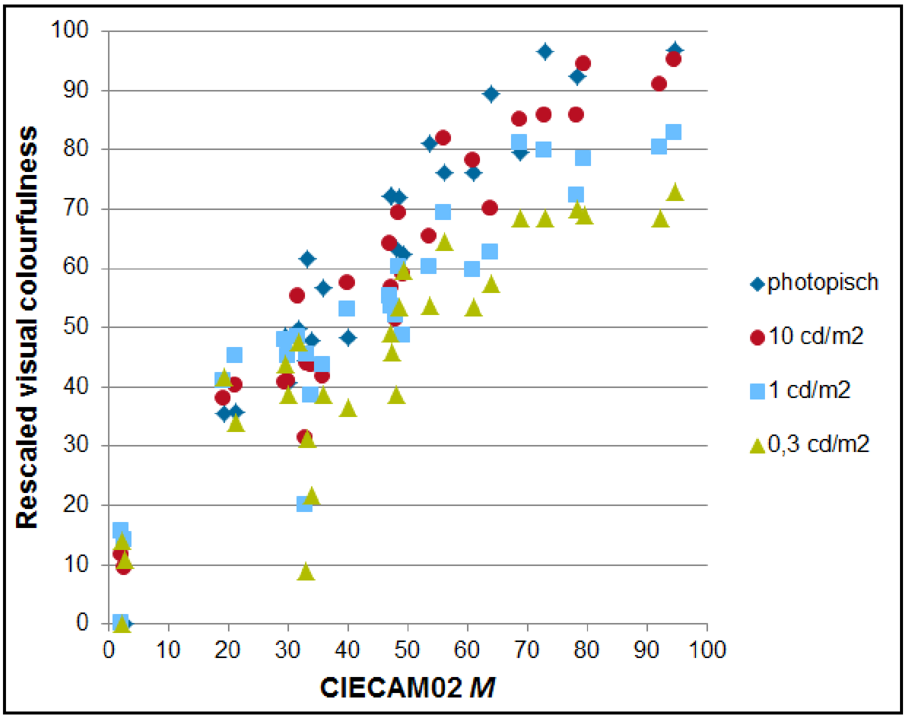

Figure 5 – Mean visually scaled colourfulness results (5 observers x 3 repetitions) as a function of CIECAM02 *M* (see the Caption to Figure 4)

As can be seen from Figure 5, rescaled visual colourfulness decreased with decreasing luminance level in a systematic but nonlinear manner. There was more decrease between 0.3 cd/m^2 and 1.0 cd/m^2 than between 1.0 cd/m^2 and 10 cd/m^2. A large deviation from the value of CIECAM02 *M* was found for the case of test colour No. 22 (unsaturated blue) which seemed to exhibit only very little colourfulness at low luminance levels. The tendency of visual mesopic lightness assessment can be seen from Figure 6.

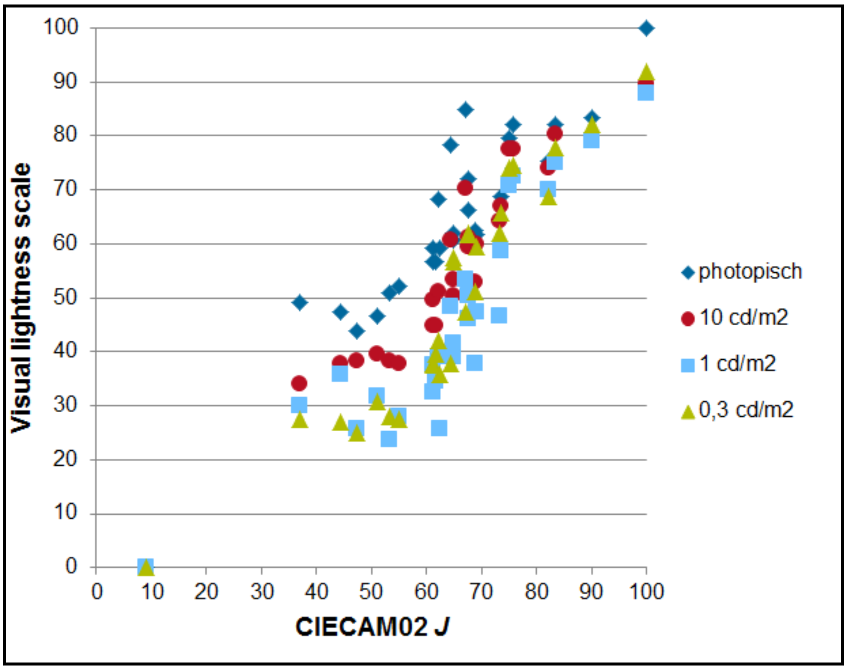

Figure 6 – Mean visually scaled lightness results (5 observers x 3 repetitions) as a function of CIECAM02 *J* (see the Caption to Figure 4)

As can be seen from Figure 6, for CIECAM02 J<60 and luminance levels lower than 10 cd/m^2, there was a significant reduction of visually scaled lightness compared to the visual photopic visual condition and to the prediction of CIECAM02 *J*. Due to the strong positive influence of saturation on lightness (Helmholtz-Kohlrausch effect), there is a large scatter of data points along the ordinate as the CIECAM02 *J* scale is virtually achromatic. In a subsequent validation experiment, not to be presented in this paper, lightness values greater than 100 were also allowed to account for this strong Helmholtz-Kohlrausch effect we experienced during lightness assessment, especially at the mesopic levels.

4 Mathematical modelling by modifying CIECAM02

As seen above, the mean answers of the subjects i.e. the average scaled values of hue, colourfulness (rescaled) and lightness were depicted as functions of the corresponding CIECAM02 correlates (*H*, *M*, *J*) by using the appropriate viewing condition parameters. It was also seen that, for mesopic levels, colourfulness was always less than predicted, in a nonlinear way. This effect was stronger for deep mesopic levels. A similar tendency was found for lightness. There were significant hue changes (between CIECAM02 prediction and visual scale values) at lower mesopic levels.

To model the above findings mathematically, two of the present authors (Bodrogi and Khanh) modified the CIECAM02 model to predict the experimentally obtained ratios J_{vis}/J and $M_{vis,resc}/M$ and differences H_{vis}-H where the index "vis" refers to a mean visual result, "resc" refers to rescaling the visual colourfulness scale and *H*, *M*, *J* represent the original CIECAM02 correlates. The modified CIECAM02 model has the following features:

- It is based on the workflow of the original model but it works with partially different parameters (e.g. exponents);
- The new *J* signal has become significantly chromatic;
- Depending on mesopic adaptation level, compressed rod signals now contribute to the *a*, *b*, *H*, *M* and *J* signals;
- 23 model parameters are varied within *plausible* ranges to get a good fit to mean visual results.

The model is currently in its development stage but a preliminary fitting result is shown in Figure 7 as an example. This preliminary result was obtained by optimizing the model parameters to obtain best fit to the mean result of 4 subjects (1 female and 3 male).

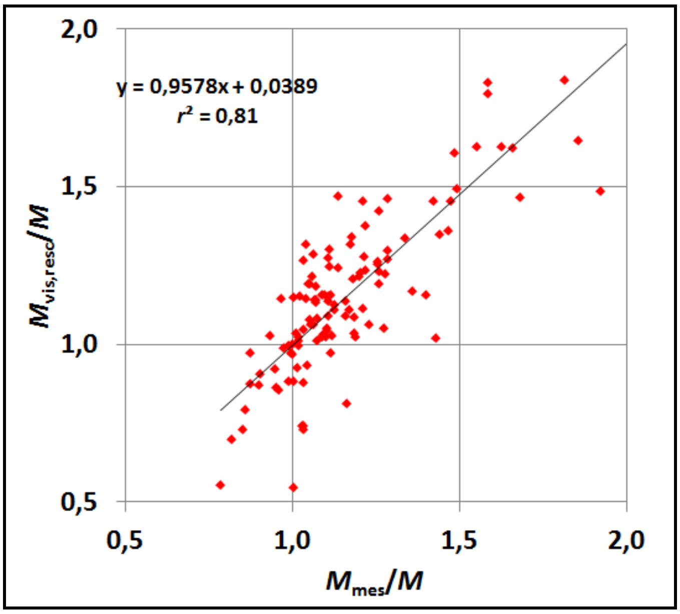

Figure 7 – The mathematical model is currently in its development stage. Here a preliminary fitting result is shown for mesopic colourfulness and to the mean answer of 4 observers. Abscissa: M_{mes} according to the modified CIECAM02 model divided by *M* from the original model (M_{mes}/M); ordinate: experimentally obtained and rescaled mean colourfulness divided by *M* ($M_{vis,resc}/M$)

5 Summary and Outlook

The refinement of mathematical modelling and a validation experiment with a chromatic visual lightness scale are currently underway. There seems to be a critical mesopic luminance value between 1 cd/m^2 and 10 cd/m^2 below which the transition point occurs where the unmodified CIECAM02 model is no more appropriate. This transition point depends on hue.

Acknowledgement: Authors would like to acknowledge Ms. Nathalie Krause who built up the device and carried out the first series of experiments.

References

FU Ch., LI Ch., CUI G., LUO M.R., HUNT R.W.G., POINTER M.R. 2012. An investigation of colour appearance for unrelated colours under photopic and mesopic vision, Color Res. Appl. 37/4, pp. 238–254.

HUNT, R.W.G. 1998. Measuring Colour, 3rd ed. Kingston-upon-Thames: Fountain Press.

HUNT, R.W.G. 1991. Revised color appearance model for related and unrelated colors. Color Res. Appl. 16, pp. 146 –165.

SHIN J. Ch., YAGUCHI H, SHIOIRI S. 2004. Change of Color Appearance in Photopic, Mesopic and Scotopic Vision, Optical Review 11/4, pp. 265-271.

OP34

ANGULAR CHARACTERISTICS OF THE SURROUNDING LUMINANCE EFFECT ON PERIPHERAL ADAPTATION STATE IN THE MESOPIC RANGE

Tatsukiyo Uchida[1,2], Yoshi Ohno[2]
[1] Panasonic Corporation, Osaka, JAPAN
[2] National Institute of Standards and Technology, Gaithersburg, Maryland USA
uchida.tatsukiyo@jp.panasonic.com

Abstract

CIE 191:2010 recommends a mesopic photometry system based on peripheral visual tasks. For implementation of the system, the visual adaptation field needs to be defined, taking into account the surrounding luminance effect on the adaptation state. A series of vision experiments in the mesopic range has been conducted to measure the surrounding luminance effect with respect to the angle between a peripheral task point and a point source (glare source). The results show that the surrounding luminance effect at the peripheral task point decreases with the angle at a larger slope than existing models, such as Stiles-Holladay equation, CIE general disability glare formula, and Stiles-Crawford equation. Thus, a new model for the surrounding luminance effect has been developed and proposed from the results.

Keywords: mesopic photometry, adaptation field, visual task performance, luminance contrast detection threshold, veiling luminance

1 Introduction

CIE has recommended a mesopic photometry system (CIE 191:2010) based on peripheral performance of tasks, such as detection, reaction time and recognition (CIE, 2010). It takes into account the Purkinje effect, which is the spectral sensitivity shift of the luminous efficiency function to shorter wavelengths at low light levels. The system properly evaluates potential luminous efficacy advantages for light sources that are rich in short wavelength components, such as light-emitting diodes (LEDs) as opposed to conventional lamps for outdoor lighting such as high-pressure sodium lamps. Therefore, it is expected to enable the lighting industry to develop and design more energy efficient and/or visually effective lighting, especially for outdoor applications.

However, some remaining issues must be resolved for the implementation of the CIE mesopic photometry system. One of the important issues is the definition of the adaptation field. The system describes the mesopic spectral luminous efficiency function $V_{\mathrm{mes}}(\lambda)$ according to the equation:

$$M(m)V_{\mathrm{mes}}(\lambda) = mV(\lambda) + (1-m)V'(\lambda) \tag{1}$$

where $V(\lambda)$ is the photopic luminous efficiency function, $V'(\lambda)$ is the scotopic luminous efficiency function and $M(m)$ is a normalization function to attain the maximum value of $V_{\mathrm{mes}}(\lambda)$ to 1. The m is a coefficient that represents the visual adaptation state, which determines the changes to the shape of $V_{\mathrm{mes}}(\lambda)$. To determine the value of m, the photopic and scotopic luminances of an adaptation field are required. The luminance of the adaptation field is referred to as "adaptation luminance." However, there is no authorized definition for the size and shape of the adaptation field to determine m.

Factors to be considered for the adaptation field definition are:

- The surrounding luminance effect (when the line of sight is fixed),
- The movement of the line of sight,
- The area of interest (AOI) in the lighting scene.

Regarding the first factor, when considering the adaptation state at a peripheral point in the retina, the surrounding luminance affects the adaptation state even though the line of sight is fixed. This effect is the narrowly-defined surrounding luminance effect. The effect includes the veiling luminance, lateral interactions within the retina, and any other factors in the visual system.

Regarding the second factor, the adaptation state is also affected by the movement of line of sight, as it relatively moves the surrounding luminance distribution around with respect to a peripheral task point in the retina. Thus, the adaptation state at a peripheral point can be considered as the spatially-weighted average with the probability function of the positions of line of sight.

The AOI is determined with respect to the lighting scene and depends on the lighting design or application. For example, if road lighting intends to illuminate a road surface, the road surface is the AOI. When one adaptation state (one value of parameter m) needs to be determined for an AOI, the adaptation luminance should be the average adaptation luminance of points in the retina that can see the AOI.

As described above, the surrounding luminance effect is the key factor for the adaptation field definition, and this paper focuses on this factor. Even though the adaptation luminance at a peripheral task point mainly depends on the local luminance at the task point (Uchida and Ohno, 2012), a previous empirical research (Uchida and Ohno, 2013) shows existence of the surrounding luminance effect that is larger than the foveal veiling luminances such as Stiles-Holladay disability glare formula (CIE, 1939) or CIE General Disability Glare Equation (CIE, 2002). A peripheral veiling luminance model, called Stiles-Crawford formula (Stiles and Crawford, 1937), shows better prediction for the experiment results.

Nevertheless, it is still not clear whether Stiles-Crawford formula can predict the surrounding luminance effects for wide viewing angle ranges. The experiment by Uchida and Ohno (2013) employed only three positions of a point source causing the surrounding luminance effect, the viewing angle between the source and the task point of which is 7°, 15°, and 30°; and Stiles-Crawford formula shows good predictions only for results at 7° and 15°.

Therefore, this empirical study aims to evaluate further details of the angular characteristics of the surrounding luminance effect by a point source on a peripheral task point in the mesopic range.

2 Experimental method

The principle of the experiment in this study was the same as the previous experiments by authors (Uchida and Ohno, 2012, 2013). The experiment measured luminance contrast detection thresholds. The threshold depends on the size and duration of the target stimuli, the background luminance when the target is presented, and the adaptation state. When all the conditions except for the adaptation state are kept constant, the luminance contrast detection threshold can represent the adaptation state (Narisada, 1995).

2.1 Set-up

The experimental set-up is shown in Figure 1. A liquid crystal display (LCD) controlled by a computer was used to present the target to be detected and the background. Neutral density (ND) filter films were placed in front of the LCD screen to reduce the luminance level to a mesopic range, but maintain high-resolution control of the luminance level by the computer. Eight white LED units were used as point sources, and were placed in front of the LCD at 4 cm from the LCD surface. Only one of the eight LEDs was turned on for an experimental condition. Each LED unit was a chip-on-board LED package with a diameter of emission surface of 15 mm. The LEDs were driven with a multi-channel DC current source controlled by the computer. The current of LED varied depending on experimental conditions, and were in a range from 2 mA to 95 mA. Care was taken so that no light from the LEDs fell on the LCD screen.

The luminance of the LCD and vertical illuminance from the LEDs at the subject's eyes were calibrated before each experiment. The subject was positioned at a viewing distance of 65 cm from the screen and fixed his/her head on a chin rest during each experimental run. At this distance, the LCD screen subtended 49° × 29° visual angle from the subject's eyes. The subject responded by clicking a mouse to record whether he/she saw the target or not.

The LCD screen presented white stimuli, which had a correlated colour temperature (CCT) of 4690 K and S/P ratio (scotopic/photopic ratio) of 2,21. CCT and S/P ratio of the LEDs were 6090 K and 1,99. The uncertainties of the measurements of CCT and S/P ratio were 70 K and 0.02 (*k*=2), respectively.

All experiments were conducted in a darkroom.

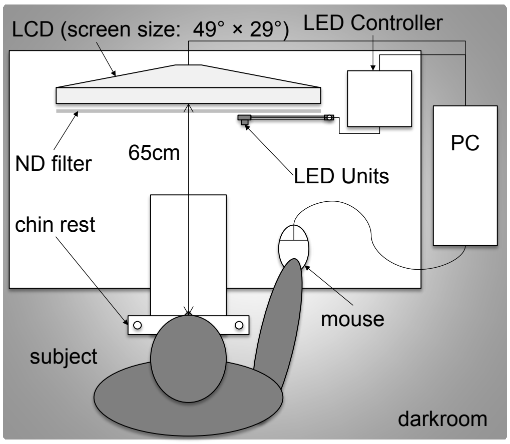

Figure 1 – Experimental set-up

2.2 Stimuli

The patterns of stimulus employed in the experiment are shown in Figure 2. The top row in the figure shows the adaptation patterns and bottom row shows the task pattern. The conditions consisted of eight point-source conditions and two reference conditions. In the point-source conditions, the point source was at eight different positions so that the visual angles between the task point and the point source were 5°, 7°, 10°, 15°, 20°, 25°, 30°, and 40°. The point source was always right above the task point, and in some cases, it was outside of the LCD screen area, but the background of the LCD was dark. There was no point source in the reference conditions. Each pattern represented a rough simulation of a road lighting scene at night-time, which has dark sky and road surface lit by a luminaire.

A fixation point during the detection task was positioned at the centre of the screen, which was marked by a cross. The target to be detected by subjects always appeared in the same position, which is lower right of the fixation point (see the bottom row in Figure 2.) The position was chosen so that the target mimicked an obstacle on a road surface and so that the fixation point avoids overlapping with the point sources right above the target. The visual angle between the fixation point and the target was 10°, which was the same as those in many experiments that became basis for CIE 191. The size of the target was 1°. The target luminance was varied between trials but was always lower than the background luminance.

The luminance of the lower half of the adaptation pattern is referred as "adaptation background luminance." It is constant at 0,2 cd·m^{-2} for all of the point-source conditions. For the reference conditions, there was no point source. The adaptation background luminance for one reference condition was 0,2 cd·m^{-2}. The adaptation background luminance of the other reference condition was 2,0 cd·m^{-2}. The luminance of the lower half of the task pattern is referred as "task background luminance." It was 0,2 cd·m^{-2} for all conditions.

2.3 Procedure and Subjects

Luminance contrast detection thresholds were measured by the random staircase method. The task for the subjects was to respond whether or not the target was seen on each experimental trial.

At the beginning of every experimental condition, subjects adapted to the adaptation pattern for five minutes. While the adaptation pattern was presented, the fixation point was moved in a 2° × 5° oval area centred at the centre of the screen every two seconds so that the point source did not excessively stimulate a fixed point on the subject's retina. This procedure was taken for consideration of photobiological safety of the subject, and was achieved by moving around the cross mark which the subject was instructed to gaze at. This procedure may affect the measurement results, but the vertical movement of the fixation point was within 2°, which was considered insignificant in most cases.

When the target was presented, the fixation point was fixed at the centre of the screen, and the task pattern (no point source) was presented for 0,6 seconds. The point source was turned off during the task pattern presentation to avoid the effect of veiling luminance by the point source (which could reduce the contrast between the target and the background) and to measure purely the effect of adaptation state. In the middle of the task pattern presentation, the target appeared for 0,2 seconds. Following the task pattern presentation, the adaptation pattern was presented again to maintain constant adaptation state. Five seconds after the subject completed each trial, the task pattern was presented again and next trial began with different target luminance. Since the time constant of the adaptation state is much larger than duration of the task pattern, these temporal changes of patterns do not affect the subject's adaptation state significantly (Narisada, 1995).

The experiment for a subject was conducted in two separate sessions. Each session consisted of four out of eight point-source conditions and both reference conditions. One of the sessions was "near point source" session, which consisted of 5° to 15° point-source conditions. Another session was "far point source" session, which consisted of 20° to 40° point-source conditions. The two reference conditions were included in both sessions. The illuminance at the subject's eyes from the point source in the near point source session was set to 3 lx, and that in the far point source session was 45 lx. These values were chosen based on previous research (Uchida and Ohno, 2013) so that the thresholds for the point-source conditions would fall between those for the two reference conditions. The point-source conditions were conducted the first, second, fifth, and sixth in a session; and the reference conditions were conducted third and fourth. The sequence of conditions was randomized under this restriction. At the beginning of each session, subjects stayed in a dark room for at least five minutes as pre-adaptation.

Eight subjects with normal vision participated in the experiment. Their ages were 27 years to 70 years.

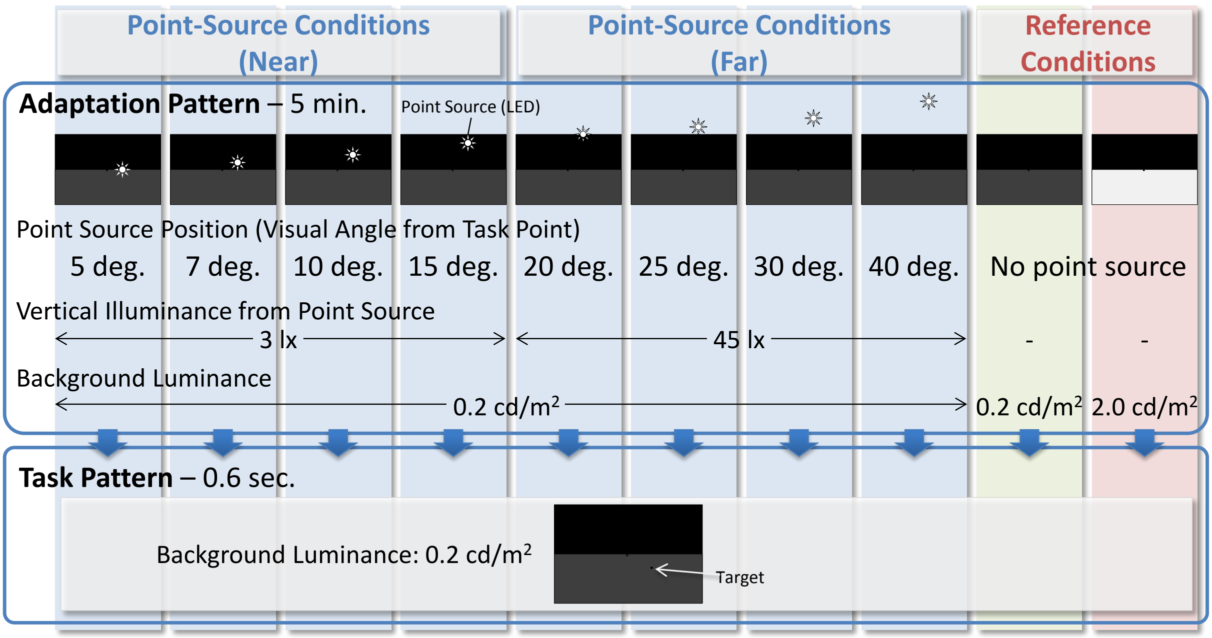

Figure 2 – Patterns of stimuli and conditions in the experiment

3 Results

Results of the experiment are shown in Figure 3 and Figure 4. These figures show luminance contrast detection threshold (ordinate) as a function of the point source position angle (abscissa). Figure 3 and Figure 4 show results of the near point source session and the far point source session, respectively. The results are the mean of all subjects' luminance contrast detection thresholds. For a comparison purpose, results of the reference conditions were plotted in the same figures, at the left end of each graph, which is at the position of 3° for Figure 3 and 15° for Figure 4, but these results are not related to these angles.

The results show that nearer point sources cause higher detection thresholds, which means lower visual performance. The reference conditions with 2,0 cd·m^{-2} show higher thresholds than the reference condition with 0,2 cd·m^{-2}. Since the adaptation luminance for the reference condition with 2,0 cd·m^{-2} is obviously higher than that of the reference conditions with 0,2 cd·m^{-2}, and since all conditions other than adaptation background luminance are the same for these two conditions, higher thresholds means higher adaptation luminance.

Note that the illuminance at the subject's eyes from the far point sources is 15 times higher than that of the near point sources. If the illuminance of the far point sources had been the same as that of the near point sources, the thresholds would have been much lower than those in the real results in Figure 4 and the effects with angle would have been too small to measure. The previous study suggests that the thresholds are linear with respect to the illuminance (Uchida and Ohno, 2013).

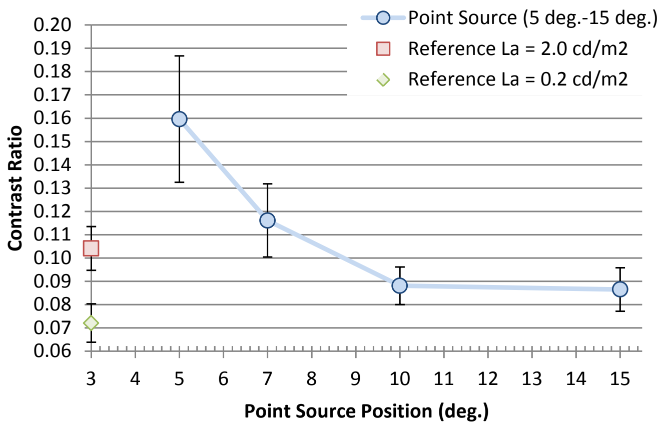

Figure 3 – Luminance contrast detection thresholds for the near point-source conditions. The error bars show the standard deviation of the mean

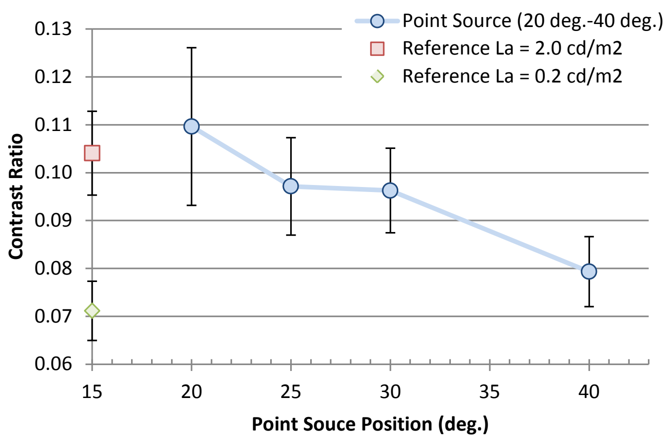

Figure 4 – Luminance contrast detection thresholds for the far point-sources conditions

4 Discussion and Analyses

The experiment results clearly show that the surrounding luminance effect depends heavily on the angle between the task point and the point source. Since the surrounding luminance effect is also proportional to the illuminance at the subject's eyes (Uchida and Ohno, 2013), the surrounding luminance effect can be expressed as:

$$L_{\text{surround}} = E \cdot f(\theta) \tag{2}$$

where L_{surround} is the surrounding luminance effect and the E is the illuminance at the subject's eyes. $f(\theta)$ is the angular function, which will be modelled finally in this study.

The previous study (Uchida and Ohno, 2013) introduced a term "effective adaptation luminance" to represent the adaptation state. It is an adaptation luminance that includes both the local luminance (the adaptation background luminance) and the surrounding luminance effect by the point source. The effective adaptation luminance is expressed as:

$$L_{\text{a,effective}} = L_{\text{local}} + L_{\text{surround}} \tag{3}$$

where $L_{\text{a,effective}}$ is the effective adaptation luminance and L_{local} is the adaptation background luminance in this study. Thus, the angular function can be calculated from the effective adaptation luminance with an equation:

$$f(\theta) = \frac{(L_{\text{a,effective}} - L_{\text{local}})}{E} \tag{4}$$

The effective adaptation luminance for the point-source conditions can be determined from the experiment results. It is known that the contrast threshold is linear with respect to the logarithm of the effective adaptation luminance (Uchida and Ohno, 2013) as:

$$C_{\text{th}} = a \log_{10} L_{\text{a,effective}} + b \tag{5}$$

where C_{th} is the contrast threshold. The constants, a and b, can be estimated from the experiment results for the reference conditions, for which both the contrast threshold and the effective adaptation luminance are known. The adaptation background luminance for the reference conditions, which is 0,2 cd·m^{-2} or 2,0 cd·m^{-2}, can be considered as the effective adaptation luminance for the reference conditions. Once the constants are determined, the effective adaptation can be calculated with Equation 4 by substituting the contrast threshold for each condition.

The angular function was determined from the experiment results by using the procedure above, and was compared with the three existing veiling luminance models, as shown in Figure 5. The models for the comparison are Stiles-Holladay disability glare formula (CIE, 1939), CIE General Disability Glare Equation (CIE, 2002), and Stiles-Crawford formula (Stiles and Crawford, 1937). The angular function determined from the previous experiment results in Uchida and Ohno (2013) is also plotted in Figure 5.

Stiles-Crawford formula shows the best prediction for the angular function from 10° to 20°, while the other two existing models show better prediction in the farther range. In a range less than 10°, all models underestimate the effects.

Since the surrounding luminance effect decreases with the angle at a larger slope than all existing models, a new model is proposed for the angular function. At present, we propose a model:

$$f(\theta) = \frac{L_{\text{surround}}}{E} = \frac{260}{\theta^3} \tag{6}$$

This model, also shown in Figure 5, can predict the empirical angular function better than the existing models. However, the proposed model still underestimates the experiment result for 5°. This is because the result for 5° was ignored to determine the parameters in the proposed model. The procedure used to determine the angular function relies on the linear function in Equation 5. However, the contrast threshold for 5° is much higher than that of the reference condition with 2,0 cd·m^{-2} adaptation background luminance. It has not been verified whether Equation 5 can be applied to such high contrast threshold or not. Therefore, the empirical angular function may have a significant error for 5° to the real angular function. Further research is needed for this point.

In this study, three geometrical parameters were fixed in the experimental conditions: the visual angle between the fixation point and the task point, the direction to the task point from the fixation point, and the direction to the point source from the task point. However, there are other combinations for these geometrical conditions in real lighting scenes. The parameters in Equation 6 may need to be modified to provide a general surrounding luminance effect equation for the outdoor lighting by taking into account those other geometrical conditions. Since the geometrical conditions for the experiment roughly mimicked that of the road lighting, the proposed model is intended to predict the surrounding luminance effect by glare sources above roads or streets, such as luminaires.

5 Conclusions

Experiments have been conducted to measure the surrounding luminance effect, in particular the effect of a glare source, on the adaptation state with respect to the angle between a peripheral task point and a point source in mesopic range. The results suggest that the surrounding luminance effect decreases with the angle at a larger slope than all existing models, such as Stiles-Holladay disability glare formula, CIE General Disability Glare Equation, and Stiles-Crawford formula.

Thus, a new model for the angular characteristics of the surrounding luminance effect has been proposed. The proposed model shows better prediction for the experimental results than the existing models. Since the experimental condition used in this study is similar to the real road/street lighting scenes with a luminaire, the proposed model is intended to predict the surrounding luminance effect by luminaires above roads or streets. To provide a general model for the surrounding luminance effect, some aspects still need to be investigated: the position of the task point, the direction to the source causing the surrounding luminance effect, and the angular characteristics in the range less than 7°.

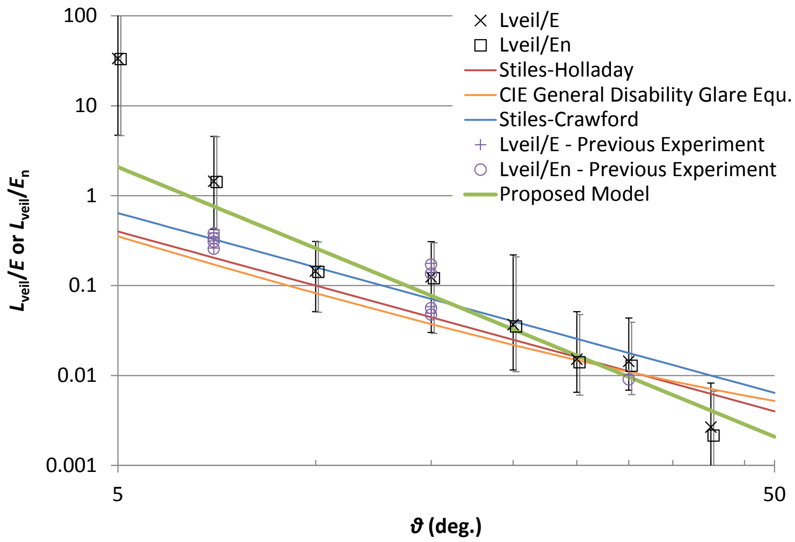

Figure 5 – Comparison of the empirical angular function of the surrounding luminance effect and models. The error bars show the standard deviation of the mean of the experimental results.

6 Acknowledgement

This study was funded by the New Energy and Industrial Technology Development Organization (NEDO). This study was conducted when Uchida was a guest researcher at NIST.

References

CIE 2010. CIE 191:2010. Recommended System for Mesopic Photometry Based on Visual Performance. Vienna: CIE.

UCHIDA, T and OHNO, Y. 2012. An Experimental Approach to a Definition of the Mesopic Adaptation Field. Proceedings of CIE 2012, 71-76.

UCHIDA, T and OHNO, Y. 2013. Effect of High Luminance Sources to Peripheral Adaptation State in Mesopic Range. Proceedings of CIE 2013, 529-536.

CIE 1939. CIE Internationale Beleuchtungskommission, Sekretariatsberichte der Zehnten Tagung, Scheveningen, 1939. Band I, 183-201.

CIE 2002. CIE 146:2010. CIE Equations for Disability Glare. Vienna: CIE.

STILES, W.S. and CRAWFORD, B.H. 1937. The effect of a glaring lightsource on extrafoveal vision.

Proc. Roy. Soc. London 122B, 255-280.

NARISADA, K. 1995. Perception Under Road Lighting Conditions with Complex Surroundings. J. Light & Vis. Env., 19, 2, 5-14.

OP35

A PILOT STUDY OF THE PHYSIOLOGICAL MECHANISM OF THE GLARE CAUSED BY LED BASED ON THE FLUCTUATION OF THE ELECTRO-OCULOGRAM

Lin Y, Liu Y, Sun Y, Qiu J
Institute for Electric Light Sources,Fudan University, Engineering Research Center of Advanced Lighting Technology, Ministry of Education, Shanghai 200433, P.R.CHINA
ydlin@fudan.edu.cn

Abstract

A pilot study was conducted to investigate the glare under LED illumination. Ten subjects were recruited to evaluate the glare under a series of light settings by using a 10-point rating scale, which is known as deBoer rating scale. When evaluating the glare, the electro-oculogram (EOG) was also recorded by an EOG amplifier, which records the position of the eye every 0.001second. It was found the average speed of the eye movement after observing the glare for 0.5 second, which was derived from the first derivative of the EOG curve, is correlated with the glare. The more serious the subject feels the glare, the faster his or her eye moves. The results found here suggest a possible physiological mechanism of the glare, which can be characterized by the average speed of the eye movement and the fluctuation of the EOG.

Keywords: glare, LED, electro-oculogram (EOG)

1 Introduction

With the development of LED industry, the properties of LED, including efficacy, colour quality, and life time, have been improved significantly. The application of LED is becoming wider and wider. The combination of LED's small size and high luminance, however, raise many concerns regarding glare.

Glare describes difficulties seeing in the presence of bright light; it can be divided into two types, discomfort glare and disability glare. When bright light enters the eye, the interreflection of light within the eyeball may reduce the contrast between visual task and background, causing glare. When the glare is so intense that vision is completely impaired, it is called disability glare; when the glare only produces difficulties in seeing the visual task, it is called discomfort glare. Both discomfort and disability glares influence people's visual perception and productivity.

Many efforts have been made to study what causes glare and how to evaluate glare, so that we can try to minimize or even avoid glare when finishing visual tasks (IES 1984; CIE 1983; CIE 1995; Hopkinson 1972; Iwata and Tokura 1998). In addition, contributions have been made to study the physiological mechanism of glare. For example, it has been found that the pupil size is able to represent the amount of stray light in the eye, so that we can also evaluate the glare based on the pupil size (Franssen et al 2007; Murray et al 2002; Stingham et al 2011).

In this pilot study, we investigate the relationship between the fluctuation of the electro-oculogram and the glare caused by LED sources based on subjective rating.

2 Methods

2.1 Experiment setting

The experiment was conducted in a full-scaled room, with a dimension of 2m × 2m × 2m. The room was enclosed by three walls and a black felt. During the experiment, the subject was seated in the centre of the room, facing a wall, which was covered by a adjustable black felt, allowing the adjustment of background illumination. One black felt was behind the participant and out of his or her field of view. The background illumination of the space was provided by four recessed LED panels. The background illumination was characterized by the illuminance level measured at position of the observer's eyes.

A horizontal track was installed at the ceiling height; an LED source having a 10° visual angle of the emitting area was installed in the track, which was employed as the source providing discomfort glare. The location of the source in the track can be easily adjusted by the experimenter. The subject was instructed to fix his or her eyes at a mark labelled on the wall, so that he or she would evaluate discomfort glare but not look at the source directly. The vertical angle between the fixation point and the glare source was 10°. The LED source was controlled by a power supply outside the room. Figure 1 illustrates the arrangement of the room.

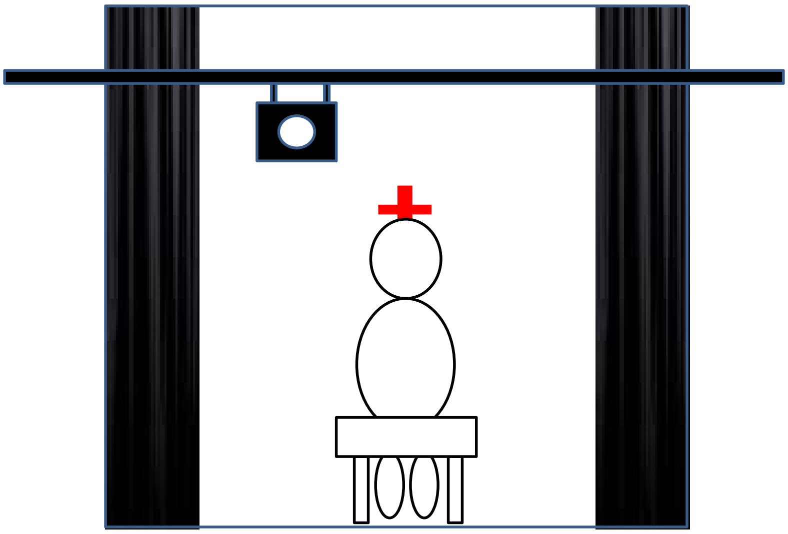

Figure 1 – Schematic diagram of the experiment room.

The independent variables for this study included the illuminance levels measured at the eye position provided by the glare source and the horizontal angle between the glare source and the fixation point. The illuminance level had four levels (20, 50, 125, and 300 lx); the angle between the source and the fixation point also had four levels (2°, 4°, 8°, and 16°). The experiment was designed as a full factorial design, so that each subject evaluated 16 different light settings. The evaluations of all 16 light settings were completed with a dark background, whose background illuminance was 0. The LED glare source had a CCT of 3300 K, whose SPD is shown in Figure 2.

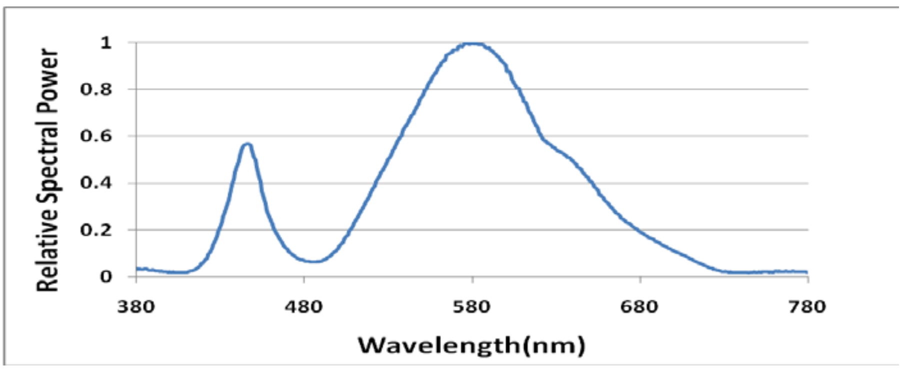

Figure 2 – The SPD of the LED glare source having a CCT of 3300 K.

The subjects also evaluated the conditions with higher background illuminance levels and under the glare source with different spectra, whose results will be discussed in another paper.

2.2 Data collection

The subjective rating of discomfort glare—deBoer rating—and the electro-oculogram were the two dependent variables for the study.

For each light setting, the subject was instructed to evaluate the discomfort glare by using a nine-point scale as described in Table 1, which is commonly identified as deBoer rating scale (deBoer and Schreuder, 1967). The description was translated to Chinese as illustrated in Table 1.

Table 1 – Ratig scale, known as deBoer rating scale, used in the experiment. (The description used in the experiment was translated into Chinese as noted).

Glare rating (deBoer rating) scale	Description
1	Unbearable (无法忍受)
2	
3	Disturbing (感到不适)
4	
5	Just admissible (刚能接受)
6	
7	Acceptable (较为满意)
8	
9	Noticeable (仅可察觉)

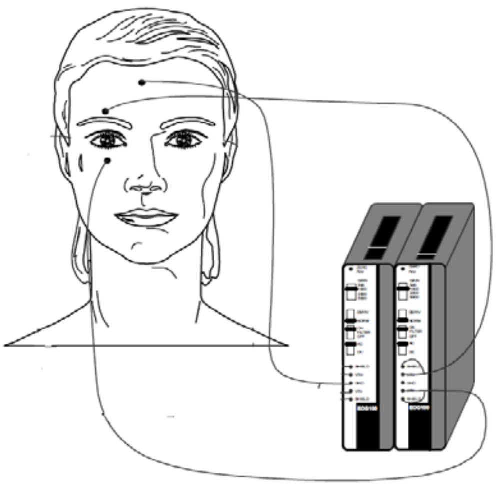

Figure 3 – Schemetic diagram showing how the EOG data was collected.

The electro-oculogram (EOG) was recorded by an electro-oculogram amplifier purchased from BIOPAC system, Inc. Three electrodes were attached around participant’s eyes, as illustrated in Figure 3, collecting and transmitting the data to the amplifier each 0.001 second. Both the amplifier collecting the electro-oculogram and the power supply controlling the LED glare source were controlled by a laptop. The amplifier provided a synchronizing trigger signal to the power supply, so that the state of the LED source and the electro-oculogram were synchronized.

2.3 Human subjects

Ten subjects (8 males and 2 females) were recruited for this study. The mean age of the subjects was 24.5 years of age with a standard deviation of 1.65. All the subjects were Chinese and had normal vision.

2.4 Procedure

Upon arrival, the experimenter escorted the subject into the room, attached the electrodes around the subject's eyes, read the instruction of the experiment to the subject, and answered the questions raised by the subject. Then the subject was instructed to fix their view at the fixation point on the wall. He or she was seated in the dark room for 10 minutes, allowing the visual system to be adapted to the dark environment. After 10 minutes, the first light setting was presented, which was on for three seconds. During that period, the experimenter instructed the subject to evaluate the discomfort glare by using the deBoer rating scale and try to not blink. After giving the rating, the glare source was turned off. After 1 second, the source was adjusted to the second light setting. After finishing the evaluation of all 16 light settings, the general illumination was changed and the subject was asked to be seated for another 10 minutes for adaptation.

3 Results and Discussions

The EOG data was extracted at each 0.01 second for analyses, which can be plotted as Figure 4. The EOG data is showing the movement of the eye.

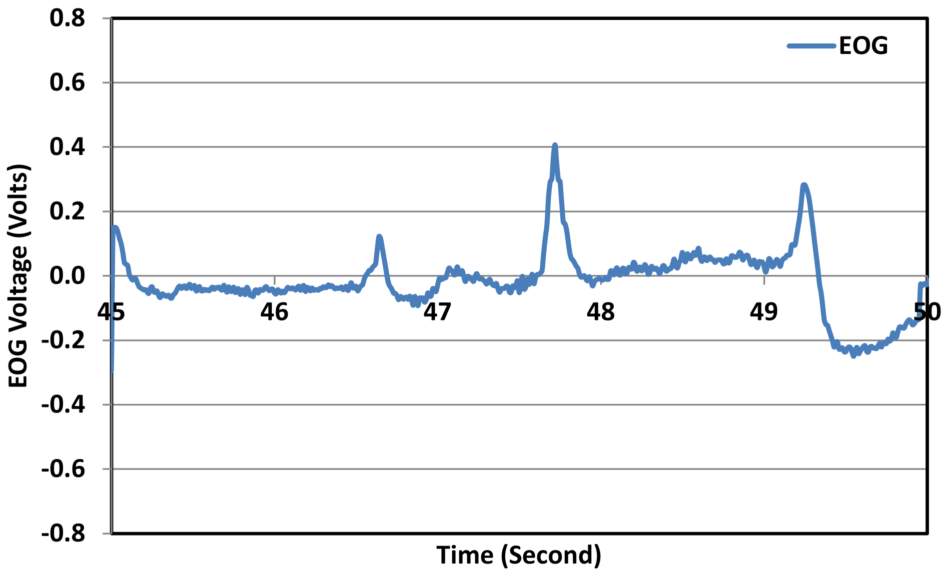

Figure 4 – Example of EOG data of a subject after seeing the glare source.

The speed of the eye movement can be characterized by the first derivative of the curve. The higher the value is, the faster the eye moved. The first derivate of the curve within the first 0.5 second after tuning on the glare source was calculated for each participant under each light setting, allowing the comparison between different light settings.The relationship between the subjective rating and the average speed of eye movement for each light setting can be plotted as Figure 5.

It can be observed that the source causing higher glare will also accelarte the movement of the eye.

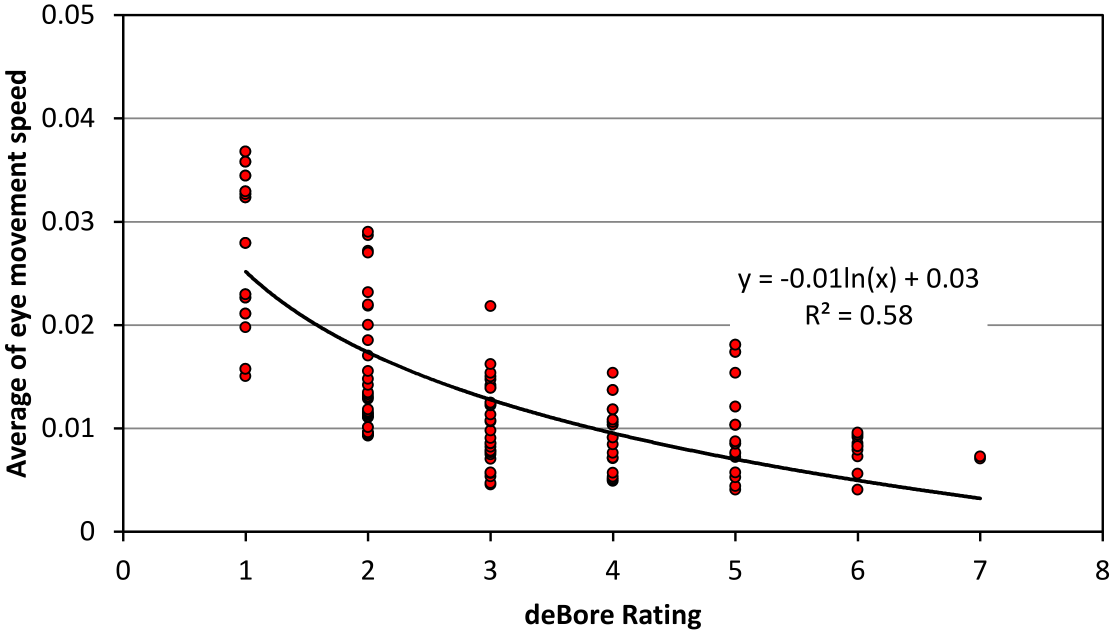

Figure 5 – The relationship between the average speed of the eye movement versus the glare as rated using deBore rating scale.

It has been found that pupil diameter decreases when glare increases (Stringham et al 2011).The results presented here shows in addition to the change of the pupil, human's eyes also move faster when glare increases, although we only focused on the movement within the first 0.5 second after observing the glare source. Further studies are necessary to see whether the movement will become faster and faster after being exposed under the glare source for a period of time.

4 Conclusion

A pilot study was conducted to investigate the possible physiological mechanism of the glare under LED illumination. Ten subjects were asked to evaluate the glare under 16 different light settings provided by LED, using a 10-point deBoer rating scale. When making evaluation of glare, the electro-oculogram was also recorded by an EOG amplifier every 0.001 second. It was found the average speed of the eye movement after observing the glare for 0.5 second is highly correlated with the glare. When the subject evaluate more serious the glare caused by the LED source, his or her eyes moved faster. The results illustrate a potential physiological mechanism of the glare, which can be characterized by the average speed of the eye movement and the fluctuation of the EOG. Further studies will be conducted to investigate how EOG will change after observing the glare source for a period of time and whether the relationship found in this pilot study is valid for other conditions.

Acknowledgement:

This work is supported by the National Basic Research Program of China (973 Program No.2010CB734102); Ministry of Science and Technology of China (Project No.2009GJC00008); Science and Technology Commission of Shanghai Municipality(Project No.09DZ1141004).

References

IES. 1984. IES Lighting Handbook. Reference Volume, New York, IESNA, 1984, pp.9-47.

CIE. 1983. Publication NO 55(TC-3.4): Discomfort Glare in Interior Working Environment.

CIE. 1995. Discomfort Glare in Interior Lighting. CIE Technical Report 117, Vienna, Austria.

deBoer JB, Schreuder, DA. 1967. “Glare as a criterion for quality in street lighting,” Trans. Illumin. Eng. Soc. 32(2), 117-135.

Franssen L, Tabernero J, Coppens JE, van den Berg T.2007. “Pupil size and retinal straylight in the normal eye”. Investigative Ophthalmology & Visual Science. 48(5).

Hopkinson RG. 1972. “Glare from daylighting in buildings”. Appl Ergonom 3(1):206-215.

Iwata T, Tokura M. 1998. “Examination of the limitations of predicted glare sensation vote as a glare index for a large source: Towards a comprehensive development of discomfort glare evaluation,” Lighting Research and Technology. 30(2), 81-88.

Murray IJ, Planinis S, Carden D. 2002. “The ocular stress monitor: a new device for measuring discomfort glares”. Lighting Research and Technology, 2002. 34(3): p. 231-242.

Stringham JM, Garcia P, Smith PA, McLin LN, Foutch BK. 2011. “Macular Pigment and Visual Performance in Glare: Benefits for Photostress Recovery,Disability Glare and Visual discomfort”. Investigate Ophthalmology & Visual SCIENCE. 52(10): p. 7406-7415.

Zhu, X., et al. 2013. “The luminaire beam-shape influence on discomfort glare for LED road lighting”. CIE Centenary Conference-Toward a new century of light. Paris, France.

OP36

TOWARDS A SYSTEM FOR DIGITAL QUANTIFICATION OF COLOUR DISCRIMINATION AND COLOUR DEFICIENCY

Tsai, Y.C. [1], Sekulovski, D. [2], Chen, H.S. [1] and Luo, M.R. [3]
[1] National Taiwan University of Science and Technology, CHINESE TAIPEH
[2] Philips Research Europe, Eindhoven, NETHERLANDS
[3] Department of Colour Science, University of Leeds, Leeds, UK
D10122501@mail.ntust.edu.tw

Abstract

Results from two experiments using a system for digital quantification of colour discrimination are presented. In the first, different psychophysical methods for establishing the Just-Noticeable Colour Differences (JND) were evaluated; in the second, the colour discrimination ability of 5 low vision observers and 30 normal vision observers from three age groups was quantified using the selected methodology. It was found that the staircase method with a forced choice performed more reliably than the method of adjustment. Also, no significant difference between the three different age groups was found, but the results showed a clear difference between the Deutanopia-type colour deficient observers and the normal colour vision observers.

Keywords: Just-Noticeable Differences, colour vision deficiency

1 Introduction

Human colour vision begins by the absorption of photons in three classes of cones. Each type is sensitive to a certain wavelength of light (red, green, and blue) and each perceived colour is therefore a mixture of stimuli of those three cone types. For colour vision deficiency (CVD) observers, any colour stimulus which possesses the cones with reduced or shifted sensitivity characteristics to the wavelength of light (Fairchild, 1998.). Those persons who have the colour vision characteristics may not distinguish the differences of certain colour combinations. Normal colour vision (NCV) is trichromatic. There are about 8% male and 0.2% female suffering from CVD (Hurvuch, 1981).

There are various colour vision tests including Anomaloscope, dichotomous hue test and pseudoisochromatic plates. The first Anomaloscope was developed in the 20th century. It was invented by the German ophthalmologist and physiologist, Willibald A. Nagel who named it Anomaloskop (Nagel, 1907). Anomaloscope is an instrument based on a Rayleigh match for checking CVD. i.e. a mixture of red and green light sources has to be matched with a yellow light source. It's the most accurate CVD diagnosing instrument used by eye specialists all around the world (Daniel, 2010.). Dichotomous hue test is based on a set of coloured plates or discs which have to be arranged in the correct order. The most famous dichotomous hue test is the D-15 dichotomous test, which was originally introduced in 1947 by Mr. Farnsworth. It belongs to a kind of arrangement test based on the theory of co-punctual points (Corn, et al. 2010.). Finally, the pseudoisochromatic plates are very quick hand-held test for various forms of CVD. It relies on the identification or non-identification of numbers or shapes against a potentially confusing coloured background. The Ishihara colour test plate is one of the most widely used methods of the pseudoisochromatic plate (Birch, 1997).

To understand each individual's colour discrimination capabilities can improve their interactions with the environment. For low colour vision, either genetic or age related, the information acquisition can be improved by providing tools to quantify the colour discrimination abilities. This can further be used to tune the information representation to the specific needs of an individual, resulting in a barrier free living and working environment not only for NCV, but also low vision (LV) observers. As a first step towards this goal, a flexible digital system for the quantification of the colour discrimination ability is needed.

The present work consists of two parts. In the first part, different psychophysical methods for scaling threshold colour-differences were investigated. The best performing method was used in the second part to perform colour discrimination experiments, both with NCV observers from different age groups and LV observers.

2 Experiment 1

To characterize an observer's colour discrimination ability, the notion of Just-Noticeable Difference (JND) is used. It is defined as the minimum value of a 'ness' that is just seen as different between a reference or standard and a sample (Engeldrum, 2000). In the case of colour discrimination, we use the distance in colour space as the 'ness'. A number of psychophysical methods can be used to measure the JND values. Two widely used methods are compared here. The first considered method was the method of adjustment. This method results in a fast determination of the JNDs, but suffers from a large experimental error and is a potential source of habituation and expectation errors. The second method used was the staircase method based on a forced choice decision. It overcomes the above limitations and can reduce the experimental error (Dixon, 1948). However, the staircase method requires a considerably longer measurement time.

2.1 Device

The experiment was conducted on a 10-bit LCD monitor, a 27 inch NEC SpectraView Reference 271. The experiment was conducted in a room without other light except the display during the experiment.

Based on measurements, a model of the device was built and the performance verified by comparing the model predictions to measurements done in a subsequent session. The difference between the modelled and measured valued was, in terms of the mean, maximum, minimum and standard deviation in CIEDE2000 ΔE_{00} units: 1.57, 1.94, 1.34 and 0.14 respectively. Moreover, the differences on all the 17 measured points had a consistent colour shift. As in the experiments the differences between colours are more important than their absolute reproduction, the calibration was evaluated as sufficient. After removing the colour shift the minimum, mean, and maximum error changed to 0.0673, 0.1712, and 0.3903 ΔE_{00} units respectively.

2.2 Procedure

Two methods for finding the threshold JND were used. In the first one, the method of adjustment, each observer can adjust freely by varying the level of colour difference until a JND is reached. The adjustment was done using a keyboard and the participants could change the level using small and large steps, where the large steps were five times larger than the small steps. Five repetitions of the measurement with the method of adjustment were used and the average value over the repetitions was used as the final result.

In the second, the staircase method, the participants had to answer a two alternative forced choice question at each presented level and the next level was decided based on their choice. Due to the two alternative forced choice (2AFC), a weighted 3:1 up:down staircase was used to converge to the 75% point (Kaernbach, 1991). The staircase procedure was run until eight reversal points were recorded and the average of the last four was used as the threshold value. After every two recorded reversal points the step size was halved. All the staircases for the same central colour point were shown with their steps intermingled.

2.3 Stimuli

Apart from the method used to find the threshold JND, the second parameter varied was the shape of the stimulus used. Two types of stimuli (see Figure 1) were used for the method of adjustment. For the staircase method, only the half circle pattern was used. The dividing line in Figure 1 was randomly arranged either horizontally or vertically. Observers had to answer the 2AFC question of whether they see the horizontal or vertical line. For both stimulus types the stimulus at the viewing distance had a spatial extend of 10° and was presented on a mid-level D65 background. For the half circle stimulus, the position of the reference was randomized at each step. For the concentric circle stimulus, the reference was always shown on the outside circle.

	Half Circle	Concentric Circle
Patterns		

Figure 1 - Two kinds of stimulus patterns used in the method of adjustment

Deviations in u'v' in ten directions from two colour centre points were used. The two colour centres had the u'v'Y coordinates (0.19, 0.46, 70) and (0.22, 0.51, 70) respectively. Both of them were selected from the colour centres of MacAdam ellipses (Wiszecky, 2000) and are located inside the monitor's gamut. Eight of the ten directions used were arranged 45° apart from 0 to 360°. The other two directions were along the Deutan confusion line (Brettel, 1997). The confusion line is the area around the colour centre where a NCV observer can correctly discriminate from the target, while a CVD (deutan) observer would confuse the colours.

Figure 2 depicts the two colour centres and the ten directions used on the CIE u'v' chromaticity diagram.

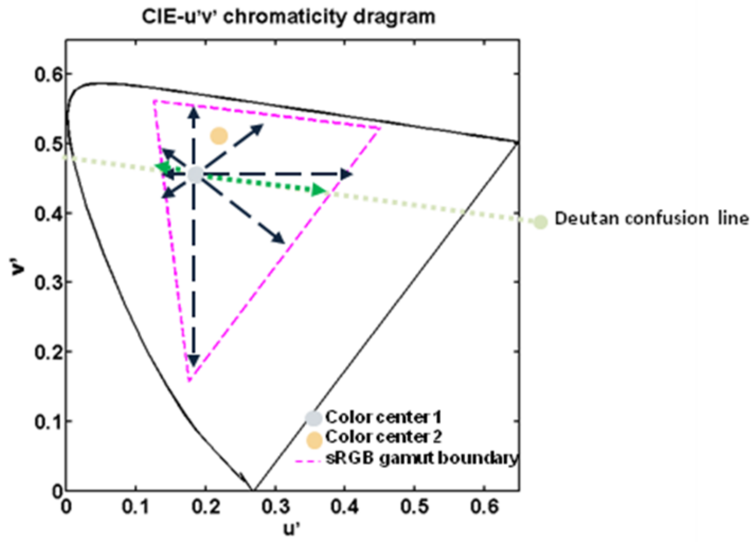

Figure 2 - The ten directions of change and the two centre colours

2.4 Observers

10 Observes aged 16 to 35 years took part in the first experiment.

2.5 Results

We present the resulting JND values in terms of Δab* from the centre colour. The L* of stimuli was fixed in the experiment so that ΔL*=0 and only Δab* is used.for each colour pair. Figure 3 shows the results for the two colour centres and the different variation of methodology and stimulus shape. The standard deviation (STD) of the result over the ten observers was also calculated in Δab*.For colour centre 1, the mean JNDs were 1.16, 1.94, 1.97 for the staircase, the adjustment method 1 (half circle) and the adjustment method 2 (concentric circle). The STD values were 0.31, 0.94 and 0.75 Δab* units in the same order. For colour centre 2, the mean JNDs were 1.30, 1.97 and 1.78 and the STD values were 0.46, 0.72 and 0.77 in the same order respectively.

The analysis results showed that both the test method and the stimulus pattern had a significant effect on the experimental results and their variance. A Bartlett K^2 test showed a significant difference in the variance between all three methods (K^2 = 62.7099, df = 2, p = 2.414e-14), as well as the two stimuli shapes (K^2 = 30.32, df = 1, p = 3.663e-08). A full linear model with *method, colour centre,* and *angle* as main factors was fit using R and analysis of variance showed a significant effect of only the main factor *method* ($F = 9.975$, $p = 0.00161$). All other main effects and interactions were not significant.

The results demonstrate that the staircase is both more sensitive and has a smaller measurement error than the method of adjustment. Moreover, for the latter method, there are significantly different results between the two kinds of stimulus pattern used. It can be concluded that regardless of the types of stimulus pattern, the staircase method outperformed the method adjustment and will be used in the second experiment.

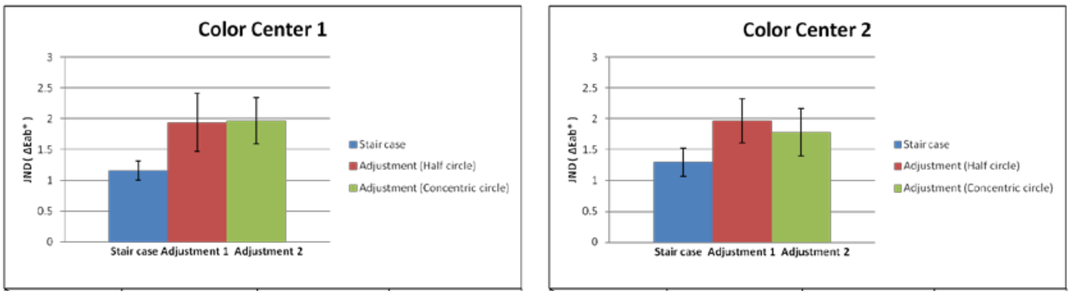

Method / Value	Stair case Color 1 (u', v', Y) = (0.19, 0.46, 70)	Adjustment Color 1 (u', v', Y) = (0.19, 0.46, 70)	Adjustment Color 1 ((u', v', Y) = (0.19, 0.46, 70)
Δab*	1,16	1,94	1,97
STD	0,31	0,94	0,75

Method / Value	Stair case Color 2 (u', v', Y) = (0.22, 0.51, 70)	Adjustment Color 2 (u', v', Y) = (0.22, 0.51, 70)	Adjustment Color 2 (u', v', Y) = (0.22, 0.51, 70)
Δab*	1,30	1,97	1,78
STD	0,46	0,72	0,77

Figure 3 - Results of Experiment 1

3 Experiment 2

The second experiment was designed to examine age related changes to colour discrimination and to compare the JND results between the normal colour vision discrimination and colour vision deficiency results. All 4 observer groups participated in this experiment.

The same device that was used in Experiment 1 was used. Only the staircase method with 2AFC was used. The same ten directions around the two colour centres as in Experiment 1 were used.

3.1 Observers

35 Observers took part in the second experiment. They were divided into four groups. Three of them were NCV observers from different age groups (16-35 years, 36-45 years and 46-60 years). Each group had 10 observers. Group 4 was the LV group and had 5 observers.

3.2 Results

As in Experiment 1, we present the resulting JND values in terms of Δab* from the centre colour. The results are depicted in Figure 4. The results demonstrate a small variation between different age NCV groups. For colour centre 1 the mean Δab* values in the different groups were 1.16, 1.01, 1.10 and 2.47 for 16-35 years, 36-45 years, 46-60 years age groups and CVD group, respectively. For colour centre 2, the mean values were 1.30, 1.30, 1.22 and 3.01 in the same order as above. The standard deviation (STD) data were calculated also in Δab* units between the ten observers in each group. For colour centre 1, the STD values were 0.31, 0.16, 0.29 and 0.67 and for colour centre 2 0.46, 0.26, 0.19 and 0.95 for the four groups in the order given above.

A full linear model with *group*, *colour centre*, and *angle* as main factors was fit using R. An analysis of variance showed a significant effect of *group* ($F = 93.093$, $p < 2e-16$), *colour centre* ($F = 12.274$, $p = 0.000489$), and an interaction effect of *group* and *angle* ($F = 7.962$, $p = 3.18e-05$). A TukeyHSD post-hoc analysis showed that on *group* only the CVD group was significantly different from the others, and there was no significant effect of age.

3.3 Discussion

The experiment results are summarized in terms of JND ellipses in \u'v' chromaticity diagram in Figure 5.

A few main conclusions can be derived from the analysis above and the Figure 5:

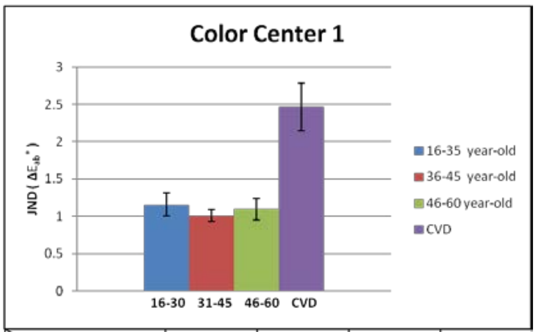

Method / Value	16-35 year-old	36-45 year-old	46-60 year-old	CVD
Δab^*	1,16	1,01	1,1	2,47
STD	0,31	0,16	0,29	0,64

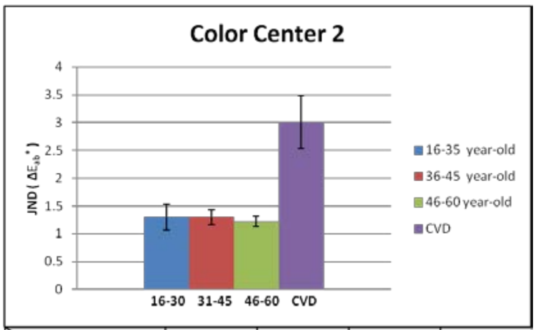

Method / Value	16-35 year-old	36-45 year-old	46-60 year-old	CVD
Δab^*	1,3	1,3	1,22	3,01
STD	0,46	0,26	0,19	0,95

Figure 4 - Results of Experiment 2

1) As expected, the results from the CVD group are significantly different from the results of the three NCV groups. Less expected was the lack of significant difference between the NCV groups. This demonstrates a lack of an age effect on colour discrimination, at least in our sample of participants that were up to 60 years old.
2) Interesting from the analysis above is the interaction effect between *angle* and *group*. It shows that different groups (LV group and NCV groups) have a different change of the JND in different directions. Figure 5 depicts this fact clearly. As expected, the deuteranomalous observers showed significantly larger JNDs on the deutan confusion line, but had comparable colour discrimination in the other directions. Visually, this results in the elongation of the CVD ellipse along the deutan confusion line.
3) The NCV groups yielded ellipses close to a circle for all age groups. It implies that u'v' space can fit the visual data well, i.e. all points in the circle having the same visual differences. Similarly, the lack of significant main effect of angle in the NCV groups demonstrates that CIELa*b* ΔE demonstrates a good colour uniformity around the two colours used and within the power of our tests.

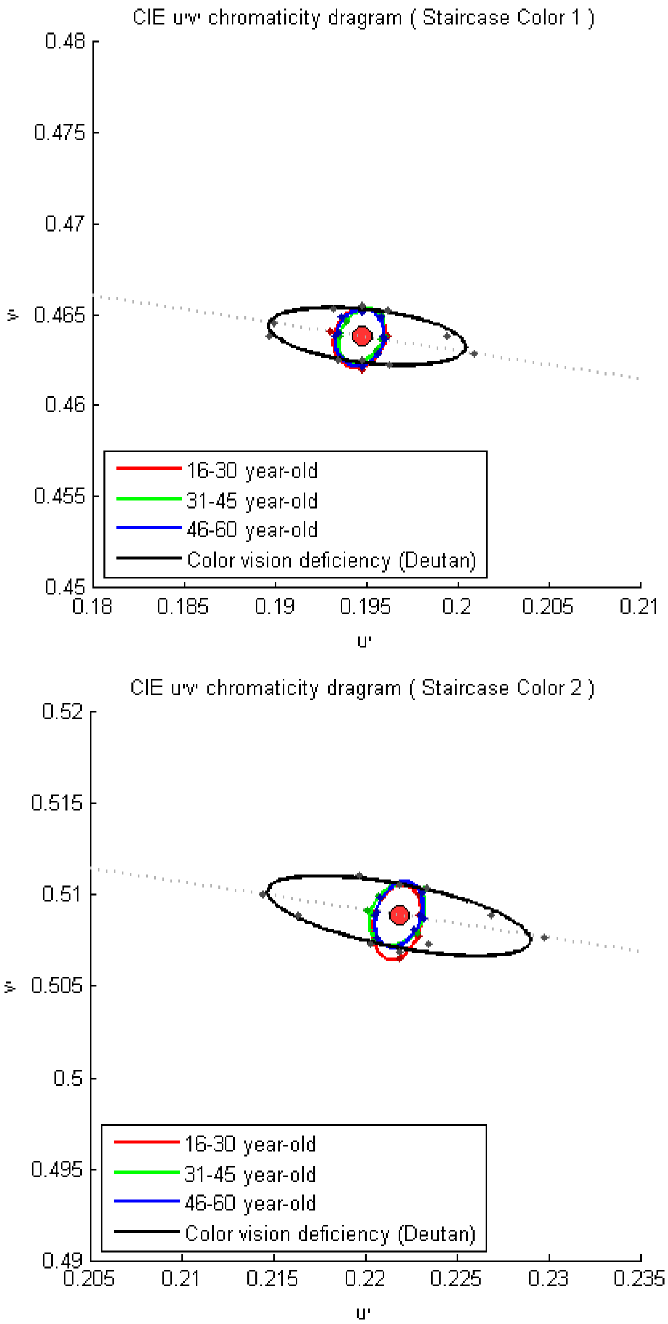

Figure 5 - Averaged JNCD ellipses for the observer groups in the study

4 Conclusions

This study is divided into two experiments. In the first part, the results showed that the staircase method is more sensitive and has a smaller measurement error than the method of adjustment. The second experiment showed a consistent colour discrimination results between 3 different age groups of normal colour vision observers. This implies a limited effect of age on colour vision, at least for observers younger than 60. In addition, colour vision deficiency observers demonstrated impaired colour discrimination along the deutan confusion line.

References

FAIRCHILD, M. D. 1998. *Color Appearance Models,* Addison Wesley, Reading, MA.

HURVUCH, L. M. 1981. *Colour Vision*, Sunderland, MA: Sinauer Associates Inc.

NAGEL, W.A. 1907. *Zwei Apparate für die Augenärzliche Funktionsprüfung: Adaptometer und kleines Spektralphotometer (Anomaloskop)*. Zeitschrift für Augenheilkunde 17.

DANIEL, F. 2010. *Color Blind Essentials*, published online on Colblindor.com.

CORN, A. L., ERIN, J. N. 2010. *Foundations of Low Vision: Clinical Functional Perspectives*, American Foundation for the Blind.

BIRCH, J. 1997. *Efficiency of the Ishihara Test for Identifying Red-Green Colour Deficiency*, Ophthalmic Physiol Opt.17 (5): 403-8.

ENGELDRUM, P. G. 2000. *Psychometric Scaling: A Toolkit for Imaging System Development*. Winchester, Mass.: Imcotek Press

DIXON, W. J., MOOD A.M. 1948. *A Method for Obtaining and Analyzing Sensitivity Data*, *Journal of the American Statistical Association*.

WISZECKY, G., STILES, W.S. 2000. *Color Science: Concepts and Methods*, Quantitative Data and Formula (2nd edition) New York: Wiley-Interscience.

BRETTEL, H., VIENOT, F., MOLLON, J.D. 1997.*Computerized Simulation of Colour Appearance for Dichromats J. Opt. Soc. Am. A*,14, 10

KAERNBACH, C. 1991. *Simple Adaptive Testing with the Weighted up-down Method*. *Perception & Psychophysics* , 49 W. 227-229

OP37

EFFECTS OF THE POSTURE OF OLED PANELS ON THE FLUX MAINTENANCE

Yamauchi, Y.[1], Hirasawa, M.[1] and Shitomi, H.[2]
[1]Graduate School of Science and Engineering, Yamagata University, Yonezawa, JAPAN
[2]Photometry and Radiometry Division, National Metrology Institute of Japan, Tsukuba, JAPAN
yamauchi@yz.yamagata-u.ac.jp

Abstract

Organic electroluminescent lighting (OLED) is expected to become one of the next generation lighting devices. In order to evaluate the performance of OLED panels, its life is one of the most important issues. As the OLED panels are surface light-emitting device, the temperature non-uniformities exist depending on the posture, and it might affect the life of the panel. If it would be the case, the posture to run the life test should be defined. In this research, we investigated the effects of the posture of OLED panels on the flux maintenance by testing three different postures in the same condition. We haven't find any distinct effects of the posture after 1500 hours of succesive operations.

Keywords: OLED, flux maintenance, posture

1 Introduction

Organic electroluminescent lighting (OLED) is expected to become one of the next generation lighting devices that will substitute conventional illuminating devices. OLED lighting has many different aspects from other devices. One of them is that an OLED panel is a 2-dimensional surface-emitting device. In order to evaluate its performance properly, standard methods should be defined and established to measure its optical properties.

CIE TC 2- 68, which started in 2010, is trying to establish those methods. Two sub-TCs (STCs) were formed in TC 2-68 and have been working on different issues in parallel. Method for measuring total luminous flux, for example, is dealt in STC-1, while flux maintenance is dealt in STC-2.

Flux maintenance, the percentage of the remaining luminous flux at a specified elapsed operating time, is one of the most important features for light sources, as it directly indicates the life of the sources, which is essential to describe its performance. It has been proposed how to measure the flux maintenance for LEDs (IES, 2008). Due to a unique feature of OLED panels being a surface light-emitting device, several factors such as heat distribution inside the panel and airflow around the panel might cause the temperature non-uniformity of the panel (Hirasawa, 2012). In the long run, that will affect the life of the panel, or flux maintenance. Theoretical analysis shows that the temperature difference of 5 to 6 degree can be expected inside of the panel when it is held vertically. Even if the panel were held horizontally, the heat distribution would be different whether the panel is held upwards or downwards.

These non-uniformities in heat distribution might cause non-uniform degradation inside a panel. However, the effects of these factors have not been clarified yet. In order to establish a standard method for evaluation of the panel life, standard experimental condition should be defined and agreed based on scientific data.

In this study, we try to find the effects of the posture of the OLED panel empirically on the flux maintenance by locating several OLED panels in different postures under the same operating conditions. We used several commercially available OLED panels to conduct the flux maintenance experiment.

2 Methods

In the experiments, three different postures were chosen to keep the panels:

i) holding a panel horizontally with the light-emitting surface upwards,

ii) holding a panel horizontally with the light-emitting surface downwards,

iii) holding a panel vertically (sideward).

The panels from the same makers were operated in the rated condition. The room temperature was kept around 25 degree. 4 different commercially available OLED panels from different makers were used as test panels for each posture. Two panels were operated in the same postures.

The OLED panels were set in a rack as shown in Figure 1.

The total luminous flux and luminance distributions were measured periodically. The total luminous flux was measured with an integrating sphere whose diameter is 1-meter, and its luminance distribution was measured with a 2D Colour Analyzer CA-2000 (Konica Minolta). We conducted measurement of OLED panels after 24, 100, 200, and 1500 hours after turning on the panels.

Figure 1 – Experimental setup

3 Results and Discussions

Figure 2 shows the normalized total flux of each OLED panel in three different postures. Each panel indicates the normalized flux measured in (a) upward, (b) downward, and (c) sideward condition. Each symbol denotes the measured values obtained from different makers. As we ran two panels in the same condition, most of the results are the averaged values of two panels, otherwise the results of a single panel are used when some defects were observed in one panel.

The results indicate that most of the panels, regardless of its makers, shows the same trends: as far as the duration (1500 hours) we have operated so far, the total flux measured haven't changed so much. It appears that the total flux maintained for all the duration. In order to make the values clear, we plotted the ratio of the flux maintenance between the initial value and that of 1500-hour operation. The results are shown in Figure 3. In this figure, we plotted the relative values for each maker. Each panel (a) to (d) corresponds to maker (a) to (d).

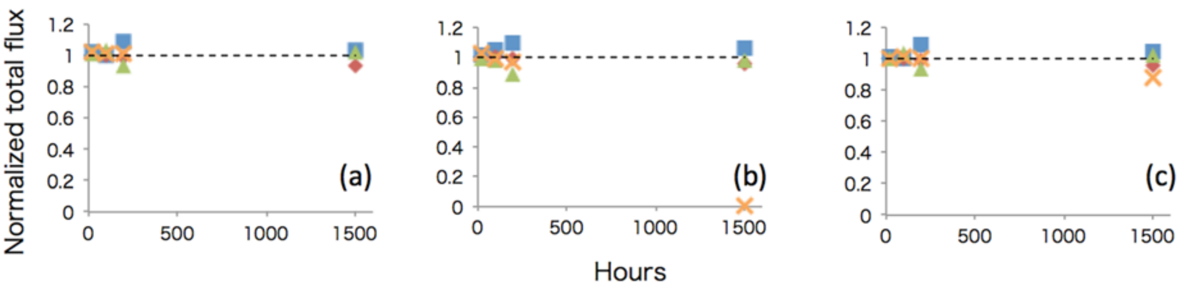

Figure 2 – Normalized total flux obtained from each posture: (a) upward, (b) downward, and (c) sideward. Each symbol denotes the data obtained from different maker.

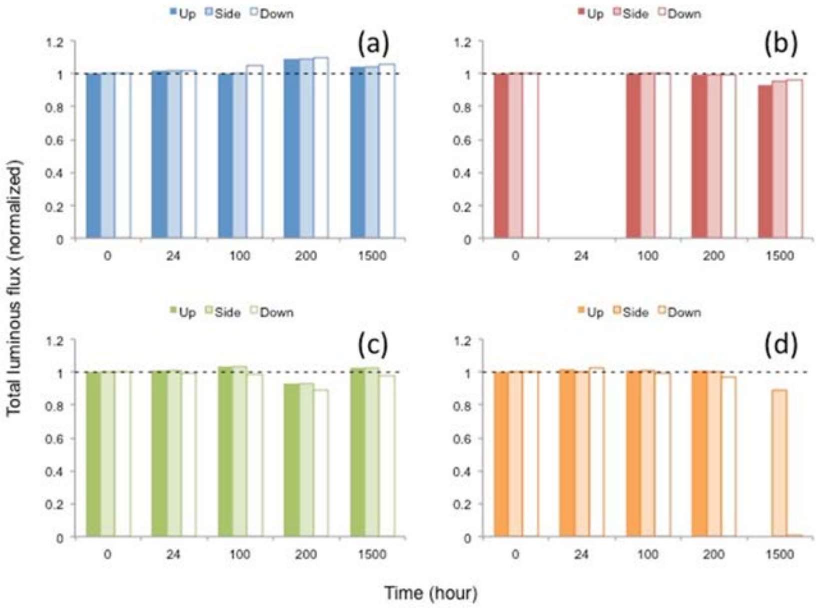

Figure 3 – Normalized total flux across the operating duration, which were obtained from each panel maker

From Figure 3, it is clearly shown that as far as the operation duration is about 1500hours, the total flux is not affected by its postures of operation. The chromaticies shifted in the same operating conditions are shown in Figure 4. The results show that there are individual differences in the change of the chromaticities depending on the makers.In order to find if any trends in detail can be observed during the operation, we extracted the data from maker (b) and (c) in Figure 5. Among all the data, the results of maker (b) and (c), and upward and sideward posture were extracted. Panels (a) and (c) are the results obtained from maker (b), while (b) and (d) obtained from maker (c). Panels (a) and (b) are the results obtained from upward condition, while (c) and (d) from sideward condition. The trends of colour shifts did not show any consistent change across the makers, but the results of each maker show the same

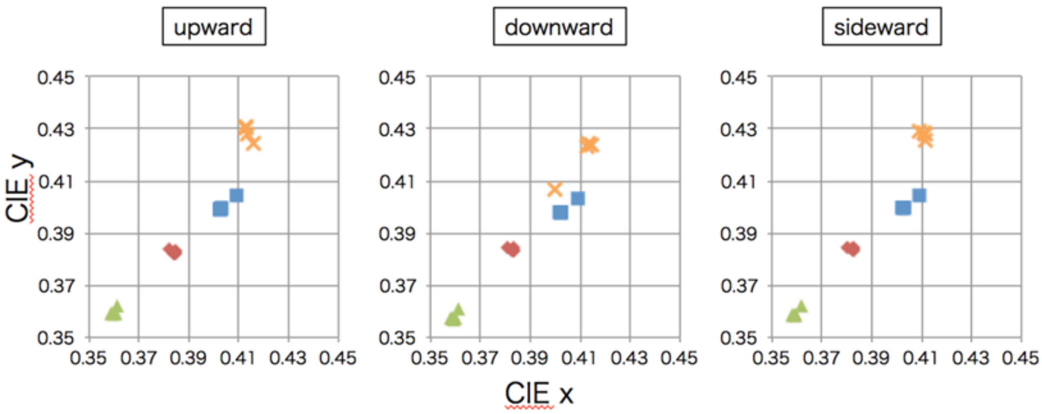

Figure 4 – Chromaticities of each OLED panels obtained from different postures. Different symbols denote the data obtained from different makers: blue squares, red diamonds, green triangles and orange crosses indicate the results obtained from maker (a) (b) (c) and (d), respectively.

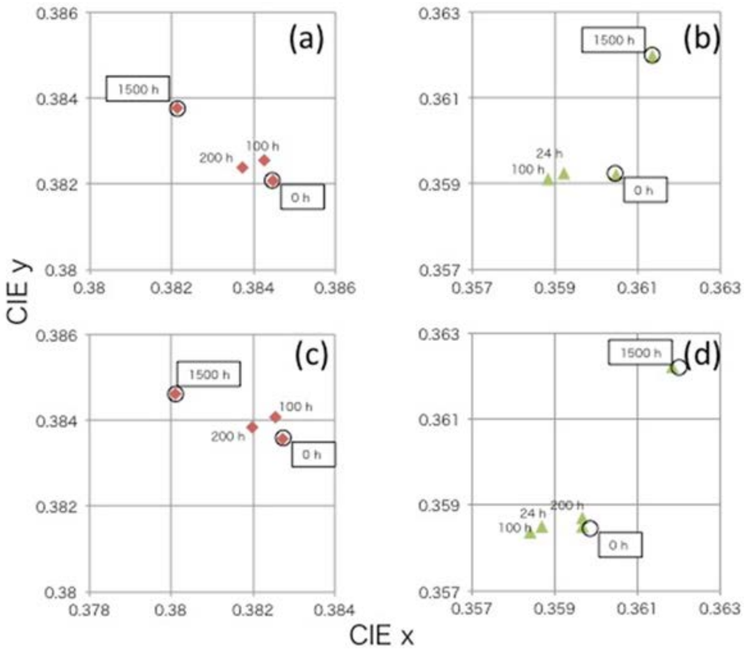

Figure 5 – Chromaticity shift of each OLED panels of maker (b) and (c).Panels (a) (b) (c) and (d) show the results obtained (a)(b) upward (c)(d) sideward. Panels (a)(c) are from maker (b) and (b)(d) are from maker (c).

trends.

4 Conclusions

Until the end of February, we have run 1500 continuous hours of operation of the OLD panels in three different postures to find if the postures of the panels affect the flux maintenance. So far, it appears that the posture doesn’t have distinct effects on the flux maintenance. We are going to continue this experiment further to check if there can be any influence owing to the posture in the long run, either in flux or in chromaticities. If any factors caused by temperature may play a role in non-uniform degradation of the panel, we expect to obtain some posture dependent change.

References

Hirasawa, M. and Yamauchi, Y., 2012. Thermal Effects on Optical Measurement of the OLED Lighting, CIE 2012, 643-646

IESNA 2008. IES LM-80-08 Measuring Lumen Maintenance of LED Light Sources.

OP40

NEW MEASURES OF LIGHT MODELLING

Veronika Zaikina[1], Barbara Szybinska Matusiak[2], Christian A. Klöckner[3]
[1,2] Department of Architectural Design, Form and Colour Studies, Norwegian University of Science and Technology, Trondheim, NORWAY
[3] Department of Psychology, Norwegian University of Science and Technology, Trondheim, NORWAY
veronica.zaikina@ntnu.no

Abstract

Most of the current lighting recommendations aim at ensuring a minimum quantity of light needed to see objects in the surrounding environment and to enable work or other activities.

Authors believe that these recommendations and measures are not a guarantee for the lighting quality. The qualitative aspects of lighting are frequently discussed topics in the lighting community. One of the issues that the currently used measures touch only sporadically is e.g. light modelling. We set up an experiment where different measures of light modelling were studied with help of High Dynamic Range Imaging technique. The analytical comparison of survey results from 32 subjects and measures obtained from luminance maps showed that the Contrast measurement (calculated with the Weber formula) and the Ratio between average luminance of the object and average luminance of the background are both good predictors for contour distinctness of the observed objects.

Keywords: Luminance maps, light modelling, luminance measurements, HDR images

1 Introduction

We live in a three dimensional space and have a fantastic aptitude for constant perception of different qualities of objects i.e. size, shape and colour, depending on the way they are viewed (Boyce, 2003). Is an adequate visibility of 3D objects important for us? Apparently yes, and moreover, it is a vital ability that enables us to see the world around and to communicate with other human beings. The current building codes for daylighting design in buildings are very simplified and use, in most countries, the daylight factor as the fundamental measure (Mardaljevic et al., 2009); other recommendations are sparse and tell very little about qualitative aspects of lighting. On the other side, research tells us that providing better recommendations is crucial because creating a comfortable and pleasant environment for occupants may increase productivity and health, may indirectly improve their home life by reducing job related stressors, and thus indirectly increase economic benefits of the companies (Aries et al., 2010).

During the past few years, researchers tried to investigate new daylighting metrics. Some studies suggest particular techniques based on standardised climate datasets, so called Climate-based daylight modelling (CBDM) and development of certain luminous quantities associated with factors related to visual comfort and quality (Mardaljevic et al., 2009). Another study dedicated to assessing of the set of metrics based on illuminance, distribution, glare and directivity and suggested that these are the most useful measures for the determination of the daylighting quality of architectural spaces (Cantin and Dubois, 2011). In both these investigations luminance measurements were included to some extent. A “Daylighting dashboard” approach was suggested in another study where eight particular daylighting metrics were analysed. The main goal was to use average illuminance, coverage, diffuse daylight, daylight autonomy, circadian stimulus, glazing area, view and solar heat gain, as a determinant measures during the conceptual phase of architectural design (Leslie et al., 2012).

The light modelling is one of several lighting quality characteristics, deprived of the attention of the researchers. With light modelling we mean the degree to which the light describes 3D-objects, so both the contour and shape are clearly visible. The better the light modelling is, the easier we distinguish 3D-objects from the background, and the more correctly we perceive its 3D-shape and their specific characteristics. A good light modelling is important in different spheres: from hospital lighting to museum or commercial lighting. The possibility to predict light modelling in particular rooms and spaces would be an undoubted advantage for architects and designers.

Some researchers tried to shed light onto the topic of light modelling earlier. Different approaches were used. One of them is illuminance measurement using a six-sided illumination meter for prediction of shading pattern of various objects or the distribution of eye illuminance at a given point (Cuttle, 2008). Another approach suggests using a particular instrument, a modelling sensor, to predict light distribution on a 3D-object, occurrence of light spots, cast shadows and to register the light direction (Matusiak, 2002).

Another rather new technique offers new options in studying light modelling characteristics, namely High Dynamic Range Imaging (HDRI). The High Dynamic Range image is a merged image of several conventional low range images taken with different exposures that contains full luminance information of the photographed region. The term “luminance map” can also be used instead of HDR images, to accentuate that the picture has been utilized specifically for the luminance measurements. The luminance-based design is a new approach to lighting design applying such pictures. It is currently being promoted by number of scientists and by CIE Technical Committee 3-45 as a perception-oriented method for lighting design (Nakamura et al., 2011). The prime advantage of this method is that the luminance is the measure that the visual perception can be most correctly described by, e.g. the perception of brightness as a function of luminance (Gilchrist, 2007).

The aim of the current study was to develop measures of light modelling by exploration of a daylit environment (the full-scale mock-up room) furnished with achromatic and chromatic 3D objects with the help of luminance mapping technique.

The hypothesis asserts that certain numerical luminance values or luminance ratios obtained from HDR images may adequately describe the modelling of daylit 3D objects as being observed by subjects.

2 Methodology

The real-life experiment consisted of the observation of 3D achromatic and chromatic objects placed in the full-scale mock-up room and simultaneous photographing of the observed environment. A previous experiment conducted by the authors showed that low saturated colours and interiors containing this type of colours could be successfully studied using luminance mapping technique (Zaikina, 2012). Therefore, it was decided to include coloured objects into the new experiment. The main data sources were subjective ratings of contour and shape visibility provided by participants in a quantitative questionnaire, graphical information i.e. drawings made by participants, and subsequently generated HDR images. In this case taking 180° HDR images or luminance maps was a method that enabled the technical-instrumental recording of the observed visual scene under the real conditions concurrently with surveying the subjects. The method of HDR Imaging is now well established and its reliability was previously tested regarding accuracy in different lighting conditions, different times of the day and representations of the different colours by a number of researchers (Inanici, 2006; Anaokar and Moeck, 2005; Chung and Ng, 2010; Cai, 2011). The experiment was conducted under the real daylight conditions, on several days, from 09:00 to 13:00. A number of female Venetian masks were chosen as 3D objects for observation. On the one hand, they are realistic enough to remind of a real human face and thus carry semantic importance for people, but nevertheless simplified and stylized so that no unnecessary noise is added to the data. On the other hand, masks possess the qualities typical for other non-face-like 3D objects: they have a well distinguishable convex shape and contain a number of small elements and details.

2.1 Experiment design

The experiment was performed in the Room Laboratory, the laboratory for construction of small full-scale spaces at the Faculty of architecture, Norwegian University of Science and

Technology, Trondheim, Norway (http://www.ntnu.edu/bff/laboratories). Data was collected during eight days under stable overcast sky conditions within two weeks of August 2013. The experimental space was a full scale mock-up room with no particular function. It was a non-specific room with one daylit opening and walls made of portable wall elements. The size of the room was 4,8 m ×4,8 m, height was 2,5 m. Two shelves were placed in the room at two different but adjacent walls. One shelf was illuminated by reflected daylight and the other shelf was illuminated by side-light from the window. The glare was avoided with the help of a partition wall constructed in front of the window. The shelves were made of box-like cells 0,5 m × 0,5 m in size, that were painted in different achromatic and equiluminanat chromatic colours. The 3D objects (Venetian masks) were also painted in the same colours as the cells. Most of the colours were low saturated: grey, pink, green; additionally white and dark grey were used. Notations of the colours according to NCS colour system can be found in Table 1.

Table 1 – Notations of the colours used in the experiment, according to NCS Colour System

Name of the colour used in paper	Dark grey	White	Green	Pink	Grey
Nominal colour nearest NCS sample	S 6005-R80B	S 0300-N	S 0520-G40Y	S 0510-R20B	S 1002-B50G

The combination of colours of the objects and colours of the cells (namely colour of the object and colour of the background) was different and unique for each cell; totally it was 18 different combinations. Positive and negative contrasts were provided for observation. The composition of the coloured objects and backgrounds was the same for both shelves, but the textures of the masks were different. The shelf with mostly diffuse lighting presented matte objects, while the shelf illuminated from the side presented glossy objects, see Figure 1. The light level in the experimental room was kept low, as it was of importance to create a situation with hardly visible objects. Two subjects observed the objects in the room and answered the questionnaires at the same time. They were sitting on adjoining chairs. The camera was placed between them at eye-level, namely at a height of 1,2 m. A set of 11 low dynamic images were taken immediately before the participants started to answer the questions. During this photographing session that lasted approximately 10 minutes, participants were able to adapt to the lighting conditions in the room.

Figure 1 – Picture showing (a) an overview of the experimental room, and (b) the plan of the experimental room

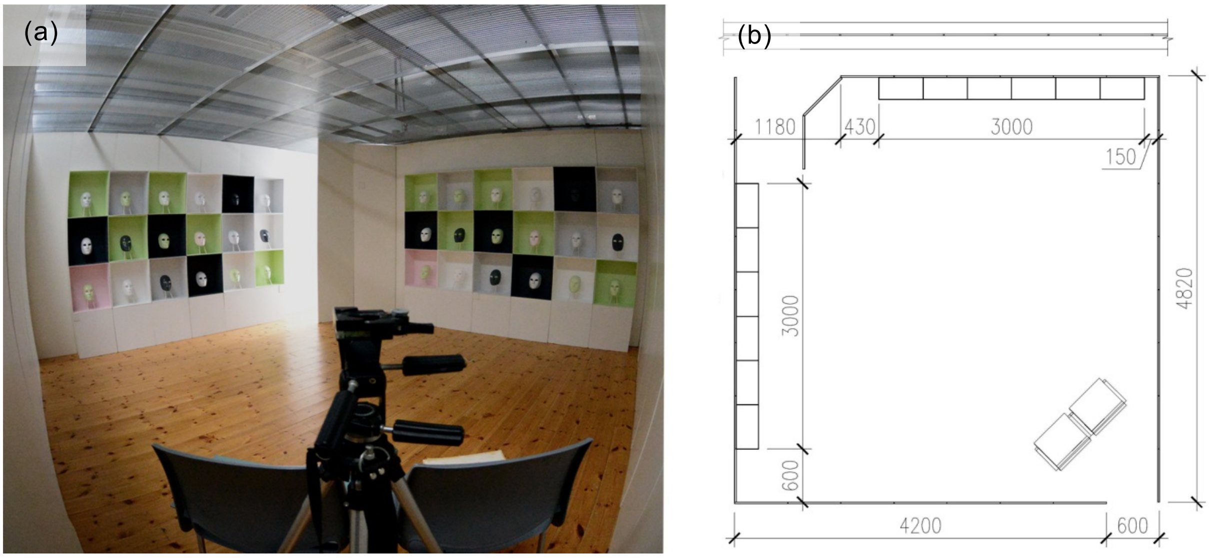

2.2 Participants

In total 32 subjects participated in the experiment. Age of the participant varied from 14 to 74, the average age was 32 years, standard deviation was 10,76. Most of the respondents were naïve with such a type of experiment; they had a different educational background and professions. Before staring the experiment, the vision of the participants was tested with the following vision tests: the visual acuity test using a Snellen chart, the Ishihara test for colour vision, a contrast sensitivity test (Vigra program); normality of 3D-vision was self-reported. According to these vision controls all the respondents had normal or corrected to normal vision and were allowed to participate in the experiment.

2.3 Questionnaire

The questionnaire consisted of two main questions:

1. How well can you distinguish the contour of the object?
2. How well can you distinguish shape and details of the object?

Both questions were asked about each of the 36 objects. The subjects were requested to mark their answers on a four-point ordinal scale with the following options:

- indistinguishable
- just distinguishable
- well distinguishable
- perfectly distinguishable

In addition, subjects specified indistinguishable and perfectly distinguishable zones at a drawing of the mask included in the questionnaire. When two participants simultaneously started the observation, one of them started with the evaluation of glossy masks while the other evaluated the matte objects first. After finishing the evaluation of one shelf with masks, they started to evaluate the second shelf without changing their position in the room. The whole procedure with one pair of the participants took approximately 1 hour.

2.4 Camera settings and manual measurements

Totally, 17 sets of 11 low-dynamic images of the observed scene were made with a Nikon D600 digital camera. To ensure of sharpness the camera was mounted on a tripod and situated between participants' chairs. The following camera settings were used: white balance – Cloudy, Auto-Bracketing – off, sensitivity – 200 ISO, auto focus – Auto, aperture – fixed, f/4. Exposure variations were achieved by varying the shutter speed in manual exposure mode with step 1 EV. All the camera settings were adjusted by dint of a computer and with the Nikon Camera Control Pro software.

For further calibration of the HDR images the manual luminance measurements were taken in four specially marked points at the observed scene. For these purposes a Minolta LS-100 luminance meter was used. Manual measurements were repeated with each new photographing session and each new pair of respondents.

All the low dynamic range images were processed and combined into HDR images with the help of the Photosphere software (Ward, 2005). After this step a calibration was applied according to the readings from the manual luminance measurements.

2.5 Measurements from luminance maps

Luminance measurements were done using two programs: the Photosphere (that was used during the preparation phase for merging of low dynamic images and calibration) and hdrscope (Kumaragurubaran and Inanici, 2013). In this particular case, both the general and the point measurements were taken in Photosphere program. Luminance measurements of multiple selected regions, complex figures and Contrast values were obtained from hdrscope software. The contrast is calculated in this program as the Weber ratio, i.e. the difference of the mean luminances of chosen foreground and background regions divided by the mean luminance of the background (Valberg, 2005), see equations 1 and 3. For convenience, we shell use the term Contrast further in this article. As a background the whole area of the cell were selected for analysis. Another measure of interest was ratio between mean luminance of the mask and mean luminance of the background (see equation 2 and 3), further will be called Ratio. The Ratio was calculated, but not generated by any of the used programs.

$$C_W = \frac{L_o - L_b}{L_b} \qquad (1)$$

where

L_o is the luminance of the object;
L_b is the luminance of the background.

$$C_R = \frac{L_o}{L_b} \qquad (2)$$

where

L_o is the luminance of the object;
L_b is the luminance of the background.

$$C_W = C_R - 1 \qquad (3)$$

where

C_R is the luminance ratio.

To the authors' opinion, this method provides a great opportunity of getting rich information based on luminance readings from different regions at the luminance maps.

3 Statistical analysis and results

In this paper the authors present the earliest results related to the first question i.e. contour distinctness.

For the statistical analysis of the data a two-level ordinal regression analysis was chosen. The experimental design with 32 participants evaluating 36 masks each resulted in a data structure where 36 evaluations were nested within each participant. To eliminate the noise that each participants' general answering patterns contributed to the data, the main analysis was conducted at the object level, but the person specific variance in the evaluations across all masks was modelled simultaneously (listed as Level 2 variance in Table 2 and 3). The regression analysis was conducted as an ordinal (and not linear) regression because the dependent variable "distinctness of the contour" had neither equidistant nor normally distributed answers across the categories.

In two separate analyses (Table 2 and Table 3) the Contrast and the Ratio were assessed as main predictors of contour distinctness and as the dependent variable, while type of the surfaces (glossy or matte), coloration (chromatic or achromatic) and order of observation were assessed as additional independent control variables. Because the characteristics of both main predictors are different below and above the zero contrast point (which is 0 for the Contrast and 1 for the Ratio) within each analysis to separate sub-analyses were conducted (left and right half of the table).

Results show that both measures (Contrast and Ratio) are equally good predictors of the distinctness of the contour of the observed masks (see Table 2 and 3).

Table 2 presents the results for the ratio of the mean luminance of the mask and the mean luminance of the background. The Ratio has a highly significant and strong negative impact on the visibility of the contour in the area of negative contrast, which means the closer the ratio approaches 1 the more difficult it is to see the contour. For positive contrasts the Ratio has a highly significant and strong positive impact, which means that the larger the Ratio value exceeds 1, the better the visibility of the contours. The type of the surface has an impact on the visibility of the contour only for dark masks on light backgrounds, but the impact is small. It means that glossiness enhances visibility of the contour of dark masks (negative contrast). Also the order of observation has a small impact for dark masks on light backgrounds. Chromaticness has a small but significant impact for light masks on dark backgrounds, where contours are slightly more difficult to see if the mask is chromatic. Figure 2 presents the probability plots for the probability to select one of the four categories (perfectly distinguishable) in the questionnaire depending on the four combinations of the control variables glossiness and chromaticness. The order effect was controlled when calculating the probabilities.

Table 2 – Regression analysis results: corellation between contour distinctness and Ratio

	Ratio ≤ 1				Ratio ≥ 1			
	B	SE	β	p	B	SE	β	p
Ratio	-10,775	1,270	-0,803	< 0,001	0,322	0,022	0,577	< 0,001
Glossiness (0=matte, 1=glossy)	1,123	0,572	0,146	0,049	0,021	0,129	0,005	0,870
Chromaticness (0=achromatic, 1=chromatic)	-0,615	0,406	-0,080	0,130	-0,324	0,134	-0,073	0,016
Order of observation (0=matte masks first, 1=glossy masks first)	-1,589	0,661	-0,213	0,016	-0,533	0,280	-0,120	0,057
Level 2 variance "contour"	1,978	0,970		0,041	0,495	0,161		0,002
$R^2_{level\ 1}$	0,764				0,332			
$N_{level\ 1}$	255				897			
$N_{level\ 2}$	32				32			

Figure 2 – Probability curve for the „perfectly distinguishable“ category of the questionnaire, four combinations of control variables, and Ratio as a main predictor

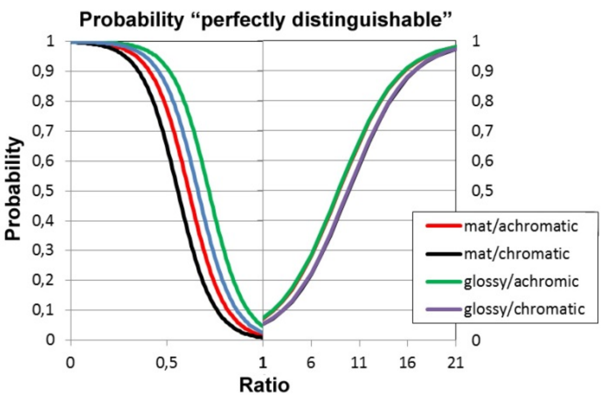

As can be seen in Table 3 and Figure 3 the results are almost identical when the luminance ratio is substituted by the Contrast as main predictor. Here the cut-off for the zero Contrast is "0". The Contrast is a highly significant and strong negative predictor for negative contrasts (better visibility the more negative the Contrast below 0 get) and it is a highly significant, strong positive predictor the more positive the Contrast is. The closer to 0, the more difficult is it to perceive the contour. Again, glossiness and order of observation have a small but significant impact for dark masks on light backgrounds, and chromaticness has a small effect for light masks on dark backgrounds.

Table 2 – Regression analysis results: corellation between contour distinctness and Contrast

	Contrast ≤ 0				Contrast ≥ 0			
	B	**SE**	**β**	**p**	**B**	**SE**	**β**	**p**
Contrast	-10,781	1,271	-0,803	< 0,001	0,341	0,023	0,569	< 0,001
Glossiness (0=matte, 1=glossy)	1,081	0,570	0,141	0,058	-0,004	0,129	-0,001	0,975
Chromaticness (0=achromatic, 1=chromatic)	-0,579	0,404	-0,076	0,152	-0,323	0,134	-0,073	0,016
Order of observation (0=matte masks first, 1=glossy masks first)	-1,572	0,657	-0,212	0,017	-0,531	0,281	-0,120	0,058
Level 2 variance "contour"	1,952	0,959		0,042	0,496	0,162		0,002
$R^2_{level\ 1}$	0,761				0,323			
$N_{level\ 1}$	255				897			
$N_{level\ 2}$	32				32			

Figure 3 – Probability curve for the „perfectly distinguishable“ category of the questionnaire, four combinations of control variables, and Contrast as a main predictor

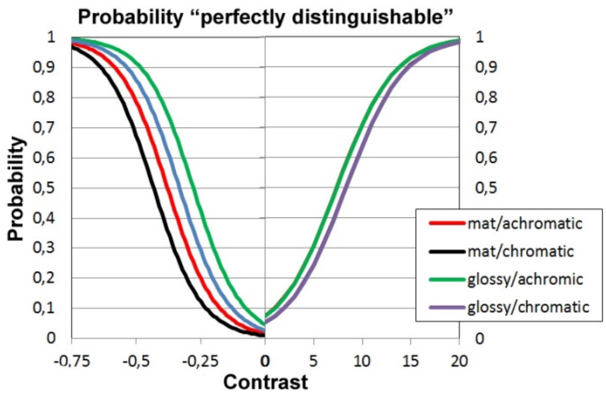

4 Discussion and conclusion

High quality lighting becomes an especially important issue in a time dominated by a dynamic technical development of new light sources and daylighting techniques. A good light modelling is one of the necessary conditions for lighting quality. It is essential both at workplaces and at homes. When we communicate with other people we need to accurately perceive various 3D-objects, especially faces; and we know that the correct interpretation of the human face expression depends on the light distribution on the face and the background.

This experiment has shown that luminance measurements could be promising predictors of light modelling. In this particular case the Contrast and the Ratio were studied as predictors of contour distinctness of the observed Venetian masks. These are measurements that are easy to perform with help of computer software, which is why they became departing point of the current experiment. Correlation of the physical luminance measurements and peoples' perceptions are complex and usually nonlinear, so they should be studied carefully. For this purposes we used a two-level ordinal regression analysis that took into account various interconnections between factors and was able to control for a number of variables, including answering style and other person related factors of the participants. The analysis shows clearly that easily measurable luminance values can predict a large amount of variance in the distinctness of the contours of the 3D objects. However, the conclusions should be tested by other researchers under other lighting conditions and/or with other objects to verify the relations with higher precision.

This article presents only the first step in the whole study. We intend to extend the testing of the different luminance measurements in terms of contour and shape visibility and distinctness. We believe the findings will provide new and useful information helping to develop modern techniques for designing qualitatively comfortable lighting.

References

ANAOKAR, S., MOECK, M. 2005. Validation of high dynamic range imaging to luminance measurements. Leukos, 2(2), 133-144.

ARIES, M., VEITCH, J., NEWSHAM, G. 2010. Windows, view, and office characteristics predict physical and psychological discomfort. Journal of Environmental Psychology, (30), 533-541.

BOYCE, P. R. 2003. Human factors in lighting, 2nd ed. London: Taylor & Francis.

CAI, H. 2011. Camera aided luminance measurement of the luminous surfaces of different light sources. AEI 2011: Building Integration Solutions. American Society of Civil Engineers, pp 272-279.

CANTIN, F., DUBOIS, M.C. 2011. Daylighting metrics based on illuminance, distribution, glare and directivity. Lighting research and technology, 43, 291-307.

CHUNG, T., NG, R. 2010. Variation of calibration factor over time for High Dynamic Range Photography in a single daylit interior scene. Light and Visual Environment, 34(2), 87-93.

CUTTLE, C. 2008. Lighting by design 2nd ed., Elsevier.

GILCHRIST, A. 2007. Lightness and brightness. Current Biology, 17(8), 267-269.

INANICI, M. 2006. Evaluation of high dynamic range photography as a luminance data acquisition system. Lighting Research and Technology, 38(2),123-136.

KUMARAGURUBARAN, V., INANICI, M. 2013. Hdrscope: high dynamic range image processing toolkit for lighting simulations and analysis. In BS2013: 13th Conference of International Building Performance Simulation Association. 3400-3407. Available at: http://courses.washington.edu/hdrscope/index.html

LESLIE. R., RADETSKY, L., SMITH, A. 2012. Conceptual design metrics for daylighting. Lighting Research and Technology, (44), 277-290.

MARDALJEVIC, J., HESCHONG, L., LEE, E. 2009. Daylight metrics and energy savings. Lighting Research and Technology, 41, 261-283.

MATUSIAK, B. 2002. A modelling sensor designed to be used in the lighting practise in cases where there it is essential to compare the modelling ability of light in an important point in a room for different lighting alternatives. Proceeding of CIE 2002, London.

VALBERG, A. 2005. Light, vision, color, Wiley.

WARD, G. 2005. Photosphere, Available at: http://www.anyhere.com.

ZAIKINA, V. 2012. Light level perception in interiors with equiluminant colours. In B. Matusiak & K. Fridell Anter Nordic light and colour. Trondheim: NTNU - The Faculty of Architecture and Fine Art, 105-122.

OP41

APPLICABILITY OF THE UNIFIED GLARE RATING AS ASSESSMENT OF DISCOMFORT GLARE SENSATION BASED ON LUMINANCE MAPS

Scheir, G.H.[1], Hanselaer, P.[1], Bracke, P.[1], Deconinck, G.[2], Ryckaert, W.R.[1]
[1] KU Leuven – ESAT – Light & Lighting Laboratory, Ghent, BELGIUM, [2] KU Leuven – ESAT - ELECTA, Leuven, BELGIUM
gertjan.scheir@kuleuven.be

Abstract

In Europe, the unified glare rating (UGR) is used to assess discomfort glare for interior lighting installations. The UGR has been developed based on uniform light sources but the applicability for non-uniform source luminance is questioned. Based on the luminance distribution of light sources, the UGR formula is alternatively calculated and interpreted. Pixels of a luminance map can be considered as an individual light source or can be grouped in several ways to form larger sources. To test its sub-divisibility, the UGR is calculated for every division of the luminance map. The validity of the formula for uniform and non-uniform sources is compared. Results show that UGR is applicable to uniform light sources but for non-uniform luminaires, UGR is dependent on the chosen division of the luminance map. The use of the UGR formula to assess discomfort glare from non-uniform light sources is questioned and the limitations for applying the UGR have been further refined.

Keywords: Discomfort Glare, UGR, Luminance Map, Luminance Camera, Sub-divisibility

1 Introduction

Discomfort glare is defined by the International commission on illumination (CIE) in the international lighting vocabulary as: “glare that causes discomfort without necessarily impairing the vision of objects” (CIE, 1987) and by the Illuminating Engineering Society of North America (IESNA) as “a sensation of annoyance or pain caused by high luminance in the field of view” (IESNA, 2000). Ever since the beginning of the previous century, researchers have attempted to quantify the amount of discomfort glare (Luckiesh and Holladay, 1925), but even now, the physiological and psychophysical mechanisms are not fully understood.

A multitude of glare indices have been developed in several fields. Glare from windows can be assessed with the Daylight Glare index (DGI) by Hopkinson (Hopkinson, 1972). Wienold and Christoffersen (Wienold and Christoffersen, 2006) further refined the DGI and proposed the Daylight Glare Probability (DGP). For the assessment of discomfort glare in interior lighting, the CIE proposed the Unified Glare Rating (UGR) (CIE, 1995). In North America, Guth developed an alternative index called the Visual Comfort Probability (VCP) (Guth, 1966, Guth, 1963). Other common glare ratings for indoor lighting are the British Glare Index (BGI) and the CIE Glare Index (CGI) (CIE, 1983). In Europe, the UGR is generally accepted for the assessment of discomfort glare in interior lighting and is included in the European standard for indoor workplace lighting EN 12464-1 (CEN, 2011).

All of the above mentioned indices are originally developed based on uniform luminaires. Non-uniform light sources were not taken into account (Cai and Chung, 2012). With a growing market share of led luminaires for interior lighting, a better assessment of discomfort glare from non-uniform light sources becomes essential. By dividing the luminous intensity, obtained from the luminous intensity distribution, by the apparent area of the luminaire, non-uniform luminaires are often approximated as uniform light sources. As an attempt to tackle some problems, the CIE developed a method for small, large and complex sources (CIE, 2002), but discussion about the validity remains (Nonne et al., 2013), as stated by a CIE reporter (CIE, 2009):

‘Your reporter has referred to UGR as a “leaky boat”. Is it time, therefore, to develop a new system rather than to try further patch the “leaks”.’

This illustrates that discomfort glare sensation from non-uniform light sources cannot be correctly assessed with traditional glare evaluating methods (Takahashi et al., 2007, Waters et al., 1995, Kasahara et al., 2006, Cai and Chung, 2012, Kim and Koga, 2004, Higashi et al., 2012, Higashi et al., 2013).

The present study is designed to evaluate the appropriateness of UGR for evaluating the degree of discomfort glare from uniform and non-uniform light sources based on luminance maps. Nowadays, luminance maps can easily be measured (Cai, 2012) and are already used for the evaluation of discomfort glare from daylight environments (Wienold and Christoffersen, 2006). Moreover, the CIE proposed (CIE, 2013) to use luminance maps for the assessment of visual discomfort for indoor applications (Blaszczak, 2003, Blaszczak, 2004, Blaszczak, 2013). Starting from a high resolution luminance map, a single large non-uniform luminaire can be divided into multiple sections and sub-divisibility of the UGR formula can be tested. The effect of different divisions of the luminance map on the calculated UGR value is studied and sub-divisibility of UGR is investigated.

2 UGR and luminance maps

The UGR is defined as (CIE, 1995):

$$UGR = 8\log\left[\frac{0,25}{L_b}\sum_{i=1}^{n}\frac{L_i^2\omega_i}{p_i^2}\right] \tag{1}$$

with

L_b the background luminance

L_i the luminance of the light source

ω_i the solid angle of the light source

p_i the Guth position index of the light source.

The sum in the UGR formula was originally intended over all luminaires in the field of view (i=1,2,...n). Each luminaire is considered as a uniform light source characterized by one luminance level, one position index and one solid angle (Figure 1: left). The formula is valid for sources with a solid angle between 0,1 and 0,0003 sr (CIE, 1995). For smaller sources as for larger and complex sources, the CIE developed an alternative formula (CIE, 2002). Glare sensation from small sources is determined by intensity rather than by luminance level and is calculated as:

$$UGR_{small} = 8\log\left[\frac{0,25}{L_b}\sum_{j=1}^{k}200\frac{I_j^2}{r_j^2 p_j^2}\right] \tag{2}$$

with

I_j the intensity of the light source

r_j the distance from the eye to the light source.

Instead of considering a light source as uniform, a large or non-uniform luminaire can be considered as a combination of multiple smaller independent light sources (Figure 1: right) and the summation in the UGR formula can be interpreted accordingly (j=1,2,…,k).

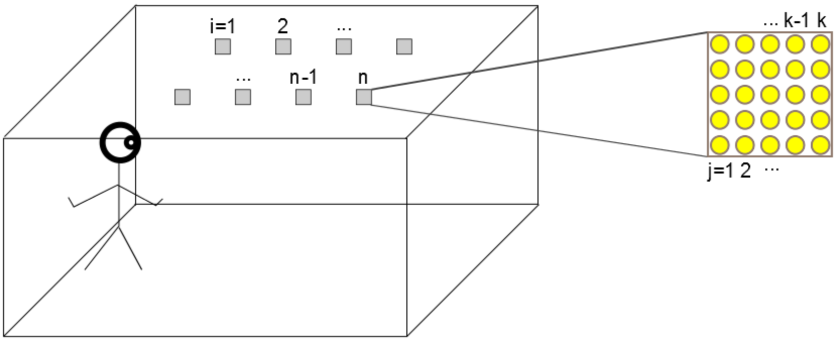

Figure 1 – Left: The sum in the UGR formula is originally intended over all luminaires in the field of view (i=1,2,…,n). Right: The summation in UGR can be interpreted alternatively by considering a source as a combination of multiple smaller sources (j=1,2,…,k).

Luminance maps can be used to test sub-divisibility since they provide information per pixel. Each pixel has a specific luminance level, solid angle and position index and different pixels can be grouped. The solid angle of a group is the sum of solid angles of all pixels within the group. The luminance level of a group is the mean of all pixels within the group and is considered uniform. By weighing the position of each pixel with its luminance value, the average position of a group is calculated and the position index can be determined.

In this experiment, several pixel grouping methods are considered:

- *Maximum*: each pixel can be considered as an independent light source, resulting in the maximum number of subdivisions for the luminance map.
- *Square*: neighbouring pixels are merged into square formations, resulting in fewer but larger groups (Figure 2: left).
- *Step*: Pixels with a luminance value in the same range are grouped (Figure 2: right). Luminance groups are generated by defining luminance boundaries resulting in luminance bins. Bin boundaries are constructed by a grayscale standard display function, developed by the National Electrical Manufacturers Association for digital imaging and communication in medicine (NEMA, 2011). The display function generates boundaries with an equal difference in perceptual luminance level between subsequent bins. By adjusting the step discussed, different luminance boundaries are generated resulting in different luminance bins.
- *Uniform*: the luminaire is considered uniform, comparable with the originally intended UGR calculation (CIE, 1995).

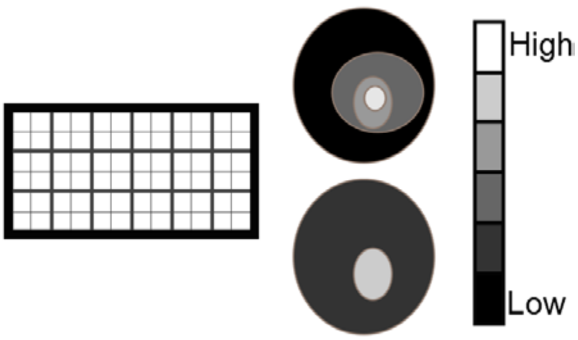

Figure 2 - Left: Neighbouring pixels are merged into square formations (in this example 72 pixels or 18 groups). Right: Pixels are grouped according to their luminance level.

For every division of the luminance map, a different amount of terms in the UGR summation will occur, possibly resulting in a different calculated UGR value. When the UGR value depends on the chosen number of subdivisions, UGR is not sub-divisible.

3 Experimental setup

To investigate the sub-divisibility of the UGR formula, three uniform and three non-uniform luminaires are considered. The uniform luminaires are (1) a naked fluorescent lamp in a white fitting, (2) a led tube with diffusor and (3) a led matrix with diffusor. As non-uniform luminaires, (4) a luminaire with 4 leds and clear optic lenses, (5) a led tube with clear optics and (6) a led matrix without any secondary optics are considered.

High resolution luminance maps (Figure 3) for all luminaires were measured with a calibrated LMK 98-4 luminance camera (TechnoTeam, 2012) mounted on a RiGO 801 near-field goniometer (TechnoTeam, 2009).

The centre of each luminaire is placed at the line of sight of the luminance camera, and thus the theoretical observer. In this experiment, the Guth position index is calculated for every pixel of the luminance map separately using a formula proposed by Levin (Levin, 1975) and used by the IESNA (IESNA, 2000). The background luminance is chosen arbitrairly at a value of 100 cd/m², comparable to the background luminance in an office.

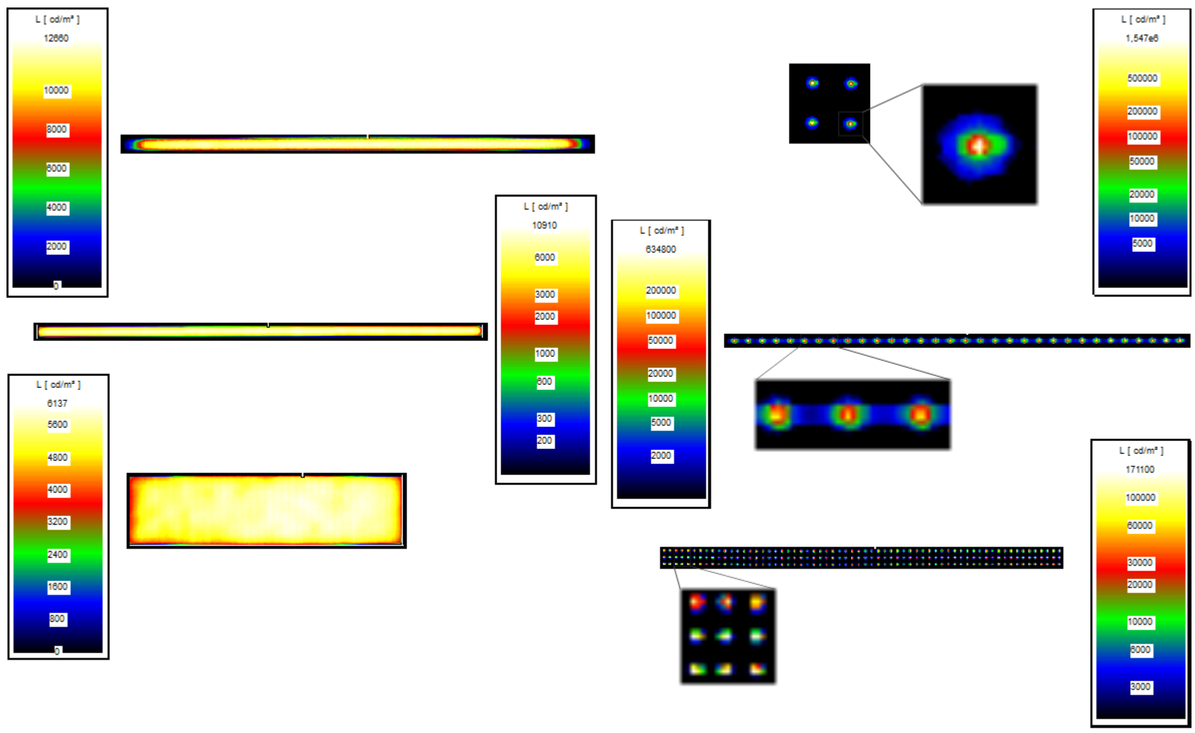

Figure 3 – Luminance map of the uniform (left) and non-uniform (right) luminaires. The uniform luminaires are a naked fluorescent lamp in a white fitting, a led tube with diffusor and a led matrix with diffusor. As non-uniform luminaires, a luminaire with 4 leds and clear optic lenses, a led tube with clear optics and a led matrix without any secondary optics are used.

4 Results and discussion

The calculated UGR value for different numbers of subdivisions of the luminance map obtained both by luminance grouping and pixel grouping in square formations is shown in Figure 4. The single group approximation of the luminance map results in the same UGR value for both grouping methods.

When dividing luminance maps, the position index of the subdivisions will not differ much from the position index of the luminaire as a whole since all light sources are not larger than 1,2 m (led tubes), seen from a distance of 1,54 m, resulting in a minimum and maximum position index of 1,0 and 1,26 respectively. For the uniform luminaires, the luminance is approximately constant. The mean luminance value of the luminaire as a whole will not differ much from the luminance values of the separate subdivisions. Hence, UGR obtained for the luminaire as a whole will not differ much from the UGR value calculated with more terms (subdivisions).

For non-uniform luminaires, when dividing luminance maps, the change in position index remains small but the luminance value of some smaller groups will be significantly larger than the mean luminance value of the luminaire as a whole. In the UGR formula, the effect of luminance is quadratic (equation 1). Subdivisions with a higher luminance value will be more important in the calculation compared to subdivisions with a lower luminance value. While the total mean luminance level remains constant, the higher the luminance value of some subdivisions, the higher the UGR value. This explains the rise in UGR for the non-uniform luminaires when the number of subdivisions increases (Figure 4).

The choice of a pixel grouping method has an effect on the maximum number of subdivisions possible. For the luminance grouping method, to maintain equal steps in perceptual luminance value, bin width must increase with luminance level and thus pixels with the highest luminance level will always be grouped in the same luminance bin. The maximum number of subdivisions for a luminance map divided in the smallest square formations possible, which is for each pixel a separate subdivision, can never be reached with the luminance grouping method (Figure 4).

The overall minimum and maximum, disregarding the number of subdivisions or grouping method, and the range of UGR values are summarized in Table 1. The range of UGR for the matrix with diffusor, led tube with diffusor and naked fluorescent lamp is 1,0, 2,1 and 1,6 respectively. Since 1 UGR unit represents the smallest noticeable difference in discomfort glare sensation and 3 UGR units correspond to a criterion step (e.g. perceptible, just acceptable, unacceptable,…) (Geerdinck, 2012), the returned UGR values are all comparable for the uniform luminaires, independent of the used grouping method or number of subdivisions. Therefore, for uniform luminaires, UGR is robust and valid. The range of UGR for the non-uniform led luminaire with clear optic lenses, the led tube with clear optics and the led matrix without secondary optics is 17,3, 12,0 and 9,1 respectively. The difference is more than three criterion steps in discomfort glare evaluation. Therefore, for non-uniform luminaires, calculating UGR based on luminance maps does not result in a single well-defined value and the applicability of UGR is questioned.

Table 1 – Minimum, maximum and range of UGR value disregarding the used grouping method or number of subdivisions.

		Minimum	Maximum	Range
Uniform	Fluorescent lamp	27,0	28,6	1,6
	Tube diffusor	22,6	24,7	2,1
	Matrix diffusor	30,3	31,2	1,0
Non-Uniform	Clear	21,5	38,8	17,3
	Tube clear	23,7	35,7	12,0
	Matrix	25,9	35,0	9,1

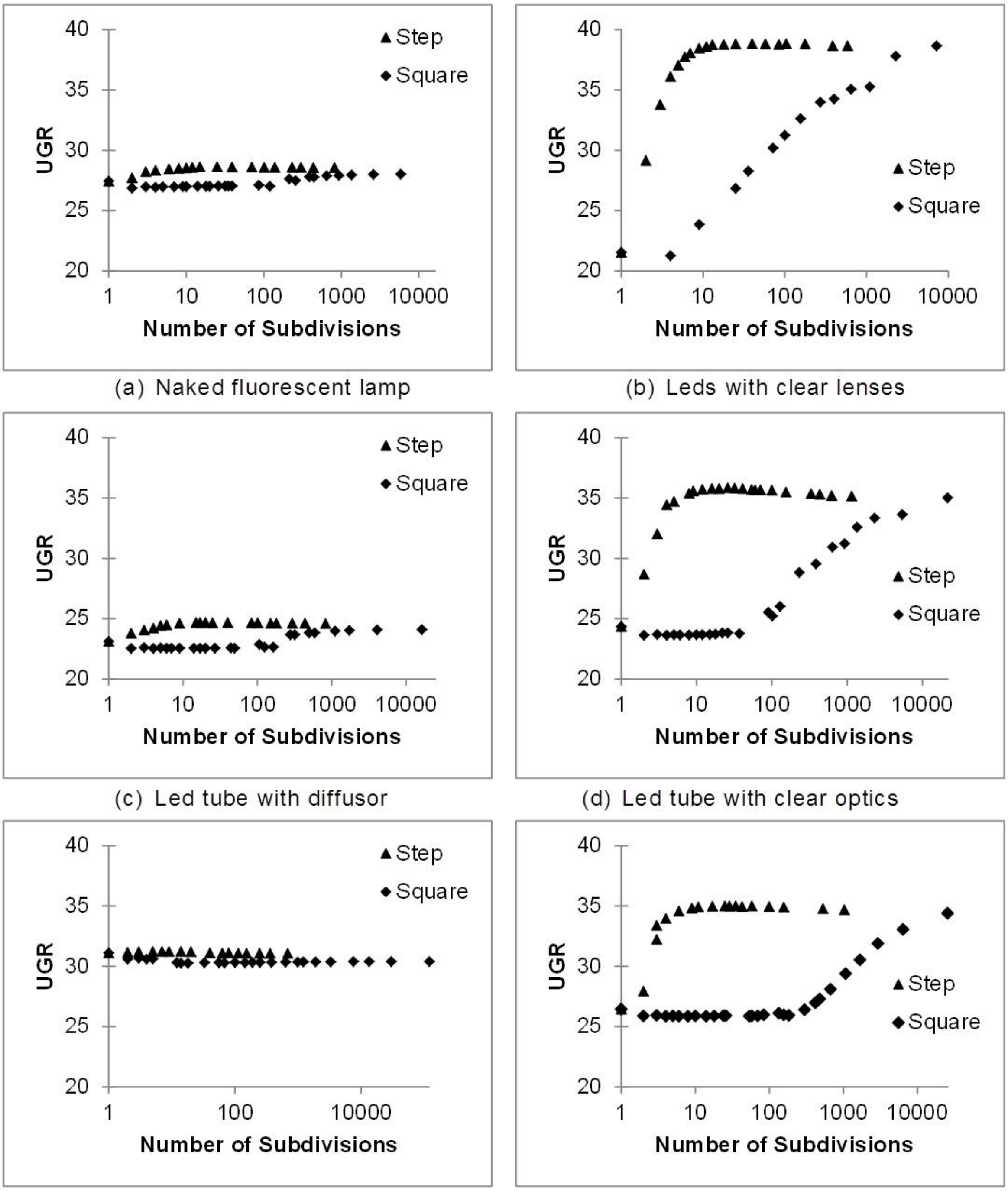

(a) Naked fluorescent lamp

(b) Leds with clear lenses

(c) Led tube with diffusor

(d) Led tube with clear optics

(e) Led matrix with diffusor

(f) Led matrix without optics

Figure 4 – Calculated UGR values for uniform (left) and non-uniform (right) luminaires. The luminance grouping is denoted as 'Step'. The pixel grouping method in square formations is denoted as 'Square'.

5 Conclusion

In this study, the sub-divisibility and applicability of the UGR has been investigated based on luminance maps. Three uniform and three non-uniform luminaires were studied and compared. Several divisions of luminance maps were obtained and UGR was calculated by considering each subdivision as a separate light source. The results are summarized as follows:

- For the uniform luminaires, difference in UGR value due to the number of subdivisions or the grouping method are smaller than 3 UGR units or 1 discomfort glare criterion.
- For non-uniform luminaires, difference in UGR value due to the choice of grouping method or number of subdivisions is larger than 9 UGR units or 3 criterion steps.

Conclusively, the use of UGR remains valid for uniform luminaires but for non-uniform light sources, the applicability of UGR is questioned.

Acknowledgements

The authors wish to thank the Hercules Foundation for funding the near-field goniophotometers as medium-scale infrastructure project (AKUL-35), ETAP for providing technical assistance and KU Leuven for funding (BAM).

References

BLASZCZAK, U. J. Idea of objective glare measurement. Photonics Applications in Astronomy, Communications, Industry, and High-Energy Physics Experiments, 2003. 317-321.

BLASZCZAK, U. J. The method of estimation of background luminance in objective glare measurements. Optical Security and Safety, 2004. 234-238.

BLASZCZAK, U. J. 2013. Method for evaluating discomfort glare based on the analysys of a digital image of an illuminated interior. *Metrology and Measurement Systems,* 20**,** 623-634.

CAI, H. 2012. High dynamic range photogrammetry for synchronous luminance and geometry measurement. *Lighting Research and Technology*.

CAI, H. & CHUNG, T. 2012. Evaluating discomfort glare from non-uniform electric light sources. *Lighting Research and Technology*.

CEN 2011. Light and lighting - Lighting of work places - Part 1: Indoor work places.

CIE 1983. CIE 055:1983. Discomfort Glare in the Interior Working Environment. Paris: CIE.

CIE 1987. *International Lighting Vocabulary,* Vienna, CIE.

CIE 1995. CIE 117:1995. Discomfort Glare in Interior Lighting. CIE.

CIE 2002. CIE 147:2002. Glare from Small, Large and Complex Sources. CIE.

CIE 2009. CIE R3-24:2009. Overhead Glare Reportership. Vienna: CIE.

CIE 2013. CIE 205:2013. Review of Lighting Quality Measures for Interior Lighting with LED Lighting Systems. CIE.

GEERDINCK, L. 2012. *Glare perception in terms of acceptance and comfort.* Graduation Report, Eindhoven University of Technology.

GUTH, S. 1963. A method for the evaluation of discomfort glare. *Illuminating Engineering,* 58**,** 351–364.

GUTH, S. K. 1966. Computing Visual Comfort Ratings For a Specific Interior Lighting Installation. *Illuminating Engineering,* 57**,** 351-364.

HIGASHI, H., KOGA, S. & KOTANI, T. The development of evaluation for discomfort glare in LED lighting of indoor work place - relationship between UGR and subjective evaluation. Proceedings of CIE 2012 Lighting Quality & Energy Efficiency, 2012 Hangzhou, China.

HIGASHI, H., KOGA, S. & KOTANI, T. The development of evaluation for discomfort glare in LED lighting of indoor work place: the effect of the luminance distribution of luminous parts on subjective evaluation. Proceedings of the CIE Centenary Conference “Towards a New Century of Light”, 2013 Paris, France.

HOPKINSON, R. G. 1972. Glare from daylighting in buildings. *Applied Ergonomics,* 3**,** 206-215.

IESNA 2000. *The IESNA Lighting Handbook*.

KASAHARA, T., AIZAWA, D., IRIKURA, T., MORIYAMA, T., TODA, M. & IWAMOTO, M. 2006. Discomfort Glare Caused by White LED Light Sources. *J. Light & Vis. Env.,* 30**,** 9.

KIM, W. & KOGA, Y. 2004. Effect of local background luminance on discomfort glare. *Building and Environment,* 39**,** 1435-1442.

LEVIN, R. E. 1975. Position Index in VCP Calculations. *Journal of the Illuminating Engineering Society,* 4**,** 99-105.

LUCKIESH, M. & HOLLADAY, L. L. 1925. Glare and Visibility. *Transactions of the Illuminating Engineering Society***,** 221-252.

NEMA 2011. Digital Imaging and Communications in Medicine (DICOM). *Part 14: Grayscale Standard Display Function.* National Electrical Manufacturers Association.

NONNE, J., RENOUX, D. & ROSSI, L. 2013. Metrology for solid-state lighting quality. *International Congress of Metrology***,** 14004.

TAKAHASHI, H., KOBAYASHI, Y., ONDA, S. & IRIKURA, T. 2007. Position Index for the Matrix Light Source. *Journal of Light & Visual Environment,* 31**,** 128-133.

TECHNOTEAM 2009. Operation Near-field goniophotometer type RiGO 801

TECHNOTEAM 2012. Werkskalibrierung LMK 98-4.

WATERS, C. E., MISTRICK, R. G. & BERNECKER, C. A. 1995. Discomfort glare from sources of non-uniform luminance. *Journal of the Illuminating Engineering Society,* 24**,** 73.

WIENOLD, J. & CHRISTOFFERSEN, J. 2006. Evaluation methods and development of a new glare prediction model for daylight environments with the use of CCD cameras. *Energy and Buildings,* 38**,** 743-757.

OP42

EVALUATING DISCOMFORT GLARE FROM WINDOWS WITH NON-UNIFORM LIGHT DISTRIBUTION

Chung, T.M., Ng, R.T.H., Yao, C.
Department of Building Services Engineering, The Hong Kong Polytechnic University, HONG KONG
tm.chung@polyu.edu.hk

Abstract

This study examined the suitability of daylight glare index (DGI), new daylight glare index (DGI_N), and daylight glare rating (DGR) for evaluating discomfort glare from windows with a non-uniform light distribution. An experiment with seven test settings was conducted in two daylit cellular offices. High dynamic range (HDR) photography was used to obtain the per-pixel luminances of the glaring sources, the window, and the background of the offices for calculating DGI, DGI_N, and DGR. The sub-divisibility and additivity of DGI, DGI_N, and DGR was tested via statistical methods. Their predictability was evaluated using 95 subjects. It was found that DGI, DGI_N, and DGR all fail in the tests of sub-divisibility or additivity, and overestimate the discomfort glare sensation from windows with a non-uniform light distribution that young people in Hong Kong may feel.

Keywords: Daylight, Discomfort Glare, High Dynamic Range Photography, Luminance

1 Introduction

On one side, daylighting in buildings provides many benefits such as saving electric lighting energy, enhancing human productivity, psychological and physiological well-being; on the other side, a high availability of daylight levels from windows may produce discomfort glare to occupants possibly causing them tending to shade the daylight from windows using curtains or blinds. In order to allow a window designed for daylighting to be used as intended, avoiding discomfort glare coming from windows is therefore very important.

Currently the CIE and major lighting codes or guidelines do not provide any recommendation on daylight glare assessment; however, there are several glare indices proposed by various researchers for predicting and evaluating discomfort glare from windows, although none of them is yet universally accepted, such as the daylight glare index (DGI), the new daylight glare index (DGI_N), and the daylight glare rating (DGR). These three glare indices commonly evaluate daylight glare using three components, and they are the glaring source luminance (L_s), the window luminance (L_w), and the background or adaptation luminance (L_b or L_a).

Discomfort glare from windows usually come from non-luminous and light-emitting surfaces which are rarely uniform. People may feel discomfort glare from the high dynamic range of luminance or extreme variation when they perceive the non-uniform light. However, when DGI, DGI_N, and DGR were developed, they did not take any possible non-uniform light distribution from the glaring sources or windows into account but simply assumed the source or window luminances to be a single value. A major reason is the lack of an effective measurement method for luminance from a non-uniform distribution.

Conventionally luminance measurement is carried out using luminance meters in a point-by-point manner. It is a tedious process and naturally suffers from random errors. More critical is that the luminance variance within the limited acceptance angle of the luminance meters is assumed averaged. However, daylight varies at all times. These assumptions greatly hinder the development of a precise glare evaluation method for daylighting. Now, these problems can be solved by the high dynamic range (HDR) photography, which uses a single consumer grade digital camera, fitted with a wide-angle lens for simulating the human binocular vision to obtain the per-pixel luminance data across a scene at one time. This paper tested the appropriateness of DGI, DGI_N, and DGR for evaluating discomfort glare from windows with a non-uniform light distribution with the aid of HDR photography.

2 The Three Daylight Glare Indices

Discomfort glare is a sensation of annoyance or pain caused by high luminance located in the visual field, which does not affect visual performance. Poor daylighting design in buildings can create discomfort glare to the occupants, which is produced by the excessive contrast between the bright daylight from windows and the generally darker background of the room. However, evaluating daylight discomfort glare is not an easy task since determining the luminance values concerned have to be executed in the shortest time due to the high daylight variability. To promote maximum use of daylight both economically and psychophysically, there is a need to develop an efficient evaluation of discomfort glare from windows.

Many studies express the degree of discomfort glare perceived as an index, e.g. VCP, BGI, and UGR for evaluating the discomfort glare from artificial lighting. However, these indices cannot be used for the prediction of discomfort glare from windows. There are two principal reasons: (i) the glare indices for artificial lighting were developed to deal with a small source, but the glare source in most daylit environments occupies a large part of visual field resulting in the increase of the adaptation level of the eye and thus the reduction of the glare sensation (Hopkinson, 1960); (ii) there is greater tolerance to mild degrees of discomfort glare from the sky seen through windows than from a comparable artificial light source with the same degree of discomfort glare perceived (Chauvel, 1982).

2.1 Daylight Glare Index

Since a discomfort glare evaluation method exclusively for daylighting is in great demand, laboratory experimental work was conducted to simulate a window by a large illuminated diffusing screen set. This light source could be extended to occupy the whole visual field and its luminance could be varied between 3,5 and 15 000 cd/m^2. The empirical results helped develop a formula to take into account the problems of adaptation and position of the source in the visual field. The formula was modified from the BGI formula so that the prediction of glare from large sources could be aligned with the prediction of glare from small sources. This formula is subsequently known as the Hopkinson-Cornell formula, expressed in Equation (1).

$$GI = \frac{L_s^{1,6}\Omega^{0,8}}{L_b + 0,07\omega^{0,5}L_s} \qquad (1)$$

where L_s is the source luminance, L_b is the background luminance, Ω is the solid angle subtended by the source modified for its position with respect to the field of view, and ω is the solid angle subtended by the source at the eye.

The predictability of Equation (1) for glare sensation from windows was verified in various studies and daylit conditions. Hopkinson (1972) conducted field experiments in classrooms and hospital wards to compare the calculated glare ratings and the perceived discomfort glare from windows using Equation (1). The degree of discomfort glare perceived from windows was found to be lower than that estimated. The hypothesis laid in Equation (1) that the visible part of the sky has a uniform luminance distribution could be blamed for the discrepancy.

Chauvel (1982) modified the Hopkinson-Cornell formula and proposed the daylight glare index (DGI), expressed in Equation (2), which becomes the most widely used index for evaluating discomfort glare from windows nowadays.

$$DGI = 10\log_{10}\left(0,478\sum\frac{L_s^{1,6}\Omega^{0,8}}{L_b + 0,07\omega^{0,5}L_w}\right) \qquad (2)$$

where L_s is the luminance of the patch of visible sky, of the obstructions, and of the ground seen through the window, L_w is the average luminance of the window, ω is the solid angle subtended by the window, and the other symbols have the same meaning as in Equation (1).

Despite its popularity, DGI was criticized by various researchers. DGI leads to a very likely confusion on the interpretation of the source and the window (Chung, 2005). In Equation (2), the “source” refers to each element of the scene visible through the window, i.e. the sky, the obstructions and the ground, while the “window” refers to all apertures visible by the observer and is considered as a single entity. If the scene seen through the window is not divided into elements such that only the sky is visible through the windows or when only the average luminance of the scene through the window is available, then the source luminance would equal the window luminance.

As DGI was modified from the Hopkinson-Cornell formula, it inherits the same problems. First, the DGI formula was created based on experiments using large artificial light sources with a uniform luminance distribution. Evaluating daylight glare in a room with simulated windows could be different from that in reality due to the greater tolerance to windows than to artificial lights. The DGI values calculated for the windows with a non-uniform luminance distribution may also differ greatly from the discomfort glare that the observer actually feels. A few researchers showed the differences between the glare evaluation under real sky conditions and that predicted by DGI (Boubekri, 1992). Waters (1995) also reported that non-uniform sources of light can cause more glare than uniform light sources when positioned perpendicular to the line of sight and less glare when located between 10˚ and 20˚ from the line of sight. Second, the glaring source with a non-uniform luminance distribution can be sub-divided in elements that can be considered with a uniform luminance value, but it has been shown that the type of sub-division influences the final result (Bellia, 2005). The validity and predictability of DGI for evaluating discomfort glare from windows with a non-uniform light distribution is still a question.

2.2 New Daylight Glare Index

Both the Hopkinson-Cornell formula and the DGI are based on experiments with uniform light sources, and overcast sky is necessarily assumed whenever adopting them. Nazzal (2000) proposed the new daylight glare index (DGI_N), expressed in Equation (3), and stated that this glare index can evaluate the discomfort glare also from direct sunlight.

$$DGI_N = 8\log_{10}\left(0{,}25\sum\frac{L_{ex}^2\Omega}{L_a + 0{,}07\sum L_w\omega^{0{,}5}}\right) \tag{3}$$

where L_{ex} is the exterior luminance, i.e. the luminance of the outdoors caused by direct sunlight, diffuse light from the sky, and reflected light from the ground and other external surfaces, L_a is the adaptation luminance, i.e. the luminance of the surroundings including reflections from the internal surfaces, and the other symbols have the same meaning as previously defined.

Nazzal (2000) also provided a protocol for obtaining the luminance values in the DGI_N, It uses three photosensors to measure the illuminance instead of the luminance directly. A sensor is positioned at the observation point and suitably shielded to receive only the light from the window. Two unshielded sensors are respectively placed close to the middle point of the window at a distance of 0,20 m from the glazing to measure the exterior illuminance and near the observation point covering a semicircular 180˚ area to measure the adaptation illuminance. Obtained illuminance values are then converted to luminances via given formulae. However, Bellia (2008) pointed out that this measuring technique cannot take the presence of zones to different luminances into account inside the window and, once set up, the shielding system is only valid for a special geometry of window, and it hits the centre respect to the line of sight.

DGI_N has two major differences with DGI and faces more criticism: (i) L_b is replaced by L_a because of the greater influence that the surrounding luminance has on the discomfort glare, but Fisekis (2003) pointed out that the contribution of the source in the adaptation term is considered twice; (ii) the source means the external source and the source luminance is recommended to measure by an unshielded meter placed near the window facing the whole external surface, but Chung (2005) argued that equating the source with the whole 180˚ external view seen at the window is not correct because the part of the external scene that is not visible to an interior observer does not contribute to the glare from the window. Besides, although the power index of the solid angle in the DGI_N equals 1, its sub-divisibility, additivity and predictability remain challenging since few studies have been conducted on these issues.

2.3 Daylight Glare Rating

Chung (2005) considered the issue of sub-divisibility in daylight glare evaluation when a large window is divided into small sources, and proposed a new formula called the daylight glare rating (DGR), expressed in Equation (4). No field experiment has yet been conducted under real sky conditions to verify the validity of DGR for evaluating discomfort glare from windows.

$$DGR = 8\log_{10}\left(\frac{0{,}088}{\left(L_b + 0.07\sum \omega^{0{,}5} L_w\right)^{0{,}88}} \sum \frac{{L_s}^2 \omega_s}{P^2}\right) \tag{4}$$

where ω is the solid angle subtended by individual divided source element, and the other symbols have the same meaning as previously defined.

Although in reality, windows usually have a complex surface with high luminance gradients, DGI, DGI_N, and DGR did not consider a non-uniform light distribution when developed, but simply assuming that the luminance distribution of the windows is somewhat a consistent. It results in that the glare ratings estimated from these indices may not be accurate to account for the subjective glare sensation. A root cause of this oversight was the lack of an efficient method for measuring luminance from a non-uniform light distribution. This problem can now be solved by the HDR photography.

3 High Dynamic Range Photography

Using HDR photography to achieve luminance mapping is rather new in lighting research. It is a sort of techniques that allows a consumer grade digital camera to record accurately a wide dynamic range of luminance between the darkest and the brightest areas of a real scene in a single image. In HDR photography, low dynamic range (LDR) photographs of multiple exposures are taken to capture a wide luminance variation of a scene and, using data fusion software, merged into a single HDR image with the luminance value of each pixel extended over the luminance span of the human visual system (Inanici, 2006). An ultra-wide angle lens is usually fitted to the camera in order to obtain the luminance across the human binocular visual field.

The multiple exposures can be achieved by changing either the aperture size or the shutter speed whereas the latter one was suggested to be a more reliable measure (Debevec, 1997). There is no recommendation on the choices of the fixed aperture size of the camera. Previous researchers ever used small to large apertures (Debevec, 1997; Xiao, 2002; Anaokar, 2005; Jacobs, 2007). There is also no recommendation about the number of LDR photographs for fusing into one HDR image. In literature, a wide variation of numbers appeared, from 4 (Xiao, 2002) or 6 (Jacobs, 2007) to 11 (Debevec, 1997) or 14 (Inanici, 2006). Theoretically, the more photographs of different exposures are used, the wider dynamic range of luminance can be obtained, and the HDR image can be of higher quality for more accurate luminance mapping.

In between the procedures of data fusion, a camera response function has to be applied. It is a curve that relates the amount of incoming light and the luminance values of the pixels in the image captured by the camera. By using computer software like Photosphere, Radiance, and Photolux, this function can be computationally derived through a self-calibration process from the series of LDR photographs. The camera response function then gives corrections to the luminance value of the HDR image, which is saved in RGBE format. The luminance of every pixel is then extracted by measuring the Y component in the CIE 1931 XYZ colour space by converting the tristimulus values of the pixels from RGB to XYZ.

Anaokar (2005) and Inanici (2006) were the pioneers to compare the per-pixel luminance values obtained by HDR photography with those measured using a point luminance meter. Both studies found that after suitable calibration processes, this technique provides a reasonably accurate method for the acquisition of a wide range of luminance across a scene within a very short period of time.

4 Experiment

An experiment was conducted in two almost identical cellular offices at the perimeter zone of a building floor occupied by the Department of Building Services Engineering at The Hong Kong Polytechnic University in the daytime on weekdays of November 2013 under different but rather stable real sky conditions. Both offices were nearly rectangular in shape with the same furnishings, and had a window on one side of the walls. One of the offices faced west and the other one faced south. Both geometry and luminance data were recorded for the offices. Figure 1 shows the layouts of the offices for conducting the experiment. The window sizes were 2,12 m x 0,70 m for both offices. The observation point was at a height of 1,2 m from the floor with a perpendicular distance of about 2,25 m from the window. Each window was divided into three equally sized sections (0,7 m x 0,7 m): high, middle, and low. Different sections of the window were shielded in the experiment, as shown in Figure 2. The shielding board was black and opaque to ensure that no daylight could penetrate through the shielded window. There were in total seven test settings. During the entire experiment, all the blinds were pulled up and all the electric lights were turned off, such that the offices were fully and solely lit by daylight.

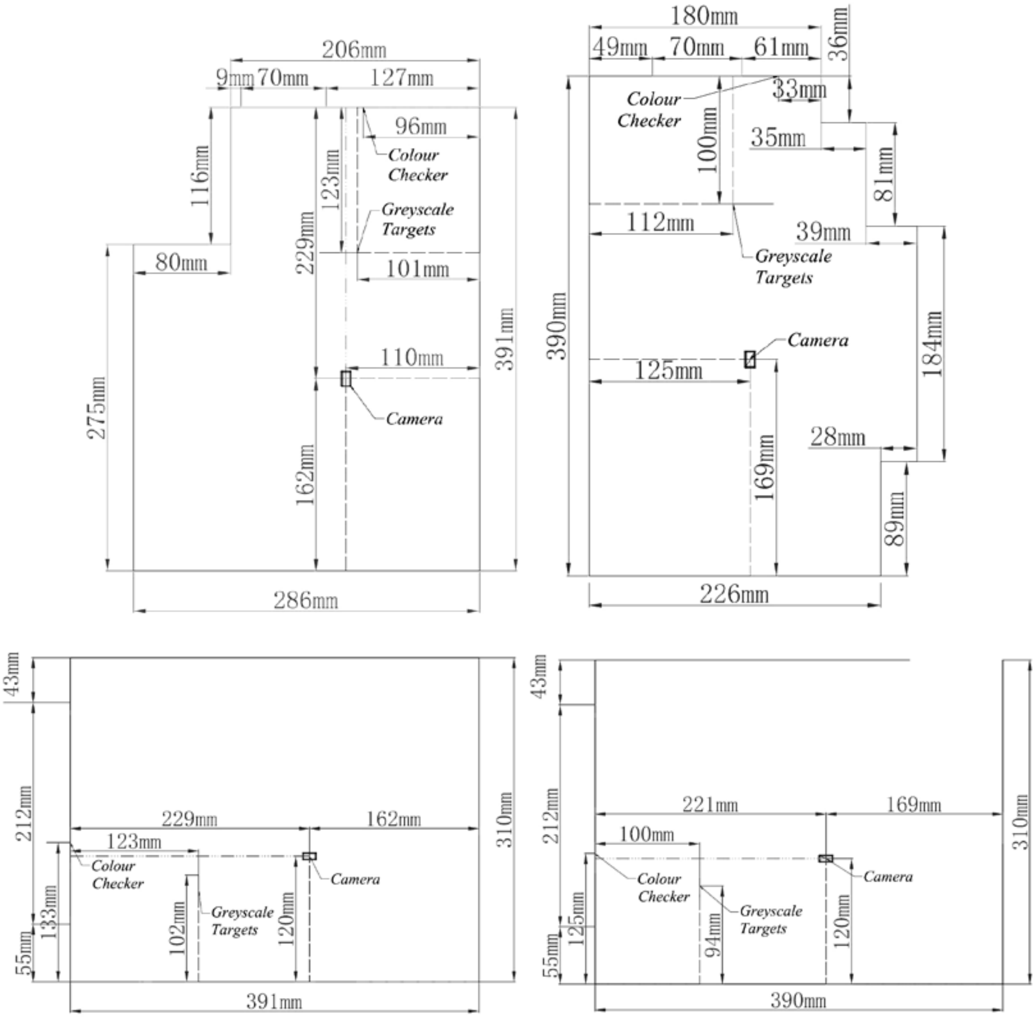

Figure 1 – The layouts of the two offices for conducting the experiment

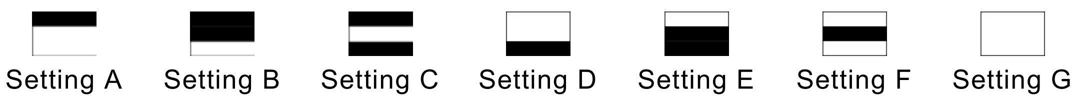

Figure 2 – The seven test settings made of shielding different sections of a window

A digital camera CANON EOS 350D fitted with Sigma zoom lens 10-20 mm F4-5,6 EX was used to obtain the luminances across the scene of each test setting. Table 1 summarizes the optimal features of the camera and lens used in this experiment. To simulate the binocular vision of human eyes, which has a visual field of 120˚ (width) x 135˚ (height), the largest angle of view 102,4˚ (circular) was used at the shortest focal length f=10 mm of the zoom lens for the HDR photography. The camera was mounted on a tripod at a height of 1,2 m from the floor and a computer software program DSLR remote Pro was used for remote control of the camera in order to, throughout the sequential photograph taking, keep all optical properties of the photographs consistent, maintain the images in alignment, eliminate noise disturbance and avoid possible camera shake. An X-Rite color checker and four paperboards with grey targets were placed within the scene.

Table 1 – Optimal features of the camera and lens used in this experiment

Feature	Setting	Feature	Setting
White balance	Daylight	Metering mode	Partial
ISO speed	100	Color space	sRGB
Size/quality	Large/fine	Exposure compensation	None
AF mode	One shot	Auto-bracket	On
AE lock button	AE lock	Drive mode	Continuous
Focal length	10 mm	Aperture size	f/5,6

The subjects of this experiment were research students and staff of the University. They might or might not have any professional knowledge about daylighting. The subjects participated in the experiment individually. He/She was invited to enter one of the test offices for conducting the experiment, where he/she was asked to sit down in a chair such that his/her eye level was at about 1,2 m high and his/her eyes were very close to the camera. The subject was briefed the objectives of the experiment. His/her general information including age and gender was collected. The experimenter also explained to him/her in detail about the meaning and sequence of words used to describe discomfort glare (i.e. imperceptible, just perceptible, perceptible, just acceptable, unacceptable, just uncomfortable, uncomfortable, just intolerable, and intolerable). To avoid any possible confusions the subjects might have about the different semantic rating scales used by different glare indices (i.e. 14-30 for DGI and DGI_N, and 7-31 for DGR), a temporary semantic scale t = 1-9 (1=imperceptible, 2=just perceptible, 3=just acceptable, 4=unacceptable, 5=just uncomfortable, 6=uncomfortable, 7=just intolerable, 8=intolerable), as shown in Figure 3, was used in this study. This linear rating scale t can be converted to the semantic scales of DGI, DGI_N, DGR using Equations (5) and (6).

$$DGI \text{ or } DGI_N = 2t + 12 \tag{5}$$

$$DGR = 3t + 14 \tag{6}$$

☐9 Intolerable ☐8 Just intolerable ☐7 Uncomfortable ☐6 Just uncomfortable
☐5 Unacceptable ☐4 Just acceptable ☐3 Perceptible ☐2 Just perceptible ☐1 Imperceptible

Figure 3 – Linear scale for subjective discomfort glare rating in the experiment

The subject was then shown the seven test settings one by one. He/She rated the perceived glare sensation from each setting, based on his/her own experiments in daily life. The order of the test settings shown to the subjects was random to prevent any effects of the sequential answering. Meanwhile, for each setting, 18 LDR photographs of different exposures were captured for the wide dynamic luminance across the scene, as shown in Figure 4, and luminances on the 18% grey on the color checker and the paperboards were measured by a conventional luminance meter (Minolta LS-100). These three tasks were carried out in parallel. The total time consumed for rating glare sensation, taking LDR photographs and measuring luminances of the grey targets for each setting was about 2 minutes. It was assumed that the change of daylight conditions within this short period of time was negligible. On average, a subject completed the whole experiment within 20 minutes.

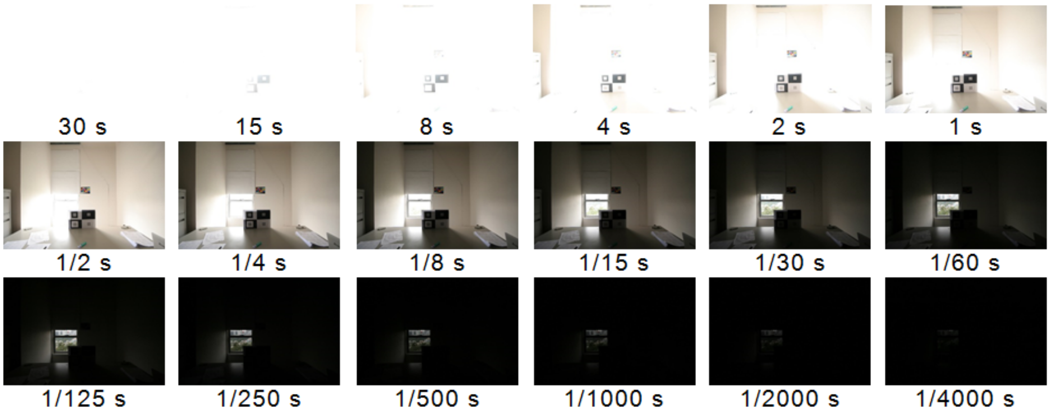

Figure 4 – The 18 low dynamic range photographs for test setting B

5 Data Processing

In the experiment, for every setting, a total of 18 LDR photographs were captured. Photosphere was adopted to merge the photographs into one HDR image. Each HDR image consists of 3456 x 2304 pixels. After the raw HDR image was formed, photometric calibration was undergone in two steps: (i) correction for vignetting effect, and (ii) luminance calibration.

Light fall-off is significant in an ultra wide angle lens for pixels far from the optical centre to the periphery. The vignetting effect of the raw HDR image should be corrected first. In this experiment, since a Canon EOS 350D fitted with Sigma lens 10-20 mm F4-5,6 EX at focal length 10 mm and aperture f/5,6 was used, the function expressed in Equation (7) was used for correcting the vignetting effect (Cai, 2011).

$$V(v) = -0.000000008088v^5 + 0.0000007465v^4 - 0.00002016v^2 - 0.003v + 1 \tag{7}$$

where v is the off-axis angle.

After both the luminances of the four 18% grey targets on the paperboards and the only one 18% grey target on the color checker physically measured by the luminance meter and the luminances of the same targets retrieved from the vignetting effect corrected HDR image were acquired, a calibration factor CF ($CF=L_{measured}/L_{HDR}$) was calculated for each grey target. A global CF_{global}, i.e. the average value of all five CFs was then used to calibrate the luminance of every pixel across the scene of the HDR image.

Once the two photometric calibration processes were accomplished, the per-pixel luminances in the HDR image were comparable to the actual luminances across the scene. These luminances obtained from the HDR photography were then used for calculating the glare ratings of DGI, DGI_N, and DGR. However, not the luminance of every pixel was useful in estimating the source, window, background or adaptation luminances. Masking the useless per-pixel luminance was therefore essential. This technique screened the useful luminances from the rest in an HDR image such that only the values of the concerned luminances were correctly remained.

6 Results and Validation of DGI, DGI_N, and DGR

In this study, a total of 95 subjects participated in 95 valid experiments. The subjective glare ratings and the calculated glare ratings of DGI, DGI_N, and DGR were obtained from 655 valid test settings. It was found for all 655 test settings, the average subjective rating was 3,93 with a standard deviation (σ) of 1,96, the average DGI was 23,96 with σ of 3,39, the average DGI_N was 25,83 with σ of 4,04, and the average DGR was 21,57 with σ of 4,33. Table 2 shows the results of the subjective glare ratings and the calculated glare ratings of DGI, DGI_N, and DGR.

Table 2 – Subjective glare ratings and calculated glare ratings of DGI, DGI_N, and DGR

		DGI	DGI_N	DGR
	Max	31,3	34,5	31,2
	Mean	24,0	25,8	21,6
	Min	13,3	13,1	8,0
	Subjective	p-value		
Max	9,0			
Mean	3,9	< 0,05	< 0,05	< 0,05
Min	1,0			

6.1 Testing predictability

In the test of predictability, the subjective glare sensation was converted from the linear rating scale t to the semantic scales of DGI, DGI_N, DGR using Equations (5) and (6) accordingly. Then, the calculated glare ratings and the converted subjective glare sensation obtained from all 655 test settings were analysed by the one-way ANOVA test. The calculated p-values were all less than 0,05. This shows that DGI, DGI_N, and DGR all overestimate the subjective glare sensation from windows with a non-uniform distribution perceived by local young people.

6.2 Testing sub-divisibility and additivity

Sub-divisibility and additivity of glare sensation are the foundation of all discomfort glare indices. The argument of sub-divisibility is that if a single large source is divided into multiple subsections for facilitating the glare calculation, it should yield the same value for any number of sub-divisions. Likewise, for additivity, if multiple light sources are assessed individually for an additive discomfort glare, they should yield the same glare rating as if they are assessed simultaneously as a whole, independent of any additions. To validate DGI, DGI_N, and DGR for evaluating discomfort glare from windows with a non-uniform light distribution, their sub-divisibility, additivity, and predictability of discomfort glare sensation were tested sequentially. In the test of sub-divisibility, two sets of DGI, DGI_N, and DGR values were calculated, namely (DGI_1, DGI_{N1}, DGR_1), (DGI_2, DGI_{N2}, DGR_2). In the first set, the window of each test setting was divided into parts of the sky, the obstructions, and the ground, if any, such that DGI_1, DGI_{N1}, and DGR_1 were calculated by treating the source luminance to be that from the patch of the sky, of the obstructions, and of the ground. In the second set, the window was regarded as a large source, where the source luminance was equal to the window luminance. DGI_2, DGI_{N2}, and DGR_2 were accordingly calculated. To validate sub-divisibility, the values of the two sets of DGI, DGI_N, and DGR were analysed using a one-way ANOVA test. The proposed null hypothesis was that the sub-divisibility of glare sensation of DGI, DGI_N, and DGR holds. The calculated p-values for DGI, DGI_N, and DGR were all less than 0,05, and thus the null hypothesis was rejected. Conclusively, the empirical data showed evidence that DGI, DGI_N, and DGR all failed the sub-divisibility test. Table 3 shows the sub-divisibility test results.

Additivity holds in the case of daylight glare if, for example, the window of setting A and the window of setting E are assessed individually for an additive discomfort glare, they should yield the same glare rating as if the window of setting G is assessed. In this test of additivity, the DGI, DGI_N, and DGR values for evaluating the discomfort glare from the windows of all seven test settings (A to G) one after the other. Then following the manner of G=A+E, G=B+D, G=C+F, G=B+C+E, A=B+C, D=C+E, and F=B+E, the data was analysed by the one-way ANOVA test again. The proposed null hypothesis was that the additivity of glare sensation of DGI, DGI_N, and DGR holds. Despite occasionally larger than 0,05, most of the p-values were generally less than 0,05, which indicated that there was a significant difference between these additions. It was concluded that DGI, DGI_N, and DGR do not have valid additivity of glare sensation. Table 4 shows the additivity test results.

Table 3 – Sub-divisibility test results of DGI_1, DGI_2, DGI_{N1}, DGI_{N2}, DGR_1, and DGR_2

	DGI_1	DGI_2	DGI_{N1}	DGI_{N2}	DGR_1	DGR_2
Max	31,3	32,8	34,5	37,2	31,2	33,7
Mean	24,0	22,4	25,8	24,7	21,6	19,7
Min	13,3	11,7	13,1	12,2	8,0	7,9
	p-value		p-value		p-value	
	< 0,05		< 0,05		< 0,05	

Table 4 – Additivity for DGI_G, DGI_A, DGI_F, DGI_{N1}, DGI_{N2}, DGR_1, and DGR_2

		DGI			
		DGI_{A+E}	DGI_{B+D}	DGI_{C+F}	DGI_{B+C+E}
Max Mean Min		33,1 27,8 20,1	30,2 26,6 20,6	31,3 27,7 19,6	32,3 28,4 20,9
	DGI_G	p-value			
Max Mean Min	30,1 25,4 16,9	< 0,05	< 0,05	< 0,05	< 0,05
		DGI_N			
		$DGI_{N;A+E}$	$DGI_{N;B+D}$	$DGI_{N;C+F}$	$DGI_{N;B+C+E}$
Max Mean Min		35,9 29,3 19,4	34,0 28,3 20,1	34,2 29,0 18,5	35,2 29,6 19,8
	$DGI_{N;G}$	p-value			
Max Mean Min	33,4 27,3 16,2	< 0,05	< 0,05	< 0,05	< 0,05
		DGR			
		DGR_{A+E}	DGR_{B+D}	DGR_{C+F}	DGR_{B+C+E}
Max Mean Min		32,3 25,0 14,1	30,6 24,1 14,7	30,6 24,7 13,1	31,4 25,2 14,3
	DGR_G	p-value			
Max Mean Min	29,9 23,3 10,9	< 0,05	0,10	< 0,05	< 0,05

	DGI_A	DGI_{B+C}	DGI_D	DGI_{C+E}	DGI_F	DGI_{B+E}
Max Mean Min	31,3 25,0 16,8	30,0 26,2 18,4	30,0 25,7 19,1	32,1 27,8 20,0	27,1 23,8 16,4	28,8 25,3 18,8
	p-value		p-value		p-value	
	< 0,05		< 0,05		< 0,05	
	$DGI_{N;A}$	$DGI_{N;B+C}$	$DGI_{N;D}$	$DGI_{N;C+E}$	$DGI_{N;F}$	$DGI_{N;B+E}$
Max Mean Min	34,5 27,0 16,8	33,3 27,7 17,4	34,0 27,9 18,9	35,1 29,3 19,2	30,4 25,4 15,9	32,2 26,9 18,2
	p-value		p-value		p-value	
	0,14		< 0,05		< 0,05	
	DGR_A	DGR_{B+C}	DGR_D	DGR_{C+E}	DGR_F	DGR_{B+E}
Max Mean Min	31,2 23,1 12,0	29,9 23,6 12,3	30,6 23,7 13,8	31,3 24,9 13,6	26,2 20,9 10,2	28,0 22,2 12,5
	p-value		p-value		p-value	
	0,39		< 0,05		< 0,05	

7 Conclusion and Discussion

Lighting researchers have been working on discomfort glare from windows for over 50 years, yet still without a reliable assessment method. DGI, DGI_N, and DGR did not consider any possible non-uniform light distribution on the windows when developed. Their validity and applicability are in doubt. There are many causes of this difficulty, including the unsuitability of conventional luminance meters for measuring luminance from a non-uniform distribution. This study tested the appropriateness of these three daylight glare indices for evaluating the discomfort glare from windows with a non-uniform distribution in cellular offices under real sky conditions with the aid of HDR photography. HDR photography is a rather new technique for mapping non-uniform light distribution. It helps to bridge the gap of acquiring per-pixel luminance across the visual field and is hoped to help restart the fundamental research of discomfort glare from windows via statistical analyses. In this study, different test settings with the different window sizes were created to test the sub-divisibility and additivity of DGI, DGI_N, and DGR. Subjective glare assessments were also collected to compare the glare ratings calculated from DGI, DGI_N, and DGR with the perceived daylight glare sensation. There are three major findings in this study: (i) DGI, DGI_N, and DGR all fail to prove having valid sub-divisibility. By treating the source luminance the same as the window luminance would yield different glare ratings. (ii) DGI, DGI_N, and DGR all fail to prove having valid additivity. By adding up glare sensation individually from multiple parts of a window of different settings would be significantly different from the glare sensation of the whole window. (iii) Current formulae of DGI, DGI_N, and DGR all overestimate the glare sensation from windows with a non-uniform light distribution that young people in Hong Kong may feel.

Acknowledgements

This work was supported by the HKSAR Government Research Grants Council General Research Fund (Project Reference: PolyU 5150/10E).

References

ANAOKAR, S., MOECH, M. 2005. Validation of high dynamic range imaging to luminance measurement. Leukos, 2, 133-144.

BELLIA, L., CESARANO, A., SPADA, G. 2005. Application of videophotometer in the evaluation of DGI in scholastic environment. International Journal on Architectural Science, 6, 82-88

BELLIA, L., CESARANO, A., LULIANO, G.F., SPADA, G. 2008. Daylight glare: a review of discomfort indexes. Visual quality and energy efficiency in indoor lighting: Today for tomorrow, International Workshop, 31 March 2008, Rome, Italy.

BOUBEKRI., M., BOYER, L.L. 1992. Effect of window size and sunlight presence on glare. Lighting Research and Technology, 24, 69-74.

CAI, H., CHUNG, T.M. 2011. Improving the quality of high dynamic range images. Lighting Research and Technology, 43, 87-102.

CHAUVEL, P., COLLINS, J.B., DOGNIAUX, R. 1982. Glare from windows: current views of the problem. Lighting Research and Technology, 14, 31-46.

CHUNG, T.M., 2005. On the calculation of daylight glare index. Proceedings of the 5th Lux Pacifica – Towards a sustainable lighting future, 24-26 July 2005, Cairns, Australia, 81-86.

DEBEVEC, P.E., MALIK, J. 1997. Recovering high dynamic range radiance maps from photographs. Proceedings of 24th Annual Conference on Computer Graphics and Interactive Techniques, Los Angeles, CA, USA, 369-378.

FISEKIS, K., DAVIES, M., KOLOKOTRONI, M., LANGFORD, P. 2003. Prediction of discomfort glare from windows, Lighting Research and Technology, 35, 360-371.

HOPKINSON, R.G. 1972. Glare from daylighting in buildings. Applied Ergonomics, 3, 206-215.

INANICI, M.N. 2006. Evaluation of high dynamic range photography as a luminance data acquisition system. Lighting Research and Technology, 38, 123-136.

JACOBS, A. 2007. High dynamic range imaging and its application in building research. Advances in Building Energy Research, 1, 177-202.

NAZZAL, A.A. 2000. A new daylight glare evaluation method. Journal of Light and Visual Environment, 24, 19-27.

WATERS, C.E., MISTRICK, R.G., BERNECKER, C.A. 1995. Discomfort glare from sources of nonuniform luminance. Journal of the Illuminating Engineering Society, 24, 73-85.

XIAO, F., DICARLO, J.M., CATRYSSE, P.B., WANDELL, B.A. 2002. High dynamic range imaging of natural scenes. Proceedings of Tenth Colour Imaging Conference: Colour Science and Engineering Systems, Technologies, and Applications. Scottsdale, Arizona, USA. 337-342.

OP43

BALANCING LIGHTING QUALITY, ENERGY EFFICIENCY AND COST IN COMBINATION WITH REAL TIME SIMULATION TECHNOLOGY

Holger Leibmann, Bert Junghans, Christian Bauer
[1-3] Zumtobel Lighting GmbH, Dornbirn, AUSTRIA
holger.leibmann@zumtobelgroup.com

Abstract

There is a wide range of possibilities to improve lighting quality, but one of the biggest challenges in the design process is to convince the decision makers on the client side.

Project networks are complex and do have a different main working focus (visual, numerical). A huge variety of different aspects have to be considered and for non specialized experts it is not easy to asses the relevance of certain criteria.

This contribution will introduce lighting design tools, which will help to present the advantages of advanced lighting solutions to the client.

The main focus on will be on the possibilities of real time simulation but this has to be seen in the context of other lighting design tools.

1 Which tools will be introduced

1.1 Hilite

Optimizing lighing quality in standard lighting design software is an iterative process. Luminaires are selected and placed in a scene. After a certain calculation time the results have to be analysed by comparing numeric values on the result pages. If the values are not satisfying the process starts again.

HILITE is a research project by VrVis Forschungs GmbH in Wien (A), Zumtobel Lighting GmbH in Dornbirn (A), Hefel Wohnbau AG in Lauterach (A) and Witsch Visuals GmbH in Höchst (A).

It is a lighting design tool that will make the optimisation of lighting quality much more efficient by using real time simulation technology that was developed and optimized for videogames, but it adds photometrical correct lighting simulation.

HILITE is not only showing the effects of changes in lighting solutions in real time, it is also able to handle measured materials (BSDF) and detailed light distributions of luminaires (e.g. individual light distribution per lens). Therefore reflexes, multi shadows or colour mixing issues with RGB LED luminaires become immediately visible.

While it is possible to achieve near realtime effects for small and medium size rooms it is also possible to reduce the calculation times for high quality simulations from several hours to less than 10 minutes compared to standard raytracing methods.

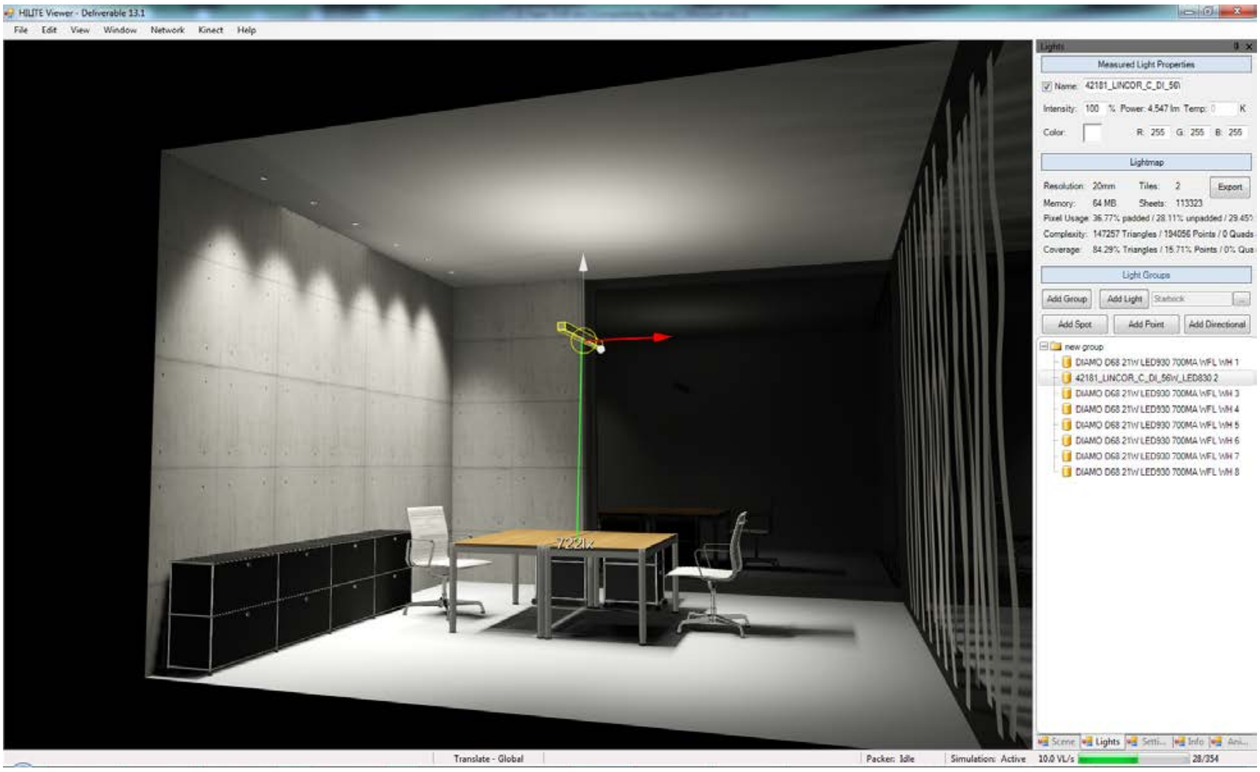

Fig. 1: Screenshot from Hilite Viewer. Simulation result ~one second after moving the main luminaire.

Fig. 2. Image of a complex scene modelled as part of a complete floor. Calculation time for final image <10min. with currently available mid range computers.

Further technical detail will be explained in Section 5 of this paper.

HILITE does make the design process far more intuitive and fun, therefore raising awareness for lighting quality with “non lighting experts” in the project process.

1.2 VIVALDI

Operating complex tools like Hilite requires expert knowledge and sufficient hardware resources. Once the lighting concept is defined, the complexity can be reduced by limiting the degree of freedom to dimming level and / or light colour of luminaire groups. Luminaire position, materials and view are fixed. On the other hand, this allows for timelines and daylight sequences to be added to the project, so that lighting design concepts that react to different requirements during the cause of a day can be developed and presented.

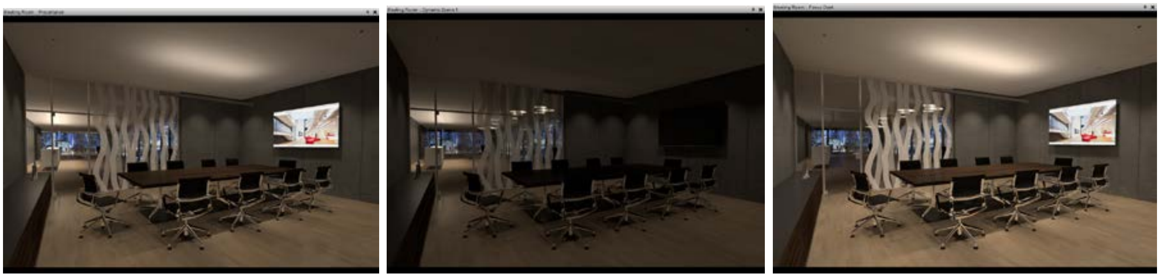

Fig. 3: Visusalisation fromVIVALDI. Different lighting scenes can be designed for the same space.

VIVALDI visualises the results in real time, while giving feedback about energy consumption and illumination levels. The advantages of HDR image formats are used to make the effects of different luminaire groups visible and to make them controllable individually. To export a project from any lighting simulation tool into VIVALDI only separate HDR images of each control group are required: Each contains the photometric information for one control group. VIVALDI is an easy to use tool that does not require substantial computing resources and while providing valuable input into the design process it also appeals to the emotional side of decision makers: They can “play” with their lighting solutions.

1.3 ecoCALC

Before making a final decision between different options, Investors will always require a credible evaluation of investment and running cost. ecoCALC is a tool to evaluate project specific lifecycle costs of lighting solutions.

In many projects ecoCALC is not primarily used as a tool for cost optimization but to analyze the impact of different lighting concepts for life cycle costs. If high quality lighting solutions with dynamic aspects are required, no short term payback times can be expected in comparison to very basic solutions. It is possible however to show that intelligent, efficient and dynamic lighting concepts have considerable saving potentials in the use stage. In many cases at least cost neutrality can be demonstrated based on the total lifecycle cost.

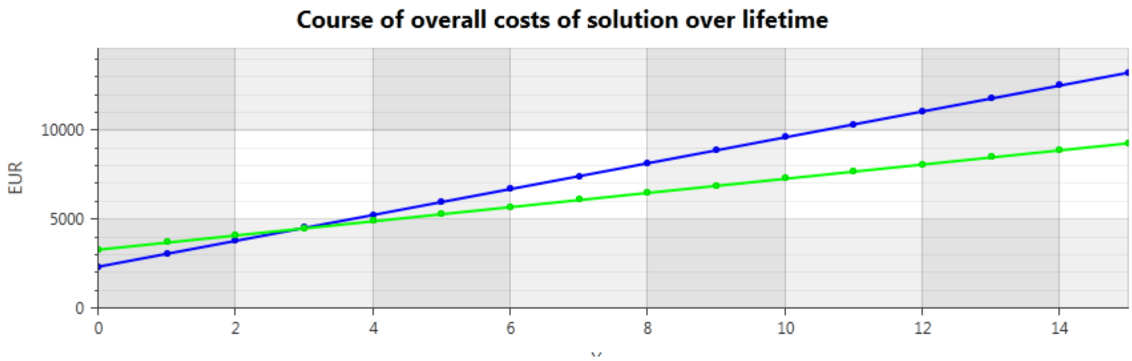

Fig. 4: Typical diagram from ecoCALC showing the amortisation time of an investment.

Even though ecoCALC does, except for the level of maintained illuminance, not take lighting quality aspects into consideration it allows designers, users or owners of buildings to accurately evaluate the impact of high quality lighting solutions on the total cost over the lifetime of the building or the installation.

2 Typical sequence of using the tools in projects

When it comes to realising lighting project with a focus on high lighting quality, strong design concepts with strong arguments backed up by scientific research will always be the backbone of every presentation.

The introduced tools can help to convince members of project networks, that don’t have their expertise in Lighting or Lighting design. Especially in early design stages, but also when it comes to stop or go decisions in later stages, interactive tools like HILITE and VIVALDI can show the advantages of high quality lighting solutions and, equally important, appeal to the emotional side of decision makers.

On the other hand most decisions in real lighting projects will be driven by financial issues. ecoCALC allows to present a credible life cycle cost analysis of all possible lighting solutions for the project. Especially lighting concepts with dynamic aspects often have saving potentials that are hidden as long as the solutions are only compared on luminaire price and data sheet level. In the early stage of the design process it can be used to quickly evaluate different concepts but also very detailed calculations are possible when it comes to final decisions between options.

In combination the tools give non experts the possibility to understand financial as well as quality aspects of lighting solutions and therefore enables them to make qualified decisions.

3 Availability

ecoCALC is freely available for download from www.zumtobel.com/ecoCALC or from www.thornlighting.com/en/products/software-downloads. The tool can be used for any luminaires, emergency luminaires or controls components of any manufacturer and is not limited to Zumtobel or Thorn products.

VIVALDI is available from www.zumtobel.com/VIVALDI in a demo version. For the full version a hardware key is required. There is a licence fee which is required to cover development costs of external partners of Zumtobel Lighting GmbH. Student Versions are available free of charge. For Details please visit www.zumtobel.com/VIVALDI.

HILITE is currently only available to be used by members of the research project, also for project work. The research project will be continued until 2016 and the aim is to create a simulation technology for commercial products.

4 Technical Details

4.1 Technical Details Hilite

4.1.1 Setup

HILITE is a research project by VrVis Forschungs GmbH in Wien (A), Zumtobel Lighting GmbH in Dornbirn (A), Hefel Wohnbau AG in Lauterach (A) and Witsch Visuals GmbH in Höchst (A).

Main focus of the HILITE Project is research into interactive real time simulation of lighting solutions using new rendering and virtual reality technologies (please refer to references).

4.1.2 Shadowmaps

Hilite is a simulation technology using optimized calculation methods for shadowmaps with GPU hardware that were developed for gaming and virtual reality to show lighting designers an interactive preview of their lighting design. The direct fraction is displayed in real time, the diffuse bounces are calculated and displayed after a short interval.

Shadow mapping means that images are projected into a room. The process can be compared to a photopraph projected with a slide projector. The projected image illuminates room surfaces and objects. These images are called “intensity maps”.

4.1.3 Intensitymaps:

To generate the maps for specific luminaires, photometric data files (LDT, IES) are converted into high dynamic range intensitymaps (EXR). These are projected into the room using shadow mapping in order to calculate the direct fraction of the lighting.

Due to the high dynamic range of these intensity maps it is possible to save complex light distributions in relatively small files (64px * 64px). A single intensitymap is sufficient for spotlights. Luminaires with more comlex light distributions require cubemaps are also optimized to be processed by the GPU.

Fig 5. Intensitymap showing luminance for different distances from the light emitting surface.

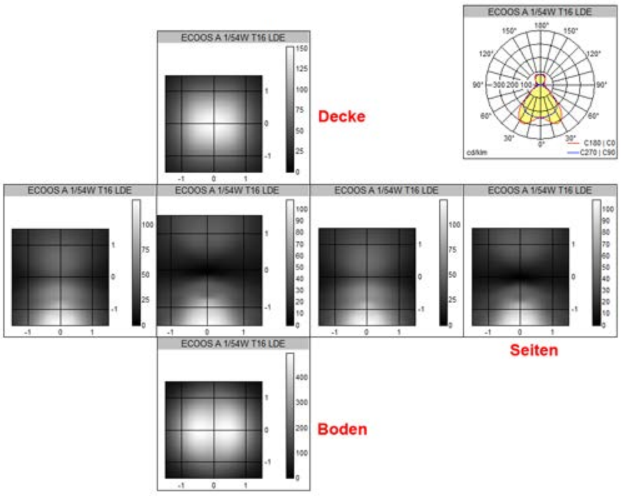

Fig 3.Typical example for a cubemap with the light distribution for a pendant luminaire with a small indirect fraction. The standard light distribution diagram in cd/klm is only added for better understanding of the cubemap.

4.1.4 Virtual Pointlights:

Hilite uses virtual point lights (VPL) to define the position of a light source. The light emitting surface is defined by polygons.

It is possible to define any quantity of VPLs for each luminaire. As LED luminaires start to replace conventional lighting technology this feature becomes more important: Every LED within a luminaire can be defined by a separate VPL with a specific light distribution and light colour. The accuracy of the simulation results is surpassing current lighting simulation software, especially when RGB luminaires are considered.

Fig 6 Separate VPLs for each LED within a luminaire

The simulation is very detailed, shadows and colour mixing for RGB luminaires can be analysed considering location, light distribution and colour of each LED within the luminaire.

Fig 7. Detailed simulation of shadows for a RGB Spot.

4.1.5 Simulation:

There are different simulation methods for direct illumination and for the diffuse bounces.

The shadowmaps that were assigned to the virtual point lights are projected into the room to simulate the direct fraction of the lighting.

Photons are emitted from the VPLs to simulate diffuse bounces. After the first contact with room surface or an object in the room, areas receiving equal numbers of photons are defined.

For the first diffuse bounce a virtual point light will be created for each of these areas. This VPL will be projected into the room using shadow mapping.

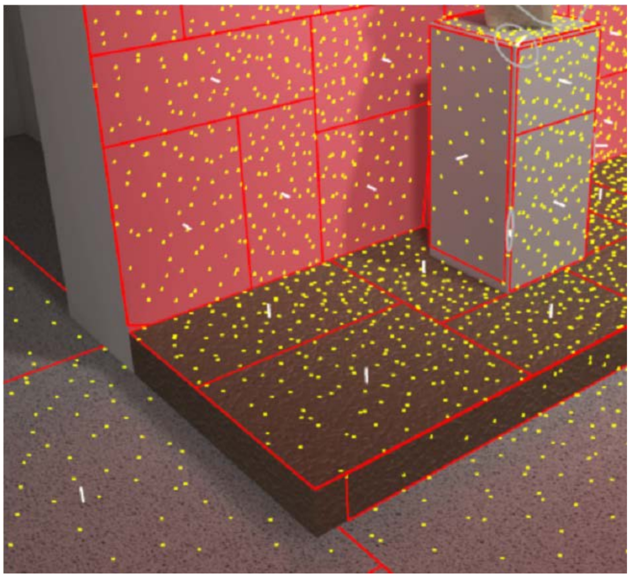

Fig 8. Photons and resulting VPLs

The method is flexible and adapts to the complexity of the geometry. The process will be repeated for the required quantity of diffuse bounces.

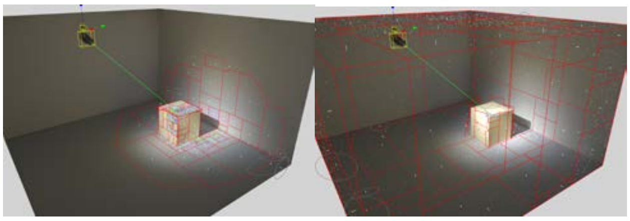

Fig 9. VPLs for the first and second diffuse bounce.

4.1.6 Lightmaps:

Hilite generates groups of luminaires that can be controlled together. The calculation results will be saved as an individual lightmap for each group of luminaires.

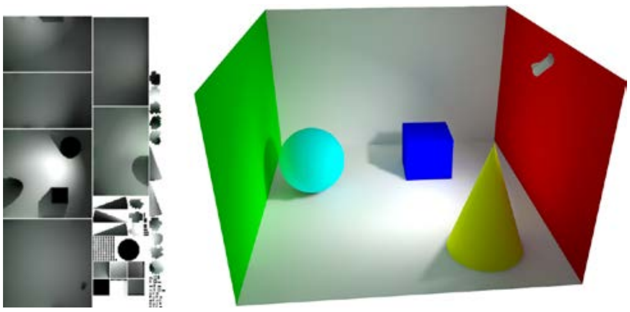

Fig10 Lightmap

Intensity and light colour for each luminaire group can be adapted without repeating the calculation. In this way it is similar to the VIVALDI functionality for interactive lighting design.

Using the fast simulation and the optimized handling for luminaire groups lighting concepts for rooms or architectural scenes can be designed in very fast, efficient and interactive way.

4.1.7 Material and Shader:

The material properties in Hilite are based on the Ward Shader Model that enables the simulation of anisotropic reflexions.

The shader was optimized for viewport rendering and the possibility of BSDF fitting was added.

Semiautomatic BSDF fitting enables the conversion of measured BSDF Date into Hilite shaders.

The material editor allows to generate complex materials (reflection fallof, fresnel, flat mirror, roughness etc.) and is already implemented.

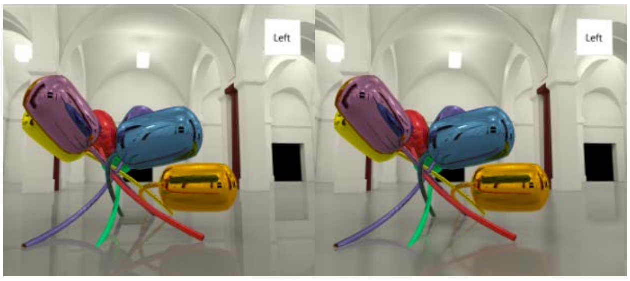

Fig 11. Different roughness of the floor in identical spaces

Depending on the shape of the object reflections can be calculated as flat reflections or as cube reflection maps. The cube maps are generated separately for each object considering the illumination of the scene.

Fig 12 The analysis of reflection on complex surfaces is possible in real time.

4.1.8 False Colour:

The false colour mode in Hilite shows the intensity of illumination.It enables the designer to optimize the luminaire positions in order to avoid unwanted shadows and to review the light distribution and light output of the selected luminaires.

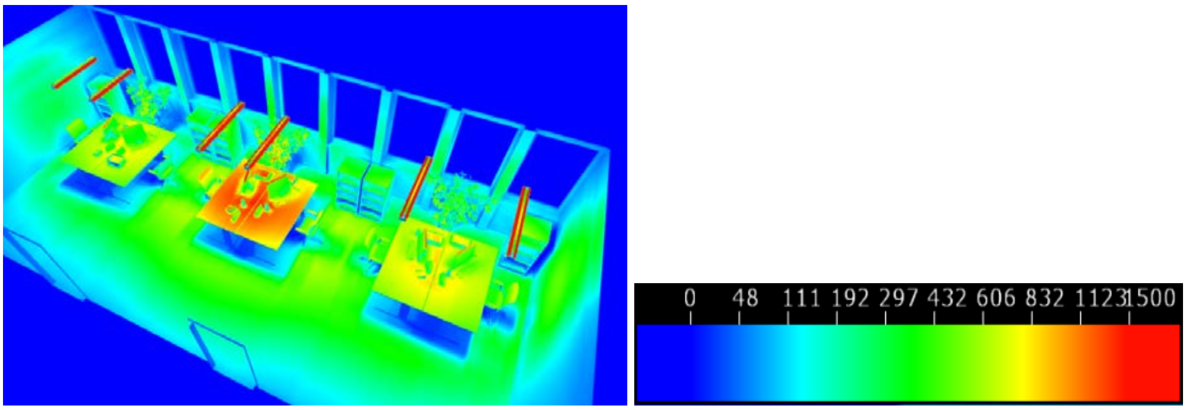

Fig 13. Comparison of a luminaire with 28W, 49W and 35W. Falsecolour mode mode available in lux or cd/m².

It is also possible to evaluate the uniformity of a lighting solution or to set a focal points as it might be desirable in exhibitions or cultural institutions.

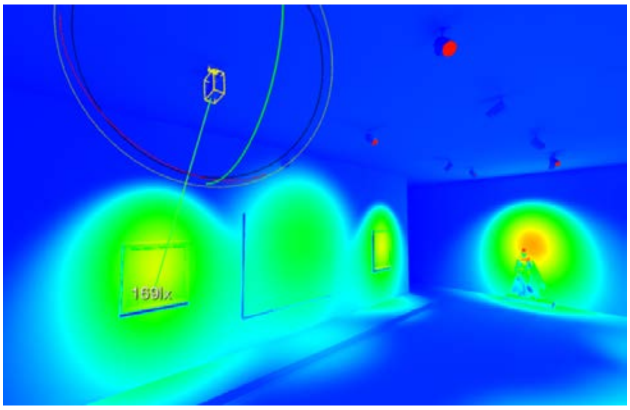

Fig 14. Interaktive positioning of luminaires in real time.

4.1.9 Recessed Luminaires:

Hilite is using intelligent masking to visualise recesses in ceilings where luminares can be located.

As this technology is faster and less complex than Boolean operations, it is ideal for larger quantities of recessed luminaires.

Fig. 15 Typical recessed luminaire with geometry.

Fig 16. Visualisation of recessed luminaires in Hilite.

4.2 Technical Details ecoCALC:

ecoCALC is able to calculate the energy consumption of lighting solutions taking into consideration complex lighting scenarios with daylight saving and different dimming levels for specific areas as well as different dynamic lighting scenarios throughout a year. The dimming characteristics of the lamps are considered in the process. Dynamic aspects like energy tariff development (evolution of energy cost) or inflation rate are taken into account.

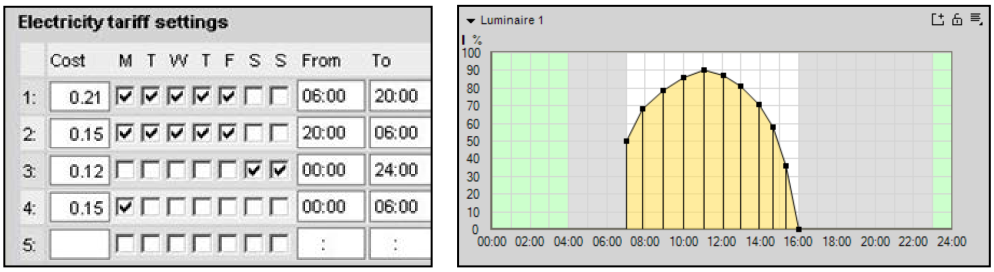

Fig 17 Definition of energy tariff and dimming curves for luminaires in ecoCALC.

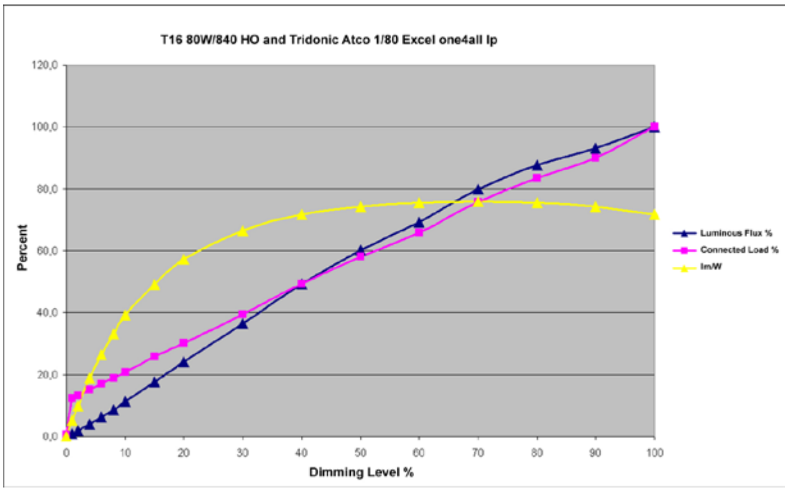

Fig 18 Dimming characteristic for a typical T16 80W lamp

When it comes to evaluating maintenance cost, ecoCALC is following the method of CIE 97, 2003 to establish the resulting illumance at project specific maintenance intervals. The maintenance intervals can be optimized in ecoCALC by linking LMF, LSF, LMMF, RSMF to project specific maintenance costs.

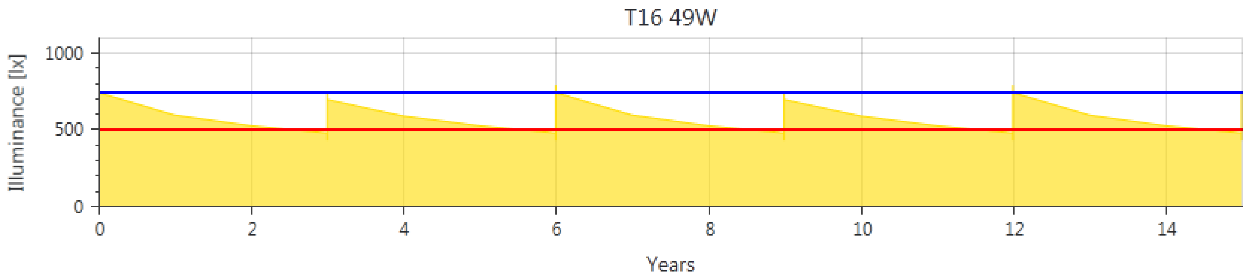

Fig 19: Course of Illumination Diagramm generated by ecoCALC.

For the lamp related maintenance factors ecoCALC contains a comprehensive lamp database with manufacturer's data for the lamp survival factor as well as for the lamp lumens maintenance factor. Advantages or disadvantages of specific lamp types can therefore be compared and the lamp selection can be optimized.

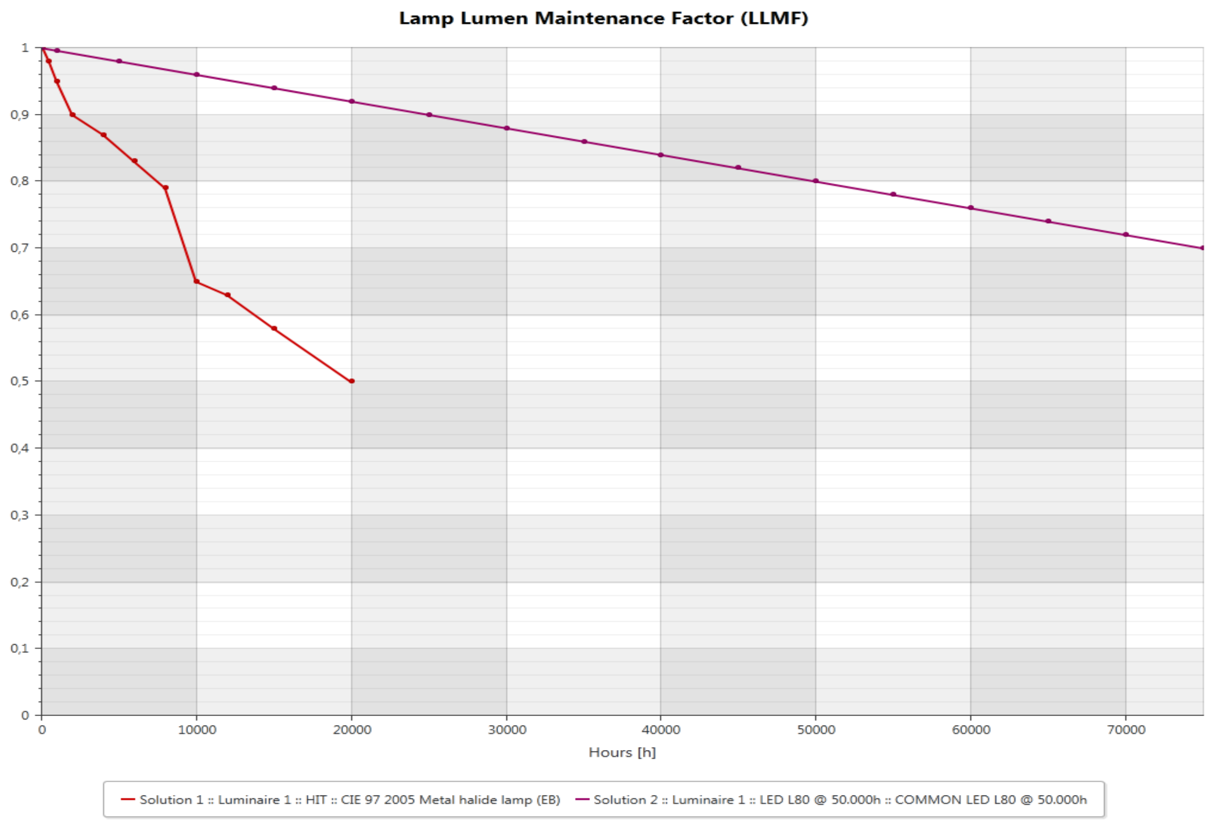

Fig 19 Course of lamp lumen maintenance factor as generated from the ecoCALC databased. Lamp data can either be used as defined in CIE 97 2005 or as declared by lamp manufacturers for specific products.

4.3 Technical Details VIVALDI:

4.3.1 The basic principle of VIVALDI

The program uses as source images, which are showing a certain room scene in a fixed perspective. Each of the images has to be congruent and is representing a single luminaire or luminaire group in its room lighting effect. Source of this images are different lighting calculation- or visualisation programs, which have to be able to export standard picture formats.

Also photographs or sketches with integrated lighting principle are suitable. The core of the application is the developed method of tonal value mapping of T&G [1].

There are three differing methods in dependency of the graphical material (simple, advanced and HDR). There is a wide range of various functions in the program. These functions are prior to photometric measurements or the quality of visual embodiment.

Each of the inserted images represents therefore a single luminaire or luminaire group in the VIVALDI project tree structure and can be influenced separately.

Lighting channels can be switched, dimmed as well as changed in his colour temperature or chromaticity.

Static and dynamic lighting concept sequences can easily be created and exportet as a movie sequence.

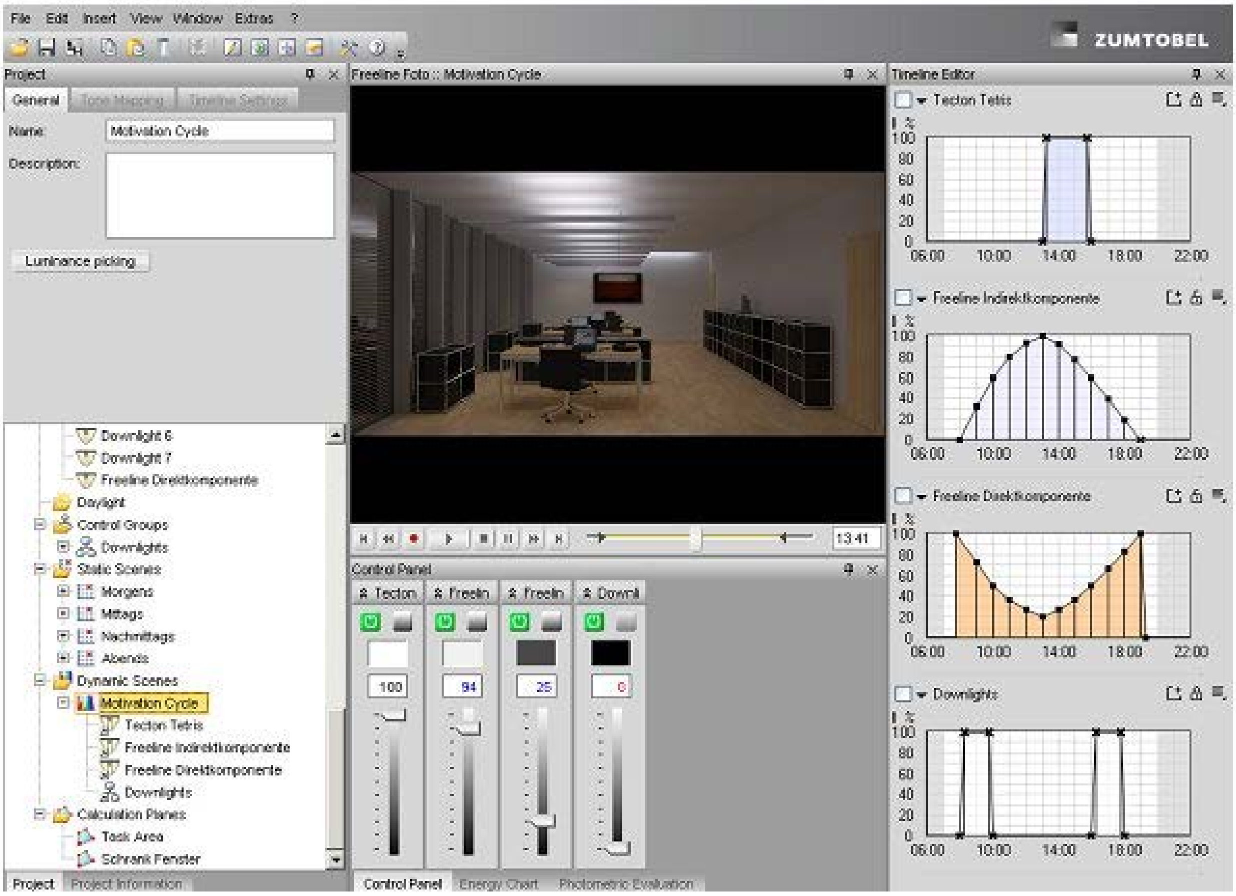

Fig 20 User interface of VIVALDI

4.3.2 Energy requirement of static and dynamic lighting solutions.

For the “lighting object channels” light technical properties (such as colour temperature, dimming value) are defined as well as an attribution regarding energetic values.

According to this features this offers the possibility to calculate the energy requirement of static or dynamic lighting scenes according to the switching or dimming characteristics.

With this method simple analysis of power input versus power output (day, week, month, year) and comparisons between various energy approaches can be verified.

4.3.3 Photometric evaluation for target value survey

With optimizing static lighting scene concepts or rather dynamic sequences, it is also required to check lighting measurement target values. VIVALDI can evaluate photometric criteria as long as information regarding luminance is part of the image information (HDR or advanced mode). If image formats like jpg or bpm are used, VIVALDI can only work on a visual level.

5 Conclusion and further developments

Currently there is a set of tools available that allows to consider most aspects when it comes to balancing lighting quality, energy efficiency and cost, linked to VR technology. For the future two further aspects will be important:

A simple tool to evaluate lighting quality and cost in very early project stages without substantial design effort. Currently a tool is developed together with Innsbruck University (A) and Bartenbach Lichtlabor (A). It allows to evaluate energy saving potentials of rooms with day- and artificial lighting systems in early design stages. The tool considers the impact of glare control as well as heating and cooling systems.

On the other hand there is the need to combine all information regarding lighting quality, efficiency and cost and makes different solutions comparable taking all aspects into account. After the publication of "Lichtqualität" (Lighting Quality) by Tralau and Dehoff for LiTG (German Lighting Society) the ELI Method to evaluate lighting quality will be used to bring the results from different tools together.

References

LUKSCH, C., TOBLER, R.F., HABEL, R., SCHWÄRZLER, M., WIMMER, M., 2013 Fast Light-Map Computation with Virtual Polygonal Lights. In ACM SIGGRAPH Symposion 2013 Paper

ANNEN, T., DONG, Z., MERTENS, T., BEKAERT, P., SEIDEL, H.-P., AND KAUTZ, J. 2008. Real-time, All-Frequency Shadows in Dynamic Scenes. ACM Trans. Graph. 27, 3, 1–8.

BAUM, D. R., RUSHMEIER, H.E., AND WINGET, J. M. 1989.Improving Radiosity Solutions Through the Use of Analytically Determined Form-Factors. In Proceedings of the 16th annualconference on Computer graphics and interactive techniques, ACM, New York, USA, 325–334.

COHEN, M. F., WALLACE, J., AND HANRAHAN, P. 1993. Radiosity and Realistic Image Synthesis. Academic Press Professional, Inc., San Diego, CA, USA.

CRASSIN, C., NEYRET, F., SAINZ, M., GREEN, S., AND EISEMANN, E. 2011. Interactive Indirect Illumination using Voxel Cone Tracing. In Symposium on Interactive 3D Graphics and Games, ACM, New York, USA, 207–207.

DACHSBACHER, C., AND STAMMINGER, M. 2005. Reflective Shadow Maps. Proceedings of the 2005 symposium on Interac-tive 3D graphics and games SI3D 05, 203.

DONG, Z., GROSCH, T., RITSCHEL, T., KAUTZ, J., AND SEIDEL,H.-P. 2009. Real-time Indirect Illumination with Clustered Vis-ibility. In Vision, Modeling, and Visualization Workshop.

FABIANOWSKI, B., AND DINGLIANA , J. 2009. Interactive Global Photon Mapping. Computer Graphics Forum 28, 4, 1151–1159.

FERNANDO, R. 2005. Percentage-closer Soft Shadows. In ACM SIGGRAPH 2005 Sketches, ACM, New York, USA, 35.

HACHISUKA, T., AND JENSEN, H. W. 2010. Parallel Progressive Photon Mapping on GPUs. In ACM SIGGRAPH ASIA 2010 Sketches, ACM, New York, USA, 54:1–54:1.

HASAN, M., PELLACINI, F., AND BALA, K. 2007. Matrix Row-Column Sampling for the Many-Light Problem. ACM Transactions on Graphics (TOG) 26, 3, 26–es.

HASSELGREN, J., A KENINE-MÖLLER, T., AND OHLSSON, L. 2005. Conservative Rasterization. In GPU Gems 2, M. Pharr and R. Fernando, Eds. Addison-Wesley Professional.

HASAN, M., KRIVANEK, J., W ALTER, B., AND BALA, K. 2009. Virtual Spherical Lights for Many-Light

T&G - Thomas & Gilles GmbH / www.t-g.de, Technical Specification VIVALDI

TRALAU, B., Bewertung der Effizienz und Qualität bei Einsatz von Lichtsteuerungen in Beleuchtungsanlagen-Anwendung des Ergonomic Lighting Indicator, OTTI 2009

DEHOFF, P., TRALAU, B., Draft Paper Lichtqualität for LitG, Germany

JUNGHANS, B., Interactive lighting design with VIVALDI for optimised lighting solutions in balance of dynamic lighting quality, energy criteria and life cycle cost aspects; Lux Europe, Istambul (T) 2009

BAUER, Ch., Hilite, LuxJunior, Illmenau (D), 2013

OP44

ACCEPTANCE STUDIES ON INTELLIGENT ADAPTIVE CORRIDOR LIGHTING

Ferenc Szabó[1], Péter Csuti[1], Renáta Kéri[1], Péter Simon[1], János Schanda[1]
Andras Kuti[2], Roland Bátai[2], László Balázs[2]
[1]Virtual Environments and Imaging Technologies Research Laboratory, Faculty of Information Technology, Department of Electrical Engineering and Information Systems, University of Pannonia, Veszprém, HUNGARY
[2]GE Hungary Ltd, Budapest, HUNGARY

Abstract

The aim of the investigation is to develop intelligent, energy efficient lighting solutions for indoor applications. The main concept is the investigation of dynamic lighting schemes and energy saving possibilities at a typical corridor of an office building. A new, intelligent lighting system with sensors has been installed at the campus of University of Pannonia. A series of visual experiments have been carried out with the participation of 30 observers. Subjects' feeling and opinion have been collected with the help of questionnaires. After the evaluation of first experimental series, a validation of the schemes and new experiments with further developed schemes have been conducted.

Keywords: lighting quality, adaptive lighting, energy efficiency

Introduction

The current economical situation and energy context requires power demand to be reduced in interior lighting. New energy efficient lighting solutions have to be developed that also provide acceptably illuminated environments for users. A current slogan that "to light only where and when it is needed" can save considerable amount of energy. It is not so easy to find reliable measurement data that would provide information how large this "considerable amount" is. Moreover, user preferences about lighting quality may vary according to the conducted activity and the user position in the building.

The European Standard 12464-1[i] prescribes for "circulation areas and corridors" the maintained illuminance at floor level to be 100 lx with an UGRL value of 28, and uniformity U_0 of 0.40 and minimum colour rendering R_a=80. The standard does not deal with intelligent type of corridor illumination, thus it does not contain any recommendation on lighting requirements near the observer and further in front of him/her.

Logadóttir et al [ii] compared conventional static lighting concept from ceiling mounted luminaires against three different types of dynamic task lighting concepts: the first providing occupant controlled task illuminance, the second concept providing occupant controlled CCT and the third providing automatically controlled CCT. Another aim was to identify which of the four lighting concepts is rated as most preferred by the test subjects. Subjects tested all four lighting concepts and questionnaires were used for rating of the concepts. Adjustable CCT of the task light was the most preferred lighting concept followed by adjustable task illuminance. Automatically controlled task CCT and conventional lighting were the least preferred. User satisfaction ratings for the lighting concepts are in the following order: adjustable task CCT, adjustable task illuminance, automatic control of task CCT and conventional lighting.

Mochizuki et al [iii,iv] tested energy saving possibilities in case of a personal lighting control system in office building in Japan. The results showed that the electrical power use for lighting was reduced by 44% in average of all the areas tested. The reduction of the electrical power use for lighting was mainly due to the turned off luminaires in the area where the occupants were absent from the office. It was found that once the occupant came to the office and turned on the luminaire which he/she could control, it was seldom switched off.

Experimental Setup

A new, intelligent lighting system with sensors has been installed at University of Pannonia. 15 luminaires with 48W fluorescent light sources divided the 50 meter length corridor into 15 zones. A series of visual experiments have been carried out with the participation of 30 observers. Homogeneity of the illuminance in the corridor was measured at 100% performance (without dimming) by defining measurement points along the corridor and cross wise. The cross wise uniformity is U_0=0.91, the length wise uniformity is U_0=0.97, both values are well over the required value of 0.4. The average illuminance value of E_v=339 lx measured during the cross sectional evaluation is three times of the required 100 lx. The average illumination of E_v=300 lx was still three times of the requirement without dimming. As a test place is a University corridor, where the students often read notice boards the system has been dimmed to fulfil 150 lx with excellent uniformity.

Table 1 – Cross section illuminance measurement results

	Measurement point IDs						E_v-min	E_v-max	E_v-ave	U_0
	A	B	C	D	E	F				
E_v [lx]	354	360	329	307	320	364	307	364	339	0.91

Table 2 – Lengthwise illuminance measurement results

	A	B	C	D	E	F	G	H	I	J	K	E_v-min	E_v-max	E_v-ave	U_0
E_v [lx]	302	302	299	297	293	290	294	298	307	310	309	290	310	300	0.97

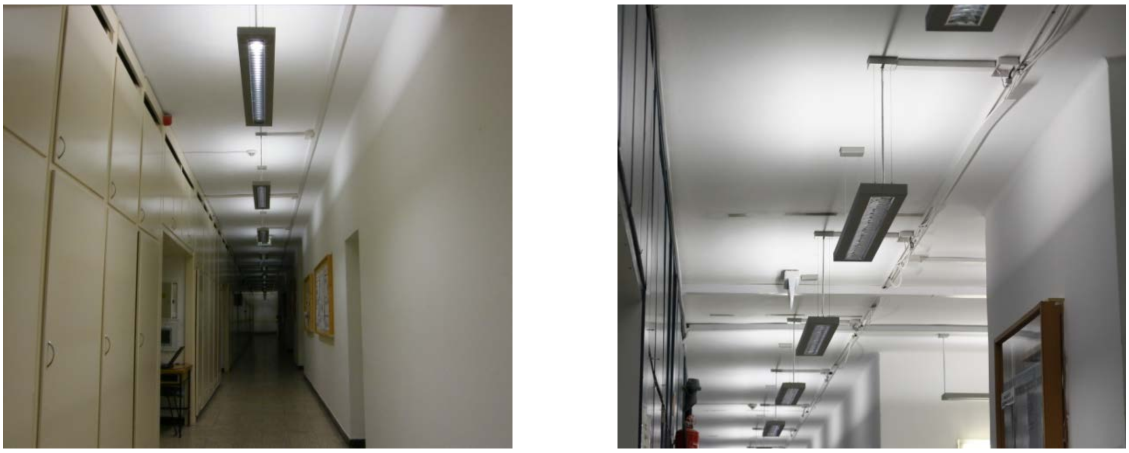

Figure 1 – University of Pannonia - test place

Test schemes used in the project’s validation phase:

This intelligent lighting development project had two phases. The first was the pilot phase where the initial lighting schemes had been developed and tested. Schemes were tuned taking into account visual comfort (e.g. illumination levels, distance lit up, flickers), and energy consumption. In this phase, it had been found out that visual comfort outperforms minimizing the energy consumption, because most of the savings can be achieved by dimming down the luminaires when the corridor is not in use. Tuning the scheme parameters by lowering holding times, and reducing illumination levels can save almost 50% in short term (comparing only active periods), but on the long run it makes no significant difference.

During the validation phase, 8 schemes have been tested and based on the results the tests schemes have been improved. In this article, authors would like to emphasize only the final results of the investigations, so only the final schemes (used in the validation phase of the project) are described. Luminaire ID #15 means the actual luminaire above the observer, smaller luminaire IDs mean luminaires farer from the observer.

(abbrevations: Sch. = Scheme, In. = Inactive level, Std. = Standard illuminance level, Ovr. = Overlighting (higher than standard level)

Table 3 – Description of schemes

luminaire ID	Illuminance level, distance lit up and holding time is equal in all two schemes, run-up time is more in case of scheme #23 (increased from 2 s in #11 to 8 s in #23)		Distance lit up is equal in length in case of #12 and #23, but it is longer in #31. Run-up time is equal in case of all three settings, holding time is increased (from 6 s in #12 to 12 s in #31)			Distance lit up is equal in length in case of #20 and #23, but in #32 all luminaires is dimming up in front of the person. Run-up time is equal in case of all three settings and holding time is increased (from 6 s in #20 to 12 s in #32)			These are the schemes which were used as a starting point in the pilot phase of the project. In case of #2 and #5, run up times ranges from 2s to 5s, and holding times from 3s to 4s. #8 and #9 were designed to minimize energy consumption, hence their timings were set to minimum (run up time is 0.9s, holding is 0.5s).			
	Sch. #11	Sch. #23	Sch. #12	Sch. #24	Sch. #31	Sch. #20	Sch. #25	Sch. #32	Sch. #2	Sch. #5	Sch. #8	Sch. #9
# 1	In. – 6 lx	In. – 6 lx	In. – 6 lx	In. – 6 lx	In. – 6 lx	In. – 6 lx	In. – 6 lx	In. – 6 lx	In. – 15 lx	In. – 15 lx	In. – 6 lx	In. – 6 lx
# 2	In. – 6 lx	In. – 6 lx	In. – 6 lx	In. – 6 lx		In. – 6 lx	In. – 6 lx		In. – 15 lx	In. – 15 lx	In. – 6 lx	In. – 6 lx
# 3	In. – 6 lx	In. – 6 lx	In. – 6 lx	In. – 6 lx		In. – 6 lx	In. – 6 lx		In. – 15 lx	In. – 15 lx	In. – 6 lx	In. – 6 lx
# 4	In. – 6 lx	In. – 6 lx	In. – 6 lx	In. – 6 lx		In. – 6 lx	In. – 6 lx		In. – 15 lx	In. – 15 lx	In. – 6 lx	In. – 6 lx
# 5	In. – 6 lx	In. – 6 lx	In. – 6 lx	In. – 6 lx		In. – 6 lx	In. – 6 lx		In. – 15 lx	In. – 15 lx	In. – 6 lx	In. – 6 lx
# 6	In. – 6 lx	In. – 6 lx	In. – 6 lx	In. – 6 lx		In. – 6 lx	In. – 6 lx		In. – 15 lx	In. – 15 lx	In. – 6 lx	In. – 6 lx
# 7	In. – 6 lx	In. – 6 lx							In. – 15 lx	In. – 15 lx	In. – 6 lx	In. – 6 lx
# 8	In. – 6 lx	In. – 6 lx							In. – 15 lx	In. – 15 lx	In. – 6 lx	In. – 6 lx
# 9	In. – 6 lx	In. – 6 lx							In. – 15 lx	In. – 15 lx	In. – 6 lx	In. – 6 lx
#10									In. – 15 lx	In. – 15 lx	In. – 6 lx	In. – 6 lx
#11									In. – 15 lx	In. – 15 lx	In. – 6 lx	In. – 6 lx
#12											In. – 6 lx	In. – 6 lx
#13			Std.-150 lx	Std.-150 lx	Std.-150 lx	Ovr.-175 lx	Ovr.-175 lx	Ovr.-175 lx			In. – 6 lx	Std.-150 lx
#14			Std.-150 lx	Std.-150 lx	Std.-150 lx	Ovr.-203 lx	Ovr.-203 lx	Ovr.-203 lx	Std.-150 lx	Std.-150 lx		Ovr.-233 lx
#15	Std.-150 lx	Std.– 150 lx	Std.-150 lx	Std.-150 lx	Std.-150 lx	Ovr.-233 lx	Ovr.-233 lx	Ovr.-233 lx	Std.-150 lx	Ovr.-233 lx	Std.-150 lx	Ovr.-233 lx

A scheme describes how the whole lighting system (in this case our corridor's lighting system) acts, when it detects movement. The closer the luminaire to the source of the movement, the higher luminaire ID it gets. For example, in case of Scheme #12, the luminaire above the user and two consecutive are going to dim up, and provide a standard 150lx illumination. From the third to eighth, illumination level is decreasing gradually down to 6lx with the ninth luminaire, which is in the inactive state (and the others following it).

Run up time means how fast a luminaire is dimming up from its' inactive state to the maximum illumination level. Holding time determines how long a luminaire retain its' dimming level (or luminaire ID) after getting a lower level, or when no movement detected.

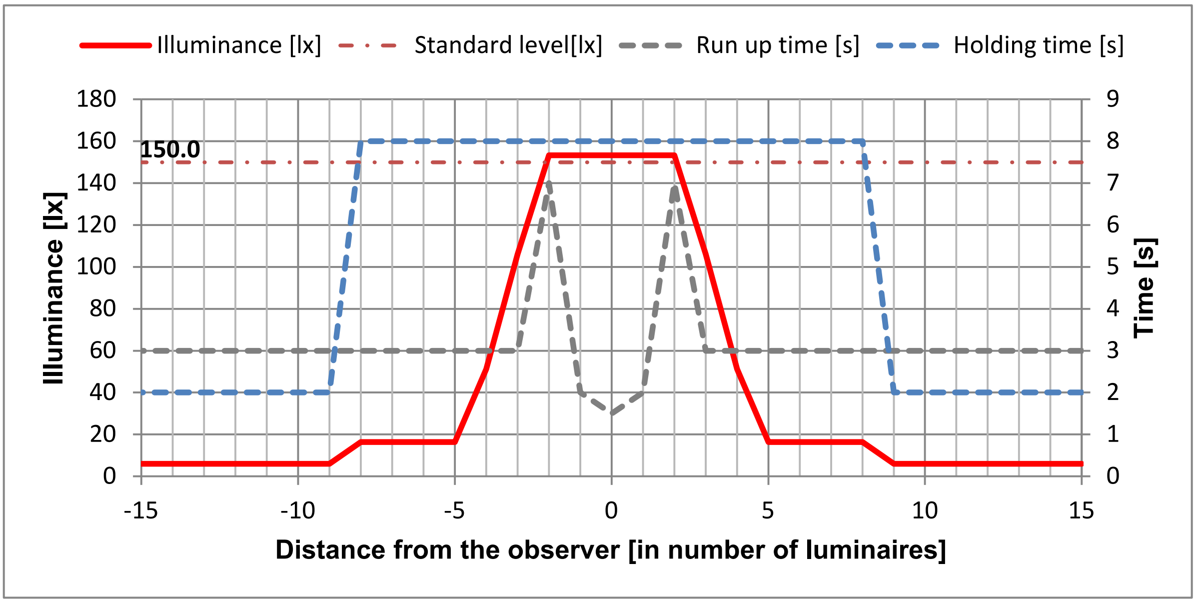

Figure 2 – Illuminance level of the corridor in case of scheme #24, after a person entered at 0 position and all the luminaires were dimmed up. Run up- and holding times were also shown.

Figure 2 shows how the lighting system acts when somebody enters the corridor and stays in one place for a while. The illuminance level shows the state, after every luminaire dimmed up to its' corresponding level. Positive values on the horizontal axis shows luminaires in front of the user, and 0 is the place where he/she actually stands. In the experimental setup, the corridor had only 15 luminaires, so this should be taken into account by cutting off the inapplicable parts of the graph.

Procedure

The tests have been performed two times with the participation of 30. The task of the test person was to walk along the corridor carefully (with possible changes in the direction of walking) and observe the standard illumination scheme (non-adaptive, constant scheme) of the corridor. After that, one of the dynamic lighting schemes was presented. After walking along the corridor he/she had to fill out a questionnaire about his/her experience on the corridor.

The questions were the following:

Q1. To what extent is the present dynamic lighting acceptable compared to the original continuous lighting?

Q2. Was the area in front of you well illuminated and clearly visible?

Q3. Was the area in front of you well illuminated when you turned back?

Q4. Have you felt any disturbing effect at the corridor (glaring, unexpected transient in luminous intensity, etc.)?

Q5. How far can you see clearly the corridor?

Different dynamic lighting patterns have been defined by changing run-up time, illuminance level at "max state" and hold time. Parameters of lighting pattern were modified systematically to find when the observers perceived distractions under the investigated scheme. A standard lighting scheme has been defined (scheme #0) without adaptive features as a reference scheme in the experiments, which realizes a homogeneous illuminance of 150 lx at the corridor according to the European standard 12464-1.

Results and discussion

1. Psychophysical tests, results

In validation phase we have defined three different schemes (scheme #11, scheme #12, scheme #20), which were further improved on the basis of observers' opinion. Only 10 observers have seen these settings and based on their 19 observations we have modified the run-up time and holding time. 30 observers saw the further developed schemes. Judgements of observers have been collected and are presented in the following figures. In corridor, schemes #0-#11-#12-#20-#23-#24-#25-#31-#32 (see table 3 for scheme descriptions) have been realized.

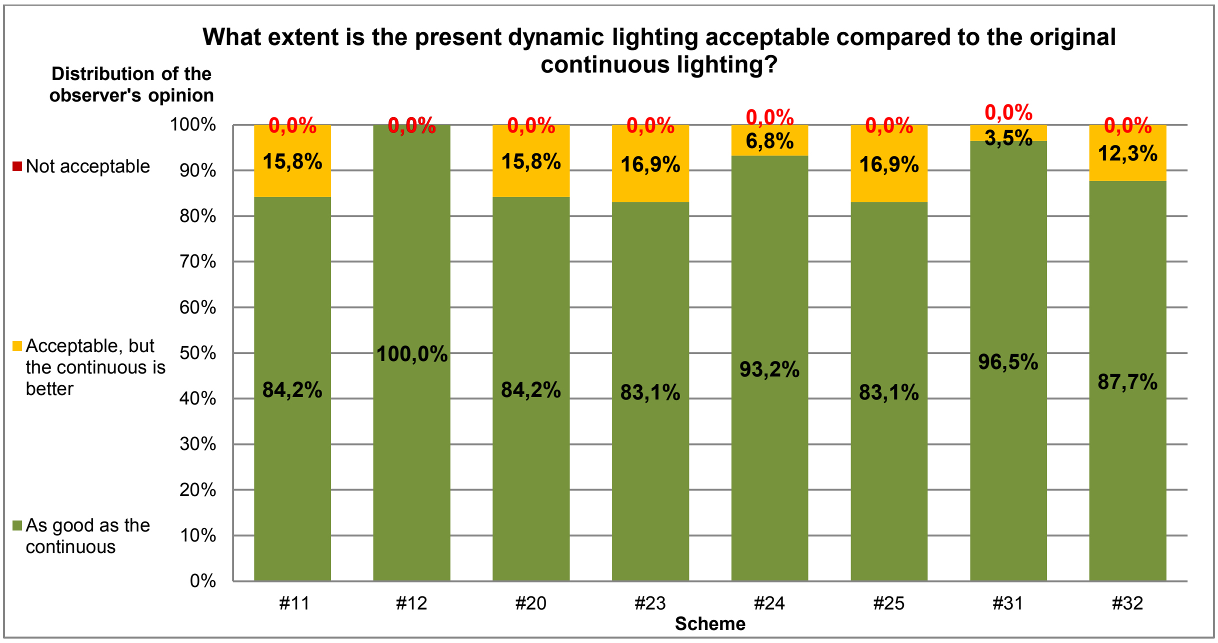

Figure 3 – Visual experiments - results

As it can be seen from the above figure all schemes are acceptable and more than 90% of the observers found the scheme #12, #24 and #31 almost as good as the continuous lighting. Observers found none of the settings unacceptable. In case of scheme #11, #20, #23, #25 and #32 more than 10% of the observers said that the actual dynamic lighting is acceptable but the continuous is better. In case of the less popular settings, either the run-up time or holding time was short, or the observers felt the illuminance level too high.

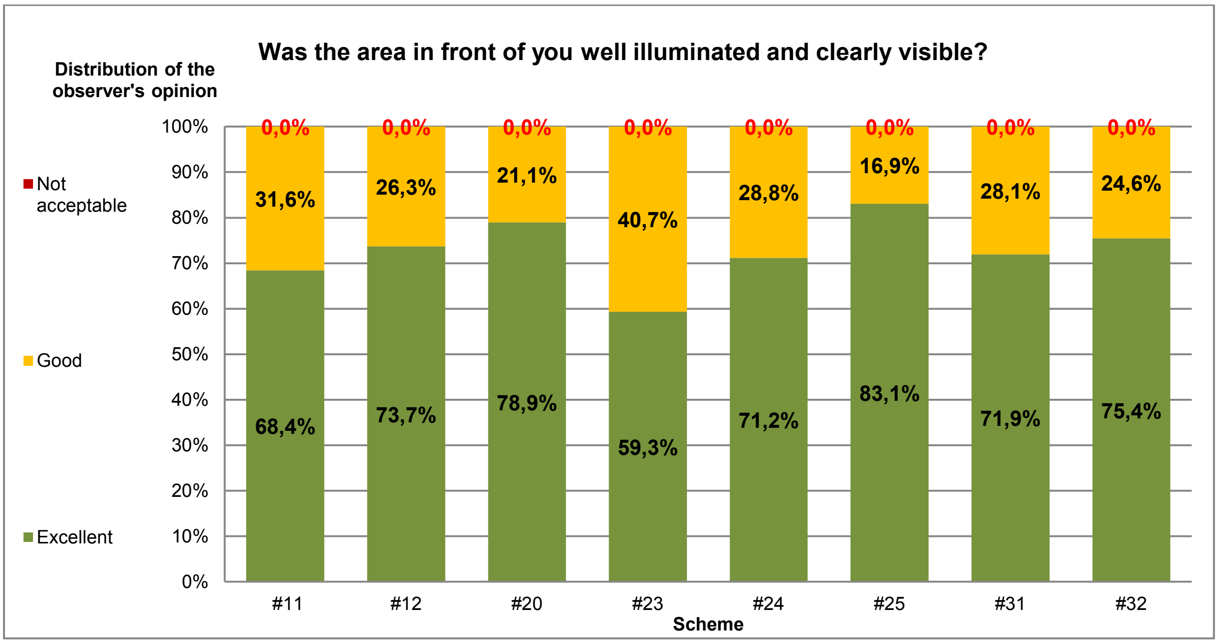

Figure 4 – Visual experiments - Results

As it can be seen from the above figure in case of all schemes the users found the scene in front of him/her well illuminated and clearly visible, so none of the settings was found to be unacceptable. In this aspect the schemes #20, #25 and #32 were the best, more than 75% of the observers found the corridor's illumination excellent. These are the schemes, where the actual and two additional luminaires were overlighting in front of the user. But in case of scheme #12, #24 and #31 more than 70% of the test persons told too that the corridor in front of him/her was excellently illuminated and clearly visible. These are the settings, where the actual and additional eight illuminants were dimmed up in front of the test person. The participants found the scheme #11 and #23 as the worst, because in these cases only five luminaires were lighting in front of the observers.

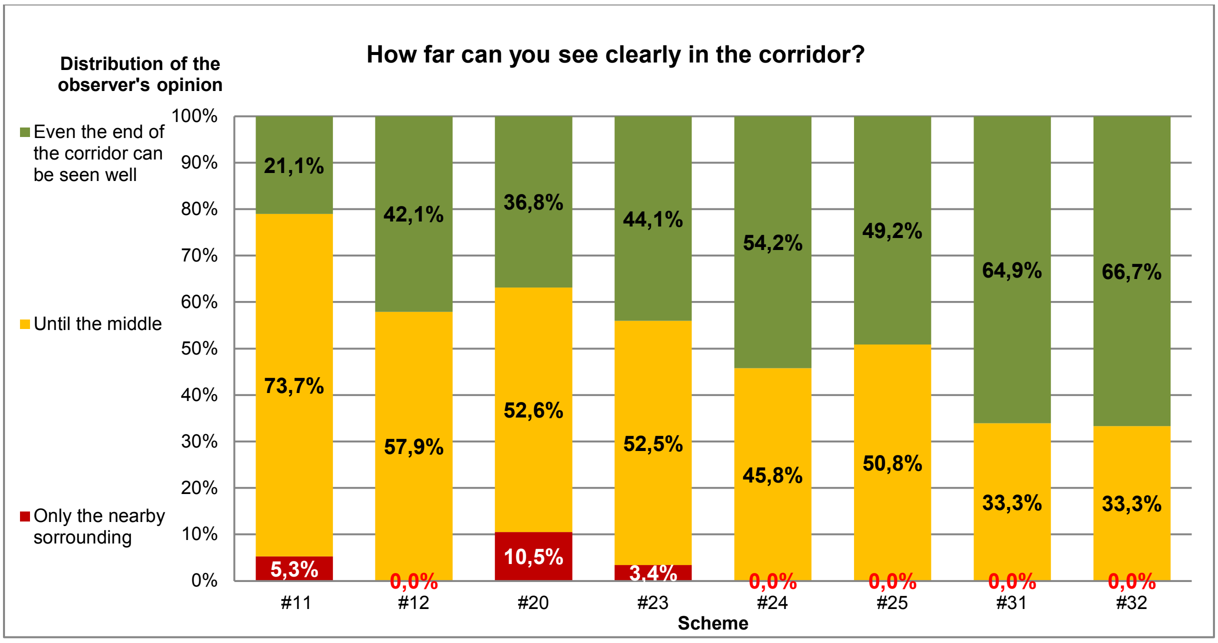

Figure 5 – Visual experiments - Results

As it can be seen from the above figure by improving the schemes the visibility of the corridor was getting better. In case of schemes #31 and #32 more than 60% of the observers have seen the end of the corridor well. These are the schemes, where all illuminants were dimmed up in front of the test person (the actual and four additional luminaires were providing illumination of at least 50 lx and the further illuminants were lighten up to 15 lx from 6 lx), while in case of the less favour settings only five or eight illuminants dimmed up in front of the observers.

Investigation of supplementary lighting at corridor ends:

In addition it has been concluded from preliminary experiments, that illuminance level at the ends of the corridor counts a lot in users' judgements of visual comfort. In case of a corridor without windows and incoming natural light with weak artificial lighting users can't see clearly the ends of the corridor, which might decrease users' comfort feeling and increase uncertainty and fear. In order to investigate this phenomenon experiments with all the eight validation schemes have been repeated with illuminated corridor endings.

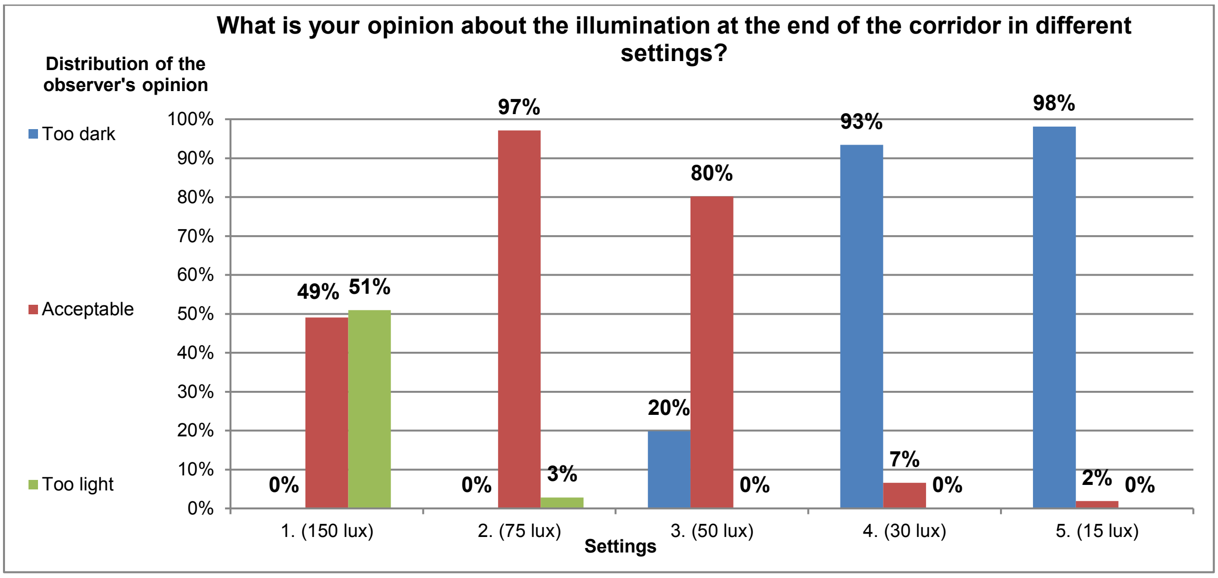

Figure 6 – Lighting level at the corridor ends - Results

As it can be seen from Figure 5, on the basis of the observers' opinion the best value was the 2nd setting, where the supplementary lighting at corridor ends was 75 lx. More than 50% of test person found the 1st setting (150 lx) too bright and they felt that the light reflected from the wall glared them. The majority of observers evaluated the 3rd setting acceptable (50 lx), but 20% of the participants perceived it to be rather dark. More than 90% of the test persons found the 4th and 5th setting too dark.

2. Energy metering: setup, tests and results

In order to measure energy consumption differences between a static and an adaptive lighting environment, a power metering system has been installed at University of Pannonia.

Energy consumption of the intelligent corridor lighting system has been measured according to two strategies:

1. One-time use measure: A test person walked through the corridor at the same speed in case of all test schemes. The time was measured from the start until all the luminaires dimmed back to their base level. For these measurements we have taken into account settings developed during the first test phase too (Scheme #2, #5, #8, #9 (see rightmost four columns in table 3), because in case of them we have experimented with shorter run-up - and holding times and with overlighting.

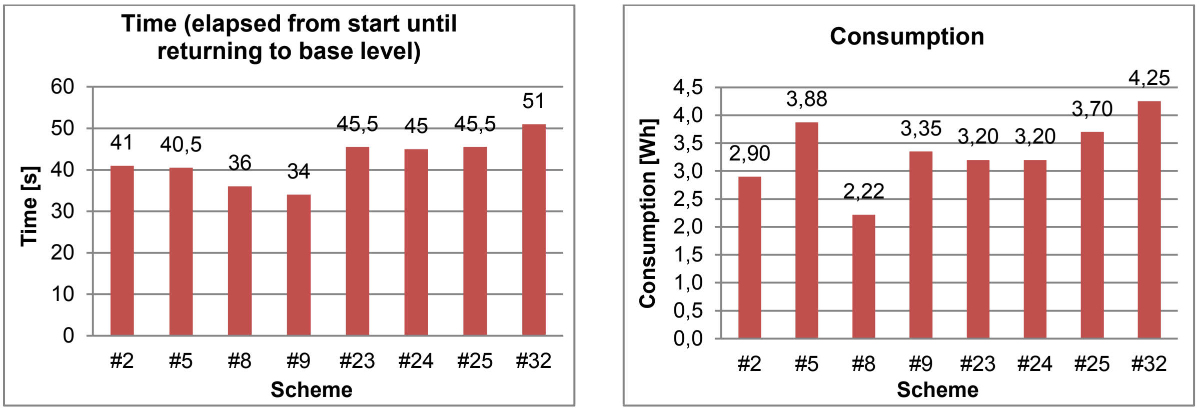

Figure 7 – Energy saving data of different schemes

As it can be seen from the consumption graph, the greatest difference is almost 50% between scheme #8 (the most economical setting, because the actual and additional only one luminaire dimmed up in front of the test person, and the run-up (0.9 sec) and holding times (0.5 sec) were minimal) and #32 (the most comfortable for the users, because all luminaires dimmed up in front of the observers, and the run-up and holding times were acceptable). But that does not imply 50% consumption reduction in long term use, because most of the time the luminaires are running on their base level. Also keeping in mind, that scheme #8 was the worst in almost all the aspects according to the results of the visual experiments, the tailoring the lighting scheme parameters by only considering the energy consumption is not practical. Also the difference in the consumption between the other schemes was not significant. That is why the lighting scheme should be optimized to users' perception and comfort.

2. Long-term tests:

Schemes are set-up at one of the two parallel corridors and continuous lighting (producing 150 lx) has been set up at the other corridor. Energy consumption has been measured during one week period.

The following diagram shows the energy saving data of the most popular scheme (#31). It was the setting, where the actual and additional eight illuminants were dimmed up in front of the test person and the holding time was longer than for the other schemes.

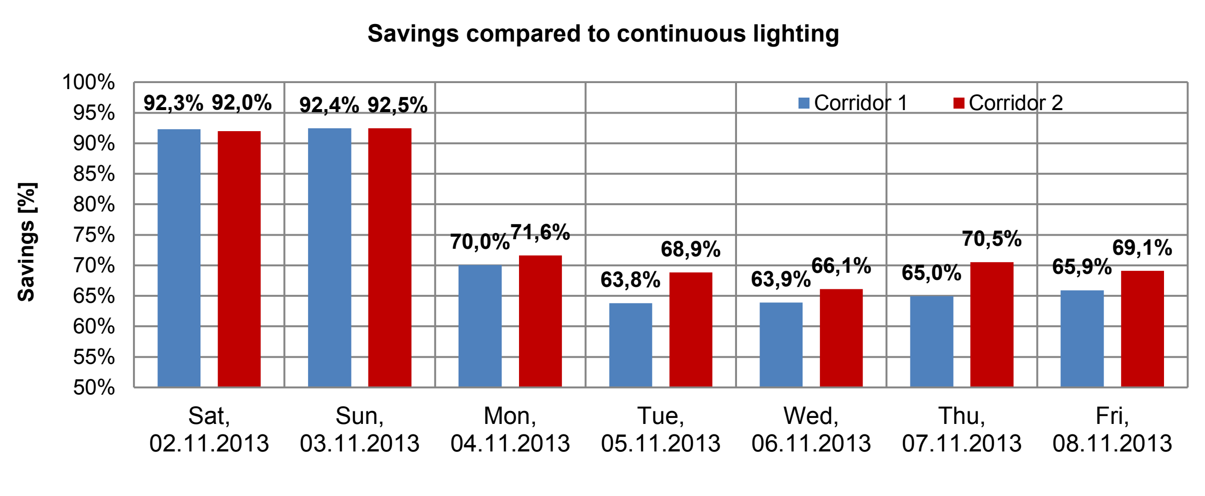

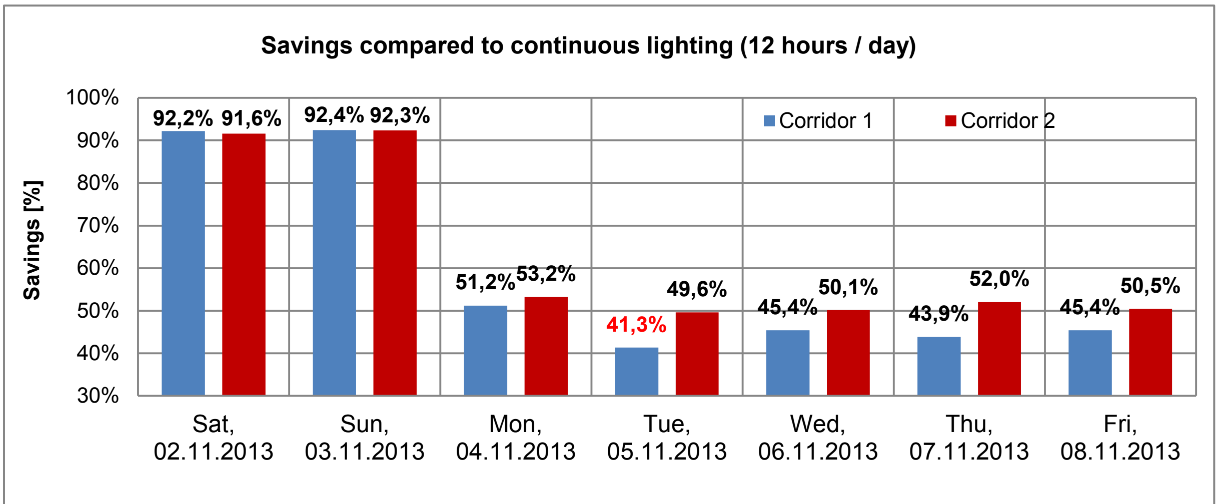

Figure 8 – Energy saving data of the most popular scheme

It can be seen that the energy savings is more than 90 % on holidays and for the other days, the savings take place between 63.8% and 71.6% for whole day measurements, and 41.3% - 53.2% when calculating with 12 hours a day.

Summarizing the results of the energy consumption measurement:

The dynamic lighting system saves at least 40% energy compared to the continuous even in worst case scenarios (maximum corridor usage, and only the most active hours taken into account). Under normal circumstances, the savings are usually more than 50%. The dynamic system can adapt itself to the corridor's traffic, hence it saves more energy without any user intervention on low usage periods (e.g. when most of the employee are on holiday).

On the long run, the measurements show no difference between the schemes consumption. What makes the energy usage vary is the rate of traffic on the corridors. This proves the conclusions made during the individual measurements of the schemes, that the lighting scheme should be optimized to users' perception and comfort, not to energy consumption.

Conclusion

Visual experiments:

- Corridor-end-lighting level between 75 lx and 55 lx is acceptable.
- The run up time of the luminaire above the user plays an important role, when entering to the corridor. This value should be between 1.5 and 2 seconds.

- The luminance level should be less or equal for the consecutive luminaires. Lowering the illuminance level while walking causes disturbance among the users.
- Overlighting makes dynamic lighting more comfortable. University of Pannonia proposes an overlighting level of 50% (225 lx), 35% (202,5 lx) and 15% (172,5 lx) for the first, second and third luminaire.

Energy metering:

- The dynamic lighting uses less energy compared to continuous because of its dynamic nature. The energy saving is achieved by dimming down the luminaires, when the corridor is not in use.
- The difference among the energy consumption of dynamic lighting schemes is not significant, and decreasing the run up and holding times makes them uncomfortable, so the schemes should be developed by preferring users' visual comfort to energy savings.
- Long term measurements show at least 40% reduction in energy consumption in worst case, and more than 50% can be achieved during normal usage.

Acknowledgement

This work has been supported by the Research and Technological Innovation Fund of the National Development Agency of Hungary, under contract number ED_12-1-2012-0008.

References

[i] European Standards 2011 Light and lighting – Lighting of workplaces – Part 1: Indoor workplaces. EN 12464-1:2011.

[ii] Logadóttir A., Iversen A., Markvart J., Corell, D. D., Thorseth, A., Dam-Hansen, C. Comparison of User Satisfaction With Four Different Lighting Concepts, CIE x038:2013. pp. 159-168.

[iii] Mochizuki E., Oikawa, D., Kim J., Tashiro H, Iida K. Effects on Energy Savings of Personal Lighting Control System in an Office Building in Japan Part 1 outline of the measurement and effects on lowering electrical power consumption for lighting

[iv] Mochizuki E., Oikawa, D., Kim J., Tashiro H, Iida K. Effects on Energy Savings of Personal Lighting Control System in an Office Building in Japan Part 2 Evaluation of Lighting Environment and Occupants' Response to Personal Lighting Control System

OP45

MEASURES FOR A BETTER QUALITY IN LIGHTING

A JOURNEY THROUGH RECENT ACTIVITIES IN APPLICATIONS AND STANDARDS

Dipl.-Ing. Peter Dehoff
Zumtobel Lighting GmbH, Schweizer Straße 30, 6850 Dornbirn, AUSTRIA
peter.dehoff@zumtobelgroup.com
Austrian representative to CEN TC 169, convenor of WG 2
President of CIE Austria

Abstract

Lighting quality is the result of a process: requirements of a user shall be in agreement with the evaluation of a lighting solution. Characteristics of a lighting evaluation and criteria for lighting design are existing and ready to be used. An extension of lighting quality is given by the importance of biological effects of lighting. Lighting quality and energy efficiency shall always be in a balance.

Keywords: Lighting quality, lighting criteria, lighting characteristics, energy efficiency, standards

1 Introduction

Lighting quality should become the equal driver as energy efficiency. For life of humans lighting quality plays an essential role. It might be difficult to measure the benefits reached by lighting quality in the same way as savings can be calculated by using energy efficient lighting solutions. On the other hand the consequences from bad lighting might be worse than expected: lesser wellbeing, lower productivity, higher cost of labour, slower recovering and less sales in retail might be a result. Sometimes people are not even aware about these consequences.

Therefore it is of higher importance to find the best way to describe what lighting quality means and how it may be achieved. It should be an essential part of standards and regulations even more than it is already incorporated.

Lighting quality is a business of many disciplines and has many stakeholders. The user, the designer, the architect, the owner, the facility manger, the manufacturer and also politicians and standard-setting experts shall be considered.

2 What is lighting quality?

> "Quality is the standard of something as measured against other things of a similar kind; the degree of excellence of something" (Oxford dictionary)

2.1 Definition of lighting quality

Interestingly:

- Lighting quality is not defined in Wikipedia where usually many expressions are described.
- Lighting quality is not defined in the ILV (International lighting vocabulary)
- Lighting quality is not defined in the European Standards EN 12665 or EN 12464

Lighting scientists have thought about lighting quality since artificial lighting became part of the daily life.

It is logical that lighting quality is not only existing of one or few parameters. One description was published by IESNA.

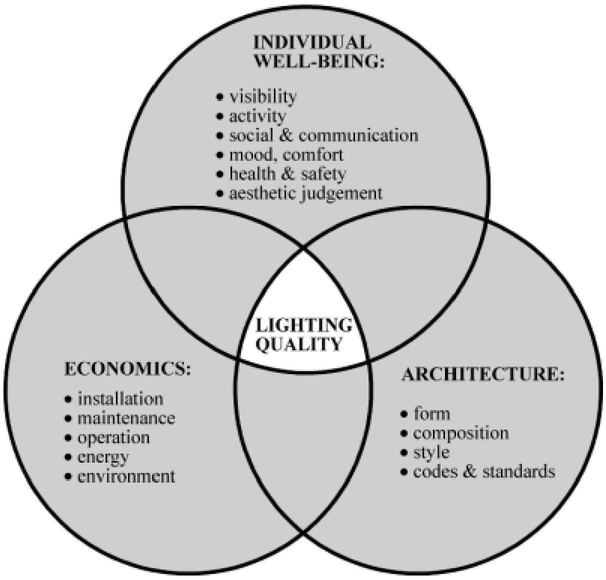

Figure 1: Lighting Quality definition developed at First CIE Symposium on Lighting Quality (Veitch, Julian, & Slater, 1998).

Lighting qualityt can be seen as the best overlap of parameters for individual well-being, architecture and economics. How may this be achieved? From the definition of "quality" it is stated that lighting quality is not an absolute measure or number. It is always measured against something else.

2.2 Process definition of lighting quality

Lighting quality is a result of lighting design process.

"The lighting designer must be able to understand the needs of the person in the space and must know how a lighting installation can help to meet them by creating the appropriate set of luminous conditions." (CIE TC 3-34)

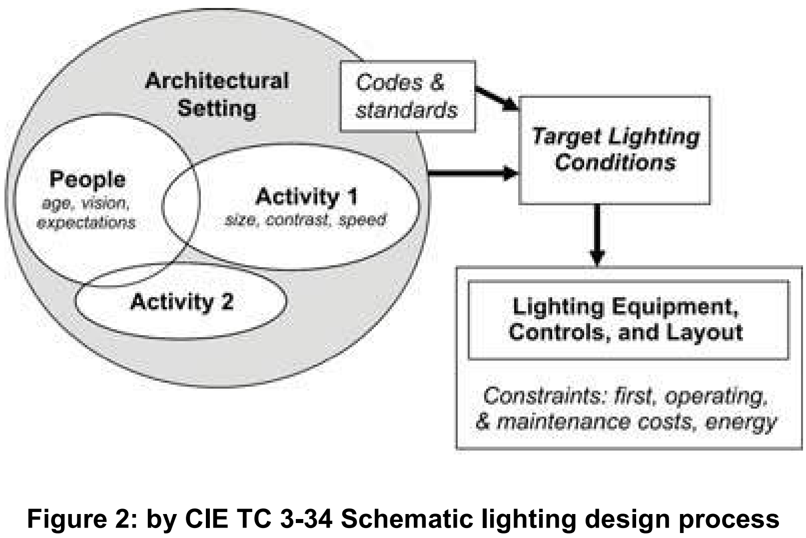

Figure 2: by CIE TC 3-34 Schematic lighting design process

2.3 Process of evaluating lighting quality

In a comprehensive draft paper (Lichtqualität, only in German) the evaluation of lighting quality is described. The process starts with an intensive determination of the requirements of a user. According to the individual assessments together with the application, f.e. office, retail or sports the requirements are systematically arranged and weighted. That is the basis for a lighting solution using specific and well described designing measures. The user has to evaluate this solution using specific characteristics. Finally an agreement must be reached between the evaluation and the requirements which is a measure for the quality of light.

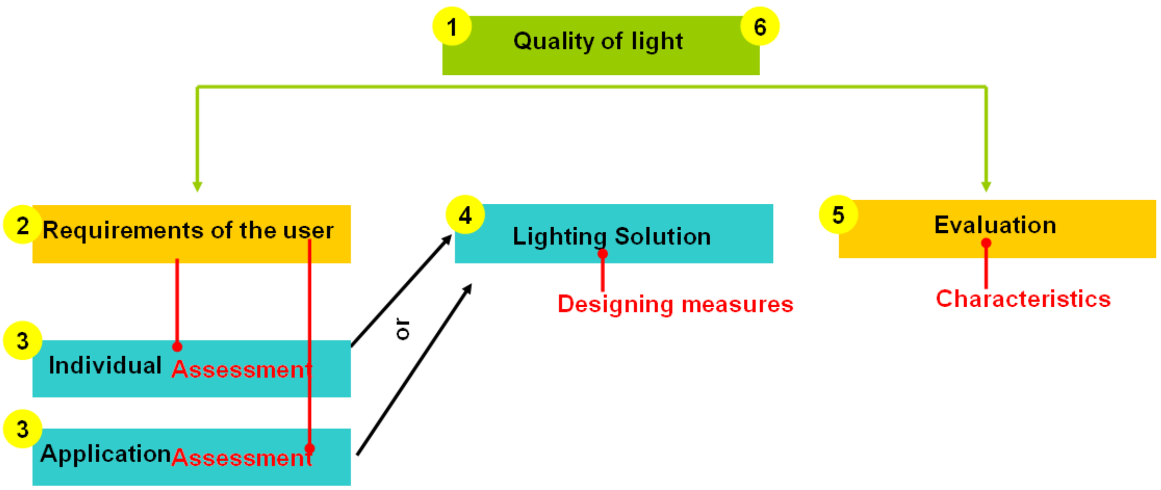

Figure 3: Process of evaluating lighting quality: requirements of the user with application and individual assessments are correlated. This results in a lighting solution (created by designing measures) which is evaluated by specific characteristics. The measure for lighting quality is the agreement between requirements and evaluation

The method developed by Tralau and Dehoff for LiTG (Lichttechnische Gesellschaft, German Lighting Society) will be published soon with all the details.

2.4 Criteria and characteristics of lighting quality

Lighting quality is the result of a process in which requirements meet the result of an evaluation. A number of characteristics are widely used to quantify and qualify the evaluation of a lighting solution. To describe the process the parameters need to be defined.

Are those parameters well known? To get a first overview the parameters as used by different authors and sources are listed in the following paragraphs.

2.4.1 Lighting quality parameters in LiTG method

In the method described above the following parameters are used:

- Requirements
  - Functional
  - Biological
  - Psychological
  - Architectural

- Designing measures
  - Amount of light
  - Size of luminous area
  - Number and position of light sources
  - Light colour
  - Light distribution
  - Spectra

Controllability
User interface

Characteristics for evaluation
Illuminance on visual task
Uniformity of illuminance
Colour contrast
Brightness contrast
Discomfort glare
Disability glare
Reflections
Colour temperature
Colour rendering
Contrast rendition
Harsh shadows
Luminances
Modelling
Flicker

The language for the requirements differs from the technical wording for the characteristics. The designing measures are dealing with lighting tasks. Characteristics are quantifiable. Their values only get a meaning when they are related to requirements. The description of the whole process allows to evaluate lighting quality.

2.4.2 Lighting quality parameters used in TC 3-34

The parameter set work out by CIE TC 3-34 “Protocols for describing lighting” is

Describing the entire set of parameters:
Person
Context
Light sources
Room Surface light levels and distribution
Task details
Task plane light distribution
High-Luminance areas
Modelling
Colour appearance
Dynamic effects

The set of descriptors is aimed to support the communication with the designer. With a common basis for communication lighting quality concepts can be better understood and developed.

2.4.3 Lighting quality parameters used by Cuttle

Cit Cuttle has developed the “Six modes of appearance” which are reproduced in TC 3-34.

The six modes are separated as

Non-located	Illuminant mode
	Illumination mode
Located	Illuminant mode
	Illumination mode
	Object mode
	Volume mode

Perceicved attributes
Brightness
Lightness
Hue
Saturation

Flicker
Pattern
Texture
Gloss
Clearness

This set of modes allows a better understanding of lighting situations.

2.4.4 Lighting criteria in standards

EN 12464 "Lighting of workplaces" is a very often used standard for lighting design within Europe. This standard is also a reference also for ISO CIE standard 8995 and other standards for lighting.

4 Lighting design criteria
4.1 Luminous environment
4.2 Luminance distribution
4.2.1 General
4.2.2 Reflectance of surfaces
4.2.3 Illuminance on surfaces
4.3 Illuminance
4.3.1 General
4.3.2 Scale of illuminance
4.3.3 Illuminances on the task area
4.3.4 Illuminance on the immediate surrounding area
4.3.5 Illuminance on the background area
4.3.6 Illuminance uniformity
4.4 Illuminance grid
4.5 Glare
4.5.1 General
4.5.2 Discomfort glare
4.5.3 Shielding against glare
4.5.4 Veiling reflections and reflected glare
4.6 Lighting in the interior space
4.6.1 General
4.6.2 Mean cylindrical illuminance requirement in the activity space
4.6.3 Modelling
4.6.4 Directional lighting of visual tasks
4.7 Colour aspects
4.7.1 General
4.7.2 Colour appearance
4.7.3 Colour rendering
4.8 Flicker and stroboscopic effects
4.9 Lighting of work stations with Display Screen Equipment (DSE)
4.9.1 General
4.9.2 Luminaire luminance limits with downward flux
4.10 Maintenance factor
4.11 Energy efficiency requirements
4.12 Additional benefits of daylight
4.13 Variability of light

This wide set of criteria allows a detailed quantification of a lighting solution. The requirements shall be fulfilled.

This extensive list of parameters show significantly that criteria for lighting design are already part of standards. With these parameters lighting quality measures are given and just should be used.

2.4.5 Lighting quality parameters for LED lighting

In a next step more and more detailed criteria will be incorporated into the standard at its next revision. A good help is given in the CIE 205 publication on "lighting quality measures for interior lighting with LED lighting systems". The emphasis is on specific parameters like

Task visibility:	uniformity of horizontal illumination reflected glare veiling reflections shadows
Visual comfort:	discomfort glare overhead glare luminance ratios visual fatigue eyestrain
Flicker and strobe	
Modelling	of faces and objects
Colour appearance:	colour rendering light colour preference object colour appearance
Consistency	of colour and luminous flux over time and space
Appearance of spaces:	room surface brightness distribution of light on surfaces
Appearance of the light source and luminaire	style integration into architecture appropriateness of appearance size, etc.

It helps to improve the overall validity of design criteria use measures for better lighting quality.

3 Lighting quality and biological effects of light

Effects of light on humans is at least twofold: the visual effects are well known and mainly covered by the above mentioned characteristics. The non-visual function is influencing the biological rhythms and the sleep and alertness reaction. These functions should also be part of lighting quality.

CIE has started very early in bringing scientists from different disciplines together. Symposia on Light and Health were organised in 2004 and 2006.

The economic effect was investigated by AT Kearney, a consulting company, in 2013. Human Centric Lighting could become a significant business opportunity. The positive aspect is that industry will develop solutions which will improve the quality of lighting for humans.

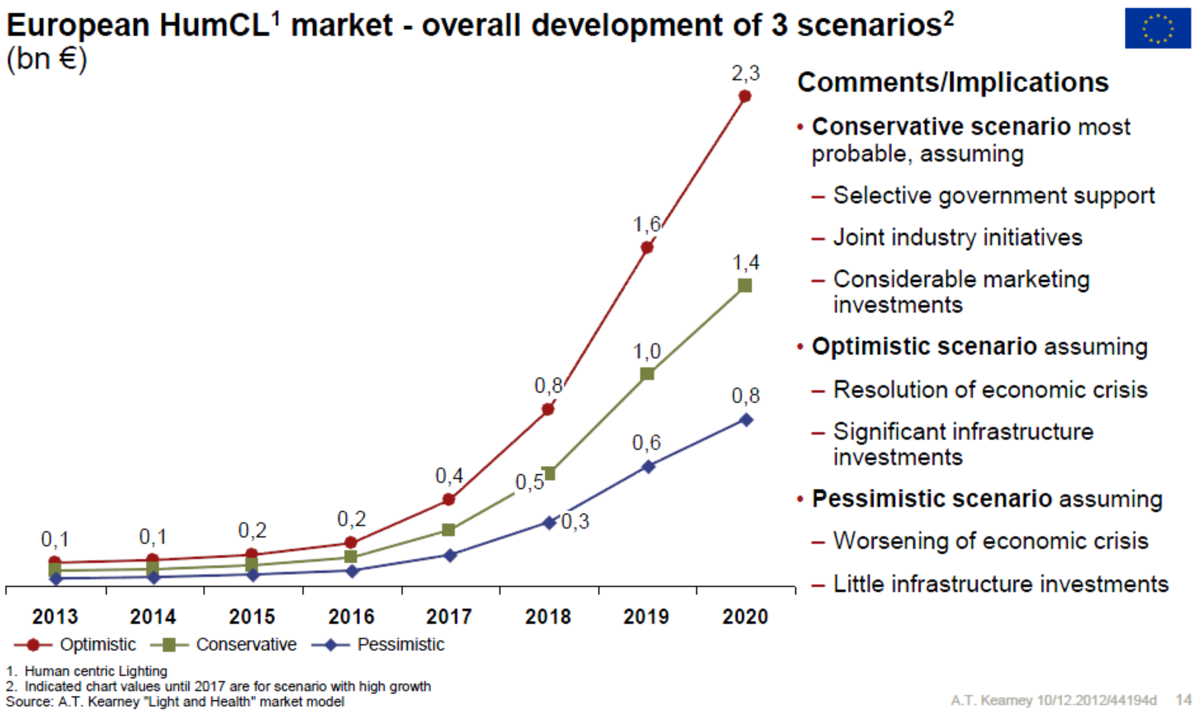

Figure 4: Impact of Human Centric Lighting on business, as investigated by ATKearney for the European market. Three scenarios show the market increase until 2020.

4 Lighting quality in application

Picture 1: Lighting of visual tasks in an office environment. Care is taken to fulfil requirements for illuminances on task areas, well-lit walls and ceiling and vertical illuminances on faces as well as modelling within the room. Daylight contributes to the room lighting.

Picture 2: Lighting of visual task in a supermarket. The customer is lead through the room, products are lit well in terms of illuminances, colour temperature and colour rendering.

Picture 3: Lighting of visual tasks in a museum. Focus is laid on the exhibited precious objects without damaging them by creating dramatic effects with best colour rendering

Picture 4: Representative lighting of an entrance area. Lighting is providing atmosphere and good visual conditions. A lighting object is also contributing to the architectural appearance of the room

The examples in pictures 1 to 4 show the fulfilment of lighting requirements in terms of measurable characteristics. These measures contribute to the lighting quality. Lighting quality is not an absolute result. It exists if the requirements of the user are fulfilled.

5 Lighting quality and energy efficiency

The standard EN 12464 defines lighting criteria while the standard EN 15193 defines requirements for energy efficiency of lighting installations. Both standards refer to each other. Therefore energy efficiency shall be reached without compromising any criteria for lighting quality.

6 Conclusion

Lighting design needs to be taken seriously. The process of meeting the requirements of a user by evaluating a lighting solution is the key. The characteristics for evaluation are many and ready to be used. This process should not be neglected by simple energy saving targets. Energy efficiency is an essential part of a lighting design process. The demand for both, lighting quality and energy efficiency, shall be kept on the political agenda of lighting strategies.

References

ISO 2002, ISO CIE S 8995: Lighting of indoor workplaces, May 2002

CEN 2007, EN 15193: Light and Lighting - Energy performance of buildings – Energy requirements for lighting, CEN, September 2007

CEN 2011, EN 12464-1: Light and Lighting - Lighting of Indoor Work Places, CEN, July 2011

CEN 2011, EN 12665: Light and lighting - Basic terms and criteria for specifying lighting requirements, CEN September 2011

CIE 2011, CIE 196: CIE guide to increasing accessibility in light and lighting, CIE Vienna

CIE 2013, CIE 205: Review of lighting quality measures for interior lighting with LED lighting systems, CIE Vienna

CIE TC 3-34 Guide to protocols for describing lighting, internal draft, unpublished

x015-1998: Proceedings of the First CIE Symposium on Lighting Quality, 9-10 May 1998, National Research Council Canada, Ottawa/Ontario, Canada

x027-2004: Proceedings of the CIE Symposium 2004 on Light and Health: Non-Visual Effects, 30 Sep. - 2 Oct. 2004, Vienna, Austria

x031-2006: Proceedings of the 2nd CIE Expert Symposium "Lighting and Health", 7-8 September 2006, Ottawa, Ontario, Canada

Human Centric Lighting: Going Beyond Energy Efficiency, Market Study by ATKearney, July 2013, published by LightingEurope and ZVEI

BOYCE, P.R. 2003. Human Factors in Lighting, 2nd ed. New York: Taylor and Francis.

CUTTLE, C. 2004: Brightness, lightness, and providing a preconceived appearance to the interior. Lighting Research and Technology, 36(3), 201-216.

DEHOFF, P: A standard for workplaces: the revised European standard EN 12464-1 "Lighting of interior workplaces", CIE 197, Proceedings of the 27th session of CIE, 2011, Sun City, South Africa

DEHOFF, P: Standards and regulations as drivers for energy efficiency and lighting quality: some European experiences, CIE x037:2012, Proceedings "Lighting quality and energy efficiency", September 2012, Hangzhou

TRALAU, B., DEHOFF, P., LIEDKE, C. Die Dimensionen der Lichtqualität: Ein neues ganzheitliches Konzept für Planung und Anwendung, Licht 2012, Berlin

VEITCH, J.A., NEWSHAM, G.R.: Determinants of Lighting Quality I: State of the Science, National Research Council of Canada, Institute for Research in Construction

OP46

INTERPERSONAL JUDGEMENTS, LAMP SPECTRUM AND TASK DIFFICULTY

Steve Fotios[1], Mengdi Dong[2], Biao Yang[1], Yandan Lin[2]

[1] School of Architecture, University of Sheffield, Sheffield, UK
[2] Institute for Electric Light Sources, Fudan University, Shanghai, CHINA
ydlin@fudan.edu.cn

Abstract

The aim of this work is to identify optimum parameters for design of lighting for pedestrians to meet their needs for interpersonal judgements, including luminance and SPD. This paper discusses three factors that affect performance of a facial recognition task – the duration and distance of observation and the task carried out – as these factors affect the interpretation of the optimum luminance and whether or not the effect of lamp spectrum is significant. For SPD, it appears that this matters if the task is difficult (e.g. limited observation duration): a better SPD (for which the best parameter still needs to be defined) allows recognition at greater distances. For luminance, this might be defined by the knee in the plateau-escarpment relationship. A new study is presented that suggests a relationship between task difficulty and facial recognition probability where task difficulty is defined as the product of observation duration and luminance.

Keywords: Interpersonal judgement, facial recognition, lamp spectrum, task difficulty

1 Introduction

One basis for the provision of road lighting in residential areas is to enable interpersonal judgements about other people - whether another person is likely to be friendly, indifferent or aggressive, in time to make an appropriate response (Caminada & van Bommel 1980; Fotios and Goodman, 2012). Analysis of the visual fixations of pedestrians using eye-tracking provides confirmation that observation of other people is a critical task (Fotios et al, in press (a)). Good road lighting should enhance the ability to make such judgements. This paper discusses evidence as to whether the visual components of interpersonal judgements are affected by lamp spectrum (SPD).

Several studies have investigated lamp spectrum and facial recognition but these lead to mixed results, with some suggesting a significant effect (e.g. Knight, 2010) while others did not (e.g. Rea et al, 2009). These data were reviewed by Lin and Fotios (2013), who concluded that an effect of spectrum is expected when the task is difficult, e.g. when the task is small (i.e. a distant person), when it observed for only a short time (e.g. ≤1000 ms), when the face is unfamiliar and when vision is deteriorated by glare.

Many past studies have investigated lighting and facial recognition, but recognition is unlikely to be the only, nor most essential, task concerning other people (Fotios & Raynham, 2011). What may be more essential is the decision as to whether it is safe to approach another person or whether they should be avoided: Willis et al (2011) found that faces exhibiting angry expressions were less approachable than those with happy expressions, and similarly for emotions conveyed by body posture. Approachability was defined as the willingness to approach a stranger in a crowded street to ask for directions, which might be considered the polar opposite of a judgement of threat intent and the resulting motivation to avoid.

Hence this paper examines experiments of facial recognition and facial expression under different lighting conditions.

2 Experimental Design

Table 1 presents a summary of the methods used in past studies. We suggest that several factors may affect task difficulty; task, duration and distance (visual size of target), in addition to luminance. There may also be an effect of glare as there is some evidence that face luminance required for pedestrian visibility increases as equivalent veiling luminance increases (Kohko et al, 2008) but that is not addressed in the current article.

2.1 Task

Two tasks that have been used in past facial recognition studies are identification (or, naming) and matching (Figure 1). The identification task requires test participants to state the name of the target person: of the tests listed in Table 1, all used photographs of celebrities. In the matching task, test participants are required to match the target person with one of a small sample of faces in a reference set.

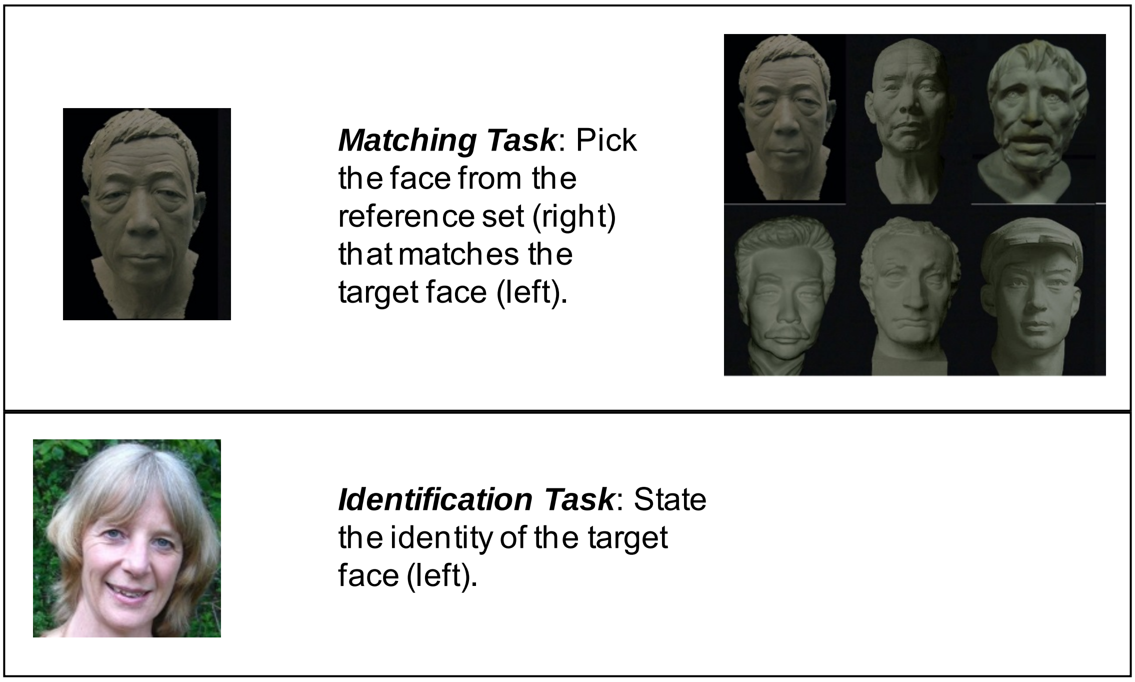

Figure 1 – Illustration of the matching and identification facial recognition tasks.

In the two studies using a matching task, mean recognition distances ranged from 12 metres (Rea et al, 2009) to 24.9 metres (Boyce & Rea, 1990). Neither of these suggested the effect of SPD to be significant. In three studies using an identification task mean recognition distances were in the range of 5.4 metres to 8.45 metres (Knight & van Kemenade, 2006; Yao et al, 2009; Knight, 2010): the target needed to be closer (i.e. of a larger visual size) to permit correct identification than found in the matching task, suggesting identification to be the more difficult task. Identification requires recollection of the name of a celebrity: whilst they need to be well-known, they appear unexpectedly. One reason that the matching task is easier is that prior inspection of the reference set raises familiarity with the faces. There is some evidence for this in the study by Persike et al (2013) who found that familiar faces were found more quickly than unfamiliar faces in a search task.

The matching task has a minimum performance above zero (e.g. a chance level of 10% if there are ten faces in the reference set) while the identification task can be reduced to a performance success of zero if the face is not correctly identified. However, recent work (see below) suggests that this difference does not explain the better performance with the matching task.

Table 1 – Methods used in past studies of inter-personal judgements

Study	Method				Effect of light level	Effect of lamp SPD
	Task	Type of target face	Distance	Duration		
Alferdinck et al., 2010	Ratings of recognisability	Real person	Set distances	Unlimited	Yes	No
Boyce and Rea, 1990	Matching	Real person	Stop-distance	Unlimited	Yes	No
Fotios, Yang and Cheal, 2013	Identify emotion conveyed	Photographs of actors portraying universally recognised expressions	Set distances	1s	Yes	Yes
Knight and van Kemenade, 2006	State name of person	Photographs of celebrities	Stop-distance	Unlimited	Not tested	Yes*
Knight, 2010	State name of person	Photographs of celebrities	Stop-distance	Unlimited	Not tested	Yes*
Lin & Fotios, 2013	State name of person	Photographs of celebrities	Set distances	1s, 3s	Not tested	Yes
Lin & Fotios, 2013	Ratings of recognisability	Photographs of celebrities	Set distances	Unlimited	Not tested	Yes
Raynham and Saksvikrønning, 2003	"*Walk towards a person until their face could be recognised*"	Real person	Stop-distance	Unlimited	Yes	Yes *
Rea, Bullough and Akashi, 2009	Matching	Real person	Stop-distance	Unlimited	Not tested	No**
Rombauts et al, 1989	Ratings of recognisability	Real person	Set distances	Unlimited	Yes	Not tested
Yao, Sun and Lin, 2009	State name of person	Photographs of celebrities	Stop-distance	Unlimited	Not tested	Yes*

Note: (i) Matching = match target face with one from a samples of reference faces. (ii) Stop distance: this requires the test participant to walk toward the target except for Boyce & Rea 1990 where the target walked towards the test participant. (iii) * In these studies there was a trend for SPD to affect recognition distance but there is no statistical analysis of differences.

An alternative task is to use ratings of recognisability (Alferdinck et al, 2010; Rombauts et al, 1989) in which the participant is instructed to make an assessment of the recognition of the face of a target person along a bipolar rating scale (e.g. *absolutely not recognisable to completely recognisable*). An advantage of this approach is that real people can be used as targets, there being no need for celebrity faces as identification is not required. Disadvantages are that ratings of recognisability are an unknown dimension, we do not know how respondents use the scale, and this may lead to a large variance.

Fotios, Yang and Cheal (2013) sought evaluations of the emotion conveyed by facial expressions. For faces there are six universally recognised expressions: anger, disgust, fear, happiness, neutrality and sadness (Etcoff & Magee, 1992). Initially, they sought a direct response as to whether the person was considered to be a threat, but these results were not found to be consistent (Fotios & Yang, 2013). Hence, instead they sought identification of the emotion conveyed.

2.2 Duration of observation

The majority of studies in Table 1 allowed an unlimited period of observation for the evaluation. Table 2 shows the results of facial recognition tasks carried out for observation durations of 0.1, 0.3, 1.0, 3.0 and 10.0 seconds using matching and identification tasks (see below). Differences between the three longer durations (1.0, 3.0 and 10 s) do not appear to be significant: performance with the two shorter durations are different from each other and from the longer durations. Observation duration matters.

Table 2 – Proportion of correctly identified faces using matching and identification tasks for different observation durations (see below). These data are for the luminance of 0.1 cd/m^2.

Task	Proportion of correct identification according to observation duration (s)				
	0.1	0.3	1	3	10
Identification	0.05	0.15	0.32	0.47	0.56
Matching	0.42	0.55	0.68	0.85	0.94

Lin and Fotios (2013) repeated an identification task using two durations of observation, 1000ms and 3000ms. The mean distances at which correct identification of identity was first found was slightly longer under 3 s observing duration than 1 s, suggesting the identification task was more difficult with the shorter exposure time. In the 1000 ms trials there was an effect of SPD, with significantly better task performance under Metal Halide lighting than under LED or HPS lighting. At 3000 ms, the results did not suggest an effect of SPD. Thus, the observation duration permitted in an experiment influences whether the an effect of SPD is likely to be revealed.

Unlimited observation is not a realistic pedestrian experience. An estimate of the typical time for which other people are centrally fixated was established by measuring fixation time in the records of an eye tracking study (Fotios et al, in press (a)) and this suggested a median fixation duration on other pedestrians of approximately 500 ms. Confirmation of this is found in the study by Jovancevic-Misic and Hayhoe (2009): the first of their 48 laps of the oval laboratory path best simulated real situations, i.e. before learning of the behaviour patterns of target pedestrians had been gained, and for these laps the fixation duration was also approximately 500 ms.

2.3 Distance

Past studies have used either a stop-distance method, or have sought judgements at one or more fixed distances: neither approach considers the needs of pedestrians.

Those studies using matching and identification tasks have tended to use a stop-distance procedure, in which the test participant walks towards a target face and stops at the distance at which they are able to meet the task instruction. This distance is used as a measured of lighting effectiveness - a greater recognition distance implies better lighting. There are several problems with the stop-distance method. First consider that the cognitive decision to stop walking following recognition requires a change in gait. The stop-distance method is subject to large errors because different targets and observers walk at different speeds and different observes take different amounts of time to make up their mind. Lighting characteristics can affect gait (Figueiro et al, 2011). Consequently, any delay in deciding that a face has been recognised can have different consequences. A step towards overcoming this is to enforce walking of a constant, slow velocity (Hayduk, 1978) but this does not appear to have been done in past facial recognition studies.

Recognition judgements can also be sought at a series of fixed distances, from which to interpolate lighting characteristics for a given decision criterion. While this was done in two studies (Alferdinck et al, 2010; Lin & Fotios, 2013) it introduced further complications: in both studies judgements were sought initially at the greatest distance with further judgements at progressively shorter distances. Instead, distances should have been experienced in a random order to offset learning effects, this exaggerated in one study (Alferdinck et al, 2010) by repeated observation of the same target. An alternative approach, when using images as targets rather than real faces, is to employ a constant observation distance but vary the size of the photograph to simulate different interpersonal distances.

From past experiments we learn the distance at which a particular task was achieved. What the results do not tell us is the distance at which interpersonal evaluations are desired by pedestrians. This distance is important as it is likely to affect estimates of the optimum luminance needed for task performance and whether or not there is a significant effect of lamp SPD.

The implication of distance can be seen in the results of the experiment by Fotios et al (2013) who sought the emotion conveyed by facial expression and body posture under three luminances, two SPD, with three interpersonal distances simulated by target size. For a 4 m distant target the optimum luminance for facial expression (as defined by transition in the plateau-escarpment relationship) was approximately 0.1 cd/m^2, while for the 10 m target it would increase to over 1.0 cd/m^2 (Figure 2) Their evaluations of body posture suggested an effect of SPD on emotion recognition for those cases are those in the middle of the luminance and distance combinations - when the task was either relatively difficult (i.e. small size and low luminance) or easy (i.e. large size and high luminance) then lamp type did not affect the task.

An understanding of the distance at which interpersonal judgements are desirable would be useful to inform interpretation of the optimum characteristics of lighting. Caminada and van Bommel (1980) suggested a requirement to recognise the face of an approaching pedestrian at a distance of 4 m, this apparently rounded from the border between the social and public zones of personal space proposed by Hall (1969). Alternative classification of personal space was reported by Cutting and Vishton (1995) who suggested three zones: personal space (up to 2 m), action space (2 m to 30 m) and vista space (>30 m). The Cutting and Vishton (1995) data are presented here to demonstrate that Hall's proposals are not definitive, and that awareness of other classifications of personal space may have lead Caminada and van Bommel towards an alternative minimum distance.

While two laboratory studies (Adams and Zuckerman, 1991; Fujiyama et al, 2005) have attempted to measure interpersonal comfort distances we do not consider the data to be credible. The results from Fujiyama et al suggest comfortable interpersonal distances that are longer (4.0 to 5.2 m) than do the results from Adams and Zuckerman (0.53 to 1.2 m):this is probably a stimulus range bias – the laboratory of larger physical size led to the larger estimate of comfort distance. Further concern is that in laboratory studies the test participants know they are being observed (Sundstrom and Altman, 1976) and are not subject to the effects of reassurance (Fotios et al, in press (b)).

Townshend (1997) proposed a minimum comfort distance of 15 m from the results of an after-dark field study in which members of the public were asked to estimate the distance at which they would be comfortable about an approaching person or group of people.This estimate of comfortable interpersonal distance compares well with the results of a pedestrian eye-tracking study, in which 40 test participants walked a 900 m urban route in daytime and after dark (Fotios et al, in press (a)). Within these records, 1538 pedestrians were visible, of whom 1128

(73.3%) were fixated at least once. Figure 3 shows the median distance at which other pedestrians were fixated, this being the median across the 40 test participants for each of the four combinations of two route sections and two times of day (daytime and after-dark). These data suggest a tendency to fixate upon other pedestrians in the range of approximately 6 m to 16m, with a mode of 10-12 m, and extreme values of up to 52 m.

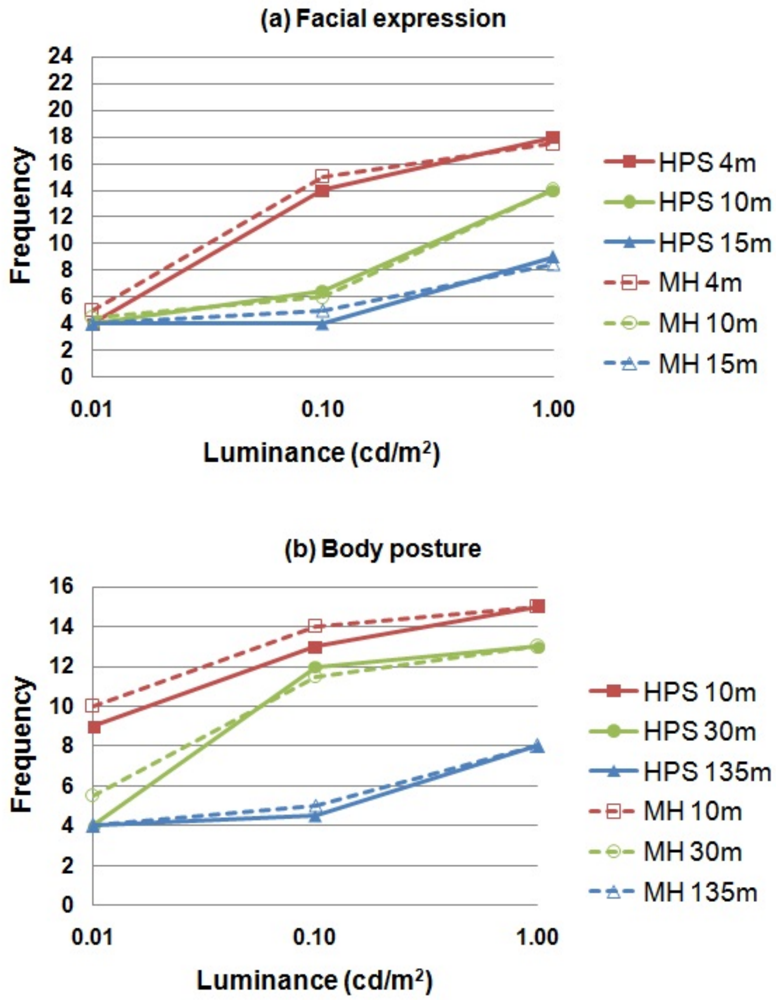

Figure 2 – Median frequencies for correct identification of emotion from facial expression (a) and body posture (b) (Fotios et al, 2013). The legends show lamp type (MH or HPS lamp) and simulated target distance.

3 Experiment to investigate difficulty

There is evidence from past work that task difficulty is influenced by luminance, the duration of observation, and the type of task. An experiment was carried out to further investigate this, measuring facial recognition with two tasks (identification and matching), three luminances (0.1, 1.0 and 10.0 cd/m^2), and five observation durations (0.1, 0.3, 1.0, 3.0 and 10 s).

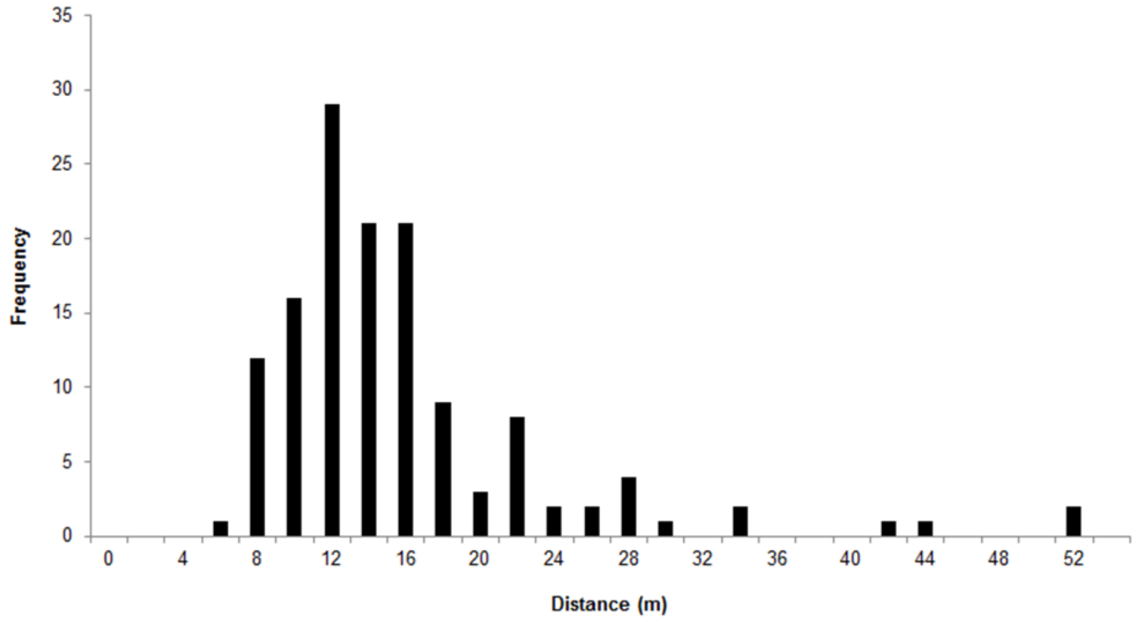

Figure 3 –Median frequency of distances at which other people were fixated whilst walking outdoors. These data are for 40 test participants, walking two route sections in daytime and after-dark (hence n=160). Note: the x-axis label of '8' (for example) represents the upper limit of distance, i.e. a bin 6<x≤8 m.

Targets were photographs presented on a display screen. For the matching task these were black and white photographs of 16 sculptures of heads. For each trial eight target faces, chosen at random, were shown on one screen in a random order. A second screen permanently displayed 10 reference faces, these including 7 of the 8 target faces and three others. For the identification task, the targets were 15 colour photographs of the faces of well-known stars in China, one photograph for each test condition, chosen from a set of 26, including the including four males and four females as were used in a previous study (Lin & Fotios, 2013). For the identification task there were no reference images.

The targets were displayed on a self-luminous screen (EIZO Color Edge CG241W, 24.1 inch display), observed from a distance of 4.5 m with the test participant's eye position fixed using a chin rest. The target images were approximately 90 mm in height, and at the 4.5 m observation distance this simulates a distance of approximately 10 m assuming a typical face height of 200 mm. The digital display allowed accurate control of observation duration and screen brightness rather than ambient light was used to vary target luminance. The matching and identification tasks were carried out separately, with test participant samples of 38 and 20 respectively. Each test participant carried out 15 trials, one for each combination of luminance and duration, and these were observed in a randomised order.

Table 3 presents results of the matching and identification tasks, these data being the proportion of correct responses. Note that for the matching task, the data include responses only for the seven faces for which there was a match in the reference set, and for these data the minimum performance expected (chance level) is 0.1. It can be seen that performance (correct identification) increases with higher luminances and longer durations, and that performance for the matching task is better than for the identification task.

Table 3 – Proportion of correct facial recognition achieved using matching and identification tasks under 15 combinations of luminance and observation duration.

Luminance (cd/m^2)	Proportion correct identification				
	Observation duration (s)				
	0.1	0.3	1	3	10
Matching task					
0.1	0.42	0.55	0.68	0.85	0.94
1	0.82	0.91	1.00	1.00	1.00
10	0.73	0.94	1.00	1.00	1.00
Identification task					
0.1	0.05	0.15	0.32	0.47	0.56
1	0.37	0.65	0.94	0.95	1.0
10	0.45	0.84	0.94	1.0	1.0

These data show clearly that the facial recognition taskis affected by both luminance and duration. Consider that task difficulty is represented by the product of luminance and duration (L*D). Figure 4 shows the relationship between the identification proportion and the logarithmic scale of L*D for the matching and identification tasks. The best fit lines, determined using a logistic fit, indicates that the product of luminance and duration provides a good model for task performance (matching: $R^2 = 0.86$, naming: $R^2=0.87$, n=15 for both).

Interpolation of Figure 4 permits estimates of optimum luminance to be made. First, assume that the minimum probability of correct identification is set at 0.85, an estimate which requires substantiation. The matching task and naming task require L*D values of 0.3 and 3.0 respectively. For the typical observation duration of 500 ms, these represent optimum luminances of 0.6 cd/m^2 for the matching task and 6 cd/m^2 for the naming task.

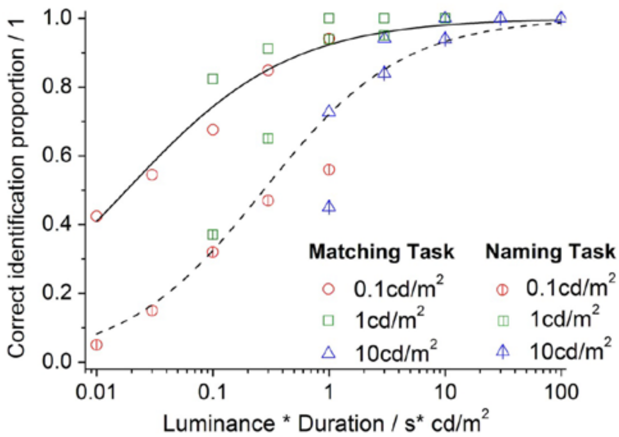

Figure 4 – Relationship between correct identification proportion and product of target luminance and observation duration for results of the matching and identification (naming) tests carried out using targets at an equivalent distance of 10 m.

4 Conclusion

This paper has discussed the relationship between facial recognition and the distance, duration and task of observation. These three factors have significant effect and thus influence interpretation of the optimum luminance required and whether there is a significant effect of SPD. A strong relationship between task difficulty and facial recognition probability has been illustrated. If the task is difficult (longer observation distance and thus smaller visual size; brief observation duration; lower luminance; unfamiliar face) a better SPD allows better recognition ability.

The aim of this work is to identify optimum parameters for design of lighting for pedestrians, from the need of interpersonal judgements, including luminance and SPD. To achieve this, it seems necessary to identify the observation distance and observation duration previously. From the past experiments, we can get some evidence that pedestrians tend to observe others at a distance in the region of 15m and with a duration of 500ms. For the factor of specific task, it was alternative. On the premise of these values, the optimum luminance for a particular correct recognition probability can be suggested according to Figure 4, resulting in 0.6cd/m^2 for the matching task and 6 cd/m^2 for the naming task.

Acknowledgement

The Sheffield contribution to this work was carried out through support from EPSRC (EP/H050817) as part of the MERLIN project.

References

ADAMS, L. & ZUCKERMAN, D. 1991. The Effect of Lighting Conditions on Personal Space Requirements. *The Journal of General Psychology*, 118, 335-340.

ALFERDINCK, J., HOGERVORST, M., VAN EIJK, A. & KUSMIERCZYK, J. 2010. Mesopic vision and public lighting – A literature review and a face recognition experiment. Soesterberg: TNO Defensie en Veiligheid.

BOYCE, P. & REA, M. 1990. Security lighting: Effects of illuminance and light source on the capabilities of guards and intruders? *Lighting Research and Technology*, 22, 57-79.

BRITISH STANDARDS INSTITUTION (BSI) BS 5489-1: 2003. Code of practice for the design of road lighting - Part 1: Lighting of roads and public amenity areas. London: BSI.

BULLIMORE, M., BAILEY, I. & WACKER, R. 1991. Face recognition in age-related maculopathy. *Investigative Ophthalmology & Visual Science*, 32, 2020-2029.

CAMINADA, J. & VAN BOMMEL, W. 1980. New lighting considerations for residential areas. *International Lighting Review*, 31, 69-75.

CUTTING, J. & VISHTON, P. 1995. Perceiving layout and knowing distances: The integration, relative potency, and contextual use of different information about depth. In: EPSTEIN, W. & ROGERS, S. (eds.) *Perception of space and motion*. London: Academic Press.

ETCOFF, N. L. & MAGEE, J. J. 1992. Categorical perception of facial expressions. *Cognition*, 44, 227-240.

FIGUEIRO, M., PLITNICK, B., REA, M., GRAS, L. & REA, M. 2011. Lighting and perceptual cues: Effects on gait measures of older adults at high and low risk for falls. *BMC Geriatrics*, 11, 49.

FOTIOS, S. & GOODMAN, T. 2012. Proposed UK guidance for lighting in residential roads. *Lighting Research and Technology*, 44, 69-83.

FOTIOS, S. & RAYNHAM, P. 2011. Correspondence: Lighting for pedestrians: Is facial recognition what matters? *Lighting Research and Technology*, 43, 129-130.

FOTIOS, S., UNWIN J., FARRALL S. (In press (b)). Road lighting and pedestrian reassurance after dark: A review. *Lighting Research & Technology*.

FOTIOS, S., UTTLEY J., CHEAL C., HARA N. (In press (a)). Using eye-tracking to identify pedestrians' critical visual tasks. Part 1. Dual task approach. *Lighting Research & Technology*.

FOTIOS, S. & YANG, B. Exploring Interpersonal Judgements between Pedestrians. 7th Lux Pacifica, 6-8 March 2013 Bangkok, Thailand. 248-251.

FOTIOS, S., YANG, B. & CHEAL, C. 2013. Effects of outdoor lighting on judgements of emotion and gaze direction. *Lighting Research and Technology*, published online as DOI: 10.1177/1477153513510311

FUJIYAMA, T., CHILDS, C., BOAMPOMG, D. & TYLER, N. 2005. Investigation of Lighting Levels for Pedestrians-Some questions about lighting levels of current lighting standards. London: Centre for Transport Studies, UCL.

HALL, E. T. 1969. *The Hidden Dimension*, New York, Anchor Books. 123-124.

HAYDUK, L. A. 1978. Personal space: An evaluative and orienting overview. *Psychological Bulletin*, 85, 117-134.

JOVANCEVIC-MISIC, J. & HAYHOE, M. 2009. Adaptive gaze control in natural environments. *The Journal of Neuroscience*, 29, 6234-6238.

KNIGHT, C. 2010. Field surveys of the effect of lamp spectrum on the perception of safety and comfort at night. *Lighting Research and Technology*, 42, 313-329.

KNIGHT, C., VAN KEMENADE, J. & DEVECI, Z. 2007. Effect of outdoor lighting on perception and appreciation of end-users. 18th Biennial TRB Visibility Symposium, Berne, Switzerland. Transportation Research Board.

KOHKO, S., KAWAKAMI, K. & NAKAMURA, Y. 2008. A study on effects of veiling luminance on pedestrian visibility. *Journal of Light & Visual Environment*, 32, 315-321.

LIN, Y. & FOTIOS, S. 2013. Investigating methods for measuring facial recognition under lamps of different spectral power distribution. *Lighting Research and Technology*, published online as DOI: 10.1177/1477153513505306

RAYNHAM, P. & SAKSVIKRONNING, T. 2003. White light and facial recognition. *The Lighting Journal*, 68, 29-33.

REA, M., BULLOUGH, J. & AKASHI, Y. 2009. Several views of metal halide and high-pressure sodium lighting for outdoor applications. *Lighting Research and Technology*, 41, 297-320.

ROMBAUTS, P., VANDEWYNGAERDE, H. & MAGGETTO, G. 1989. Minimum semicylindrical illuminance and modelling in residential area lighting. *Lighting Research and Technology*, 21, 49-55.

SUNDSTROM, E. & ALTMAN, I. 1976. Interpersonal relationships and personal space: Research review and theoretical model. *Human Ecology*, 4, 47-67.

TOWNSHEND, T. 1997. Safer City Centres: The Role of Public Lighting. In: OC, T. & TIESDELL, S. A. (eds.) *Safer city centres: Reviving the public realm*. London: Paul Chapman Publishing Ltd.

WILLIS, M., PALERMO, R. & BURKE, D. 2011. Judging approachability on the face of it: the influence of face and body expressions on the perception of approachability. *Emotion*, 11, 514-23.

YAO, Q., SUN, Y. & LIN, Y. 2009. Research on Facial Recognition and Color Identification under CMH and HPS Lamps for Road Lighting. *LEUKOS*, 6, 169-178.

OP47

URBAN ARCHITECTURAL LIGHTING IN CHINA: AN INSPIRING QUALITATIVE STUDY TO DEMONSTRATE ITS DISTINCTIVENESS AND ALSO SIMILARITIES TO INTERNATIONAL PRACTICES

Yang Xiu[1], Hao Luoxi[2], Lin Yi[2], Yan Caijie[1], Demirdes Nurullah Haldun[1]

1. Philips Research China, Shanghai, CHINA
2. College of Architecture and Urban Planning, Tongji University, Shanghai, CHINA

Shawn.yang@philip.com

Abstract

Thanks to rapid penetration of LED based lighting applications, China became one of world's most attractive playground for local and international lighting application experts, lighting designers, urban planners, landscape architects, etc. The important contribution of this study would be to demonstrate and compare the current application practices of urban architectural lighting in China with its few decades past in view of key cultural aspects that might have impact on preferences of lighting designers, DMUs and end users. International lighting professionals could benefit from such a high inspiring fast transformations in urban architectural lighting application in China. By means of this information, this study aims to interact with international practice and contribute to international application knowledge base by suggesting broad perspective for expected future developments in Chinese urban lighting concepts. Based on findings of qualitative field study, future application trends are also suggested.

Keywords: Urban architectural lighting, current situation, urban lighting elements, application trend

1 Background

Since the 1980s, the design and construction of Chinese urban architectural lighting have been gone through the "lighting-up" phase, which means from no lighting to lighting by any means thanks to the Chinese reform and open-up. Then in later years, around 2000, transitioned to the phase contending in beauty and fascination recently, in other words "City Beautification", arriving at a more rational phase that turning to pursue the lighting quality and environmental conservation and aim at solving the practical problems and fulfilling the practical demands.

The transition and evolution of Chinese urban architectural lighting firstly benefit from the fast development of economy since Chinese reform and open-up, which has been improving peoples' living standard and give them more economic capability to pursue their cultural life. Additionally, the rapid expansion of urbanization demanded modern urban architectural lighting. The development of liberal economy also helped the urban architectural lighting can develop freely and rapidly.

Secondly, the urban architectural lighting is also deeply influenced by history and culture of China. As we know, the historical accumulation and the profound Chinese culture, have crucial influence on peoples' aesthetic value and habits gradually and unconsciously. For instance, the Chinese tradition that people likes lively atmosphere, red or purple color and festivals decorated with lanterns, all have leavening influence on urban architectural lighting.[1]

Thirdly, the improvement of science and technology also plays a vital role in the evolution. More and more new lighting sources and related technologies have been invented and applied, enriching the methodology of urban architectural lighting. Especially the development of LED technology and its unique advantages compared with traditional lighting resources, broadly promoted the application of LEDs in urban lighting, such as in architecture, squares, parks and green areas. Additionally, LEDs are also widely applied in urban functional lighting applications, improved the diversity and richness of urban landscape lighting.

Another motivation is the increasing lighting education for people who are devoted to lighting application. Because, in the first decade of development of the Chinese urban lighting, lighting design was done by some experts indirectly linked to lighting, such as landscape designers, electrical engineers, architects, etc. who get their design skills and experience totally from practice rather than professional trainings. During that phase, as mentioned above, most illuminating engineers followed the “lighting-up” principle. Consequently, more and more practical projects were implemented. Some urban lighting planning theories and lighting design methodology were gradually come out afterwards. Some universities and lighting communities also set up dedicated lighting classes and gradually the urban lighting practice improved from wild attempts to more normalized and knowledge-based.

Besides, local government also gave full support and promoted series of recommendations as guidance. At the beginning of the present century, China had held many important international activities, for instance Beijing 2008 Olympic Games, Shanghai 2010 Word Expo, Guangzhou 2010 Asian Games and Xian 2011 International Horticultural Exposition etc. The Government has also taken their leading role in the urban design and construction, which greatly contributed to enhance urban lighting applications.[2] In the meanwhile, the government has also introduced various regulations and recommendations to normalize the urban lighting design and installation mainly by “urban lighting master plan”. Moreover, some relevant national standards of lighting applications, such as "Code for lighting design of urban nightscape (JGJ / T 163-2008)" and "urban lighting management regulations" and so on, were released, to monitor and instruct urban lighting application activities efficiently.

The rapid development of urban lighting practice has also brought a lot of issues for applications, such as lighting pollution resulted from redundant illumination, exaggerated use of colored light, imbalanced lighting levels, glare, excessive applications of drastically changed dynamic lighting and the trend of using LED screens as building façade, etc. Besides this, the selection and application of lighting products for urban landscape are greatly influenced by the price. Due to the fast-growing urban lighting market, unfortunately many products of low price which are far from even “good-enough quality” are in use today.

All these issue, have significant negative effects on humans daily life, i.e light trespass and discomfort glare. In addition, the lack of associated lighting researches, also lead to the lack of beneficial guidance and basis in lighting applications. On the contrary, as already from the beginning of 20th century, in Europe and in United States, there were many dedicated organizations and expert circles working and discussing how to improve the quality of lighting applications and enhance people’s lives by lighting, e.g. The Illuminating Engineering Society of North America (IESNA) in 1906; The British Illuminating Engineering Society (IES) in 1909; The German Lighting Society (LiTG) in 1912 in Berlin, The “Association Francaise de l’Eclairage” (AFE) in 1930.In 1913, after various small establishments already as from 1900, Commission Internationale de l’Eclairage (CIE) was born to mainly provide an international forum for all matters relating to the science and art of lighting.

So, in spite of the fact that rapid upgrading of urbanization in China, urban lighting still need more space for growth and improvement by means of experience and guidance.

2 Study

This qualitative study was carried out mainly by implementing three study elements; literature research, field study and expert interviews. For field study, more than 10 Chinese cities in different regions with different economic levels have been visited, such as Shanghai, Beijing, Guangzhou, Hangzhou, Guilin, Taizhou, Chengdu, Harbin, Dalian, Xinjiang etc. to survey the current urban architectural lighting situations and talk to the end-users. Meanwhile, many nr of people who has expert influence have been interviewed e.g. lighting consultants, lighting designers, urban planners and DMUs in government bodies. Details of the questionnaires, answers and information exchanged during these interview sessions are compiled in a separate report and listed here below under ref. 3.[3] Briefly, urban architectural lighting application situation in the past, present and in the future were discussed during these interview sessions.

Thanks to different background of the co-authors, we could comprehensively understand the past and the current situation of urban architectural lighting practices in China, After analysing all qualitative and experience based data relevant mainly for China environment, we also tried to find similarities to and differences from international practice and briefly presented in this paper with sample visuals.

3 The characteristics of Chinese urban architectural lighting

Chinese territory widely differs from one region to another, having different local circumstances and customs. Therefore even in different cities, different levels of economic development plays a key role in urban architectural lighting design and installation strategies. Decades of rapid economic development contributed to the prosperity of the urban landscape lighting. In this part, the current situation of Chinese urban architectural lighting will be analyzed comparing it with international practice from the viewpoint of lighting application master planning, design & products; the root causes of these problems and future trends will also be briefly discussed.

3.1 Lighting master planning

With the rapid development of Chinese economy and urbanization during last two decades, the urban lighting installations have also of expanded considerably and led to adopt lighting master planning (with close guidance of the government) to prevent chaos and confusion in large scale lighting applications, take Guilin as an example (See figure 1).[4] Related government documents also conducted each city to have its own urban lighting master plan. Urban lighting master plan plays an important role in promoting and regulating the development of Chinese urban lighting.

However, establishment of urban lighting master planning is not mature enough yet and sufficiently standardized and rigorous. Sometimes, important key principles are decided only according to planners' subjective judgments.

Figure 1 – Guilin lighting master planning (2010-2020)

3.2 Lighting design

In China, demand for preparation of a lighting design generally is in very short time because of the rapid implementation of the construction work and the dynamic urban development which sometimes leads to immature lighting design solutions. Consequently, it is difficult to always ensure the appropriate quality of the lighting design due to lack of lighting project experience of some developers. Sometimes, lighting design work lags behind the construction of the project for which it is done. Even a lot of lighting designs are completed while the construction of the site is ongoing. The main urban elements which could be the subject for architectural lighting application are: building, square, structures, green areas, water, etc.

3.2.1 Façade lighting

Building is one of the most important carriers of the urban landscape lighting. Overall, the current lighting effect of building in China contends in beauty and fascination. In Chinese practice, The lighting of buildings is becoming more and more brighter, more and more colorful and the extensive use of dynamic light with adjacent buildings compete with each other.

However, because of the economic and geographical differences in China, lighting design and installation also show significant differences in different cities. In economically backward areas, the situation of building lighting is disordered. In those areas, because of the lack of unified planning, façade lighting depends on the wishes of the owners, and even sometimes it is just done to the purpose of unconsciously lighting-up. In the cities where high level of economic development achieved, high-quality architectural lighting design for building facades, which is adapted to the surrounding environment and rational expression of the architectural characteristics of the building is demonstrated successfully. Figure 2 shows two different façade lightings.

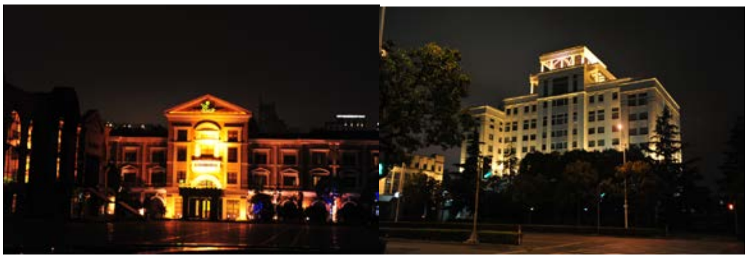

Figure 2 – Façade lighting is different from economically backward areas (the right) and developed areas (the left)

Figure 3 – Contour lighting for building façade along with Yueshan Road in Jilin

For the choice of façade lighting methods, contour lighting and flood lighting are widely used. Bunches of neon tubes and recently LED stripes are selected for contour lighting (see figure 3). Bulky floodlighting luminaires are selected for the front lighting of buildings. Both of them generally consumes great amount of energy. In floodlighting scheme, due to not well controlled light distribution, the amount of spill-light is usually rises up to even 1/3 of the total luminous flux.

Figure 4 – Dynamic and colorful façade lighting of Science & Art Culture Center in Suzhou

Figure 5 – The GreenPix media wall in Beijing

Generally speaking, although there is lack of creativity and innovative solutions on lighting effects, most of them can lighten the structure of buildings. Currently the luminance or the illuminance of lighting buildings far exceeds Chinese standards and regulation. A government report points out the lighting values of 69% of surveyed buildings are higher than the standard value (See figure 4).[5] Many years ago, the CCT of most façade lighting cases are very low with the yellow color, mainly due to the application of sodium lamp which is cheaper. In recent years, color temperature range of façade lighting varies widely, from 2000K-6500K but mostly neutral color temperature ~4000K. In addition to that, thanks to the rapid development of LED lighting technology, dynamic and colorful lighting solutions are widely applied to façade lighting.

Presently, “media façade” type of lighting is an important trend for architectural urban lighting (See figure 5).[6] LED luminaires are mounted directly on the facade of the buildings, which make too bright surface and consequently serious issues for discomfort glare and light nuisance. Market demand for miniaturization and integration of luminaires/light sources into architectural elements is increasing rapidly.

3.2.2 Lighting for Square

In China, square Lighting is a prerequisite to ensure public activities at night. However, functional lighting level in general is not sufficient and lack of landscape lighting. Most of the squares have just functional lighting, with inadequate illuminance level and poor uniformity. Some squares use supplementary spotlights which causes excessive brightness non-uniformities with serious glare. Some squares use lots of custom-made luminaires with special appearance but in improper scale and shape, cause not good lighting effects of squares. This is mainly due to Chinese rapid urban renewal and construction, while landscape lighting design is often lagged behind or ignored during construction.

There are mainly two types of squares in China, the “public square” invested by government (See figure 6), and the other, “commercial/leisure square” (See figure 7), by the property developer. The lighting quality of the former square is depended on the lead of the government departments who rarely engage an independent professional lighting design team for public squares. Lighting of squares can be renewed when big events are carried out with the novel lighting schemes. Colorful light is used and even image projectors are frequently used in square lighting. [7-8]

For the lighting of commercial/leisure square, in general, independent lighting designers are engaged in order to improve the quality of the project and the property value, by means of appropriate lighting methodology, the good choice of color, suitable lighting control, inviting lighting atmosphere creation.

Figure 6 –Tianfu public square in Chengdu

Figure 7 –Tianyi commercial square in Ningbo

3.2.3 Lighting for Plant

Plant lighting is one of the most important parts of urban landscape lighting. Almost all of the urban landscape lighting will involve the plant lighting. The current dominant lighting method relatively simple that is, spot lighting from bottom-up with the luminaires mounted under the plants, or mounted on the trunk, to illuminate the crown of the plant and achieve the effect of lighting. Other lighting methods are less used, e.g. silhouette lighting effects. Secondly, there is excessive lighting for plant. In order to illuminate the trees in practical applications, high-power luminaires are used. Sometimes, even all plants on a small hill are illuminated for the sake of eye-catching night-time beautification. However, these kinds of applications sometimes causes serious light nuisance and might disturb people, also greatly effect on the natural growth of plants. Coloured light, especially green colour is preferred for plant lighting in China with the purpose of emphasizing of the natural green colour, but the visual effect sometimes is a bit theatrical and exaggerated.

Figure 8 – Plant lighting around Gulong Lake in Guilin

3.2.4 Lighting for structures

Structures, e.g. bridge, viaduct, monument, tower, etc. are important elements as landmarks of urban landscape as well as nightscape. China has fewer urban structures than other countries. Currently, the common practice is to use colourful lighting to display the importance and of the structures and conceal their clumsy forms (See figure 9).

3.2.5 Lighting for Water

According to the theory of Chinese "Feng Shui", water is source of everything on earth, so in urban landscape design, water is indispensable. In water lighting, illumination of water surface and the edge is essential. Nowadays, in China, few highly innovative demonstrations of underwater lighting can be found. [9]

The lighting of water edge usually goes with the scenery along the bank. Most cities in China tend to provide the bank with man-made revetment, thus for the sake of highlighting the water front, designers like to employ wall washers to light up the upright walls, or install linear and direct view luminaires alongside the bank (See figure 10).

Figure 9 – Bridge under Bailang River in Weifang

Figure 10 – Water front nightscape in Shaxian

4 Overview on International practice and comparison

As already mentioned above, expert level individual and group studies have already been carried out internationally for many years to elaborate and improve the quality of lighting applications, not only from functional perspective, but equally important from the perspective of improving peoples' lives with lighting. Currently Continental Europe is faced with challenges of maturity and sustainability. There is a challenging need to build a new collective identity across different areas of metropolises. The dialog between contemporaneity and history – fundamental for countries like France, Italy and Spain – is addressed, mostly by means of master planning, but also at the level of design details. Current innovation focus is the integration of high-tech system solutions for individual lighting systems for urban environments. This will create opportunities for new lifestyle statements. [10]

In China, the extreme use of light for urban entertainment and communication in 1st tier landmark cities might soon need to meet a more fundamental challenge, that of the requirements of eco-impact and environmental sustainability.

This is a problem manifested by wild, uncontrolled growth, by radical urban change and metropolitan fragmentation, by the risk of environmentally destructive and ultimately "difficult to live" cities. The solution to such a problem lies in the identification of sustainable strategies, practices and solutions. A new urban lighting planning for people, one to truly inspire the People's Republic of China and the other countries of the continent, could be a part of the solution. Currently, a transition period is clearly observed to reconcile between history and the future, individuals and the collectivity, the personal sphere and the social dimension push urban design in new directions. Here, urban architectural lighting could have the opportunity to connect to people's needs and wants, above all with an eye to sustainability.

Besides observations about current situation, to let readers to evaluate the differences and the similarities visually in two parts of the world, some application examples are given below (See figure 11~18):

Figure 11 — Xian Theatre in Shanxi, China

Figure 12 — Louvre Museum in Paris, France

Figure 13 – National Centre for the Performing Arts in Beijing, China

Figure 14 – Guggenheim Museum in Bilbao, Spain

Figure 15 – Sichuan TV Tower in Chengdu, China

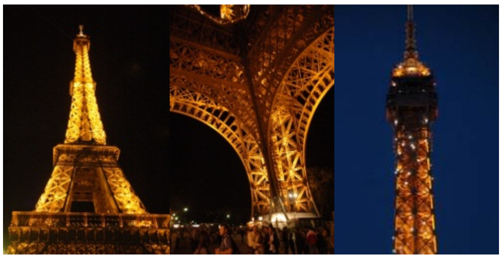

Figure 16 – Eiffel Tower in Paris, France

Figure 17 – Tianyi Square in Ningbo, China

Figure 18 – Finsbury Avenue Square in London, UK

5 Future trends

With the development of science technology and the improvement of social, Chinese life-style have also changed considerably. We are living in the "Information", boosted with social media offerings, with the great help and rapid growth of Mobile Internet recently, Big Data, Social Network, We-Media, e-commerce, digitalization in Lighting becomes hot topics and made great impact on development of traditional industry. The development of future urban lighting will closely capture the times, basing on these new technologies, focusing on human natures which are the basic purpose of urban lighting, keeping balance of development and protection which is an ultimate theme, making use of crossover cooperation which is an effective method for nightscape innovation, and leading to a diversify development in the future.[11] The design and production of the luminaires would also be affected by 3D print technology.

Digitalization

Currently, social networking services greatly change our lives compare to the past and will definitely be pushed by further innovations from the lighting industry. With rapid development of mobile internet in China, people would be able to select their favourite lighting and participate to create the environment by mobile internet at any time via intelligent lighting system. Therefore, the digitalization of lighting will be the important part of our future lives with digital products, digital solutions and digital services.

Green lighting

Green lighting is one of important strategy for China. How to balance between energy efficiency and lighting quality is an eternal topic. As Dr Ann Webb said "Good lighting brings safety, security and a better quality of life to all but needs to be supplied in a task-dependent manner, that is of a quantity and quality appropriate to the task, and with the minimal use of resources." High efficient products are only one part of energy saving from product level. Even energy management systems and adjacencies proper applications have big contribution to sustainable development for the future.

Humanization and individualization

The basic purpose of urban lighting is to realize a comfortable and beautiful lighting environment for human being. Urban architectural lighting should pay much more attention to the public needs of people, including safety and health. Normally, individual needs would rarely be expressed in public area, but personal favourites have increasing potential to contribute to urban lighting. In China, humanization and individualization trends are important but priority is not given yet. There is strong expectation that these trends for urban architectural lighting will be taken into priority list in the near future.

Crossover application concepts

Crossover has become a popular word, means that it gets benefits from traditional to modern, from east to west, from hardware to software, from the visible to invisible. In the rapid development of Chinese urban nightscape, it brings more and more demands for lighting applications. Existing conventional lighting application mind-set, conservative lighting design methodology and even marketing tools are unable to meet current needs. Therefore, maybe crossover cooperation could become an important method for the future development of urban lighting. Art is one of important field for crossover cooperation with urban lighting, such as atmosphere lighting, lighting installation art works, interactive lighting, light sculpture, projection lighting, and so on.

Miniaturization & Embedded

For urban architectural lighting, it is in great need of the luminaires of small size, narrow beam angle and high power with short distance mounted. In the future, LED products would be integrated into architecture to become a kind of building material.

6 Discussion

As explained above, although there are current differences between Chinese and International Urban Architectural Lighting practices, thanks to globalization, in terms of technology, social networking, digitalization of Lighting and rapidly growing cultural interactions considerably expanded thanks to booming transportation network between even distant countries and regions, gradual convergence in urbanization concepts and in-turn in lighting application concepts is witnessed. In the near future, further to as we do today, as we use the same equipment, as we eat the same food, as we wear the same type of clothes, as we aware and inspired on real time broadcasting, similar preferences and practices would be demonstrated with of course the tint of cultural effects.

References

[1] Liu Yizheng. 2010. The history of Chinese culture. Changsha: Yuelu Publishing.

[2] Luoxi Hao, Xiu Yang, Kun Zeng, Qiying Jin. 2012. The exploring and practice of Chinese urban master planning and construction: Review on Chinese urban lighting planning of 20 years (中国城市照明规划的探索与实践——中国城市照明规划 20 年回顾). China Illuminating Engineering Journal, 23(z1).

[3] Philips. 2013. Report of urban architectural lighting in China. Shanghai.

[4] Luoxi Hao, Haihong Gu, Yi Lin, Xiu Yang, Qiying Jin, Yaodong Chen, Meng Zhang, Meiqi Fu. 2013. Guilin City Urban Lighting Master Plan[C].The proceeding of the 7th LUXPacifica 2013‘Cultural lighting’, Bangkok.

[5] Ministry of Housing and Urban-rural Development of the People’s Republic of China. 2009. Code for lighting design of urban nightscape (JGJ/T 163-2008). Beijing.

[6] Philips. 2009. Light & Emotions: Exploring lighting cultures 47 Conversations with lighting designers.

[7] Gang Song, Caijie Yan. 2013. The qualitative evaluation of lighting quality in urban square lighting. Proceedings of CIE centenary conference ”Towards a New Century of Light”, Paris.

[8] Gang Song, Kangjun Liu, Dong Zheng. 2012. Urban street lighting application investigation and subjective evaluation. Proceedings of CIE 2012 "Lighting Quality and Energy Efficiency", Hangzhou.

[9] Yi Lin, luoxi Hao, Xiu Yang. 2013. The Lighting Design Practice of Beishan Road from an urban design perspective[C].The proceeding of the 7th LUXPacifica 2013‘Cultural lighting’, Bangkok.

[10] Philips. 2007. City, People, Light.

OP48

THE IMPORTANCE OF DEVELOPING A CITY STREET LIGHTING MAP

Djokic, L.S.[1], Kostic, M.B.[2], Kostic, N.M.[3]
[1] University of Belgrade, Faculty of Architecture, Belgrade, SERBIA, [2] University of Belgrade, Faculty of Electrical Engineering, Belgrade, SERBIA, [3] University of Belgrade, Technical Faculty in Bor, Bor, SERBIA
lidija@arh.bg.ac.rs

Abstract

The paper presents reasons for an advanced city street lighting map, which, for each city road, street and pedestrian path, contains the information on lighting classes valid during various night periods with their duration, as well as on the recommended lamp type. This data is based on the required performance, energy efficiency and economics of the street lighting solution. The procedure for developing a city street lighting map, divided into three steps, as well as the description of the map graphics, are also given.

Keywords: City Street Lighting Map, Lighting Class, Lamp Type.

1 Introduction

A city street lighting map usually assumes an urban presentation in which the streets are differentiated according to their lighting class. Such a document is generally prepared for two reasons. It contains and, therefore, offers the information on the street lighting class which is the initial and crucial data necessary for lighting design. It also serves as a basis for standard designs for streets of the same lighting class and morphology (width of street, and height and configuration of surrounding buildings), providing financial savings and easier maintenance. However, more information provided by the city lighting map can additionally simplify the design process and also contribute to visual comfort and city beautification. The additional information refers to lamp type (its colour of light and colour rendering), which influence the quality of the urban nightscape. It can also include the street lighting classes relevant during late night and early morning hours with their duration, which is important if light control devices or systems are planned in the future. The determination of different lighting classes on the same street during the night is a time consuming and financially demanding task, but it considerably helps to initiate measures of light control, providing significant energy savings.

The following question could emerge at this point: what is the purpose of a street lighting map if city streets have been illuminated for quite some time? Actually, there are several convincing answers. Nowadays many cities are undergoing street lighting reconstructions replacing energy inefficient high-pressure mercury luminaires with high-pressure sodium (HPS), metal-halide (MH) or LED luminaires. The quality of such actions is based on the information regarding the street lighting class. For fifteen years street (road) lighting classes have usually been determined using the procedure set in CIE Technical Report 115 (CIE 115, 1995), which was based on a small number of influencing factors. Besides, there were no quantitative criteria which would reduce the extent of subjective evaluation done by the lighting designer. As a result, different designers often categorized the same street into different lighting classes, causing a significant difference in the number of poles and luminaires. Just to be on the safe side, and not endanger traffic safety, or for other reasons, designers frequently chose a more demanding lighting class, which is why many cities have very intensive street lighting. The city of Belgrade, Serbia, represents a typical example of such an approach. Fortunately, the recently published CIE Technical Report 115-2010 (CIE 115-2010, 2010) narrows down uncertainties for lighting designers, justifying the necessity for developing a city street lighting map.

Another reason in favour of an upgraded city lighting map can be derived from the fact that through the last decade the need for rational use of energy and financial management led to a reduction of luminance levels corresponding to the lighting classes, especially in the developed countries (IESNA RP-8-00, 2005).

Therefore, we propose the development of a city street lighting map presenting an urban street network in which all roads, streets or pedestrian paths of equal lighting class are shown by the same colour, while the differentiation of lamp type (depending on the desirable colour of light and colour rendering) is shown through hatches. In addition, we recommend an electronic map which would offer additional information regarding all lighting classes referring to each of the streets, together with the time periods for which they are valid. Such information can easily be gained by clicking on a street (road) under consideration.

2 Energy efficiency and the economic aspect

The optimal choice of the procedure for determining the street (road) lighting class upon which the photometric requests are dependant, dominantly influences the energy efficiency and economics of the lighting solution. Energy efficiency of the solution also considerably depends on the type of light source, which should be determined within the city lighting map, as well.

For the selection of the street (road) lighting class, the following two procedures (methodologies) are broadly used: the one presented in the recently published CIE document (CIE 115-2010, 2010), and the one given in the European norm (CEN/TR 13201-1, 2004). Although the latter contains quantitative criteria which facilitate the selection of the lighting class for motorized traffic (M lighting class), the authors of this paper do not consider that the introduced lighting subclasses are necessary, since the photometric calculations are not very precise (the determination of the maintenance factor and road surface reflection class, which significantly influence the pole spacing, is usually made in an arbitrary way). Therefore, the authors modified the table from CIE 115-2010, 2010 which relates to the selection of lighting classes for motorized traffic, adding some quantitative criteria generally taken from CEN/TR 13201-1, 2004, aiming to minimize the effect of subjective evaluations of the lighting designer (see Table 1).

According to CIE 115-2010, all streets and roads for motorized traffic (with the maximum allowed velocity of over 40 km/h) are categorized into six M lighting classes (M1 – M6), depending on: speed, traffic volume and composition, separation of carriageways, intersection density, parked vehicles, ambient luminance and visual guidance/traffic control (traffic lights, traffic signs, traffic marks on the street (road) and traffic regulations). Table 1 contains possible values (weighing values) of all of the above mentioned parameters. The lighting class can be calculated by using the following formula:

$$M = 6 - V_{ws}, \tag{1}$$

where Vws denotes the sum of all eight weighing values. If the calculated M value is not an integer, the next lower whole number should be used, which assumes the application of stricter lighting criteria.

For the selection of the lighting class of a street intended for pedestrian and low speed traffic areas ($v \leq 40$ km/h), particular lighting criteria based on the pedestrian needs are determined.

As well known, pedestrian visual tasks and needs significantly differ from those which refer to the drivers. The pedestrian speed is much lower, and their attention is focused on the immediate surroundings. While drivers see objects on the street (road) as dark silhouettes, pedestrians watch their details and faces of people they meet. Therefore, lighting criteria related to pedestrian and low speed traffic areas are separately determined. CIE 115-2010 offers a table containing the relevant lighting criteria for this purpose, as well as the corresponding P lighting classes (P1 - P6), which the authors of this paper recommend due to the simplicity of its use.

Table 1 – Parameters for the selection of M lighting class according to CIE 115-2010 (numerical values in the second column which relate to traffic volume and composition are taken from CEN/TR 13201-1)

Parameter	Options	Weighing value
Speed	Very high (v > 120 km/h)	1
	High (80 < v ≤ 120 km/h)	0.5
	Moderate (40 < v ≤ 80 km/h)	0
Traffic volume (in both directions)	Very high (over 40000 vehicles/day)	1
	High (25000 – 40000 vehicles/day)	0.5
	Moderate (7000 – 25000 vehicles/day)	0
	Low (4000 – 7000 vehicles/day)	-0.5
	Very low (up to 4000 vehicles/day)	-1
Traffic composition	Mixed, with high percentage of non-motorized	2
	Mixed	1
	Motorized only	0
Separation of carriageways	No	1
	Yes	0
Intersection density	High*	1
	Moderate	0
Parked vehicles	Present	0.5
	Not present	0
Ambient luminance	High	1
	Moderate	0
	Low	-1
Visual guidance/traffic control	Poor	0.5
	Moderate or good	0

*If the interchange spacing is shorter than 3 km or if there are more than 3 junctions per km.

3 Choice of lamp type

Colour of light and colour rendering significantly contribute to the ambient appearance. Spaces in which people gather and those with intensive pedestrian traffic generally require warm-white light and excellent colour rendering, which contribute to the feeling of comfort. This is why MH lamps with a ceramic discharge tube characterized by the correlated colour temperature (CCT) of 3000 K are adequate not only for the illumination of pedestrian paths, but also for streets in the immediate surroundings of residential buildings, as well as for the illumination of downtown areas due to the density of their pedestrian traffic.

For the illumination of streets and roads outside the downtown area, due to a reduced density of pedestrian traffic, HPS lamps are recommended. Although characterized by poor colour rendering, they provide satisfactory conditions for normal motorized traffic. Their significant advantages are high energy efficiency and long life.

It can be expected that in the near future LED luminaires with not only optimal technical and photometric indicators, but also with an acceptable price, will be developed, enabling their broad use in all domains of public lighting. Then, wherever the lighting map shows luminaires with HPS lamps, appropriate LED luminaires of CCT of 3000 – 4000 K can be installed instead. White LEDs (4000 K) are generally recommended due to their higher luminous efficacy. Another reason for their use is represented by the fact that higher CCT contributes to concentration and awakeness.

For those streets in which luminaires with MH lamps with a ceramic discharge tube are foreseen, adequate substitutes would be LED luminaires with CCT of 3000 – 4000 K. This range satisfies the different needs and preferences in ambients located in both warm and cold areas.

4 The procedure for developing a city street lighting map

The first step: Based on the criteria from Table 1 (referring to street (road) lighting class for motorized and mixed traffic), or the criteria presented in the appropriate table from CIE 115-2010 referring to pedestrian street lighting class, for each road, street or pedestrian path an appropriate lighting class is determined: of type M (for roads and streets for motorized and mixed traffic) or of type P (for pedestrian streets or paths in parks and along waterways, as well as those belonging to specific ambiences).

For each road, street or pedestrian path the determination of the lighting classes relevant during late night and early morning hours, as well as their duration, is also recommended.

The second step: The lamp type should be determined for each road, street or pedestrian path, regarding colour of light and the need for colour rendering (see Section 3).

The third step: The city street lighting map should present all roads, streets and pedestrian paths of equal lighting class with the same colour, according to the corresponding legend. Different lamp types should be shown using hatches, also presented in the legend.

5 Conclusions

This paper presents reasons for the development of an advanced city street lighting map, which will contain the following information regarding each city street and road: lighting classes relevant during various night periods with their duration and adequate lamp type.

Even though the described street lighting map is intended mostly for functional lighting, it is also valuable for urban ambiences, which certainly contribute to the overall urban image and its presentation. One of the purposes of this type of a street lighting map is to stress the urban concept. The stratification done within the map, regarding the adequate application of the light colour, its intensity and colour rendering, should segregate spaces of different character and enable comprehensive recognition of individual city zones.

References

CEN 2004. CEN/TR 13201-1. Road Lighting – Part 1: Selection of Lighting Classes. Brussels: CEN

CIE 1995. CIE 115. Recommendations for the Lighting of Roads for Motor and Pedestrian Traffic. Vienna: CIE.

CIE 2010. CIE 115-2010 (2nd edition). Lighting of Roads for Motor and Pedestrian Traffic. Vienna: CIE.

IESNA 2005. IESNA RP-8-00. Roadway Lighting. New York: IESNA.

OP49

A GLARE DETECTION SYSTEM WITH A DIGITAL CAMERA FOR HUMAN CARE

Pei-Jung Wu[1], Jeng-Han Wu[2], Shiau-En Luo[2], Yi-Huai Xiao[2], Bao-Jen Pong[3], Shao-Wei Hsu[3], Chien-Yue Chen[2]*

[1]Institute of Imaging and Biomedical Photonics, National Chiao Tung University, Tainan, CHINESE TAIPEI

[2]Department of Electronics Engineering, National Yunlin University of Science and Technology, Douliu, CHINESE TAIPEI

[3]Center for Measurement Standards Industrial, Industrial Technology Research Institute, Hsinchu, CHINESE TAIPEI

*chencyue@yuntech.edu.tw

Abstract

Taking pictures with a general camera, such pictures are converted with programs for the environment luminance in order to establish a luminance measurement system. The luminance of the dazzling areas is substituted into glare rating (GR), through quantification, to examine the glare standard. Ordinary pedestrians and passers-by are further proceeded questionnaire survey to establish a glare detection system by examining the similar feelings about signboards, street lamps, and flashing neon lights in the environment to GR.

Keywords: Glare, Luminance, Digital camera, HDR image.

1 Introduction

Everywhere on roads, the flicker of neon signboards and large LED banners could cause discomfort of drivers' or passers-by's eyes and easily result in accidents. Such light could result in discomfort of human eyes; however, people do not know whether the glare caused by such luminance conforms to the standard.

Problems caused by overusing lighting systems are regarded as light pollution, which is classified into flashing light, sky glow, and glare [1].Glare is caused by the luminance of light source higher than the average luminance in an area or the dazzling or discomfort resulted from uneven luminance distribution in the environment. Distinct glare would affect human eyes to different extent and could harm eyes and cause eye diseases.

This study therefore aims to examine the conformity of the luminance in public environments to the glare index and integrate the research data and questionnaire survey to establish a glare detection system. The public would then pay more attention on the issue of light pollution as the luminance in an environment exceeding the glare index could be easily detected by a camera.

2 Method

A digital camera is used for taking pictures with different shutter time, and such pictures are integrated into a High Dynamic Range (HDR) picture with image processing software. As HDR photography could catch broader luminance change than a static one does [2], a chromaticity coordinate could be used for the conversion to acquire the luminance value, which is substituted for the equation of camera parameters to calculate the real environment luminance in the picture. The glare index could be acquired by substituting the luminance into the glare evaluation equation. The glare index of the picture is objectively analyzed the glare evaluation standard, while the questionnaire survey is subjectively proceeded with passers-by for further comparing the statistical results.

The human-factor experiment is based on measurement in this study that the measurement is first preceded and the image viewed by the participant is taken with a camera. The image is then synthesized into an HDR image for comparing with the questionnaire result. The experiment is preceded in two parts of 1. measuring the luminance in the measured location and calculating the glare evaluation and 2.understanding the participant's perception of viewing luminance through questionnaire survey for the statistical data. The experimental flow is shown in Fig.1.

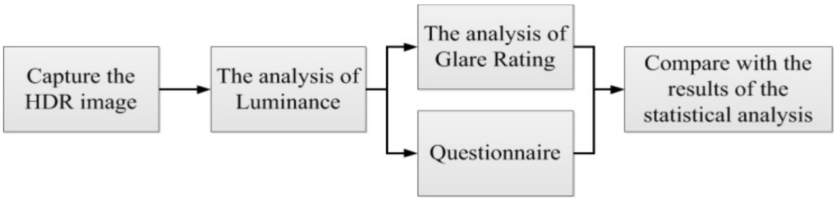

Figure 1- Experimental flow

2.1 Analysis of true luminance of image

The pictures taken by a digital camera should be converted into an image with 2D array pixels. The pixel of each image appears a value, which shows the light intensity at the point. The true luminance of the image is acquired by multiplying the value with a calibration constant Kc [3]. The equation is show as below.

$$N_d = K_c \left(\frac{tS}{f_s{}^2}\right) L_s \qquad (1)$$

N_d Digital number (value) of the pixel in the image;
K_c Calibration constant for the camera;
t Exposure time,(s);
f_s Aperture number;
S Sensitivity of the film;
L_s Luminance of the scene(cd/m^2);

2.2 Conversion of glare index

CIE 112 glare evaluation equation is utilized in this study [4]. When the luminance ratio between the light source and the background is large, the calculated glare value is obvious. Glare rating (GR) in the glare equation stands for the glare index.

The smaller glare index reveals the less stimulation on human eyes. The luminance in this experiment is acquired by calculating the image. The parameters for the glare equation contain Lvl the light source luminance (cd/m2) and Lve the background luminance (cd/m2), equation 2. The luminance of the image is first calculated the mean; the light source luminance presents the value larger than the mean, while the background luminance reveals the value smaller than the average. The glare index therefore could be acquired.

$$GR = 27 + 24\, log_{10}\left(L_{vl}/L_{ve}{}^{0.9}\right) \qquad (2)$$

After acquiring the GR value, the glare index is further evaluated according to the glare rating in Table 1. Based on the idea of glare evaluation, the environment luminance could be calculated, and the probability of glare at different locations could be distinguished.

Table 1–Glare rating

	Glare Rating (GR)
Unbearable	90
	80
Disturbing	70
	60
Just admissible	50
	40
Noticeable	30
	20
Unnoticeable	10

2.3 Conversion of glare index

Inputting the camera parameters in equation 1, the luminance at each point of the image pixel could be acquired with MATLAB for the luminance distribution diagram, from which the location with the most luminance distribution could be clearly viewed. Since the light source luminance and the background luminance appear strong contrast, it is where glare the most easily generates. From the glare distribution, the areas exceeding the glare index could be recognized that the glare evaluation index at various locations could be further analyzed.

3 Results

Figure 2 shows the original image shot by the camera, and Figure 3 displays the HDR image after conversion. With comparison, the HDR image luminance is more nature and true. Substituting the value into MATLAB, the luminance and glare distribution diagram could be acquired, Figure 4 & 5, from which the signboard and the light source on the top are the major light source. With analyses, the light source luminance appears between 0.01 cd/m2 and 0.068 cd/m2, and the glare evaluation index shows in 25-50, presenting that the glare resulted from light source could be easily noticed and would cause discomfort on human eyes.

This study discusses the relations between the luminance of a general digital camera pixels and the true luminance. Since the general digital camera pixels could not express the true luminance and the surrounding environments or the selection of shooting locations could result in influence, errors would appear in the conversion. For this reason, the questionnaire survey is used for the comparison in this study in order to discuss the conformity of glare evaluation areas to the perception of human eyes, Figure 6. Total 26 participants, 12 males and 14 females, are tested, which conforms to the number of people for human-factor experiments. The score in the questionnaire is from 1 to 5. The higher score means that the subject strongly agree with the feeling. The questionnaire result shows that light sources can easily dazzle and tire human eyes. Such a result also conforms to the calculated glare evaluation result.

Figure 2 –Original captured

Figure 3–HDR image

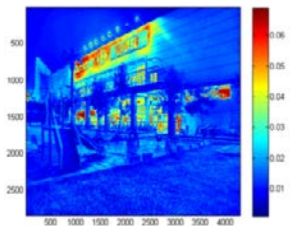

Figure 4 –Luminance distribution

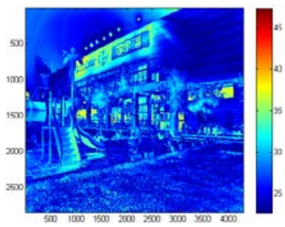

Figure 5 –Glare index distribution

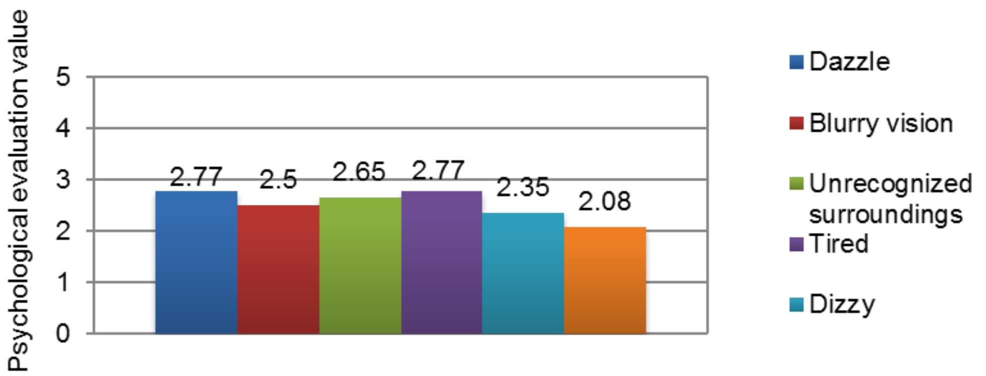

Figure 6 –Statistics of glare rating

4 Discussion

This study aims to examine the conformity of the glare index of large-scale banner light source to the standard and present the luminance distribution of the shot image to calculate the glare index. Since the general digital camera pixels could not express the true luminance and the surrounding environments or the selection of shooting locations would cause effects, errors are likely to appear on the conversion. The questionnaire survey is therefore applied to analyzing the conformity between the glare evaluation and the direct view with human eyes. It also confirms the feasibility of analyzing glare with digital cameras that the system is simple and handy.

5 Conclusion

A general digital camera is used for taking pictures with different exposure time, which are converted into an HDR image for simulating the distribution of true luminance through the program. CIE 112 glare evaluation is further utilized for the calculation, and the acquired glare index is used for judging the measured environment reaching the light pollution standards so as to rapidly examine light pollution. The questionnaire survey is applied to the comparison so that the research results could be used for subjectively and objectively examining light pollution. The successive studies are expected to increase the number of participants so as to acquire more data and reduce errors. Moreover, the system allows the public being easily aware of the harm of light pollution and could benefit more people.

References

Rubiño M, Cruz A, Garcia JA, Hita E, “Discomfort glare indices: a comparative study,”Applied Optics,Vol. 33, Issue 34, p.p. 8001-8008 ,1994

Evaluation of high dynamic range photography as a luminance data acquisition system,”Lawrence Berkeley NationalLaboratory, Lighting Research Group,Berkeley, California,USA,Lighting Res.Technol vol 38.2 p.p.123-136,2006

“Measuring Luminance with a Digital Camera,”Peter D.Hiscocks, P.Eng, 2011

CIE 112,“Glare evaluation system for use within outdoor sports and area lighting,” 1994.

OP50

SIMULTANEOUS MEASUREMENTS OF GLARE AND FLICKER PROPERTIES OF ENVIRONMENTAL LIGHTINGS

Pong, B.J.,[1*], Hsu, S.W.,[1], Chung, T.Y.,[1], Wu K.N.,[1]
[1]Industrial Technology Research Institute/Center for Measurement Standards, Hsinchu, CHINESE TAIPEI
*bjpong@itri.org.tw

Abstract

Nowadays, the assemblage lightings or billboards made by LED have considerable performance in brightness and contrast, and may produce uncomfortable visual experience for the glare and/or flicker. In our previous studies, we have performed separately temporal and spatial measurements on the flashing LED billboards with simple patterns. The objective parameters flicker index (*FI*) and unified glare rating (*UGR*) can be used to express the subjective evaluation results with simple equations.

Because the actual lighting environments are more complex than the former experiments, the simultaneous measurements on the temporal and spatial variations on the LED lighting or billboard with complicated patterns are required. A novel analysis method on the flicker and glare characteristics of the measurement results will be presented. Therefore the purpose of this work is to systematically study the problem with a new method on an assemblage LED lighting and a LED billboard with various light distributions and/or contents.

Keywords: Simultaneous measurements, Temporal and spatial variations, Glare, Flicker

1 Methods

The experimental set up is shown in Figure 1, the images of LED billboard are controlled through a controller, where eyes represents the human perception experiment (please refer to [Lai P.Y., 2013]), where glare and flicker are measured by temporal imaging luminance measurement device (TILMD) simultaneously. A Canon-600D digital single-lens reflex (DSLR) camera with a 10 mm to 22 mm lens is calibrated as the TILMD to measure the temporal imaging luminance of the lighting environment. The MOV files with resolutions of 1920x1280 and frame rate of 60 Hz is taken by the TILMD, and then converted to serial imaging luminance with a Labview program. The luminances of lightings (L_s), background luminance (L_b), and vertical illuminance (E_v) of each frame can be calculated with the definitions in our previous work [Hsu, S.W., 2013]. The temporal *UGR* is calculated by average of UGR of several frames in a short period. Because of the light transient adaption of vision, a causal weighting function named transient adaption function (TAF) is used to calculate temporal *FI* by integration of product of E_v and TAF.

A commercial LED billboard, shown in Figure 2, is used for the experiments under various highest luminances (L_h) of the billboard and environmental illuminances (E_e). The video contents to the billboard are edited as portrait, landscape, artificial, animal, plant, food, art, technology, and assemblage lighting-like, as shown as Figure 3. An assemblage LED lighting is selected as the flashing illuminant to be tested. There are five flashing modes, six flashing periods, six digital level, and six measurement distances for the experiments.

TILMD filming the image of target scene, e.g. as shown as Figure 4, and transferred into the luminance distribution, and then calculate three parameters, which are the background luminance, the luminance of target light source, and the total illuminance, respectively. These parameters are used to calculate the *UGR* [CIE 1995] and the *FI* [DILAURA, D. 2011]. The luminance distribution of the target scenes are temporal varied, it must amend the definition of *UGR* and *FI*, in which the temporal unified glare index $UGR(t)$ (since it is the time-average value, so sometimes expressed as $UGR_a(t)$) and temporal flicker index $FI(t)$ are defined as equation (1) and equation (2), respectively.

$$UGR(t) = \frac{\int_{-\infty}^{t} UGR(\tau)v(t-\tau)d\tau}{\int_{-\infty}^{t} v(t-\tau)d\tau} \tag{1}$$

$$FI(t) = \frac{\int_{-\infty}^{t} \max[E(\tau)-\bar{E}(t),0]w(t-\tau)d\tau}{\int_{-\infty}^{t} E(\tau)w(t-\tau)d\tau} \tag{2}$$

where

$UGR(\tau)$ is an unified glare rating at specific time τ

$v(t-\tau)$ is a FWHM of 0.033 seconds Gaussian function, after Fourier transformation of differential function of this function, it is similar to 30 Hz low-pass filter, and seems relevant to the human eye critical flicker fusion frequency (referred to as CFF).

$\overline{E}(t)$ is a time-average illuminance expressed as equation (3):

$$\bar{E}(t) = \frac{\int_{-\infty}^{t} E(\tau)w(t-\tau)d\tau}{\int_{-\infty}^{t} w(t-\tau)d\tau} \tag{3}$$

$w(t-\tau)$ is the TAF described at previous paragraph, which is a FWHM of 0.033 seconds Gaussian function

$E(\tau)$ is the total illuminance at specific time τ

In accordance with the previous analysis temporal comfort rating (*CF*) is expressed as equation (4):

$$\text{Comfort Rating} = a \cdot UGR(t) + b \cdot \log(FI(t)) + c \tag{4}$$

where weighting factors a=-0.213, b=-2.09, c=7.00, respectively. The weighting factors used [Hsu, S.W., 2013] are the same as our previous work, where score of *CF* is the defined similar to De Bore glare rating scale [De Boer, J.B. 1976] as shown as table 1.

Table 1 – De Bore's and CF 9-point scale

De Bore glare rating	*CF*	Description
1	1	Unbearable
3	3	Disturbing
5	5	Just acceptable
7	7	Satisfactory
9	9	Just noticeable

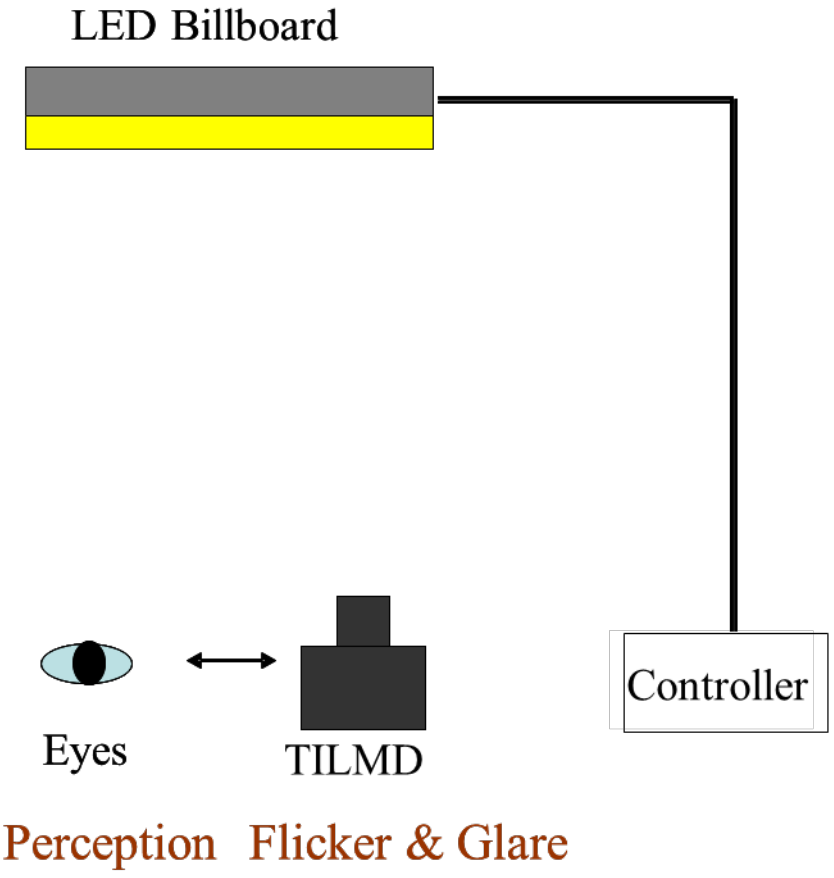

Figure 1 – Schematic measurement set up diagram of flicker and glare experiments

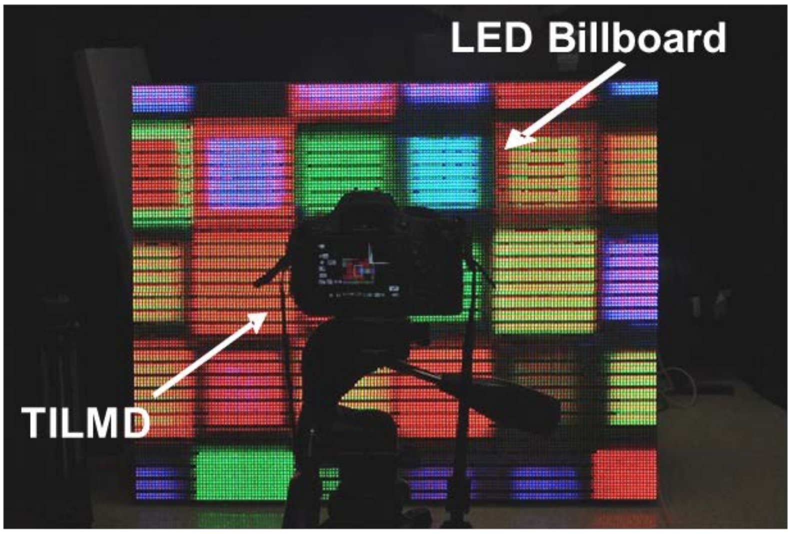

Figure 2 – Glare and flicker measurement set-up example of LED billborad by TILMD

Portrait (video 1)	Landscape (video 2)	Artificial (video 3)
		
Animal (video 4)	Plant (video 5)	Food (video 6)
		
Art (video 7)	Technology (video 8)	Assemblage lighting-like (video 9)
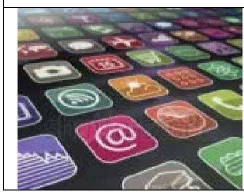		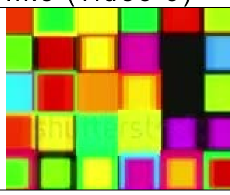

Figure 3 – Night catagories of video contents

Figure 4 – Target scene of flicker and glare measurements of LED billboard

2 Results

In this section, a LED billboard and an assemblage LED lighting are the targets under measurement, where the simultaneous measurement results of glare and flicker will be shown.

2.1 LED billboard

We can get $UGR_a(t)$, $FI(t)$, *CF* for measurements on each video content in accordance with equation (1), equation (2), and equation (4), respectively. Figure 5 shown the results for L_h =2000 cd/m^2, there are grey image clips between video contents which indicated by dash line. *CF* is mostly less than 5 for video contents of portrait (video 1) and assemblage lighting-like (video 9), *CF* is partly less than 5 for video contents of landscape (video 2), artificial (video 3), art (video 7) and technology (video 8), and *CF* is mostly larger than 5 for the rest contents.

As expected, the *UGR* of the experiments is a linear combination of the logarithms of L_s and $1/L_b$. The local maximums of *UGR* are mostly at the situations where the light outputs from the LED billboard are too bright. The obtained *FI* is a linear function of variance of E_v, and the local maximums of *FI* are generally at the large changes of the outputs from the billboard.

For L_h = 5000 cd/m^2, *CF* is decreased about 1.1 for all video contents. It is expected that the empirical equation can be revised to a more accurate form after comparisons of the results in this work and ergonomic tests in the future.

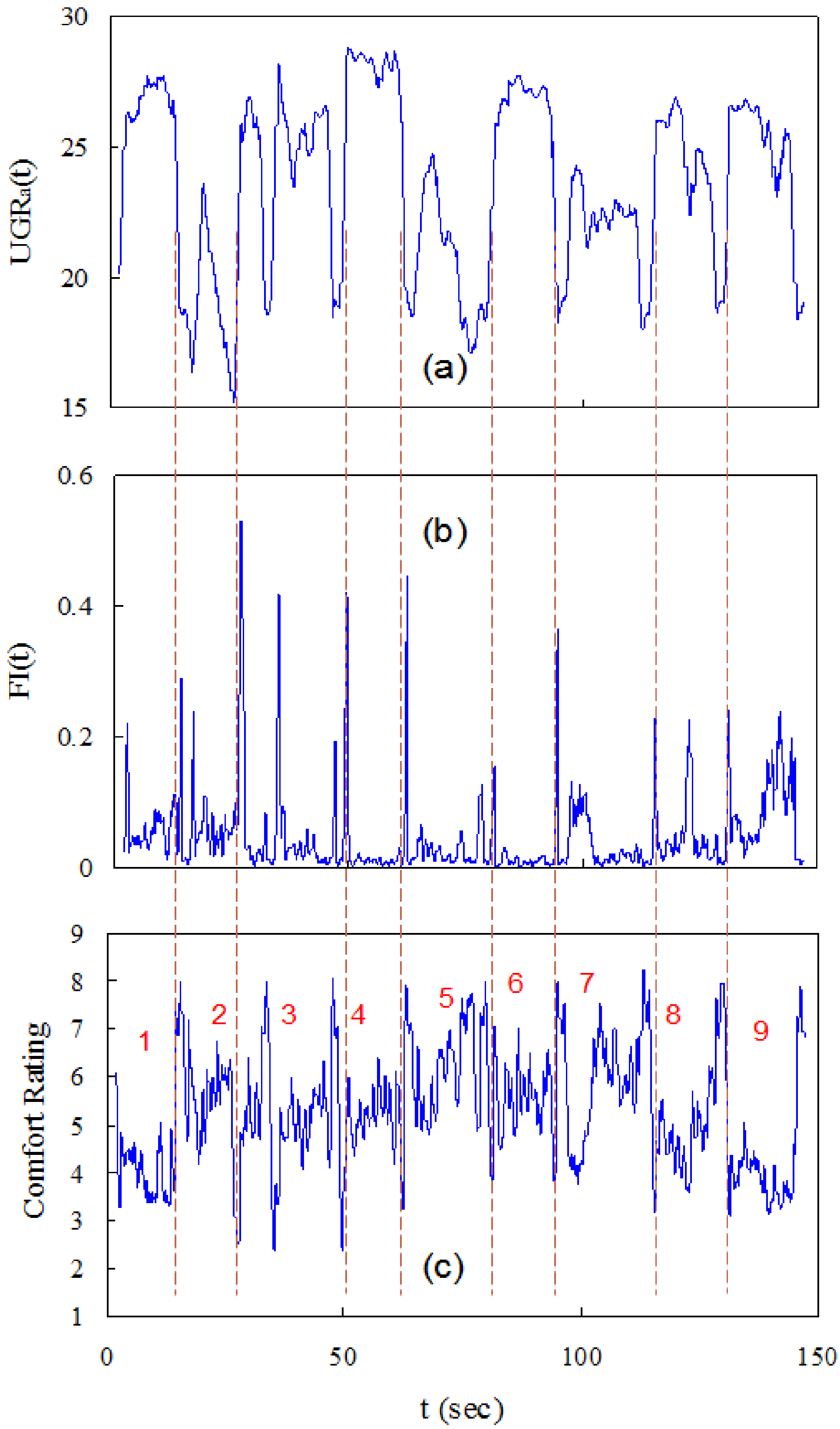

Figure 5 – (a)temporal *UGR*, (b) temporal *FI*, and (c) temporal comfort rating of 9 videos.

2.2 Assemblage LED lighting

Compared with visual perception, the overall comfort rating would be as the minimum in the flashing period. The rank of minimum *CF* for the flashing modes is from synchronous flash (i), radial stack (v), argument stack (vi), radial scan (iii), to argument scan (ii), as shown as Figure 6, where corresponding minimum values are about 3, 4, 4.6, 4.9, and 6.7, respectively. Figure 7 shown the picture took at one of the assemblage LED lighting flashing mode, which is radial stack mode.

For the variation of flashing periods, there are 0.25 sec, 0.375 sec, 0.5 sec, 0.75 sec, 1 sec and 1.25 sec of period with flashing mode of argument scan. It is observed that the variation of minimum *CF* is not obvious for these periods. For the variation of output grey levels, there are 255, 170, 128, 102, 85 and 51 of output grey levels with flashing mode of argument stack. It is observed that *CF* is smaller when output grey lever is larger. For the variation of observation distance, there are 1.65 m, 2.53 m, 3 m, 3.21 m, 4.28 m, 4.92 m of observation distance with flashing mode of synchronous flash. It is observed that *CF* is smaller when observation distance is shorter.

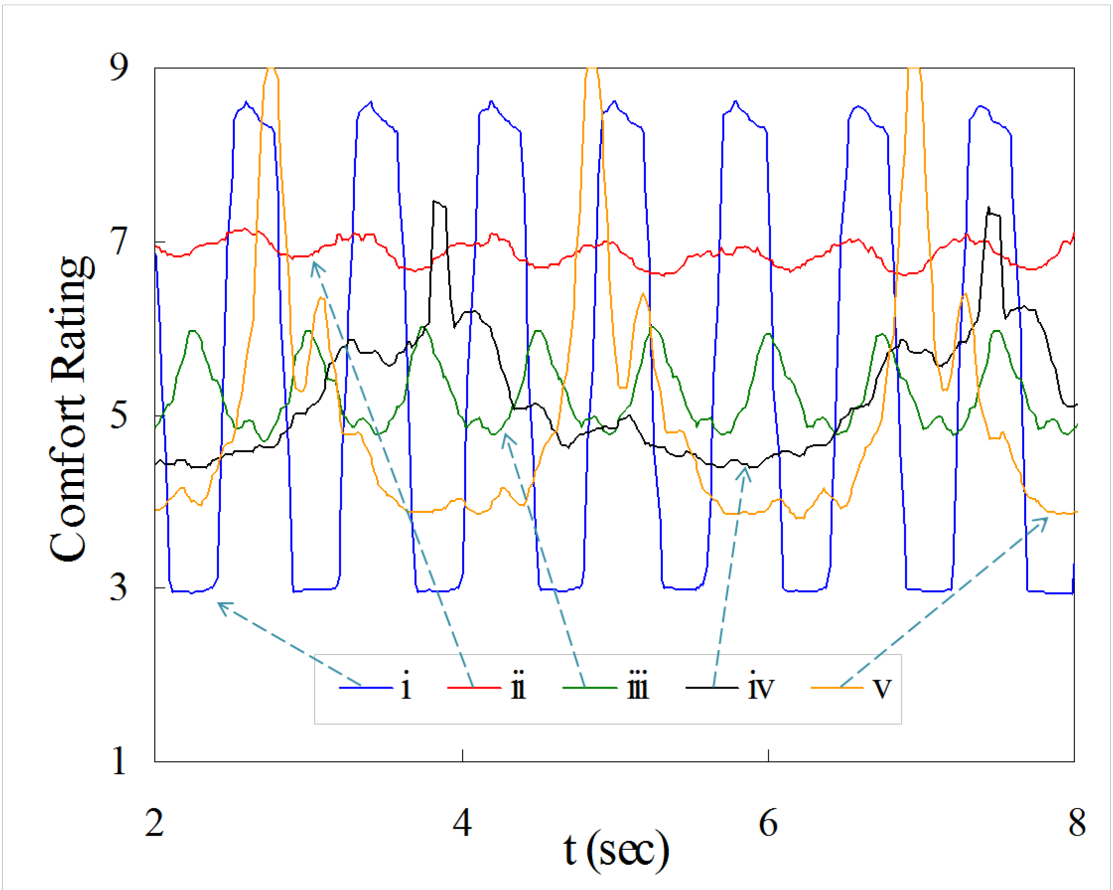

Figure 6 – Temporal comfort rating of assemblage LED lighting.
Where curve i is synchronous flash mode, curve ii is argument scan mode, curve iii is radial scan mode, curve vi is argument stack mode, curve v is radial stack mode.

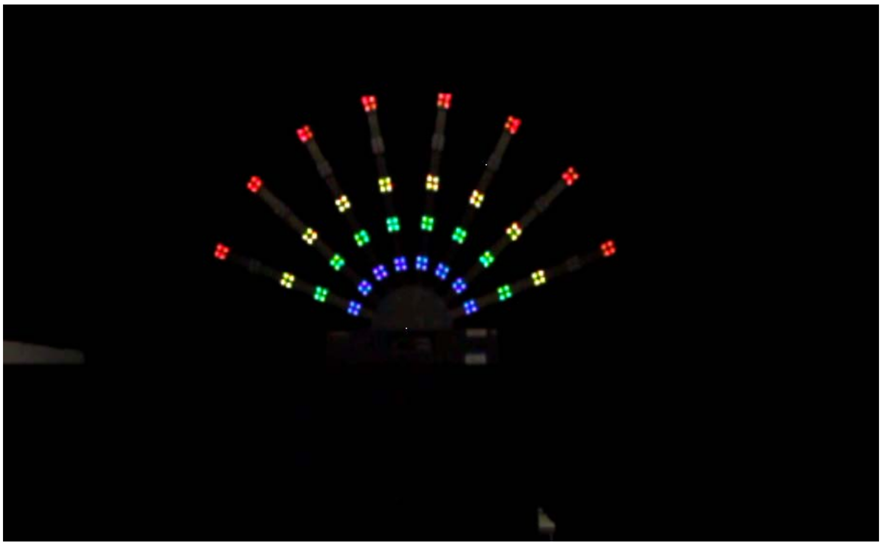

Figure 7 – Assemblage LED lighting at radial stack mode

3 Conclusions

Flicker and glare can be respectively generalized as excessively temporal and spatial contrast of light. Their influences to visual perception are important and are still under examined, especially for the LED lighting environments. In this work, we have proposed a simultaneous measurement and analysis method of these two features by a TILMD. This method is used to study the LED billboard with concrete scenes, and the assemblage LED lighting with various conditions. The results of the experiments show that this method would be an alternative approach for the related studies about light pollution from LED lightings.

References

LAI, P.Y., WEN, C.H., PONG, B.J., LUO, M.R. 2013. Investigation of Discomfort Glare of RGB LED Billboard at Night. *Proceeding of CIE Century Conference "Towards a New Century of Light"*, pp.442-451, Paris, France, April 15 and 16, ISBN 978-3-902842-44-2.

HSU, S.W., CHUNG, T.Y., PONG, B.J., CHEN, Y.C., HSIEH, P.H., LIN, M.W. 2013. Relations Between Flicker, Glare, and Perceptural Ratings of LED Billboards under Various Conditions. OP58, *Proceeding of CIE Century Conference "Towards a New Century of Light"*, pp.428-434, Paris, France, April 15 and 16, ISBN 978-3-902842-44-2.

De Boer, J.B. 1967. Visual perception in road traffic and the field of vision of the motorist. In Public Lighting. Eindhoven, Netherlands: Philips Technical Library.

CIE 1994. CIE 112:1994. Glare evaluation system for use within outdoor sports and area lighting. Vienna: CIE

CIE 1995. CIE 117:1995. Discomfort Glare in Interior Lighting. Vienna: CIE

CIE 2003. CIE 150:2003. Guide on the limitation of the effects of obtrusive light from outdoor lighting installations. Vienna: CIE

DILAURA, D., Houser K., Mistrick, R., Steffy Gary 2011. THE LIGHTING HANDBOOK 10th ed.. New York: IESNA

OP51

A NOVEL APPROACH ON OUTDOOR SPORTS LIGHTING DESIGN METHODOLOGY AND ITS VALIDATION BY SENSITIVITY ANALYSIS

Nath, D.[1], **Mazumdar, S.**[2], Mukhopadhyay, S.[3]
[1] Future Institute of Engineering & Management, Kolkata, INDIA, [2] School of Illumination Science Engineering & Design, Electrical Engineering Department, Jadavpur University, Kolkata, INDIA, [2] Philips Lighting Academy, Philips Electronics Pvt. Ltd., New Delhi, INDIA
[1]dipayan_nath@yahoo.co.in, [2]saswati.mazumdar@gmail.com,
[3]sudeshna.mukhopadhyay@philips.com

Abstract

The sports lighting design is a dedicated task and is confined to the experienced professionals. This proposed algorithm is a novel methodology towards changing the conventional trial and error basis designing approach by predefining the illumination values on the field grid points at the initial stage of design and accordingly the light source photometry is defined. The sensitivity analysis is done through hardware based setup and feeding real time data into the algorithm for simulation based response and hence successful qualitative validation of the algorithm. The performance of the algorithm is also verified by tracing the photometric distribution of MR16 lamp from the real-time data through simulation and that too is compared with the actually measured photometry of the MR16 lamp by Mirror Distribution Photometer. Subsequently for the real time experiments, the power is drawn from *Constant Voltage Constant Frequency* power supplies to maintain the power quality.

Keywords: Simulation based Modelling, Sensitivity analysis, Validation, Performance Evaluation, Spherical surface

1 Introduction

The sports lighting design, for both types, i.e. indoor and outdoor sports lighting, there are standards available, like – IESNA[7], CIE[9] etc. Also different sports authorities have their own standards like – ICC, FIFA. These standards define the quantitative and qualitative lighting parameters for different types of sports but the design methodology remains trial & error basis as the lighting design software are nothing but only calculating tools. Luminaires are aimed manually, without any specific idea of range of aiming angles, to achieve the defined lighting parameters for the concern sports. After each design approach, the output results from the software are checked with the reference values as set by the standards[7][8][9]. If the results do not match, the designing procedure starts from the beginning by aiming the individual luminaires.

This proposed algorithm gives a new approach of designing methodology. By this algorithm, at the initial stage, the illumination distribution pattern on the grid points, on the field, can be defined. This feature makes the algorithm robust in nature for designing of different types of sports lighting facilities. Also this algorithm is developed by considering initially point sources of light. The photometric distribution characteristics of any point source can be traced for any predefined horizontal illumination values on the field grid points and overall horizontal uniformity of the field by this algorithm. However to validate the algorithm, sensitivity analysis is done[3][10] by changing the input parameter of the system and correspondingly observing the output response of the system. During the validation of the algorithm the intensity of the point source is gradually increased and the change in response of the system in terms of standard deviation of horizontal illumination on the field grid points, average horizontal illumination and uniformity is observed. The simulation based results are verified with the hardware based setup to validate the algorithm.

The assumed point source is considered to be at the centre of a *hypothetical spherical surface*. However, this point source will be resolved into *'n'* numbers of point sources by tracing the intensity distribution pattern on the sphere surface to achieve the predefined illumination pattern on the field. Thus, this paper elaborates the proposed algorithm for this new designing methodology and also reviews the advantages of application of this algorithm instead of present tools that are used for lighting design.

2 Present Sports Lighting Designing Methodology

The present day outdoor sports lighting design is done by different lighting designing software, like – Calculux, AGI32, Europic etc. The steps for designing any outdoor sports lighting facility can be divided into four basic steps. *Step I* starts with selecting the lighting recommendations in terms of horizontal, vertical illumination, uniformity & glare rating as per *Class & Group of play*[8][9]. According to the recommended values of illuminating parameters, the approximate quantity of luminaires are calculated for a given sports lighting area by lumen method calculation. In *Step II*, the luminaire mounting arrangements are selected based upon provided data or considering all relevant constrains. *Step III* is the process of lighting design by any lighting design software which is a trial & error approach. In *Step IV,* the design output is checked with the reference, i.e. whether the quantitative & qualitative illumination parameters are matching with the standards[7][8][9] or not. If it matches, then the design gets selected as the optimized design, otherwise the designing procedure starts again from the beginning by aiming individual luminaires.

In this designing process, it is difficult to form any particular illumination distribution patters on the field, i.e. to follow the predefined illumination values on the grid points of the field from the initial stage of design. *For example*, in case of cricket stadium lighting design, the maximum illumination is required on the centre, pitch, area but on the other hand in the football stadium the pattern of illumination on the grid points are to be equally distributed. So it is the user or lighting designer, who has to do the design in trial & error basis to achieve any particular illumination distribution pattern on the field as well as the desired quantitative and qualitative illumination parameters on the field.

Also it is difficult to say, in how many attempts a lighting design can be made perfectly, as the lighting design software does not have any optimization characteristics, rather these are calculating tools only. It is the human feedback which comes into play during the designing process and hence the experience of the designer comes into count. Also the guide lines[9] are there to restrict the maximum aiming angle of luminaire, to avoid glare and light pollution. Whereas there are no luminaire aiming guide lines related to achieve any particular illumination values and patterns on the ground. Figure 1 shows typical flow chart of lighting design process by present lighting designing software.

In practice, at the time of doing outdoor sports lighting design by any lighting designing software, initially only one mast is designed with the luminaires aimed at the ground. Then with respect to that aimed luminaires of one mast, rest of the masts, rather luminaires, are made in symmetrical arrangement. When the average illumination level due to the contribution of single mast is known, the average illumination level due to the contribution of all other masts can also be roughly calculated. Generally the total average illumination will be equal to the average illumination achieved by single mast luminaires, multiplied by the total number of masts.

In this entire design procedure, it can be concluded that the lighting designing software is used as calculating tool only; however the optimization of design is done by the experience of the user. The lighting designing software also does not have artificial intelligence to provide any guidance path to the users to make sports specific or more precisely to say, ground illumination pattern specific design. The entire methodology of designing is on trial & error basis.

2.1 Structure of the Algorithm

The proposed algorithm starts from the fundamental point of making the sports lighting designing process trial & error free. The structure of this proposed algorithm is elaborated in Figure 2. By this new methodology of design there is no requirement of individual luminaire aiming. The mast quantity, luminaire mounting height and mast locations are given as input to the algorithm. According to the horizontal illumination on the grid points, the photometric distribution pattern of individual point source on each mast can be traced. This method also takes care of overall and transverse uniformity on the field as the horizontal illumination values on the field grid points are predefined. Later, with the development of the algorithm, this point source will be resolved into 'n' number of point sources per mast. Thus in this entire sports lighting design process there will not be any trial and error to fix the individual luminaire aiming angles to achieve any recommended illumination level on the ground. The working structure of the algorithm is described in the consecutive steps of *Initializations* and *Calculations*.

2.2 Algorithm: Initialization

For outdoor sports lighting design, only the direct component of light is considered from the light source[6]. The calculation can be done by the use of basic lumen method. However to start the design procedure, the parameters that are to be incorporated are – field dimensions, mast height, mast quantity, mast locations, considered grid structure on the field, absorption loss factor and maintenance factor. To begin with, field dimension of 6x10 units is assumed alongwith 1x1 unit grid structures. The centre of the field is considered to be at (0,0) co-ordinates. There are four numbers of masts and each is having a height of 5unit. The masts are located at a distance of 2units from the consecutive field side-ends. To make the algorithm generalized, all the dimensions are made unit free. At the initial state, every mast is assumed to have a single point source. The intensity distribution patterns or photometric distribution of all the sources are not considered. Also there is spherical surface which is considered to be surrounding the point source. The point source is assumed to be located at the centre of the sphere. Now it is considered that all the grid points on the ground are illuminated by the ray of light[1], coming out from the single point source as shown in Figure 3 by the lines.

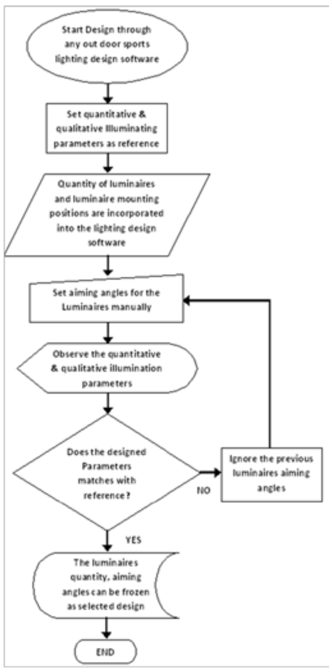

Figure 1 – Present Design Methodology

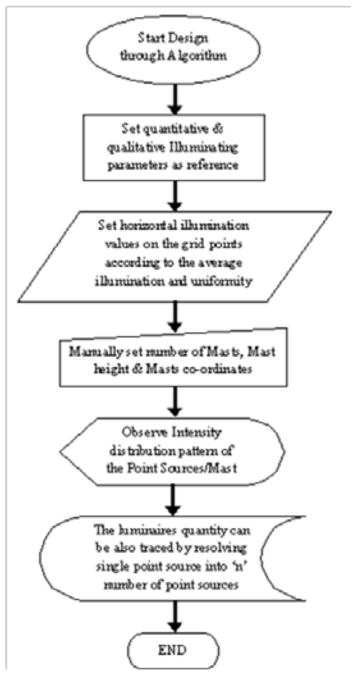

Figure 2 – Proposed Design Methodology

2.3 Algorithm: Calculations

The designing approach begins with the initialization of any arbitrary horizontal illumination pattern on the grid points on the ground. The average horizontal value of this distribution is chosen to be 1/4th of the actual required average horizontal illumination on the ground. A single point source is considered on a single mast to generate this pattern and value of average horizontal illumination on the field. According to the distribution of initial horizontal illumination pattern on the field, the intensity pattern of the point source is traced by Equation 1[11].

$$I(i,j)_{Point\,Source} = \frac{E(i,j) \times d(i,j)^2}{AL \times MF \times \cos\theta(i,j)} \quad (1)$$

Where

E	is the individual horizontal illumination values on the grid points
d	is the point source to individual grid point distance
AL	is the absorption loss
MF	is the maintenance factor
Θ	is angle of incident on individual grid points
(i,j)	indicates the dimension of the field grid matrix. Hence the intensity distribution pattern can also be calculated for all the point sources.

It is interesting to mention that now the point source is represented in the form of a matrix. The point source matrix dimension will be same as the dimension of grid point's matrix on the field. It can also be said that the light rays which is coming out of the point source to illuminate the entire ground will enclose certain part of the sphere surface. Also it is very obvious that this enclosed surface will be represented by a matrix having dimension equal to the number grid point dimension on the field. This can be well described from Figure 4 which is indicating the light rays coming out of the point source and enclosing the spherical surface. The intensity distribution pattern on the sphere surface can also be traced by Equation 2.

$$I(i,j)_{Sphere} = \frac{E(i,j) \times (d(i,j) - r)^2}{AL \times MF \times \cos\theta(i,j)} \quad (2)$$

Where r is the radius of the sphere and other symbols are synonymous with Equation 1.

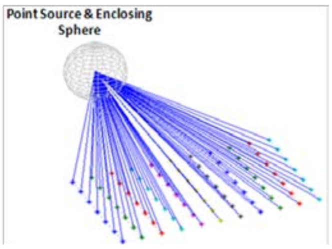

Figure 3 – Grid point on the field and spherical surface surrounding the point source

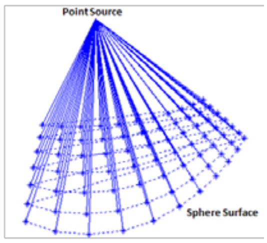

Figure 4 – Light rays enclosing spherical surface

Thus with respect to initial illumination pattern on the grid points, now there are two intensity distribution matrixes, Point source intensity distribution matrix denoted as $I_{Point\ Source}$ & intensity distribution on the sphere surface noted as I_{Sphere}.

It is considered that the field is to be designed with four point sources, placed upon four masts. Thus with respect to the initially calculated point source, the other three point sources are placed in symmetry. The point sources are made double axis symmetry with respect to the centre of the field. However this can be described through Figure 5. The mentioned Point Source 1 is the initially designed point source. Whereas the Point Source 2, Point Source 3 & Point Source 4 are made in symmetrical arrangement with respect to the Point Source 1. The average horizontal illumination on the field is due to the contribution of all four point sources and that can be calculated. Also it is to be mentioned that the pattern of illumination distribution on the field will be same as the initially described pattern.

The horizontal illumination on the field grid points, due to individual point sources, can be calculated by Equation 3[11].

$$E(i,j)_{P1} = \frac{I(i,j) \times AL \times MF \times \cos\theta(i,j)}{d(i,j)^2} \quad (3)$$

Where $E(i,j)_{P1}$ is the horizontal illumination values on the field grid points due to the contribution of Point Source 1. The intensity distribution of Point Source 1 is denoted by $E(i,j)_{P1}$ In similar way, $E(i,j)_{P2}$, $E(i,j)_{P3}$, $E(i,j)_{P4}$ can also be calculated.

However the horizontal illumination values on the grid points are denoted by E(i,j) matrix and each element of the matrix is the algebraic summation due to the contribution from all four point sources, as in outdoor lighting design only direct component of light from the source is considered. It is calculated by the Equation 4 where E(i,j) is the dimension of the field grid point's matrix.

$$E(i,j) = E(i,j)_{P1} + E(i,j)_{P2} + E(i,j)_{P3} + E(i,j)_{P4} \qquad (4)$$

Whereas the average horizontal illumination value on the field is calculated by Equation 5.

$$E_h = \sum E \big/ (i \times j) \qquad (5)$$

Where E_h is the average horizontal illumination values on the field due to contribution of all point sources, $E(i,j)_{P1}$, $E(i,j)_{P2}$, $E(i,j)_{P3}$, $E(i,j)_{P4}$ are the horizontal illumination values on the ground due to point source 1, 2, 3 & 4 respectively.

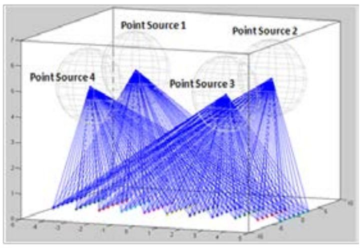

Figure 5 – Four point sources are placed in symmetry with respect to the field

3 Sensitivity Analysis: Method of Algorithm Validation

The next phase of algorithm in on the latest tools and techniques required for *performance evaluation*[10] of intelligent reasoning system. Performance evaluation serves mainly two objectives. First, one can test: whether the designed system performs satisfactorily for which it is built. This is called *validation*[2][10]. Secondly, evaluating the performance, it can be determined whether the tools and techniques have been properly used to model *"the expert"*. This is called *verification*[10]. The validation of an expert system is carried out by qualitative means. *Sensitivity analysis* is a popular method for qualitative validation.

Sensitivity analysis means change in response of a system, when there is even a small change in its input excitation[1][10]. Thus from the sensitivity analysis of two identical systems, the accuracy of one system with respect to other can be concluded. Thus to validate[3][10] the algorithm, three systems are considered – first is the *simulation based model.* In this model, initially the grid points are defined with some arbitrary horizontal illumination values and according to that the point source photometry is traced. The second one is a miniature *real-time setup of the simulated model.* Here a ground is considered in same dimension with simulation based model. Four 50W MR16 lamps (as point sources) are mounted on four poles and the ground is illuminated due to the contribution of all the lamps. In the third system, i.e., *simulated based real-time model*, the illumination pattern on the field is measured by keeping one MR16 lamp in 'ON' condition and that is the initially defined illumination pattern in simulation based model. By changing the intensity of the source, both in real-time and simulated model, the sensitivity analysis is done to validate the algorithm[3][10].

3.1 Validation of Algorithm: Simulation vs Real Time Result

In this simulation based model, the input parameter is the intensity of the point source. The intensity of the point source has been traced and represented by the matrix $I(i,j)_{\text{Point Source}}$, where (i,j) represents the dimension of the matrix. All the individual values of the intensity matrix are uniformly increased by 50 candelas per simulation. Thus after every simulation, a new intensity matrix is formed which is denoted by $I(i,j)_{\text{Point Source}}$ and has been described by Equation 6. In the similar way the intensity matrixes for all the point sources are increased uniformly.

$$I(i,j)_{Incresing} = I(i,j)_{Point\,Source} + 50 \qquad (6)$$

The responses of the simulated based model system are (a) standard deviation[12] of the horizontal illumination values on the grid points, (b) average horizontal illumination, (c) minimum horizontal illumination, (d) maximum horizontal illumination, (e) horizontal overall uniformity ($E_{minimum}/E_{average}$) and (f) horizontal transverse uniformity ($E_{minimum}/E_{max}$).

The standardized sports lighting design parameters[7][8][9] are horizontal illumination, vertical illumination, horizontal & vertical uniformity (overall/transverse)[5] and glare rating. Initially this algorithm is formulated to deal with horizontal illumination and its relative parameters. However depending upon the validation and performance of the algorithm by sensitivity analysis, the vertical illumination and glare rating controlling parameters will be incorporated. The calculation of standard deviation on the horizontal illumination on the grid points has significance. Standard deviation (S.D.)[12] is the measure of dispersion, i.e. S.D. may be defined as ‘Root-Mean-Square-Deviation from arithmetic mean’, shown in Equation 7[12]. S.D. of the horizontal illumination values on the grid points shows the deviation characteristics with respect to increasing intensity of the point sources.

$$S.D.(\sigma) = \sqrt{\frac{1}{n}\sum(x_i - \bar{x})^2} \qquad (7)$$

A new set of responses emerges after every simulation which is plotted against the increasing average intensity values of all point source. All the above mentioned responses are shown in Figure 6(a)-6(f).

It is interesting to observe that as the intensities of the point sources are increased uniformly, the responses, like standard deviation, average illumination, minimum illumination and maximum illumination of horizontal illumination on the field show increasing characteristics. The nature for both the uniformity factors, are initially increasing in nature which get saturated after certain number of simulations.

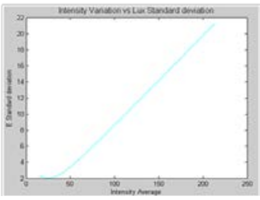

Figure 6(a) – Intensity vs Standard Deviation for Horizontal illumination values

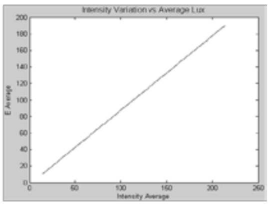

Figure 6(b) – Intensity vs Average Horizontal illumination values

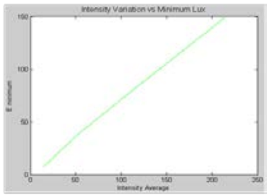

Figure 6(c) – Intensity vs Minimum Horizontal illumination values

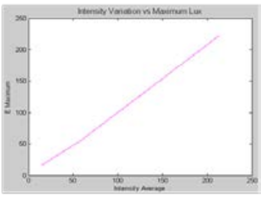

Figure 6(d) – Intensity vs Maximum Horizontal illumination values

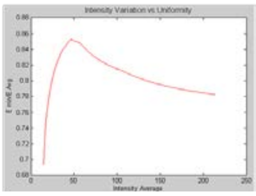

Figure 6(e) – Intensity vs Overall Horizontal Uniformity values

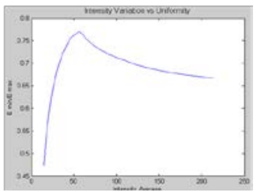

Figure 6(f) – Intensity vs Transverse Horizontal Uniformity

Figure 6 – Simulated results for Sensitivity responses on the horizontal grid points of the field

3.2 Validation of Algorithm: Simulation vs Real Time Result

To *validate the performance*[1][4] of the proposed algorithm, a miniature real-time setup of the simulated model is prepared. The dimensional unit values of the field, mounting height of the luminaires, are kept identical with the simulation based model, although in real time the units are considered in foots. Halogen MR16, 50Watt lamps, with reflectors, are chosen as point sources for the real-time based simulated model.

The halogen lamp produces light by the principle of incandescence. Any variation of the supply power can change the output characteristics of the lamp. To avoid such consequences, during the measurement operation, the lamps are powered through *CVCF (Constant Voltage Constant Frequency)* modules. It is observed that if the voltage across the source is increased gradually, the intensities of the MR16 lamp at 0^0, 10^0, 20^0 vertical angles do increase which is evident from Figure 7.

The photometric distributions of the MR16 lamp are measured in the span of 150 volt to 230 volt at an interval of 5 volt. It is observed that, the nature of the photometric distribution remains identical with the increase of peak intensity values of MR16 lamp. This is evident from Figure 8. Thus the point source in simulation based model can be represented by halogen MR16 lamp in real-time as the intensity can be increased uniformly with the gradual increase of voltage across the lamp. Another advantage of selecting MR16 lamp is the nature of the photometric distribution remains identical with the increase of the peak intensity of the lamp.

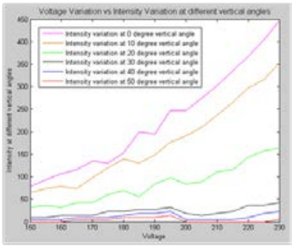

Figure 7 – Voltage variation vs Intensity variation of MR16 lamp

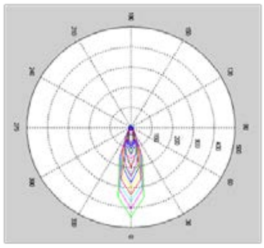

Figure 8 – Photometric distribution of 50W MR16lamp at different voltage levels

However to replicate the simulation based model in real-time, an area is considered of 6ft x 10 ft dimension. The entire area is divided uniformly into 1ft x 1ft grid points. Thus the dimension of grid point's matrix on the field is (7x11), i.e. total 77 points. There are total four numbers of MR16 lamps mounted at the height of 5ft on four different poles. The locations of the poles are kept identical with the simulation based model. All four MR16 lamps were kept on at 150 volt and the horizontal illumination values were measured on the grid points. At an increment of 5 volts, this measurement process gets repeated upto 230 volt. Now from the measured horizontal illumination values, the set of responses are extracted, i.e. (a) standard deviation[12] of the horizontal illumination values on the grid points, (b) average horizontal illumination[7][8], (c) minimum horizontal illumination, (d) maximum horizontal illumination, (e) horizontal overall uniformity ($E_{minimum}/E_{average}$) and (f) horizontal transverse uniformity ($E_{minimum}/E_{max}$). These responses are plotted against increasing average intensity values of the MR16 lamp at different voltage levels. The following Figures 9(a)-9(f) show the sensitivity analysis response for the real-time setup of the simulated model.

In the next phase of validation[1][10], a real-time based simulation method is used. At the initial stage of the algorithm, an arbitrary horizontal illumination distribution pattern was considered on the field grid points. According to that, the intensity distribution matrix for a single point source was traced. Then after, other three point sources were made in symmetry with respect to first point sources to get the total summation of horizontal illumination levels on the field grid points. In this phase only one MR16 lamp is kept at 'ON' condition and the measurements of horizontal illumination on the grid points were taken. This real-time data is fed to the algorithm to generate the photometric distribution characteristics of the simulation model based point source. However the MR16 lamp photometry from the simulated data is to be generated from the intensity distribution matrix. This matrix is calculated from the horizontal illumination values on the grid points by Equation 1[11]. The MR16 lamp is mounted on the vertical plane. The light source is also adjusted to some horizontal and vertical aiming angles with respect to the field. Thus the highest horizontal illumination value on the field grid points is located and is considered to be the nadir point for the point source. The luminaire has double axis symmetrical photometric distribution. Thus the diagonal grid points, corresponding to the maximum illumination value, are considered as the plane for photometry distribution measurement of the MR16 lamp. The incident angles corresponding to these points are calculated. The intensity values at angles corresponding to the diagonal grid points are used to form the photometry of the source. To get the distribution of the point source on the field, the intensity values are divided by the square of the distance between the point source to nadir point[11].

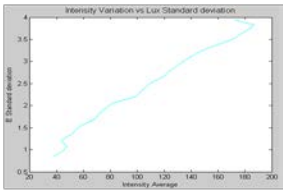

Figure 9(a) – Intensity vs Standard Deviation for Horizontal illumination value

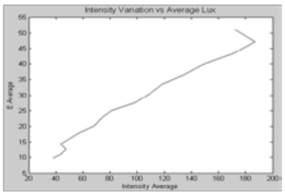

Figure 9(b) – Intensity vs Average Horizontal illumination values

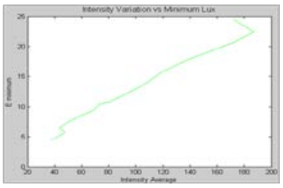

Figure 9(c) – Intensity vs Minimum Horizontal illumination values

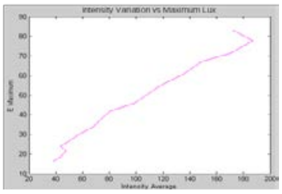

Figure 9(d) – Intensity vs Maximum Horizontal illumination values

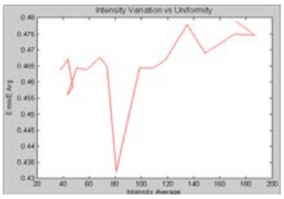

Figure 9(e) – Intensity vs Overall Horizontal Uniformity values

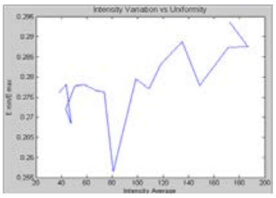

Figure 9(f) – Intensity vs Transverse Horizontal Uniformity

Figure 9 – Real-time results for Sensitivity response on the horizontal grid points

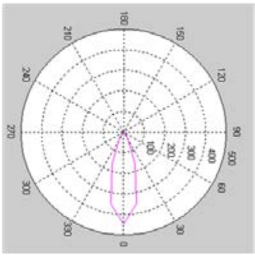

Figure 10 – Photometric Distribution of MR16 lamp, measured in Mirror Distribution Photometer

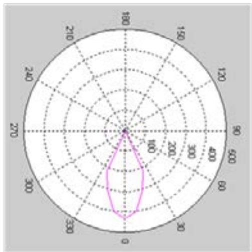

Figure 11 – Photometric Distribution of MR16 lamp, traced by algorithm from real-time data

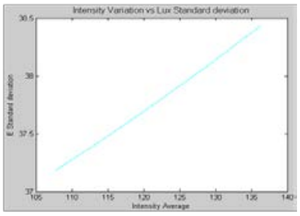

Figure 12(a) – Intensity vs Standard Deviation for Horizontal illumination values

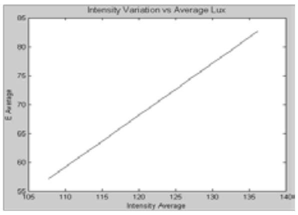

Figure 12(b) – Intensity vs Average Horizontal illumination values

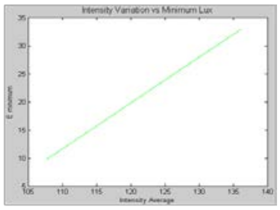

Figure 12(c) – Intensity vs Minimum Horizontal illumination values

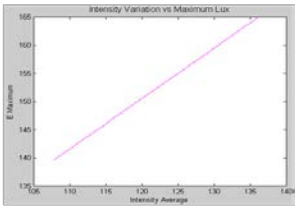

Figure 12(d) – Intensity vs Maximum Horizontal illumination values

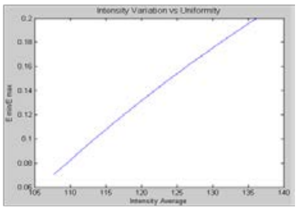

Figure 12(e) – Intensity vs Overall Horizontal Uniformity values

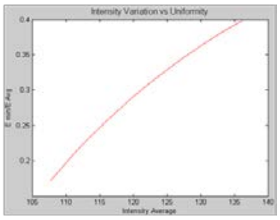

Figure 12(f) – Intensity vs Transverse Horizontal Uniformity values

Figure 12 – Simulated results from Real-time data for Sensitivity responses on the horizontal grid points of the field

The measured photometric distribution pattern of MR16 lamp by Mirror Distribution Photometer is shown in Figure 10 and Figure 11 shows the photometry of the simulation based model point source. From Figure 10 and Figure 11 it is seen that the accuracy percentage of the algorithm to trace the peak intensity of the source is *96.47%*. The reason of photometric variation is due to lack of available simulating points.

Thereafter tracing the single point source intensity distribution pattern matrix, three other sources are placed symmetrically with respect to the traced point source. Again applying Equation 6, the point source intensity is uniformly and gradually increased per simulation. These real-time based simulated results are plotted in Figures 12(a)-12(f).

4 Result Analysis

During the sensitivity analysis of real-time data, the intensity of the MR16 lamp is varied in the span of 150 volt to 230 volt. Similarly the horizontal illumination values on the grid points have increased. The range of variation of average horizontal illumination value on the field is traced. Within this range, the simulation of the algorithm is also done. However the sensitivity analysis[1][3][10] for all three cases, i.e. *simulation based model*, *real-time model* & *simulated based real-time model* shows almost identical natures for the standard deviation, average horizontal illumination, minimum horizontal illumination and maximum horizontal illumination against variable average intensity. In general it can be concluded from the characteristic curves that as the intensity of the source increases, the standard deviation of horizontal illumination values on the grid points also increases. The same phenomenon works for average, minimum and maximum horizontal illumination on the field. Thus the sensitivity analysis draws conclusive results for the proposed algorithm. The change of input or change of intensity of the point source changes the response of the systems in identical nature.

However the trend of uniformity (overall/transverse)[5] against variable intensity does not show much similarity. There are two possible reasons; *firstly*, all the four MR16 lamps could not be aimed at same horizontal and vertical angles. This is evident from the data table of any measured horizontal illumination values on the field. A typical measurement of horizontal illumination values on the grid points, at 230 volts, shows dissimilarities of illumination values at the four corner points. Also the maximum illumination value appears at the (5,7) co-ordinate of the grid points of the field. However according to the symmetrical arrangement of the luminaires, it was supposed to arise at (4,6) co-ordinate, i.e. at the middle of the field grid points, as the field grid point dimension is (7,11). It is referred in Table 1. *Secondly*, at the time of simulation, the intensity of the source was uniformly increased, i.e. all the values of the matrix were uniformly increased. However, at the time of real-time application, the intensity of the point source does not increase uniformly at all the vertical angles. It can be made evident from Figure 7. At the vertical angles 0^0, 10^0 the intensity is stiffly increasing with respect to intensity at 30^0,40^0 and 50^0 vertical angles as plotted against increasing terminal voltage of the lamp. Thus the increase of the intensities of MR16 lamp at all vertical angles is not uniform. Due to the effect of this irregular photometric distribution, the overall horizontal uniformity and transverse uniformity on the field becomes irregular too. However this irregular variation does not impact the objection of validation.

Table 1 - E_h values on the grid points due to single MR16 lamp at 230V

	1	2	3	4	5	6	7	8	9	10	11
1	24.5	34.8	45.4	51.4	56.6	55.6	56.6	51.1	44.2	33.2	26.3
2	26.3	40.5	51.9	59.5	64.5	65.1	67.5	63.2	51.9	38	25.6
3	27.9	48.8	56.2	66.2	72.3	73.6	77.1	72.2	57.7	42.1	27.9
4	29.7	42.1	53.7	66.4	75.9	80.2	83.2	75.1	62.2	43.6	28.8
5	30.2	41.2	50.9	57.9	70.9	80.9	83.4	77.1	62.6	45	28.8
6	29.7	39.8	48.3	52.6	54.4	63.7	72.1	68.4	55.2	38.4	26.7
7	28	36.6	43.2	46.3	46.7	50.2	51.1	53.6	45.4	34.2	27.3

5 Conclusion

By this novel approach, as discussed in this paper, the sports lighting designing methodology can be changed. Due to application of this algorithm, the sports lighting designing approach will not be trial and error basis and also the sports lighting designing efficiency will certainly not be dependent on the experience of the designer or user. It is also significant to mention that by this proposed algorithm the grid point to point illumination can be made predefined and accordingly the source intensity distribution pattern can be designed. With the defined illumination pattern on the field grid points, every designing approach can be made sports facility specific. The success of validation of the algorithm by sensitivity analysis is also significant. The identical nature of the responses from all the three systems indicates high performance simulated model of real-time system. The algorithm also shows high accuracy of replicating real-time based luminaire photometry to simulated model of point source.

Now in practice it is difficult to design a single luminaire with such intensity distribution characteristic for a large ground if the required illumination levels are very high. In further development, the application of *source distribution* is to be done. The point source intensity distribution of the point source can also be traced on the sphere surface and single point source can be resolved into ‘n’ number of point sources to achieve that intensity distribution on the spherical surface. The vertical illumination and glare rating parameters are to be added to evolve with an intelligent self optimizing algorithm.

References

[1] LENDERINK, E. STEHOUWER, P. 2008. Optimization, sensitivity analysis, and robust design using response surface modeling. *Illumination Optics,* Proc. SPIE 7103, 710302.

[2] CHOI, K. P., ZHANG L. 2004. Sensitivity analysis and efficient method for identifying optimal spaced seeds. *Journal of Computer and System Sciences*, Volume 68, Issue 1, Pages 22–40

[3] NANNICINI, T. 2007. Simulation–based sensitivity analysis for matching estimators. *The Stata Journal*, Volume 7 Number 3: pp. 334-350.

[4] KUMAR, P., JAMIL, M., THOMAS, M. S., MOINUDDIN, A. 2000. Sensitivity analysis of fault quantities. *International Journal of Electrical Power & Energy Systems*, Volume 22, Issue 2, Pages 147–153.

[5] HOUSER, K.W., WEI, M., ROYER,M.P. 2011. Illuminance uniformity of outdoor sports lighting. *LEUKOS The Journal of the Illuminating Engineering Society of North America*, 7:221-235.

[6] BRONS, J.A., BULLOUGH, J.D., REA, M.S. 2008. Outdoor site-lighting performance: A comprehensive and quantitative framework for assessing light pollution. *Lighting Research and Technology*, 40, page 201-224.

[7] BS EN 12193:2007. Light and lighting. Sports lighting.

[8] IESNA RP-6-01. Recommendation for Sports and Recreational Area Lighting.

[9] CIE169:2005. Technical Report, Practical Design Guidelines of Sports Events for Colour Television and Filming.

[10] KONAR, A. 1999. *Artificial Intelligence and Soft Computing – Behavioural and Cognitive Modeling of Human Brain* (page no.612).London. CRC.

[11] SIMMONS, R.H., BEAN, A.R. 2001. *Lighting Engineering Applied Calculations*. Architectural Press.

[12] DAS, N.G. 2008. *Statistical Methods - Combined Edition (Volumes I&II)*. Tata McGraw-Hill Education Pvt. Ltd.

OP52

ADJUSTABLE POWER LINE IMPEDANCE EMULATOR FOR CHARACTERISATION OF ENERGY-SAVING LIGHTING PRODUCTS

Tuomas Poikonen[1,2], Teemu Koskinen[2], Hans Baumgartner[2], Petri Kärhä[1,2], and Erkki Ikonen[1,2]

[1] Centre for Metrology and Accreditation (MIKES), Espoo, FINLAND
[2] Metrology Research Institute, Aalto University, Espoo, FINLAND
tuomas.poikonen@mikes.fi

Abstract

We have developed an adjustable power line impedance emulator (APLIE) for characterisation of electrical power consumption of AC-operated energy-saving lamps. The passive single-phase LCR-network can emulate impedance curves of low-voltage power distribution networks in the frequency range of DC – 1 MHz. The device is connected in series with the regulated AC voltage source and the lamp under measurement in order to reduce the sensitivity of the lamp electronics to the output impedance of the AC voltage source. Test measurements conducted for a group of energy-saving lamps showed that some lamp electronics are very sensitive to changes in the source impedance. A difference of 1.2 % was measured for the efficacy of a compact fluorescent lamp (CFL), when using different impedance settings. The APLIE can be used as a versatile tool for characterisation of the electrical behaviour of energy-saving lamps, as well as for developing a fixed impedance stabilisation network for efficacy measurements.

Keywords: Luminous efficacy, energy-saving lamp, electrical power, source impedance

1 Introduction

Luminous efficacy [lm/W], defined as the luminous flux produced by a lamp divided by its electrical power consumption, is used for determining the energy efficiency of light sources [1]. Luminous flux can be measured using an integrating sphere or a goniophotometer. Electrical power measurement of AC-operated energy-saving lighting products, such as LED-lamps or CFLs, is challenging because they contain various types of built-in power converters for driving the LEDs or the fluorescent tubes. Such lamps draw non-sinusoidal current pulses at each power line cycle, producing harmonic distortion to the electrical network [2]. In addition, the high total harmonic distortion (THD) and low power factor of the lamps cause increased uncertainty in the electrical power measurement [3,4]. Due to the insufficient stability and distortion properties of low-voltage power lines, testing laboratories use regulated AC voltage sources for operating the lamps. Depending on the manufacturer, the output impedance of the AC voltage source can be different at two different testing laboratories. A problem arises, when the impedance of the AC voltage source is coupled with the power converter of the energy-saving lamp. The operation of the lamp electronics may thus depend on the effective impedance, and differences of several percents in the measured efficacy can occur depending on the lamp type and the measurement equipment used [3].

We have developed an adjustable power line impedance emulator (APLIE) that stabilises the impedance of the luminous efficacy measurement setup in order to allow different types of AC voltage sources to be reliably used for supplying energy-saving lamps of large variety. The APLIE contributes to reducing the most important uncertainty component in the luminous efficacy measurements. Impedance stabilisation networks for measurement of electromagnetic compatibility (EMC) would be commercially available, but they are not directly suitable for measurements of energy-saving lamps, for which the most interesting frequency range is 50 Hz – 200 kHz [3,4].

2 Efficacy measurement setup

Our luminous efficacy measurement setup is shown in Figure 1 and the corresponding uncertainty budgets in Table 1. The luminous flux and relative spectral radiant flux are measured using a 1.65-m integrating sphere, equipped with a photometer head and a spectroradiometer. The setup is based on the absolute integrating sphere method [5].The lamp under measurement is driven with a 500 VA programmable AC voltage source with a typical THD of voltage smaller than 0.1 %. The electrical power consumption is measured using a 1 MHz power analyser. Characterisation of the setup and a group of LED-lamps has been described in [4] before taking the APLIE in use.

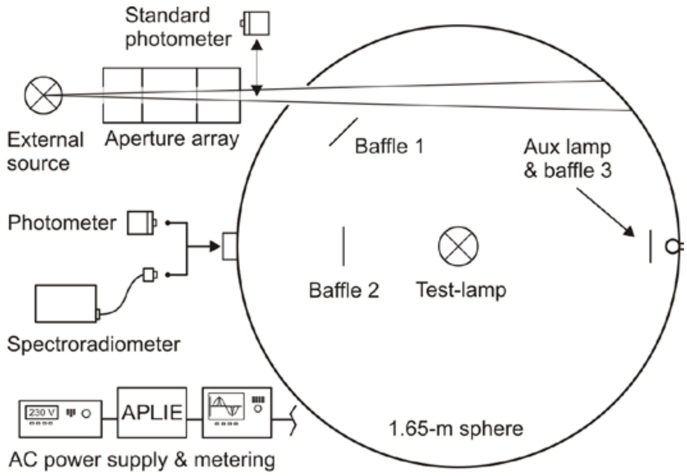

Figure 1 – Luminous efficacy measurement setup [4].

The relative expanded uncertainty of luminous efficacy for a typical LED-lamp with stable built-in electronics is 1.2 % (k = 2). The most important uncertainty contributions are related to the realisation of the luminous flux scale and the electrical power measurement. The latter uncertainty is heavily dependent on the characteristics and stability of the lamp electronics, and needs to be determined for each lamp individually. Lamps with THD above 200 % and power factors below 0.4 can be problematic, causing temporal variations up to 1 % in the measured electrical power [4]. Achieving low measurement uncertainty of luminous efficacy with all lamps available in the market is challenging. Developing methods and tools for electrical power characterisation of energy-saving lamps is thus highly important.

Table 1. Uncertainty budget of the luminous efficacy measurements [4].

Source of uncertainty of efficacy	Relative standard uncertainty [%] Problematic lamp (achieved)	Stable lamp (achieved)	Anticipated with improvements
Measurement setup			
Luminous flux responsivity	0.3	0.3	0.2
Drift of the sphere photometer	0.1	0.1	0.1
Stability of the AC-power supply	0.2	0.1	0.1
Luminous efficacy measurement			
Stability of the luminous flux	0.1	0.1	0.1
Stability of the built-in electronics	1.0	0.2	0.1
Electrical power measurement	0.9	0.3	0.2
Photocurrent measurement	0.1	0.1	0.1
Spectral mismatch correction	0.2	0.2	0.2
Self-absorption correction	0.2	0.2	0.1
Spatial nonuniformity correction	0.1	0.1	0.1
Combined standard uncertainty	1.4	0.6	0.4
Expanded uncertainty (k = 2)	2.9	1.2	0.9

3 Adjustable impedance emulator

The adjustable power line impedance emulator (Figure 2) will be used for characterisation of the electrical power consumption of energy-saving lighting products. The passive single-phase LCR network can emulate various impedance curves found in typical low-voltage power distribution networks, to which the lamps are connected in normal operation. The APLIE is connected in series with the AC voltage source and the lamp under measurement (Figure 1). The instrument weighs about 15 kg, and its volume is 485 x 355 x 500 mm^3.

Figure 2 – Adjustable power line impedance emulator (APLIE).

The model of the LCR circuit used in the APLIE was developed on the basis of the data published on power line impedances in several different countries around the world [6–11]. In addition, the impedance of the wall sockets in the campus area of Aalto University was measured at the fundamental frequency of 50 Hz. The data were then combined, and used to calculate average, minimum and maximum curves for the power line impedances to be simulated. The circuit proposed by Zhao and Rietveld [3] was simulated as well, and was found to produce an impedance curve close to the calculated average. Therefore, we decided to use the circuit model by Zhao and Rietveld as the basis of our device to be further developed.

Special care was taken in the selection of components to obtain the aforementioned average, minimum and maximum impedance curves of the simulated model. The resistances of the wiring and switches were minimised. Air-gapped coils and capacitors designed for high-speed switched mode applications were used. Some of the filter components were removed from the actual circuit to avoid impractically large reactive power requirement for the AC voltage source. The APLIE consumes only 4 W of active power, and 100 var of reactive power from the AC voltage source, when no load is connected. The maximum continuous load current that can be used is 25 A. The impedance responses of the APLIE were characterised in the frequency range of DC – 1 MHz. At the average setting, the impedance is approximately 0.5 Ω at 50 Hz, and gradually increases to 100 Ω at 1 MHz. The impedances of the minimum and maximum settings differ from the average by up to one order of magnitude. In addition to the three basic curves, the impedance can be adjusted at three different frequency bands using the switches in the front panel.

4 Test measurements

Test measurements were carried out for 5 LED-lamps, a CFL, and an incandescent lamp using our luminous efficacy measurement facility of Figure 1 [4]. The electrical power consumptions of the lamps were measured and the waveforms were sampled for analysis. As expected, the efficacy measured for the incandescent lamp was found to be insensitive to changes in the source impedance. For the CFL, the largest difference obtained in the efficacy with different impedance settings was 1.2 %. The shapes of the current waveforms and the harmonic contents of three LED lamps changed significantly with different impedance settings, although the changes in the efficacy were smaller than 0.1 %. It was found that when the APLIE was in use and configured for the average impedance, the output of the AC voltage source was stable and the sporadic phenomena found with some lamp types disappeared. For one of the lamps measured, the standard deviation of the electrical power consumption dropped to half of that measured without the APLIE. A larger group of lamps needs to be tested to make general conclusions on the behaviour of various lamp electronics.

5 Conclusions

The developed impedance emulator can be used as a versatile tool in the research of electrical power characterisation of AC-operated energy-saving lamps. In addition, it can be used for developing a fixed impedance stabilisation network that, in the future, could be used by testing laboratories [3]. The test measurements support the need to develop such a network, as the difference of 1.2 % in the luminous efficacy measured for the CFL with different source impedance settings is as large as the expanded uncertainty reported earlier for luminous efficacy of LED-lamps with stable electronics [4]. Measurement results for a larger group of energy-saving lamps will be presented at the conference.

References

1. IES 2008 IES LM-79-08. Approved Method: Electrical and Photometric Measurements of Solid-State Lighting Products. New York: IES.

2. YE, Z. et al. 2008. A topology study of single-phase offline AC/DC converters for high brightness white LED lighting with power factor pre-regulation and brightness dimmable. In Proceedings of IEEE Industrial Electronics Conference, 1961–1967.

3. ZHAO, D. et al. 2012. The influence of source impedance in electrical characterization of solid state lighting sources. In Proceedings of IEEE Precision Electromagnetic Measurements Conference, 300-301.

4. POIKONEN, T. et al. 2012. Luminous efficacy measurement of solid-state lamps. *Metrologia*, 49, S135–S140.

5. Ohno, Y. 1998. Detector-based luminous-flux calibration using the absolute integrating-sphere method. *Metrologia* 35, 473–78.

6. Nicholson, J. R. et al. 1973. RF impedance of power lines and line impedance stabilization networks in conducted interference measurements. In Proceedings of IEEE Transactions on Electromagnetic Compatibility Conference, 84-86.

7. Malack, J. A. et al. 1976. RF impedance of United States and European power lines, In Proceedings of IEEE Transactions on Electromagnetic Compatibility Conference, 36-38.

8. Neto, J. P. L. et al. 2003. In-door power-line impedance measurement up to high frequency (10 kHz – 70 MHz). In Proceedings of IEEE 7th International Symposium on Power-Line Communications and Its Applications, 243-247.

9. Knop, A. et al. 2009. High frequency grid impedance analysis with three-phase converter and FPGA based tolerance band controller. In Proceedings of IEEE Compatibility and Power Electronics Conference, 286-291.

10. Marcus, I. U. et al. 2011. The influence of the network impedance on the nonsinusoidal (harmonic) network current and flicker measurements. In Proceedings of IEEE Transactions on Instrumentation and Measurement Conference, 60, 2202-2210.

11. Sigle, M. et al. 2012. On the impedance of the low-voltage distribution grid at frequencies up to 500 kHz. In Proceedings of IEEE International Symposium on Power Line Communications and Its Applications, 30-34.

OP53

LUMINOUS FLUX AND COLOUR MAINTENANCE INVESTIGATION OF INTEGRATED LED LAMPS

Corell, D.[1], Thorseth, A.[1], Dam-Hansen, C.[1]
DTU Fotonik, Technical University of Denmark, Roskilde, DENMARK
andt@fotonik.dtu.dk

Abstract

This article will present an investigation of the luminous flux and colour maintenance of white LED based retrofit lamps. The study includes 23 different types of integrated LED lamps, covering 18 directional and 5 non-directional. Luminous flux and colour data for operation up to 20000 h has been measured, and will be presented. Data for the first 6000 h of operation is used for studying extrapolation method and results are compared with experimental data for operation over 19000 h. It has been further examined when catastrophic failures occurred.

Keywords: LED, LEDi, retrofit, lumen maintenance, colour maintenance, lifetime

1 Introduction

As inefficient light sources such as the incandescent light bulb and halogen light sources are being phased out, there is a need for efficient and durable replacements lamps. The market has been flooded with LED based retrofit lamps for replacement of these. Manufacturers of LED lamps generally promise a very long lifetime or luminous flux maintenance and a high efficiency. Since the luminous flux depreciation of LED lamps is not only determined by the LED components but also by the electronics, connections, thermal/mechanical construction and the optics, it is unlikely that the luminous flux maintenance will be well described by LM-80 measurements and TM-21 extrapolations for luminous flux depreciation of the LED components contained in the LED lamp.

This investigation was part of a larger test study of the quality of LED retrofit lamps (LEDi lamps) commercially available on the market in Denmark in 2010 and 2011. This was done in order to be able to evaluate and describe the lifetime / luminous flux maintenance of these types of Solid State Lighting (SSL) products, a number of the LED lamps where selected for a long term experimental study looking at the luminous flux and colour maintenance over long term operation and to evaluate current ways of predicting luminous flux output.

2 Method

LED lamps covering 18 types of directional lamps and 5 types of non-directional LED lamps were chosen for this study, covering both 12 V DC and 230 V AC units. The number of samples of each type of LED lamp varied from 1- 6 pieces and a total of 48 samples were measured. The SSL products had power consumption below 8 W and were supplied by industrial partners in the project “LED lighting quality program”.
The LED lamps were set up for continuous operation in an air-conditioned room, with an ambient temperature of approximately 22 ± 3 deg. C. Half of the products were oriented with base up, the rest with base down. The lamps were monitored 2-3 times weekly to detect sudden failures. All the LED lamps were tested for their photometric and colorimetric properties using a 1 m sphere spectroradiometer system for total spectral flux measurements. The lamps were shifted from the continuous operation to the sphere, so fast that only a short time for stabilization in the sphere was needed. Measurement procedures were preferably set up to apply to LM-79, with some tolerances exceeding this standard. The measurements were done initially at 0 h, at 500 h and 1000 h and subsequently every 1000 h until 6000 h of operation. This follows the recommendations for luminous flux maintenance testing in the IEC/PAS 62612 (ICE, 2009). By February 2014 half of the products have been running for

19500 hours, the rest for 24000 hours. Only results for up to 20000 h of operation will be presented in this paper.
An extrapolation method (IES, 2011) used to estimate LF maintenance for values at operation times up to 36000 h was investigated this method was compared with measured values at 20000 hours.

3 Results and discussion

In this section the results will be presented and discussed.

3.1 Luminous Flux Maintenance:

A total of eight LED series was measured in this maintenance testing, each series contains 3-6 LED units of the same product, information about each series can be found in Table 1, and the luminous flux of these has been averaged at each measurement hour. The luminous flux vs time for four of these LED series is shown on Figure 1. The uncertainty of each time is found using propagation of uncertainty, the error bars in Figure 1 represents this uncertainty. This uncertainty is calculated by taking the luminous flux of each sample multiplied with its uncertainty squared. Afterwards they are summed together and the square root of this is taken and finally dividing with the amount of unfailed samples at each point equation (1) shows how this is calculated:

$$\sigma_{\phi,n}(t) = \frac{\sqrt{\sum((\phi_n(t) \cdot \sigma_n(t))^2)}}{n} \tag{1}$$

where

$\Phi_n(t)$ = averaged normalized luminous flux output at time t.

$\sigma_n(t)$ = Uncertainty of the measurement at time t.

n = Amount of samples at time t.

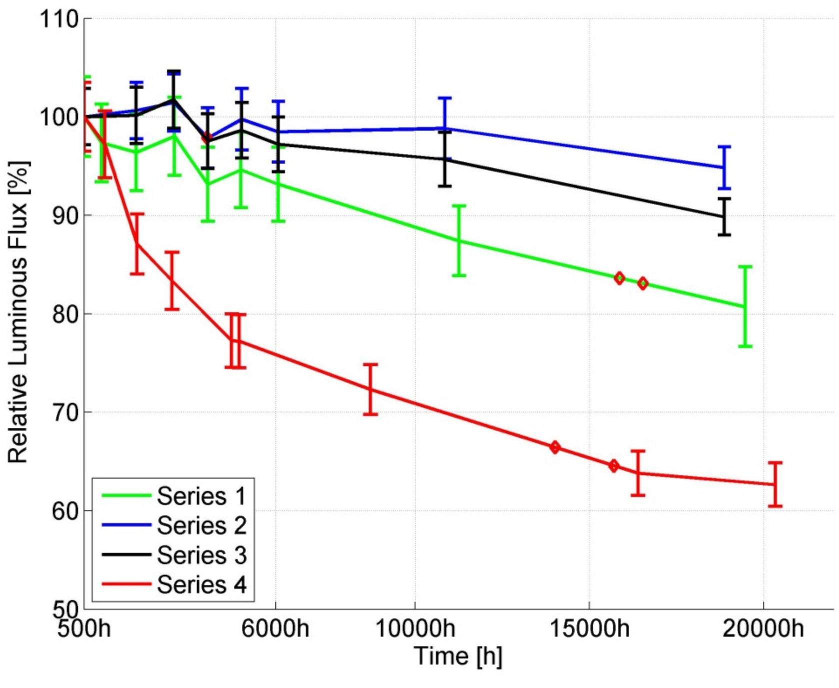

Figure 1 – Normalized measured luminous flux vs Time for 4 LED series, with error bars showing the variation among samples compounded with the measurement uncertainty, diamonds indicates that a light source from this series failed

For the majority of samples the luminous flux measured at 6000 h was above 85 % of the initial value. Due to markedly large variations in the luminous flux from 0 to 500 h, ranging from a range +/- 10 % and up to 55 % for one sample, it was decided to use the values at 500 h as the initial value, and the subsequent measurements have been normalized according to the luminous flux at this time, equivalent to a 500 hour burn-in.

Table 1 - The properties for the LED product in the chosen/example series

Series #	No. of samples	Wattage	Voltage	Type
Series 1	3	3.7 W	230 V	Directional
Series 2	6	3.7 W	230 V	Directional
Series 3	6	4.6 W	230 V	Directional
Series 4	4	5.9 W	230 V	Non-Directional

Only light sources that are alive are used in the averaging and calculation of the uncertainty. If a light source from one of these series failed, the time stamp of occurrence is marked with a red diamond (With an accuracy of 2-3 days).

3.2 Extrapolation Method

The extrapolation method suggested by IES in TM-21-11 (IES, 2011) can be used for data sets above 6000 h, using values for at last 5000 h of data, meaning that data from 1000 h to 6000 is used to predict the life time of LEDs. The following formula is used for the curve fit, to predict the LED life time:

$$\phi(t) = \beta \cdot e^{-\alpha t} \qquad (2)$$

where

t	=	operation time in hours
Φ(t)	=	averaged normalized luminous flux output at time t
α	=	projected initial constant derived by the least squares curve fit
β	=	decay rate constant derived by the least squares curve-fit.

Figure 1 has been extended with this curve fit data (dashed lines), Figure 2, and it is seen that the luminous flux prediction fits reasonably well for series 1-3 after 19000 h within 10%, for series 4 the prediction is off by more than 40%, in order to get a more accurate prediction one could use more time data.

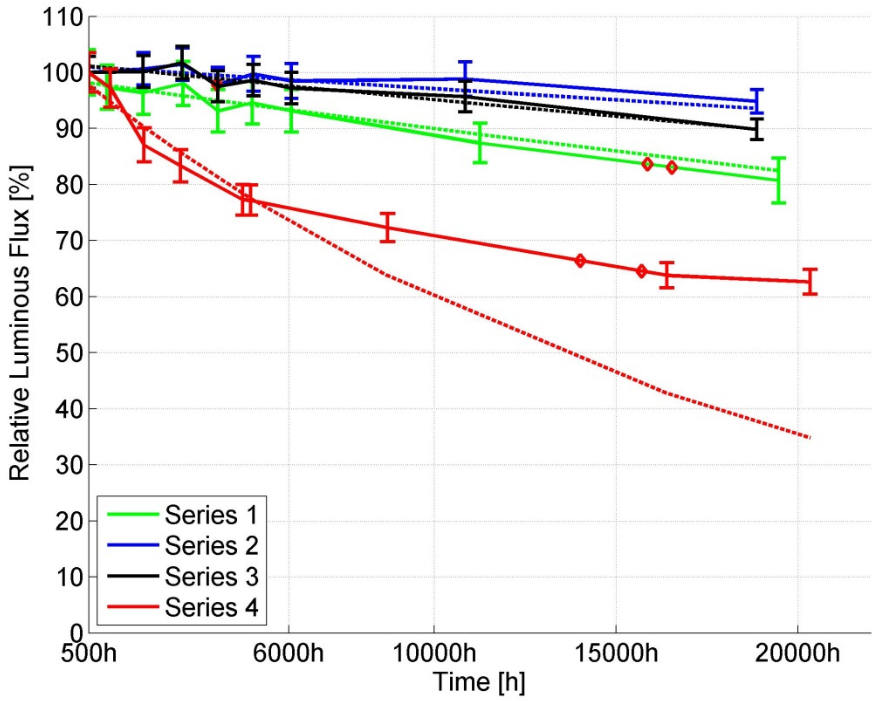

Figure 2 – comparison of normalized measured luminous flux vs time for 4 LEDs series, and exponential extrapolations (dashed lines) fitted to the measurements using 1000-6000 hours data to create the fit

The deviation between the luminous flux values obtained by the measurements and the extrapolation method, for the surviving LED sources, is seen in Figure 3. The predicted values are compared to the measured luminous flux values around 19000 hours. It is seen that the deviation for a small majority of the sources lies within 1-10 %, and only a minority lies above 40 %. This deviation could be decreased even further if data from test hours above 10000 hours is used in the extrapolation, especially the predication for series 4 would be improved.

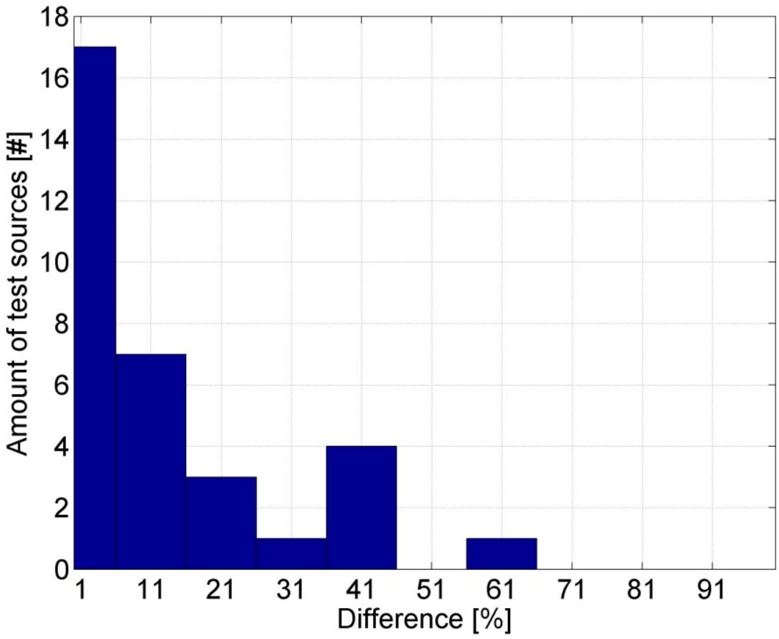

Figure 3 - Histogram showing the difference in %, between the extrapolated luminous flux values and the measured luminous flux values for the surviving sources around 19000 hours

3.3 Colour Maintenance

When looking at the colour maintenance for the LED lamps, a large change in the (x,y)-chromaticity coordinates is observed for a majority of the samples. The change in chromaticity is for some of the light sources, so large that the Duv becomes larger than 5.4 10^{-3}, indicating that reddish or greenish tint of the white light will be observable (Bieske & Schierz, 2010).
Figure 4 shows how the four series behaves as a function of time, where the purple circle is the starting point at 0 hours (when the light source is turned on for the first time), the circles around this point is the least noticeable difference circles, if the chromaticity change stays within the first of these, the change cannot be perceived by a normal human observer, if it goes into the second circle the change is perceivable (Bieske & Schierz, 2010).
It is seen that for series 2 and 3 the change in chromaticity is very small, meaning that the colour difference between the light at 19000 h compared with 0 hours for these series are very low, this is not the case for series 1 and 4, in which the chromaticity changes a lot. This observation is also in agreement with what can be seen when comparing Figure 4 and Figure 5 with Figure 1, the series that are most stable, with the least number of failed light sources, is also the ones that have the smallest change in the chromaticity. Interesting to note is that we see both increase and decrease in colour temperature for the series that are most unstable, when looking at Figure 5, there seems to be no connection between the colour temperature changes and the stability of the light sources.

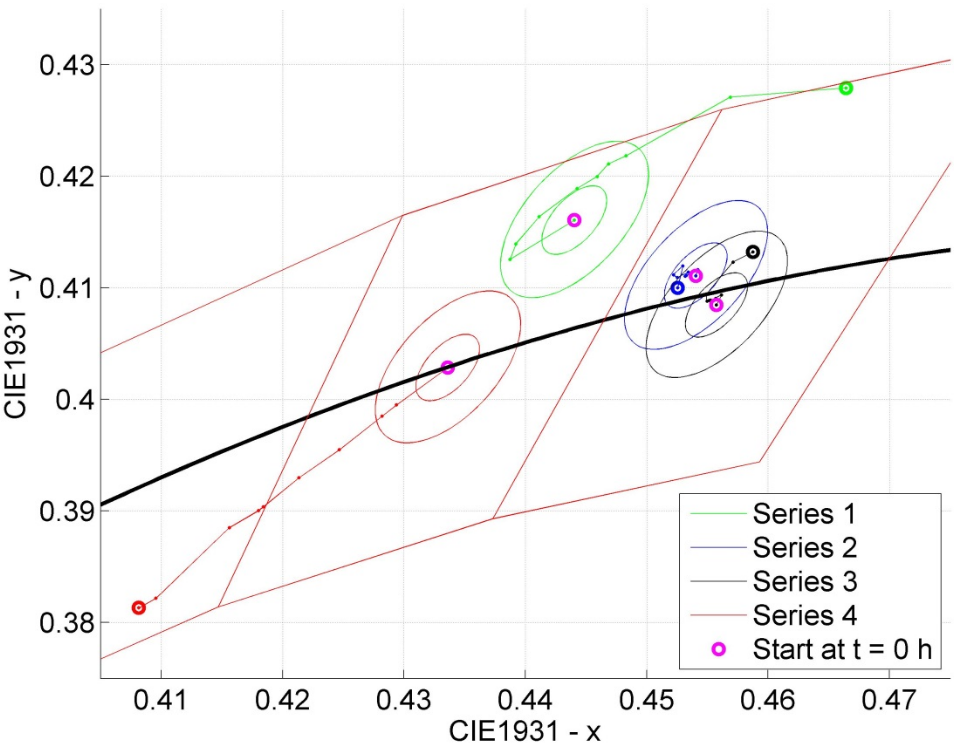

Figure 4 - Chromatic coordinates vs time for 4 LED series incl. just noticeable difference circles, the red quadrangular are the chromaticity standard quads from (ANSI, 2008), the solid black line is the planckian locus. The measurement end points, the coloured circles, are at 19000 hours.

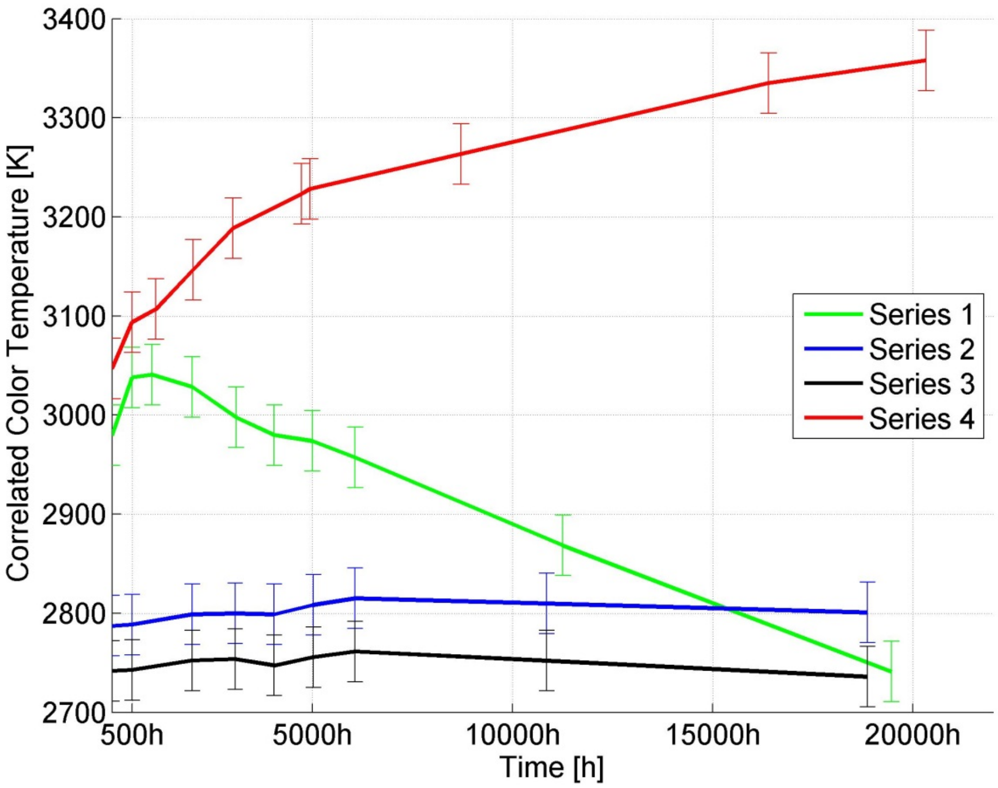

Figure 5 - The correlated colour temperature vs. time for the 4 lamp series

3.4 Critical Failures

Out of the 48 samples in the test, 13 samples showed catastrophic failures within the 19000 hours. In Figure 6 the failures have been grouped according to time, and it is seen that the majority of these failed after 10000 hours. 8 out of the 13 samples that failed were non-directional light sources, and the rest was directional, 8 of these were non-directionals and 5 came from the same series.

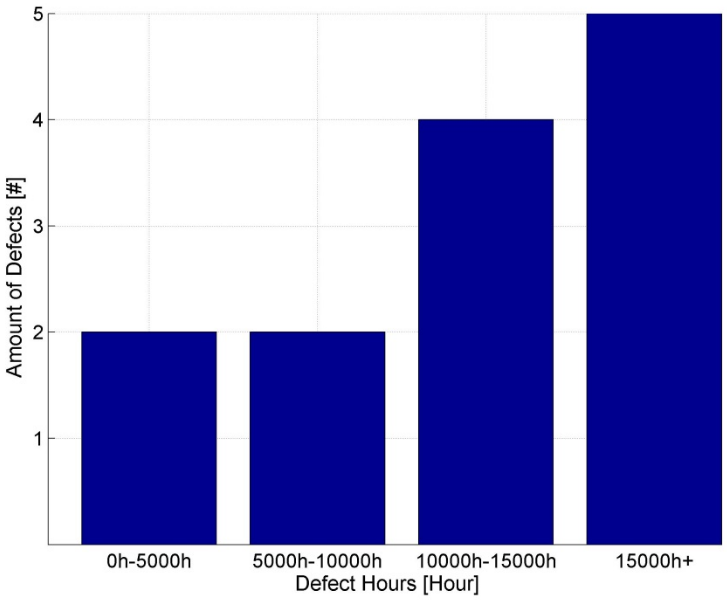

Figure 6 - The amount of failures vs time for all the 48 LED products used in the test

4 Conclusion

This research gives a valuable dataset for luminous flux and colour maintenance for operation up to 20000 h for a group of 23 types of integrated LED lamps, covering 12 V DC and 230 V AC, and both directional and non-directional lamps. A reasonably good agreement with the luminous flux measurements at 19000 hours and the extrapolated values were observed, for 17 of the lamps, the difference is within 10%. For the remaining 16 this was not the case. This indicates that using only the first 6000 hours of luminous flux data for the luminous flux prediction of the LED lamps would not work for all lamps. One solution would be to use more luminous flux time data to give a more accurate prediction. This would not safeguard against sudden failures though, there does not seem to be any relationship between the luminous flux behaviour for the products and when a product fails. One of the more stable series of products (if looking only at the first 6000 hours) measured in the project all failed between 9000 and 15000 hours. This makes it increasingly difficult to predict their lifetime by looking at the luminous flux behaviour alone. A total of 13 out of the 48 products used in this test have failed, by February 2014 the majority of these after 10000 hours, most of these non-directional lamps. However, it should be noted that we only measured 48 LED products and that the sample sizes for the eight series were minor (3-6), in order to give a more accurate description of the challenges with predicting the life time of LED products, the sample size should be large. The products tested in this project where developed from 2010 and 2011, so it is expected that better and improved LED products may have reached the marked by today.

Funding

The authors acknowledge the financial support for the project “LED lighting quality program” (PSO 342-035) by Elforsk under the Danish Energy Association.

Bibliography

ANSI. (2008). {ANSI NEMA ANSLG C78.377-2008}: Specifications for the Chromaticity of Solid State Lighting Products.

Bieske, K., & Schierz, C. (2010). Dynamic Lighting - Perception of lumunous colour variation. *Proceedings of CIE 2010 "Lighting Quality and Energy Efficiency"* (pp. 290-297). CIE.

ICE. (2009). *IEC/PAS 62612 Self-ballasted LED-lamps for general lighting services - Performance requirements.* International Electrotechnical Commission.

IES. (2011). TM-21-11 Projecting Long Term Lumen Maintenance of LED Light Sources. *TM-21-11 Projecting Long Term Lumen Maintenance of LED Light Sources*. IES.

OP54

MEASURING CHARACTERISTICS OF LEDS BY MONITORING TURN-ON TRANSIENT BEHAVIOURS

Yang, T.H.[*1], Tang, C.S.[1], Ding, T.J.[2], and Chou, H.Y.[1]
[1] Department of Optics and Photonics, National Central University, Chungli, CHINESE TAIPEI, [2] Department of Electro-Optical &Energy Engineering, Mingdao University, Pettow, CHINESE TAIPEI
thyang@dop.ncu.edu.tw

Abstract

By analysing the measurement data in detailed, the important characteristics including the luminous efficiency, the illumination chromaticities, the light decay, the thermal resistance, etc. can easily be found in a short time. Thus, an efficient method to evaluate the performance of LEDs is proposed and verified. Most of the essential characteristics of LEDs can be found by monitoring the turn-on transient behaviours.

Keywords: LEDs, luminous efficiency, junction temperature, electric current, forward voltage, transient behaviours, emission spectrum.

1 Motivation

Recently, more and more applications of light-emitting diodes (LEDs) technology are continuously increasing around our daily life, such as the vehicle headlamps (POHLMANN, 2007), the backlight module for the LCD panels (ANDREAS, 2004), and so on. Moreover, LEDs have promising potential to be the main light source for the general lighting in the future due to many advantages such as small size, energy saving, etc. (SCHUBERT, 2005). However, the quality of the products span to a very wide range. How to efficiently evaluate the quality of the LEDs products has become an urgent and practical subject. As being one of the most promising new light sources, the light-emitting diodes (LEDs) have been applied for many practical applications. The LED penetration to the common daily life is getting significant. LEDs actually take great advantages of power saving, vivid colours, tuneable lightness over other light sources. However, it is still of some mysteries in LEDs that how to reach the optimal balance among efficiently inputting electric energy, reducing the waste heat, and harvesting most of light. Considering of wide-spreading applications in smart lighting, it is getting urgent to well study the detailed lighting mechanism in LEDs.

Currently, most of the important characteristics of LEDs are difficult to measure in an efficient way. However, all the important characteristics are very crucial for evaluating the performance of LEDs. The measurements are often very time-consuming such as not acceptable to implement in the practical industrial mass-production. Most of the time is spent on approaching the status of the thermal equivalence. Those important characteristics are including the luminous efficiency, the illumination chromaticities, the light decay, the thermal resistance, and so on. The essential source of the complexity in measurement results from the dependence of the characteristics upon the driving electric current and the junction temperature of LEDs. In fact, during the transient stage after turning on, the optic, the thermal, and the electric properties are all dynamically involved in LEDs. Therefore, all the important characteristics can be identified and traced out via the monitoring on the transient behaviours of LEDs. An efficient method of evaluating the performance of LEDs can be proposed and applied to wide-spread applications.

2 Method

An integrated measuring system as shown in Figure 1 is established to collect necessary data for evaluating the performance of LEDs. By measuring all the optic, the thermal, the electric, and the chromatic performance in the same time with a high sampling rate during the transient stages, the essential characteristics of LEDs dynamically changing as the times goes are monitored. According to the conventional forward voltage method (Xi, 2004, CHHAJED, 2005, CHOU, 2008), the junction temperature, Tj, can be detected by measuring the instant electric forward voltage of the LED samples under the constant electric current driving.

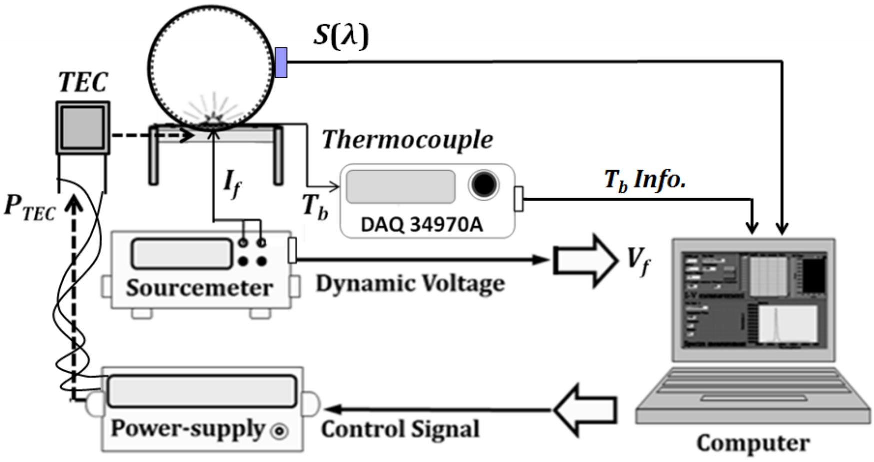

Figure 1 – Measurement system for collecting the optic properties of LED samples under different driving condirionts of various electric currents and diversed junction temperatures.

3 Results

Firstly, we measure the forward voltage of LEDs under the diverse driving condition of the controlled junction temperatures from 30 °C to 100 °C and the electric currents from 0.10 A to 1.00 A. With each fixed driving electric current I_f, the forward voltages of LEDs follow the linear relation to the junction temperature T_j as shown in the figure 2(a). It is easy to model the relation between the forward voltages and the junction temperatures in terms of the driving electric current as expressed in Eq. (1). With Eq. (1), it is convenient to monitor the instant junction temperature T_j simply by the electric driving current I_f and the voltage V_f.

$$\mathrm{T_j}(\mathrm{I_f},\mathrm{V_f})=\frac{\mathrm{V_f}-\left(b_{2T_j}\cdot \mathrm{I_f}^2+b_{1T_j}\cdot \mathrm{I_f}+b_{0T_j}\right)}{\left(m_{3T_j}\cdot \mathrm{I_f}^3+m_{2T_j}\cdot \mathrm{I_f}^2+m_{1T_j}\cdot \mathrm{I_f}+m_{0T_j}\right)} \quad (1)$$

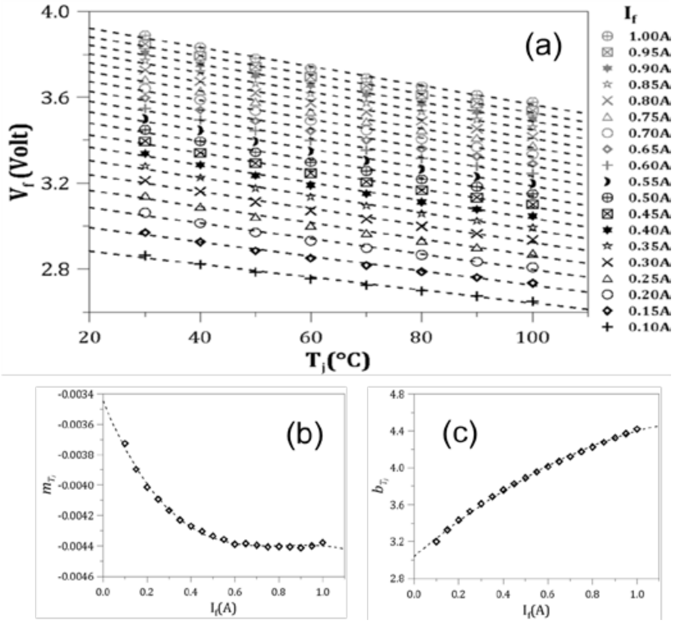

Figure 2 – (a) Linear relation between forward voltage and junction temperature with diversed electric driving current. (b) The slopes and (c) the intercepts of the linear relation in (a) versus the driving electric current.

Secondly, the turn-on transient behaviours of LEDs are monitored only the electric properties, and the thermal properties can be analysed. Figure 3 shows that the junction temperatures rapidly increase as the time goes, then quickly saturate at a fixed level. The output optic power Po decreases as the junction temperature increasing, too.

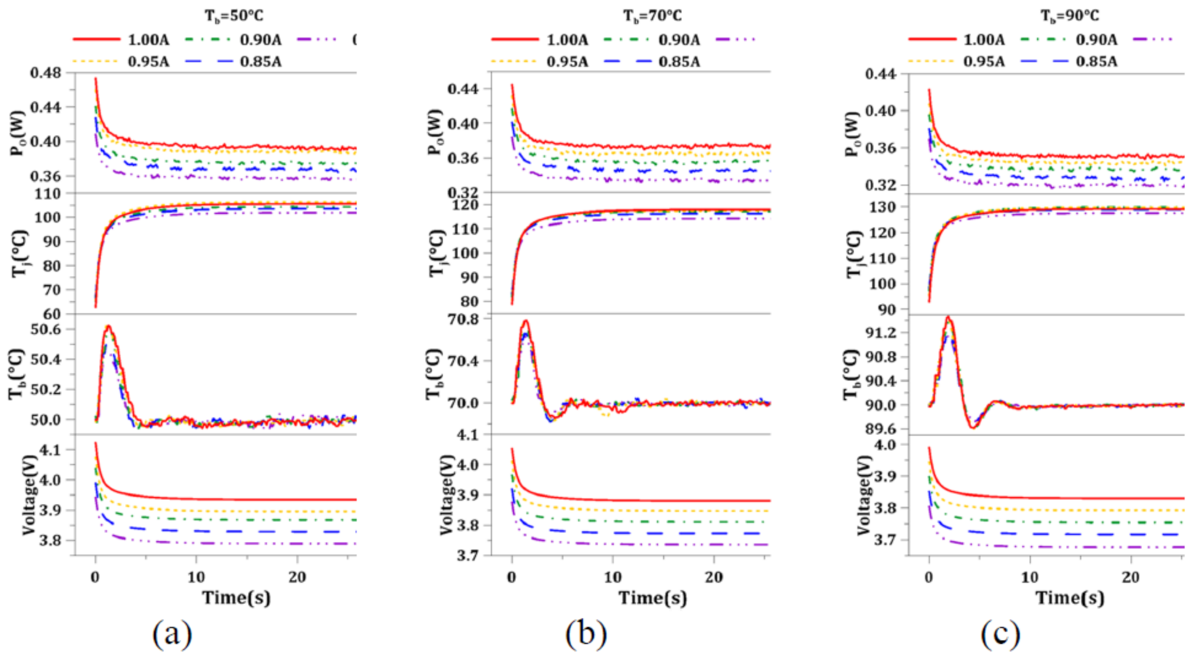

Figure 3 – All the turn-on transient behaviours of LEDs are analysed under various driving electric currents and different contrlled board temperatures of (a) 50 °C, (b) 70 °C, and (c) 90 °C.

Furthermore, the output optic behaviours of LEDs are identified as four featured characteristics by Eq. (2) and as shown in figure 4.

$$S(\lambda)=\frac{2A_0}{e^{\frac{-(\lambda-\lambda_C)}{B_L}}+e^{\frac{(\lambda-\lambda_C)}{B_R}}}, \quad (2)$$

where

A_0 is the peak optic power;

λ_c is the peak wavelength;

B_L is the left-half bandwidth;

B_R is the right-half bandwidth.

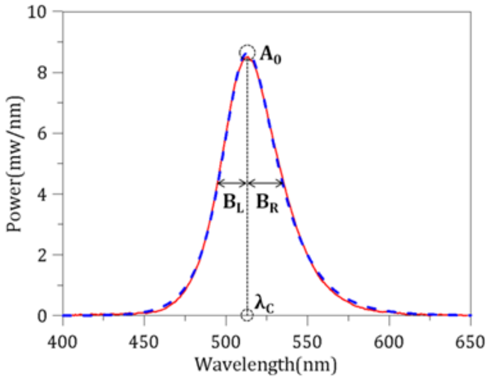

Figure 4 – A typical emission spectrum of colour LED. The optic emission spectrum can be featured by only four characteristics, A_0, λ_c, B_L, and B_R. The curve of the spectrum is convenient to be represented by Eq. (2).

With aid of Eq. (1) and (2), we can compared between the short term transient behaviours and the long term steady behaviours by few featured characteristics, i.e. A_0, λ_c, B_L, and B_R. Typical results of common cases are shown in Figure 5 as the time evolves.

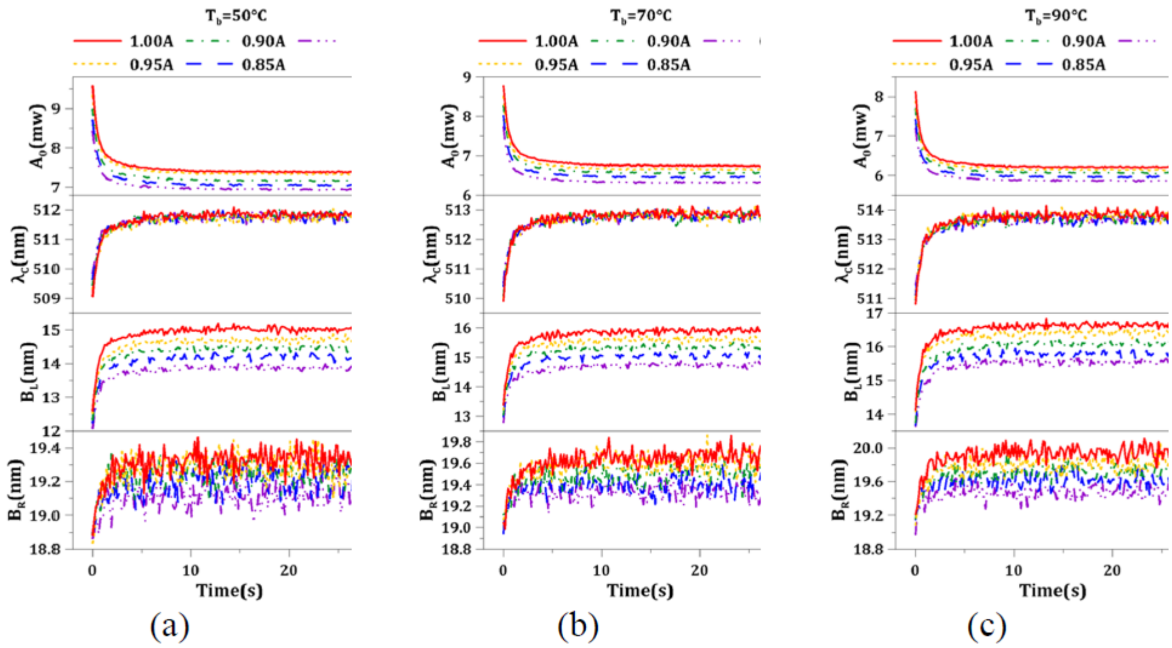

Figure 5 – The typical changes of A_0, λ_c, B_L, and B_R as time evolves. The LED chip board temperature is controlled at (a) 50 °C, (b) 70 °C, and (c) 90 °C.

As compared the turn-on transient behaviours to the long term steady behaviours, it is obviously concluded they all follow the same dynamics. Figure 6 presents the same dynamics in LEDs. Therefore, it strongly implies the fact that we can monitor the performance of LEDs simply by the turn-on transient behaviours. After analysing the measurement data in detailed, the important characteristics including the luminous efficiency, the illumination chromaticities, the light decay, the thermal resistance, and so on, can easily be found in a short time.

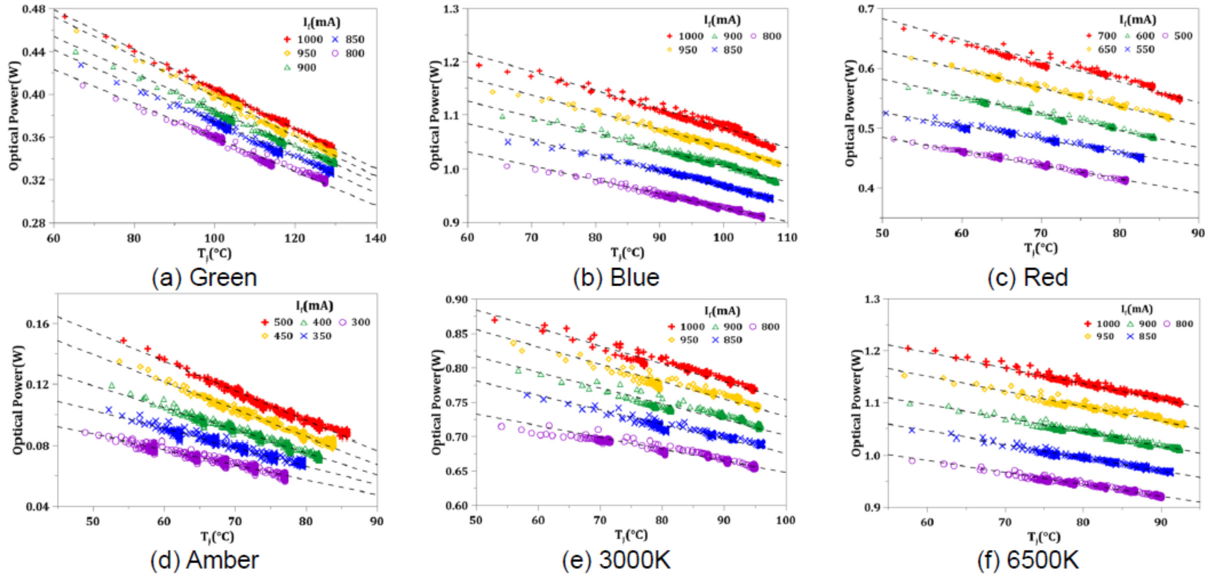

Figure 6 – The turn-on transient dynamics of LEDs are compared to the long therm steady behaviours for (a) green (b) blue (c) red (d) amber (e) warm white and (f) cool white LEDs. Under the same operation conditions, two dynamics follow the same tendency.

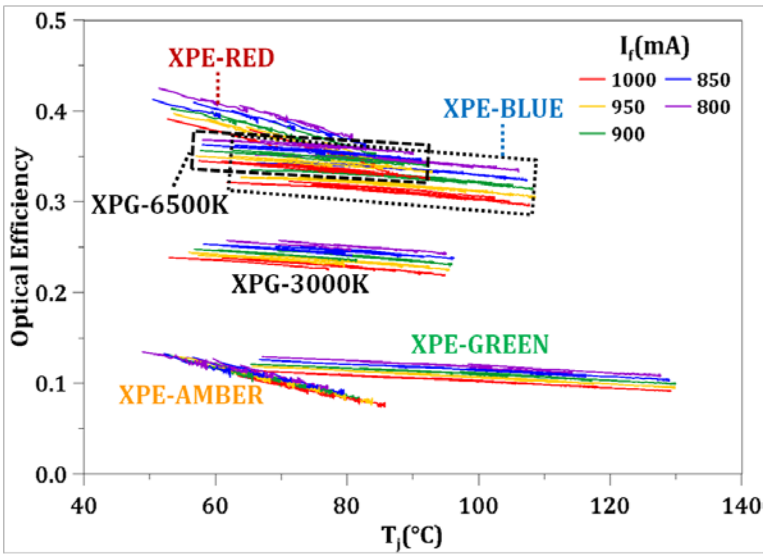

Figure 7 – Optical efficiency versus junction temperature with different driving electric currents for green (XPE-GREEN), blue (XPE-BLUE), red (XPE-RED), amber (XPE-AMBER), warm white (XPG-3000K), and cool white (XPG-6500K) LEDs. The data are collected from the turn-on transient stage and the long term steady stage of LED operations.

4 Conclusion

An efficient method to evaluate the performance of LEDs is proposed and verified. Most of the essential characteristics of LEDs can be found by monitoring the turn-on transient behaviours. As shown in figure 7, one of the important performance of LEDs, optical efficiency, can be easily mapped out as different driving conditions of various electric currents and junction temperature for diverse LEDs.

Acknowledgement

This study was partly sponsored by the National Science Council, Taiwan, under the grant numbers of NSC 102-3113-E-008-001, NSC101-2911-I-008 -501, NSC 101-2221-E-008-108, and NSC 102-2221-E-008 -066, , and Energy Technology Program for Academia, Bureau of Energy, Ministry of Economic Affairs 102-E0606.

References

POHLMANN, W. 2007. High Performance LED Lamps for the Automobile: Needs and Opportunities, Proc. SPIE 6797, 67970D.

ANDREAS, S. 2004. LEDs, New Light Sources for Display Backlighting, OSRAM OPTO Semiconductors.

SCHUBERT, E. F. 2005. Solid-State Light Sources Getting Smart, Science. 308, pp.1274-1278.

Xi, Y. 2004. Junction-Temperature Measurement in GaN Ultraviolet Light-Emitting Diodes Using Diode Forward Voltage Method, App. Phys. Lett. 85, 2163—2165.

CHHAJED, S. 2005. Junction Temperature in Light-Emitting Diodes Assessed By Different Methods, Proc. SPIE 5739, 16-24.

CHOU, H. Y. 2008. Dependence of Emission Spectra of LEDs upon Junction Temperature and Driving Current, J. Light & Vis. Env. 32(2), 133-136.

OP55

DEVELOPMENT OF 2π TOTAL SPECTRAL RADIANT FLUX STANDARDS AT NIST

Yuqin Zong[1] and Haiping Shen[2]
[1] National Institute of Standards and Technology, Gaithersburg, Maryland, USA
[2] Fudan University, Shanghai, CHINA
yuqin.zong@nist.gov

Abstract

We have developed a new, reflector lamp based 2π transfer standard for total spectral radiant flux (TSRF) scale in the spectral range from 360 nm to 1100 nm. Correlated colour temperature of the standard lamp is 3000 K. Spectral aging rate is ±0.3 % for 24 h operation time. The 2π standard lamp has a near Lambertian beam pattern. Relative expanded uncertainty (k=2) of the 2π standard lamp is between 1.3 % (in the visible region) and 2.9 % (in the ultraviolet region).

Keywords: 2π standard lamp, total spectral radiant flux, integrating sphere, spectroradiometer.

1 Introduction

Integrating spheres equipped with a spectroradiometer are commonly used for measurement of light emitting diodes (LEDs) and solid-state lighting (SSL) products for total spectral radiant flux to obtain photometric, radiometric, and colorimetric quantities. Such sphere-spectroradiometer measurement systems are typically calibrated against total spectral radiant flux standards. There are two types of measurement geometries: 4π and 2π. In a 4π geometry a light source is placed at the centre of a sphere. While in a 2π geometry the light source is mounted on a port of a sphere. Depending on the measurement geometry, a 4π or 2π total spectral radiant flux standard is required for calibration of such a sphere-spectroradiometer system.

A 4π total spectral radiant flux standard, based on a 75 W quartz tungsten halogen lamp, was developed in 1997 at NIST which covered the spectral range from 360 nm to 830 nm [1] and was extended to 300 nm to 1100 nm in 2011 with expanded uncertainties between 1 % to 3 % (k=2) depending on the wavelength range.

For measurement of 2π LEDs (such as high-power LEDs) and 2π SSL products a 2π geometry sphere is more convenient than a 4π geometry sphere. Hence 2π geometry spheres are preferred by calibration laboratories and recommended by many national and international standard testing documents. However, 2π total spectral radiant flux standards are not available from National Metrology Laboratories at present time. To address the urgent need we recently developed a compact 2π total spectral radiant flux standard based on a 20 W tungsten halogen reflector lamp. The 2π standard lamp covers the spectral range from 360 nm to 1100 nm.

2 Description of a 2π standard lamp for total spectral radiant flux

Similar to a 4π standard lamp, an ideal 2π transfer standard lamp for TSRF should have a smooth spectral power distribution, high correlated colour temperature (CCT) (>3000 K), low aging rate, high reproducibility, and good long term stability.

A 2π sphere is typically small (less than 0.5 m diameter typically), thus, a small, low wattage lamp is preferred as a 2π standard lamp. Several tungsten halogen reflector lamps have been evaluated to see if they are feasible to be used as 2π transfer standards. Currently we use a compact (37 mm diameter), 12 V, 20 W tungsten halogen aluminium reflector lamp as the 2π transfer standard. The nominal CCT of the reflector lamp is 3000 K and total luminous flux is 250 lm. The rated average life of the reflector lamp is 2000 h and it allows to be operated in any orientation. A custom lamp housing with a four-wire socket is designed for operating this standard lamp.

The ideal beam pattern for a 4π standard lamp is isotropic. In contrast, the ideal beam pattern for a 2π standard lamp is Lambertian. Unfortunately commercial tungsten halogen reflector lamps with a large beam angle are not available. Therefore, we replaced the window of the 20 W tungsten halogen aluminium reflector lamp with an optical diffuser to convert its narrow beam pattern to a near Lambertian beam pattern. A photograph of the modified tungsten halogen aluminium reflector lamp (the 2π TSRF transfer standard) and a lamp housing are shown in Figure 1.

Figure 1 – Photograph of the 2π TSRF transfer standard lamp and its lamp housing

Beam pattern of the 2π standard lamp is symmetric. Figure 2 shows a measured beam profile of the 2π standard lamp which is close to that of a Lambertian source.

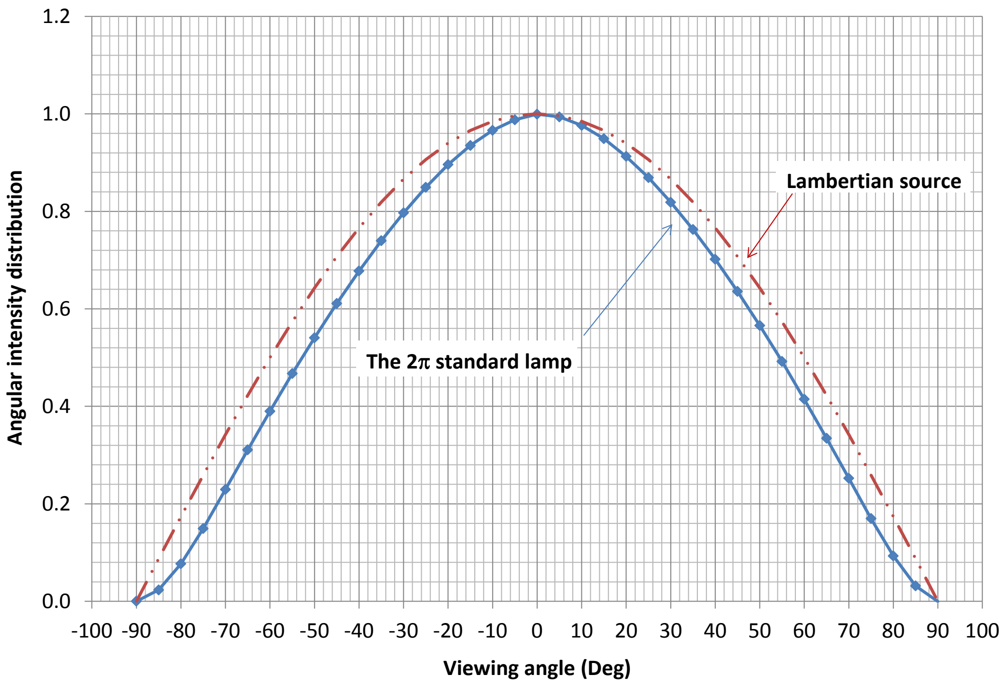

Figure 2 – Measured beam profile of the 2π standard lamp

Aging curves of spectral radiant intensity of the 2π standard lamp at four wavelengths of 430 nm, 555 nm, 720 nm, and 830 nm are shown in Figure 3. The starting points at t = 0 are set to be 1.000 for 430 nm, 1.005 for 555 nm, 1.010 for 720 nm, and 1.015 for 830 nm, so that the curves are not overlapped. The aging curve for CCT is shown in Figure 4. After an initial stabilization time (approximately 10 min) spectral radiant intensity changes slowly over time due to aging. Change of the spectral radiant intensity is within ±0.3 %, and the change of CCT is less than 2 K for 24 h operation.

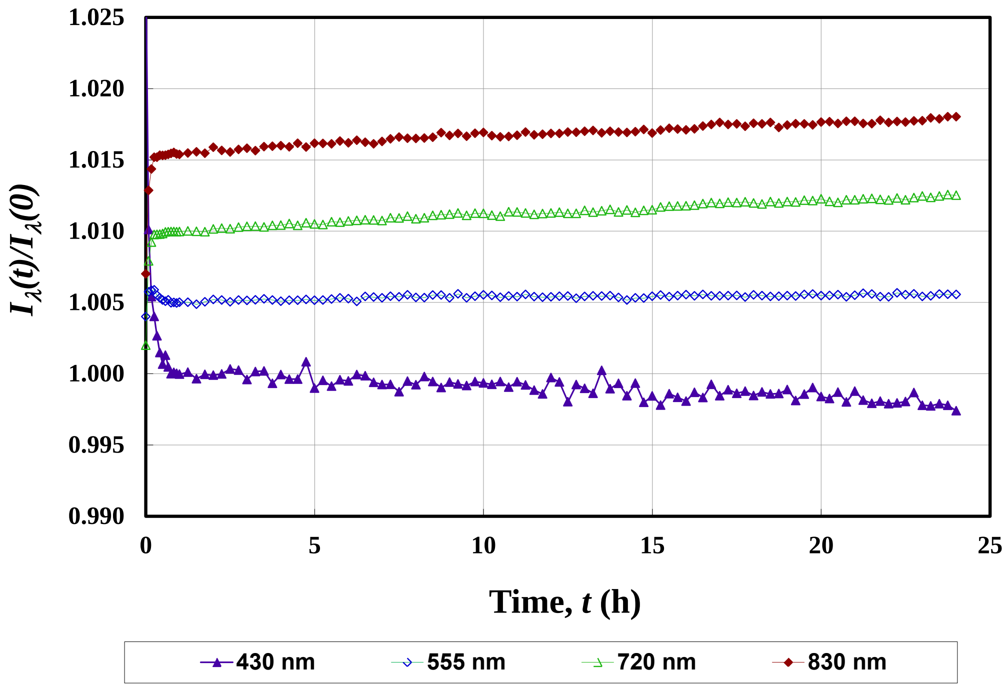

Figure 3 – Aging of spectral radiant intensity over 24 h operation time

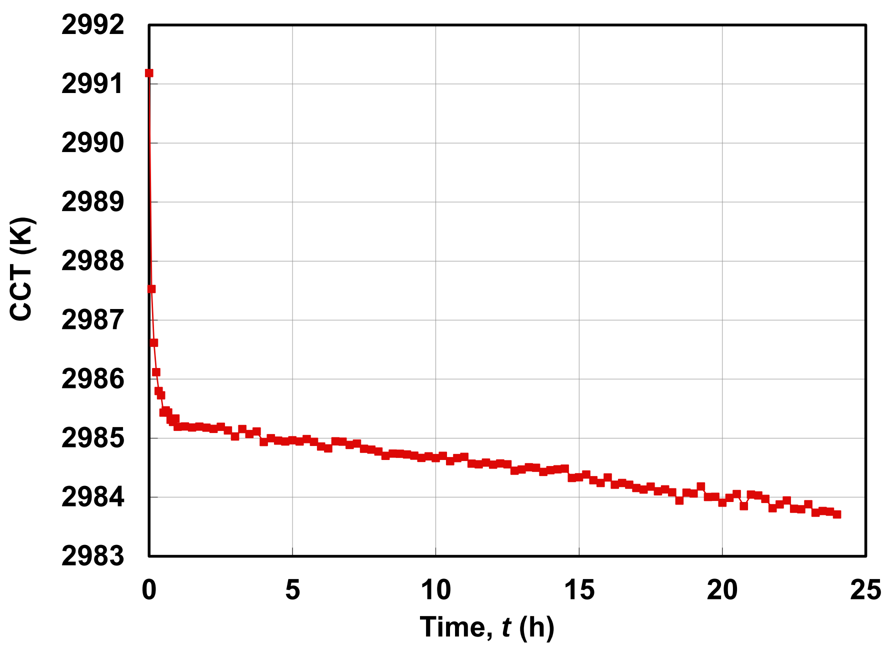

Figure 4 – Aging of CCT over 24 h operation time

3 Calibration of 2π TSRF standard lamps

A 2π TSRF standard lamp is calibrated using a way similar to that used for calibration of a 4π TSRF lamp. To determine the TSRF, a 2π standard lamp is first measured at many angles using a gonio-spectroradiometer for the relative spectral radiant intensity distribution, $I_{\lambda,\mathrm{rel}}(\lambda,\theta,\varphi)$. The scaling of $I_{\lambda,\mathrm{rel}}(\lambda,\theta,\varphi)$ is set arbitrarily, but is fixed during measurements of the lamp at every angle so that relative change of the lamp's intensity with different angles is measured accurately. After the measurements of $I_{\lambda,\mathrm{rel}}(\lambda,\theta,\varphi)$, the 2π TSRF standard lamp is then calibrated for total luminous flux, Φ_v , using the NIST 2.5 m absolute integrating sphere [2] to determine the scaling factor, k_scale. The TSRF, $\Phi_\lambda(\lambda)$, is obtained using Equations 1 and 2,

$$\Phi_\lambda(\lambda) = k_\mathrm{scale}\int_{\varphi=0}^{2\pi}\int_{\theta=0}^{\frac{\pi}{2}} I_{\lambda,\mathrm{rel}}(\lambda,\theta,\varphi)\sin\theta\,\mathrm{d}\theta\,\mathrm{d}\varphi\,, \tag{1}$$

$$k_\mathrm{scale} = \frac{\Phi_\mathrm{v}}{K_\mathrm{m}\int_{\lambda=0}^{\infty}V(\lambda)\int_{\varphi=0}^{2\pi}\int_{\theta=0}^{\frac{\pi}{2}} I_{\lambda,\mathrm{rel}}(\lambda,\theta,\varphi)\sin\theta\,\mathrm{d}\theta\,\mathrm{d}\varphi\,\mathrm{d}\lambda}\,, \tag{2}$$

where K_m (=683 lm/W) is the maximum spectral luminous efficacy, $V(\lambda)$ is the spectral luminous efficiency, and θ and φ are polar coordinates of the gonio-spectroradiometer. As indicated in the above two equations, the scaling of $I_{\lambda,\mathrm{rel}}(\lambda,\theta,\varphi)$ is cancelled, and the absolute scale of $\Phi_\lambda(\lambda)$ is determined by total luminous flux, Φ_v, making $\Phi_\lambda(\lambda)$ consistent with the NIST luminous flux scale. Thus, the TSRF scale realized at NIST is based on both the NIST spectral irradiance scale and NIST total luminous flux scale.

The gonio-spectroradiometer used for the calibration is shown in Figure 5. It is composed of a 3-axis scanning mechanism, a fast, cooled (-10° C), charge-coupled device (CCD) array spectroradiometer, and a motion control/data acquisition computer. The 3-axis scanning mechanism consists of a short arm for the lamp holder (used to set up the orientation of a standard lamp), a long arm for rotation of the irradiance head of the spectroradiometer around the θ axis, and a lamp holder which rotates around the φ axis. The dead angle of θ due to the mechanism of the lamp holder is ±3 degrees (that is, θ covers from 0 to 177 degrees). For measurement of 2π lamps the required scanning angle, θ, is only from 0 to 90 degrees, thus the dead angle does not cause any problem. Both scanning motors for θ and φ axes stop when an optical measurement takes place. The total measurement time for a 2π standard lamp is approximately one hour with a scanning angle interval of 5 degrees for θ and 10 degrees for φ.

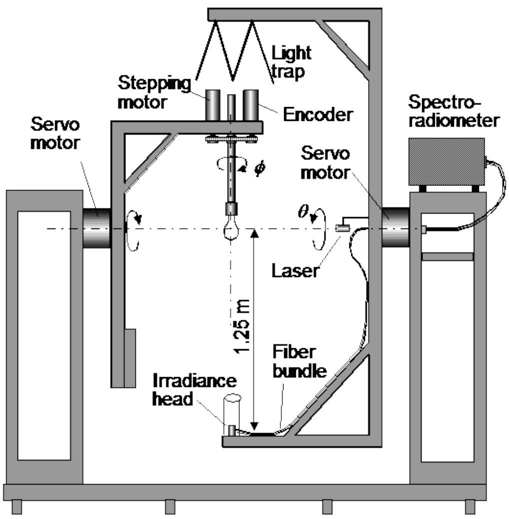

Figure 5 – Illustration of the NIST gonio-spectroradiometer

An irradiance head (a 15 mm diameter UV-VIS-NIR diffuser) is mounted on one end of the long arm (for θ) with a rotation radius of 1.25 m, and a light trap is mounted on the other end of the long arm. A hood is mounted on the irradiance head to minimize the errors arising from scattered ambient stray light. The irradiance head has an approximate cosine response within the field of view limited by the hood.

The CCD array spectroradiometer is placed on the fixed frame of the gonio-spectroradiometer. A 1.5 mm core diameter, 5 m long quartz fiber bundle is used to couple the rotating irradiance head to the stationary array spectroradiometer. The twisting effect of the fiber bundle on the responsivity of the spectroradiometer was tested to be less than 0.1 %. The spectroradiometer is calibrated against two FEL spectral irradiance standard lamps [3] when the long arm for the irradiance head is rotated to be horizontal (θ =90°).

The signal response nonlinearity of the spectroradiometer was characterized and corrected. In addition, the spectroradiometer was also characterized and corrected for errors from stray light using the stray-light correction matrix method [4]. The stray-light corrections are applied for all optical measurements including the standard FEL lamp measurements (for relative spectral irradiance responsivity calibration) and the 2π standard lamp measurements at every rotation angle. The correction for stray-light errors is critical for reducing the uncertainties in the UV region.

4 Uncertainty of 2π TSRF standard lamps

The uncertainty of a 2π TSRF standard lamp is analysed following the international recommendation [5] and is shown in Table 1.

Table 1 – Uncertainty budget for a 2π TSRF standard lamp

Component	Type	Standard uncertainty (%)							
		360 nm	380 nm	400 nm	450 nm	555 nm	750 nm	950 nm	1100 nm
Scaling factor, k_{scale}, i.e., total luminous flux of a standard lamp	B	0.25	0.25	0.25	0.25	0.25	0.25	0.25	0.25
Total uncertainty of the reference FEL lamps	B	0.54	0.51	0.48	0.43	0.35	0.27	0.22	0.19
Performance of the gonio-spectroradiometer	B	0.63	0.36	0.26	0.22	0.22	0.32	0.51	0.84
Calibration of the gonio-spectroradiometer	B	0.91	0.60	0.34	0.25	0.25	0.25	0.33	0.59
Measurement of a standard lamp	A	0.53	0.52	0.29	0.25	0.25	0.25	0.30	0.39
Reproducibility and long term stability of a standard lamp	A	0.50	0.35	0.30	0.25	0.25	0.25	0.30	0.40
Combined relative uncertainty (%)		1.46	1.10	0.81	0.69	0.65	0.65	0.81	1.21
Expanded relative uncertainty of total spectral radiant flux (%) (*k*=2)		**2.9**	**2.2**	**1.6**	**1.4**	**1.3**	**1.3**	**1.6**	**2.4**

5 Summary

We have extended the TSRF transfer standard lamps from 4π to 2π. The new 2π standard lamp is a near Lambertian source. It has a CCT of 3000 K and covers the spectral range from 360 nm to 1100 nm with the uncertainty from 1.3 % to 2.9 % depending on the wavelength region. The aging rate is ±0.3 % for 24 h operation time.

References

[1] ZONG, Y. and OHNO, Y. 2007. Realization of total spectral radiant flux scale and calibration service at NIST. CIE 26th Session – Beijing 2007, D2 179-182.

[2] OHNO, Y. and ZONG, Y. 1999. Detector-Based Integrating Sphere Photometry, Proc., 24th Session of the CIE, 1999, 1, Part 1, 155-160.

[3] YOON, H. W., GIBSON, C. E., and BARNES, P. Y. 2002. Realization of the National Institute of Standards and Technology detector-based spectral irradiance scale, Appl. Opt., 2002, 41, 5879-5890.

[4] ZONG, Y., BROWN, S. W., JOHNSON, B. C., LYKKE, K. R., and OHNO, Y. 2006. Simple spectral stray light correction method for array spectroradiometers, Appl. Opt., 2006, 45, 1111-1119.

[5] ISO 1993. Guide to the Expression of Uncertainty in Measurement.

OP57

GLARE EVALUATION OF OUTDOOR TENNIS COURT FLOODLIGHTING USING HIGH DYNAMIC RANGE PHOTOGRAPHY

Chung, T.M., Cheung, H.D., Ng, R.T.H., Chow, P.M.
Department of Building Services Engineering, The Hong Kong Polytechnic University, HONG KONG.
tm.chung@polyu.edu.hk

Abstract

This paper presents the glare rating measurement for an outdoor tennis court in The Hong Kong Polytechnic University using the high dynamic range (HDR) photography. This technology, which uses a consumer grade digital camera to obtain the luminance across the field at pixel level, allows precise and quick on-site measurement of parameters required by the CIE basic glare evaluation formula. Glare rating (GR) values which quantify the glare sensation due to floodlighting were obtained both by HDR photography and conventional measurement method using illuminance meter. The measurement results and data acquiring procedures of both methods are compared and discussed. Besides, subjective glare sensations were collected from 50 players via questionnaires.

Keywords: High Dynamic Range Photography, HDR, Glare Rating, Floodlighting, Tennis Court

1 Introduction

Not only should the floodlights in an outdoor tennis court provide adequate light level, appropriate light distribution and suitable colour rendering for players, match officials and spectators to have clear vision after dark, causing no visual discomfort or disability to persons inside the court is of the same importance in the lighting design. Particular attention should be paid to glare restriction in the lighting design of outdoor tennis courts.

Glare appears in the visual field when the luminance of the light sources is much above the average ambient luminance. It would produce adverse psychological effects to humans, such as impairing their vision of objects and/or causing discomfort. In terms of a sport ground, existence of glare could even affect the performance of the players and the judgement made by the match officials. As recommended by the SLL Lighting Handbook, the Glare Rating (GR) should be used to estimate the degree of glare for outdoor sports and area lighting. For an outdoor tennis court, it should not exceed 50 for Class I and Class II courts and 55 for Class III courts (SLL, 2009). The International Commission on Illumination (CIE) suggests using the basic glare evaluation formula which gives a GR value at a fixed observer position (CIE, 1994). The formula consists of the veiling luminance produced by the environment in front of the observer and veiling luminance produced by the light sources, whose equivalent value can be calculated from the illuminance on the observer’s eye produced by each individual light source. The measurement of these illuminance values involved the use a shade to enclose the light beam coming from a particular light source and eliminate any other light sources in the field of view. It demands preparation of the shade before conducting the measurement and on-site adjustment of the shade. As it is common to have more than one floodlights mounted on a light mast, it is very difficult and impractical to measure the illuminance contributed by each light source.

With the development of digital photography, the high dynamic range (HDR) technology can be employed to measure the photometric parameters required for GR evaluation. The HDR photography uses a single consumer grade digital camera, fitted with wide-angle lens simulating the human binocular vision and mounted on a tripod at the observer position in the tennis court, to obtain the luminance of light sources across the scene at pixel level at one time. With the information available in the site, such as the distance between the center of the light source and the observer’s eye, and the dimensions and the aiming angles of the light source, the per-pixel luminance of each light source obtained from the HDR photos can be converted to illuminance at the observer due to that small patch, in unit of pixel, of light.

The evaluation of glare sensation using the conventional method, which requires the use of a shade to enclose each light source, and the HDR photography method are demonstrated for an outdoor tennis court in The Hong Kong Polytechnic University. The measurement results and data acquiring procedures of both methods are compared and discussed. Besides, subjective glare sensations were collected from about 50 players via questionnaires. Using the HDR photography, the per-pixel luminance of each light source across the scene is obtained for acquiring the illuminance at the observer in a faster, more reliable and more efficient manner. This method could predict glare sensation and act as an alternative method for glare evaluation of outdoor tennis court lighting as well as other outdoor sports and area lighting.

2 Basic Glare Evaluation Formula

According to the CIE definitions, glare is defined as the condition of vision in which there is discomfort or a reduction in the ability to see details or objects, caused by an unsuitable distribution or range of luminance, or to extreme contrasts (CIE, 2011). It is usually classified into discomfort glare and disability glare. The former is the glare that causes discomfort without necessarily impairing the vision of objects. The latter is the glare that impairs the vision of objects without necessarily causing discomfort.

Disability glare depends mainly on the quantity of light falling on the eye and is relatively unaffected by the luminance of the source; whereas in the case of discomfort glare, source luminance is one of the major contributory factors. It is generally accepted that disability glare is caused by light scattered in the eye, forming a luminous veil over the retinal image of adjacent parts of the scene. The luminous veil over the retina can be described by a veiling luminance, which reduces the luminance contrasts of the image of the field of view on the retina and therefore causes the contrast of an object to fall below threshold so that the object is not seen, or the contrast to be reduced to near threshold so that the target object is difficult to be seen. The veiling luminance depends on the intensity and distance of the glare source which together determine the illuminance at the eye caused by the glare source, and the angle between the glare source and the line of sight.

As discomfort glare is a subjective sensation and there is no known cause for discomfort glare, it is not well understood as disability glare. Suggestions of causes for discomfort glare range from fluctuations in pupil size due to bright light source in field of view to distraction caused by glaring lights that attract the eye resulting in directing the gaze towards these disturbing lights and the stress on the extra-ocular (facial) muscle surrounding the eye. It is generally agreed that discomfort glare produced by an individual source depends on the source luminance, solid angle subtended by the source, angular displacement of the source and general field luminance controlling the adaptation level of the observer's eye. In many cases, disability and discomfort glare occur together. Disability glare and discomfort glare are two different effects or outcomes of the same stimulus pattern, namely a wide variation of luminance across the visual field.

Investigations on glare sensation in sport field lighting have shown that the veiling luminance produced by the luminaires (L_{vl}) and the veiling luminance produced by the environment (L_{ve}) correlate best with the glare assessments in outdoor sports and area lighting (Tekelenburg, 1982). Although these investigations were studies into the effect of discomfort glare, the correlating parameter L_{vl} has also been used for the description of disability glare and therefore the above two parameters (L_{vl} and L_{ve}) are used to describe the general glare within outdoor sports and area lighting by CIE. Based on these investigation results, CIE recommends that Glare Rating (GR), which can be calculated from L_{vl} and L_{ve}, should be used to quantify the glare directly from the luminaires of an outdoor lighting installation (CIE, 1994; CIE, 2005). The GR values may be different for each observer position and for each different viewing direction. For a given observer position and a given viewing direction, below eye level, the GR value can be evaluated using the basic glare evaluation formula which is expressed as follows:

$$GR = 27 + 24\log\frac{L_{vl}}{L_{ve}^{0,9}} \tag{1}$$

L_{vl} is the equivalent veiling luminance produced by the light from the luminaires which is directly incident on the eye. This equivalent veiling luminance (in cd/m^2) can be calculated by:

$$L_{vl} = 10\sum_{i=1}^{n}\frac{E_{eye-i}}{\theta_i^2} \tag{2}$$

where $E_{eye\text{-}i}$ is the illuminance (in lux) on the observer's eye, in a plane perpendicular to the line of sight, produced by the i^{th} light source; θ_i is the angle (in degrees) between the observer's line of sight and the direction of light incidence of the i^{th} light source on the eye (1,5° < θ_i < 60°); n is the total number of light sources. The value of $E_{eye\text{-}i}$ is the illuminance contributed from one light source. If it is possible to switch off all the other light sources, then $E_{eye\text{-}i}$ can be easily measured by an illuminance meter mounted on a tripod at the observer position aiming along the observer's line of sight (usually assumed to be 2° downward from the horizontal). However, it is usually not practical for an outdoor space, especially where the area is illuminated by some other lighting surrounding the site, like the street and road lighting which is impossible to be switched off. Therefore a shade is usually used along with the illuminance meter to enclose the light beam coming from each light source and eliminate any other light sources in the field of view. The shade should be either tailor-made or adjusted on-site for each light source. It should be noted that the actual veiling luminance, and therefore the glare sensation, experienced by any given observer is a function of a number of aspects of their eyes and thus is very variable between subjects. In general, the older the subject is the worse problems they are likely to have with glare. Equation (2) gives the amount of veiling luminance typically found for a subject with good eyesight in the age range from 20 to 30.

L_{ve} is the equivalent veiling luminance caused by light reflected towards the eye by the environment, such as the area in front of the observer. It can be calculated by equation similar to Equation (2) above by treating the environment as consisting of many light sources.

$$L_{ve} = 10\sum_{i=1}^{n}\frac{E_{eye-i}}{\theta_i^2} \tag{3}$$

The calculation of L_{ve} is a complex process involving breaking down the luminous field into a series of small elements, finding the illuminance that they cause at the eye of the observer and the angle between them and the direction of view, and calculating its value using Equation (3). It is even more difficult and impractical than the measurement of $E_{eye\text{-}i}$ for the calculation of L_{vl}. Therefore another simplified method for the calculation of L_{ve} is recommended by CIE. The following equation can be used when the background viewed by the observer is the area illuminated by the light sources.

$$L_{ve} = 0{,}035\frac{E_{h-av}\rho}{\pi} \tag{4}$$

where $E_{h\text{-}av}$ is the average horizontal area illuminance (in lux) and ρ is the reflectance of the area assuming diffuse reflection.

By using Equations (1) to (4) above, GR can be calculated for each observer position and each viewing direction. Observer positions can be located individually according to the use of the site, or placed along some calculation grids with maximum distance between points as recommended by international lighting codes (SLL, 2012). The viewing directions could be chosen individually for all observer positions or a fixed number of viewing directions could be selected assuming rotation in equal angular steps. By calculating the GR values for all observer positions and viewing directions, an average GR value can be used to evaluate the glare sensation experienced within the outdoor area lighting. It can be considered to have values between 0 and 100 with higher values indicating greater glare. For an outdoor tennis court, it should not exceed 50 for Class I and Class II courts and 55 for Class III courts (SLL, 2009).

3 High Dynamic Range photography

The evaluation of GR involves the measurement of $E_{eye\text{-}i}$ which is the illuminance on the observer's eye contributed from one of the light sources, excluding any other light sources in the field of view. The conventional method is to use an illuminance meter together with a shade to measure $E_{eye\text{-}i}$. The measurement has to be repeated for each light source and the aiming angle of the shade enclosing the illuminance meter also has to be adjusted correspondingly.

Another alternative method to measure $E_{eye\text{-}i}$ is available with the technology of High Dynamic Range (HDR) photography. It is a kind of techniques that allows a wide dynamic range of luminance between the darkest and the lightest area of a real scene to be recorded accurately in a single image. A series of low dynamic range photographs with different exposure settings is taken to capture a wide luminance variation of a scene and, using data fusion software, merged into a single HDR image with the luminance value of each pixel extended to over the luminance span of the human visual system (Inanici, 2006). With the advanced development of this technology, the luminance within the field of view could be obtained using a consumer grade digital camera with an ultra-wide angle lens in a quick and inexpensive manner.

In order to capture the darkest and lightest area of the scene, multiple photographs are taken with different exposure settings by changing either the aperture size or the shutter speed. There was no clear recommendation about the choices of aperture size of the camera. Previous researchers ever made use of small to large apertures (Anaokar, 2005; Debevec, 1997; Jacobs, 2007; Xiao, 2002). Besides, there is also no technical recommendation on the number of low dynamic range photographs for fusing into one HDR image. There was a side variation of this number, from 4 (Xiao, 2002) or 6 (Jacobs, 2007) to 11 (Debevec, 1997) or 14 (Inanici, 2006). In theory, the more photographs are fused into an HDR image, the wider dynamic range of luminance can be obtained and the HDR image can be of higher quality for more accurate luminance mapping.

For data fusion of ordinary photographs into an HDR image, a camera response function has to be applied. It is a curve that relates the amount of incoming light and the luminance values of the pixels in the image captured by the digital camera. By using computer software like Photosphere, hdrgen, Radiance and Photolux, this function can be computationally derived through self-calibration process from the series of low dynamic range photographs. The camera response function then gives corrections to the brightness value of the HDR image which is saved in RGBE image format. The luminance value of a pixel is then extracted from the measure of the Y component in the CIE 1931 XYZ colour space by converting the tristimulus values of that pixel from RGB to XYZ.

The HDR photography technology is now widely used for capturing the luminous environment of a space. This technique is promising for wide data collection within a short period time. Some of the researches utilizing this technology are studies about the discomfort glare sensation in a daylit interior space (Hirning 2014; Suk, 2013) and studies about luminance and illuminance mapping (Bellia, 2011; Bellia, 2013).

4 Methodology

This research involves calculations of Glare Ratings for different observer positions in an outdoor tennis court in The Hong Kong Polytechnic University using both the conventional method and HDR photography technology. The conventional method measure $E_{eye\text{-}i}$ by hand held illuminance meter, while the HDR method calculates $E_{eye\text{-}i}$ from the luminance values extracted from the HDR images. The measurement results and data acquiring procedures of both methods are compared and discussed. Besides, subjective glare sensations were collected from about 50 players via questionnaires.

4.1 Tennis Court

The sports ground being studied is located inside the campus of The Hong Kong Polytechnic University. It consists of two tennis courts with standard dimensions of 23,8m in length and 11,0m in width. The space between the two courts is 5,6m wide. Four 9m high light masts, which are installed 4,3m away from the court, are used to illuminate the whole area. Four 1500W metal halide floodlights are installed on each light mast. Figure 1 shows the layout of the sports ground. Glare Rating values at positions P1 to P8 in tennis court TN2 were studied. The viewing direction at these observer positions are shown by arrows in Figure 1.

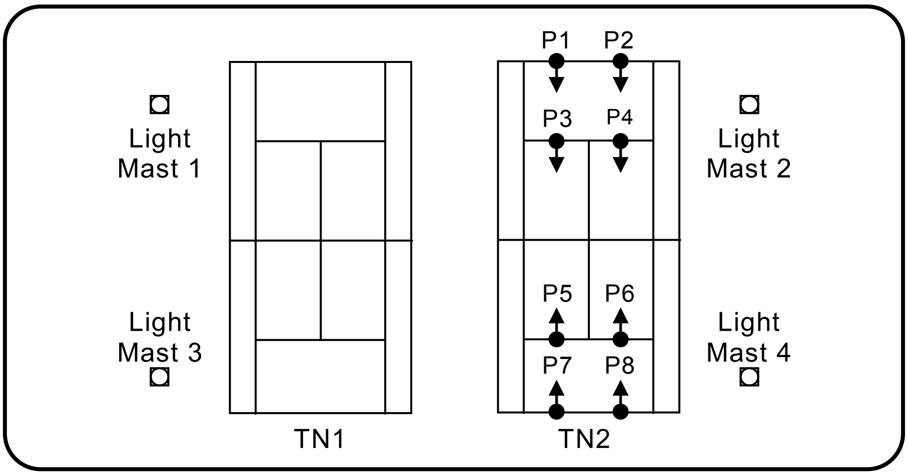

Figure 1 – Layout of the tennis court and the observer positions

4.2 Glare Rating Measurement by Conventional Method

Glare Rating values at observer positions P1 to P8 were evaluated using the conventional method. Theoretically the illuminance on the observer's eye, $E_{eye\text{-}i}$, should be measured individually for each lamp on the light masts using an illuminance meter, so that the illuminance measured is contributed from the light beam coming from that lamp only and any other light sources in the field of view are excluded. However, it is very difficult and impractical to use a shade to include the light beam coming from one lamp and maintain the illuminance meter aiming 2° downward from the horizontal along the observer's line of sight. Therefore, in order to proceed the measurement practically, it is assumed that the four lamps on each of the light mast were located close enough to each other and far away enough from the observer so that they could be treated as one light source. The value of $E_{eye\text{-}i}$ was then measured by the illuminance meter installed inside the shade which encloses the light beam from the four lamps on one light mast. The veiling luminance L_{vl} was then calculated by the equations modified from Equation (2).

For measurement points P1, P2, P3 and P4:

$$L_{vl} = 10\left(\frac{E_{eye-LM3}}{\theta_{LM3}{}^{2}} + \frac{E_{eye-LM4}}{\theta_{LM4}{}^{2}}\right) \tag{5}$$

For measurement points P5, P6, P7 and P8:

$$L_{vl} = 10\left(\frac{E_{eye-LM1}}{\theta_{LM1}{}^{2}} + \frac{E_{eye-LM2}}{\theta_{LM2}{}^{2}}\right) \tag{6}$$

$E_{eye\text{-}LMi}$ is the illuminance (in lux) on the observer's eye, in a plane perpendicular to the line of sight, produced by the light mast number i. θ_{LMi} is the angle (in degrees) between the observer's line of sight and the direction from the centre of the four lamps on the light mast number i to the observer's eye. Figure 2 explains the parameter for the calculation of L_{vl}.

For the veiling luminance produced by the environment (L_{ve}), it can be estimated using Equation (4). The average horizontal illuminance ($E_{h\text{-}av}$) of the tennis court TN2 was measured to be 588lx and the average reflectance of the area (ρ) was measured to be 0,16. After the calculation of L_{vl} and L_{ve} the value of GR can be evaluated by Equation (1).

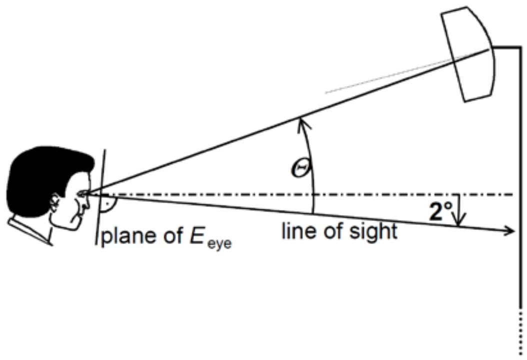

Figure 2 – Parameters for the calculation of L_{vl} (conventional method)

4.3 Glare Rating Measurement by HDR Photography

The veiling luminance L_{vl} was calculated from $E_{eye\text{-}i}$ using Equation (2) in the conventional method and $E_{eye\text{-}i}$ was directly measured by illuminance meter. An alternative method is suggested here for the calculation of $E_{eye\text{-}i}$ by the luminance of the light source from the observer's viewing angle. By assuming the light source to be perfectly diffusing, $E_{eye\text{-}i}$ can be estimated by the following equation:

$$E_{eye-i} = L_{HDR-i} \times \frac{A_i \cos\phi_i \cos\theta_i}{D_i} \tag{7}$$

where

L_{HDR-i}	is the luminance of the i^{th} light source extracted from HDR images (in cd/m^2);
A_i	is the illuminating surface area of the i^{th} light source (in m^2);
θ_i	is the angle between the observer's line of sight and the direction of light incidence of the i^{th} light source on the eye (in degrees);
ϕ_i	is the angle between the observer's line of sight and the aiming direction of the i^{th} light source (in degrees);
D_i	is the distance between the i^{th} light source and the observer's eye (in m).

The above parameters are explained in Figure 3. The magnitude of $L_{HDR\text{-}i}$ could be measured by a luminance meter provided that the acceptance angle of the meter is small enough to enclose the light source only. Otherwise, the average luminance of the light source as well as part of the background would be measured. Taking an example using typical professional luminance meter like the Konica Minolta LS-100, the acceptance angle is 1°. A light source with dimension of 0,6m should be measured with a maximum distance of 34,4m away from it. In this research, the values of $L_{HDR\text{-}i}$ were measured by utilizing the HDR photography technology.

A consumer grade digital single-lens reflex camera (Canon EOS 350D) fitted with ultra-wide angle lens (Sigma 10-20mm F4-5,6 EX DC HSM) was used. It was mounted on a tripod to keep optical properties consistent, maintain the image in alignment, eliminate noise disturbance and avoid possible camera shake throughout the sequential photograph taking. The lens' aperture and focal length were adjusted and kept constant before taking the photographs. The whole course of photograph taking was controlled by an external computer program called DSLR Remote Pro which altered the shutter speed for each photograph in the series. In this study, a total of 18 photographs in sequence of shutter speeds ranging from 1/4000s to 30s with step of 1 exposure value (EV) were taken for each observer's position P1 to P8. Figure 4 shows a set of photographs taken at one of the positions. It is noted that although altering either the aperture size or the shutter speed could vary the exposure values, the camera was set to aperture priority mode with a fixed aperture size so that exposure variations where achieved by varying shutter speed in automatic exposure bracketing mode, which was reported to be more reliable (Debevec, 1997; Mitsunaga, 1999).

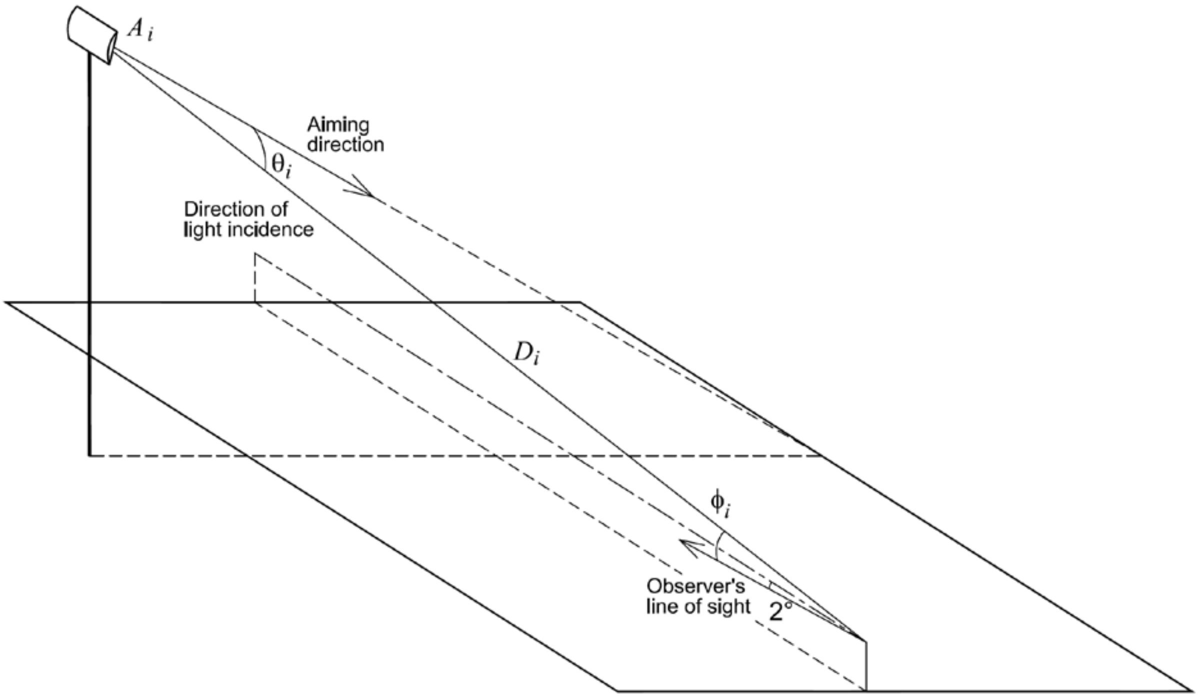

Figure 3 – Parameters for the calculation of L_{vl} (HDR method)

Figure 4 – The 18 low dynamic range photographs for position P1

For each observer position, an HDR image was generated by fusing the 18 photographs of multiple exposures and then the luminance values of pixels could be extracted from the HDR image. Calibration is required when converting the luminance values extracted from the HDR image to the real luminances within the scene. The X-Rite ColorChecker chart which consists of 24 standardized coloured and greyscale targets was used for the luminance calibration. A calibrated hand held luminance meter was used to perform the physical luminance measurement for each target of the ColorChecker chart, so that a calibration factor could be calculated. In this way, the veiling luminance L_{vl} and L_{ve} were then calculated using Equations (2) and (4), and GR value was found by Equation (1).

5 Results and Discussion

The GR values for observer's positions P1 to P8 were calculated by both the conventional and HDR methods. The results are summarised in Table 1. The GR values range from 12 to 28. As recommended by the same CIE standard, the GR numbers in the table are given without decimal fractions. The deviation of the GR values calculated by the HDR method from the corresponding values by the conventional method varies from -2 to +7. It shows that the HDR method overestimates the GR values for some of the observer's positions in this tennis court, provided that the conventional method gives the correct GR values. The average values of GR are 20 and 17 as calculated by the HDR method and the conventional method respectively. The GR values can be between 0 and 100 with higher values indicating greater glare. A GR value of 10 indicates a glare sensation of "unnoticeable", while 30 indicates "noticeable" as suggested by the CIE standard (CIE, 1994). As recommended by the SLL Lighting Handbook, for an outdoor tennis court GR should not exceed 50 for Class I and Class II courts and 55 for Class III courts (SLL, 2009). Therefore, the glare performance of this tennis court should be very satisfactory as predicted by calculation with measured illuminance and luminance by both conventional and HDR methods.

Table 1 – Calculated GR values

Observer position	HDR Method GR_{HDR}	Conventional Method GR_M	GR_{HDR} - GR_m
P1	12	13	-1
P2	17	16	+1
P3	20	18	+2
P4	18	17	+1
P5	28	22	+6
P6	15	17	-2
P7	24	18	+7
P8	22	15	+7
Average	20	17	+3

In order to compare the prediction by quantitative measurement and subjective sensation of glare performance, a questionnaire survey was conducted for users of this tennis court. A total of 50 completed questionnaires were collected. The age groups of the respondents include ≤20 (12%), 21-30 (26%), 31-40 (12%), 41-50 (22%) and >50 (28%). About half of them (42%) need to wear visual aid of contact lenses or spectacles. More than 75% of the subjects used the tennis court more than once a month. When they were asked to assess the lighting environment of the court, nearly half (48%) of them expressed that the overall brightness of the court is a "little too dim". Based on the lighting measurement in this study, the average horizontal illuminance on the ground level of the tennis court was found to be 588lx, while the recommended illuminance values are 500lx, 300lx and 200lx for Class I, II and III outdoor tennis court with reference to SLL Lighting Handbook. As for the comfort of the lighting environment, more than half (60%) expressed "neutral" for their sensation. When they were asked about the frequency of light offending their eyes, 54% selected "sometimes". 62% of the total number of respondents claimed that the direction of the offending light was from "above eye level". As for the glare level experienced by the players, 28%, 48% and 16% of them expressed the level to be "disturbing", "just admissible" and "noticeable" respectively. The rest of the subjects found the glare to be "intolerable" or "barely perceptible". Table 2 gives the summary of the questionnaire result in this study.

Table 2 – Questionnaire results

1. Overall brightness of the court:		2. Comfort of the lighting environment:		3. Awareness of light offending eyes:	
Too bright	0%	Very uncomfortable	4%	Very often	4%
A little too bright	4%	Uncomfortable	16%	Often	18%
Just right	38%	Neutral	60%	Sometimes	54%
A little too dim	48%	Comfortable	20%	Rarely	24%
Too dim	10%	Very comfortable	0%	Very rarely	0%
4. Direction of the offending light:		**5. Glare level experienced in the game:**			
Above eye level	62%	Intolerable	4%		
Near eye level	18%	Disturbing	28%		
Below eye level	10%	Just admissible	48%		
No offending light	10%	Noticeable	16%		
		Barely perceptible	4%		

From the questionnaire survey results, it seems that the glare performance of the floodlighting in this outdoor tennis court was not very satisfactory. Over 30% of the respondents claimed that the glare level to be "disturbing" and even "intolerable". It contradicts with the GR calculation that the average GR values were found to be 20 and 17 using the HDR and conventional methods respectively. A GR value of 10 represents the glare sensation of "unnoticeable", while a value of 30 represents "noticeable". According to the GR calculation, the glare sensation within this tennis court should be just noticeable. A rather large deviation was found between the glare sensation level predicted by quantitative assessment of GR values and the subjective glare sensation collected by questionnaire survey. It has been pointed out earlier in this paper that Equation (2) gives the amount of veiling luminance typically found with a subject with good eyesight in the age range from 20 to 30. In the questionnaire survey, about half of the respondents need to wear visual aid and only 26% fall into this age group. Therefore, the glare sensation predicted by GR values which rely on the calculation of L_{vl} by Equation (2) could result in certain error.

The inadequate prediction of glare sensation from GR values implies the possible deficiency of this quantitative glare assessment method. The accuracy of glare sensation prediction from GR values is not the focus of this study. However, the wide variation of glare sensation by the respondents and the considerable difference between the quantitative and subjective measurement of glare sensation may suggest that the HDR method used for GR calculation may still be workable. Although it overestimates the GR values for some of the observer's positions in this study, the amount of overestimation could be insignificant when it is compared to the possible error of predicting glare sensation from GR values. Besides, the HDR method offers an alternative to capture the luminance of all the glare sources in the visual field within a short period of time using consumer grade digital camera. This method is more practical compared to the conventional method which requires illuminance measurement at observer's eye separately for each light source using a shade to enclose the light beam coming from that light source eliminating any other light sources in the field of view.

6 Conclusion

The glare sensation due to floodlighting in an outdoor tennis court in The Hong Kong Polytechnic University was studied by Glare Rating values which were measured by both the conventional method as well as an alternative method utilizing the HDR photography technology. The HDR method obtains the luminance of light sources across the scene at pixel level at one time. It allows precise and efficient on-site measurement of parameters required for GR calculation by the CIE basic glare evaluation formula. The measurement results and data acquiring procedures of both methods were compared and discussed. In this study, the difference of Glare Rating values estimated by the HDR method and the conventional method varies from -2 to +7. It shows that the HDR method overestimates the Glare Rating values for some of the observer's positions in this tennis court. Further studies will be carried out to study the accuracy of predicting E_{eye} using HDR method by comparing with the illuminance measurement under a controlled lighting environment, so that E_{eye} due to each light source could be measured more accurately without using the shade. Besides, the feasibility of estimating the veiling luminance produced by the environment, L_{ve}, by using the HDR method will also be studied. The luminous field could be divided into a series of small elements and the illuminance due to each of the small element could be estimated from its luminance value, so that L_{ve} could be calculated by Equation (3).

Acknowledgements

This work was partially supported by the HKSAR Government Research Grants Council General Research Fund (Project Reference: PolyU 5150/10E).

References

ANAOKAR, S., MOECH, M. 2005. Validation of high dynamic range imaging to luminance measurement. Leukos, 2, 133-144.

BELLIA, L. SPADA, G., PEDACE, A. 2013. Lit environments quality: A software for the analysis of luminance maps obtained with the HDR imaging technique. Energy and Buildings, 67, 143-152.

BELLIA, L., MUSTO, M., SPADA, G. 2011. Illuminance measurements through HDR imaging photometry in scholastic environment. Energy and Buildings, 43, 2843-2849.

CIE 1994. CIE 112:1994. Glare Evaluation System for Use within Outdoor Sports and Area Lighting. Vienna: CIE.

CIE 2005. CIE S 015/E: 2005. Lighting for Outdoor Work Places. Vienna: CIE.

CIE 2011. CIE S 017/E: 2011. ILV: International Lighting Vocabulary. Vienna: CIE.

DEBEVEC, P.E., MALIK, J. 1997. Recovering high dynamic range radiance maps from photographs. Proceedings of 24th Annual Conference on Computer Graphics and Interactive Techniques, Los Angeles, CA, USA, 369-378.

HIRNING, M.B., ISOARDI, G.L., COWLING, I. 2014. Discomfort glare in open plan green buildings. Energy and Buildings, 70, 427-440.

INANICI, M.N. 2006. Evaluation of high dynamic range photography as a luminance data acquisition system. Lighting Research and Technology, 38, 123-136.

JACOBS, A. 2007. High dynamic range imaging and its application in building research. Advances in Building Energy Research, 1, 177-202.

MITSUNAGA, T., NAYAR, S.K. 1999. Radiometric self calibration. Proceedings of the IEEE Conference on Computer Vision and Pattern Recognition. Fort Collins, Colorado, USA, 374-380.

SLL 2009. The SLL Lighting Handbook. London: The Society of Light and Lighting.

SLL 2012. The SLL Code for Lighting. London: The Society of Light and Lighting.

SUK, J.Y., SCHILER, M., KENSEK, K. 2013. Development of new daylight glare analysis methodology using absolute glare factor and relative glare factor. Energy and Buildings, 64, 113-122.

TEKELENBURG, J. 1982. Evaluation of glare in sports-field lighting. International Lighting Review, 3, 68-71.

XIAO, F., DICARLO, J.M., CATRYSSE, P.B., WANDELL, B.A. 2002. High dynamic range imaging of natural scenes. Proceedings of Tenth Colour Imaging Conference: Colour Science and Engineering Systems, Technologies, and Applications. Scottsdale, Arizona, USA. 337-342.

OP59

A SENSE OF WASTE: LIGHT URBAN DESIGN TACTICS

- A Qualitative Approach to Outdoor Urban Public Space - OUPS! - Lighting Design –

José Nuno Sampaio
KTH, Stockholm, SWEDEN
jnpdsf@kth.se

Supervision: Peta Sjölander (KTH), Bosse Westerlund (Konstfack)

Abstract

Taking a post-humanistic perspective, here presented an approximation between Lighting Design and Urban Design through tactical manoeuvres proposing qualitative Design principles. These tactics support appropriate quality urban lighting to help mitigate Light Pollution.

From a Lighting Design and pedestrian perspective, which cannot be addressed by lighting motorized traffic (CIE, 2010), this paper ambition is to establish a constructive dialogue between designers and those involved with urbanity. Everyday specialists such as citizens, astronomers, biologists, engineers and other organized Dark Sky defenders are considered. Reaching the lighting industry and general public, the qualities of the city by night and the reduction of waste may be discussed.

A qualitative approach to public space lighting detects that no form of lighting pollution has a simple explanation. Pollution as a consequence of human activity seems to result from the fragile intersection between many driving forces, mostly human driven, strongly rooted on the economic and ecological side of urban life.

Keywords: Design, Quality, Senses, Urban, Dark-Sky

1 Introduction

People reflect about light as much as fish reflect about water. (Sampaio, 2013a) The human being is progressively becoming an *urban-being* and the future of the species seems to increasingly depend on potentials of sustainable cities, their extension, flexibility and mutability. Inner city per capita levels show better results on energy use, waste management and CO2 emissions (EC, 2009)

As an introduction to a qualitative approach to lighting, tactical manoeuvres are proposed as the case-studies under a research lens “Light Urban Senses”, first introduced at CIE 27 session South Africa in 2011 as a poster and now developed:

- LED technology in a test installation: Analysis international cooperation
- Lighting Design meets Urban Design: International Competition
- Starlight Foundation : Quality Lighting and Light Pollution mitigation through design criteria

1.1 Energy waste and Light Pollution

From the Design perspective, referring to a *SENSE OF DARKNESS* (Sampaio, 2013b), a proposal for a Light Pollution definition:

" That amount of lighting that, by waste or bad design, does not contribute in any way positively to human night-time activities." (Sampaio, 2011)

Under this light and in respect to one of the oldest sciences in human time: Astronomy, means that artificial lighting that positively contributes to human night-time activities at the same time not emitting light upwards, is not to be considered a pollutant by itself.

1.2 Field Studies over three outdoor lighting diametric extremes

Empirical Observations, ethnographical studies inscribed at the Grounded Theory. (Bowen, 2006) (Glaser,1978)

A - Shanghai, People’s Republic of China - One Landmark of the Night

Resulting of an invitation from Aalto University Design Factory based in Shanghai, China, a lighting design workshop was launched and produced. The work visit allowed the analysis of the *nightscape* of one of the fastest growing metropolis on Earth in 2011.

B - San Pedro de Atacama, Republic of Chile - The Fundamental Darkness

Part of field-studies in order to ethnographically experience the lighting optimal conditions and their absence, San Pedro de Atacama was analysed. The international ALMA project is located in this region, considered one of the driest and more remote locations on the planet, this is one of the best places on Earth to do astronomical science in 2012.

C - Brasilia, Republic of Brazil - The planning of the Modern City

Part of field-studies in order to ethnographically experience the lighting optimal conditions and their absence, Brasilia was analysed. Still a question to be answered: have we ever been modern or are we still living modern? From a pedestrian perspective and what is it like to be one, and just be, walk, move, sit, linger in the landmark city of Brasilia. Built from scratch in the late 1950's and inaugurated in 1960, Brasilia became a symbol of an era and, actually, the city exists during nigh time but rarely referred until 2012.

These empirical observations allowed the confirmation that *A Sense of Darkness* (Sampaio, 2013) has a cultural dimension which Urban Planning Modernity (Modernism or the International Style) has not taken into account when neglected the pedestrian.

2 Cases of study

Taking the perspective of the Pedestrian, a “Light Pedestrian”, the technical report *“CIE 115:2010 - Lighting of Roads for Motor and Pedestrian Traffic”* (CIE, 2010) is perceived as the initial platform for the following cases of study analysis.

2.1 LED Project Art installation “Amber Drops” - Gdansk, Poland

Project LED Light in Public Space (2010-2012)

How successful case in use of LED technologies in people’s public adoption?

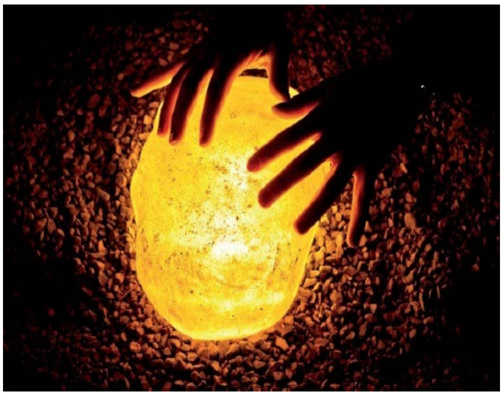

Figure 1: Image from project "Amber Drops", Gdansk, Poland

Post-occupancy evaluation of the site installation accomplished with the local partners, lead us to conclude (Sampaio,2011a):

*1 - Sense of **Direction*** *- Notion of **Mobility***

The *Pedestrian Path Network* (PPN) in the city of Gdansk gains a new route: a previously avoided urban space has been transformed in an activated public place. People now use the new installation area.

*2 - Sense of **Scale*** *- Notion of **Proportionality***

The site specific conditions have adapted best to the human scale which relates to the floor elements and the sitting benches. The heavy viaduct over the installation area has lost oppressive influence.

*3 - Sense of **Play*** *- Notion of **Reality***

The tactile light elements placed in the sand invite the touch and trigger curiosity. Working as a metaphor, the *amber drops* refer to a symbolic representation of such a local / regional character, suggesting poetry on site.

*4 - Sense of **Participation*** *- Notion of **Identity***

The international competition where the project results from invites the community in a certain voluntary engagement for submitting a proposal, especially evident in a work based on a local character reference.

*5 - Sense of **Value*** *- Notion of **Responsibility***

Art interventions implemented in public space under these premises seem to be well received by the local citizens who manifest their approval. Their interest shows a greater commitment with the shared place.

2.2 Nordic Urban Lighting Design Competition - Stavanger, Norway

"Light Urban Senses" (Sampaio, 2011a) criteria combined with Urban Design.

How two different design communities join to successfully design urban space?

The 2011 two awarded entries for relating Urban Design disciplinary main driving forces (or pillars) and outdoor Lighting Design guide-lines: "Light a Life" and "Staging Urban Space"

Figure 2: Entry Awarded 2nd Place, titled: "Light a Life"- First slide

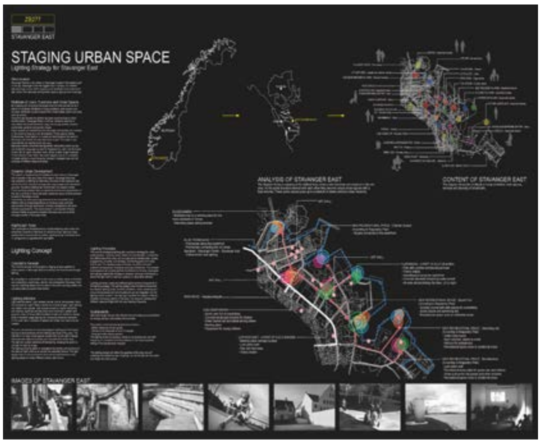

Figure 3: Entry Awarded 3rd Place, titled: "Staging Urban Space"- First Slide

The awarded entries successfully related the Urban Design driving forces (left) with the proposed Lighting Design proposed guide-lines (right). Security and safety have been included due to the topic sensitivity at present time even if, as previously mentioned, the discussion does not follow this as main concern but ambitions at going much beyond (Sampaio et al,2011):

PERMEABILITY	*1 - Sense of Direction*	*- Notion of Mobility*
LEGIBILITY	*2 - Sense of Scale*	*- Notion of Proportionality*
MOOD MANAGEMENT	*3 - Sense of Play*	*- Notion of Reality*
READABLE EDGES	*4 - Sense of Participation*	*- Notion of Identity*
INFRASTRUCTURE	*5 - Sense of Value*	*- Notion of Responsibility*
ACCESSIBILITY	*0 - Sense of Security*	*- Notion of Safe Use*

Both entries developed taking these *Light Urban Senses* as main driver and show evidences of producing meaningful results when relating them with Urban Design disciplinary pillars. (Sampaio et al, 2011))

These two competition awarded entries and the level they exhibit clearly indicate it is possible to design lighting for *OUPS*! (Outdoor Urban Public Space) taking into consideration the Five *Light Urban Senses* we have initially proposed, and that these are enough pertinent to produce lower light levels.

2.3 Alqueva Dark Sky - Alqueva, Portugal : The Mediator Design Concept

Starlight Foundation, “Dark Sky Alqueva”, and the criteria for a IDA Reserve.

How lighting technology meets economy through tourism and astronomy?

Figure 4: Alqueva Starlight Reserve – Municipality Reguengos de Monsaraz, Alentejo, Portugal

The “Dark Sky Alqueva” is the first ever “Starlight Tourist Destination” implemented in the world. This certification is awarded by the Starlight Foundation and supported by UNESCO and UNWTO. This winning candidate differentiated itself due to the over-arching list of cultural attractions, including the largest concentration of Megalithic monuments, well-known by their astronomically influenced orientation.

This Dark-Sky Reserve comprises six different urban municipalities, and many more stake-holders, and is currently in the process of application for IDA certification (International Dark-Sky Association) being the research activity this adequate adaptation of the existing lighting conditions to the dark-sky criteria.

This research cooperation in the process involves the process and methodology for an extensive “Lighting Inventory and Guide-lines” and deals closely with Lighting Technologies, process which will be examined through the “Light Urban Senses” scope, an early result of this research project once again put to test. The Mediator Design concept rises from the role the designer assumed as a mediator between apparently contrasting interests. When effectively mediated all interests tend to be possible in the same direction: quality of lighting.

The inventory and strategic guide-lines contemplate (1) – General Lighting – Public, (2) – Scenic Lighting – Decorative and (3) – Commercial Lighting – Private. This document is submitted to Regional Development Coordination Commission.

The European Commission has highlighted this project including it at the report “Enhancing the Competitiveness of Tourism in the EU - An Evaluation Approach to Establishing 20 Cases of Innovation and Good Practice”. Taking into account “Tourism” is the largest service industry in the planet this distinction should not be underestimated as the Lighting industry future fate may depend on the shift from a “product industry” towards becoming a “service industry”.

“*The Astrotourism Society*” has been founded and further research on urban lighting to follow the Mediator concept, put to practice in field-studies on a global scale.

3 Conclusions

A SENSE OF WASTE represents an understanding of the potential value of building trust on darkness. There is an economic and ecological potential on cooperation with Dark Sky organizations, which are receptive for lighting design.

Energy efficiency and an effective reduction of a sense of insecurity may result from addressing other priorities such as the “Light Urban Senses” guidelines.

Tactics is clearly knowing what to do when there is something to be done (Lovejoy, 2008), out of the jurisdiction of the designer, who tactically finds collaborations in order to test design concepts and principles. Outdoor lighting for public places in the urbanity is found a *transdiciplinary* issue.

Cooperation highlights the role of the designer as a MEDIATOR defining the criteria for quality, revealed possible to design using the guidelines “Light Urban Design Senses” and Urban Design complementarity.

European Commission “Precautionary Principle” (EC, 2011) could be considered when lighting outdoor urban areas, especially when “accelerating the deployment of” LED lighting lacks arguments on health issues.

Field studies based on Qualitative Research and Grounded Theory are fundamental to understand how people may identify themselves with diametric opposed lighting conditions.

Outdoor Urban Lighting Design approaching tourism has an ecological and economic impact and instead of considering “conflict zones” (CIE, 2010)) the areas where pedestrians meet motorized traffic; these should be regarded as opportunity areas both for design and the future of the lighting industry.

References

BOWEN, G. A. . (2006). Grounded Theory and Sensitizing Concepts. *International Journal of Qualitative Methods*. 5 (3), 12-23.

CIE (2010). CIE 115:2010 - Lighting of Roads for Motor and Pedestrian Traffic. *Technical Report*. 2nd Edition (9), p15-16-17.

EC EUROPEAN COMMISSION. (2009). *Sustainable and responsible business.* Available: http://ec.europa.eu/enterprise/policies/sustainable-business/documents/eco-design/legislation/framework-directive/index_en.htm. Last accessed 18th February 2013.

EC EUROPEAN COMMISSION. (2011) *Communication on “Precautionary Principle”*. Available at: http://europa.eu/legislation_summaries/consumers/consumer_safety/l32042_en.htm. Last accessed 15th February 2013.

GLASER, B. G. (1978). *Theoretical sensitivity: Advances in the methodology of grounded theory.* Mill Valley, CA: Sociology Press.

LOVEJOY, D. (2008). *Moral victories: the story of Savielly Tartakower*. London: Mullumbimby, N.S.W. : Echo Publications. 123.

SAMPAIO, J.N.. (2011a). “LIGHT URBAN DESIGN STRATEGIES: THE CITIES' USERS AND URBAN SENSES -- A QUALITATIVE APPROACH TO OUTDOOR URBAN PUBLIC SPACE LIGHTING": *Proceedings of the twenty seventh (27th) Session of the CIE South Africa 2011 International conference,* Sun City, pp.1201-1207.

SAMPAIO, JN. (2011). *The Light Pollution: Definitions.* Available: http://www.idaquebec.org/en/la-pollution-lumineuse/definitions/. Last accessed 15th February 2013.

SAMPAIO, J.N.; IVERSEN, Håkon. (2011). *Nordic Urban Light Design Competition 2011 – The Manual.* Available: http://nordicurbanlightdesign.org/. Last accessed 07th February 2013.

SAMPAIO, J.N.. (2013a). *Lighting/ Space Design - Thursday, July 04, 2013.* Available: http://znunosampaio.blogspot.pt/2013/07/blog-post.html. Last accessed 20th September 2013.

SAMPAIO, J.N.. (2013b). SENSE OF DARKNESS. *ALAN2013 - First International Conference on Artificial Light at Night - Conference Proceedings*. 43

SAMPAIO, J.N.. (2013). Light Urban Design Tactics: The Cities' Users and Urban Senses. *10th European Academy of Design Conference - Crafting the Future*. 2 (Track 2), 46-47.

Photographic Credits References: *Figure 1: Laznia Centre for Contemporary Art, Gdansk; Figure sequence 2-3: NUDA Nordic Urban Design Association; Figure sequence 4: Alqueva Dark Sky reserve.*

OP60

ECO-GREENERGY WIND-SOLAR HYBRID RENEWABLE ENERGY LIGHTING AND CHARGING SYSTEM

W. T. Chong[1], W.K. Muzammil[1,2], A. Fazlizan[1], H. Taheri[1], M. Gwani[1], S.C. Poh[1]
[1]Department of Mechanical Engineering, University of Malaya,
50603 Kuala Lumpur, MALAYSIA
[2]School of Engineering and Information Technology, University Malaysia Sabah,
88400 Kota Kinabalu, Sabah, MALAYSIA
chong_wentong@um.edu.my (W.T. Chong)

Abstract

An innovative outdoor lighting and charging system powered by a shroud-augmented vertical-axis-wind-turbine (VAWT) and solar photovoltaic (PV) panel is disclosed. It combines a hybrid renewable energy generation system, energy-saving lighting (LED) and rain water collector. The novel omni-direction-guide-vane (ODGV) is designed to surround the VAWT for wind power augmentation. It is used to guide incoming airflow and creates a venturi effect to increase the wind speed before the wind-stream interacts with the wind turbine blades. The ODGV improves the starting behaviour of the VAWT, and is able to augment the wind energy by 3,48 times. The solar PV panels can be mounted on the top surface of the ODGV for solar energy generation. Additionally, the solar panel integrated platform can serve as a rainfall catchment area. The green energy generated from the wind-solar hybrid system is utilized to power outdoor lights or may be stored in a battery.

Keywords: Hybrid renewable energy, vertical axis wind turbine, guide-vane, on-site energy generation.

1 Introduction

Renewable energy sources, i.e. wind and solar energy are recognized as potential sources for free, clean and inexhaustible energies. Interests in renewable energy generation from researchers worldwide are driven by the increasing demand of energy from plethora of industries. However, the use of fossil fuel reserves are creating a number of adverse effects on the environment. Hence, research and development on the use of green technology exacts great responsibilities from researchers, academicians and investors alike to sustain the environment for future generations.

Wind power technology has improved since the past few decades in which the capacity of a wind turbine has increased from the classical 250 W to 5 MW. As of 2012, the Alta Wind Energy Center in California, United States of America, is the largest wind farm in the world that has a combined installed capacity of 1020 MW. In the UK, a 500 MW offshore wind farm will be constructed by the year 2017 (Mishra, 2013). Meanwhile, it was reported that on-site energy generation in urban areas using wind turbines and solar energy systems have high potentials. However, due to the presence of high-rise buildings, urban areas generally have weak and turbulent wind conditions (Knight, 2004). Thus, in order for wind energy systems to be used in urban regions, these disadvantages must be overcome.

In low wind speed regions, i.e. Malaysia which experiences low and unsteady wind speeds, are more suitable for wind turbines with lower cut-in wind speed. A drag-type vertical-axis-wind-turbine (VAWT) possesses great advantages and is particularly suitable to be used in a turbulent environment. Its characteristics include low cut-in wind speed, good starting behaviour and simplicity in fabrication (Eriksson et al., 2008, Peacock et al., 2008). Furthermore, for a wind turbine to be used in an urban area, there are a few obstacles researchers need to solve before it can be suitably implemented. Some such issues include acoustic pollution, structural issues, safety problems, blade failures, electromagnetic interference and visual pollution (Knight, 2004, Oppenheim et al., 2004).To overcome these issues, this paper introduces an innovative design of a lighting and charging system which incorporates an omni-direction-guide-vane (ODGV) integrated with a VAWT and solar photovoltaic (PV) system for on-site standalone power generation. The ODGV is designed to improve the performance of a wind turbine in terms of rotational speed, self-starting behaviour of the wind turbine (reduces the cut-in speed of the incoming airflow) and power output.

2 Eco-Greenergy Design and Principles

The study presents an innovative idea of combining hybrid wind-solar energy generation, energy-saving lighting and rain water collection system into one compact design. The harmoniously integrated hybrid concept that links wind turbine, solar photovoltaic panel and a shroud-augmentation device called the ODGV is useful to cover load demand under varying weather conditions. Moreover, the ODGV improves the performance of the wind energy generation system and overcomes the disadvantage of low wind speed in Malaysia by guiding the airflow and creating a venturi effect to increase the natural wind-stream speed before it interacts with the wind turbine. The general arrangement of this system is shown in Figure 1.

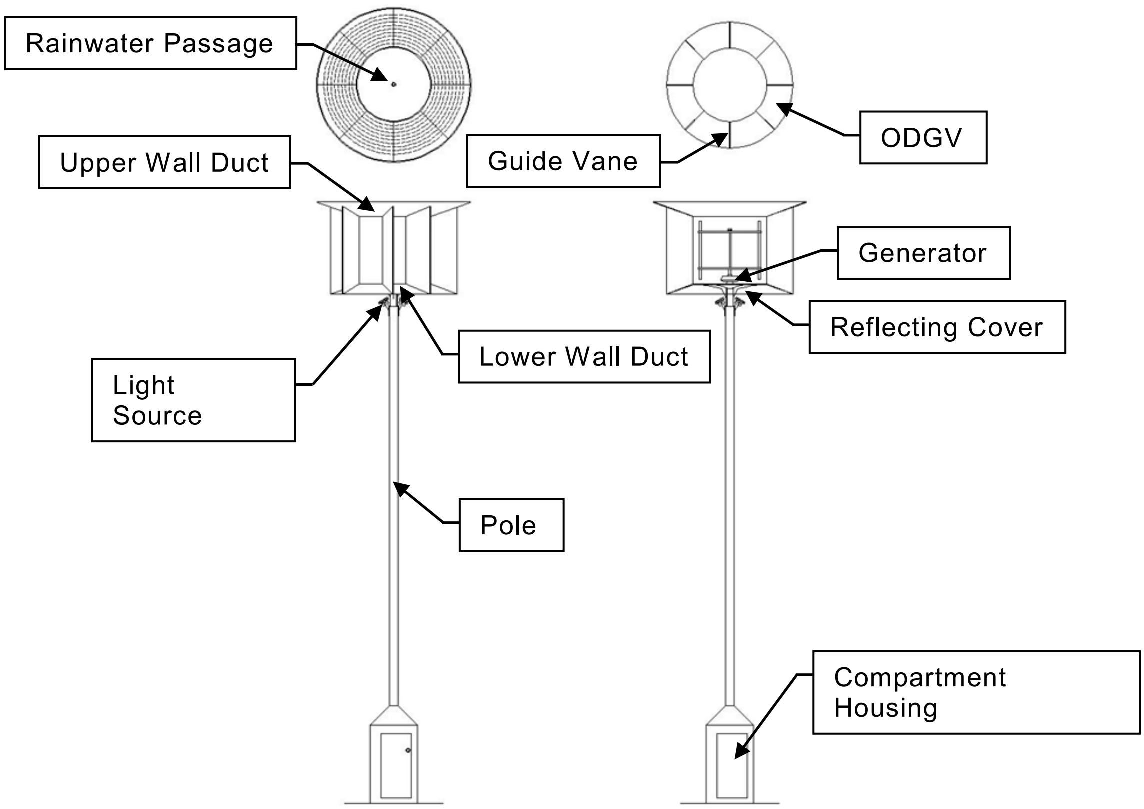

Figure 1 – General arrangement of the Eco-Greenergy wind-solar hybrid renewable energy lighting and charging system

The ODGV comprises of an upper wall duct, lower wall duct and a number of guide vanes. The wind turbine is shrouded by the ODGV. Multiple number of guide vanes surround the wind turbine to guide the oncoming wind stream from all directions. The guide vanes together with the surfaces of the upper and lower wall ducts (inclined/declined at certain angles) form the channels through which the wind stream passes before it interacts with the wind turbine. Additionally, the guide vanes surrounding the VAWT prevents the blade to fly off which may cause injuries to the surrounding people, and thus enhancing the security feature of the system. As presented in Figure 2, the guide vanes can be designed and adapted in various forms i.e. curve plate, straight plate or multiple segmented straight plates with constant or variable thicknesses. The wind turbine for the system is a vertical axis wind turbine. It can be in any form of new or existing VAWTs (drag-type or lift-type) or a combination of VAWTs, i.e.

Darrieus coupled with S-rotor wind turbine. The driveshaft of the VAWT is directly connected to the generator to minimize mechanical losses.

The inclination angle of the upper and lower duct walls are preferably 20 degrees from the horizontal plane. The cross-sectional area of the intake of the ODGV is preferably two times ore more than the cross-sectional area for the guide vanes' exit. By inducting higher wind speed into the wind turbine, smaller and lighter rotating parts of wind turbine can be used to create the same power output, with lesser load on the bearing of turbines and reduced moment of inertia for better starting behaviour. Also, apart from reducing the cost for the whole system, using a smaller sized wind turbine can eliminate or further minimize any electromagnetic interference and noise level issues caused by large wind turbines with longer blades.

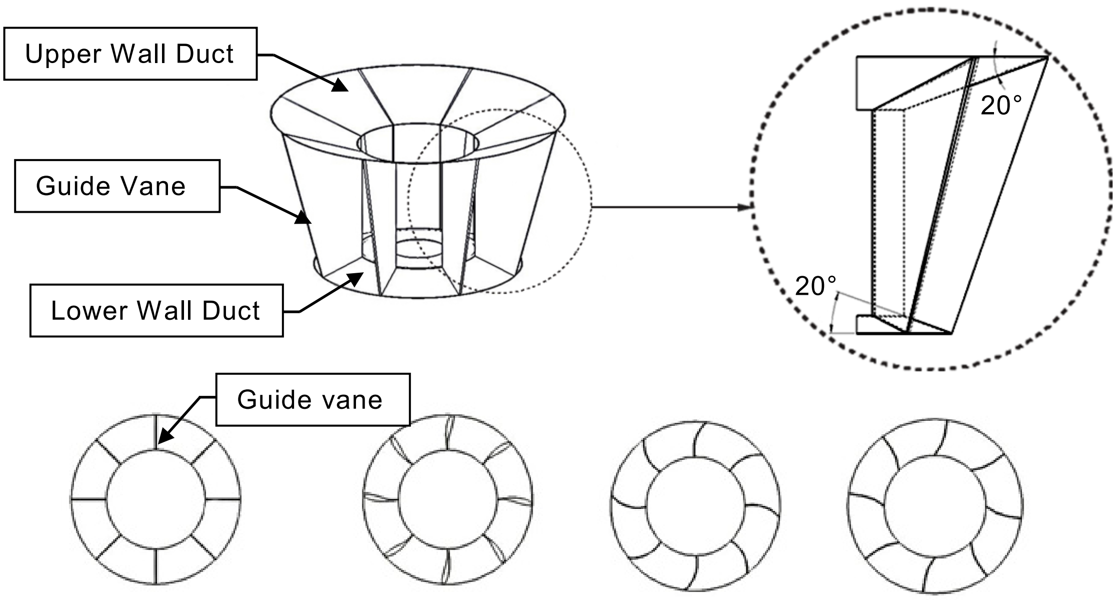

Figure 2 – Omni-direction-guide-vane (ODGV)

The solar energy generation system is strategically placed on top of the upper wall duct of the ODGV. Multi-sector arrangement of the radially inclined solar cells on top of the upper wall duct is used to harness solar energy from multiple angles of the sun. The energy generated from the VAWT and solar cells is used to power the light source. Any excess energy generated from the system can be stored in a battery which can be used to supply energy for other electrical appliances or fed into the grid line. As an option to benefit from the heavy rainfall of the Malaysian climate, a rainwater harvesting feature can be added into the system. The inclined panels of the upper wall duct directs the rainwater to flow towards the centre of the ODGV and through a rainwater passage that share a centre axis as the VAWT. A water mesh can be fitted at the mouth of the passage to filter foreign objects. The rainwater may be stored and used for watering plants or flushing of the wind turbine. It can also be treated, stored and used for general purposes.

In order to minimize power consumption, LED is adapted as the light source due to its durability and efficiency. Multiple LEDs can be adapted to be fitted under the reflecting cover. The bottom cover of the ODGV is designed to reflect light and thus enhances the LED light distribution. It also can be used as a thermal heat sink for the LED. The pole can have heights in the range of 2 m to 30 m above ground level. An artist's impression of the system is shown in Figure 3.

Figure 3 – An artist's impression of the Eco-Greenergy wind-solar hybrid renewable energy lighting and charghing system

3 Experimental Study

The experiment was conducted to show that the ODGV fitted on the Eco-Greenergy wind-solar hybrid renewable energy lighting and charging system can improve the performance of the wind turbine. In the following sub-sections, the ODGV design to be used in the experiment is presented, wind tunnel testing was carried out and the results from the experiment are tabulated and discussed.

3.1 Omni-direction-guide-vane design

The design shown in Figure 4 is used for the experimental study of the ODGV and its effects on the performance of the VAWT. The ODGV has four pairs of guide vanes, with each pair tilted at angles of 20° and 55° as shown in Figure 5. The guide vane pairs are designed equally spaced from each other, and around a cylinder with tapered feature at the outer radial band. The radial placement of the guide vanes permits the wind to be captured from all directions without the use of a yawing mechanism.

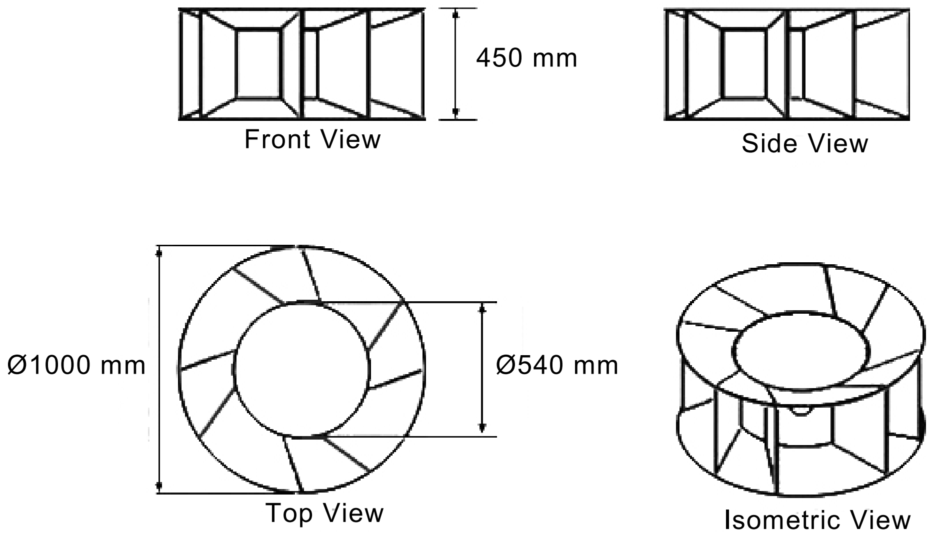

Figure 4 – ODGV dimensions(Chong et al., 2013)

3.2 Preliminary test

An initial testing was conducted to simulate oncoming airflow in a real world environment where the wind stream is swirling and turbulent. Oncoming wind stream from three different directions, i.e. 0°, 30° and 60° were simulated through the use of three industrial fans arranged in parallel. An ODGV model with dimensions shown in Figure 4 was used to enclose a Wortmann FX630137 5-bladed VAWT. The experiment concluded that the ODGV increased the rotor rotational speed to about two times more than a bare VAWT. This significant result proves that the ODGV can improve the performance of a wind turbine.

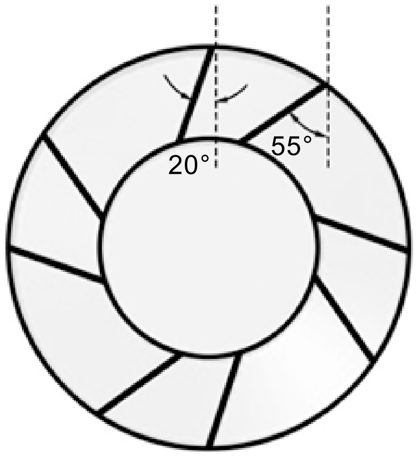

Figure 5 – Orientation of the guide vanes (Chong et al., 2013)

3.3 Wind tunnel test

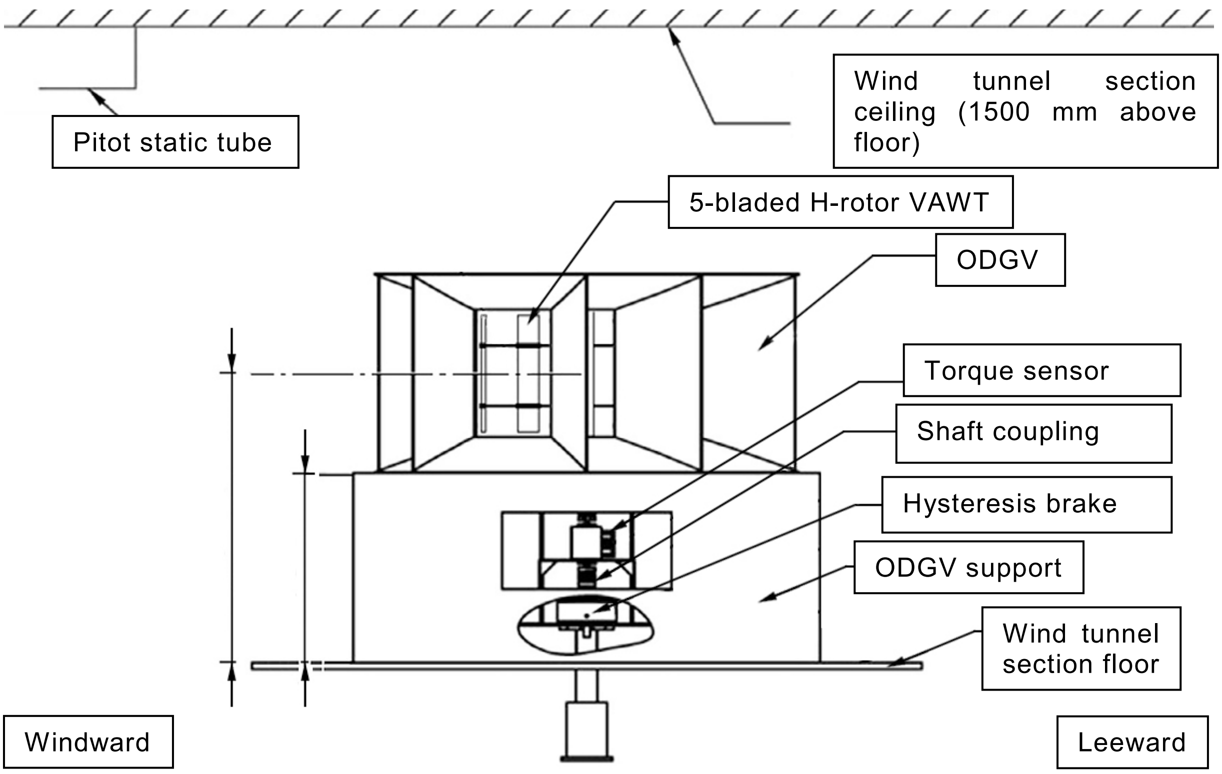

Figure 6 – A schematic side view of the experimental test rig in a wind tunnel (Chong et al., 2013)

A wind tunnel test was conducted at the Aeronautics Laboratory, University Teknologi Malaysia. Similarly, the ODGV and VAWT parameters from the preliminary test were used in the wind tunnel test, as shown in Figures 4 and 5. Figure 6 illustrates the experimental set-up of the VAWT which is shrouded by the ODGV. Two different configurations were carried out during the experiment:

- A bare VAWT without ODGV
- An ODGV integrated VAWT

Initially, the wind speed in the wind tunnel was increased steadily until the VAWT started to rotate. This is to assess the self-starting characteristics of the wind turbine for both of the configurations. The wind turbine for this initial assessment was subjected to the inertia and bearing friction only (no external load). Subsequently, in order to evaluate and compare the rotational speed and power generated by the wind turbine for both the configurations, a 6 $m \cdot s^{-1}$ wind speed was used for the following experiments. Hysteresis brake was used to apply loads on the shaft rotor. By adjusting the brake, the load exerted on the shaft is increased steadily until it reaches the maximum when the rotational speed of the rotor is stabilized. The maximum torque and power generated by the wind turbine is recorded and calculated accordingly.

4 Results and Discussions

4.1 Self-starting behaviour

The results from the assessment of self-starting behaviour of the VAWT are tabulated in Table 1. Under the same test conditions, the bare wind turbine started to rotate at a recorded wind speed of 7,35 $m \cdot s^{-1}$. Meanwhile, the ODGV integrated VAWT self-started at a reduced wind speed of 4 $m \cdot s^{-1}$. With lower self-starting wind speed, the ODGV improves the performance of the wind turbine and increases the operating hours of the wind energy system. At 6 $m \cdot s^{-1}$ wind speed, the ODGV integrated VAWT recorded a maximum rotational speed of 256 rpm, as opposed to the maximum rotational speed of 91 rpm recorded by the bare VAWT. Hence, by using the ODGV, the rotor rotational speed of the wind turbine was increased by about 182%.

Table 1 – Assessment of self-starting characteristics of a bare VAWT and an ODGV integrated VAWT (Chong et al., 2013)

Parameter	ODGV integrated VAWT	Bare VAWT
Self-starting wind speed, $m \cdot s^{-1}$	4,00	7,35
Maximum rotational speed (at 6 $m \cdot s^{-1}$), rpm	256	91

4.2 Wind turbine performance

Table 2 shows the summary of the VAWT performance for both the configuration types. As discussed previously, the wind speed of the wind tunnel was set to 6 $m \cdot s^{-1}$. The bare VAWT produced a maximum torque of 11,25 mN·m at a steady rotational speed of 77,4 rpm. As a result, 0,1252 W was generated after calculating the losses due to bearing friction.

Table 2 – VAWT performance results at a wind speed of 6 $m \cdot s^{-1}$ (after applying hysteresis brake load) (Chong et al., 2013)

Parameter	ODGV integrated VAWT	Bare VAWT	Augmentation ratio
Maximum torque, mN·m	23,64	11,25	2,10
Rotational speed, rpm	144,4	77,4	1,87
Power generated, W	0,4352	0,1252	3,48

The ODGV integrated VAWT recorded a maximum torque of 23,64 mN·m at a steady rotational speed of 144,4 rpm. Thus, 0,4352 W of power was produced. The augmentation ratios in power generated and maximum torque by comparing both of the configuration types are 3,48 and 2,10 respectively.

5 Conclusion

This paper introduces a novel invention designed to utilize wind and solar energy to provide power for outdoor lighting. The outdoor light system comprises of a pole, an omni-direction-guide-vane (ODGV) and a light source (LED lamp) fitted at the lower part of the ODGV, where a reflecting cover shrouds the light source to enhance its luminosity and provide better light distribution. On top of the ODGV, optimum surface area and orientation for solar panel and rain water collector are incorporated into the design. A vertical axis wind turbine (VAWT) is enclosed within the ODGV, in which the ODGV has multiple flow channels formed by the guide vanes, upper and lower wall ducts inclined at an angle in 20° from the horizontal plane. The guide vanes are designed to create a venturi effect and thus the speed of the natural wind-stream entering the wind turbine is intensified. From the wind tunnel testing, the ODGV successfully improved the self-starting characteristics of the VAWT. At a wind speed of 6 $m \cdot s^{-1}$ in the wind tunnel, the rotor rotational speed recorded an increase of 182% at free-running condition. Furthermore, the power output at maximum torque for the ODGV integrated VAWT is 3,48 times higher than the bare VAWT. Assessment of both of these wind turbine configuration types (bare and integrated ODGV) with both having the same specifications (blade length, swept area and aerofoil profile) reveals that the ODGV integrated VAWT improves on the many disadvantages of a bare VAWT. Additionally, the hybrid system covers the varying load demand under the unpredictable nature of the weather. Thus, the novel concept introduced in this study promotes the use of renewable energy in urban areas and thus can be implemented to reduce greenhouse gas emissions by minimizing the dependencies on fossil fuel reserves for energy generation.

Acknowledgements

The authors would like to thank the University of Malaya for the assistance provided in the patent application of this design (Patent no: PI 2013700243), and the research grant allocated to further develop this design under the University of Malaya Research Grant (RP015C-13AET) and Postgraduate Research Grant (PG047-2012B). Special appreciation is also credited to the Ministry of Education Malaysia (MOE) for the research grant (Fundamental Research Grant Scheme, FRGS – FP053-2013B).

References

CHONG, W. T., FAZLIZAN, A., POH, S. C., PAN, K. C., HEW, W. P. & HSIAO, F. B. 2013. The design, simulation and testing of an urban vertical axis wind turbine with the omni-direction-guide-vane. *Applied Energy,* 112**,** 601-609.

ERIKSSON, S., BERNHOFF, H. & LEIJON, M. 2008. Evaluation of different turbine concepts for wind power. *Renewable and Sustainable Energy Reviews,* 12**,** 1419-1434.

KNIGHT, J. 2004. Urban wind power: Breezing into town. *Nature,* 430**,** 12-13.

MISHRA, S. 2013. *500MW Galloper offshore wind farm gets greenlight* [Online]. Available: http://www.greenwisebusiness.co.uk/news/500mw-galloper-offshore-wind-farm-gets-greenlight-3955.aspx [Accessed 13th Feb 2014].

OPPENHEIM, D., OWEN, C. & WHITE, G. 2004. Outside the square: Integrating wind into urban environments. *Refocus,* 5**,** 32-35.

PEACOCK, A. D., JENKINS, D., AHADZI, M., BERRY, A. & TURAN, S. 2008. Micro wind turbines in the UK domestic sector. *Energy and Buildings,* 40**,** 1324-1333.

OP61

BENCHMARKING THE ENERGY EFFICIENCY OF ROAD LIGHTING

Dionyz Gasparovsky[1], Roman Dubnicka[1], Jana Raditschova[1]
[1]Slovak University of Technology, Faculty of Electrical Engineering and Information Technology, Bratislava, SLOVAKIA
dionyz.gasparovsky@stuba.sk

Abstract

Energy efficiency of lighting systems belongs to one of the most discussed topics in lighting engineering today. Satisfying required lighting quality criteria as pre-condition, lighting systems should be also designed with respect to the least energy consumption and optimized investment/operational costs. Energy demand is in close relation with carbon dioxide emissions, decrease of which is a global target. Energy saving measures concern both existing and new objects and can be divided to product oriented and system oriented. In the field of lighting, system based legislative and normative measures are well developed and actually being improved for energy performance of buildings (in CIE covered by TC3-52). Energy efficiency criterion is here represented by the well-known numerical indicator LENI.

For public lighting systems the standardization is still in progress. There are several approaches and assessment systems published up to now. The mainstream approach is equivalent to LENI used for buildings, i.e. based on kWh per meter square of the area to be lit. Unlike in buildings where the indicator has to be combined with other sub-systems, in public lighting there are no such restrictions and the indicator can be related also to the lighting level. It is in question how to combine luminance and illuminance based designs within the same lighting system (e.g. carriageway and parallel sidewalks) and whether specified, target or calculated values of the luminous parameters should be taken. Each of the option has benefits as such as shortcomings. Current discussions are released from finding an universal indicator, split to a couple of indicators is rather expected to be the most probable outcome. *Power density* as one of them, is based on the installed power related to area and luminous parameter. *Annual energy consumption indicator* is the other one and relates the lighting profile (as variation of power with time) to the same area as power density.

This paper aims to compare different approaches and assessment systems. Benchmarking of energy efficiency demands for big number of calculations to obtain a bulk of data that can be scaled accordingly to the energy performance. Selection system for calculation arrangements is suggested in this paper. Several lighting situations are combined with different road profiles, lighting system geometries and luminaire types including different lamps and quality of optics. Thus the indicators can be proved on numerous examples, giving a large set of data in result. Sample calculations for the most common situation with particular input data are also presented in the paper.

Keywords: energy efficiency, public lighting, roadlighting, lighting network

1 Introduction

Energy performance of lighting in buildings is expressed through the LENI indicator[1] in kWh/m^2. It is obvious and easy to imagine figures of energy consumption per square metre as an “energy density”. In buildings, besides lighting also other significant specific energy consuming appliances come to the scheme of assessment, i.e. building thermal protection (envelope), heating and hot water preparation, and air conditioning if installed. This means that the figure of energy performance has to be combined from all the mentioned sub-systems and for this reason the lighting part cannot be related to the photometric requirement, for example in kWh.lx^{-1}.m^{-2} or this can be only as an additional indicator.

Unlike LENI, public lighting is free of any such limitation. The indicators of energy performance can be defined in any appropriate way. Some indicators are being used since a longer time. It is expected that the European Commission will issue a directive on energy efficiency of public lighting like EPBD[2]. Energy performance indicators, which should be the basement for assessment, are to be defined by expert groups. A mandate is given also to the technical committee CEN TC169. Workgroup WG12 of this committee actually prepare the full set of standards for public lighting – EN 13201[3]. While first 4 parts are revisions of the previous editions, Part 5 on energy performance is a brand new part. Definitions of energy performance indicators, as subject of the EN 13201-5, are currently in preparation and are expected to be published in the middle of 2015.

2 Energy performance indicators

Until the standardization on energy performance of public lighting began, several approaches on assessment of energy efficiency were known. Further concepts have been elaborated during the standardization process. Concepts and approaches can be summarized briefly as follows:

- **Installed power per road length P_L in kW/km:** Used in many of available lighting software. This indicator does not consider different road widths. It is calculated from the system power of luminaire used and number of luminaires per kilometre taken from spacing of the installation.
- **Installed power per road area P_A in W/m^2:** Used in many of available lighting software. It is a simple power density.
- **Lighting Energy Numerical Indicator LENI in kWh/m^2:** Approach inherited from the EPBD is today used provisionally in some countries or by some experts. However, there is no methodology how to take into calculations the lighting control because situation in buildings, for which the LENI concept was derived, is different.
- **Street Lighting Energy Efficiency Criterion SLEEC in kWh/lx/m^2:** This is the most complex indicator that integrates all the necessary factors – lighting control and operational profiles, photometric parameter and area of the illuminated target. Nevertheless, this indicator in its complexity failed to succeed in scaling as resulting figures did not reliably distinguish between worse and better installations, what concerns their energy efficiency.
- **Power Density Indicator PDI in W/lx/m^2 and Annual Energy Consumption Indicator AECI in kWh/m^2:** This pair of compound indicators is included in the current draft of European standard, but still not closed as a definitive selection. The previous SLEEC concept is here split into two indicators that should alway be used together. PDI stands for istalled power density while AECI expresses the energy consumption density.
- **Luminous efficacy η in lm/W:** This alternative approach is reciprocal to the previously mentioned indicators, with different input data. Luminous efficacy of the lighting installation accounts for losses of luminous flux along path from the lamp to the illuminated target and comprises of efficacy of the lamp, optical efficiency (L.O.R.) of the luminaire, maintenance factor (MF) and utilisation factor (UF).
- **Other approaches:** Besides the main stream concepts, there are also other studies performed by different authors, e.g. [4].

Except of luminous efficacy, the indicators are based on three inputs:

- **System power of luminaires (W):** Power of all components associated with the illuminated area and necessary for the functioning of the system shall be included in calculation, i.e. power of lamps, ballasts, control gears, drivers, lighting controls etc. If for calculation an elementary area of road section between two consecutive luminaires is considered, identical to the calculation field, only power of one of the luminaires is to be included (or half of the two luminaires).
- **Area as a target of illumination (m^2):** In general it can be an elementary area identical to the calculation field (see the previous comment) or it can be a full length of the lighting installation – in case of straight roads. Indicators are applicable also for any areas of regular or irregular shape like squares, parks, pedestrian walk zones etc.

- **Luminous parameter (usually lx):** Discussions are still ongoing wether specified, target or calculated values should be used and how to deal with roads designed to luminance.

All variants have pros and contras but for the sake of simplicity, a proper selection should be agreed. Using specified values it can be impossible, in some situations, to compare lighting systems with the fixed geometry (e.g. refurbishment) when none of the parameters will differ. But using calculated values it is more difficult to prevent the overlit of road and this is the reason why PDI should never be used stand alone but together with AECI. Actually, calculated values are preferred against specified or target.

SLEEC was previously split to L-based and E-based indicator according to the design criterion. The same can be applied to PDI. However, having too many variants complicates the practical assessment of installations. If specified values are used for calculation, luminance can be converted to illuminance through the luminance coefficient Q_0, what is not an ideal solution because roads optimized to luminance and having beneficial reflectance properties will loose. If calculated values are used, even for roads optimized to luminance, illuminance calculated on the same calculation field and grid of points can be used, what is another arrgument for preferring calculated photometric values.

Power density indicator (PDI) for an area divided into sub-areas can be calculated with the following formula:

$$D_P = \frac{P}{\sum_{i=1}^{n} \overline{E}_i \cdot A_i} \tag{1}$$

where

D_P	is the power density indicator (W.lx^{-1}.m^{-2});
P	is the system power of the lighting installation used to light the relevant areas (W);
$\overline{E}_i$	is the calculated maintained average horizontal illuminance (lx);
A_i	is the size of the sub-area "i" lit by the lighting installation (m^2);
n	is the number of sub-areas to be lit.

If the required lighting class changes during the night and/or through the seasons (e.g. reductions due to decreased traffic density, changes in the visual environment etc.), the PDI should be calculated separately for each of the lighting classes. It means that for the same lighting installation several values of PDI can be provided.

Annual Energy Consumption Indicator (AECI) shall be calculated with the following formula:

$$D_E = \frac{\sum_{j=1}^{m} P_j \cdot t_j}{A} \tag{2}$$

where

D_E	is the annual energy consumption indicator for a road lighting installation (Wh.m^{-2});
P_j	is the operational power associated with the jth period of operation (W);
t_j	is the duration of jth period of operation profile when Pj is consumed, over a year (h);
A	is the size of the area lit by the same lighting arrangement (m^2);
m	is the number of periods with different operational power P_j.

m shall also consider the period over which the quiescent power is consumed. This period would generally be the time when the lighting is not operational i.e. daylight hours and any night time period when the lighting is not lit.

3 Selection system for sample calculations

Calculation of energy performance indicators are needed to acquire real figures for different combinations of road profiles, lighting system geometries and luminaires that are common in practice. Sample calculations should create an imagination on absolute values and their variation and to aid how to distinguish between more and less energy efficient solutions.

To follow these objectives, selection of the components and selection of their combination have been performed. The scheme of selection is presented in Fig. 1. Number of road profiles to be analyzed is the minimum indicated. Single-side arrangement of lighting system will be the standard, other geometry types will be tested only for a limited selection of profiles. At least 10 luminaire types will be proved, but the selection of luminaires is open-ended. For single-side lighting systems and few other systems the number of possible combinations is about 1000. For skilled person it takes around 10 minutes to find the optimum solution, what makes in total 167 man-hours for all combinations. Instead of this approach, specific selection of situations can be made to study the quality of luminaires, influence of the lighting class or road width, lamp type used, etc.

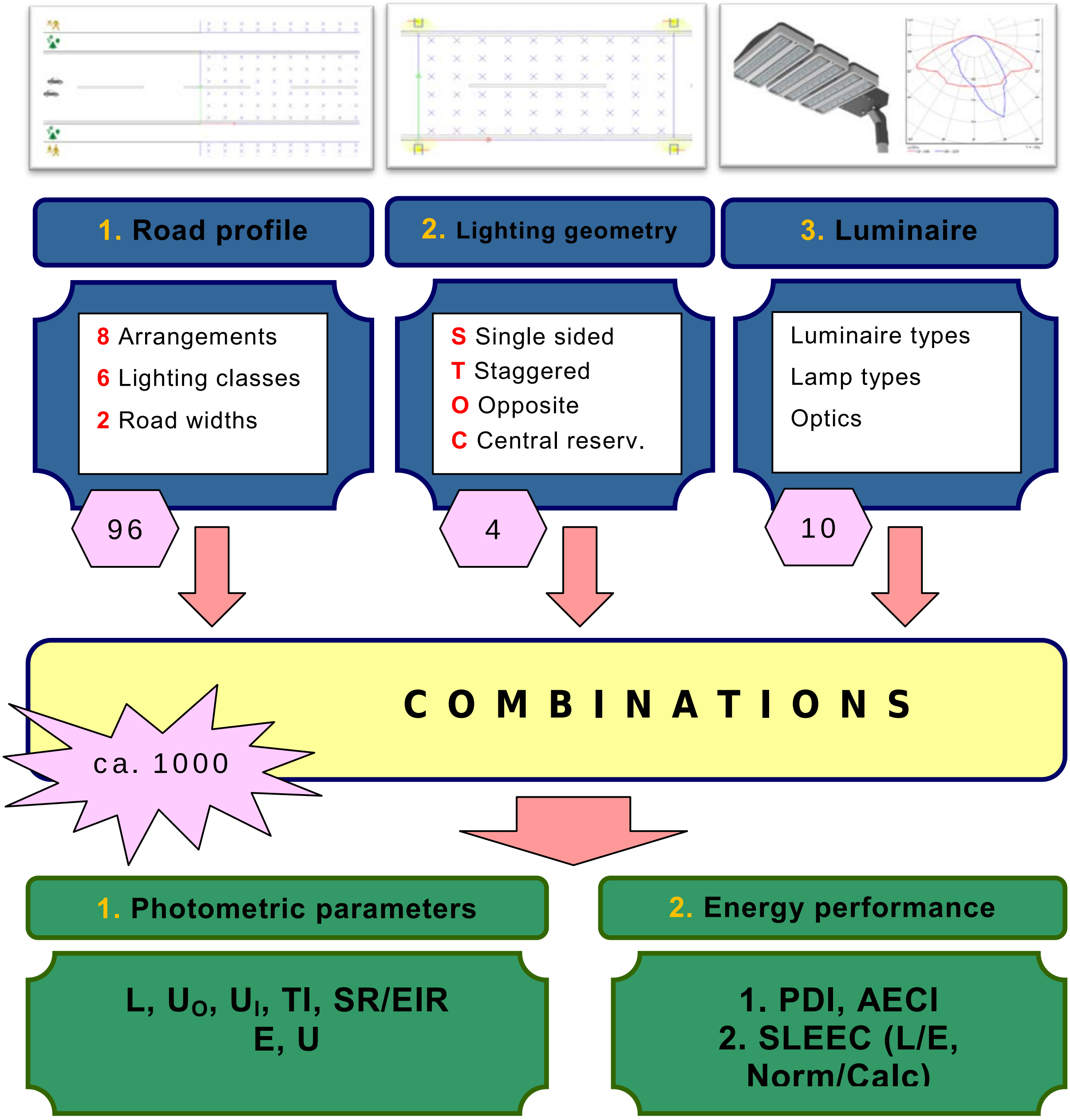

Figure 1 – Flow chart of the selection system for sample calculations

Basic arrangements of **road profiles** are depicted in Figure 2. For each arrangement, 2 road widths are chosen and combined with different lighting classes: M1 to M6 for the carriageway and corresponding lighting class for the concurrent sidewalks.

Arrangement of the lighting system is generally single-sided and for selected situations staggered, opposite and central reservation arrangements will be tested. Luminaires will not be tilted. Arm overhang is ranged from 0 to 2 m with the step 0,5 m. Mounting height will be set within the range 5 to 14 m (step: whole numbers) and the spacing of poles will be sought between 20 to 60 m (step: 1 m). For each calculation, the geometry will be optimized with preference given to the spacing in order to enlarge the illuminated area as much as possible and to have thus the energy performance indicators as low as possible. Mounting height and arm length affects to the indicators only indirectly.

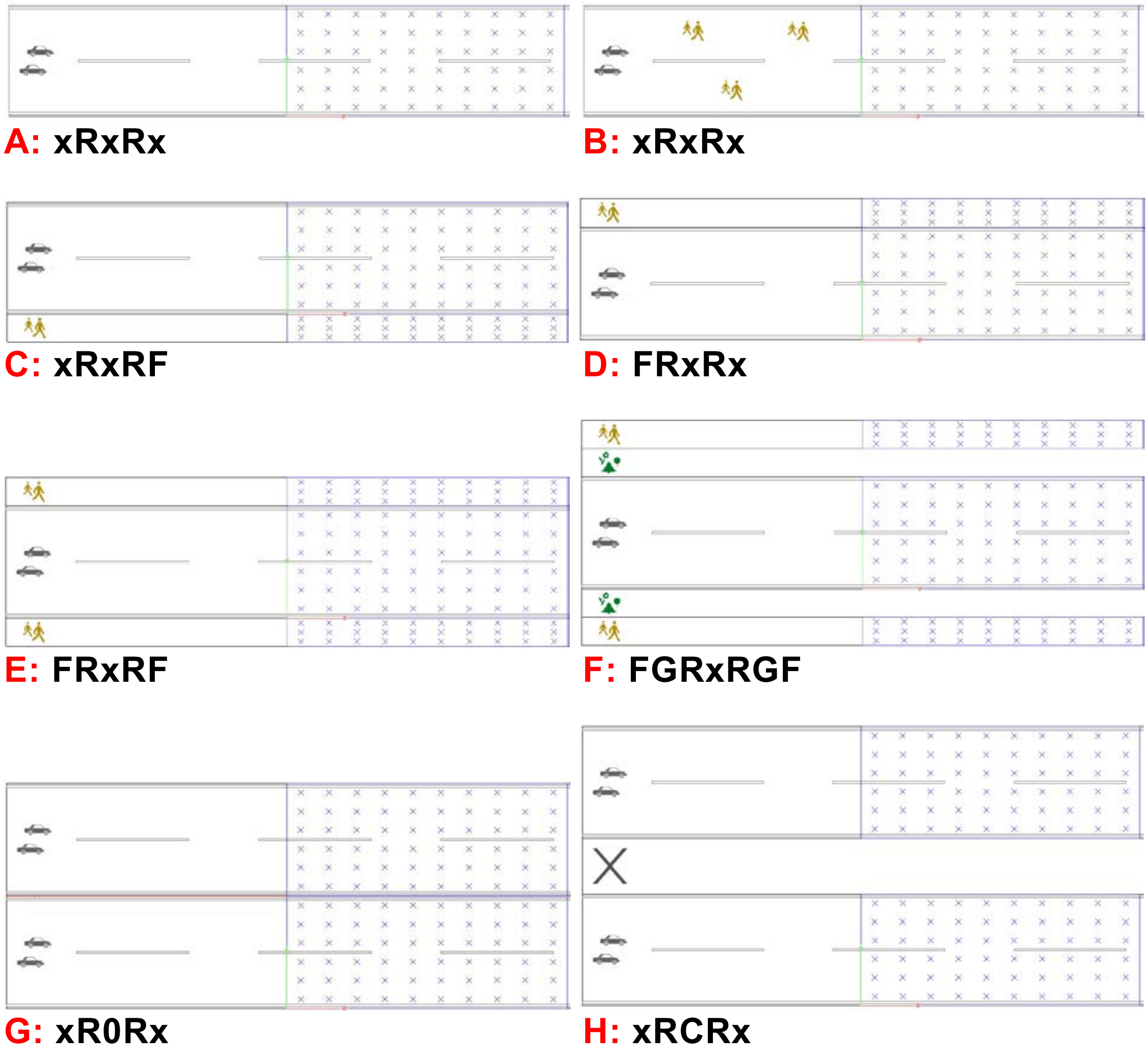

Figure 2 –Typical road arrangements for the calculation of energy performance indicators

Key:

A: Pattern “xRxRx” (two-lane road for motorized traffic)

B: Pattern “xRxRx” (road with mixed motorized and pedestrian traffic and without footpaths)

C: Pattern “xRxRF” (road and footpath on the side of lighting arrangement)

D: Pattern “FRxRx” (road and footpath on the opposite side to the lighting arrangement)

E: Pattern “FRxRF” (road and two footpaths on both sides)

F: Pattern “FGRxRGF” (road and two footpaths on both sides separated from carriegeway by a grass strip)

G: Pattern “xR0Rx” (road with dual carriageway without central reservation)

H: Pattern “xRCRx” (road with dual carriageway with central reservation)

Set of **luminaires** for calculations are chosen to cover the possible options. Low-cost or sophisticated luminaires incorporate reflecting diffuser or high-quality smooth or faceted reflectors, respectively. Lamp types comprise ellipsoidal and tubular high-pressure sodium lamps, mercury lamps, metal halide lamps, LEDs, PL-L type compact fluorescent lamps and possibly low-pressure sodium lamps for some situations, not including incandescent lamps as these are not used in public lighting since long times. For a particular road profile several lamp wattages of the same type can be tested. Lamp position in the luminaire, where adjustable, will be optimized and not taken as the option. Bottom cover made of flat glass and polycarbonate will be distinguished.

4 Example of calculation of DPI and AECI

Examle for the situation F: Two lane road with sidewalks on both sides and grass strips separating footpath from carriageway.

Two luminaires are installed per pole: Luminaire P_R for illumination of road and distant (left) footpath partially also illuminates the right footpath. An additional luminaire P_F is used for illumination of the left footpath. Note that power of both luminaires are included in calcullation just once.

Voltage regulator is installed for reducing the light level to 50 % with corresponding decrease in power by 30 % (reduction coefficient is then k = 0,7) in times when traffic volume is lower – 23:00 to 4:00. Annual operation time is thus devided to 2 175 h of full operation (t_{full}) and 1 825 h on reduced level (t_{red}).

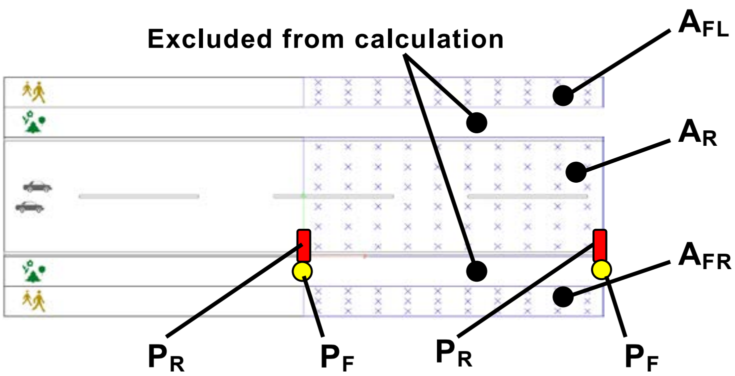

Figure 3 – Situation and description of parameters for calculation of PDI and AECI for the situation F as an example

Formulae (1) and (2) for the calculation of energy performance indicators become the form:

$$D_P = \frac{P_R + P_F}{E_{FL}A_{FL} + E_R A_R + E_{FR}A_{FR}} \qquad D_E = \frac{(P_R + P_F)(t_{full} + k.t_{red})}{A_{FL} + A_R + A_{FR}}$$

Using particular figures:

Width of road:	**6 m**	Lighting class for road:	**ME3c** (1,00 cd.m^{-2})	
Width of footpath L:	**2 m**	Lighting class for footpath L:	**S3** (7,50 lx)	
Width of footpath R:	**3 m**	Lighting class for footpath R:	**S3** (7,50 lx)	
Width of grass strip L:	**2 m**			
Width of grass strip R:	**5 m**			
System power P_R:	**114 W** (HPS 100 W)			
System power P_F:	**61 W** (HPS 50 W)			
Mounting height for P_R:	**12 m**	Spacing for P_R: **30 m**	Overhang: **1,5 m / 0°**	
Mounting height for P_F:	**8 m**	Spacing for P_F: **30 m**	Overhang: **-1,5 m / 180°**	
Maintenance factor:	**0,80**			
Road surface:	**R3**			
Area A_R:	**180 m^2**			
Area A_{FL}:	**60 m^2**			
Area A_{FR}:	**90 m^2**			

Photometric calculation have been performed using the Dialux computer program, giving the results as shown in the Table 1.

Table 1 – Photometric results of the calculation

Symbol	Unit	Description	Calculated	Required
Carriageway				
L_{av}	cd.m^{-2}	Maintained luminance of road surface	1,13	≥ 1,00
U0	1	Overall uniformity of illumination	0,80	≥ 0,40
Ul	1	Longitudinal uniformity of illumination	0,78	≥ 0,50
TI	%	Threshold Increment	3	≤ 15
SR	1	Surround Ratio	0,69	≥ 0,50
E_{av}	lx	Average illuminance of road surface	18	-
E_{min}	lx	Minimum illuminance of road surface	10	-
E_{max}	lx	Maximum illuminance of road surface	25	-
Left footpath				
E_{av}	lx	Average illuminance of the footpath	9,56	≥ 7,50
E_{min}	lx	Minimum illuminance of the footpath	6,47	≥ 1,50
Right footpath				
E_{av}	lx	Average illuminance of the footpath	11,50	≥ 7,50
E_{min}	lx	Minimum illuminance of the footpath	6,78	≥ 1,50

Combining photometric parameters with power and geometry data, DPI and AECI indicators can be calcuated as follows:

$$D_P = \frac{114W + 61W}{9,56lx.60m^2 + 18lx.180m^2 + 11,50lx.90m^2} = \mathbf{0{,}0361\ W.lx^{-1}.m^{-2}}$$

$$D_E = \frac{(114W + 61W)(2175h + 0,7.1825h)}{60m^2 + 180m^2 + 90m^2} = \mathbf{1,831\ kWh.m^{-2}}$$

This example is a case study of the calculation of energy performance numerical indicators based on the DPI and AECI compound parameters. Using this pair of parameters, different lighting designs for the same road profile can be directly compared between each other and thus the optimum solution can be chosen when simultaneously considering the installation and operational costs. The same time, DPI and AECI can be also well indicative for a self-standing assessment of a lighting system, i.e. its comparison to an average standard or stated limits presented as the energy performace scale. This is, however, a subject of future works.

Table 2 – Luminaire specifications and lighting arrangement parameters

No.	Luminaire	Opt	Pos	Lamp	Ver	P_l	P_n	Φ	H	S	t
						W	W	lm	m	m	m
1	SGS102			H		250	274	12 700	7	29	2
2	SGS102			S	PP	100	114	10 200	7	23	1
3	SGS102			S	PP	150	169	17 000	9	33	2
4	SGS102			S	TPP	100	114	10 700	7	27	2
5	SGS102			S	TPP	150	169	17 500	9	37	2
6	SGS104		4	S	TPP	100	114	10 700	8	30	1
7	SGS104		5	S	TPP	150	169	17 500	10	42	2
8	SGP340		2	H		250	274	12 700	8	26	2
9	SGP340	FG	5	M		100	114	8 300	7	22	1,5
10	SGP340	PC	5	M		100	114	8 300	7	23	1
11	SGP340	FG	4	M		150	169	12 500	8	29	2
12	SGP340	PC	5	M		150	169	12 500	8	27	2
13	SGP340	FG	3X	S	TPP	100	114	10 700	8	29	1
14	SGP340	PC	3X	S	TPP	100	114	10 700	8	30	0,5
15	SGP340	FG	4	S	TPP	150	169	17 500	10	42	0,5
16	SGP340	PC	4	S	TPP	150	169	17 500	10	43	0
17	BGP340			L			108	11 040	8	38	0
18	BGP340			L			90	9 200	8	33	0,5
19	BGP340			L			73	7 360	8	27	0,5
20	BGP340			L			55	5 520	8	20	0,5

Key:

Opt: Optics (FG = Flat Glass, PC = Polycarbonate)

Pos: Lamp position in the luminaire

Lamp: Lamp type (H = Mercury, S = Sodium, M = Metal Halide, L = LED)

Ver: Lamp version (PP = ellipsoidal, TPP = tubular)

$\mathbf{P_l}$ – Lamp wattage (W)

$\mathbf{P_n}$ – Luminaires system wattage (W)

Φ – Luminous flux of the luminaire

H – Mounting height (m)

S – Spacing (m)

t – Overhang (m)

The indicators can be applied for an installation element between two consecutive lighting poles (identical with the calculation field) or for a road section. For practical use, DPI gives too small numbers and can be presented with a 10^{-3} multiplier.

5 Sample calculations for benchmarking

In this paper, results of sample calculations are illustrated for a particular road profile similar to that used as a case study in section 4, with only difference in width of grass strips, here equal to 1 m. For this profile and lighting requirements (ME3c for carriageway and S3 for footpaths), different luminaires and lighting arrangements have been proved as shown in Table 2. Results of calculated photometric parameters and energy performance indicators are in Table 3. Based on the results, Table 4 presents a basic scaling of the indicators. It must be taken into account that values of indicators are statistically still not enough significant and further calculations will be needed. The scaling is valid for the F situation with particular road width and ME3c lighting class only.

Table 3 – Calculation results of photometric parameters and energy performance indicators

No.	L_C	E_C	E_L	E_R	P_L	P_A	SLEEC	PDI	AECI
	cd.m^{-2}	lx	lx	lx	kW/km	W/m^2	kWh/lx/m^2	W/lx/m^2	kWh/m^2
1	1,00	17	8,17	9,24	9,590	0,8589	0,2588	64,69	3,4357
2	1,02	19	8,35	10,46	5,016	0,4506	0,1223	30,58	1,8024
3	1,01	17	10,08	11,22	5,239	0,4656	0,1315	32,87	1,8623
4	1,05	18	8,76	7,68	4,332	0,3838	0,1137	28,42	1,5354
5	1,07	18	11,06	9,51	4,732	0,4152	0,1152	28,79	1,6609
6	1,12	18	7,66	7,73	3,876	0,3455	0,1037	25,94	1,3818
7	1,15	17	12,23	7,71	4,056	0,3658	0,1076	26,90	1,4632
8	1,01	19	10,21	10,49	10,686	0,9580	0,2541	63,53	3,8322
9	1,03	19	9,35	7,62	5,244	0,4711	0,1332	33,31	1,8843
10	1,00	19	7,96	8,18	5,016	0,4506	0,1284	32,09	1,8024
11	1,03	19	8,58	11,20	5,915	0,5298	0,1415	35,37	2,1191
12	1,00	17	11,63	10,08	6,422	0,5690	0,1610	40,25	2,2761
13	1,03	19	9,95	7,52	3,990	0,3574	0,1005	25,12	1,4295
14	1,04	19	8,30	7,91	3,876	0,3455	0,0985	24,62	1,3818
15	1,07	18	11,10	8,74	4,056	0,3658	0,1029	25,72	1,4632
16	1,00	16	11,21	8,44	4,056	0,3573	0,1094	27,34	1,4292
17	1,05	16	7,53	9,95	2,916	0,2584	0,0807	20,17	1,0335
18	1,06	16	8,94	7,63	2,790	0,2479	0,0798	19,94	0,9917
19	1,04	16	8,79	7,52	2,774	0,2458	0,0794	19,86	0,9832
20	1,06	16	8,98	7,67	2,750	0,2500	0,0803	20,08	1,0000

Key:

L_C – Luminance of the carriageway (W)
P_L – Installed power per road length (kW/km)
P_A – Installed power per road area (W/m^2)
E_C – Illuminance of the carriageway (lx)
E_L – Illuminance of the left footpath (lx)
E_R – Illuminance of the right footpath (lx)

		Two least efficient solutions
		Two most efficient solutions

Table 4 – Scaling of benchmarks for the situation under consideration

Energy Class	P_L	P_A	SLEEC	PDI	AECI
	kW/km	W/m^2	kWh/lx/m^2	W/lx/m^2	kWh/m^2
A - B	≤ 4	≤ 0,35	≤0,10	≤ 28	≤ 1,4
C - D	4 - 6	0,35 - 0,5	0,10 - 0,15	28 - 34	1,4 - 2
E - F	6 - 8	0,50 - 0,75	0,15 - 0,20	34 - 40	2 - 3
G	≥ 8	≥ 0,75	≥ 0,20	≥ 40	≥ 3

6 Conclusions

Standardization of energy performance indicators for public lighting systems are still in progress. Definitions presented in this paper have to be thus deemed as report of interim situation and the most probable version of the future standard. One of the objectives of the standard under preparation is to provide also benchmark values of the indicators. To do this, it is necessary to perform a bulk of sample calculations. Selection of road profiles, lighting system arrangements and geometries, luminaire types and operational profiles to be used in combinations, is now prepared and calculations are ongoing.

Acknowledgements

This publication is the result of the project implementation:
Research centre of light and lighting technology, ITMS 26220220150,
supported by the Research & Development Operational Programme funded by ERDF.

Operačný program VÝSKUM a VÝVOJ

Agentúra Ministerstva školstva, vedy, výskumu a športu SR pre štrukturálne fondy EÚ

Podporujeme výskumné aktivity na Slovensku/
Projekt je spolufinancovaný zo zdrojov EÚ

Európska únia
Európsky fond regionálneho rozvoja

References

1. EN 15193:2007 Energy performance of buildings. Energy requirements for lighting
2. Directive No. 2010/31/EC of the European Parliament and of the Council on Energy Performance of Buildings. Brussels, 2010
3. EN 13201: Road lighting (group of standards), 2004
4. PRACKI, P.: A proposal to evaluate road lighting energy efficiency. LUMEN V4 2012.
5. CIE 115: Lighting of Roads for Motor and Pedestrian Traffic, 2010
6. SOKANSKY, K. & NOVAK, T.: Energy savings in public lighting. Przeglad Elektrotechniczny, 84(8), pp. 72 - 74, 2008
7. SOKANSKY, K., NOVAK, T. & BLAHA, Z.: Assessment of parameters of lights for public lighting. Proc. of the 10th International Scientific Conference Electric Power Engineering 2009, VSB TU Ostrava: Ostrava, pp. 194 - 196, 2009
8. SKODA, J. & BAXANT, P. The reduction in electricity consumption through proper lighting. In proc.: EPE - Electric Power Engineering 2009. Brno University of Technology: Brno, pp. 1 – 4, 2009

OP62

HIGH ACCURACY IMAGING COLORIMETRY

Richard Young[1], Jürgen Neumeier[1]
[1] Instrument Systems GmbH, Munich, GERMANY
Young@instrumentsystems.com

Abstract

The spectral responsivity requirements for a basic colorimeter and the benefits for extension to 6 channels are described. Matrix methods allow the combination of the 6 channels to give improved agreement to the CIE colour matching functions. This gives more accurate results for virtually all sources.

Colour difference vector plots are used throughout to clearly show results and allow visual comparisons. The techniques of optimising the adaptive matrix to CMF spectral values or to specific colour parameters are demonstrated.

Results of a study are presented for a set of 22 LED and filtered incandescent sources, measured using spectroradiometers and imaging colorimeters employing the traditional 4-filter construction and a new 6-filter construction. Results are compared, demonstrating the benefits of the enhanced 6-filter construction for general measurements.

Keywords: Photometry, Colour, Colorimeter, Colorimetry, Imaging, High accuracy, Adaptive, Matrix, LED, Source, Measure, CMF, Study

1 Introduction

Imaging colorimetry has gained popularity due to its ease of use and potential for making sophisticated automated analysis (JENSON 2013). Exact alignment is generally not required and multiple regions may be compared and processed.

The imaging colorimeter provides CIE X, Y and Z tristimulus values and derivative colour quantities such as CIE xyz, u′v′, L*a*b*, CCT etc. It employs filters to match the response to the CIE colour matching functions $\bar{x}, \bar{y}, \bar{z}$. As the $\bar{x}$ CMF has two peaks it is often split into two channels so a 4-filter colorimeter is used to represent the three CMFs.

Spectral mismatch of the colorimeter responses relative to the CMFs means the accuracy of measurement varies with the spectrum of the device under test (EPPELDAUER 1998). The closer the spectrum to the calibration source the more accurate the measurement. As calibrations are frequently made using white incandescent sources, LEDs and coloured sources often give large errors in measurement. An exception to this is when matrix correction methods are used to correct display measurements. Here, there are generally three primaries of the display that are mixed to give the test colour and hence there is a limited variation in spectra. The matrix method of correction (OHNO 1997) is now commonly applied to such measurements but if the spectrum is completely unknown this method cannot be used. Matrix methods can still be applied to improve results in specific cases (SCHANDA 2008, KOSZTYÁN 2008, KOSZTYÁN 2010)

If the number of colour detection channels is increased to six, the correction matrix can now be optimised across a large set of sources and no inherent assumption of spectrum is required.

2 Optimising spectral responses

The colour matching functions (CMFs) defined by CIE provide the basis of most measurements of colour quantities. These are shown in Figure 1 as solid lines. A practical colorimeter aims to reproduce this spectral response using a combination of filters and detectors and although the match can be close it is never exact. An example of the match is given as broken lines in Figure 1. This example is of a 4-filter colorimeter, where the double peaks of the CIE x colour matching function is realised using 2 channels on the colorimeter (X_1 and X_2). One can see in this example that around 560 nm the Z channel of the colorimeter is much higher than the CIE z CMF and the X_2 channel is lower than the CIE x CMF. For narrow band sources such as LEDs that emit in this region, large errors in colour values can result from this mismatch.

One way of improving the match is to combine the channels. We can see that the high Z-channel response around 560 nm roughly corresponds to the Y-channel peak wavelength, so by combining the Z- and Y- channels in optimum proportions a closer match to the CIE z CMF may be obtained.

This can be represented mathematically by a simple matrix product:

$$\begin{bmatrix} \hat{X} \\ \hat{Y} \\ \hat{Z} \end{bmatrix} = \begin{bmatrix} X_1{}' \\ X_2{}' \\ Y' \\ Z' \end{bmatrix} \cdot \mathbf{M} \tag{1}$$

where

$\hat{X}, \hat{Y}, \hat{Z}$ are the measured tristimulus values or spectral elements of combined responses

$X_1{}'$, $X_2{}'$, Y', Z' are the measurements from the colorimeter channels

$\mathbf{M}$ is the 3 x 4 adaptive matrix of factors for the combinations of channels

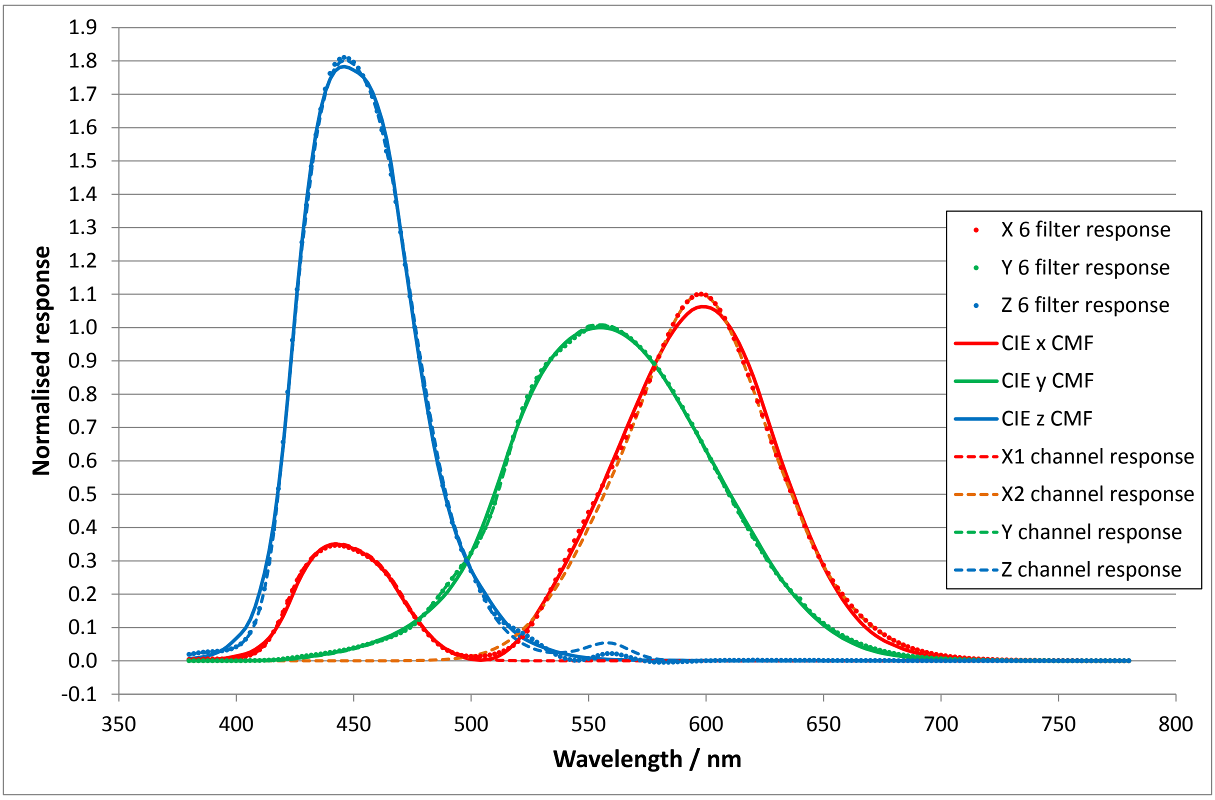

Figure 1 - Colour matching functions and examples of implementation. CIE CMFs (solid), 4-channel colorimeter example (dashed lines) and 6-filter colorimeter example (points).

There is a limit to how well this works however, since correcting the 560 nm response is likely to make the 530 nm response, which is already low, worse. There are many possible optimisations of the adaptive matrix therefore and each depends on the spectrum of the source to be measured. Often the spectrum of the source to be measured is unknown or one of a range of possibilities; here some compromise combination is required that minimises the errors from each source.

If a 5th channel is added to the colorimeter, the possibilities for optimisation are greatly increased. However, the improvement will still be around the peak wavelength response of the extra channel. By adding a 6th channel a broader optimisation can be attempted, making it much less dependent on the spectrum of the source.

The effective response then becomes:

$$\begin{bmatrix} \hat{X} \\ \hat{Y} \\ \hat{Z} \end{bmatrix} = \begin{bmatrix} X_1{}' \\ X_2{}' \\ Y' \\ Z' \\ K' \\ L' \end{bmatrix} \cdot \mathbf{M} \qquad (2)$$

where

K', L' are the measurements from the additional channels

$\mathbf{M}$ is a 3 x 6 adaptive matrix of factors

The response of these extra channels would typically be single peaks at appropriate wavelengths to correct errors in the other 4 channels but this is not a strict requirement. Narrow band responses may introduce local corrections but be of limited general use. The optimum responses of these extra channels therefore should be matched to the errors in the basic four channels. An example of using 6 channels to conform to the CIE CMFs more exactly is given in Figure 1, where the match is dramatically improved in both the 530 nm and 560 nm regions.

For general matching it is useful to look at colour errors. These can be represented visually by vector arrows on a colour difference vector plot such as those shown in Figure 2. Here, the true (measured using a quality spectroradiometer for real sources or calculated for simulated sources) coordinates are shown as circles and measured coordinates are at the tip of an arrow originating in the circle. The length of the arrow indicates the magnitude of the difference and the direction of the arrow indicates the direction of change. For many quality systems the arrows would be too short to assess clearly, so it is common to magnify them by some scaling factor to highlight the differences. Figure 2 for instance shows the vector scale is 3, indicating the arrows are 3 times longer than actual. When comparing errors, the shorter the arrow the lower the error.

The sources represented in Figure 2 include both real and simulated sources. There are a set 20 nm FWHM Gaussian distributions the represent pseudo-monochromatic source such as LEDs and these can be seen around the outer edges close to the monochromatic locus. A further set of 20 coloured and white LEDs, plus four white and filtered incandescent sources, are included and these are distributed at the edges and towards the middle of the diagram.

There is a clear general improvement resulting in lower errors for all sources when going from a 4-channel to a 6-channel colorimeter. The only limitation is that those spectral components lying beyond the wavelength range of the additional filters cannot be corrected in this general way so the errors are the same for both systems.

The colour difference vector plots in Figure 2 are for least squares optimisations to the CMF spectra and as such they are perhaps the most general. However, this requires knowledge of the spectral responsivities of each channel.

3 Optimising colour errors between sources

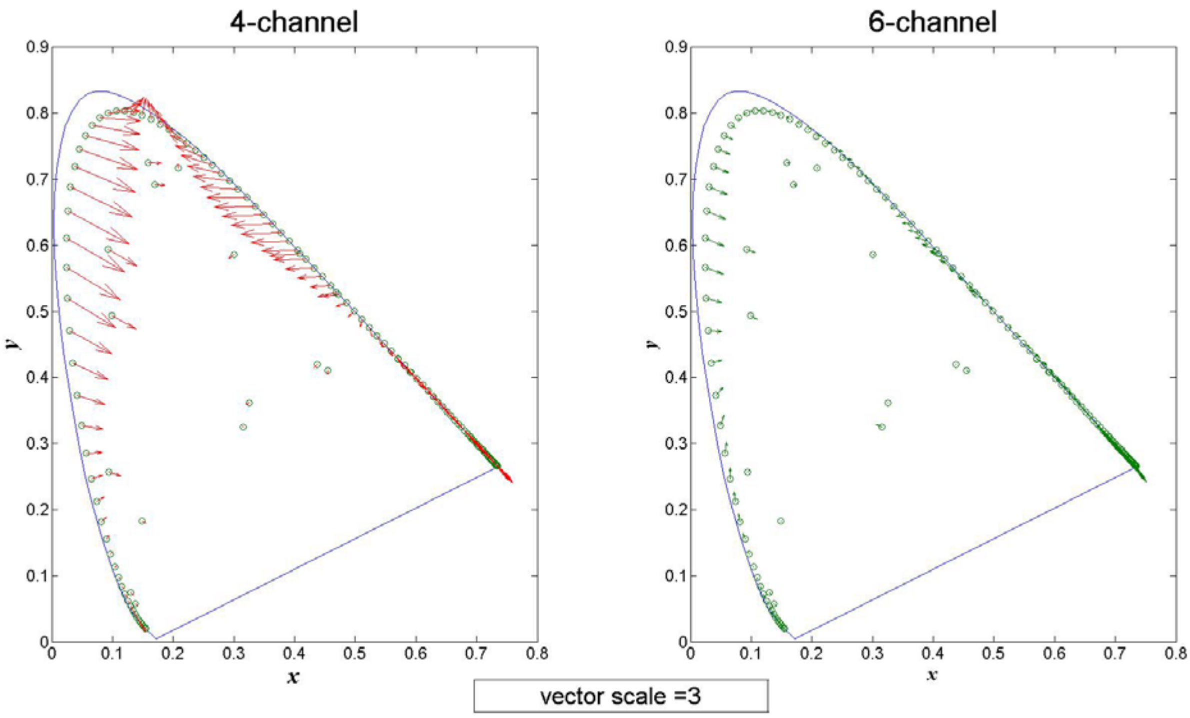

Figure 2 – Colour difference vector plot in CIE xy space for the errors in measurement of various sources using 4-channel (left) and 6-channel (right) imaging colorimeters. The vectors are enlarged by the scale shown for clarity of comparison.

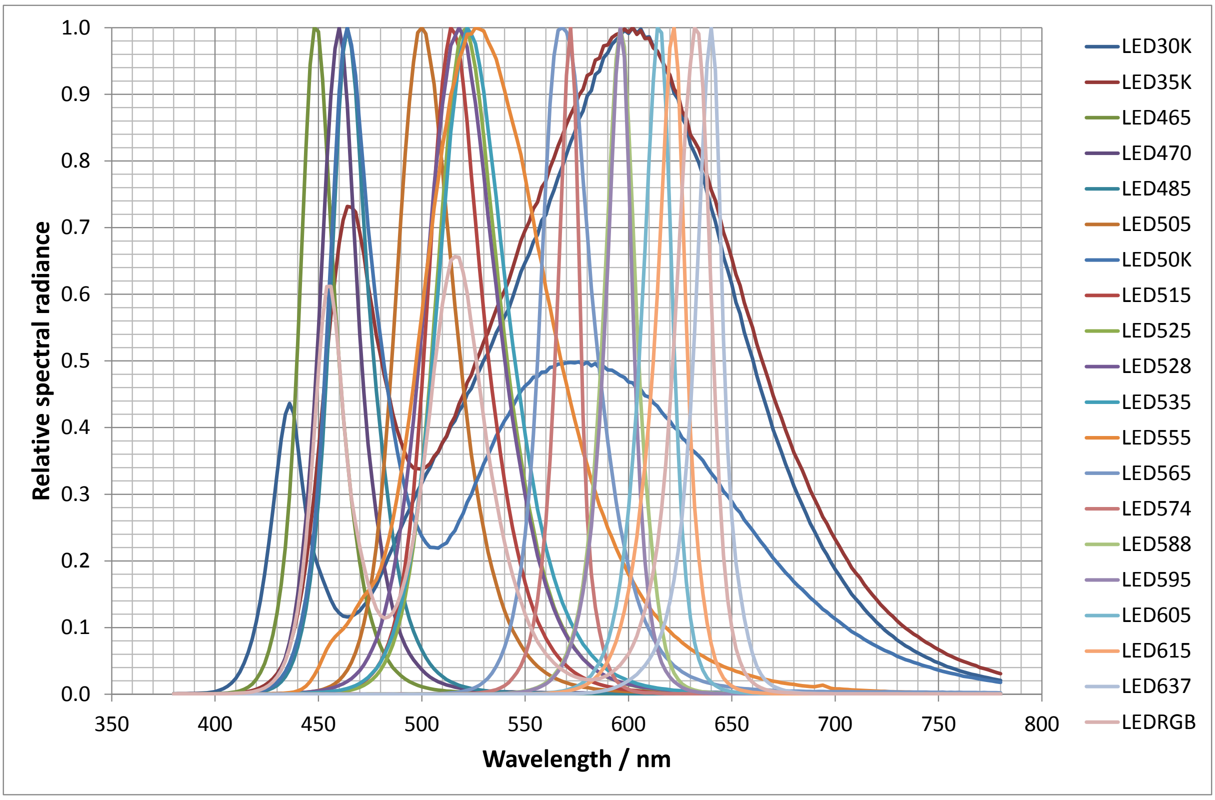

Figure 3 - Spectra of training sources.

If specific types of spectral sources are anticipated in the measurement then examples can be used (a training set) to minimise errors across the set. This no longer requires the spectral responsivities of the channels but instead requires that the tristimulus values of the training set are known. The optimisation can be for any specific derivative colour space or output quantity, e.g. CCT.

The training set should represent the typical variation in measured sources, such as those presented in Figure 3.

Figure 4 shows examples of where a training set is used. The plot on the left is for the least squares matching of the CMFs. Some sources among the training set show small errors whereas other show very large errors in Δx, Δy, $\Delta u'$, $\Delta v'$. By optimising the matrix to reduce the large errors, some of the small errors are made worse, as shown in Figure 4 (right) but a better all-round performance is obtained.

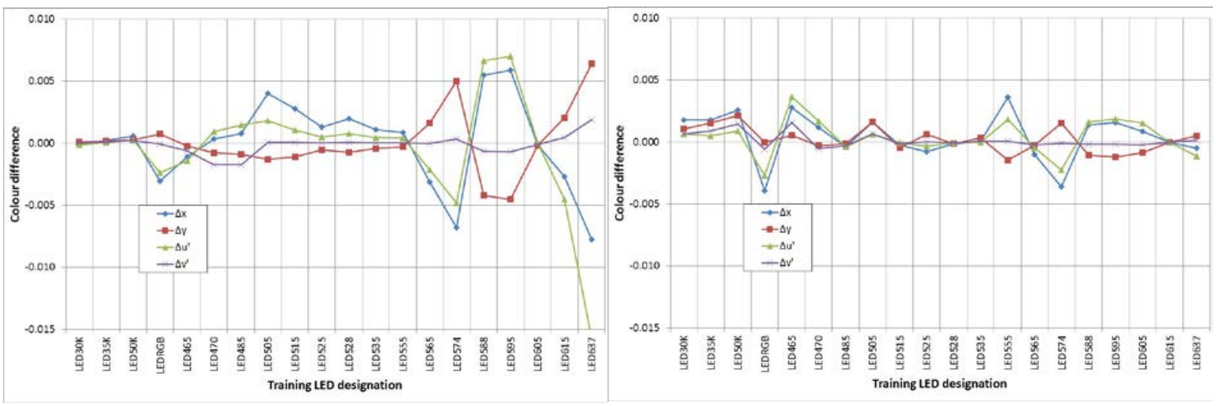

Figure 4 - Colour differences obtained by optimising the matrix for least squares fit to CMFs (left) and lowest average delta xy distance (right)

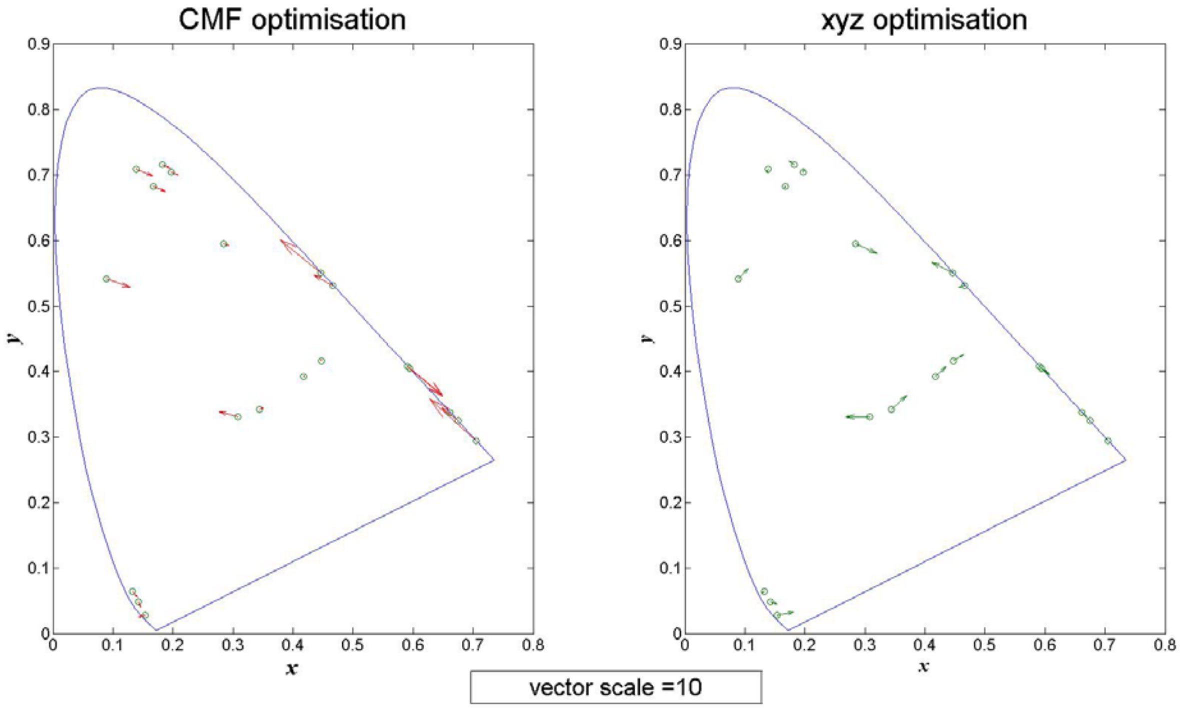

Figure 5 - Colour difference vector plot of training sources corresponding to those shown in Figure 4. Note the vector scale = 10 for clarity.

This can also be seen in the colour difference vector plot of Figure 5. Here we can see that for the CMF optimisation, the white sources near the centre of the plot show low errors (with the exception of the RGB LED) but red LEDs give large errors. When the CIE xy optimisation is performed the red LEDs have much lower errors but the error for white LEDs has increased.

The optimisation has consequences for the measurement of other sources however, especially those outside the gamut of the training set. Figure 6 illustrates that errors may increase for some sources near the monochromatic locus.

It is important therefore that the training set includes all the desired sources to be measured. However, some sources might be considered more important than others in terms of accuracy, and this can be accommodated using weighting factors in the optimisation.

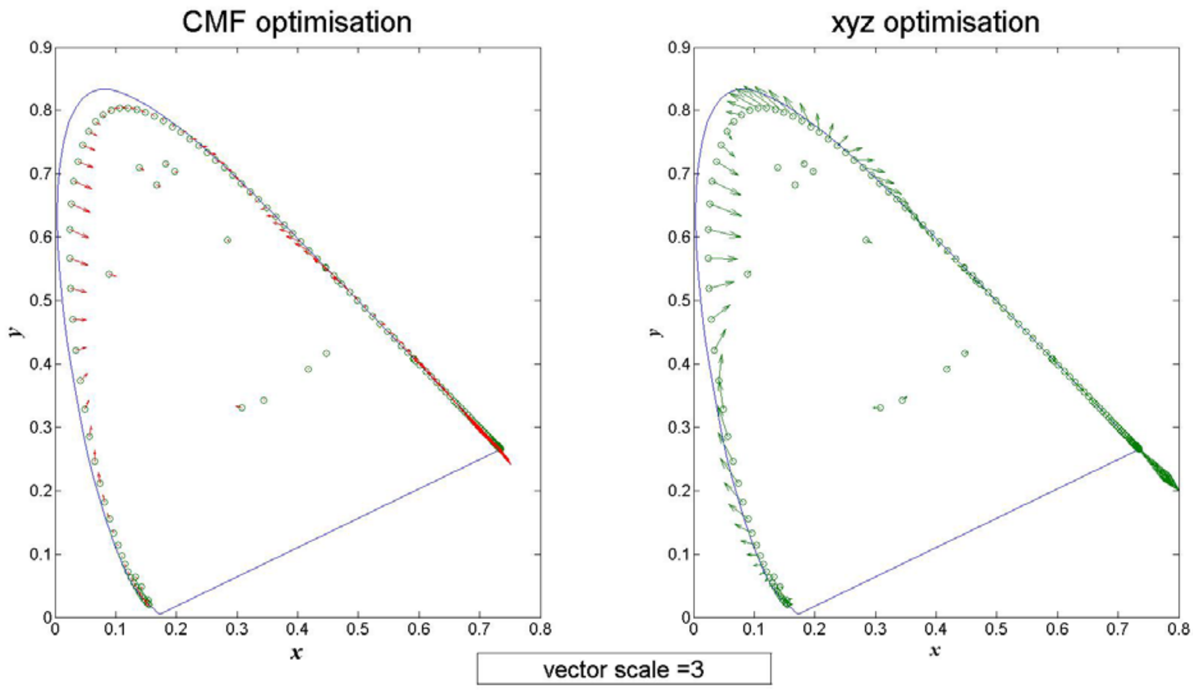

Figure 6 - Colour difference vector plots corresponding to the optimisations in Figure 4. This is the same as Figure 5 but with simulated sources added and the vector scale = 3 to prevent overshoots outside the plot area.

Obviously, there can be as many adaptive matrices as there are output parameters, so each can be individually optimised. However, if this is done then it should be noted that they are no longer related by normal transforms and should not be interconverted.

4 Study of test sources

A study of 22 samples including LEDs and filtered incandescent sources, which were not included in the training set, was made. Each source was measured using a quality spectroradiometer and a colorimeter possessing the basic 4 filters (normal) or 6 filters (enhanced). The 6 filter system was optimised for minimum xy differences.

Figure 7 shows the results of the study as colour difference vector plots. Note that the vector scale is 10 to clearly show the errors involved. Although white sources are accurately measured with the 4-channel system, coloured sources give large errors. In contrast, the errors for all sources are small using the 6-filter system.

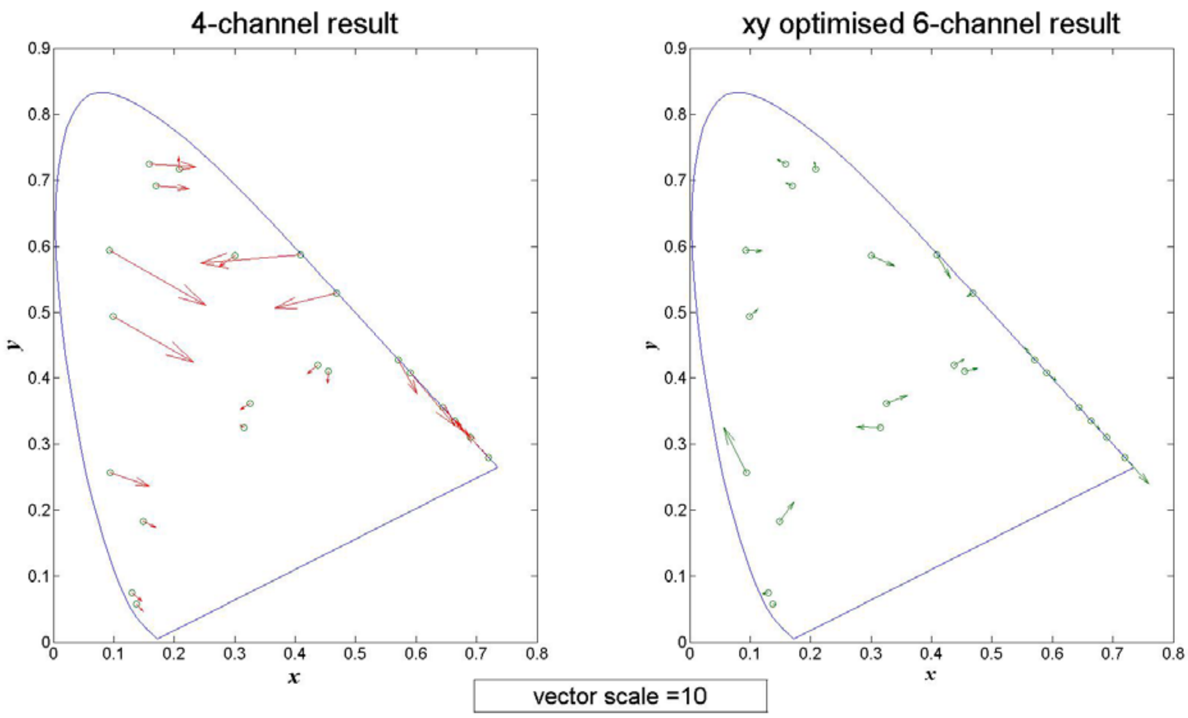

Figure 7 - Study results using a 4-channel filter (left) and 6-channel optimised systems (right).

5 Conclusions

A colour difference vector plot is an effective visualisation tool to appreciate the errors inherent in measurements of sources. When compared to a 4-channel imaging colorimeter, a 6-channel system dramatically decreases errors for most sources.

Optimisation of the adaptive matrix can be generalised for all sources by a least squares fit to CIE colour matching functions. This optimises the effective responsivity of the system and does not require prior knowledge of the source to be measured. It does require values for the channel spectral responsivities however.

If however, knowledge of the tristimulus values for sources is available, the adaptive matrix can be optimised to a specific output parameter, e.g. CIE xy, uv or u′v′ chromaticities, CCT, colour rendering index etc. The spectral responsivities of channels are no longer required. Optimisation using a training set and a target algorithm will generally reduce errors but for some sources, especially outside the gamut of training sources, errors may increase. Optimisation can include weighting if some sources are more important than others in terms of accuracy.

A study of 22 samples, including LEDs and incandescent sphere sources, verified the benefits of using an enhanced (6-channel) instead of a normal (4-channel) system.

References

EPPELDAUER, G.P. 1998: Spectral Response Based Calibration Method of Tristimulus Colorimeters, J. Res. Natl. Inst. Stand. Technol. 103, 615

JENSEN, J.J. 2013. Advantages and Applications for the Use of Imaging Colorimeters, Proc., CORM 2013 Conference, CORM

KOSZTYÁN, Z.T., EPPELDAUER, G.P., SCHANDA, J.D. 2010. Matrix-based color measurement corrections of tristimulus colorimeters, Applied Optics, 49, 12, 2288-2301

KOSZTYÁN, Z.T., STURM, S., MÜLLER, D., SCHANDA, J. 2008. Decreasing Colour Measuring Systematic Error in Image Taking Tristimulus Colorimeters, CIE x033:2008, Proc. CIE Expert Symposium on Advances in Photometry and Colorimetry, 21-25.

OHNO, Y., HARDIS, J.E. 1997. Four-Color Matrix Method for Correction of Tristimulus Colorimeters, Proc., IS&T Fifth Color Imaging Conference, 301-305

SCHANDA, J.D., KOSZTYÁN, Z.T. 2008. Industrial colorimetry with image resolution, Proc., Bulg. Colour Conference, Varna, 1-5

OP63

A NOVEL CONTINUOUS SCANNING METHOD FOR GONIOSPECTRORADIOMETRY

Li, S., **Chen, C.**, Li, Q., Pan, J.
EVERFINE INSTITUTE OF OPTOELECTRONICS
everfine@everfine.net

Abstract

The traditional scanning mode for goniospectroradiometry is the step rotating mode. This mode is widely used and accepted, but it does cost long measurement time. A novel continuous scanning method will be introduced in this paper. Using this method, the goniospectroradiometer is performing the measurement while rotating. Measurement simulations are given, the simulation results indicate that the continuous scanning method is time-saving and effective.

Keywords: goniospectroradiometry, continuous rotating scanning, step rotating scanning, time-saving

1 Introduction

The measurement for spatial distribution of spectroradiometric quantities for radiation sources is very informative and valuable since the radiometric quantities, photometric quantities and colorimetric quantities can be calculated from the spectroradiometric quantities. Especially for LEDs, the uniformity of spatial chromaticity distribution (IES, 2008[1]) and the risk of the photobiological safety (IEC, 2006[2]) can be both evaluated by the goniospectroradiometry.

For the measurement, the goniospectroradiometer is commonly used. The traditional measurement scanning is typically based on the step rotating (SR) mode which means the scanning procedure is “rotate - stop and measure - rotate” (CIE, 1996[3]). However, this scanning mode costs much measurement time and causes instability during the switch between start and stop of goniospectroradiometer. Furthermore, the long measurement time results in that the drift of the radiation source cannot be negligible and increases the measurement errors.

This paper will introduce a novel scanning method based on continuous rotating (CR) mode for goniospectroradiometry. Using this CR mode, the goniospectroradiometer will rotate smoothly and uniformly in a measurement plane and cost less measurement time. Typical distributions of spectroradiometric quantities and CCT of some LEDs are simulated and measured by both the CR mode and the SR mode. The simulation results indicate that the CR mode is time-saving and can also keep high measurement accuracy comparing with the SR mode. The CR mode is another practical solution for goniospectroradiometry of LEDs in addition to the SR mode.

2 Principle of CR mode

For CR mode, the goniospectroradiometer is rotating while conducting measurement. The angle range of measurement can be called the signal integration interval (SII). The measured value is in fact the average integration result in the SII and the sampled angular position is the middle of the SII. An operation interval lies between two SIIs. Fig. 1 gives the schematic of CR mode.

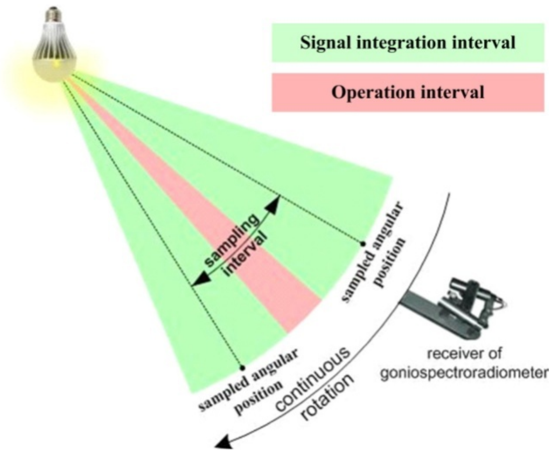

Figure 1 – The schematic of CR mode

Here gives the formula expression of CR mode to specify its principle. The measured signal can be expressed as

$$g_m(C,\hat{\gamma}_i)=\int_{\gamma_i}^{\gamma_i+a(C,\gamma_i)} g(C,\gamma)/a(C,\gamma_i)\,d\gamma \tag{1}$$

$$\gamma_i=\gamma_0+\sum_{j=0}^{i} a(C,\gamma_i)+i\,a_o(C,\gamma_i)\ ,\ \hat{\gamma}_i=\gamma_i+\frac{a(C,\gamma_i)}{2} \tag{2}$$

where, γ_0 is the start angular position of one C measurement plane. $\hat{\gamma}_i$ is the i-th sampled angular position, γ_i is the start angular position of the i-th SII $a(C,\gamma_i)$, $g(C,\hat{\gamma}_i)$ and $g_m(C,\hat{\gamma}_i)$ are the real and measured signals at $\hat{\gamma}_i$, respectively. $a_o(C,\gamma_i)$ is the OI between two consecutive SIIs for goniospectroradiometer to obtain the measurement data, decide the next start position of measurement, calculate the integration time of next SII and send the measurement start signal. The corresponding rotation time is called operation time $t_o(C,\gamma_i)$. The sampling interval $a_I(C,\hat{\gamma}_i)$ can be expressed as

$$a_I(C,\hat{\gamma}_i)=\frac{1}{2}\big(a(C,\gamma_i)+a(C,\gamma_{i+1})\big)+a_o(C,\gamma_i) \tag{3}$$

which is shown in Fig. 2.

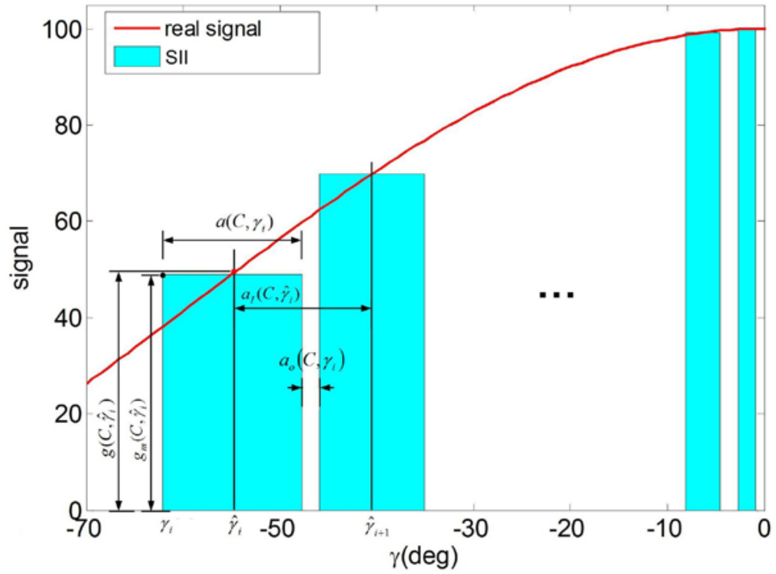

Figure 2 – The principle of CR mode

3 One implementation of CR mode requiring radiometric pre-measurement

The measured signal by goniospectroradiometer is spectral radiant intensity or spectral irradiance which is high dimensional. However, it is hard to use such high dimensional data to determine the SII and OI. Therefore, here gives two simplified methods: one is to concentrate the signal at certain wavelength where the variation of the signal is the most drastic; the other is to convert the high dimensional data to a one-dimensional index such as CCT.

For the CR mode, the sampling interval $a_I(C,\hat{\gamma}_i)$ is determined by the SII and OI and varies with them. The rotation speed of goniospectroradiometer ω(C) varies for different C measurement planes and keeps constant in each C measurement plane. It can be determined by the minimal integration time t_{min} and minimal SII a_{min}.

$$\omega(C) = \frac{a_{\min}}{t_{\min}} \tag{4}$$

The minimal integration time should be determined by the strongest spectral signal measured by goniospectroradiometer. The integration time t_{min} should ensure the reading of the strongest spectral signal to have good SNR.

In order to find the angle position where the strongest spectral signal lies and obtain absolute signal distribution, a pre-measurement by a gonioradiometer is done at each C measurement plane. Then, angular distribution of the readings related to the radiant quantities y(C,γ) can be obtained and the angle position of strongest signal γ_m can also be obtained, the corresponding maximal readings is defined as y_{max}. Then SII at different angle positions can be calculated based on a_{min}, y_{max} and y(C,γ).

$$a(C,\gamma_i) = \begin{cases} \dfrac{a_{\min} y_{\max}}{y(C,\gamma_i)} & \left(\dfrac{y_{\max}}{y(C,\gamma_i)} \le k_a\right) \\ k_a\, a_{\min} & \left(\dfrac{y_{\max}}{y(C,\gamma_i)} > k_a\right) \end{cases} \tag{5}$$

where k_a is the coefficient which prevent the SII become too large.

The OI $a_o(C,\gamma_i)$ can be determined by the latest variation of the measured signal. If the variation is drastic, OI should be decreased to a small range. Otherwise, OI can be expanded. However, the expanded range cannot be too large since the large OI will lead to the missing of important sampled position. According to the above mentioned requirement, the determination rules of OI can be quite a lot. Here gives a simple realization:

$$a_o(C,\gamma_i) = k \cdot a_{\min} \;,\; k = f\left(\frac{|g_m(C,\hat{\gamma}_i) - g_m(C,\hat{\gamma}_{i-1})|}{g_m(C,\hat{\gamma}_i)}\right) \tag{6}$$

where the $f(\cdot)$ is a decreasing function of $|g_m(C,\hat{\gamma}_i) - g_m(C,\hat{\gamma}_{i-1})| / g_m(C,\hat{\gamma}_i)$.

4 Simulation and Discussion

A radiometric and CCT distribution of a LED lamp at a C measurement plane is simulated which is shown in Fig. 3. The CR mode requiring radiometric pre-measurement is used.

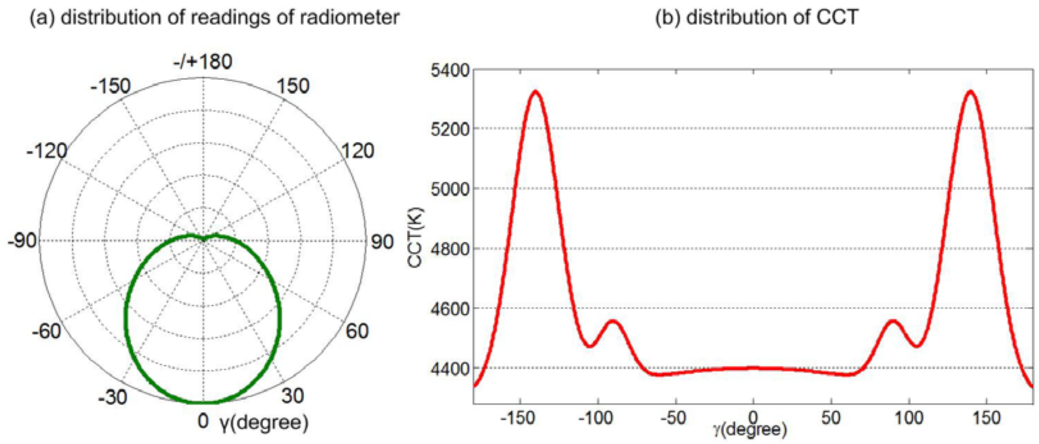

Figure 3 – The readings of radiometer and CCT distribution of simulated LED source

The minimal SII a_{min} is set to be 0.5°, k_a to be 10, the corresponding integration time is supposed to be 50ms. Then the rotation speed of goniospectroradiometer ω(C) is 10°/s. The distribution of SII and OI are given in Fig. 4. The real signal and measured signal are shown in Fig. 5. Fig. 6 gives the relative error between the real signal and measured signal. The maximal sampling interval is 10.5°, the minimal sampling interval is 2.5°.

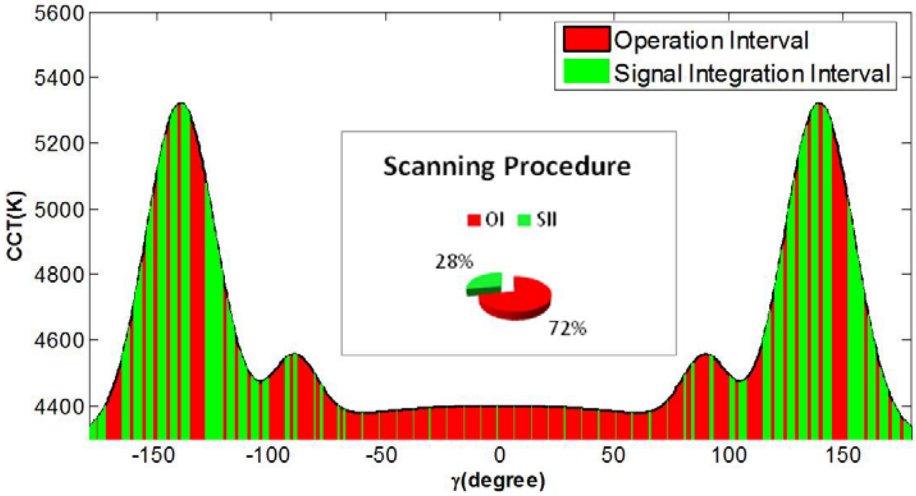

Figure 4 – The distribution of SII and OI

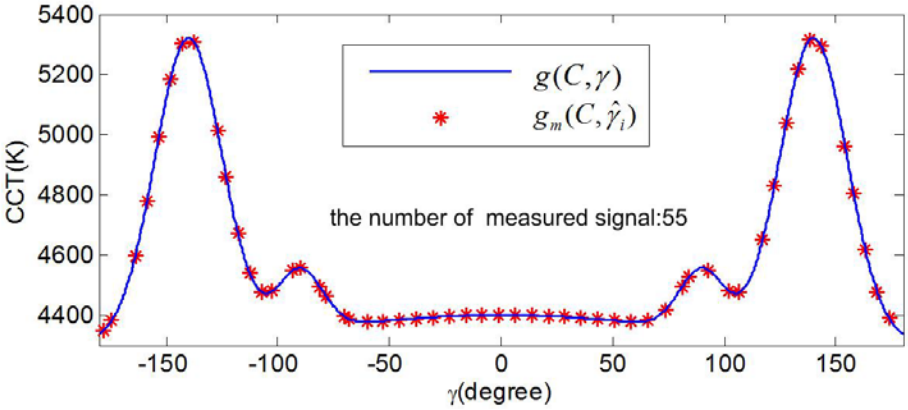

Figure 5 – The real signal and measured signal

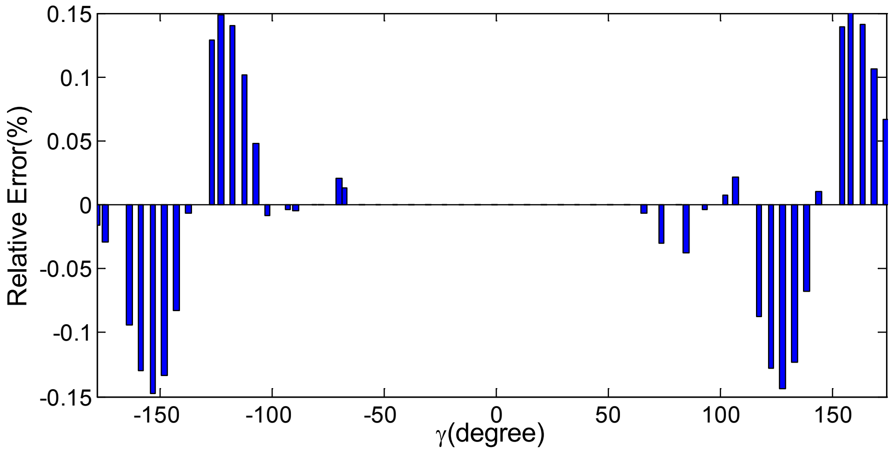

Figure 6 – The relative error between $g_m(C,\hat{\gamma}_i)$ and $g(C,\hat{\gamma})$

This C measurement plane of simulated LED lamp is also scanned with SR mode. Supposing its sampling interval is the same as the minimal sampling interval of CR mode, which is 2.5°, the time for moving from one sampling position to next sampling position and the stability of the switch between start and stop of goniospectroradiometer is 2s, the average time for adjusting the integration time at one sampling position is 2s. Then, the total time of SR mode can be calculated, which is 576s. For CR mode, supposing the pre-measurement by the gonioradiometer costs 60s, the acquirement of t_{min} costs 20s. Then, the total time for scanning is 116s which is much less than the total time of SR mode.

Based on the simulation results, it can be concluded that the advantages of CR mode are time-saving, fast adjustment of integration time and variable sampling interval. The fast adjustment of integration time is realized based on the radiometric pre-measurement and the minimal integration time t_{min}. The variation of sampling frequency is realized by the change of OI. When, the variation of measured signal is drastic, the OI is controlled to be a small range. Otherwise, the OI is larger. This determination can prevent too many sampling times at the angle range where the measured signal changes a little and make sure that the sampling times is enough at the angle range where the measured signal has drastic variation.

5 Another implementation with no pre-measurement

In this implementation, the head of the gonioradiometer and the receiving optics of goniospectroradiometer are both equipped on the rotation arm. The head of the gonioradiometer is just before the receiving optics of goniospectroradiometer along the rotation direction, which makes possible that the real time reading of gonioradiometer can be used to adjust the integration time of goniospectroradiometer. More research and work will be done for the realization of this implementation.

6 Conclusion

For goniospectroradiometry, the scanning method with CR mode is significant, since the smooth rotation not only reduces the instability during the switch between start and stop of goniospectroradiometer but also saves more measurement time. This mode will be a better choice for goniospectroradiometry than the SR mode for industry measurement.

References

[1] IES 2008. IES LM-79-08 Electrical and Photometric Measurements of Solid-State Lighting Products. New York: IES.

[2] IEC 2006. IEC 62471/CIE S009 Photobiological Safety of Lamps and Lamp Systems. Geneva: IEC.

[3] CIE 1996. CIE 121:1996 The Photometry and Goniophotometry of Luminaires. Vienna: CIE.

OP64

GONIOPHOTOMETRIC CHARACTERIZATION OF OPAQUE CONSTRUCTION MATERIALS (COOL MATERIALS)

G.Rossi[1], P. Iacomussi[1],M. Zinzi[2], E. Carnielo[2]
[1] INRIM, Torino, ITALY, [2] ENEA, Roma, ITALY
g.rossi@inrim.it

Abstract

In recent years the construction materials manufacturers introduced into the market an increasing number of innovative external coatings of roofs and facades, called *cool materials.* These materials have high solar reflectance values compared to conventional building materials. This propertie guaranties reduced solar radiation absorption and a limitation in surface temperature that normally rises in presence of high solar loads. Generally they have smooth surfaces with a reflection mode that presents a not negligible regular component. In this perspective the reflectance behaviour on incidence angle plays an important role on the estimation of solar gains and in lighting engineering applications. However its angular dependence is generally not well specified, while its knowledge is important because materials with similar shapes can appear differently to their visual appearance attributes. The paper introduces a method to compute the reflectance values of *cool materials, considering a reduced number of measurement directions* in order to calculate more accurately the energetic flows involved in the energy balances of buildings, to evaluate their visual impact under different lighting and viewing conditions and their behaviour considering the light pollution problem.

Keywords: e.g. Cool materials, BRDF, Reflectance, lighting engineering, solar gain.

1 Cool materials

The urban and the built environments play a crucial role in defining sustainable patterns in cities. Energy, environment and public health strategies need to be carefully addressed at urban level since it is expected that four of five EU citizens will live in urban areas by 2030 (IEA 2008, IEA 2009). The global warming emphasizes the consequences of urban sprawl: ambient temperatures increase with more frequent heat waves, with a longer duration. A typical effect of this condition is the Urban Heat Island (UHI) phenomenon, defined as the increase in urban air temperature compared to surrounding rural areas. UHI mainly depends on the modification of the land surface in the urban area, where the vegetation is replaced by built surfaces (typically paved roads and buildings), characterised by high solar absorption, high impermeability and thermal properties, which enhance the energy storage and the heat release, as well as by anthropogenic activities (GOLDREICH, Y. 2006, HASSID, S. 2000, HUANG, L. 2008, TAHA, H. 2000). The UHI also impacts the building energy and peak demand for cooling (KOLOKOTRONI, M. 2006, HASSID, S. 2000).
Cool materials are characterised by high solar reflectance and are able to remain cooler under the solar radiation, comparing to conventional materials of the same colour. These materials are also characterised by high infrared emissivity making them able to emit and dissipate the stored heat. These characteristics allow the material to reduce its surface temperature, with the consequent reduction of the heat released to the outdoor air by convection (mitigation the urban heat island effect) and to the built environment (reduction of the building cooling demand). Many recent studies demonstrate the benefits of cool materials at building and urban level (SYNNEFA, A. 2007, AKBARI, H. 1997, ZINZI, M. 2010, SYNNEFA, A. 2006, CARNIELO, E. 2013).
The solar reflectance is the key parameter to predict the thermal response of construction materials, however most of thermo-physical models consider constant the solar reflectance of surfaces during the daylight at every incidence angle of direct beam solar radiation assuming that each surface is lambertian (constant distribution of hemispherical radiance and independent by the incidence angle). This assumption may not be valid for some materials not

perfectly diffusive, especially at high incidence angle of direct radiation beam. This issue induces an overestimation of solar gains. Angular and directional properties of the reflectance are, as a consequence, needed to predict the thermal behavior of conventional and cool materials in a more accurate way.
The wide use of these materials has an impact in the lighting conditions of the urban area too. The directional distribution of the reflect light can modify their visual impact under different lighting and viewing conditions and, during night, can influence the light pollution level, changing the fraction of light diffused upwards.

2 Goniophotometry of materials

The knowledge of the reflection factor (a parameter that describes how much energy is reflected without specifying its directional distribution) allows a first estimation of the levels of illumination or irradiation due to the fraction of daylight (solar and sky light) or artificial light (during the night) reflected by the material. For more accurate calculations and simulations, the presence of preferential directions of reflection requires a goniometric characterization of the material reflection properties. This characterisation is generally obtained through the spatial measurement of the luminance (or radiance) coefficient *q,* indicated also as BRDF (Bi-directional Reflectance Distribution Function) (CIE 1979, CIE 1987).

BRDF measurements are very time consuming, the available databases consider a reduce set of material typologies and the metrological traceability of these data are often unknown. If not required by specific standard requirements, usually manufactures give global parameters only, like reflectance in the visible and solar regions and colorimetric coordinates.

Because of the time involved in goniophotometric and gonioradiometric measurements, it is interesting to find the best compromise between measurements time and details of results, identifying the minimum number of measurements necessary for a knowledge of BRDF, sufficient for the accurate evaluation of the material behaviour in thermal and lighting applications.

In this research, samples with different behaviour in reflectance (mostly Lambertian, mostly regular, diffuse regular and backscattering) were tested for their reflectance characteristics considering 4 different incidence angles (8°, 30°, 45° and 60°) and measuring the luminance coefficient *q* on the same plane of incidence. This was done to highlight the change of properties (from diffuse to specular) while increasing the inclination of the incident light. These measurements are carried out using the INRIM goniophotometer for materials characterization, considering only a relatively small number of measurement directions and measuring *q* in the visible range. The 15 samples measured were classified considering the above-mentioned four behaviours. The paper describes in details the measurements results of a sample for each category and proposes a simplified methodology to obtain the directional hemispherical reflectance values from the measured luminance coefficient values acquired in one (or two) plane(s). These results are compared with the measured values of directional - hemispherical reflectance carried out using an integrating sphere at ENEA.

2.1 The INRIM goniophotometer for material characterisation

The INRIM goniophotometer for material characterisation is an improved version of a previous design, ROSSI G. 1991. It is completely computer controlled and allows photometric measurement for any orientation of lighting and reflecting axes with reference to the sample axis. The reference coordinate system is on the sample surface, its origin is coincident with the rotating centre of the goniometer. Eight different movements are available to arrange the sample in all possible space orientation (Figure 1 and Figure 2).

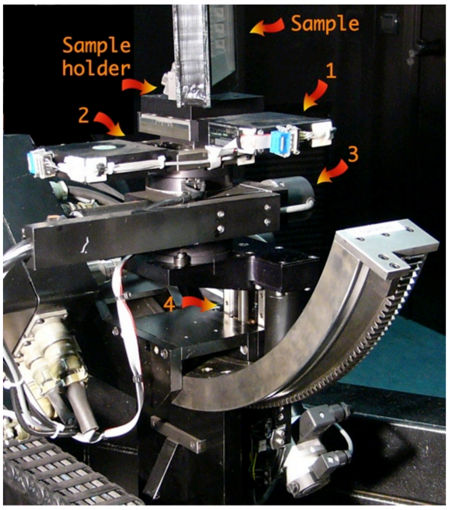

Figure 1 INRIM goniometer: mechanical movements of the sample

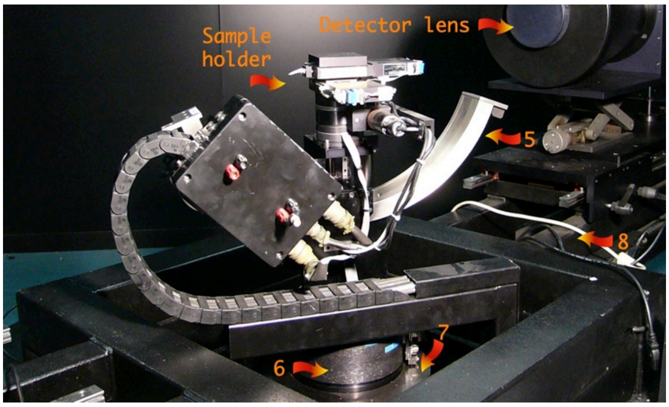

Figure 2 INRIM goniometer: the remaining mechanical movements, number 8 is for detector movement

The uncertainty on the linear position is about 10^{-2} mm, while 0,01° is the repeatability for angular rotations. The small deformations of the mechanical structure and the alignment accuracy allow to reach uncertainty of 0,1° on the definition of incidence and observation angles.

The luminance coefficient $q(\theta_i,\theta_o,\phi_i,\phi_o)$ is evaluated using a CCD camera (ROSSI G. 1995).

$$q(\theta_\mathrm{i},\theta_\mathrm{o},\phi_\mathrm{i},\phi_\mathrm{o}) = \frac{L(\theta_\mathrm{o},\phi_\mathrm{o})}{E(\theta_\mathrm{i},\phi_\mathrm{i})} \tag{1}$$

Where:

L is the luminance measured in the direction of observation (θ_o, ϕ_o);

E is the illuminance on the sample when lighted from the direction (θ_i,ϕ_i).

Both illuminance and luminance are measured with the CCD detector, therefore its calibration in SI units is not necessary and the luminance coefficient is related only to the ratio of exposure time (*T*) and of pixels counts (*C*) by a geometrical factor (*G*) when the source (subscription *s*) and the sample (subscription *o*) luminances are measured BO N. 2008.

$$q(\theta_\mathrm{i},\theta_\mathrm{o},\phi_\mathrm{i},\phi_\mathrm{o}) = G(\theta_\mathrm{i},\phi_\mathrm{i})\,\frac{C_\mathrm{o}\,T_\mathrm{s}}{C_\mathrm{s}\,T_\mathrm{o}} \tag{2}$$

2.2 Sample description

From the set of measured samples, four samples have been chosen as representative of different reflectance behaviour and considered in details in this paper. The different reflectance behaviours are:

1. mainly lambertian: no evidence of a specular or prevalent component in the reflection behaviour;
2. mainl regular with an evident reflection component in the regular direction;
3. regular diffusing: the reflection is mainly concentrated in the plane opposite to the incidence one, but no regular component is clearly recognizable;
4. backscattering: the reflection is mainly concentrated in the same plane of incidence, but it is not clearly recognizable a retroreflected component.

The list of samples and behaviours is summarized in Table 1.

Table 1 - Samples identifications

Behaviour	Sample no.	Type	Sample description	Sample surface
Mainly lambertian	8296	Normal	Concrete	
Mainly regular	8285	Cool	Smooth polyvinylic membrane – light gray	
Regular diffusing	8284	Cool	Rough polyvinylic membrane – gray	
Backscattering	8298	Normal	Clay brick	

The luminance coefficient of all samples has been measured in the observation plane ϕ_0=0-180° for four different directions of incidence: (θ_i=8°, ϕ_i=180°), (θ_i=30°, ϕ_i=180°), (θ_i=45°, ϕ_i=180°), (θ_i=60°, ϕ_i=180°).

3 Measurement results

For each sample the luminance coefficient graphs are provided in the following figures. The measurement uncertainty of the luminance coefficient measured values is 1,5%.

In all samples, as the incidence angle increases, the regular component increases too in a more or less relevant way. Therefore the above classification of samples reflectance behaviour must be considered qualitative and, often, referred to performances for angles of incidence less than 45 °.

The increase of the luminance coefficient in a given direction implies that, at equal illumination on the surface, the brightness will be higher in that direction than in others. From the lighting engineering point of view this feature is very interesting for buildings appearance, road light and lighting pollution calculations, as well as glare and veiling luminance ones, especially if the material is used in tunnel surroundings or in road lighting when mesopic conditions are considered.

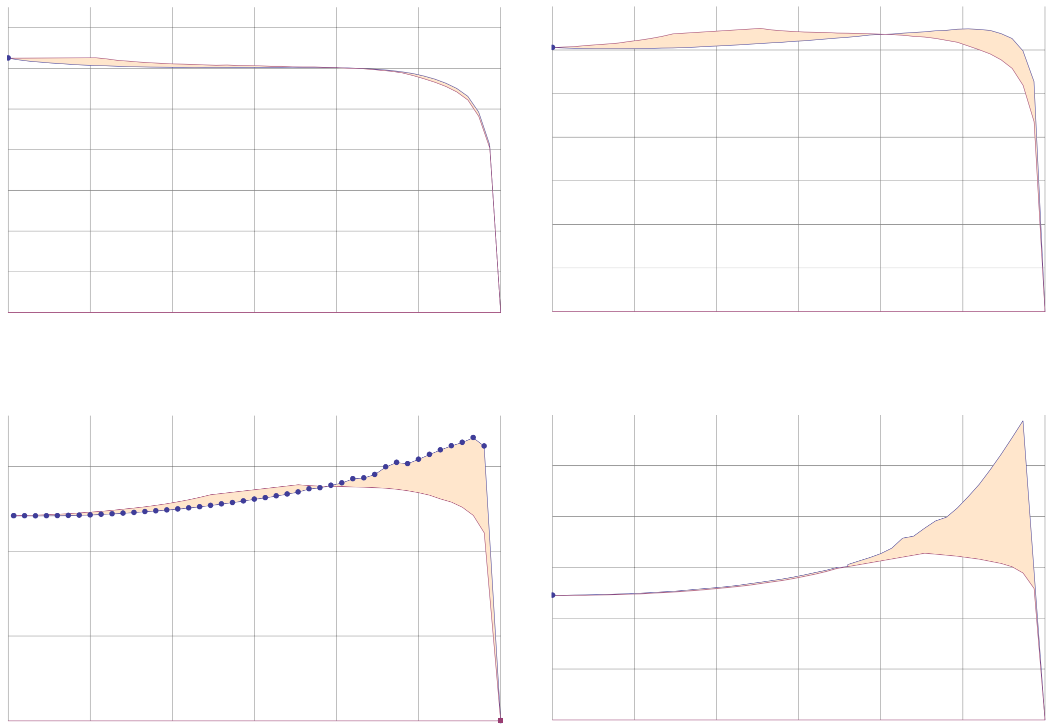

Figure 3 Luminance coefficient of sample 8296. Comparison between the two measured planes

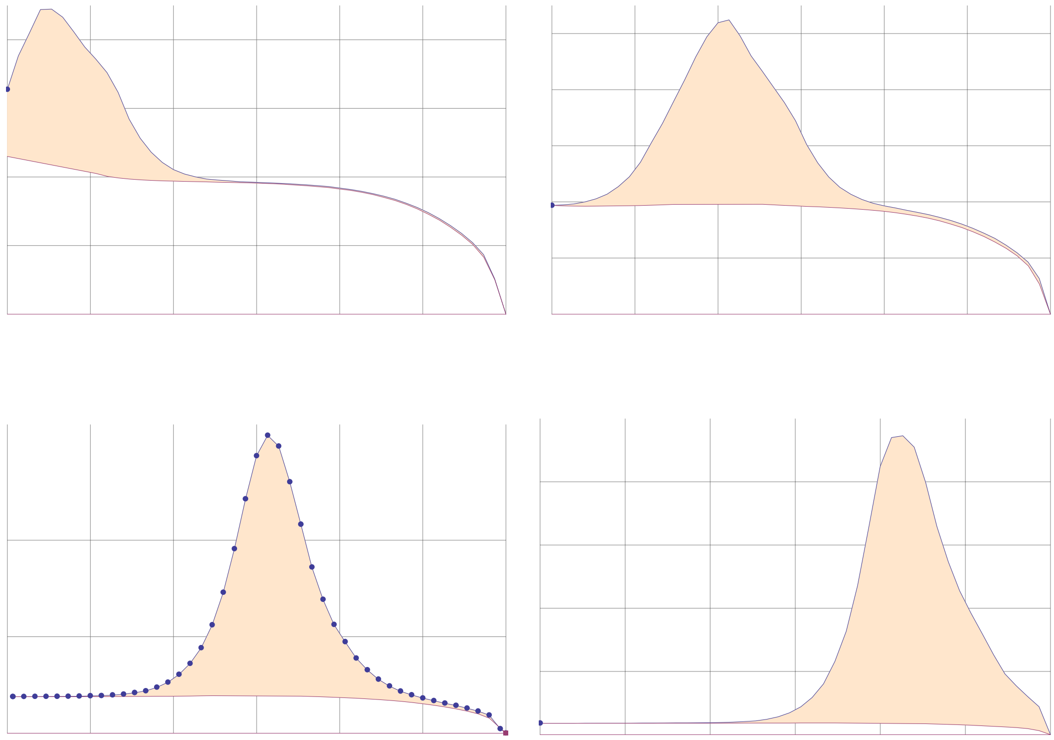

Figure 4 Luminance coefficient of sample 8285 Comparison between the two measured planes

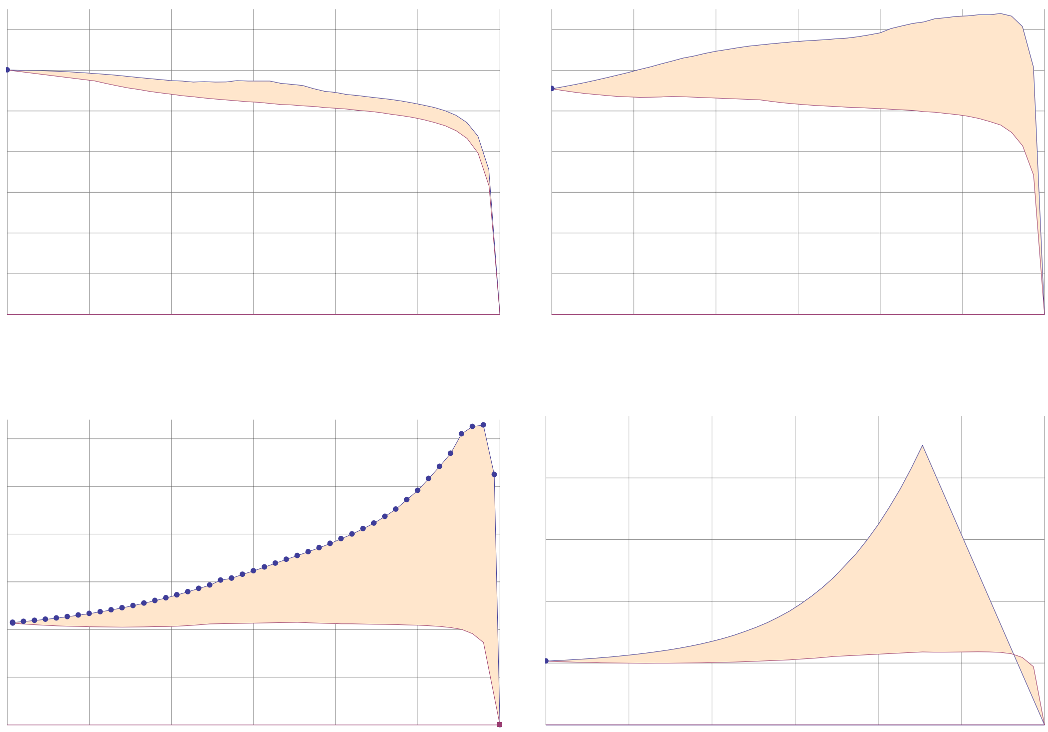

Figure 5 Luminance coefficient of sample 8284. Comparison between the two measured planes

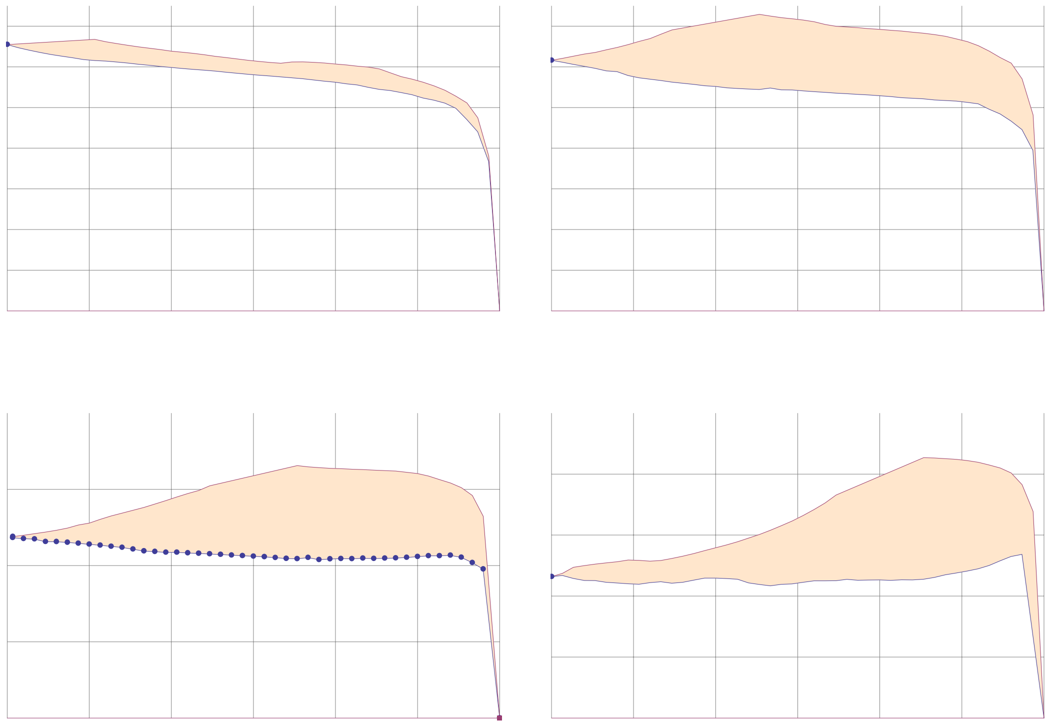

Figure 6 Luminance coefficient of sample 8298. Comparison between the two measured planes

3.1 Directional hemispherical factor

The directional-hemispherical reflectance factor, $\rho(\theta_i,d)$ can be calculated from the luminance coefficient data with the following numerical integration:

$$\rho_{\theta_i,\mathrm{d}} = \int_{\phi_o=0}^{2\pi} \int_{\theta_o=0}^{\frac{\pi}{2}} q(\theta_i, \theta_o, \phi_i, \phi_o)\, \cos\theta_o\, \sin\theta_o\, \mathrm{d}\theta_o\, \mathrm{d}\phi_o \tag{3}$$

where incidence and observation directions are as in (1).

Because the luminance coefficient has been measured only in the observation plane ϕ_0=0-180°, in order to numerically integrate the data, some approximations, related to the reflectance behaviour of the sample, are needed and should be verified. The hupetheses applied are described in Table 3.

The identification of regular and diffuse component is the largest source of uncertainty in the approximation used because was arbitrarily obtained comparing the results in the two measured half-plane. The calculated results are shown in Table 4.

The directional-hemispherical reflectance factor calculated by numerical integration has been compared to the measured directional-hemispherical reflectance factor obtained using the integrating sphere of the ENEA laboratory. The discrepancies are between 5% (materials with mainly lambertian reflectance) and 20% (materials with backscattering reflectance).

The ratio "total reflectance over diffuse reflectance" is an indicator of the relevance of the diffuse component at the growing of the incidence angle θ_i. As a matter of facts, as the inclination of the solar rays increases, the material behaviour changes from diffuse to specular, with an increase of the reflected regular component respect to the diffuse component. If this behaviour is associated to a cooling material of high solar reflectance, the advantages in reducing the UHI could be greater, if the reflected energy goes upward and not toward other buildings or road surfaces. Generally this advantage is underestimated because thermo-physical models consider only a lambertian behavior of the solar reflectance (constant distribution of hemispherical radiance independent by the incidence angle).

It is well known that the reflected component of road lighting installation light is the main part of the luminous flux that creates lighting pollution, because in urban area the luminaries are shielded by buildings (SOARDO, P. 2008). Considering, as a reference situation, a lambertiant material used for vertical surfaces (facades) or for horizontal surfaces (roof of low buildings), the vertical backscattering surfaces increase the luminous flux upward at high angles (respect to the horizon), while mainly regular or regular diffusing material in horizontal surfaces increase the luminous flux upward at low angles (the more important in increasing the sky artificial luminance). However, this flux can be shielded by higher buildings and a correct analysis of the variation of the luminance level due to the wide introduction of these materials can be done only by statistical models under development.

Table 2 - Description of approximation for solving the numerical integration

Reflectance behaviour	Approximation hypotheses
Mainly lambertian	The measured values of luminance coefficient in the ϕ_i=180° are extended to 90° ≤ ϕ_o < 270°, while measured values for ϕ_i=0° are extended to 0° ≤ ϕ_o < 90° and 0° ≤ ϕ_o < 90°
Mainly regular	The regular component is clearly identified and considered symmetrical around the direction of regular reflection. For the diffuse component, the same hypothesis of “mainly lambertian” material is used.
Regular diffusing	The regular component is clearly identified but it is not symmetrical around the direction of regular reflection. The measured shape of the peak in the plane ϕ_o=0° is used as weight function to reduce the *q* values also for the other azimuthal coordinates. For the diffuse component, the same hypothesis of “mainly lambertian” material is used.
Backscattering	As for “regular diffusing” but the reference plane for the peak shape is ϕ_o=180°.

Table 3 - Calculated directional-hemispherical reflectance factor

Sample No.	Calculated $\rho(\theta_i,d)$ for incidence θ_i=8°, ϕ_i=180°			Calculated $\rho(\theta_i,d)$ for incidence θ_i=30°, ϕ_i=180°			Calculated $\rho(\theta_i,d)$ for incidence θ_i=45°, ϕ_i=180°			Calculated $\rho(\theta_i,d)$ for incidence θ_i=60°, ϕ_i=180°		
	Total	Diffuse component	Ratio Diffuse/Total	Total	Diffuse component	Ratio Diffuse/Total	Total	Diffuse component	Ratio Diffuse/Total	Total	Diffuse component	Ratio Diffuse/Total
8296	0,309	0,309	0,999	0,322	0,311	0,965	0,341	0,319	0,937	0,365	0,344	0,943
8285	0,505	0,497	0,983	0,515	0,492	0,955	0,529	0,491	0,928	0,566	0,470	0,832
8284	0,278	0,274	0,988	0,284	0,270	0,953	0,292	0,275	0,940	0,312	0,282	0,905
8298	0,313	0,310	0,991	0,329	0,319	0,970	0,351	0,319	0,909	0,382	0,325	0,851

4 Conclusions

A set of cool and traditional materials has been measured in the visible range in order to verify if the lambertian assumption could be used to describe their reflection behaviour. This simplified assumption may not be correct for some materials not perfectly diffusive, especially at high incidence angle.

The results clearly show that goniometric investigations are absolutely necessary for more accurate evaluation of appearance (brightness) and thermal load calculation of materials used in urban area.

If the luminance coefficient is measured just in the incidence plane and some simplifying assumptions are adopted, the directional-hemispherical reflectance factor calculated by numerical integration has accuracies between 5% and 20%. Higher accuracies require more complex mathematical models or the measurement in a new plane accurately selected considering the results of the first measured plane.

References

AKBARI, H. 1997. Peak power and cooling energy savings of high albedo roofs. *Energy and Buildings*. 25, 117-126.

BO, N. 2008. CCD detector for diffusing materials and retroreflector. CIE Proceedings Expert Symposium, Torino 2008.

CARNIELO, E. 2013 Optical and thermal characterisation of cool asphalts to mitigate urban temperatures and building cooling demand. *Building and Environment*. 60, 56-65

CIE1979 CIE 44:1979. Absolute Methods for Reflection Measurements. Paris CIE

CIE1987 CIE 17.4:1987 CEI 50-845:1987. International Lighting Vocabulary. Genève CIE CEI.

GOLDREICH, Y. 2006. Ground and top of canopy layer urban heat island partitioning on an airborne image. Remote Sensing Environment. 104, 247-55

HASSID, S. 2000. The effect of the heat island on air conditioning load. *J. Energy Build.* 32(2), 131-141.

HASSID, S. 2000. The effect of the Athens heat island on air conditioning load. *Energy Build*. 32, 134-41.

HUANG, L. 2008. A fieldwork study on the diurnal changes of urban microclimate in four types of ground cover and urban heat island of Nanjing. *Build Environ*. 43,7-17.

IEA 2008. World energy outlook 2008. Geneva. International Energy Agency.

IEA 2009. World energy outlook 2009. Geneva. International Energy Agency;

KOLOKOTRONI, M. 2006. The effect of the London urban heat island on building summer cooling demand and night ventilation strategies. *Solar Energy*. 80(4), 383-92.

ROSSI, G. 1991. A new gonioreflectometer. CIE Proceedings 22nd Session, Melbourne 1991, pp 59-60

ROSSI, G. 1995. Photometric Characterization of Materials Through Gonioreflectometry. CIE Proceedings 23rd Session, New Delhi 1995, pp. 91-94

SOARDO, P. 2008. Compatibility of road lighting with star visibility. Lighting Research and Technology. 40. 307-322

SYNNEFA, A. 2006. A study of the thermal performance and of reflective coatings for the urban environment. *Solar Energy*. 80,968-981.

SYNNEFA, A. 2007. Estimating the effect of using cool coatings on energy loads and thermal comfort in residential buildings in various climatic conditions. *Energy and Buildings*. 39(11), 1167-1174.

TAHA, H. 2000. Meteorological and air quality impacts of heat island mitigation measures in three U.S. Cities. *Lawrence Berkeley National Laboratory R*eport. Berkeley. CA.

ZINZI, M. 2010. Cool materials and cool roofs: Potentialities in Mediterranean buildings. *Advances in Building Energy Research*. 4, 201-266.

OP66

UNCERTAINTY BUDGET ASSESSMENT FOR PRACTICAL ASSESSMENT OF THE RETINAL HAZARD OF EXTENDED LIGHT SOURCES IN ACCORDANCE WITH IEC 60825 AND IEC 62471 GUIDELINES

S.R.G. Hall[1], P. Miller[1], **T.M. Goodman[1]**, N. Haigh[2], D. Chan[2]

[1] National Physical Laboratory, Teddington, UK

[2] LUX-TSI Ltd, UK

simon.hall@npl.co.uk

Abstract

The rapid pace of technology has produced devices that have some characteristics of both lasers and “non-laser” devices .Examples of these optical sources are high brightness light emitting diodes and supercontinuum laser sources. This has led to an explosion of interest in the practical evaluation of the photobiological hazard posed by broadband extended light sources. The various photobiological safety standards, such as CIE S009, IEC 62471 and IEC 60825, provide indicative diagrams and information concerning the practical evaluation of the photobiological hazard potential of these sources. These involve:

- measurement of the spectral radiance and irradiance of the source under defined geometric conditions (these allow for factors such as the minimum size of image that can be formed on the retina and the effect of eye movements);
- weighting the results with a defined action spectrum (which allows for the relative spectral effectiveness of optical radiation for the specified photobiological effect) to determine the exposure hazard value (EHV); and
- comparison of the EHV with defined permissible limits (i.e. conditions under which it is believed that nearly all individuals in the general population may be repeatedly exposed without adverse health effects).

However, although these standards describe the measurement procedures and processes for determining the EHV for the source in question, the determination of the uncertainty associated with these measurements is seldom discussed. This paper will present an approach for establishing an uncertainty budget for assessment of photochemical and photothermal retinal hazards, based on evaluation of the practical limitations of the measurement equipment and procedures used and their impact on the measurement results. In particular, a simple software based stochastic process will be described, which allows the influence of the various uncertainty contributors to be explored dynamically; this helps to ensure that attention is paid to the most important contributory factors (such as field stop placement, spectral resolution etc.) so as to minimise the uncertainty associated with the determination of the EHV.

The use of this approach to determine the blue light hazard EHV for a white LED will be presented as an example. Based on this analysis, it will be shown that certain measurement uncertainties (such as the wavelength calibration of the spectroradiometer) have very little impact on the EHV, while others (such as the area of the field stop) are much more significant. This information could be helpful in preparing improved guidance for measurement procedures and for assessing ‘typical’ uncertainties for a given measurement set-up.

1 Introduction

The general philosophy for testing against a safety standard should involve the measurement of the device characteristics and an assessment of the uncertainty of those measurements. The conservative criterion for pass or fail should be:

$$Effective\ EHV = EHV(measured) - EHV(Uncertainty)$$

where EHV is the effective hazard value, which can be variously taken as the Acceptable Emission Limit (AEL) for laser devices or the Exposure Limit (EL) for non-laser sources.

The ever-increasing demand for optical radiation safety related testing is driven by both regulation (e.g. European Union ‘Artificial Optical Radiation Directive’ safety requirements) and appreciation of the potential hazard of these new sources. Examples include: lamps (UV); LEDs (UV, VIS, NIR) and high brightness LED lighting. In addition, the influence of the spectral composition of light on human circadian rhythms has recently exited interest; current research in this area involves the manipulation of the spectral power distribution of light sources to change the level of employee alertness and has the potential, for example, to alleviate jet lag and or reduce depression due to seasonal affective disorder.

2 Optical Hazard Testing

There are two main testing approaches for these sources: IEC 60825-1 ed2.0 Safety of laser products - Part 1: Equipment classification and requirements:2007; and IEC 62471 ed 1.0:2006 Photobiological safety of lamps and lamp systems.

The comparison of these methodologies highlights the differences built into the standards. These are due to simplifications and compromises used to simplify analysis; the damage caused by optical radiation is independent of the method of production but is changed by the optical characteristics of the source. The two ‘core’ measurement parameters are: spectral irradiance and spectral radiance, with measurements made over a defined ‘field of view’ where *‘field of view’* ≅ *‘acceptance angle’*. Various wavebands need to be considered, as indicated in Table 1.

Table 1: Optical wavelength hazard bands

IEC 62471 Hazard Band	Wavelength Range (nm)	Measurement Type
Actinic UV Skin & Eye	200 to 400	Irradiance
Eye UV-A	315 to 400	Irradiance
Blue Light ‘small’ source	300 to 700	Irradiance
Blue Light ‘extended’ source	300 to 700	Radiance
Retinal Thermal	380 to 1400	Radiance
Retinal thermal (weak stimulus)	780 to 1400	Radiance
Infrared hazard to eye	780 to 3000	Irradiance
Skin thermal hazard	380 to 3000	Irradiance

A double monochromator system (Figure 1) can provide an accurate measurement of the spectral power distribution of a source provided that the system has been well characterised. However, often this type of measurement is impractical due to the bulky and expensive nature of these systems. Array spectrometers are widely used but require ‘stray light’ correction due to the array detector’s spectral response profile. Greater attention is required to the ambient temperature deviation from the calibration temperature for measurements in the near infra-red for silicon arrays as the band gap is approached.

Several different measurement configurations can be used, depending on the quantity being measured and the hazard being considered: examples are shown in Figures 2 to 4.

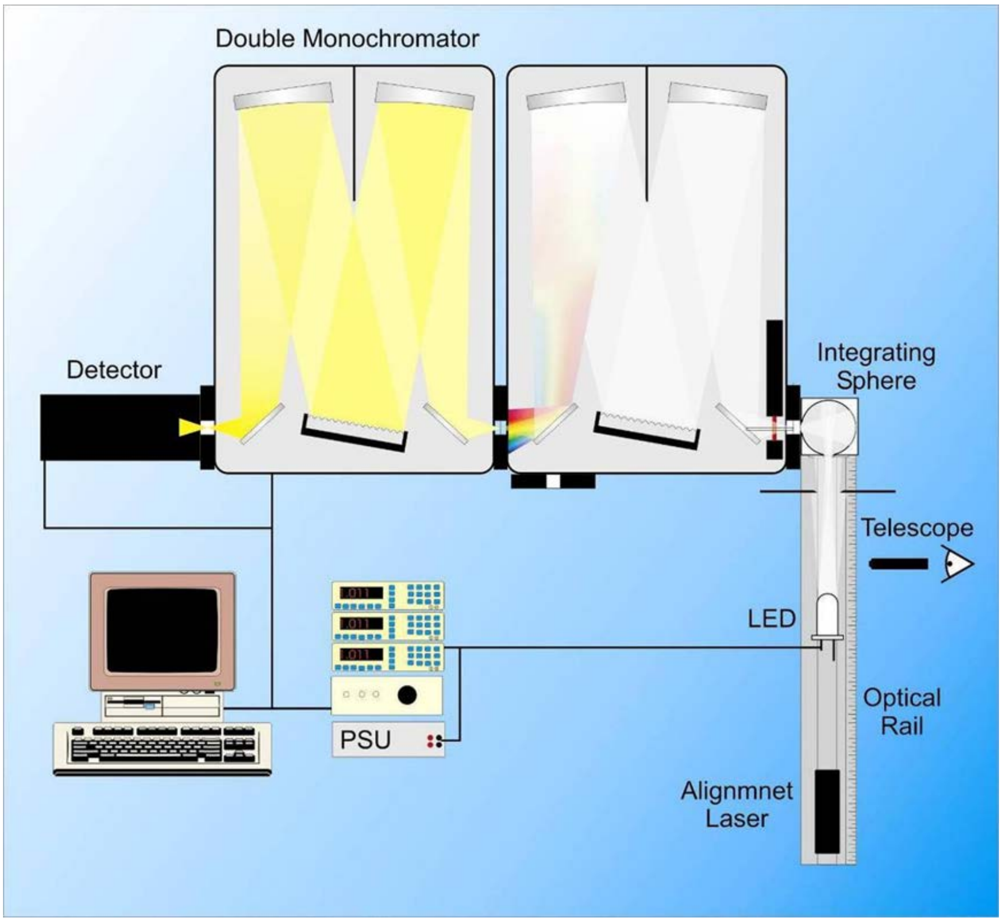

Figure 1: Spectral Radiometry - Double monochromator method

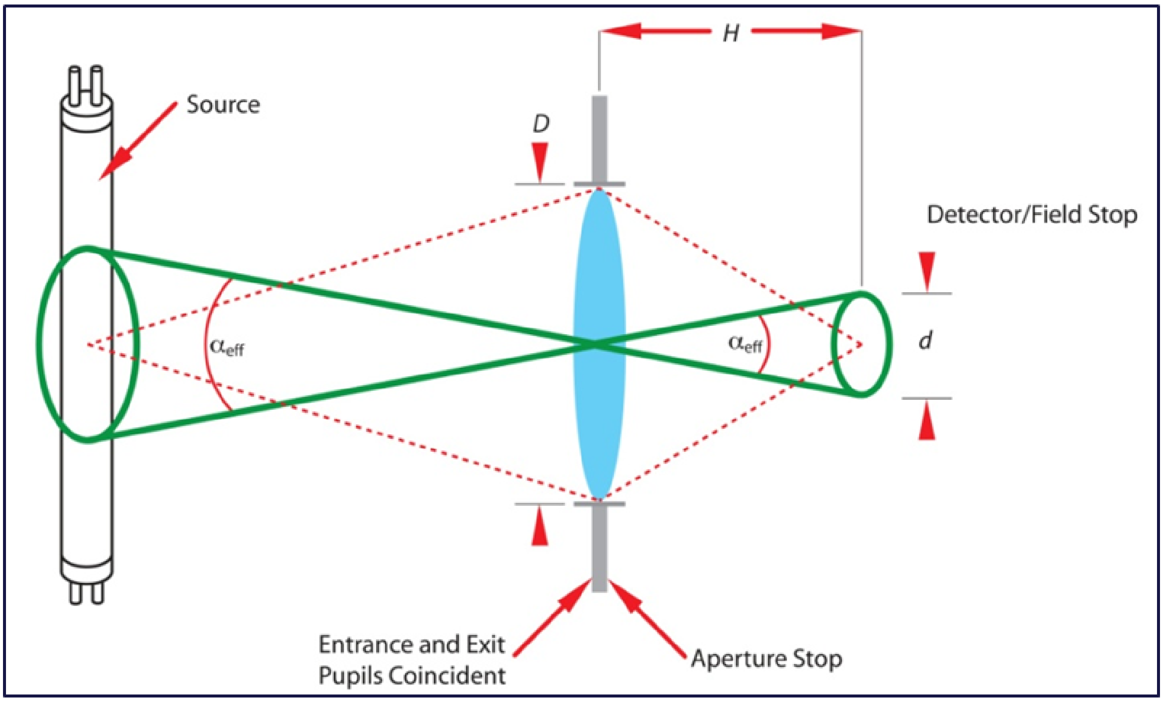

Figure 2: Test setup for radiance testing using IEC 62471 using a lens

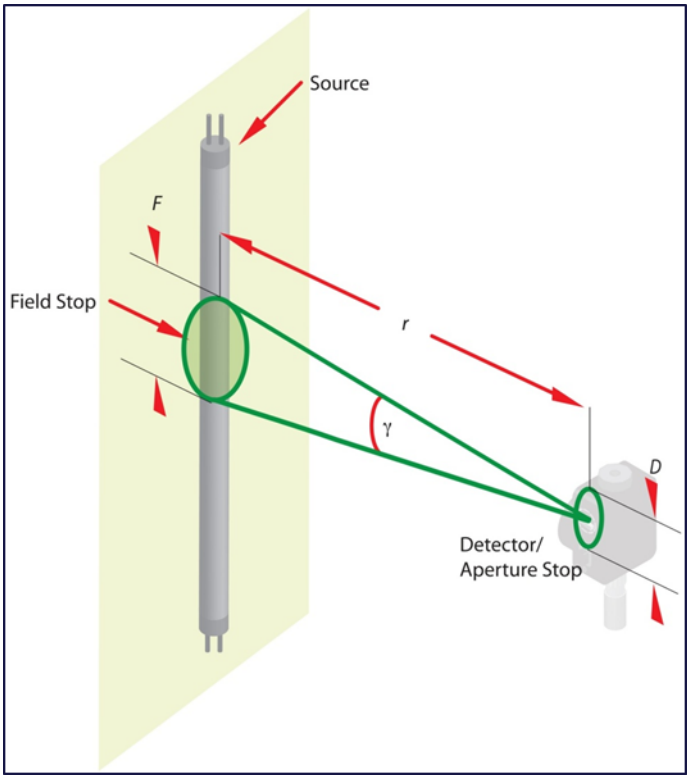

Figure 3: Alternative test method for source radiance: this requires the field stop to be placed close enough to the apparent source location to not alter the required field of view.

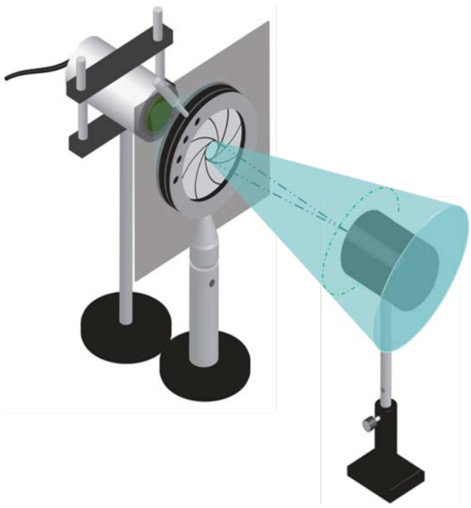

Figure 4: An example of a radiance measurement with commonly available laboratory components (not to scale)

3 Practical measurement

3.1 Defining the irradiance from the collected radiant power

At the core of any optical radiation safety analysis is a need to determine or measure the irradiance at a suitable plane that simulates where the beam is incident on human skin or eye. The irradiance is defined as the power per unit area, where for IEC 62471 analysis:

- The power is the optical radiation coupled through a test aperture
  - The test aperture (also called the ‘aperture stop’) is located just in front of the detector or optical power meter sensor
  - The aperture stop may also be defined by the detector diameter
- The area for the irradiance calculation is determined from the diameter of the aperture stop

Figure 5 shows from a practical perspective, how the irradiance is physically realised in an optical radiation safety test regime. Figure 6 shows how the irradiance is defined from the properties of the beam.

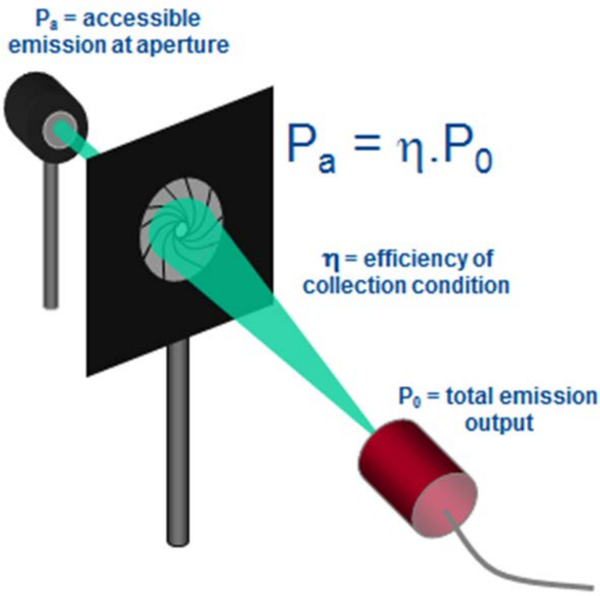

Figure 5: Practical irradiance measurement

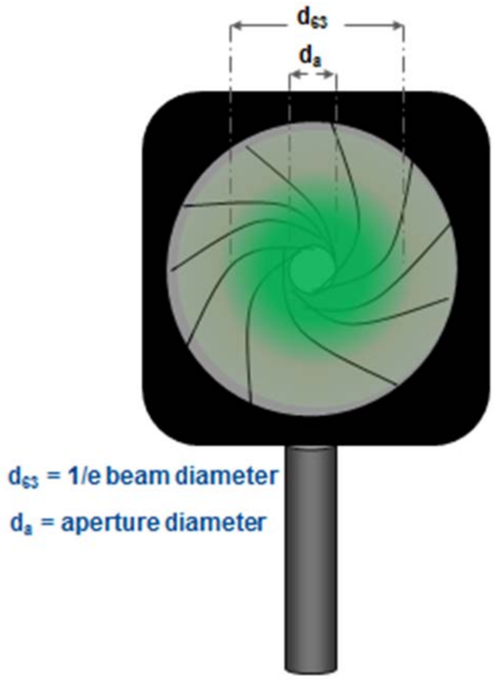

Figure 6: Irradiance = Power per unit detector area

3.2 Irradiance coupling

To effectively measure the radiant power it is required that there is uniform irradiance at the aperture stop. In this case the coupled power increases quadratically with stop diameter, but irradiance stays constant with changing aperture diameter, If we consider the situation where the irradiance has a Gaussian profile at the aperture stop, as is often the case with laser-type sources, the coupled power decreases exponentially with increasing stop diameter and the irradiance falls with increasing stop size. To try to combat this effect IEC 62471-1 recommends that a 7 mm diameter aperture is used unless the irradiance at the detector is spatially-uniform.

Table 2: EHV versus Detector Aperture Stop

Beam Divergence		d_{63} at 200 mm	Practical Stop Diameter	Gaussian Coupling Efficiency	Accessible Emission	EHV	Aperture Stop Irradiance
mrad	deg	mm	mm	%	uW		$W.m^{-2}$
100	6	20	6.9	11.2	30.8	0.97	0.80
		20	7	11.5	31.7	1.00	0.82
		20	7.1	11.8	32.5	1.02	0.84
500	29	102	6.9	0.457	30.8	0.97	0.80
		102	7	0.470	31.7	1.00	0.82
		102	7.1	0.483	32.6	1.03	0.84

Typically 2-3% EHV change per 100 micron diameter uncertainty

3.3 EHV versus detector aperture stop

As the aperture stop diameter is increased the detected radiant power should increase. Calculation of the EHV assumes a defined stop diameter e.g. 7.0 mm aperture stop at 200 mm distance. The use of a slightly larger aperture stop setting will overestimate the EHV result by typically 2 % to 3 %. The EHV increase for a Gaussian spatial profile beam at a stop that is set incorrectly by + 100 µm produces a conservative EHV outcome.

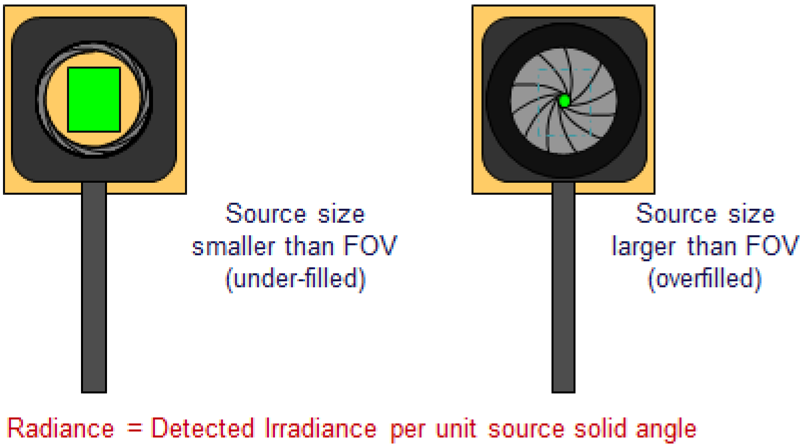

Figure 7: Spatially Averaged Radiance

The choice of the correct aperture stop size may depend on the risk category. Consider Blue Light Hazard (BLH) testing, for example. For the Exempt Condition, the following are specified:

- Exposure Time = 10000 s
- Acceptance Angle γ = 100 mrad (‘field of view’)

This implies a 20 mm diameter field stop located over the source

For Low Risk Condition, the conditions are:

- Exposure Time = 100 s
- Acceptance Angle γ = 11mrad

This implies a 2.2 mm diameter field stop located over the source.

The field stop diameter accuracy will clearly influence the resultant radiance result. The IEC 62471 standard Test Method recommends an ‘imaging’ setup as shown in figure 2 and as a practical arrangement (baffles removed for clarity) in figures 8 and 9.

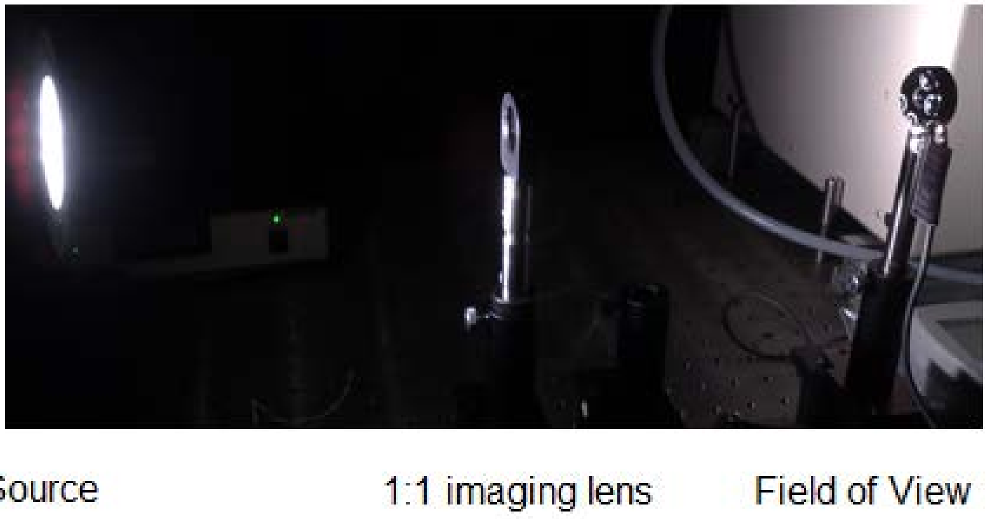

Figure 8: Low Risk BLH Imaging Method

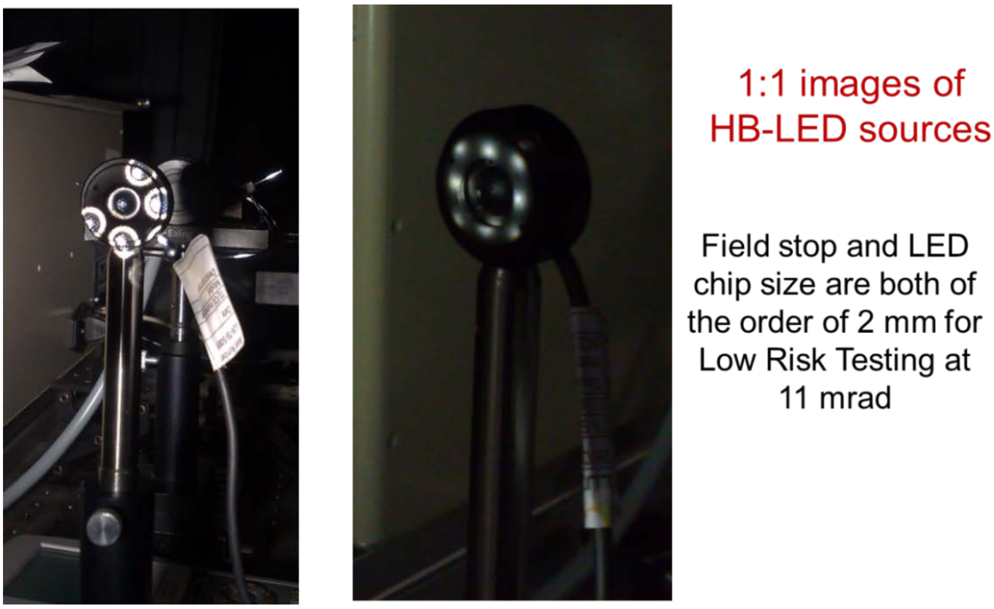

Figure 9: Low Risk BLH Imaging Method

The smaller the required acceptance angle,γ the higher the accuracy requirement on the field stop diameter setting (and its location within the field of view). The stop size uncertainty implies uncertainty of power coupled through the field stop, this results in increased uncertainty in radiance and EHV value.

If we assess the EHV due to power coupled through the field stop we find that the 11 mrad field stop can substantially vignette certain source types. If we assume a source exitance Gaussian spatial profile on the field stop, we find through the simulation that there is typically a 5% EHV change per 100 μm field stop diameter increase (Table 3). If, however, we assume a source with a uniform exitance spatial profile on the field stop, we find that there is typically a 10% EHV change per 100 μm field stop diameter increase (Table 4). A conservative approach to determination of the EHV would be to use slightly larger field stop setting than that specified in the standard.

Table 3: Simulation of Gaussian Profile Stop Coupling: 11 mrad FOV – Gaussian Coupling

Required Field of View (mrad)	Test Distance (mm)	Assumed Field Stop Diameter (mm)	Nominal LED Chip Diameter (mm)	Gaussian Coupling Efficiency (%)	Gaussian Coupled Power (uW)	EHV
11	200	2.1	2	70.18	36.5	0.95
11	200	2.2	2	66.8	38.4	1.00
11	200	2.3	2	73.33	40.1	1.04

Table 4: 11 mrad FOV – Uniform Coupling: Simulation of Uniform Exitance Profile Field Stop Coupling

Required Field of View (mrad)	Test Distance (mm)	Assumed Field Stop Diameter (mm)	Nominal LED Chip Diameter (mm)	Uniform Irradiance Coupled Power (uW)	Relative EHV
11	200	2.1	2	35	0.91
11	200	2.2	2	38.4	1.00
11	200	2.3	2	42	1.09

4 Uncertainty evaluation

For any measurement, a full uncertainty budget using both type A and B uncertainties should always be available, evaluated in accordance with the ‘Guide to Uncertainty in Measurement’. An estimate of the uncertainty due to the various influences in the measurement process can be simply produced by variation of input quantities and observing the effect upon the final result. This can be done conveniently with specially designed software. This paper uses an NPL designed package ‘Eyelight’ which has been licenced and developed by Lux-TSI.

4.1 Example of BLH uncertainty evaluation using sensitivity analysis

Radiance measurement depends upon: solid angle; field of view; acceptance angle; field stop diameter; spectral radiant power(or energy); wavelength; apparent source location (distance). The sensitivity of the final result to changes in each of these parameters must be determined in order to evaluate the uncertainty associated with this result.

As an example we used a several representative source spectral power distributions:

a. 440 nm indigo blue LED,

b. High brightness cool white LED,

c. Ultraviolet LED

In the first step, we adjusted the source metrics in the ‘Eyelight’ software to yield EHV = 1.0, see Figure 10.

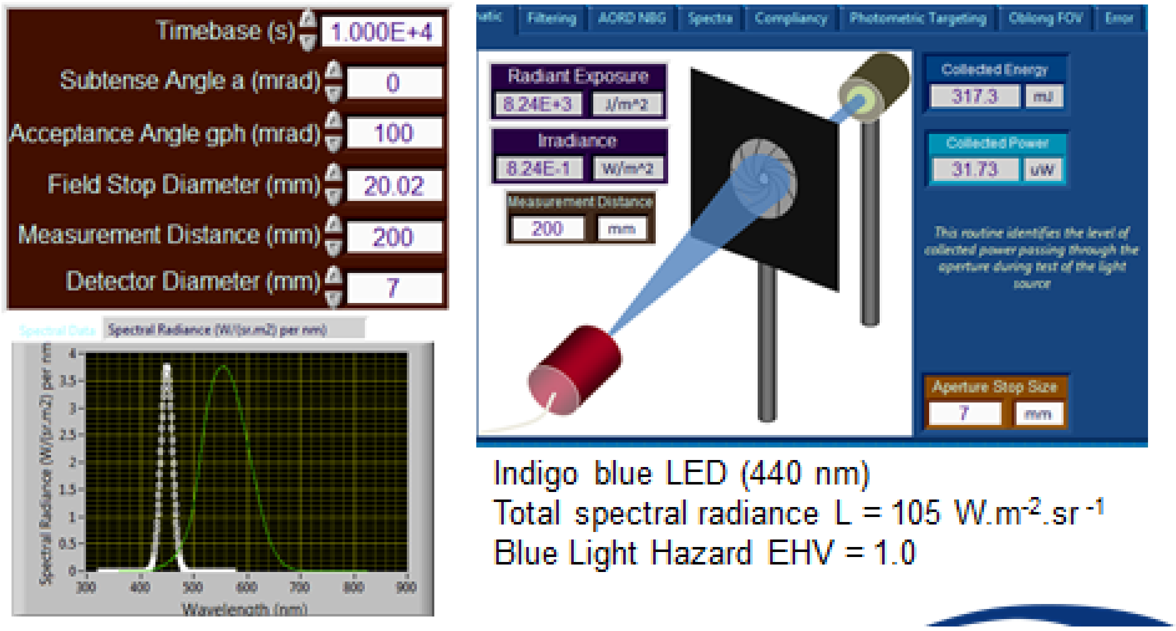

Figure 10: Metric scaling to produce an EHV=1

We then varied the measurement parameters and noted the influence upon the EHV Value. This was converted to a percentage difference to produce the uncertainty associated with a known degree of change for each parameter.

The influnce of translating the spectral power distribution up and down the wavelength scale with respect to the action spectra in theIEC 62471 standard was also investigated (Figure 11). The procedure for this was to define the spectrum of the light source and then to laterally displace it across the wavelength scale and to plot the resultant change in the EHV. In Figure 12 it can be seen for this example an uncertainty of 1% was introduced for every 10 nm offset.

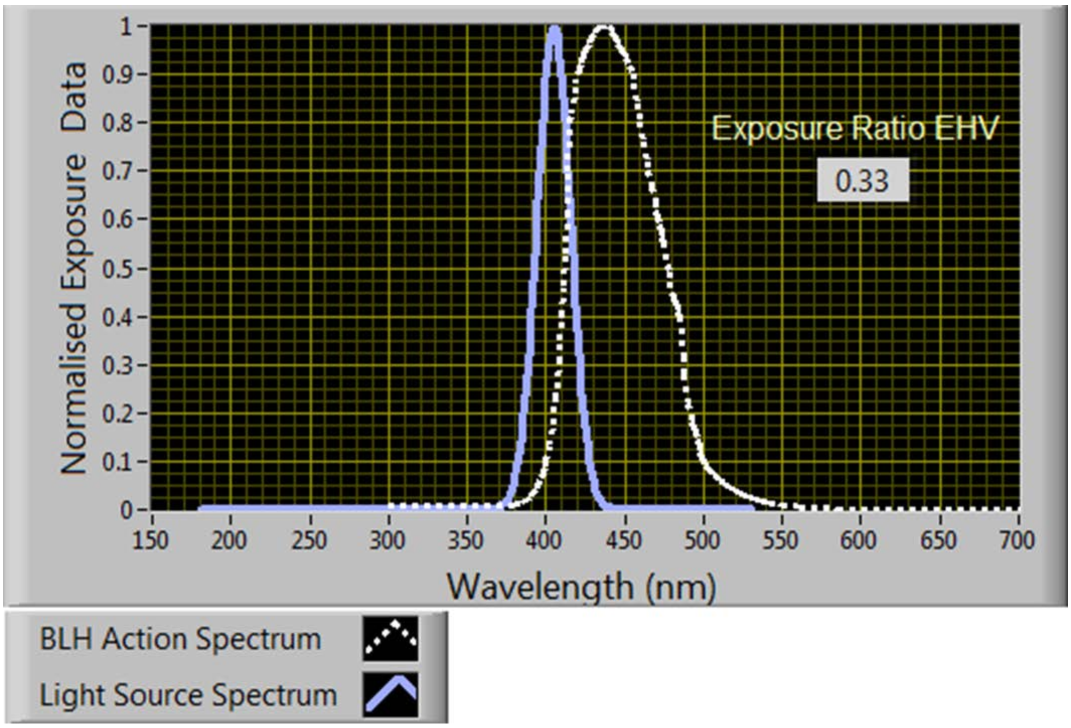

Figure 11: translating the spectral power distribution of a blue diode up and down the wavelength scale

,

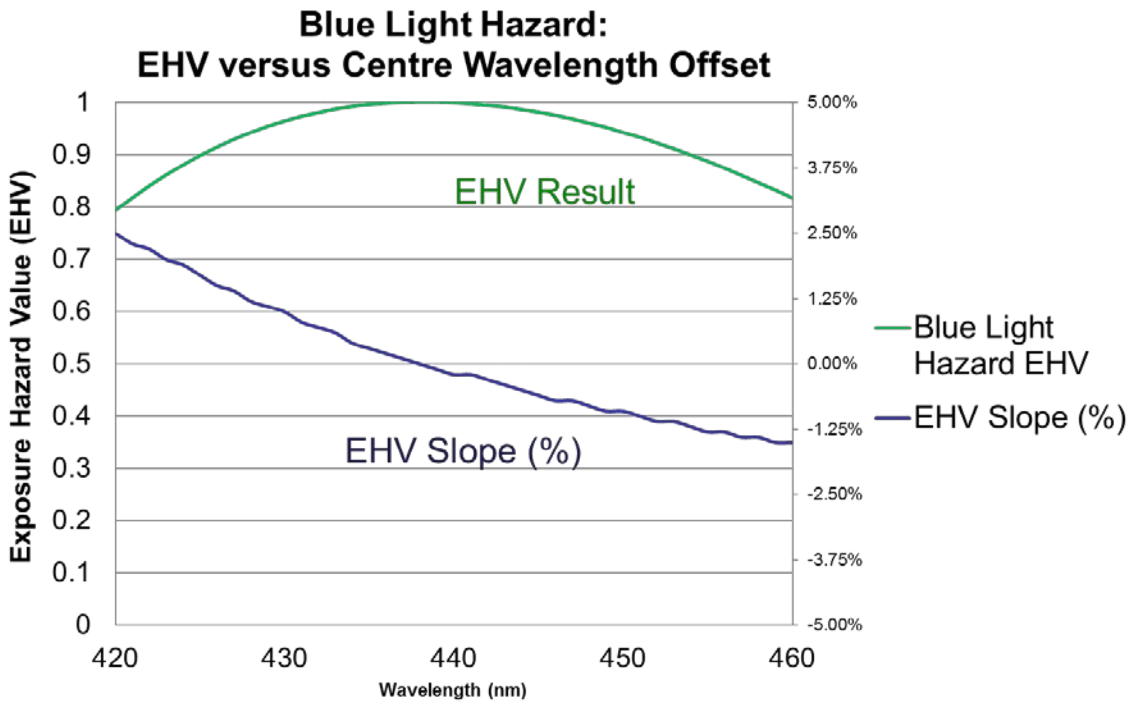

Figure 12: EHV – Spectral Analysis

A further source of uncertainty can be in the over- or under-estimation of the source spectral bandwidth. In Figure 13 the software analysis shows a 2% change for just 5 nm increase in the Full Width Half Maximum (FWHM) spectral bandwidth.

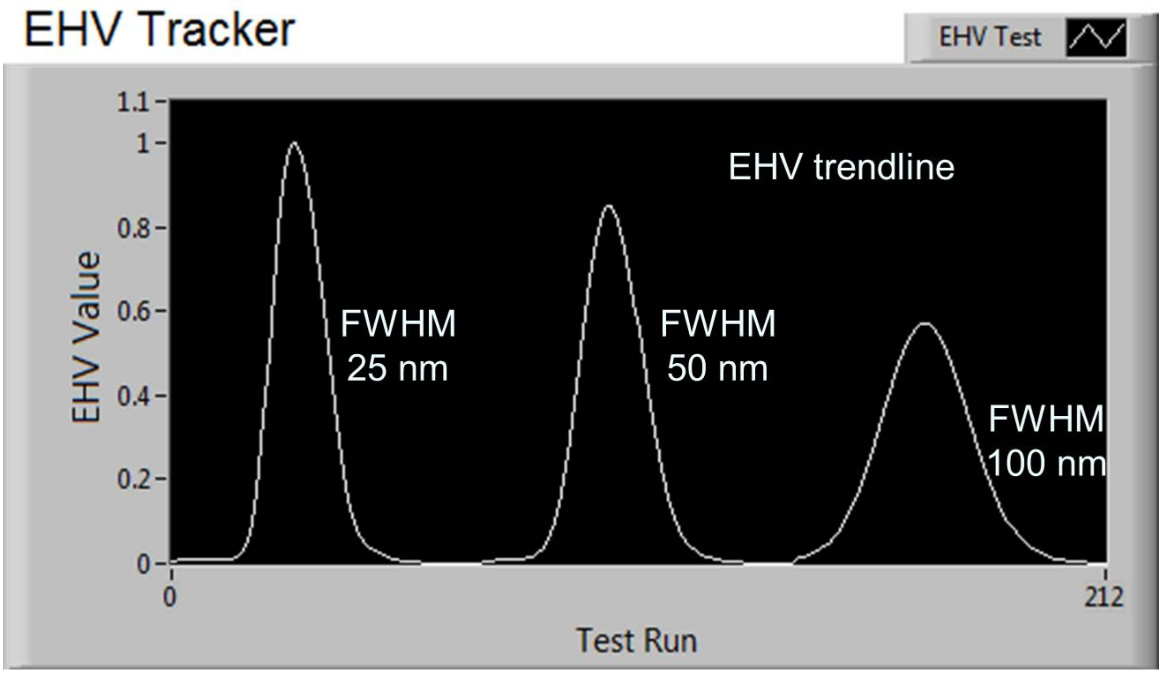

Figure 13: Dynamic EHV Tracking as the source spectral bandwidth is changed

One of the largest sources of uncertainty is due to the field stop diameter uncertainty. As an example, consider an LED chip evaluated at 200 mm for 'Low Risk' Blue Light Hazard LED EHV. For the purposes of this analysis, we assume:

- o LED Chip diameter is 2.0 mm
- o Gaussian ‘exitance’ profile
- o Field Stop at 200 mm has a diameter of 2.2 mm

Analysis using the ‘Eyelight’ software gives the results shown in figure 14 i.e. typically 5% EHV change per 100 μm field stop diameter increase.

.

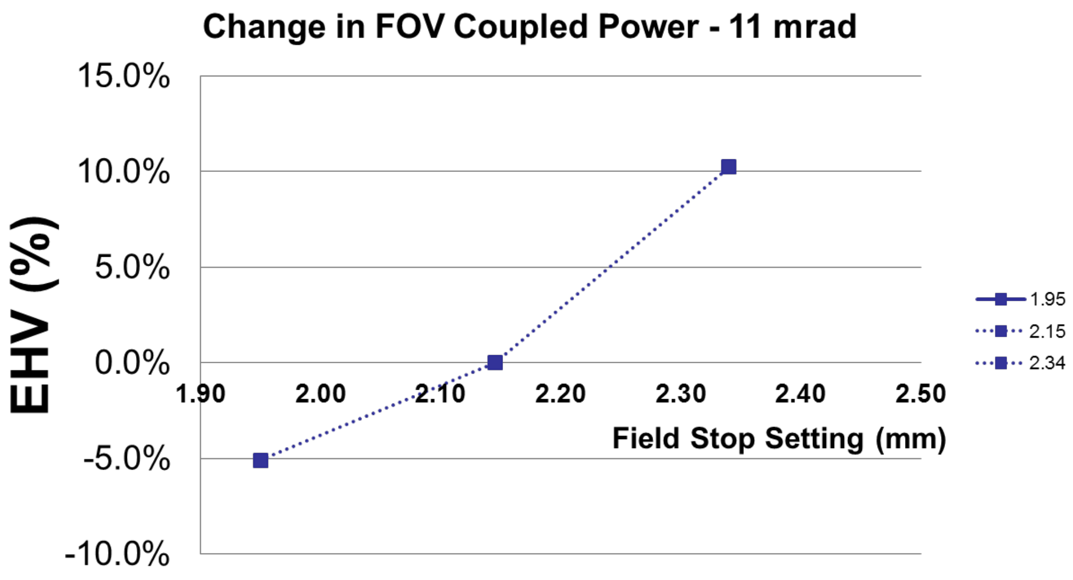

Figure 54: Calculated data (FOV = 11 mrad)

5 Conclusions

The evaluation of the optical radiation safety EHV requires an uncertainty value to be reported to give confidence in the quality of the assessment. The adoption of a conservative approach to measurement is recommended to ensure collection of a slightly larger proportion of the radiant power and hence a slight over-estimation of the EHV.

An approach to uncertainty estimation using sensitivity analysis has been described. An advanced software simulation process is beneficial to avoid substantial manual calculation that would otherwise be required for this approach to uncertainty estimation.

The spectral ‘sliding’ & stop size ‘dithering’ techniques presented can provide useful insights into the measurement system and can help to ensure that attention is paid to the most important contributory factors (such as field stop placement, spectral resolution etc.) so as to minimise the uncertainty associated with the determination of the EHV.

Table 5: Typical 62471 EHV uncertainties

Parameter	Influence on Blue Light Hazard Exposure Hazard Value
Centre wavelength	≈ 1% per every 10 nm offset
Spectral Linewidth	≈ 2% per every 5 nm FWHM spread
Spectral radiant power	≈ 2 to 5% depending on detector type
Irradiance (Area of detector)	≈ 2 to 3% per 100µm @ 7 mm detector diameter
Radiance (area of field stop)	≈ 5 to 10% per 100µm @ 2.2 mm diameter (Low Risk Testing at 11 mrad FOV)

References

ICNIRP 2013,*Health Phys*, "Guidelines on Limits of Exposure to Laser Radiation of Wavelengths between 180 nm and 1,000 µm" 105(3):271-295;

ICNIRP 2013,*Health Phys,* "Guidelines on Limits of Exposure to Incoherent Visible and Infrared Radiation". 105(1):74-96;

Haigh N.R, Hall S.R.G. "LED Safety - Blue Light Hazard Analysis of LED Devices" The 5th China International Exhibition & Forum on Solid State Lighting, Shenzhen, China, 2008

Hall, S., Crane, L. and Gibbs, D. "Investigation of a measurement technique to determine the apparent source size for light emitting diodes" National Physical Laboratory.

Ward, B. Europtics Ltd. for HSE. Research report 345. (RR345) (RR 345) WEB VERSION ONLY. 2005, ISBN 0717661083 http://www.hse.gov.uk/research/rrhtm/rr345.htm

PP01

A TEST OF COLOUR RENDERING EVALUATION

Rizzi A.[1], Bonanomi C.[1], Fumagalli S.[2]
[1] Dept. of Computer Science, Univerisità degli Studi di Milano, ITALY
[2] ENEA UTTEI-SISP, Ispra, ITALY
Alessandro.Rizzi@unimi.it, Cristian.Bonanomi@unimi.it, Simonetta.Fumagalli@enea.it

Abstract

From the sixties the scholar community is researching on new colour rendering indices to improve the one originally proposed. An important impulse of this research comes from the new types of light sources, like LED. Starting from the idea that, so far, the best colour rendering evaluator available is our vision system itself, here we present an experiment performed with human observers to assess the appearance preservation of colour under a set of light sources. The test protocol uses both 2D and 3D reference objects in order to have different kinds of surface complexity. The results are compared with the standard CRI.

Keywords: Colour Rendering, Colour Preference, Colour Appearance.

1 Introduction

The problem of the changes in the colour of objects induced by changes in the illuminant spectrum has a renewed attention with the advent of new types of lighting devices. The method to measure such change, called Colour Rendering Index (CRI), dates back in the sixties when CIE proposed a procedure to specify the properties of visual rendering of a light source (CIE, 1965), later updated in 1974 (CIE, 1974) and in 1995 (CIE, 1995).

In several cases the CRI does not return a value in accordance with the human visual system perception, as discussed in many studies (Joist-Boissard 2009; Brückner, 2009; Sandor, 2006).

The problem with the new type of lighting is that these light sources have a low Colour Rendering Index, but a pleasant visual appeal and a preservation of colour appearance better than what indicated by CRI.

One of the difficult tasks is to obtain a CRI able to scale changes in the colour shift proportional to our vision. In this work we present a simple experiment to check how the rendering of colour is preserved according to a magnitude scale made by observers and to what extent this scale fits with standard CRI.

2 The experiment

The main goal of this work is to collect data about the variation in colour appearance due to changes in the illuminant. We are interested to compare the scaling of the values of both rendering indices computed and estimated by observers. Regarding the scaling, we are interested in checking if the scale is “linear” to our perception of colour shift; in other words, if the scaling formula of CRI matches with the observers’ judgment.

In searching for observers’ judgment we have to deal with two main problems: the magnitude estimation of perceived shift that controls the scaling and the cognitive effect of the personal understanding of the problem.

In the experiment, we propose to the observers a method in two steps to support them in the magnitude estimation process and to prevent, as much as possible, the cognitive bias, impossible to eliminate but statistically compensated.

2.1 Experiment setup

The experiment involved 48 observers, 21 females and 27 males. Before running the experiment we tested the observers with the Ishihara plates, to check their colour vision.

We run two variants of the experiment. In the first one we used two-dimensional Macbeth Color Checker, while in the second one we used a three-dimensional plastic brick toys. In both cases the aim was to compare the colour samples, observed under a reference light source and under a test light source.

The use of a 3D object involves introducing shadows and inter-reflections, created by complex geometries. This is an important difference, that insert important cues for our vision system (McCann, 2014).

We run the experiments in wood boxes built on purpose, with size: 1m x 1m x 0.8m. The inside of each box is covered with white paper. The upper part of the box is screened with a panel, to avoid that direct light reaches the observer’s eyes. In each test box are housed two light sources, only one at a time is turned on.

The experiments are conducted in a dark room without time limits. The observers accomplished the experiment after an adaptation period to the light.

2.2 Light sources

We have tested six light sources: three fluorescent, one halogen, and two LED lamps. Another halogen light source has been used as reference, with a colour rendering index equal to 100. In table 1 we report some of the features of the used light sources. The last line of the table (“Experiment”) specifies if the light source has been used in the Macbeth Color Checker (2D) or the plastic brick toys (3D) experiment.

Table 1 – List and properties of the light sources used in the experiments

Light source	A	B	C	Reference	D	E	F
Type	Fluo.	Fluo.	Fluo.	Halogen	LED	LED	Halo. IRC
Power (W)	20	11	11	42	8	3	30
Flux (lm)	1250	650	600	630	345	270	806
Lux (lx)	913	546	457	390	338	171	470
CCT	2849	6246	4109	2476	3033	2955	2712
Experiment	3D	2D+3D	3D	2D+3D	3D	2D+3D	3D

As it can be noticed, the light source labelled as B has a CCT of 6246 K, very different from the others. We decided to test it as an extreme condition.

The fluorescent lamps are turned on more than 20 minutes before the measurements and before starting the test, to guarantee the stabilization of emitted flux.

2.3 The samples

In the 2D experiment we used two Macbeth Color Checkers (MCCs). The first MCC is observed under an halogen light source, considered as the reference. The second MCC is placed under two lamps to test: a fluorescent light source (B) and an LED light source (E).

In the 3D experiment the Macbeth Color Checkers are replaced with four plastic brick identical constructions, with the purpose to create a three dimensional scene with shadows and inter-reflections. In this case, observers are asked to examine six coloured bricks (orange, green, white, blue, yellow, red) part of the toy, showed in figure 1.

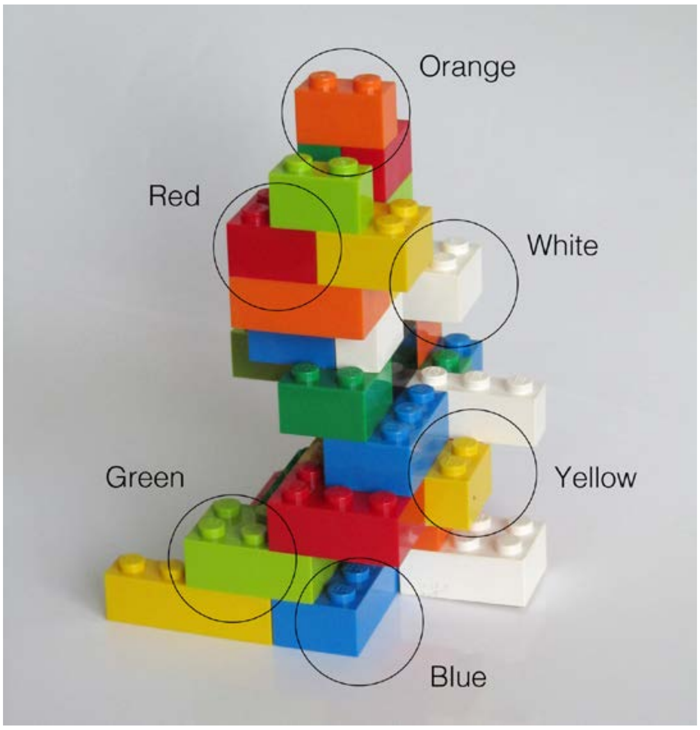

Figure 1 – Samples of the 3D experiment.

2.4 Testing procedure

We let the observers adapt to the average luminance level, similar in all the boxes. There are no biological evidences of sensory adaptation to the colour of the light. Colour constancy is mainly the result of brain activity. This allows us to watch simultaneously different boxes that generate in our vision system various colour appearances according to the spatial distribution of luminance (Land, 1977; McCann, 2005).

In the questionnaire we have recorded some personal data (sex, age, eye colour, class attended, any vision problems, and use of lenses or glasses during the experiment) and the evaluation of the differences for each pair of colours. The question asked is "How much the patch colour is similar ?". To help observers to estimate colour differences we proposed them a two-stage approach: at the first stage we asked for a qualitative assessment of the colour shift, then we asked to assign to their qualitative evaluation a score, according to the value ranges reported in table 2.

Table 2 – Qualitative and quantitative evaluation method of the patches colour differences.

The patches are:	Qualitative evaluation	Quantitative evaluation
Identical	ID	100
Similar	SIM	80-99
Different	DIF	50-79
Very different	VD	1-49
Completely different	CD	0

The purpose of the preliminary qualitative assessment is to help observers in their choices. Observers could always correct their answers.

2.5 Results of the 2D experiment

We tested the Macbeth Color Checker under two light sources. In figure 2 we plotted the results in order to compare the average scores under the two lights of each corresponding patch. The first column of each pair of bars corresponds to the evaluation of the patch under the fluorescent light source (B), the second column corresponds to the evaluation of the patch under the LED light source (E). For an easier identification the bar colours are similar to their 24 actual colours.

Patches have a significant visual difference under the two lamps. The columns labelledA1 and A2 report the average score, among the 24 patches. The average score of the user estimation for the fluorescent lamp is 72 (A1), while in the case of the LED the total average value raises to 80 (A2).

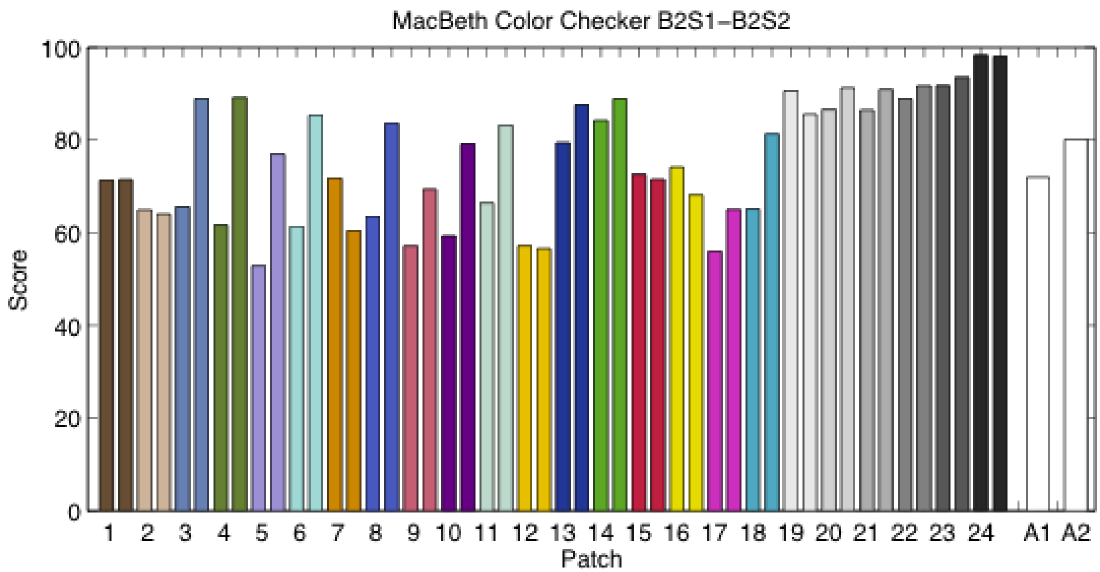

Figure 2 – Comparison of the average score of the individual patches about the 2D experiment. The first column of each pair of bars corresponds to the average evaluation of the patch under the fluorescent light source (B), the second column corresponds to the evaluation of the patch under the LED light source (E).

It can be noticed how the patches number 3-4-5-6-8-9-10-11-18 have a higher similarity score when observed under LED light source (second bar of each pair) than when observed under the fluorescent light source. On the contrary the yellow-orange patches (7-12-16) receive a better rating if observed under the fluorescent light source.

Finally, it is possible to note that achromatic patches (columns 19-24) received better scores (above 80) than the chromatic ones.

2.6 Results of the 3D experiment

In the second experiment, we have used four identical plastic brick toys, placed (with the same orientation) in four light booths, three of which containing each one two test light sources, while the fourth contained the reference light. Six coloured bricks were considered: orange, green, red, white, blue and yellow (see figure 1).

The ranking (from higher to lower) of the light sources resulting from the observers estimate is: F (91), A (86), C (82), D (81), B (78), E (70).

3 A comparison between the perceptual rendering indices and the calculated index

In table 3 we show the standard CRI of the light sources tested as well as the indices estimated by the users.

Table 3 – Comparison between the calculated and perceived colour rendering

Light source	A	B	C	D	E	F
Type	Fluo.	Fluo.	Fluo.	LED	LED	Halo. IRC
Std. CRI	80	83	78	83	63	98
User: 2D	**-**	**72**	**-**	**-**	**80**	**-**
User: 3D	**86**	**78**	**82**	**80**	**70**	**91**

In the following the results for every light sources:

A: the observers give a score of 86 for the 3D experiment. The standard CRI gives to the light a score around 80, in line with the result of the observers.
B: in this case both the 2D and 3D experiments have been performed. The results of the observers are comparable (72 and 78 respectively). The standard CRI overestimates the results (83).
C: On the contrary of the previous case, the calculated CRI underestimate the observers result.
D: the Cri gives a good approximation of the observers' perception.
E: also in this test both the 2D and 3D experiments have been performed. However in this case the trend of the perceptual result is reversed: in the 2D experiment the result is 80 while in the 3D experiment it is 70. The CRI underestimates the results.
F: The CRI overestimates the result. This is due to the fact that the halogen light source has a spectrum that can be approximated with a black body radiation. Therefore the reference light source is almost identical to the light source to test.

The Pearson correlation coefficient, between the users' answers and the CRI is 0.875.

4 Conclusions

In this paper we have presented a test with observers, comparing a set of colour samples observed under a reference light source and under a test light source. In the first experiment two-dimensional objects have been used, while in the second one we have replaced them with three-dimensional objects in order to introduce shadows and inter-reflections as in everyday scenes.

In the second part, we have compared the quantitative estimates made by the observers with the standard CRI value.

Future studies will extend this comparison with a wider set of CRIs.

References

BRÜCKNER, S., BODROGI, P., KHANH, T.Q. 2009. Colour Rendering of new white LED light sources visual tests. *Proc. of 11 Lux Europa*. 397–404.

CIE 1965. CIE 13:1965. *Method of measuring and specifying colour rendering properties of light sources*. Vienna.

CIE 1974. CIE 13.2:1974. *Method of measuring and specifying colour rendering properties of light sources*. Vienna.

CIE 1995. CIE 13.3:1995. *Method of measuring and specifying colour rendering properties of light sources*. Vienna.

JOST-BOISSARD, S., FONTOYNONT, M., BLANC-GONNET, J. 2009. Colour Rendering Of Led Sources: Visual Experiment On Difference, Fidelity And Preference. *CIE Light and Lighting Conference with special emphasis on LEDs and Solid State Lighting.*

LAND, E.H. 1977. The Retinex Theory of Color Vision, *Scientific American*, 237, 108-128.

MCCANN, J.J. 2005. Do humans discount the illuminant? *Proc. SPIE, Human Vision and Electronic Imaging X*, 9–16.

MCCANN, J.J., PARRAMAN, C., RIZZI, A. 2014. Reflectance, illumination, and appearance in color constancy. *Frontiers in Psychology,* 5:5.

SANDOR, N., SCHANDA, J. 2006. Visual Colour-rendering experiments. *Light Res. & Tech*, 38, 225-239.

PP03

A STUDY ON THE COLOR APPEARANCE OF CLOTHING UNDER VARIABLE COLOR TEMPERATURE AND ILLUMINANCE OF VARIOUS LIGHT SOURCES INCLUDING LED LAMPS

1st Eun Jung LEE[1], 2nd Takayoshi Fuchida[2]
[1] Dongduk women's university, Seoul, KOREA of 1st author, [2] Graduate School of Joshibi University, Kanagawa, JAPAN of 2nd author
lej624@gmail.com

Abstract

This study focuses on evaluating product color appearance under given conditions; base lighting including LED lamps, various kinds of spot-lighting and level of illuminance varied by each apparel brand. Furthermore, we are going to look through which lighting can emphasize product color appearance in color-scientific way. In this study, we performed CIECAM02 Q-aM-bM calculations for the analysis of the color appearance of RED, YELLOW, GREEN, BLUE from high to low illuminance for the combination of the test lamps illuminances used in the subjective experiment. Also we compared the correlation of 'colorfulness coordinate system' and the difference of each lighting and illuminance for counter color size. It turned out that there was the chance to discuss the connection between each experimental result in the future. This suggests the new path to further studies in the foreseeable future.

Keywords: Color Appearance, Ambient and Spot-Lighting, Apparel Brand Illuminance, CIECAM02

1 Introduction

1.1 Background and Purposes of Research

Lighting in the apparel stores has its 3 bigger purposes; reappearance of apparel colors, effective showing, and energy-efficiency. Lighting, which is especially in the effective showing purpose, is set up based on the brand-focusing VMD concept. VMD, which shows the products in visual-friendly way and also stimulate consumers to buy them, not only represents the expert methods of visualized product showing but also exposes the communicative unification of store infrastructure such as product design, display and store interior which are the basic constituents to build up the brand images for consumers.

Even though the products are taken high in their brilliancy, the poor store VMD reflecting the poor store VMD which cannot reflect the fashion brand with leaving out essential factors when they are sold to consumers cannot carry the products' original functions, nor produce the ultimate profitable results from marketing.

In the area of apparel store VMD, images from clothes of each fashion brand and its image concepts are decided such as [light], [brilliant], or [showy], and store design is conducted to highlight these product images.

For these matters, lighting as well as the pin-pointed apparel products is highly considered in its importance and it has the role to magnify features of products' color and fabric precisely and properly when it comes to whether lighting is needed and show them to consumers. This and the following sections and sub-sections shall serve as an example how to structure a paper.

In apparel stores with lighting setup with various Correlated Color Temperature(CCT) and illuminance, clothing items with various colors and fabric are found.

While the studies on color consciousness and color rendering property or other studies on sensitive image under light source color and CCT difference are originally conducted, it is apparently hard to find the studies on how different the clothing item's color appearance is under the store setup of each lighting method and illuminance level in its practical and relative color appearance difference centered area in the key word of 'fashion' only.

Traditionally, high color rendering propertized lighting has been used in apparel stores. Because it will be helpful for consumers to find the products' charms by high color rendering effect of color appearance which is different from each observer's eyes. We can suggest many cases that the clothing products have variable color appearance under different in-store lighting though the products have same color and fabric. Whoever watches the clothing items in stores, color appearance for the same clothing is changeable due to store lighting and showing method. For most of the cases, it seems that lighting designers' personal sensitivity is casually relied upon when it comes to the store lighting and showing based on each fashion brand VMD concept. Color appearance is so deeply related with the products' images that it is supposed to be complicated. Images above such as 'light', 'brilliant' and 'showy', example, are featured in different color appearance manner. To figure out which impact would be shown if each lighting and illuminance is differently facilitated is necessary for store VMD. Besides, for consumers, fashionable which is proper to TPO(Time, Place, Occasion) will get genuine help from knowledge of the connectedness between lighting setup and color appearance.

This study aims at the following purposes; to evaluate color appearance by different illuminance in each fashion brand category and to achieve coloric scientific verification on which setup of lighting and illuminance will beautifully highlight each color appearance for targetted apparel products.

2 Methods of Experiments

2.1 Experiment Samples

In practical apparel stores, plain and cubic displays are separated in products playing formation. In the previous study, women' basic blouse was chosen as the sample for color appearance estimation. This sample was supposed to be plainly displayed on the in-store clothing organizers with its average size of 220mm×280mm. Making cubic displaying scenes modelized in this study, which were the sleeveless dresses, the experiment samples, which were the sleeveless dresses, were proportioned to quarter of human body size due to its validity eyesight so that observers can easily take levels of whole color appearance under experiments' setup conditions<Figure 1>. The experiment samples, which were 100% 40 yarn-numbered, cotton broad-clothes were designated to 6 colors, including 4 chromatic RED, YELLOW, GREEN, BLUE colors, which are similar to vivid tone(PCCS), and 2 achromatic WHITE, BLACK colors.

Figure 1 – Color of the 6 quarter of human body size Samples

In<Figure 2>, the spectrum reflection rations, which were evaluated using Spectrum colorimeter(Konica Minolta CM-3700d), for six different sample colors under D65 lighting source were marked.

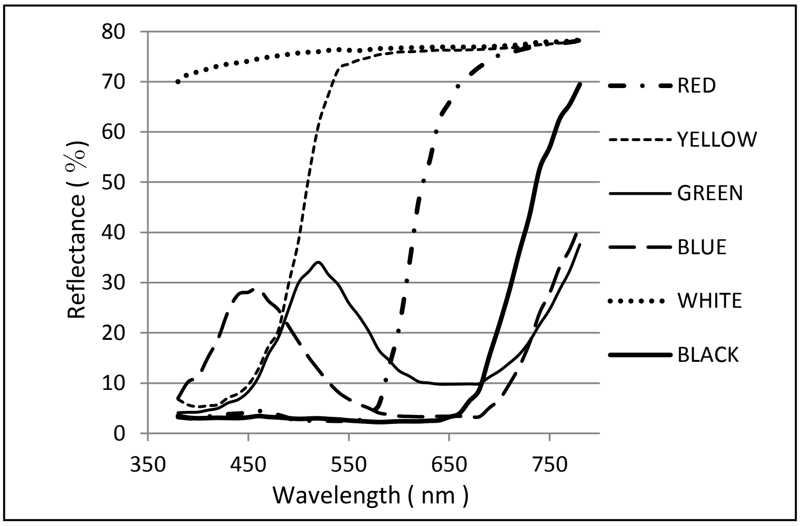

Figure 2 – Spectral reflectance for the color of the 6 textile samples under D65 illuminant

2.2 Experiment Lighting Setup

2.2.1 Experiment Lighting and Illuminance Factors

Experimental lighting and illuminance were set up based on the preliminary survey targeting women' apparel stores; from department stores, shopping malls to fashion brand off-line boutiques.

Illuminance in ambient lighting set up were varied to 1200 lx, 700 lx and 300 lx upon each women' apparel chops such as Young Casual, Mrs. Formal and Prêt-à-Porter for these lighting lx results, the additional exrimental conditions facilitating spot lighting on the ceiling were 2400 lx, 1600 lx and 800 lx. So, in this, evaluation on color appearance was palnned to be conducted by classifying lighting setup differences from these 3 women' apparel shops. In the following proceeding, these expert will be used; one is Y・C high illuminance for Young Casual, M・F medium illuminance for Mrs. Formal, P・P low illuminance for Prêt-à-Porter.

Each sort for experimental lighting in <Table 1> andeach spectral distribution level in <Figure 3> is shown. Used lamps and their sorts and numbers, CCT(K), Ra values and output lx observed under these 3 lighting setups are shown in <Table 2>.

Table 1 – Lamps used

Lamp name	Maker : Type	Correlated color temp*. (K)	Ra*	Lamp species named
Incandescent	TOKI : GW110V100WG125K	2600	98	*I*
Fluorescent	NEC : 60WEEA15EDF	6700	88	F_1
Fluorescent	NEC : 100WEFG25ECF	6700	88	F_2
Neutral white color LED	KFE JAPAN : LB07-E26CW	5000	70	*f*
Electric lamp color LED	KFE JAPAN : MB07-E26WW	3000	72	*i*

* Product specification values. Ra denotes the general color rendering index.

Table 2 – Characterization of lightings

Lighting Notation	Lighting for	Lamp combination	Correlated color temp*. (K)	Ra	Illuminance used for impression evaluation (lx)
		Lightings with Y・C high , M・F medium, or P・P low illuminance			
I	ambient	*4I , 2I , 1I*	2600,2600,2580	98,98,98	1200,700,300
F	ambient	*2F₂ , 1F₂ , 1F₁*	6800,6780,6670	88,88,89	1200,700,300
I+f	spot	*4I + 2f , 2I + 2f , 1I + 1f*	3900,3890,3200	90,78,78	2400,1600,800
F+f	spot	*2F₂ + 2f , 1F₂ + 2f , 1F₁ + 1f*	5800,5650,5560	77,76,73	2400,1600,800
I+i	spot	*4I + 2i , 2I + 2i , 1I + 1i*	2780,2770,2690	84,76,76	2400,1600,800
F+i	spot	*2F₂ + 2i , 1F₂ + 2i , 1F₁ + 1i*	4780,4770,4760	76,75,72	2400,1600,800

※ Y・C high : Young casual-high illuminance. ※ M・F medium : Mrs. Formal-medium illuminance.

※ P・P low : Prêt-à-Porter-low illuminance.

2.2.2 Color Appearance-Experimental Booth

Subjective evaluational observation booths, which were 2-space-dividened boxes having a center compartment between each side, were paved with N5.0 non-luster fabric<Figure 3(A)>.

2 kinds of ambient lightings were set up<Figure 3(B)>.

For the experimental samples, LED spot-lightings with the 60 degrees downward angle were facilitated on the ceiling right in front of the booths.

Each lighting is randomly controlled by using switches. The illuminance of lighting setup was changed with differentiating the lighting usage electricity and lighting numbers, whose setup was identical with each experimental illuminance. In this experiment, each experimental illuminance in <Table 2> is identical with the experimental sample spot-related illuminance on the parallel plain. The lighting usage electricity and setup lighting numbers were collaborated according to the possibilities in <Table 2>. This experimental set up has the CCT and Ra values which were estimated within the same visual distance from observer's naked eyes. This reflection ration of the white-colored plate(380nm~780nm) on the experimental table was calculated using spectrum radiation(Co. TOPCON SR-3AR).

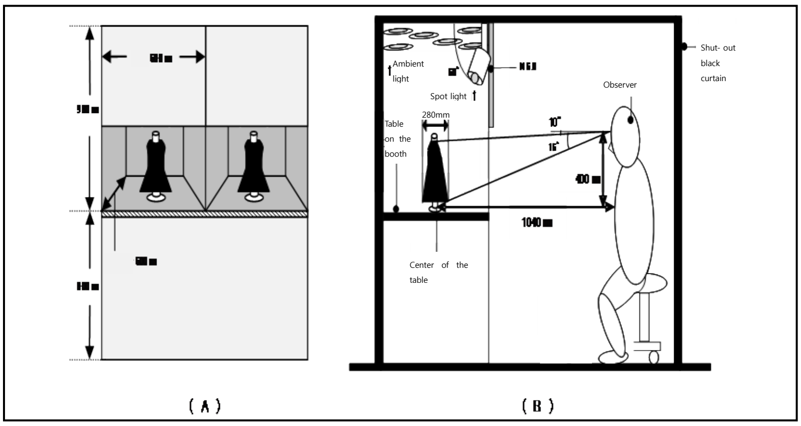

Figure 3 – The booth for the impression evaluation

Randomized estimations for illuminance showed the difference up to 3% within the average. This illuminance was estimated on each sample for color appearance experimentation(based on JIS Z 8726-1990).

Lighting from the outer space was blocked by the shut-out black curtains wrapping the whole experimental booths and cells occupied by observers <Figure 3(B)>.

2.3 Evaluation of Color Appearance

2.3.1 Methods for Evaluation of Color Appearance

Color appearance evaluation were conducted, based on 5-step-standards by evaluation terms, for the subjective evaluation on relative color appearance taken from the 2 experimental samples under each lighting and illuminance setup. This was set up with 13 evaluating-related adjectives<Table 3> based on the preliminary survey(Eun Jung Lee, 2011). <Figure 4>

Observers gave points to color appearance of identical experimental samples in the different booths with each different lighting setup; zero point on ‘Neither of them’, one point on ‘Slightly left lateral’ or ‘Slightly right lateral’, and two points on ‘Yes’.

For example, observers watched the right booth RED dress sample and described that this sample under the experiment spot light, comparing it to the one under the experiment ambient light, had lighter-colored image.

Table 3 – 13 evaluating-related adjectives

1. light	5. cool	9. prefer	13. showy
2. brilliant	6. clear	10. natural	
3. pale	7. glossy	11. gay	
4. beautiful	8. feeling texture	12. fresh	

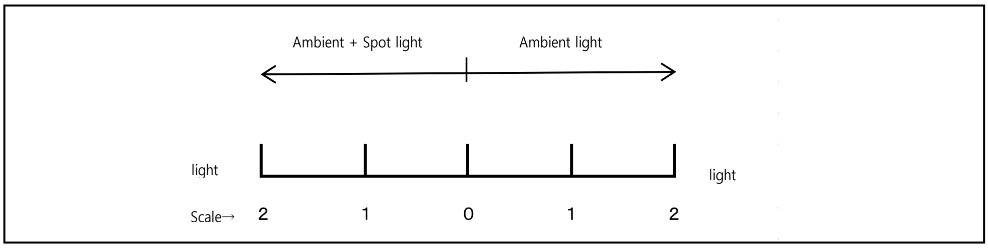

Figure 4 – A measure used in the impression evaluation

3 Results and Discussions

3.1 Colors of Experimental Sample

results of subjective evaluation on color appearance, in which the background color is gray, were for 6 experimental sample colors. The comparison results between setups of I-ambient lighting for Red(A) and I + f spot lighting were exemplified. For the same proceeding in Red(B) the comparison results form evaluation for color appearance between setups of F – ambient lighting and F + f spot lighting. There results for 3 sorts of illuminance were collectively listed in figure 5.

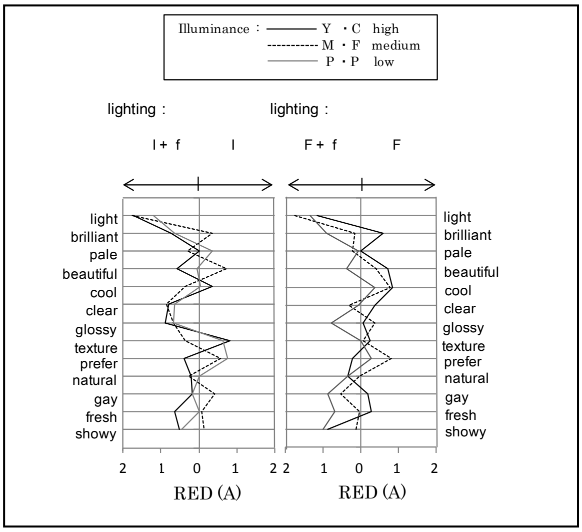

Figure 5 – A The difference of the color impression between base lightings and the spot lightings with the neutral white color LED lamp

(A) : RED impression for the I+f and I lighting environment shown in Table 2.

(B) : RED impression for the F+f and F lighting environment shown in Table 2.

Taking into consideration on Red(A), for every potential in-shop lighting setups, the color appearance term [light] is even lighter under spot lighting. This resulted from increasing illuminance by spot lighting. The same went for [clear], [fresh] appearance. But, for [fresh] and [showy] appearance, the emphasizing effect of color appearance by spot lighting is varied by each in-shop-categorized illuminance. For example, [brilliant] appearance is emphasized under spot lighting setup in P.P low illuminance.

However, in Y.C high and M.F average illuminance, the ambient lighting setup conversely featured [brilliant] appearance. For this same emphasizing effect, the color appearance on [beautiful], [feeling texture], [prefer], and [fancy] was strongly appeared under the ambient lighting setup by spot lighting.

Taking into consideration on Red(B), the term [light] was similarly even lighter under spot lighting among all of the in-shop setups, same as the results from Red(A). However, the other color appearance results, under spot lighting setup, were varied in their emphasizing patterns.

From these explanations, it was suggested that spot lighting setups, especially for Red color appearance, were not always said as effective on color appearance emphasizing for every color, even though there were equipped with different color appearance term and added by spot light under ambient lamp in the researching environment.

The verified expertise in this study were extracted from <Table 4> and replotted into <Table 5>. These expertise included lighting source color which has the emphasizing effect for maximum color appearance from each sample color, illuminance level and colors.

Emphasizing effect of color appearance on both RED and BLUE are highly affected by ambient lighting I and F. For example, the I effect of color appearance exaggeration on R, and F effect on B.

Exaggeration of color appearance under another lighting setup, consisting of I, F added with spot light, was nearly ranged between I and F.

From the results above, when it comes to the target color, it was suggested that to opt for the illuminance and lighting setups with cautiousness is inevitable<Table 5>.

Table 4 – Impression emphasis effect by base and spot lightings

○ : An impression emphasized. × : An impression lessened.

I : Incandescence lamp lighting. F : Fluorescence lamp lighting.

f : Neutral white color LED lighting. i : Electric lamp color LED lighting.

Color	RED						YELLOW						GREEN						BLUE						WHITE						BLACK						Total (○/30)
Lighting environment	Ambient		Ambient + Spot				Ambient		Ambient + Spot				Ambient		Ambient + Spot				Ambient		Ambient + Spot				Ambient		Ambient + Spot				Ambient		Ambient + Spot				
Base Lighting	I	F	I	F	I	F	I	F	I	F	I	F	I	F	I	F	I	F	I	F	I	F	I	F	I	F	I	F	I	F	I	F	I	F	I	F	
Spot Lighting			f		i				f		i				f		i				f		i				f		i				f		i		
Young Casual shop high illumination environment																																					
light	○		○	○	○				○	○	○	○			○	○	○	○		○	○	○	○					○	○	○			○		○		21
clear	○		○		○	○			○	○		○		○	○	○	○	○		○		○				○		○		○		○	○	×	×		19
showy	○			○	○				○	○	○				○	○	○	○		○	×	○					○	○	○				○				16
gay	○				○				○	○	○				○	○	○	○		○	×	○				○		○	○	○					×		15
brilliant	○		○	×	○	×			○	○	○				○	○	○			○		○	○					○	○				○	×		×	15
fresh	○		○		○				○	○					○	○	○	○		○		○				○	×	○	○				○				15
glossy	○		○		○					○					○	○		○		○	×	○						○	○	○			○			×	13
prefer	○				○	×	○			○	○	○	○		○	○					×	○	×				×	○					○	×		×	12
beautiful	○				○	×			○	○	○									○	×	○						○		○				×	×	×	9
cool					×			○	○	×				○	×		×	×			×		×			○	×		×			○	○		×		6
natural				○	○								○												○		○										5
texture			×		○	×	○		×			×	○					×					×		○								×	×		×	4
pale											×								○		○			×					×				×	○			3
Total (○/13)	9	0	5	3	11	1	2	1	8	9	6	3	3	2	8	8	6	6	1	8	2	9	2	0	2	4	2	9	6	5	0	2	8	1	1	0	153 / 390
Mrs. Formal shop middle illumination environment																																					
light	○		○	○	○	○			○	○	○	○			○	○	○	○		○	○	○	○	○			○	○	○	○			○	○	○	○	26
glossy	○		○		○					○	○	○			○					○	○		○				○	○	○	○			○	○	○	○	18
gay	○				○		○		○	○	○	○			○	○		○		○	○					○	○	○	○	○			○				18
showy	○				○		○		○	○	○	○			○	○	○	○		○	○			○			○		○	○	○			×			18
clear	○		○			○			○			○		○						○	○			○		○	○			○		○	○			○	15
brilliant	○				○		○		○	○	○									○	○						○			○		○	○				12
cool		○		×				○		×	×	○		○		×	×			○	○	×	×	○		○	○	×	×			○	○	×	×		11
fresh	○								○	○	○	○			○		×			○	○					○	○							×			10
beautiful	○		×				○				○				×	×	×			○	○	×	×				○	×	×					×	×	×	6
prefer	○		×	×		×	○				○					×				○	○	×	×					×						×	×	×	5
pale		○			×			○			×				×				○		×				○		×				○		×				5
texture						×	○				○	×	○									×			○			○									5
natural									×		○	×	○								×				○		×										3
Total (○/13)	9	2	3	1	5	2	6	2	6	6	10	7	2	2	5	3	2	3	1	10	10	1	2	4	3	4	9	4	4	6	1	4	6	2	2	3	152 / 390
Prêt-à-Porter shop low illumination environment																																					
light			○	○	○	○		○	○	○	○	○		○	○	○	○	○		○	○	○	○	○		○	○	○	○	○		○	○	○	○	○	29
fresh	○		○	○		○		○	○		○	○			○	○	○	○		○	○	○	○	○		○	○	○	○						○		22
pale	○		○			○			○	○	○	○		○	○	○	○	×		○		○	○			○	○	○	○	○						○	20
glossy										×	×		○			×			○		○				○		×	×	×		○			×			19
texture	○		○			○			○	○	○	○		○	○	○	○	×		○		○	○			○	○	○	○	○							19
natural	○		○						○	○	○			○	○	○	○	○		○		○	○			○	○	○	○								17
brilliant				○	○			○		○	○			○		○	○			○		○	○			○		○	○	×		○		○			16
showy	○		○	○					○	○	○	○		○	○	○	○	○		○		○				○		○	○			○		○			10
beautiful	○			×					○		○	○				○				○		○	○	×				○	○				×	×		×	10
clear					×	×		○	×		○	×		○	×			×		○	×	○				○	×	○		×		○	×			×	8
gay	○								○		○	○				○	○			○			○	×				○	○				×			×	5
cool					○				×		×		○				×				○				○		○	×									5
prefer				×			○			×			○				×					×		×													2
Total (○/13)	7	0	6	4	3	4	1	4	8	6	10	7	3	7	6	9	8	4	1	10	4	9	8	2	2	8	6	10	9	3	1	4	1	3	2	2	182 / 390

Table 5 – Lighting environment emphasizing the color impression.

Shop illuminance	RED		YELLOW		GREEN		BLUE		WHITE		BLACK		Color impression term emphasized
Y・C high illuminance	I	I+i (I+f)		I+f F+f (I+i) (F+i)		I+f F+f I+i F+i	F	F+f (I+i) (F+i)		I+f F+f I+i (F+i)		I+f	light clear showy gay brilliant glossy
M・F medium illuminance	I	(I+f) (F+f) I+i (F+i)		I+f F+f I+i F+i		I+f F+f I+i F+i	F	I+f (F+f) (I+i) (F+i)		I+f (F+f) I+i (F+i)		I+f (I+i) (F+i)	
P・P low illuminance		I+f (F+f) (I+i) (F+i)		I+f F+f I+i (F+i)	F	I+f F+f I+i	F	(I+f) F+f I+i (F+i)	F	I+f F+f I+i		(I+f) (F+f) (I+i) (F+i)	light fresh pale texture showy natural brilliant

( ): Lightings with no impression depressed at least, but not always emphasized.

3.2 Expectation of Experimental Sample Color under Lighting Lamp using the CIECAM02

The 3 sorts of illuminance levels used in this study of color appearance evaluation, added with the CIECAM02(CIE Color Appearance Model 2002) analysis values, calculated the expected (aM, bM) output for color appearance on sample colors(RED, YELLOW, GREEN, BLUE) which were ranged from high(1200 lx) to low(300 lx) illuminance and plotted the aM and bM coordinate onto <Figure 6>.

In the CIECAM02 color adaptation model, the only chromatic color which was likely to be adapted under the lighting lamp changed. However, since isochromatic colors , without any special case such as chromatic-colored lighting lamp, have the premise that they are shown as literally isochromatic as they are, that the expectation on color showing by CIECAM02 from sample colors(WHITE, BLACK) were excluded from this experiment.

The 2 tristimulus values of experimental light source and values 4 chromatic color samples were used for plotting Gamut Area surrounded by RYGB.

The expectation value for color appearance under an incandescent light lamp shows the characteristics of an incandescent light source emphasized by RED tristimulus value. Diversely, under a white-colored fluorescent light lamp, YELLOW and GREEN tristimulus values were strongly featured with their light sources.

In <Figure 6>, it is shown that the 300 lx plot is relatively far detached from the other 1200 lx, 700 lx plots without any exception under every source of light.

That the RED color differences were huge under the both of light sources is ascribed to that the color appearance is affected by each different illuminance. As long as it goes up along high illuminance, the colorfulness follows the pattern. And in the opposite pattern, the colorfulness decreases when it goes down from high to low illuminance(CIE Publication 17.4. 02 – 40). This phenomenon is well defined as Hunt Effect(1952). Composed of the coordinate area of each illuminance, Gamut Area deeply relates to how widely each illuminance can give out reappearance of colors.

Under the I lighting setup, the increases in colorfulness from R/G color were firmly detected.(Especially high in the R changes)

Under the F lighting setup, it was the Y colorfulness increased that showed the most apparent pattern and later changed into G color.

From the G color, F lighting changed into Y lighting lateral way, rather than I.

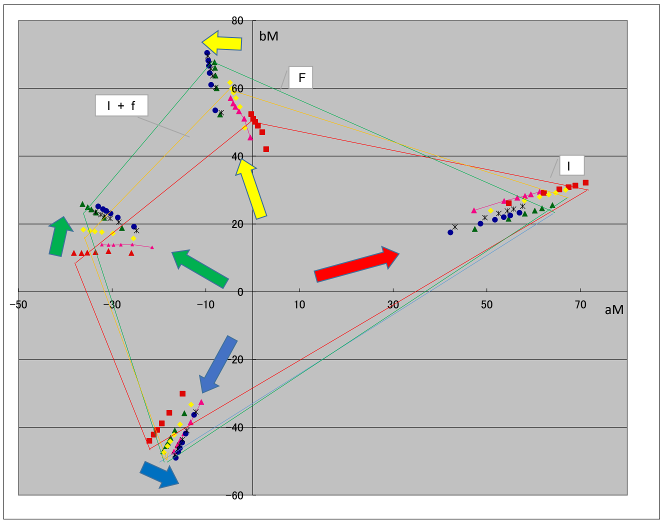

Figure 6 – color appearance emphasizing, the corresponding relation between aM – bM and colorfulness by the CIECAM02

From the B color, the changes in colors were detected under I and F lighting setups.

For example in this experiment, the color appearance evaluation [showy] suggested the corresponding relation between the changes in illuminance and the results form subjective evaluation in the following areas; R, G, Y, and B area.

In the apparel shops categorized by each different light sources and illuminance variation, the results of color appearance evaluation showed the corresponding relation with the colors in sight based on the CIECAM02–standardized interpretation.

4 Conclusion

In this study, 13 evaluation image terms were used to verify the emphasizing effect of color appearance, with the purpose to identify how the different ambient lighting setups, which are white and incandescent-colored and sometimes even more varied in the shops(Young Casual, Mrs. Formal, Prêt-à-Porter fashion brand categorized products would affect the color appearance for each apparel product.

It was verified that the emphasizing effect of color appearance on each experimental sample was relatively different upon lighting, illuminance and the product color itself.

Throughout the examples in <Table 4>, it was suggested that the emphasizing effect of color appearance is shown under the ambient lighting setups. This will be highly considered to become the part of standards for facilitating relative ambient and spot lighting setups to enhance the color appearance emphasizing.

In the real shop areas, multiple color choice is common for lighting effect(color reappearance). So, the method of comparison and conclusion using the various factors such as multi color balance or correlation in colorfulness area and the size of Gamut Area is necessary.

From the expectation results of color appearance (aM, bM) on sample colors(RED, YELLOW, GREEN, BLUE) ranged from high to low illuminance calculated by CIECAM02 under each different illuminance level, the results from the average subjective evaluation could be related to the comparison of differences between correlation of colorfulness plots and lighting and illuminance in Gamut Area. This well shows the likelihood of further researching and continual future studies.

The potential future study aims at the emphasizing effect of color appearance resulting from more variables under spot lighting which contains the ambient lighting setup in the apparel shops. Also, this would exceed the results of this current study with its even more various evaluation terms which could have an impact on image examination by careful lighting facilitation.

References

Lee, E. J. 2011. *Fundamental Study on Effect of Lightings on Color Impression Emphasis of Clothing (in Japanese)*, A Doctoral Dissertation, Graduate School of Fashion and Living Environment, Bunka Gakuen University.

CIE(1987). CIE Pub. 017.4 International lighting vocabulary. 4th ed. CIE

CIE Technical Report(2004). a Colour Appearance Model for Colour Management Systems : CIECAM 02. CIE 159

PP04

A STUDY ON THE EVALUATION METHOD OF COLOUR RENDERING PROPERTIES OF MUSEUM LIGHTING AT LOW ILLUMINANCE

Nakajima Yuki.[1], Fuchida Takayoshi.[1]
[1] Graduate School of Joshibi University of Art and Design, Kanagawa, JAPAN
122105@isis.joshibi.jp

Abstract

The purpose of this study is to clarify colour rendering properties at low illuminance and also to try to develope the new calculating method to evaluate the colour rendering values taking into consideration of illuminance.

The subjective experiment on colour appearance of the two-colour combinations (the set of the pairs of two colour chips) and the mosaic colour samples (mosaic colours) illuminated by the test and the reference light sources with different illuminance was carried out. The result showed that the subjective evaluation of colourfulness, brightness, and preference under the LED white light source（Ra19）composed of R/G/B LED chips at 700 lx and 10 lx was higher than those under the other light sources (the fluorescent lamp with Ra96, the LED lamp of blue LED and yellow phosphor with Ra82, the warm-white fluorescent lamp with Ra60). It was suggested that the current CIE Ra or Ri would not be sufficient when colour rendering properties of narrow band mixed-LEDs were evaluated especially at low illuminace level.

To examine whether the current CRI are appropriate or not for subjective evaluation of colour appearance at very low illuminance, we tried to verify the several calculation methods of the colour rendering values taking into consideration of illuminance. As the result, it was shown that the colour rendering properties of LED lighting at very low illuminance level could be evaluated by the Gamut Ratio (GR) or the Feeling of Contrast (FCI).

Keywords: LED, Colour Appearance, Colour Rendering, CIECAM02

1. Introduction

In recent years, LED lamps have started to be used for museum lighting whose colour rendition should be very important. It has been well known that museum lighting would cause colour fading or thermal damages against artworks by its ultraviolet and infrared radiation. As the spectral power distributions of LED lamps are different from those of conventional light sources (fluorescent lamps and incandescent lamps), colour appearance under LED light sources seem to change from under other conventional light sources.

The colour rendering properties of LED lamps should be carefully examined when these lamps are used in a place that emphasizes colour appearance such as museum. The lighting environment of museum should also be carefully controlled not to give any damage against deterioration of artworks. The CIE publication CIE 157:2004 (CIE 2004) recommended the appropriate illuminance levels and the limiting exposure to control of damage to artworks by optical radiation. In case of the exhibition of Japanese paintings for example, illuminance level is regulated to constrain at low illuminance, under 50 lx of the most severe case not giving colour fade damage as little as possible.

Brightness and colourfulness of chromatic objects decreases when illuminance decreases, whose effect is known as the Hunt effect (Hunt 1952). At the viewpoint of appreciation of artworks at museum, low illuminance means the decrease of colour appearance because artworks will lose brightness and colourfulness at low illuminance.

The present ISO/CIE standard (CIE 2001) recommends museum lighting needs Ra80 at the minimum. However, the Colour Rendering Index (CRI) is not including illuminance effect. Good colour reproduction needs high illuminance at least several hundred lux even though the high CRI lamp. It should be focussed on whether the current CRI are appropriate or not for subjective evaluation of colour appearance at very low illuminance

Although the problems on the colour rendering properties of LED light sources have been pointed out on subjective evaluation as well as on the calculation method of colour rendition, the CIE colour rendering indices (Ra,Ri) is not include illuminance effect for its basic definition. The issue is whether the current colour rendering index is suitable or not for measuring colour reproduction of artworks of museum.

The purpose of this study is to clarify colour rendering properties at low illuminance and also to try to recommend the new calculating method to evaluate the colour rendering values taking into consideration of illuminance.

2. Experiment 1

2.1 Experiment

The subjective experiment of affective feeling evaluation on the two-colour samples (the set of the pairs of two colour chips) and the polychromatic colours sample (denote as mosaic colour sample) illuminated by each test light source with different illuminance levels using the Semantic Differential method (seven categorized scales) was carried out.

The experiments were performed by a haploscopic viewing method using the subjective evaluation booth (Figure 1) composed of the adjacent two boxes, the reference at the left and the test at the right. The wall of the booth was painted in N6. The lamps were installed at the top of each boxes. Illuminance of the test box was set at 700 lx or 10 lx on the top of the desk, and the reference side was fixed at 700 lx shown in Figure 2. The observer evaluated subjectively the feeling of the colour pair and the polychromatic colours sample in the test side (the right eye) as comparing with the feeling of the same colour pairs in the reference side (the left eye).

The six kinds of adjective pairs (Figure 3) was employed for affective evaluation. The four kinds of light sources were used for the experiment, the conventional fluorescent lamps (denote as FL-EDL and FL-WW), the blue LED and yellow phosphor type-LED light source (denote as LED-BY) and the LED light source composed of red, green and blue LEDs (denote as LED-RGB). The relative spectral power distributions and CCT, *Ra, R9* of the lamps are shown in Figure 4 and Table 1.

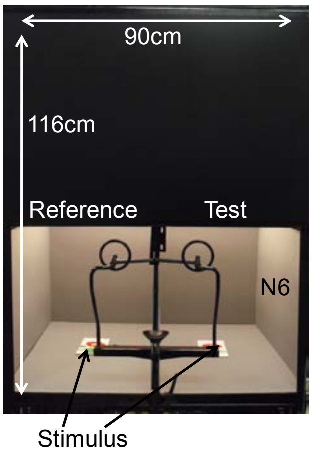

Figure 1 – The viewing booth

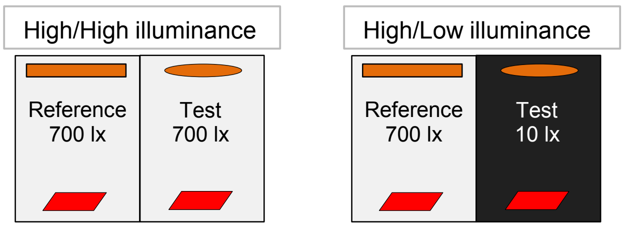

Figure 2– Illuminance of the reference and the test field

（－）←→（＋）
dislike-like
dirty-beautiful
uncomfortable-comfortable
dark-bright
sober-flashy
dull-vivid

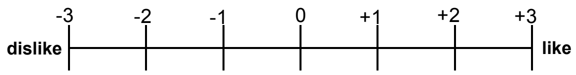

Figure 3－the adjective pairs for the evaluation

Table 1 – CCT,Ra,R9 of the light sources used in the experiments

Reference light source（CCT）	***Ra***	***R₉***
FL-EDL（3600K）	96	95
Test light sources（CCT）	***Ra***	***R₉***
LED-RGB（2880K）	19	-186
LED-BY（3060K）	82	12
FL-WW（3500K）	60	-94
FL-EDL（3600K）	96	95

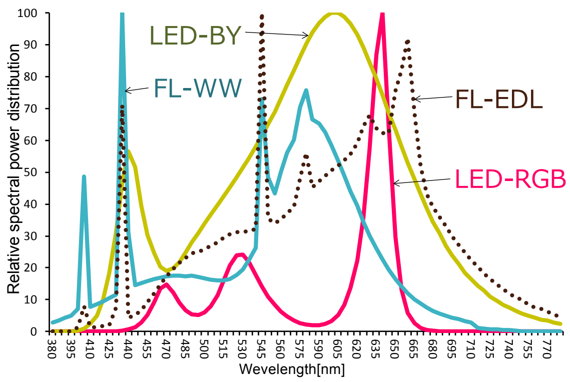

Figure 4 – The relative spectral power distributions of the light sources

We used the mosaic colour sample of red, yellow, green, blue natural mineral pigments and gold leaf used for Japanese paintings in this study. Each colour patch (5×5cm) was arrayed on a black hard board shown in Figure 5 (left). The spectral reflectance and CIECAM02 a_M-b_M colourfulness coordinate of each sample is shown in Figure 5 (right), Figure 6.

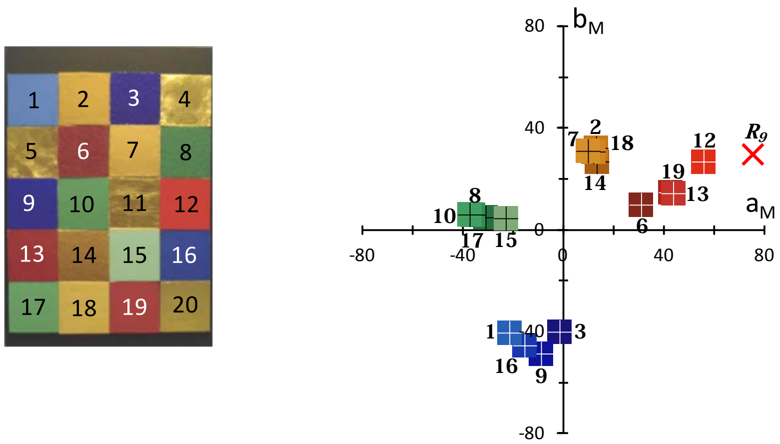

Figure 5 – The mosaic colour sample(left), aM-bM colourfulness coordinates of each colour (right)

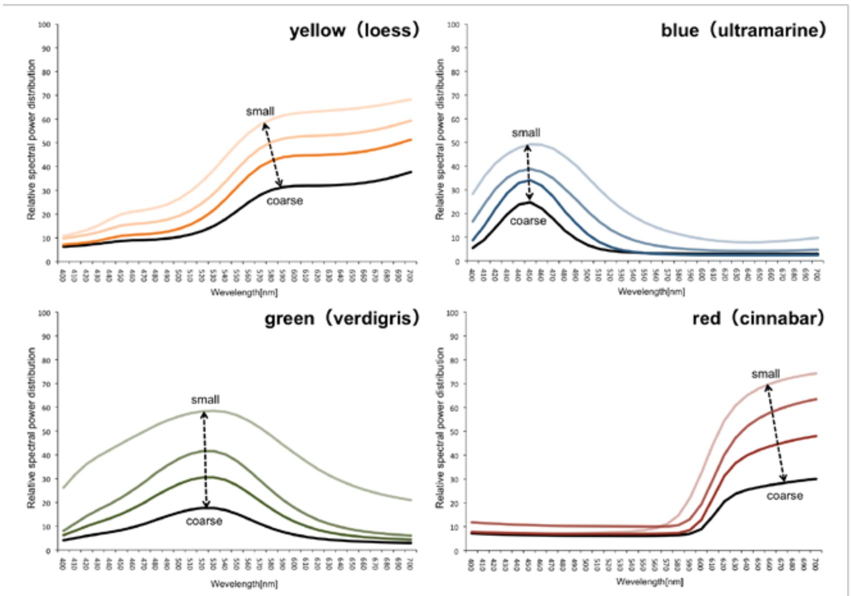

Figure 6 – The spectral reflectances of the red/yellow/green/blue sample

2.2 Results

Figure 7 is the result of our previous report at CIE2013 Paris Conference showing the total average profile of the subjective evaluation of the red-green two-colour combinations and those of the blue-yellow pairs under 10 lx of LED-RGB, and 700 lx of LED-BY and 700 lx of FL-WW. It is very interesting results that each profile line under each test light source for different illuminance is almost overlapping. In other words, this result shows that the feeling of two-colour combinations under LED-RGB at 10 lx is almost the same with the feeling under LED-BY and the warm white fluorescent lamp at 700 lx.

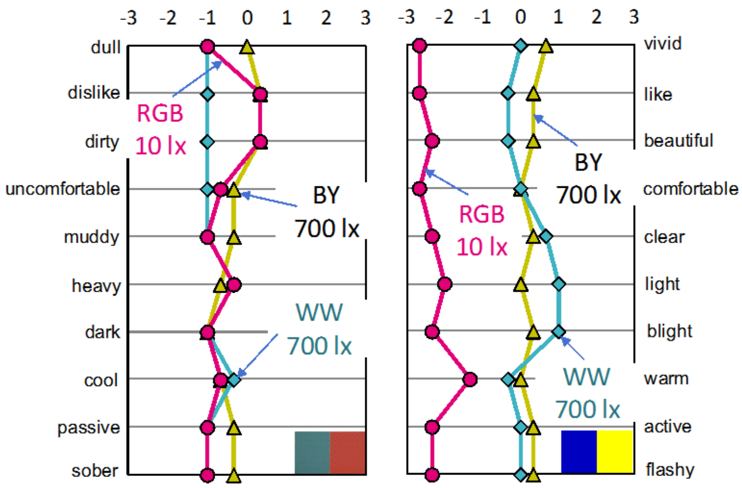

Figure 7 – Profiles of the subjective evaluation under each light sources and illuminance level (the two colour combinations)

Figure 8 shows that the affective evaluation of the mosaic colour sample was strongly influenced by illuminance. At low illuminance (10 lx) the subjective evaluation became decrease because the colour appearance was desaturated by the Hunt effect. Furthermore, it was shown that the affective evaluation was influenced by the spectral power distributions of the light sources. The subjective feeling under the LED-RGB illumination was higher than the other test light sources at all illuminance level.

It is reported that the colour rendering index *Ra* indicating colourimetric fidelity does not correlate with preferred lighting conditions. As indicated in our study, it is clear that LED-RGB lighting with very low Ra19 looks bright, beautiful and preferable at low illuminance as well as at high illuminance compared with the other light sources.

Figure 9 shows the relationship between *Ra* and *R9* and the subjective evaluation of "bright-dark" and "vivid-dull". As shown in Figure 9, it is obvious that the subjective result under LED-RGB lighting does not correlate with Ra and R9. Therefore when evaluating colour appearance at different illuminance including white LED lighting, the current colour rendering evaluation method is not sufficient and the other indices deriving from the different method from the current *Ra* and *Ri* will be required.

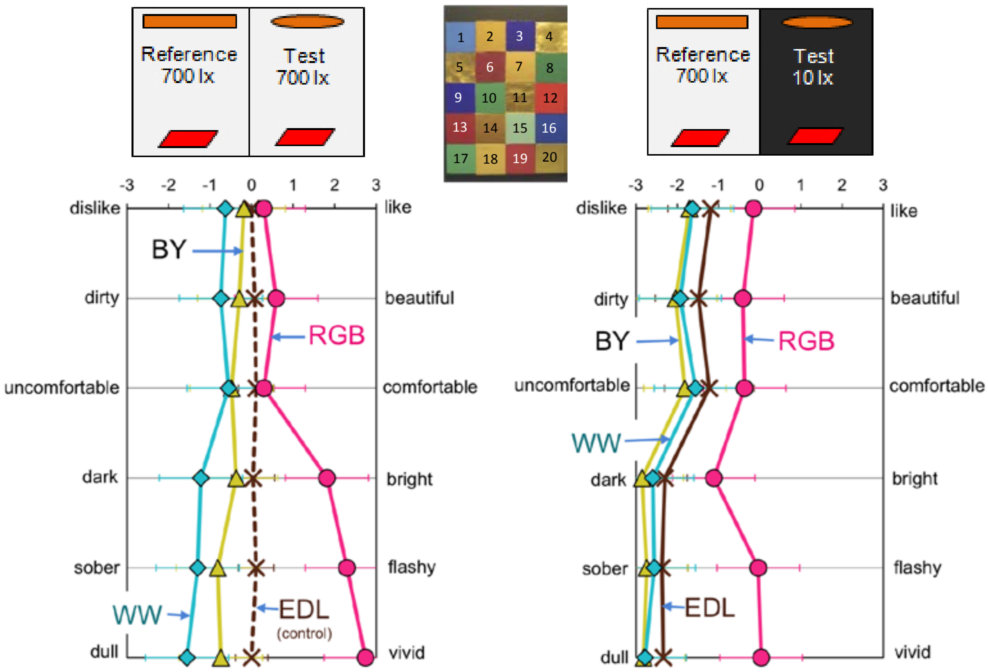

Figure 8 –Profiles of subjective evaluation of the mosaic colour samples under each light source and illuminance level.

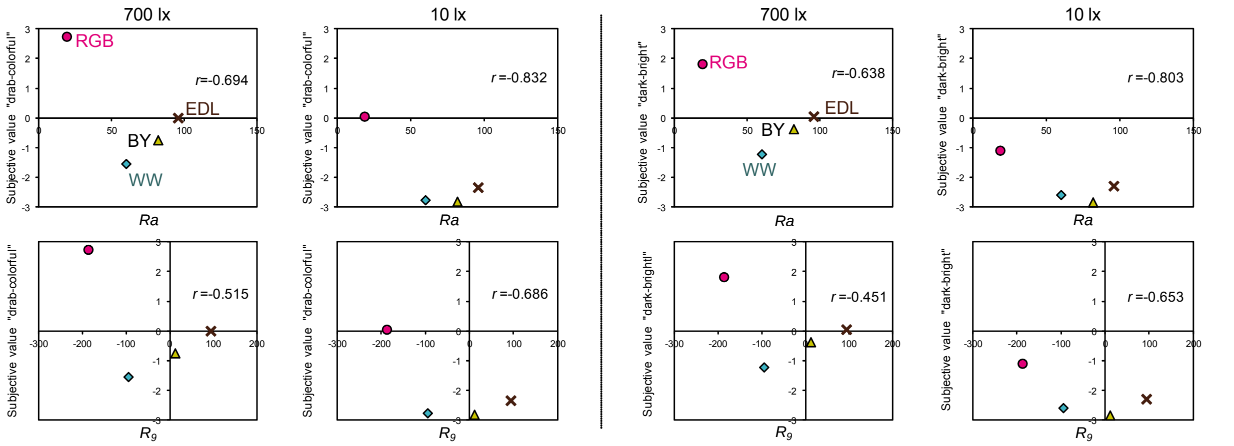

Figure 9 –Relationship between the subjective evaluation (left:vivid-dull, right:bright-dark) and Ra／R9

3. Experiment 2

3.1 Experiment

To examine whether the current CRI are appropriate or not for subjective evaluation of colour appearance at very low illuminance, we tried to verify the several calculation methods of the colour rendering values taking into consideration of illuminance.

We examined first the colourimetric fidelity based caluculation methods.

①Ra（J-$a_M b_M$）

②Ra（Q-$a_M b_M$）

③Ra（E,J-$a_M b_M$）

④Ra（E,Q-$a_M b_M$）

⑤Ra（CRI-CAM02UCS (Luo, Cui, Li 2006)）

⑥Ra(CRI2012 (Smet, Schanda, Whitehead, Luo 2012))

Next, the caluculation methods based on the gamut ratio (GR) and the feeling of contrast (FCI) (Hashimoto, Yano, Shimizu, Nayatani 2007) were examined.

⑦GR（Gamut Ratio）

⑧FCI(J-$a_C b_C$)

⑨FCI(J-$a_M b_M$)

⑩FCI(Q-$a_M b_M$)

These expressions were calculated in the new colour space of CIECAM02 (CIE 2003) or CIECAM02-UCS (Luo, Cui, Li 2006). CIECAM02 and CIECAM02-UCS be able to predict colour appearance including illuminance.

The procedure is as follows:

(a) The tristimulus values XYZ of the test light sources and the reference light source with the same correlated colour temperature with the test were calculated,

(b) The tristimulus values of each test colour samples under the reference and the test light sources were calculated.

(c) J, Q, C, M, $a_C b_C$, $a_M b_M$ and a_M'b_M' of CIECAM02 or CIECAM02-UCS under each illuminance (1000 lx, 10 lx) were calculated using the parameters in Table 2.

Table 2 – CIECAM02 parameters for calculation

parameter	value
Y_b	20
F	1
N_c	1
c	0.69
L_A(1000 lx)	63.66
L_A(10 lx)	0.64

3.2 Results

The results indicated that the current CRI based on colour fidelity was not correlated with the affective evaluation of the mosaic colour sample under low illuminance. In other words, the current CRI could not evaluate the colour rendering properties at low illuminace.

The colour rendering values considering illuminance parameters based on the gamut ratio (GR) and the feeling of contrast (FCI) were correlated to the colour appearance results of the two-colour pairs under even low illuminance as well as high illuminance. The colour rendering values with illuminance effects based on GR and FCI could be the one of the best methods calculating colour rendering values when changing illuminace.

4. Conclusion

(1) The colour appearance (brightness, vividness, etc.) of the mosaic colour sample changes depending on illuminance and decreases at low illuminance.

(2) The current *Ra* or *Ri* cannot express the colour appearance of the mosaic colour sample under low illumination.

(3) LED-RGB lighting has the effect of making the colour appearance of chromatic objects more colourful and more vivid compared with other light sources at very low illuminance (10 lx).

(4) As an appropriate index showing colour feeling of the chromatic objects under different illuminance, it is conspicuous that the indices based on the GR (Gamut Ratio) or the Colour Contrast will have a good correlation with the subjective evaluations.

Table 3 – The various colour rendering indices in consideration of illuminance

Light sources		***Ra***	**①Ra(J-$a_M b_M$)**	**②Ra(Q-$a_M b_M$)**	**③Ra(E,J-$a_M b_M$)**	**④Ra(E,Q-$a_M b_M$)**	**⑤Ra(CRI-CAM02UCS)**	**⑥Ra(CRI2012)**
FL-EDL(L)	EDL 1000lx	96	97	97	96	96	97	99
Ref:P3062	EDL 10lx		59	-337	46	-481	53	48
LED-RGB(L)	RGB 1000lx	19	56	55	42	41	42	38
Ref:P2878	RGB 10lx		61	-335	48	-478	52	42
LED-BY(L)	BY 1000lx	82	85	85	80	80	81	84
Ref:P3064	BY 10lx		58	-338	44	-482	50	45
FL-WW	WW 1000lx	60	71	70	61	60	61	59
Ref:P3500	WW 10lx		52	-339	36	-487	39	33
test colors		CIE/JIS 8 test colors(No.1-8)	CIE/JIS 8 test colors(No.1-8)	CIE/JIS 8 test colors(No.1-8)	CIE/JIS 8 test colors(No.1-8)	CIE/JIS 8 test colors(No.1-8)	CIE/JIS 8 test colors(No.1-8)	CIE/JIS 8 test colors(No.1-8)
chromatic adaptation transform		von Kries	CAT02	CAT02	CAT02	CAT02	CAT02	CAT02
color space		CIE1964 $U^*V^*W^*$	CIECAM02(J-$a_M b_M$)	CIECAM02(Q-$a_M b_M$)	CIECAM02(J-$a_M b_M$)	CIECAM02(Q-$a_M b_M$)	CIECAM02(J'-a_M'b_M')	CIECAM02(J'-a_M'b_M')

Light sources		**⑦GR（Gamut Ratio）**	**⑧FCI(J-$a_C b_C$)**	**⑨FCI(J-$a_M b_M$)**	**⑩FCI(Q-$a_M b_M$)**
FL-EDL(L)	EDL 1000lx	101	114	122	117
Ref:P3062	EDL 10lx	46	110	43	22
LED-RGB(L)	RGB 1000lx	123	183	204	192
Ref:P2878	RGB 10lx	57	178	64	33
LED-BY(L)	BY 1000lx	98	101	106	102
Ref:P3064	BY 10lx	45	97	40	21
FL-WW	WW 1000lx	83	74	77	73
Ref:P3500	WW 10lx	38	71	30	16
test colors		CIE/JIS 8 test colors(No.1-8)	RYGB（FCI）	RYGB（FCI）	RYGB（FCI）
chromatic adaptation transform		CAT02	CAT02	CAT02	CAT02
color space		CIECAM02($a_M b_M$)	CIECAM02(J-$a_C b_C$)	CIECAM02(J-$a_M b_M$)	CIECAM02(J-$a_M b_M$)

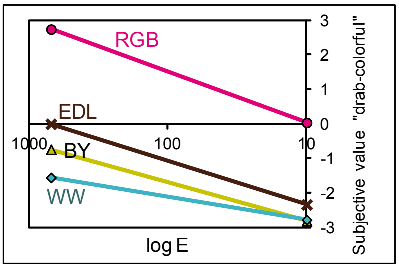

■ Top: Relationship between the subjective evaluation and illuminance (log E)

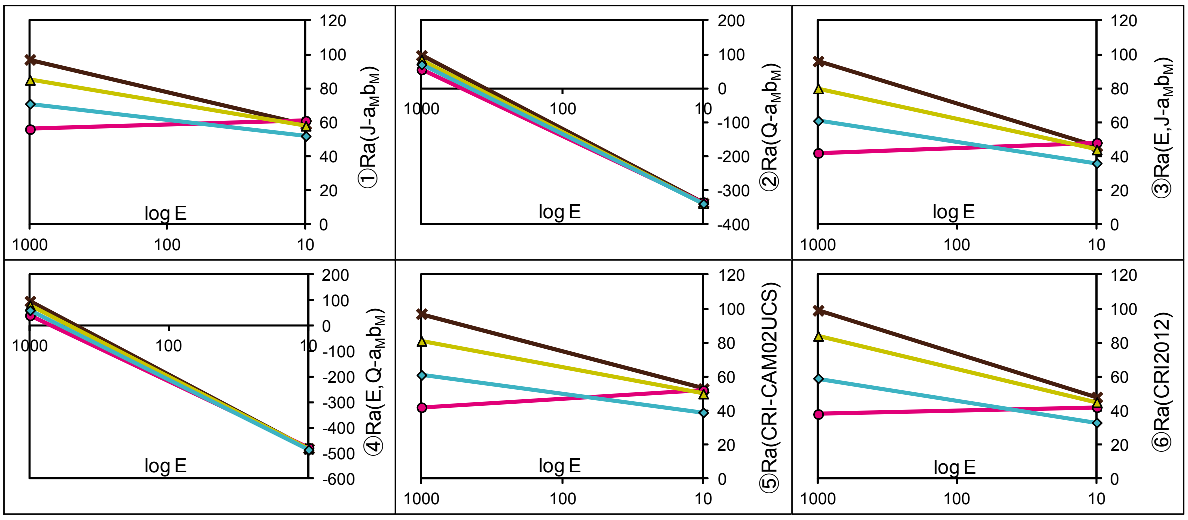

■ Middle: Relationship between the colour rendering indices (①②③④⑤⑥) about colourimetric fidelity in consideration of illumination and illuminance (log E)

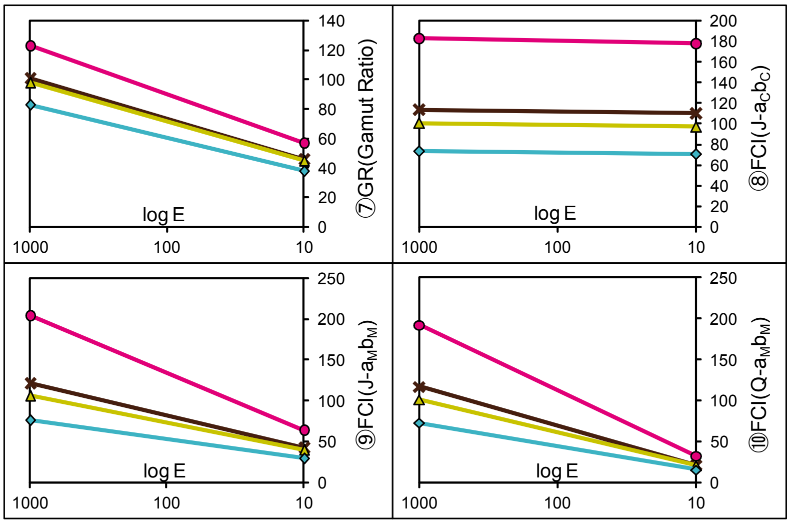

■ Bottom: Relationship between the colour rendering indices (⑦⑧⑨⑩) about Gamut area, Colour Contrast in consideration of illumination and illuminance (log E)

Figue 10 – Relationship between illuminance (log E) and the subjective evaluation, the various colour rendering indices in consideration of illuminance

Top : Relationship between subjective evaluation and illuminance (log E)
Middle: Relationship between the colour rendering indices (①②③④⑤⑥) about colourimetric fidelity in consideration of illumination and illuminance (log E)
Bottom: Relationship between the colour rendering indices (⑦⑧⑨⑩) about Gamut area, Colour Contrast in consideration of illumination and illuminance(log E)

Acknowledgement

We would like to express our sincere appreciation and gratitude to Dr.Kenjiro Hashimoto, Fellow of the Illuminating Engineering Institution of Japan, Japan Colour Research Institute and KONICA MINOLTA INC. for their support. We also thank to the students of Graduate School of Joshibi University of Art and Design for their observer participation to our subjective experiment.

References

CIE 2004. CIE 157:2004. Control of damage to museum objects by optical radiation. Vienna: CIE.

HUNT, R. W. G. 1952. Light and dark adaptation and the perception of colour. J. Opt. Soc. Am., 42, 190-199.

CIE/ISO 2001. ISO 8995-1:2002(E)/CIE S008/E: 2001: Joint ISO/CIE Standard: Lighting Work Places-Part 1: Indoor [incl. Technical Corrigendum ISO 8995: 2002/Cor. 1:2005(E)] CIE.

LI, C., LUO, R. M., LI, C., CUI, G. 2012. The CRI-CAM02UCS Colour Rendering Index, Colour Res. Appl., 37, 161-167.

SMET, K. A. G., SCHANDA, J., WHITEHEAD, L., LI, C., LUO. 2012. CRI2012: A proposal for updating the CIE colour rendering index, Lighting Res. Technol. 2012; 0: 1–21

HASHIMOTO, K., YANO, T., SHIMIZU, M., NAYATANI, Y., 2007. New methode for specifying colour-rendering properties of light sources based on feeling of contrast, Colour Res. Appl., 32, 361-171.

CIE 2004. CIE 159:2004. A colour appearance model for colour management systems: CIECAM02. Vienna: CIE.

LUO, R. M., CUI, G., LI, C. 2006. Uniform Colour Spaces Based on CIECAM02 Colour Appearance Model, Colour Res. Appl., 31, 320-330.

PP05

COMPUTATION AND EVALUATION ON DUV PROPERTY OF LED LUMINAIRES

Huang, S.G.[1]**,** Liu, L.[1], Chen, Y.[1]

[1]National Center of Supervision & Inspection on Electric Light Source Quality (Shanghai) [1]Shanghai Alpha Lighting Equipment Testing Ltd. (SALT), Shanghai, CHINA

huangsungang@163.com

Abstract

In this paper we introduced the definition of Duv (anther important dimension of chromaticity) which was first defined in ANSI_NEMA_ANSLG C78.377-2008. Based on the definition and the discussion of three classic calculating methods of Duv, an equal-interval method for optimizing Duv calculation is proposed. Comparing the results of these above-mentioned methods by MATLAB, it is proved the newly proposed method improves the accuracy as well as the speed of the Duv calculation. Besides we also investigate the products applied for the Energy Conservation Certification to evaluate the Duv property and find out large Duv play an important role on products failed the Energy Conservation Certification. At last, the article analyzes the CCT and CRI do not tell the whole story of color quality and call all society to pay attention to Duv as well as CCT and CRI.

Keywords: Colorimetry, Chromaticity diagram, Solid state lighting, Duv algorithm, LED, Colour quality

1 Introduction

The LED-based solid state lighting (SSL) with the high energy-efficient, high color quality white light, long life time and colorful light source has the potential to revolutionize the lighting industry which is developed quickly in recent years. The progress in LED lighting industry can best be measured by efficiency and pricing. As report, the lumen efficiency of white LED source has achieved 231 lumens per watt and is available to break the 300 lumens per watt with low color quality [1]. The pricing which determines the competitive ability of LED products is affected by many factors, from the cost of materials to various subsidies. But in number, the price falls a lot in recent 10 years [1].

Light-emitting diodes (LEDs) which are not inherently white light source emit light in a very narrow range of wavelengths in visible spectrum and they are widely applied at exit signs, traffic lights and decoration engineering. However, to be used as general light sources, white light with high color quality is needed. Duv [2] (anther important dimension of chromaticity) has become an important metric of color quality in many standards [3, 4] (such as GB/T 29294-2012) as well as correlated colour temperature (CCT) [5,6] and Colour rendering index (CRI). Thus, the computation on Duv property of LED luminaires is indispensable and urgently required in chromaticity test.

In former years, for color quality information of lighting products only CCT and CRI are often used and Duv is not shown though it is also critical [7, 8]. So Duv is not available in some commercial instruments, and it is often asked how to calculate it [9]. Furthermore, many commercial instruments have different calculation method and different computation result. The curve fitting method [10] has little computation but with only acceptable accuracy and the point by point method [11] has the best accuracy but with large calculations. Our research group based on the definition and the discussion of three classic calculating methods of Duv try to find the balance between the accuracy and the speed of calculation. In this paper, an equal-interval method for optimizing Duv calculation is proposed. Comparing the results of these above-mentioned methods by MATLAB, it is proved the newly proposed method improves the accuracy as well as the speed of the Duv calculation. We also investigate the products applied for the Energy Conservation Certification to evaluate the Duv property and find out large Duv play an important role on products failed the Energy Conservation Certification. At last, the article analyzes that the CCT and CRI do not tell the whole story of color quality and call all society to pay attention to Duv as well as CCT and CRI.

2 Computation results of different commercial software

Many instrument manufacturers calculate the Duv and display it on their software after a spectrum test. Unfortunately, the Duv has not been defined by CIE and no recommend computation method has been approved. Different manufacturer has different computation method and even different comprehension on Duv. The △Duv is introduced to indicate the absolute value of the difference between different instrument manufacturers while the △Duv% is the index that represent how much the computation difference △Duv influence the qualification evaluation. And the △Duv% is defined as the following formula: △Duv%=100%×△Duv/tolerance, where the tolerance is 0.012 (±0.006) which was defined in ANSI_NEMA_ANSLG C78.377-2008.

Table 1.Comparison between E* and P*

sample	x	Y	Duv(E*)	Duv(P*)	△Duv	△Duv%
1	0.4294	0.3956	-2.33E-03	-2.40E-03	7.00E-05	0.58
2	0.3790	0.3800	1.91E-03	1.80E-03	1.10E-04	0.92
3	0.3620	0.3640	-2.22E-04	-3.00E-04	7.80E-05	0.65
4	0.3443	0.3522	6.01E-04	5.00E-04	1.01E-04	0.84
5	0.3401	0.3721	1.20E-02	1.19E-02	1.00E-04	0.83

The E* is an instrument manufacturer in China, and the P* is an instrument manufacturer in Australia.

The computation results of Duv on the basis of the same chromaticity coordinate (x, y) between manufacturer E* and P* are shown in table 1. The CCT of the chromaticity coordinates is selected from about 3000K to 5500K, and according to the results shown in table 1, the biggest Duv difference △Duv between E* and P* is 1.10E-04 while the biggest △Duv% is 0.92%.

Table 2.The comparison between L* and P*

sample	x	y	Duv(L*)	Duv(P*)	△Duv	△Duv%
1	0.4338	0.4099	2.30E-03	2.80E-03	5.00E-04	4.17
2	0.4007	0.3799	4.00E-03	-3.80E-03	7.80E-03	65.00
3	0.3892	0.3679	7.10E-03	-6.60E-03	1.37E-02	114.17
4	0.3591	0.3665	1.50E-03	2.10E-03	6.00E-04	5.00
5	0.342	0.3537	1.70E-03	2.40E-03	7.00E-04	5.83

The L* is an instrument manufacturer in USA, and the P* is an instrument manufacturer in Australia.

The software from manufacturer E* and L* can not calculate Duv directly based on a spectrum or a chromaticity coordinate (they can only calculate the Duv property after a spectrum test). So comparing the computation methods of Duv between E* and L* is a tough thing. Table 2 shows the computation results of Duv on the basis of the same chromaticity coordinates (x, y) between manufacturer L* and P*. The chromaticity coordinates are another group of coordinates of which CCT is ranging from about 3000k to 5000K. We were shocked at the difference of Duv calculated by instrument manufacturer L* and P* according to table 2. The biggest Duv difference △Duv is 1.37E-02 and the △Duv% is 114.17% which means the calculate difference is bigger than the tolerance which was defined in ANSI_NEMA_ANSLG C78.377-2008. In the chromaticity diagram, we can see the coordinate (0.3892 0.3679) is below the Planckian locus, and the Duv should absolutely negative. The biggest Duv difference is 7.00E-04 which can influence the qualification evaluation significantly (the △Duv% is about 5.83%) even we eliminate the sample 2 and sample 3 (the Duv of these two samples should sign "-" before the computation values of manufacturer L*).

The computation results from different instrument manufacturers distribute in a large scope and one manufacturer even do not sign the "-" before its computation result which can be identified obviously in the chromaticity diagram (the chromaticity coordinate is below the Planckian locus). Thus an effective method and acceptable computational accuracy should be recommended urgently, otherwise products with qualified Duv will be judged to below the standard meanwhile the products with unqualified Duv will calculate to up to the standard.

3 Classic calculating methods on Duv

As the definition in ANSI_NEMA_ANSLG C78.377-2008, the Duv is the closest distance from the Planckian locus on the (u', 2/3v') diagram, with + sign for above and – sign for below the Planckian locus. The chromaticity of white light can be expressed by chromaticity coordinates such as (x, y) and (u', v'), but according the coordinates, we can not know the color quality of the white light. However, the chromaticity of white light expressed by CCT and the distance from the Planckian locus Duv is an effective and intuitive way.

3.1 Point by point method

According to ANSI_NEMA_ANSLG C78.377-2008, the Duv is defined based on the (u, v) chromaticity diagram. Thus, before calculate the distance from the Planckian locus Duv, the chromaticity coordinates (x, y) should be first translated to (u, v). Their relationship is described by the following equations:

$$\begin{cases} u = \dfrac{4x}{-2x+12y+3} \\ v = \dfrac{6y}{-2x+12y+3} \end{cases} \tag{1}$$

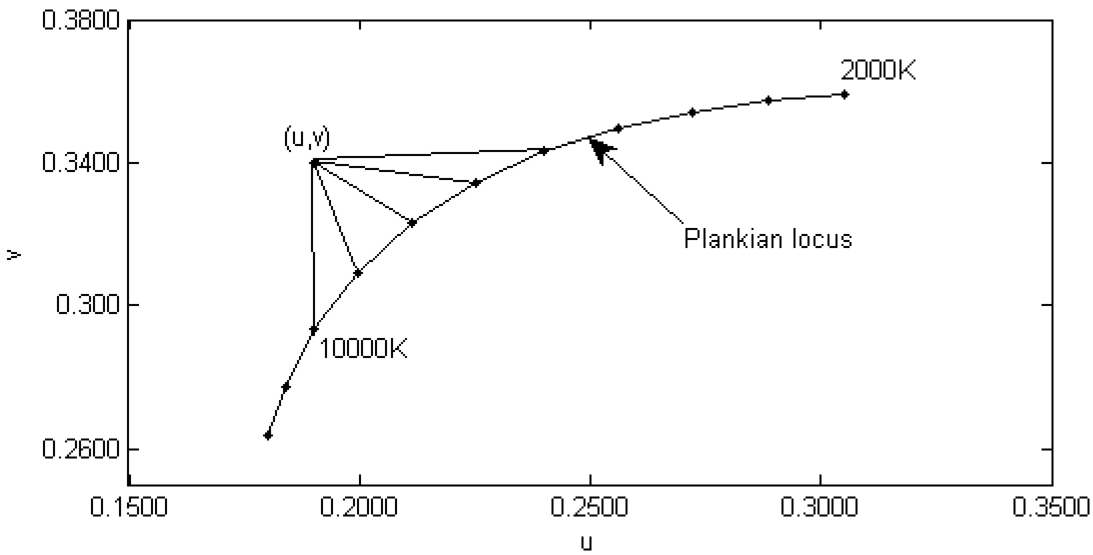

Fig.1 The Planckian locus in the CIE 1960 chromaticity diagram

The point by point method is calculating all the distances from the chromaticity coordinates (u, v) of white light to each point on the Planckian locus based on 1960 chromaticity diagram shown as figure 1. And then find the shortest distance which is the Duv of the white light.

The point by point method cost huge computational resource and take a lot of time though it has high accuracy results. Take the white LED for example, the CCT range of white LED is from 2000K to 10000K, take the interval as 1K, and 8001 distances should be calculated and more calculated amount should be taken to find the shortest distance.

3.2 Curve fitting algorithm

The curve fitting algorithm is widely used in CCT computations []. This method is using curve fitting technology to find the analytical function of the Planckian locus. The closest distance from the chromaticity coordinates to the Planckian locus can be calculated easily by Newton-type iterative method based on the analytical function of the Planckian locus. The CCT during 1000K to 10000K can be expressed as []:

$$T = -437n^3 + 3601n^2 - 6861n + 5514.31 \qquad (2)$$

Where $n = (x - 0.3320)/(y - 0.1858)$, $x = 9u/(12 + 6u - 24v)$, $y = 3v/6 + 3u - 12v$ as we know the correlated color temperature, the chromaticity coordinates on the Planckian locus can be found and the Duv is the distance between these two coordinates.

The curve fitting algorithm cost little computational resource, but it can't always fit the Planckian locus well especially in the high CCT region. The more difference between the curve fitting locus and Planckian locus, the worse results of Duv will be calculated.

3.3 Triangular solution [8]

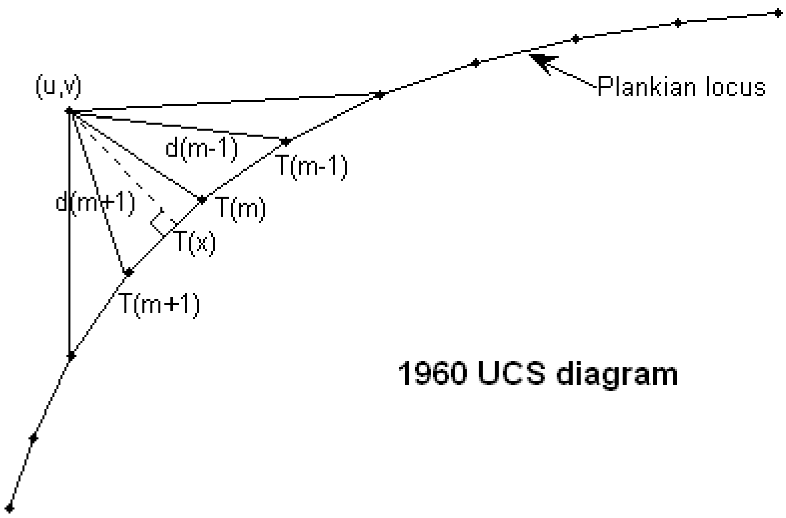

Fig.2 Triangular solution of Duv computation

The triangular solution of Duv computation is an approximate treatment method. We should first create a table of distance d (i) to Planckian locus on 1960 UCS diagram shown as figure 2. And then find the closest point in the table. At last, solve the triangular for the neighboring 2 points shown in figure 3.

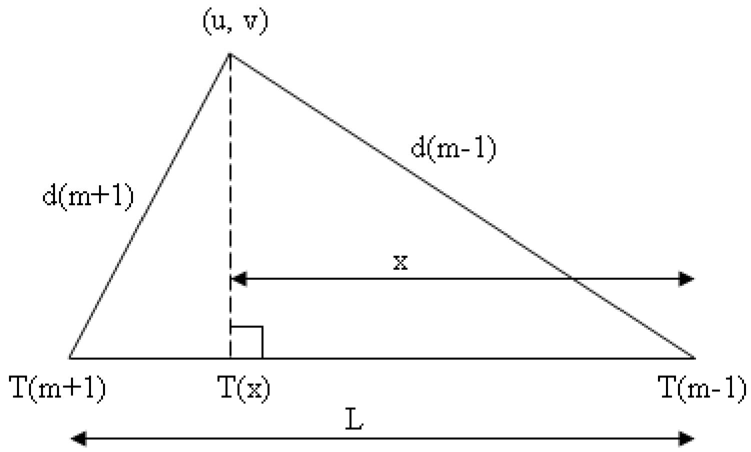

Fig.3 The approximate triangular on Duv computation

As the d (m+1), d (m-1) and L are calculated, the x can be deduced:

$$\mathrm{x} = \frac{d^2(m-1) - d^2(m+1) + L^2}{2L} \tag{3}$$

Using the Pythagorean Theorem, the Duv can be expressed as:

$$\mathrm{Duv} = \pm(d^2(m-1) - x^2)^{1/2} \tag{4}$$

Where $\pm$ is + sign for chromaticity coordinates (u, v) above and – sign for chromaticity coordinates (u, v) below the Planckian locus.

4 The Equal-interval method on Duv

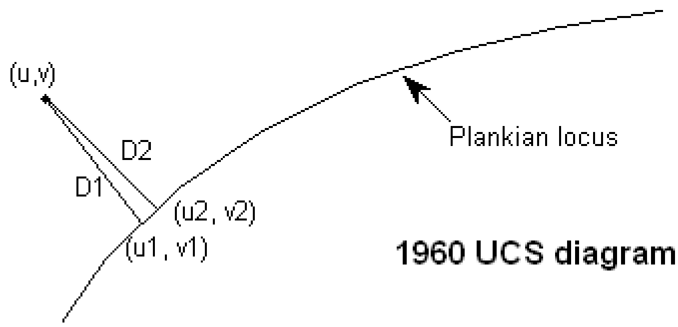

Fig.4 Equal-interval solution of Duv computation

The equal-interval method is dividing the Planckian locus into N equal-interval sections, then calculating the distances from the chromaticity coordinates (u, v) to each section end point, finding the shortest distance D1 and its corresponding coordinates (u1, v1) on the Planckian locus which is the end point of the M section shown in figure 4, finding the coordinates (u2, v2) on the Planckian locus which is larger 1K than the coordinates (u1,v1) and then calculate the distance D2 from (u, v) to (u2, v2). Comparing D1 with D2, if D1<D2, dividing the M section into N equal-interval sections and repeating the previous steps, otherwise dividing the M-1 section into N equal-interval sections and repeating the previous steps.

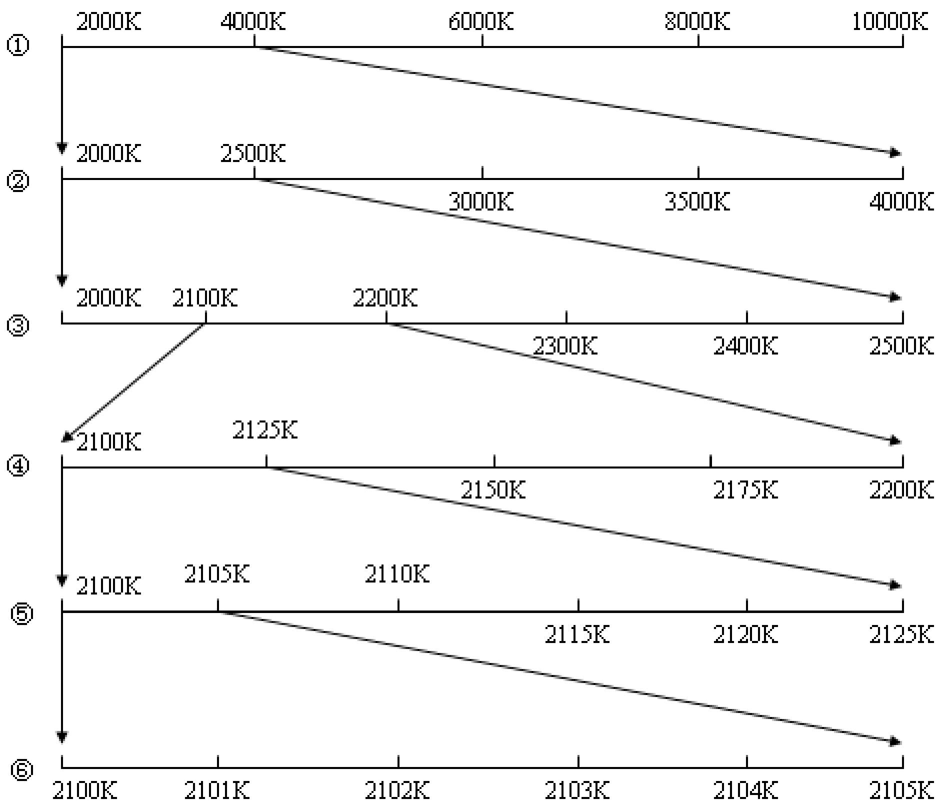

Fig.5 Six steps of equal-interval partitioning at 2000K to 10000K

To reducing the calculated amount, taking a 2102K white LED for example. The CCT range of white LED is from 2000K to 10000K, dividing the CCT rang into 4 sections, calculating the chromaticity coordinates (u, v) to each end point of sections and finding the shortest point is during 2000K to 4000K, dividing the section 2000K to 4000K into 4sections and finding the shortest point is during 2000K to 2500K, repeating the previous step, after 6 steps dividing, the interval between sections is 1K, after comparing each distance, the 2102K is the shortest point. The Duv is the distance between the chromaticity coordinates (u, v) to the coordinates which corresponding 2102K on the Planckian locus.

5 Comparison analyses of different methods on Duv computation

5.1 The computation results of points on tolerance quadrangle

In the initial stages of commercialization, the SSL products are considered to be for replacement of existing fluorescent lamps and luminaires as well as those of incandescent lamps, the chromaticity specification was developed. As the SSL technology are still at their early stage, control and stability of chromaticity of light are not well established. The quadrangles representations of the chromaticity specification of SSL products are shown in figure 6 [2].

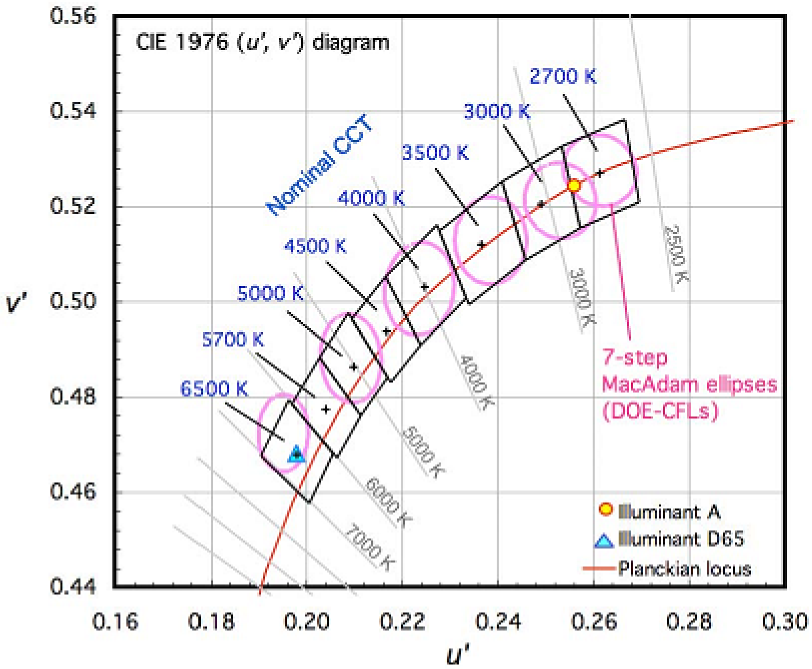

Fig.6 The chromaticity specification of the SSL products

Six points on tolerance quadrangle were selected and the calculate results of the four different algorithms are shown in the table 3. The △t is the average time that the algorithm calculate the Duv of chromaticity coordinates takes. From the table 3, the 'curve fitting algorithm' takes the least time, meanwhile the 'point by point method' and the 'Equal-interval method' have the best accuracy. The 'Equal-interval method' takes little time but have the best accuracy (in some sense, the 'Equal-interval method' is a simple version of the 'point by point method').

Table 3 The comparison of the four different algorithms on Duv calculation

sample	1	2	3	4	5	6	△t(s)
X	0.4813	0.4562	0.4147	0.3548	0.3222	0.3068	/
Y	0.4319	0.4260	0.3814	0.3736	0.3243	0.3113	/
Duv(Q)	6.00E-03	6.00E-03	-6.00E-03	7.00E-03	-4.00E-03	-3.00E-03	/
Duv(P)	6.00E-03	6.00E-03	-6.00E-03	7.00E-03	-4.00E-03	-3.00E-03	0.09734
Duv(C)	6.00E-03	6.00E-03	-5.99E-03	6.98E-03	-4.00E-03	-3.02E-03	0.00001
Duv(T)	6.02E-03	6.02E-03	-5.98E-03	6.99E-03	-4.00E-03	-3.02E-03	0.00394
Duv(E)	6.00E-03	6.00E-03	-6.00E-03	7.00E-03	-4.00E-03	-3.00E-03	0.00353

The Duv(Q) are the values in theory, as the points are on tolerance quadrangle, the Duv values are 6.00E-03, 6.00E-03, -6.00E-03,7.00E-03, -4.00E-03, -3.00E-03, separately. The Duv(P) is the value calculated by the 'point by point method'. The Duv(C) is the value calculated by the 'Curve fitting algorithm'. The Duv(T) is the value calculated by the 'Triangular solution'. The Duv(E) is the value calculated by the 'Equal-interval method'.

The rest points of the tolerance quadrangle were calculated by the four different calculation algorithms and the results are the same as the results shown in table 3. The 'curve fitting algorithm' takes the least time and have acceptable results while the 'Equal-interval method' has the best accuracy and takes little time.

5.2 The computation results of white LED

Table 4.The comparison of the six different algorithms on Duv calculation of white LED

sample	1	2	3	4	5	⊿t(s)
x	0.4294	0.379	0.362	0.3443	0.3401	/
y	0.3956	0.38	0.364	0.3522	0.3721	/
Duv(E*)	-2.33E-03	1.91E-03	-2.22E-04	6.01E-04	1.20E-02	/
Duv(P*)	-2.40E-03	1.80E-03	-3.00E-04	5.00E-04	1.19E-02	/
Duv(P)	-2.36E-03	1.94E-03	-2.10E-04	6.13E-04	1.19E-02	0.09829
Duv(C)	-2.36E-03	1.94E-03	-2.24E-04	6.20E-04	1.19E-02	0.00001
Duv(T)	-2.35E-03	1.94E-03	-2.07E-04	6.16E-04	1.19E-02	0.00406
Duv(E)	-2.36E-03	1.94E-03	-2.10E-04	6.13E-04	1.19E-02	0.00340

The samples in the table 4 is selected from the table 1 whose CCT (correlated color temperature) is from about 3000K to 5500K. The Duv(P) which adopt the ‘point by point method’ has the best accuracy but cost huge computational resource and takes the maximum time. The Duv(E) which adopt the ‘Equal-interval method’ has the same accuracy as the ‘point by point method’ but takes much less time. The computational results from manufacturer E* and P* have some difference (not huge) to the results from ‘point by point method’. The ‘curve fitting method’ takes the least time and has acceptable results may be can be used in estimation.

The five samples in the table 5 is selected from the table 2 whose CCT (correlated color temperature) is from about 3000K to 5000K. From table 5, we can find that the results from manufacturer P* have little different to the results from ‘point by point method’, meanwhile the results from manufacturer L* have huge different to the results from any other algorithm. Moreover, the manufactory L* even do not sign the “-” before its computation result which can be identified obviously in the chromaticity diagram (the chromaticity coordinate is below the Planckian locus).

Table 5.The comparison of different algorithms on Duv calculation of white LED

sample	1	2	3	4	5	⊿t(s)
x	0.4338	0.4007	0.3892	0.3591	0.342	/
y	0.4099	0.3799	0.3679	0.3665	0.3537	/
Duv(L*)	2.30E-03	4.00E-03	7.10E-03	1.50E-03	1.70E-03	/
Duv(P*)	2.80E-03	-3.80E-03	-6.60E-03	2.10E-03	2.40E-03	/
Duv(P)	2.77E-03	-3.80E-03	-6.61E-03	2.03E-03	2.30E-03	0.09502
Duv(C)	2.77E-03	-3.81E-03	-6.61E-03	2.04E-03	2.31E-03	0.00001
Duv(T)	2.77E-03	-3.82E-03	-6.60E-03	2.03E-03	2.31E-03	0.00411
Duv(E)	2.77E-03	-3.80E-03	-6.61E-03	2.03E-03	2.30E-03	0.00362

In a word, the ‘Equal-interval method’ with the same accuracy as the ‘point by point method’ but takes much less time should be recommended as the main algorithm urgently. The error of Duv results calculated by ‘Equal-interval method’ comes from two aspects: one is the interval you divided the Planckian locus, the smaller you divided the interval is, the more accuracy of Duv would be. The other is the accuracy of the chromaticity coordinates you calculated the Duv based on. In addition, the commercial software from instrument manufacturers should be compared carefully, software from manufacturer L* should be modified, otherwise products with qualified Duv will be judged to below the standard meanwhile the products with unqualified Duv will calculate to up to the standard. Besides, the ‘curve fitting method’ can calculate the Duv of chromaticity coordinates quickly and with acceptable accuracy can be used in estimation and other low accuracy region.

6 The importance of Duv property

Duv is defined in ANSI_NEMA_ANSLG C78.377-2008 as the closest distance from Planckian locus on the CIE 1960 chromaticity diagram, with + sign for above and – sign for below the Planckian locus. It has become an important metric of color quality in many standards (such as GB/T 29294-2012) as well as CRI and CCT. The CCT, CRI and Duv are the three dimensions of chromaticity to evaluate the colour quality of LED luminaires. The light with high CRI do not means it has high colour quality, in some case; light with high CRI can also has large Duv property such as sample 1 and sample 2 in table 6. The samples in Table 6 whose spectrum distribution are in figure 7 shows light with high CRI but different spectrum distribution at nominal CCT 5000K have different Duv. Sample 1 and sample 2 with Duv 1.20E-02 and 1.17E-02 are out of the colour tolerance at 5000K which means light from sample 1 and sample 2 has low colour quality.

Table 6 The three dimensions of chromaticity of LED luminaires

sample	x	y	CCT	Ra	Duv
1	0.3400	0.3722	5240	82.8	1.20E-02
2	0.3386	0.3703	5284	83.0	1.17E-02
3	0.3475	0.3559	4925	84.3	1.18E-03

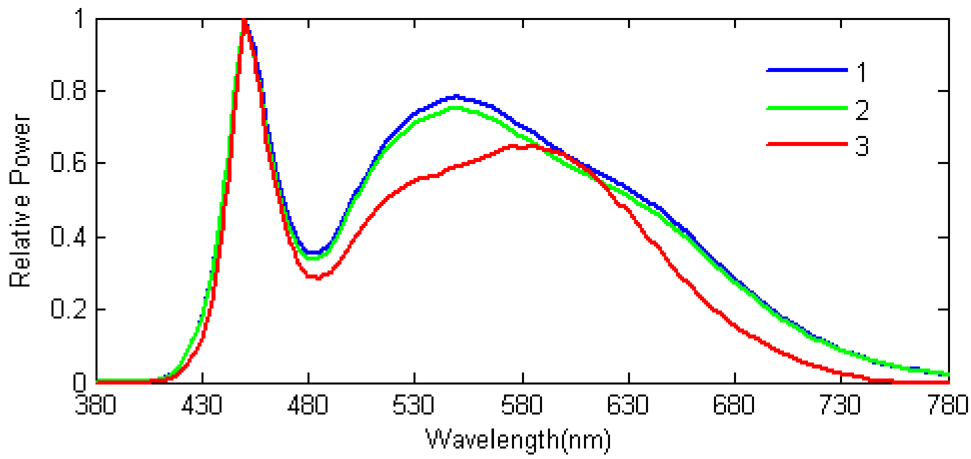

Fig.7 The spectrum distribution of LED luminaires

The Energy Conservation Certification for LED luminaires has conducted for 3years in china, hundreds of preoducts have applied for this certification, and many of them failed. We investigate the luminaire effecacy, lumen maintaince performance, CCT, CRI, Duv and stability of CRI and found out large Duv property plays an important role on products failed Energe Conservation Certification. So we should pay more attentions to the Duv property of LED luminaires as well as CCT and CRI

7 Conclusions

This paper has studied on the Duv property of LED luminaires. Duv as defined in ANSI_NEMA_ANSLG C78.377-2008 is the closest distance from Planckian locus on the CIE 1960 chromaticity diagram. The comparisons of Duv calculations of different commercial software were studied in first section and different software has different computation method on Duv. An effective computation method on Duv should be recommended. Three classic calculating methods of Duv were introduced and an equal-interval method for optimizing Duv calculation is proposed in second section. After comparing the results of different computation method by MATLAB, it is proved the newly proposed method improves the accuracy as well as the speed of the Duv calculation. At last, we analyze the CCT and CRI do not tell the whole story of color quality and call all society to pay attention to Duv as well as CCT and CRI.

References

[1] Haitz, R., Jeffrey, Y. T. January 2011. Solid-state lighting: ‘The case’ 10 years after and future prospects. *Physica status solidia.* Volume 208, 17-29.

[2] NIST 2008. ANSI_NEMA_ANSLG C78.377-2008. Specifications for the chromaticity of solid state lighting products.

[3] SAC/TC 2012. GB/T 29294-2012. Performance requirements for LED downlights. Shanghai: SAC/TC.

[4] CQC 2013. CQC3128-2013. Energy conservation certification criteria for LED downlights. Beijing: CQC.

[5] CIE 1989. CIE 17.4 1989. International Lighting Vocabulary. Vienna: CIE.

[6] Gardner, J. L. March 2000. Correlated colour temperature-uncertainty and estimation. *Metrologia,* Volume 37, 381-384.

[7] CIE 1995. CIE 13.3 1995. Method of measuring and specifying colour rendering of light source. Vienna: CIE.

[8] CIE 2007. CIE 177 2007. Colour rendering of white LED light source. Vienna: CIE.

[9] Ohno, Y. S. October 2013. Practice use and calculation of CCT and Duv. *The journal of the illuminating Engineering Society of north America.* Volume 10, 47-55.

[10] McCamy, C.S. April 1992. Correlated color temperature as an explicit function of chromaticity coordinates. *color research & application,* volume 17, Issue 2, 142-144.

[11] Robertson, A. R. May 1968. Computation of correlated color temperature and distribution temperature. *Journal of the optical society of America,* volume 58, 1528-1535.

PP07

REACTION TIME MEASUREMENTS TO PERIPHERAL STIMULI ON UNIFORM AND NON-UNIFORM BACKGROUNDS UNDER MESOPIC LIGHT LEVELS

Cengiz, C., Puolakka, M., Halonen, L.
Aalto University, Lighting Unit, School of Electrical Engineering, Espoo, FINLAND
can.cengiz@aalto.fi

Abstract

Definition of the visual adaptation field in night-time driving conditions is needed in order to implement the CIE 191 system for mesopic photometry. In order to determine the size and shape of the adaptation field, new data must be created using experimental setups where the stimuli and the background can be controlled. For this purpose, reaction times to achromatic circular stimulus appearing at different eccentricities (from -75˚ to 75˚) were measured on uniform and non-uniform backgrounds under mesopic light levels. Ten subjects (mean age 28) participated in the experiment. The results concerning both the uniform and non-uniform fields indicate that reaction times to stimulus at far periphery under mesopic light levels are affected by the local luminance of the visual task. However, the luminance distribution of the backgrounds has also effect on reaction times and number of the missed targets. Further studies are needed to verify the results by applying dynamic backgrounds.

Keywords: Mesopic, Photometry, Reaction time, Visual field, Adaptation

1 Introduction

Mesopic photometry includes methods for evaluating visual perception at low light levels (from 0.005 cd/m^2 to 5 cd/m^2). The CIE 191 system of mesopic photometry was published in 2010. (CIE, 2010). Defining the visual adaptation field in terms of its extent and shape is an important goal in order to implement this system for outdoor lighting.

Reaction time measurement is one of the techniques applied to assess the visual performance at mesopic light levels. It refers to the question ‘how quickly the target is detected’ (Eloholma, 2005), which has been studied by adopting different experimental setups (Walkey, 2007). In these studies target eccentricities were below 15˚. In driving conditions miscellaneous stimuli appear also at far periphery. In this study target eccentricities between -75˚ to 75˚ were used.

In reaction time measurements, the background applied is an important factor to assess adaptation conditions of the subjects. In some studies (Walkey, 2006; Eloholma, 2006), uniform backgrounds were applied to measure reaction times. However, it is also necessary to analyse the effect of background non-uniformity on visual performance since the visual scene in driving at night includes various luminances. Therefore, the comparison between the visual performance in uniform and non-uniform backgrounds should provide information for defining the adaptation state. In this study, reaction times for stimuli at larger eccentricities were measured to see the effects of background luminance, luminance uniformity and target location on visual performance. The results are presented to be adopted in estimation of the visual adaptation field at mesopic levels.

2 Methods

A large screen illuminated by three projectors was used to create the background and the stimuli (Figure 1). The screen provides a visual field subtending 180˚ x 44˚. The background spectrum was white (Figure 2). The background luminance ranged from 0.1 to 1 cd/m^2 and the contrast between the background and the target was 0.7.

The contrast value is calculated by the following equation:

$$C = (L_b - L_t)/L_b \quad (1)$$

where C is the contrast, L_b is the background luminance and L_t is the target luminance.

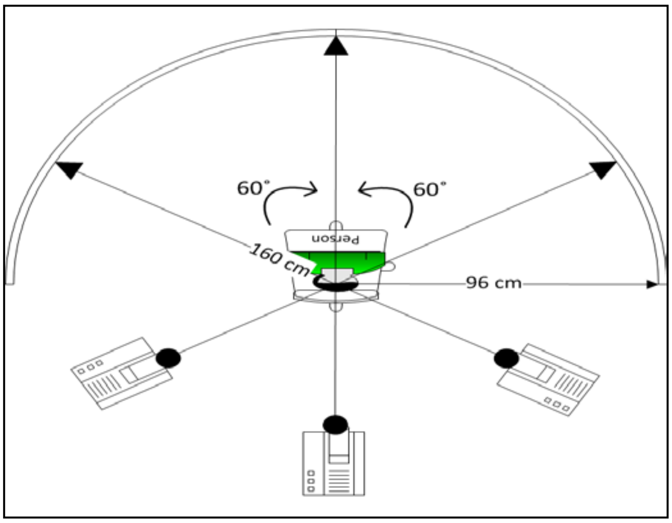

Figure 1 – The experimental setup. The distance between the subject and the fixation point is 96 cm. The distance between the projector and the corresponding central point of the projection is 160 cm. The angle between projectors was 60˚.

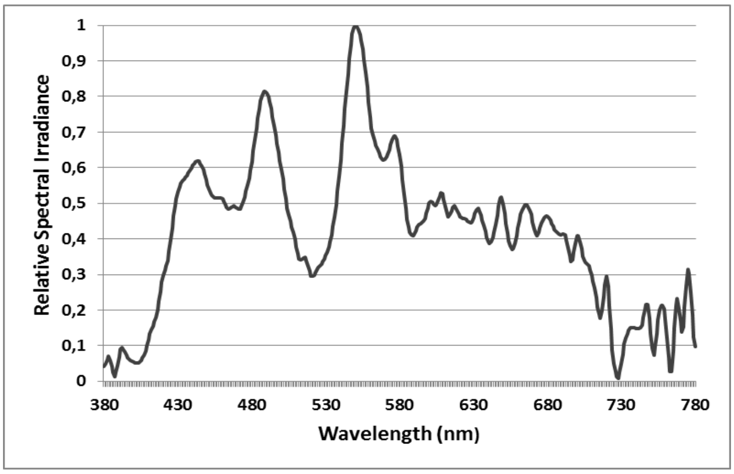

Figure 2 – Spectral power distribution of the background light.

Ten subjects (mean age 28; 5 females and 5 males) participated in the experiment. Achromatic stimuli with the size of 1,5˚ appeared at eccentricities -75˚, -45˚, -10˚, 0˚, 10˚, 45˚, 75˚ were imposed to the background. The order of the stimuli appearance was randomized. The subjects adapted the background light for 10 minutes.

Two uniform and three non-uniform backgrounds were used. Figure 3 shows the five backgrounds used in the experiment. The luminance of the uniform backgrounds were 0,1 and 1 cd/m^2. For non-uniform backgrounds, three different figures (elliptical, road scene and windscreen) with 1 cd/m^2 luminance were imposed to the uniform background with 0,1 cd/m^2 luminance.

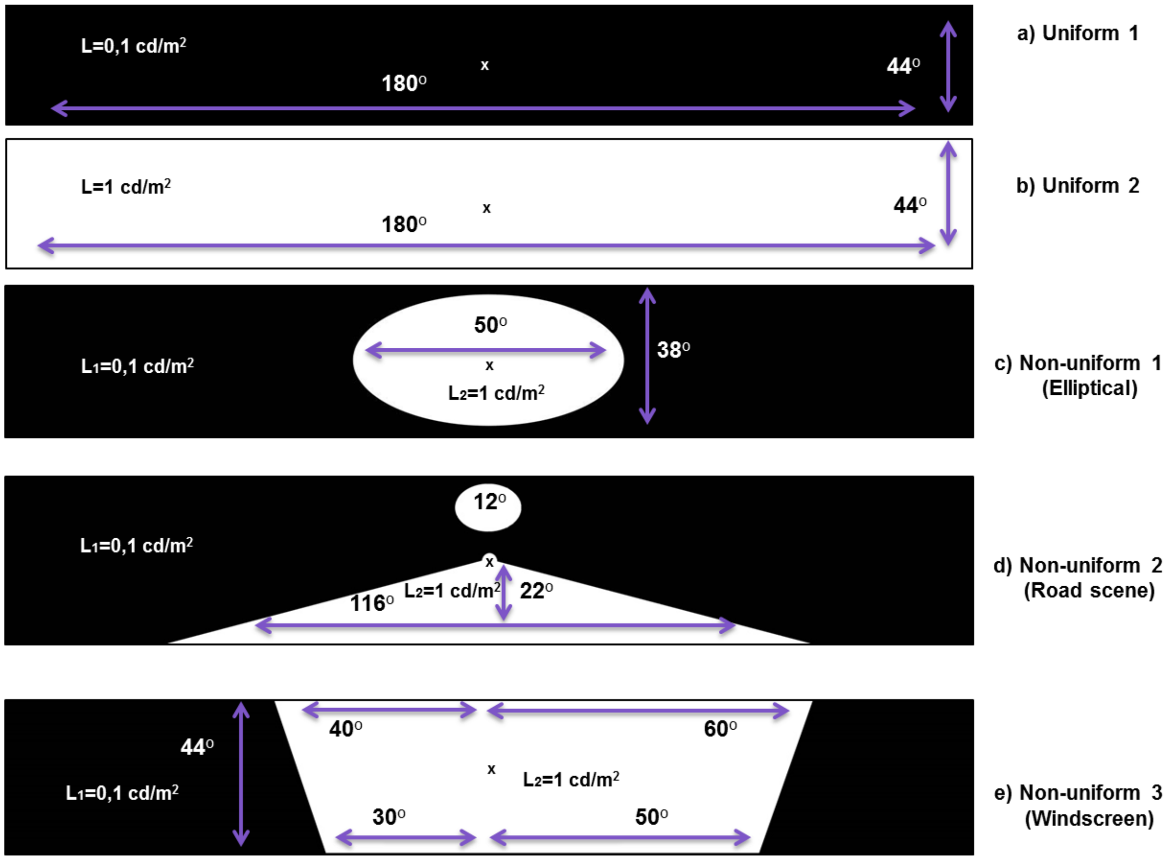

Figure 3 – Two uniform and three non-uniform backgrounds applied in the experiment. The luminance of the white area is 1 cd/m^2 and the luminance of the black area is 0,1 cd/m^2.

The non-uniform backgrounds simulate an elliptical shape of the visual field and a road scene and windscreen of the car, respectively. The reason for using different backgrounds was to analyse the effect of the adaptation luminance pattern on visual performance.

After adapting to the background, the subjects were asked to press the button when detecting the stimulus. The time between the stimulus appearance and the subject's response were recorded as the reaction time. The duration of the stimulus appearance was 1500 ms. Reaction time recorded as 1500 ms was regarded as a missed target. The time between stimulus appearances was randomized. Exceptionally short reaction times were discarded from the results to eliminate anticipatory.

3 Results

Reaction times for stimuli appearing at eccentricities of -75˚, -45˚, -10˚, 0˚, 10˚, 45˚, 75˚ for all backgrounds are presented in Figure 4. As expected, the stimulus location affected the reaction times and the number of missed targets. The reaction times increase with increasing eccentricity for most of the backgrounds. For the second non-uniform background (road scene), reaction time is significantly higher than other backgrounds at 0˚ eccentricity. The only missed target recorded at that eccentricity was also recorded in the second non-uniform background. It can be attributed to the complexity of the scene in the adaptation task.

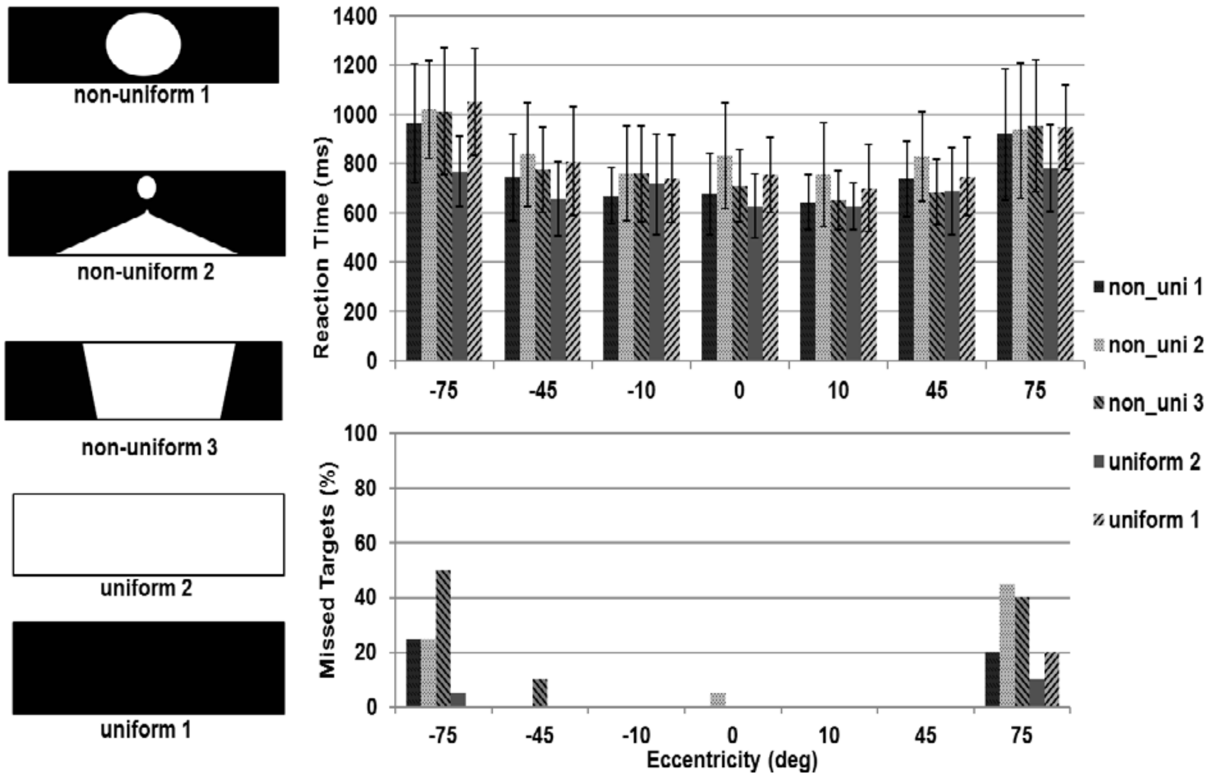

Figure 4 – Reaction times and the number of the missed targets for all backgrounds.

Two background luminances were used: 0,1 and 1 cd/m^2. The values refer to the black and white areas of the backgrounds, respectively, as shown in Figure 4. The results indicate that reaction times to stimulus at far periphery (-75˚, -45˚, 45˚ and 75˚ eccentricities) depend on the local luminance of the stimulus rather than on the uniformity of the background. In other words, for a stimulus appearing at 45˚eccentricity, stimulus luminance is 0,17 cd/m^2 in the backgrounds of uniform 1 (0,1 cd/m^2), non-uniform 1 (elliptical) and non-uniform 2 (road scene), whereas it becomes 1,7 cd/m^2 in uniform 2 (1 cd/m^2) and non-uniform 3 (windscreen) based on Equation 1. The results indicate that reaction times to targets appearing at far periphery which have same target luminance were similar. However, luminance distribution of the background affects reaction times to stimuli at -10˚,0˚ and 10˚ eccentricities. Luminance distribution effect is also visible on number of the missed targets at -75˚and 75˚ eccentricities as shown in Figure 4.

The statistical analysis of reaction time and number of the missed targets was performed with two way of analysis of variance (ANOVA) (Table 1). Eccentricity and background affect both reaction time and number of the missed targets. Although, the effect of the luminance is not significant on reaction time, the interactions show that the combinations of luminance, eccentricity and background have effect on reaction times as well as three-way interaction of these parameters. Eccentricity, luminance and background have significant effect on number of the missed targets. Comparison of the eccentricity effect on reaction times was analysed by conducting post hoc Bonferroni test. This statistical method also indicates that difference in reaction times is significant for -75˚, -45˚, 45˚ and 75˚ eccentricities.

Table 1 – Results of statistical analysis (ANOVA) in terms of *p*-values (significance criterion: *p* < 0,05) for reaction time and missed targets.

Source of variation	*p*-values	
	Reaction time	Missed targets
Eccentricity	0,000	0,000
Luminance	0,251	0,038
Background	0,000	0,000
Eccentricity x Luminance	0,020	0,000
Eccentricity x Background	0,000	0,000
Luminance x Background	0,029	0,373
Eccentricity x Luminance x Background	0,008	0,935

4 Discussion

The results indicate that the target luminance, location and luminance distribution of the background affect the reaction times at mesopic light levels. The difference in reaction times between the stimulus at eccentricities 0˚ and 10˚ was small, except for the second non-uniform (road scene) background. The differences in reaction times for foveal stimuli may be due to the luminance distribution of the background. The effect of stimulus location and luminance on reaction times was most visible at -75˚, -45˚, 45˚ and 75˚.

Reaction times to stimuli at far periphery are affected by the local luminance of the stimulus appeared on the screen. It supports the local adaptation approach presented in the previous studies (Uchida, 2012)

As expected, the number of missed targets was higher at eccentricities 75˚ and -75˚ for all backgrounds. The effect of luminance distribution is stronger on the number of the missed targets. For example, half of the subjects missed the target appearing at -75˚ at the third non-uniform (windscreen) background, whereas there were no missed targets at the same eccentricity for the first uniform background (0,1 cd/m^2) although both stimuli have same luminance.

The high increase of the number of the missed targets at -75˚ and 75˚ eccentricities for non-uniform backgrounds indicates that the luminance distribution of the adaptation task affects visual performance against peripheral stimuli. In other words, detection of targets at -75˚ and 75˚ is more difficult in non-uniform backgrounds than uniform backgrounds. In real driving conditions, there are various stimuli with different luminances. Thus, if the visual performance against peripheral stimuli is considered as one of the parameters to estimate the shape and the size of the visual adaptation field, the extension of the visual adaptation field is expected not to cover areas beyond eccentricities -75˚ and 75˚.

5 Conclusions

Applying the stimulus at different eccentricities onto the background under mesopic light levels is a reliable method to define the visual adaptation field in terms of its shape and the area it covers. The luminance distribution of the background and the local luminance of the stimulus play critical roles for the speed of target detection in far peripheral vision. Considering the reduction of the number of the detected targets at -75˚ and 75˚ eccentricities in non-uniform backgrounds, the visual adaptation field is expected to cover the area extending less than those eccentricities based on the visual performance against the targets with corresponding size and contrast. However, by considering targets with larger size and higher contrast and also the visual tasks which are different from reaction time, it is not straightforward to suggest the abovementioned area in terms of its extension. Further studies are needed for verifying the results in dynamic backgrounds simulating real night-time driving conditions with different visual tasks.

References

CIE 2010. CIE 191:2010. Recommended System for Mesopic Photometry Based on Visual Performance. Vienna: CIE.

ELOHOLMA, M., Viikari, M., Halonen, L., Walkey, H., Goodman, T., Alferdinck, J., Freiding, A., Bodrogi, P., Varady, G. 2005. Mesopic models – from brightness matching to visual performance in night-time driving: a review. *Lighting Research and Technology*, 37 (2), 155-175.

WALKEY H., Orrevetelainen, P., Barbur, J., Halonen, L., Goodman, T., Alferdinck, J., Freiding, A., Szalmas, A. 2007. Mesopic visual efficiency II: reaction time experiments. *Lighting Research and Technology,* 39, 335-354.

WALKEY H.C., Harlow J.A., Barbur J.L. 2006. Characterising mesopic spectral sensitivity from reaction times. *Vision Research,* 46, 4232-4243.

ELOHOLMA, M., Ketomäki, J., Orreveteläinen, P., Halonen, L. 2006. Visual performance in night-time driving conditions. *Ophthalmic and Physiological Optics,* 26 (3), 254-263.

UCHIDA, T., Ohno, Y. 2012. An experimental approach to a definitiron of the mesopic adaptation field. Proceedings of CIE 2012 Lighting Quality and Energy Efficiency, Hangzhou, China, September 19-21 2012, 71-76.

PP08

VISIBILITY EVALUATION FOR FACE OF PERSON STANDING UNDER LED STREET LIGHTING ENVIRONMENT

Michico Iwata[1], Miyoshi Ayama[2], Shunsuke Kohko[3], Toshihide Mori[4], Hisaki Itsuki[5], Nobuhiro Kyoto[6], Youko Inoue[7], Etsuko Mochizuki[8], Toshihiro Toyota[9], Hiroaki Hattori[10], Takako Kimura[11], Yasuhiro Kodaira[12]

Setsunan University[1], Utsunomiya University[2], Iwasaki Electric Co., Ltd. [3], JAPAN
Panasonic Corporation[4], Inaba Electric Work Co., Ltd[5], GS Yuasa International Ltd. [6], JAPAN
Nara Women's University[7], Chiba Institute of Technology[8], JAPAN
Industrial Research Institute of Shizuoka Prefecture[9], Seiwa Electric MFG. Co., Ltd. [10], JAPAN
Stanley Electric Co., Ltd.[11], Koito Electric Industries, LTD[12]. JAPAN

michico@led.setsunan.ac.jp

Abstract

In this research, we performed the field experiments during night to determine the effect of LED street lighting on pedestrian visibility. A total of five different LED sources were used: three different luminous flux levels and two different types of mounted diffusion filters. We also added two other types of lights for comparison: fluorescent light and HID mercury vapour lamp. We used human faces as the objects of visibility evaluations. The first finding of our research was that a 1,000 lm LED light and a 2,000 lm LED light with an 80° diffusion plate provided low illumination of the object surface, and had lower evaluation values than did the other lights. Our second finding was that the evaluation values for 2,000 lm LED light; 3,000 lm LED light; and 2,000 lm LED light with 20° diffusion plate were higher than the first two LED lamps and about the same as that of fluorescent lamp. Our third finding was that HID mercury vapour lamps had the highest evaluation among any lighting type employed in the experiment.

Keywords: Outdoor Lighting, Discomfort Glare, White LED, Visibility

1 Introduction

In daily life, street lighting plays a very important role in ensuring safe mobility and preventing crimes at night. Fluorescent lights and mercury vapour lamps have conventionally been used for street lighting, but in recent years, LED lighting has gained immense popularity. However, LED lighting is often blamed for dazzling pedestrians having discomfort glare, which results in problems such as lower visibility of objects in street environments.

The purpose of the study is to provide data that will help the creation of good street environments using LED illumination. Field experiment was carried out to study the effect of LED street lighting on pedestrian visibility and discomfort glare. This study reports the results of visibility rating. Discomfort glare experiment is reported in the other study[1)], and Iwata M. et al examined evaluations with elderly people and visually impaired people[2)].

2 Experiments

The first type of light source we selected was for a LED lamp enabling variable light control (Panasonic model NNY20425 LE1). We subjected these lights to current control in order to set three luminous flux conditions (3,000; 2,000; and 1,000 lm) and added two more conditions by mounting diffusion plates with diffusion angles of 20° and 80° on the 2,000 lm LED light. Thus, we prepared five LED light sources for testing.

To compare LED lighting with conventional lighting, we added two more lighting conditions by preparing a fixture with a fluorescent light mounted therein and a conventional HID mercury vapour lamp light source (GS Yuasa model MR-330TB). As shown in Table 1, the tests were conducted using a total of seven test light sources.

Table 1 Light sources examined in the experiment

LED lighting	LED（5000K）3000 lm
	LED（5000K）2000 lm
	LED（5000K）1000 lm
	LED（5000K）2000 lm + Lens diffusion plate (20° diffusion angle)
	LED（5000K）2000 lm + Lens diffusion plate (80° diffusion angle)
Conventional lighting for comparison	HID mercury vapour lamp(HF100X)
	Fluorescent light (type FHT57)

Experiments were conducted on a factory ground in Nara, Japan, at night, from 16 through 19 October 2012. The test street simulated a community street shared by pedestrians and vehicles in a residential neighbourhood. We set a street width of 5 m for each light source and an average horizontal illuminance of 5 lx on the street surface. All the light sources were mounted on light poles at a height of 4.5 m above the ground that is a typical height for street lights in residential area in Japan.

Twenty-one observers participated the experiment. They had visual acuity of at least 0.7 on the Japanese scale, in each eye. Results from one male observer and one female observer who reported absolutely no glare or who reversed the order of the evaluation in their answers were excluded from the analysis. As a result, evaluations from 19 test observers, 11 males and 8 females, were used for the data analysis.

The test object for visibility evaluation was a human face placed at a height of 1.5 m at a position 5 m further in front of a light source in front of each test subject. Observers were instructed to answer how clearly visible the face's eyes, nose, and mouth were by marking the correspondent position in the 7-step linear evaluation scale shown in Figure 1.

The evaluation positions were the six points indicated by A, B, C, D, E, and F in Figure 2. Table 2 shows the distance from each location to the light source in front of the subject. Starting from Point A (the farthest point), the observers approached the test object for evaluation while recording their evaluations. The distance between the observers and the test object at each evaluation position is obtained by adding a value of 5 m to the distance indicated in Table 2.

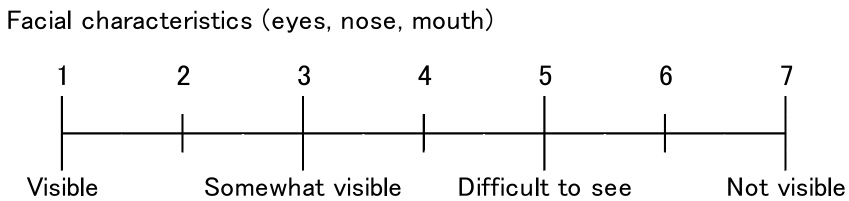

Figure 1 Scale for evaluating visibility of facial characteristics

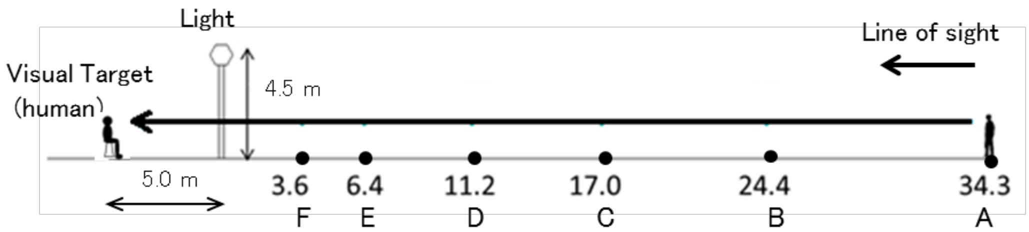

Figure 2 Layout of light source, visual target and observing positions A to F

Table 2 Distance of visual target and observing positions A to F from the light in metres

Evaluationpoint	Distance(m)
A	34.3
B	24.4
C	17
D	11.2
E	6.4
F	3.6

3 Experimental Results

Figure 3 shows the relationship between evaluation distance and average visibility evaluation for each of the seven light sources. As shown, the evaluation results for all the light sources decrease as the observation distance increases. However, curves do not overlap perfectly The differences among the light sources are as follows. The evaluations for the 1,000 lm LED light and 2,000 lm LED light with the 80° diffusion plate are roughly the same and lower than those for the other lighting types. The evaluation results for four lighting types (fluorescent light; 2,000 lm LED light; 3,000 lm LED light; and 2,000 lm LED light with 20° diffusion plate) are roughly the same and higher than those for the aforementioned two lighting types. HID mercury vapour lamps have the highest evaluation of any lighting type.

Figure 4 shows the relationship between preocular illumination and visibility evaluation. As shown, visibility evaluation has a very high correlation with preocular illumination. Using preocular illumination (x), visibility evaluation (y) can be estimated from the formula $y = -1.4557 \log(x) + 5.276$ ($r^2 = 0.91$). Since preocular illumination decreases as the evaluation distance increases, this trend can be inferred to match the relationship to evaluation distance. For the same preocular illumination, the 1,000 lm LED lighting type has the highest evaluation.

Figure 5 shows the relationship between evaluation distance and equivalent veiling luminance, and Figure 6 shows the relationship between equivalent veiling luminance and visibility evaluation. As shown in Figure 5, the equivalent veiling luminance is the lowest for 1,000 lm LED lights but relatively high for fluorescent lights and HID mercury vapour lamps. In addition, for all the light sources, the equivalent veiling luminance is higher at Point E than at Point F (directly under the lights), and there is almost no difference in the equivalent veiling luminance at Points A–D, with values lower than those at Points E and F. The relationship between equivalent veiling luminance and visibility evaluation shown in Figure 6 indicates that visibility evaluation tends to increase as equivalent veiling luminance increases for each lighting type. However, visibility evaluation is more strongly affected by evaluation distance than by equivalent veiling luminance.

Table 3 shows the vertical-plane illumination of the test object for each lighting type. The values vary according to lighting type: the lowest for 1,000 lm LED lights (6.17 lx) and the highest for HID mercury vapour lamps (16.75 lx).

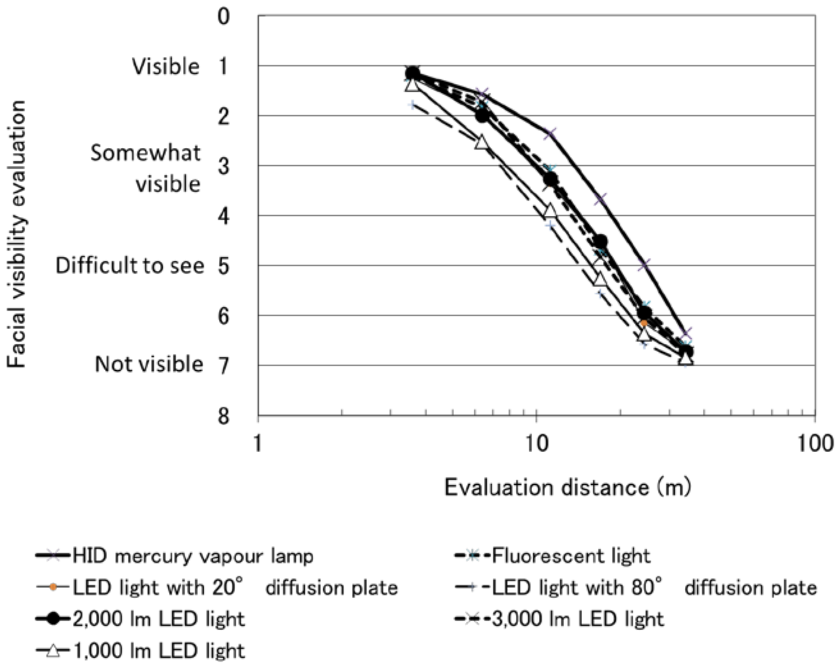

Figure 3 Relationship between evaluation distance and visibility evaluation

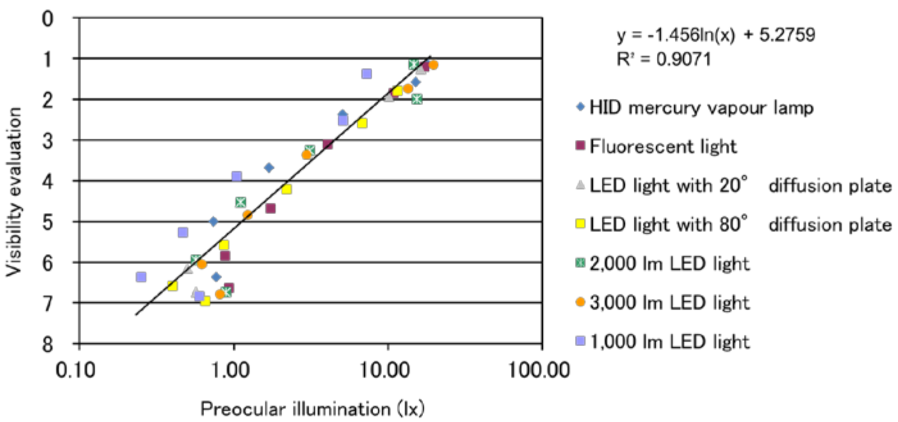

Figure 4 Relationship between Illuminance at the observer's and visibility evaluation

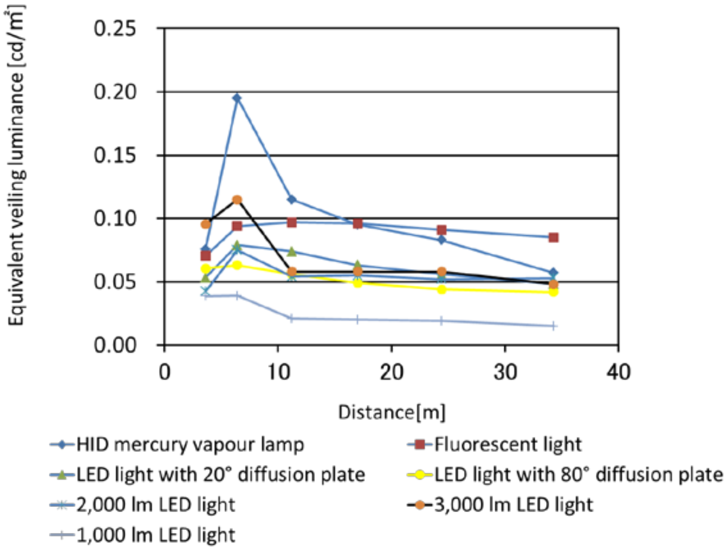

Figure 5 Relationship between evaluation distance and equivalent veiling luminance

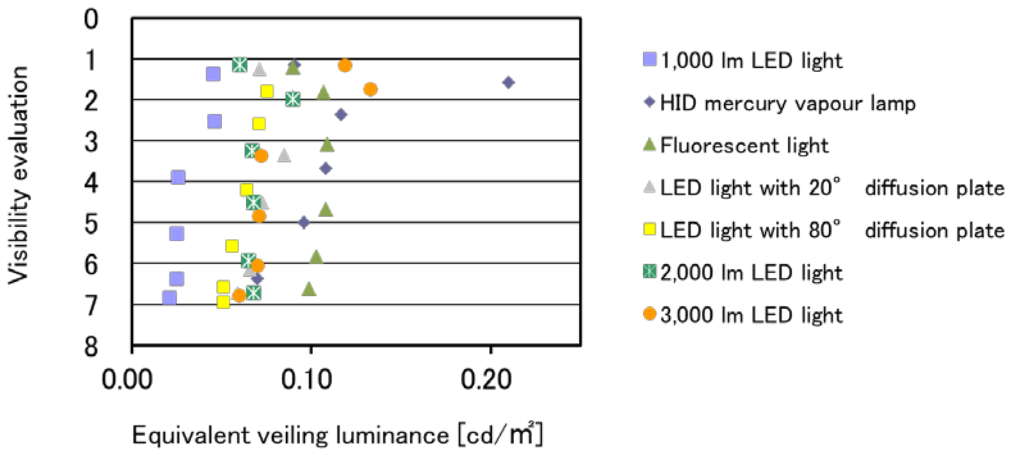

Figure 6 Relationship between equivalent veiling luminance and visibility evaluation

Table 3 Vertical Illuminance at the test object

①	LED (5000K) 3000 lm	16.57
②	LED (5000K) 2000 lm	15.14
③	LED (5000K) 1000 lm	6.17
④	LED (5000K) 2000 lm + Lens diffusion plate (20° diffusion angle)	13.26
⑤	LED (5000K) 2000 lm + Lens diffusion plate (80° diffusion angle)	9.14
⑥	HID mercury vapour lamp (HF100X)	16.75
⑦	Fluorescent light (type FHT57)	14.08

Figure 7 shows the relationship between the vertical illuminance at the test object, i.e., human face, and visibility evaluation. Point F with the least distance between the observers and the test object, has the highest evaluation value, and Point A with the largest distance has the lowest evaluation value. For all observing positions, evaluation values of the group where the illuminance at the test object is higher than 13 lx, are slightly higher than those of which the illuminance at the test object is lower than 10 lx. For all the evaluation positions, evaluations tend to be higher when surface illumination of the test object is higher and lower when the surface illumination is lower; however, the 2,000 lm LED light with the 80° diffusion plate has a lower evaluation value than does the lower-illumination 1,000 lm LED light.

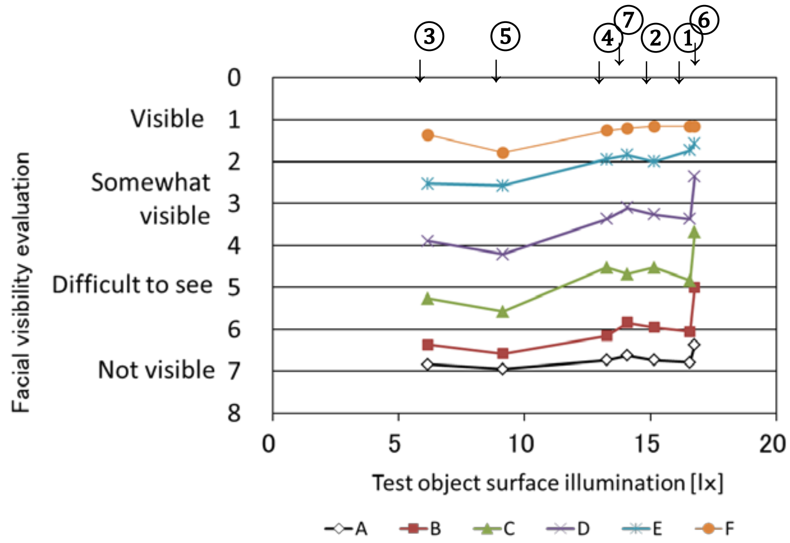

Figure 7 Relationship between illuminance at the visual target and visibility evaluation

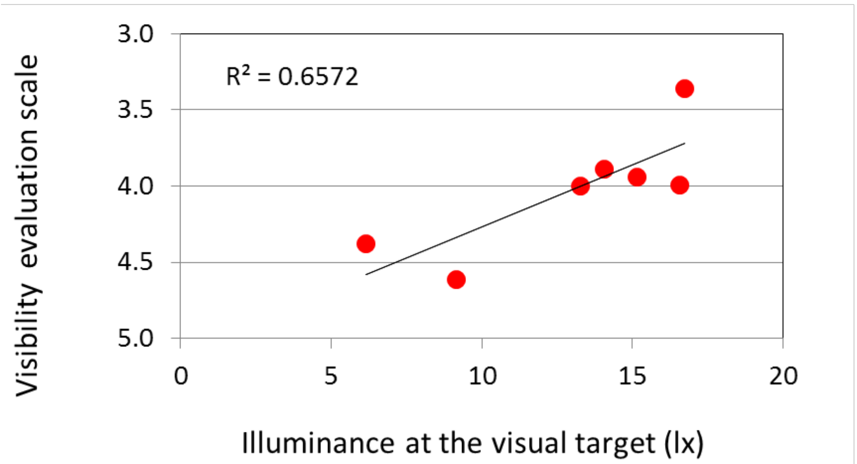

Figure 8 Relationship between the illuminance at the visual target and grand average of visibility evaluation

Figure 8 shows the relationship between the vertical illuminance at the test object, i.e., human face, and the grand average of visibility evaluation. As shown in Figure 3, shape of visibility curves as a function of the distance from the light source is similar for all light sources. Thus the grand average is a simple index for performance of each light source. As shown in Figure 8, general tendency is the larger the illuminance at the test object, the higher the visibility, with a high correlation (R^2 = 0.6572). This is reasonable that the human face under higher illuminance is easier to be seen. However, our results do not show a simple monotonous relation. Inverse relation is found between 1,000 lm LED Light and the 2,000 lm LED light with the 80° diffusion plate. The illuminance of the former is lower than that of the latter, while visibility evaluation of the former is higher than the latter. Also, the four lamps, fluorescent light, 2,000 lm LED light, 2,000 lm LED light with the 20° diffusion plate, and .3,000 lm LED light show nearly the same values in visibility evaluation, although their illuminance varies from 13.26 lx to 16.57 lx. Therefore, some factor(s) other than the illuminance at the test object, such as luminance or luminance distribution of the face, is needed to explain the results of these light sources.

In this experiment, discomfort glare was evaluated using the rating method similar to deBoer's glare scale. Figure 9 shows the relationship between visibility evaluation and glare evaluation for Point D. For all the light sources, greater glare results in a lower visibility evaluation. For the same glare evaluation, the visibility evaluation is high for HID mercury vapour lamp, and the lowest among all the light sources are the 2,000 lm LED light with the 80° diffuser and the 1,000 lm LED light. It is interesting that order of glare evaluation among the four lamps of which visibility evaluation value is 3.9 or 4.0, is LED2000, LED3000, LED+20deg diffuser, and FL, which is roughly opposite to the illuminance at the test object in this group. This suggests that the luminous flux of LED2000 and LED3000 is effective to keep the illuminance at the test object larger than 15lx, however, it causes discomfort glare to observers to give negative effect on the visibility resulting the same level of visibility as the light sources of lower illuminance such as LED+20deg diffuser and FL.

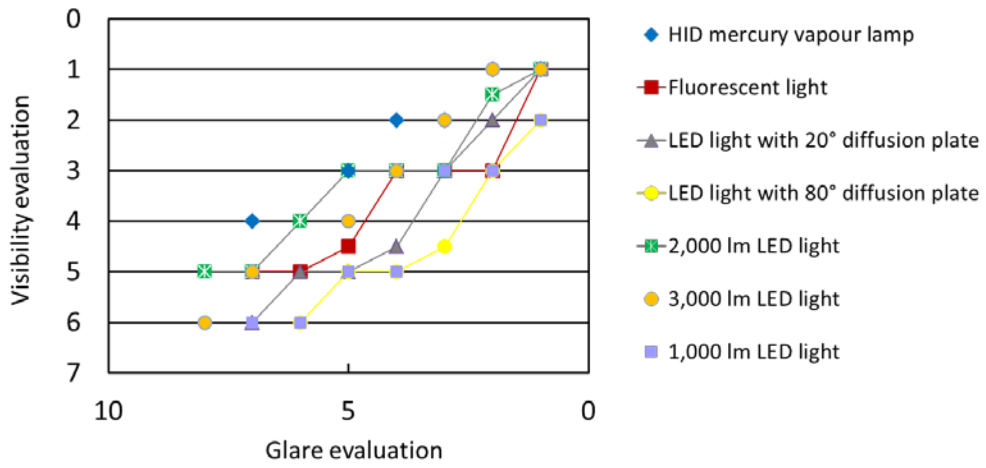

Figure 9 Relationship between glare evaluation and visibility evaluation at Point D

4 Summary

In order to provide data for designing high visibility and glareless LED street lighting, visibility and discomfort glare evaluation experiment was carried out in the night field using various light sources. In this paper, visibility experiment was reported. For LED light source, 3 luminous flux levels, 1000lm, 2000lm, and 3000lm were employed. For 2000lm condition, 2 different diffusers, diffusion angle of 20deg and 80deg, were attached to the light source. Thus, a total of five different conditions were made for LED lights. In addition to them, fluorescent light and HID mercury vapour lamp were utilized as comparisons. Visibility of a human face sitting under the light source was evaluated at 6 different positions with the distance of 3.6 to 34.3 m from the light source.

HID mercury vapour lamps had the highest evaluation among any lighting type employed in the experiment, main reason of this might be the highest Illuminance at the test object. However, we can not conclude that the illuminance at the test object is a single factor for visibility evaluation. LED1000lm and LED2000lm + 80deg diffuser showed the reverse relation, and the four sources, LED2000, LED3000, LED+20deg diffuser, and FL, discomfort glare seems to give negative effect on the visibility evaluation. Further study is expected to clarify the relations between probable factors for better pedestrian visibility to design safe, secure, and comfortable environment during night.

Acknowledgements

This research was conducted by the "Research & Investigation Committee on Glare of LED Lighting Fixtures in Outdoor Lighting Environments" of the Illuminating Engineering Institute of Japan under entrustment of JLEDS. We hereby express our sincere gratitude to the JLEDS, the Committee and all concerned.

References

1) Kohko S. et al.: Glare of LED Lighting in Outdoor Environment, Proceedings of the CIE 2014 Lighting Quality & energy Efficiency (accepted).

2) Iwata M. et al.: Experiment to Evaluation Visibility with Street Luminaires with Different Upward Light Output Ratios and the Use of Calculated Veiling Luminance to Determine Contrast Performance, J. L. V. E, Vol.35, No.1, 2011

PP09

THE STUDY OF BANDPASS CORRECTION IN ARRAY SPECTROMETER MEASUREMENT

Fu, H.K., Liu, Y.L., **Chou, P.T.**
Industrial Technology Research Institute, Chutung, Hsinchu, CHINESE TAIPEI
hkfu@itri.org.tw, itriA10269@itri.org.tw, PTChou@itri.org.tw

Abstract

The accurate measurement of spectrum makes the accurate calculation of chromaticity and obtains the accurate photometry. The correction of spectrum is the important process to obtain the accurate measurement. Many correction technologies are studied to improve the array spectrometer measurement. In this study, we focused on bandpass correction of an array spectrometer with Hg-Ar lamps to eliminate the spreading bandwidth. The correction method is by taking the line spectra of Hg-Ar lamp as the bandpass function and fixing the spectrum by deconvolution. The spectra with bandpass correction could decrease $\Delta u'v'$ from 2% to 20% in the measurements of different lights. This method provides a quick and intuitive way to do bandpass correction and can be used in array spectrometers which have similar bandpass function in different wavelengths.

Keywords: Photometry, Array Spectrometer, Measurement, Chromaticity

1 Introduction

The spectrometer is a basic equipment to analyse the photometry and chromaticity in visible light. There are two kinds of spectrometers based on different collecting light techniques. One is the scanning spectrometer which collected light by a single channel detector, such as photomultiplier tube (PMT), silicon detector with rotating the mirror to scan the spectrum. Because of the scanning mechanism, the scanning spectrometer needs a period of time to collect light. It is hard to analyse the unsteady light for a scanning spectrometer. The other is the array spectrometer which collected light by a charge-coupled device (CCD) without any other mechanical motions. The array spectrometer has the advantage of simultaneously collecting light in all spectra. It is convenient for production inspection. However, the spectrum resolution of array spectrometer depends on the specification of CCD and the simultaneously collecting light system may cause stray light. For quick analysis of spectrum, we focus on the array spectrometer in this study.

The accuracy of array spectrometer depends on three elements. First is the specification of hardware, such as the resolution of CCD, the linearity of CCD, the cooling system of CCD, the quality of grating, the reduction of the stray light, and so on. Second is the exactitude of spectrum correction, for example, the setup of standard light source, the experience of correction people, and the procedure of correction. With careful consideration, these can reduce the measurement uncertainty. Third is the advanced correction of spectrum. In general correction procedure, there are the corrections of frequency response and wavelength position. In real use, there are more complex conditions needed to be considered, such as stray light correction [1]. The addition of proper algorithm is needed to increase the accuracy of measurement. In this study, we focused on bandpass correction of an array spectrometer with Hg-Ar lamps to eliminate the spreading bandwidth. This method provides a quick and intuitive way to do bandpass correction, and can be used in array spectrometers which have similar bandpass function in different wavelengths.

2 Method and Theory

The correction procedures with the addition of proper algorithm can be divided into the correction of wavelength position, the linearity correction of CCD, the elimination of noise and dark current, the bandpass correction, the stray light correction, and the correction of frequency response. These correction procedures include the establishment of correction data and the calculation of established correction data and measured data. The procedures of establishing correction data are composed of five steps. In the first step, the wavelength position of CCD pixels is corrected by the line spectra of Hg-Ar lamp. In the second step, the linearity data of CCD are established by a steady light source with known intensities in several light current levels. In the third step, the bandpass correction data are established by the line spectra of Hg-Ar lamp with mathematical calculation. In the fourth step, the stray light correction data are established by several wavelengths of lasers. In the final step, the mentioned established data were used to establish the correction data of frequency response by a traceable standard light.

Then, the calculation of established correction data and measured data are composed of seven steps. In the first step, the measured raw data were collected from array spectrometer. In the second step, the elimination of dark current is processed by the dark current measurement. In the third step, the wavelength position data are applied to the dark current eliminated data. In the fourth step, the linearity correction data of CCD are applied to the wavelength position corrected data. In the fifth step, the bandpass correction data are applied to the CCD linearity corrected data. In the sixth step, the stray light correction data are applied to the bandpass corrected data. In the final step, the correction data of frequency response are applied to the stray light corrected data. The relation of correction models and measured data can be described by the following equations,

$$D_{\mathrm{meas},i} = g(\sum_j h_{i,j} S_j L_j + D_{0,i} + n_i) \quad , \tag{1}$$

$$\lambda = f(i) \quad , \tag{2}$$

$$L_j = L_e + L_s \, . \tag{3}$$

Where i, j are the pixel number; L_j is the stray light corrected data; λ is the wavelength; $D_{\mathrm{meas},i}$ is the measured data; L_e is the real light data; L_s is the stray light data; f function is the relation between wavelength and CCD pixel; g function is the CCD linearity corrected relation; $h_{i,j}$ is the interaction coefficient of different pixels; S_j is the frequency response coefficient; $D_{0,i}$ is the dark current data; n_i is the the noise data. Therefore, the correction procedures are based on the mentioned equations. Through these correction procedures, the measured data return to the real light data.

In order to obtain the measured raw data of high signal to noise ratio, the entrance slit width of spectrometer increases. However, the increase of slit width broadens the light pass which broadening the collected wavelength on the CCD pixels. Therefore, the resolution of wavelength on the CCD pixels decreases. This phenomenon is enhanced when collecting narrow band width light. There are several mathematic methods to reduce this phenomenon by Stearns and Stearns approximation, inverse matrix, and deconvolution. The concept of Stearns and Stearns approximation is based on using the weighted averages method of self and nearby pixel data to return the original data of detected signals [2]. The inverse matrix and deconvolution are matrix calculation and convolution calculation, respectively. Considering the convenience of calculation and experiment and the accuracy of experiment provided from literature, we adopt the deconvolution method to do the bandpass correction.

In general, the full width at half maximum (FWHM) of line spectra of Hg-Ar lamp is under 0.2 nm which is smaller than the spectral resolution of array spectrometer. Theoretically, each line spectrum of Hg-Ar lamp is ideally detected by one or two CCD pixels. Therefore, the measured line spectra are normalized and averaged to be the basis function of bandpass correction to do deconvolution calculation. The convolution equation is defined as

$$g(\mathrm{x}) = f(\mathrm{x}) * h(\mathrm{x}) = \int f(\mathrm{x}-\mathrm{t}) h(\mathrm{t}) d\mathrm{t} \, . \tag{4}$$

Where f function is an ideal pulse function; h function is the measurement of spectrometer; g function is the measured signal which caused by the convolution of an ideal pulse function and measurement system. In other words, the line spectrum of Hg-Ar lamp is the pulse function. There are many methods to do deconvolution calculation. Considering the steady and general application, we adopt the Richardson-Lucy algorithm to do recursion to approach the original data [3]. The recursion algorithm is defined as

$$f_{i+1}(\mathrm{x}) = f_i(\mathrm{x})\left(\frac{g(\mathrm{x})}{f_i(\mathrm{x}) * h(\mathrm{x})} * h(-\mathrm{x})\right). \tag{5}$$

3 Results and Discussion

The bandpass correction data are established by a Hg-Ar lamp connected an array spectrometer with an optical fibre. From the measured raw data, the top and nearby pixels of line spectra are analysed. Then, all of spectra are normalized and averaged to be the basis function of bandpass correction. These correction data can be used to do the bandpass correction of spectrum. Based on advanced correction procedure, we adopt a low-end array spectrometer with and without bandpass correction to test the correction results. The high-end array spectrometer with standard correction procedure developed by manufacture is used for reference standard. The experiment is taken by comparing with and without bandpass correction measured photometric and chromatic values of four colour light-emitted diodes (LEDs). Four colours are blue, green, red, and white. The measured line spectra are normalized and averaged as shown in Fig. 1.

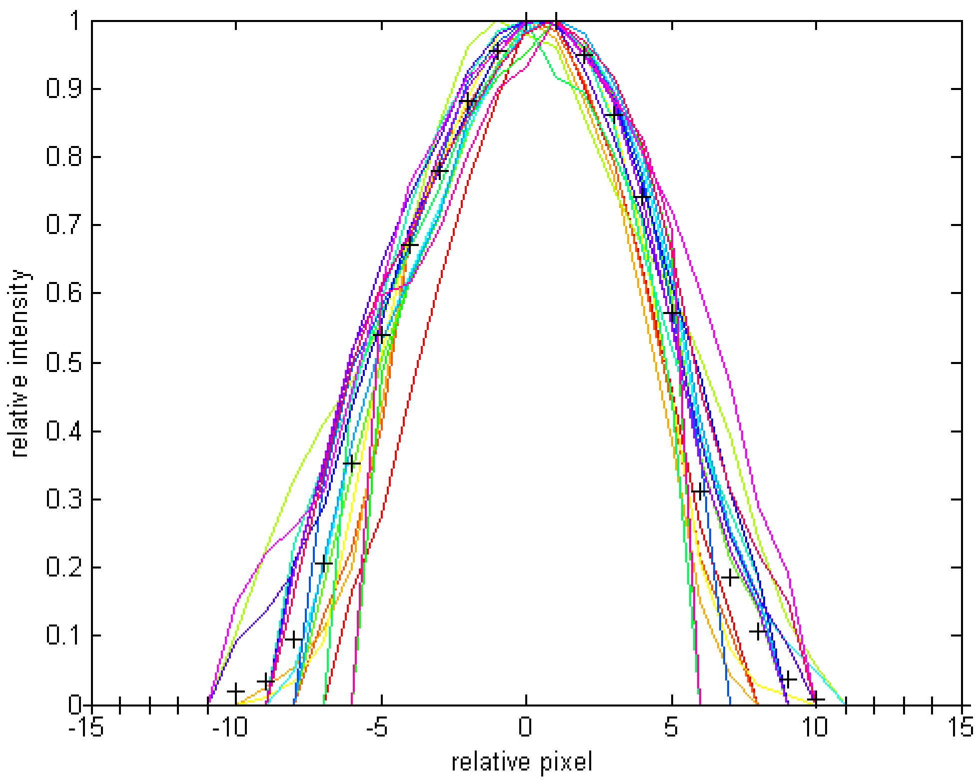

Figure 1 –The measured line spectra, „+“ is the averaged spectrum.

The experimental results without bandpasss correction list in table 1. The experimental results with bandpasss correction list in table 2. The Y is the luminous flux. The x and y are the colour coordinates of CIE 1931. The u' and v' are the colour coordinates of CIE 1976. The spectra with bandpass correction could decrease $\Delta u'v'$ from 2% to 20% in the measurements of different lights. The maximum correction result, about 20%, is the green LED. The minimum correction result, about 2%, is the red LED. The accuracy of luminous flux also increases.

This method provides a quick and intuitive way to do bandpass correction and can be used in array spectrometers which have similar bandpass function in different wavelengths.

Table 1 – The comparison of without bandpasss correction and reference standard.

	blue	green	red	white
Y (lm)	0,131159	0,170036	0,690822	0,259831
ΔY (lm)	-0,00035	0,000931	-0,00124	0,000645
x	0,065077	0,705324	0,306487	0,247513
Δx	0,000464	-0,00288	-0,00078	0,001406
y	0,000778	0,001668	0,001231	0,003709
Δy	-0,000016	-0,000016	-0,000014	-0,00000016
u'	0,149103	0,061143	0,521749	0,190684
$\Delta u'$	-0,00067	0,000533	-0,00025	-0,000072
v'	0,166456	0,57066	0,520823	0,4087
$\Delta v'$	0,000891	-0,00046	-0,00065	0,001156
$\Delta u'v'$	0,001114	0,000703	0,000696	0,001158

Table 2 – The comparison of with bandpasss correction and reference standard.

	blue	green	red	white
Y (lm)	0,131128	0,169744	0,690899	0,259752
ΔY (lm)	-0,00038	0,000639	-0,00116	0,000566
x	0,06501	0,705811	0,306408	0,247422
Δx	0,000396	-0,00239	-0,00086	0,001315
y	0,000777	0,001668	0,001231	0,003709
Δy	-0,000016	-0,000016	-0,000014	0,00000016
u'	0,1491	0,061003	0,521916	0,190659
$\Delta u'$	-0,00067	0,000393	-0,000083	-0,000097
v'	0,166319	0,570724	0,520797	0,40862
$\Delta v'$	0,000754	-0,0004	-0,00068	0,001076
$\Delta u'v'$	0,001009	0,000557	0,000681	0,00108

4 Conclusion

The accurate measurement of spectrum makes the accurate calculation of chromaticity and obtains the accurate photometry. The correction of spectrum is the important process to obtain the accurate measurement of spectrometer. In this report, we adopt the deconvolution method to do the bandpass correction and use the Richardson-Lucy algorithm to do recursion to approach the original data. The spectra with bandpass correction could decrease $\Delta u'v'$ from 2% to 20% in the measurements of different lights. This method provides a quick and intuitive way do bandpass correction of spectrum.

References

1. Zong, Y. et al. 2006. Simple spectral stray light correction method for array spectroradiometers. Appl. Opt., 45(6), 1111-1119.

2. Gardner, J. L. 2006. Bandwidth correction for LED chromaticity. Color Research and Application, 31(5), 374-380.

3. Eichstadt, S. et al. 2013. Comparison of the Richardson Lucy method and a classical approach for spectrometer bandpass correction. Metrologia, 50, 107–118.

PP14

ZERNIKE POLYNOMIALS FOR PHOTOMETRIC CHARACTERIZATION OF LEDS

Velázquez, J.L., Ferrero A., Pons A., **Campos J.**, Hernanz M.L.
Departamento de Imágenes, Visión e Instrumentación Óptica, Instituto de Óptica, CSIC, Madrid, SPAIN
jl.velazquez@csic.es

Abstract

The group of optical radiation measurements (GIMRO), in the Institute of Optics of the Spanish National Research Council (IO-CSIC), has developed a method based on Zernike polynomials to analyze photometric properties of Light Emitting Diodes (LEDs) from measurements of the angular luminous intensity distribution. It has been used eighteen LEDs of three different manufacturers with different optical characteristics to demonstrate the performance of this method. The procedure basically consists in fitting a linear combination of Zernike polynomials to measurements of the emission angular distribution. Since the Zernike polynomials describe the wavefront, the fitting parameters (the coefficients corresponding to the each Zernike term) can be easily related with the total luminous flux, the divergence of the emission by the full width at half maximum (FWHM), the anisotropy and the direction of the emission optical axis.

Keywords: High-Power LED, Zernike Polynomials, Angular Distribution, Luminous Intensity, Luminance, Divergence, Total Flux, Anisotropy, Optical Axis.

1 Introduction

Zernike polynomials are used in many cases by its versatility to describe different phenomena. In this work we present a methodology to describe the photometric properties of LEDs with the Zernike polynomials. These polynomials are a complete set of orthogonal polynomials over the interior of the unit circle and, thus, they allow aberration function to be expanded in a power series.

The group of optical radiation measurements (GIMRO), in the Institute of Optics of the Spanish National Research Council (IO-CSIC), has developed a method based on Zernike polynomials to analyze, from measurements of the angular luminous intensity distribution, photometric properties of Light Emitting Diodes (LEDs) such as total luminous flux, the divergence of the emission by the full width at half maximum (FWHM), the anisotropy and the direction of the emission optical axis. Luminous intensity measurements carried out by the goniophotometer developed at IO-CSIC were used to demonstrate the performance of this method. Eighteen LEDs from different manufacturers and with different optical characteristics (6 Luxeon Rebel, 7 Cree Xlamp and 5 Osram Golden Dragon high-power LEDs) were selected for this purpose.

2 Description of the goniophotometer

The goniophotometer (Velázquez J.L. et al., 2013) developed at IO-CSIC (Fig. 1) consist of a photometer temperature-stabilized P11S0T manufactured by LMT Lichtmesstechnik GmbH for measure the illuminance emitted by the LED. This photometer has a circular detection area of 100 mm^2, with a non-cosine-correction diffuser. A baffle was used to prevent from the stray light from the environment. The photometer is placed in a displacement stage on an optical bench, which allows the distance between the tip of the LED and the photometer to be accurately determined. LEDs to be characterized are located in a rotation system, which is composed of two URS75BPP stepper motor-based rotation stages of Newport Company. According to its manufacturer, their angular motion range is 360º, being 1º the minimum increase in the displacement. It also has a positioning accuracy of 0.003º ± 0.015º and a rotation eccentricity of 3 μm ± 1.5 μm. These stages provide the system with two degrees of freedom θ and φ (azimuth and spherical polar coordinates). To correct the small displacements from the centre of rotation, the system has four linear displacement stages with an accuracy of 1.00 mm ± 0.01 mm. Two stages are in the horizontal plane and two stages are in the vertical plane as it sees in the figure 1. LEDs are positioned in the vertical rotation stage with a system of temperature-stabilized to control the flux emitted. Considering everything mentioned here the illuminance of the LED can be measured in any direction, except in a small occlusion field behind the source.

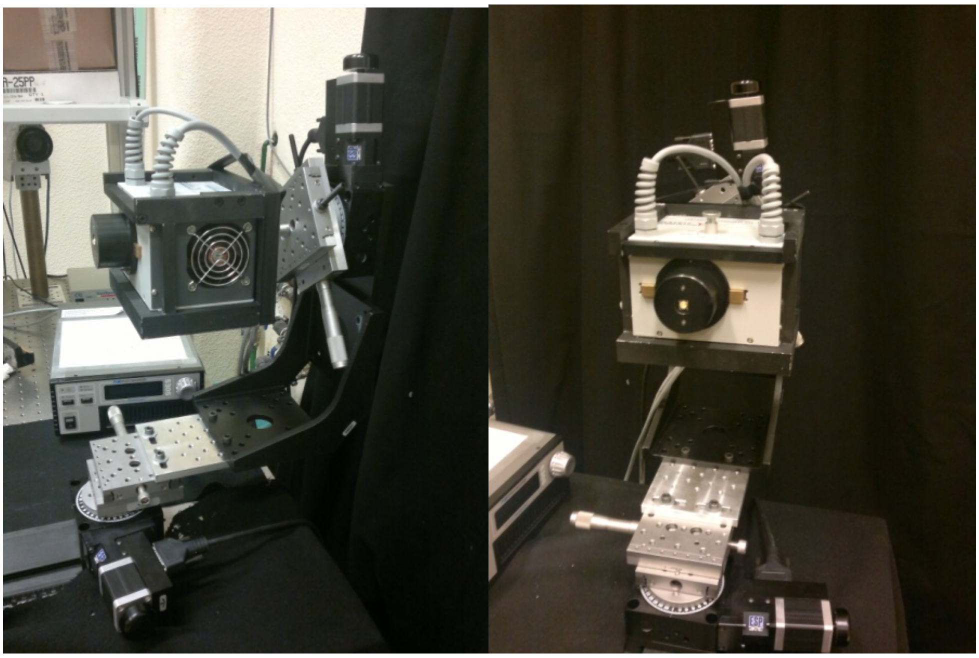

Figure 1 - Goniophotometer developed at IO-CSIC.

3 Description of the emission angular distribution by Zernike polynomials

Luminous intensity angular distributions $I(\theta,\varphi)$ may be expressed as a linear combination of properly chosen polynomials $Z(\theta,\varphi)$ as:

$$I(\theta,\varphi) = \sum_i c_i Z_i(\theta,\varphi) \tag{1}$$

where c_i is a weighting coefficient which depends on the angular distribution. If each polynomial $Z(\theta,\varphi)$ can be related with a specific property of the emission, the set of values c_i will define the emission angular distribution and it will allow its important characteristics to be described.

In order to fit experimental data of emission angular distributions, we decided to choose the well-known Zernike polynomials (Born M. et al 1975), which are used in many cases by its versatility to describe different phenomena. These polynomials are a complete set of orthogonal polynomials over the interior of the unit circle and, thus, they allow aberration function to be expanded in a power series. The Zernike polynomials are initially defined in polar coordinates (ρ,ϑ). We have expressed them in spherical coordinates (θ,φ), by using the transformation:

$$\theta = \operatorname{asin}\rho \tag{2.a}$$

$$\varphi = \vartheta \tag{2.b}$$

to expand the luminous intensity angular distribution in power series. Using this transformation of the Zernike polynomials it is possible to express the angular emission of LEDs as a summation of well-known polynomials, whose corresponding weights allow the photometric properties and quantities of the LED emission to be interpreted and estimated in a straightforward way.

From goniophotometric measurements on eighteen high powers LEDs the following nine Zernike terms were identified as the most relevant to fit the angular distribution of the luminous intensity (see Fig. 2) of this kind of LEDs:

$$Z_0^0 = 1 \tag{3.a}$$

$$Z_1^{-1}(\theta,\varphi) = 2\sin\theta\sin\varphi \tag{3.b}$$

$$Z_1^1(\theta,\varphi) = 2\sin\theta\, cos\varphi \tag{3.c}$$

$$Z_2^{-2}(\theta,\varphi) = \sqrt{6}\sin^2\theta\sin(2\varphi) \tag{3.d}$$

$$Z_2^0(\theta) = \sqrt{3}(2\sin^2\theta - 1) \tag{3.e}$$

$$Z_2^2(\theta,\varphi) = \sqrt{6}\sin^2\theta\cos(2\varphi) \tag{3.f}$$

$$Z_3^{-1}(\theta,\varphi) = \sqrt{8}(3\sin^3\theta - 2\sin\theta)\sin\varphi \tag{3.g}$$

$$Z_3^1(\theta,\varphi) = \sqrt{8}\left(3\sin^3\theta - 2\sin\theta\right)\cos\varphi \tag{3.h}$$

$$Z_4^0(\theta) = \sqrt{5}(6\sin^4\theta - 6\sin^2\theta + 1) \tag{3.i}$$

Where $Z_0^{\ 0}$ is usually referred in Optics as the constant term, $Z_1^{\ -1}$ as the vertical tilt, $Z_1^{\ 1}$ the horizontal tilt, $Z_2^{\ -2}$ the oblique astigmatism, $Z_2^{\ 0}$ the defocus function, $Z_2^{\ 2}$ the vertical astigmatism, $Z_3^{\ -1}$ the vertical coma, $Z_3^{\ 1}$ the horizontal coma, and $Z_4^{\ 0}$ the primary spherical. We will call, C_{Cons}, C_{TiltV}, C_{TiltH}, C_{AstigO}, C_{Def}, C_{AstigV}, C_{ComaV}, C_{ComaH}, C_{Sph} respectively, to the weighting coefficients associated to those terms.

Thus, a relatively simple expression to model the emission angular distribution for each LED as function of the spherical coordinates and these weighting coefficients.

$$I = C_{Cons} + C_{TiltV}Z_1^{-1} + C_{TiltH}Z_1^1 + C_{AstigO}Z_2^{-2} + C_{Def}Z_2^0 + C_{AstigV}Z_2^2 + C_{ComaV}Z_3^{-1} + C_{ComaH}Z_3^1 + C_{Sph}Z_4^0 \tag{4}$$

Since the Zernike polynomials describe the wavefront, by fitting the luminous intensity to Zernike polynomials (letting weighting coefficients as free parameters), some intrinsic properties of the emission are obtained, as the divergence, the optical axis, the total luminous flux and the anisotropy.

3.1 Divergence

LED's divergence is given by the Full Width at Half Maximum (FWHM). This value is obtained by using only those polynomials independent on φ in Eq. (4) to calculate the luminous intensity.

3.2 Optical axis

The optical axis is the axis of rotational symmetry of the emitted flux, and do not coincide always exactly with the geometrical axis referred to the LED mount. The optical axis direction is defined by its spherical coordinates (θ_0,φ_0) and determined from the two Zernike polynomials related with the tilt aberrations (vertical and horizontal), which can be used to quantify the average slope in both the X and Y directions.

3.3 Anisotropy

We will define two kinds of anisotropies, both of them representing the variations of emission with the azimuthal angle (φ), and in consequence, excluding variations due to the divergence of the LEDs. The first type of anisotropy, $A_1(\theta)$, is defined as the relative standard deviation of $I(\theta,\varphi)$ with fixed polar angle θ, and it can be calculated from the variation due to the Zernike terms with just φ-dependence, which depends on the coefficients, C_{TiltV}, C_{TiltH}, C_{AstigO}, C_{AstigV}, C_{ComaV} and C_{ComaH}. Therefore, this kind of anisotropy has to be expressed a deviation value for each polar angle.

The second type of anisotropy, *A*, is calculated as the standard deviation of $A_1(\theta)$, and it is represented by only one deviation number. Thus, *A* will be a generic parameter that defines the degree of anisotropy of the LED, and that is independent on its divergence.

3.4 Total luminous flux

The total luminous flux Φ of the LED is calculated by integration of Eq. (4) with integration limits (0,π/2) for the polar angle and (-π,π) for the azimuthal angle. After the integration, the φ-dependent terms are cancelled and the total luminous flux is given by the very simple equation:

$$\Phi = 2\pi\left(C_{Cons} + \frac{1}{\sqrt{3}}C_{Def} + \frac{1}{\sqrt{5}}C_{Sph}\right) \tag{5}$$

4 Results

The performance of the Zernike polynomial in the reconstruction of the experimental data for two different LEDs is shown in Fig.2. As can be appreciated in both figures, the constant, the defocus and the primary spherical terms are the most relevant in the reconstruction of the angular distribution of the luminous intensity, while the other terms are close to zero.

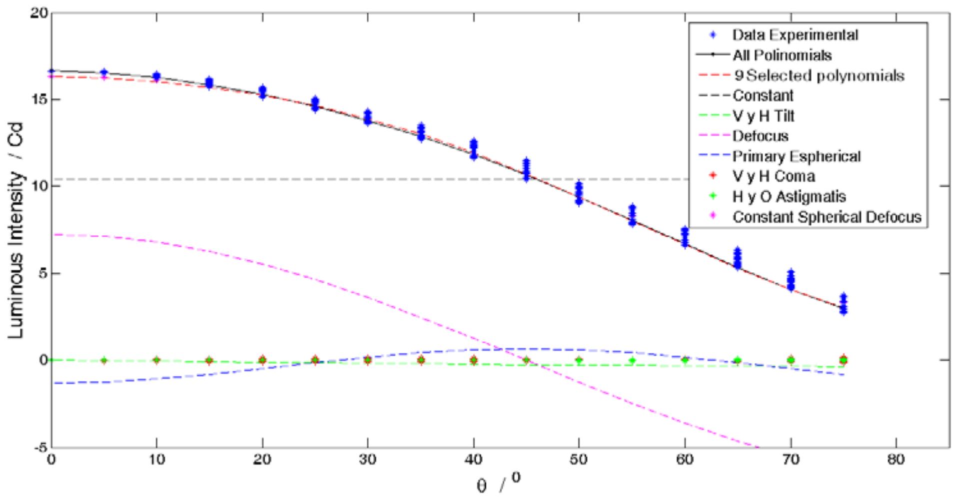

a)

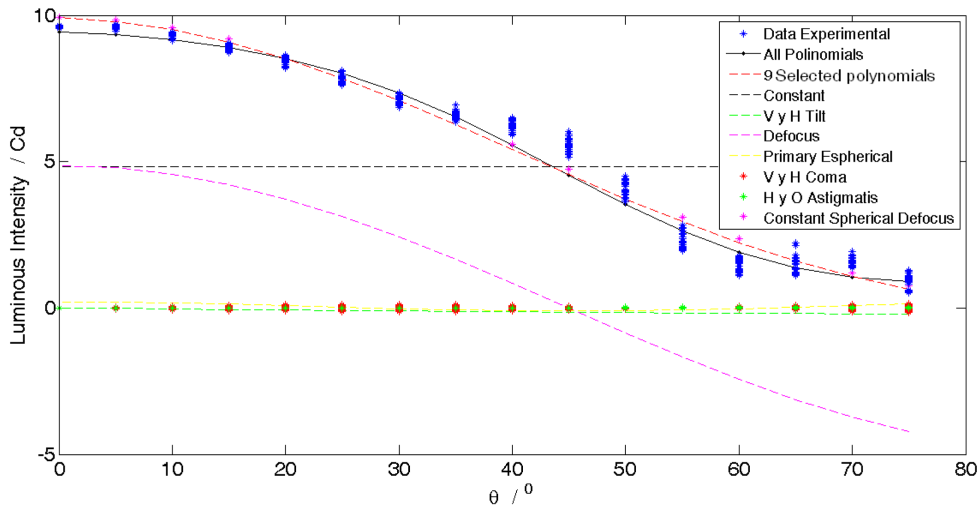

b)

Figure 2: Contribution of different Zernike terms to the total luminous intensity. a) Luxeon Rebel LED, b) High-power blue Cree LED.

Parameters describing intensity angular distributions are shown in Table 1.

FWHM values are given both for calculated by the Zernike formalisms from the experimental measurements and for the specifications from the manufacturer, values which are not given from Osram and which are given as a constant by Cree and Luxeon (90º and 125º, respectively). In the case of Osram's LEDs, we obtained a constant value of 180º, which means that we did not found divergence.

Table 1: Parameters describing luminous intensity angular distributions

	FWHM /°		Optical axis /°		Anisotropy (%)	Total flux /lum	
	Exp.	Spec.	θ_0	φ_0		Exp.	Spec.
CREE							
Polar White	80.4	90	2.8	209.7	11.8	84.6	80.6
White	81.8	90	2.5	187.7	14.5	72.5	73.9
Warm White	76.8	90	5.3	194.0	12.9	41.6	45.0
Neutral White	75.6	90	6.8	47.8	13.3	54.3	56.0
Blue	83.0	90	3.0	99.0	6.8	20.1	18.1
Red	73.4	90	8.3	124.2	15.9	38.1	39.8
Green	92.4	90	6.3	161.0	21.0	64.1	51.7
LUXEON							
Polar White	105.7	125	7.5	89.6	4.7	75.8	50.0
Warm White	118.1	125	3.0	70.7	9.2	45.5	50.0
Neutral White	111.8	125	3.4	170.8	4.6	48.4	50.0
Blue	116.5	125	3.6	168.0	7.4	30.0	23.5
Red	121.3	125	1.4	155.3	4.3	57.4	50.0
Green	113.5	125	2.6	212.3	5.0	86.0	80.0
OSRAM							
White	180.0	--	1.0	111.4	1.0	113.5	--
Warm White	157.3	--	0.8	48.0	2.8	88.9	--
Blue	180.0	--	2.1	144.0	1.1	20.8	--
Red	180.0	--	0.2	88.3	1.2	50.8	--
Green	180.0	--	2.2	125.5	2.6	74.1	--

The calculated spherical coordinates of the optical axis (θ_0,φ_0), given in the fourth and fifth columns, allow the deviation between the optical axis and the mechanical axis (θ=0º) to be assessed. This deviation is lower for Osram's LEDs than for Cree's and Luxeon's.

Anistropy (sixth column) is really small for high-divergent Osram's LEDs, and much higher for low-divergent Cree's LEDs, which may reveal some correlation between these two descriptors, although, as previously described, the anisotropy factor was defined to be dependent only on variations with azimuthal angle.

Finally, total luminous fluxes are given both for calculated by the Zernike formalisms from the experimental measurements (Eq. 5) and for the specifications from the manufacturer. Important deviations are found which need to be explained yet in future research.

5 Conclusions

It has been shown that it is possible to interpolate and describe the emission angular distribution of LEDs using a reduced set of Zernike polynomials. The selected polynomials are those related to the commonly known as tilt, astigmatism, coma, primary spherical and defocus aberrations.

Since Zernike polynomials are well-documented, the set of the calculated weighting coefficients will characterize completely the emission angular distribution of any LED. Expressions to calculate variables as FWHM, optical axis, total flux or anisotropy can be derived using these coefficients.

This approach to deal with photometric measurements of emission distributions of LEDs has been examined by measuring and analyzing eighteen LEDs from different manufacturers and with different optical characteristics (6 Luxeon Rebel, 7 Cree Xlamp and 5 Osram Golden Dragon high-power LEDs).

References

Born M, Wolf E, 1975, Principles of Optics: Electromagnetic Theory of Propagation, Interference and Diffraction of Light, 5 ed., England:Pergamon Press.

Velázquez J.L, Ferrero A, López M, Pons A, Villamarín A, Campos J and Sperling A, 2013, Angular distribution of the averaged luminous intensity of low power LEDs transfer standards, 8th Iberoamerican Optics Meeting and 11th Latin American Meeting on Optics, Lasers, and Applications, edited by Manuel Filipe P. C. Martins Costa, Proc. of SPIE Vol. 8785, 87858

PP16

COMPARISON OF STRAY LIGHT IN SPECTROMETER SYSTEMS USING A LOW COST MONOCHROMATIC LIGHT SOURCE

Thorseth, A.[1], Lindén, J.[1], Dam-Hansen, C.[1]
[1] DTU Fotonik, Technical University of Denmark, Roskilde, DENMARK
andt@fotonik.dtu.dk

Abstract

We present an experimental setup that is under development for automated stray light characterization of spectrometers. The setup uses a tuneable monochromator which enables this characterization on relatively cost low equipment. We present the measured line spread functions for two spectrometers, one low-end and one mid-range.

Keywords: Spectroradiometry, Line spread functions, Stray light correction

1 Introduction

With the introduction of new light sources such as LEDs and LED systems that can have large variations in the spectral power distributions, spectral characterization of these light sources becomes increasingly important. Additionally there is an increased interest in controlling the amount of UV light received from daylight, within many healthcare applications.

These changes have resulted in an increase in the interest in accurate and comprehensive measurements of spectral characteristics both in lighting research and the lighting industry. Recent years have also seen development of small and relatively inexpensive handheld spectrometers. However mid-range and low-end spectrometers will often have problems with performance on several issues, such as low sensitivity, high dark noise and finite and asymmetric bandpass. A prominent example of these problems is stray light, e.g. from the second order diffraction from the diffraction grating, which can be seen as a signal with the double wavelength of the main signal on the detector array. For normal visible range use in typical LED application this effect will cause a shift from the strong blue peak to the red region, which will typically lower the measured correlated colour temperature and increase the measured colour rendering index. In this work we have used a probe light source based on a diffraction grating monochromator to that is necessary to make the stray light correction, instead of the tuneable laser systems used by Zong et al. (Zong, et al., 2006). Monochromatic light sources based on conventional light sources and monochromator systems are much less costly than tuneable lasers, as they are based on the same technology as the spectrometers. The bandwidth is much larger for monochromators using diffraction gratings. However, for corrections involving wavelength shifts much larger than the bandwidth, this will have little influence. For the specific application to LED, Heidel and Marchl (Heidel & Marchl, 2013) presented an increase in accuracy of chromaticity coordinates by a factor of two, using the method developed by Zong et al. However, this was done for a high-end spectrometer that was moved to the institution having the tuneable laser for the construction of the correction matrix. We think it would be useful to have a method that could be applied more easily and be affordable for low end and low cost spectrometers.

2 Method

Stray light in the context of array spectrometers is light incident on the detector that is measured to have a wavelength other than the actual wavelength due to it arriving on other parts of the detector array, corresponding to other wavelengths. To characterize an array spectrometer for stray light a tuneable monochromatic light source is needed. Ideally measurement of a monochromatic light source would give a single value for the pixel corresponding to the wavelength of the incoming light and zero for all other pixels. However, in practise stray light such as second order diffraction will contribute to signals on other parts of the sensor array. In this section we describe the experimental setup and the theory used to make a preliminary analysis of the results.

2.1 Experimental setup

The setup consists of broadband light source Deuterium and Halogen light source (Ocean Optics DH-2000), which is fibre coupled to an optical fibre. The light source is equipped with a computer controlled shutter. The optical fibre is then coupled to an Acton SpectraPro 2150i computer controlled monochromator. The monochromatic light from the output port of the monochromator is coupled to the optical fibre input of the spectrometer to be characterised. The spectrometer integration time and measurement trigger is controlled from the computer. A double lens F# matchers are used for optimum in and out-coupling to the monochromator, which is an F/4 system. The setup can be seen in Figure 1.

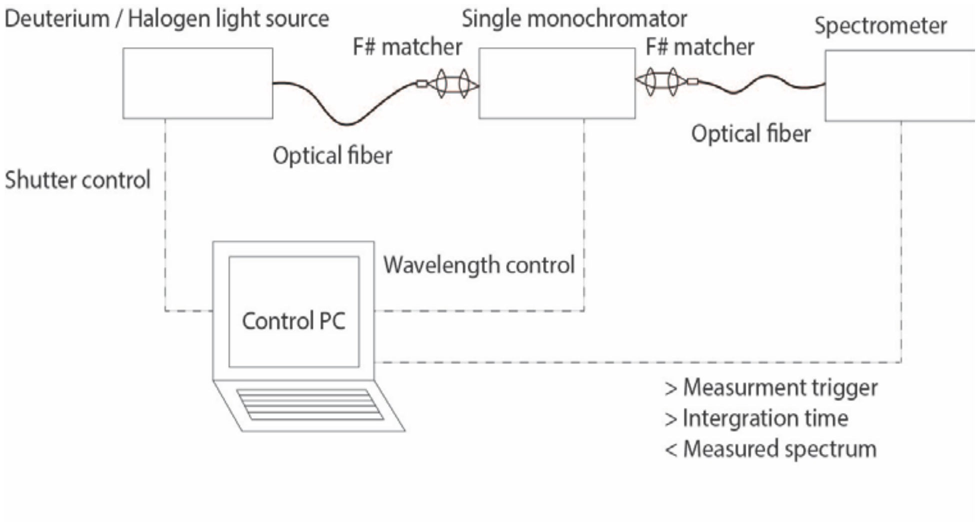

Figure 1 - Experimental setup

2.2 Experimental procedure

To get a satisfactory characterization of the probe light from the monochromator the signal on the detector must be high compared to the thermal noise and with small intervals between the probe wavelengths. This requires long integration time or a powerful light source. Since the throughput of the monochromator is limited the integration time must be long yielding total characterisation times of several hours. Normal time constraint therefore makes it necessary to automate the measuring process.

To be able to make this measurement in an automated way the whole process including the spectrometer under test has to be remote controlled. The procedure which is implemented in LabVIEW is depicted in Figure 2. First the monochromator is set to the probe wavelength. Then an initial guess of a useful integration time is sent to the spectrometer and the measurement is initiated. In order to get a high dynamic range for the measurements the integration time has to be changed according to the power of the probe beam. A measurement with integration time τ_1 is recorded and if the signal peak S_{peak} is between the maximum signal S_{max} and $0.8S_{max}$ the signal is accepted; if not a new integration time τ_2 is set, according to the following formulae

$$\tau_2 = 0.99\tau_1 \frac{S_{max}}{S_{peak}} \tag{1}$$

If the sensor signal is saturated the integration time is reduced by a factor of ten, according to the formulae

$$\tau_2 = \frac{\tau_1}{10} \tag{2}$$

The factor of 1/10 is used to achieve a fast reduction of the signal strength without reaching the noise level, and the factor 0.99 is used to avoid unintentionally reaching saturation. We have found that this method is useful to achieve a fast convergence towards a useful integration time within a few iterations (Thorseth, 2011).

Most spectrometers require that a dark measurement is taken whenever the integration time is changed and since few low-end spectrometers are equipped with an automated shutter, the characterization system has be equipped with a shutter control, to be able to automatically shut the light off for the dark measurement. This is used to record the background signal consisting of electrical sensor noise and ambient light that is irrelevant for the characterization. The background is recorded as an average over 10 measurements. Thereafter the shutter is deactivated to allow for the main signal to be recorded as an average over 10 measurements. The process can now be repeated for a new wavelength setting of the probe light wavelength on the monochromator.

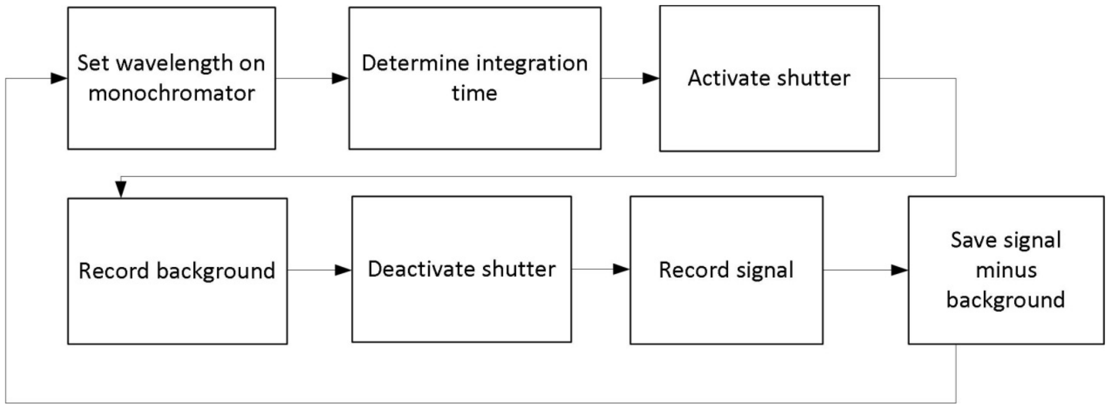

Figure 2 – Experimental procedure

The spectrometers used in this work are: A low cost miniature spectrometer, with no cooling referred to as the low-end spectrometer and useable for the visible range. And a mid-range spectrometer, with a cooled sensor and UV and near-IR capabilities, referred to as the mid-range spectrometer.

2.3 Stray light calculations

From the line spread functions we can calculate the bandwidth, by finding the full width half maximum (FWHM). When using laser lines as probe beams the bandwidth of the source becomes negligible. However, the bandwidth of the monochromator is about 1 nm, which will cause a considerable convolution with the spectrometer bandpass.

One way to calculate the stray light f_{stray} is to sum up all N pixel signals S_i which has been normalized to the maximum value. Using the signal from a monochromatic light source where the pixels near the bandpass are enumerated b (Young, 2013).

$$f_{stray} = \frac{\sum_{i \neq b}^{N} |S_i - B_i|}{N \sum_{i}^{N} |S_i - B_i|}, \tag{3}$$

where B_i is the background signal. In this instance we take the absolute value of the signal because for non-cooled sensors the electrical noise is contributing a large amount of negative values to the summation, which can drown out stray light signals. The near-band pixels can be defined in various ways. In this paper we use two different of ways to characterise the stray light using equation (3). Here the near-band pixels are defined as being within 1·FWHM and 10·FWHM on both sides of the centroid, respectively.

The line spread functions can be used to make a stray light correction matrix as showed by Zong et al. (Zong, et al., 2006). The correction is made by forming a matrix from the line spread functions with the pixels inside the bandpass set to zero.

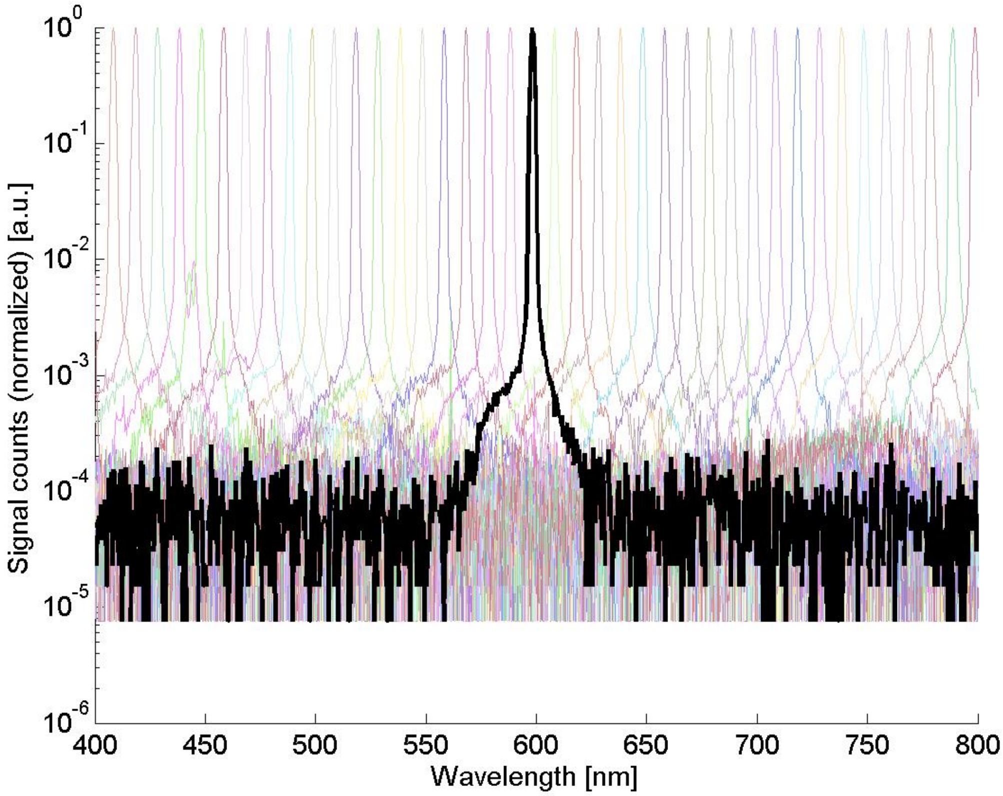

Figure 3 – Measured line spread functions for the low-end spectrometer. The highlighted spectrum is there to show the lower part of the signal.

3 Results

Using the automated monochromator setup we are able to automatically probe the line spread function of the spectrometers. Measurements have been performed for wavelength intervals of 1 nm. An example is shown in Figure 3 for a low-end spectrometer with probe beams shown at every 10 nm from 400 to 800 nm and one measurement highlighted to show the lower part of the signal. The signals shown on the figure are absolute values to visualize the level of noise below zero. Figure 4 show similar data for the mid-range spectrometer.

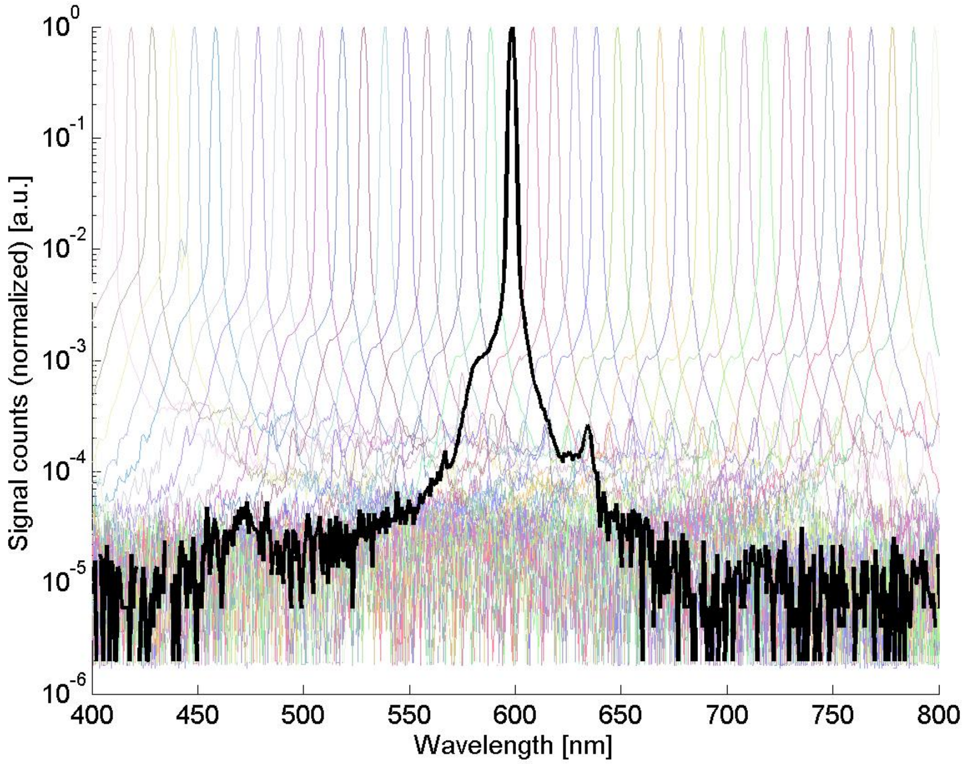

Figure 4 – Measured line spread functions for the mid-range spectrometer. The highlighted spectrum is there to show the lower part of the signal.

From this data it is for instance possible to find the FWHM of the line spread function for the spectrometer. In Figure 5 the FWHM have been calculated for all probe wavelengths, and is shown as a function of centroid wavelength.

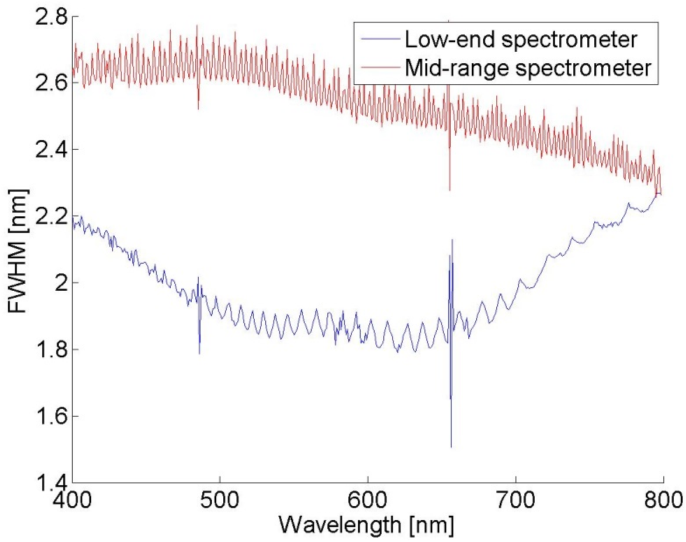

Figure 5 – Full width half maximum of the signals measured on two different spectrometers

Figure 6 shows the stray light characteristic f_{stray} calculated with equation (3) with 2·FWHM (close to the band) and 20·FWHM (far from the band) as near-band pixels, for all the measured line spread functions.

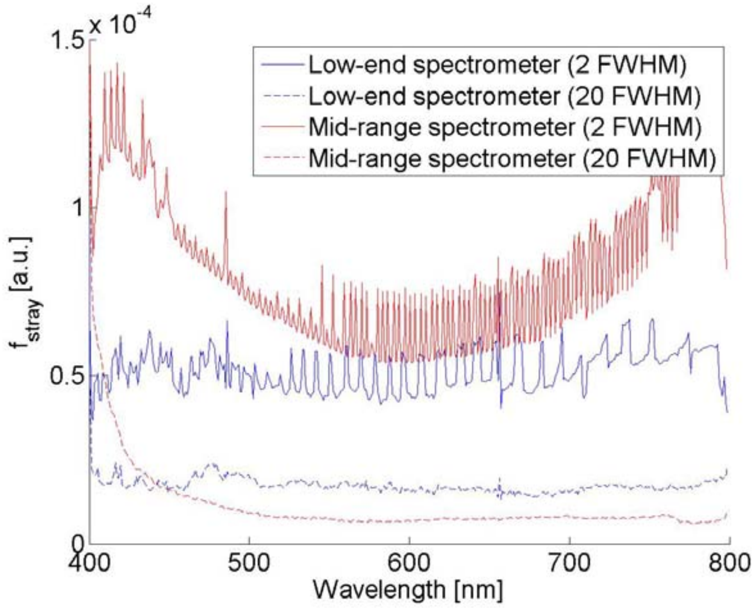

Figure 6 - Stray light calculation for the two spectrometers using equation (3), with the near-band filter is set to a width of 2·FWHM and 20·FWHM

The results can be used for stray light correction as shown by Zong et al. (Zong, et al., 2006). Figure 7 shows the values of the stray light correction matrix with probe beams from 400 to 800 nm for the low-end spectrometer, while Figure 8 shows the resulting matrix for the mid-range spectrometer. The limited wavelength range presented here is due to second order diffraction in the monochromator that in the current set causes a signal indistinguishable from stray light in the spectrometer.

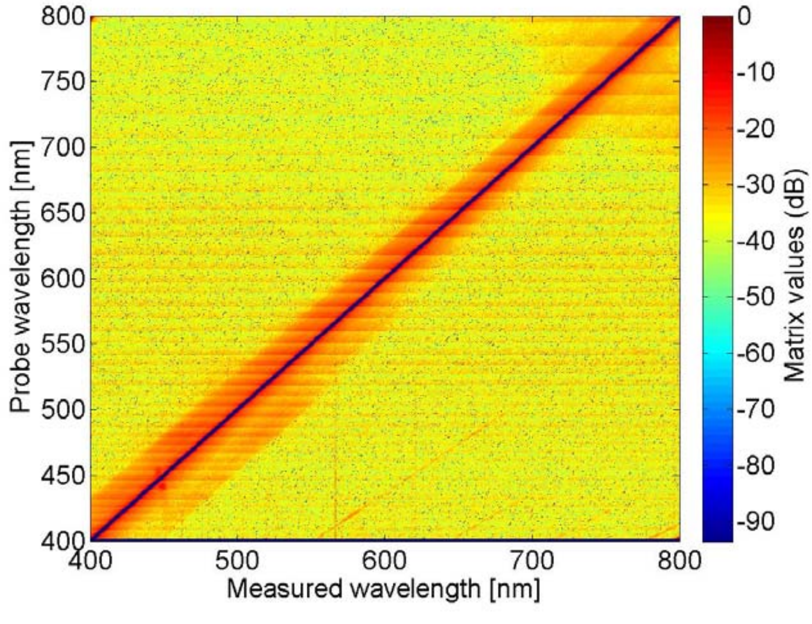

Figure 7 – Stray light matrix of low-end spectrometer

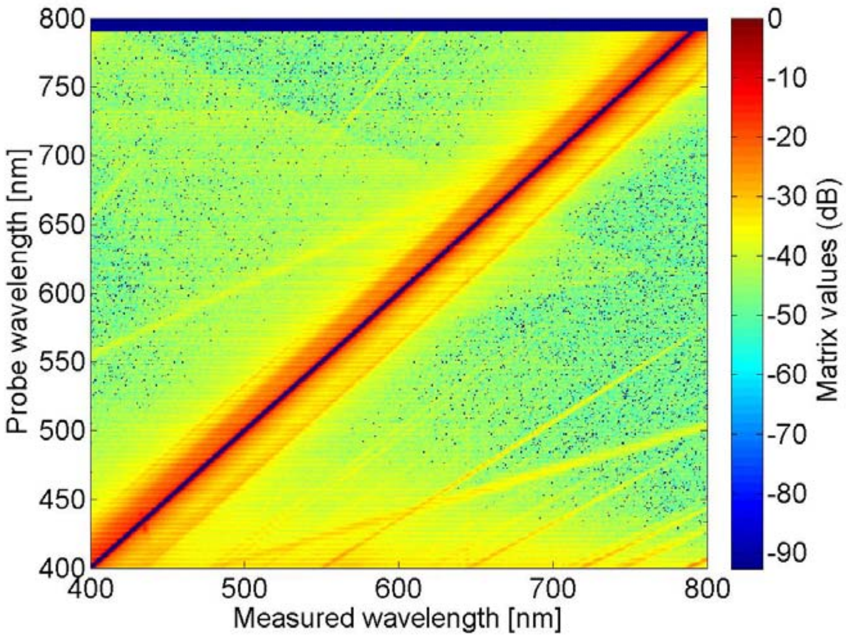

Figure 8 – Stray light matrix of mid-range spectrometer

4 Discussion

As previously stated this experimental method is not suitable to characterize the bandpass of the spectrometer, unless this is very large, due to the comparably large bandpass of the monochromator, but it should be possible to measure the stray light that is incident far from the probe light. With this knowledge we can now compare the two spectrometers that have been measured. It is seen from Figure 3 and Figure 4 that the low-end spectrometer has an overall higher background signal level, most likely due to the lack of cooling. However, the low part of the bandpass is much higher for the mid-range spectrometer. This is evident both in Figure 4 and in Figure 6 where the stray light characterized by $f_{stray}$for the mid-range spectrometer is higher than for the low-end spectrometer for the 2·FWHM calculation. On the other hand the f_{stray} goes notably down for the mid-range spectrometer when moving away from the probe light wavelength using the 20·FWHM calculation. The apparent underperformance by the mid-range spectrometer is caused by the fact that we have only probed a small part of the much larger wavelength range that has not been utilized in this work. However, it is evident that for instance in LED lighting applications where most of the light will be between 400 nm and 800 nm, the low-end spectrometer has some characteristics that are as good as the mid-range spectrometer. The noise level on the other hand is markedly different, Figure 7 show that the low-end spectrometer has a higher level of noise. The bandpass is also clearly visible as a ridge around the removed diagonal. The horizontal lines are likely caused by the change in the integration time within the tolerance given by the algorithm described in section 2.2, which will change the signal to noise ratio. The stray light matrix shown in Figure 8 show that the dark noise is considerably less, however, other features are visible which are clearly related to the incoming light; ridges with positive slopes running alongside the signal from the probe beam. It is our goal to develop the setup and procedures to account for and correct these effects.

5 Conclusion and outlook

We have presented a setup to measure the line spread functions of array spectrometers, involving equipment with a relatively low cost. The automation of the setup enables a measurement to be made without human interference and with durations of a few hours. The setup is still under development and we will be working on extending the wavelength range and increase the amount of light through the monochromator, to decrease measurement time even further. It is also our intension to characterize a range of different spectrometers. Further possibilities would be to apply the matrix correction method on reference measurements of for instance LED spectra to test whether the results of the measurement method is suited for a correction calculation. With knowledge of the line spread function it could also for example be interesting to use Richardson-Lucy deconvolution (Eichstädt, et al., 2013) on a measured spectrum, to increase the optical resolution below the bandpass, due to the fact that even hand held spectrometers now can be equipped with considerable computational power.

Acknowledgements

This research was made possible by a grant to the Center for LED metrology from the Danish Agency for Science, Technology and Innovation.

References

EICHSTÄDT, S. et al., 2013. Comparison of the Richardson--Lucy method and a classical approach for spectrometer bandpass correction. *Metrologia,* 50(2), p. 107.

HEIDEL, G. & MARCHL, W., 2013. *Practical experiences with stray light correction on array spectrometers for LED-production.* Paris, CIE, pp. 211-222.

THORSETH, A., 2011. *Characterization, Modeling, and Optimization of Light-Emitting Diode Systems.* Ph.D. Thesis red. Copenhagen: Technical University of Denmark.

Young, R., 2013. *Personal communication.* Paris.

ZONG, Y. et al., 2006. Simple spectral stray light correction method for array spectroradiometers. *Appl. Opt.,* 45(6), pp. 1111-1119.

PP17

DEFINING LUMINOUS INTENSITY DISTRIBUTIONS OF LED LUMINAIRES BY THE MEASUREMENT OF ROTATING LUMINAIRE GONIOPHOTOMETERS

Dubnicka Roman[1], Csuti Peter[2], Schanda Janos[2], Szabo Ferenc[2], Rusnak Anton[1], Grinaj Lukas[1], Lipnicky Lukas[1]
[1]Department of Electrical Power Engineering, Faculty of Electrical Engineering and Information Technology, Slovak University of Technology, Bratislava, SLOVAKIA,
[2]University of Pannonia, Department of Electrical Engineering and Information Systems, Virtual Environments and Imaging Technologies Research Laboratory, Veszprem, HUNGARIA
Contact email address: roman.dubnicka@stuba.sk

Abstract

The paper deals with the measurements of various types of LED luminaires by means of goniophotometers with rotating luminaire performed at two independent photometric laboratories situated at University of Pannonia in Hungary and Slovak University of Technology in Slovakia. Furthermore, results of measurements provide comparison of measurement of luminous intensity distribution curves (LIDC) and total luminous flux for LED luminaires of two different independently constructed goniophotometers with rotating luminaire. Also these measurements will serve for comparison with preliminary results of LIDC of luminaires by other types of goniophotometers described by the CIE document extended of near-field goniophotometer measurements what is also still often discussed theme about possibility to use of this novel approach of goniophotometry for use of LIDC measurements.

Keywords: Goniophotometry, LED luminaires, LIDC measurement

1 Introduction

At the present two important standards about LED luminaires are under preparation beside the already issued and approved document LM-79. In these documents broader scope is dedicated to goniophotometry of LED sources respective LED luminaires. In laboratories there are existing goniophotometers of various types according to CIE 121:1996 The Photometry and Goniophotometry of Luminaires. Very often discussed topic is the use of a goniophotometer of type A i.e. with rotating luminaire for LED products. This type of goniophotometer is widely used in many photometric laboratories for its favourable price and moderate space requirements.

During the measurement the work position of the luminaire changes with every rotation of the goniophotometer. There exists doubt how large the error is, compared to sytems, where the luminaire is not changing in Earth’s gravitational field. Auxiliary photometer has to be used for possible corrections at the measurement. In the papers is very hard to find something about position of this photometer. Therefore decision was on laboratory agreement how to perform measurement with it. Three LED luminaires were chosen as comparison batch each with different LIDC to show also the influence of different types of luminaires. We show also how big the influence is when measuring a luminaire in the so-called false C-planes where the inverted luminaire's luminous part is twisted by 90° and so it is aimed towards photometer head.

After performing the comparison between the laboratories results were compared to catalogue values of luminaires which were derived from measurements done by using C-plane goniophotometers where the position of the luminaire is kept unchnged in the Earth’s gravitational field. The whole comparison measurement procedure, described below, was properly arranged and discussed at the laboratories before starting any measurements. Additionally, also the electrical quantities of luminaires were measured at each laboratory.

2 Batch of luminaires

For this comparison measurement three different LED luminaires were chosen, each signed with unique IDs. The first subject was marked as L1 which was a square shaped office lighting LED luminaire with dimensions of 60 cm by 60 cm with diffuser, the second subject was marked as L2 which was a refurbished old type luminaire with two LED retrofit tubes of type T8 and with a length of 120 cm covered by linear prism and the third subject was marked as L3, which was a downlight LED luminaire with clear glass surface. Pictures of the luminaires is shown in Figure 3.

Figure 3 – Pictures of luminaires used in the comparison measurement from left L1, L2 and L3

Electrical parameters have been as follows. L1 has rated power 42 W, L2 has rated power 49 W and L3 has 31 W rated power. Each of the luminaires had own driver ready for supplying by AC voltage 230 V.

Luminaires have been before comparison properly burned to stabilise their photometric parameters. The subjects of the representative batch for this comparison were chosen from purposes which are usually and often used in common lighting installations. Also luminaire refurbished with LED tubes as replacement for fluorescent tubes into old fashion luminaire was chosen because this is common practice at the present. It was forbidden to clean luminous parts of luminaires before the measurement.

3 Measurement setup and procedure of comparison

Two independently constructed goniophotometers with rotating luminaire were used for comparison measurements. At University of Pannonia it was used for measurements in false C-planes (first polar axis of luminaire in horizontal direction)with step motors and at Slovak University of Technology in Bratislava was used self-made goniophotometer with possibility to measure all planes defined in CIE standard. The measurement setups for both laboratories are described below. All procedures and equipment used for measurements was properly calibrated with traceability to national or international standards.

The chosen subjects were measured in bilateral comparison by the following scheme. The first measurement was performed at the University in Slovakia after that a measurement was performed at the University in Hungary and at the end of the comparison again a measurement at the University in Slovakia was performed to check possible drifts of measured comparison batch of luminaires due to transport. Each laboratory followed requirements according to European standard EN 13032-4. A unified Excel sheet was created were the measured parameters have been entered by the laboratories. According to agreement between laboratories, measurements were completed in C-planes with 15° steps with gamma step 2,5°.

At the measurement was demanded for each laboratory to use auxiliary photometer or photometer by which the correction of values due to changing of working position of luminaire could be done. Each laboratory had individual testing procedure which followed as it performs tests of luminaires as usual. Measurement setups both of laboratories are described in the following sections.

3.1 Measurement set-up at University of Pannonia

Depiction of the goniophotometer system with rotating luminaire can be seen in Figure 1. The distance between luminaire and detector varied during the tests. For the downlight (L1) and the 60 cm by 60 cm luminaire (L3) 5 m measurement distance was used, this distance in case of the 120 cm luminaire (L2) was 15 m. The distance measurement was carried out by a laser distance meter which has typical measuring accuracy of ±1 mm for both distances.

On the photometer was mounted a stray light corrector tube to exclude light reflections falling onto the detector's surface from unwanted directions. The detector's tilt alignment was done by aiming an attachable laser pointer (which is always perpendicular to the detectors surface) on the centre of the mounted luminaire. The $V(\lambda)$ fitting of the used photometer had an f_1' quality index value of 1,2% and the luminous responsivity had a value of 2,375 nA/lx.

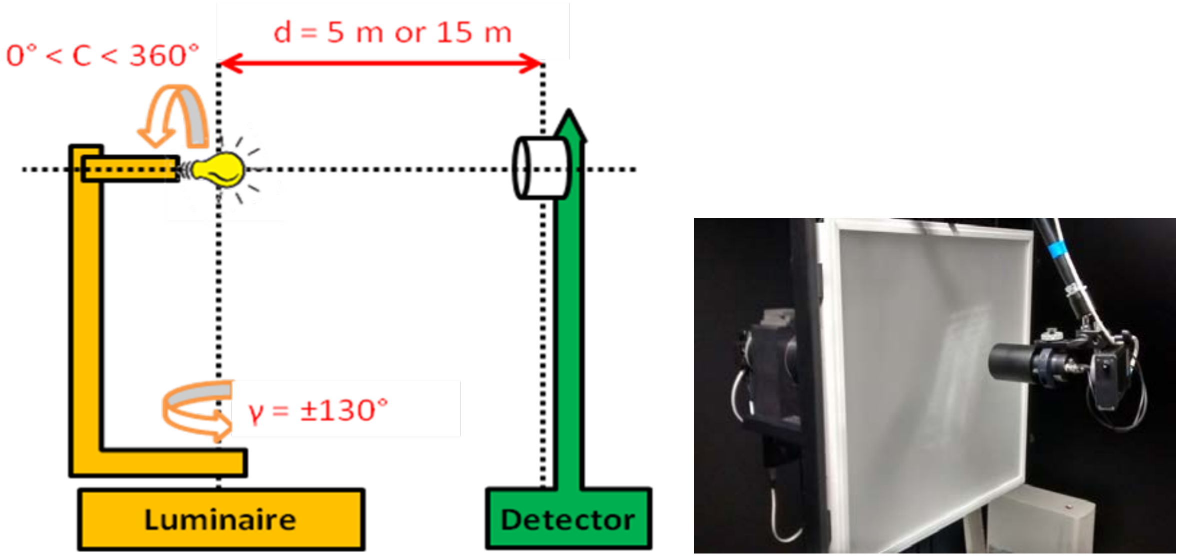

Figure 1 – Scheme of goniophotometer set-up at University of Pannonia in Veszprém

The goniophotometer's vertical axis angular position gives the elevation values (γ) and has a rotation range of ±130° (with angular resolution of 0,1° and with an elevation step of Δγ=2,5°) from which we used γ = 90° elevation stop value by testing subjects L1 and L3. In case of luminaire L2 we used a higher elevation stop of γ = 120° to catch scattered light from the cover glass of the luminaire. The horizontal axis provided the C-plane settings of the test from C = 0°to C = 360° with angular resolution of 0,1° in this case also. Rotation step was ΔC = 15°.

To position the auxiliary detector in a way that it will measure only the luminaire's emitted light and at the same to ensure that it won't influence the measurement result is impossible. To overcome the problem we separated the two measurements. We measured the luminaire position influence on the measurement results at a second round of measurement right after the real measurement. We positioned the auxiliary detector seen in the right hand picture in Figure 1.

To measure the electrical parameters a digital power meter with 200 kHz conversion rate and 16 bit A/D was used. The 50 Hz sinusoidal mains voltage of the luminaire was supplied by our mains stabilizer device.

3.2 Measurement set-up at Slovak University of Technology in Bratislava

Depiction of goniophotometric system with rotating luminaire can be seen in Figure 2. One axis defining C-planes passes through the photometric centre perpendicular to luminous part of each luminaire and rotating by this axis are defined C-planes. Second axis defining gamma angles passes through photometric center perpendicular to first axis but in contrast with laboratory in Hungary it is horizontally oriented. In the center of arm of goniometric system is mounted holder for luminaire under test. On each arm of it is placed properly calibrated digital inclinometer with resolution 0,1° to set C-planes and gamma angles.

In front of the luminaire at a distance where the inverse square law can be assumed to be true the photometer head of the illuminance meter is placed. The photometer head of the used illuminance meter is a Class L device according to DIN 5032-7 which satisfies requirements defined in the standards with $V(\lambda)$ fitting quality index f_1' under 1,5%. Distance between reference plane of photometer head and photometric centre was measured by calibrated laser distance meter. To ensure that photometer head and photometric centre is situated at same self levelling cross laser was used. Stabilised one-phase programmable power supply CHROMA 61505 with possibility to measure electric parameters of tested luminaires including ballast was used. Spectrum analyser ELCOM placed between power supply and tested luminaire including ballast was employed to perform harmonic analysis, possible distorted waveforms due to electronics, THD-u and THD-I with bandwidth complies standard.

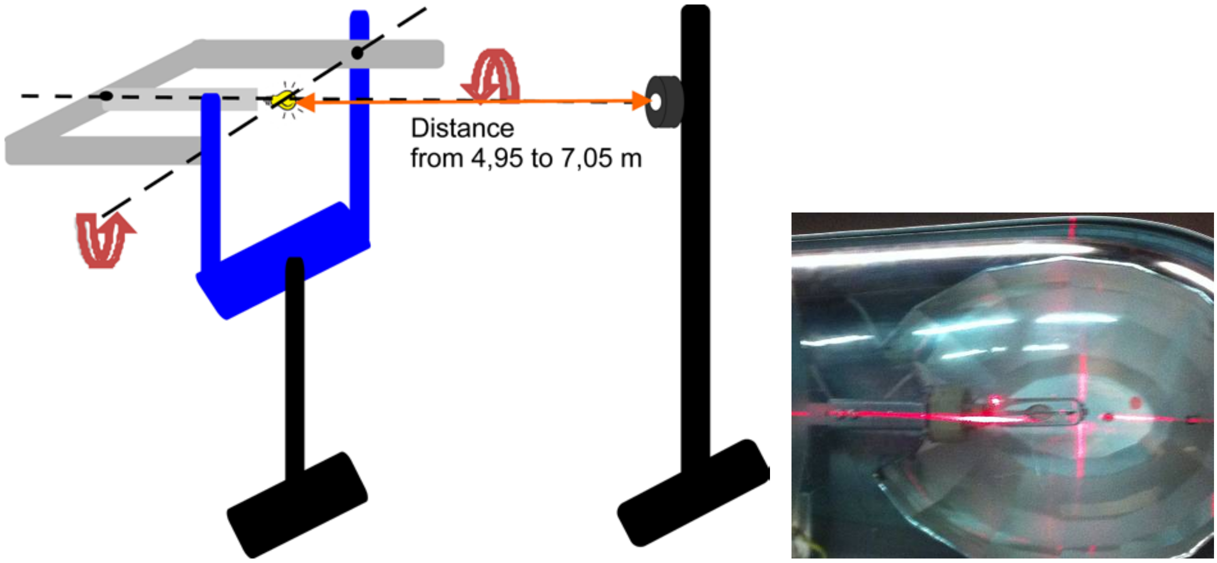

Figure 2 – Scheme of goniophotometer set-up at Slovak University of Technology in Bratislava

After the measurement of LIDC the photometer was placed directly at the centre on luminous part of luminaire to investigate the influence of the changing of the luminaire's working position. The photometer head was fixed to avoid any displacement of it on the surface and so to influence the correction results. The signal from photometer has been recorded to the template and normalised to the value of C=0° and gamma 0° they were used to correct the values of LIDC. The influence of the correction was the most markable at the measurement of the second luminaire L2.

Measurement was performed at three distances. Distance at measurement of luminaire L1 was 7,05 m, L2 was 6,66 m and luminaire L3 at 4,59 m.

4 Results

In tables below the results from comparison measurements each of tested luminaire by the participating laboratory can be seen.

Table 1 – Results of measurement for luminaire L1

	Total luminous flux Φ (lm)	Power including ballast P (W)	Power factor PF	Luminous efficacy η (lm/W)
University of Pannonia	3692	49,3	0,96	75,4
Slovak University of Technology	3681	48,8	0,97	74,9
Catalogue measured values	3784	49,0	0,96	77,2

Table 2 – Results of measurement for luminaire L2

	Total luminous flux Φ (lm)	Power including ballast P (W)	Power factor PF	Luminous efficacy η (lm/W)
University of Pannonia	3790	42,2	0,93	89,6
Slovak University of Technology	3724	42,0	0,91	88,7
Catalogue measured values	3678	42,1	0,93	87,4

Table 3 – Results of measurement for luminaire L3

	Total luminous flux Φ (lm)	Power including ballast P (W)	Power factor PF	Luminous efficacy η (lm/W)
University of Pannonia	1337	31,3	0,95	42,7
Slovak University of Technology	1315	31,1	0,96	42,3
Catalogue measured values	1319	31,0	0,96	42,5

In the header fields of each table the measured parameters are listed. In the two rows of each table are listed names of Universities with measured values of each parameter. In the third row values are shown, which can be considered as reference values for total luminous flux because as it was mentioned above these parameters were measured by C-type goniophotometer without changing operating position.

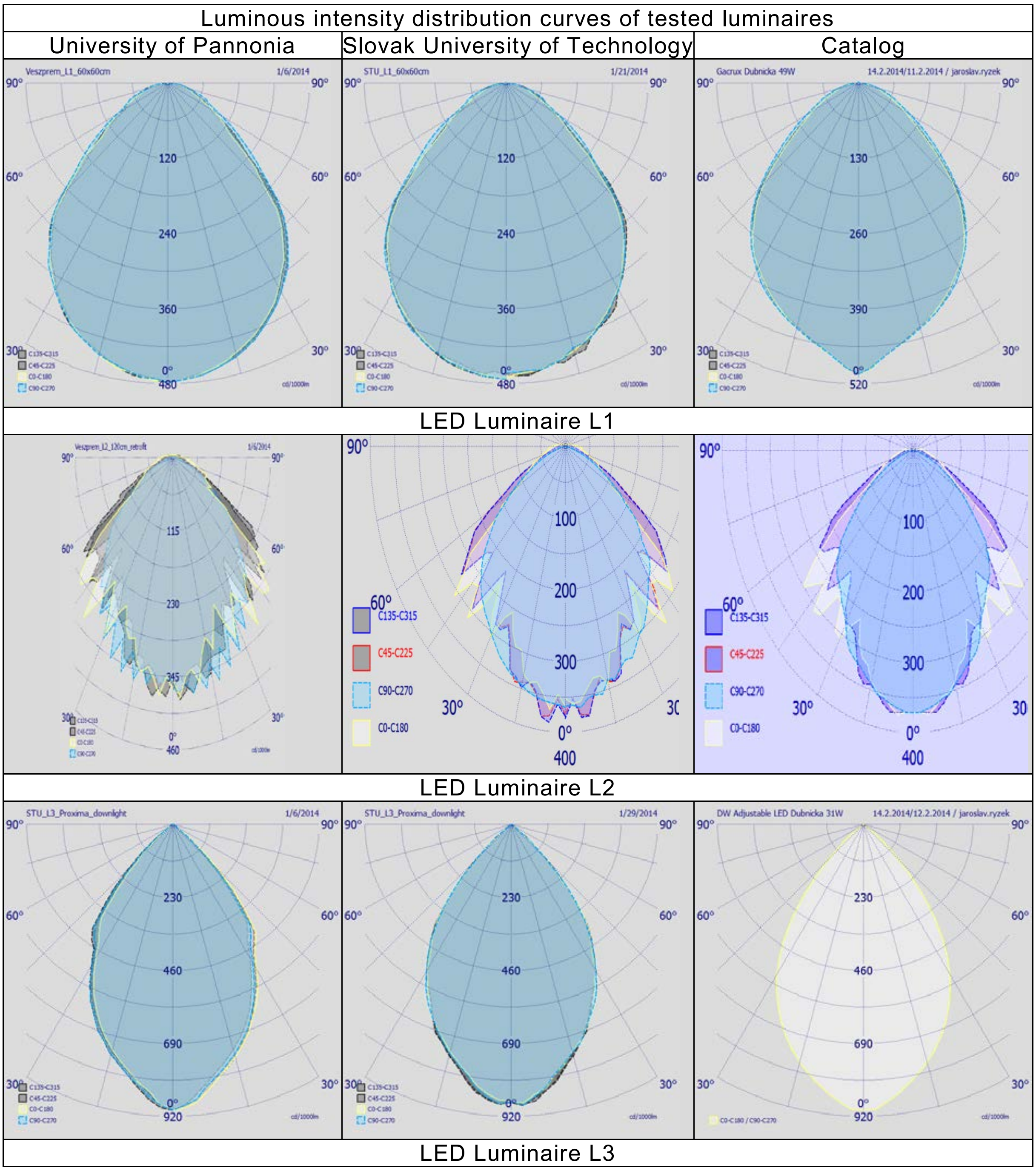

Figure 4 – LIDC results from comparison measurement

The luminous intensity distribution curves for each tested luminaire can be seen in Figure 4. It is shown for some additional C-planes, not - as usual - only for C0-C180 and C90-C270 to see how consistent the measurements are.

5 Uncertainty of measurement

For each measurement setup the relative expanded uncertainty (k=2) for luminous intensity in one direction, assuming normal distribution (what corresponds approximately to 95% confidence interval) was estimated.

Table 4 – Uncertainty budgets for measurement set-ups of laboratories

x_i contribution	distribution	University of Pannonia u_{rel} / %	Slovak University of Technology u_{rel} / %
Photometric scale of photometer head	normal	1,5	2,0
Drift from last calibration	rectangular	0,4	0,5
Linearity of photometer head	rectangular	0,4	0,2
Spectral error of photometer head	rectangular	1,4	1,8
Fatigue of photometer head	rectangular	0,2	0,2
Distance measurement	normal	0,4	0,4
Resolution	normal	0,05	0,05
Reproducibility	normal	0,6	0,7
Straylight	normal	0,6	1,1
Stability of power supply	rectangular	0,1	0,1
u_c		2,35	3,1
U (k = 2)		**4,7**	**6,2**

Measurement uncertainty was stated according to BIPM GUM document. Concrete contributions were assumed at the estimation of uncertainties of each measurement set-up with associated probability distributions.

6 Conclusions

Bilateral comparison of luminous intensity distribution curves measured by two independent photometric laboratories was performed. From the results of comparison it can be seen that total luminous flux of tested batch of luminaires deviation from reference value, that was stated as catalogue values, comply with stated expanded uncertainty declared by each laboratory. Electricity parameters were additionally determined but no uncertainty budget or estimation was performed. From Tables 1-3 can be seen deviations from reference values in the range of 1%. Very interesting deviations were found in measurement of luminous intensity distributions curves of tested luminaires. Especially for luminaire L2 are deviations significant, especially for plane C90-C270. It can be affected by the fact that measurements have been performed at different distances where peaks were not found at measurements of Slovak University of Technology and neither by the Catalogue laboratory where a near-field goniophotometer was used. Also possible influence of near-field technology it can be seen in pictures at the measurements of luminaire L1 where at the 0° gamma angle was found unexpected shape of LIDC. For future work this influence will be investigated by comparing more goniophotometer systems with different technologies and types. Furthermore investigation of the influence of these results to real realisations of lighting installations should be performed, to link photometric measurements to the practice.

Further on it is worth mentioning that only one case of influence of changing working position of LED luminaire monitored by correction photometer was found. It was for luminaire with LED retrofit tubes L2 where corrections had the most significant influence to the result. For other luminaires L1 and L3 corrections of measured values were negligible in comparison with uncertainty of measurement.

Acknowledgments

We acknowledge the financial support of the Hungarian State and the European Union under the TAMOP-4.2.2.A-11/1/ KONV-2012-0072.

This publication is the result of the project implementation:
Research centre of light and lighting technology, ITMS 26220220150,
supported by the Research & Development Operational Programme funded by ERDF.

Operačný program VÝSKUM a VÝVOJ

Agentúra Ministerstva školstva, vedy, výskumu a športu SR pre štrukturálne fondy EÚ

Podporujeme výskumné aktivity na Slovensku/
Projekt je spolufinancovaný zo zdrojov EÚ

Európska únia
Európsky fond regionálneho rozvoja

References

GRUM F., BECHERER R. J., 1979 „*Optical radiation measurements vol. 1: Radiometry*,“ Academic Press: 1979

OSA/AIP, Handbook of Applied Optics, Edited by Casimer DeCusatis, Chapter 1 (1997)

CIE 1996. CIE 121:1996. The Photometry and Goniophotometry of Luminaires. Vienna: CIE.

DIN 1985. DIN 5032-7. Photometry; classification of illuminance meters and luminance meters. Berlin: DIN

CIE 2012. CIE DS 023/E:2012. Characterization of the Performance of Illuminance Meters and Luminance Meters. Vienna: CIE.

BIPM 2008. JCGM 100:2008. Guide to the expression of uncertainty in measurement, Paris: BIPM

PP18

MEASUREMENT AND EVALUATION ON FLICKER OF LED LIGHTING SOURCES BASED ON THE EYE'S TEMPORAL PERCEPTION

Jianping Wang[1] Xiangping Ye[2] Kun Hu[2] Zhengfei Zhuang[3]
1 Zhejiang University Sensing Instruments Co., Ltd. Hangzhou, CHINA.
2 National Testing Center for Optical Radiation Safety of Photoelectric Products, Huizhou, CHINA.
3 Guangdong Sensing Optical Technology Co., Ltd. Foshan, CHINA.

Abstract

With the development of technologies, the excavation of new values of LEDs has been paid close attention in the lighting industry, including energy saving in dimmable lighting, human well-being and positive photobiological effects. It leads to a lot of new LED products with dynamic performance quickly enter into the market, which has largely satisfied with the requirements of human being on light. But at the same time, it also brings us new issues. In these products, the intensity of the light will varies with the time, and the corresponding flicker will be harmful to human, including visible flicker (low frequency) and stroboflash (high frequency). Especially on high-speed running status, flicker may bring fatal safety problem.

In this paper, comparing the current methods we will introduce a new method considering human eye's perception for measuring and evaluating the flicker of LED lighting sources. In this method, we measure the light output as a function of time, then use Fourier analysis to compute flicker spectrum power intensity as a function of frequency, and weighted it with the eye's temporal perception function, finally calculate flicker levels and report the frequency and flicker level of the highest flicker peak. And in this paper, we also compare our evaluation results with tradition measuring methods including percent flicker and flicker index. Lastly, we analyze the value and feasibility of the method for characterizing the flicker of LED lighting sources.

Key words: IDMS; Eye's Temporal Perception; Flicker index; Percent flicker.

1 Introduction

With the rapid development of electronic industry, human eyes often exposed to the AC fluorescent bulbs, LED lighting sources and display screen. New technology brings convenience on people's work and life, but also arouses a potential hazard to human health. Flicker, the Illuminating Engineering Society of North America (IES) Lighting Handbook defines– the most commonly used term – as "the rapid variation in light source intensity" [1]. LED flicker has its potential human impacts, which range from distraction or mild annoyance to neurological problems. The effects of flicker are dependent on the light modulation characteristics of the given source, the ambient light conditions, the sensitivity of the individuals using the space, and the tasks performed. Low-frequency flicker can induce seizures in people with photosensitive epilepsy, and the flicker which exist in office lighting has been linked to headaches, fatigue, blurred vision, eyestrain, and reduced visual task performance for certain populations. Flicker can also produce hazardous phantom array effects—which may lead to distraction when driving at night, for example—or stroboscopic effects, which may result in the apparent slowing or stopping of moving machinery in an industrial setting [2].

The photometric flicker found in electric light sources is typically periodic, with its waveforms characterized by variations in amplitude, average level, periodic frequency (cycles per unit time) and shape. Percent Flicker and Flicker Index are metrics historically used to quantify flicker. Percent Flicker is better known and easier to calculate, but Flicker Index has the advantage of being able to account for differences in waveform shape (or duty cycle, for square waveforms). Both metrics account for amplitude variation and average level, but since both are based on the analysis of a single waveform period, neither is able to account for differences in periodic frequency. Measuring and reporting flicker is not a standard practice for commercial light sources. Although industry bodies have developed flicker metrics, they have not produced complementary standardized measurement procedures to ensure appropriate comparisons of reported values.

In this paper, we will introduce a new method for measuring and evaluating the flicker of LED lighting sources which considered the human eye's perception, and we will also calculate the flicker index of light source and analyze the value and feasibility of the method for characterizing the flicker of LED products.

2 Experimental setup

In this paper, FP-210, which produced in Zhejiang University Sensing Instruments Co., Ltd., was used to acquire and store the signals of the LED lighting sources. Fig. 1 depicts principle of FP-210. The integrating sphere (1 meter diameter) equipped with a photomultiplier tube (PMT) with a response rate of 2μs, and the evaluation results show on the PC.

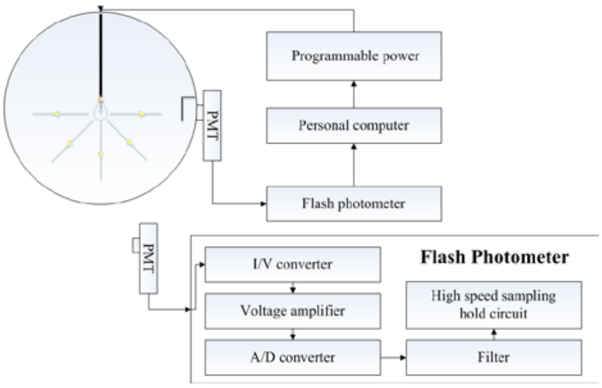

Figure 1-Principle diagram of FP-210

3 Materials and methods

Human perception of light flicker is affected by frequency, percent flicker, duty cycle, waveform shape, and correlated color temperature (CCT), among which, frequency is the major factors[3]. Two metrics proposed by IESNA lighting experts were used to measure the severity of flicker in our test setup: percent flicker and flicker index. Percent flicker is a measure of the depth of modulation of flicker and is calculated using the following formula:

$$\text{Percent Flicker} = (\max - \min) / (\max + \min) \times 100\% \quad (1)$$

Flicker index is a lesser known metric that accounts for the different shapes or duty cycles that the periodic waveforms of AC lighting can have. It is calculated using the following formula with reference to the figure 2.

$$\text{Flicker index} = \text{Area1} / (\text{Area1} + \text{Area2}) \quad (2)$$

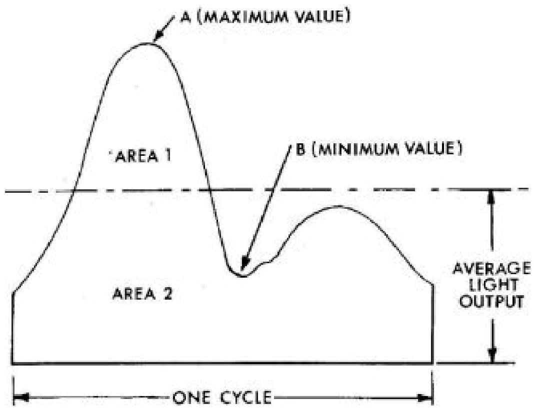

Figure 2-Defining Flicker Index and Percent Flicker[4]

Flicker characterization also mentioned in IDMS published by the SID's ICDM working group. This includes the fast fourier transform (FFT) method of calculating dominant flicker frequency and weighted flicker level to match the approximate temporal flicker sensitivity of the human eye (Table 1). In this method, we measure the light output as a function of time, then use Fourier analysis to compute flicker intensity as a function of frequency, and weighted it with the eye's temporal perception function, finally calculate flicker levels and report the frequency and flicker level of the highest flicker peak.

Table 1-Flicker Weighting Factors

Frequency:Hz	Scaling: dB	Scaling: Factor
20	0	1.00
30	-3	0.708
40	-6	0.501
50	-12	0.251
60	-40	0.010

Note: Use linear interpolation between the listed frequencies.

"Scaling:dB" is equivalent to "Scaling: Factor"

4 Results and discussion

In this part, we obtained three typical LED lighting sources which produced in country A, country B and country C, respectively. And the corresponding electronical parameters are 220V/50-60Hz, 110-220V/50-60Hz and 220V/50Hz. In the process of measuring, firstly, the transient photometer (FP-210) parameters were set to sampling interval 50 μs, frequency 20000 Hz and 4000 sampling points. And we employed the standard lamp for calibration and dark current correction. Then we lighting the tested LED lamps in the integrating sphere, and obtained the results after lighting the lamps for 15 minutes. Figure 3 to 5 show the frequency spectrum analysis on LED lighting sources from country A, country B and country C. Table 2. show the electronical parameters and measurement results of three typical LED lighting sources. From figure 3 to 5, we can find that the power of frequency spectrum had reached the maximum near 100Hz. But in fact the human eyes do not detect such a high frequency flicker, so only low frequency harmonic component is keeping when weighted with the eye's temporal perception function. Form figure 3 to 5 and table 2, we can find the parameters of flicker depth, percent flicker and flicker index do not accurately evaluate the real flicker level because they can not consider the effect of the eye's temporal perception function or other physical factors. For percent flicker, it gave the same evaluation (100%) on the LED lighting source from country A and country B which own distinct flicker level. For flicker index, it could provide a more reliable evaluation method than percent flicker. The flicker index 0.5519 represents the lamps from country A has the strongest flicker level which quadrate with the fact. Unfortunately, it also can not distinguish the flicker level of other two types LED lamps from country B and country C. Only the IDMS method makes up the deficiencies of the above parameters and reflects the real flicker level from different countries.

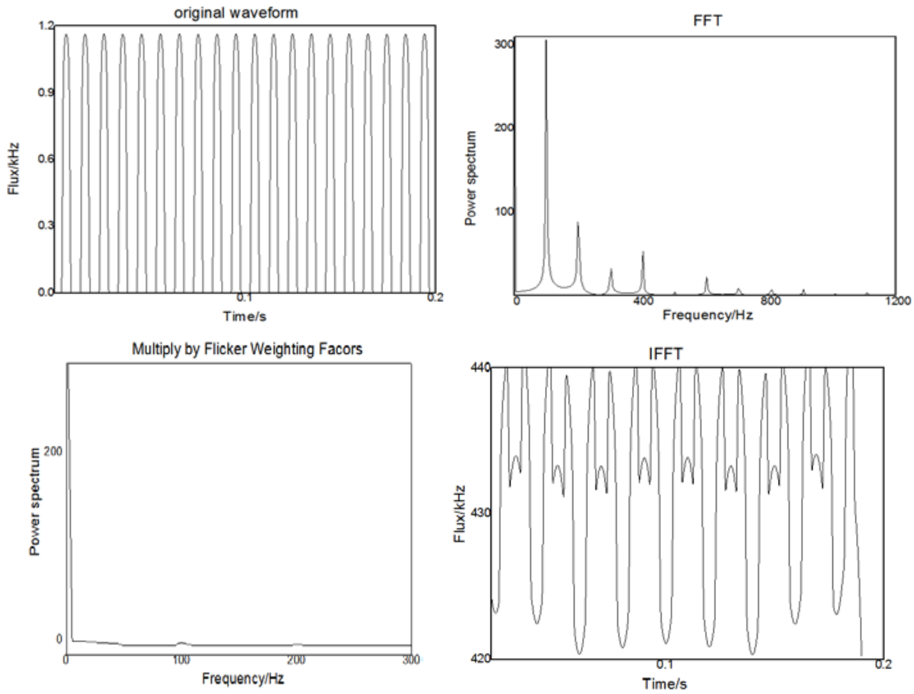

Figure 3-Frequency spectrum analysis on LED lighting source (Country A)

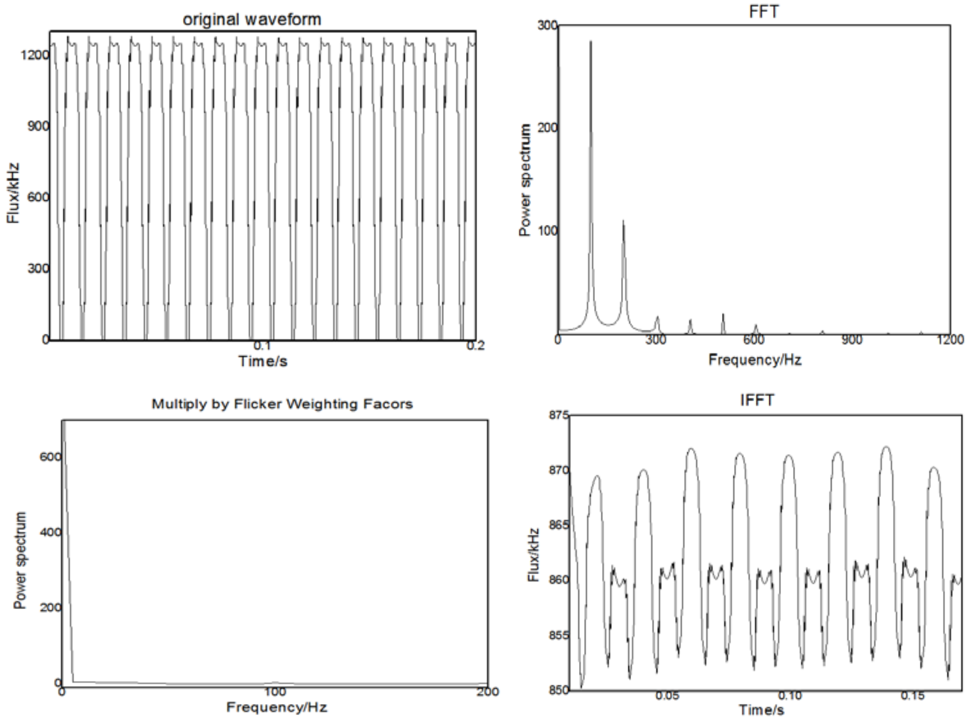

Figure 4-Frequency spectrum analysis on LED lighting source (Country B)

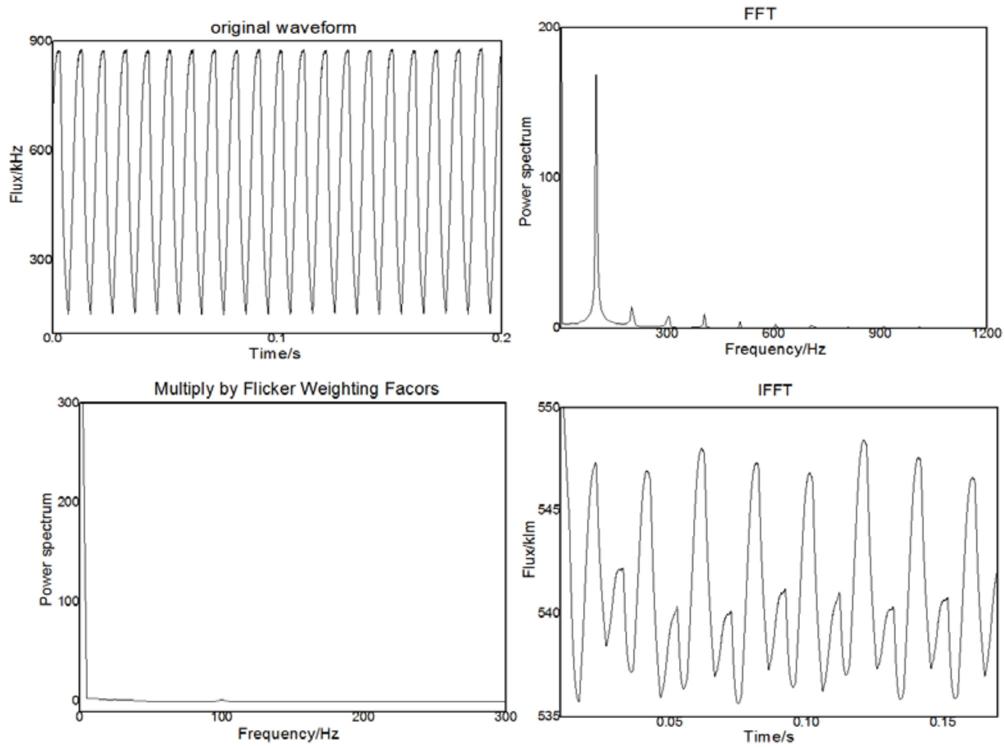

Figure 5-Frequency spectrum analysis on LED lighting source (Country C)

Table 2-Electronical parameters and measurement results of three LED lighting sources

Producing country	Power supply specifications	Flicker depth	Percent Flicker	Flicker index	IDMS evaluation Flicker (dB)
Country A	220V/50-60Hz	0.0068	1.0000	0.5519	-33.79
Country B	110-220V/50-60Hz	0.0005	1.0000	0.2556	-40.92
Country C	220V/50Hz	0.0330	0.7015	0.2179	-38.79

5 Conclusion

In this paper, FP-210 offered the traditional flicker evaluation parameters percent flicker and flicker index, and also offered the parameter which considered the effect of the eye's temporal perception function. In conclusions, the traditional methods percent flicker and flicker index could only give a partly correct evaluation results. Our new method makes up the deficiencies of traditional ways. And the LED flicker level from country A is stronger than that from country C, LED lighting source from country B own the weakest flicker, the result is consistent with actual situation, and better than the traditional methods.

References

[1] REA M.S., The IESNA Lighting Handbook, 9th Edition. Illuminating Engineering Society, New York, New York, 2000.

[2] WANG J., MOU T. An Evaluation method for lighting flicker based on frequency spectrum analysis. Opto—Electronic Engineering. 39(11): 32-36, 2012.

[3] BULLOUGH J. D., HICKCOX K. S., KLEIN T. R. and NARENDRAN N., "Effects of flicker characteristics from solid-state lighting on detection, acceptability and comfort," Lighting Res. & Technol. 43(3):337-348, 2011.

[4] FARRELL J E, BRIAN L BENSON and CARL R TTAYNLE. Predicting flicker thresholds for video display term inals[J]. Proceedings of the SID (S0036-1496), 28(4) : I1—15, 1987.

[5] Information Display Measurement Standard (IDMS), section of 10.5, 180-181.

PP19

EVALUATION OF RELATIONSHIPS BETWEEN TEMPERATURE AND ELECTRICAL PROPERTIES FOR SSL PHOTOMETRIC MEASUREMENTS

Godo, K.[1], Numata, T[1]., Zama, T.[1]
[1]NMIJ/AIST 1-1-1, Umezono, Tsukuba, Ibaraki, JAPAN,
kenji-goudo@aist.go.jp

Abstract

We have developed a measurement facility which allows real-time, simultaneous evaluation of temperature and electrical properties of LED lamps (We call “multi thermostatic system”). By using the multi thermostatic system, a relationship of these parameters has been investigated.

Keywords: SSL, LED lamp, temperature property, electrical property, output impedance

1 Introduction

Rapidly, Solid State Lighting (SSL) products such as LED lamps are replacing traditional light sources for energy saving. Therefore, accurate evaluation of luminous efficacy (of these SSL products), which is an index of the energy saving defined by total luminous flux and electrical power consumption, is becoming important. The LED lamp is generally comprised of LEDs and an AC/DC driver circuit, the AC/DC driver circuit has a big influence on evaluation of luminous efficacy like LED elements. Also, a total luminous flux and electrical power of LED lamp strongly depend on ambient temperature and case temperature of it. This means that careful investigations of relationship between the total luminous flux, the temperature properties and the electrical properties of LED lamps are necessary for an accurate evaluation of their luminous efficacy. Moreover, also in uncertainty evaluation for SSL measurement, those evaluations are indispensable.

In this study, we have developed a measurement facility which allows real-time, simultaneous evaluation of temperature and electrical properties of LED lamps (We call “multi thermostatic system”). Then, by using the multi thermostatic system, a relationship of these parameters has been investigated.

2 Development of the multi thermostatic system

Figure 1 shows the schematic diagram of the multi thermostatic system for measurement of temperature and electrical properties of LED lamps. The system is based a thermostatic

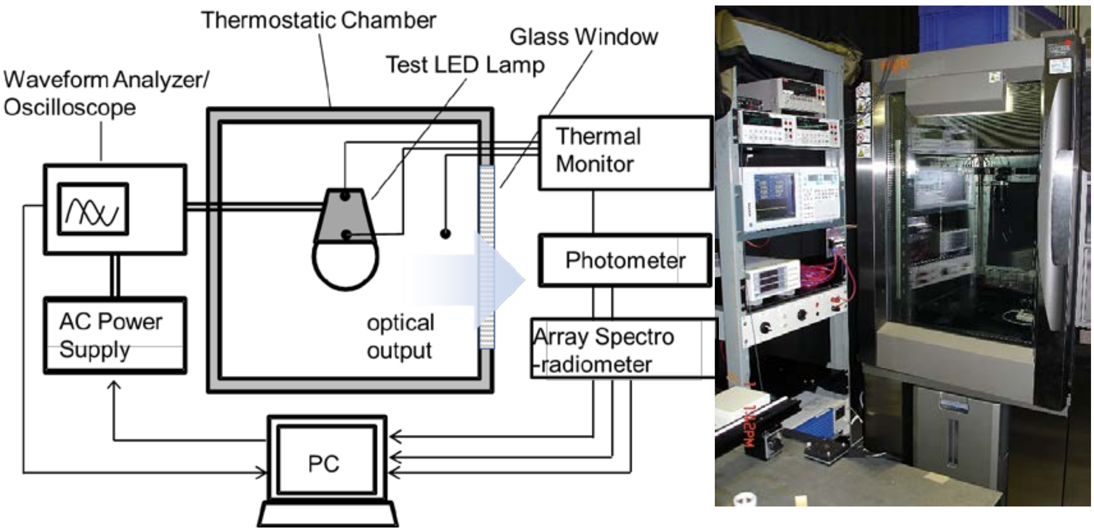

Figure 1 – NMIJ multi thermostatic system

chamber whose front panel is constructed by a glass window. A test LED lamp is set in the thermostatic chamber. To monitor temperatures of the test LED lamp, multiple thermistor probes are attached to the test LED lamp (shown in fig 2). One of the reasons that not only the temperature of the thermostatic chamber but also the temperature of the test LED lams measures is to confirm the temperature of the test LED lamp being stable after the temperature of the thermostatic chamber changes. As we show it in fig 2, a temperature stabilization time of the test LED lamp is different from a stabilization time of the thermostatic chamber. A stabilized AC power supply, a waveform analyzer and optical measurement instruments (a photometer and array spectro-radiometer) placed outside of the thermostatic chamber allow real-time measurement of the electrical quantities (current, active power and waveform) and the optical quantities (luminous flux and spectrum) of the test LED lamps under various temperature conditions. Also to investigate an electric impedance effect of AC power supply, an extended cable is easily attached to the AC power supply.

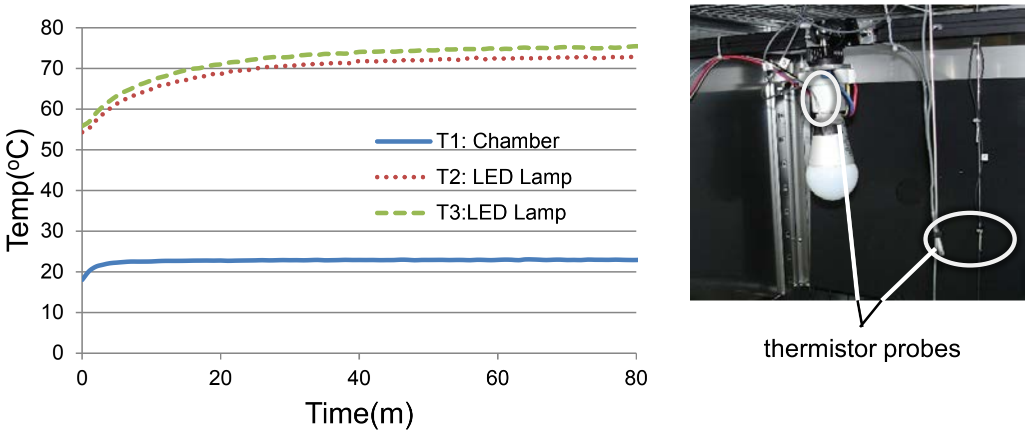

Figure 2 – Temperature monitor results after the thermostatic chamber temperarure change

3 Measurement results

We evaluated the temperature and the electrical properties of five test LED lamps. Sample A, sample B and sample C are omnidirectional type LED lamp, sample D and sample E of test LED lamps are beam type LED lamps.

3.1 Temperature properties of LED lamps

Figure 3 shows the evaluation results of temperature properties of the test LED lamps. Figure3 (a) indicate the result of sample A, and figure 3 (b) shows sensitivity coefficients of each parameter (electric current, active power and luminous flux) against the chamber temperature.

Generally, the sensitivity coefficient of luminous flux for LED is about 0.1 %/oC - 0.2 %/oC.

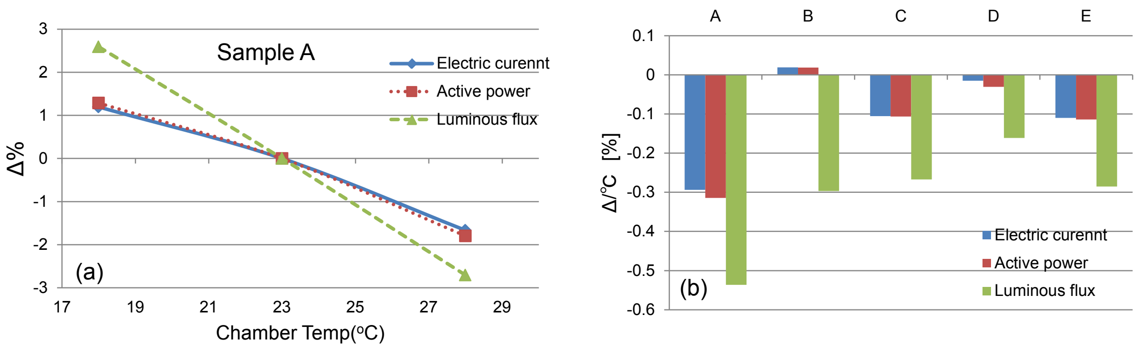

Figure 3 – Temperature properties of the test LED lamps

Frome the sensitivity coefficient of LEDs, the sensitivity coefficient of the test LED lamp are bigger than it of LED, the influence of the AC/DC driver circuit is strong, and those individual differences of the AC/DC driver circuit are big.

3.2 Input Voltage dependence of LED lamps

Figure 4 shows the input voltage dependency of the test LED lamps properties (electric current, active power and luminous flux). Figure4 (a) indicate measurement results of sample C, and figure 4(b) indicate sample D, respectively. In sample C, the electric current change to reverse direction against change of the input voltage, therefore there are few changes of the active power and the luminous flux of sample C. The other, in sample D, the electric current change to same direction against change of the input voltage, there are big changes of the active power and the luminous flux of sample

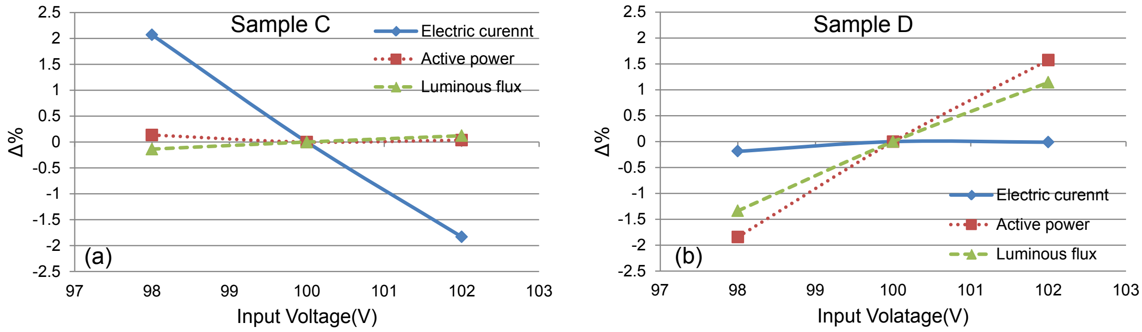

Figure 4 – Input voltage dependency of the test LED lamps properties ((a) sample C, (b) sample D)

4 Output Impedance effect of AC power supply

Figure 5 shows the evaluation results of output impedance effects of AC power supply. Figure 5 (a) shows sensitivity coefficients of each parameter (electric current, active power and luminous flux) against the output impedance of AC power supply. Our AC power supply can easily change the output impedance. Electric current of Sample B and sample D are influenced by the output impedance. But, generally, commercial AC power supply doesn't have big output impedance, the situation such as above experiment result is less likely to occur. However, a cable length from an AC power supply to a LED lamp included in output impedance effect, too. Figure 5 (b) shows the cable length influence in active power of sample D. As the cable length gets longer, the active power greatly changes and becomes unstable. However, the change is decrease at 20 m.

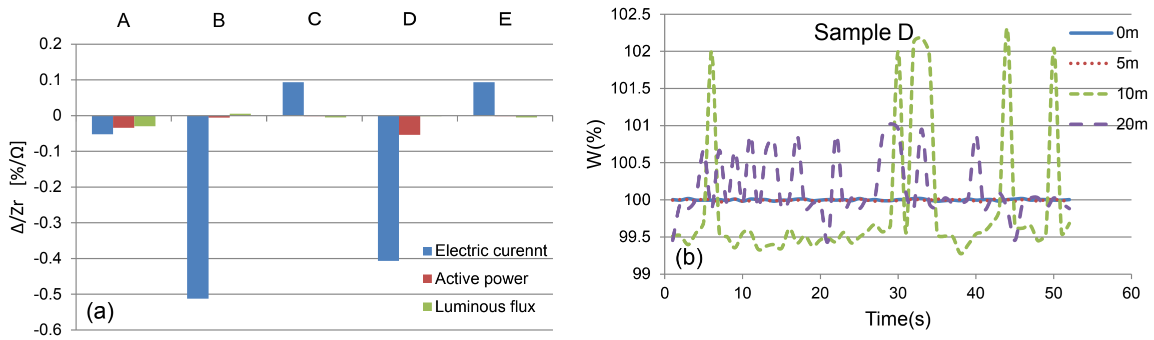

Figure 5 – Output Impedance effect of AC power supply

5 Conclusion

We developed a new measurement facility for evaluation of temperature properties and electrical properties of LED lamps. Our measurement results showed that these properties change depending on LED type or test conditions. And, the measurement results indicated that not only output impedance of AC power supply but the cable length from an AC power supply to a test LED lamp is influence electrical properties of LED lamps.

References

MARTINSONS, C. et al., 2013, INFLUENCE OF CURRENT AND VOLTAGE HARMONIC DISTORTION ON THE POWEOR MEASUREMENT OF LED LAMPS AND LUMINAIRES, *PROCEEDINGS of CIE Centenary Conference "Towards a New Century of Light"*, p290-p299.

D. Zhao, et al., 2013, GUIDELINES FOR TRACEABLE MEASUREMENTS OF ELECTRICAL PARAMETERS OF SSL, EMRP-ENG05-1.1.3 .

E.FRED,2003, Light-Emitting Diodes second edition(p106), UK, Cambridge.

PP21

BEAM PROPAGATION RATIO PARAMETERS, TRACEABLE TO NATIONAL MEASUREMENT STANDARDS

S R G Hall[1], S D Knox[1], M Shaw[1], **T M Goodman**[1]
[1] National Physical Laboratory, Teddington, UK
simon.hall@npl.co.uk

Abstract

In many laser and non-laser applications the M^2 beam propagation factor is key to understanding system performance and photobiological hazard potential. The accepted M^2 measurement methodology involves sampling the beam width at several positions along the direction of propagation using a camera which is translated with respect to the source. However this approach can be slow and typically requires a large measurement setup which is not practical in many situations. A number of other techniques have been proposed and implemented in commercial instruments, each having limitations in terms of size or performance. In this poster we describe a novel compact device which incorporates a liquid lens to allow fast, accurate and flexible measurement of M^2.

Keywords: photobiological hazard

1 Introduction

The measurement of beam propagation parameters is essential for the wide ranging use of lasers in industry, medicine and academia. There are a number of methods available for measurement of the diameter of a beam as well as its far-field divergence. The basic principles for those methods have been established in an ISO standard series 11146 [1][2][3]. However commercially available devices to measure laser parameters such as M^2 beam propagation ratio, divergence, Rayleigh distance and waist diameter are usually slow, cumbersome and difficult to align.

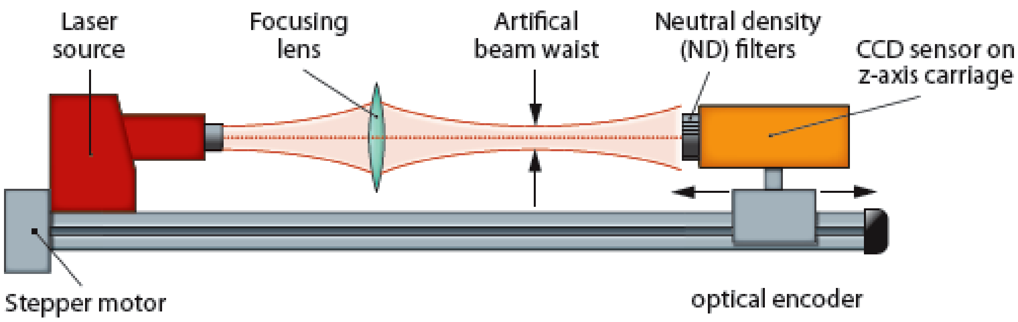

Figure 1 – ISO 11146 recommended measurement by moving array detector with respect to lens

2 New technique for measurement of M^2

The problems with these existing approaches has led NPL to develop a novel compact device which incorporates a liquid lens to allow fast, accurate and flexible measurement of M^2. The design concept was to remove the need for a movement stage, required to allow beam widths to be sampled as the stage moves through the laser caustic, and replace the fixed lens used in the standard configuration with one which can vary its optical power in response to a changing input voltage. The lens is constructed from two different drops of immiscible liquid, one electrically conducting, one insulating. The drops sit on top of each other in a conic ring of metal. When an electrical charge is applied to the metal ring the conductive liquid changes its electro-wetting characteristics, leading to a change in the radius of curvature of the interface between the liquids and so changing the power of the lens.

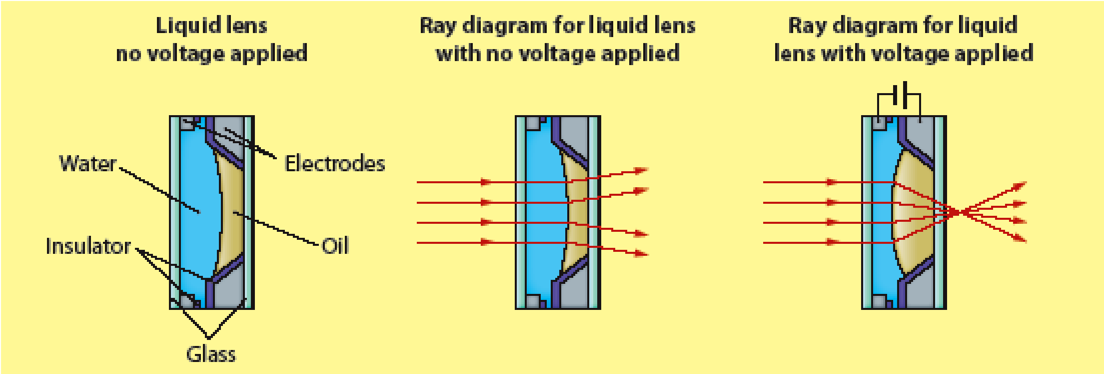

Figure 2 – Operation of liquid lens

For this prototype a conventional convex lens was used to increase the optical power of the liquid lens. A low profile and high pixel-density CCD sensor was incorporated to allow the liquid lens to be placed close to the detection array. The distances between the lenses and camera were initially chosen to optimise the dynamic range of the device.

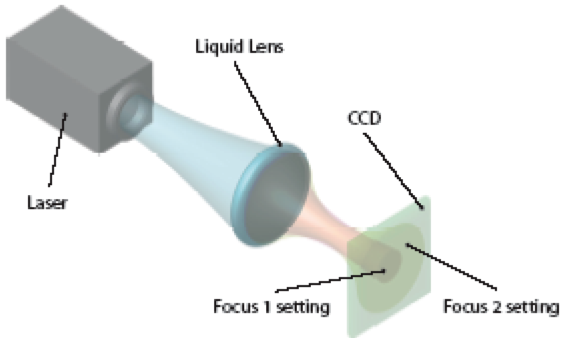

Figure 3 – Prototype device using a variable power lens, removing the need to translate the array detector

Figure 4 – Photograph of prototype device using a liquid lens

3 Characterisation and calibration

The components used to create the device were well characterised to allow a stable and predictably accurate prototype to be produced. The relative positions of the components were located and measured using cat's-eye reflections of a beam from a Zygo interferometer. This information was required to construct a Zemax software model of the device as the complex nature of the liquid lens excluded the option of a thin lens geometrical optics approximation. The standard ISO 11146 fixed lens system was modelled alongside the variable power liquid lens system and the results compared for Gaussian propagation of a TEM00 M2 beam using the physical optics capability of the program.

A precision amplifier system was produced by NPL which demonstrated low hysteresis and good linearity. This had to supply up to 60V to the lens to exploit its maximum dynamic range. The unit was calibrated and the uncertainty in the calculation of the high voltage (HV) output (lens driving voltage) from the measured monitor voltage is negligible with respect to focal length changes of the driven lens. The liquid lens was calibrated for focal power accuracy and linearity against a set of fixed lenses. A lens calibration system was constructed using a Shack-Hartmann wavefront sensor to allow the wavefront error and focal length to be measured across the liquid lens adjustment range (Figure 5). This shows that the focal length changed reproducibly with applied voltage and that the wavefront error was within acceptable limits for laser beam measurements.

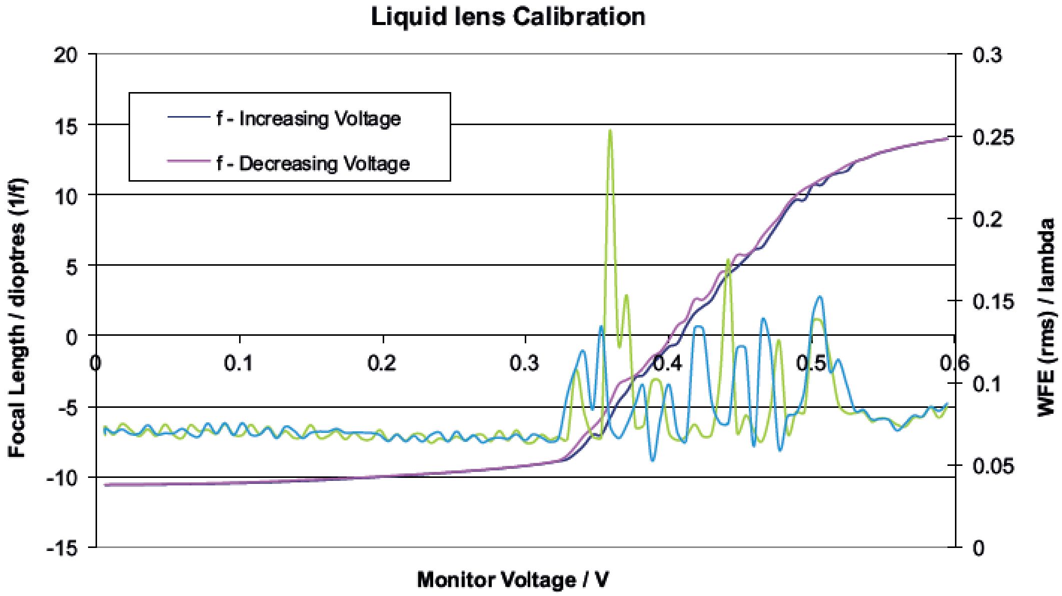

Figure 5 – Focal length change with applied voltage and corresponding wavefront error using a Shack-Hartmann wavefront sensor

4 Practical validation

In order to validate the new method, a comparison was made between the liquid lens prototype system and a standard ISO 11146 system, using a laser interferometer to measure component positions with a positional accuracy of ±0.01 mm [4] – see Figure 6. This showed good agreement between the standard approach and the liquid lens method, as shown in Table 1, and confirmed that the liquid lens approach offers a reliable, compact and fast technique for traceable calibration of beam propagation ratio measurements..

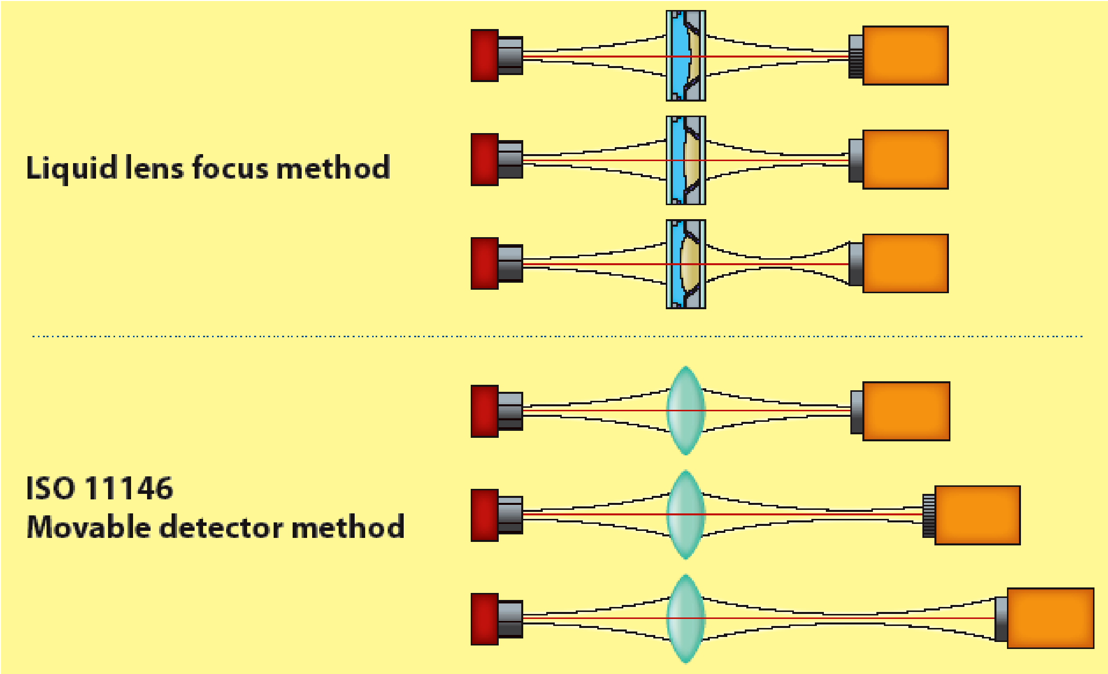

Figure 6 – Comparison between new method and ISO 11146 method

Table 1 – Results of comparsion

	M^2 device	Uncertainty +/–	ISO	Uncertainty +/–
M^2	1,054	0,122	1,099	0,0296
Divergence / mrad	16,827	1,234	15,093	0,2571
Raleigh Distance / mm	3,00	0,155	3,89	0,0468
Waist diameter / mm	0,05	0,003	0,059	0,0007

5 Conclusions

We have outlined a novel device that opens up new opportunities for laser control [5]. It is compact and capable of fast traceable measurements for the calibration of beam propagation ratio measurement devices.

6 Acknowledgements

This work was funded by the Physical Program of the National Measurement System in the Department for Business Innovation and Skills.

The expertise of Pravin Patel (NPL) is acknowledged for the design and construction of the low hysteresis HV amplifier.

References

[1] EN ISO 11146-1:2005 Lasers and laser-related equipment – Test methods for laser beam parameters – Beam widths divergence angle and beam propagation factor

[2] EN ISO 11146-2:2005 Lasers and laser-related equipment Test methods for laser beam widths divergence angles and beam propagation ratios General astigmatic beams

[3] PD ISO/TR 11146-3:2004 Lasers and laser-related equipment Test methods for laser beam widths divergence angles and beam propagation ratios Intrinsic and geometrical laser beam classification propagation and details of test methods

[4] Hall S R G, Robinson D, Knox S D, Yang H, Scott A M, Woods S C, A J Turner and Lewin A. 2007. Improvement and Commissioning of a Novel Technology for the Measurement of Laser Beam Profiles Proc. SPIE Photonics West, Laser Resonators and Beam Control IX conference (San Jose, CA: SPIE)

[5] SRG Hall. Method and system for measuring the propagation properties of a light beam. PCT patent application WO2010125344

PP23

SUPERCAPACITOR AS A SOURCE FOR AUTONOMOUS EMERGENCY LUMINAIRE

Novak, T., Sokansky, K., Carbol, Z.
Department of electrical engineering, VSB – Technical University of Ostrava, CZECH REPUBLIC
karel.sokansky@vsb.cz

Abstract

In this article, authors are describing possibility of supercapacitor usage for powering emergency luminaires. Basic facts about modern supercapacitors and fundamental characteristics are provided initially. Analysis of usage such supercapacitors in emergency lighting and suitable luminaires follows. Prototype of emergency escape lighting luminaire powered by 3000F supercapacitor was created. For this purpose authors made capacity calculation and simulation of discharging characteristic. Then results of prototype measurements are described. Finally pros and cons of supercapacitor usage are summarized, with prediction of future growth.

Keywords: Emergency lighting, supercapacitor, LED luminaire

1 Introduction

In connection with the development of nanotechnologies in recent years there have been created new possibilities of power accumulation on the principle of electric charge accumulation on the capacitors electrodes. These high capacity capacitors are called supercapacitors, also SuperCaps or UltraCaps. Even if the capacitors have been known for a long time they have improved so much in the recent years (especially surfaces of electrodes and dielectric materials) that can be meaningfully used for accumulating energy for a longer period. Mostly they are used currently to back up data in electronic memories and similar devices with low power consumption. The newly found usage is when starting a drive with high currents, in the DC link converters, in the reduction of peak demand and in the traffic engineering in accumulation of vehicles braking energy that will be used in their next moving off (e.g. Mazda6).

In connection with the LED light sources the supercapacitors seem ideal backup power supply for emergency lighting luminaires.

Advantages:

- Lower power consumption by LED
- Long life- time
- Reliable operation at low temperatures

Disadvantages:

- Higher cost than conventional accumulators
- Larger sizes of accumulators

2 General Description of Supercapacitors

Supercapacitor, unlike various accumulators (NiCd, Pb, NiMH, Li-Po, Li-Ion, etc.) does not use the electrochemical principle to accumulate the power. It transforms power into electric field energy between two electrodes.

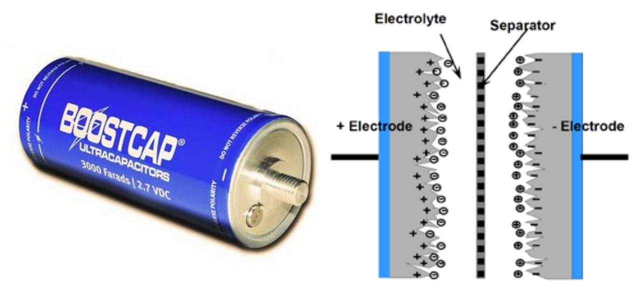

Figure 1 – Supercapacitor Maxwell BCAP3000 and supercapacitor inner structure [1]

These are dominantly made of carbon powder coated on aluminum foil. One gram of powdered carbon has a surface area up to 2000 m^2 [2]. Positive and negative electrodes are separated by a separator consisting of a polypropylene film. Free room is filled with liquid electrolyte. The maximal voltage of supercapacitor depends on it. The operating voltage and the maximal one is about 2-3V. The large surface of electrodes, the small distance between them and high electric solidity of electrolyte and separator create conditions for the relatively high capacity of the supercapacitors. The capacity is directly proportional to the electrodes surface and inversely proportional to their distance:

$$C = \varepsilon_0 \cdot \varepsilon_r \cdot \frac{S}{d} \tag{1}$$

The amount of energy that can be accumulated:

$$W = \frac{1}{2} \cdot C \cdot U^2 \tag{2}$$

It is worth emphasizing that the amount of accumulated energy depends on the square of the voltage. Therefore the voltage has the greater impact on the accumulated energy than the capacity does. For example supercapacitor 2.7V / 2500F is able to store the same energy as a supercapacitor 2.5V / 3000F.

A significant advantage of supercapacitors is that the voltage changes are relatively little during their discharge.

$$\frac{W_{0.5}}{W_1} = \frac{\frac{1}{2} \cdot C \cdot \left(\frac{1}{2} \cdot U\right)^2}{\frac{1}{2} \cdot C \cdot U^2} = \frac{\frac{1}{4} \cdot U^2}{U^2} = \frac{1}{4} \tag{3}$$

Equation 3 shows that the reduction in voltage of the capacitor from the initial voltage by half causes the release 75% of the accumulated energy. The change of the certain (above described) parameters may occur due to aging. They are affected by time or number of cycles.

Due to the very low temperature solidification of the electrolyte the supercapacitors can operate at temperatures as low as -40°C and even higher working temperatures do not have a marked influence on capacity. There is only a change of a value of the replacement series resistance (Resr). However, this resistance is not an important parameter for emergency lighting due to low labor currents, since it arises only minimal voltage drop (see Fig. 2) and therefore its warming is negligible too. Maximal operating temperature of supercapacitors is 65°C so it is higher than at the conventional battery cells.

Supercapacitors´ lifetime is influenced by applied voltage and by ambient temperature. For example, at rated voltage and temperature 25°C there is after 88 000 hours (about 10 years of operation) the loss of capacity about 15%. With increasing of temperature by every 10°C the loss of the capacity is multiplied. At 35°C, which is considered as maximal when the device is being installed, the loss of capacity after ten years of operation is the maximum up to 30%. Number of cycles has the impact on the capacity reduction as well (1 million cycles cause a loss of capacity by about 20%). However, when using to supply emergency luminaires the number of cycles for the expected lifetime is less than one thousand. Supercapacitors are permanently under the supply voltage and the discharging occurs only when there is a voltage failure. This mode will have only a minimal effect on the capacity loss. Due to the high lifetime of supercapacitors it will not be necessary to change them during all time when the emergency luminaires are being used. This provides the advantages of enabling permanent installation into luminaires and especially in reducing the cost of maintenance (replacing the standard accumulators).

The great advantage of supercapacitors is their high efficiency. There are not electrochemical reactions as at the conventional accumulators. In applications with low operating current, the total efficiency of the cycle (charging / discharging) is up to 98%, depending on operating current. This allows us to achieve a very high efficiency of the device operation.

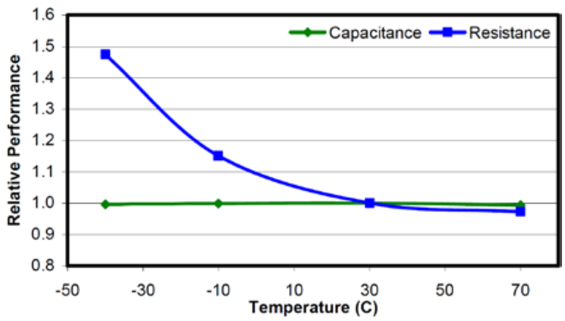

Figure 2 – Supercapacitors parameters temperature dependence [2]

3 The Behaviour of Supercapacitors for Power LED Lighting

When calculating the required capacity and the number of articles we start from the substitute scheme and the supercapacitor discharge characteristics (see Fig. 3).

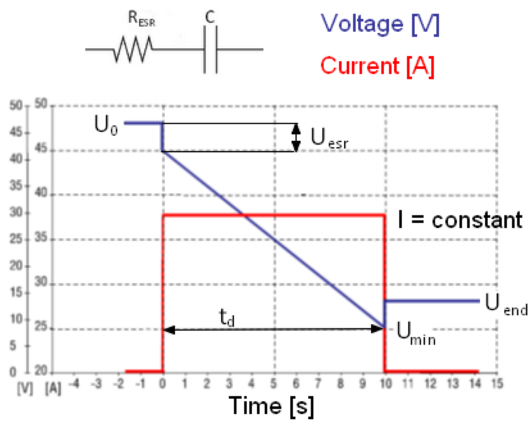

Figure 3 – Substitute scheme of the supercapacitor and discharge characteristics of supercapacitor [4]

where

U_0	is the initial voltage of charged capacitor
U_{esr}	is the voltage drop at the equivalent series resistance
U_{min}	is the the minimal usable voltage
U_{end}	is the voltage after load disconnection
t_d	is the discharge time
I	is the constant discharge current

Besides its capacity the supercapacitor has its spare internal resistance Resr that causes a voltage loss Uesr while discharging.

$$U_{esr} = R_{esr} \cdot I \tag{8}$$

This loss reduces the amount of usable energy from the capacitor:

$$\Delta W = \frac{1}{2} \cdot C \cdot \left[U_0^2 - (U_{\min} + U_{esr})^2 \right] \tag{9}$$

The amount of resistance depends on the type of supercapacitor, number of supercapacitors and their connections. The maximal voltage loss Uesr occurs at the maximal current that will flow through the circuit at the minimal voltage of the capacitor. The calculation takes into account the efficacy of the converter. Internal resistance Resr is bigger in cells with lower capacity. For the calculation we have chosen the supercapacitor with capacity of only 2000F:

$$U_{esr\max} = R_{esr} \cdot I_{\max} = R_{esr} \cdot \frac{P}{U_{\min} \cdot \eta} \tag{10}$$

$$U_{esr\max} = 0.58 \cdot 10^{-3} \cdot \frac{1}{0.8 \cdot 0.7} = 0.001V \tag{11}$$

In applications for charging of the emergency LED lighting, because of low operating currents, Uesr will not be taken into account due to its small size.

4 Design of Power Connection of the Emergency LED Luminaire with Supercapacitor

Theoretical calculation of the supercapacitor capacity was done for LED light source of power 1W, supplied by a constant operating current 350mA and voltage of 3.3V. The LED of 1W power and high luminous efficacy (e.g. 125lm/W) is an adequate light source in combination with good-quality optics designed for the lighting of emergency exits. The effectiveness of optical parts of such a good-quality luminaire is more than 70%. Due to the exact distribution of the luminous flux and its sufficient quantity (over 90lm), such luminaires (when meeting the standard values for emergency lighting) can illuminate the standard corridor with an emergency exit of length longer than 10m. The lifetime of LED modules is not limiting in case of emergency lighting, because it is considered a lighting period of maximum of 1000 hours in the lifetime of the luminaire.

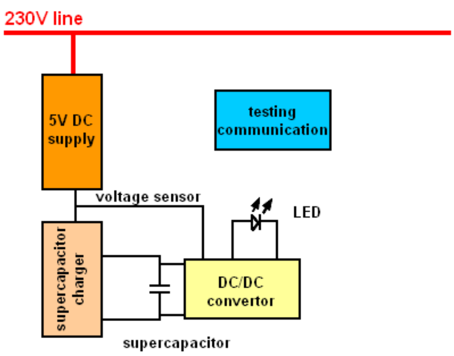

Figure 4 – Block scheme of a supercapacitor powered luminaire

Table 1 – PARAMETERS OF SUPERCAPACITOR MAXWELL BCAP3000

Capacity / Voltage	3000 F / 2,7 V
Production tolerance	-0% up to +20%
Operation temperature	-40°C up to +60°C
Available power	3.04 Wh
Lifetime	1 million cycles
Length / diameter	138 mm /61 mm
Weight	0.51 kg

The design of a power connection and the choice of appropriate circuit converters as well as power supplies for LED are essential for the functionality and efficiency of the whole system. For the circuit it is necessary to use DC / DC converter, because supercapacitor voltage decreases when discharging. When choosing a suitable circuit it is important to monitor the minimal operating voltage of the converter Umin, which will set the amount of usable energy from the capacitor. Used converter must have the highest efficiency possible at the required output current in the range of input voltage.

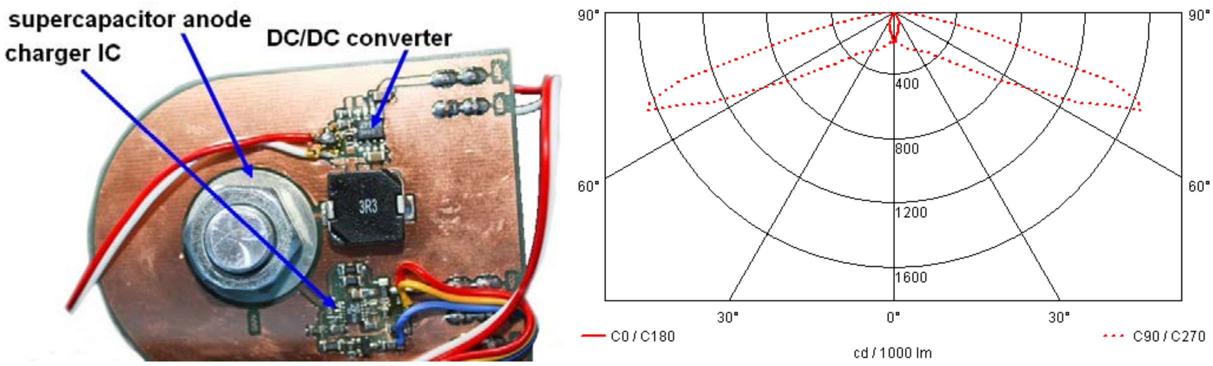

Figure 5 – PCB of prototype of a supercapacitor powered luminaire, luminous intensity distribution curve of prototype for emergency escape roads

To ensure a constant luminous flux coming from LED it is the best if the circuit keeps a constant output current. As it is apparent from the volt-ampere characteristics of the power LED it is necessary to choose the current source, not the voltage source for the power supply. Based on the knowledge of LED module power and used circuit we must decide whether to use one or more supercapacitors. Using multiple supercapacitors leads to increased voltage, therefore to reduction of current flowing through the circuit, and also to the reduction of internal losses. On the contrary, there is a higher price of supercapacitors (even if they are of half capacity) and the need to use a voltage balancer, which will be in charge of balancing the voltage on the capacitors so that there is no exceed working voltage, which could damage the supercapacitor. Based on the survey of the present converter circuits and supercapacitors offer the suitable solution seems to be to use a supercapacitor for 1W LED or more pieces for more efficient light sources. The Fig. 4 shows a block scheme of the designed emergency luminaires.

5 Calculation of a Supercapacitor Capacity

The calculation of a suitable supercapacitor size comes after the circuit and sources design. From the above mentioned the following quantities will be relevant for the calculation:

The minimal operating voltage converters: $U_{\min} = 1V$

The initial voltage of charged supercapacitor: $U_0 = 2.7V$

Permitted voltage loss of the supercapacitor:

$$\Delta U = U_0 - U_{\min} = 2.7 - 1 = 1.7V \tag{13}$$

Supplied constant power: $P = 1W$

Efficiency of DC / DC converter: $\eta = 0.8$

Average current consumption:

$$I_{avg} = \frac{I_{\max} + I_{\min}}{2} = \frac{\frac{1}{1 \cdot 0.8} + \frac{1}{2.7 \cdot 0.8}}{2} = 0.86A \tag{14}$$

Supercapacitor aging factor (capacity decline in 10 years): $k = 0.7$

Required time of luminaire lighting: $t = 3600s$

According to the above mentioned explanation (see equation 11) there will be neglected a component of the voltage loss at the internal resistance (Uesr). Since the current increases almost linearly during discharging, the instantaneous current can be replaced by and average current Iavg and express the required capacity of the supercapacitor:

$$C = \frac{I_{avg} \cdot t}{\Delta U} = \frac{0.86 \cdot 3600}{1.7} = 1821F \tag{15}$$

The following equation takes into account the capacity loss during the projected lifetime of a luminaire (10 years):

$$C_{final} = \frac{C}{k} = \frac{1821}{0.7} = 2602F \tag{16}$$

From the supercapacitors offer there was chosen the closest higher capacity 3000 F. For an example of such a supercapacitor it was chosen the type Maxwell BCAP3000 with the parameters listed in Tab I.

6 Experimental 1W LED Emergency Luminaire with 3000F Supercpacitor

For verification of theoretical calculations, prototype of emergency luminaire with 1W white LED and 3000F supercapacitor Maxwell BCAP 3000F was constructed. There was used integrated DC/DC converter LTC3490, which maintains constant output current for LED, 350 mA. For supercapacitor charging, LTC4425 IC was used.

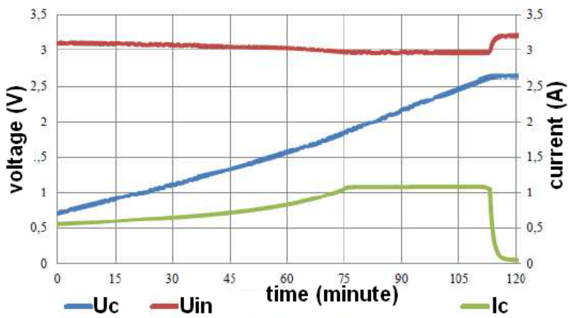

Figure 6 – Charging of 3000F supercapatitor by LTC4425 IC

For testing purposes, charging current of supercapacitor was limited to 1A, IC`s maximum is 3A. Maximum charging current is also automatically limited by IC based on voltage difference between input and output, to prevent overheating.

In this specific case, supercapacitor was charged from 0.7V to full voltage 2.7V in 110 minutes.

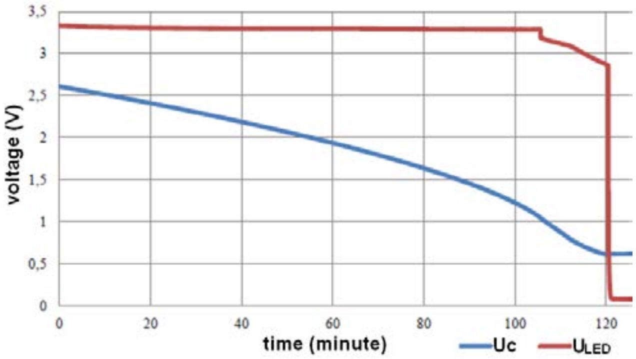

Figure 7 – Voltage course during discharging

In descripted connection 1W white LED of last lighting in nominal values for 106 minutes. Then capacitor voltage was too low for LTC3490 IC and it was not able to keep constant voltage. During discharge phase only voltage sensors were used to avoid influence to ICs and results distortion.

Supercapacitor was discharged from 2.6V to 1V. It was used 85% of accumulated energy, according to formula (3). Because supercapacitor is the most expensive part of luminaire, for practical usage this must be improved to keep competitive ability with battery powered luminaires.

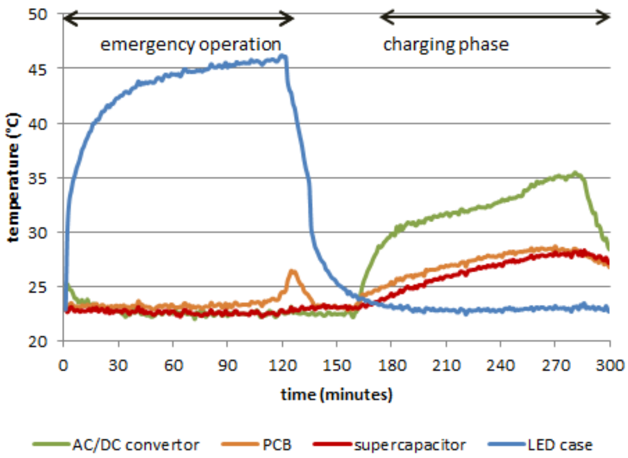

Figure 8 – Results of thermal measurement of prototype

Prototype went through thermal measurement at ambient temperature 23°C. Measurement was realized by wire thermocouples.

At left side of Fig. 7, there is visible higher temperature of LED emergency operation phase. Between 120-135 minute temperature rise of DC/DC convertor temperature rise is significant, which is caused by lowering efficiency and higher input current.

During charging phase, AC/DC 230V/5V converter produced the most of heat. Temperatures of supercapacitor and PCB with soldered ICs have also slightly raised.

Electrical part was connected with optical part, which consisted of reflector and lens designed for emergency escape roads lighting. Therefore optical efficiency was lower, 73%. Nominal luminous flux of luminaire was 91 lm. Because of precise optical distribution, prototype is capable of illuminating 3m height emergency escape road of length up to 13m.

7 Conclusions

From above mentioned it is clear that the supercapacitor is fully usable in practice for supplying the autonomous emergency lighting luminaires equipped with LEDs.

Emergency lights supplied by the supercapacitors will be applicable for:

- emergency escape lights and anti-panic luminaires with a operation period of one hour,
- luminaires with LED light sources and with a good directing of luminous flux,
- autonomous supplying.

The disadvantages of this solution are:

- higher investment cost,
- bigger dimensions of supercapacitor and then the whole luminaire,
- unavailability of higher capacity for longer operation time or for the usage of LED higher power consumption.

With the increasing specific power of LEDs this solution has a great potential for the future.

Acknowledgment

This article was prepared with the support of the project "Usage of LED technology in industrial lighting applications," SP2014/77, by institution of VSB-TU Ostrava.

References

[1] YADAV, A.; KHAIRE, B. 2013. Overview of Supercapacitor. *International Journal*, 2013, 3.6.

[2] EN 50172. 2004 – Emergency escape lighting systems.

[3] EN 1838. 2000: Lighting applications – Emergency lighting.

[4] DUDA, V. 2010 *Využití superkapacitorů v trakčních pohonech*, M.S. thesis, University of Pardubice, Czech republic.

[5] ltracapacitor Technology for Worldwide Energy Storage and Power Delivery Applications [online]. [cit. 2014-01-12]. Available from WWW: <http://ecadigitallibrary.com/pdf/CARTSUSA09/3.0.pdf>.

[6] SKODA, J., BAXANT, P., KRBAL, M., SUMEC, S., PAVELKA, T. 2013. Photometry of LED sources, *Przeglad Elektrotechniczny*, 89 (6), pp. 341-344, ISSN: 00332097.

[7] GASPAROVSKY, D; SMOLA, A; MACHA, M; JANIGA, P. 2012. New Approach to Determination of Luminaire Maintenance Factor Curves for various Conditions. *LIGHT & ENGINEERING 2012*, vol: 20, Issue: 2, pp. 17-26, ISSN: 0236-2945.

[8] Materials from Maxwel company [online]. [cit. 2014-01-12]. Available from WWW: <http://www.maxwell.com/products/ultracapacitors/product.aspx?PID=D-CELL-SERIES>.

PP25

DAYLIGHT DESIGN PERFORMANCE BY USING HONG KONG REPRESENTATIVE SKIES

Ho, J.C.K.[1], Ng, E.[2], Chan, P.W.[3]
[1]Institute of Environment, Energy and Sustainability, The Chinese University of Hong Kong, Hong Kong SAR, CHINA
[2]School of Architecture, The Chinese University of Hong Kong, Hong Kong SAR, CHINA
[3] Hong Kong Observatory, Hong Kong SAR, CHINA
justinckho@gmail.com

Abstract

This study compares the daylight design performance by using Hong Kong Representative Skies (HKRS) to Perez All-Weather Sky Model. Based on the evaluation of sensitivity of Vertical Sky Component, it is demonstrated that the HKRS could give better results comparing with Perez all-weather sky model. A reduction in error of approximately 9 –25% could be expected, depending on the orientation of a surface.

Keywords: Hong Kong Representative Skies, Perez All-Weather Sky Model, Vertical Sky Component

1 Introduction

During the last decade, detailed measurements of daylight availability have been made throughout the world. Hong Kong participated fully in this programme. A task now is to reduce the data into information and guidelines for practical use. A better use of daylight is a crucial factor in sustainable design. The Commission Internationale de l'Eclairage (CIE) publishes an international standard method for classifying sky brightness patterns(CIE, 2003). It is known as the CIE General Sky, and its purpose is not only to provide an agreed method of analysing measured data but to make possible international comparison of daylight climates. This is a key aim both in daylighting research and in practical applications(He and Ng, 2012; Wittkopf, 2007).

Ng et al.(2007a) established the “Hong Kong Representative Sky” (HKRS) based on the CIE General Sky type definitions. The subset consists of three sky types, namely this includes CIE General Sky type 1, 8 and 13, representing overcast, partly cloudy and clear sky, respectively. The HKRS suggests that the daylight climate could be characterized by a small subset of standard types without significant loss of accuracy and provides a better basis for estimating vertical sky component (VSC) as compared to the CIE Overcast Sky model(Ng et al., 2007a). To obtain a better estimate of VSC , Ng et al. (Ng et al., 2007b) developed a method to predict daylight availability dynamically based on forecasts of weather observatory for Hong Kong(Ng et al., 2007b). This study aimed to assess the daylight design performance in terms of VSC by comparing Hong Kong Representative Skies (HKRS) to Perez All-Weather Sky Model.

2 Data

For HKRS, sky data with 10-min intervals were collected from the International Daylight Monitoring Programme (IDMP) research class station in The Chinese University of Hong Kong (22˚25´N, 114˚12´E). The sky luminance distribution data were measured with an EKO sky scanner (MS-321LR). This study included the sky luminance scan data collected from June 2003 to May 2005, but excluded the period during September 2003 to October 2003, and 15 November 2004 to December 2004 due to instrument malfunction. The sky scanner measures the luminance of 145 points of the sky dome(Tregenza, 1987), rejecting any over 50 kcd/m2. After quality control, all the sky luminance scans were fitted to the CIE standard general sky based on Tregenza’s method (Tregenza, 2004) by our previous work (Ng et al., 2007a).

3 Sensitivity of Vertical Sky Component

3.1 Hong Kong Representative Skies

The CIE standard general sky defines a set of luminance distributions, ranging from the heavily overcast sky to the cloudless clear sky including the previously recommended CIE standard overcast sky and CIE standard clear sky (CIE, 2003). The 15 standard general skies include five clear, five partly cloudy and five overcast sky types (Table 1).

Table 1 – CIE General Sky Type description (CIE, 2003)

Type	Luminance Distribution
1	CIE Standard Overcast Sky, Steep luminance gradation towards zenith, azimuthal uniformity
2	Overcast, with steep luminance gradation and slight brightening towards the sun
3	Overcast, moderately graded with azimuthal uniformity
4	Overcast, moderately graded and slight brightening towards the sun
5	Sky of uniform luminance
6	Partly cloudy sky, no gradation towards zenith, slight brightening towards the sun
7	Partly cloudy sky, no gradation towards zenith, brighter circumsolar region
8	Partly cloudy sky, no gradation towards zenith, distinct solar corona
9	Partly cloudy, with the obscured sun
10	Partly cloudy, with brighter circumsolar region
11	White-blue sky with distinct solar corona
12	CIE Standard Clear Sky, low luminance turbidity
13	CIE Standard Clear Sky, polluted atmosphere
14	Cloudless turbid sky with broad solar corona
15	White-blue turbid sky with broad solar corona

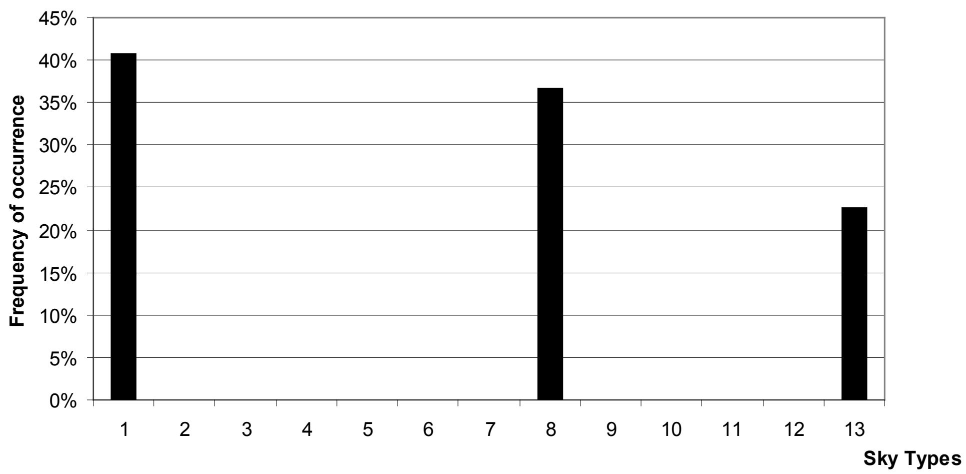

Figure 1 – Frequency distribution of three Hong Kong Representative Skies

Our previous study proposed three standard skies (sky type 1, 8 and 13) as Hong Kong Representative Skies for Hong Kong, representing the overcast, partly cloudy and clear sky, respectively (Ng et al., 2007a). The HKRS suggests that the daylight climate could be characterized by a small subset of standard types without significant loss of accuracy and provides a better basis for estimating vertical sky component (VSC) as compared to the CIE Overcast Sky model. Figure 1 shows the frequency distribution of the subsets of three Hong Kong Representative Skies.

3.2 Calculating VSC

Perez all-weather sky model (Perez et al., 1993) currently is the most widely used sky model for dynamic annual daylight simulations(Reinhart et al., 2006; Walkenhorst et al., 2002). This section exams the influence of HKRS on estimating Vertical Sky Component (VSC) comparing to Perez all-weather sky model. For the purpose of simplicity, the estimation regarding VSC refers to unobstructed windows facing four cardinal directions. Vertical Sky Component (VSC) is the measure of sky light incident on a vertical plane and is a good indication of potential good daylighting. VSC is defined as the ratio of the vertical diffuse illuminance (E_v) at a point (usually center of a window) to the unobstructed horizontal diffuse illuminance available (E_h) at the same point on a horizontal plane:

$$VSC = \frac{E_v}{E_h} \tag{1}$$

Step 1: Calculating the vertical illuminance (E_v)

For an unobstructed window surface, the amount of daylight is mainly determined by luminance from the sky. Furthermore, the area of sky visible through a window has the most significant influence on the internal light. The total diffuse illuminance on a point on a surface is by adding the contribution of the illuminance (ΔE_{vp}) from each small patch of sky (Tregenza and Waters, 1983):

$$E_v = \sum_{p=1}^{145} \Delta E_{vp} \tag{2}$$

where,

$$\Delta E_{vp} = D_p L_p \Delta S_p$$

where,

L_p is the luminance of the sky patch at altitude α_p and azimuth φ_p;

ΔS_p is the angular size of the sky patch;

D_p is the daylight coefficient which in this case (an unobstructed window) depends only the geometry of the window. D_p for an unobstructed vertical surface facing azimuth φ_v is given by:

$$D_p = \begin{cases} \cos\alpha_p \cos(\varphi_p - \varphi_v) & When\ 0 \le \alpha_p \le \frac{\pi}{2}, \quad -\frac{\pi}{2} \le \varphi_p - \varphi_v \le \frac{\pi}{2} \\ 0 & otherwise \end{cases} \tag{3}$$

Step 2: Calculating the horizontal illuminance (E_h)

The calculation of horizontal illuminance is based on the method outlined in Tregenza (Tregenza, 2004). The horizontal illuminance from patch p is given by:

$$E_{hp} = \frac{\pi L_p}{n_p} \left(sin^2\left(\frac{b_p \pi}{15}\right) - sin^2\left(\frac{(b_p - 1)\pi}{15}\right) \right) \qquad \text{when } 1 \le b_p \le 7 \tag{4}$$

and

$$E_{hp} = \pi L_p \left(1 - sin^2\left(\frac{7\pi}{15}\right)\right) \qquad when\ b_p = 8 \tag{5}$$

where b_p is the band containing patch p; n_p is the number of patches in band b_p; L_p is the luminance of a sky patch.

The total horizontal illuminance is given by:

$$E_h = \frac{S_d}{2\pi} \sum_p E_{hp} \tag{6}$$

where

$$S_d = \sum_p \left(sin\left(\frac{b_p\pi}{15}\right) - sin\left(\frac{(b_p - 1)\pi}{15}\right)\right)\left(\frac{2\pi}{n_p}\right) \tag{7}$$

Table 2 – Error analysis based on the HKRS and Perez all-weather sky model

		East	West	North	South
HKRS	RMSE	0.0902	0.0803	0.0730	0.0685
	RMSE %	24	24	21	19
Perez all-weather sky	RMSE	0.1170	0.1102	0.0773	0.0813
	RMSE %	31	32	23	23
Reduction in Error (%)		23	25	9	17

4 Results and conclusions

Table 2 shows the error observed in the four cardinal directions when VSC is estimated using the HKRS and Perez all-weather sky model against the observed VSC. The results show that the HKRS could give better results comparing with Perez all-weather sky model. A reduction in error of approximately 9 –25% could be expected, depending on the orientation of a surface. The hourly HKRS can be used to assess the annual daylight performance of buildings in high-density Hong Kong to provide the “real” daylight performance during a whole year.

5 Acknowledgements

The work described in this paper was fully supported by a grant from the Research Grants Council of the Hong Kong Special Administrative Region, China. (Project no. CUHK 415711).

References

CIE 2003. Spatial Distribution of Daylight - CIE Standard General Sky. Standard CIE S 011/E:2003.

HE, J.Z., NG, E. 2012. Predicting sky types and zenith luminance from the cloud index derived from geostationary satellite data. Light. Res. Technol. 44, 139–148.

NG, E., CHENG, V., GADI, A., MU, J., LEE, M., GADI, A. 2007a. Defining standard skies for Hong Kong. Build. Environ. 42, 866–876.

NG, E., GADI, A., WONG, F., MU, J., GADI, A., LEE, M. 2007b. Predicting daylight availability dynamically based on forecasts of a weather observatory. Light. Res. Technol. 39, 69–80.

PEREZ, R., SEALS, R., MICHALSKY, J. 1993. All-weather model for sky luminance distribution–Preliminary configuration and validation. Sol. Energy 50, 235–245.

REINHART, C.F., MARDALJEVIC, J., ROGERS, Z. 2006. Dynamic daylight performance metrics for sustainable building design. Leukos 3, 7–31.

TREGENZA, P.R. 1987. Subdivision of the sky hemisphere for luminance measurements. Light. Res. Technol. 19, 13–14.

TREGENZA, P.R. 2004. Analysing sky luminance scans to obtain frequency distributions of CIE Standard General Skies. Int. J. Light. Res. Technol. 36, 271–281.

TREGENZA, P.R., WATERS, I.M. 1983. Daylight coefficients. Light. Res. Technol. 15, 65–71.

WALKENHORST, O., LUTHER, J., REINHART, C., TIMMER, J. 2002. Dynamic annual daylight simulations based on one-hour and one-minute means of irradiance data. Sol. Energy 72, 385–395.

WITTKOPF, S.K. 2007. Daylight performance of anidolic ceiling under different sky conditions. Sol. Energy 81, 151–161.

PP28

OUTDOOR MEASUREMENT ON LUMINOUS EFFICACY OF WINDOW

Daisuke Ito[1]
[1] Institute of Technologists, Saitama, JAPAN
ito@iot.ac.jp

Abstract

Heat flows around windows are largely affected by solar radiation. Thus, the control of sun radiation through window is very important. Several kinds of glass for controlling and distributing sunlight and daylight and reducing the air conditioning load have been developed (Ito et al 2010). For measuring luminous efficacy of window, a simplified method was proposed. The purpose of this study is to propose a simplified measurement method for luminous efficacy of window. The applicability of the method was tested with a low emissivity glass, and a double glass. The measurements were conducted in Saitama on sunny days. The reliability of this method was checked in natural condition. This method is helpful to choose a glass for a window.

Keywords: Luminous Efficacy of Window, Glass for Window

1 Introduction

Heat flows around windows are largely affected by solar radiation. Thus, the control of sun radiation through window is very important. On the other hand, the requirement of daylight for indoor lighting have been increasing as one of the effective strategies for energy conservation today. Several kinds of glass for controlling and distributing sunlight and daylight and reducing the air conditioning load have been developed. For measuring luminous efficacy of window, a simplified method was proposed. Special apparatuses were used to measure those optical properties. The apparatuses were possibly too complex, for the precision required in practical use. The purpose of this study is to propose a simplified measurement method for luminous efficacy of window.

2 Measurement method

2.1 Measurement boxes

This method needs simple apparatus complexes to measure luminous efficacy of window. The integrating sphere was used for measuring visible transmittance of window. The measurement box with room air conditioner was used for measuring solar heat gain coefficient. Figure 1 shows measurement boxes. The left box is the measurement box with room air conditioner and the center box is integrating sphere for measurement of visible transmittance , while the right one is integrating sphere for calibration.

2.2 Measurement condition

The low emissivity glass which has a microscopically thin, transparent coating reflecting long-wave infrared energy is compared with double pane glass. The measurements were conducted in Saitama (139.5 degrees in longitude, 36.1 degrees in latitude) on sunny days (7th and 19th December 2012). When luminous efficacy of window was measured, a window facing south was used for the case with sunlight.

2.3 Measurement items

Table 1 shows measurement items. The global illuminance, the outside vertical illuminance on the outside window surface and the integrating sphere illuminance are measured by illuminance maters (Konica Minolta, T-10). The global solar radiation and the vertical solar radiation on the outside window surface are measured by pyrometers (EKO, MS-402). The air temperature and surface temperature are measured by thermo couples. The electric power for air conditioning system is measured by wattmeter.

Figure 1 – Measurement boxes

Table 1 – Measurement items

Measurement item	Device for measuring
Outside air temperature Inside air temperature Surface temperature Water temperature for air conditioning system	Thermo couple
Global illuminance Outside vertical illuminance Integrating sphere illuminance	Illuminance maters (Konica minolta, T-10)
Global solar radiation Vertical solar radiation	Pyrometers (Eko, MS-402)
Electric power for air conditioning system	Wattmeter
Volume of flow	Flow meter

3 Results

3.1 Global illuminance and global solar radiation

Figure 2 shows results of global illuminance and global solar radiation. During the measurement for the south facing window with direct sunlight, vertical illuminance on the outside window surface ranged from 29000 to 94000 lx, global illuminance ranged from 20000 to 60000 lx, vertical solar radiation on the outside window surface ranged from 387 to 900 W/m^2,and global solar radiation ranged from 170 to 540 W/m^2.

3.2 Luminous efficacy of window

Luminous efficacy of window is calculated as follows.

$\eta w=(\eta d*\tau g)/Hg$

ηw: luminous efficacy of window
ηd: luminous efficacy of daylight
τg: visible Transmittance
Hg: solar heat gain coefficient (ISO 2003)

Figure 3 shows results of the luminous efficacy of low emissivity glass and double-pane glass. The average luminous efficacy of the low emissivity glass was 170 lm/W and that of the double-pane glass was120 lm/W respectively.

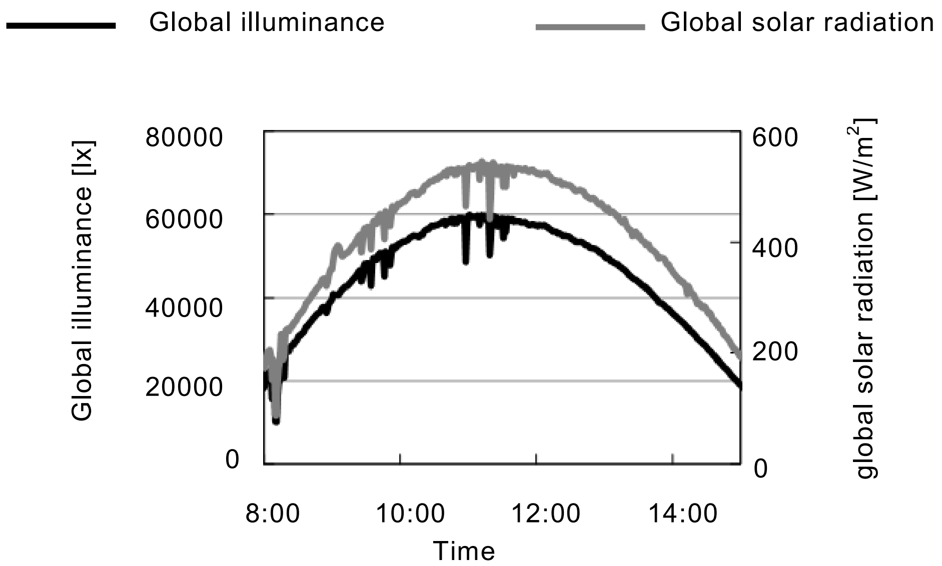

Figure 2 – Luminous efficacy of low emissivity glass and double-pane glass

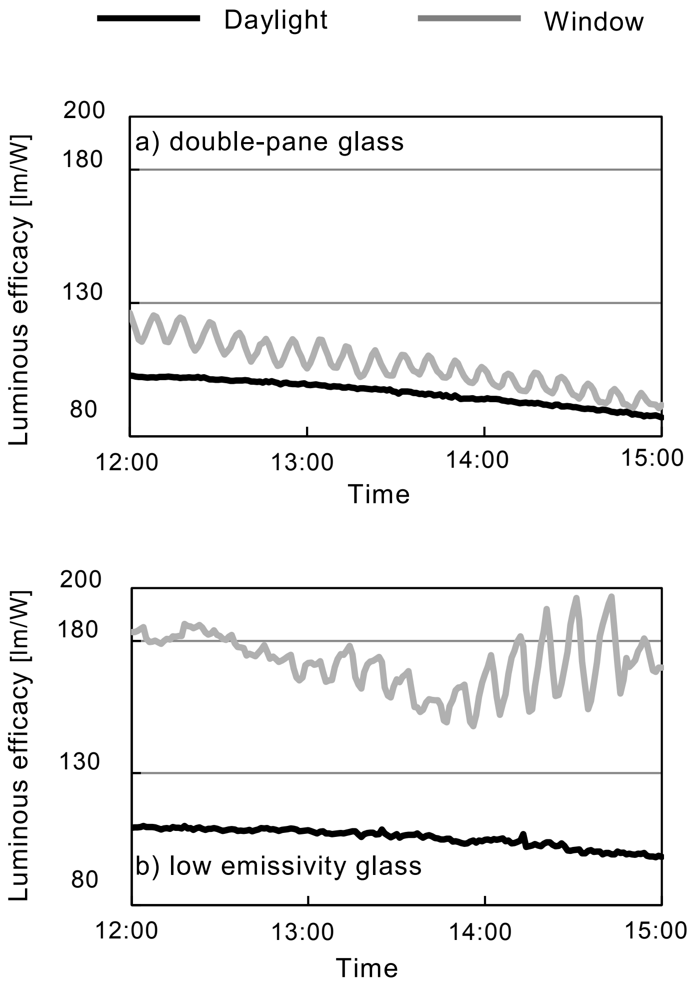

Figure 3 – Luminous efficacy of low emissivity glass and double-pane glass

4 Conclusions

Using this method, the luminous efficacy of window was measured. The applicability of the method was tested with a low emissivity glass, and a double glass. Also the reliability of this method was checked in natural condition. It was considered this simplified method produces results within acceptable engineering accuracy in many cases.

A suitable glass for a window is chosen depending on the desired amount of glare, outside view and the air conditioning load affected by the usage of the room. Thus this method is helpful to choose a glass for a window.

References

ITO, D., TAKEDA, H., ASHIE, Y. and HUJIMOTO, T. 2010: Survey on optical and thermal property of solar shading technique for existing window and numerical simulation on load reduction effect in air-conditioning system, Aij Journal of Technology and Design, pp. 185-190, vol. 16, no. 32

ISO 2003. ISO 15099-2003: Windows and door – Thermal transmission properties-Detailed calculations: ISO.

PP29

THE COMPOSE OF REFERENCE SKY MODEL SUPERIMPOSED ON THREE TYPICAL SKY COMPONENT

Bian Yu*[12] MaYuan[3] Yu Daxing[1] Gao Fei[1]

1. School of Architecture, South China University of Technology (SCUT), Guangzhou, Guangdong, CHINA, aryubian@163.com;
2. State Key Laboratory of Subtropical Building Science, SCUT, Guangzhou 501641, Guangdong, CHINA;
3. College of Architecture & Urban Planning, Guangdong University of Technology, Guangzhou, Guangdong, CHINA, mayuan0714@163.com

Abstract

This work try to define the reference sky model of southern China: using a fisheye lens digital camera to capture sky images continuously in year-long term, and develop program to obtain sky luminance distribution data from images, the statistical processing will define three most occurrence standard model as typical sky model, and the linear component of which superimposed the reference sky model.

Keywords: reference sky model; typical sky; fish-eye lens camera

1 Introduction

Design for day-lighting is of growing concerns. In the lack of definite reference of sky conditions, lots of the day lighting simulation is based on CIE Overcast sky, which does not truly represent the sky conditions. This research is mainly focus on the sky pattern of subtropical area in China, and Guangzhou is the central city of Southern China, which is in the subtropical area with highly luminous climates. This topic is based on the scanned sky pattern data of Guangzhou and proposed an assumption that a sky model superimposed by three standard sky model components which could approximately fit the average real sky luminance distribution, and this structure will benefit to establish a simpler dynamic day-lighting simulation progress.

2 CIE standard sky model

The luminance pattern of the sky depends on location, weather, climate, and it changes during the day and with the position of the sun. CIE proposed 15 standard General Sky luminance distributions at 2003 (CIE Standard CIE S011/E:2003), which model the sky under a wide range of conditions, from heavily overcast sky to cloudless clear sky.

Examination shows that the standard set of luminance distributions gives a good overall framework for categorizing actual skies, include the subtropical area with highly luminous climate.

15 sky patterns are too much to apply in day lighting simulation progress, and some patterns are seldom present in selected area. Find out 3 most occurrence sky patterns and set them as the standard sky patterns in this area is the basic work to establish a more accurate sky pattern.

* Corresponding Author Name: Bian Yu
Affiliation: School of Architecture, South China University of Technology
e-mail: aryubian@163.com

3 Southern china representative sky

3.1 Method

To achieve the sky luminance, fish-eye lens digital camera was used, and it is an adequate method which would adopted in research program without sky-scanner.

Fig.1. Test Devices: Fisheye Lens Digital Camera and luminance Meter

The instrument used in this program, as shown in Fig.1, consists of a Fish-eye lens digital camera, PC, a luminance meter, horizontal illuminance data measurement, water-proof mask (not shown in Fig). The fish-eye lens towards the Zenith and the upper side of viewfinder towards North, the camera was set to record sky image every 10 min in fixed position and the images store in PC, meanwhile an illuminance meter measure the horizontal illuminance data every 10min. This measurement start at Dec. 8th, 2012, and captured more than 30,000 sky images (include night time), only few time was interrupted because the storm weather and instrument errors.

The sky scan work in Guangzhou is in process, the research instruments are set in the roof of research building of state key lab of subtropical building science, South China University of Technology, Guangzhou. (Latitude: 23.2N; Longitude: 113.3E)

3.2 Define the Typical Sky Types

Define the 3 typical sky types are mainly based on the frequency of occurrence, after more than one year sky scan work, the observed sky luminance measurements will show 3 most occurrence sky types, and which will define as the typical sky types in the whole year.

Sky images were processing to 500*500 pixel square images. The research team developed a computer program that extracts the luminance data (relative value) from 145 sections in the digital photos. The value got from the image section was transferred to luminance of sky element (relative value) by the position angle (ω).

The scanned image will transfer to sky luminance map through the computer process, as shown in fig.2, and then the observed luminance values will compare with each CIE standard sky type in 145 sections. The minimum RMS error over the whole sky will select to be the fit standard sky type.

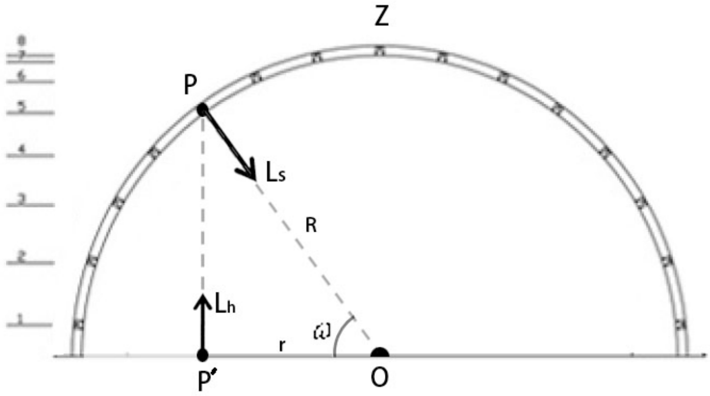

Fig.2. liner relation of luminance between sky element and corresponding image unit

As it is seen in the fig.2, the relation between the luminance of sky element P to the centre and the horizontal luminance of its horizontal projection element P' conforms to the formula (1). This research measures luminance of 145 points of sky and divide to eight levels. Therefore, the angle (ω) and the eight overall values are known.

$$L_s = \frac{L_h}{\sin \omega} \quad (1)$$

Through this research, it is found that the logarithm of the sky luminance within a certain threshold and the image grayscale logarithm are with linear relation and which also associated with different devices and shooting parameters. In this research, the choosing shooting parameter is (f8.0, shutter 1/2000, ISO100) which has been demonstrated so as to guarantee the liner relation of the shy luminance and gradation of image. The data of the paper are all relative values of shy luminance. Therefore, the analysis of the levels of gradation of the graphic images can help get relative values. Just like the fig.3 indicates, after acquisition of image, they have been processed and transformed to a sky luminance distribution.

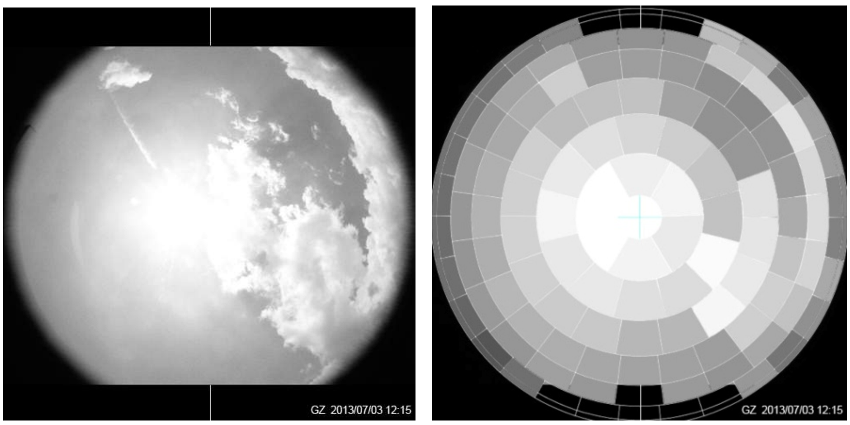

Fig.3. Sky Photo (left) and corresponding luminance map (right)

The CIE Standard General Sky defines a set of luminance distributions, which model the sky under a wide range of conditions. The relative RMS error where a particular sky was the best-fit in comparison to the base case where the complete sets of 15 standard skies were used, therefore, CIE characterizes three standard sky types, namely Typical Sky Model 1, 2, 3.

3.3 Real sky type based on 3 most occurrence sky types

The real sky type is superimposed on the linear component of the standard sky type, and the factor "K" is define as the frequency of occurrence during the 3 standard sky types. Fig.4 shows the Real sky type in China subtropical area is superimposed on the linear component of 3 standard sky types, and Linear factor "K" is define as below.

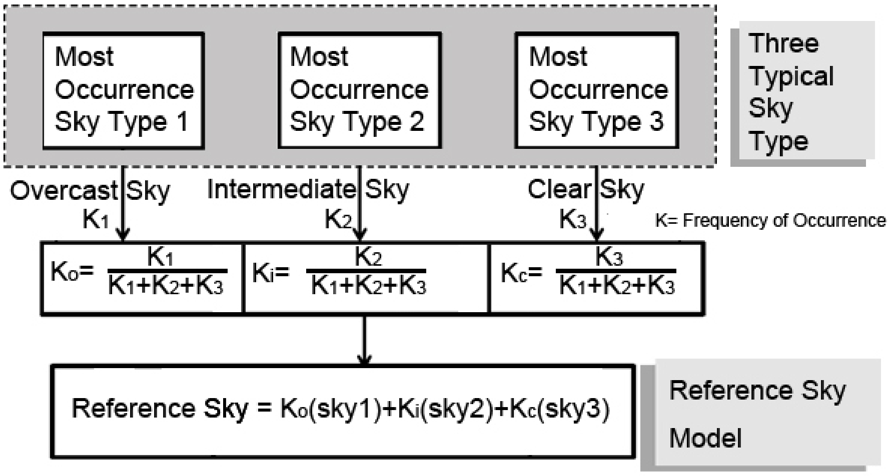

Fig.4. Real sky type of china subtropical area

$$CSRS = Ko(Sky1) + Ki(Sky2) + Kc(Sky3) \tag{1}$$

$$K_o = \frac{K_1}{K_1 + K_2 + K_3} \tag{2}$$

$$K_i = \frac{K_2}{K_1 + K_2 + K_3} \tag{3}$$

$$K_c = \frac{K_3}{K_1 + K_2 + K_3} \tag{4}$$

K1: the frequency of occurrence of Sky type1 during the whole year.
K2: the frequency of occurrence of Sky type2 during the whole year.
K3: the frequency of occurrence of Sky type3 during the whole year.

Ko, Ki, K: the linear factor of standard sky type.

4 Data Analysis

This research has been started from Dec. 8th, 2012, until now, more than 30000 images have been collected, including night light. The research is mainly in spring and autumn days of China subtropical area, starting from March 20th, 2013 to September 23rd, 2013 (excluding the night light images), and obtains 10736 valid images. Among them, 5331 images from March 20th to June 21st and 5405 images during the following days until September 23rd. After processing all these images, some data can be figured out as following:

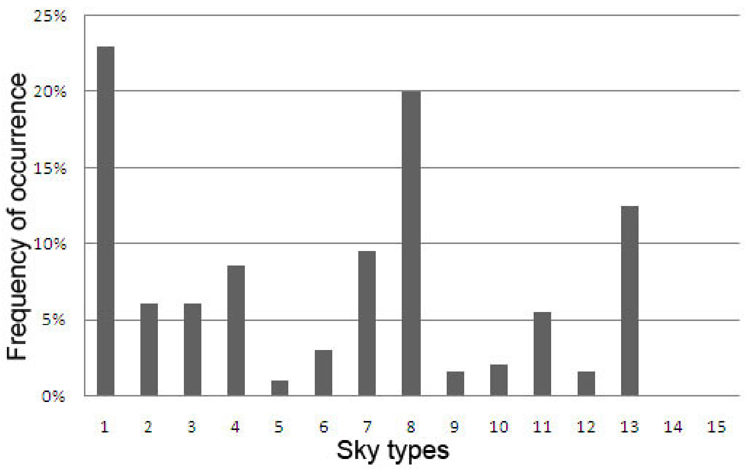

Fig.5. occurrence frequency of sky type during research time

Based on the analysis on sky luminance of China subtropical area in spring and summer, fig 5 shows the occurrence frequency of 15 standard sky models. In the fig.5, the sky type one, eight and thirteen are with high occurrence frequency, respectively 23%, 20% and 13%. So according to such result, these three sky types are defined as three standard sky models.

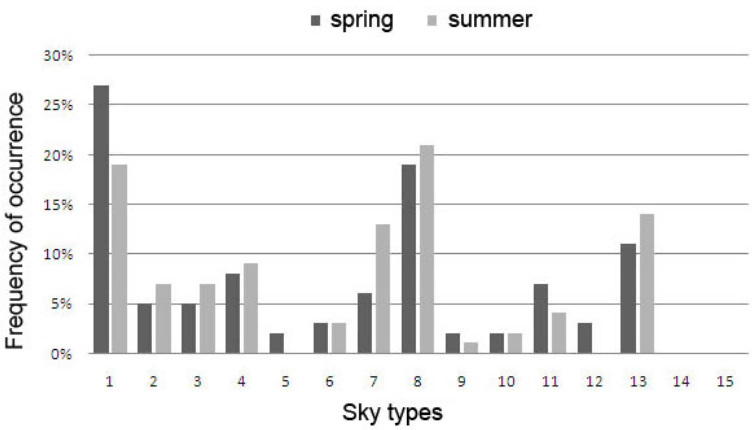

Fig.6. occurrence frequency of sky type respectively in spring and summer time

Dividing the testing data to two groups of spring and summer sky types, that comes like fig.6. And fig.6 also shows that the occurrence of sky type one, eight and thirteen are still the top three types, respectively 27%, 19% and 11% in spring and 19%, 21% and 14%. According to the above statistics, Ko, Ki and Kc are easily figured out as follow:

Chart.1. the frequency of occurrence of sky type Ko 、Ki、Kc

Time frame	Sky type	K value
First half year	1	0.41
	8	0.36
	13	0.23
	1	0.47
springtime	8	0.33
	13	0.20
	1	0.35
summertime	8	0.39
	13	0.26

In conclusion, the CSRS which represented by Guangzhou's is as follow:

Spring CSRS=0.47(sky 1) +0.33(sky8) +0.20(sky13)
Summer CSRS=0.35(sky 1) +0.39(sky8) +0.26(sky13)

CIE puts forward 15 types of sky luminance models and the sky type 1, 8 and 13 are the typical ones.

5 Data Analysis

Using a fisheye lens digital camera capture sky images continuously in year-long term, the reference sky models during spring and summer time of China southern areas represented by Guangzhou are as below:

Spring CSRS=0.47(sky 1) +0.33(sky8) +0.20(sky13)
Summer CSRS=0.35(sky 1) +0.39(sky8) +0.26(sky13)

The research program is in processing, and the sky model superimposed on three standard sky types will help to improve the assistant design and day light analysis tool which implicated in China subtropical area, and provide a more accurate result of day lighting simulation.

By far, the research is still in progress, after attaining all the data of sky luminance of the whole year round, further study on reference sky model could be carried out. And furthermore, reference models that reflect the average sky luminance value of each season, each month and each hour, which will definitely be fit for set up a dynamic model collection of a year-long term. The sky models are with limited quantity, but they provide a more accurate result of day lighting simulation in a year-long term, which also provide basic statistics and theoretical support for studying dynamic lighting analysis simulation technology.

Acknowledgements

The work was supported by National Nature Science Foundation of China (Project No: 51208205) & State key laboratory of subtropical building science (Project No: 2013ZC17 & 2011KB279)

References

[1]. CIE Standard (CIE S011/E:2003) Spatial distribution of daylight----CIE Standard general sky, CIE Vienna, 2003.

[2]. Edward Ng, Vicky Cheng, Defining standard skies for Hong Kong, Building and Environment, 42 (2007), P866–876.

[3]. Trengenza PR. Analysing sky luminance scans to obtain frequency distributions of CIE standard General Skies. Lighting Research and Technology 2004:36(4):271-81.

[4]. Christoph F. Reinhart, Sebastian Herkel, The simulation of annual daylight illuminance distributions, Energy and Buildings, Volume 32, Issue 2, July 2000, Pages 167–187.

[5]. He J, Edward Ng, Using Satellite-Based Methods to Predict Daylight Illuminance for Subtropical Hong Kong, Lighting Research and Technology, CIBSE, United Kingdom, 2010:42(2), P135-148.

[6]. J. Mardaljevic. Climate Based Daylight Analysis[J]. CIE Division 3, October 2008.

[7]. J.L. Torres, M.de Blas, Sky luminance distribution in Pamplona (Spain) during the summer period, Journal of Atmospheric and Solar-Terrestrial Physics,72 (2010) 382-388.

[8]. 沈天行,张九红. 利用图像数字化处理研究标准全云天空下采光系数[J] . 照明工程学报, 2006, 17 (2) :28- 32.

[9]. 何荥,翁季 等.用鱼眼镜头数码相机测试天空亮度分布[J].重庆大学学报’2010’33(7):129-134.

PP30

LIGHTING DESIGN FOR MITIGATING VEILING REFLECTION IN INDOOR SWIMMING POOL

Chan, T.K.C.[1], Tsang E.K.W.[1],
[1] Parsons Brinckerhoff (Asia) Ltd., Hong Kong SAR, People Republic of CHINA
chan.thomas@pbworld.com

Abstract

Swimming pool is one of the most important recreational facilities among different sport activities in Hong Kong. Recently, it has occasionally been reported that veiling reflection in swimming pool might affect or delay the lifeguard in life rescue. A comprehensive study was hence initiated by relevant local government departments. After a systematic review on local and overseas design practices and related standards, it is found that only a small number of documents provide useful information on the issue of veiling reflection. Furthermore, this information is descriptive and provides general principles only. Designers might need lot of validation studies like conducting simulations and a deep understanding on the water behaviours during design process. It has become a major hurdle for most of the building professionals in reducing the occurrence of veiling reflection within an indoor swimming pool. It is found that the major techniques in reducing veiling reflection are controlling the angle of incidence of light, relative location between lifeguards and light sources and the intensity and distribution of light. This paper outlines the key findings on veiling reflection through a series of literature review, site visit, parametric analysis and engagement process. A design guideline was developed based on the findings and the key principles adopted in this guideline are discussed.

Keywords: Swimming Pool, Veiling Reflection, Glare, RADIANCE, Design Guidelines

1 Introduction

Swimming is one of the most favourable sport activities in Hong Kong. According to the Census and Statistics Department (2011), swimming was ranked as the fourth most favourable sport. Swimming pools were ranked as second when considering sport facilities most often used in the vicinity of home. More importantly, about 13.5% of Hong Kong citizens consider that among all city sport facilities, swimming pools are the most insufficient. Today, many swimming pools are currently being designed and constructed. To cope with the sustainable development and local green building practices, natural ventilation and daylighting design features have become two of the major design considerations in swimming pool development.

Safety of swimming pool is of the prime concern for the general public. According to the World Health Organization (WHO, 2004), drowning is the third largest type of unintended death causing 382,000 fatal accidents globally. In Hong Kong, there are 36 drowning cases per annum and 7% of them occurred in swimming pools (Centre for Health Protection, 2012).

During the implementation of green building design strategy, one of the induced problems for these environmentally-friendly designs is the problem of veiling reflection. Veiling reflection reduces the visibility of those looking at the pool above it. In effect, lifeguards are rendered unable to see swimmers underneath the water surface. This kind of reflection is caused by a higher luminance of reflected light from the water surface compared with the pool basin. According to WHO (2006), poor water visibility is one of the causes for drowning. It makes objects underneath the water surface difficult to see or even invisible. One of the potential risks of veiling reflection is reducing the visibility of lifeguards and hence delaying the time for life rescue. Existing indices such as unified glare rating and daylight glare index are used for artificial and natural lighting, respectively. However, these kinds of performance indices are not applicable to handle veiling reflection in swimming pool. In view of life safety, the Architectural Services Department (ArchSD) and Leisure and Cultural Services Department (LCSD) decided to develop a design guideline to alleviate the problem of veiling reflection in swimming pools.

Chan et al. (2013) described the approach of using simulation technique in the study of veiling reflection in indoor swimming pool for different daylighting design. And in another study, Chan and Tsang (2013) reviewed the implications of major design parameters in lighting design on the visual environment of indoor swimming pool. In this paper, the major physical phenomena, major influential factors and the design solutions were discussed.

2 Study approaches

The research study is aimed to include the views from different stakeholders with building professional and academia. It includes a survey on existing literature, and review current design and performance of indoor swimming pool, numerical analysis to study the impact of different design parameters and consulting the stakeholder for their opinions and views. The flow of the study is shown in Figure 1.

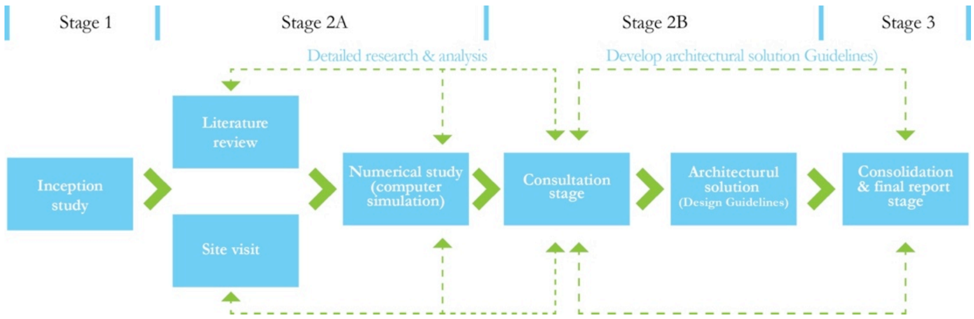

Figure 1 – Study approach

2.1 Literature review

There are in total 17 literatures being studied and classified into five categories based on their purposes and coverage. They are discussed below:

a) Licensing and legislative requirement

This type of standard relates to statutory or licensing purposes. These standards are focused on basic facilities provisions especially relating to safety and hygiene purposes without addressing major technical consideration on neither controlling reflection nor lighting design. The Hong Kong Special Administrative Region Government (1961), and the Food and Environmental hygiene department (n.d.) are classified into this category.

b) Professional design guidelines

Some professional bodies like ArchSD (2009), FINA (n.d.) and Society of Light and Lighting (2009) have issued a few design guidelines. These guidelines are widely adopted by professional and are considered as easy to use. However, these design references are not written specifically for the natural or artificial lighting system of swimming pool. Instead, they usually provide general considerations that allow the designers to complete the study with ease.

c) Filming and broadcasting requirement

Broadcasting in sport venue is not uncommon. The lighting environment for swimming pools with broadcasting purpose has higher requirements than that of normal leisure pools. The vertical illuminance and uniformity are additional criteria for artificial lighting design for sport venue designed for broadcasting. The CIE (1989), CIE (2005) and Ministry of Construction (2007) belong to this category.

d) Comprehensive design guidelines

Sometimes more in-depth design guidelines like Standards Australia (2007), CIE (1984), Illuminating Engineering Society of North America (2001), Sport England (2011) and Chartered Institution of Building Services Engineers (1990) are written specifically for designing swimming pools or sport venues. Descriptions on special considerations on materials and treatment of different objects within the venue like water in swimming pool are also introduced. The influences of the built environment to the players can also be found in these standards.

e) Operation guidelines

Operation guidelines are not written based on technical considerations for architects and building designers. It is focused on the view of swimming pool staffs and actual operation of swimming pool. They also provide suggestions for operation to handle undesirable swimming pool lighting environment. In this study, LCSD (2011), Health and Safety Executive (2003), Irish Water Society (2010) and Lifesaving Society (2012) were reviewed.

2.2 Site visit

Eight indoor swimming pools were visited. Four of them are under the management of the LCSD and designed or supervised by the ArchSD. These four newly built swimming pools can reflect the current design practices of the industry.

Other two local swimming pools which were constructed by a private developer and a sport institution respectively were visited. The design practices of these swimming pools are different from those in public sector. For example, the private swimming pool has great concerns on ceiling height and luxury design. The institutional indoor swimming pool is designed according to the requirements of the FINA which provides a high level of functionality compared with the leisure pools. Their design concepts are different from public sector and are worth for studying.

Two swimming pools outside Hong Kong were also visited and studied. These two swimming pools are located in Shenzhen and Macau which are closed to Hong Kong. They were originally constructed for holding international competitions. After the games, these two overseas swimming pools were revamped and opened for public access. It is believed that these two overseas swimming pools enjoyed the same climate as Hong Kong but involved with different types of design practices which might inspire the Hong Kong designers.

2.3 Numerical Study

In this study, RADIANCE (Ward and Shakespeare, 1998) was used to conduct simulation. Two generic pools based on the standard swimming pool design in Hong Kong were developed for this study. Sky conditions are an important parameter for daylighting study. Sky luminance distribution pattern is intertwined with the geographical location and climate. In the past decade, the Commission Internationale de L'Eclairage (CIE) published 15 General Skies to represent major sky luminance distribution patterns over the world. Li et al. (2011) has found that three general skies, No. 1, 8 and 13 were most commonly found in Hong Kong which represents overcast, intermediate and clear sky respectively. Different setting for the swimming pool is evaluated against these three general skies.

A higher resolution in the simulation time step can increase the accuracy of the study. However, to employ an hour-to-hour simulation is very time consuming and might take over several years to complete the study and is not feasible to complete the study within the project duration. So measures were taken to reduce the computational time by an important sampling approach, which was used to select characteristic solar positions and 42 solar positions were identified. Several bins were selected based on the cumulative frequency of solar altitude. These selected solar altitude and azimuth were presented in the table. Under this arrangement, the root mean square difference for the angular distance is only about 7.1° which will not affect the accuracy of study.

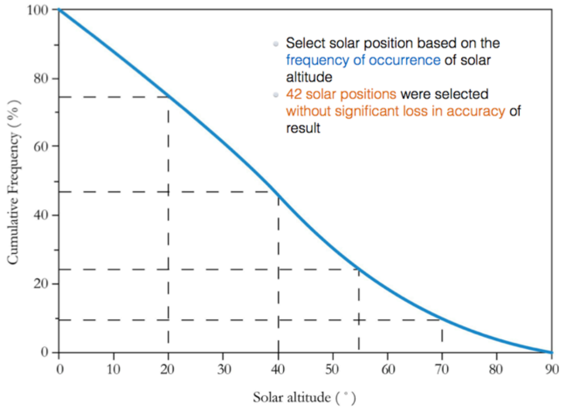

Figure 2 – Cumulative frequency of solar altitude in Hong Kong

2.4 Consultation

The preliminary results from the study were presented to over 100 stakeholders coming from profession building designer such as architect, engineers, surveyors, lifeguards associations, management and planning departments together with other end-users. The stakeholders have openly discussed the findings of the study and compromise several design solutions during the consultation period and provided further recommendations for the completion of study.

3 Major physical phenomena in indoor swimming pools related to reflection and glare

Through the above process, several physical phenomena and design challenges were identified. Major items were grouped into the following four categories and the recommended design solution to be discussed later would be focused on this four major areas.

Figure 3 – Major physical phenomena in swimming pool (top left: veiling reflection; top right: reflected image on water surface; bottom left: glare affects the lookout post; bottom right: reflected light on water surface causes eyestrain

3.1 Veiling Reflection

Veiling reflection is the most significant design challenge which occurs in swimming pools. It is caused by a higher luminance level on water surface than that of the pool basin. Once veiling reflection occurs, the visibility of lifeguards towards the water basin is greatly reduced. For most of the time, these lifeguards are not able to see the bottom of the pool. And it might create potential risks of life rescue occasionally. Among the four problems identified in this section, veiling reflection is the most dangerous one which should be eliminated as much as possible. However, it is also known that this is a physical phenomenon, which cannot be totally avoided.

3.2 Reflected image on water surface

Water is a good reflector. No matter how small amount of light is being reflected, image must be formed on water surface. The major concern is whether these reflected images are noticeable or not. These reflected images would distract lifeguards' attention from swimmers underneath water surface. It will be more appearance for a swimming pool with a deeper colour tile on the pool basin especially when there is large contrast between the colour of indoor surfaces.

3.3 Direct glare from natural and artificial lighting

Glare can be prevented in most of the building designs, for example, office. However, under most circumstance, building professionals do not specifically focus on the effects of glare in relation to lifeguards and hence this kind of problems might occur in swimming pools occasionally. This kind of glare can be discomfort glare or disable glare. Both of them affect the lifeguards in carrying out their duties and might impair their visions. This problem is more commonly found in sidelight and indirect artificial lighting system.

3.4 Indirect glare from water surface

Swimming pool is different from most of other building designs. There is a large surface of water which is a reflector like a mirror. Many designers are not aware of light, which can also be viewed from below via reflection on water surface. Luminaries especially the one without any shielding is more significant in inducing this phenomenon. Not only the problem associated with direct glare, it is dizzier and annoying when the water is undulating and sometimes it causes eyestrain.

4 Most influential design parameters

Two major governing parameters were identified. The first one is the angle of incidence for light which governs the amount of light being reflected. The second one is the vision of eye.

4.1 Angle of incidence

As the smaller the angle of incidence is, the lesser the fraction of reflection is. In Figure 4, the reflectance has a sharp increase after 50°. Turbinated water surface has a variation of angle of incidence under turbinated water surface of ±20˚ (Standard Australia, 2007; CIE, 1984, IESNA, 2001; CIBSE, 1990). It means that the actual angle of incidence is between 30˚ and 70˚ (50˚ ± 20˚). In this Design Guidelines, a limitation on 50° angle of incidence is chosen. The reason of not further reduction on the angle of incidence is due to the fact that further reduction causes difficulty in selecting appropriate light fittings and unreasonable height of ceiling height.

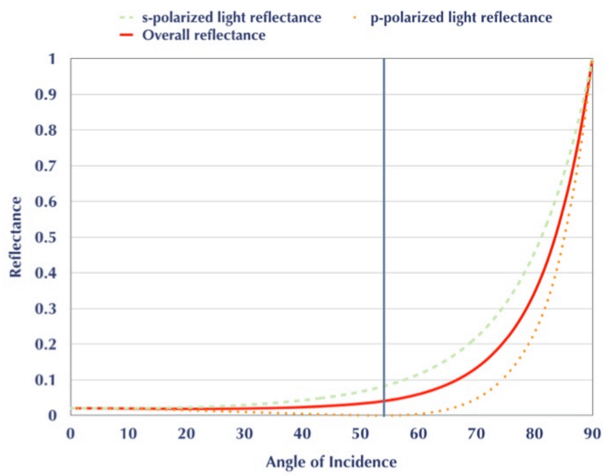

.

Figure 4 – Relationship between reflectance and angle of incidence

4.2 Field of view

Lighting should not be located directly within the lifeguards' field of view, and some analysis on the field of view of human being was conducted. Major of our activities are within 30° from eye of sight and this region is called "near field" (refer to Figure 5). Our visual system is most sensitive to 2° (solid angle which is equivalent to about 6.05° angular distance) around the foveal vision (from sight of line), where major reading activity will happen in this small region. From the area between 30° and 60°, it is known as the "far field" which the sensation of the light is much less than the near field. All zones are affecting the human comfort. However, complete elimination of light fittings within field of view is not feasible under current knowledge and technologies. After considering the dimension of swimming pools, it is believed that only avoiding light fitting within the foveal vision is practical.

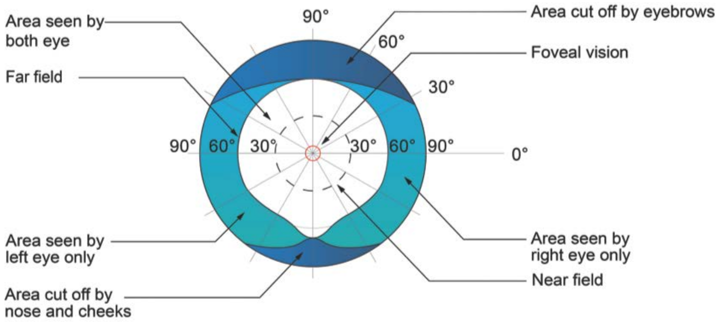

Figure 5 – Field of view of human vision

5 Development of design solutions

There are five major areas identified as the most effective measures to mitigate veiling reflection and glare. Each of them is discussed one by one.

5.1 Window Setback

As the distance between window and pool edge increase, the intensity of light fallen on water surfaces decrease, the magnitude and area of veiling reflection decreased (As found in Figure 6). So an appropriate setback of window can mitigate the veiling reflection. However, it is not able to determine the exact setback through numerical analysis or literature review. So the government and those stakeholders agreed that twice the window top height (commonly used to define daylight zone and parameter zone in practice) is used as design reference.

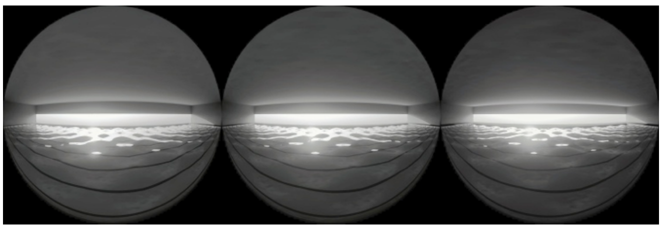

Figure 6 – Veiling reflection and the distance of window setback (Left to right: 0.5x, 1x and 2x of window top height)

5.2 Window location

Window location determines the area and degree of veiling reflection. In relation to the window location, the place where window is attached and the level of window are the most determining factors. When the window is located in the longitudinal side, more veiling reflection is observed especially the lookout post is usually located along the longitudinal side. The relative veiling reflection created on the water surface affects the lifeguards in carrying out their duties. Comparing, when the windows are located in the short end, the area covered with veiling reflection is less. Also after consulting the opinions from lifeguards association, it is found that the location affected by such veiling reflection is more acceptable since the drowning cases less frequently occurred in these locations.

When it comes to the height of window, it is suggested that the window should be placed in the lower part of the wall even the veiling reflection is more serious than that of high-level window. This is based on the concerns raised from lifeguards association that veiling reflection formed in the middle of the pool is more dangerous to the swimmers and affects the lifeguards in carrying out their duties.

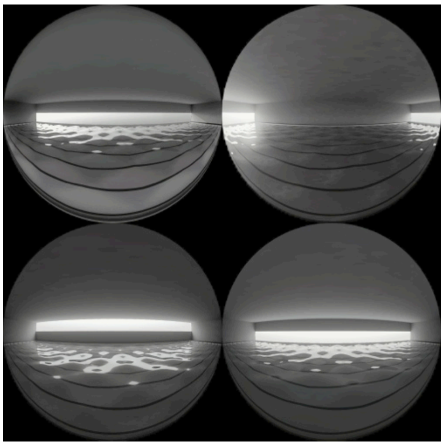

Figure 7 – Location of window (top left: window at the long end; top right: window in short end; bottom right: window at high level; bottom left: window at low level)

5.3 Surface reflectance

It is found that pool basin reflectance is the most important parameter in determining the clearness of image formed on water surface. A higher luminance on water surfaces from wall forms a clear image on the same luminance from pool basin. A series of simulation were conducted to identify the relationship between wall and pool basin surface reflectance. By changing the reflectance of wall and pool basin together with the agreement with the stakeholders, it is found that if the pool basin's surface reflectance is set to 0.7, the optimal reflectance for wall is 0.5.

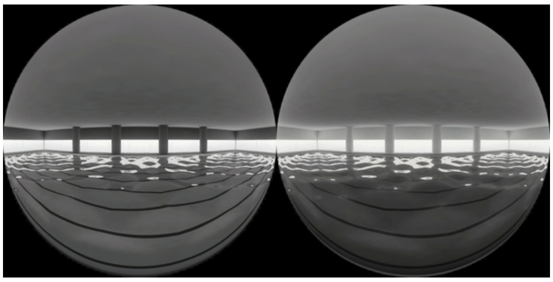

Figure 8 –basin reflectance and image (left: high pool basin reflectance eliminates the image; right: clear image forms for low pool basin reflectance and high wall reflectance)

5.4 Rooflight

Rooflight is an effective means dealing with veiling reflection on pool surface. It is found that there is no relevant design reference. A series of simulation is conducted to identify the requirement of size of rooflight, transmittance of windows and rooflight. Based on the simulation results and consultation with the relative lifeguards association, it is found that the rooflight should not be less than 50% of the roof area in order to illuminate the pool basin and hence reduce veiling reflection. It is also found that if the window has a transmittance over 0.6, it is very difficult to eliminate the veiling reflection by rooflight as the luminance reflected from water surface is very high. Hence, the transmittance of rooflight should be 0.2 higher than that of windows.

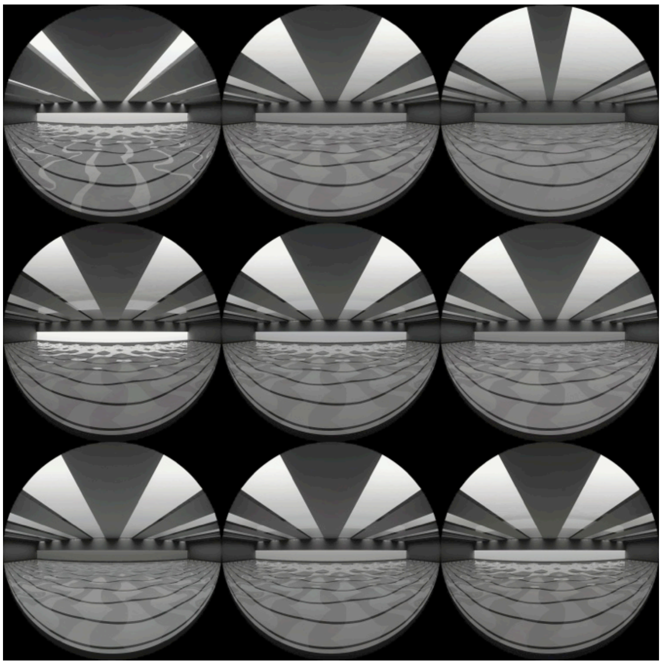

Figure 9 – The Study on rooflight (top: size of rooflight; middle: tranmittance of rooflight; bottom: transmittance of window)

5.5 Artificial lighting

It is found that improper locations of light fittings cause eyestrain, hotspot, glare and maintenance problem (see Figure 10). It is found that the major governing factor in lighting design is the height of swimming pool. It is found that different lighting system has its own ceiling height requirement. If the ceiling level is too low, for sidelight system, the angle of incidence increases, veiling and hotspot to increase eyestrain may then be found. For indirect system, since there is requirement on the minimum vertical distance between light source and deflector, the low-level lighting will be a glare sources for spectators and lifeguards. Similarly, direct lighting system needs an additional space for maintenance platform. The Design Guidelines also provided calculation method to determine the minimum mounting height of each lighting systems.

Figure 10 – Problem associated with lighting system (left: eyestrain caused by reflected light on water surface; middle: hotspot; right: viewing spotlight directly)

6 Conclusions

This paper has briefly reviewed the physical phenomena and design challenges related to light reflection and glare found in indoor swimming pool. Among all, the veiling reflection is the most dangerous since it induces difficulties for lifeguards in carrying out their duties. Other challenges included reflected image on water surfaces, glare caused by lighting system and reflected light on water surface. Their implications on how lifeguards will be affected in carrying out their duty are also described. Two major considerations in controlling the angle of incidence and locating the lighting system out of the view of lifeguards are also highlighted. This information is transformed to building design guidelines for building professional to follow.

Five major measures including window setback, window location, surface reflectance, rooflight and architectural design for artificial lighting system are also introduced. This study and the Design Guidelines are accomplished based on building design practices in Hong Kong within 8-month consultancy period. It is only a snapshot and pioneer study. Further review such as development of performance index and performance based design approaches are required. Nevertheless, it is believed that this study has summarised the views from professional and swimming pool operators which can enrich the knowledge of building designers.

Acknowledgements

The work is supported by the ArchSD and LCSD of the HKSAR Government. The authors would like to express their sincere thanks to the above departments for the approval of the publications.

References

Architectural Services Department of the HKSARG, 2009, "*Design Guide for Public Swimming Pool*". Hong Kong: Architectural Services Department of HKSARG.

Chan, T.K.C., Li, K.S.K., Tong, K.C.F., Tsang, E.K.W. 2013. Global illumination simulation technique in developing guidelines to mitigate veiling reflection in indoor swimming pools. *In proceedings of 13th Conference of International Building Performance Simulation Association*, Chambery, France, 26-28 August 2013, 3019-3026.

Chan, T.K.C., Tsang, E.K.W. 2013. Safety in lighting design for indoor swimming pool. *In proceedings of 2013 International Lighting Symposium*, Hong Kong, People Republic of China, 18 October 2013, 10-15.

Census and Statistics Department of the HKSARG. 2011. *Public views on Education Reform & Public views on the provision of sport facilities*, Thematic household survey report no. 47. Hong Kong: Census and Statistics Department of the HKSARG.

Centre for Health Protection. 2012. *Epidemiology and prevention of unintentional drowning*. Non-communicable diseases watch, 5(7). Hong Kong: Department of Heath, Hong Kong Special Administrative Region Government.

Chartered Institution of Building Services Engineers. 1990. LG4:1990: *Lighting Guide Sport*, London: Chartered Institution of Building Services Engineers.

Commission Internationale de l'Eclairage. 1984. CIE 62-1984: *Lighting for Swimming Pool*, CIE Central Bureau, Vienna, Austria.

Commission Internationale de l'Eclairage. 1989. CIE 83-1989: *Guide for the lighting of sport events for colour television and film systems*, CIE Central Bureau, Vienna, Austria.

Commission Internationale de l'Eclairage. 2005. CIE 169:2005: *Practical Design Guidelines for the lighting of sport events for colour television and filming*, CIE Central Bureau, Vienna, Austria.

"*Swimming Pools Regulation*" 1961. Chapter 132CA. Hong Kong: HKSARG.

Federation Internationale de Natation, n.d. *Facilities Rules*, FINA [online] Available from: http://www.fina.org/H2O/index.php?option=com_content&view=category&id=88:facilities-rules&Itemid=184&layout=default [Accessed August 2012].

Food and Environmental Hygiene Department of the HKSARG. n.d.. *Requirement of Lighting Provision for Swimming Pool Licence*. Hong Kong Special Administrative Region: Food and Environmental Hygiene Department of the HKSARG.

Health and Safety Executive. 2003. *Managing health and safety in swimming pools*, 3rd Edition, HSG179, Surrey: Sport England and Health and Safety Executive.

Illuminating Engineering Society of North America, 2001, IESNA RP-6-01: *Recommended Practice for Sports and Recreational Area Lighting*, USA: Illuminating Engineering Society of North America.

Irish Water Safety. Institute of Leisure & Amenity Management, Swim Ireland, 2010. *Swimming Pool Safety Guideline*, 2nd Ed, Galway: Irish Water Safety.

Leisure & Cultural Services Department of the HKSARG. 2011. *Operational Requirements for Heated Swimming Pool Facilities*, Hong Kong: Leisure & Cultural Services Department of the HKSARG.

Li D.H.W., Tang H.L, Cheung K.L., Lee E.W.M., Cheng C.C.K. 2011. "Sensitivity analysis of climatic parameters for sky classification", *Theoretical and Applied Climatology*, 105(3-4), pp.297-309.

Lifesaving Society. 2012. *Public Aquatic Facility Safety Standard*, Lifesaving Society, Canada.

Ministry of Construction. 2007. *Standard for lighting design and test of sports venues*, JGJ 153 – 2007. China Architecture and Building Press, Beijing. [In Chinese].

Society of Light and Lighting. 2009. *The SLL Lighting Handbook*, London: Chartered Institution of Building Services Engineers and Society of Light and Lighting.

Standards Australia. 2007. AS 2560.2.5 – 2007: *Sports Lighting Part 2.5: Specific Applications – Swimming Pool*, Standards Australia, Sydney.

Sport England. 2011. *Swimming Pools Design Guidance Note*, Revision 3, London: Sport England.

Ward G., Shakespeare R. [eds.]. 1998. "*Rendering with RADIANCE – The art and science of lighting visualization*", San Francisco: Morgan Kaufmann Publishers.

World Health Organization. 2004. *The world health report: 2004: changing history*, Geneva, Switzerland: World Health Organization.

World Health Organization. 2006. *Guidelines for safe recreational water environments. Volume 2, Swimming pools and similar environments*, Geneva, Switzerland: World Health Organization.

PP31

DAYLIGHT DESIGNS FOR HOSPITAL UNDER SUBTROPICAL CLIMATE

Chan, T.K.C.[1], Tsang E.K.W.[1],
[1] Parsons Brinckerhoff (Asia) Ltd., Hong Kong SAR, People Republic of CHINA
chan.thomas@pbworld.com

Abstract

Hospital is an energy-intensive building and lighting system consumes a significant part of the total building energy consumption. In recent years, lots of energy efficient measures have been incorporated into high-grade hospital during the design and construction stages. Hence, the energy consumptions of hospital buildings have been changed substantially. Under this development trend, a comprehensive study was conducted to review the built environment and energy usage of hospital in subtropical region. The design of building envelope, building services system, combined heat and power plant and new green building features were evaluated against standard design practices. This paper presents a part of the study which specifically addressing the concerns of natural lighting on the visual quality and its implication on energy consumption. It is found that Low-E IGU has become the major glazing in new hospitals. And under such arrangement, low solar heat gain and high visible transmittance can be achieved without the installation of shading device. Also the glazing area for hospital development seems higher than other type of building. The visual performance was assessed by RADIANCE in order to understand the indoor lighting environment, like illuminance level, different arrangements of glazing, indoor surface finishing and layout plan. It is found that most of in-patient ward can achieve satisfactory indoor daylight level, but for wards with 6 or more bed, better design strategies are needed.

Keywords: Hospital, RADIANCE, daylight factor

1 Introduction

Daylight is an effective approach in creating a pleasant visual environment and providing an opportunity for energy saving. Daylight is considered as the best source of lighting with good colour rendering and its quality is the one light source that most closely matches human visual response. Windows served two roles in hospital bedded area for transmitting daylight and providing connection with external environment for patient (SLL, 2008). Rea et al.(2002) found that the spectral composition of daylight is different from most electric lighting. It can maximise the melatonin suppression response and can improve the circadian photobiological activation. Baker and Steemers (2002) stated that without daylight, circadian cycle slows down by about 1.1 hours per day. Baker (2000) also found that a poorly daylit building is a contributory factor for Sick Building Syndrome and affects the phase synchronising ability of light. Another study on student behaviour towards natural light showed that a high morning cortical level had positive effects on sociability and hormone patterns of students (Küller and Lindsten, 1992). Furthermore, a study by Joarder and Price (2013) suggested that an increase in 100lux for daylight level can reduce 7.5hour of a patient stay in hospital after coronary artery bypass graft surgery. It seems that daylight might have positive impacts on recovery for a number of illnesses.

Hospital being one of the most energy intensive developments among different building types, understanding the daylight availability in different wards can provide indication for building designer to explore the energy saving opportunity.

Recently, there is an increasing demand in the healthcare services. In 2012, hospitals under the Hospital Authority provide 27,062 beds and manage over 7.6 million patient days a year (Hospital Authority, 2011; Hospital Authority 2013). And Hospital Authority proposed using a public-private partnership approach in the healthcare services to cope with the increasing demand (Hospital Authority, 2011). In this paper, 4 different hospitals cover public, private and public-private partnership developments were analysed. Their major design characteristics which affect daylighting performance were discussed. And by computer simulation technique, the daylight factor and the average daylight factor were computed and briefly discussed.

2 Survey sample and parameters affect daylight

A total four hospitals were selected for the study. The criteria were listed as below:

i. The hospital were completed or to be completed between 2013 and 2016.

ii. The hospitals cover private and public development

iii. The hospital must have at least one floor with in-patient bedded ward.

iv. Day-care hospital and clinic were excluded in this study.

v. The newly designed hospitals must have obtained the approval from Building Department for construction.

The design documents including drawings, specifications, design report and construction information were collected. In order to retain building anonymity, they are designated Hospital 1, Hospital 2 and so o and summarised in Table 1. After study these hospitals' characteristics, it is more valuable to study the daylight performance of ward then others functional room of building since the major focuses of the hospitals are different. The surveyed hospitals cover new development, redevelopment of existing hospital and new extension of an existing hospital. The developers includes local authorities, local and overseas private sector investment. The number of bed provided by each development is ranged from about 50 to 350. It is observed that for private development, more wards are designed for single bedded to about 3 beds with a few wards having 4 to 5 beds. It seems that the design of the private invested hospitals is target for mid-class consumers with a higher standard of living. While for the public sector, the room number is ranged from 6- to 8-bed ward with a higher density to fulfil the ever increasing demand in medical services in Hong Kong. Since the variety of their natures, it is believe that the surveyed samples should be able to represent the current practices of hospital design in Hong Kong as well as nearby regions. Three major categories viz. building orientation and area, glazing type and window area are discussed.

Table 1 – Design characteristics of surveyed hospitals in Hong Kong

	Hospital 1	**Hospital 2**	**Hospital 3**	**Hospital 4**
Development Sector	Private	Private-public funding	Public	Private
Building Nature	Redevelopment	New development	Redevelopment	Extension
Year complete	2014	2016	2013	2015
Total number of floor	9	9	12	28
Number of ward floor	3	4	2	9
Floor area (per ward floor)	1,500	18,700	4,800	2,000
No of bed	51	349	260	193
Floor to floor height	3.75	4.5	4.5	4.2
Building Window to wall ratio	47%	49%	43%	52%
Major window orientation	Northeast and Southwest	East and west	North and south	East and West
Glazing Type	IGU	IGU	IGU	IGU
Shading Coefficient	0.35	0.26	0.42	0.4
Visible transmittance	0.42	0.48	0.4	0.5

	Hospital 1	Hospital 2	Hospital 3	Hospital 4
Shading devices	Nil	Nil	Nil	Nil
Ward detail	1-bed ward Area: 9-30m^2 Window to floor area ratio: 23-54%	1-bed ward Area: 16-42m^2 Window to floor area ratio: 49-108%	6-bed ward Area: 52-58m^2 Window to floor area ratio: 17-18%	1-bed ward Area: 20-138m^2 Window to floor area ratio: 23-54%
	2-bed ward Area: 21-24m^2 Window to floor area ratio: 17-23%	2-bed ward Area: 16-26.24m^2 Window to floor area ratio: 26-29%	7-bed ward Area: 52-55m^2 Window to floor area ratio: 17-19%	2-bed ward Area: 24-28m^2 Window to floor area ratio: 32-35%
	4-bed ward Area: 34-40m^2 Window to floor area ratio: 24-27%		8-bed ward Area: 54-57m^2 Window to floor area ratio: 14-15%	3-bed ward Area: 38-41m^2 Window to floor area ratio: 20-23%
	5-bed ward Area: 48.5m^2 Window to floor area ratio: 24%			

2.1 Building orientation and area

The orientation of building and its windows affected the capture of daylight into building. Traditionally, building designer preferred north-south orientation which enables capture of daylight without overheating. Another school of thought believing morning sunlight can improve circadian activities for patients. Unfortunately, there is no available design guideline recommending the favourable orientation of windows in ward. The major façade orientation as shown in Table 1 found that most of them do not show the preference on orientations of hospital. The surveyed hospitals cover all directions. It is believed that similar to the consideration of building orientations in commercial building is more subjected to site constraints (Li and Tsang, 2008). The geometrical arrangement of hospital concerns about the logistic flow within the hospital and traffic nearby to increase the efficiency of handling emergency cases and reduce the unnecessary travel for patients rather than the micro-climate.

The increase in interior surface area of the building reduces the reflected light flux within the building and usually has a lower lighting level. In this study, the ward areas were analysed. It is found that in general, private-funded hospitals have a smaller number of bed per ward, but the area per person is larger than that of public sectors. As indicated before, the target patients of public and private hospital are different. Apart the 1-bed ward, it is found that the averaged area per bed is 8-15m^2 per person for private hospital. While for public hospital, the average area per bed is about 7.5-8.5m^2 per bed. And the area of 1-bed ward varies from 9-135m^2 per bed. Even in the same hospital, the size of 1-bed ward can be changed by nearly seven times. The wards are mainly located in the perimeter zone of the building which can capture more daylight. And even the area of ward in private hospital is larger, but the hospital usually located the bed and major working area closed to the windows which enable to patients experience better daylighting environment.

2.2 Glazing type

Glass controls the amount of daylight being admitted into the building. In principle, the daylight level especially the daylight factor is directly proportional to the transmittance of windows glazing. Hence, glazing is always a major parameters affecting indoor illuminance level. In these four hospitals, it is found that all of them are equipped with insulated glazing unit (IGU) with low-e coating. Low-e glass contains a thin coating of metal oxide substantially cutting down heat gain without proportionally reducing daylight transmittance. It should be pointed out that low-e glass is effective in terms of minimizing solar heat gain when there is short wave radiation (i.e. East and West orientations). In the survey, it is found that Low-e IGU is commonly used in hospital design compared with commercial building. A plausible explanation is that hospital has a greater concern on acoustic and hence the employment of IGU (double glazing) is more commonly found in hospital. It can found that the hospital currently employ some glazing with a visible transmittance (VT) around 0.4 to 0.5 with a relatively low shading coefficient of about 0.25-0.4. And with these high-performance glazing, shading devices cannot be found in new hospital development.

2.3 Window area

For a given glazing type, the critical factor determining the daylight entering a building is the window area. According to the Hong Kong Building Regulation, the required window area should be more than one-tenth of the floor area of the room. Window area is commonly represented by the window-to-wall ratio (WWR) that is expressed as the ratio of the total area of windows to the overall gross facade areas including windows. It is found that, the building has a WWR around 40-55%. Currently the increase in area of glazing is highly due to the low-e IGU can effectively control the heat gain through the fenestration.

The area of window to ward floor area ratio is also studied, it is found that as the number of bed for the ward increases, the percentage of glazing area to floor area tend to decreased. For most of the wards in private hospital, the percentage of glazing to floor area is over 20% and for several 1-bed wards, the percentage can be over 100%. While for the public sector, the percentage of glass to floor area is merely achieved 20%. The high level of this value is due to the fact that all in-patient wards are located in perimeter zones with a comparatively less depth of rooms.

3 Daylight factor analysis by computer simulation approach

Based on the characteristic of described in Section 2, further analysis were conducted to understand the indoor daylight performance of wards in hospital. Several stereotypes were fabricated and the indoor daylight factors were calculated. The 1-, 2-, 3-, 4-, 5- and 8-bed ward were simulated by RADIANCE.

3.1 Model descriptions

In total, there are 6 models were fabricated. Their geometry are based on the resulted of surveyed hospitals. For 1-bed to 5-bed wards, floor and glazing area are based on current design of private hospitals as it is uncommon to find a ward with small number of bed in public sector. For the 1-bed ward, the minimum sized is used as the range of this type of ward is very large and it is not a good assumption to using oversize ward as study reference. Also we found that the design characteristic for 6-, 7- and 8-bed wards are similar, so only the 8-bed ward is study and the stereotype is based on public hospital arrangement. The floor to ceiling height is assumed to be 2.7m based on their fitting-out drawings and proposals from interior designers. Details of the simulation models can be found in Table 2 and Figure 1.

Table 2 – Dimension of ward being simulated

	Area (m^2)	Window to floor area ratio (%)	Dimension (W x L)
1-bed ward	16	49	3.8m x 4.2m
2-bed ward	25	32	4m x 6.25m
3-bed ward	38	22	4.5m x 8.5m
4-bed ward	37	26	6.9m x 5.4m
5-bed ward	49	24	7m x 7m
8-bed ward	56	15	6.9m x 8.05m

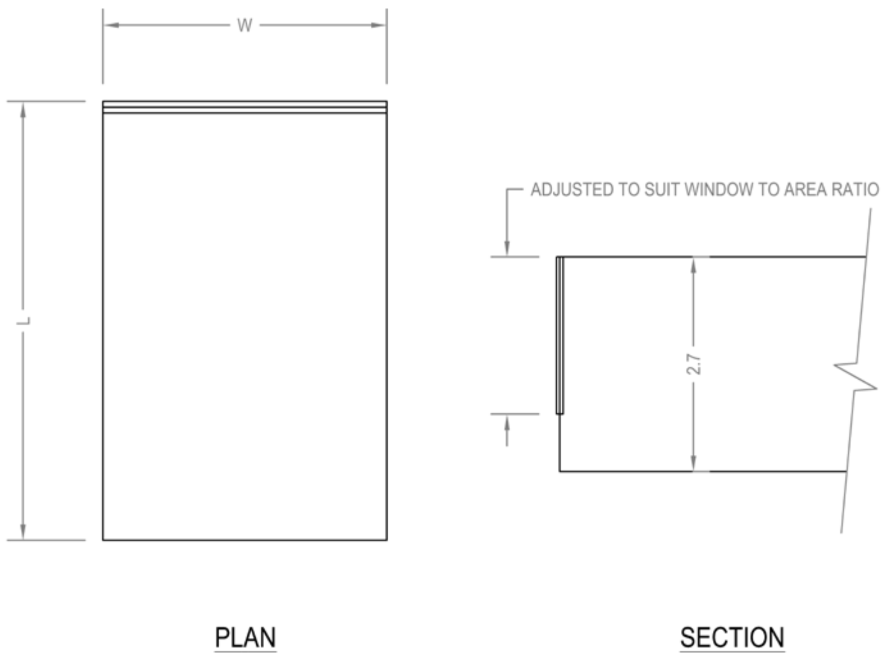

Figure 1 – Typical layout of ward for simulation study

Since not all finishing are completed at this moment, so the reflectance of the major surfaces, like ceiling, wall and floor are 0.7, 0.5 and 0.2 respectively.

3.2 Model descriptions

RADIANCE (Ward and Shakespeare, 1998) is a computer simulation package for simulating and visualizing lighting in and around architectural environments using the backward ray-tracing technique. It is a well-established lighting program that has been used by a number of researchers (Reinhart and Herkel, 2000; Li and Tsang, 2005). It has been reported that RADIANCE simulations can produce more close prediction to real building measurements comparing with a number of daylighting software packages (Gugliermeti et al, 2001). The built-in ''Gensky' sub-program was used to generate the CIE overcast sky conditions for indoor illuminance calculations. The key simulation parameters for daylight illuminance determinations are the number of reflections and resolution of the inter-reflection calculation, which are referred to the ambient parameters. Convergence tests were conducted to obtain the settings for ambient parameters such that the accuracy and simulation time of the ray-tracing calculations in RADIANCE can be reduced to an acceptable level. Table 3 summarises the ambient parameter settings for these six wards.

Table 3 – Ambient setting of simulation

Ambient parameters	Setting
Ambient division	2048
Ambient sampling	1024
Ambient accuracy	0.08
Ambient resolution	1024
Ambient bounces	6

4 Daylight performance of hospital wards

Daylight performance is usually evaluated in terms of average daylight factor. It is expressed as the ratio of indoor illuminance level to the horizontal illuminance under an unobstructed overcast sky. As pointed out in CIBSE (1999), an averaged daylight factor over 5% can ensure a space is adequately day lit and under most situations, artificial lighting are not required for normal office hour. While for a space of average daylight factor of 2% or below, the interior looks gloomy and artificial light is frequently required during daytime. In SLL

(2008), there is no specific suggestion for daylight level for ward. So the average daylight factors were computed for study and the results are listed in Table 4. It is found that the typical 1-bed ward can achieve an average daylight factor of 5% or more. It means that the ward is adequately daylit and under most of the time, no artificial light is required. For other type of wards, it is also found that the average daylight factor is between 4.39% and 3.31%. It is more likely that the indoor space can enjoy a reasonable amount of daylight and artificial lighting is required occasionally.

Table 4 – Average Daylight factor for different ward

	Average daylight factor (%)
1-bed ward	6.27
2-bed ward	4.39
3-bed ward	3.31
4-bed ward	4.00
5-bed ward	3.97
8-bed ward	3.47

Apart form average daylight factor, the centreline daylight factor for different wards is also analysed. Figure 2 shows the daylight factor along the centreline for these six types of ward. It is found that the daylight factor drops as distance from window increases. As expected, the ward with a smaller floor area like the 1-bed ward has a higher daylight factor than other type of wards as it has a high window to floor area ratio and smaller area of internal surfaces. As the number of bed in ward increase, the internal daylight factor decreased. The exceptional cases in this study are 4-bed and 8-bed wards. In the 4-bed ward, it has a relatively large room width and hence the window height becomes shorter. So the daylight captured per unit length near the window wall is smaller. Similar observations were found for the 8-bed ward due to small window to area ratio. For all wards, distance within 3.5m from window can achieve a daylight factor over 2%. However, for narrow and deep ward like the 3-bed ward and some highly dense ward (8-bed ward) have very low daylight factor at the back of the ward which is smaller than 1%. It is recommended that the designer should review the design of these ward and interior design need to locate the beds in the ward with care.

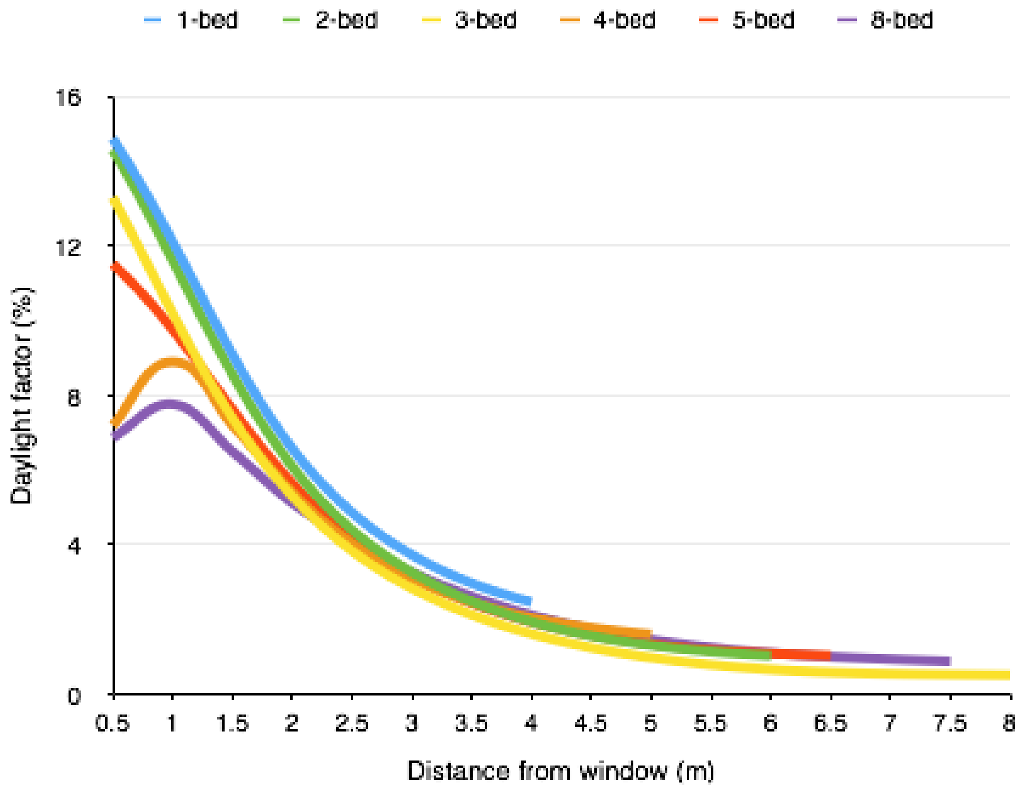

Figure 2 – Centreline daylight factor for different wards

5 Conclusion

In this study, four hospitals with in-patient ward to be completed between 2013 and 2016 were analyzed to understand the current hospital design practices. It is found that the design of hospital invested by private and public have several differences. Usually, private built hospitals tend to provide wards with less number of beds. While for the public sectors, they tend to build wards can accommodate more beds. The average area per patient for public hospital is smaller than that for the private one.

The location of ward seems to suit the functional design instead of the consideration of daylighting and other built environment or energy issues. In all surveyed building, low-E IGU is used in most buildings it can reduce solar heat gain (shading coefficient of 0.26-0.4) without a significant reduction in the visible transmission (visible transmittance of 0.0.4-0.5). Compared with most existing hospital using tinted glass, the patient can expect more daylight in new hospitals. All hospitals have very high window to wall ratio of about 50% which larger than other type of buildings. It may be due to the employment of Low-e IGU. The design of each wards were also analysed. It is found that for those wards with less bed, the window area to floor area ratio is higher and in general, this ratio decreases as the number of bed increases which drops from nearly 50% for a 1-bed ward to less than 15% for an 8-bed ward.

The average daylight factor and centreline daylight factor is also analysed. It is found that 1-bed ward has sufficient daylight with about 6% average daylight factor and artificial lighting does not need to be frequently used. For other types of ward, the average daylight factor is over 2% and will not look gloomy. For the daylight factor along the centreline, it is found that the daylight factor decrease as distance from window increase. And within 3.5m from window, the daylight factor are able to exceed 2%. For some wards with inadequate natural light, new design is recommended and interior designers need to aware of the variation of indoor daylight level among the ward.

This study is only the preliminary review of current design. More comprehensive study is being prepared for relevant authorities to implement in new projects.

Acknowledgment

The authors would like to express their thanks to designers and different consultant team in supplying related design and construction documents for this study.

References

BAKER, N., STEEMERS, K. 2002. Daylight design of buildings. London: James & James (Science Publishers) Ltd.

CIBSE, LG10 1999: Daylighting and window design, London:CIBSE.

GUGLIERMETI, F., GRIGNAFFINI, S., BISEGNA, F. 2001. Computer simulations, full and scale model measurements as design tools to assess daylight factor in underground open space. In Proceeding of Istanbul 2001 – International Lighting Congress, 519-526, Istanbul Technical University, Istanbul, Turkey, 12-14 September 2001.

Hospital Authority, 2011. Annual Plan 2011-2012, Hong Kong: Hospital Authority

Hospital Authority, Hospital Authority Statistical Report 2011-2012, Hong Kong: Hospital Authority

JOARDER, A.R., PRICE,A.D.F., 2013. Impact of daylight illumination on reducing patient length of stay in hospital after coronary artery bypass graft surgery, Lighting Research and Technology, 45, 435-449.

KÜLLER K., LINDSTEN C., 1992. Health and behaviour of children in classrooms with and without windows. Journal of Environmental Psuchology.12, 305-317.

LI, D.H.W., TSANG, E.K.W. 2005. An analysis of measured and simulated daylight illuminance and lighting saving in a daylit corridor. Building and Environment, 40, 973-982.

LI, D.H.W., TSANG, E.K.W. 2008. An analysis of daylighting performance for office buildings in Hong Kong. Building and Environment, 43,1446-1458.

REA, M.S., FIGUEIRO, M.G., BULLOUGH J.D., 2002.Circadian photobiology: an emerging framework for lighting practice and research. Lighting Research and Technology,34, 177-190.

REINHART C.F., HERKEL, S. 2000. The simulation of annual daylight illuminance distributions – a state-of-the-art comparison of six RADIANCE-based methods. Energy and Buildings, 32, 167-187.

SLL, 2008. Lighting Guide 2: Hospitals and health care buildings, England: The Society of Light and Lighting

WARD, G.L., SHAKESPEARE, R. 1998. Rendering with Radiance. The art and science of lighting visualization. Los Altos, CA: Morgan Kaufmann.

PP32

MUSEUM LIGHTING WITH LEDS: LED LIGHTING FOR THE SISTINE CHAPEL

Ferenc Szabó[1], Péter Csuti[1], János Schanda[1]

[1]Virtual Environments and Imaging Technologies Research Laboratory, Faculty of Information Technology, Department of Electrical Engineering and Information Systems, University of Pannonia, Veszprém, HUNGARY

Abstract

The European Commission founded a pilot flagship project (LED4ART), which has the aim to demonstrate that high quality and energy efficient museum lighting based on LEDs is possible in 2014. The place of demonstration is one of the top ten museums in the world: the Sistine Chapel in the Vatican. A consortium consists of 6 partners from 5 countries are in charge of renewing the lighting system of the Sistine Chapel. Members of the consortium are OSRAM, the Vatican City State, OSRAM Italy, the Energy Research Institute of Catalonia (IREC), Fabertechnika and University of Pannonia. The role of the Virtual Environment and Imaging Technologies Research Laboratory in this project is to determine the LED spectral power distribution in order to present the world-famous frescoes to the visitors in the form as the artist imagined them. Beside this aspect, art preservation and energy efficiency are still important issues. The project has been started in 2012 with the evaluation of the old lighting system and going to reach the final aims in the first half of 2014. On-site measurements have been done in the Sistine Chapel, spectral optimization of LED spectra has been done according to modern colorimetric practice. In this paper, the most important results of the onsite measurement sessions are presented.

Keywords: museum lighting, light quality, energy efficiency

Introduction

In the field of illuminating artworks, there are two special requirements against lighting: optimal lighting should minimize irreversible damage of artworks and should provide the most preferred appearance of them[i]. Hence these two conditions can not be hold together, one should define a compromise to save the artworks as far as possible and provide their preferred appearance to the visitor of the museum at the same time. The present ISO/CIE standard[ii] requires for museum lighting 300 lx average illuminance, with an UGR_L glare index of 19 and general colour rendering index R_a=80. For museum lighting obviously colour fidelity lighting is of importance, as one certainly does not want to distort the perceived colours compared to those as conceived by the painter, even if some observer would find the painting “nicer” under a light source with preferred colour rendering. The only exceptions might be if by the methods of illumination one tries to “restore” the fading of some pigments[iii], or if one would like to compensate the lower colourfulness perceived due to the lower illumination of the painting by increasing the gamut area produced by the illumination (but these are exceptional cases and one has to deal with them most carefully).

For paintings of historic importance not the most pleasing illumination should be selected, but an illumination as the painter had seen his piece of art under the illumination he/she had used to create the picture[iv]. Emphasis was on natural illumination, designers could not put major emphasis on artificial lighting quality. At the time of building the Sistine Chapel, artificial lighting existed only as a form of candle light. There are anecdotes that Michelangelo painted parts of frescos by candle light, but certainly he selected his paints under daylight of high illuminance; no colour discrimination – even for a master as Michelangelo – is possible under candle light. For this reason we expect that colours of the frescos in Sistine Chapel have been chosen by “Mediterranean” daylight. Centuries later, first lighting designs were made with gas lighting in museums, but soon electrical lighting with incandescent lamps became the standard. The existing lighting system of the Sistine Chapel has two operation modes: general lighting for visitors during opening hours of the Vatican Museum. Gala lighting system is switched on only for special occasions (e.g. mass with the pope).

General lighting system is realized by backlighting of the windows. Behind each of the 12 windows of the chapel 12 metal halide lamps (150W each) are installed. In front of the historical window glass a UV filter and diffuser is installed. The most efficient way to increase the transparency would be the replacement of the window glass. However due to the fact that the windows are partly still original, a replacement is not possible.. Due to the roughened surface of the glass and the filter the total transparency is only 20 to 25 %. The emission is therefore diffused and the beam is directionless. For the gala lighting system 40 halogen lamps (30 x 500W, 10 x 1000W) are installed on a handrail in a height of 11 m. In addition to these luminaires further eight halogen lamp luminaires are switched on, which are integrated into the general lighting system. The down-lights produce considerable heat and glare to the observer if he/she intends to look at the frescos on the ceiling. On the other side the inadequate illumination of the ceiling is also obvious.

On-site measurements

In order to evaluate the current lighting system and make it comparable to the new LED lighting system, on-site measurements had been taken in Sistine Chapel. Measurement sessions have been organized late in the evening after sunset, so no daylight from outside had entered the Chapel during measurements. Since the Museum closes at 6 pm, no visitors were present during the measurement sessions.

Illuminance measurements of the floor area

The measurements were performed by three groups, who divided up the floor area among themselves. The three hand held illuminance meters were compared to each other, and it was confirmed that the individual differences of readings were within ±1.5 %. A 2 by 2 m network was laid on the floor, and the illuminance in every point was taken, both under normal and gala illumination. Thus measurements were made in 7 columns from the left side of the Chapel (looking towards the altar), and 20 rows, where 13 rows are between the altar and the dividing fence, and 7 rows are outside of the fence.

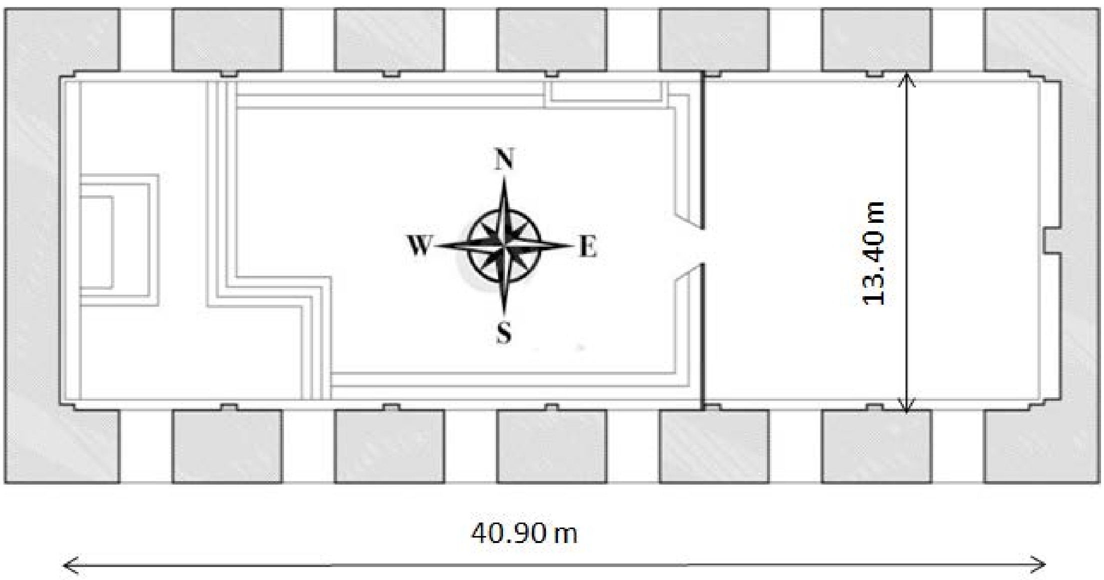

Figure 1 - Ground plan of the Sistine Chapel

1 Illuminance measurement under normal illumination

Figure 2 shows the measured illuminance values. In the fourth column at row A and B stands the altar, where no measurement was made. In column I and J no measurements could be taken, as there a scaffold stood to reach higher locations in the Chapel. In Column 7, row T and S stands the organ keyboard, again not accessible for measurement. Line N was very near to the fence, the data are only approximate, as the fence screened the light, and partly one had to take measurements on the top of the bank that stands adjacent to the fence.

Measurements showed illuminance values below 13 lx, partly quite low values. Although low floor illuminance helps to provide contrast to the lighting of the frescoes, the new lighting system should provide much higher values.

2 Illuminance measurement under gala illumination

Figure 2 shows illuminance data for the gala illumination, in lx. The values are much higher as for the normal illumination, actually high enough to perform reading/writing tasks.

	1.	2.	3.	4.	5.	6.	7.
A	79.6	112.6	54.1			81.0	72.0
B	105.3	158.8	220.0		196.0	108.0	71.5
C	124.7	233.0	272.0	299.0	280.0	188.5	95.5
D	138.0	268.0	357.0	363.0	327.0	234.0	131.0
E	167.9	301.4	391.0	385.0	324.0	257.0	175.0
F	176.8	315.0	407.0	325.0	352.0	280.0	209.0
G	179.8	282.0	349.0	347.0	322.0	256.0	207.0
H	178.1	281.0	333.0	337.0	303.0	231.0	190.0
I	172.2	287.0	327.0	309.0	273.0	219.0	160.0
J	168.0	286.0	303.0	299.0	236.0	154.0	
K	170.5	284.0			241.0	145.0	66.0
L	180.7	271.0	257.0		220.0	134.0	63.0
M	176.7	267.0	241.0	198.1	192.0	111.0	66.0
N	99.3	161.7	170.0	109.0	142.0	103.0	55.0
O	139.8	236.0	212.0	218.0	180.4	127.4	77.0
P	174.6	262.0	250.0	223.0	206.0	149.1	88.0
Q	171.7	259.0	275.0	261.0	234.0	161.2	102.0
R	146.2	236.0	264.0	257.0	235.0	144.3	89.0
S	126.3	195.7	238.0	231.0	213.0	116.2	
T	98.7	166.8	196.0	191.0	180.0	126.0	
U	87.4	147.2	177.0	147.0	132.0		

Figure 2 - Measured illuminance (in lx) under gala illumination

Table 1 shows the average illuminance values for the different parts of the Chapel under gala illumination. Table 2 shows the average illuminance levels in different part of the Sistine Chapel.

Table 1 - Statistical analysis of the illumination in each column, under gala illumination

Column	1	2	3	4	5	6	7
E_{av} (lx)	146.8	238.6	264.7	264.7	239.4	166.3	112.8
E_{min} (lx)	79.6	112.6	54.1	109.0	132.0	81.0	55.0
E_{max} (lx)	180.7	315.0	407.0	385.0	352.0	280.0	209.0
$e_1=E_{av}/E_{max}$	0.8	0.8	0.7	0.7	0.7	0.6	0.5
$e_2=E_{min}/E_{av}$	0.5	0.5	0.2	0.4	0.6	0.5	0.5

Table 2 - Average values of different parts of the Chapel under gala illumination, in lx

E_{av}. near to altar	234.4
E_{av}. inner part. without altar	213.7
E_{av}. total inner part	217.0
E_{av}. exterior part	139.8

Illuminance measurements of the walls

Direct illuminance measurement on the walls would be possible only in the lower part of the Chapel, in the part of the wall that is partly covered by an acrylic panel, and partly painted drapes. To reach higher lying parts of the wall for illuminance measurement an indirect method was chosen: Part of the wall was covered with a white cloth the reflectance of which was separately measured, and the luminance of this cloth was measured with an image taking luminance measuring camera: Canon D450 USB, with TechnoTeam software and calibration. Figure shows the reflected luminance in false colour representation. The green area corresponds to 1.5 cd/m^2.

Assuming a Lambert reflection characteristic of the fabric, the luminance of the fabric is

$$L = \frac{\rho E}{\pi} \quad (1)$$

and thus

$$E = \frac{L\pi}{\rho} \quad (2)$$

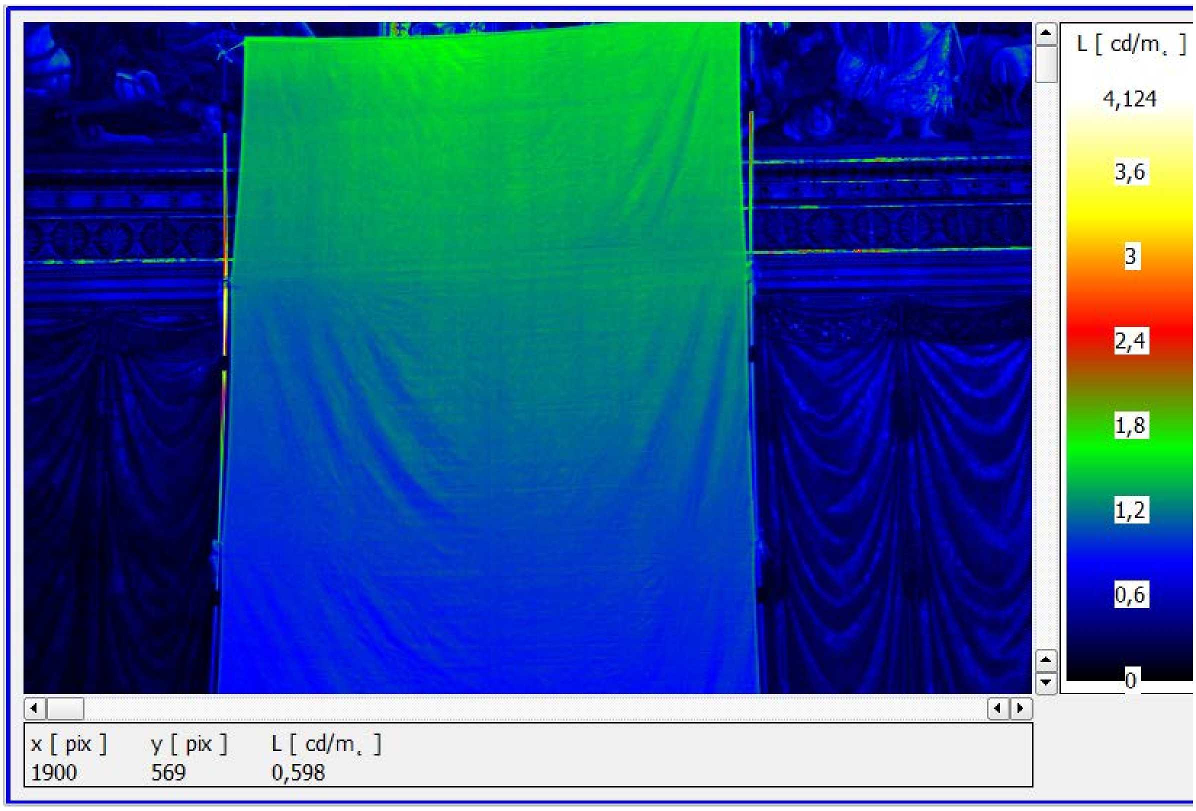

Figure 3 - False colour image of the cloth hanging in front of the Botticelli fresco.

The falls colour image (Figure 4) shows that in the lower area of the fresco the luminance is as high as 2.5 cd/m^2, corresponding to about 10 lx, but the lower part goes beyond 1 cd/m^2, that corresponds to about 4 lx illumination.

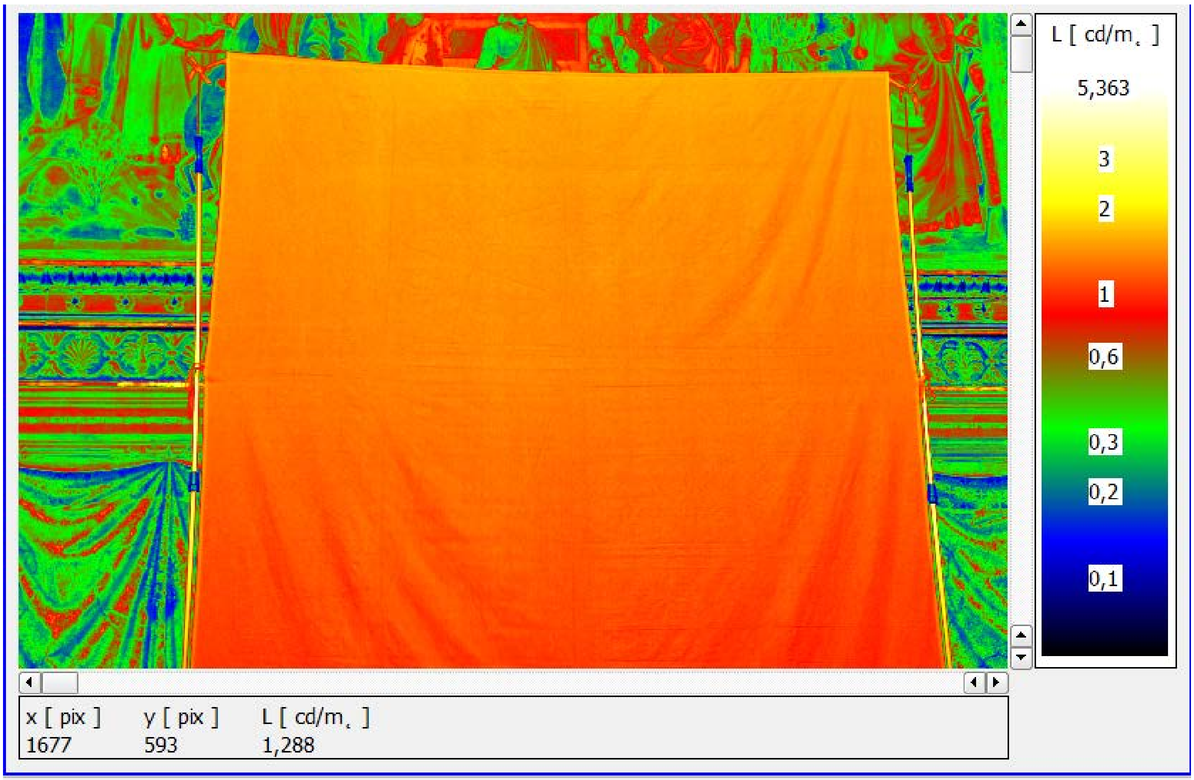

Figure 4 - False colour image of the cloth hanging in front of the Rosselli fresco.

Spectral measurements

Pigments of paints used in frescoes from XVth century are very different from the pigments of current paints; hence reflectance of these paints is highly different. Current light source colour quality metrics use test samples from XXth century, hence none of them is able to provide good prediction in case of the frescoes of Sistine Chapel. To be able to investigate how well colours will be reproduced by the new LED illumination the reflectance spectra of characteristic pigments had to be determined. In situ measurements were made to get a feel how different the reflectance spectra of the fresco pigments were, compared to the used in current colour rendering calculation programs.

Technique of taking the reflectance spectra

In the Chapel no measurements with a spectrophotometer could be used that would touch the fresco. Instead of that we used a theatre projector to illuminate a small part of a fresco, where that colour was used, the spectrum of which we intended to determine. This illumination was done from a distance of several metres, illuminating the fresco obliquely, to avoid the regular reflection from the painting. As far as possible we tried to irradiate under 45° and observe perpendicularly. The observation was done using a Minolta 2000 spectroradiometer. Figure 5 shows the general arrangement for taking the measurements. The projector irradiates a small part of the fresco from a horizontal distance of a_1, and under an angle α_1. d_1 is the distance between the projector and the fresco element. The distances and angle between the fresco element and the spectroradiometer have and index 2. In determining the reflected radiation these distances and angles have been taken into consideration. To determine the spectral power distribution of irradiation, a PTFE white standard was used, the reflectance spectrum of which was about 98 % and flat in the visible part of the spectrum.

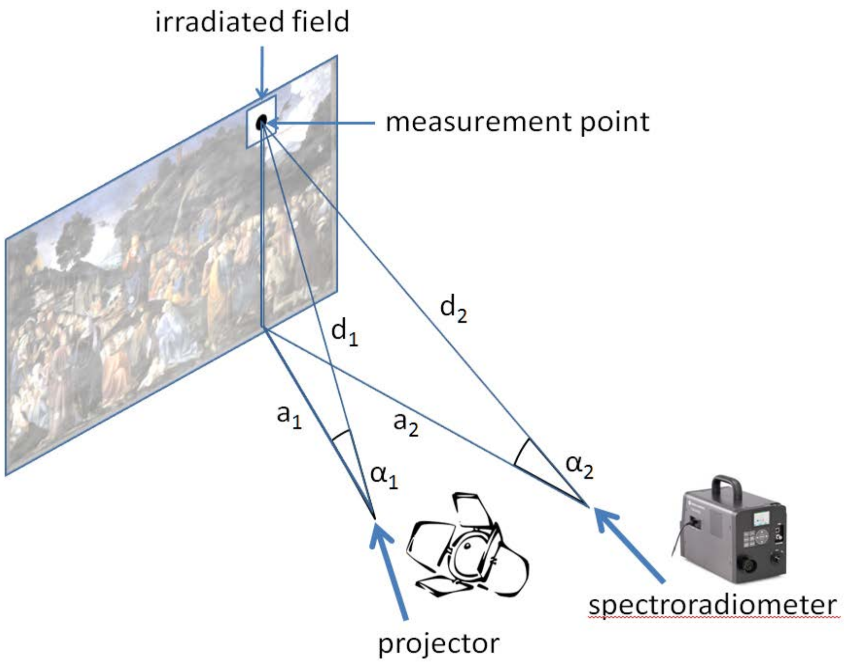

Figure 5 - Arrangement for performing the measurements.

For archiving the measurement results a detailed booking system was set up. Table 3 shows a small excerpt from this book-keeping. For every spectrum taken with the Minolta spectroradiometer information on the image, the predetermined point in the image (meas. point), the angles of illumination obliquely and horizontally (with these values the measured radiance had to be corrected, cos-correction), and information on the parallel taken simple photographic image (for eventual identification of measurement points).

Table 3 - Measurement results book-keeping

Name of picture	meas.point	spectroradiometer meas #	oblique	horizontal	image
No.1. Last judgement	11	1	18.17	14.38	5868
	12	2	17.77		5869
	13	3	16.66		5870

To get a feeling on the data taken, Table 3 shows an excerpt of the underlying spectral data in table form. To get to the reflectance spectra, the projected area of the image had to be calculated based on the angles as shown in Table 3 and the reflectance of the single measurement point calculated taking the measured radiance of the PTFE standard into consideration.

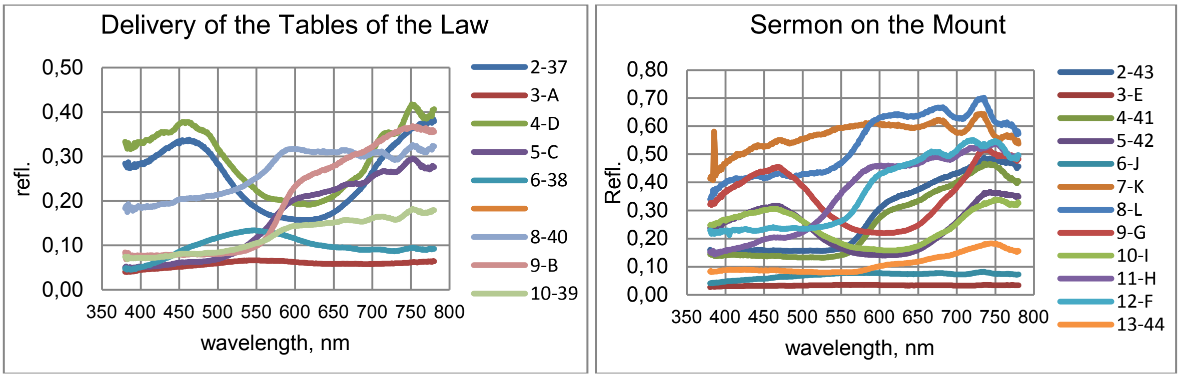

Figure 6 - Spectral reflectance of pigments in the „Delivery of the Tables of the Law" and the „Sermon on the Mount" frescos.

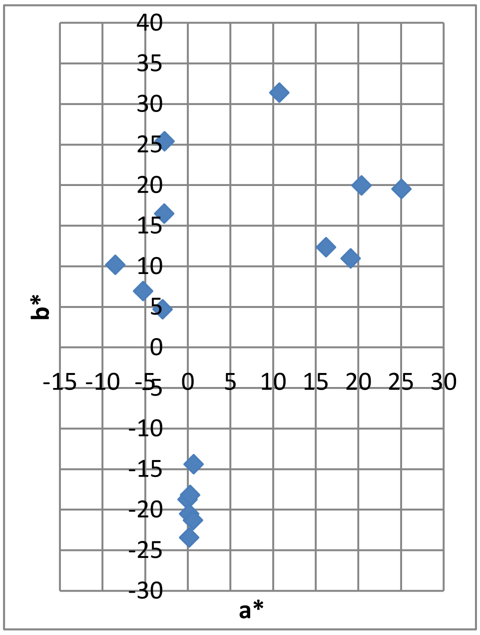

Selection of spectra for colorimetric calculations

The final task was to select spectra for evaluating the colour rendering properties of the new LED based lighting system. The CRI2012 colour fidelity program uses 16 reflectance spectra to determine a general colour fidelity index. Thus we selected from the measured pigment spectra such spectra the colorimetric properties of which showed big chroma and were distributed around the colour circle. Unfortunately in the purple area no adequate spectra were found. The a*, b* co-ordinates of the selected samples are seen in Figure 7.

Figure 7 - a*, b* co-ordinates of the selected 16 spectra.

Optimization of LED spectrum

The next task was to select the LEDs to be used in the lighting system of the Sistine Chapel. The curators of the Vatican Museum required an illumination with a correlated colour temperature not higher than 3500 K, and for the realization of such a large scale illumination the number of different LEDs had to be kept in reasonable limits. Thus it was agreed to provide an adjustable lighting using warm white colour LEDs and red, green and blue supplementary LEDs. An optimization program was developed using the above determined reflectance spectra to find from a high number of LEDs with different spectral characteristics such LEDs that would provide good CIE colour rendering [v] , good Colour Quality Index [vi], minimal colour difference compared to the appearance of fresco colours under daylight illumination. According to our measurement results and spectral optimization, minimal colour difference compared to the appearance of fresco colours under daylight illumination could be achieved by mixing the light of a kind of warmwhite LED with blue LED (peak at 466 nm), turquoise LED (peak at 500 nm), red LED (peak at 659 nm). The so selected LED spectra are shown in Figure 8.

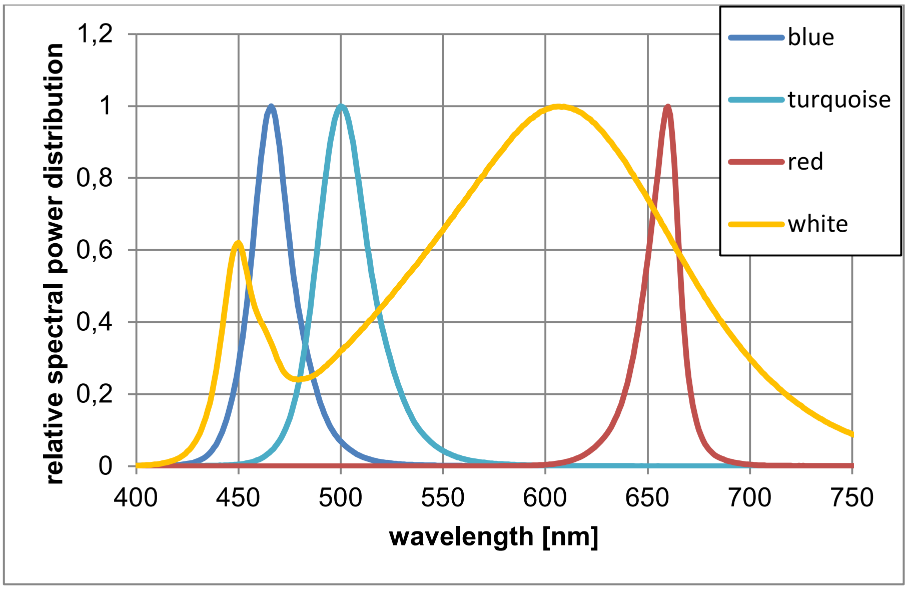

Figure 8 - Spectra of primary LED channels in the final luminaire.

The four spectra provide a further dimension of freedom for the optimization. Two alternative paradigms were selected for this optimization: using the CRI2012 program[vii] and minimizing the colour distortion between the CIECAM02-UCS[viii], [ix] coordinates illuminating the paint samples under daylight and L_a=100, and correlated colour temperature of 3500 K and L_a=30. More detailed results on this are to be found in[x].

Conclusion

By investigating the existing lighting system of the Sistine Chapel, we can conclude that in case of gala illumination the glare is too high and it provides a heavy thermal load. The floor illumination in case of normal lighting is very low, below standard levels. For the new illumination higher levels are recommended. The evenness of the illumination is adequate. The floor illumination with gala illumination provides adequate visibility for reading and writing in the main area of the Chapel. The vertical illumination on the side walls of the Chapel in case of normal lighting is low, but enough for foveal vision. Thus colours of frescos are visible, but at the lower end of photopic vision. The fresco illuminance is in the order of 10 lx. At lower parts of the walls the illuminance drops to 3 to 5 lx. For the new lighting system one can recommend that the fresco illumination should be approximately ten times higher as the present one. Task of the fresco reflectance spectrum investigation was to determine whether the fresco pigments produce further requirements in selecting optimal LED spectrum to illuminate the Sistine Chapel frescos. In situ reflectance spectra measurements were performed in the Chapel on frescos painted by Michelangelo, Botticelli and Rosselli. LEDs are attractive light sources for museum lighting. By using composite LED systems, consisting from some white LEDs (blue plus yellow phosphor) blue, green and red additional LEDs, one can optimise the spectrum in such form that the colour distortion between the perceived colours under daylight (D65 in our present example) and the museum lighting (3500 K CCT in the present example) should be minimised.

Acknowledgement

This research was supported by EU ICT-PSP-2010-5 project (grant number: 297262) entitled High Quality and Energy Efficient LED Lighting for Art (LED4ART).

References

[i] Cuttle C. Light for Art's Sake: Lighting for Artworks and Museum Displays. Amsterdam: Butterworth-Heinemann, 2007

[ii] ISO: Lighting for work places – Part 1. Indoor, *ISO 8995-1/*CIE S 008/E, First ed.:2002-05-15.

[iii] Berns, R.S.: Rejuvenating the appearance of cultural heritage using color and imaging science techniques. In: Proc. AIC Colour 05, Granada, Spain.2005, pp. 369–374 (2005)

[iv] Schanda, J., Csuti, P., Szabó F. Colour fidelity for picture gallery illumination, Part 1: Determining optimum LED Spectra, under publication.

[v] CIE Technical Report (1965) Method of measuring and specifying colour rendering properties of light sources, 1st ed. Publication CIE 13 (E-1.3.2).

[vi] Davis W, Ohno Y (2005) Toward an improved color rendering metric. Proc. SPIE 5941 59411G1-G8.

[vii] Smet KAG, Schanda J, Whitehead L, Luo RM (2013) CRI2012: A proposal for updating the CIE colour rendering index. Lighting Res. & Technol. 45:689-709 2013.

[viii] CIE (2004) A Colour Appearance Model for Colour Management Systems: CIECAM02. CIE Publ. 159:2004.

[ix] Luo MR, Li Ch (2007) CIE color appearance models and associated color spaces, in Colorimetry, Understanding the CIE System, ed. J Schanda, Wiley-Interscience 2007.

[x] SCHANDA, J. 2014 What is colour fidelity in museum lighting? this conference.

PP34

VISUAL IMPRESSIONS OF COLOURED LED LIGHTINGS IN AN INDOOR SPACE

Yinqiu YUAN, Li-Ling LEE, Ming-Shan JENG, Shih-Pu CHEN
Industrial Technology Research Institute, Hsinchu, CHINESE TAIPEI
AlinaYuan@itri.org.tw

Abstract

The study aims to investigate the relationship between the hue of coloured LED lighting and human observer's visual impression. To achieve the goal, a psychophysical experiment was conducted in a non-window room illuminated with coloured LED lights. A RGB LED lamp was used for generating visual stimuli. 10 young observers participated in the experiment. Each of them was asked to evaluate all light samples in terms of 25 scales. The results suggest that there were three underline factors of visual impression of a space illuminated in coloured LED. The three underline factors can be denoted by "naturalness", "feminineness" and "young". The results also show that light samples in white and yellow regions appeared natural; light samples in yellow, red and purple regions looked feminine; in terms of young, lights of white, purple and blue were rated as young.

Keywords: Visual Impressions, Coloured LED Lighting, Indoor Space

1 Introduction

Colour can evoke viewer's emotional responses in certain ways (Ou et al, 2004). In any built environments, colour scheme, including objective colours and lighting colours, plays an important role for design practices. Since the late 90's, the relationship between objective colour and viewer's emotional response has been studied. These researches shared a similar lighting condition, i.e. the test samples were illuminated by CIE standard lighting sources, such as D65 in the studies of Ou's (2004) and Sato's (2000). These lightings generally appeared cool white. Regarding the influence of coloured lighting on induced viewer's emotional responses, in the area of colour and lighting research and application, it has become a hot topic recently. The majority related research focused on comparing the effects of warm or cool white lighting between selected lighting sources, such as florescent lamp and LED lamp, in terms of perceived spatial traits (e.g. Atli et al. 2012) and vision efficiency (e.g. Kubo et al., 2012). Although the findings indicated that the perceived geometry characteristics and quality of viewing conditions could be different under lightings with different values of compared colour temperature (CCT), the general emotional responses evoked by a coloured lighting has been barely revealed in these researches.

Recently, some researchers went further by using specific coloured lightings, for example red, blue, yellow and green LEDs (e.g. Dresp, 2004, Huang, 2009, Yamadaki et al, 2012), in their experiments. The experimental results provided evidence that different coloured lightings may have different influence on viewer's emotional responses. For example, according to the work of Yamadaki and his colleagues (2012), in an office environment, blue and red lights made the observers felt uncomfortable, while orange light or an incandescent light are psychologically suitable for relaxation and could evoke a warm feeling. This was supported by many others (e.g. Guo et al, 2012, Nagashima et al, 2012, Ishida et al, 2011). Nevertheless, these findings can hardly form an overall understanding of coloured light influence on human observer's emotional responses, as the investigated scales in the precious studies did not cover a wide range of human emotional responses induced by colour.

To address these issues, the present study used LED lights with independent red, green and bule channels to illuminant an non-window room space (2.4m×1.7m). A group of 10 young people in Taiwan Industrial Technology Research Institute were invited to participate in the experiment. The effects of hues on perceived colour emotion scales were investigated.

2 Methods

2.1 Scales of investigation

Experiment 1 intends to investigate the impacts of hue of coloured LED lightings on human observer's from widely used colour emotion word pairs (Ou, 2004). The 24 scales include boring/interesting, cool/warm, sad/happy, plain/splendid, narrow/spacious, unfriendly/friendly, uncomfortable/comfortable, styleless/stylish, feminine/masculine, dislike/like, nervous/relax, unfamiliar/familiar, passive/active, dangerous/safe, hard/soft, unhealthy/healthy, old/young, dirty/clean, country-style/city-styled, private/disclosure, dim/bright, unnatural/natural, stale/airy, and childish/mature, facial skin colour not preferred/preferred. As the observers were all Chinese speakers, the original word pairs written in English translations are made by the experimenter in reference to Far East English-Chinese Dictionary during the experiment.

2.2 Experimental room and viewing condition

A small white-painted room (size in 2.4m×1.7m) is used as the experimental room. A LED lamp with independent red, green and blue channels is recessed in the middle of the ceiling. During the experiment, a touch screen panel produced by htc is used for controlling hue of the LED lighting. A group of common household stuff including an office chair, a mirror and a round coffee table on which displaying a bunch of artificial flowers, fruits and small ceramic statures are used as room decorations.

The viewing stimuli include 5 coloured lights (Red, Green, Blue, Yellow and Purple) and 2 white lights (a RGB white without CCT value and a CCT=4000K white light). All of the test light samples have middle-level saturation. During the experiments, all the viewing stimuli were repeated. Therefore, there were 2x7 = 14 viewing stimuli in total for each of the observer. Figure 1 shows the 7 test LED light samples plotted in CIE1931 colour space chromaticity diagram with a white circled dot stands for one light sample.

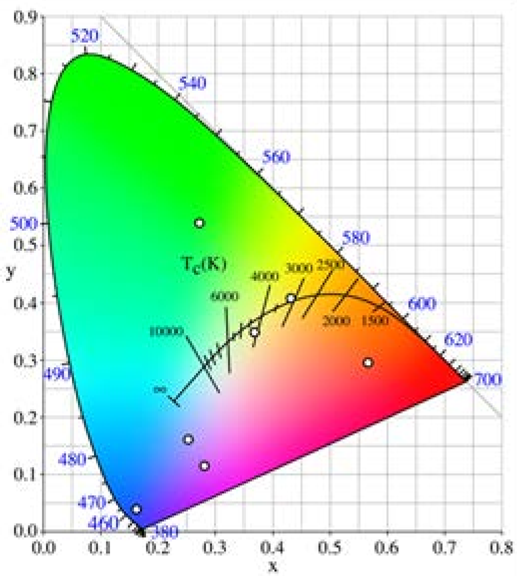

Figure 1 – The 7 test LED light samples used in the experiment

2.3 Observers

Ten young Taiwanese (aged under 40) equally spread in both genders participate in Exp1. All of them are staff in Industrial Technology Research Institute of Taiwan (ITRI), and are examined with Ishihara's test for colour deficiency.

2.4 Psychophysical experiment

Experiment 1 is performed in a room without window and illuminated with a controllable LED lighting varying in hue. Before the experiment, each observer is explained about the procedure of the test. In the experiment, the observer is firstly shown the instruction of the experiment as shown below (the instruction is written in Chinese as all the observers are native Chinese speaker), and then demonstrated the examination by the experimenter before the observer processes the test on his/her own.

During the test, each observer is required to sit on a chair in the center of the test room facing forward. The test room is lighted in each hue of red, green, blue, yellow and purple for two times individually and randomly. Each scene is presented for about 10 seconds for the observer being able to fully adapt himself/herself to the light. For each scene, the observer is asked to rate the scene in terms of each of 26 scales on a six-point force choice polar scale. In the whole period of experimental time, each observer remains sitting in the test room until the test finishes. The experiment takes about 45 minutes to complete for each observer.

3 Results And Discussion

Results of the experiment suggest that there were three underline factors of visual impression of a space illuminated in coloured LED.

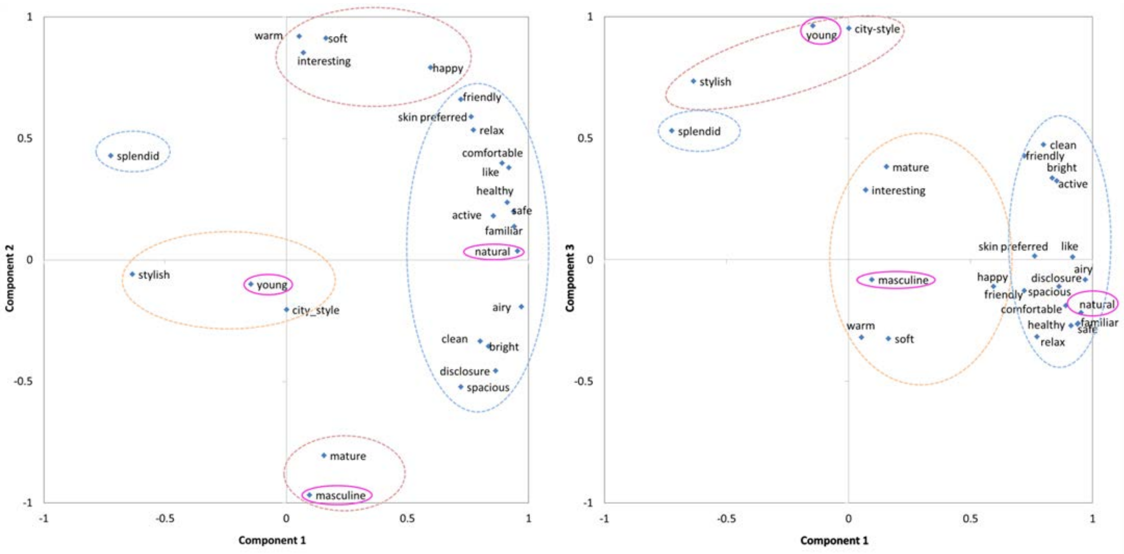

Figure 2 – Component plot of visual impression of coloured LED lightings: (a) Component 1 plots against Component 2, (b) Component 1 plots against Component 3

The three underline factors can be denoted by “naturalness”, “feminineness” and “young” (circled in solid pink lines in Figure 2(a) and (b)). The correlations of the 25 scales are illustrated in Figure 2(a) and (b), with highly correlated scales being circled in the same colour of blue for Component 1, red for Component 2 and yellow for Component 3. In terms of visual impression of naturalness, the result suggested that in CIELUV space, lights in white and yellow region (red circled area in Figure 3 (a)) appeared natural while the rest appeared unnatural. For feminineness, lightings in the region of yellow, red and purple (circled in red in Figure 3 (b)) looked feminine while the rest appeared masculine. For young, lightings of white, purple and blue (circled in red in Figure 3 (c)) were scored positively as young while the rest were rated old.

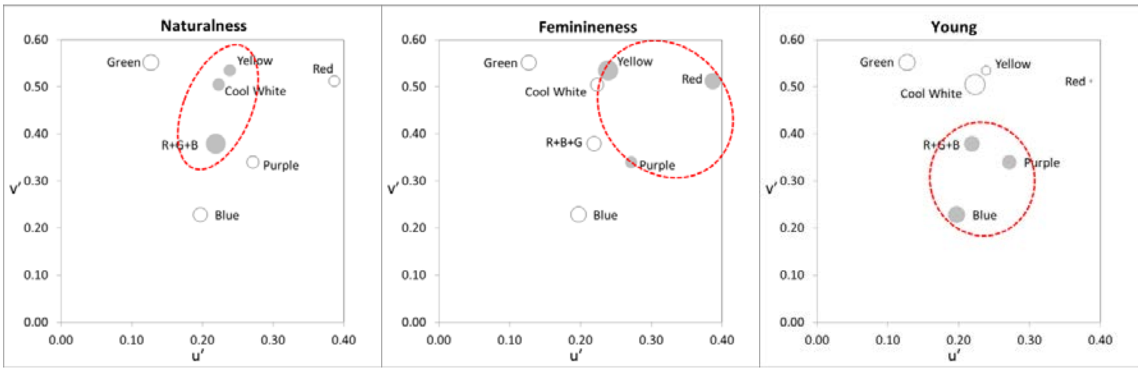

Figure 3 – The six hues in the CIELUV space, filled bubbles indicate positive values and open bubbles indicate negative values. Bubble size for each hue represents factor score of (a) naturalness, (b) feminineness and (c) young.

4 Conclusions

The results suggest that there were three underline factors of visual impression of a space illuminated in coloured LED. The three underline factors can be denoted by "naturalness", "feminineness" and "young". Hue of coloured LED lighting influenced visual impression for the indoor space in terms of the three underline factors. The outcomes of the current study are useful for LED lighting design for indoor spaces, such as shopping stores and family homes.

Acknowledgements

This work was supported by the Bureau of Energy, Ministry of Economic Affairs (103-E0201).

References

Atli, D., Sekulpvski, D., Oligunturk, N., Seuntiens, P. 2012. Effects of colour and chromatic light on depth perception. AIC 2012 interim meeting, 184-187.

Dresp., B., Cuibal, C. R. 2004. Interaction of color and geometric cues in depth perception: When does "red" mean "near"? Psychological research. , 69, 30-40.

Guo, Y., Saito, M., Nakamura, M., Nagashima, K. 2012. Physiological and psychological responses to color lights under cold environmental condition. Journal of the color secience association of Japan, 36, 226-227.

Huang, K. C. 2009. Effects of colored lights, spacing between stimuli, and viewing distance on error in a depth-matching task. Perceptual and motor skills. , 108, 636-642.

Ishida, T., Mori, B., 2011. Harmonious color group characterized by a colored light source. Proceedings of the midterm meeting of the international colour association, 213-216.

Kubo, C., Yamagishi, M., Ayama, M., Yamaba, K. 2012. Readability of colored text on a colored background under LED lighting and Fluorescent lighting. AIC 2012 interim meeting, 148-151.

Nagashima, K., Yoda, T., Yagishita, T., A. Taniguchi, T., Hosono, K. Kanosue. 2002. Thermal regulation and comfort during a mild-cold exposure in young Japanese women complaining of unusual coldness. Journal of applied physiology, 92, 1029-1035.

Ou, L. , Luo, M. R., Woodcock, A., Wright, A. 2004. A Study of Colour Emotion and Colour Preference. Part I: Colour Emotions for Single Colours. Color research & application, 29(3), 232-240.

Ou, L., Luo, M. R., Woodcock, A., Wright, A. 2004. A Study of Colour Emotion and Colour Preference. Part II: Colour Emotions for Two-Colour Combinations. Color research & application, 29(4), 292-298.

Sato, T., Kajiwara K., Hoshino H., Nakamura T. 2000. Quantitative Evaluation and Categorising of Human Emotion Induced by Colour. Advanced colour science technology, 3, 53-59.

Yamaguchi, S., Okuda, S., Saito T. 2012. Preferable LED Lamps for Appearance of Skin Color of Human Face. AIC 2012 interim meeting. 446-449.

Yamasaki, G., Sunaga S., Seno T., Kozaki T. 2012. Examination of a suitable lighting for a nap in a resting room of an office. AIC 2012 interim meeting, 458-461.

PP35

LIGHTING QUALITY OF ENERGY EFFICIENT ILLUMINATION OF SCHOOL BOARDS

Dionyz Gasparovsky[1], Jana Raditschova[1], Roman Dubnicka[1]
[1]Slovak University of Technology, Faculty of Electrical Engineering and Information Technology, Bratislava, SLOVAKIA
dionyz.gasparovsky@stuba.sk

Abstract

Illumination of school boards is essential to capture the attention of pupils, to perform their visual task efficiently and accurately, and to avoid undesired phenomena like glare or fatigue. It is obvious that luminance levels depend on illuminance and reflectance, thus the lighting system has to account for school board type. In contrast to dark backrounds used before, whiteboards are preferred, in general, today. Old-fashioned blackboards are often replaced by whiteboards without adjustment of the lighting. This upgrade usually results to dramatic change of luminance levels. Current standards on illumination of workplaces do not distinguish between dark and white boards. In result, new or refurbished lighting systems in classrooms do not suit the visual needs of users. For improvement of standard requirements there is, however, lack of sufficient knowledge on what attributes the quality lighting with the best possible energy efficiency should fulfil.

This paper brings to the public newest results of investigation in the field of schoolboard lighting aimed at analyses of photometric parameters on boards and their surroundings lit by optimized lighting systems. Illuminance is studied versus luminance for all common types of school boards. The information presented in this paper comprise partial analyses and findings ellaborated within the framework of a complex research on school board lighting.

Keywords: school board lighting, school lighting, illumination of black board, illumination of white board, lighting in classrooms, lighting quality

1 Introduction

Lighting quality in classrooms is highly important for the health of children and taking into account short-term actions it determines the learning performance and concentration. Attention of pupils is usually focused on the front board which intermediates them all the essential information. During normal teaching process the visual task is often swapped from board to desk and vice versa what also determinates the adaptation of eyes. Therefore, illumination level of boards and desks as well as their surroundings should be harmonized in order to avoid unpleasant and undesired luminance distribution.

Up to now, in existing buildings there are still many older-type luminaires in operation, providing uneven illumination by means of incandescent lamps or uniform but low-level illumination by fluorescent lamps behind diffusers. On the other hand, current lighting standards (like CIE S008 and EN 12464-1) require to satisfy vertical illuminance 500 lx on boards. This can be done by contemporary energy-efficient luminaires with fluorescent lamps and assymetrical luminous flux distribution. It is not only a energy saving measure but also a mean how to provide much higher quality of illumination in classrooms. To follow this objective, many classrooms in schools and other educational buildings undergo renovation. After several years of activities in this application field, there are many positive feedbacks but also some negative experience. Study presented in this paper is based on numerous measurements of boards before and after modernization as well as on feedback of lighting users.

It is necessary to point out that the standard requires the same illuminance on black board, green board and whiteboard. Illuminance, however, is not the right attribute of good and pleasant illumination, both in terms of visual performance and visual comfort. Today, white boards are preferred against dark boards enabling to use coulourful and dustless markers. But too illuminated white boards give high luminances that may cause glare of users.

2 Background

2.1 Normative requirements

Normative requirements are set in the standard CIE S 008[1] which in Europe is implemented in the EN 12464-1[2], Table 5.36. Maintained illuminance shall be at least 500 lx with uniformity 0,7 or better, Ra minimum 80 and UGR shall be below 19. Specular reflections shall be prevented. Presenter/teacher (in front of the board) shall be illuminated with suitable vertical illuminance, not specified in particular numbers. These requirements to an equal extent apply to black, green and white boards (Fig. 1).

Usage of dark boards (green or black) versus white boards depends on choice of negative or positive contrast between the foreground and the background. White boards are undoubtly much more energy efficient because better reflect light. Dark boards absorb the essential part of incident luminous flux which is only reflected from white chalk writings or drawings. On the other hand, the latter provides more visual comfort than large board area with high luminance level. Dark board itself is also better percepted against background of the front wall and clearly marks out the “working area” to which one has to focus his attention. Edges of white boards are “lost” in the plane of front wall. Nevertheless, advantages of dustless and easier to use and clean white boards lead to their preference against dark boards, not taking into account illumination characteristics as the core criterion.

Experience with lighting installations in class rooms with white boards showed that users, both teachers and pupils, are unsatisfied with high luminance levels at about 500 lx of average illuminance. Extent of visual discomfort was often declared by users so high that they stopped to use the dedicated illumination of school board, and only the main lighting system in class room was kept in operation. User reactions need to be regarded, but these may express individual preferences and as such should not be oversignificated.

Figure 1 – Green board, black board and white board in class rooms

2.2 Previous illumination techniques

Illumination of school boards in existing lighting installations in schools and similar educational buildings is typical for the time period in which the lighting was installed or renovated. Oldest luminaires which are still in operation can be dated back to 1950. Not taking into account individual specific deviations, standard lighting solutions can be recognized as follows:

- **No specific illumination of school board** (Fig. 2a)
- **Pair of luminaires for incandescent lamps with zonal reflector** (Fig. 2b): reflectors (Fig. 3b) help to create more uniform lighting of board’s vertical plane from a point light source. However, illumination is highly uneven, bright light spots are visible in the higher parts of the front wall, often above the board (Fig. 3a).
- **Line arrangement of luminaires for fluorescent lamps with diffuser** (Fig. 2c): common single lamp fluorescent luminaire is not specifically dedicated for this illumination task.

Due to diffuser, illumination of board is uniform but luminous flux is not efficiently directed towards the board and thus the real contribution (in addition to the general illumination of classroom) is neglectable.

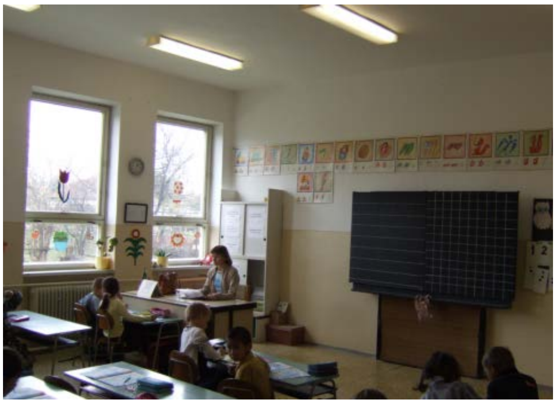

a) No specific illumination

b) Incandescent lamps and zonal reflectors

c) Fluorescent diffuser luminaires

d) Bare fluorescent lamps

e) Assymetrically shaded luminaires

Figure 2 – Different techniques of school board illumination

a) Light spots from zonal reflectors

b) Luminaire for incandescent lamp with zonal reflector (left) or reflecting diffuser (right)

Figure 3 – Illumination of school board with pair of luminaires for incandescent lamps

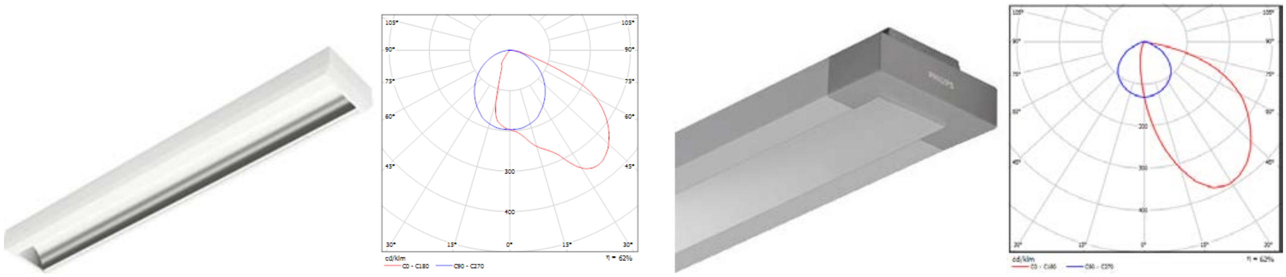

a) Examples of luminaires for fluorescent lamps with assymetrical optics suitable for illumination of school boards

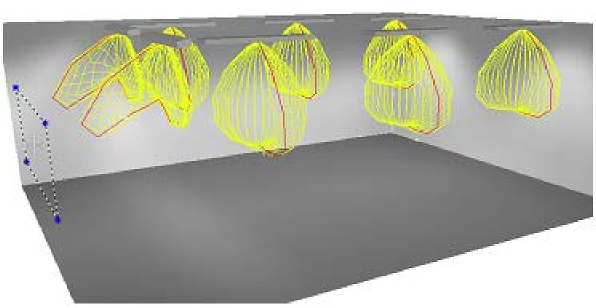

b) Luminous flux distribution

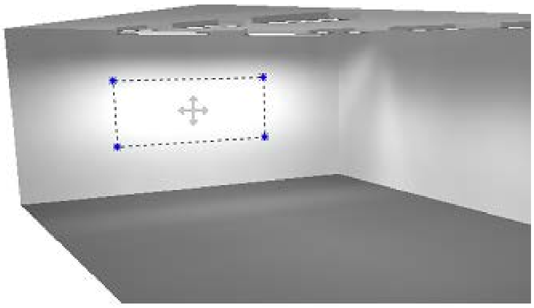

c) Computeral visualization

d) Lighting installation

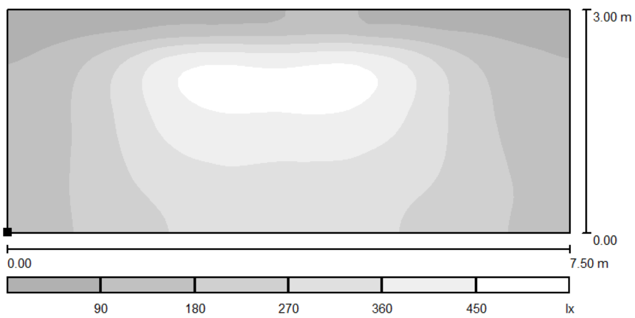

e) Distribution of illuminance on the wall

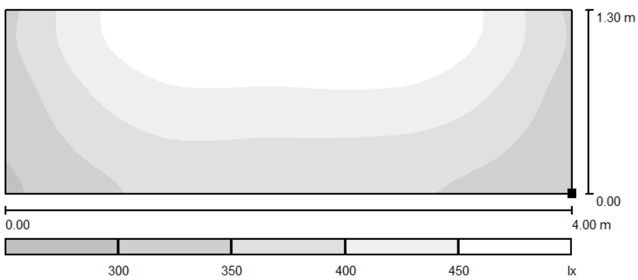

f) Distribution of illuminance on the board

Figure 4 – Example of the most common recent illumination technique

- **Line arrangement of luminaires for fluorescent lamps without any optics** (Fig. 2d): visible bare lamps provide higher luminous flux than with a diffuser but glaring is too high. Lighting quality is similar than in the previous case.

- **Line arrangement of luminaires for fluorescent lamps with a shade** (Fig. 2e): the shade on one side of luminaire prevents from glare and its inside painting acts as a reflecting diffuser to direct luminous flux from lamps toward the plane of board. This solution provides much better illumination, however, it is not common.
- **Line arrangement of luminaires for fluorescent lamps with louvres:** can be found in newer installations. Single lamp luminaires are not specifically dedicated for illumination of vertical planes. Half of luminous flux is directed away from the board.

2.3 Present technical solutions

The most common illumination technique is depicted in Figure 4. Because school board is a vertical plane, the best technical solution comprise the installation of luminaires with asymmetrical reflectors (Fig. 4a).

Normally a pair of luminaires is used in a linear arrangement. For short boards a single luminaire is sufficient. Spiral-shape based reflector efficiently directs the luminous flux towards the board and prevents from glare on the other side. However, this solution also has several shortcomings, listing two of them:

- Luminaires are intended to be mounted on ceiling or suspensions, mounting height can be thus set as desired but luminaires can hardly be tilted.
- To provide uniform vertical illuminance asymmetrically, lamp need to be positioned precisely according to the reflector. All such luminaires are therefore manufactured as single lamp luminaires. Luminous flux from a single lamp is not sufficient to provide 500 lx illuminance, regardless on the flux (or wattage) of lamp used. The only solution of this problem is to install two luminaires side by side (parallel) to each other to double the luminous flux. However, installation costs are then doubled as well and this approach is usually rejected by investors.

Case study calculation presented in Fig. 4 by means of a pair of 1x 80 W luminaires showed the difficulty to reach the 500 lx level although, as seen in Fig. 4c, the luminous flux is efficiently used up to illuminate the area of school board almost from edge to edge. At the maintenance factor f_M = 0,80, resulting maintained illuminance is calculated as 405 lx with uniformity of U = 0,73.

2.4 Previous research results

In the framework of auditing of schools and educational buildings, illuminance on school boards have been measured in the 3 x 3 grid of points for old lighting systems. Nearly 100 buildings have been audited, in each building 2 – 3 school boards have been measured. Results of measurements published in [3] and [4] have been used as pre-study to acquire opinion on the lighting quality of old systems, tu support the necessity of re-construction and to run a more complex research on illumination of school boards. Besides other parameters, lighting systems in the state before refurbishment are still subjected to the measurement of illuminance but the grid density was increased to 3 x 9 points.

3 Methodology

Research on illumination of school boards is based on gathering data from numerous measurements of lighting systems. Evaluation of the satisfaction of users or similar methods based on observers are not in scope of the current research. Research objectives comprise different lighting regimes, position of observers for measurement of luminance, analysis of the critical detail of different sizes, comparison of the lighting quality before and after renovation, comparison of calculated and real parameters etc. This paper is focused on partial research tasks passing attention to the crucial parameters of illumination – illuminance, luminance and reflectance. Description of the research methodology is hereby limited to the studied subjects only.

Up to now, two school buildings in Bratislava have been completely measured both before and after refurbishment of lighting systems. Big cluster of data is still being processed, thus in this paper only results for one object in the state after re-construction are being presented.

Identification of the object is: Primary school in Bratislava, Pankúchová street, where all 30 school boards – 29 green and 1 white, have been measured. In the other building, black boards and white boards are prevailing, but results are yet unavailable.

Boards have been duly cleaned before the measurement to avoid increase of luminance on chalk residues. Illuminance has been measured in the grid of 27 points as illustrated in Fig. 6. The grid was only marked on the rim of boards not to disturb the measurement of luminance which was measured simultanously (Fig. 5). Luminance was measured from the rear wall in the centre of its width, in height of 1 m corresponding to the average eye height of sitting pupils. Differences in eye height around the chosen value is not significant and can be neglected. Other positions of observers have been also measured but not included in this paper. Lighting system was put into operation at least 15 minutes before the measurement and both the main lighting system and the school board dedicated luminaires have been switched on.

To assess the perception of information on school boards, text containing ABC and an additional "X" letter in three sizes according to different age of pupils, as commonly used in the teaching process, have been written and centered on the board (Fig. 5). The three sizes correspond to: first two classes, transient from 4th to 5th class (1st and 2nd degree of primary education) and last two classes. Image captured for the luminance analysis shows this text, the whole school board and sufficient area around the board, where illuminance has also been measured in points depicted in Fig. 6 – X_A, X_B, X_C, Y_2 and Z_2.

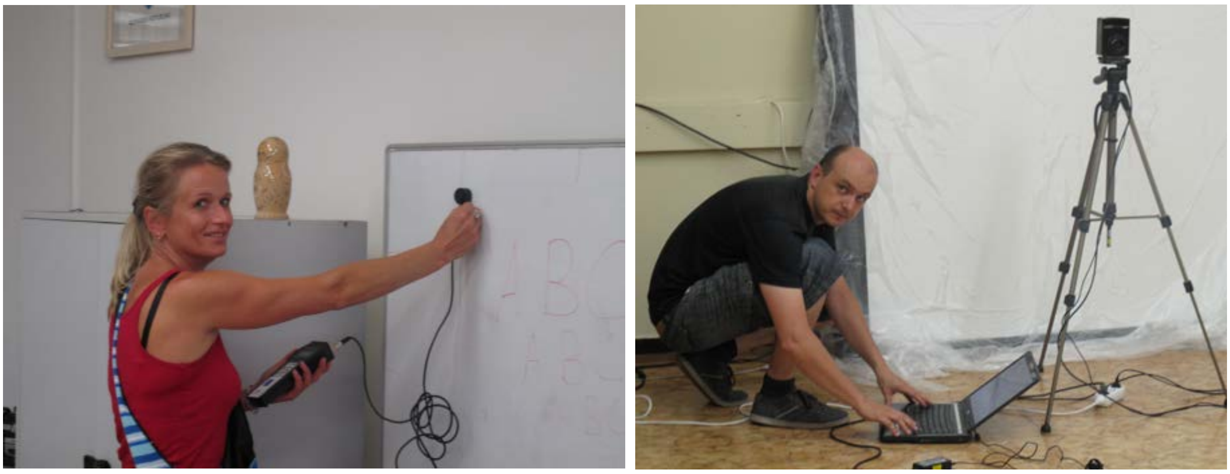

Figure 5 – Measurement of illuminance (left) and luminance (right) of school boards

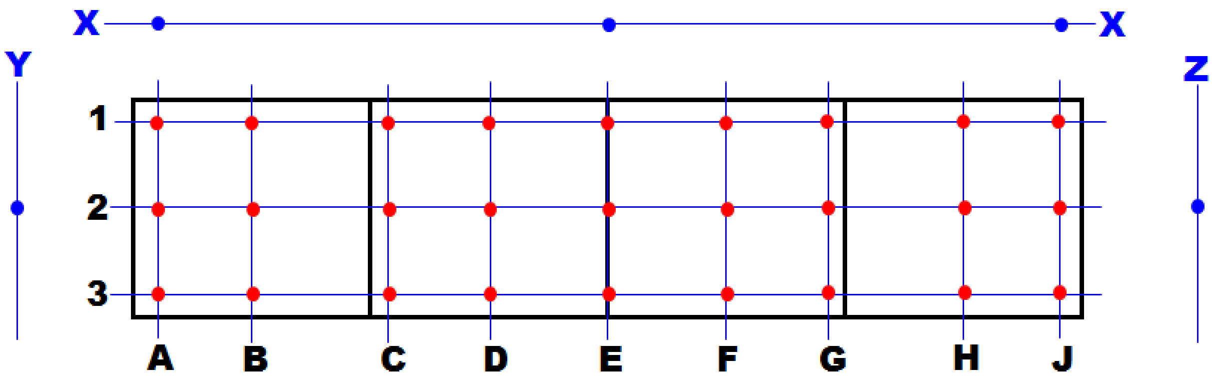

Figure 6 – Grid points on the board plane

4 Results & Discussion

Measurement results for maintained illuminance E_m, maintained luminance L_m, uniformity of illuminance U_E and luminance U_L are presented in Table 1 for green boards and in Table 2 for a single white board. Reflectance of school boards has been calculated from the measured values of luminance and illuminance, taking into account diffuse nature of reflection, as follows:

$$\rho = \frac{\pi L}{E} \tag{1}$$

For white board the reflection is semi-specular but for aims of this particular investigation the differences can be neglected. Reflectance has been calculated in individual points, Table 1 shows the average values.

Luminance in specific points around the board have been acquired and analyzed as well. The results are summarized below.

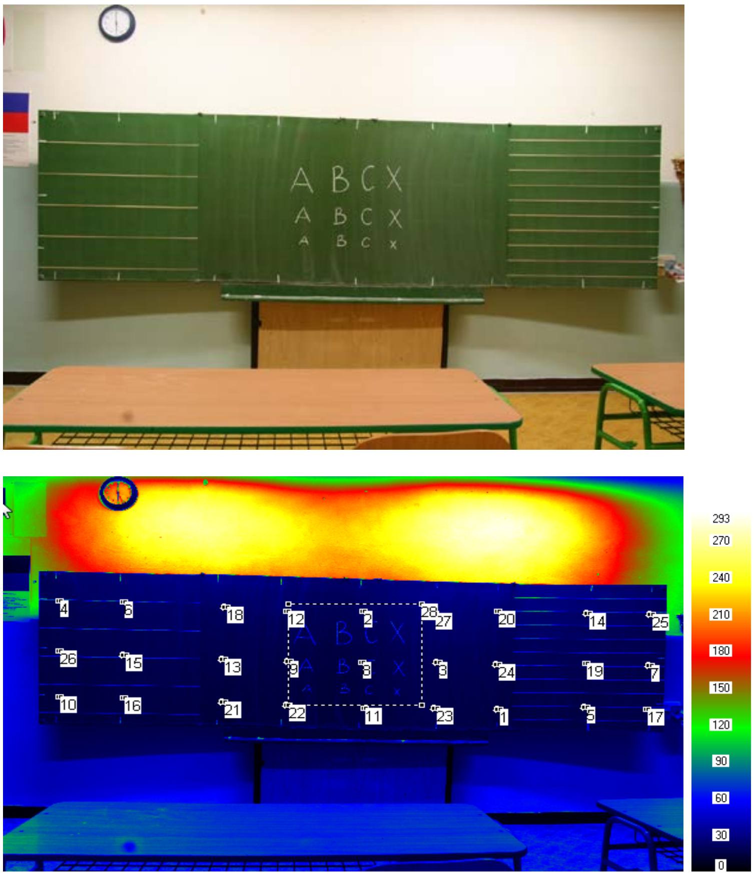

Figure 7 – Green board in the room No. 1 and its luminance map

<u>Average luminances</u> taken from the measurement of 29 green boards:

Wall over the board: **250 cd.m^{-2}**

Board background: **20 cd.m^{-2}**

Board foreground (text): **50 cd.m^{-2}**

Wall surrounding the board: **60 cd.m^{-2}**

White sheet of paper attached to the board: **140 cd.m^{-2}**

Table 1 – Results of measurement of the illuminance on schoolboards

Room No.	E_m (lx)	U_E	L_m ($cd.m^{-2}$)	U_L	ρ
2	540,4	0,742	21,67	0,685	0,126
1	576,5	0,739	21,48	0,716	0,117
18	778,9	0,763	17,24	0,642	0,070
230	521,8	0,782	18,60	0,718	0,112
231	662,3	0,752	21,16	0,712	0,100
99	576,9	0,754	18,35	0,781	0,100
96	544,7	0,688	17,81	0,805	0,103
94	522,0	0,826	23,64	0,811	0,142
95	553,4	0,804	18,80	0,713	0,107
97	555,7	0,812	20,76	0,837	0,117
108	486,7	0,775	15,01	0,782	0,097
109	564,8	0,825	18,63	0,758	0,104
110	530,3	0,815	14,85	0,784	0,088
111	509,3	0,830	15,71	0,885	0,097
112	539,7	0,719	16,57	0,772	0,096
82	550,0	0,647	18,43	0,757	0,105
83	548,4	0,682	24,64	0,746	0,141
85	564,9	0,735	21,04	0,765	0,117
86	540,2	0,750	19,37	0,780	0,113
74	545,1	0,754	22,27	0,741	0,128
77	579,3	0,615	19,46	0,780	0,106
78	500,9	0,759	34,64	0,494	0,217
79	528,7	0,817	17,03	0,827	0,101
55	489,1	0,738	16,61	0,732	0,107
56	507,9	0,693	27,89	0,563	0,173
57	488,7	0,745	16,40	0,753	0,105
58	543,5	0,782	19,08	0,771	0,110
214	478,0	0,590	16,77	0,657	0,110
215	501,3	0,672	19,74	0,701	0,124
Average	**545,8**	**0,745**	**19,78**	**0,740**	**0,115**
MIN	478,0	0,590	14,85	0,494	0,070
MAX	778,9	0,830	34,64	0,885	0,217
StDEV	**58,2**	**0,062**	**4,11**	**0,079**	**0,027**

Table 2 – Results of measurement of the illuminance on schoolboards

Room No.	E_m (lx)	U_E	L_m (cd.m^{-2})	U_L	ρ
232	447,7	0,884	100,41	0,889	0,705

Over the table there is an intense light spot although maximum luminous flux is directed to the board plane. Ratio of luminance between the white wall and green board is more than 10:1. Luminance of the white chalk writing is as much as 50 cd.m^{-2} with contrast 2,5:1 to the background but blank white sheet of paper (reflectance 80 %) has luminance much higher. Letter lines are thin and their reflectance is only about 25 – 30 %. Luminance value similar to foreground has the wall around the board, painted light green.

Figure 8 – White board in the room No. 232 and its luminance map

Average luminances taken from the measurement of 1 white board:

Wall over the board: **90 cd.m^{-2}**

Board background: **100 cd.m^{-2}**

Board foreground (text): **70 cd.m^{-2}**

Wall surrounding the board: **110 cd.m^{-2}**

For white board the situation is different. Luminance of the board and white walls around are approximately the same. Letter lines are here very thin, too. Contrast of the text against background is 0,7 in comparison to 0,4 for green boards, i.e. much worse. It is because the trace of black ink is not solid enough, mainly at faster movement of pen.

5 Conclusions

Information presented in this paper should be considered as interim results of study on illumination of school boards, being a part of a comprehensive research in this area. In the current stage, data are being processed, sorted and analyzed from different points of view. Further gathering of data is continuously running but only for certain missing school board types and some special illumination techniques from the past are sought. Basic collection of measured data is, however, already finished. The aim is to have about 100 – 120 school boards measured, in total.

Results showed that luminance distribution maps of illuminated green boards and white boards are significantly different. But for the same school board type, the results are comparable with very small deviations from the average. Reflectance of white board is 70 % while reflectance of green board is about 10 %. Reading of green board is more comfortable but less energy efficient. It can be expected that due to advantages of white boards these will be preferred but to create a good visual environment of users, specific requirements should be set up not only for illumination. For example, to highlight the board on the front wall a darker painting of the wall can be recommended.

Acknowledgements

This publication is the result of the project implementation:
Research centre of light and lighting technology, ITMS 26220220150,
supported by the Research & Development Operational Programme funded by ERDF.

Operačný program VÝSKUM a VÝVOJ

Agentúra
Ministerstva školstva, vedy, výskumu a športu SR
pre štrukturálne fondy EÚ

Podporujeme výskumné aktivity na Slovensku/
Projekt je spolufinancovaný zo zdrojov EÚ

Európska únia
Európsky fond regionálneho rozvoja

References

1. ISO 8995-1:2002(E)/CIE S 008/E:2001. Joint ISO/CIE Standard: Lighting of Work Places - Part 1: Indoor. Vienna: CIE 2001.

2. EN12464-1:2011. Light and lighting – Lighting of workplaces. Part 1: Indoor work places. Brussels: CEN 2011.

3. GAŠPAROVSKÝ, D. - SMOLA, A. 2013. Illumination of School Boards in Educational Buildings. In Proc: LUX EUROPA Krakow 2013: 12th European Lighting Conference. Krakow, Poland, September 17-19, 2013. Warszawa: Polski Komitet Oświetleniowy SEP, 2013. ISBN 978-83-910849-6-0. pp. 547-553.

4. GAŠPAROVSKÝ, D. - LIESKOVSKÁ, L.: Characteristics of the Illumination of School Boards. In Proc: Svetlo - Light 2013: 20th International Lighting Conference. Podbanské, Slovakia, 23.-25.10. 2013. Bratislava: KONGRES Management s.r.o., 2013. ISBN 978-80-89275-35-9. pp. 156-165.

PP37

ILLUMINATION SYNTHESIS AND PLAYBACK BY A LIGHT PLAYER

Dmitri Simonian, **Steven Paolini**
Telelumen LLC, Saratoga CA, USA
steve@telelumen.com

Abstract

Since the last century industry and science have been making great progress in creating and qualifying light sources that approximate natural illumination. Improvements in LED and phosphor technologies have made it possible to achieve impressive luminous efficiency and high colour rendering by commercially available luminaires. More recently, lighting community has begun thinking about new things that can be done with LED lighting. Light sources with illumination spectra designed for specific purposes, such as Xicato Vibrant Series (Xicato, 2013) or GE Reveal (GE Lighting, 2013), have emerged. We discuss the next generation of highly tunable light sources built to create useful, accurate, and time-varying illumination. A full day of sunlight on the beach, or light around sunset, or light under tree canopy on a windy day, are just a few examples of what is now possible.

Keywords: Electronic Illumination Systems, Quality of Light, Colour Tuning, Light Player, Colour Vector

1 Multichannel luminaires

Luminaires capable of reproducing a variety of lighting conditions generally have 3 or more independently controllable light channels, where each channel is an electrically connected set of LEDs of a particular type. A luminaire controller defines drive levels on each light channel. A drive level can be set by duty cycle in the case of pulse-width modulation (PWM) control, by DC current in the case of amplitude modulation (AM) control, or both. Combined PWM/AM control is desirable for high dynamic range of luminous output.

A luminaire with a larger number of independently controllable light channels is capable of producing a greater variety of spectral shapes. One may be wondering why this is necessary. A large fraction of visible gamut is available with just three independently controllable light channels, for example: red, green and blue. By adjusting drive levels the colour point of light emitted by the luminaire can be brought to match any desired colour point within the gamut defined by the three channels.

A basic three-channel luminaire is capable of synthesizing a desired (target) light in the sense that the target and the synthesized illumination will appear indistinguishable to one’s eye so long as one is looking directly at the two light sources or at reflections of the two light sources by a neutral white diffuser. Synthesized and target light may have dissimilar spectra but they will appear the same to one’s eye if their tristimulus values match. Three degrees of freedom provided by a 3-channel luminaire are adequate for matching three tristimulus values.

Even though target and synthesized illumination may have matching tristimulus (or, equivalently, matching luminous fluxes and colour points), the colours of a scene under target and synthesized illumination will not match in the general case. Perceived colour of light emitted by a source is fully defined by its tristimulus values. Perceived colour of light reflected by an object is defined by the spectral power distribution of the incident light and by the reflectance spectrum of an object.

Therefore, additional degrees of freedom (more light channels) are required for reproducing not only the appearance of the target light, but also the appearance of a scene illuminated by the target light.

Illumination may be worth reproducing for various reasons: it may be pleasant and comforting (e.g., sunset), or may be interesting because it is not easily found in daily life (e.g., light under water), or may be specific to a certain event (e.g., light during a solar eclipse, light emitted by a ball lighting), or may be practical (e.g., lighting tuned to "improve" the appearance of vegetables at a grocery store; lighting tuned to suppress or encourage melatonin production). A software-controlled luminaire is also capable of creating time-changing illumination conditions, for example, synthesizing a full day of sunlight.

2 The method of illumination synthesis

Let's formulate mathematically the goal of reproducing desired lighting by an M-channel luminaire. In the discussion that follows we introduce certain new terms that are defined in the appendix.

In order to reproduce the desired illumination we could decide to minimize the root-mean-square (RMS) difference between the desired and the synthesized spectral power distributions (SPD) by varying drive levels of an *M*–channel luminaire. If target spectral power distribution could be fit by the spectra emitted by *M* channels with high accuracy, all photometric characteristics would match, and thus minimizing RMS difference would be a valid objective. In reality *M* is a small number – for example, between 4 and 16 –and a good fit to target would in general be difficult to achieve due to a limited variety of spectral shapes that can be formed as linear combinations of channel spectra.

A more relevant optimization goal could be formulated as follows: minimize RMS differences between three-dimensional colour points (tristimulus values) of target and synthesized lights reflected by colour standards taken from a certain test palette.

Presumably, the colours of the palette are chosen to represent the coloured objects of the scene. The palette may also be generic, for example, a set of 15 saturated colours of CQS test samples (Davis, Ohno, 2010), or an original set of 8 CRI test samples. The following expresses the objective function of the fidelity of light reproduction:

$$F = \sum_{v=1}^{V} w_v \left(\mathbf{t}_s^v - \mathbf{t}_t^v \right)^2 \tag{1}$$

Here $\mathbf{t}_t^v$ is the colour point (a row-vector) of sample v from the test palette illuminated by the target light, and $\mathbf{t}_s^v$ is colour point of sample v from the test palette illuminated by the synthesized light. Colour point components for sample v can be found as scalar products of 3 colour matching functions with the spectrum of light reflected by a test sample. There are V samples in the test palette, so index v runs from 1 to V. Weights w_v are all set to 1 by default, but can be adjusted to reflect the relative importance of reproducing the appearance of certain colour samples, or to account for non-uniformity of the colour space.

Colour points of samples illuminated by synthesized light $\mathbf{t}_s^v$ depend on channel drive levels, and therefore, the merit function in Equation (1) a function of *M* drive levels.

In most cases minimization of the merit function will have to be done under the constraint of matching the tristimulus values of target and synthesized light. Another way to express this constraint is to require that the colour point of target and synthesized light reflected by a perfect white colour sample match:

$$\mathbf{t}_t^0 = \mathbf{t}_s^0 \tag{2}$$

Index 0 in Equation (2) signifies the "zeroth test sample" of the palette – an ideal white reflector.

To cast the definition of the merit function into a form suitable for a straightforward iterative minimization, we introduce the concept of a "colour vector". A colour vector is a characteristic of emission spectrum with respect to the chosen colour palette. It is defined as a vector of tristimulus values of light reflected by colour samples of the test palette. This vector is a compact representation of spectral power distribution. It is also a lossless representation with respect to the chosen colour palette. A colour vector has 3V components:

$$\mathbf{r} = [\ \mathbf{t}^1 \quad \mathbf{t}^2 \quad \ldots \quad \mathbf{t}^V\ ]^T \tag{3}$$

We now form a luminaire colour matrix $\mathbf{R}$ by stacking M colour column-vectors, one for each light channel, each normalized by the channel drive level:

$$\mathbf{R} = [\ \mathbf{r}_1 \quad \ldots \quad \mathbf{r}_M\ ] \tag{4}$$

Now the colour vector of synthesized light is $\mathbf{r} = \mathbf{Rk}$ where k is a column-vector of M drive levels, and the merit function from (1) can be written in the form of RMS difference between the target and synthesized colour vectors:

$$F(\mathbf{k}) = \left|\mathbf{r}_t - \mathbf{Rk}\right|^2 \tag{5}$$

Merit function F is then minimized iteratively with respect to drive level vector $\mathbf{k}$. In some cases the components of the luminaire colour matrix $\mathbf{R}$ depend on drive levels, and the matrix has to be recalculated continually in the course of iterative minimization.

3 Example luminaires and the accuracy of illumination synthesis

Let's now consider a 5-channel luminaire comprising red, green, blue, phosphor-converted amber, and neutral white LEDs. In Figure 1 we show target daylight at colour temperature of 5000K and 1000 lumens vis-à-vis the light emitted by this luminaire synthesized to match the appearance of 15 colours of the CQS test palette under this target light.

The plots in Figure 1, 2, and 3 should be read as follows:

In the top left plot, the desired (target) SPD is shown by a blue curve, and the SPD synthesized by the luminaire to match the target is shown by a black curve. The horizontal axis is wavelength in nm. Synthesized SPD is a sum of emission spectra of luminaire channels at optimum drive levels calculated by minimization of the merit function in Equation (5) under the constraint of Equation (2).

The CIE (x, y) plot (top right) shows the colour point of the desired light (blue cross), the colour point of synthesized light (open black square), and colour points of channel spectra (gray circles). The area of a gray circle is proportional to the luminous flux contributed by the corresponding channel. For example, referring to Figure 1, the green channel contributes 144 lumens to the total luminous flux of 1000 lumens; the phosphor-converted amber channel contributes 5 lumens, and so on.

The bottom right plot shows a portion of (x, y) color space.

Lastly, coloured circles in the bottom left plot represent the colour points of the CQS palette illuminated by target light, in a*, b* axes of CIELAB colour space. Circle radius is 2 just noticeable differences (JND). Black contour with open circles represents rendering of this palette by synthesized light. If centers of open circles fall within the coloured circles, appearance of colour standards under the synthesized light is less than 2 JND away from target. White point for La*b* calculations is fixed at 5000K in all figures. It is worth mentioning that we use CIELAB colour space to visualize the solution obtained by our method of light synthesis, but the method itself does not rely on CIELAB color space. Only the most basic information, namely, three color-matching functions, is needed to solve the merit function minimization problem.

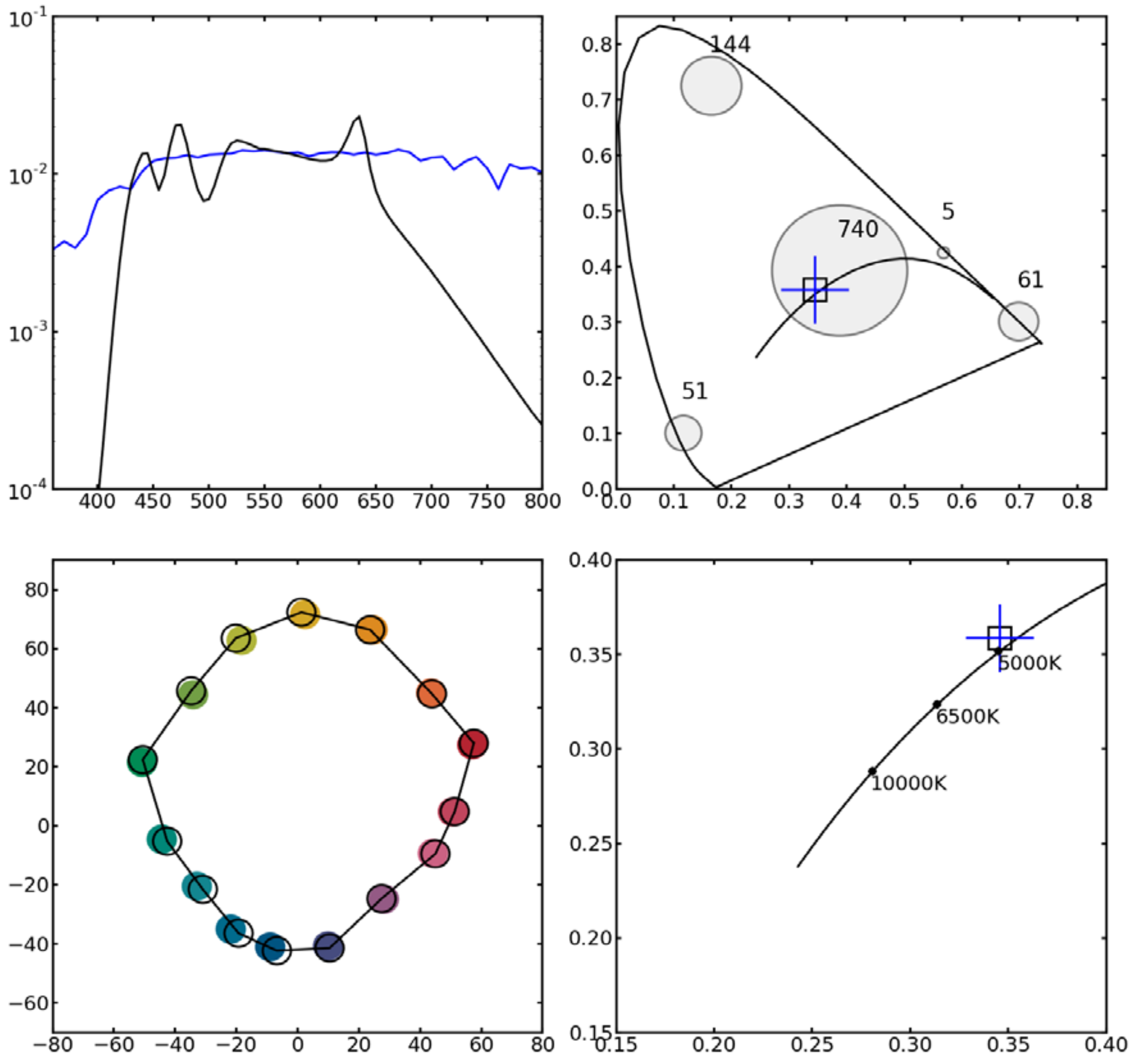

Figure 1– 1000 lumens of 5000K daylight synthesized by a 5-channel luminaire

The SPD match in Figure 1 would generally be considered poor, but since our eyes are not spectrometers, the fidelity of light reproduction should be evaluated on the basis of appearance of the colour palette. Looking at the La*b* plot (bottom left), we conclude that the apparent colour point of each colour standard in our palette when illuminated by the synthesized light is within 1JND of that when illuminated by the target light. In other words, even though SPD shapes of the two spectra are quite dissimilar, the appearances of the colour palette under synthesized light and under target light are nearly identical. This justifies the choice of optimization goal formulated in Equation (**5**).

To illustrate the importance of the number of degrees of freedom of the light source, let us consider light under water, and try to reproduce the lighting 50 ft below the ocean surface. We calculate the target as a product of daylight spectrum at 5000K and the absorption spectrum of 50ft of water, using the water absorption coefficient (Buiteveld, 1994). Water predominantly absorbs long wavelengths, causing strong attenuation of red and yellow at such depths. An attempt to accurately replicate the underwater lighting by a 5-colour luminaire is presented in Figure 2. Now looking at La*b* plot (bottom left) we conclude that the approximation of the underwater lighting is marginal. Rendering of warm colours (yellow, orange, red) is particularly inaccurate: the difference between target and approximation is up to 8 JND. The reason for this is that no light channel of this luminaire has a spectral shape appropriate for reproducing the sharp attenuation of emission above 600nm: the spectra of both phosphor-converted LEDs are too broad, while red, blue and green direct LEDs have no emission around 600nm.

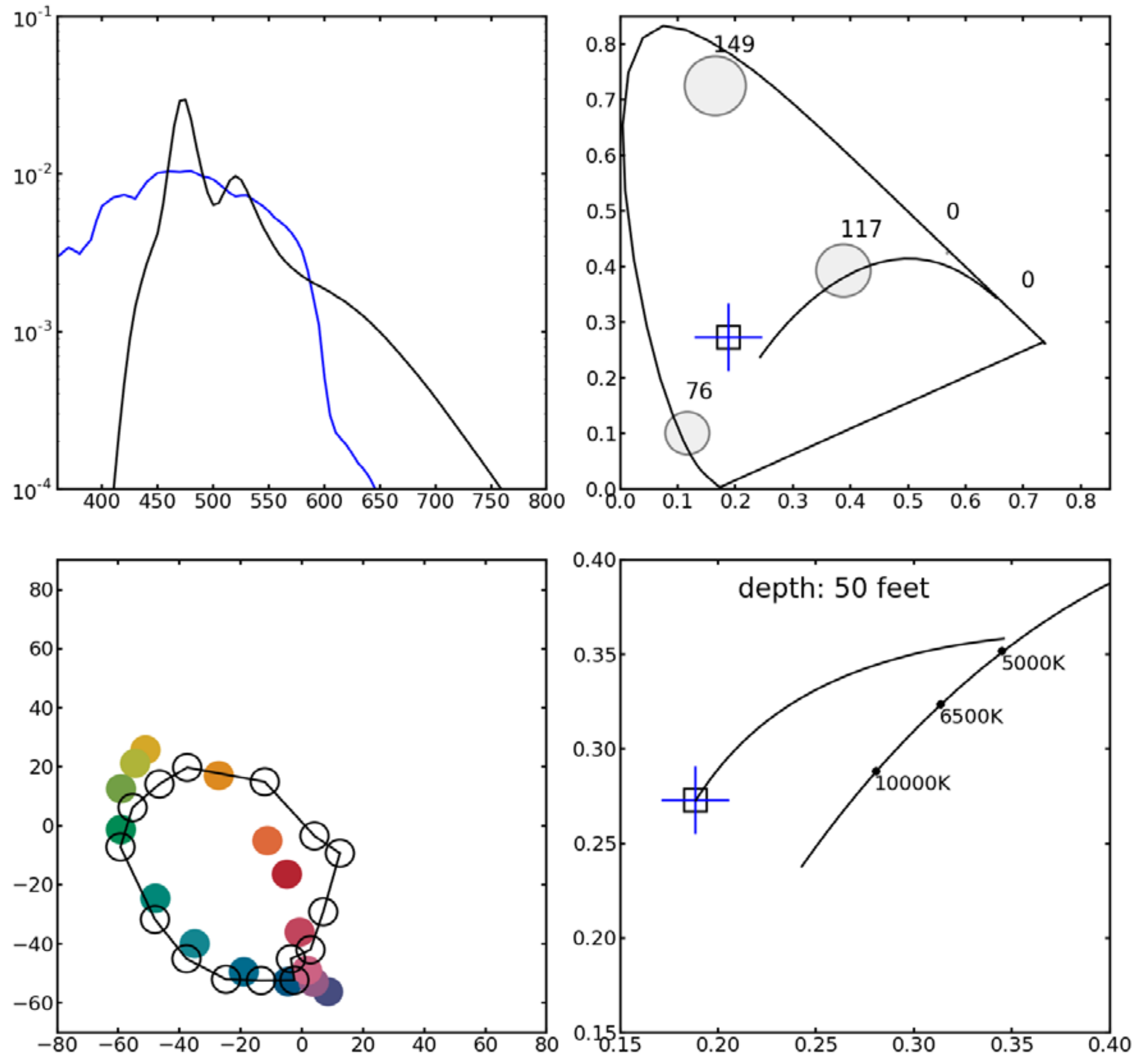

Figure 2– Natural light 50 feet under the ocean surface synthesized by a 5-channels luminaire

If we construct a light source with a larger number of appropriately chosen channels, we will gain adequate tenability to accurately reproduce the desired underwater lighting. The result in Figure 3 is produced by a 9-channel light source comprising royal blue, blue, cyan, green, deep green, amber, phosphor-converted amber, red, and neutral white LEDs.

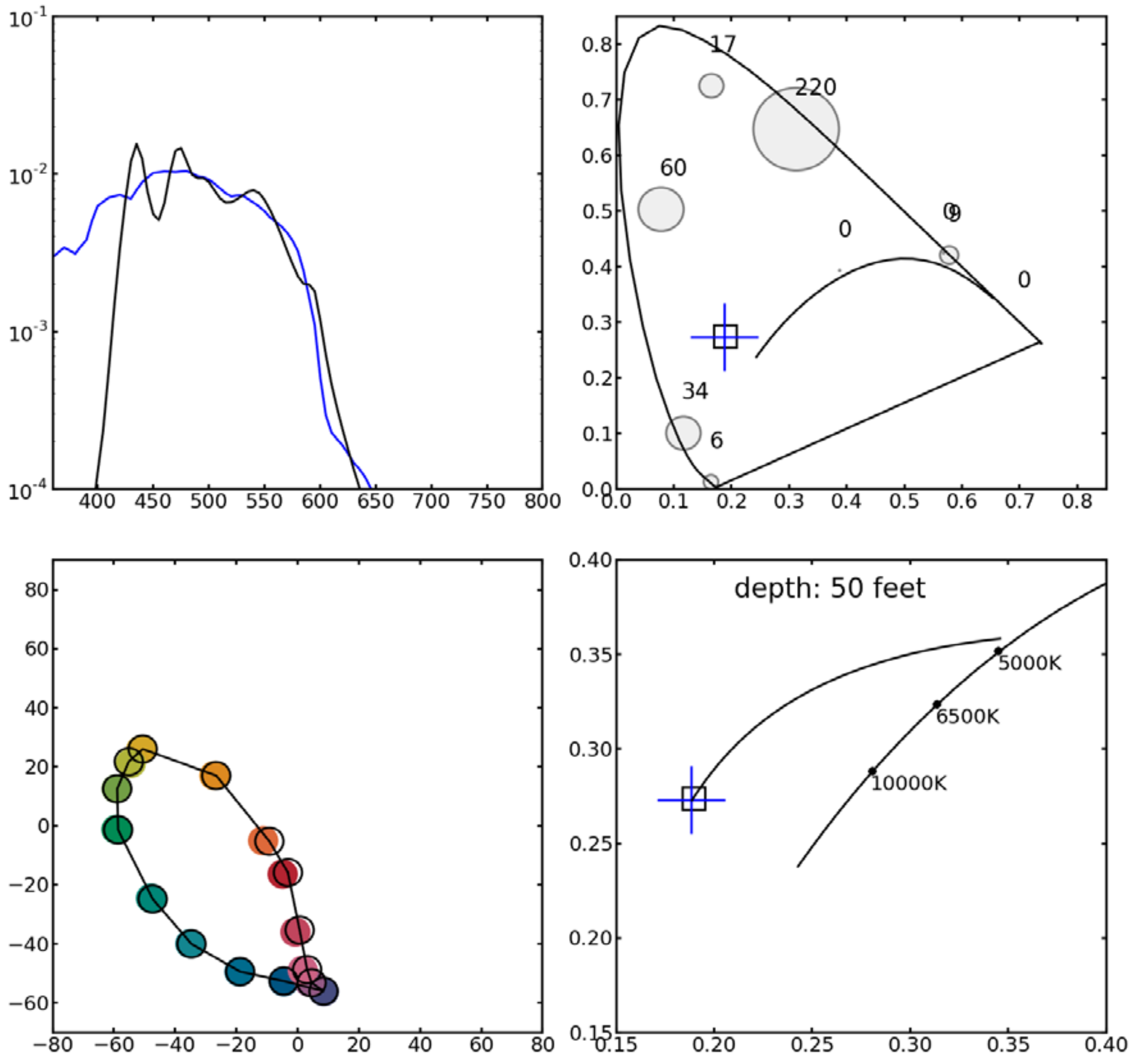

Figure 3– Underwater lighting synthesized by a 9-channel luminaire

Having a total of 7 direct LEDs among 9 channels allows us to replicate the attenuation of sunlight at wavelengths longer than 600nm (top left plot of Figure 3) accurately enough to achieve exact reproduction of the appearance of the colour palette, since all test samples of a palette are within 1JND of target (bottom left plot in Figure 3).

How many and what kind of independently controllable light channels are adequate depends on the allowable inaccuracy of colour rendering, the variety of target lighting spectra, and cost. 5 channels in our first example are adequate for synthesizing natural sunlight. The component LEDs of this luminaire were chosen to provide “narrow” channels for broad gamut (direct red, green, and blue), as well as “broad” channels (phosphor-converted white and amber) for acceptable colour rendering in a broad range of CCT.

To illustrate the point of the previous paragraph, a series of daylight and thermal spectra with colour temperatures between 1000K and 8000K were synthesized by a 5-channel luminaire according to the optimization goal in Equation (5). Contributions to luminous flux by different channels are shown in Figure 4.

Colour rendering measured by CRI is excellent between 1800K and 6500K. In this range: R_a> 90 and R_9> 50. All channels are necessary for this degree of light reproduction accuracy: each channel contributes at least 10% of the total flux at its wavelength of maximum contribution.

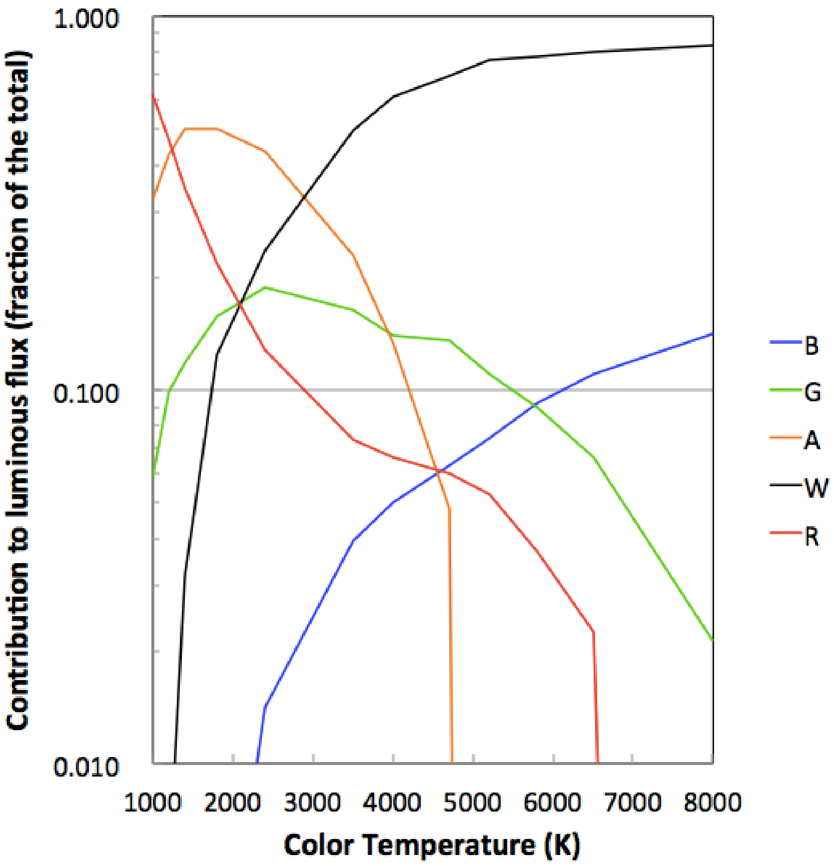

Figure 4– Contributions of red, green, phosphor-converted amber, white, and red channels of a 5-channel luminaire to synthesized white light with colour temperatures from 1000K to 8000K

Daylight at 8000K synthesized by this 5-channel luminaire has R_a =86 and R_9 = 72. By contrast, the 9-channel luminaire considered above can synthesize a much better approximation of daylight at 8000K with colour rendering indices R_a = 99 and R_9 = 98. This shows that adding properly selected light channels to the luminaire extends the range of colour temperatures where synthesized light has adequate colour rendering.

As we saw in the example of light underwater, a larger number of channels may be required to synthesize special lighting. In certain applications hybrid channels may be formed by electrically connecting dissimilar LEDs, in order to alter the shape of channel emission spectra without increasing the number of independently controllable channels.

Summary

We provide a general method of approximating useful time-varying or constant lighting by modern electronic illumination systems.

Existing light quality metrics are inadequate, as the gamut of sources and/or reflectors are limited to a few standard cases. We propose a general solution to maximizing light quality as it applies to arbitrary lighting conditions. It allows for any desired illumination and any set of colour reflectors to serve as the target, and for any set of sources to synthesize the best solution for the target. Target illumination could be, for example, time-varying light of a dimmable incandescent lamp, or a full day of sunlight, or shimmering candle light. The colour reflectors could be a set of ripe fruit, or a palette of CQS test samples, or a set of paints. The best solution minimizes the differences between the tristimulus values of target and synthesized light reflected by the colours of the palette. We provide examples that illustrate the effect of adding colour channels on the accuracy of light synthesis. By applying our method, designers of modern electronic luminaires can reproduce any time-varying composition of illumination effects with high fidelity.

Appendix – Definition of terms used in this paper.

Channel spectrum: Spectral power distribution of light emitted by an independently controllable channel of a multichannel luminaire, at a certain drive level.

Colour vector: A vector of tristimulus values of a given light reflected by colour samples of the test palette. This vector is a compact representation of spectral power distribution. The colour vector has $3V$ components, where V is the number of colours of the test palette.

Luminaire channel: One of a number of independently controllable light sources within a luminaire.

Luminaire colour matrix: a $3V$ rows by M columns matrix of colour column-vectors of M light channels, with each colour vector normalized by the corresponding channel drive level.

Target colour vector: A colour vector that corresponds to the desired (target) illumination.

Test palette: A collection of reflective samples with known spectral reflectances. Examples of test palettes are: an expanded set of 14 CRI colour samples, 15 CQS colour samples, or a proprietary set of reflective samples.

References

BUITEVELD, H., HAKVOORT, J. M. H., DONZE, M. 1994. The optical properties of pure water, SPIE Proceedings on Ocean Optics XII, 2258, 174--183, (1994).

DAVIS, W., OHNO, Y. 2010. Color quality scale, Optical Engineering 49(3), 033602, March 2010

GE LIGHTING 2013.GE Lighting Reveals New LED Bulb as Its Chief Innovation Manager Shares Glimpse of What’s Ahead, pressroom.gelighting.com/news

XICATO 2013. Xicato’s Colour Scientists Design New Light for Richer, More Vivid Colors, www.xicato.com

PP38

GOALS FOR ENERGY EFFICIENT LIGHTING PUT INTO HIERARCHY

Monica B. Säter
Department of Architecture, Chalmers University of Technology, Gothenburg, SWEDEN

Abstract

This paper shows some data from a post doc project performed at Chalmers in Gothenburg,

Sweden. In the project was the design of energy efficient lighting analyzed and was related to models and goals for lighting design. The result of the analysis reveals that energy efficient lighting often is seen as a change from a non energy efficient light source to a more energy efficient alternative. But energy efficient lighting needs to be seen from a broader perspective to fully contribute to a decrease of direct and indirect negative effects by the use of artificially emitted photon flows. Not only the production of electrical power used for lighting, is a burden for nature (indirect effects). The use of artificially photon flows can in the same way give negative consequences for human diurnal rhythm and be a disturbance for the life of animals, plants and to eco systems as well (direct effects). Despite the use of an energy efficient light source that decrease the amount of energy used for lighting, the problem with a negative impact on humans and nature from artificially emitted photon flows is still not fully solved.

1 Introduction

In this study was the way daylight appeared in a space during 2013 analyzed and the precise need for a complementary lighting manually designed hour by hour during the test days. In the beginning of the study was the energy saving lighting design process (E-LDP) and eco lighting design process (ECO-LDP) developed. Based on E-LDP was a lighting application installed and followed during a year. Data was analyzed and combined with the result from a literature review. When data from the study were evaluated, the result was compared to other models for lighting design. The models were used theoretically in the same daylight measured during the year. Energy use for the year was calculated. It was evaluated if goals about a pleasant space, support for the user psychologically, physiologically and visually (PPV) and energy efficiency where fulfilled or not. From the work with the lighting application in the study were the analysis originated about hierarchy in goals for energy efficient lighting design and performed as a part of the study.

1.1 Direct and indirect negative effects

The design of the energy efficient lighting application can be done in many ways. When old lighting applications are renovated or new are installed, it is a costly process and it is an advantage if this is done in a way that reduces both direct (impact from artificially emitted photon flows) and indirect negative effects (from the production of energy) of the use of lighting for both indoor and outdoor environments. If the indirect negative effects are reduced in a way that increases the direct negative effects, the investment in a new lighting application is not done in a fully successful way.

1.2 We are not alone on the planet

How to design energy efficient lighting is concerned the four steps of the lighting design process and the interaction between man, light, colour and space. But it concerns not only direct effects on humans from artificially emitted photon flows. We are not alone on the planet. The ways lighting applications are designed and being used, have a direct impact on animals and plants and ecosystems as well. As an indirect effect are the production of energy a burden for humans, animals, plants and ecosystems as well through the impact on the climate. For urban areas is the energy saving lighting design process developed in the project and for non urban areas, the eco lighting design process (ECO-LDP).

1.3 A two folded perspective

The way we design energy efficient lighting for the indoor and outdoor environment need to handle the direct impact from artificially emitted photon flows on humans and animals, plants and ecosystems as well as the indirect negative effects on nature of the production of electricity. From this two folded perspective (direct and indirect effects) can strong arguments be found for how to design the future energy efficient lighting application and evaluate if some goals are more important than others.

2 Methods

2.1 The development of the project

Phase 1.The development of the process of lighting design for energy efficiency (E-LDP) and eco-lighting design process (ECO-LDP).

Phase 2. Literature review.

Phase 3.The development of the lighting application.

Phase 4. The analysis of the way the daylight appeared during the year. The evaluation of when and where to use the three part system of the installed lighting application. Measurement of the ambient light for 23 occasions 8.00 a.m.-19.00 p.m. during the year.

Phase 5. Analyse of data from the study.

Phase 6. Criteria´s for the control of the lighting application where developed.

Phase 7. The future more advanced application was described. E-LDP and ECO-LDP was developed further.

Phase 8. The way the lighting was used was analyzed and values for when to switch on and when to switch off the lighting were developed.

Phase 9. The impact from the use of the lighting design process for energy efficient lighting in reduction in energy use where estimated nationally and on a European level (will be published in a future article).

2.2 E-LDP the lighting design process for energy efficient lighting (indoor environment)

E-LDP indoors. Introduction to the design: Theory as a start into the process. Theory about comparisons between models for lighting applications according to energy use. Evaluation of the fulfillment of goals when the specific model is used according to a pleasant space, support of the user psychologically, physiologically and visually.

Step1: The space is evaluated.

Step 2: The user´s needs are evaluated.

Step 3: The design of the daylight (shadings) and the complementary electrical lighting and the synchronization of them are performed. The design of the part of the lighting application placed opposite to the windows. The design of the part of the lighting application put in the ceiling. The design of the task lighting.

Morning: Daylight is used for ambient light the way it appears in the space. Complementary lighting is used if daylight does not contribute to a pleasant space. At first is the inner part of the space lit. If this is not enough the lighting application in the ceiling is lit.

Day: Daylight is used for ambient light the way it appears in the space. Complementary lighting is used if daylight does not contribute to a pleasant space. At first is the inner part of the space lit. If this is not enough the lighting application in the ceiling is switched on.

Afternoon: Daylight is used for ambient light the way it appears in the space. Complementary lighting is used if daylight does not contribute to a pleasant space. At first is the inner part of the space lit. If this is not enough the lighting application in the ceiling is switched on.

Step 4: Design of the lighting application as a system.

Completion: Evaluation if goals are fulfilled for a pleasant space, support psychologically, physiologically and visually and for energy efficiency

2.2.1 E-LDP, lighting design process for energy efficient lighting (outdoor environment)

In urban areas is the process developed towards the human need of a pleasant space and a safe visual orientation and a life without disturbance from unwanted lighting at the dark period of the day and night and throughout the year. In non urban areas can the ECO-LDP process be used that in a better way cope with the needs of not only humans need for light but the need of a dark night for animals and plants too.

E-LDP outdoors: Introduction to the design: Theory as a start into the process. Comparisons between models for lighting applications according to energy use. Evaluation of fulfillment of goals when the specific model is used according to a pleasant space, support of users living at the space, walking and driving.

Step1: The space is evaluated.

Step 2: The expected user´s needs are evaluated (living, walking, and driving).

Step 3: The design of the complementary electrical lighting as well as the synchronization of daylight and the complementary lighting are performed. Reasons to the design can be found in history, the present situation and in a future perspective of scheduled changes.

Morning: The complementary lighting follows the sunrise and stays on the lowest level for a pleasant space and for a safe visual orientation (lover than pleasant). The complementary lighting is taken away when daylight is enough.

Day: The complementary lighting stays during the day on the lowest level for a pleasant space and for a safe visual orientation, if needed.

Afternoon: Complementary lighting is used again if daylight does not contribute to a pleasant space and by that gives a visual support of the user.

Night: The level of light is as low as possible (moonlight is preferable during very late hours) but still being pleasant and give support for a safe visual orientation. Houses are protected from lighting entering gardens and houses.

Step 4: Design of the lighting application as a system.

E-LDP Completion: Evaluation if goals are fulfilled or not. The evaluation is concerned a pleasant space, support of a safe visual orientation, not being disturbed at night by lighting and for energy efficiency.

2.3 Literature review

In the post doc project was a literature review performed concerning methods for lighting design for energy efficiency and direct and indirect effects of the use of artificially emitted photon flows.

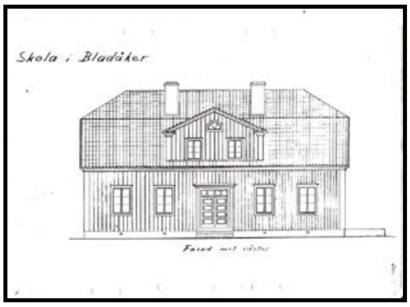

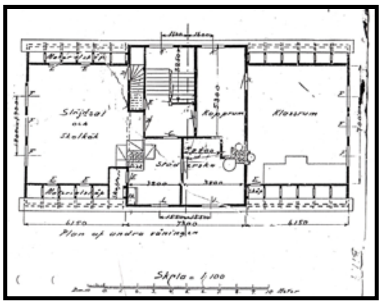

Figure 1 – Bladaker school

Figure 2 – The space used in the study (right part)

2.4 The lighting application

The space used in the study (Figure 2 Klassrum, the right part of the floor plan) was together with the lighting application seen as an interaction model. A lighting application was developed by the use of the lighting design process for energy efficient lighting and was followed during a year. Two times per month under 2013 was the ambient light measured vertically and horizontally every hour 8.00 a.m. - 19.00 p.m. in the afternoon (with the exception of January that had only one test day due to a late start of the project financially). Critical values for when to fill in daylight where recorded under the test days during the year. The ambient lighting was evaluated and the daylight filled in manually with a complementary electrical lighting when needed and only in the parts of the space that were evaluated as to dark. In this model was an active lighting used during the day and a more relaxing lighting during the afternoon. It was a three part system. Active wall lighting, relaxing wall lighting and relaxing lighting in the ceiling. In the work with the application were goals for energy efficient lighting developed.

2.5 The lighting application used in the study

The floor area, 54 m² (see picture above the right part of the floor plan named Klassrum. 3 Windows, size120cm x240 cm. 2 luminaries on the wall opposite to the windows equipped with LED (8,1W x7=56, 7/54 m². = 1,05W/m². 2 Luminaries on the wall equipped with Halogen (42Wx6=252/54 m²=4,66W/m²). 8 luminaries in the ceiling (down lights) equipped with Halogen 20Wx8=160W. 160W/54m²= 2,96 W/m².

2.6 A lighting application followed during a year

The lighting application was installed and the way the ambient light appeared in the space during the year were evaluated and measured. Daylight was filled in manually with a three part system in order to get an ambient light that contributed to a pleasant and safe space. Basic principles for dynamic control of the ambient light related to daylight where developed and tested during the year. The result of the study where compared to alternative models for lighting design theoretically used in the same lighting conditions as measured during the year.

2.7 Models for lighting design compared to each other

The chosen lighting design models, used in the study, were compared to each other. It was evaluated if they contributed to a pleasant space, a good support of the user psychologically, physiologically and visually and to energy efficiency**.**

2.8 Goals for lighting design

Data from the literature review and data about the way the ambient light appeared in the space studied during the year was put together and combined with the comparison between all models used for lighting design in the study. From this material was goal for lighting design written down and sorted out as more or less important.

3 Results

The method used for lighting design, the process performed and the goals the lighting designer strives towards, can by research, be developed and described.

3.1 Direct and indirect impact from the use of energy efficient lighting in the indoor environment

Negative effects from the indoor lighting, affect humans in two ways. Directly trough photon flows emitted by a light source that deviate from daylight in the way daylight appears at the space and on the time of the day. Indirectly by the production of electricity used for lighting that have a negative effect on nature and the climate.

3.2 Impact from the use of indoor and outdoor lighting

In the indoor environment, the use of daylight and a complementary electrical lighting represent quality of life and support for a safe visual orientation. But the use of lighting in a positive way need to be balanced towards how to avoid a direct negative impact on diurnal rhythm from the complementary electrical lighting and to decrease the indirect negative effect generated by the production of electricity used for lighting.

3.3 Impact from the use of energy efficient lighting in the outdoor environment

As for the indoor environment outdoor lighting affects humans, animals and plants in two ways. At first in a direct way trough photon flows emitted by a light source that deviate from daylight and indirectly by the production of electricity used for lighting that is a burden for nature and the climate. In the outdoor environment, the use of a complementary electrical lighting represents, as for indoor lighting, quality of life and a support or a safe visual orientation. But the need for outdoor lighting ought to be balanced towards the need of a decreased direct negative effect through the stress on diurnal rhythm not only for humans but for animals, plants and ecosystems as well and to the reduction of the indirect effects that are related to the production of electricity.

The direct negative effects of indoor lighting affects users on an individual level mostly. The direct negative effects from lighting in the outdoor environment is more severe and concern in a more complex way those humans, who live in the area as well as animals, plants and ecosystems.

3.4 Low direct and indirect effects from energy efficient lighting

Energy efficient lighting should be designed in a way that gives low direct and indirect negative effects for humans, animals, plants and ecosystems. This can be done by mimicking daylight in spectral composition, by the time when the lighting application are used and in the level of light used. If so, the human need for quality of life and for safe visual orientation by the use of lighting can in a better way be balanced against humans, animals, plants and ecosystems need for a support for life and diurnal rhythm, by the dark night.

3.5 Goals for an energy efficient lighting application put into hierarchy (indoors)

Based on the literature review and the analysis of the lighting application used in the study during the year and alternative models for lighting design was the following scheme for the design of the energy efficient lighting application developed for the indoor environment.

Reduction of direct negative effects (indoors)

- *The work with the design of the energy efficient lighting should have as a first goal, to reduce direct negative effects on those who use the indoor lighting.*

- The first goal is fulfilled by the use of daylight as much as possible. The user need to get the psychologically, physiologically and visually support from daylight under as many hours as possible during the year.

- It is also fulfilled by the use of a complementary electrical lighting with an energy efficient light source only lit when needed and in a restricted way.

- When daylight does not contribute to a pleasant and visual secure level of ambient light in the space the daylight should be completed with a carefully designed daylight mimicking, complementary electrical lighting.

- This complementary electrical lighting should be seen as ambient light for everybody and be completed with the individual task lighting seen as an individual tool for work.

- The level of complementary lighting that is designed to be pleasant and secure in the indoor environment for dark conditions, should in a dynamic way be increased to a higher level during daytime when daylight can be seen through the windows and differences between the ambient light in the indoor environment is on a low level (unpleasant) compared to the daylight that can be seen in the visual field of the user.

- When no daylight can be seen in the visual field, the level of light seen as pleasant and secure is lower. The exact level of light is dependent on the contrast situation in the space and the user´s needs for a safe visual orientation in the space.

Reduction of indirect negative effects (indoors)

- *The work with the design of the energy efficient lighting should have as a second goal, to reduce indirect negative impact from the use of indoor lighting.*

- This can be done by working with the direct negative effects in a successful way. Here the need for lighting is defined. The way we design and use the application have a direct effect on the indirect negative effects.

3.6 Reduction of direct negative effects outdoors

- *The work with the design of the energy efficient lighting should have as a first goal, to reduce direct negative impact on those who live around the outdoor lighting application.*

- The first goal is fulfilled by the use of daylight as much as possible. The different types of users living in the area need to get the psychologically, physiologically and visually support from daylight under as many hours as possible during the year.

- It is also fulfilled by the use of a complementary electrical lighting with an energy efficient light source only lit when needed and in a restricted way.

- When daylight does not contribute to a pleasant and visual secure level of ambient light in the space the daylight should be completed with a carefully designed daylight mimicking complementary electrical lighting.

- This complementary electrical lighting should be seen as visual security for humans.

- The level of complementary lighting that is designed to be pleasant and secure in the outdoor environment for dark conditions, should in a dynamic way be decreased to a lower level during night time.

- When no daylight can be seen in the visual field, the level of light seen as pleasant and secure is lower. The exact level of light is dependent on the contrast situation in the space and the user´s needs for a safe visual orientation in the space.

Reduction of indirect negative effects

- *The work with the design of the energy efficient lighting should have as a second goal, to reduce indirect negative impact from the use the indoor of lighting.*

- This can be done by working with the direct negative effect in a successful way. Here the need for lighting is defined and the ways we use the application have a direct effect on the indirect negative effects.

3.7 Goals for energy efficient lighting

- *Decrease direct negative effects* from indoor and outdoor lighting by the increased use of daylight (when possible).
- *Decrease direct negative effects* from indoor lighting by the decreased use of complementary lighting and by energy efficient daylight-mimicking light sources emitting an activating photon flow in the morning and an relaxing photon flow in the afternoon and by a pleasant level of light as low as possible and related to daylight outside when daylight is not enough as ambient light (low when low outside for support of the diurnal rhythm).
- *Decrease direct negative effects* for the outdoor environment by the decreased use of complementary lighting and by energy efficient daylight-mimicking light sources emitting an activating photon flow in the morning and an relaxing photon flow in the afternoon and by a pleasant level of light as low as possible.
- *Decrease indirect negative effects* for indoor and outdoor environments by the reduction of direct negative effects.

4 Discussion

4.1 Discussion of methods

The methods used were literature review, lighting analysis and measurements of vertical and horizontal illuminance and luminance.

4.2 Lighting analysis and measurements

Light analysis is a key-knowledge in research in lighting design. When research is based on analyzes of the way the light appears in the space during the day and the year, the research is rooted in the human experience of the space.

4.3 Measurements of a small spot

The measurement of the photon flow on a small spot is not direct related to the human visual experience. Instead photon flows are interacting by transmission, absorption and reflection (TAR) with the surfaces in the space. The photons carry information to the visual sight and to a selection process of the information and some information is used as input to the human brain.

4.4 Lighting analysis is a holistic approach to lighting design

When research is based on lighting analysis this is a holistic approach to the human experience that is three dimensional and relative and fit into an annual rhythm and of a constant change of the natural photon flow and the human changed response during the day through the impact of the diurnal rhythm to the external trigger.

4.5 An atomistic approach to lighting design

When research in lighting design is based on measurements of photon flows emitted into the space the approach is atomistic and not related to the human experience. If this atomistic approach and the measurements only valid for a certain space is used in general for spaces with an altered contrast situation and by that in another situation according to transmission, absorption and reflection (TAR) there will be a misfit in-between the lighting, the space, and the user.

4.6 Increased information about negative effects

The number of articles that describes direct negative effects of the use of artificially emitted photon flows, increases. The articles about indirect negative effects of the use of lighting related to the production of electricity are also increasing. The two problems are connected to each other and can be improved by an increased use of daylight.

4.7 An increased use of daylight

Not all spaces have well-functioning openings for windows and use methods to handle glare and heat related to sunshine and daylight. Despite many spaces do not have an ideal daylight situation, daylight should be used as much as possible. Problems according to the use of daylight should be solved, if possible.

4.8 Indirect problems increase and direct problems decrease

If the reduction of indirect negative effects of the use of energy efficient lighting are accomplished by a method that increases the direct negative effects for humans, animals and ecosystems the problem with the use of lighting are not finally solved. An increase of direct effects as a result of the decrease of the indirect effects should be avoided.

5 Conclusion

The way the lighting design models fulfill goals can be described and be related to a reduction of direct negative effects on humans, animals, plants and ecosystem, by the use of artificially emitted photon flows and to the indirect effects of the production of electricity. When the direct negative effects, seen from a broad perspective, are decreased, the indirect negative effects are reduced at the same time. If only focusing on the reduction of the indirect negative effects there is a risk that this can be done in a way that increases the direct negative effects.

5.1 Goals for lighting design put into hierarchy

- ***Goal 1.Decrease of the direct negative effects of the use of electrical lighting***

- *Use daylight as much as possible and mimic daylight*
  The need for quality of life, safe visual orientation and efficiency at work need to be supported in a way that do not hurt the user in diurnal rhythm in the indoor environment or human users, animals, plants or ecosystems in the outdoor environment. This perspective is not static and by that are levels of light when dark outside as low as possible.
- *Balance the need and risk of electrical lighting*
  The need for electrical lighting should be balanced towards the risk of the use of the lighting.

- ***Goal 2. Decrease of the indirect negative effects of the use of electrical lighting***

- *Decrease of the use of electrical lighting by an increased use of daylight*
  Daylight should be used as much as possible for ambient light in the indoor environment. The increased use of daylight for ambient light decreases both the direct and indirect negative effects of the use of complementary electrical lighting.

- *Decrease the use of the complementary electrical lighting by design*
  It is in the same way of great importance to design the application in a way that uses the complementary electrical lighting as little as possible. The design of the application in this way decreases both the direct and indirect negative use of complementary electrical lighting.

- *Decrease the use of energy for lighting through more energy efficient light sources*
  The change of the light source to a more energy efficient alternative is needed as well, but should be used in combination with the design of an increased use of daylight and a decreased use of electrical lighting.

- *Decrease the use of energy through a combination of lighting design and a better technique*
  When a lighting application designed to increases the use of daylight and to reduce the time when the complementary electrical lighting is switched on, is combined with modern lighting technique mean for energy W/m²&h will decrease and by that both direct and indirect negative effects of the use of a complementary electrical lighting.

5.2 Future work

Models for lighting design need to be evaluated from estimated energy potentials and be compared to each other with the ambition to collect more information about mean for energy use W/m²/h during the year.

References

ARIES, M. B.C., AARTS, M. P.J., HOOF, VAN. J. 2013. Daylight and health: A review of the evidence and consequences for the built environment published online 7 November 2013. Lighting Research and Technology The online version of this article can be found at: DOI: 10.1177/1477153513509258

BADIA, P., MYERS, M., BOECKER, M., CULPEPPER, J. 1991. Bright light effects on body temperature alertness, EEG and behavior. Physiology and behavior, Vol 50 pp, 583-588.

BEAUPRE, S. BOUDREAULT, P-L. T. LECLERC, M. 2010. Solar-Energy Production and Energy-Efficient Lighting: Photovoltaic Devices and White-Light-Emitting Diodes Using Poly(2,7-fluorene), Poly(2,7-carbazole), andPoly(2,7-dibenzosilole) Derivatives . Advanced Materials 2010, 22, E6, E27

CAOCHEN, C. (2007). Alerting effects of light. Sleep Medicine Reviews (2007). 11, 453-464

EDELL-GUSTAVSSON, U., EK, A-C. 1992. The relevance of sleep, circadian rhythm and life-style as related to a holistic theory of health. Scand J Caring Sci Vol. 6, No. 1 1992.

FOSTERVOLD, K., LARSEN, P., LILLELIEN, E. MJÖS, T., BERG, M. (2010). Conference proceedings CIE.

PAULEY, S.M. (2004). Lighting for the circadian clock: resent research indicates that lighting has become a public health issue. Medical Hypotheses 63, 4 (2004)

RICH, C., LONGCOR, T. 2006. Introduction. I: Rich C, Longcore T (red). Ecological Consequences of Artificial Night Lighting, ss 1-13. Island Press, Washington. Chapter 2. BEIER, P. 2006. Effects of artificial night lighting on terrestrial mammals.

RYCKERT, .WR., LOOTENS, C., GELDOF, J., HANSELAER, P. 2010. Criteria for energy efficient lighting in buildings. Energy and buildings, 2010 - cat.inist.fr

SÄTER, M. 2012. Equilibrium. User Centred Lighting Design. Towards the development of a lighting design that is individually psychologically, physiologically and visually supportive. Department of Architecture. Chalmers University of Technology.

SÄTER, M. 2014. Model to optimized energy efficiency in lighting applications offices and open-plan offices. Post doc project. Chalmers Publication Library (in Swedish)

WEVER, R. (1979) *The Circadian System of Man*: Results of Experiments under Temporal Isolation. New York: Springer-Verlag

PP39

LIGHTING DESIGN PROCESS FOR ENERGY EFFICIENT LIGHTING

Säter M.B.
Chalmers Technical University
Department of Architecture Gothenburg SWEDEN

Abstract

This paper is based on data from a post doc. project, performed during 2013 (Säter 2014) on Chalmers in Sweden. The project showed that a well experienced lighting designer that use modern lighting technique in a creative way and an energy saving lighting design process (E-LDP) developed within the project, can create an lighting application that at the same time save energy and enhance the light-related support of the user. The project is theoretically positioned within theory about the interaction in-between man, light, colour and space (MLCS) that was developed in a Thesis (Säter 2012) performed prior to the post doc project. Mean for energy used during the 23 test days (spread over the year), was low.

Keywords: Lighting design process for energy efficient lighting; phased start for lighting

1 Introduction

In the study was a lighting application developed that only used the exact amount of complementary lighting that was needed to keep a pleasant space during 2013.

The exact need for a complementary lighting where developed hour by hour, manually. In the study was the E-LDP and eco lighting design process (ECO-LDP) defined during the initial start of the project and then further described later in the project. Based on E-LDP was the lighting application used in the study developed and installed. The application used daylight to its full extent and used the phased start of the three part lighting application system. Data where analyzed and combined with the result from a literature review. Models for lighting design where theoretically used in the same daylight as measured during 2013. The mean for energy use during the year where compared between the models. If goals where fulfilled about a pleasant space, support of the user psychologically, physiologically and visually (PPV) and energy efficiency, where analyzed.

1.1 Lighting design

Lighting design, a work task by many within the building process have a great potential to contribute to a decrease of the amount of electricity used in the world today. If daylight is used in the indoor environment for ambient lighting in an optimized way and if the ongoing change of lighting technique towards more energy efficient alternatives is combined with the use of the handicraft lighting design, the potential for energy savings will increase.

1.2 All four steps should be professionally performed

If all four steps in the lighting design process are performed in a professional way, the urgent need of reduction of energy used for lighting can be managed without a high risk for rebound effects.

1.3 Obstacles for the development

It is a problem that knowledge is needed from many areas in the work with the lighting design process. To guarantee that the lighting design process is professionally performed in all four steps, knowledge in how to design a pleasant space, support of the user, use daylight and the complementary electrical lighting and use lighting technique, need to be represented in the work with the process.

1.4 Describe the process

When the work tasks within the process are described, it will be easier, to point out what to do and connect the work task to the right competence.

1.5 Models for income

The development of the work with lighting design is not in line with the common model of income for the lighting industry that focuses in a high extent on step four of the lighting design process. Although this fact, the way lighting applications are designed, need to be developed towards a professionally performance of the whole lighting design process. The professional performance will make it possible for the lighting industry to contribute more to the urgent reduction of energy used globally. From an ethical perspective, the future claims an increase in the efforts of reduction of energy used for lighting.

2 Methods

2.1 The development of the project

Phase 1.The development of the process of lighting design for energy efficiency (E-LDP) and the eco lighting design process (ECO-LDP).

Phase 2. Literature review.

Phase 3.The development of the lighting application.

Phase 4. The analysis of the way the daylight appeared during the year. The evaluation of when and where, use the three part system of the installed lighting application. Measurement of the ambient light for 23 occasions in-between 8.00 a.m. - 19.00 p.m. during the year.

Phase 5. Analyse of data from the study.

Phase 6. Criteria´s for the control of the lighting application where developed.

Phase 7. The future more advanced application was described. E-LDP and ECO-LDP was further developed.

Phase 8. The way the lighting where used was analyzed and values for when to lit and when to switch off the lighting were developed,

Phase 9. The impact from the use of the lighting design process for energy efficient lighting in reduction in energy use where estimated nationally and on a European level (will be published in a future article).

2.2 E-LDP the lighting design process for energy efficient lighting (indoor environment)

E-LDP indoors: Introduction to the design: Theory as a start in to the process. Theory about comparisons between models for lighting applications according to energy use. Evaluation of fulfillment of goals when the specific model is used according to a pleasant space, support of the user psychologically, physiologically and visually and energy efficiency.

Step1: The space is evaluated.

Step 2: The user´s needs are evaluated.

Step 3: The design of the daylight (shadings) and the complementary electrical lighting and the synchronization of them are performed. The design of the part of the lighting application placed opposite to the windows. The design of the part of the lighting application put in the ceiling. The design of the task lighting.

Morning: Daylight is used for ambient light the way it appears in the space. Complementary lighting is used if daylight does not contribute to a pleasant space. At first is the inner part of the space lit by luminaries on the wall. If this is not enough the lighting application in the ceiling is switched on.

Day: Daylight is used for ambient light the way it appears in the space. Complementary lighting is used if daylight does not contribute to a pleasant space. At first is the inner part of the space lit by luminaries on the wall. If this is not enough, the lighting application in the ceiling is switched on.

Afternoon: Daylight is used for ambient light the way it appears in the space. Complementary lighting is used if daylight does not contribute to a pleasant space. At first is the inner part of the space lit by luminaries on the wall. If this is not enough the lighting application in the ceiling is switched on.

Step 4: Design of the lighting application as a system.

Completion: Evaluation if goals are fulfilled for a pleasant space, support of the user, psychologically, physiologically and visually and for energy efficiency

2.2.1 E-LDP the lighting design process for energy efficient lighting (outdoor environment)

For urban areas is the process developed towards the need of the human user of a pleasant

space and a safe visual orientation and a life without disturbance from unwanted lighting when dark outside. In non urban areas can the ECO-LDP process be used and in a better way cope with the needs of not only humans but the needs of animals and plants too.

E-LDP outdoors. Introduction to the design: Theory as a start into the process. Comparisons between models for lighting applications according to energy use. Evaluation of fulfillment of goals when the specific model is used according to a pleasant space, support of users living, walking and driving in the space.

Step1: The space is evaluated.

Step 2: The expected user´s needs are evaluated (living, walking, and driving)

Step 3: The design of the complementary electrical lighting as well as the synchronization of daylight and the complementary lighting is performed. Reasons to the design can be found in history, the present situation and in a future perspective of scheduled changes.

Morning: The complementary lighting follows the sunrise and stays on the lowest level for a pleasant space and for a safe visual orientation (lover than pleasant). The complementary lighting is taken away when daylight is enough.

Day: The complementary lighting stays during the day on the lowest level for a pleasant space and for safe visual orientation, if needed.

Afternoon: Complementary lighting is used again if daylight does not contribute to a pleasant space and gives a visual support to the user.

Night: The level of light is as low as possible (moonlight is preferable during very late hours) but still pleasant and gives support for a safe visual orientation. Houses are protected from outdoor lighting entering gardens and houses.

Step 4: Design of the lighting application as a system.

E-LDP Completion: Evaluation if goals are fulfilled or not. The evaluation is concerned a pleasant space, support of a safe visual orientation, and protection from unwanted light at night and for optimized energy efficiency.

2.3 Literature review

The literature review was concerned the design of energy efficient lighting and direct and indirect negative effects of the use of lighting in indoor and outdoor environments.

2.4 The lighting application

The space used in the study (Figure 2 Klassrum, the right part of the floor plan) was together with the lighting application seen as an interaction model. A lighting application was developed by the use of the lighting design process for energy efficient lighting and was followed during a year. Two times per month under 2013 was the ambient lighting measured vertically and horizontally every hour 8.00 a.m. -18.00 p.m. in the afternoon (with the exception of January that had only one test day due to a late start of the project financially). Critical values for when to fill in daylight where recorded under the test days during the year. The ambient lighting was evaluated and daylight filled in manually with a complementary electrical lighting when needed and only in the parts of the space that were evaluated as unpleasant. In this model was an active lighting used during the day and a more relaxing lighting during the afternoon. It was a three part system. Active wall lighting, relaxing wall lighting and relaxing lighting in the ceiling.

2.5 2.5. The lighting application used in the study

The floor area, 54 m² (see picture above the right part of the floor plan named Klassrum. 3 Windows, size 120x240 cm. 2 luminaries on the wall opposite to the windows equipped with LED (8,1W x7=56,7/54 m². = 1,05W/m². 2 Luminaries on the wall opposite to the window equipped with Halogen (42Wx6=252/54 m²=4,66W/m²). 8 luminaries in the ceiling (down lights) equipped with Halogen 20Wx8=160W. 160/54m²= 2,96 W/m².

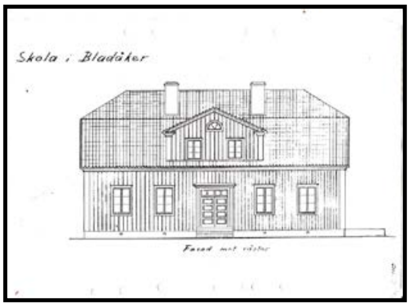

Figure 1 – Bladaker school

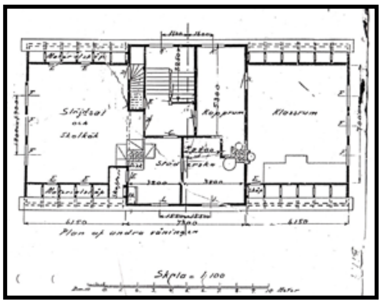

Figure 2 – The space used in the study (right part)

2.6 The practical application, version 1 and 2

Version 1part 1. Active wall lighting: Two luminaries on the inner wall opposite to the windows equipped with LED, were used for an active light 8.00 a.m.-13.00 p.m. when needed. Designed to fill in daylight in the inner part of the space to keep the level of a comfortable light. Large sized (130cmx30cmx30cm and 100cmx 30cmx30cm) white paper luminaries equipped with LED 8,1Wx4+ LED 8,1Wx3.

Version 1part 2.Comfortable wall lighting: Two luminaries on the inner wall opposite to the window equipped with Halogen were used 13 p.m.-19.00 p.m. when needed. Designed to fill in daylight in the inner part of the space and to keep the level of a comfortable ambient light. White paper luminaries (130cmx30cmx30cm) equipped with Halogen 42Wx3+ Halogen 42Wx3.

Version 1 part 3. Comfortable ceiling: The 8 luminaries in the ceiling equipped with Halogen were used 8.00 a.m-19.00 p.m. when needed. Designed to secure the level of a comfortable lighting when daylight and the lighting in the inner part of the space was not enough. Down lights equipped with Halogen 20Wx 8.

Version 2 part 1. Active wall lighting: Two luminaries on the inner wall opposite to the window equipped with LED 8,1Wx4+ LED 8,1Wx3 were used for an active light 8.00 a.m-13.00 p.m.

when needed. Designed to fill in daylight in the inner part of the space to keep the level of an active ambient light. White paper luminaries (130cmx30cmx30 cm and 100cmx30cmx30 cm).

Version 2 part 2. Comfortable wall lighting: Two luminaries on the inner wall opposite to the window equipped with fictive LED with a spectral composition close to the incandescent and were used 13 p.m.-19.00 p.m. when needed. Designed to fill in daylight in the inner part of the space to keep the level of a comfortable light. Large sized (130cmx30cmx30 cm) white paper luminaries. Fictive LED 8,1Wx4+8,1Wx3. Fictive spectral composition for a relaxing light close to the incandescent.

Version 2 part 3. Comfortable ceiling: The 8 luminaries in the ceiling where equipped with fictive LED with a spectral composition close to the incandescent and used in-between 8.00 p.m.-19.00 p.m. when needed. The application was designed to secure the level of a comfortable lighting when daylight and the lighting in the inner part of the space was not enough for ambient light. Down lights. Halogen 160W converted into LED (theoretically) in a way that gave the same amount of lumens.

2.7 Alternative interaction models

Theoretically and based on the data about the appearance of the ambient light during the year collected in the study, was the two versions of the lighting application developed in the study, compared to each other. Then 5 other models for lighting design was tested towards the data collected in the study about the ambient light from daylight in the space during 2013. The five models represent different criteria´s for the design of the lighting application and where compared within the same lighting situation during the year.

2.8 Alternative models for lighting design

Old office. Mean for energy use theoretically in the recorded daylight conditions in the study during the year were12 W/m²/h. The interaction model where used as a reference.

Office 500/500 LED. Mean for energy use theoretically in the recorded daylight conditions in the study was 9,8 W/m²/ h. The application where theoretically designed towards a predesigned level of 500 Lux on the working table and in the same way for the rest of the floor.

Office 500/250 LED. Mean for energy use theoretically in the daylight conditions recorded in the study were 7,3 W/m²/ h. The application where theoretically designed towards a predesigned level of 500 Lux on the working table and for 250 Lux on the level of the table for the rest of the floor.

Office 100 Lux on the wall. Mean for energy use theoretically in the daylight conditions recorded in the study, were 4, 3 W/m²/ h. The application where theoretically designed towards a predesigned level of 100 Lux on the wall measured at 184 cm above the floor plane.

Office 500/250+ daylight control. Mean for energy use theoretically in the daylight conditions recorded in the study were 2,96 W/m²/ h. The application where theoretically designed towards a predesigned level of 500 Lux on the working table and for 250 Lux on the level of the table for the rest of the floor. The hour the complementary artificial light was in use were estimated based on data from the study.

Office 200 Lux on the wall+ daylight control. Mean for energy use theoretically in the daylight conditions recorded in the study were 2, 45 W/m²/ h. The application were theoretically designed towards a predesigned level of 500 Lux on the working table and for 250 Lux on the level of the table for the rest of the floor. The hour the complementary artificial light was in use were estimated based on the data from the study.

Study model Version 1. LED/HALOGEN 30-50 Lux on the wall. Daylight control performed manually. Mean for energy use in the daylight conditions recorded in the study, 1, 97 W/m²/ h.

Study model Version 2. LED/LED, 30-50 Lux on the wall. Daylight control performed manually. Mean for energy use in the daylight conditions recorded in the study, 0, 61 W/m²/ h.

Study model Version 2:1. LED/LED, 30-50 Lux on the wall. Daylight control performed manually. Presence detector was added (supposed to give -10%). Mean for energy use in the daylight conditions recorded in the study, 0, 55 W/m²/ h.

2.9 Evaluation of fulfillment of goals for the models for lighting design.

The models for lighting design where compared to each other and it was evaluated if goals for the use of the process where fulfilled or not.

2.9.1 A pleasant space

High fulfilment: A space lit with a complementary electrical lighting that follows the level of daylight in the space and fill in with a low level of light that emphasize the space in a pleasant way.

Low fulfilment: A space lit with a complementary electrical lighting that do not follow the level of daylight in the space and fill in with a low level of light that do not emphasize the space in a pleasant way.

2.9.2 Psychological support of the user

High fulfilment: Daylight and the complementary electrical lighting contribute to a pleasant space.

Low fulfillment: Daylight and the complementary electrical lighting do not contribute to a pleasant space.

2.9.3 Physiological support of the user

High fulfillment: The users spend their time in daylight as much as the daylight conditions in the space allow them to do. The user have a complementary electrical lighting that is activating in the morning when needed and have a relaxing complementary artificial lighting in the afternoon, when needed. The complementary electrical lighting follows the levels of daylight in a way that is appropriate for the contrast situation in the space and has a spectral composition that in a rough way are related to the changes in the spectral composition in daylight during the day.

Low fulfillment: The complementary lighting is used in a way that keeps a predesigned value for level of light. The user has a complementary electrical lighting that is activating. The complementary electrical lighting do not follow the levels of daylight in a way that are appropriate for the contrast situation in the space and do not have a spectral composition that in a rough way are related to the changes in the spectral composition in daylight during the day.

2.9.4 Visual support of the user

High fulfillment: The daylight is shaded out and do not contribute to the experience of visual discomfort. Daylight and complementary electrical lighting designed in relation to the contrast situation in the space. The user have a visual support from their task lighting that goes from a low to a high level (0-2000 Lux) and is when possible surrounded by an ambient light experienced as on a lower level compared to the level of light on the working table.

Low fulfillment: The daylight is not shaded out and risks contribute to the experience of visual discomfort. Daylight and complementary electrical lighting is not designed in relation to the contrast situation in the space. The user have only a limited support from their task lighting and is always surrounded by an ambient light experienced as on higher or on the same level compared to the level of light on the working table.

2.9.5 Energy efficiency

High fulfillment: Energy efficiency is achieved by the use of both design for an optimized energy efficient lighting application and the use of modern lighting technique.

Low fulfillment: Energy efficiency is not achieved by the use of design for an optimized energy efficient lighting application only by the use of modern lighting technique.

2.10 Measurements

Wall: Vertical illuminance and luminance, 19 measurements points on the wall, 184 cm above the floor. Measured every hour 8.00 a.m-19.00 p.m. during test days.

Floor: Horizontal illuminance, 9 measurements points on the floor. Measured every hour 8.00 a.m.-19.00 p.m. during test days.

Window: Vertical and horizontal illuminance and luminance. 6 measurements points around the windows measuring the experience of glare. Measured when daylight was evaluated as disturbing during test days. Critical values were collected.

3 Results

3.1 E-LDP the lighting design process for energy efficient lighting (indoors)

The E-LDP: indoors where developed in the study. See methods for more information.

3.1.1 E-LDP the lighting design process for energy efficient lighting (outdoors)

The E-LDP: outdoors where developed in the study. See methods for more information.

3.2 The application developed in the study,

3.2.1 Ambient light

The ambient light was measured during 2013 8.00 a.m. – 19.00 p.m. under the following test days: 31.1, 1.2, 27.2, 26.3, 29.3, 24.4, 30.4, 24.5, 27.5, 29.6, 30.6, 29.7, 30.7, 29.8, 31.8, 25.9, 30.9, 24.10, 25.10, 27.11, 28.11, 16.12, and 17.12.

The measurements were performed during 11 hours per day at 10 occasions and for 253 hours in 2013. Daylight was enough for ambient lighting in 190/253 hours and needed to be completed with electrical lighting for 63/253 hours during the 23 test days.

3.2.2 The lighting from the wall 8.00 a.m.-13.00 p.m., 13.00 p.m.-19.00 p.m.

The lighting in the inner part of the space on the wall opposite to the window called the active wall where used 8.00 a.m.-13.00 p.m. for 19/253 hours.

The lighting in the inner part of the space on the wall opposite to the window called the comfortable wall where used 13.00 a.m.-19.00 p.m. for 44/253 hours.

3.2.3 The lighting from the ceiling 8.00 a.m.-19.00 p.m.

8.00 a.m.-13.00 p. was the lighting in the ceiling used for 6/253 hours.

13.00 p.m.-19.00 p.m. was the lighting in the ceiling used for 36/253 hours.

3.3 The total need for a complementary electrical lighting

As a total was the complementary electric lighting used in 63/253 hours. Task lighting was separated from the ambient lighting and designed to be used when needed and was not used under the test days.

3.4 A pattern of the need of a complementary lighting

There was no need for a complementary electrical lighting 8.00 a.m.-19.00 p.m. from 24 of April to 31of August 2013. The daylight only needed to be filled in during morning and afternoon in January, February, March, September, October and November during the test days. In December was the inner lighting on the wall opposite to the window used during the test days 22/22 hours and for 15 /22 hours was the lighting from the ceiling added.

3.5 Comparison between the lighting application in the study and to other models for lighting design

The lighting design models developed in the study where theoretically used in the ambient light from daylight in the space during 2013. In this way all models here mentioned was compared to each other based on the same data about daylight. They had a mean for energy use during 2013 from 12 W/m²/h,9.8 W/m²/h, 7.3 W/m²/h, 4, 3 W/m²/h, 2, 96 W/m²/h, 2.45, 1, 97 W/m²/h, 0, 61 W/m²/h, 0,55 W/m²/h. In what way the models for lighting design fulfilled goals of a pleasant space, a good support PPV for the users and according to energy efficiency, were evaluated.

The Old office. Mean for energy use theoretically in the recorded daylight conditions in the study during the year were 12 W/m²/h. The lighting design model was used as a reference.

Office 500/500 LED. Mean for energy use theoretically in the recorded daylight conditions in the study were 9,8 W/m²/h. The application was theoretically designed towards a predesigned level of 500 Lux on the working table and in the same way for the rest of the floor.

Office 500/250 LED. Mean for energy use theoretically in the daylight conditions recorded in the study were 7,3 W/m²/h. The application was theoretically designed towards a predesigned level of 500 Lux on the working table and for 250 Lux on the level of the table for the rest of the floor.

Office 100 Lux on the wall. Mean for energy use theoretically in daylight conditions recorded in the study were 4,3 W/m²/h. The application was theoretically designed towards a predesigned level of 100 Lux on the wall measured 184 cm above the floor plane.

Office 500/250+ daylight control. Mean for energy use theoretically in the daylight conditions recorded in the study were 2,96 W/m²/h. The application was theoretically designed towards a predesigned level of 500 Lux on the working table and for 250 Lux on the level of the table for the rest of the floor. The hour the complementary artificial light was used were estimated based on the data from the study.

Office 200 Lux on the wall+ daylight control. Mean for energy use in the daylight conditions recorded in the study, 2,45 W/m²/ h. The application was theoretically designed towards a predesigned level of 500 Lux on the working table and for 250 Lux on the level of the table for the rest of the floor. The hour the complementary artificial light was in use were estimated based on the data from the study.

Study model Version 1. LED/HALOGEN 30-50 Lux on the wall. Daylight control performed manually. Mean for energy use in the daylight conditions recorded in the study were 1,97 W/m²/ h.

Study model Version 2. LED/LED, 30-50 Lux on the wall. Daylight control performed manually. Mean for energy use in the daylight conditions recorded in the study were 0, 61 W/m²/ h.

Study model Version 2. LED/LED, 30-50 Lux on the wall. Daylight control performed manually. Presence detector added (supposed to give -10%). Mean for energy use in the daylight conditions recorded in the study were 0,55 W/m²/ h.

3.6 Comparison of fulfillment of goals for the models for lighting design used in the study.

Table 1.

Lighting design models High fulfilment Low fulfilment	Mean W/m²/h during 2013 23 test days	Pleas-ent space	Psych supp	Phys supp	Visual supp	Eneff
The Old office Static level of light.	12,4 W/m²/ h					L
Office 500/500 Lux. LED. Static level of light.	9.8 W/m²/ h	M	M	L	M	L
Office 500/250 Lux. LED. Static level of light.	7,3 W/m²/ h	M	M	L	M	L
*Office 100 Lux on the wall. LED.*Static level of light.	4.3 W/m²/ h	L	L	L	L	M
Office 500/250 Lux. LED + daylight control Static level of light.	2,96 W/m²/ h	M	M	L	M	M
Office 200 Lux. on the wall+ daylight control. LED. Static level of light	2,45 W/m²/ h	M	M	L	M	L²
Study model Version1. LED/ HALOGEN 30-50 Lux on the wall. Daylight control performed manually. Dynamic level of light, follows daylight.	1.97 W/m²/ h	H	H	H	H	H
Study model Version 2. LED/LED 30-50 Lux on the wall. Daylight control performed manually. Dynamic level of light, follows daylight*	0,61 W/m²/ h	H	H	H	H	H
Study model Version 2. LED/LED, 30-50 Lux on the wall. Daylight control performed manually. Presence detector added theoretically. Dynamic level of light, follows daylight*	0,55 W/m²/ h	H	H	H	H	H

*Daylight was the ambient light. When daylight did not contribute to a pleasant space it was filled in manually to a predesigned level of light appropriate to the contrast situation in the space that was comfortable in dark conditions.
L² When used in dark conditions the mean for energy use is 8.6Wm²/h. This can be compared to E-LDP when used in dark condition have a mean for energy use of 2,44Wm²/h.

3.7 Fulfillment of goals

When the models for lighting design was compared to each other according to if they contributed to a pleasant space, a psychological, physiological and visual support for the user, it was found out that the lighting design application done by the E-LDP and when all four steps in the lighting design process was professionally performed and based on lighting analysis gave the lowest mean for energy use and contributed at the same time to the highest scores for a pleasant space, a god support for the user PPV.

3.8 Development of a system that compensate for differences in the experience of level of light in the visual field.

The level of light outdoors is high during daytime. Daylight in the visual field will be compared to the experienced level of light indoors. When the difference between daylight outdoors and level of ambient light in the indoor environment is too big, the experience of the indoor environment will be gloomy. A system was developed to solve the problem based on dynamic criteria's for lighting control. This will be further described in a future article. In this article will also measured data from the study be published.

4 Discussion

4.1 Discussion about methods

Literature review, lighting analysis and measurement of vertical and horizontal illuminance and luminance, were used as methods.

4.2 Lighting analysis and measurements

This project is based on the analysis of the appearance of daylight and the design of the complementary lighting during a year. When analysing the way light appears in a space the researcher stays within the human visual experience of the space. When measuring the constantly changing photon flow of daylight, the recorded values are not connected to the human visual experience of the space. Lighting analysis is the basic tool for research in the human experience of the space. This is a study done without (naive) subjects. The experienced lighting designer (the researcher) has instead focused on the evaluation of daylight and the need for complementary lighting. Design is to handle the complexity in a holistic way. It is balancing between contradictory needs of daylight and the complementary lighting and to associate to common knowledge about design that is accepted. The naive subject's gives information about contradictory needs and differences in preferences but this type of information is not design. The design need to be based on all types of information according to being a human staying in a space and then be balanced together in a well functioning way.

4.3 Discussion of results

The result is although it is based on the way daylight appeared in the space during the 23 test days only based on reality for the application performed in the study. For the other models of lighting design used in the study is the energy use done as estimated energy potentials based on the same daylight data as for the application in the study.

4.4 The need for lighting in the morning

Maybe it is a surprise to see that lighting was not needed as ambient light 8.00 a.m.-19.00 p.m. for four months in Sweden in the application developed in the study.

4.5 The need for lighting in the afternoon

A complementary lighting was needed in the afternoon with a declining number of hours from 31 January to 29 of March and then the need for lighting came back 25september with an increasing number of hours and estimated to disappear again late in March 2014. This type of pattern of the need for lighting is important to evaluate to avoid that lighting is used when not needed.

4.6 More precise data

It is likely that an increased number of test days in a more precise way reveal data about the need for a complementary electrical lighting during the year.

4.7 The need for lighting when dark outside.

In a space with well functioning openings for daylight appropriate for the space is lighting only needed when daylight indoors is not enough to keep the lowest level of light that contributes to a pleasant space. Humans need to stay in a low level of light and in a comfortable spectral composition close to daylight in the evening otherwise they will not feel at comfort and might get a negative impact on the diurnal rhythm.

5 Conclusion

5.1 E-LDP

E-LDP where developed within the study. The comparisons between different models for lighting design where used theoretically in the same daylight conditions that was measured in the project during 2013. Estimated energy potentials were performed.

5.2 E-LDP, a low mean for energy used and a good support of the user

The combination of the use of the E-LDP and modern lighting technique resulted in a lighting solution that when used had the lowest mean for energy use during the year (2013) compared to other fictive lighting design models. In the same way gave this lighting application a pleasant space and a good support for the user (table 1.)

5.3 E-LDP, optimization through research in the design of connection between interaction factors

When research in the interaction between man, light, colour and space is performed regarding the design of the lighting application this is a holistic approach that handles the four steps of the lighting design process and strive to design well-functioning connections between the interaction factors (MLCS). Research performed with this approach is useful to develop optimized energy efficient lighting applications and to avoid developing strategies for energy efficiency that lead to a bad reuptake or/and rebounds effects.

5.4 E-LDP, research in the interaction between man, light, colour and space, MLCS

Research about the interaction between MLCS is valuable for society. If the result from the study is used there is a theoretical potential to reduce the amount of electricity used for lighting.

5.5 Reduction of energy use in reality

In reality not all spaces have well functioning opening for daylight so the potential for a reduction of the energy used for lighting is hard to estimate. But the result have the possibility to inspire to use daylight as much as possible in ambient light, use dynamic criteria’s for controlling the light and to use the complementary electrical lighting, as less as possible.

5.6 Use all four steps in the LDP

The use of all four steps of the LDP in a professional way is not in line with the common model for income in the lighting Industry. It is an ethical issue to optimize the way lighting design are performed towards an increased energy efficiency with at the same time a good support for the user and by that a low risk for rebounds effects caused by the way the technique are used.

5.7 Future work

Further research about the interaction between MLCS have the possibility to increase the knowledge about how to design light in an energy efficient way and at the same time increase the support for the user.

Acknowledgement

The project was financed by the Swedish Energy Agency and the Bertil and Britt Svensson Foundation for Lighting Technique and is here gratefully acknowledged.

References

SÄTER, M. 2014. 2014 Model for an optimized energy efficiency in lighting applications offices and open-plan offices. Post doc project. Chalmers Publication Library (in Swedish)

PP40

ASSESSMENT ON LIGHTING QUALITY AND ENERGY CONSERVATION FOR LIGHTING ENVIRONMENTAL EXPERIENCE DESIGN OF A CONVENIENCE STORE

Cheng, C.C. [1] , Hu, C.J.[1] , Wu, H.Y. [1] , Chao, N.T.[1] , and Hsiao, T.C.[2]
[1] Industrial Technology Research Institute, Hsinchu, CHINESE TAIPEI
[2] Taiwan FamilyMart Co.,Ttd, Taipei, CHINESE TAIPEI

Abstract

Buildings account for 40% of global energy consumption and 30% of global greenhouse gas emissions. Therefore, widespread adoption of building environment renovation focused on lighting quality and energy-saving can benefit global carbon dioxide reduction. This study reveals three design issues creating an environmental lighting experience that combines daylight and artificial lighting using the example of a Taiwanese convenience stores in the Xinying Service Area of Taiwan, and where lighting quality meets the European standard EN 12464-1 while simultaneously satisfying electricity conservation needs. Numerical simulation and in-situ measurements have found that lighting experience design could achieve approximately a 20% reduction in electricity consumption associated with lighting.

Keywords: Lighting environmental experience design; lighting quality; energy saving

1 Introduction

According to statistics from 2012, the four major domestic convenience store chains in Taiwan together have a total of 9,879 stores, and the density of convenience stores in Taiwan thus is among the highest in the world, at up to one store per 2,360 people. Based on 2012 retail statistics from Taiwan, the two main domestic convenience stores have achieved strong revenue growth of up to 10%. The reason for this revenue growth relates to the exploration of merchants to satisfy consumer needs, and the engagement of a new generation of convenience stores from 2008 to supply advanced shopping experiences. In addition, because of remaining open for 24 hours of convenience stores, lighting represents up to 16% of their total electricity consumption. According to commercial lighting research conducted by the U.S. Department of Energy [1], the preliminary strategy used to reduce lighting energy consumption is to replace high-efficiency equipment, but currently the advanced strategy is to discuss how to derive a high-quality environment that incorporates lighting design and smart lighting control to cater to peak and off-peak customer volume. Therefore, this study reveals three design issues on lighting environmental experience based on the lighting requirements of European standard EN 12464-1, using the example of a convenience store in the Xinying Service Area of Taiwan. The example focuses on the need to simultaneously provide a high-performance environment and conserve electricity.

2 Methods

The results of lighting environment and the verification of illuminance levels were determined using the DIALux ray-tracing lighting simulation and rendering program. The steps involved in this study are:

First, to simulate the original lighting design of a Taiwanese convenience store in the Xinying Service Area, and thus provide a comparable reference for lighting quality and lighting energy use.

Second, to reveal three scenario designs on lighting environmental experience with the smart lighting control based on the peak and off-peak periods of customer volume, and involving the combination of daylight and artificial lighting.

Third, to set the lighting requirements of design according to European standard EN 12464-1 for the lighting of indoor work places, which set limits on minimum illuminance and uniformity of illuminance throughout task areas, surrounding areas, backgrounds, walls and ceilings [2].

Fourth, to evaluate the three scenario designs related to lighting environmental experience to determine whether lighting quality and electricity conservation needs can be better satisfied than in the original lighting design.

3 Results and Discussion

3.1 Site Plan of the Design Case Study

Figure 1 (left) displays a convenience store located in the Xinying Service Area of Taiwan, with the dimensions: width 10 m x length 15 m, and floor-to-ceiling height 2.15 m. The orientation of the room is 45° in a northeasterly direction at latitude 23.3°N and longitude 120.3°, and the room has unilateral side-lighting. The wall area that is open to natural light comprises 1/9 of the floor area, and has the dimensions: width 8.0 m x height 2.0 m. The windows are double glazed with horizontal louvers inside. Figure 1 (right) depicts that the store space comprises three major parts, namely the till area, sales area, and office area. The sales area is further differentiated into a peripheral area closely to the window and hot food zoon.

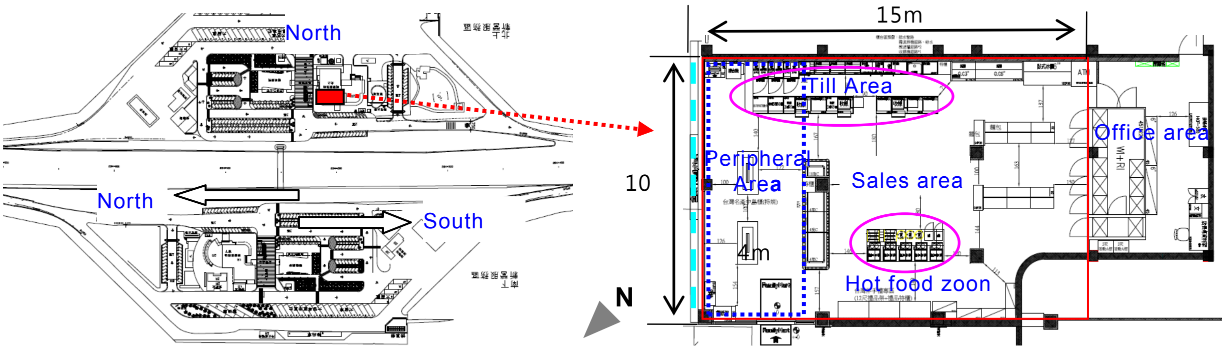

Figure 1 Convenience store layout in the Xinying Service Area

3.2 Original lighting design

Original lighting design in this convenience store, which is shown in Fig. 2 (left), uses T5 fluorescent lamps throughout the sales space, simultaneously uses T5 fluorescent slim lamps washing the surrounding walls to create a space atmosphere.

Numerical simulation shown in Fig. 2 (right) revealed the issues, there are: (1) the illuminance levels throughout the sales area are 300-350 lx below the lighting requirements. (2) the illuminance above fresh food counter is exceeding to 1,000 lx owing to Inadequate layout of luminaries. (3) the Illuminance level of merchandise shelf with 185 lx is insufficient for visual demand. (4) sunshine through the window in the morning will interrupt the eyes of consumer while facing east.

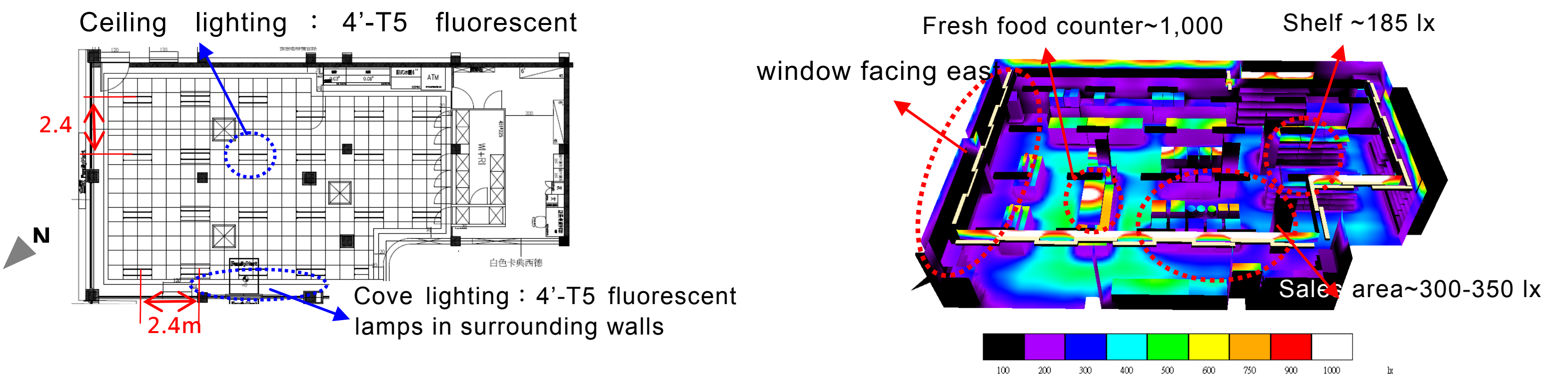

Figure 2 Original lighting layout of convenience store

3.3 Lighting environmental experience Design

Convenience store chains recently have switched their focus from increasing store numbers to improving the quality of store environment. In the new generation of convenience stores, lighting design has progressively evolved from simply supplying illuminance to shaping the atmosphere. The lighting in a commercial store can help creating an atmosphere that emphasizes the character of the store and makes it a desirable shopping destination, and hence it is important not to compromise the visual aspects of a lighting installation simply to reduce energy consumption. This requires the consideration of appropriate lighting systems, equipment, controls and the use of available daylight.

3.3.1 Scenario Design

The design issues on lighting environment experience in this study include: (1) to provide three scenario designs, namely daylight, warm night, homecoming, with cove lighting washing peripheral walls to create an atmospheric space, and to make the hot food zone a focal point, (2) to introduce daylight and integrate it with artificial lighting, (3) to align the luminaries layout to the merchandize shelf to obtain appropriate illuminance for ambient lighting.

Three lighting scenario designs are described in Fig. 3.

1) The first scenario: daylight during 06:00-18:00, using T5 LED luminaries with 6,000K white light to provide uniform ambient lighting for the sales area simultaneously with the use of cove lighting with 6,000K white light by washing peripheral walls to create a bright atmosphere.
2) The second scenario: warm night during 18:00-22:00, with the cove lighting converted to 3,000K warm light in parallel with 3,000K in the hot food zone to create a relaxed shopping atmosphere.
3) The third scenario: homecoming during midnight hours, specifically 22:00-06:00, when the customer volume is low. Parts of the cove lighting are turned off in this scenario, with only the cove lighting in the till area being conserved, to consider energy saving and safety in the till area and thus create an atmosphere of returning home attractive to those who are still out at this late hour.
4) Hot food lighting focal point: hot food lighting with colour temperatures of 3,000K and 6,000 K enables the use of the appropriate light colour to emphasize the tastiness of hot foods and make the hot food zone a focal point. Figure 4 displays the hot food lighting design.

Three scenario designs	a. scenario I: daylight 06:00-18:00	b. scenario II: warm night	c. scenario III: homecoming 22:00-06:00
Cove lighting	6,000K	3,000K	Turn off except for the till
Hot food zone lighting	3,000		
Ceiling lighting (in peripheral area)	smart lighting control	6,000K	
Ceiling lighting (in sales area)	6,000K		

Figure 3 Scenario designs with colour temperature

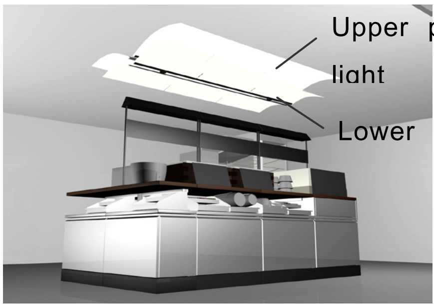

Figure 4 Hot food lighting design

5) Introduce daylight and integrate it with artificial lighting: adjusting the louvers within the window according to sky conditions to introduce daylight and dimming the luminaries via a lighting control system in peripheral area during the daytime. Figure 5 shows the introduction of daylight and the light dimming control system.

Figure 5 Introduction of daylight and light dimming control system

3.3.2 Lighting requirements

In this study of convenience stores, the lighting design is based on a task-ambient design that supplies task lighting throughout work areas such as the till area and hot food zone, while ambient lighting provides relatively low illuminance in the whole sales region. The lighting requirements refer to the European standard EN 12464-1 for the lighting of indoor work places [2], such as retail premises, which sets limits on minimum illuminance and uniformity of task areas, surrounding areas, backgrounds, walls and ceilings, as listed in Table 1. Table 2 lists the lighting requirements of three scenario designs.

1) Illuminance of Ambient lighting

According to EN 12464-1 the illuminance of the sales area as an ambient lighting must be related to task lighting to provide a well-balanced illuminance distribution in the visual field. This study sets the illuminance for the floor of sales area at 300 lx to 500 lx.

2) Illuminance of Task lighting

The illuminance of task areas, included the till area and hot food zone, was set at 500 lx to 700 lx.

3) Illuminance of the walls /ceiling (background)

Based on the research of Newsham et al. (Newsham, 2005) on visual lightness, the preferred average luminance in a horizontal band 40° wide should be >=30 cd/m2.

Conventional wall and ceiling surfaces can be approximately described by lambertian reflectance, where luminance results from illuminance according to Eqn. (1).

$L = \rho \bullet E/\pi$...... (1), where

L is the luminance of a surface;

E is the illuminance on a surface;

ρ is the reflectance of a surface.

Typical reflectance of ceiling/wall surfaces are 70% and 50%, and the illuminance of the background in the visual field calculated using Eqn. (1) is set from 150 to 200 lx for the walls and from 100 lx to 150 lx for the ceiling.

4) Uniformity of illuminance

Uniformity of Illuminance described in terms of minimum-to-average values quantifies the illuminance distribution of a surface. Greater uniformity ratio can minimize visual fatigue. This study requires illuminance uniformity over the work area to exceed 0.6, and the ratio is set to 0.4 for the sales area.

Table1 Lighting requirements for retail premises according to EN 12464-1

Type of area, task or activity	E_m (lx)	UGR_L	U_o	R_a
Sales area	300	22	0.4	80
Till area	500	19	0.6	80
Wrapper table	500	19	0.6	80

Where,

E_m indicates the maintained illuminance (lx)
UGR_L represents the unified glare rating limit
U_o is the illuminance uniformity
R_a denotes the minimum colour rendering indices

Table 2 Lighting requirements for three scenario designs

Scenarios	Lighting requirements	Luminaries／Color temperature
Scenario I : daylight (06:00-18:00)	1. Ambient lighting in the whole sales area • Floor, 300-500 lx • Wall, 150-200 lx • Ceiling, 100-150 lx • Illuminance uniformity >0.4 2. Task lighting in the till area and hot food zone • Working plane, 500-750 lx • Illuminance Uniformity >0.6 • Color Rendering (Ra)>80	• Ceiling lighting ： T5 LED dimmable lamps with 6,000K, integrated with smart lighting control in the peripheral area • Cove lighting：T5 LED slim lamps with 6,000K • Hot food lighting：LED panel lamps, included with 3,000K and 6,000K
Scenario II: warm night (18:00-22:00)		• Ceiling lighting：same with Scenario I • Cove lighting ：T5 LED slim lamps with 3,000K • Hot food lighting：same with Scenario I
Scenario III : homecoming (22:00-06:00)		• Ceiling lighting：same with Scenario I • Cove lighting ：T5 LED slim lamps with 3,000K, turned off except for the till area during midnight hours • Hot food lighting：same with Scenario I

3.4 Lighting Simulation and Evaluation

The results of lighting environment and verification of illuminance levels were determined using the DIALux ray-tracing lighting simulation and rendering program.

3.4.1 Simulation set-up

– Ceiling luminaries use T5 LED lamps, which are dimmable, together with available daylight through windows in the peripheral area, and non-dimmable lighting in the sales area. The layout of ceiling luminaries, which is shown in Fig. 6, is parallel to the window in the peripheral area (at a depth of 4m from the window) and parallel to the merchandise shelf to enhance the ambient lighting. Additionally, cove lighting in the surrounding walls uses a LED slim lamp to create a sense of space. Figure 7 shows these LED luminaries and luminous intensity distributions.

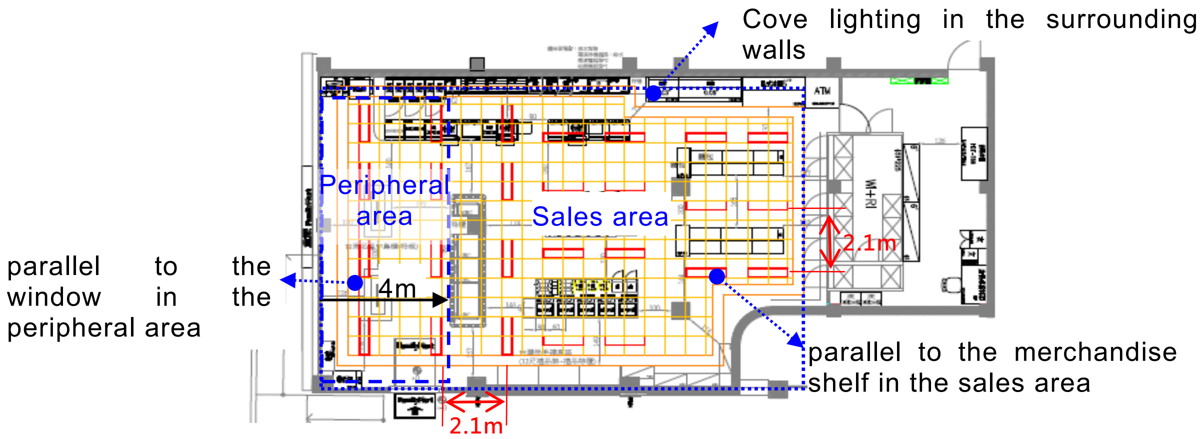

Figure 6 Luminaries layout of new lighting design

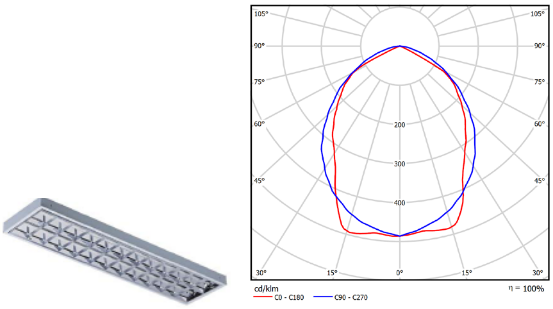

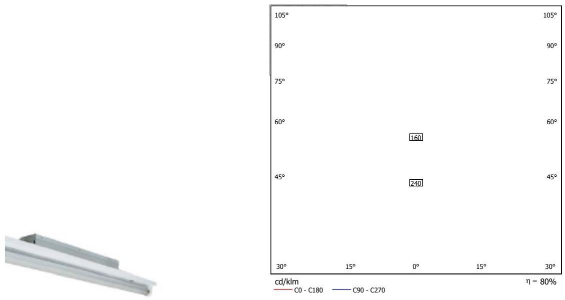

a. Ceiling luminaries with T5 LED lamps ; b. Cove luminaries with T5 LED lamp

Figure 7 Luminaries with luminous intensity distribution

– Reflectance values of major surfaces in the convenience store are chosen based on the IESNA lighting handbook [3] and are: 0.7 for the ceiling, 0.5 for the walls, and 0.3 for the floor and furniture. Table 3 lists the properties of major surfaces, as well as their reflectance and the shading coefficient of the windows.

Table 3 Description of major surfaces in the convenience store

Surface	Description	Reflectance	Shading Coefficient
Ceiling	White mineral gypsum	0.7	-
Walls	White/Green plastic polished panels	0.5	-
Floor	Polished porcelain tile	0.3	-
Merchandise shelf	Aluminum panels coated with light grey paint	0.3	-
Windows with louvers inside	8mm clear glass +15mm air +5mm clear glass, 12mm horizontal light yellow louvers inside	0.4	Open/SC ~0.75 Close/SC ~0.19

3.4.2 Simulation results

The illuminance levels of three scenario designs were calculated at the floor, background wall, and ceiling for ambient lighting in the sales area, and at the height of 0.8 m above the floor for task lighting at the cashier counter and hot food table. Moreover, available daylight was exclusively assessed in overcast skies during early morning in the spring to represent the available illuminance of daylight.

Table 4 lists the simulation results, and the illuminance distributions of the three scenario designs were depicted as the attached figures of Table 4, which indicate illuminance levels with false colour rendering.

1) Scenario I : daylight

   – The illuminance levels for ambient lighting, including that of the floor, wall and ceiling in the peripheral area due to daylight introduction could achieve 785 lx, 388 lx and 422 lx, which reveal plenty of daylight and all match the set illuminance levels of 300-500 lx, 150-200 lx, and 100-150 lx.

   – The illuminance levels for ambient lighting, including that of the floor, wall and ceiling in the sales area could achieve 489 lx, which also match the illuminance level of 300-500 lx. Additionally, illuminance uniformity reaches up to 0.5, which matches the need for uniformity of 0.4 in ambient environment.

- The illuminance levels for task lighting of the cashier counter in the till area could achieve 743 lx. Additionally, illuminance uniformity reaches up to 0.75, corresponding to the minimum requirement of more than 0.6 for the task area.

2) Scenario II : warm night

- The illuminance levels for ambient lighting, including the floor, wall and ceiling throughout the sales region, given artificially supplied directive lighting, could achieve 447 lx, 168 lx and 111 lx, all of which match the set illuminance levels of 300-500 lx, 150-200 lx, and 100-150 lx. Additionally, illuminance uniformity reaches up to 0.59, in accordance with the minimum requirement of more than 0.4 for the ambient environment.
- The illuminance levels for task lighting over the cashier counter could achieve 618 lx, and illuminance uniformity reaches up to 0.79, corresponding to the minimum requirement of more than 0.6 for the task area.

3) Scenario III : homecoming

- The illuminance levels for ambient lighting, including that of the floor, wall and ceiling throughout the sales region, and for cove lighting except for the till area, could achieve 410 lx, 159lx and 106 lx, and thus in all cases matched the set illuminance levels of 300-500 lx, 150-200 lx, and 100-150 lx. Additionally, illuminance uniformity reaches up to 0.6, matching the minimum requirement of 0.4 for an ambient environment.
- The illuminance levels for task lighting over the cashier counter could achieve 618 lx, and illuminance uniformity reaches up to 0.79, corresponding to the minimum requirement of more than 0.6 for the task area.

4) Hot food zone lighting

- Hot food lighting needs to be supplemented by more than 500 lx while surrounding ceiling luminaires supply a hot food table 256lx. The illuminance levels for task lighting over the hot food table while supplying led panel lamps could achieve 823 lx, and that for the area surrounding the hot food zone could reach 419lx, all of which values match the set illuminance levels of 500-750 lx and 300-500 lx. The simulation results were presented in Table 5.

Table 4 Simulation results based on three scenario designs

Scenario design	Simulation results	Illuminance distribution
Scenario I : daylight (06:00-18:00)	1. Ambient lighting <u>Peripheral area</u> • Floor, 785 lx • Wall, 388 lx • Ceiling, 422 lx • Illuminance uniformity 0.5>0.4 <u>Sales area</u> • Floor, 489 lx • Illuminance uniformity 0.7>0.4 2.Task lighting • Cash counter, 743 lx • Illuminance uniformity 0.75>0.6	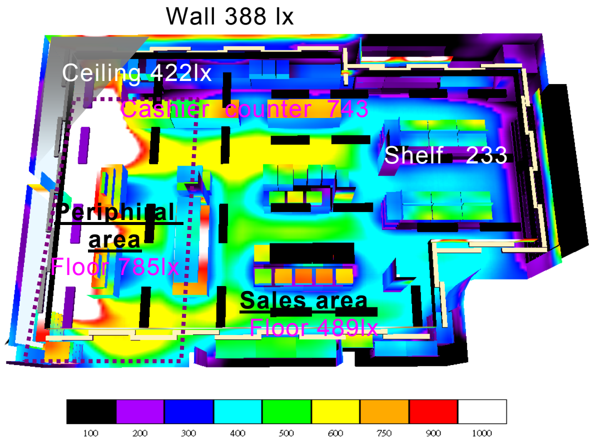
Scenario II: warm night (18:00-22:00)	1. Ambient lighting • Floor, 447 lx • Wall, 168 lx • Ceiling,111 lx • Illuminance uniformity 0.59>0.4 2. Task lighting • Cash counter, 618 lx • Illuminance uniformity 0.79>0.6	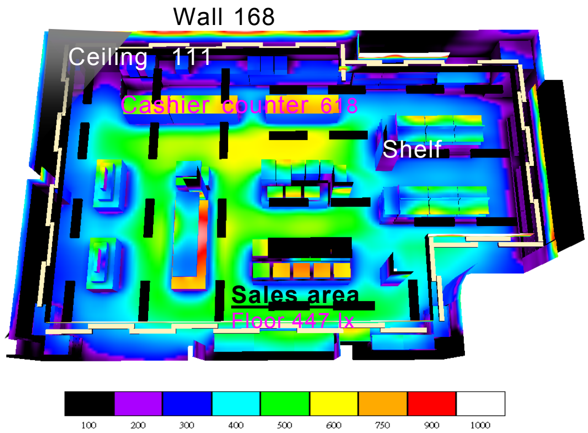
Scenario III : homecoming (22:00-06:00)	1. Ambient lighting • Floor, 410 lx • Wall, 159 lx • Ceiling, 106 lx • Illuminance uniformity 0.6>0.4 2. Task lighting • Cash counter, 614 lx • Illuminance uniformity 0.79>0.6	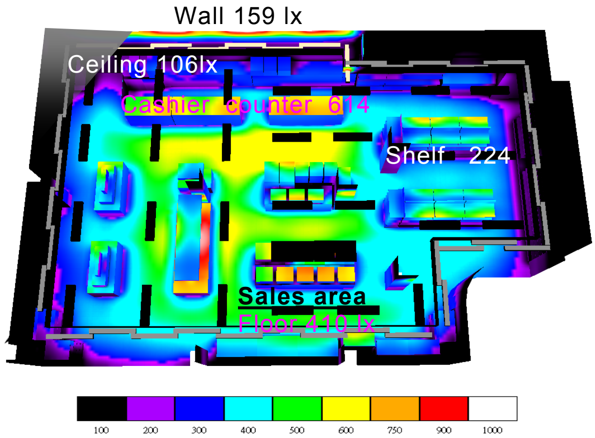

Table 5 Simulation results for the hot food table and its surrounding area

Items	Lighting requirements	Turn off hot food lighting	Turn on hot food lighting
Hot food table	500-750 lx	256	663
Surrounding area of hot food zoon	300-500 lx	367	400

3.4.3 Evaluation of energy saving

The scenario designs involved in the lighting environment experience were evaluated if electricity conservation is more progressive than in the original lighting design.

Comparison of Tables 6 and 7 reveals that the lighting environmental experience design could achieve 20% electricity reduction in annual lighting energy use relative to the original lighting design of the convenience store by using LED lamps throughout sales area, integrating daylight with smart lighting control in the peripheral area, and adjusting the intensity of cove lighting depending on scenario designs.

Table 6 Lighting energy consumption of original lighting design

Zone items	Specification of luminaries			Lighting energy consumption		
	Luminaries style	Watts	Numbers	Watts	hr/day	kWh/yr
Till area	4’x2’ T5 fluorescent luminaries(5,000K)	65	4	260	24	2,278
Peripheral area	4’x2’ T5 fluorescent luminaries(5,000K)	65	6	390	24	3,416
Sales area	4’x2’ T5 fluorescent luminaries(5,000K)	65	20	1,300	24	7,402
Cove lighting	4’-T5 fluorescent slim lamp (3,000K)	35	35	1,225	16	7,154
				2,720		20,250

Table 7 Lighting energy consumption of lighting environmental experience design

Zone items	Specifications of luminaries			Lighting energy consumption			
	Luminaries style	Watts	Numbers	Watts	hr/day	Dimming time (hr/day)	kWh/yr
Peripheral area	4’x2’ T5 LED dimmable luminaries (6,000K)	50	8	400	12	12	2,978
Sales area	4’x2’ T5 LED luminaries (6,000K)	50	19	600	24	0	8,322
Hot food zoon	LED panel lamp (3,000K and 6,000K)	6	18	108	24	0	946
Cove lighting	4’-LED slim lamp (6,000K)	15	38	570	12	0	2,497
	4’-LED slim lamp (3,000K)	15	31	465	4	0	679
	4’-LED slim lamp (3,000K) in till area	15	7	105	12	0	460
Cove lighting	2’-LED slim lamp (6,000K)	9	5	45	12	0	197
	2’-LED slim lamp (3,000K)	9	4	36	4	0	53
	2’-LED slim lamp (3,000K) in till area	9	1	9	12	0	39
				2,073			16,171

4 Conclusions

This study reveals three scenario designs involving lighting environmental experience using the example of a Taiwanese convenience store in the Xinying Service Area. The design issues examine in this study include: (1) to provide three scenario designs, namely daylight, warm night, homecoming, with cove lighting washing the surrounding walls to create an atmospheric space, and to make the hot food zone a focal point, (2) to introduce daylight and integrate it with artificial lighting, (3) to align the luminaries layout to the merchandize shelf.

Numerical simulation revealed that: (1) the illuminance levels for ambient lighting, including the floor, wall and ceiling, all match those of 300-500lx, 150-200lx, and 100-150lx. (2) the illuminance levels for both the cashier counter and hot food zone reach 500-700lx, and thus correspond to the recommended illuminance level for task lighting. (3) illuminance uniformity reaches the minimum requirements of 0.4 for the ambient environment and 0.6 for the task area.

Additionally, lighting environmental experience design could achieve a 20% reduction in annual lighting energy use relative to the original lighting design. The lighting environmental experience design analyzed in this study can not only satisfy the need for a high-performance lighting environment, but also can reduce electricity consumption for lighting.

Acknowledgements

This publication is the result of the project implementation: the Smart Sensing Network Technology and Service Development (102-EC-17-A-02-01-0617) funded by the Department of Industrial Technology/MOEA, R.O.C(Taiwan)

References

[1] C. Jones, Lighting the Way to Zero Net Energy, the DOE Commercial Lighting Solutions, 2008.

[2] CEN EN 12464-1:2011 Light and lighting - Lighting of work places - Part 1: Indoor work places published by the European national standards institute CEN 2011

[3] The Lighting Handbook, Illuminating Engineering Society of North America, Tenth Edition, 2011.

PP41

PROPOSAL FOR GUIDELINE OF VERIFICATION LIGHTING SYSTEMS ACCORDING TO ISO 8995-1:2002(E)/CIE S008/E:2001

Dubnicka Roman, Gasparovsky Dionyz, Raditschova Jana
Department of Electrical Power Engineering, Faculty of Electrical Engineering and Information Technology, Slovak University of Technology, Bratislava, SLOVAKIA
roman.dubnicka@stuba.sk

Abstract

The paper deals with proposal of guideline for verification of indoor lighting systems from real field trials. In the paper is presented proposal or outline of unified system according to standards ISO 8995-1:2002/CIE S008/E:2001 with possibility to transform in some form of guideline or recommendation which users can follow for unified verification measurement to control of realisations of lighting designs. Paper also describes measurement of all important photometric parameters described in this standard i.e. maintained illuminance level, uniformity and also treats about measurement of other parameters like discomfort glare from luminaires defined by UGR, CCT and luminance measurements at the specific workplaces.

Keywords: Indoor lighting, Lighting design, Field photometric measurement, Photometry

1 Introduction

After realisation of lighting design according to international standard ISO 8995-1:2002(E)/CIE S008/E:2001 implemented for example in some national or regional standards for example in Europe EN 12464-1 for indoor lighting shall be performed verification of the lighting system of workplaces. Until now it was not created unified guideline or recommendation at CIE or ISO level how to perform verification beside on some national standards or legal documents. Some of these documents at national level quite often do not describe directly how to perform verification measurement but just describe instrument requirements and they do not treat about procedure how to do it. It should be kept in mind that in some countries is verification of the lighting design realisation one of the condition to have building permission of building owner and shall be performed or when some reconstruction of indoor lighting system of indoor workplaces was done. To have good indoor lighting system of indoor workplaces is very important for health and well-being of the persons especially for workplaces with long-term staying of persons. At the present CIE standard S008 for indoor lighting is under revision and in the near future will be released new version of this document. In it is also included one very interesting note about necessity of verification indoor systems which are performed by lighting designers by means of lighting simulation tools. Some discrepancy between simulations and realisation of designs was showed in some papers. Therefore verification of lighting system should be performed by the field measurement of photometric parameters after realisation of lighting design.

It is photometric measurement of parameters of indoor lighting system which are declared in this standard. One of the problems is to define proper illuminance measurement grid and choosing appropriate instruments for performing of measurements. Even more people who perform these measurements do not treat about accuracy of measurement and they use photometric devices which are not properly metrologically characterised. Users rely on values from certificates but they quite often do not know how to treat with them. Furthermore they quite often not express uncertainty of the measurement which is very important for confident measurement. Each of the problems described above should be unified in one international guideline for practice to define step by step to help people who are dealing with field photometric measurements or consumers who want to verify lighting design to underpin good practice in lighting engineering. The last argument is why to do this document also clearly define procedure for verification of lighting design by field measurement when some discrepancies occur between design and realisation. It would undoubtedly help on disputes arising with bad practice in lighting design and also avoid long discussion in conflict situations i.e. between lighting designer and customer. At the CIE level is place in the frame of the Division 3 which concerns about indoor lighting designs to create technical committee which in connection with experts from lighting engineering and metrology it can be solved problem how to perform good practice in field trials. At the end of procedure this document could be implemented in relevant standards to underpin good practice at the verification of indoor lighting system.

2 Verification field measurement

In this chapter are described necessary steps which shall be done before field measurement. The verification of the indoor lighting system shall be performed with the appropriate instrumentation and measurement grid to verify all necessary parameters given in the standard. It is divided in two subsections where they are listed instruments, devices and proposal of the measurement grid what is needed in the measurement procedure.

2.1 Devices and accessories for field measurement

According to standard for indoor workplaces it shall be verified by field measurement following parameters

- maintained illuminance level E_m
- uniformity of illuminance in the workplace U_0
- discomfort glare rating from luminaires installed in indoor workplace ***UGR***
- Correlated colour temperature (CCT) T_c
- Colour rendering index R_a

For the measurement of listed parameters is necessary to ensure appropriate instrumentation. It is very briefly described also in the standard. The emphasis is to choose proper illuminance meter and luminance meter. The measurements of the other parameters are not recommended in the standard. For example at the present for measuring discomfort glare rating UGR are commonly used image photometers the use of which has still an increasing trend. The CCT is can be measured by spectroradiometers especially with CCD array detectors which are easy portable. In connection of measurement of CCT by spectroradiometers it can be verified Ra index from spectral measured data in the visible spectral range. These devices can serve also for measuring relative spectral power distribution what can be used for spectral mismatch corrections of illuminance or luminance meter adapted to the V(λ) function. Illuminance level measurement can be also performed by means of already above described spectroradiometers with cosine corrector on the fibre optics entrance.

2.1.1 Illuminance meters

At the present lot of lluminance meters are exist on the market with different quality. User of the illuminance meter shall have good knowledge about his instrument to minimize errors in the measurement process. The scheme of illuminance meter for the measurement of the horizontal or vertical illuminance is shown in the picture Figure 1. One of the most common errors is exactly due to wrong using of illuminance meters because usually users rely on indicated values on the display unit of the photometer. Therefore proper metrological characterisation of the illuminance meter is necessary before measurement. In some countries e.g. Slovak Republic or Czech Republic when persons are authorised for verification measurement of indoor (outdoor) lighting system especially in the workplaces their illuminance meters shall be verified with traceability to national standards before measurement. It means that illuminance meters belong to the field legal metrology. Using non-verified illuminance meter is against the law and user can be persecuted if some official measurements performed. Based on the verification procedure is further decided by laboratory if illuminance meter comply with law regulatory requirements of the instrument. This condition is directly implemented in the law system of each country.

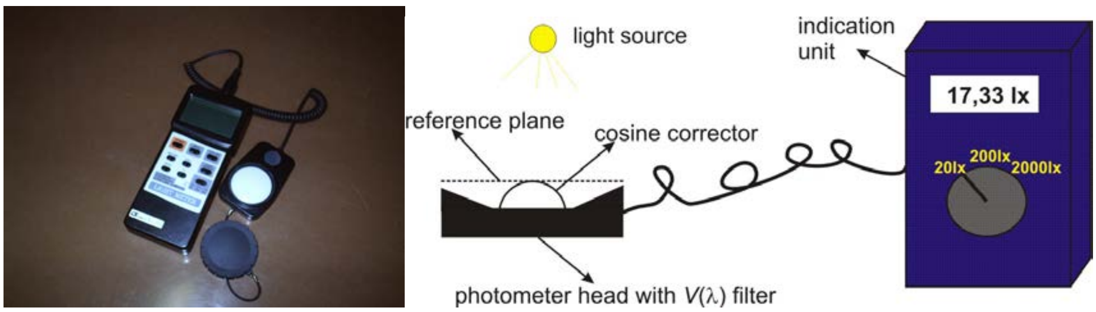

Figure 1 – Scheme of illuminance meter for the measurement of the planar illuminance

Unfortunately, quite often producers of illuminance meters declare common quality indicies which have been tested on the one piece of device to predict that these parameters are valid on whole production series. Even more users usually avoid verification procedure because they do not want spend money for whole procedure and they like rely on producer data which as it was mentioned above do not meet real values. Thus the verification of used devices in the measurement process ensure better quality of the measurement under assumption that user knows how to deal with his or her devices. The verification consists from calibration of following basic parameters of illuminance meter as

- Calibration of photometric scale - linearity
- Directional response of the photometer with cosine diffuser to the incident radiation
- Temperature dependence of the illuminance meter
- Spectral responsivity of the illuminance meter
- Fatigue of the illuminance meter

Each of the listed parameter can be found as quality index in the standard CIE S 023/E:2013. Measurement procedure should be performed also according to this document. The verified parameters represent metrological characteristics of illuminance meter which can significantly influence the measurement result. The calibration of them shall be performed by national metrologic institute or authorised laboratory for verification of illuminance meters. Sometimes it is needed to measure also other than planar illuminance what is defined for example in the new version European standard EN 12464-1 indoor workplaces where is requirement of measuring cylindrical illuminance. These types of illuminance meters are produced by some producers with special photometer head with cylindrical diffuser and before measurement they shall be also verified according to the measurement procedure described in the CIE standard.

2.1.2 Luminance meters

These devices are used for measurement of luminance as another important photometric parameter. It is very important measurement due to spatial luminance distribution information from the measurement in the place of indoor lighting system. On the market it can be found lot of various types of luminance meters with different view angle determined by used the optic system. They can be simply constructed in combination with illuminance meters when on the photometer head is mounted optics or baffles to determine particular view angle.

Also luminance meters as it was mentioned at illuminance meters should be properly metrologicaly characterised to avoid big measurement errors due to imperfections which are connected with these devices.

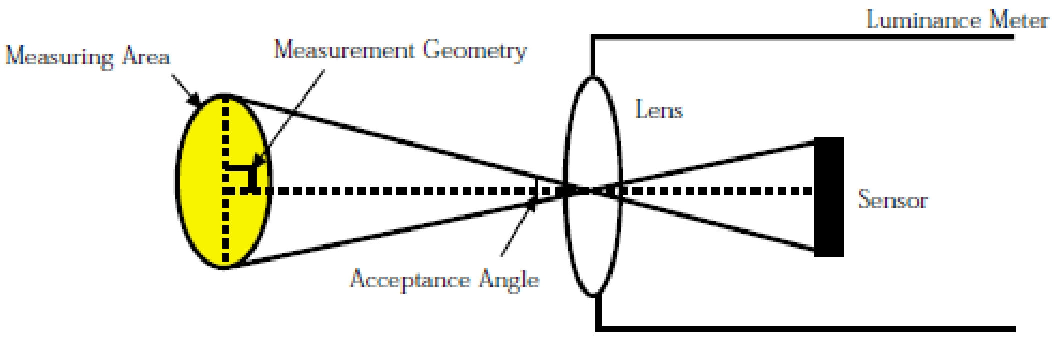

Figure 2 – Scheme of luminance meter

The verification should consists from calibration of following basic parameters of luminance meter as

- Calibration of photometric scale – linearity
- Directional response of the luminance meter
- Temperature dependence of the luminance meter
- Spectral responsivity of the luminance meter
- Focusing distance of the luminance meter

Luminance meters with view angle 1° or with smaller field view used at the special task areas. Requirements for luminance meters is defined in the standard ISO 8995-1:2002(E)/CIE S008/E:2001.

2.1.3 Image photometers

At the present this type of photometer is commonly used by many users for field measurement of luminance distribution of measured places in the practice. It means till just recommended parameters like UGR is can be measured not just be computed as it describes standard for indoor workplaces. The scheme of construction of image photometers is shown in the picture Figure 3. From the aquired image it is easily investigated spatial luminance distribution from the investigated position and thus according to mathematical relations in the document CIE 117:1995 Discomfort Glare in Interior Lighting.

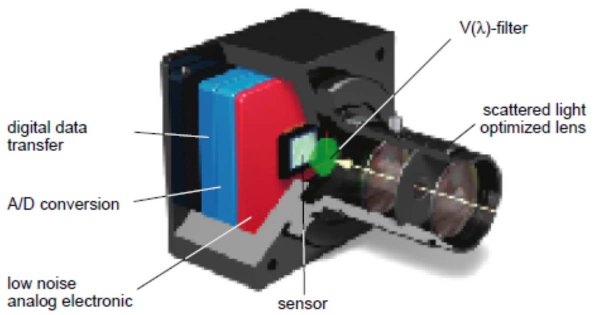

Figure 3 – Example of filter wheel image photometer or camera image photometer

In the Figure 3 are shown typical image photometers used in the practice. Their using is based on the CCD technology where image is acquired throughout optical system of each device. From these devices can be determined also colorimetric parameters of measured place, but user should be aware about the principle by means of the image photometer detect radiation falling on CCD chip. The first using filter wheel where X, Y, Z filters are mounted into the rotating wheel and for each of this filter is image acquired. Combination of these images can be established colour map of the image with photometric information ensured by Y filter what represent according to measurement geometry luminance photometric quantity. The second camera image photometer has RGBG matrix mounted on the CCD chip and after that by mathematic interpolation is picture processed. Both of described principles has advantages and disadvantages but common problem is spectral responsivity of these devices in the visible spectrum range which are not perfectly adapted to spectral matching functions defined in the CIE colorimetry. Among others also in the processing enter other problems connected with optical system and time of acquiring image where saturation of CCD chip can be reached what negatively influence measured values. Therefore using proper additional optics like grey filters is recommended and also proper modes for acquiring of image is necessary set so as user could avoid these errors. Especially for camera image photometers are very sensitive if big contrasts in the image occurred.

2.1.4 CCD spectroradiometers

The spectroradiometric measurements were usually used in laboratories for example desktop spectroradiometers using grid as disperse element in Czerny-Turner geometry. On the market we can find lot of types of spectroradiometers with different construction and different detection system consist detectors with various spectral responses. In the verification procedure of indoor lighting system should be used spectroradiometers which are simply portable and spectral information over whole spectral region to have on real time instead of scanning wavelength by wavelength i.e. time consumable measurement. This advantage provides still forthcoming and improving spectroradiometers with CCD array detector. CCD array element has area where are small areas so-called pixels defining resolution of instrument. For each pixel belong wavelength region with some bandwidth In the Figure 4 is layout the most common used commercial CCD array spectroradiometers.

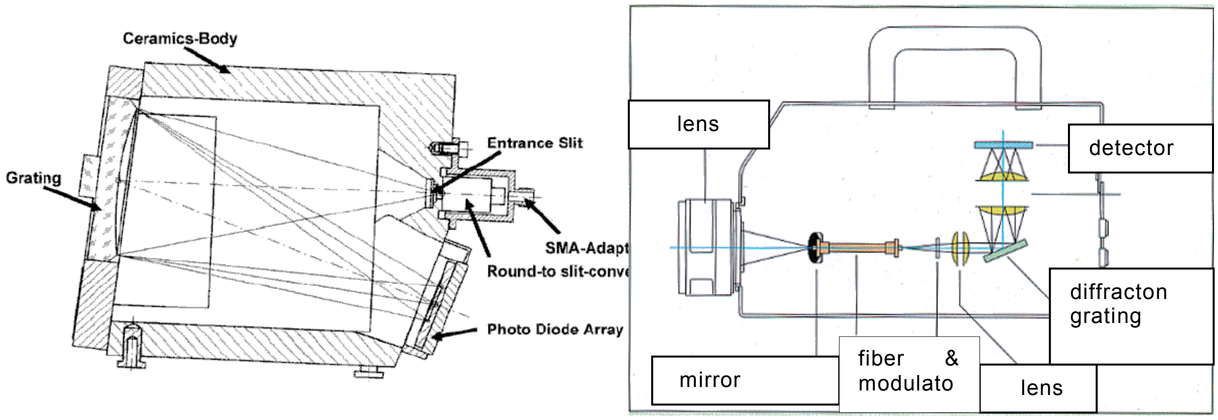

Figure 4 – Examples of CCD array spectroradiometers

The advantage of using CCD array spectroradiometers is undoubtedly clear. They shall be used for spectral power distribution of light sources in the measured place. Then data from spectroradiometric measurement in connection with measurement of illuminance or luminance can serve as spectral mismatch corrections of illuminance or luminance meters what in some level eliminates this error. Furthermore from spectral data it can be determined Ra index or CCT if necessary in some special cases.

2.1.5 Other devices

For distance measurement, environmental measurement i.e. temperature or humidity, voltage measurement in the plugs is necessary to use other devices which by means of could be measured desirable quanities e.g. distance between measurement points in the grid, temperature and humidity in the measured place or to hold photometer head of illuminance meter or fibre optics of spectroradiometer it shall be used tripod to ensure reliable measurement in the prescribed height above the floor and avoid shading which can negatively influence results of measurement. For measurement of environmental conditions in the measured place shall be used temperature/humidity meter. The voltage shall be performed by proper portable multimeter. These devices shall be properly calibrated with traceablity to national or international standards. These values are very important for corrections which they are coming from temperature coefficients of used devices described above.

2.2 Measurement grid

One of the very important aspects at the verification is choosing right measurement grid where verification of photometric parameters of lighting system is performed. The basic parameters are average maintained illuminance level at the task area $\overline{E}_m$ and uniformity of the illuminance U0 in the task area. The standard recommends perform control measurement in the grid as it was used in lighting design. This condition can not be very often obeyed especially for older lighting systems where lighting design is unknown. The measurement grid of verification control illuminance grid shall be designed according to relationship

$$p = 0{,}2 \times 5^{\log_{10} d} \quad (1)$$

where

d is the longer dimension of the calculation area (m), however if the ratio of the longer to the shorter side is 2 or more then *d* becomes the shorter dimension of the area

p is the maximum cell grid size (m);

For smaller areas sometimes result from relation is huge number of cells for verification which can be maybe reduced to the number which would satisfy and sufficient for verification of illuminance level in the workplace.

Table 1 – Results of analysis of the illuminance grid

Analysis	Interval of calculated average maintained illuminance level from chosen grids $\overline{E}_m$ (lx)	Interval of calculated uniformity of illuminance level from chosen grids U_0
EN 12464-1 p = 0,25m to 0,75m excluding 0,5m band from wall **56 to 487 measurement points**	(756lx ; 788 lx)	(0,36 ; 0,59)
EN 12464-1 p = 0,5m **112 measurement points**	762 lx	0,38
Number n = 1,78 Maximum error 10% **9 measurement points**	(590 lx ; 894 lx)	(0,59 ; 0,92)
Number n = 1,78 Maximum error 5% **18 measurement points**	(780 lx ; 820 lx)	(0,52 ; 0,71)

But preliminary results from investigation of various proposals of girds show that formula is the best possible in comparison with other approaches what is shown in the Table 1 where intervals of computed values of parameters in the verification various possible designs of grids investigated in research work at Slovak University of Technology in Bratislava (Dubnicka R. et al (2013),Bled). The reference value for maintained illuminance level was taken reference value 787 lx. Based on this work can be said that 4 % measurement error can be assumed as maximum error. For uniformity it should be done more deeply investigation because variance of this parameter is bigger than usually assumed uncertainty of this parameter and results shows that results are very different for different verification grids which can be designed.

3 Measurement procedure of verification

The following photometric parameters of indoor lighting system shall be verified what means verification of the calculations performed by means of lighting simulation tools DIALUX or RELUX what is commonly used by lighting engineers in preparation of the lighting design. It is maintained illuminance $\overline{E}_m$ of the particular indoor workplace

$$\overline{E}_{\mathrm{m}} = \frac{\sum_i E_i}{n} . MF \tag{2}$$

where

E_i	is the illuminance of the i-th measurement point in lx;
n	is the numbers of measurement points of grid;
MF	is the maintenance factor MF;

the uniformity of illuminance U0 in the workplace

$$U_0 = \frac{E_{\min}}{\overline{E}_{\mathrm{m}}} \tag{3}$$

where

$E_{\min}$	is the illuminance of the i-th measurement point in lx;
$\overline{E}_{\mathrm{m}}$	is the maintained illuminance level in lx;

and UGR given by the formula defined by CIE document

$$UGR = 8.\log\left[\frac{0{,}25}{L_{\mathrm{b}}} . \sum \frac{L^2 . \omega}{p^2}\right] \tag{4}$$

where

L_b	is the background luminance (cd.m^{-2});
L	is the luminance of the luminous parts of each luminaire in the direction of the observer's eye (cd.m^{-2});
ω	is the solid angle of the luminous parts of each luminaire at the observer's eye (sr);
p	is the Guth position index for each luminaire (displacement from the line of sight);

First step before the verification measurement of indoor lighting system will be performed all notes about the workplace shall be done by the person who will perform verification. Notes shall be written in the way that everyone independent who would like to repeat the verification measurement based on notes it could be repeated. It means description of whole lighting system i.e. informations about luminaires, reflectance of surfaces if they are diffuse it can be performed measurement according to the formula

$$\rho = \frac{L_{\mathrm{V}} . \pi}{E_{\mathrm{V}}} \tag{5}$$

where

L_{V}	is the luminance emerging from surface element in cd.m^{-2};
E_{V}	is the illuminance falling on the surface element in lx;

further notes shall be done about layout of measured place with dimensions, design of measurement grid (number of measurement points, layout on the ground or place where it was performed), photo documentation from the place, description of daylight openings (windows, roof skylights etc.), and installation height of luminaires.

After doing all necessary notes of the workplace the measurement can start. The photometer head of illuminance meter shall be adapted to illuminance level in the measurement place before measurement and simultaneously measurement of voltage in the plugs can be done. Meanwhile can be designed measurement illuminance grid where will be measured illuminance level at each level for determining average of maintained illuminance level and uniformity of illuminance in the workplace. The measurement of the illuminance if possible should be repeated three times to estimate uncertainty type A. If a lot of measurement points are designed due to dimension of the workplace the repetition of the measurement only in a few measurement points is sufficient performing measurement. If portable spectroradiometer can be used then measurement of spectral power distribution of light sources can be performed for evaluation of CCT and also for spectral mismatch corrections. At the end of verification by the image photometer it should be acquired images for each work position in the workplace to evaluate luminance distribution in the workplace and UGR.

If the measurement of all parameters has been carried out then next step is post-processing of measured data. It means applying all known corrections to the measured values according to calibration certificates of used devices.

The spectral mismatch correction factor of measured light source Z due to imperfect spectral responsivity (Figure 5) of the photometer head of both illuminance and luminance meter shall be done according to mathematic formula derived from document CIE standard

$$\mathrm{SMFC}(\mathrm{Z}) = 1 - \frac{\dfrac{\sum_{380}^{780} S(\lambda)_A \cdot V(\lambda) \cdot \Delta\lambda}{\sum_{380}^{780} S(\lambda)_A \cdot s_{rel}(\lambda) \cdot \Delta\lambda}}{\dfrac{\sum_{380}^{780} S(\lambda)_Z \cdot V(\lambda) \cdot \Delta\lambda}{\sum_{380}^{780} S(\lambda)_Z \cdot s_{rel}(\lambda) \cdot \Delta\lambda}} \qquad (6)$$

where

$S_A(\lambda)$ is the spectral power distribution of illuminant CIE A at which calibration was performed;
$S_Z(\lambda)$ is the spectral power distribution of measured light source;
$s_{rel}(\lambda)$ is the spectral responsivity of photometer head;
$V(\lambda)$ is the spectral sensitivity of human eye.

Multiplying of measured values by SMFC reduces spectral mismatch error of photometers or image photometers. Quite often is spectral power distribution of light sources unknown because not everyone has spectroradiometer. When this case occurs then it shall be assumed theoretical spectrum of different sources and computed SMFC for each of this source. The biggest computed SMFC represent the maximum error of spectral mismatch error and it can be used as number for uncertainty analysis. Special attention should be focused when coloured light sources are measured especially in the blue or red spectral region where 60 % or 70 % error can be reached. By simulation of LED blue source and worse spectral responsivity of illuminance meter from Figure 5 was computed SMFC 0,27 i.e. when 100 lx indicates unit of meter with this SMFC it means real illuminance level at 27 lx.

The second factor which can significantly influence results is directional responsivity of illuminance meter. It is due to fact that in the workplace can angle of incident of light onto acceptance area of the photometer head be so large that using qualitative index f_2 do not sufficient. This qualitative index comes from basic assumption of diffuse light source falling from all incident angles uniformly and integration over all incident angles from 0° to 85°. Therefore it is necessary to analyse or estimate based on experience the origin of light incident on acceptance area of the photometer head for example in the case when for example falling onto acceptance area under angle over 50° where measurement error due to directional response will be larger in comparison with assumption just index f_2.

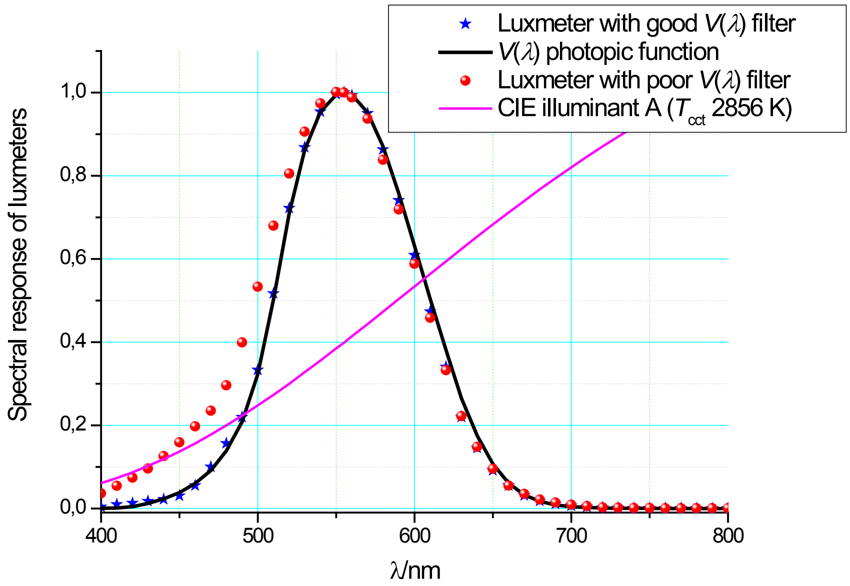

Figure 5 – Spectral responsivities of photometers of different quality

The last contribution to the results can occur from environmental conditions in the case when for example measurement is performing at ambient temperature different from calibration. Then it should be assumed temperature coefficient of photometer head if it is not temperature stabilized. For Si photodiode is common temperature factor approximately 0,1% or 0,2% from measured value. After using all corrections can be determined parameters which were under verification process.

4 Relation between uncertainty and standards values

At the end of the post-processing it shall be stated overall uncertainty measurement for each parameter. It is commonly underestimated and avoided, but without expression of uncertainty of measurement it can not be decided if photometric parameters verified in the measurement process comply with standard requirements or not. Relation between of uncertainty measurement and values prescribed by the standard shall be clearly stated when it can be said that lighting system is OK or not. From the measured values properly corrected shall be subtracted uncertainty of the measured parameter from the result to follow the worst case what can occur. After that it can be compared to the standard value and it can be said that lighting system parameter complies with 95% probability when normal distribution is assumed. It means, when it was measured maintained illuminance level 575 lx with estimated relative uncertainty 10 % from measured value then the worst case is

$$575 \text{ lx} - (0{,}09*575) \text{ lx} = 523{,}3 \text{ lx}$$

When it was measured maintained illuminance level of the usual office then standard requirement is 500 lx and the lighting system clearly complies with standard condition. But when we assume larger uncertainty in the case when for example illuminance meter with worse quality is used after that it can not be clearly stated that maintained illuminance level comply to standard ISO 8995-1:2002(E)/CIE S008/E:2001. In this way should be compared all measured parameters.

5 Conclusions

In the paper was depicted briefly verification procedure of indoor workplace lighting system which can be done with described instrumentation and brief guide how to measurement should run. The proposal about treatment of measured value and uncertainty of measurement is coming from law from Slovak Republic. In the future is worth considering to create technical committee for creation of detailed guideline for lighting systems according to ISO 8995-1:2002(E)/CIE S008/E:2001. Especially the emphasis should be focused on the problematic of evaluation of the uncertainty in the verification guideline because a lot of people do not have good knowledge about this problematic and thus push these people to perform reliable measurement. It was shown that value assigned to measurement result is very important for decision if the parameter prescribed by the standard meet requirements or not. Furhermore they can be avoided many controversial situations over the world by means of unification verification procedure at CIE level.

6 Acknowledgments

This publication is the result of the project implementation:
Research centre of light and lighting technology, ITMS 26220220150,
supported by the Research & Development Operational Programme funded by ERDF.

Operačný program VÝSKUM a VÝVOJ

Agentúra
Ministerstva školstva, vedy, výskumu a športu SR
pre štrukturálne fondy EÚ

Podporujeme výskumné aktivity na Slovensku/
Projekt je spolufinancovaný zo zdrojov EÚ

Európska únia
Európsky fond regionálneho rozvoja

References

GRUM F., BECHERER R. J., 1979 „*Optical radiation measurements vol. 1: Radiometry*," Academic Press: 1979

OSA/AIP, Handbook of Applied Optics, Edited by Casimer DeCusatis, Chapter 1 (1997)

Dubnicka R. et al (2013), ANALYSIS OF ILLUMINANCE GRID AT VERIFICATION OF THE INDOOR LIGHTING BY MEANS OF FIELD MEASUREMENT, Lighting engineering 2013, Bled, Slovenia

Dubnicka R. et al (2013), RELATION BETWEEN THE GRID FOR CALCULATION/MEASUREMENT AND RESULTING LUMINOUS PARAMETERS FOR ILLUMINATION OF INDOOR WORKPLACES. CIE Midterm session 2013 "Towards a new century of Light": Paris

Dubnicka R. et al (2013), USING OF CCD BASED FIBRE OPTIC SPECTRORADIOMETERS IN PHOTOMETRIC MEASUREMENTS UNDER DIFFERENT CONDITIONS, CIE Midterm session "Towards a new century of Light", Paris: 2013

CIE 1995. CIE 117:1995. Discomfort Glare in Interior Lighting. Vienna: CIE.

CIE 1996. CIE 121:1996. The Photometry and Goniophotometry of Luminaires. Vienna: CIE.

CIE S 023/E:2013. Characterization of the Performance of Illuminance Meters and Luminance Meters. Vienna: CIE.

BIPM 2008. JCGM 100:2008. Guide to the expression of uncertainty in measurement, Paris: BIPM

CEN 2012, EN 12464-1. Lighting of workplaces Part 1: Indoor workplaces. Brussels: CEN TC 169 Light and Lighting

PP42

INFLUENCE OF ACCURACY LUMINOUS INTENSITY DISTRIBUTION MEASUREMENT ON LIGHTING DESIGN REALISATIONS

Dubnicka Roman, Gasparovsky Dionyz, Raditschova Jana
Department of Electrical Power Engineering, Faculty of Electrical Engineering and Information Technology, Slovak University of Technology, Bratislava, SLOVAKIA
roman.dubnicka@stuba.sk

Abstract

Paper concerns about problematic of expression of uncertainty measurement of LIDC in connection of lighting design of lighting systems. Even more it analyses influence of this parameter assign to the result of measurement to the lighting designs photometric parameters for either indoor or outdoor systems. At the end of paper is introduced analysis which can serve for new treatment about uncertainties at the photometric measurements and can also find solution for other parameters which are measured with their uncertainties as their influence on parameters to be interesting for lighting engineering field.

Keywords: Luminous intensity distribution curves, Lighting design, Uncertainty of measurement

1 Introduction

By means of goniophotometry are measured luminous intensity distribution curves (LIDC) of luminaires. These measurements are important for lighting designers who use results from these measurements for lighting desings of indoor or outdoor lighting system. Uncertainty of luminous intensity distribution of luminaires is at the present big unknown. Metrologists involved in the field of goniophotometry still try to find the way how to express the uncertainty of LIDC measurement by one number. Till now it could not be found agreement among this community what expression should be used. As it was mentioned goniophotometry is close connected with lighting designs for indoor or outdoor lighting systems. Therefore it can be possible inluence of uncertainty measurement of LIDC of luminaires on photometric parameters which are important for lighting designers. Simultaneously it can solve problem to improve of knowledge of lighting designers or customers who concerns about LIDC of luminaires. They could much easier to predict possible errors influenced by these measurements. Thus lighting designers can do better lighting designs what can avoid possible inconveniences which sometimes occurs at realisations. Furthermore avoiding these problems can be saved lot of money which can be as result of improper design.

The results from performed in research work can serve as background for future work how to express and treat influence of uncertainty measurement of LIDC of luminaires connected through practical treatment and interest from side of lighting engineers how to treat photometric measurements of luminaires i.e. uncertainty of measurement will not serve as invisible or not important number on the test reports or testing results of photometric laboratories. After that either accredited or not accredited photometric laboratory will not vaste anymore with time on uncertainty evaluation of measurement at the LIDC measurements of luminaires.

2 LIDC of investigated luminaires

The LIDC of luminaires should characterise spatial properties of luminaires which serve as input data for another processing by lighting engineers who prepare lighting design of installations either indoor or outdoor lighting. Therefore these data should be as much reliable as can be because they are linked through lighting computations to real photometric parameters which shall follow different standards or legal requirements. LIDCs of luminaires in the form interchangeable files in different forms depend on region over the world for example in Europe it is EULUMDAT photometric data file or in North America and Australia it is widespread IES photometric data file. These files serve as data for lighting engineers for lighting computations of indoor, outdoor or public lighting systems to compute photometric parameters as they are defined in standards e.g. EN 12464 part 1 Indoor lighting of workplaces, EN 12464 part 2 Outdoor lighting of workplaces or EN 13201 for Road lighting. Five types of luminaires with different LIDC were investigated. Four are intended to use for indoor lighting installations and one is for road lighting installation with LEDs. The LIDC of each luminaire is shown in picture Figure 1.

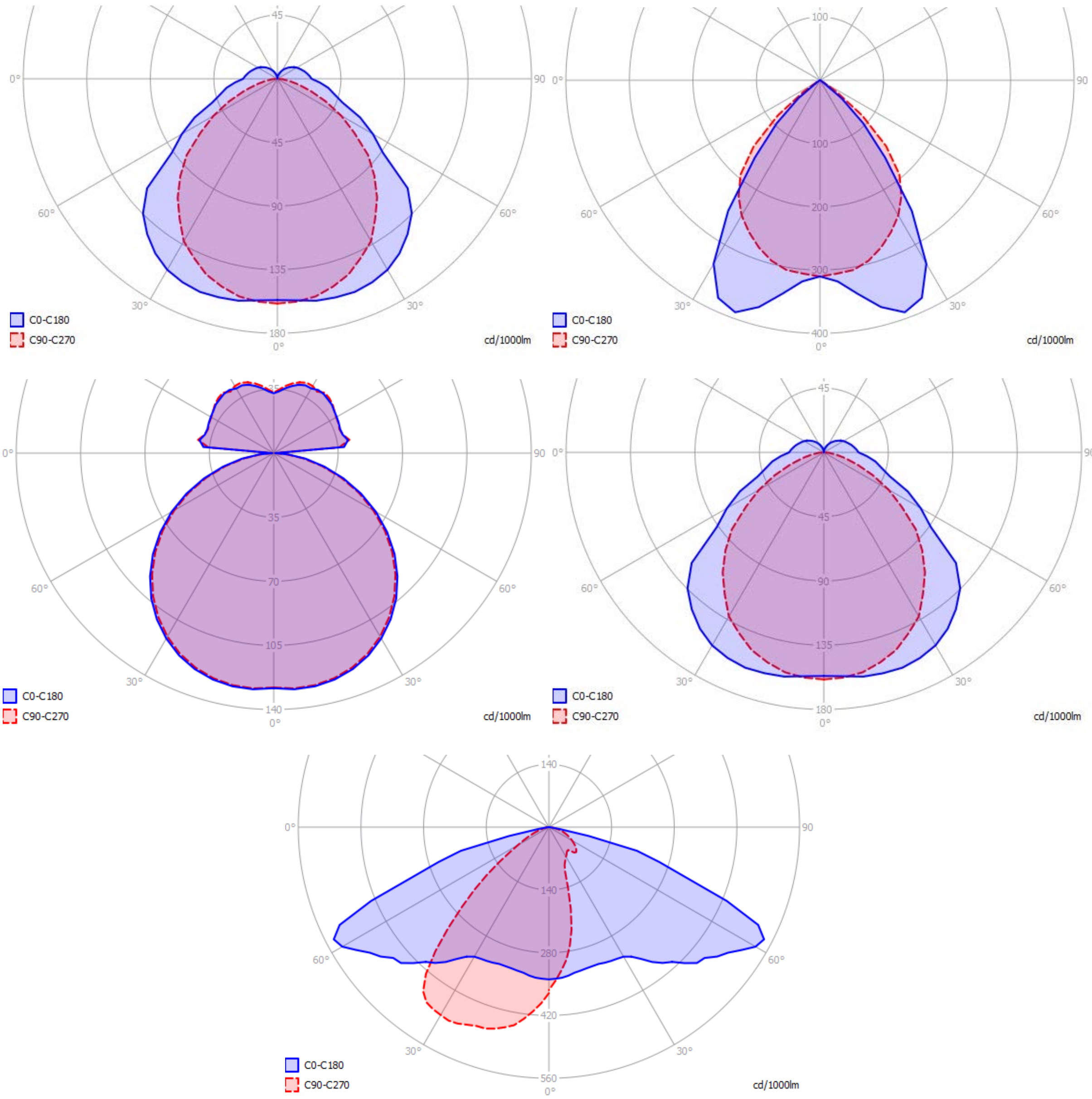

Figure 1 – Pictures of LIDC of investigated luminaires

Purpose of investigation it was to choose luminaires with different LIDC and with different downward and upward luminous flux fraction to show influence of accuracy of measurement to realisation of lighting system. For each luminaire was simulated by means of Monte-Carlo method various possible LIDC and each variant were perfromed lighitng computations of photometric parameters for lighting system. Due to the comparison purposes for indoor lighting luminaires was used one layout of the office room. The position of each luminaire in the simulations was invariant i.e. in the lighting calculations was assumed only various shape of LIDC. In the simulation of LIDCs of luminaires was assumed with relative expanded uncertainty of measurement U = 9 %. Into simulations was accounted both dependence and independence of luminous intensity in each direction of LIDC of investigated luminaire. It was also assumed model of the worst case which may realistically occur.

3 Lighting simulation tool calculations

Data from simulations described above were used for computations of photometric parameters of real situations. The indoor luminaires were situated into model of usual office and roadlight was in one type of road class. The 3D visualisation of models is shown in picture Figure 2.

Figure 2 – 3D visualisation of the room model and the road model

The following photometric paramters were computed. For indoor lighting it was maintained illuminance $\overline{E}_m$ of chosen indoor workplace

$$\overline{E}_{\mathrm{m}} = \frac{\sum_i E_i}{n}.MF \tag{1}$$

where

E_i is the illuminance of the i-th measurement point in lx;
n is the numbers of measurement points of grid;
MF is the maintenance factor MF;

and the uniformity of illuminance U_0 in the workplace

$$U_0 = \frac{E_{\min}}{\overline{E}_{\mathrm{m}}} \tag{2}$$

where

$E_{\min}$ is the illuminance of the i-th measurement point in lx;
$\overline{E}_{\mathrm{m}}$ is the maintained illuminance level in lx;

In the simulation with roadlight luminaire were computed photometric parameters according to EN 13021 which are average luminance on the road surface Lav, uniformities U0 a Ul for each road class. The calculations were performed by means of lighting simulation tool DIALUX what is commonly used by lighting engineers in preparation of design.

4 Results

In tables below, Table 1 and Table 2, it can be seen results from calculations of photometric parameters in DIALUX for investigated luminaires.

Table 1 – Results of calculations of parameters in DIALUX

	Luminaire No.1				Luminaire No.2				Luminaire No.3			
	Range of computed values		Range of computed values		Range of computed values		Range of computed values		Range of computed values		Range of computed values	
Parameter	E_{min} lx	E_{max} lx	r_{min} %	r_{max} %	E_{min} lx	E_{max} lx	r_{min} %	r_{max} %	E_{min} lx	E_{max} lx	r_{min} %	r_{max} %
Calculated values	384	471	85	87	449	549	75	76	595	728	58	60

Table 2 – Results of calculations of parameters in DIALUX

	Luminaire No.4				Luminaire No.5			
	Range of computed values		Range of computed values		Range of computed values		Range of computed values	
Parameter	E_{min} lx	E_{max} lx	r_{min} %	r_{max} %	L_{min} cd.m^{-2}	L_{max} cd.m^{-2}	$U0_{min}$ %	$U0_{max}$ %
Computed values	428	524	86	87	1,55	1,89	42	43

5 Conclusions

The paper analyses influence of accuracy of the measurement LIDC of luminaires and its impact to the lighting design. From preliminary results for chosen luminaires it can be said at all investigated luminaires with various LIDC that the uncertainty of measurement significantly influence result of lighting design computations i.e. also practical realisation of assumed lighting system. The recommendation for lighting designers from presented results in the tables it can be take under consideration uncertainty of measurement of LIDC of used luminaire in one direction because values lies around mean value of each range from computation. This number in that way should be directly involved into lighting computations to avoid complications due to bad lighting design. The most changing photometric parameters occur in maintainted illuminance for indoor luminaires and average luminance for roadlight luminaire. Uniformities in both cases is invariant towards various luminaires LIDC simulations because range of the computed values lies in the range of assumed uncertainty of measurement. They should follow the rule that variance of possible values from calculation around mean value is approximatelly even to uncertainty of measurement of luminous intensity in one direction. In the future work it is necessary investigate concrete problems in the measurement of spatial characteristics of luminaires and perform simulation in various indoor or outdoor models with more complicated shape of LIDC. Also influence for various symmetry should be investigated because this simplification in the measurement of LIDC of luminaires to save time, but on the other hand that laboratories risk

6 Acknowledgments

This publication is the result of the project implementation:
Research centre of light and lighting technology, ITMS 26220220150,
supported by the Research & Development Operational Programme funded by ERDF.

Operačný program VÝSKUM a VÝVOJ

Agentúra
Ministerstva školstva, vedy, výskumu a športu SR
pre štrukturálne fondy EÚ

Podporujeme výskumné aktivity na Slovensku/
Projekt je spolufinancovaný zo zdrojov EÚ

Európska únia
Európsky fond regionálneho rozvoja

References

GRUM F., BECHERER R. J., 1979 „*Optical radiation measurements vol. 1: Radiometry*,“ Academic Press: 1979

OSA/AIP, Handbook of Applied Optics, Edited by Casimer DeCusatis, Chapter 1 (1997)

CIE 1996. CIE 121:1996. The Photometry and Goniophotometry of Luminaires. Vienna: CIE.

BIPM 2008. JCGM 100:2008. Guide to the expression of uncertainty in measurement, Paris: BIPM

CEN 2012, EN 12464-1. Lighting of workplaces Part 1: Indoor workplaces. Brussels: CEN TC 169 Light and Lighting

CEN 2012, EN 12464-2. Lighting of workplaces Part 2: Outdoor workplaces. Brussels: CEN TC 169 Light and Lighting

CIE 2005. CIE 97:2005. Guide on the Maintenance of Indoor Electric Lighting. Vienna: CIE.

Dubnicka R. et al (2013), RELATION BETWEEN THE GRID FOR CALCULATION/MEASUREMENT AND RESULTING LUMINOUS PARAMETERS FOR ILLUMINATION OF INDOOR WORKPLACES. CIE 2013 "Towards a new century of Light": Paris

PP43

SPECTRORADIOMETRIC ANALYSIS OF SKY TYPES ACCORDING TO CIE DOCUMENT CIE S 011/E:2003

Dubnicka Roman[1], Rusnak Anton[1], Komar Ladislav[2], Darula Stanislav[2], Smola Alfonz[1]
[1]Department of Electrical Power Engineering, Faculty of Electrical Engineering and Information Technology, Slovak University of Technology, Bratislava, SLOVAKIA
[2]Institution of Construction and Architecture, Slovak Academy of Sciences, Bratislava, SLOVAKIA
roman.dubnicka@stuba.sk

Abstract

Sky types are defined as the luminance distribution on a sky vault, although only 15 standardized types are using in various fields of research. They can be used in different areas of life - building physics, medical and other areas. Luminance as the photometric quantity is based on the spectral values using the V(λ) function, and is the key parameter for sky luminance distribution. Nowadays it does not exist knowledge of the spectra of all sky types. Contribution will try to give an idea how to behave several types of sky. Presented article discusses possibility of measuring spectral characteristics of a daylight and its evaluation. It shows the selected spectral power distributions. The paper presents experimental measurements aimed to basic colorimetric parameter and shows the relation between luminance and correlated colour temperature of the sky type. Even more it shows a concept how to behave several hemispherical luminance distributions.

Keywords: radiometric measurements, spectral power distribution, CIE sky types, CCT, luminance

1 Introduction

Spectral power distribution is formed by the decomposition of the radiation energy on the spectral components and creates the base of all quantitative parameters reported in lighting technology in the visible spectral range from 380 nm to 780 nm. Quantitative photometric parameters as luminance, illuminance etc. are derived from the spectral power distribution and their knowledge are important in interior lighting for buildings using daylight as the alternative energy saving solution. Solar radiation transmitting radiant energy is used not only as a renewable resource, but it is also important for visual perception of natural light by the human eye. The atmosphere changes the spectral power distribution and it affects the photometric and colorimetric parameters. Current studies have gradually defined various parameters. The lighting engineering recognizes two views of solar radiation i.e. in terms of spectrum of solar radiation utilized in colorimetry through defined daylight sources and the view in terms of the luminance distribution of the sky, which is variably spread over the surface of the hemisphere. These two approaches of the solar radiation can solve several current topics such as physiological action of light on human circadian rhythm, spectral simulation of daily light exterior and interior conditions, etc. Spectral prediction is one of the unsolved problems of mixing natural and artificial light. Future of lighting engineering is based just on a relative spectral distribution so that will be achieved the desired level of spectral power distribution in space and faithfully simulate daylight. This trend will be adapted and even more computing programs that will work with spectral mathematical methods. The current model of sky provides fifteen types of luminance distribution on the hemisphere. The introduction of the mathematical model is focusing on photometric parameters. Sphere of spectral characteristics for the distribution of luminance on the sky hemisphere is remained unexplored up to now.

2 Theoretical procedure of measurement and evaluation of spectral characteristics

In the measurements it can be assumed several key factors: the climatic conditions of the location, viewing angle, angular height of the sky element, position of sun, sky type, the time necessary for the measurement execution. The usage is established on mathematical apparatus according to ISO 15469:2004 - CIE S011/E:2003 (CIE, 2003). Climatic conditions can affect the resulting values in terms of uncertainty of measurement. Input data in the measurement is the spectral irradiance $E_e(\lambda)$ of the incident radiation reaching the sensor. For each element on the hemisphere it is possible to determine irradiance E_e of selected band spectral power distribution and the equation below is valid

$$E_e = \sum_{\lambda_1}^{\lambda_2} E_e(\lambda).\Delta\lambda \tag{11}$$

Evaluation algorithm is based on the input data set of experimental measurements. Obtained data from measurement are processed by the CIE standard describing 15 sky types. Analysis of sky elements is determined by spectral distribution, which was verified by a mathematical method for the reconstruction of the spectral characteristics of daylight. Radiance of element $I_e(\lambda)$ is given by

$$I_E(\lambda) = \frac{\mathrm{d}\phi_e(\lambda)}{\mathrm{d}\Omega} \tag{2}$$

where Φ_e (W.s^{-1}) is the radiance power and angle $\mathrm{d}\omega$ (sr) is the solid angle. For differential of the spectral irradiance E_e using the inverse square law next relation is valid

$$\mathrm{d}E_e(\lambda) = \frac{\mathrm{d}I_e(\lambda)}{r^2} = \frac{L_e(\lambda).E_e(\lambda).\mathrm{d}A\cos\theta}{r^2} = L_e(\lambda)\mathrm{d}\omega \tag{3}$$

where $L_e(\lambda)$ is the spectral radiance and solid angle is replaced by the parameter distance r between the sensor and the element on the hemisphere. Integration $L_e(\lambda)$ through the surface area *A* is expressed by the direction of radiation $a^2 sin\theta d\theta d\varphi$, therefore the overall intensity of the radiation spectrum $E_e(\lambda)$ is written as follows:

$$E_e(\lambda) = \int_0^{2\pi}\int_0^{\pi/2} L_e(\lambda)(\theta,\varphi)\cos\theta\sin\theta.\partial\theta.\mathrm{d}\varphi \tag{3}$$

By identifying the sky elements in the spectral level it is possible to do analysis of sky types. Determination of the real type of sky parameters is based on the time and date of measurement, e.g. position of the sun on the hemisphere. Measured spectral characteristics of sky types are processed for different sky conditions in regard to the experimental spectral characteristics. Determination of the irradiance on a horizontal plane for sky luminance distribution can be described as (Noriko, 2005)

$$E_e(\lambda) = \sum_{i=1}^{145} \pi \frac{E_{ei}(\lambda)}{\omega}(\cos^2\gamma_{up} - \cos^2\gamma_{down}) \tag{5}$$

Equation (5) is a global spectral irradiance on the horizontal plane by the distribution of elements in the hemisphere and it includes the size of the amplitude of individual elements. Angles γ_{up}, γ_{down} represent defined almucantars of the elements, $E_{ei}(\lambda)$ is the spectral irradiance from a given element.

Determination of the calculation method is based on principal component analysis (PCA) (Simmons, 1963). This method uses the reconstructed spectral characteristics of representative sky types and creates spectral components of daylight $S_0(\lambda)$ to $S_2(\lambda)$. PCA method has proven to be most suitable in terms of spectral characteristics of the reconstructions. Current calculation method is also used for the CIE daylight sources. The

CIE model verification serves as a basis for determining the spectral characteristics of sky types based on the value of CCT (Robertson, 1968).

Spectral characteristics of sky elements were measured by the radiometric system (Komar et al., 2013). The measurement is based on scanning sky elements for the selected almucantar and azimuth, a prerequisite for the measurement is a traceability to the measurement geometry. Number of measured elements in the case of luminance distribution is 145. All elements are covering almost 70% of the hemisphere. When evaluating element is considered to be a light source whose parameters are measured at all points in the same area, i.e. it is considered as a point light source.

3 Results of scanning by the spectral scanner

The relative gradation and indicatrix function (CIE, 2003) is possible express for radiometric measurement. The coefficients *a,b,c,d,e* are becoming depend on wavelength. Then coefficients have form: *a(λ), b(λ), c(λ), d(λ), e(λ)*. It is valid

$$f(\chi,\lambda) = 1 + c(\lambda)\left[\exp(d(\lambda)\chi - \exp(d(\lambda)\frac{\pi}{2})\right] + e(\lambda)\cos^2\chi \tag{6}$$

Radiometric interpretation of gradation function is analogic (CIE, 2003) and it is valid

$$\frac{\varphi(Z,\lambda)}{\varphi(0^0,\lambda)} = \frac{1 + a(\lambda).\exp\left(\frac{b(\lambda)}{\cos Z}\right)}{1 + a(\lambda).\exp\left(b(\lambda)\right)} \tag{7}$$

In Figure 1, the function of L_a/L_z indicates the realistic mathematical calculation according to CIE 2003/ISO standard. Base curve ratio achievable element and the element of zenith L_a/L_z based on luminance, so a given curve will always advise to the average of all spectral functions to express indicatrix, or gradation waveforms. Description of the spectral decomposition indicatrix and gradation functions was not currently studied. To illustrate the spectral curves, basic sky types; clear and overcast are presented on Figure 1. It indicates a relation with a defined evaluation based on the luminance. Luminance is related with the spectral sensitivity of the human eye V(λ). The shape of the curve V(λ) has an impact on the photometric interpretation. For the indicatrix spectral dependence, the interval of the wavelengths of the red part of the spectrum is dominant. The lower angular distances from the sun occurs scattering investigated interval of spectral wavelengths. With increasing distance from the sun on the solar almucantar leads to overlap indicatrix curves. This causes a lot of radiant energy from the sun, which exceeds the level of energy in the higher distance from the sun. The sun as the energy source has a thermal emitter and has equal energy spectral distribution. Predominant part of the energy emission in direct sunlight is in the red spectral wavelength region. CIE mathematical model computes spectral characteristics of daylight indicating a dependence of the spectral range with lots of incident energy. This theoretical assumption does not apply. Spectrum of the overcast sky is presented and the spectral characteristics of the blue light predominates. Gradation function of spectral studied wavelengths on Figure 1 is a vertical spread on the solar meridian. It occurs otherwise than in the case of spectral indicatrix functions. In the site of zenith angle 90° are the spectral curve intervals consistent with increasing distance from the zenith to the horizon and there can be seen a scattering of wavelength intervals. A specific case is the overcast sky, which is azimuthally uniform and the sun has absolutely no impact on radiated spectral characteristics of diffuse sky. Diffuse sky behaves as uniformly glowing object with a certain luminance gradation on the hemisphere.

Scattering of the spectral intervals of gradation function is minimal and in some gradation levels reaches higher energy in the blue and violet spectral interval. Indicatrix and gradation spectral functions have impact for determining the presence of direct sunlight. It occurs at wavelengths above 500 nm. Overcast sky has minimal scattering spectral bands at different χ, Z. Finding decomposition of wavelengths for each spectral region the color of the curve indicates the character of the radiation of the sky hemisphere. As a result of determining the type of the sky is a standardized way of spectral irradiance distribution of elements on the sky hemisphere. Processing relationship for spectral irradiance is obtained. Calculation provides amplitude to the final shape of the spectral power distribution.

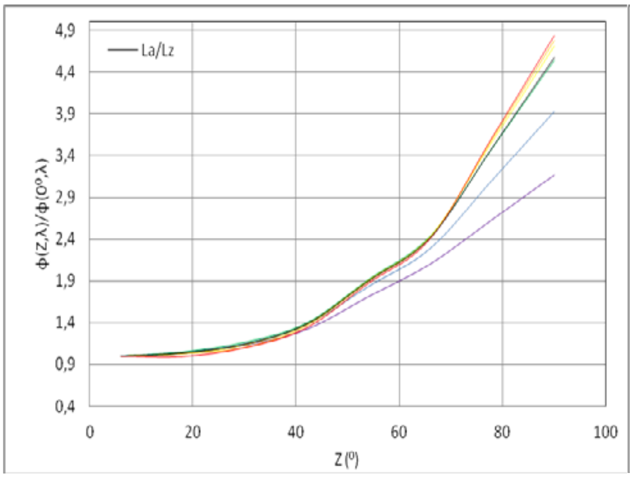

Spectral gradation of clear sky

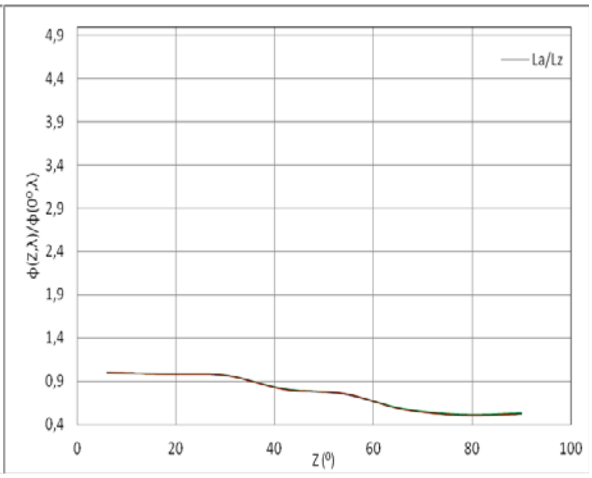

Spectral gradation of overcast sky

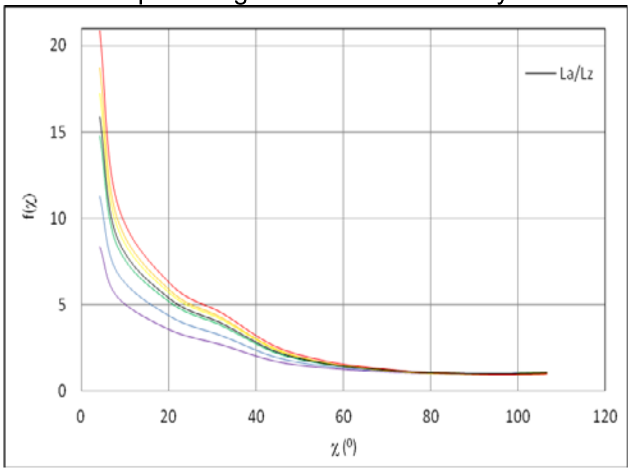

Spectral indicatrix of clear sky

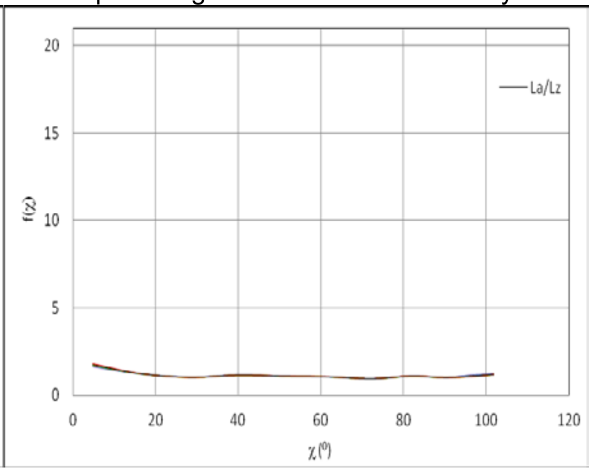

Spectral indicatrix of overcast sky

Figure 1 – Spectral decomposition of distribution ranges

Reported sky types are selected on the basis of the highest rate of R^2 with defined types of sky. Luminance distribution of sky is choosing on the basis of the homogeneity of the hemisphere, i.e. solar meridian for the left and right side should be about the same, so that indicatrix and gradation function achieve similar properties. From the measurements were obtained fourteen sky types. None evaluated type was type is designated V.5. Sky types I.1 to III.1 characterize sky without direct sunlight. Reconstructed spectra indicate a predominance of wavelengths in the range from 300 to 500 nm.

Sky types III.2 to IV.3 are with filtered sunlight, where the hemisphere is partially covered by clouds. This group is to asses difficult in terms of spectral characteristics. The character of the hemisphere creates together with dynamic marching different variations of spectra. Waveforms on Figure 2a), show which range is able to acquire sky types. For a more comprehensive study of this group it shuld be suitable to measure hundreds of skies. Sky types IV.4 to VI.6 are as much as possible affected by direct sunlight. The amplitude of solar radiation in the spectral ranges 500 nm or more is reflected, it comes to the energy increase in spectral value. Historical measurements of spectral characteristics were composed of multiple measurements across the world. Time diversity of the measurements in terms of luminance variations of the sky type, is manifested in indicatrix and gradation functions. Considering minimum altitude of the sun on the hemisphere ($\gamma_s \geq 6^o$) removes this error. For all measured and evaluated skies coefficients *a, b, c, d, e* were recorded together with the coefficient of determination R^2. Sky type with the highest compliance was taken into account as a representative type of the sky shown on Figure 2b).

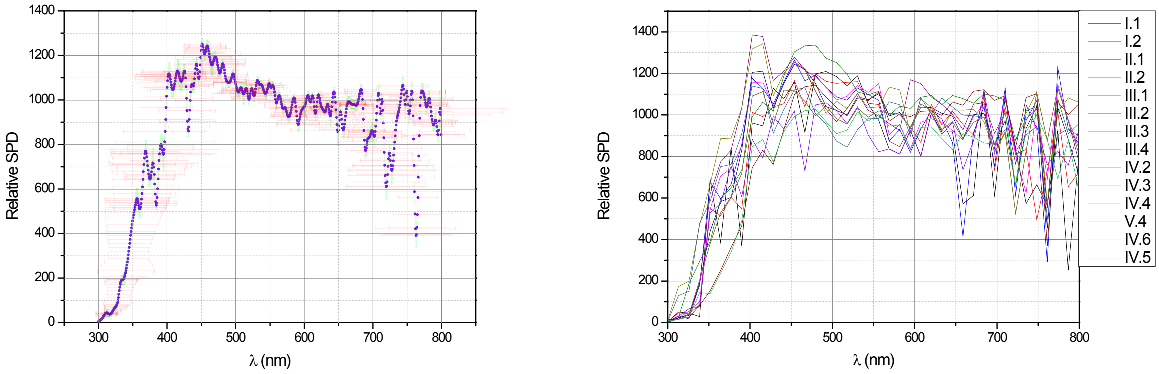

a) b)

Figure 2 – a) Average spectral power distribution from sky types with scatter of values, b) Spectral characteristics

Verification was performed for fourteen representative spectral types, which were measured and evaluated. Analysis of the characteristic vectors $V_{1,n}$ indicates the spectral waveforms abstractness except vector V_1 and subsequent feature vectors can reach negative values.

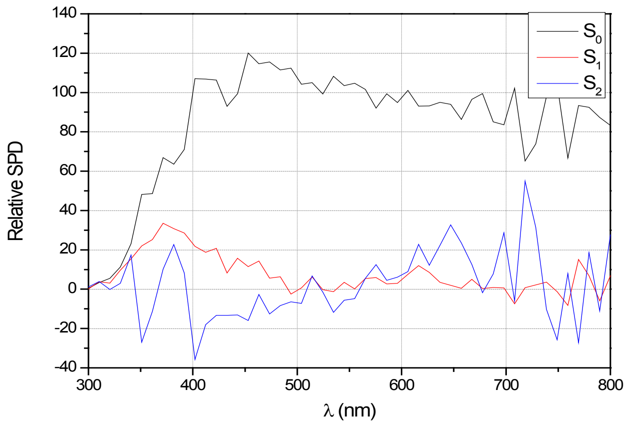

Figure 3 – SPD of daylight components calculated from reconstitution of sky type.

Waveforms of vectors are approximately equal to the evaluation of daylight mathematical model CIE, to their discrete form. Reverse relationship of the spectral power distribution of daylight has been verified for sky types. Using the procedure of PCA daylight components S_0, S_1, S_2 were obtained.

Component of daylight S_0 represents the average value determined by the spectral distribution of all wavelengths. Waveform on Figure 3 shows S_1 and S_2 components. Expression of component S_2 is a curve given by scanning the spectral characteristics of high-resolution measurements. The components are expressed by cubic spline interpolation method. In evaluating the spectral distribution manifests compressed sample wavelength. The difference between the model and real curves in the wavelength range 300-330 nm is caused by supplementing the original authors of the UV measurements, Figure 4.

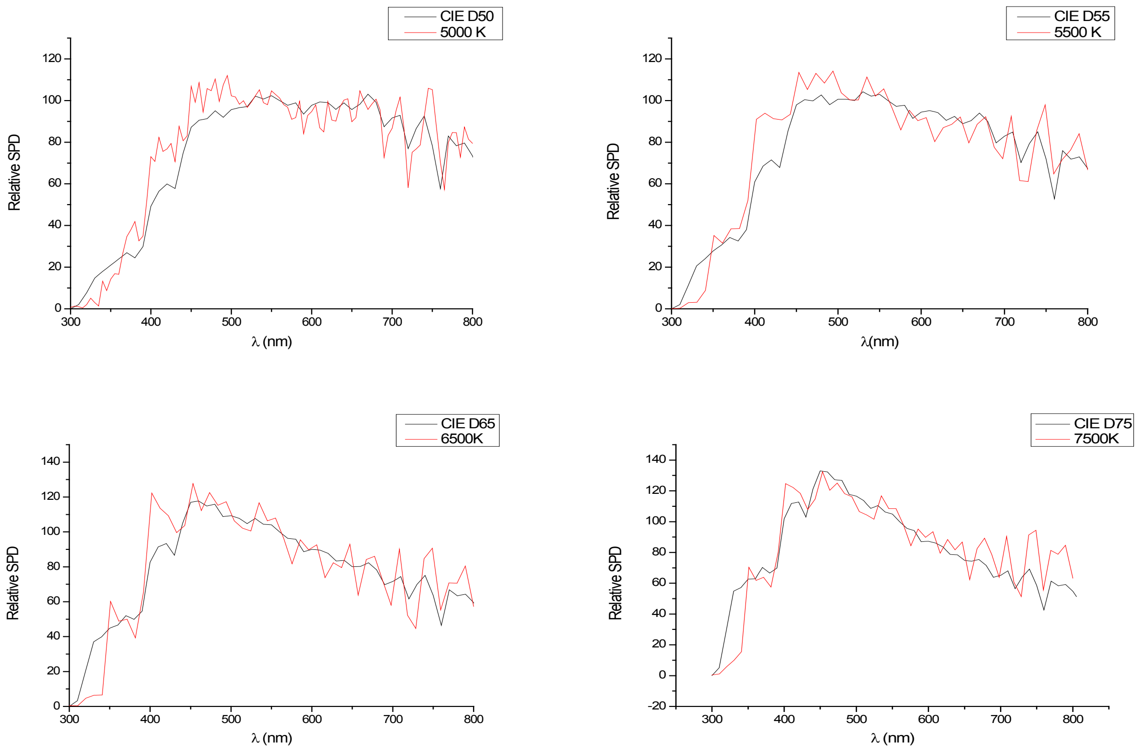

Figure 4 – Spectral power distributions of daylight light sources D50, D55, D65, D75 deriving from S_0, S_1 a S_2

4 Daylight curve in chromaticity diagram

Luminance distribution of sky types are indirectly linked to the defined colorimetry of daylight. Standard overcast sky is assigned in list of luminance distribution of sky as I.1. From the current standard are not verified the values of colorimetric parameters.

Table 1 Parameters of daylight equation $y=a+bx+cx^2$

Type of evaluation	Count of elements / sky	a	b	c
Global	89	-0,132	2,166	-2,220
Sky patch	12 905	-0,166	2,401	-2,576

Table 1 shows measurements of daylight and presented by expression of daylight curve by polynomial equation of the second degree. Table was completed by measuring a set of data. Those are the two cases: the composition of the resulting spectral irradiance to the global irradiance and the elemental expression of all tested types of sky, see Figure 5. The measured sky I.1 to VI.6 covers the whole spectrum of colours. The majority of the measured elements located or surrounds curve of daylight. At the global colorimetric measurements of the sky the elements that do not meet requirement of distance from daylight curve or Planckian locus were not included into the evaluation. The amplitude of energy of these elements achieves low energy levels. Sensing of elements occur the substance of radiation hemisphere in its parts. Spectral measurements of the diffusion system in combination with the direct measurement of radiation lead to different variations of the chromatic coordinates. Group of sky types I.1 to III.1 have CCT below the maximum of limit of model CIE. The chromaticity coordinates of types III.2 to IV.3 are distributed on curve of daylight. Chromaticity coordinates, which are located at wavelengths of red and outside curve of daylight have physical nature in direct. In clear sky types, IV.4 to VI.6, chromaticity coordinates are scattering mainly in blue region, which occurs on opposite hemisphere from that where sun is located. Elements of clear sky achieve CCT = 20 000 K. Evaluation sky from reconstructed global radiation are valid for condition $\Delta uv \leq 5,4 \times 10^{-2}$ In case of measurements the 62 %

from all elements meet this condition. It is about 8 000 elements. The relative expanded uncertainty of spectral radiometric measurement was estimated as U ~ 11 %. The reported expanded uncertainty of measurement is stated as the standard uncertainty of measurement multiplied by the coverage factor k = 2, which for a normal distribution corresponds coverage probability of approximately 95%. The standard uncertainty of measurement has been determined in accordance with GUM document (BIPM, 2008).

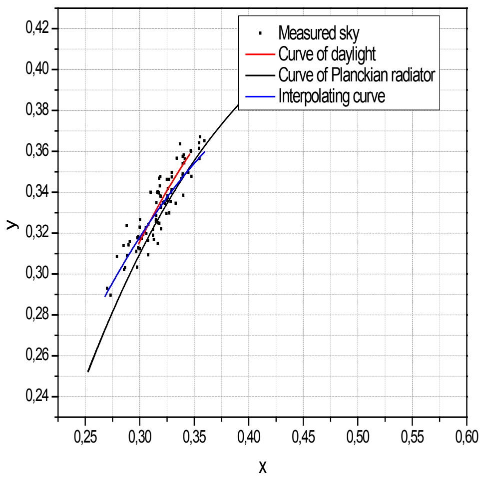

a)

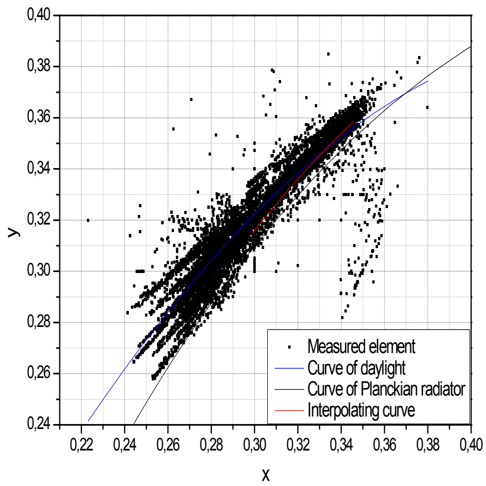

b)

Figure 5 – Daylight curve a) of reconstructed sky type, b) of measured elements on hemisphere.

5 Conclusion

Spectral characteristics compositing of the 145 sky elements come into wavelength regions whose form are not consistent with the predicted spectral power distribution of the various regulations and standards. The amplitude of the analyzed elements is showing in these spectral intervals atypical spectral power distribution. When measuring almucantar, the angular height of 60 and 180 depending on the solar almucantar may occur outside parasitic spectral distribution over the ground. Indicatrix and gradation function in assessing the sky type are a quality control system. Functions are mathematically formulated and adequately present type of sky. Overall, the functions can be described up to 36 skies, combining the indicatrix and gradation functions we can get sky type, which is not established by standards. By composition of 145 elements in the hemisphere is possible to get a representative form of spectral power distribution.

Analysis of the data of different authors demonstrated possible imperfection of mathematical method of daylight curve. Presentation of the method forms equation with a perfect parallel with the curve of Planck radiator. In a real environment with real measurements of solar radiation the chromatic coordinates may not be always placed on the daylight curve.

The original authors of the experimental observations of daylight curve measurements performed in different ways: direct, diffuse and reflected measurement of solar radiation. By the methods of measurement were captured possible states of daylight and subsequently were analyzed by the method of principal components.

Comparing both types of evaluation polynomial equation daylight confirms that atmospheric conditions are variable and one prediction equations describe the ideal state of daylight in the chromatic diagram.

Acknowledgements

The first, second and last authors of the paper were supported by the agency VEGA MŠVVaŠ SR under Grant No. VEGA 1/0988/12 “Energy efficiency of lighting systems in buildings”. The third and fourth author of the paper were supported by the APVV Agency under the Contract No. APVV-0177-10 and also by Grant Agency VEGA under contract No. 2/0029/1.

References

CIE. 2003. *Spatial Distribution of Daylight – CIE standard general Sky CIE S 011/E:2003*, Vienna: CIE, ISBN: 0580436101.

KÓMAR L., RUSNÁK A., DUBNIČKA R. 2013. Analysis of diffuse irradiance from two parts of sky vault divided by solar meridian using portable spectral sky-scanner, *Solar Energy*, 96, p.1-9. ISSN: 0038-092X, 2013.

NORIKO U. et al. 2005. Estimation of horizontal illuminance by measured sky luminance distribution, *Building simulation 2005, Ninth international IBPSA conference*, Montreal, Canada, p. 1271, 2005.

ROBERTSON A.R. 1968. Computation of correlated color temperature and distribution temperature, *Journal of the Optical Society of America*, 58, p.1528-1535 ISSN:1084-7529.

SIMONS, J. L. 1963. Application of characteristic vector analysis to photographic and optical response data, *Journal of the Optical Society of America*, 53, p.968–974, ISSN:1084-7529,

BIPM. 2008. JCGM 100:2008, GUM 1995 with minor corrections, *Evaluation of measurement data – Guide to the expression of uncertainty in measurement*, first edition, p.10 – 27.

PP44

PREFERABLE LIGHTING CONDITIONS FOR MIGRAINEURS TO RELAX IN ROOM

Shino Okuda[1], Akari Kagimoto[1], Muneto Tatsumoto[2], Katsunori Okajima[3] and Koichi Hirata[2]
[1] Doshisha Women's College of Liberal Arts, Kyoto, JAPAN,
[2] Dokkyo Medical University, Utsunomiya, JAPAN,
[3] Yokohama National University, Yokohama, JAPAN
sokuda@dwc.doshisha.ac.jp

Abstract

Lighting is an important factor for creating relaxing environment for both migraineurs and non-migraineurs. This study aims to reveal the preferable lighting condition for migraineurs to relax in a room. We conducted an experiment of subjective evaluation on preferable brightness in a mock-up experimental room. The room was equipped with nine LED down-lights and five fluorescent lamps on the ceiling. Subjects were asked to adjust the intensity of the light using a light controller so as to be their preferable brightness under four kinds of light source conditions. The results show that migraineurs statistically prefer lower illuminance and lower colour temperature as compared with non-migraineurs, and that preferable illuminance under the condition of LEDs is lower than that of fluorescent lamps for both migraineurs and non-migraineurs.

Keywords: migraine, preferable brightness, subjective experiment

1 Introduction

Lighting is an important factor to achieve relaxation in a room. The atmosphere in a room depends on what kind of luminaires, level of illuminance and correlated colour temperature (CCT) are used. The ranges of the illuminance and CCT for relaxing alone and for talking to a person have been measured in the mock-up room with fluorescent lamps (Nakamura, Karasawa, 1999). It has been also reported that, using a method of ascending adjustment, preferable illuminance for relaxation is very low (20-50lx) (Ishida, Inoue, 2005). In addition, it has been reported that low CCT and relatively low illuminance are favoured for relaxation on the basis of the experimental results using the scale model of a house (Oi, Takahashi, 2007), and that preferred illuminance and CCT level under RGB LED lighting are almost similar to those under RGB fluorescent lamps (Oi, Lu, Takahashi, 2009).

Preferable lighting conditions depend on physiological characteristics such as gender, age, chronic disease and so on. About 20% of women ranging from twenty to forty years old have migraine (Sakai, Igarashi, 1997), and about 40% of migraineurs have migraine headache triggered by light stimulation (Kelman, 2007). Migraineurs are more sensitive to glare than non-migraineurs (Aiba, Tatsumoto, Eda, Ishikawa, Ayama, Hirata, 2011) and to the light of 480nm which is the peak wavelength of intrinsically photosensitive retinal ganglion cell (ipRGC) (Tatsumoto, Eda, Ishikawa, Ayama, Hirata, 2013).

The purpose of this study is to reveal the preferable lighting conditions for migraineurs when they seek relaxation in a room. We conducted an experiment with subjective evaluation under LED and fluorescent lighting conditions.

2 Methods

Figure 1 illustrates a plan and a section of the experimental space. We made a mock-up living room whose space of 2.6 meters by 2.6 meters was consisted of a wooden floor and a white (N9) wall. It was furnished with a sofa, a low table and some shelves, and it was also equipped with nine LED down-lights (3000K or 5000K) or five fluorescent lamps (3000K or

5000K) on the ceiling. Figure 2 shows the spectral distribution of each light source under the illuminance condition of 400lx.

Subjects sit on the sofa in the experimental room. They were asked to adjust the intensity of the light using a light controller. They adjusted their preferable brightness by using an ascending and descending methods. Each subject repeated 3 times each ascending series and descending series under four kinds of light source conditions. Participants were classified into two groups, migraineurs and non-migraineurs, by medical screening on the basis of the International Classification of Headache Disorders. They were forty females in their twenties, and the half were migraineurs and the half were non-migraineurs.

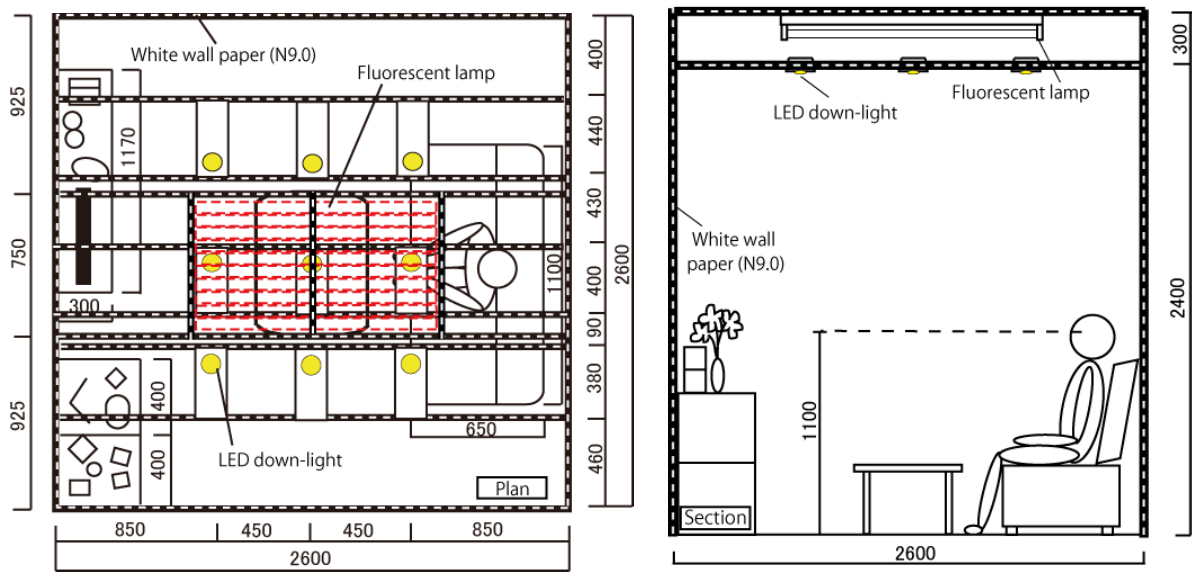

a) Plan b) Section

Figure1 – Experimental space

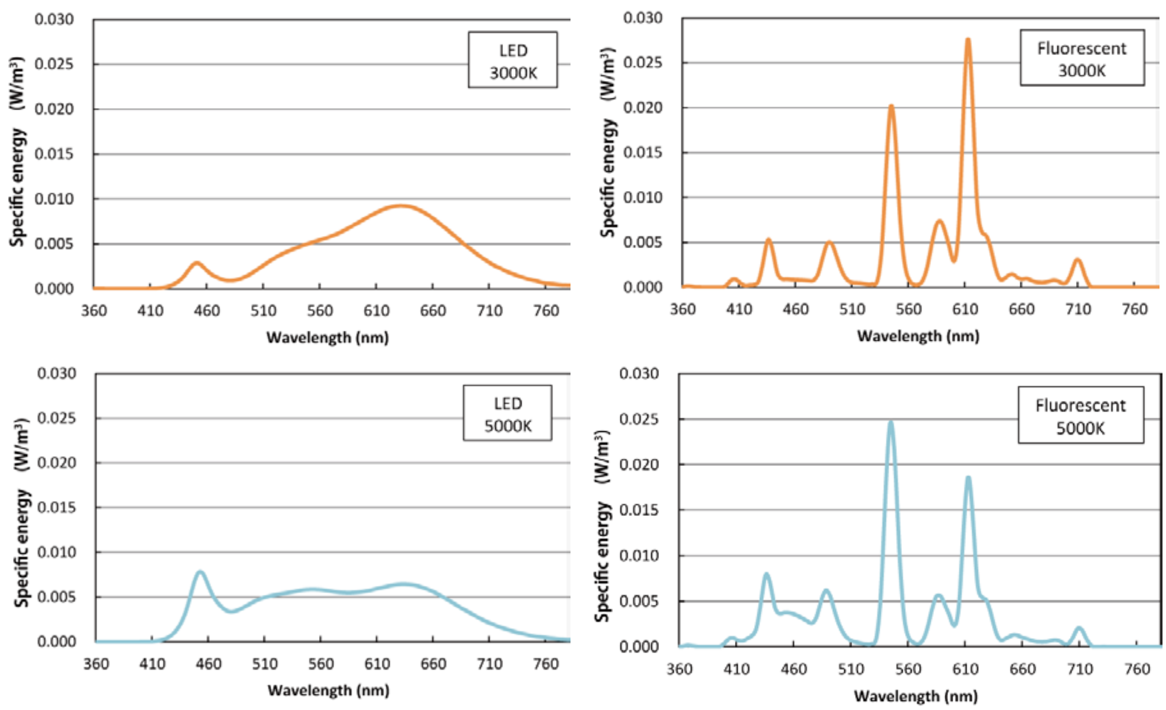

Figure 2 – Spectral distribution under each light source.

3 Results and discussion

Figure 3 shows the average values of illuminance adjusted to preferable brightness by ascending and descending adjustments under the LED lighting and fluorescent lighting conditions. It was shown that the adjusted illuminance by descending is higher than that by ascending in each lighting condition. These results suggest that migraineurs prefer lower illuminance and lower CCT as compared with non-migraineurs in any light source. Preferable illuminance range under the condition of LED lighting is lower than that of fluorescent lighting in each CCT condition for both migraineurs and non-migraineurs.

Table 1 shows the average values of all acquired data of the preferred illuminance under each lighting conditions. The average vertical illuminance values measured on the face of migraineurs are 199lx under the lighting conditions of 3000K LED lighting, 182lx under 5000K LED lighting, 305lx under 3000K fluorescent lighting, and 287lx under 5000K fluorescent lighting. On the other hand, those for non-migraineurs were 280lx under 3000K LED lighting, 251lx under 5000K LED lighting, 461lx under 3000K fluorescent lighting, and 407lx under 5000 K fluorescent lighting. There are statistical differences between the preferable illuminance values for migraineurs and that for non-migraineurs.

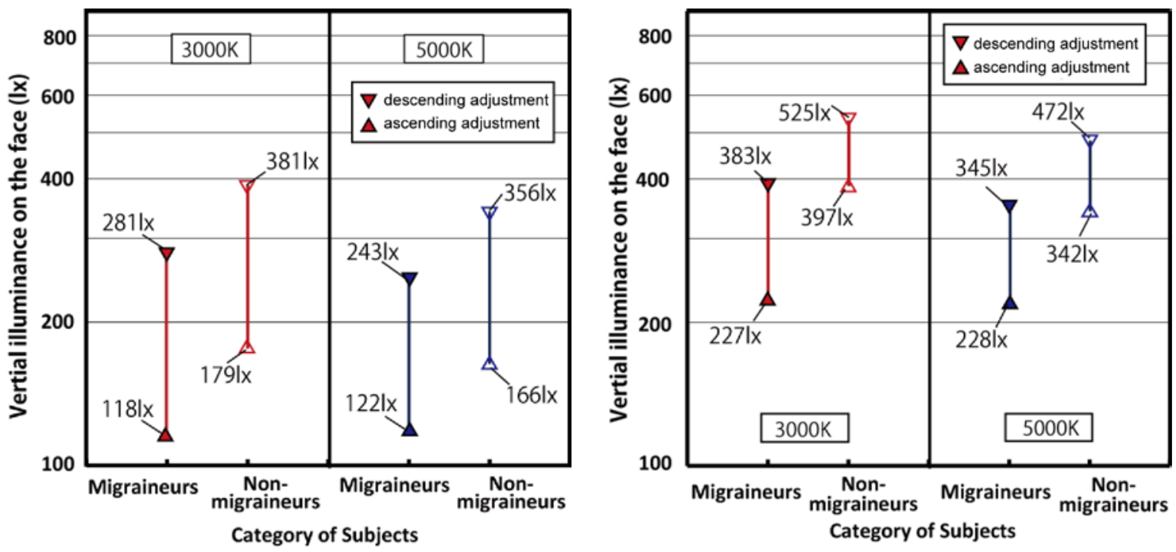

a) LED lighting b) Fluorescent lighting

Figure3 – Evaluation results of preferable illuminance on the face

Table1- Statistical results on the significant difference between the preferable illuminance for migraineurs and that for non-migraineurs

Light source conditions	Preferable illuminance for migraineurs	Preferable illuminance for non-migraineurs	*p*-value
LED lighting 3000K	199(lx)	280(lx)	0,006**
LED lighting 5000K	182(lx)	251(lx)	0,027*
Fluorescent lighting 3000K	305(lx)	461(lx)	0,004**
Fluorescent lighting 5000K	287(lx)	407(lx)	0,016*

*p<,05 **p<,01

4 Conclusions

Migraineurs preferred lower illuminance and lower CCT than non-migraineurs under both LED and fluorescent lighting conditions. In addition, both migraineurs and non-migraineurs tended to favour lower illuminance under LED lighting condition than fluorescent lighting condition.

Acknowledgments

This study was supported by JSPS KAKENHI GRANT Number 25282006. I would like to thank Sayo Aikawa and Chihiro Tanaka in D.W.C.L.A. for helping this experiment.

References

NAKAMURA, H., KARASAWA Y., 1997. Relationship between Illuminance / Color Temperature and Preference of Atmosphere. *Journal of Light & Visual Environment*, 23-1, 29-38

ISHIDA, K., INOUE, Y., 2007. Study on Lighting for the Relaxation, *Proceedings of 26th session of the CIE*, 337-340

OI, N., TAKAHASHI, H., 2007. Preferred Combinations between Luminance and Color Temperature in Several Settings for Daily Living Activities, *Proceedings of 26th session of the CIE*, 330

OI, N., LU, B., TAKAHASHI, H., 2009. A comparison between Fluorescent Lamp and LED on the Preference of Indoor Illuminance and Color Temperature; Scale Model Experiments Assuming Living Rooms, *Proceedings of the 6th Lux Pacifica*, 123-126

SAKAI, F. and IGARASHI, H., 1997. Prevalence of migraine in Japan; national wide survey. *Cephalalgia*, 17 (1), 15-22

KELMAN, L., TANIS, D., 2007. The triggers or precipitants of the acute migraine attack. *Cephalalgia*, 27 (5), 394-402

AIBA, S., TATSUMOTO, M., EDA, T., ISHIKAWA, T., AYAMA, M., HIRATA, K., 2011. Discomfort glare caused by light source in migraine. *Proceedings of 2011 Annual Conference of the Illuminating Engineering Institute of Japan*, 184 (written in Japanese)

TATSUMOTO, M., EDA, T., ISHIKAWA, T., AYAMA, M., HIRATA, K., 2013. Light of intrinsically photosensitive retinal ganglion cell (ipRGC) causing migraine headache exacerbation. *Cephalalgia*, 33 (Supp 8), 2

PP45

PROPOSAL OF LIGHTING METHOD IN CLASSROOM OF PRIMARY SCHOOL CONSIDERING THE TEACHERS' BRIGHTNESS SENSATION

Suzuki,N.[1], Mochizuki, E.[2] Oikawa, D.[2]
[1] ENDO LIGHTING CORP, Tokyo, JAPAN, [2] Chiba Institute of Technology, Chiba, JAPAN
n_suzuki@m1.endo-lighting.co.jp

Abstract

In primary schools, the energy use for lighting accounts for about half of the total enegy use. It is usual that all of the ceiling luminaires are lighted on by the teachers, even if the students judged supplementary artificial light is not necessary.

The purpose of this study is to propose the new lighting method in classrooms which contribute the visual comfort of the teachers and energy saving. This paper reports the results of the field measurement conducted in a real primary school for four months. As a result, lightening the rear wall of the classroom by the wall washer luminaires uniformized the luminance distribution within the teachers' visual field and raised their brightness. It was also identified raising the teachers' brightness might decrease the hours when the ceiling luminaires on the window side lighted on.

Keywords: teachers' brightness, brightness of the rear wall, luminance uniformity, electrical power consumption.

1 Introduction

It has been said that energy use for lighting accounts for nearly half of the total energy use in primary schools. It is recommended to introduce daylight in classrooms and to light off the ceiling luminaires in accordance with the amount of daylight not only for energy savings but also for environmental learning of the students.

In our previous study, it was identified that ceiling luminaires in classrooms of primary schools were controlled by the students of the higher grades, still the teachers regularly lighted on luminaires as they entered the classroom regardless of the outside condition (Mochizuki et.al. 2010). It was also identified that even in the cases when the students judged the ceiling luminaires could be lighted off for enough brightness on the desk, more than half of the teachers judged the ceiling luminaires could not be lighted off even if they sensed the desk was rather bright. One of the reasons of this could be supposed that the teachers might sense the classroom darker because of the high luminance contrast between the window side and the corridor side of the classroom when looking around the classroom from the entrance of the classroom. It can be supposed that lowering luminance contrast within the teachers' visual field is important to enhance their brightness sensation and that might lead to reduce unnecessary lighted luminaires.

The purpose of this study is to identify how to design the lighting environment in classrooms of primary schools from the viewpoint of the luminance distribution within the teachers' visual field. In this paper, the results of the field experiment identifying the effects of the wall lighting for the rear wall of the classroom on the teachers' visual environment and those on energy conservation are reported.

2 Experimental method

Experimental conditions and measurement methods are described in the following.

2.1 Profile of the experimental classrooms

A field experiment was conducted in the four classrooms of S primary school in Kawasaki city, Japan. Figure 1 and Table 1 show the profile of experimental classrooms. All of the target classrooms had windows oriented south. Two of them were located on the ground floor, the classrooms for the 5th grade, and the others were on the second floor, the classrooms for the 4th grade. Each classroom was divided into two types (Type A and B). The Type A was the reference rooms, only ceiling luminaires wewe mounted on the ceiling. On the other hand, the the Type B was the test rooms, three pairs of the wall washer luminaire with tubular LED lamp of 29,8 W and 5000 K, were mounted to light the rear wall of the classroom in addition to the ceiling luminaires. The field experiment was conducted during the second term, from the end of August till the end of December 2013.

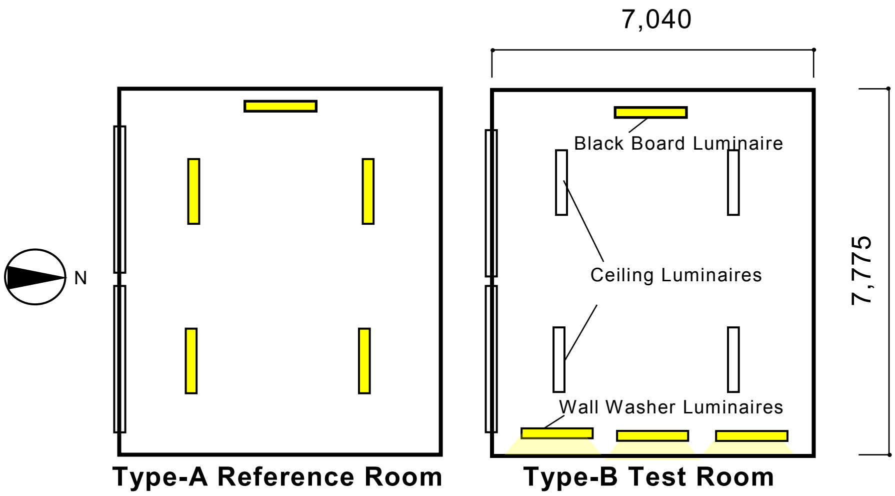

Figure 1 - Plan of the classrooms

Table 1 - Lighting fixtures mounted in each experimental room

	Type-A Reference Room		Type-B Test Room	
	Electrical power consumption (W/Unit)	Number of the fixutures	Electrical power consumption (W/Unit)	Number of the fixutures
Black Board Luminaire	36,0	1	36,0	1
Ceiling Luminaire mounted on the Window side	72,0	2	72,0	2
Ceiling Luminaire mounted on the Aisle side	72,0	2	72,0	2
Wall Washer Luminaire	None	None	29,8	3

For the classrooms of the Type A, only teachers were asked to judge whether the ceiling luminaires were necessary or not and to light on/off. On the other hand for the classrooms of the Type B, both the teachers and the students were asked to light on/off just as they always did on every occasion when they judged to light on the ceiling luminaires.

2.2 Questionnaire for the actual operation on the luminaires

Prior to the field measurement, a questionnaire was conducted to identify the evaluation of the lighting environment by the teachers and the actual operation of the ceiling luminaires and the curtain in each classroom. As results all sixteen answers wer obtained. Figure 2 shows the result of the questionnaire about the occasions to light on the luminaires. It was identified that all of the teachers lighted on the ceiling luminaires at the moment of entering the classroom. There were much possibilities that they had the habit of lighting on all of the luminaires without any considerations about their visual environment. It was indicated that there was a necessity to improve their habit of operation of the luminaires above all.

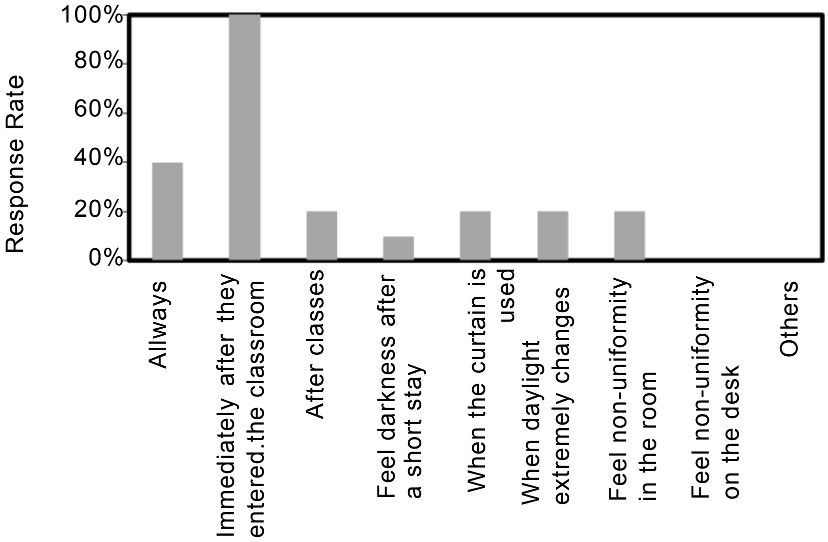

Figure 2 - Occasions to light on the luminaires （multiple answers, N=10）

2.3 Environmental measurement method

Figure 3 shows the measurement scenes. Illuminance logger (HIOKI 3640) was set under each ceiling luminaire to record the illuminance at intervals of 2 minutes to sense the state of each luminaire (lighted on/off). A panel which calls the teachers' and the students' attention to stop and consider about the lighting on the ceiling luminaires was settled beside the lighting control panel at the entrance of each classroom. In the cases when the teachers or the students lighted on the ceiling luminaires, they were asked to choose the reasons why they lighted on the ceiling luminaires by filling out the sheets of the questionnaire, which were settled near the lighting control panel.

In addition to the measurement, subjective evaluation of the lighting environment in each classroom and the measurement of the luminance distribution by using luminance camera (Luminocam, Kozo Keikaku Engnierring) in each classroom was conducted every month.

Illuminance logger was mounted under the fluorescent lamp.

Asked the teachers and the students.to think whether they really needed to lihgt on the ceiling luminaires.

Asked to record the teachers and the students the reasons why they lighted on the ceiling luminaires every class.

Figure 3 - Measurement scenes

3 Results and discussion

3.1 Change in lighting environment by wall washer luminaires

Horizontal illuminance on the desk (700 mm high from the floor, at intervals of 1 m, KONICA-MINOLTA illuminance meter T-10M), and luminance distribution from the viewpoints of the teachers (at the entrance and on the platform, 1.5 m from the floor, Luminocam) were also measured in each classroom with each lighting condition on August 23, 2013. Figure 4 shows some examples of the luminance distribution from the viewpoint of the teachers standing on the platform. It can be seen that the luminance distribution of the rear wall in the reference room was rather large, the upper side of the rear wall is slightly dark and the lower side of the rear wall was bright. On the other hand, the luminance distribution of the rear wall in the test room was quite smaller, both of the luminance of the upper side and that of the lower side of the rear wall was quite uniform. Comparing the measurement data in the reference room where all ceiling luminaires and the black board luminaire were lighted on and that in the test room where only the ceiling luminaires on the aisle side, the black board luminaire and the wall washer luminaire were lighted on, it was shown that the horizontal illuminance of both classrooms were over 300 lux, higher enough than the recommended illuminance in JIS Z 9110.

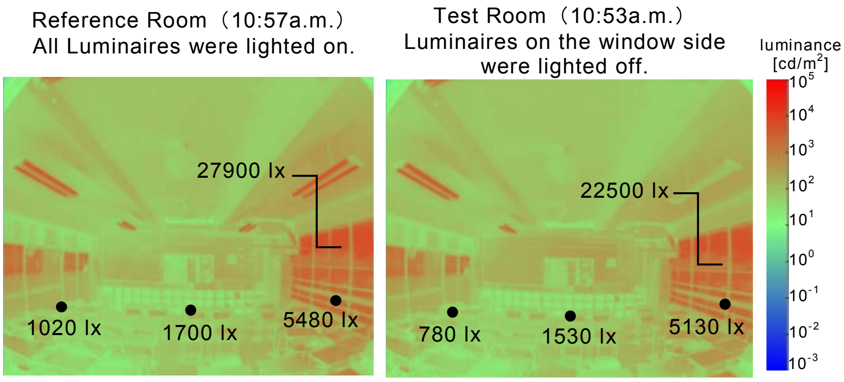

Figure 4 - Luminance distribution from the viewpoint of the teacher standing on the platform

Table 2 summarizes the result of a luminance uniformity on the desk and standard deviation of the luminance from the viewpoint of the teachers standing on the platform in each lighting condition. It can be seen that standard deviation of the luminance in the lighting condition No. 3 is lower than thet in the lighting condition No.5 nevertheless the illuminance uniformity was approximately the same. From the results of the questionnaire for the teachers, it was also identified that lightening the rear wall by the wall washer luminaires added the spatial brightness of the teachers in the classroom, the students had pleasure that their works of art displayed on the rear wall looked more impressive. It was suggested that uniformalising the luminance distribution had good affects on the visual comfort from viewpoint of the teachers.

Table 2 – Result of measurement in each lighting condition

Lighting Condition	Black Boards Luminaire	Wall Washer Luminaire	Luminaire of the window side	Luminaire of the aisle side	Electrical Power Consumption (W)	Illuminance Uniformity	Luminance Standard Deviation
1	Off	Off	Off	Off	0,0	0,233	475
2	**ON**	**ON**	Off	Off	125,4	0,277	469
3	**ON**	**ON**	Off	**ON**	269,4	0,306	573
4	**ON**	**ON**	**ON**	**ON**	413,4	0,298	681
5	**ON**	Off	**ON**	**ON**	324,0	0,345	672
6	**ON**	Off	Off	**ON**	180,0	0,254	670

3.2 Effects on energy saving by the wall washer luminaires

Figure 5 compares the time when the ceiling luminaires on the window side were lighted on and that on the aisle side were lighted on. In the reference room, both of them were approximately the same, that is all of the ceiling luminaires were lighted on when the classroom was occupied. On the other hand, the time of when the luminaires on the window side in the test room was shorter than that on the aisle side for several days. It can be predicted that improving the luminance distribution in the classroom may raised the teachers' brightness in the classroom and reduced the number of the lighted ceiling luminaires.

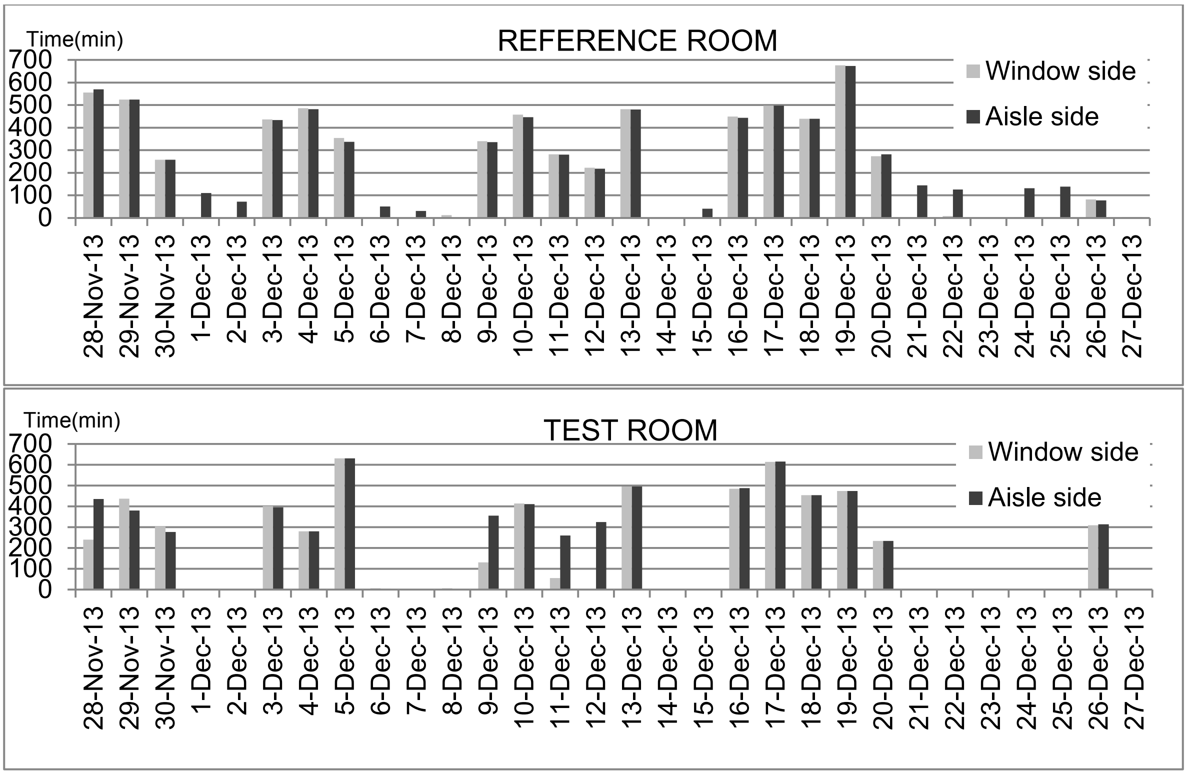

Figure 5 - Comparison of the time when the ceiling luminaires were lighted on

The total electrical power use in the test room per day was calculated. Table 3 shows the relationship between the total electrical power consumption in the test room on 28 November, 9, 11 and 12 December when the ceiling luminaires on the window side were lighted off and that under the supposition that all of the ceiling luminaires were lighted on when occupied as usual. It could be suggested that in the case when the ceiling luminaires on the window side could be lighted off by increasing the luminance on the rear wall and uniformizing luminance distribution in the classroom, the total electrical powere use for lighting in the classroom could be reduced to some extent.

Table 3 – Comparison of electrical power consumption

	Electrical power consumption (kWh/day)	
Date	Actual test room	Test room under supposition that the all luminaires were lighted on
28 Nov 13	2,53	2,35
9 Dec 13	1,92	1,92
11 Dec 13	1,30	1,40
12 Dec 13	1,47	1,76
Average	1,80	1,86

4 Conclusion

In this study, field measurement was conducted to identify the effects of lightening the rear wall of the classroom with the wall washer luminaires on the teachers' visual comfort and energy saving. The results showed that lightening the rear wall in the classroom by the wall washer luminares improved the luminance distribution within the teachers' visual field and raised the teachers' brightness in the classroom. That might lead the teachers to light off the ceiling luminaires on the window side. It can be suggested that lightening the rear wall can improve the visual comfort of the teachers without additional energy consumption.

Acknowledgement

We are deeply grateful for Mr. Miyagawa and Mr. Takayama, the members of Municipal Board of Education of Kawasaki city, for their supports to our investigation.

References

Mochizuki, E., Koike, K. and Ikeda, S. 2010. Possibility Saving Electrical Power Consumption in Elementary School. Proceeding of CIE2010 " Lighting Quality and Energy effesiency", pp.205-209.

JIS2011. JIS Z 9110-2011 General rules of recommended lighting levels. Japan: JIS

PP46

A MODIFIED DISCOMFORT GLARE INDEX FOR GREEN BUILDINGS

Hirning, M.B.[1], Isoardi, G.L.[1], Cowling, I.[1]
[1] Queensland University of Technology, Brisbane, AUSTRALIA
m.hirning@qut.edu.au

Abstract

This study presents the largest-known, investigation on discomfort glare with 493 surveys collected from five green buildings in Brisbane, Australia. The study was conducted on full-time employees, working under their everyday lighting conditions, all of whom had no affiliation with the research institution.

The survey consisted of a specially tailored questionnaire to assess potential factors relating to discomfort glare. Luminance maps extracted from High Dynamic Range (HDR) images were used to capture the luminous environment of the occupants. Occupants who experienced glare on their monitor and/or electric glare were excluded from analysis leaving 419 available surveys. Occupants were more sensitive to glare than any of the tested indices accounted for.

A new index, the UGP was developed to take into account the scope of results in the investigation. The index is based on a linear transformation of the UGR to calculate a probability of disturbed persons. However all glare indices had some correlation to discomfort, and statistically there was no difference between the DGI, UGR and CGI. The UGP broadly reflects the demographics of the working population in Australia and the new index is applicable to open plan green buildings.

Keywords: Discomfort Glare, Green Buildings, Lumiance Mapping

1 Introduction

Controlled use of daylight has the potential to provide both health and energy benefits in commercial buildings. Used as a supplementary light source, daylight can provide energy savings through increased thermal and lighting efficiency (Boyce, 2003); (Galasiu, 2006). Positive non-visual health benefits of natural light include increased well-being, alertness and sleep quality (Van Bommel, 2006); (Webb, 2006).

In Australia, building designers are encouraged, through the sustainability rating system, Green Star (GBCA, 2013), to design spaces which deliver these benefits to occupants. Built on existing international systems, BREEAM (UK) and LEED (US), a six-star rated building indicates world leadership in environmental design. It has been demonstrated that if occupant comfort is rated highly, green buildings can achieve significant energy savings and increased perception of productivity (Thomas, 2010). However, studies both in Australia and overseas show little evidence that overall levels of occupant comfort and satisfaction in lighting or thermal comfort are greater in ‘green’ rather than conventional buildings or that they achieve the energy consumption predicted in the design stage (Paul, 2008); (Abbaszadeh, 2006); (Leaman, 2007).

Discomfort glare is a phenomenon arising from high luminance contrasts or unsuitable luminance distributions in the visual field causing discomfort. Much of the research into discomfort glare involves very small sample sizes, comprising largely of students from the researching institution or no subjective data at all (Shin, 2012); (Nazzal, 2001); (Suk, 2013). The traditional indices, such as the DGI, persist, despite their inconsistencies, as there is a lack of statistically significant research to enable their replacement. Many researchers agree there is a lack of adequate knowledge to effectively predict discomfort glare in practical situations (Clear, 2013); (Galasiu, 2006). The ability to predict discomfort glare in complex lighting environments, if possible, would be invaluable for daylighting design in green buildings.

This study presents the largest known investigation of discomfort glare in green buildings. Data were collected from five buildings located in Brisbane, Australia and its immediate surrounds. Two of the buildings were five star rated green buildings, the other three buildings were six-star rated. Each of the buildings was specifically designed to include daylight as a significant lighting component as well as provide occupant comfort. A total of 493 surveys on discomfort glare were conducted. Each survey involved a questionnaire on discomfort glare and an accompanying luminance map extracted from High Dynamic Range (HDR) images.

A major obstacle in quantifying discomfort glare has been the difficulty in analysing complex lighting distributions. Previous researchers could only use time-consuming, point-by-point luminance measurements to assess a lighting scene (Hopkinson, 1972). Accurate assessment of luminance distributions within real environments would have been very difficult due to the dynamic nature of daylight. However, with current digital imaging technology techniques, such as high dynamic range (HDR) imaging, luminance distributions of spaces are able to be captured quickly and analysed on a pixel-by-pixel basis (Reinhard, 2005). This allowed a thorough comparison of major glare indices through the analysis of luminance maps and subjective responses.

2 Methodology

This research involved collecting a large number of luminance maps along with questionnaire data to study occupant discomfort in open plan office spaces under daylight conditions. Subjective user assessments were conducted in five green star rated buildings using the building's tenants. In total, 493 complete surveys (questionnaire and associated luminance map) were collected. The majority of surveys correspond to a unique individual. Only 25 occupants completed the survey twice.

2.1 Buildings

Two of the buildings were high rise office buildings located in the Brisbane central business district (CBD), with partially obstructed urban views. The other three were located in isolated industrial areas, providing unobstructed nature views. Only two of the buildings had external shading on the façade and all had internal shading and large floor to ceiling windows.

The building interiors were all open plan office spaces with a few private offices for supervisors. The work tasks of employees in each of the buildings varied greatly, from administration and IT to graphic design and architectural drawing. The surveys were conducted sporadically over 14 days from February to October 2012, covering the seasons of Autumn, Winter and Spring. The buildings were granted anonymity as a condition of unrestricted access to them.

2.2 HDR Image Calibration

The luminance distribution of an occupant's field of view was derived from HDR images. A calibrated HDR image can be used to represent the luminance distribution of any environment. All that is required is a digital camera fitted with a fisheye lens and the appropriate software (Reinhard, 2005); (Inanici, 2006). HDR imaging is a useful tool that has the ability to capture luminance values within 10% accuracy across a wide range of luminances and sources (Inanici, 2004); (Cai, 2011). The camera used to acquire all HDR images in this study was the Nikon Coolpix 8400 Digital Camera. In order to capture a subjects field of view the FC-E9 Fisheye lens (focal length = 5.6 mm, 190° field of view) with equidistant projection properties was attached to form a camera lens system.

HDR imaging requires multiple exposure images of the same scene. In order to acquire luminance maps suitably accurate for glare analysis, photometric calibration of the camera and lens system is required (Krawczyk, 2005); (Hirning, 2010a). Hirning et al provides extended details of the method used to produce the calibrated luminance maps used in this study (Hirning, 2010b). Multiple exposure images of the same scene are combined using a self-calibration algorithm to create a single HDR image with relative luminances (Robertson, 2003). Corrections for vignetting and absolute luminance are then applied to HDR images from which an accurate luminance map can be extracted.

Absolute luminance was spot-calibrated in test scenes using a Topcon BM7 Luminance Colour Meter. Further calibrations were applied to correct for vignetting, which is the reduction in brightness registered by pixels far away from the optic axis. An equidistant fisheye causes vignetting because light rays incident at large angles to the optic axis are projected onto a larger area of the imaging plane than those passing through the optical axis. Once acquired, all calibrations remain valid for any subsequent HDR images created by the same camera lens system using the same image settings.

The calibration procedure used the program pfstools and its extension pfscalibration for HDR image creation and calibration (Mantiuk, 2007). The system is able to capture a wide range of luminance values to within 8% accuracy in the laboratory.

2.3 Questionaire

Figure 1 is the questionnaire used in each occupant survey, which has been adapted slightly from a questionnaire used in a previous investigation (Hirning, 2013). The questionnaire is designed to be quick and easy to complete, however it must also capture the important information required. Questions were structured so that a person of a non-technical background could provide a meaningful answer, avoiding answers requiring much interpretation. The questions were all checkbox, making it easy for occupants to fill out quickly. The most significant part of the questionnaire is the glare indication diagram, which assesses whether discomfort glare is being experienced at the time of survey. The occupants only requirement is to indicate where in the field of view, if at all, there is uncomfortable light.

2.4 Data Collection

The survey was conducted only on fine days with very little or no cloud. No surveys were conducted under overcast or partly cloudy conditions. Clouds moving across the sun create rapidly changing lighting conditions which interfere with HDR image capture. Participation in the survey was completely voluntary. Every effort was made to survey all occupants who were accessible in the open plan areas of the buildings. The method of collecting data was to ask a single or group of occupants to participate in the survey. The electric lighting was left on during the survey, consistent with the lighting conditions under which the occupant normally worked. Directly after the questionnaire was completed the physical (HDR) data were collected. The fisheye lens was positioned approximately at the same location and view direction as the subject’s eye when seated performing the glare assessment.

2.5 Statistical Analysis

Statistical data analysis was used to investigate current glare indices to assess their suitability as glare prediction models in open plan green buildings and to create a new index if required. This was achieved by calculating the linear correlation (through coefficient of determination, r^2) between each index and percentage discomfort.

In this investigation there were only two possible response levels to glare; comfort or discomfort, with a large number of observations. Reporting a correlation that is comparable to other large data sets is necessary when discussing statistical significance of the data. However, coefficient of determination (r^2) is not a good measure to assess categorical response data. To overcome this, responses were grouped together and a percentage (or probability) of people experiencing discomfort calculated for each group. The method converts the two-level categorical data into quantitative data via the creation of ordered “groups”.

Initially, all potential glare predictor variables (i.e. glare indices) were calculated for each survey. Surveys were then ordered numerically with respect to the value of one selected predictor variable. The ordered surveys were combined into “groups” with numerically adjacent surveys (i.e. those with similar predicted values). The mean value of the predictor variable in each group was calculated, as well as the percentage discomfort (being the ratio of discomfort surveys to total surveys for each group). These two values create a data pair for each group. Then coefficient of determination is calculated to assess if there is a significant correlation between the predictor variable and percentage discomfort.

Glare indices were determined using Evalgare (Wienold et al., 2012). The location and solid angle subtended by the screen was used as input to Evalglare. Thus Evalglare produced a default circular task zone (used for background luminance) of equivalent size and location to the screen (Figure 2).

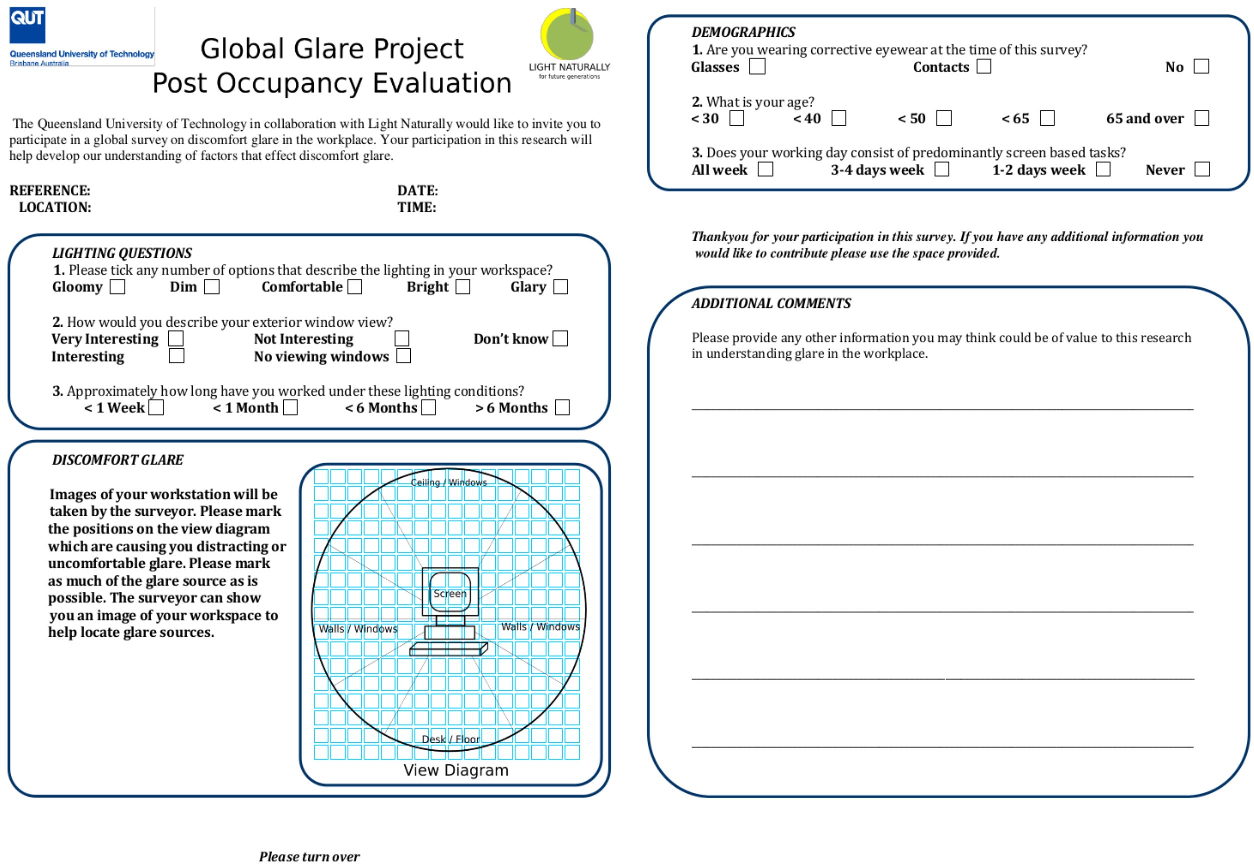

Queensland University of Technology Brisbane Australia

Global Glare Project
Post Occupancy Evaluation

LIGHT NATURALLY for future generations

The Queensland University of Technology in collaboration with Light Naturally would like to invite you to participate in a global survey on discomfort glare in the workplace. Your participation in this research will help develop our understanding of factors that effect discomfort glare.

REFERENCE: **DATE:**
LOCATION: **TIME:**

LIGHTING QUESTIONS

1. Please tick any number of options that describe the lighting in your workspace?
Gloomy ☐ **Dim** ☐ **Comfortable** ☐ **Bright** ☐ **Glary** ☐

2. How would you describe your exterior window view?
Very Interesting ☐ **Not Interesting** ☐ **Don't know** ☐
Interesting ☐ **No viewing windows** ☐

3. Approximately how long have you worked under these lighting conditions?
< 1 Week ☐ **< 1 Month** ☐ **< 6 Months** ☐ **> 6 Months** ☐

DISCOMFORT GLARE

Images of your workstation will be taken by the surveyor. Please mark the positions on the view diagram which are causing you distracting or uncomfortable glare. Please mark as much of the glare source as is possible. The surveyor can show you an image of your workspace to help locate glare sources.

DEMOGRAPHICS

1. Are you wearing corrective eyewear at the time of this survey?
Glasses ☐ **Contacts** ☐ **No** ☐

2. What is your age?
< 30 ☐ **< 40** ☐ **< 50** ☐ **< 65** ☐ **65 and over** ☐

3. Does your working day consist of predominantly screen based tasks?
All week ☐ **3-4 days week** ☐ **1-2 days week** ☐ **Never** ☐

Thankyou for your participation in this survey. If you have any additional information you would like to contribute please use the space provided.

ADDITIONAL COMMENTS

Please provide any other information you may think could be of value to this research in understanding glare in the workplace.

Please turn over

Figure 1 – Discomfort glare questionnaire handed out to occupants

3 Results

3.1 Survey Response Data

The survey data consisted of 493 complete surveys. Hirning et al provides details the collected frequencies for all response categories gathered from the questionnaire (Hirning et al, 2014). An occupant response was classified as experiencing discomfort if a glare source was indicated on the view diagram in the questionnaire and comfort otherwise. In total 242 (49%) surveys were classified as discomfort and 251 (51%) as comfort.

The location of a building was used to infer window view type independently of occupants. For buildings located within the CBD, view type was classified as Urban. Conversely, buildings that were located in isolated industrial areas, surrounded by mostly grass, trees or water and without the presence of nearby buildings, view type was classified as Nature. During data collection, glare sources indicated on the view diagram were recorded as occurring from either daylight or electric source (Table 1).

Table 1 – Total counts for glare source characteristics inferred from HDR images

Source Type	Total Counts		Daylight Glare	Total Counts
None	250		Window	167
Daylight	222		Reflected	61
Electric	21		Task/Screen	63

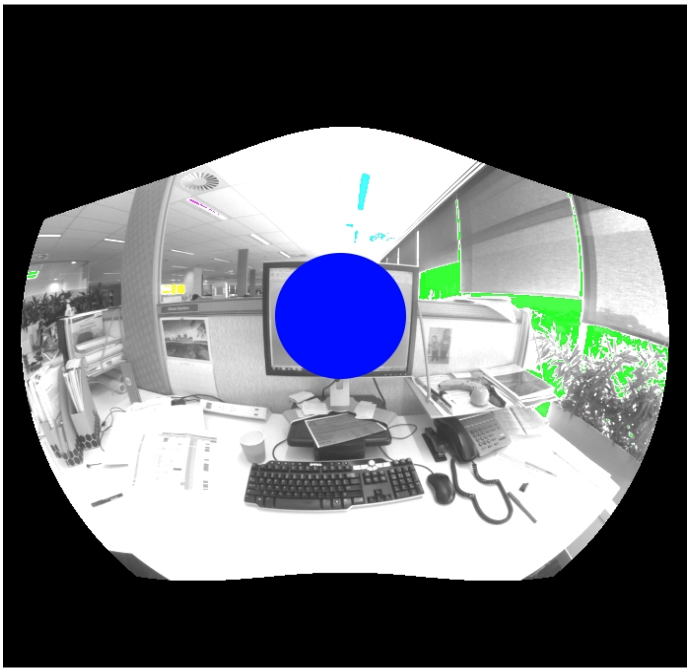

Figure 2 – Example of the evalglare task zone investigated (coloured blue). The fisheye image is no longer circular as it has been cropped to Guth's total field of view.

During post-processing, using HDR images and the view diagrams, glare from daylight was further subdivided. This included whether glare originated from the window, was reflected from an internal surface, or was due to direct sunlight. In addition, if glare (electric or daylight) impacted the task area (i.e. computer screen or keyboard), this was categorised as Task/Screen glare. Some occupants only allowed imaging of their monitor background, clearing any material on their screen as they conducted sensitive work. These surveys (of which there were 83) were identified during post-processing as they do not display the original task under which the questionnaire was conducted (Screensaver).

3.2 Statistical Analysis of Glare Indices

The major glare indices were investigated for their linear correlation to percentage discomfort under various conditions. Glare indices were calculated with Evalglare using the default background multiplier of five. Task luminance was used as the adaptation or background luminance (L_b) in the calculation of glare indices. A region of brightness in the field of view was presumed a glare source if its average luminance was fives times greater than the task luminance. Occupants with screen glare and electric glare were excluded from further analysis.

In addition to the major glare indices, many parameters and combinations of parameters were investigated for their correlation to discomfort. However, the established glare indices performed significantly better than all other tested predictor variables. Table 2 shows the coefficient of determination for selected glare predictor variables. A fixed sample size of 419 was now used to establish 21 groups with a group size of 20 (see Section 2.4.1). Glare indices were determined using Evalgare using the task luminance multiplier of five. Correlations for each metric are compared to the DGI using Fisher-Z transformation to assess statistical significance (m = 21).No glare index was statistically more significant than another. The Fisher-Z transformation was used to compare the Pearson-r correlations. The p-values for comparing the DGI to the other glare indices is displayed in the final column of Table 2. The logarithm of both average luminance and vertical illuminance display appropriate linear relationships and high correlations (0.685 and 0.657) respectively. It is not surprising then that all glare indices have similar correlations as they in general produce a metric based on the logarithm of luminance. The DGP, which has a very strong linear dependence on vertical illuminance, obtained a lower correlation than most of the other indices due to the low correlation of vertical illuminance (0.387). It was again found that the logarithm of vertical illuminance provided a much higher correlation to discomfort (0.657).

Table 2 – Coefficient of determination for the major glare indices.

Index	r^2	Z	p
DGI	0.738	-	-
DGP	0.683	0.33	0.74
UGR	0.739	-0.01	0.99
CGI	0.771	-0.23	0.82
VCP	0.502	1.18	0.24
E_v	0.387	1.61	0.11
L_{av}	0.420	1.50	0.13
L_{screen}	0.0007	2.84	0.0045
$\log(E_v)$	0.657	0.48	0.63
$\log(L_{av})$	0.685	0.32	0.75

Screen luminance appears to be completely uncorrelated to discomfort (Table 2). It was expected that screen luminance would provide an adaptation luminance, which in turn would produce some effect on discomfort. However, large variations in screen luminance between occupants did not occur, especially compared to other parameters such the average field of view or glare luminance. Almost all occupants in a building have the same monitors, which are all about the same brightness level. Thus there was not enough variation in screen or task luminance to be able to observe an effect on discomfort. However this may provide an important simplification for predicting glare in office-type buildings. Figure 3 shows the results produced using no-task zone for the UGR with a background multiplier of five. Other forms of glare equations were tested by modifying the coefficients and exponents of the glare indices. However this did not produce any higher correlations than those already achieved.

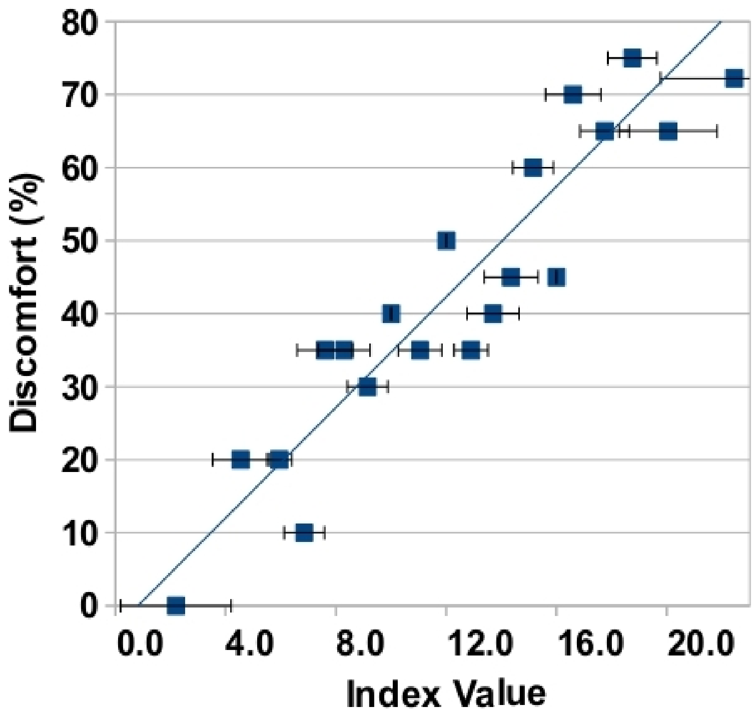

Figure 3 – UGR with no task zone and background multiplier of five.

3.3 Other Factors

Data collected from the questionnaire were also used to investigate other factors that may possibly impact discomfort glare;

• Age

• (View) Interest

• Eye (Correction)

The UGR (without a task zone and background multiplier five) was used to help investigate these other categorical factors. The UGR was chosen because it is the least complicated index to calculate and does not require illuminance measurements. It also has the nice property of additivity of glare source area's i.e. solid angle has a exponent of one (ω^1) (Einhorn, 1966). The DGI and CGI do however produce statistically identical results.

Multiple linear regression was used to analyse the effect of these various factors on discomfort glare. The results are displayed in Table 3. The top section of the table displays R, R^2, adjusted R^2 and the standard error (SE) of the model with m = 419. The middle section displays the total sum of squares (SS), degrees of freedom (df), mean square error (MS), F-statistic (F) and p-value (p) for the model. The bottom section of the table displays the coefficient summary which includes the unstandardised regression coefficients (B) and their standard error (SE), the standardised regression coefficients (β), t-score (t) and p-value (p).

Table 3 – ANOVA for Selected Glare Model

Model Summary

R	R^2	Adjusted R^2	SE
0.41	0.17	0.16	0.45

ANOVA

	SS	df	MS	F	p
Regression	16.99	4	4.25	20.97	0.00
Residual	83.67	414	0.20		
Total	100.67	418			

Coefficients

	B	SE	β	t	p
(Const)	-0.0389	0.077	0.00	-0.50	0.61
UGR	0.0320	0.0036	0.40	8.85	0.00*
Age	-0.0059	0.023	-0.01	-0.26	0.80
Eye	-0.0083	0.024	-0.02	-0.35	0.73
Interest	0.0367	0.020	0.08	1.81	0.07**

* Indicates significant p-values < 0.05

** Indicates weakly significant p-values < 0.10

Table 3 shows that the glare index was the only statistically significant predictor of discomfort. View Interest showed weak significance (p-value = 0.07) in the model. However, the factor has a very large standard error (0.020) which is 54% of the regression coefficient (0.0367). There is too much error in the coefficient to warrant including this factor in the final model (Equation 1). In light of these results the most effective method for predicting discomfort in open plan office buildings are the current glare indices, UGR, CGI and DGI. Equation 1 presents the UGR transformed to a probability prediction scale from its categorical ratings. A regression coefficient of 3.2×10^{-2} has been applied to the original UGR equation and renamed the Unified Glare Probability (UGP) (Equation 1).

$$UGP = 0.26 \log_{10} \frac{0.25}{L_b} \sum \frac{L_s^2 \omega_s}{P^2} \tag{1}$$

4 Discussion

Similar to many other investigations into discomfort glare, there were large variations in individual perception of discomfort. This variation in survey responses was large enough that the exponents and coefficients of the glare indices were somewhat invariant to discomfort correlation. The UGR was thus chosen to represent the general form of the equation due to its simplicity and additivity of glare source areas (Einhorn, 1966). The categorical scale of the UGR was modified to a probability and termed the UGP (Unified Glare Probability). The probability represents the percentage of disturbed persons under a particular light scene.

The probability scaling is more applicable than the previous categorical scalings of the index, which have proven unreliable in real environments. Though occupants were not required to estimate a magnitude of discomfort during this investigation, anecdotal evidence from the survey suggests that occupants who indicated discomfort are equivalently rating “just uncomfortable” to “uncomfortable”. No occupant is experiencing intolerable glare. Employees in these buildings had flexible working hours and majority of the occupants had worked under their lighting conditions for over six months. Occupants have an acute awareness of the time of day when glare becomes intolerable. At these times occupants simply make sure they are not required at their desk.

Three factors were tested alongside the UGR relating to age, eye correction and view interest. It was discovered that none of these factors were statistically significant. This suggests that only physical luminance and solid angle parameters influence discomfort glare. However, Table 3 showed view interest to have a statistically weak influence within the model. Other research has shown that view type and view interest do influence the subjective appraisal of discomfort glare (Tuaycharoen, 2007); (Yun, 2011). The results of this investigation do not conclusively disagree with those results. The DGP also showed a weak improvement in correlation when age was applied to the equation (Wienold, 2012). There may have been other factors, not accounted for in this study which have a significant influence on discomfort, however measuring and accounting for more of these types of factors could be problematic.

5 Conclusion

This study presents the largest known general investigation on discomfort glare with 493 surveys collected from five green buildings located in Brisbane, Australia, under clear skies. The study was conducted at the occupants own workplaces, all of whom had no affiliation with the research institution. The data thus reflects the screen-based work tasks, lighting variations and occupant demographics present in these environments. Discomfort glare was highly prevalent within the green buildings investigated, 49% of occupants surveyed reported some discomfort at the time of survey.

The investigation revealed occupants were more sensitive to glare than any of the current indices could account for. A new index, the UGP, was developed to take into account the scope of results in the investigation (Equation 1). The index is based on a linear transformation of the UGR to calculate a probability (or percentage) of disturbed persons. The index uses the average field of view luminance for the background (L_b) and a background multiplier of five to determine glare sources ($L_s \geq 5L_b$). The final result produced an r^2 value of 0.87. However, all glare indices had some correlation to discomfort. Statistically, there was no significant difference in correlation between the DGI, UGR and CGI.

$$UGP = 0.26 \log_{10} \frac{0.25}{L_b} \sum \frac{L_s^2 \omega_s}{P^2} \tag{1}$$

All glare indices tested in this investigation severely underestimated discomfort. The experimental circumstances under which the UGP and all other glare indices were developed is an important consideration in their application. The UGP is the only large study conducted in green open plan office buildings using non-affiliated office workers. Therefore, it is the appropriate index to assess discomfort glare for screen-based tasks in open plan office buildings, under clear sky conditions in sub-tropical climates.

References

ABBASZADEH, S., ZAGREUS, L., LEHER, D., HUIZENGA, C. 2006. *Occupant satisfaction with indoor environmental quality in green buildings.* Proceedings of Healthy Buildings, Lisbon.

BOYCE, P., HUNTER, C., HOWLETT, O. 2003. *The Benefits of Daylight through Windows*.Technical Report. Lighting Research Center, Rensselaer Polytechnic Institute. Troy, New York.

CAI, H., CHUNG, T.M. 2011. *Improving the quality of high dynamic range images*. Lighting Research and Technology 43, 87–102.

CLEAR, R.D. 2013. *Discomfort glare: What do we really know?* Lighting Research and Technology 45, 141–158.

EINHORN, H.D. 1966. *A new method for the assessment of discomfort glare*. Lighting Research and Technology 1, 235–47.

GALASIU, A.D., VEITCH, J.A. 2006. *Occupant preferences and satisfaction with the luminous environment and control systems in daylit offices: A literature review*. Energy and Buildings 38(7), 728–742.

GREEN BUILDING COUNCIL OF AUSTRALIA (GBCA), 2013. Online. Available: http://www.gbca.org.au/green-star/green-star-overview/ (Accessed: June 2013).

HIRNING, M., COYNE, S., COWLING, I. 2010a. *The use of luminance mapping in developing discomfort glare research*. J. Light & Vis. Env 34, 101–104.

HIRNING, M., ISOARDI, G., COWLING, I. 2014. *Discomfort glare in open plan green buildings*. Energy and Buildings 70, 427–440.

HIRNING, M., ISOARDI, G., COYNE, S., COWLING, I. 2010b. *Applying the use of high dynamic range imaging pipelines to discomfort glare research.* Proceedings of CIE 2010 Lighting Quality and Energy Efficiency, Vienna, Austria, 14–17th March. pp. 767–775.

HIRNING, M.B., ISOARDI, G.L., COYNE, S., GARCIA HANSEN, V.R., COWLING, I. 2013. *Post occupancy evaluations relating to discomfort glare: A study of green buildings in Brisbane*. Building and Environment 59, 349–357.

HOPKINSON, R. 1972. *Glare from daylighting in buildings*. Applied Ergonomics 3.

INANICI, M., GALVIN, J. 2004. *Evaluation of High Dynamic Range Imaging as a Luminance Mapping Technique*. Technical Report 57545. Lawerence Berkley National Laboratory. Berkley.

INANICI, M.N. 2006. *Evaluation of high dynamic range photography as a luminance data aqcuisition system*. Lighting Research and Technology 38, 123–136.

KRAWCZYK, G., GOESELE, M., SEIDEL, H.P. 2005. *Photometric Calibration of High Dynamic Range Cameras*. Technical Report MPI-I-2005-4-005. Max-Planck-Institut für Informatik.

LEAMAN, A., BORDASS, B. 2007. *Are users more tolerant of 'green' buildings?* Building Research & Information 35, 662–673.

MANTIUK, R., KRAWCZYK, G., MANTIUK, R., SEIDEL, H.P. 2007. *High dynamic range imaging pipeline: Perception-motivated representation of visual content.*Human Vision and Electronic Imaging XII, SPIE, San Jose, USA

NAZZAL, A.A. 2001. *A new daylight glare evaluation method: Introduction of the monitoring protocol and calculation method*. Energy and Buildings 33, 257–265.

PAUL, W.L., TAYLOR, P.A. 2008. *A comparison of occupant comfort and satisfaction between a green building and a conventional building*. Building and Environment 43,1858–1870.

REINHARD, E., WARD, G., PATTANAIK, S., DEBEVEC, P. 2005. *High Dynamic Range Imaging: Acquisition, Display and Image-Based Lighting*. Morgan Kaufmann. 502 p, San Francisco.

ROBERTSON, M.A., BORMAN, S., STEVENSON, R.L. 2003. *Estimation-theoretic approach to dynamic range enhancement using multiple exposures*. Journal of Electronic Imaging12, 219–228.

SHIN, J.Y., YUN, G.Y., KIM, J.T. 2012. *View types and luminance effects on discomfort glare assessment from windows*. Energy and Buildings 46, 139–145.

SUK, J.Y., SCHILER, M., KENSEK, K. 2013. *Development of new daylight glare analysis methodology using absolute glare factor and relative glare factor*. Energy and Buildings 64, 113–122.

THOMAS, L.E. 2010. *Evaluating design strategies, performance and occupant satisfaction: a low carbon office refurbishment*. Building Research & Information 38, 610–624.

TUAYCHAROEN, N., TREGENZA, P.R. 2007. *View and discomfort glare from windows*. Lighting Research and Technology 39, 185–200.

VAN BOMMEL, W.J. 2006. *Non-visual biological effect of lighting and the practical meaning for lighting for work*. Applied Ergonomics 37, 461–466.

WEBB, A.R. 2006. *Non-visual effects of light*. Energy and Buildings 38, 721–727.

WIENOLD, J. 2012. *New features of evalglare*. Online. Presented at the 11th International Radiance Workshop, Copenhagen; Available: http://www.radiance-online.org/community/workshops/2012-copenhagen/Day3/Wienold/rad_ws_2012_evalglare_newfeatures.pdf (Accessed: August 2013).

WIENOLD, J., REETZ, C., KUHN, T. 2012. *Evalglare, Version 1.08*. Fraunhofer Institute for Solar Energy Systems (ISE), Germany, http://www.ise.fraunhofer.de/radiance (Accessed: January 2013).

YUN, G.Y., SHIN, J.Y., KIM, J.T. 2011. *Influence of window views on the subjective evaluation of discomfort glare*. Indoor and Built Environment 20, 65–74.

PP47

Evaluation Method Research on Discomfort Glare of LED Products

Wu, Y.[1], **Hua, S.M.**[1], **Zhang, W.**[1], **Liu Q.**[1], **Zhang, D.B.**[1], **Xin, H.Z.**[1]
[1]National Lighting Test Centre, Beijing, CHINA.
wuyang@nltc.cn

Abstract

For the traditional lamps or luminaires used in interior lighting environment, the evaluation metric United Glare Rating (UGR) is usually used. With the fast development of SSL lighting technology, LED products has became more and more popular in people's daily life. It seems that, if compared with the glare value calculated by UGR method, people feel more discomfort glare from some of the LED lighting. In this paper, we first did some subjective experiments, to check this, which were based on the comparison method. Then, objective calculation and comparison were then made, trying to make some improvement to the evaluation metrics. With the improved evaluation method, discomfort glare characteristics of the products are expected to be evaluated and rated. This may help the consumers to distinguish and then select the good lighting products with less discomfort glare, which could then help to promote the application of the energy efficient LED lighting products with good lighting quality. Based on this, large sample size experiments are still going on to improve the research.

Keywords: Discomfort Glare, UGR, LED Products, Comparison Method

1 Introduction

The CIE publication 17.4-1987 "International Lighting Vocabulary" defined discomfort glare as: *glare which causes discomfort without necessarily impairing the vision of objects* [1]. The discomfort glare is a significant quality evaluation index for interior lighting design. In the actual lighting environment, the probability of discomfort glare is very large, and it affects human's vision psychology and physiology seriously in the long period of discomfort glare pollution. Therefore, the discomfort glare control has been a very focus in lighting design, especially for LED lamps or luminaires.

Due to the difference of luminous principle and emitting structure between the traditional products and LED products, luminous characteristics have large differences. The luminance uniformity is very good but the luminance is relative low for traditional products. While LED products have more advantages than traditional products, such as higher luminance, smaller luminous surface and volume, more flexible in lighting design. However, the luminance uniformity of LED products is not so good, which leads to more discomfort glare than traditional products.

According to the research on the glare luminaires with non-uniform luminance distribution, C.E. Water et al. [2] found that discomfort glare is largely dependent on the position of glare sources in the observer's field of view and luminance uniformity. In 2007, Lee Chang-Mo et al. [3] studied subjective appraisal of discomfort glare which was based on UGR for luminaires (radius=0.1 m) using white LED modules with uniform and non-uniform luminance in interior room, and the results showed that greater discomfort glare was caused by the light source with non-uniform than that with uniform luminance as the higher was as the average luminance in an environment with low background luminance. In addition, the results also demonstrated that the UGR is not applicable for the light sources with non-uniform luminance. In 2009, Seung-Gyun Jung et al. [4] did an experiment for adjustment of UGR formula through subjective evaluation under non-uniform and relative uniform luminance luminaires. It was shown that luminance uniformity had big influence to discomfort glare, and two regression equations has been obtained by regression analysis method. Higashi, H. et al. [5] studied the relationship between UGR and subjective evaluation in LED lighting and found that it was difficult to design using the UGR in LED lighting due to the luminance uniformity on luminous part. Also the UGR formula has been modified to develop a new evaluation method for discomfort glare.

Based on the above studies, it could be concluded that the original UGR formula for traditional light sources should be unsuitable to evaluate the products with non-uniform luminance distribution. In this paper, subjective experiments were conducted firstly to check the difference. Based on the results, objective calculation was then performed, which was trying to check the gap, and then improve the evaluation method to correct this..

2 Experiment setup

In this study, subjective experiments were conducted to evaluate the discomfort glare of lighting products, including LED and traditional lighting sources. A comprehensive evaluation method based on subjective assessment and objective physical quantities was used in this study.

2.1 Evaluation method

In this study, a comprehensive evaluation method was used. It consists of measurements of objective physical quantities (average luminance, luminance uniformity and luminance distribution) and subjective evaluation (UGR values) in typical lighting environment.

For the physical quantities, the luminance uniformity (U_L) and luminance distribution were tested by a LMK mobile advanced 550D, and the average luminance (L_{ave}) was tested by a Gonio. For the subjective evaluation, as comparison method, the specially made uniformed reference lighting sample and different LED downlights were evaluated by subjective observers. Then the subjective evaluation values (UGR_s) from the comparison-subjective observation, and the calculated values (UGR) using the UGR formula were compared. The correction method was then considered based on the difference $\Delta UGR = (UGR - UGR_s)$.

The improved evaluation method is expected to be used for the discomfort glare characteristic evaluation of the single product. Based on this kind of lighting quality evaluation of products, the evaluation of lighting application could also be considered and evaluated.

2.2 Experiment samples

In this experiment, 14 download luminaires including 1 incandescent, 1 compact fluorescent lamp (CFL), and 12 typical LED downlights were chosen as experiment samples. In general, the samples were divided into two parts: the downlights with and without diffusers, and some downlights include cut off angle and some not.

2.3 Experiment design

The space of the room is 7m*2.5m*2.9m (L*W*H). The doors and the windows have been covered with white (in)-black (out) curtain to avoid the exterior light entering into the room. In addition, the walls were painted white, and the reflectance of all the surfaces is within the range specified in CIE S 008/E-2001: Lighting of Indoor Work Places.

As a subjective methodology, semantic differential scaling is usually used to evaluate the discomfort glare. But in the actual experiment process, the subjective observers could not exactly distinguish the specific grating easily, especially for the boundary between very close gratings. Therefore, in order to avoid the amphibolous judgements, a reference downlights has been designed and introduced into this experiment. It is used to simulate the traditional lighting source which has good luminance uniformity. The uniformity ($U_L = L_{min}/L_{ave}$) of reference lamp is larger than 0.8. The luminance of the reference luminaire could be continuously adjustable from low to high values by controlling the current with a DC power supply.

According to the on-site measurements in typical lighting environment with a PR 670, such as classrooms, shopping malls and living rooms, the average background luminance is 30 cd/m^2. In this experiment room, the background luminance (L_b) could be controlled at constant value (L_b=30 cd/m^2) by two fluorescent luminaires which are also continuously adjustable.

There are six viewing angles: 75°, 65°, 55°, 45°, 30° and 0°. The definition of the view angle is shown in Figure 1, and the observers see the luminaires in the direct view. For every luminaire at each angle, the subjective observer should compare the discomfort glare of experimental sample and reference luminaire until they feel the same feeling. The position index of this experiment is fixed at 1.0 due to the direct view.

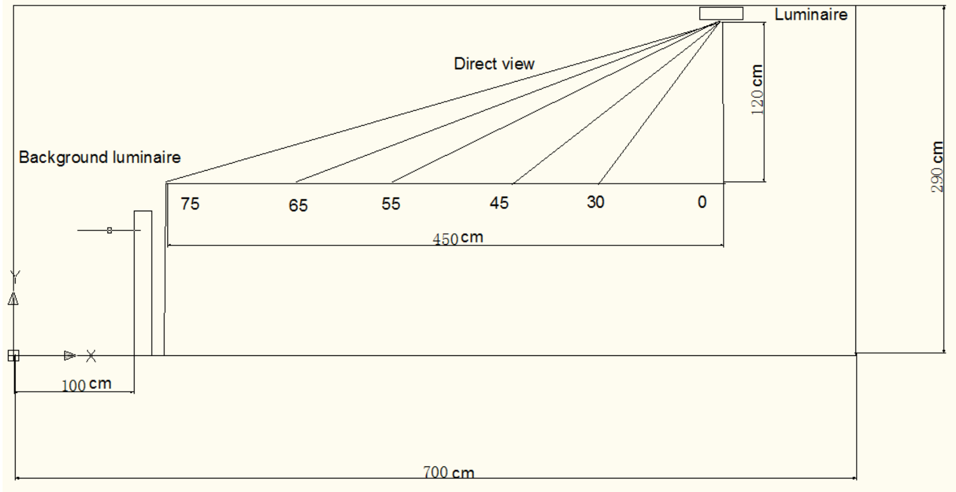

Figure 1 – Schematic overview of the experiment

Figure 2 shows the whole experimental scene in this study. In this scene, the left luminaire is the experiment sample, and the right luminaire is the reference one. A vehicle was made to carry the subjective observers and a chin-rest is used to keep the fixed height for every observer.

Figure 2 – The experiment scene

2.4 Subjective observers

The research in this paper is based on the first stage subjective experiments. For this stage, 5 males and 6 females worked as the subjective observers, and two of them are without glasses. The average age is 29 years, and the scope is from 23 years to 54 years.

2.5 Experiment procedure

The experimental procedures are listed as following:

(1) The subject enters in the room and adapts the background luminance for 1 minute.

(2) The subject sits on the vehicle at one angle position and put the head on the chin-rest, and the subject is to view directly the left luminaire and the reference luminaire,

respectively. Then the experiment support person adjusts the current of the reference luminaire.

Note1: In order to avoid the overlay of discomfort glare from the other luminaire, the subject should shelter from the interruption light using a baffle when viewing one luminaire.

(3) The subject is then requested to make one's comparison assessment of the discomfort glare of the two luminaires, and then confirm the same feeling. At the same time, the experiment support person records the current of the DC power supply.

(4) Then the subject will be pushed to next angle, and the above procedure is repeated each time.

(5) After 6 angles are finished, the subject would have a rest for 10 minutes.

(6) Then the new luminaire would be replaced randomly and the above procedure is repeated each time.

3 Results

The UGR values of the experimental samples were calculated by the following formula (CIE 117, 1995) [6]:

$$UGR = 8\log\left(\frac{0.25}{L_b}\sum\frac{L^2\omega}{p^2}\right) \tag{1}$$

where

L_b is the background luminance (cd/m^2);

L is the luminance of the luminous parts of each luminaire in the direction of the observer's eye (cd/m^2);

ω is the solid angle of the luminous parts of each luminance at the observer's eye (sr),

and P is the Guth position index for each luminaire (displacement from the line of sight).

The discomfort glare of the experimental samples evaluated by subjects at six angles has been transferred into the current of reference luminaire. The relationship between current and luminance for reference luminaire has been calculated by luminance distribution burning at different current using an extrapolation method. Therefore, the subjective evaluation values (UGR$_s$) of the experimental samples could be calculated using the parameters of reference luminaire at different currents. In the experiment process, the subjects compared the experimental samples and reference luminaire very easily, and the amphibolous judgements did not appear in the whole experiment.

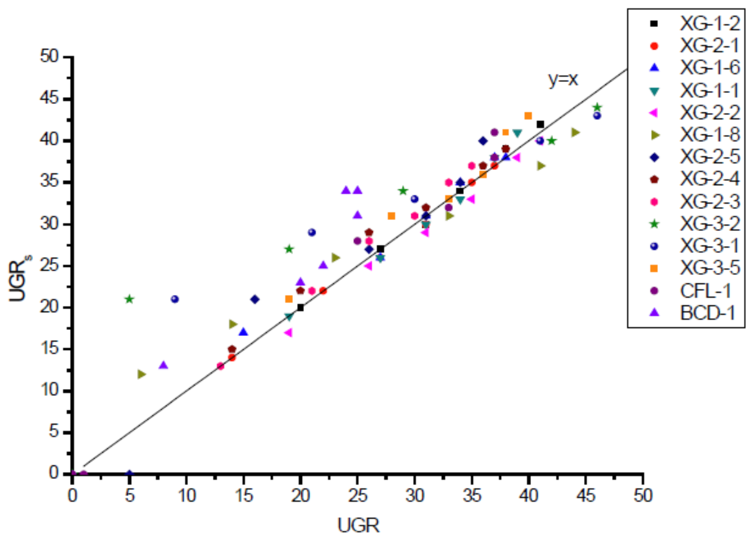

Figure 3 – The UGR values and the UGR$_s$ values

According to the above formula, the UGR values and UGR_s values (mean of all subjects's evaluation values) of the experimental samples were shown in Figure 3. It could be seen that most UGR values are smaller than UGR_s values, especially for the LED luminaires. This conclusion has been proved by C.E. Water, Lee Chang-Mo and Seung-Gyun Jung, et al [2, 3, 4]. It demonstrates that the UGR formula could not be used for evaluating the discomfort glare of non-uniformity LED luminaires and it should be modified further.

In order to judge which parameter is the main affecting factor for the difference between UGR and UGR_s, the correlation coefficient (R) was calculated and the results are shown in Table 1.

Table 1 –The correlation coefficient (*R*) between different parameters and the difference △UGR(UGR- UGRs)

	L_{max}(cd/m^2)	$U_{L1(Lmin/Lave)}$	$U_{L2(Lmin/Lmax)}$	$U_{L3(Lave/Lmax)}$	△UGR
L_{max}(cd/m^2)	1	/	/	/	/
$U_{L1(Lmin/Lave)}$	-0.35	1	/	/	/
$U_{L2(Lmin/Lmax)}$	-0.28	0.89	1	/	/
$U_{L3(Lave/Lmax)}$	-0.36	0.68	0.86	1	/
△UGR	0.03	-0.46	-0.40	-0.44	1

The above results demonstrate that R of maximum luminance (L_{max}) is the smallest, and the luminance uniformity is larger than L_{max}. It proves that the discomfort glare is mainly dependent on the luminance contrast in the field of view. Therefore, the luminance uniformity has a correlation better than L_{max} and this conclusion is same with Higashi, H. et al. [5]. While the $U_{L1(Lmin/Lave)}$ was chosen as the new evaluate parameter for the discomfort glare, which is different from Higashi, H. et al[5] who chose the $U_{L3(Lave/Lmax)}$. In addition, the negative values indicate that the bigger of the luminance uniformity, the smaller of △UGR.

The above results demonstrate that if the luminance uniformity is added in the UGR formula as a new affecting parameter, the discomfort glare could be evaluated more accurately, especially for LED lighting products. Based on the original UGR formula and the above subjective evaluation results, a new formula UGR_n was obtained in this study, as following:

$$UGR_n = 8\log\left(\frac{0.25}{L_b}\sum\frac{f(L,U_L)^2\omega}{p^2}\right) \tag{2}$$

$$f(L,U_L) = 3319 - 6785 * U_L^{0.5} + 16 * L^{0.5} * Ln(L) \tag{3}$$

where

U_L is the luminance uniformity of each luminaire in the direction of observer's eye at each angle, and it is equal to minimum luminance (L_{min}) over average luminance (L_{ave}).

Note 2: The other parameters are the same as UGR.

Figure 4 shows the relationship between the UGR_n values calculated using new formula UGR_n and the UGR_s values. The results shows that the UGR_n formula shorts the difference between UGR values calculated using original UGR and UGR_s values a lot. The color symbols in Figure 4 is very close to the line y=x.

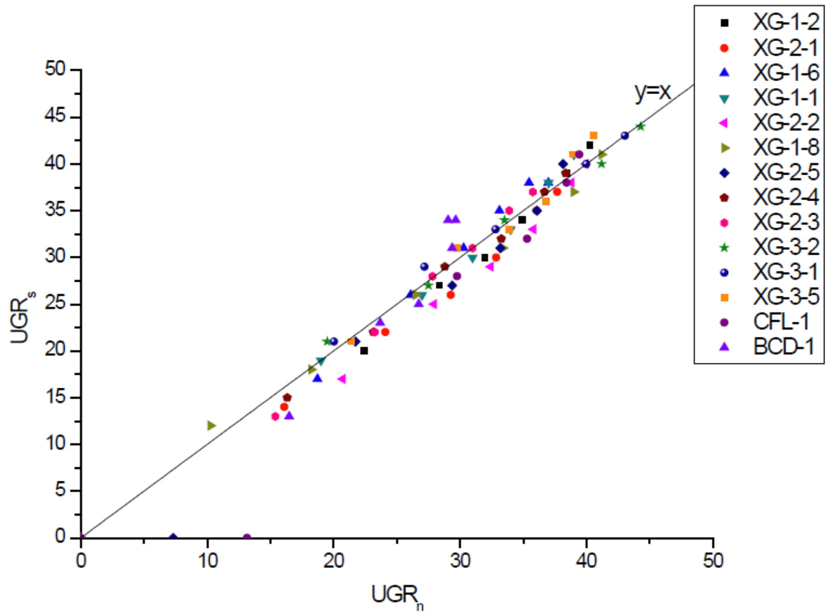

Figure 4 – The UGR_n values and the UGR_s values

4 Conclusions

According to the experiment results and analysis, it could be concluded as following:

- The reference luminaire is firstly to be used as an evaluation tool instead of semantic differential scaling and obtained good effects for subjective assessment.
- The subjective assessment results show that most UGR values are smaller than UGR_s values, especially for the LED luminaires. It demonstrates that the UGR formula should be unsuitable in evaluating the discomfort glare of non-uniformity LED luminaires.
- The discomfort glare is mainly dependent on the luminance contrast in the field of view, and the luminance uniformity has a correlation better than L_{max} for UGR.
- The modified formula UGR_n using luminance uniformity U_L as a new parameter has been obtained and it is based on the original UGR formula and the above subjective evaluation results. The shorten difference between UGR_n and UGR_s proved that it is able to evaluate discomfort glare in both LED and traditional lighting effectively and accurately.

Since quantity of the subjective observers is limit in this stage, and it may affect the correction in this research, large sample quantity experiments are still going on to verify the experiment method, and also check the accuracy of the analysis and correction.

Experiment research as above is just the first step to make improvement or correction to the traditional evaluation method. Further study based on luminance and its distribution is also going on to make the evaluation more from principal aspect.

5 Acknowledgements

This research has been supported by the national high technology research and development program, and the project No. is 2011AA03A113.

References

1. CIE 1987. CIE 17.4: 1987. International Lighting Vocabulary, 4th ed.
2. Waters, C. E. 1995. Discomfort Glare from Sources of non-uniform luminance. Journal of the Illuminating Engineering Society, 24-2, 73-85.

3. Lee, C. M., Kim, H. 2007. A study on the estimation of discomfort glare for LED luminaires. CIE 26th session, Beijing.

4. Jung, S. G., Cho, Y. I., Kim, H. 2009. A study of UGR for non-uniform luminance source. Proceedings of LUX EUROPA 2009(Istanbul), 9-9, 553-558.

5. Higashi, H., Koga, S., Kotani, T. 2012. The development of evaluation for discomfort glare in LED lighting of indoor work place-relationship between UGR and subjective evaluation. Proceedings of CIE 2012 “Lighting Quality and Energy Efficiency”, CIE x037, 706-712.

6. CIE 1995. CIE 117:1995. Discomfort Glare in Interior Lighting.

PP48

MUSEUM LIGHTING ENVIRONMENT: BUILD UP PERCEPTION ZONE MAPS ON LED ILLUMINATION

CHOU, C. J. [1], LUO, H. W. [2], CHEN, H. S.[3], and LUO, M. R.[4]
[1] Graduate Institute of Color and Illumination Technology
[2] Graduate Institutes of Applied Science and Technology
[3] Graduate Institute of Electro-Optical Engineering
[1,2,3] National Taiwan University of Science and Technology, CHINESE TAIPEI
[4] Colour, Imaging Design Centre, University of Leeds, UK
m10025009@mail.ntust.edu.tw

Abstract

Two experiments were conducted to collect the visual appearance data under different illumination conditions according to correlated color temperature (CCT) and illuminance level. Experiment 1 was carried out to investigate the impact of LED illumination conditions on visual perceptions in a viewing cabinet. Experiment 2 is the same as Experiment 1 except that it was performed in a real museum. It was found that the results between the two experiments were similar, indicating little difference between viewing environment on visual perceptions. The data were combined to establish the perception zone maps in CCT and illuminance plane.

Keywords : LED, Museum lighting, kruithof's rule, perception zone map

1 Introduction

LED sources are well positioned to museums due to its little UV and IR energy for conservation and low energy consumption. However, the appearance perceptions of LED lighting in museums have not been clearly understood. In 1941, Kruithof [1] proposed a method to achieve the "pleasure" effect based on a plot of correlated color temperature (CCT) against illuminance level for indoor lighting design, in which pleasing region was identified [2]. The illuminations of his experiment were fluorescent and incandescent lamps. The Kruithof's rule [3] showed that a higher CCT and higher illuminance level would make observers feel pleasant. This is also true for a lower CCT and a lower illuminance level. According to the CIE guideline [4] and the Kruithof's rule, the CCT of the pleasant zone should cover approximately 2700K to 4000K. And this range of CCT is also applicable for museum lighting. The paper is aimed to find the appropriate combinations of CCT and illuminance level suitable for museum lighting. Consequently, a novel concept of perception zone map similar to pleasant zone in the Kruithof's rule is proposed in this paper

2 Experimental Design

The aim of the present study is to investigate the visual appearance and atmosphere perceptions of novel illumination conditions for museum lighting and examine in the hope that LED sources could replace traditional lightings used in the museum. Two experiments were included in the present study. Their experimental conditions will be discussed in the following sections.

2.1 Paintings

Six hand-painted duplicated Fine Art Museum paintings were selected in Experiment 1, including oil paintings, watercolors and oriental paintings. Each category included indoor and outdoor contents. Table 1 shows the 6 paintings studied.

Table 1 - The 6 paintings used in Experiment 1

(Collected by Taipei Fine Arts Museum)

	oriental paintings	Water color	Oil painting
Indoor Scene			
	Artist's Mother at Fifty, 1959, by LIANG, shiow-chung	Portrait of Miss Sun, 1952, by LI, Che-Fan	Still Life, 1988, by KOO, Chung-Kuang
Outdoor scene			
	Lonely Boat, 1984, by OU, Haonian	East Gate, 1981, by LI, Che-Fan	Street Scene on a Summer Day, 1927, by CHEN, Cheng-Po

Three paintings (see Table 2) were used in Experiments 2, in which two of them were supplied by the museum, and the other one was "Still Life" used in Experiment 1.

Table 2 - The 3 paintings were used in 2nd experiment

(Provided by CHIMEI Museum)

		
Feeding Time, 1881, by Julien Duper, French	A Still Life with a Bottle, a Pewter Plate and an Earthenware Bowl, 1984, by Henk, Helmantel	Still Life, 1988, by KOO, Chung-Kuang
authentic work	authentic work	duplication

2.2 Light Source

Commercial white LEDs and a Telelumen® system were used in the present study. The latter is a lighting system including 16 narrow band LEDs to construct the spectral power distributions (SPDs) of light sources including those in blackbody. In the present study, 2700 K, 3500 K, 4000K, 5000K and 6500K were investigated and each of them had 3 illuminance levels (50, 150 and 300 lx). Five commercial white LEDs (3000K, 4000K, 5000K, 5500K (R_a of 87) and 5500K (R_a of 72)) were also studied at 100 lx. A total of 20 illumination conditions were studied in Experiment 1. Figure 1 shows the SPDs of the light sources used in the experiment.

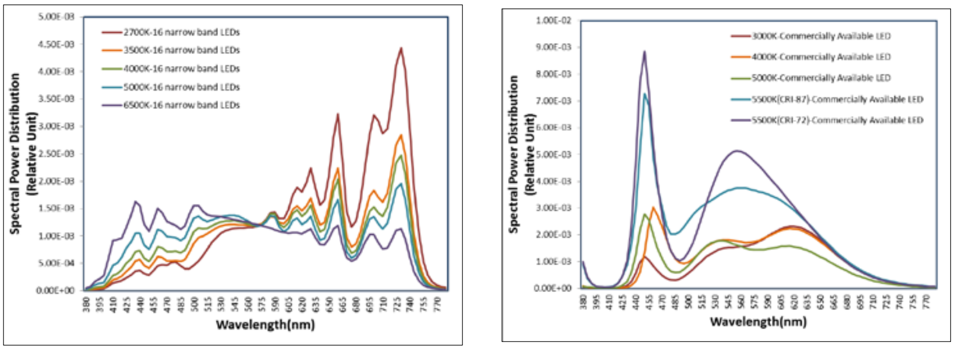

(a) SPDs of simulated daylights (b) SPDs of commercial white LEDs

Figure 1 - SPDs of experimental light sources

Experiment 2 was conducted at CHIMEI museum, which is located in the south of Taiwan, Tainan. Nine sets of illuminants were produced again using the Telelumen system, including 3 CCTs (3000K, 4000K, 5000K) at 3 illuminance levels a(50, 200, 500 lx). Four commercial LED illuminants with CCTs of 3000K, 4000K, 5500K (R_a of 72) and a 5500K (R_a of 87) were also used. All the white LED illuminants were set at 200 lx. Besides, a fluorescent lamp with high CRI general widely used in the gallery was also studied. The SPD of the fluorescent lamp is shown in Figure 2. In total, 14 lighting conditions were used.

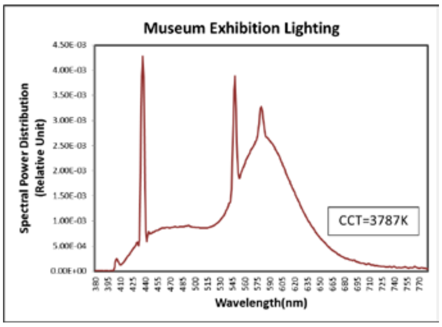

Figure 2 - The SPDs of the exhibition fluorescent lamp

2.3 Observers and experimental environment

Experiment 1 was conducted at the Lab of NTUST. All of the duplicated paintings were illuminated in a light cabinet. Observers took part in the experiment including 15 engineering students (8 males and 7 females) and 15 art and design students (7 males and 8 females). Observers were asked to make judgments on a chair having at a distance of 100 cm from the light cabinet.

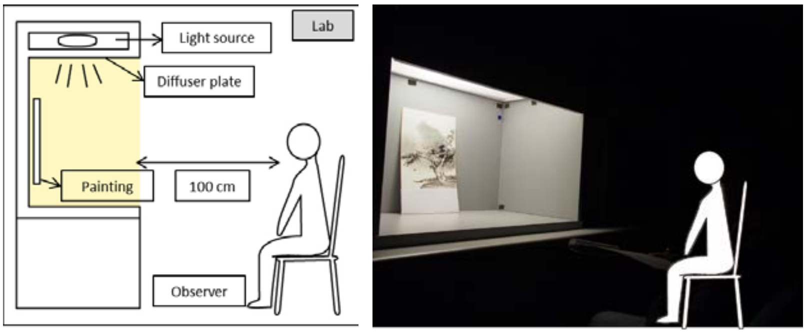

Figure 3 - Light box environment

Experiment 2 was conducted at the gallery of CHIMEI museum. Observers took part in Experiment 2 including 10 experts in art-field (5 males and 5 females) and 8 naive observers (4 males and 4 females). They viewed the paintings at a distance of 100~400 cm from the paintings on the wall. Observers were free to sit on the chair or stand up to observe paintings clearly.

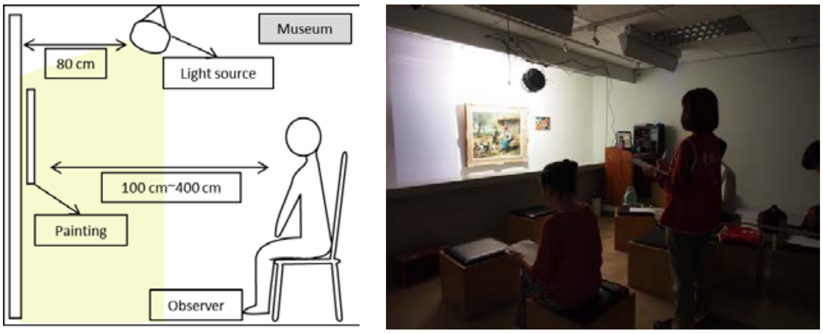

Figure 4 - Museum environment

2.4 Psychophysical Experiment

As mentioned earlier, the goal of this study is to define the relationship of visual perceptions at varying CCTs and illuminance levels. In Experiment 1, 11 semantic differential scales were designed according to perceived appearance and atmosphere perception: colorful/dull, bright/dark, clear/blur, warm/cold, and relax/tense, soft/hard, pleasant/unpleasant, natural/unnatural, active/passive, classic/modern, comfortable/uncomfortable, respectively. Observers were asked to assess paintings using the categorical judgment method via a 6 categorical-point scale. The eleven scales used were consisted of 6 categories (e.g. for bright-dark scale, the 6 categories are: 1- very dark, 2- dark, 3- a little dark, 4- a little bright, 5- bright, 6- very bright). In Experiment 2, 10 semantic differential scales were used, in which pleasant/unpleasant, clear/blur, classic/modern were replaced by high visibility /low visibility and lively/boring.

3 Results and Discussion

3.1 Principle Component Analysis (PCA)

PCA was used to analyze experimental data. A semantic map was also generated to show the relationship among the perception attributes. Table 3 shows the results of factor loadings for Experiments 1 and 2. It can be seen that two components, named *visibility* and *warmth,* were extracted for both experiments. In other words, the original 11 scales can be reduced to only 2 underlying dimensions. This also indicates that Experiment 1 results were similar to those of Experiment 2. Different environments and different paintings made little difference to visual perceptions. This can be clearly seen from the component plot in Figure 5, i.e. the scales in the same component are closely located together.

Figures 6a shows the component plot of the 20 experimental lighting conditions in Experiment 1, which were based on the average scores of paintings estimated by observers. Figure 6b shows the component plot of the 14 experimental lighting conditions in Experiment 2. The results in both figures indicate that the 1st component was highly correlated with illuminance and the 2nd component was highly correlated with CCT. According to these results, the “pleasant” perception is decreased with a reduction of illuminance level, while the “soft” perception is reduced under cooler sources.

Table 3 - Component loadings for the semantic scales

Experiment 1			Experiment 2		
Scale	Component		Scale	Component	
	1st Visibility	2nd Warmth		1st Visibility	2nd Warmth
Pleasant	0.98	0.17	**Bright**	0.99	0.1
Comfortable	0.97	0.17	High Visibility	0.98	0.15
Colorful	0.97	0.22	**Colorful**	0.95	0.28
Bright	0.95	-0.24	**Active**	0.88	0.42
Clear	0.93	-0.36	Lively	0.83	0.52
Natural	0.9	0.37	**Comfortable**	0.71	0.59
Active	0.84	0.51	**Soft**	0	0.99
Relax	0.71	0.68	**Warm**	0.27	0.93
Soft	0.12	0.99	**Relax**	0.49	0.8
Classical	0.23	0.97	**Natural**	0.56	0.74
Warm	0.3	0.94			

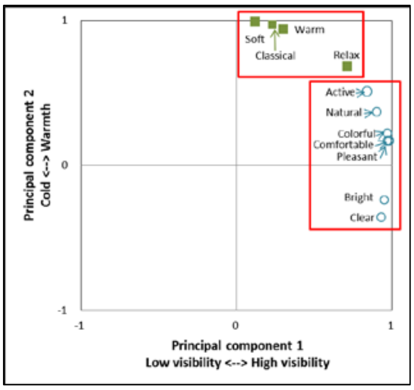

Experiment 1 of light box environment

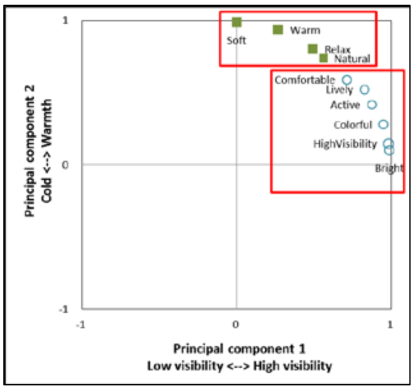

Experiment 2 of real museum environment

Figure 5 - The component plots of semantic scales

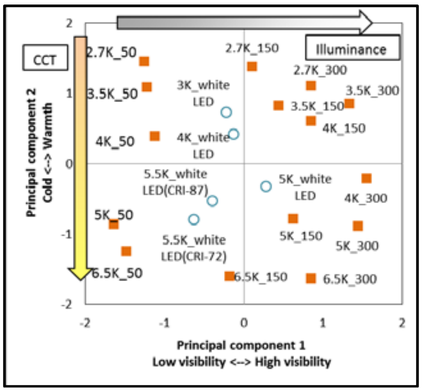

(a) Experiment 1 of light box environment

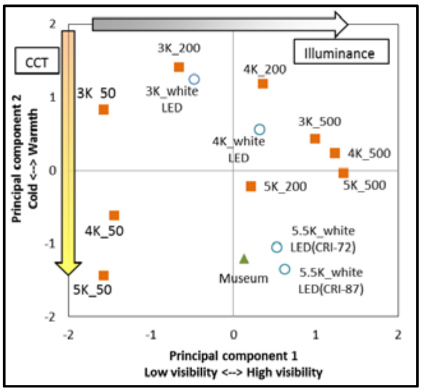

(b) Experiment 2 of real museum environment

Figures 6 - The component plots of lighting conditions

3.2 Analysis of Variance (ANOVA)

ANOVA was applied to investigate the impact of five variables (CCT, illuminance, gender, education background and type of painting) on visual perception. The results are summarized in Table 4. It shows that visual perceptions were significantly affected by three parameters (CCT, Illuminance and types of painting) and by the interactions between CCT and illuminance, and between illuminance and gender.

Table 4 - ANOVA results of the 1st experiment for emotion reaction of the paintings were illuminated by different CCTs and illuminance

Pleasant			Soft		
Source	F-value	p-value	Source	F-value	p-value
CCT	25.981	0.000*	CCT	252.952	0.000*
Illuminance	655.829	0.000*	Illuminance	4.53	0.011*
Type of painting	16.381	0.000*	Type of painting	2.489	0.029*
Gender	0.917	0.338	Gender	0.399	0.527
Education background	0.026	0.873	Education background	8.478	0.004*
CCT * Illuminance	7.183	0.000*	CCT * Illuminance	4.385	0.000*
CCT * Type of painting	1.438	0.046*	CCT * Type of painting	1.251	0.148
CCT * Gender	2.778	0.007*	CCT * Gender	1.481	0.169
CCT * Education background	2.186	0.033*	CCT * Education background	1.710	0.102
Illuminance * Type of painting	3.458	0.000*	Illuminance * Type of painting	1.455	0.150
Illuminance * Gender	3.352	0.035*	Illuminance * Gender	15.865	0.000*

* means the source has a significant difference ($p<0.05$)

Experiment 2 was conducted at the real museum, where one oil painting was used in Experiment 1 was also utilized. It was used to analyze the effect due to different viewing environments (i.e. light cabinet in the NTUST laboratory or real museum gallery). The ANOVA results are given in Table 5. The results show that lighting type and experimental site had no significant effect on the different observers participated in the two experiments. This again confirmed our earlier finding that the visual perceptions for viewing paintings are not affected by the viewing environment.

Table 5 - ANOVA results for the combined data

Bright			Soft		
Source	F-value	p-value	Source	F-value	p-value
CCT	4.743	0.000*	CCT	50.298	0.000*
Illuminance	262.647	0.000*	Illuminance	0.667	0.615
Gender	6.163	0.013*	Gender	6.883	0.009*
Education background	0.07	0.792	Education background	1.525	0.217
Lighting type	0.014	0.905	Lighting type	0.022	0.883
Site	2.702	0.101	Site	1.257	0.263
CCT * Illuminance	3.187	0.000*	CCT * Illuminance	1.672	0.068
CCT * Gender	3.669	0.001*	CCT * Gender	0.531	0.811
CCT * Lighting type	6.309	0.012*	CCT * Lighting type	0.022	0.883
Illuminance * Gender	3.491	0.008*	Illuminance * Gender	2.668	0.031

* means the source has a significant difference ($p<0.05$)

3.3 Perception Zone Map

As mentioned earlier, the Kruithof rule was useful to identify “pleasant zone” in the illuminance and CCT plane. This concept is further developed to build “perception zone” here. The zone map is aimed to exhibit the impact of illuminance and CCT on different visual perceptions. Table 6 shows the 7 perception zones corresponding to visual perceptions according to the two components (components 1 and 2) found in the last section. In each zone map, a boundary locus was drawn, which was determined by drawing curves across the data corresponding to 3.5 in the categorical point (the neutral point in each scale).

It can be seen that all perceptions in the visibility component are obviously affected by illuminant, i.e. the boundary divides the two “negative” and “positive” regions across illuminance with little influence from CCT. For example, the “bright-dark” zone map covers about 100 lx to 150 lx of illuminace level, and there was little effect from CCTs. For “soft-hard” zone map, it covers approximate 4000K ~ 5000K of CCT, which had little effect on illuminance. In addition, the “warm-cold” and “relax-tense” zones correspond to the CCT range of 4000K ~ 5600K and 3700K ~ 6000K, respectively.

It was found in Experiment 1 that the “comfortable” and “pleasant” perceptions agree well with each other. For “colorful-dull” and “comfortable-uncomfortable” zone map, the boundary lies approximately between 75 lx and 150 lx and had little effect from CCT. This result seems disagree with the Kruithof rule, which shows a positive correlation between CCT and illuminance in the comfort zone (a brighter and a cooler source, or a dimmer and a warmer source will be more pleasant).

Table 6 - Perception zone maps of the 1st and 2nd experiments

<table>
<tr><td colspan="4">(a) Component 1 (72.2%)</td></tr>
<tr><td>Bright-Dark</td><td>Colorful-Dull</td><td>Comfortable-Uncomfortable</td><td>Active-Passive</td></tr>
<tr>
<td>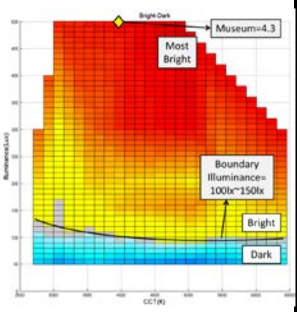
</td>
<td>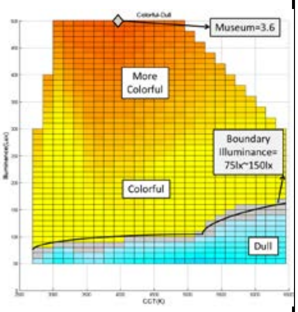
</td>
<td>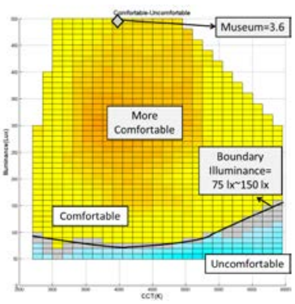
</td>
<td>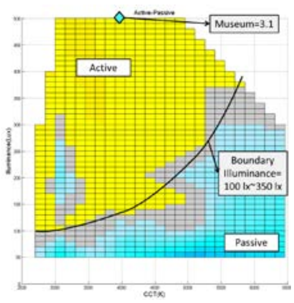
</td>
</tr>
<tr><td colspan="4">(b) Component 2 (20.4%)</td></tr>
<tr><td>Soft-Hard</td><td>Warm-Cold</td><td colspan="2">Relax-Tense</td></tr>
<tr>
<td>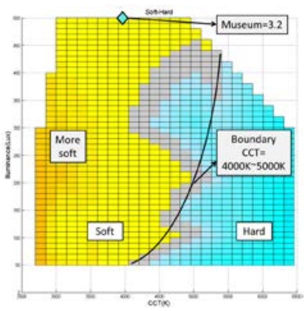
</td>
<td>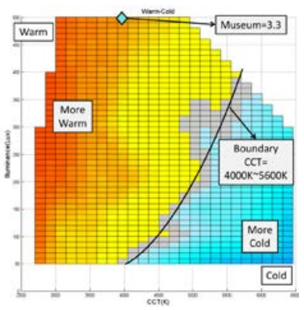
</td>
<td colspan="2">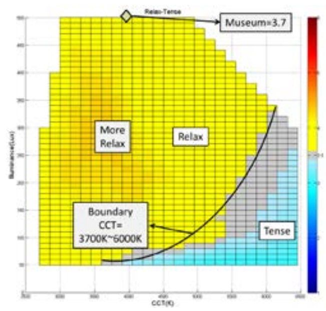
</td>
</tr>
</table>

4 Conclusion

The aim of the present study is to investigate the effect of illumination conditions on visual perceptions. Two experiments were conducted. It was found that Experiments 1 and 2 results had good agreement and both CCT and illuminance had big impact on all visual perceptions. All the perception scales can be reduced to two dimensions: visibility and warmth. This implies that the visual perceptions are not affected by the viewing environment.

Similar to the Kruithof rule, perception zone maps were established to define the negative and positive perception by a boundary in the illuminance and CCT plane. They were established base on combined data of Experiments 1 and 2.

Acknowledgements

Special thanks to the Taipei Fine Arts Museum for supporting this research in providing digital files of paintings. And thanks to the CHIMEI Museum for assisting this research in providing authentic work of paintings and space for performing experiment.

References

[1] KRUITHOF, A. A. 1941. Tubular luminance lamps for general illumination. Philips Tech. Rev., 61-33.

[2] VIENOT, F. DURAND, F. and MAHLER, E. 2009. Kruithof's rule revisited using LED illumination. Jour. of Modern Optics, 56, 1433-1446.

[3] CIE 2004. CIE 157:2004. Control of damage to museum objects by optical radiation, Vienna: CIE.

[4] DAVIS, R. G. and GINTHNEW, D. N. 1990. Correlated color temperature, illuminance level and the Kruithof curve. J. Illum. Eng. Soc., 19, 27-38.3.

[5] BERNS R. S. 2011. Designing white-light LED lighting for the display of art: a feasibility study. Color Res. Appl., 36. 324-334.

PP49

INFLUENCES OF FLICKER CHARACTERISTICS FROM LIGHTING SYSTEMS ON HUMAN PERCEPTION

Wei-Cheng Chao, Pei-Ting Chou, I-Ping Chang, Fei-Chang Hwang, Shu-Mei Yang
Electronics and Optoelectronics Research Laboratories, Industrial Technology Research Institute, CHINESE TAIPEI

Abstract

A systematic study was conducted aiming to assess effects of flicker characteristics under different lighting conditions on human perception and to minimize negative visual and non-visual impacts of flicker from different lighting systems. To study efficiently, Box-Behnken Design (BBD) of experimental designs (DOE) for response surface methodology (RSM) was utilized to rate the relative impact of flicker frequency, amount of modulation, duty cycle, illumination and solid angles on visual and non-visual perception and acceptability. Simultaneously, this study could generalize prescriptions for the flicker under different lighting conditions to minimize negative visual and non-visual impacts of flicker under lighting systems.

1 Introduction

1.1 Purpose

This study attempts to assess effects of flicker characteristics under different lighting conditions on human perception. Furthermore, this study is presently working on prescriptions for the luminous flicker from different lighting conditions to minimize negative visual and non-visual impacts of flicker from lighting systems.

1.2 Background and Motivation

Lighting is an important environmental factor when considering human perception, health and safety, visual comfort and workplace design. But how well do we really understand the implications of lighting on these factors? When one attempts to digest the enormous volume of information of the past century regarding recommended lighting conditions, one begins to see that these recommendations are varied, not extensively tested and often apply to a very limited set of luminous conditions. In a world with flicker which increasingly challenges technological boundaries, it is important that the factors and limits which affect human perception and visual comfort are well understood in order to design and evaluate new lighting system. Human visual sensitivity to flicker depends upon a number of factors, including the frequency, modulation amount, duty cycle, illumination and solid angle. Therefore, this study designs an experiment to assess the relative impact of these factors on visual and non-visual perception and acceptability and attempts to minimize negative visual and non-visual impacts of flicker from different lighting systems.

2 Method

To finish this experiment, the systematic procedure was developed (Figure 1). This procedure started with literature review, followed with planning and setting up ergonomics experiment, doing this ergonomics experiment, and ended with developing flicker rating. Detailed information on each item is listed below.

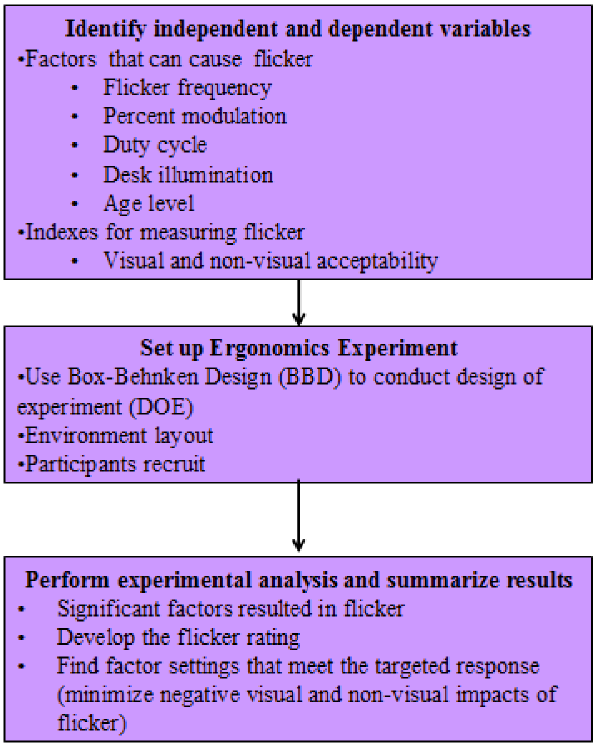

Figure 1 Systematic procedure for flicker rating

1) Identify independent and dependent variables

Flicker is the rapid modulation of light in a cyclical manner. Human visual and non-visual sensitivity to flicker depends upon a number of factors, including the flicker frequency, percent modulation (the difference between maximum and minimum light output divided by the sum of the maximum and minimum light output), duty cycle, desk illumination, and age level. This study identified these five factors in Table 1 as independent variables.

Table 1 Independent variables of this study

Factors	Levels
Flicker frequency	-1:60, 0:120, 1:150 Hz
Percent modulation	-1:50%, 0:75%, 1:100% flicker
Duty cycle	-1:10%, 0:20%, 1:30%
Desk illumination	-1:400, 0:600, 1:800 lx
Age level	-1:20~21, 0:22~45, 1:46~60

After reviewing the literature, Table 2 indicated that direct perceptions, indirect perceptions, satisfaction, subjective physiological effect, objective physiological effect, and task performance could be regard as criteria (Dependent variables) to judge effects of flicker characteristics under different lighting conditions on human reaction.

2) Set up Ergonomics Experiment

In a dark-painted windowless room at National Taiwan University of Science and Technology, a workstation containing a laptop computer, a clipboard taking letter size paper and a task luminaire was set up (Figure 2).

Response surface methods (RSM) are powerful optimization tools in the arsenal of statistical design of experiments (DOE). Therefore, five-factor, three-level Box-Behnken Design (BBD) of RSM of DOE was employed to establish a cause-and-effect relationship between a number of independent variables (factors) and a dependent variable (response) of interest and to determine the settings of the factors to achieve an optimum value of these responses. This study uses a five factors quadratic model and the data matrix generated by Minitab. For each experimental session, all of the conditions in Table 3 were presented in a randomized order. Upon entering the laboratory and signing an informed consent form approved by Joint Taiwanese Institutional Review Board, 46 volunteer subjects (24 females/22 males, aged 20–55 years) participated in the study. Subjects wore corrective lenses if necessary. No subjects who reported a history of migraines or epileptic seizures participated in the study.

Table 2 Dependent variables of this study

Category	Description
Direct perceptions	Q1: How acceptable was the stroboscopic effects under this lighting condition while using the computer? (-2: very unacceptable, -1: somewhat unacceptable, 0:neither acceptable nor unacceptable, +1:somewhat acceptable, +2: very acceptable)
	Q2: How acceptable was the stroboscopic effects under this lighting condition while looking directly at the luminaire?
	Q3: How acceptable was the stroboscopic effects under this lighting condition while looking at point A?
Indirect perceptions	Q4: How acceptable was the stroboscopic effects after you were asked to shift your gaze between points A and B in the room?
	Q5: How acceptable was the stroboscopic effects after you were asked to wave your hand underneath the luminaire?
Subjective physiological effect	Q6: How tired was your eyes now?
	Q7: How discomfortable was your head now?

View of the test laboratory from the subject's seating position

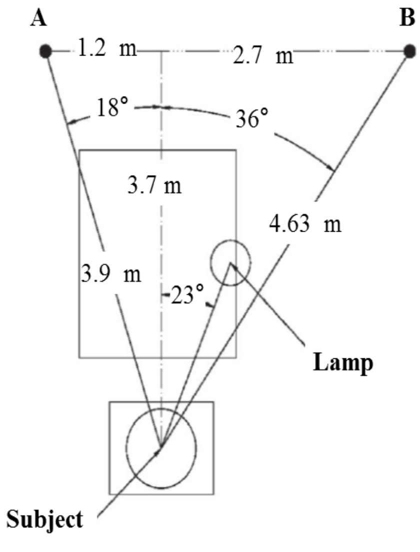

Approximate angular positions of objects in the subject's field of view

Figure 2 Experimental Layout

Table 3 (part1) Matrix of independent variables of BBD of this study

StdOrder	RunOrder	Flicker frequency -1:60, 0:120, 1:150 (Hz)	Percent modulation -1:50%, 0:75%, 1:100% (flicker)	Duty cycle -1:10%, 0:20%, 1:30%	Desk illumination -1:400, 0:600, 1:800 (lx)	Age level -1:20~21, 0:22~45, 1:46~60
46	1	0	0	0	0	0
1	2	-1	-1	0	0	0
10	3	0	1	0	0	-1
36	4	1	0	0	0	1
37	5	0	-1	0	-1	0
45	6	0	0	0	0	0
15	7	-1	0	1	0	0
9	8	0	-1	0	0	-1
6	9	0	0	1	-1	0
44	10	0	0	0	0	0
16	11	1	0	1	0	0
7	12	0	0	-1	1	0
31	13	0	0	-1	0	1
39	14	0	-1	0	1	0
40	15	0	1	0	1	0
27	16	-1	0	0	1	0
5	17	0	0	-1	-1	0
23	18	0	-1	1	0	0
3	19	-1	1	0	0	0
2	20	1	-1	0	0	0
26	21	1	0	0	-1	0
29	22	0	0	-1	0	-1
33	23	-1	0	0	0	-1
25	24	-1	0	0	-1	0
28	25	1	0	0	1	0
41	26	0	0	0	0	0
32	27	0	0	1	0	1

Table 3 (part 2) Matrix of independent variables of BBD of this study

StdOrder	RunOrder	Flicker frequency -1:60, 0:120, 1:150 (Hz)	Percent modulation -1:50%, 0:75%, 1:100% (flicker)	Duty cycle -1:10%, 0:20%, 1:30%	Desk illumination -1:400, 0:600, 1:800 (lx)	Age level -1:20~21, 0:22~45, 1:46~60
20	28	0	0	0	1	1
13	29	-1	0	-1	0	0
8	30	0	0	1	1	0
42	31	0	0	0	0	0
17	32	0	0	0	-1	-1
11	33	0	-1	0	0	1
4	34	1	1	0	0	0
24	35	0	1	1	0	0
14	36	1	0	-1	0	0
12	37	0	1	0	0	1
21	38	0	-1	-1	0	0
30	39	0	0	1	0	-1
35	40	-1	0	0	0	1
43	41	0	0	0	0	0
38	42	0	1	0	-1	0
19	43	0	0	0	-1	1
22	44	0	1	-1	0	0
34	45	1	0	0	0	-1
18	46	0	0	0	1	-1

3) Perform experimental analysis and summarize results

In this study, BBD was used for response surface optimization with five independent variables (flicker frequency, percent modulation, duty cycle, desk illumination, and age level) at three levels. Deigns using BBD are usually very efficient in terms of the number of required runs and therefore are less expensive to run compared to central composite design (CCD). The design points fall within a safe operating limit, within the nominal high and low levels, as BBD does not contain any points at the vertices of the cubic region. This could be advantageous when the factor-level combinations are prohibitively expensive or impossible to test because of the physical process constraints. We perform experimental analysis and summarize results as the following.

- Effect of flicker frequency, percent modulation, duty cycle, desk illumination, and age level on each dependent variable

The significance of each coefficient was determined by P value, and the smaller the P-value, the more significant are the corresponding coefficient is. Data in Table 4 showed that flicker frequency ($P < 0.05$) has the strongest effect on direct perceptions, indirect perceptions, and subjective physiological effect.

- The good set of conditions that will meet all the goals

The Minitable 14 software used searches for a combination of factor levels that simultaneously satisfy the requirements placed on each of the responses and factors. Optimization requires that goals (i.e., none, maximum, minimum, target, or in range) are set for the variables and response where all goals then get combined into one desirability function. To find a good set of conditions that will meet all the goals, the five variables (1) flicker freq. (1:150 Hz), (2) percent modulation (1:100%), (3) duty cycle (-1:10%), (4) Desk illumination (-1:400), and (5) Age level (-1:20~21) were set within range while dependent variables were set at Table5. By applying the desirability function approach, the optimum level of various parameters was obtained as showed in the data set: (1) flicker freq. (1:150 Hz), (2) percent modulation (1:100%), (3) duty cycle (-1:10%), (4) Desk illumination (-1:400), and (5) Age level (-1:20~21). Figure3 showed desirability ramps that were developed from optimum points via numerical optimization.

Table 4 P value of combinations of independent and dependent variables

	Direct perceptions			Indirect perceptions		Subjective physiological effect	
Independent/dependent variables	Q1	Q2	Q3	Q4	Q5	Q6	Q7
Flicker freq.	0.001**	0.033**	0.10*	0.010**	0.573	0.05**	0.001**
Percent modulation	0.372	0.781	0.107	0.107	0.573	0.209	0.133
Duty cycle	0.550	0.171	0.583	0.783	0.195	0.187	0.035**
Desk illumination	0.764	0.781	1.000	0.783	1.000	0.655	0.752
Age level	0.550	0.406	0.583	0.107	0.195	0.840	0.728
Flicker freq.*Flicker freq.	0.098*	0.073*	0.05**	0.002**	0.033**	0.782	0.246
Percent modulation* Percent modulation	0.341	0.308	0.347	0.684	0.711	0.423	0.679
Duty cycle*Duty cycle	0.941	0.632	0.892	0.684	0.146	0.414	0.708
Desk illumination*Desk illumination	0.130	0.538	0.499	0.087*	0.579	0.098*	0.806
Age level*Age level	0.508	0.945	0.892	0.892	1.000	0.313	0.851
Flicker freq.*Percent modulation	0.081*	0.033**	0.003**	0.107	0.264	0.655	1.000
Flicker freq.*Duty cycle	0.081	0.104	0.276	0.035**	0.453	1.000	0.529
Flicker freq.*Desk illumination	0.550	0.578	1.000	0.582	0.453	0.374	0.529
Flicker freq.*Age level	0.081*	1.000	0.276	0.276	0.453	0.374	1.000
Percent modulation*Duty cycle	1.000	1.000	1.000	1.000	0.140	0.374	0.067*
Percent modulation*Desk illumination	1.000	1.000	1.000	1.000	1.000	0.187	0.213
Percent modulation*Age level	1.000	0.10*	1.000	0.582	1.000	0.988	0.931
Duty cycle*Desk illumination	1.000	1.000	1.000	1.000	0.453	1.000	0.529
Duty cycle*Age level	0.550	1.000	1.000	0.582	0.264	0.374	0.213
Desk illumination*Age level	1.000	1.000	1.000	1.000	0.140	0.187	0.529

Table 5 The range of response optimization

	Goal	Lower	Target	Upper	Weight	Import
Q1	Maximum	0.0	2	2	1	1
Q2	Maximum	0.0	2	2	1	1
Q3	Maximum	0.0	2	2	1	1
Q4	Maximum	0.0	2	2	1	1
Q5	Maximum	0.0	2	2	1	1
Q6	Minimum	-2.0	-2	0	1	1
Q7	Minimum	-2.0	-2	0	1	1

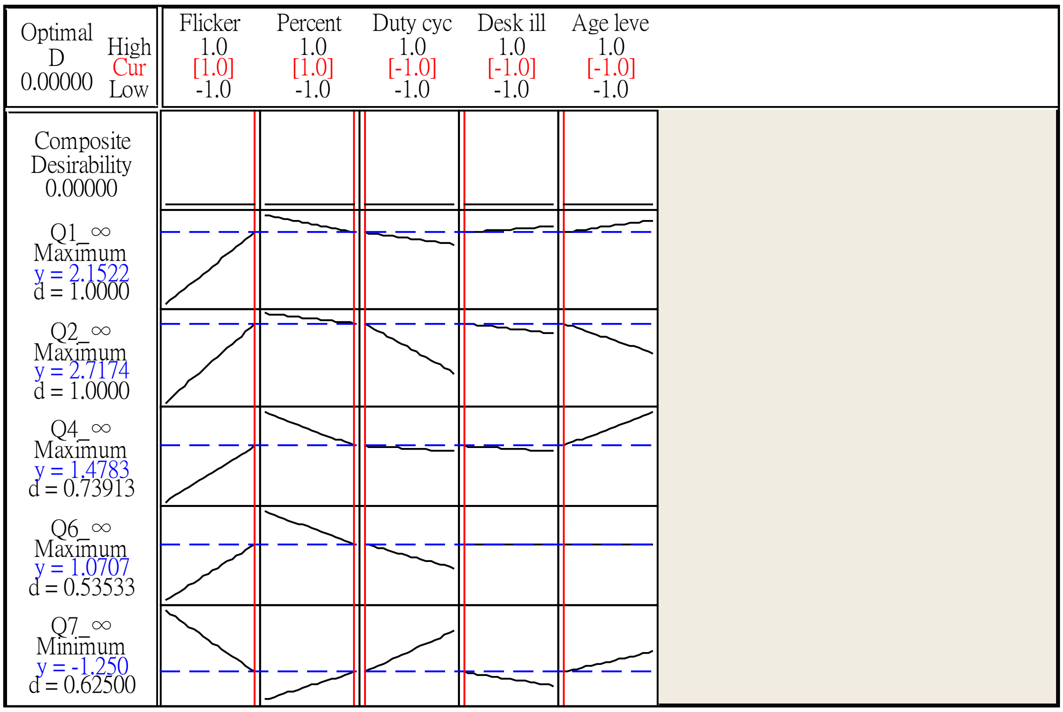

Figure 3 Desirability ramp of response optimization

3 Conclusion

The experimental design approach using BBD was successfully applied in the prescription for the luminous flicker under different lighting conditions to minimize negative visual and non-visual impacts of flicker from lighting systems. According to the results, flicker frequency ($P < 0.05$) has the strongest effect on direct perceptions, indirect perceptions, and subjective physiological effect. By applying the desirability function approach, the optimum level of various parameters was obtained as showed in the data set: (1) flicker freq. (1:150 Hz), (2) percent modulation (1:100%), (3) duty cycle (-1:10%), (4) Desk illumination (-1:400), and (5) Age level (-1:20~21).

PP51

ENVIRONMENTAL INFLUENCE ON BACKGROUND LUMINANCE PREFERENCE OF COMPUTER USE AT HOME

Sheng Peng[1], Kangjun Liu[1], Shu-Guang Kuai[1], Weixi Zhou[1], and Xiaodan Tang[1]
Yang Shen[2], Xingtao Zhou[2]
[1] Philips Research China, Shanghai, CHINA
[2] Department of Optometry & Refractive Surgery, Eye & ENT Hospital, Fudan University, Shanghai, CHINA
sheng.peng@philips.com

Abstract

There are many different guidelines on illumination level for work with VDTs. Most of the previous work put their focus on professional spaces with high desktop illuminance. For a low illuminance environment, it is not fully studied on VDTs. For example, many home lighting conditions have illuminance below 100lux, comparing with 500lux in office. The adaptation condition for visual comfort may yield different preferences. It is generally understood that offering a certain amount of background light could be a solution to help relieve eye fatigue. However, home background may become very different from the background defined in previous experiments with the assumption of a wall close to the display. It is not clear by having a wall in distance from the display, whether or not same level of visual comfort as having a wall close by can still be realized with back lighting. In this study we investigated the background influence on visual comfort levels by comparing illuminated VDT background ‘with wall’ and ‘without wall’ at home, using no back lighting as the control condition. The results suggest that even with a wall in distance, back lighting can still be effective to improve visual comfort and relieve eye fatigue for computer use at home.

Keywords: Visual comfort, Screen-background luminance, CVS

1 Background

Visual comfort has been an important subject of considerable research in relation to displays. Within the environment of workspace, ergonomics lighting may become very important to affect workplace efficiency [1,2,3]. Previously there have been a lot of studies on visual fatigue of operators who requires daily use of computer terminals and report computer vision syndromes (CVS) [4,5,6] such as, dry eyes, eye irritation, blurred vision and double vision.

While the large majority of research has addressed the question of ergonomics lighting for professional spaces, relatively less attention has been put on home scenarios. In general, many home lighting conditions have illuminance below 100lux, comparing with 500lux in office. The adaptation condition for visual comfort may yield different preferences for visual comfort. It is also understood that offering suitable background light could be a solution to help relieve eye fatigue. [7,8]. However home background may become very different from the background defined in previous experiments with the assumption of a wall close to the display[7]. It is not clear by having a wall in distance from the display, whether or not same level of visual comfort as having a wall close by can still be experienced with background lighting.

The objective of this study is to understand the preferred surrounding lighting environment for computer use at home with a wall close by the back of the display (‘with wall’ condition) and with a wall in distance from the display (‘without wall’ condition) using dark condition without a back lighting as the control.

2 Experiment

A laptop (Dell16400) with a 14-inch LCD display was used in this experiment. Four dimmable LED strips were mounted on the back of the computer screen to provide background luminance (Figure 1, left panel). The back lighting creates a uniform distribution on the wall close by the computer. The control environment was created by turning off the back lighting with the wall close by the screen. Participants sat in front of the display screen (1400*900 pixels, 30.7cm*19cm, frame rate of 60 hz) at a 60 cm viewing distance. By turning the participants for 180° facing the other side of the wall, we made another setup with a same model laptop on a table which has a wall in distance (~3m) to the back of the screen.

Figure 1. Experiment setup with back lighting and the lighting effect of back lighting on the wall

The screen and background luminance were measured by a calibrated 2D luminance camera (Cannon EOS550D). We pre-defined three conditions: movie, game and web. In each of these conditions, we selected one typical picture to present on the display and calculated the mean luminance of the entire display. The background luminance was defined as the average luminance of surrounded area extending to 26 ° in the upper visual field and 26° in the left and right visual fields (same luminance measurement method as in reference [7]).

The average screen luminance values for the three scenarios are movie: 16 cd/m2, game: 28 cd/m2, web page: 64 cd/m2. The intensity of the LED light sources was controlled by a dimmer which could adjust the background luminance to 16 calibrated discrete levels: 0 cd/m2, 12 cd/m2, 26 cd/m2, 40 cd/m2, 55 cd/m2, 69 cd/m2, 84 cd/m2, 98 cd/m2, 112 cd/m2, 127 cd/m2, 141 cd/m2, 154 cd/m2, 169 cd/m2, 183 cd/m2, 197 cd/m2, 212 cd/m2. The calibration was made with the wall close by the display. For the wall in distance condition, same level settings were used, so that we can compare the different preference levels of 'with wall' and 'without wall' close by as in Figure 2.

Figure 2. The setup of a laptop 'with wall' and 'without wall' close by the screen

60 young adult participants (30 male, 30 female, mean age = 26.8 ± 3.4) took part in the experiment. They all have normal or corrected-to-normal vision and gave their informed consent before the data collection.

Each participant has to do a tuning of the light setting (excluding the case without back lighting) to their preferred level for three screen viewing activities including watching a movie frame, a game picture and a web page. Then the participant will give visual comfort assessment based on a nine scale scoring questionnaire as shown in Table 1.

Table 1. Visual comfort rating scale

Score	Description
1	Very uncomfortable
2	
3	Uncomfortable
4	
5	Just acceptable / Just OK
6	
7	Comfortable
8	
9	Very comfortable

The assessments were repeated for each of the 9 stimuli. The three screen luminance levels (movie, game, web) and three ambient conditions (no back lighting, with wall, without wall) were randomized in the experiment. The total assessment takes around 15 minutes to complete for each participant. The procedure allowed the participants to take a close comparison among the three different ambient conditions, therefore could answer the question of whether or not under ‘without wall’ condition one can still realize the similar level of visual comfort as ‘with wall’ condition and even understand how better they are comparing with ‘no back lighting’ condition.

3 Results

An analysis of variance (ANOVA) was performed with the software package SPSS version 21 on the ratings of visual comfort levels. The visual comfort level was used as the dependent variable, whereas the ambient condition and screen luminance were selected as fixed factors, and subjects as a random factor. As in Table 2, the ambient condition ($F= 213.861$, $p<0$) and screen luminance ($F=4.362$, $p=0.013$) both have significant influence on the overall visual comfort, so does the interaction of the two factors ($F=3.383$, $p=0.10$). As illustrated in Figure 3, the visual comfort level of viewing without backlight condition is much lower than with backlight condition; while with backlight, with wall and without wall has no significant difference.

Table 2. Tests of Between-Subjects Effects

Dependent variable:

Source	df	F	Sig.
ambient condition	2	213.861	.000
screen luminance	2	4.362	.013
subject	59	3.566	.000
ambient condition * screen luminance	4	3.383	.010

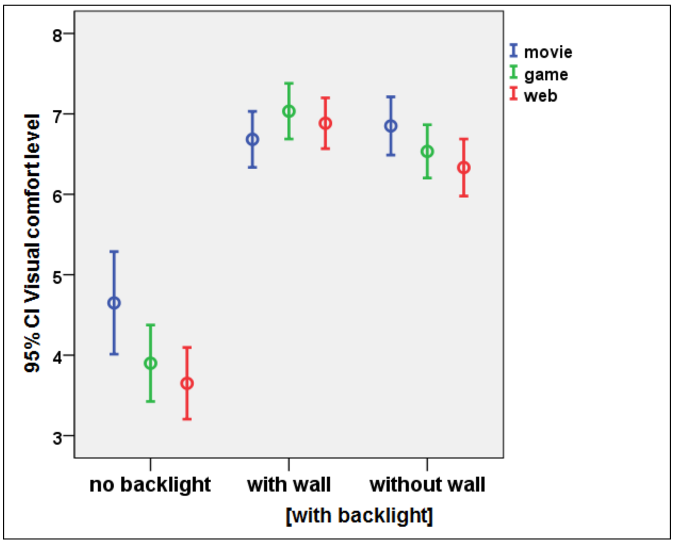

Figure 3. Visual comfort level with different ambient conditions and screen luminance

4 Discussion

Screen-background luminance difference has been believed an important factor that contributes to visual discomfort in watching computer screen. Our results indicate that providing a suitable background light clearly demonstrates the benefits for visual comfort compared with a dark environment, which is consistent with previous findings reported by the literature. Based on the results, we built up a solution that positions light sources on the back of computer screen to offer additional light for compensating screen-background luminance difference. To implement that, the solution should comply with environment at home. One of the important factors is that the wall in home scenarios can reflect light back. When the wall is close to the screen background, the reflection can generate a relative uniformed lighting background in a vertical surface. While a wall is far from the screen, there is no vertical surface. Since the distance to a wall is uncertain at home, it is important to understand whether and how much the distance to a wall can affect human visual comfort. In this study, we compared comfortable levels of three conditions, 1) no backlight: without background lighting; 2) with wall: the wall is close to the computer screen; 3) without wall: the wall is far away from the computer screen.

The condition without a wall could affect human visual comforts in two aspects. First, a wall can reflect a certain amount of lighting rays to human eyes. Without it, the background looks less bright. In addition, the brightness level of upper part and lower part of background are not equal. In the lower part, desk can reflect lighting rays to human eyes making it look brighter while the top part is relatively darker. The non-uniformity could be another important factor inducing discomfort and is much harder to be addressed. In our experiment, we noticed that for the ‘without wall’ condition, participants need to turn the light to a higher level to reach the similar visual comfort level as they did in the condition ‘with wall’ (Figure 2). It compensates for the brightness level of two conditions. Interestingly, the overall comfort levels are not significantly different between two conditions. The results indicate that once matching preferred brightness level, the non-uniformity play little roles in visual comfort. The results confirm that positioning lighting sources at the back of a computer screen would be an effective way to improve visual comfortable in watching a computer screen.

5 Conclusions

This study provides statistic evidence on back lighting can improve visual comfort level for computer use at home. It also shows that for variety of different home ambient environment, it is also possible to experience the similar visual comfort level for ‘with wall’ and ‘without wall’ conditions. This work may help home ergonomic lighting design for computer use and further work of more quantitative photometric measurements may be used to derive guidelines of interior lighting design.

Acknowledgments

We would like to thank Dr. Ingrid Heynderickx from Philips Research Laboratories and Technical University of Eindhoven in Eindhoven, Netherlands for her continuous support and advice on this work.

References

1. Conlon, E., Lovegrove, W., Hine, T., Chekaluk, E., Piatek, K., and Hayes-Williams, K. "The effects of visual discomfort and pattern structure on visual search" Perception 27, (1998) pp.21-33.

2. Gur, S., and Ron, S. "Does work with visual display units impair visual activities after work?" Documenta ophthalmologica. Advances in ophthalmology 79, (1992), pp.253-259.

3. Kurimoto, S., Noro, K., Matsuoka, S., Yamamoto, S., Komatsubara, A., and Iwasaki, T. "The working adaptation in visual display terminal (VDT) workers" Journal of UOEH 8 Suppl, (1986) pp.227-264.

4. Blehm, C., Vishnu, S., Khattak, A., Mitra, S., and Yee, R.W. "Computer vision syndrome: a review" Survey of ophthalmology 50, (2005) pp.253-262.

5. Portello, J.K., Rosenfield, M., Bababekova, Y., Estrada, J.M., and Leon, A. "Computer-related visual symptoms in office workers", Ophthalmic & physiological optics : the journal of the British College of Ophthalmic Opticians 32, (2012) pp.375-382.

6. Rosenfield, M. "Computer vision syndrome: a review of ocular causes and potential treatments", Ophthalmic & physiological optics : the journal of the British College of Ophthalmic Opticians 31, (2011) pp.502-515.

7. Peng, S., Liu, K., Chen,Y., Kuai, S.-G., Heynderickx, I., “Visual comfort lighting for computer use at home” Proc CIE Centenary Conference “Towards a New Century of Light”, Paris, France, May. 2013, pp. 668-672.

8. Sheedy, J.E., Smith, R., Hayes, J., "Visual effects of the luminance surrounding a computer display", Ergonomics, 48, (2005), pp.1114-1128

PP52

THE INFLUENCE OF ELAPSED TIME AND ILLUMINANCE/COLOR TEMPERATURE ON THE SUBJECTIVE EVALUATION OF INTERIOR LIGHTING

1st Hiroshi Takahashi[1], 2nd Satoshi Misawa[2], 3rd Takashi Irikura[2]
[1] Kanagawa Institute of Technology, Atsugi, Kanagawa, JAPAN,
[2] Shibaura Institute of Technology, Toyosu, Tokyo, JAPAN
htakahashi@ele.kanagawa-it.ac.jp

Abstract

The illuminance and color temperature of a light source affect the perceived impression of interior lighting. People generally prefer a low color temperature (i.e., warm colors) in interior spaces with low illuminance, and a high color temperature, (i.e., cool colors) in interior spaces with high illuminance. This phenomenon is expressed by the Kruithof curve, which describes the relation between the illuminance and color temperature of a light source. However, there are issues with the Kruithof curve. Therefore, the aim of the present study was to clarify the influence of elapsed time on the subjective evaluation of interior lighting. Two different scale models were used in this study. Each subject is assumed the activity of relaxing in the living room and evaluates orally in this experiment. The results show the perception of comfort with regard to the interior space tended to increase with elapsed time.

Keywords: Elapsed Time, Illuminance, Color Temperature, Interior Lighting

1 Introduction

The illuminance and color temperature of a light source affect the perceived impression of interior lighting. People generally prefer a low color temperature (i.e., warm colors) in interior spaces with low illuminance, and a high color temperature, (i.e., cool colors) in interior spaces with high illuminance. This phenomenon is expressed by the Kruithof curve, which describes the relation between the illuminance and color temperature of a light source(1). However, there are issues with the Kruithof curve. In previous research, a subjective evaluation of the impression of the lighting environment formed immediately after entering a room was carried out, since this is the time when the strongest and most important impression is formed(2), (3). However, due to chromatic adaptation, the human impression of the lighting environment is expected to change with time. If the manner in which such changes occur was understood, a lighting environment could be designed that more closely mimics real life. Therefore, the aim of the present study was to clarify the influence of elapsed time on the subjective evaluation of interior lighting.

2 Experiment

Figure 1 shows the experimental apparatus. Two different scale models were used in this study. The first was a standard room and the second was an evaluation room. Both models were constructed from white (N9.5) styrene boards and were 1/10 scale models (W 360 mm×D 450 mm×H 240 mm) of a living room. A 60-mm-diameter round shape imitating a ceiling light was formed in the center of the ceiling and diffusion paper was used to diffuse the light from a metal halide lamp. Color filters were used to adjust the color temperature of the light source, and were combined so that the correlated color temperature had a deviation (Δuv) of less than 0.005 from the blackbody locus.

The Semantic Differential (SD) method was used to evaluate the impressions of the subjects. Five pairs of words (comfortable/uncomfortable, warm/cool, preferred/unfavorable, natural color appearance/artificial color appearance, and calming/restless) were employed in this study. Figure 2 shows the evaluation scale. Table 1 shows the experimental conditions. The subjects were seven males in their 20s. Each subject is assumed the activity of relaxing in the living room and evaluates orally in this experiment.

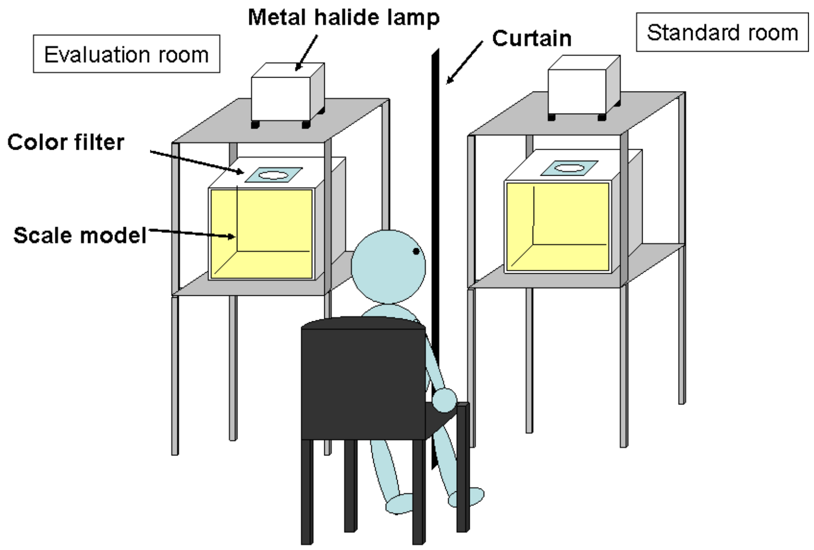

Figure 1 – Experimental apparatus

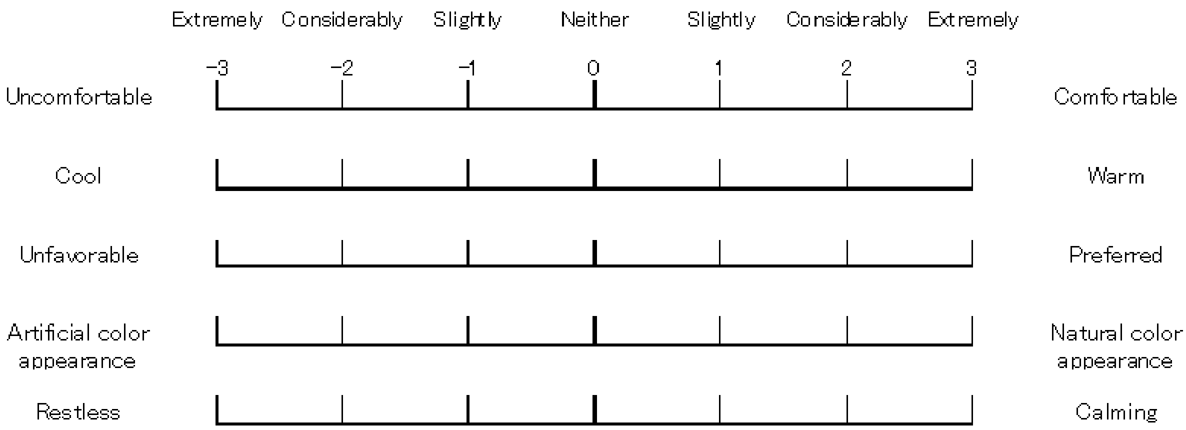

Figure 2 – Evaluation scale

Table 1 – Caption of Table 1

Standard room condition	200lx, 4200K
Light source	Metal halide lamp
Illuminance [lx]	200, 500
Color temperature [K]	2000, 2500, 3000, 3900, 4200, 5000, 6500

The experiment procedure was as follows:
(1) The subject was given 5 minutes to adapt to the standard room.
(2) The subject then observed the evaluation room for a specified period of time (0, 2, 4, 6, 8 and 10 minutes) and performed an evaluation.

(3) The subject was allowed to adapt to the standard room again and then observed the evaluation room of the other lighting condition.
(4) Steps (1) to (3) were repeated.

3 Results and Discussion

The results for one of the subjects included extreme values, which were considered as defective values. Therefore, the results were processed by using the average of the results for the remaining six subjects. Figure 3 and Figure 4 show the results of characteristic.

Figure 3 shows the relationship between the elapsed time and the comfort evaluation score. For an illuminance of 200 lx, the color temperature has a tendency to increase with elapsed time, and converges around the score of 1.2, which shows that "the environment is slightly comfortable" after 10 minutes; however, there are significant differences in the comfort evaluation score at 0 minutes. It is thought that the effect of the difference in color temperature on comfort is smaller because the color adaptation level is high as the elapsed time increases.
For 500 lx, a similar convergence tendency is not observed, but the color temperature does maintain a constant value after a few minutes. Although the evaluation score shows a tendency to increase with elapsed time, it is suggested that the influence of the difference in color temperature on comfort is larger than compared with that of the 200 lx case.
The influence of color temperature on comfort is considered to be large for high values of illuminance, since the difference in the comfort evaluation score at 500 lx is larger than that at 200 lx after 0 minutes. Moreover, a high illuminance condition is considered that chromatic adaptation is completed quickly, since the comfort evaluation score stabilize after several minutes.

Figure 4 shows the relationship between the elapsed time and warmth evaluation score. For 200 lx, the impression of warmth (color temperature: 2000 K and 2500 K) is almost constant with elapsed time. Although there is a tendency to gradually feel the warmth with elapsed time for a color temperature of 3000 K or more, the warmth evaluation score remains almost constant after 10 minutes. Moreover, the difference in the warmth evaluation score of each color temperature decreases with elapsed time.
For 500 lx, the change in the impression of the warmth with elapsed time for all of the color temperature conditions is small.
The impression of warmth is considered to have a great influence on the impression formed by the subject after entering the room, and therefore, the impression of the warmth of the interior space is considered to have a tendency as large as that for high illuminances and low color temperatures.

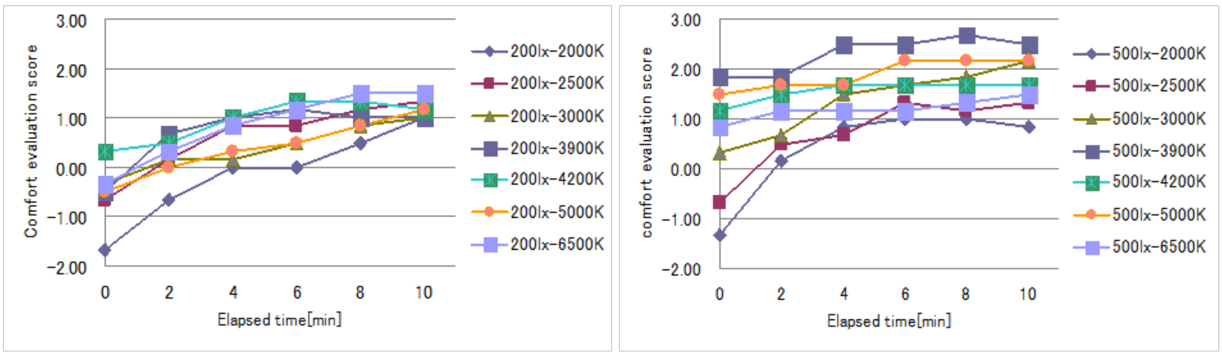

Figure 3 – Relationship between the elapsed time and the comfort evaluation score

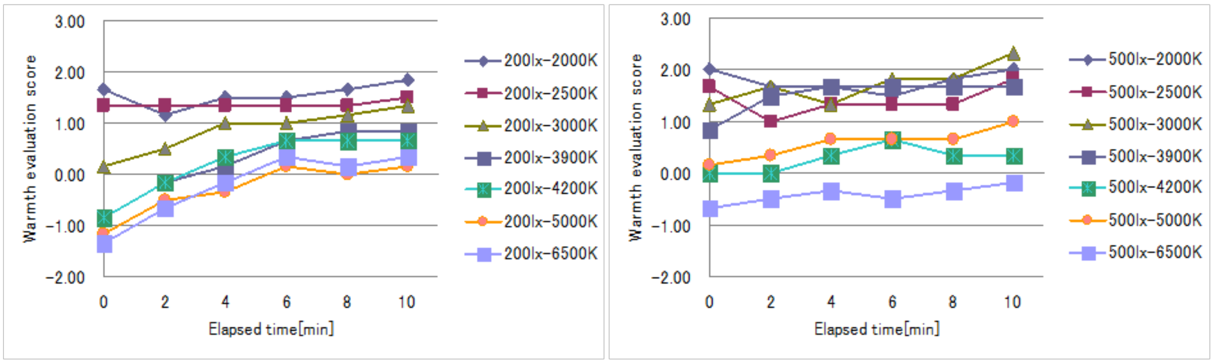

Figure 4 – Relationship between the elapsed time and warmth evaluation score

Here we compare the experimental results with the Kruithof curve referring to the method of Nakamura et al[(2)]. Figure 5 shows a comparison for 0 minutes. The white and gray areas of the Kruithof curve represent the comfortable and uncomfortable areas, respectively. The size of each circle represents the magnitude of the comfort. For 500 lx, the size of the circles in the comfortable area is relatively larger than those in the uncomfortable area. This shows that the results are in fair agreement with the Kruithof curve. For 200 lx, there are only slight differences in the sizes of the circles between the comfortable area and uncomfortable area. This shows that the results differ from the Kruithof curve.

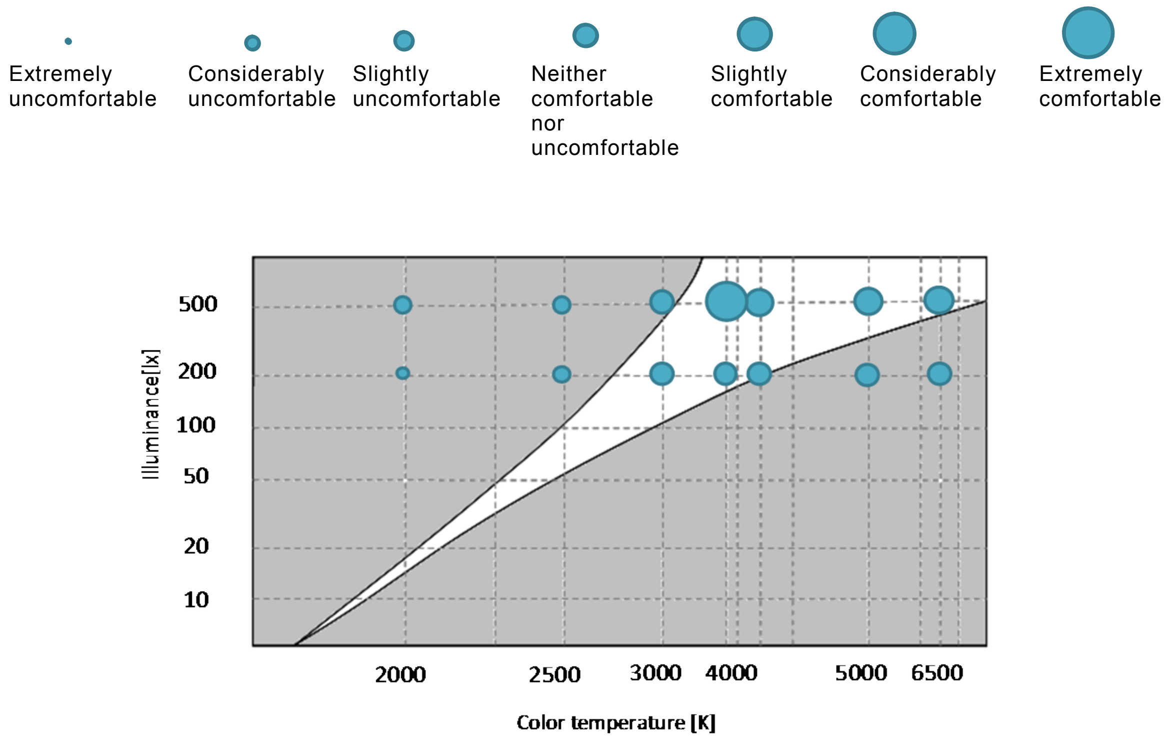

0 minute

Figure 5 – Comparison with Kruithof curve

4 Conclusion

The influence of the elapsed time on the subjective evaluation of interior lighting was investigated by conducting subjective evaluation tests with small-scale models.

The results are summarized as follows:

(1) The perception of comfort with regard to the interior space tended to increase with elapsed time.
(2) The high illuminance condition indicates to be completed more quickly chromatic adaptation.
(3) The perception of warmth is strongly influenced by the initial impression, and this tendency is as large as high illuminance and low color temperature.

References

(1) A.A.KRUITHOF. 1941, Tubular Luminescence Lamps for General Illumination, *Philips Technical Review* 6, pp.65-96

(2) NAKAMURA, H. and KARASAWA, Y. 1997, Relationship between Illuminance/Color Temperature and Preference of Atmosphere, *Journal of the Illuminating Engineering Institute of Japan*, Vol.81, No.8A, pp. 687-694

(3) OI, N., KASAO, M. and TAKAHASHI, H. 2007, The preference of the indoor illuminance and color temperature : Scale model experiment assuming daily activity, *Journal of Environmental Engineering, AIJ*, No.614, pp.87-92

PP54

ENERGY EFFICIENT AND STUDY PROMOTING LIGHTING AT HIGH SCHOOL: PRELIMINARY RESULTS.

Govén T.[1], **Gentile N.**[2], Laike T.[2], Sjöberg K.[2]
[1] Fagerhult AB, Stockholm, SWEDEN, [2] Lund University, Lund, SWEDEN
Contact: niko.gentile@ebd.lth.se

Abstract

A correct lighting solution guarantees appropriate working conditions, while saving energy. Today it is well-known that the light influences our visual perception, our emotions and our biological system, thus our health and productivity. Four identical classrooms of a high school in Helsingborg, Sweden, were equipped with two different lighting concepts: classic pendants with T5 fluorescent tubes and a new diffuse light LED system. A grand total of 72 students aged between 17 and 18 years, were occupying the rooms over the academic year. The light environment, the electricity consumption, the students' feelings and their circadian rhythm were monitored. Compared with the fluorescent installation, the LED system appears to do not have negative effects on the students, all the while saving energy.

Keywords: LED, circadian rhythm, school students, photobiological effects of light.

1 Introduction

A very recent resolution from the European Parliament set a binding EU 2030 energy efficiency target of 40%, where the cost-effectiveness of the undertaken actions has a key role (European Parliament, 2014). The efficiency improvement in lighting appears to be among those measures, as sustained by (Enkvist et al., 2007) . Focusing on Sweden, about 14 TWh/year are consumed for electric lighting, mostly in the commercial and public sector (Belysningsbranschen, 2012). For school buildings in particular, in 2007, the Swedish Energy Agency published an important report concluding that the average electricity consumption for lighting in educative facilities was 21,4 kWh/m2y (Energimyndigheten, 2007). At the time of the study, most of the installations used fluorescent lamps with conventional ballast. Although in the recent years an improvement of electric lighting installation in schools has been observed, the saving margins are still promising. Most of the saving potential is offered by the implementation of robust lighting control systems and by the use of new efficient light sources (Dubois and Blomsterberg, 2011), such as, for example, solid state lighting. Nonetheless, together with technical improvements and energy savings, lighting design should be driven by human psychological and biological factors, which nowadays are widely recognised as relevant (Boyce, 2003). Reasonably, those factors become of utmost importance for a sensitive category such as school pupils.

In the near future, a massive lighting retrofit towards the use of lighting emitting diodes (LED) technology will likely take place. Therefore, investigating the effects of this new technology on students' biology and emotions becomes more and more interesting. In this perspective, a field study which aimed to compare a fluorescent with a LED lighting installations was set-up. During a full academic year, a number of high school Swedish students used the two proposed lighting solutions. Through questionnaires (emotions and light experience), saliva analysis for cortisol concentration (circadian rhythm) and the logging of electricity use (energy), the subjective and objective lighting environments were evaluated.

This work presents the preliminary results of the above mentioned field study. The first part of the paper describes in details the experimental set-up, while the second part is dedicated to the main results obtained so far. The third and final section gives space to discussion about the findings and it addresses some major conclusions.

2 Methods

During the academic year 2012/2013, 116 students from four classes of a technical high school situated in Helsingborg, Sweden, were involved in this study. Among those, 72 (age 17-18 years, male =54, female = 18), actually took part to the measurements. Although minor daily moving in different rooms in occasion of some courses, each class mainly used a specific classroom, which was subject of the investigation. For one year a logging system recorded the presence of people and the electricity use for lighting in the four investigated classroom, with a pace of a record every 2 minutes. The individuals were called for three psychological and biological assessments (morning, noon and afternoon), occurred in five occasions (November, January, February, March and April).

2.1 Geometry and light environment

Four identical classrooms with sidelight windows facing south-west were investigated (Figure 1). The rooms are located at the second floor of the school building and they present a GWR (Glazing-to-Wall Ratio) of about 70%. They all present the same white painted walls and the furnishings are identical, included the heavy dark red canvas for solar protection. The floor is covered by a smooth dark grey rubber mat, while the visible ceiling is realized in white plasterboard. The educators teach from a platform slightly higher than the floor level. A desk, a pulpit and a big whiteboard are positioned on the platform. The classes have about 25 desks available for the pupils. The daylight factor is very similar among the rooms and it is higher than 2 for about 80% of the room deepness.

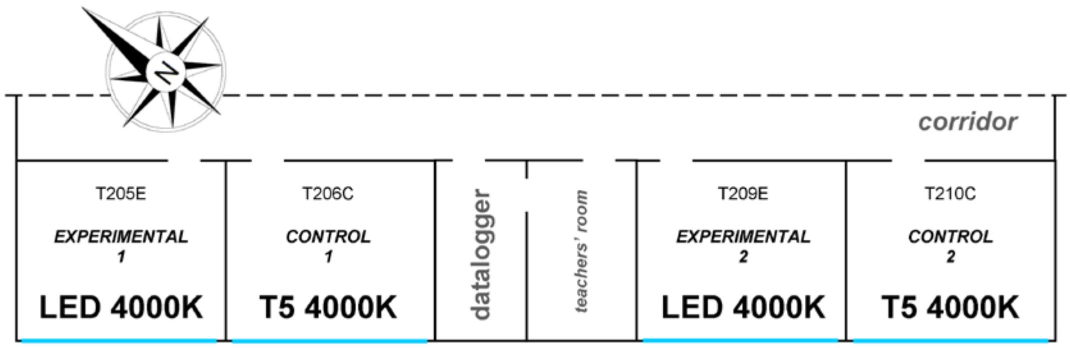

Figure 1 – Plan of the investigated classrooms

Two of the classrooms were refurbished with fluorescent T5 pendants, while the other two were retrofitted with a diffuse LED system prototype. The T5 rooms acted as control rooms and are hereinafter indicated as T206C and T210C, while the LED are considered experimental rooms and are hereinafter named T205E and T209E. Both the lighting solutions provided an average illuminance of 500 lux on the working space and they have a correlated colour temperature of 4000K.

Figure 2 – Two of the LED (left) and T5 (right) investigated classrooms

Nevertheless, because of the different design concept, the ambient lighting differs in the control and experimental case. The cylindrical illuminance as well as the ceiling and wall luminance are reported in Table 1.

Table 1 – Main characteristics of the two studied electric light environments

	Averaged horizontal illuminance	Cylindrical illuminance[a]		Ceiling luminance	Wall luminance	Ambient illuminance in the field of view[b]
		Room centre 1,2m height	Teacher position 1,5m height			
Control T5	500 lx	225 lx	350 lx	115 cd/m^2	75 cd/m^2	310 lx
Experimental LED	500 lx	315 lx	510 lx	210 cd/m^2	100 cd/m^2	420 lx

Through a wall switch next to the entrance door, the occupants can turn on the light and choose their preferred lighting scene setting. The available options for the LED experimental classrooms are: “normal” with an average of 500 lux horizontal illuminance at the work plane, “computer-based task” with 300 lux and “AV/projector”. The ambient light design is supposed to guarantee an appropriate luminance on the whiteboard. For the control T5 rooms, which have a down-light design, the options are: “normal + WB” mode, with 500 lux horizontal illuminance at the work plane plus an additional fluorescent tube over the whiteboard, “normal” where the whiteboard light is excluded and “AV/projector”.

For completeness, also the other school classrooms, not object of the study, were briefly analyzed by annotation of the illuminance at a reference point. It is interesting to see that the illuminance varied between 530 and 1200 lux in the other rooms, which used a series of different light sources, with a preponderance of T12 fluorescent tubes, often partially worn. This indicates that even the control room used in this field study represents a well-improved refurbishment compared with the existing situation.

NOTE [a] in Table 1 the cylindrical illuminance refers to the students and teacher in sitting position. Since the teacher’s desk is located on a lifted platform, the teacher face is higher (about 1,5 m from the floor) than the students’ faces (about 1,2 m from the floor)

NOTE [b] in Table 1, the ambient illuminance in the field of view is defined for this study as the averaged sum of the averaged maintained illuminance reaching the following six surfaces/planes in the classroom: working plan, ceiling, front and back walls, left and right walls.

2.2 Emotional and biological assessment

Whilst the investigation of energy use in the four classrooms was conducted for over one solar year, the subjective assessment of psychological and biological factors was limited to 6 consecutive months, during which the daylight availability was significantly changing (Table 2). The measuring days were scheduled by prioritising the daylight conditions, a mid-week day, time-space from holidays and the students’ availability. As in field studies several unforeseen occurrences may happen, some days saw a lower participation, typically due to recurring seasonal ailments. Furthermore, during the first day of examination, a constant decreasing number of participants was observed from the morning till the afternoon. Thus, in the following occasions it was decided to offer refreshments after the last afternoon samples to encourage the attendance.

Table 2 – Number of participants in each phycho-biological sampling

	9.00		12.00		15.00	
	LED	T5	LED	T5	LED	T5
2012-11-21	27	34	25	30	22	23
2013-01-23	16	32	16	29	19	27
2013-02-14	23	32	23	33	13	24
2013-03-21	19	31	19	27	17	26
2013-04-09	22	28	21	30	14	33

During each sampling, the students were hosted in groups of 12 in a specifically set up room where they were received by the school nurse and one of the author of this work (Figure 3). The subjects were requested to fill in a survey. The survey consisted in two main parts. The first part consisted on a validated questionnaire for assessing the emotions (Küller, 1991). In the second part, the light experience was evaluated through a series of items in a 7-points scale (Küller and Wetterberg, 1993). In addition, during the afternoon occasion, the survey was enlarged with a further survey which aimed to highlight specific harassments, such as glare, visible flickering from the light or even sleeping annoyances.

Figure 3 – Students during one of the sampling

Simultaneously to the questionnaire filling, the students chewed a Sarstedt Salivette cotton swab for cortisol measurement. The cotton swab were preserved in a freezer and later sent to a qualified laboratory for the analysis. Because of the dependency of cortisol concentration from several variables different from lighting, the students were continuously recommended to do not eat or drink any sour food or beverage during the sampling day. Also, the daily schedule of the school activities was carefully annotated. The outdoor sky conditions completed the set of additional information for the measurement.

3 Results

3.1 Energy use

At the present time, only the autumn-winter logged data have been treated (from 2012-08-20 to 2013-03-12). Hence, the results refers to the saving potential only, since the energy use would be overestimated because of the typical higher use of electric lighting during the dark months. The logged data of electricity consumption for lighting were clustered in different categories, corresponding to the designed scene settings. For each setting, the power absorption was measured (Table 3).

Table 3 – Number of participants in each phycho-biological sampling

	Measured absorbed power [W]			
	T205E	T206C	T209E	T210C
Normal	477	539	454	542
Bild	322	477	311	479
AV/projector	178	304	167	393
Standby	11	7	11	7

The frequency of occurrence of each scene setting delineated the typical pattern of use for the specific classroom (Table 4). The patterns include nights, weekends and holidays.

Table 4 – Number of participants in each phycho-biological sampling

	Pattern during the logged period				Pattern with the electric light on				
	T205E	T206C	T209E	T210C	T205E	T206C	T209E	T210C	Average
Normal	5,90%	3,00%	6,30%	1,40%	76,50%	31,20%	76,90%	24,90%	52,38%
Bild	1,10%	5,70%	0,60%	4,00%	13,90%	60,00%	7,20%	69,40%	37,63%
AV/projector	0,70%	0,80%	1,30%	0,30%	9,60%	8,80%	15,80%	5,70%	9,98%
Standby	92,20%	90,40%	91,80%	94,10%					

Despite the considerable lower power use of the LED system with lights on, a higher absorption in standby mode was observed. This, along to a very low occupancy rate (all the classrooms are empty over 90% of the time), led to just 0,78% of energy savings. When investigating the reasons, it was found that at the installation time (summer 2012) some delays in the prototype development forced the light installers to use four provisional drivers/luminaire for the LED classrooms, which had sizeable parasitic losses (0,09 A/luminaire). According with the manufacturer, today LED system for the same type of luminaire only uses two drivers with a total parasitic current of 0,04 A/luminaire. Future systems are expected to suppress close to 0 the standby losses by cutting the current to the light fixtures when the switch is operated. Thus, a projection of the savings without standby was done. With reference to the pattern in Table B, the potential saving of the two LED classrooms raises to 15,06%. Finally, since the differences in the scene setting patterns play an important role in the final electricity use, the savings could be calculated also in relation to an average observed pattern, obtained as arithmetic average of the four classrooms' patterns (Table 4). In the hypothesis of null standby power, the potential saving results to be 23,63%.

3.2 Psychological assessments

The students from the four classrooms were clustered in two groups representing the T5 and LED users. As first assessment, both the grades in the national tests and the absenteeism rate of the students were checked, resulting in no significant differences among the two groups. So far, no major time and season depended trends in the questions answers were found. On the other hand, some differences were individuated in the general lighting experience. Since the tendency was irrespective of time and day, the set of answers were combined in a single elaboration. The perceived quantity of light showed a significant difference in the two systems (N = 735, p=0,000), with a higher evaluation of the LED (mean = 4,97, σ = 0,98) in respect to the T5 (mean = 4,85, σ = 1,04) (Figure 4). The results suggest that the ambient lighting solution proposed in the experimental classrooms helps to perceive as more illuminated the space.

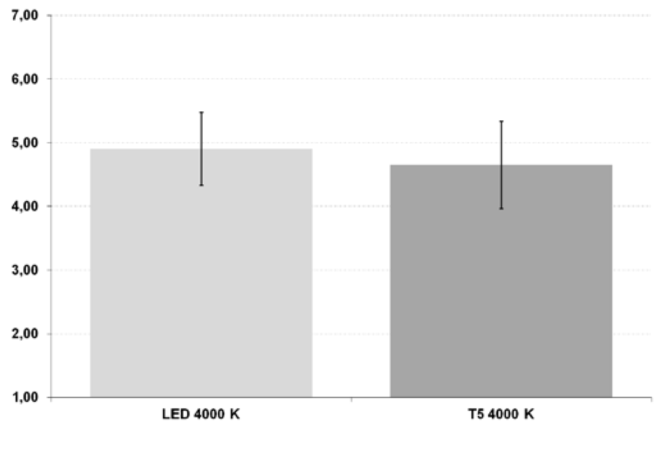

Figure 4 – Perceived quantity of light

When asked to answer to the direct question "how good can you see with this light?", the students appeared to be pretty satisfied with both the lighting solutions (Figure 5). Nevertheless, a significant higher appreciation of the LED system was found (N = 735, p =

0,000). In addition, the pupils seem to be more unanimous when judging the experimental classrooms (mean = 6,07, σ = 0,87) instead of the T5 (mean = 5,65, σ = 1,35). The lack of time and season dependency of the answers suggests that the score should not be related to enthusiasm for the innovative lighting system or other transient circumstances.

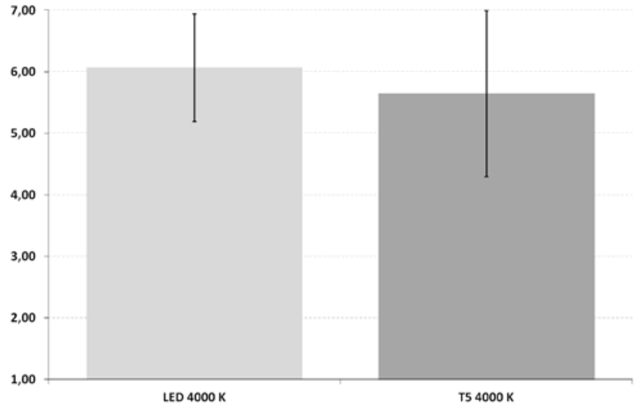

Figure 5 – How good can you see in this light?

3.3 Biological aspects

The analysis of the cortisol concentration during the day and seasons drew attention to a relatively strong linkage between the darker (typically October-January) and the lighter season. A significant effect of the different electric lighting solution during the day was observed in November (N = 44, p = 0,046) and January (N = 39, p = 0,028), while no correlations were found during the later samples, when the daylight availability was higher. It is interesting to see that e.g. in March (N = 40, p = 0,845) the cortisol concentration among the two groups of students are pretty much identical, which suggests a highly predominant effect of the natural light on the pupils' circadian rhythm (Figure 6).

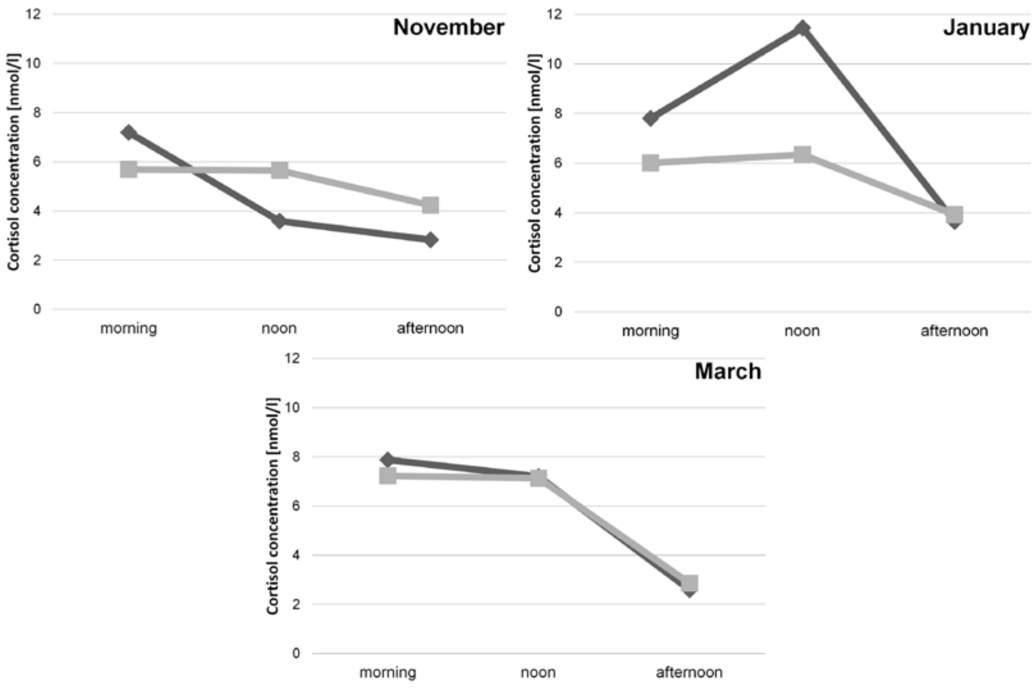

Figure 6 – Cortisol concentration during the sampling day in November, January and March

The higher cortisol concentration for the LED group during the morning sample suggests a greater boost for the experimental room. In January, an unexpected peak in cortisol during the noon measurement was justified by mean of one of the LED classes going out of the building for reaching the school gym. Even though the day was characterized by a very low global illuminance (overcast sky), the daylight should have raised the cortisol concentration of the children. Apart for this specific point, the experimental group appears to suppress the cortisol regularly while approaching the night. In the control group the trend is less marked. Finally, during the spring the suppression is more regular and it follow the normal daily variation.

4 Discussion and conclusions

At the present time, the solid state lighting appears to represent an important share of the next future lighting market. The energy saving potential is promising and the efforts in reducing energy consumption for the human activities persuades to a massive switch to this new technology. However, it should be always take in mind that light, among other factors, plays an essential role in our health and well-being. Consequently, the blind pursuing of higher savings could be just as bad as their missed achievement. In this work, the preliminary results of the outcomes of a new LED lighting solution on the emotions and the biology of school pupils was investigated.

On the energy side, it appears fundamental to design systems with reduced or even null standby energy consumption in rarely or irregularly occupied spaces. The preliminary results of this study showed that the higher luminous efficacy of the LED system could be neutralized by unexpectedly high parasitic losses due, in the specific case, to an out-of-date driver. Even a small discrepancy between the design and implementation stages could led to unforeseen results. On the other hand, the LED system could achieve substantial savings, as high as 23,63% when compared to the fluorescent T5 installation, which is already a relatively energy efficient solution. The T5 lighting tube with direct/indirect light distribution is today commonly used in Nordic countries and it is considered as one of the best performing. The same T5 system was also evaluated has very efficient in a previous similar study performed in London (Sansal, 2012, Govén et al., 2011). Not to be forgotten that the psychological assessment have highlighted a greater light quantity perception in the experimental classrooms, most probably due to the different lighting design. As consequences, the energy use may be further reduced by decreasing the light levels, though the option needs to be tested against the variation of users’ response. The general appreciation of the LED installation was also higher in the proposed experiment, whilst both the proposed systems scored pretty high results. In matter of biological effects, the assay of the electric light influence on the circadian rhythm represents a particularly hard task in field studies, because of the greater contribution of natural light, even during the winter. Nevertheless, some differences were noted during the dark season, when the experimental classrooms appeared to be more accommodating in helping the students to follow their daily natural hormonal cycle.

Overall, these preliminary findings suggested that the introduction of a solid state lighting in school classrooms would not be harmful for the pupils well-being, while could led to considerable energy savings, when the installation is properly done. In comparison to the more widespread fluorescent installation, whether the new LED systems could actually produce benefits on the students’ well-being and performance has to be still determined. Although the tendency was towards a better appreciation of the latter, it is hasty to reach conclusion at this step of the study.

This work will continue to develop with the addition of the missing energy data, as well as with a deeper analysis of the psychological items and of the cortisol concentration results.

Acknowledgment

The authors wish to express their gratitude to the students, the headmasters, the teachers, the nurse of Tycho Brahe School of Helsingborg for their enthusiastic participation in the project and their tolerance during the measurements. This project is supported by The Swedish Energy Agency.

References

BELYSNINGSBRANSCHEN 2012. En ljusare framtid. *Att spara energi och miljö med smart belysning.* Stockholm: Belysningsbranschen.

BOYCE, P. R. 2003. *Human factors in lighting*, 2nd ed. New York: Taylor and Francis.

DUBOIS, M. C. & BLOMSTERBERG, A. 2011. Energy saving potential and strategies for electric lighting in future North European, low energy office buildings: A literature review. *Energy and Buildings,* 43**,** 2572-2582.

ENERGIMYNDIGHETEN AND BOVERKET 2007. *Energianvändning & innemiljö i skolor och förskolor - Förbättrad statistik i lokaler, STIL2*. Eskilstuna: Statens energimyndighet.

ENKVIST, P., NAUCLÉR, T. & ROSANDER, J. 2007. A cost curve for greenhouse gas reduction. *McKinsey Quarterly,* 1**,** 34.

EUROPEAN PARLIAMENT 2014. *Resolution of 5 February 2014 on a 2030 framework for climate and energy policies (2013/2135(INI).* Strasbourg: European Parliament.

GOVÉN, T., LAIKE, T., RAYNHAM, P. & SANSAL, E. 2011. Influence of ambient light on the performance, mood, endocrine systems and other factors of school children. *CIE 27th session, Sun City, South Africa,* 112.

KÜLLER, R. 1991. Environmental assessment from a neuropsychological perspective. *Environment, cognition and action: An integrated approach***,** 111-147.

KÜLLER, R. & WETTERBERG, L. 1993. Melatonin, cortisol, EEG, ECG and subjective comfort in healthy humans: impact of two fluorescent lamp types at two light intensities. *Lighting Research and Technology,* 25**,** 71-80.

SANSAL, K. 2012. *Time-dependent effects of indoor lighting on well-being and academic performance.* UCL (University College London).

PP55

A STUDY OF THE SWITCHING FREQUENCY FOR VARIOUS PHOTOELECTRIC ON-OFF APPROACHES BASED ON MEASURED DAYLIGHT DATA

Danny H. W. Li[*1]
[1] Building Energy Research Group, Department of Civil and Architectural Engineering, City University of Hong Kong, Tat Chee Avenue, Kowloon, Hong Kong SAR, CHINA
bcdanny@cityu.edu.hk

Abstract

In a well day-lit space when the daylight intensity is far more than the required value, photoelectric switching can result an excellent energy saving. However, a problem with the switching control type is the frequent and rapid switching of lights on and off, particularly during the unstable sky conditions when daylight levels are fluctuating around the switching lighting level. This can annoy occupants and lessen lamp life. The paper studies three variants of photoelectric switching control, namely differential, switching time delay and daylight time delay controls. The results show that they can reduce the number of switching operations. The annual average number of switch offs per day using differential, switching time delay and daylight time delay can be dropped to 2.5, 4 and 1.2, respectively. The findings support that an appropriate photoelectric switching control should be adopted for lamp fittings installed in well day-lit spaces.

Keywords: Photoelectric, Switching frequency, On-off controls, Daylight, Atrium

1 Introduction

Daylighting is an essential sustainable development in modern architecture in creating a pleasant visual environment and alleviating the problems of energy issues. Daylight is the best source of light for good color rendering and its quality is the most closely matches human visual responses. The amount of daylight penetrating a building is mainly through window openings which provide the dual function not only of admitting light for indoor environments with a more attractive and pleasing atmosphere, but also allowing people to maintain visual contact with the outdoor spaces. From the energy- and cost-saving viewpoint, the arguments for daylight are strong. The energy savings derived through the use of day-lighting not only facilitate the sparing use of electric lighting and reduced peak electrical demand, but also reduce cooling loads and offer the potential for smaller air-conditioning plants to be built (Li et al., 2002; Li et al., 2005). In circulation spaces such as corridors, people expect the way ahead to be lit adequately. Many studies have been reported that in day-lit corridors, photoelectric lighting controls can result excellent energy savings (Li and Lam, 2003; Slater et al., 1996). It is argued that photoelectric controls should be installed for electric lightings installed in day-lit areas. Energy saving can be attained when the illuminance levels from lamp fittings are larger than the design values. It can be achieved using appropriate daylight-linked switching or dimming lighting controls. In a well day-lit room when daylight intensities are far more than the required levels, the energy reductions from photoelectric switching controls can be more than those from the photoelectric dimming controls (Li et al., 2006). However, a problem with the switching control type is the frequent and rapid switching of lights on and off, especially during unstable sky conditions when daylight levels are fluctuating around the switching illuminance. This annoys occupants and reduces the lamp life. There are a few variants including differential switching or dead-band, switching-linked time delay and daylight-linked time delay to limit the number of switching on and off (Littlefair 2001). Core daylighting, that is daylight provision in areas situated at considerable distances from facades

- Corresponding author: Tel: +852-34427063; fax: +852-34420427. E-mail:bcdanny@cityu.edu.hk

and windows, is currently one of the main challenges in sustainable building design (Linhara, 2010). An atrium allows daylight to penetrate into the core of a building, contributing not only cultural and architectural content, but also the potential to resolve many environmental issues (Hung and Chow). Daylighting is one of the basic components of passive solar building design and its estimation is essential (Chel et al., 2010). Studies have been conducted on the effect of atrium characteristics on daylight levels on the atrium floor and along working planes in adjoining spaces (Wright and Letherman, 1998). Daylight may vary substantially with every floor. With shallow atria or the spaces on the top few floors, more incident light is received from the sky while the daylight levels in deep atria of the lower atria spaces are chiefly influenced by reflected light (Aizlewood, 1995). This paper studies the switching frequency for different daylight-linked lighting switching controls. Measured daylight illuminance data of an atrium building were used for the analysis. The performance in terms of lighting energy reduction and the number of switching were simulated and evaluated. The findings are reported and design implications discussed.

2 Photoelectric switching controls

A photoelectric switching control is designed to switch electric lighting on and off automatically as the daylight level falls and rises through a predetermined level. There are a few variants to lower the number of switching (Littlefair, 1998). The basic variant of the on-off control is the ‘differential switching or dead-band’ photoelectric control that has two switching illuminance levels: one at which the lights are switch on (E_{on}), and another, higher illuminance, at which the lights are switched off (E_{off}). The main advantage is that it can reduce rapid switching on and off when the illuminance swings around the desired level. Also, it makes switching off less obtrusive, as it is performed when daylight represents a higher proportion of the illuminance to which the eye is accommodated. It is very important to set appropriately the two switching illuminance values which affect both the number of switching and the electric lighting energy consumption. There is no simple analytical expression for lighting use under a differential switching control. To a good approximation, the fraction of the working year that electric lighting would be off under an on-off control is simply given by the fraction of the working year that the daylight threshold illuminance level (E_{mean}) which is the average of the two switching illuminances E_{on} and E_{off}. Another technique to decrease the number of switching is to introduce a time delay into the process. Two different types of time delay namely switching-linked and daylight-linked time delays are categorized. The switching-linked time delay only allows switching off until the pre-set delay had to elapse after the last switch on. For daylight-linked time delay, the lighting could only be switched off when the daylight illuminance had exceeded the target value for the pre-set time period. Delay in switching on is not considered as it could lead to illuminances falling well below desired levels.

3 Background information

The study was based on the daylight illuminance data recorded in an institutional building between January 2012 and June 2013. The institutional building is a purpose-built, 13-storey block located on the periphery of a Hong Kong industrial zone situated along the southern coast of China within the subtropical region at latitude of 22.3N° and longitude of 114.2E°. The institution is surrounded by buildings in three cardinal orientations (i.e. north, south and west), with a highway to the east. The building was designed with a skylight and an enclosed stepped atrium to harvest daylight. The stepped atrium increases daylight and improves sky views by splaying the well walls away from the vertical, but the sky component and hence the daylight factor of the lower floors are significantly reduced (Samant 2010). Figure 1 presents the vertical section of the building. The atrium dimensions are 11.5m x 9.5m x 40.7m (height). The lower floors of the atrium between 2/F and 9/F are typical classrooms, with the four open corridors surrounding the atrium. The upper part, from 10/F and 13/F, is a cubic atrium (i.e. 15m x 15m x 15m) and consists of mainly mechanical and office rooms. There is a glazed skylight with a building integrated photovoltaic (BIPV) system installed on the atrium roof aperture. The skylight constitutes around 40% of the plan area obstruction (PAO), which is defined as the percentage of roof blockage when viewed from a plan perspective with the focal point at infinity. Totally, 67 numbers of ceiling-mounted energy-efficient T5 fluorescent tubes, with rated power ranging from 14W to 35 W were installed for the corridors at every floor. Daylight-linked dimming controls were used in the corridors at 9^{th} floor. The system detected both the reflected electric light and the daylight values to give a ‘closed loop’ control. The recorded lighting levels were sent to the dimmable electronic ballasts which adjust the light outputs of the lamp fittings accordingly. Four photoelectric sensors were mounted on the ceiling of the four corridors to record the light intensity. The daylight performance and energy use due to the daylight-linked dimming controls in the 9/F corridors were examined and reported (Chow et al., 2013; Li et al., 2014). There are three additional ceiling mounted photoelectric light level sensors installed respectively along the same plummet line from 6/F to 8/F to record the daylight illuminance. The data were transmitted to a logging system for storage. The recorded illuminance readings only provided the daylight availability for the corridors and the sensor itself did not form any part of the lighting controls. The present study analyzed the three types of control algorithm, namely differential switching, switching linked time delay and daylight linked time delay photoelectric controls based on the daylight illuminance data measured in the 7^{th} Floor.

4 Analysis and simulation

The daylight illuminance was recorded at 2.5 min intervals from 9:00 am to 6:00 pm each day between February 2012 and July 2013. It is inevitable that there would be some short periods of missing data due to different reasons including instrumentation malfunction and power failure. Totally, there are 216 daylight illuminance readings recorded in each day. The analysis was on daily basis. The daylight illuminance data for the whole day would not be used for the study if there were some missing data. Considerable efforts were made to obtain a continuous record of data and in all about 85536 readings (i.e. 396 days) were collected for the study. In every case the illuminance levels at a particular time were assumed to have applied for the whole of the time interval (i.e. 2.5 minutes) since the previous scan. As mentioned (Littlefair, 2001) such an assumption in practice might lead to a slight underestimate of the switching numbers during periods of very substantial daylight illuminance variation (on a less than 2.5 minutes timescale). For every photocell the daylight illuminance at each time was checked and if this was less than the target illuminance E_t, the control was assumed to have kept the lights on since the last scan. If it was larger than the E_t the lights were assumed to have been off. At the end of the working day, the percentage of time the lights off was computed. The number of switch off was counted by keeping a record of when the control changed state. The switch off at the end of the day was not included in these totals. If at 09:00 the daylight illuminance was above the switching on illuminance then the lighting was assumed to be switched off at first. It should be pointed out that no electric lighting was actually used under the switching controls. The analysis and results were carried out by calculation according to the measured daylight illuminances. It is assumed that ‘perfect’ control, switching exactly when daylight reached the target E_t.

Table 1 - Energy saving and number of switch offs per day under simple switching controls

	Percentage of Lighting energy use		Number of switch offs per day	
	105 lux	150 lux	105 lux	150 lux
Jan	67.3	53.4	6.9	7.8
Feb	84.6	68.6	6	5.2
Mar	82.6	72.3	6.1	5.6
April	86.6	76.6	5.9	6.4
May	88.1	80.1	5.8	6.7
Jun	89.3	80.9	5.3	6.8
Jul	80.3	68.5	8.3	10.2
Aug	81.4	70.4	4.8	7.4
Sep	78.3	66.7	7.1	6.9
Oct	79.4	67.7	4.9	5.7
Nov	71.1	59	8.2	9.1
Dec	50.6	36.9	8.6	7.6
Annual	78.3	66.8	6.5	7.1

Table 1 presents the percentage of lighting energy saving and the average number of switch offs per day at 7th Floor for simple switching controls. Two E_t of 105 and 150 lux were set. It can be seen that the percentage of lighting energy saving with E_t of 105 lux ranges from 50.5% in December to 90% in June. The annual average number of switch offs per day is 6.5 which implies at least 13 switching operations in one day if the number of switch on is included. When E_t is 150 lux, the energy saving reduces but the switching frequency increases. The lighting energy saving for the whole year is 66.8% and the maximum average number of switch offs in a day is 10.2 occurring in July. Such a large number of switching operations could cause in considerable annoyance to occupants. To reduce the switching frequency, three variants of on-off control namely differential switching, switching linked time delay and daylight linked time delay photoelectric controls were examined. Table 2 gives the energy use and the number of switching under differential switching of 100/110 lux and 100/150 lux controls. Similar lighting energy savings were computed with the annual values of 78.1% and 67.3% for 100/110 lux and 100/150 lux controls, respectively. Less switching frequency is observed. An increase of illuminance differential reduces the frequency of switching. The annual average number of switch offs per day for 100/150 lux was 2.5 which is two thirds lower in number than for the standard on-off 150 lux controls. It should be pointed out that standard on-off switching is not used in practical situation. For a closed-loop control, the interior photocell receives direct and indirect light from the lamps and natural light. The photocell would switch the lights off immediately after they were switched on as the photocell responded to the extra illuminance provided by the lamp fittings.

Table 2 - Energy use and number of switch offs per day under differential switching controls

	Percentage of Lighting energy use		Number of switch offs per day	
	100/110 lux	100/150 lux	100/110 lux	100/150 lux
Jan	66.9	53.7	6.7	2
Feb	84.5	73.8	5.9	2
Mar	82.8	71	5.4	1.7
April	86.4	76.9	5.7	2.1
May	88	81.6	5.8	2.9
Jun	89.3	82.9	5.2	2.8
Jul	79.9	70.8	8.2	4.1
Aug	81.2	70.6	4.6	2.6
Sep	78.1	64.7	7.1	2.5
Oct	79.4	65.4	4.9	1.3
Nov	70.9	59.3	8.1	3.6
Dec	50.2	36.6	8.3	2.1
Annual	78.1	67.3	6.3	2.5

Another way to reduce the frequency of switching operations is to introduce a time delay into the process. Table 3 shows the energy saving and switching performances for switching illuminance of 150 lux under two switching linked time delay where switching off cannot occur till at least 5 and 30 minutes after the last switch on. For the 5 minutes time delay, the energy saving is close to the 100/150 lux differential control but the average switch offs are more than double. The minimum average number of switch offs per day is 4.7 appearing in February. When the time delay is extended to 30 minutes, both the lighting energy saving and number of switch offs per day decrease. The annual energy saving drops to 57.8% and the number of switch offs per day in most months is not more than 4. It seems that the time delay switching control is an alternative for consideration. Likewise, the same daylight dataset was used to determine the performance under daylight linked time delay control. Table 4 summaries the lighting energy reduction and switching frequency under 5 and 30 minutes time delay. The results show that the 5 minutes daylight linked time delay control are comparable to the 30 minutes switching linked time delay control in terms of both energy and switching aspects. The percentage of lighting energy reduction and the average number of switch offs per day for the whole year are 61.2% and 4, respectively. If 30 minutes time delay is adopted, the annual lighting energy saving lowers to 41.4% but the average number of switch offs per day significantly drops to 1.2. The findings reveals that for the same time delay, the switching linked control will allow more energy reduction than the daylight linked version but the latter will give less number of switching operations. It should be pointed out that the lower number of switching operations with the daylight linked time delay means that a shorter delay time can be used. It implies that a daylight linked time delay can result less energy use for the same number of switching operation, provided an appropriate delay time is selected.

Table 3 - Energy use and number of switch offs for E_t=150 lux under switching linked time delay controls

	Percentage of Lighting energy use		Number of switch offs per day	
	5 minutes delay	30 minutes delay	5 minutes delay	30 minutes delay
Jan	52.2	45.9	6.8	3.7
Feb	68	63.1	4.7	3.1
Mar	71.5	65.4	5.1	3.3
April	75.6	68.5	5.8	3.5
May	78.8	70.7	6	3.4
Jun	79.4	70	5.9	3.4
Jul	66.7	55.4	9.1	4.9
Aug	69.1	59.8	6.5	3.9
Sep	65.4	57.3	6.2	3.7
Oct	66.9	60.6	5.3	3.1
Nov	57.6	48.3	8.3	4.7
Dec	35.8	28.7	6.9	3.9
Annual	65.6	57.8	6.4	3.7

Table 4 - Energy use and number of switch offs for E_t=150 lux under daylight linked time delay controls

	Percentage of Lighting energy use		Number of switch offs per day	
	5 mins delay	30 mins delay	5 mins delay	30 mins delay
Jan	47.5	29.6	3.7	1.1
Feb	64.6	47.2	2.8	1.1
Mar	67.9	50.1	3.3	1.1
April	71.6	54.1	3.6	1.1
May	74.8	54.7	3.8	1.2
Jun	75.6	54.2	4	1.2
Jul	60.6	36.2	5.5	1.3
Aug	64.4	40.2	4.8	1.4
Sep	61.2	39.4	4.5	1.3
Oct	63.3	46.5	3.2	1.2
Nov	51.9	29.1	4.9	1.1
Dec	31.3	15.3	3.4	1
Annual	61.2	41.4	4	1.1

5 Conclusions

Field measurements of the daylight illuminance in atrium corridors were undertaken. Based on the measured daylight availability, a number of daylight linked switching controls namely the simple, differential, switching delay and time delay on-off controls were analysed. Their performances in terms of lighting energy reduction and number of switching were simulated and evaluated. Under the simple on-off control, the energy saving could be very good but the frequent switching would be unaccepted. Based on the simulated results, the three variants of the switching control can reduce the number of switching with similar energy use. Using 100-150 lux differential switching control, the annual percentage saving and number of switch offs per day are 67.3% and 2.5, respectively. With the same time delay, the switching linked time delay control can give more lighting energy reduction and larger number of switch offs than the daylight linked time delay control. However, provided an appropriate delay time is chosen, daylight linked time delay controls can result less energy use than switching linked version with the same number of switching frequency. The annual number of switch offs per day under 30 minutes daylight linked time delay control is only 1.2. Photoelectric electric lighting controls are appropriate building energy conservation schemes and should therefore be widely applied in day-lit areas.

Acknowledgements

The work described in this paper was fully supported by a General Research Fund from the Research Grant Council of the Hong Kong Special Administrative Region, China [Project no. 9041777 (CityU 116312)].

References

AIZLEWOOD, M. 1995. The daylighting of atria: a critical review. ASHRAE Trans. review of prediction. 101, 841-857.

CHEL, A., TIWARI, G.N., SINGH, H.N. 2010. A modified model for estimation of daylight factor for skylight integrated with dome roof structure of mud-house in New Delhi (India) Applied Energy, 87(10), 3037-3050.

CHOW, S.K.H., LI, D.H.W., LEE, E.W.M., LAM, J.C. 2013. Analysis and prediction of daylighting and energy performance in atrium spaces using daylight-linked lighting controls. Applied Energy, 112:1016-1024

HUNG, W.Y., CHOW, W.K. 2001. A review on architectural aspects of atrium buildings. Architectural Science Review, 44(3), 285-296.

LI, D.H.W., LAM, J.C. 2003. An investigation of daylighting performance and energy saving in a daylit corridor. Energy and Buildings, 35(4), 365-373.

LI, D.H.W., LAM, J.C., WONG, S.L. 2002. Daylighting and its implications to Overall Thermal Transfer Value (OTTV) determinations. Energy, 27(11), 991-1008.

LI, D.H.W., LAM, J.C., WONG, S.L. 2005. Daylighting and its effects on peak load determination. Energy, 30(10),1817-1831.

LI, D.H.W., LAM, J.C. 2003. An investigation of daylighting performance and energy saving in a daylit corridor. Energy and Buildings, 35(4), 365-373.

LI, D.H.W., LAM, T.N.T., WONG, S.L. 2006 Lighting and energy performance for an office using high frequency dimming controls. Energy Conversion and Management, 47(9-10), 1133-1145.

LI, D.H.W., CHEUNG, A.C.K., CHOW, S.K.H., LEE, E.W.M. 2014. Study of daylight data and lighting energy savings for atrium corridors with lighting dimming controls. Energy and Buildings

LITTLEFAIR, P.J. 1998. Predicting lighting energy use under daylight linked lighting controls. Building Research and Information, 26(4), 208-202.

LITTLEFAIR, P.J. 2001. Photoelectric control: the effectiveness of techniques to reduce switching frequency. Lighting Research and Technology,33(1), 43-58.

LINHARTA, F. 2010. Performance of anidolic daylighting systems in tropical climates – parametric studies for identification of main influencing factors. Solar Energy 84(7):1085-1094.

SAMANT, S. 2010. A critical review of article published on atrium geometry and surface reflectances on daylighting in an atrium and its adjoining spaces. Architectural Science Review, 53(2):145-156.

SLATER, A.I., BORDASS, W.T., HEASMAN, T.A. 1996. People and lighting controls. BRE information paper IP 6/96. Garston: CRC.

WRIGHT, J., LETHERMAN, K. 1998. Illuminance in atria: review of prediction methods. Lighting Research and Technology 30(1), 1-10.

PP56

USE OF A COMPACT CCD CAMERA FOR CONTINUOUS MEASUREMENT OF SKY LUMINANCE DISTRIBUTION AND THE CLASSIFICATION OF THE CIE SKY TYPE

Kobav, **M.B.**[1] Bizjak, G.[1]
[1] University of Ljubljana, Faculty of Electrical Engineering, Ljubljana, SLOVENIA
matej.kobav@fe.uni-lj.si

Abstract

Energy saving is very popular in all areas. In the field of lighting is especially important since power LEDs appeared on the market. LEDs promise almost miraculous savings. Unfortunately, it is seldom aware that you can save energy with proper building design and their good window openings design to ensure minimum dependence on artificial lighting. This means the proper layout, orientation and design of window openings. If we would like to correctly simulate daylight already in the planning stage, we also need relevant information about the sky and the spatial distribution of the luminance of the sky. For this purpose, we developed a new device that enables a stable and continuous measurement of the sky luminance distribution and the classification of the CIE sky type. The article presents the use of a compact CCD camera as a sky scanner and the conclusions

Keywords: Daylight, Sky Luminance distribution, Overcast sky, Clear sky, Intermediate sky

1 Introduction

In year 2005 an EKO sky scanner was installed at the IDMP station in Lyon (France) for a period of one year. Since the sky scanner was borrowed only for one year it was necessary to develop another way how to produce sky luminance distribution maps. First we were using compact cameras Nikon Coolpix 990 and Coolpix 5000 as a substitute for sky scanner. Main problem with compact cameras was the influence of environment. It was practically impossible to leave the camera outside since it was not protected against rain and humidity. Another problem was also direct sunlight. With compact cameras the CCD is exposed to the incoming light all the time. Also when a camera is in "stand by" mode, waiting for a picture to take. Only one day camera was used in a sunny conditions and the CCD got burned. There was a noticeable trace of the position of the sun on every picture. The CCD was permanently damaged. Soon after that we started to think about a new substitution for a sky scanner and we came to an idea to work with compact CCD cameras that can be connected directly to computer and remotely operated.

2 Selection of a CCD camera

For us it was most important to find a camera in the affordable price range and the camera should be easily connected to computer and remotely operated from LabVIEW. We decided to use camera from a company Imaging source, type DFK 51AUC03 (Figure 1) and fish eye lens from company Lensation type Lensagon BF5M11920 1/3.2" 1.19 mm IR MP (Figure 2).

Figure 1 – Compact CCD camera

Figure 2 – Fish eye lens

In this USB colour camera a Micron 1/3.2" 2 Mp CMOS digital image sensor is installed. The shutter is an electronic rolling one. Resolution of a CCD is 1600 x 1200 and with use of fish eye lens the size of used area is 1150 x 1150. Dynamic range of the A/D converter is 10 bit and dynamic range of the output image is 8 bit. Camera allows manual adjustments of exposure time in range from 1/10.000 to 4 seconds, adjustments of gain in range 0 to 18 dB and adjustments of white balance in range -6 dB to +6 dB.

Viewing angle of the fish eye lens is 185^0.

3 Images from CCD camera

Since the dynamic range of an image captured with this CCD camera is only 8 bit, the range of pixel values is only from 0 to 255. In order not to lose information about the brightest pixel the exposure must be adjusted so that the maximum pixel value is not exceeded. When taking images of sky luminance distribution under overcast skies the range from 0 to 255 could be enough, but if we are capturing the sky luminance distribution under clear skies with direct sunlight or under intermediate skies with multiple reflections of light between clouds, then the mentioned range is not enough. The only solution is to take several images with different exposure value (EV).

Figure 3 – Images of clear sky captured with CCD camera and fish eye lenses (different exposure time)

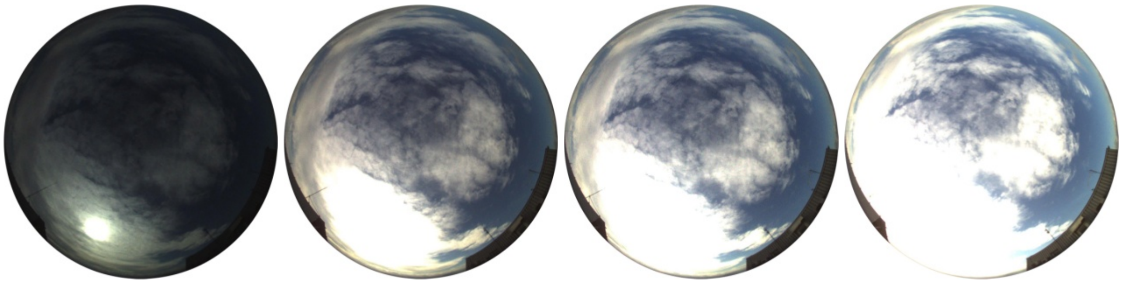

Figure 4 – Images of intermediate sky captured with CCD camera and fish eye lenses (different exposure time)

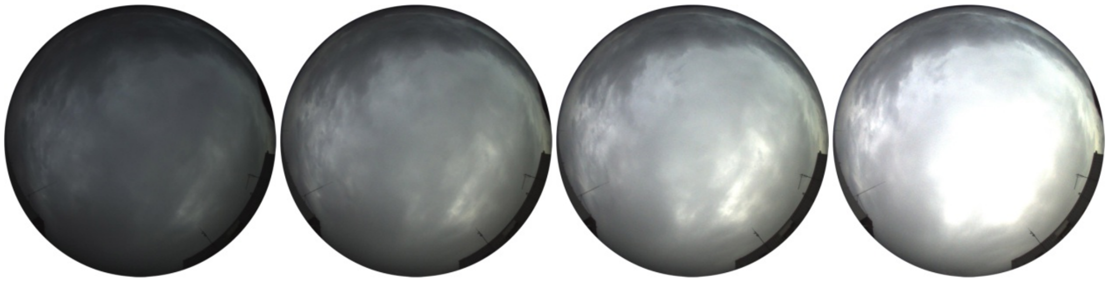

Figure 5 – Images of overcast sky captured with CCD camera and fish eye lenses (different exposure time)

4 Principle

Image captured with this camera is in color. To get the luminance of a measured point in the sky we have to convert color image from RBG color space into CIE Lab color space. Since we ignore the color information, the brightness or pixel value is proportional to the luminance [COUTELIER, B. 2003].

With normal digital cameras exposure value is defined by equation 1:

$$EV = 3.32\, log_{10}\left({}^{N^2}/_{t}\right) \tag{1}$$

where

- EV is exposure value
- N is the relative aperture (f-number)
- t is the exposure time (shutter speed)

Since this camera does not have a mechanical shutter like it is known from normal digital cameras, we are not dealing with normal exposure value. As mentioned before with this camera it's possible to adjust exposure time and gain. Gain on a CCD camera represents the conversion factor from electrons into digital counts. Gain is expressed as the number of electrons that get converted into a digital number. Gain value should be adjusted to maximize the dynamic range of the image.

Brightness of a pixel or pixel value is proportional to the number of electrons that are released when photons hit the sensor [HISCOCKS, P.D. 2011]. When we introduce all parameters of the camera we get next equation:

$$\mathrm{L}^* = \mathrm{K_C} \cdot \mathrm{t} \cdot \mathrm{G} \cdot \mathrm{L_S} \tag{2}$$

where

- L^* is brightness of a pixel or pixel value
- K_C is the calibration coefficient
- t is the exposure time (shutter speed)
- G is the gain

5 Calibration

The calibration of the camera was carried out in dark room with the reference integrating sphere (Figure 4). The luminance of the light emitting area could be adjusted in range of 10 cd/m^2 to 10.000 cd/m^2. Correlated color temperature is 2856 k (i.e. illuminant A), which is used as reference for the calibration of photometers. Homogeneity of the luminous area is sufficient for calibration purposes.

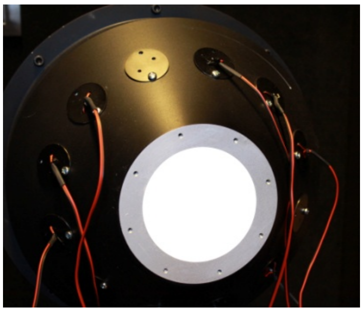

Figure 6 – Reference integrating sphere

In the first part of the calibration we set the exposure time to a constant value and altered only gain. With the constant luminance value on the sphere opening it was possible to confirm that brightness of the pixel is proportional to the gain. In the second part of the calibration we set the gain to a constant value and altered only exposure time. In this part we confirmed that brightness of the pixel is proportional to the exposure time. In the last part of calibration we set the exposure time and gain to a constant value and altered luminance of the luminous area of the integrating sphere. In all cases luminance was measured with luminance meter Jeti Specbos 1200 as a reference luminance.

In this part of the research we did not take into account problems with vignetting. Problems with vignetting will be solved in further research. In the calibration process we measured only pixels in the middle of the image.

When the calibration was finished it was possible to create absolute luminance maps for each image. For every sky scan we take 5 images with deferent settings of exposure time and gain. The first image is captured in automatic mode and than two underexposed and two overexposed images are captured. The entire process of capturing all 5 images takes about 10 seconds.

6 Luminance tables

The signal noise and thereby the quality of a CCD sensor dictated to use averaging of an array 3x3 pixels. From the original image with approximately 1 MIO useful pixels we finish with about 115.000 elements, which proved to be more than sufficient.

For each 3x3 array in a single image we calculated average pixel value (average value of all 9 pixels). Since the dynamic range of an image is 8 bit pixel values are in range from 0 to 255. Underexposed pixels have values 0 and saturated pixels have values 255. For those pixels it's impossible to calculate luminance with Equ. 2 since they are practically not defined.

For each set of 5 images luminance values are calculated as an average value of luminance values for each array of pixels. If one or more array pixel values (on the same position) from those 5 images are zero, then array from this image is not used for calculation of average. If pixel values from all 5 images are 0, than this array is marked as "underexposed".

If one or more array pixel values (on the same position) from those 5 images are 255, then this array is neglected. If all pixel values in an array from all 5 images are 255, than this array is marked as "saturated".

When all luminances are calculated a luminance map is calculated. Luminance map can be presented with false color graph or with graph in shades of gray (Figure 7).

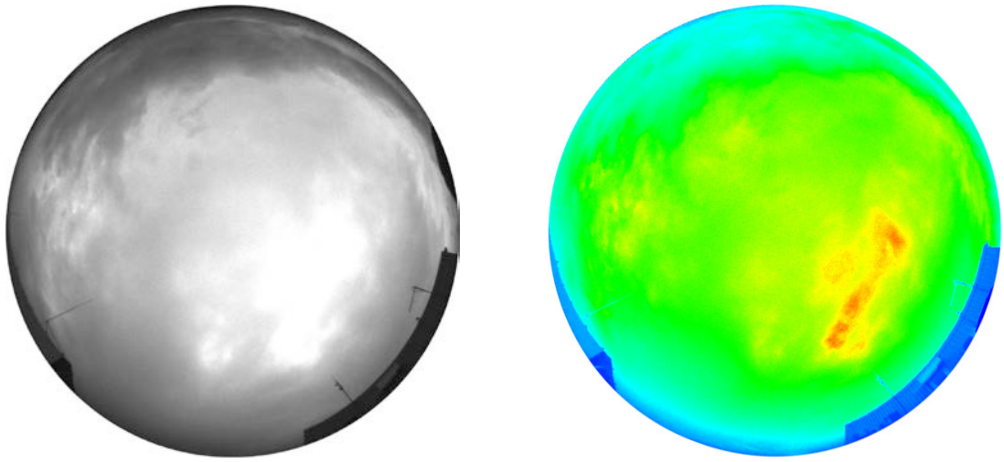

Figure 7 – Luminance map in shades of grad and in false colours

7 Defining CIE Sky type

Beside presentation of the sky luminance map we can also derive CIE sky type based on CIE S 011/2003 standard [CIE 2003]. CIE sky type is based on gradation and indicatrix function. Determination of the gradation and indicatrix group is based on calculation of luminance ratio between two elements on every almucantar. Since there are 6 gradation and 6 indicatrix groups, we come to 36 combinations but only 15 of them are listed in the CIE standard. Since some of combinations are really rare, we provide the table how to include 36 combinations in 15 standard CIE sky types. From sky luminance map we define gradation and indicatrix group. The method is the same as described in [KOBAV, M.B. 2013].

8 Future work

The camera and the LabVIEW program are working fine and the whole system is ready to be used. For now is the main problem that we have to solve in future is an appropriate case to keep the camera in a warmed up and humid place. Another problem is direct sunlight. If we want to perform measurement also under clear skies it's necessary to protect CCD against direct sunlight for longer time. The easiest way is to install shadow ring.

9 Conclusion

In our paper we describe the complete analysis of the use of compact CCD camera for continuous measurements of sky luminance distribution. With the analysis of sky luminance maps it's possible to define the gradation and indicatrix group directly from the sky scan. The results of the gradation and indicatrix group can be used together with transformation table to derive CIE sky type.

References

[CIE 2003] CIE S 011.1/E:2003. Spatial distribution of daylight – CIE standard general sky. Vienna: CIE

[KOBAV, M.B. 2013] Characterization of the sky scanner measurements based on CIE and ISO standard CIE S 011/2003. Lighting Res. Technol. 45. 504–512

[COUTELIER, B. 2003] Luminance calibration of the Nikon Coolpix 990 digital camera. Proceedings of the CIE Conference. San Diego: CIE, 2003.

[HISCOCKS, P.D. 2011] Measuring luminance with digital camera. http://www.ee.ryerson.ca/~phiscock/astronomy/light-pollution/luminance-notes.pdf.

PP58

INVESTIGATION AND STUDY ON DAYLIGHTING SITUATION OF THE SCHOOL GYMNASIUM

1st **Yawei Yao**[1], 2nd Mingyu Zhang[1]
[1] School of Architecture, Tianjin University, Tianjin, CHINA
yaoyawei891121@163.com

Abstract

In this paper, the research object is the school gymnasium in Tianjin region. Through a series of in-depth researches which present the necessary parameters and questionnaires for users, we can get the status of school gymnasium lighting quality in Tianjin area and establish the lighting quality database of Tianjin school gymnasium. Then, combined with the daylight quantity and quality indicators (daylight factor standard value is 2.0) which are mentioned in the newly revised “Standard for Daylighting Design of Buildings” (GB50033-2013), we analyze the lighting quality in school sports buildings in Tianjin. All of our work will be refined as the basic reference for the study which is aimed to improve the lighting quality of school gymnasium.

Keywords: School gymnasium, Daylighting, Design standard, Evaluation and analysis

1 Introduction

School gymnasium is an indispensable part of school infrastructure, it not only the main places of everyday teaching and sports training, but also has the game, places of public health functions. In recent years, with the development of our national economy, living standards continue to improve, what greatly increase the intensity of physical activity, and residents have higher requirements on the stadium's environmental quality. With the concept of "green sports architecture" deepening, energy conservation has become an important aspect of sports architecture design. Meanwhile, the school gymnasium with a "quantity", "body mass", "high-frequency" characteristics, and the energy consumption of artificial lighting and defects of the lighting quality are becoming increasingly serious. Rational use of natural light can not only reduce energy consumption of artificial lighting, but also provides the user with a good indoor environment. It can be seen from visual function test that the human eye has a higher visual effect and feel more comfortable and wholesome in natural light than under artificial light[1]. For the stadium construction, the use of natural lighting also help raise the level of sports training and competition. Thus, the rational use of natural daylight for lighting and rational design of daylighting opening to avoid lighting quality defects has become an important way to solve the energy consumption of sports construction. At present the main reference of lighting design and evaluation of sports construction is "Standard for Daylighting Design of Buildings " GB50033-2013 (Hereinafter referred to “SDDB”), newly promulgated in 2013. In the newly design standards, light quantity and quality indicators have new requirements, and daylight factor standard values changed from the lowest value to the average. This paper combines the new standard, based on the research of the lighting quality of Tianjin school gymnasium, evaluates and analysis the lighting quality of school sports construction, and provides a basis for optimizing the lighting quality of school gymnasium.

2 The Research Content and Methods

2.1 The purpose and object of the research

- Purpose: To investigate the situation of natural daylight quality in Tianjin school gymnasium.
- Object: Tianjin University Gymnasium, the new Tianjin Polytechnic University Gymnasium, the old Tianjin Polytechnic University Gymnasium, Tianjin Normal University Gymnasium

(Main Hall), Tianjin Normal University Gymnasium (Gym), Tianjin University of Technology Gymnasium, the old Nankai University Gymnasium.

Table 1 – Stadium Basic Situation

Gyms	The main form of light opening	Function
Tianjin University Gymnasium	Skylight	Badminton
The new Tianjin Polytechnic University Gymnasium	Skylight	Badminton
The old Tianjin Polytechnic University Gymnasium	Skylight	Badminton
Tianjin Normal University Gymnasium (Main Hall)	Skylight	Badminton
Tianjin Normal University Gymnasium (Gym)	Side windows	Gymnastics
Tianjin University of Technology Gymnasium	Side windows	Basketball
The old Nankai University Gymnasium	Side windows	Badminton

2.2 Research Content

- Time: October 2013 - December 2013, 10:00 AM ~ 2:00 PM
- Instrument: Handheld luminance meter (konnica minolta Ls-100) , Illuminance meter (XYI-III digital illuminance meter) , Rangefinder (Leica Disto D5), Camera (CANON 7D, etc.).

Figure 1 – Illuminance Meter, Luminance Meter, Rangefinder

- Contents: building size, the size of the venue and lighting opening, physical testing: indoor and outdoor horizontal illuminance, window luminance, wall brightness.
- Method: Tested under conditions of natural light, and exclude the interference of artificial lighting. Tested under normal lighting opening circumstances. Illuminance measurement is uniform distribution method, each point spacing 3m to 4m, covering the activity field area and the field around 1 m; Luminance measurement method using uniform points method, 4 to 6 points on each side wall cloth.

3 Statistics and Analysis on surveys results

3.1 Data processing

The further calculation can be carried out according to measurement parameters, and the calculation method is shown below.

$$C_i = \frac{E_i}{E_0} \times 100\% \quad (1)$$

C_i is the points' lighting factors;

E_i is the indoor horizontal illuminance;

E_0 is the outdoor horizontal illuminance;

$$C_{ave} = \frac{1}{M \times N} \sum C_i \tag{2}$$

C_{ave} is the average value of lighting factors;

C_{min} is the minimum lighting factor

M is the number of longitudinal distribution points;

N is the number of lateral distribution points.

$$\mathrm{U} = \frac{C_{min}}{C_{ave}} \tag{3}$$

U is the uniformity of lighting;

C_{ave} is the average value of lighting factors;

C_{min} is the minimum lighting factor

$$\mathrm{DGI} = 10 \log \sum G_n \tag{4}$$

$$G_n = 0.478 \frac{{L_s}^{1.6} \Omega^{0.8}}{L_b + 0.07 \omega^{0.5} L_s} \tag{5}$$

$$\Omega = \int \frac{d\omega}{p^2} \tag{6}$$

$$\mathrm{p} = \exp\left[\left(35.2 - 0.31889\alpha - 1.22e^{-2\alpha/9}\right)10^{-3}\beta + \left(21 + 0.26667\alpha - 0.002963\alpha^2\right)10^{-5}\beta^2\right] \tag{7}$$

DGI is the discomfort glare index of window

G_n is the dazzled constant;

L_s is the window brightness(cd/m^2) ;

L_b is the background brightnesscd/m^2;

ω is the solid angle between window and calculation point(sr);

Ω is the solid angle considering the correction of window position(sr);

p is the gus position index;

α is the angle between window's diagonal and vertical direction;

β is the angle between window' center and observers' eyes;

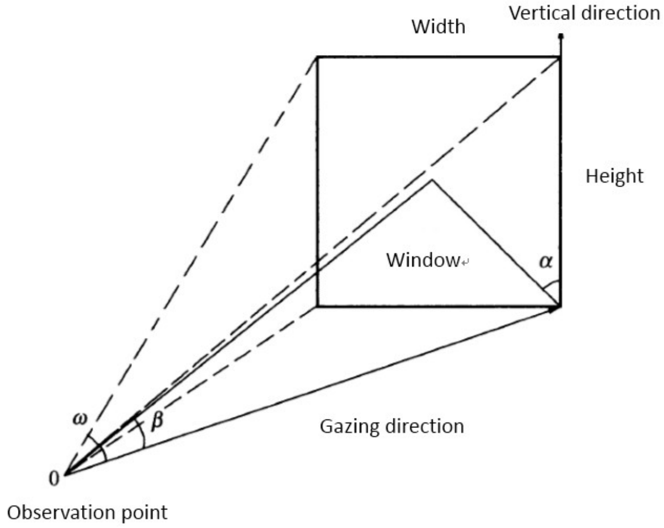

Figure 2 – Schematic Plot for Discomfortable Dazzled Calculation of Windows

3.2 Data comparison and analysis

3.2.1 National standard

According to the current SDDB, which is short for Standard for Daylighting Design of Buildings (GB50033-2013), the normal values of the side lighting factor and indoor natural lighting are 2.0% and 300lx. Meanwhile, the normal values of the top lighting factor and indoor natural lighting are 1.0% and 150lx. According to SDDB, the gymnasium's lighting level is defined as Ⅳ, and the corresponding discomfortble glare index of window is 27. In SDDB, the top lighting uniformity is defined as 0.7. Otherwise, the side lighting uniformity is not defined for the great change of illuminance.

3.2.2 Data comparison

Considering the data from all gymnasiums, the comparison is conducted on the average illuminace, the average value of lighting factors, the lighting uniformity and window' discomfortable glare index (DGI).

- Indoor average illuminance

The comparison about indoor average illuminance between these gyms is shown as the figure 3. The lateral lighting normal value is defined as 300lx, and the top lighting normal value is defined as 150lx. It's obvious that only the new Tianjin Polytechnic University Gymnasium, whose average illuminace is 48.53lx, cannot satisfy the standard.

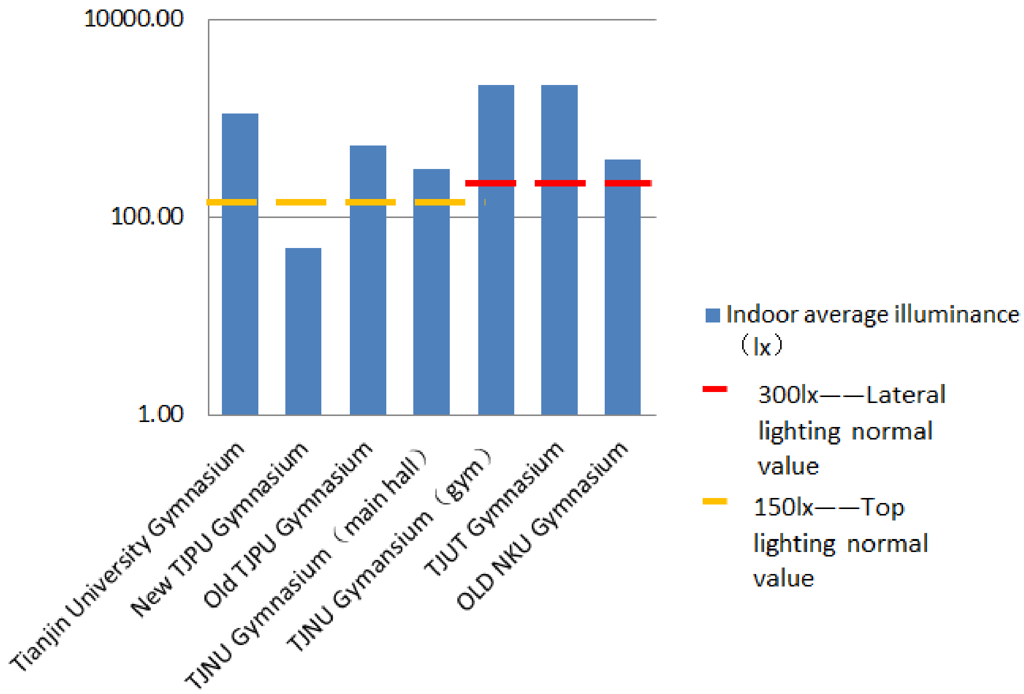

Figure 3 – Indoor Average Illuminance Comparison (lx)

- Average value of lighting factor

The figure 4 indicates the comparison about the average value of lighting factors in each gymnasium. The measurement criteria of the side and the top lighting normal values are 2.0% and 1.0%. According to the Fig 4, the average values of Tianjin University Gymnasium, the old Tianjin Polytechnic University Gymnasium, Tianjin Normal University Gymnasium (Main Hall), Tianjin University of Technology Gymnasium respectively are 2.3650%, 1.2585%, 5.7275% and 5.0503%. What's more, these four gymnasiums also fit the indoor illuminance normal value. However, the average value of lighting factor in the new Tianjin Polytechnic University Gymnasium is 0.1577%. This value is much lower than design value, which means the lighting is seriously deficient.

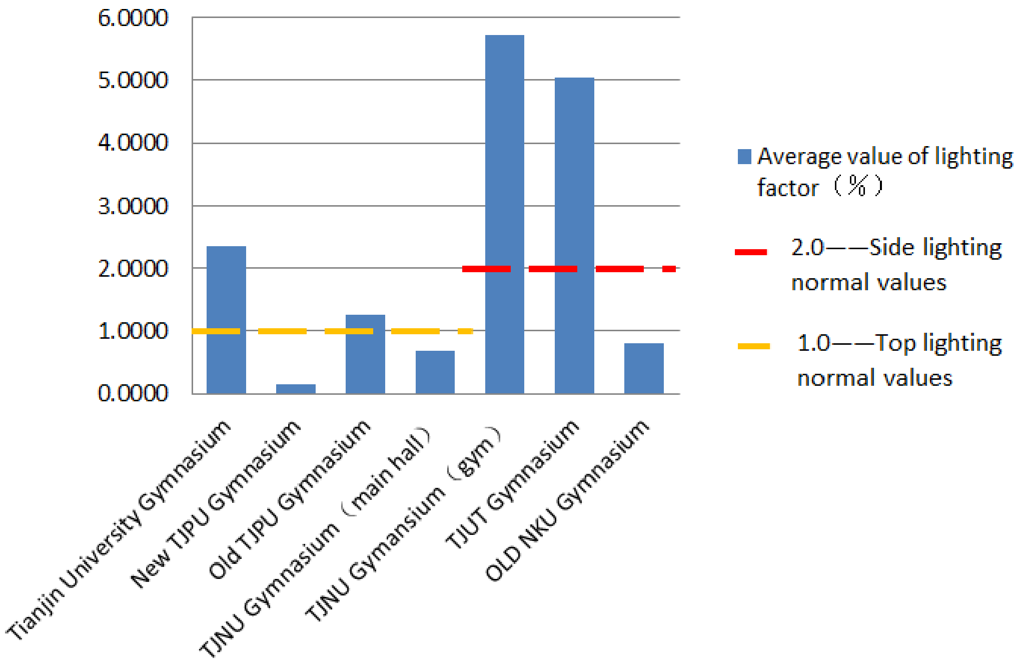

Figure 4 – Average Value of Lighting Factors Comparison (%)

- Lighting uniformity

Figure 5 has shown the comparison about lighting uniformity of Tianjin University Gymnasium, the old and new Tianjin Polytechnic University Gymnasiums and Tianjin Normal University Gymnasium (Main Hall), which give priority to top lighting. It's obvious that except the new Tianjin Polytechnic University Gymnasium whose lighting uniformity is 0.7561, the rest 3 gymnasiums cannot meet the normal value of lighting uniformity. And, the old Tianjin Polytechnic University Gymnasium's lighting uniformity is 0.1762 that is much lower than normal value.

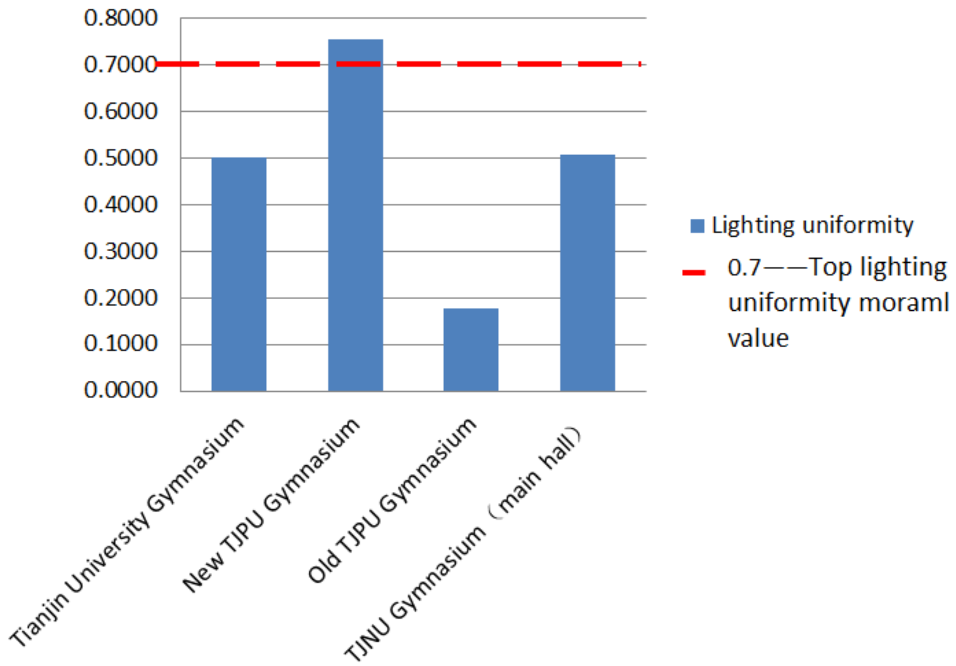

Figure 5 – Lighting Uniformity Comparison

- Window's discomfortable glare index (DGI)

The comparison about DGI in the gymnasiums prior to side lighting is shown in the figure 6, and the normal value of DGI is 27. As shown in Fig 6, the DGI of Tianjin University of Technology Gymnasium is 24.78 lower than normal value, which meets the design standard. Otherwise, the DGIs of Tianjin Normal University Gymnasium (Gym) and the old Nankai University Gymnasium are 32.81 and 33.40 higher than normal value, which is beyond design standard.

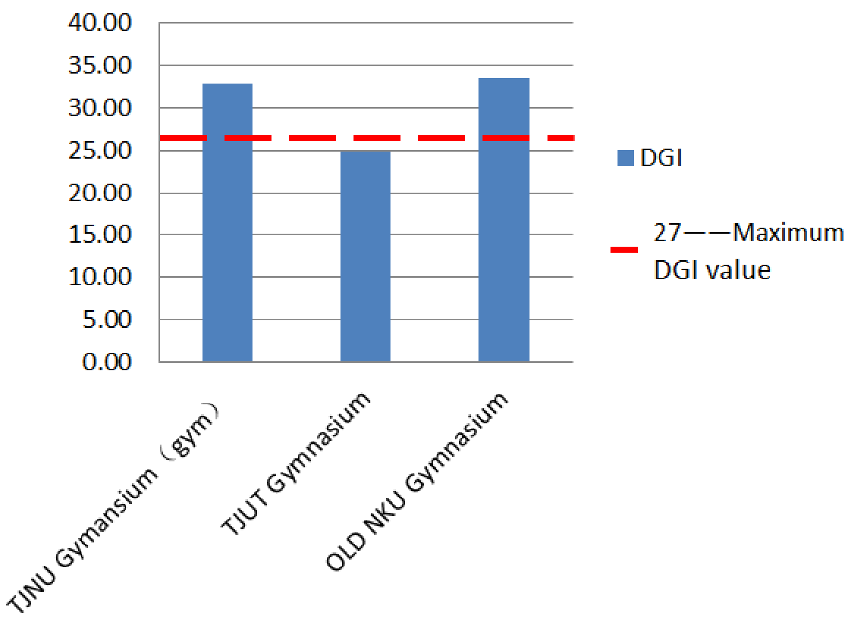

Figure 6 – DGI Comparison in Main Lighting Windows

3.2.3 General analysis

The data of the lighting surveys are concluded in table 2.

Table 2 – Comprehensive Table Statistics

Main daylight opening forms	Gyms	Indoor average illuminance	Lighting factors average value (%)	Lighting uniformity	DGI
Skylight	Tianjin University Gymnasium	1111.57	2.3650	(0.5020)	——
	The new Tianjin Polytechnic University Gymnasium	(48.93)	(0.1577)	0.7561	——
	The old Tianjin Polytechnic University Gymnasium	527.95	1.2585	(0.1762)	——
	Tianjin Normal University Gymnasium (Main Hall)	303.37	(0.6848)	(0.5076)	——
Side windows	Tianjin Normal University Gymnasium (Gym)	2162.12	5.7275	——	(32.81)
	Tianjin University of Technology Gymnasium	2169.11	5.0503	——	24.78
	The old Nankai University Gymnasium	379.33	(0.7899)	——	(33.40)

Note: Brackets indicate that does not meet the standard requirements.

According to the results of surveys on each gymnasium, it's obvious that those gymnasiums which adopt skylights for the main lighting opening forms cannot meet the normal value of lighting uniformity and average lighting factors. However, the gymnasiums using side windows always cannot meet DGI normal values. Meanwhile, based on the feelings of testers, most gymnasiums cannot provide high-quality light environment for the sports activities. The lack of the special index for lighting in gymnasium in the original design standard results in the lack of professional lighting design.

4 Case analysis and simulation optimizing

Taking the gymnasium of Tianjin Normal University(main hall) for example, from the result of the investigation of current situation, we try to optimize the simulation result by the soft of Ecotect.

4.1 The introduction of gymnasium

The Tianjin Normal University gymnasium (main hall) use east –west rectangular skylights as its' main daylight opening, in the east, and west sides, each side use a row of high windows as auxiliary daylight opening. (The west side of the high window keep closed throughout the year)

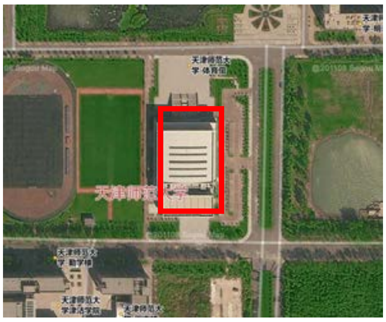

Figure 7 – The Surrounding Situation of Tianjin Normal University Gymnasium

Figure 8 – The Skylight of Tianjin Normal University Gymnasium (Main Hall)

Figure 9 – The East Side High Windows of Tianjin Normal University Gymnasium (Main Hall)

This measurement of the gymnasium finished on December 11 in 2013, sunny. According to the survey data, figure 10 is a False Color image of level of indoor intensity of illumination drawing by SIGMAPLOT, and the result shows us that the gymnasium can reach the standard of indoor average illumination. While cannot meet the daylight factor and the standard lighting uniformity, so the subjective evaluation is a “regular”. The high windows in the east and west sides offer enough light to the indoor space, which give us a qualified horizontal illumination. However, it also causes poor lighting uniformity and fails to reach the standard value of lighting uniformity, for the Illumination in the north area is higher than the south area.

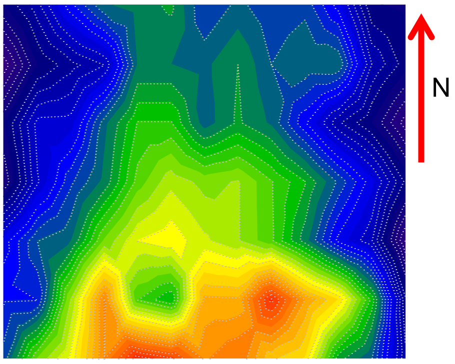

Figure10 – Tianjin Normal University Gymnasium (Main Hall) indoor horizontal illuminance (lx)

4.2 Simulation optimizing

4.2.1 Model Building

The simulation bases on a model under the condition of CIE standard clear sky.

The simulation result should be based on a particular time of December 21, 12 noon, while loading the meteorological data of Tianjin area as at the same time.

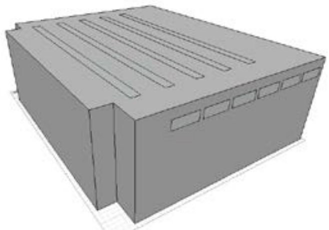

Figure 11 – Model

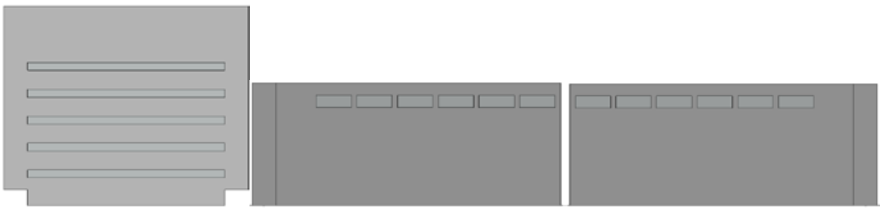

Figure 12 – The Top Surface, East Facade, West Facade

- Original model:

Based on the three-dimensional venues model, we use Ecotect to determine the indoor light environment simulation. The simulation results are as follows: the average of lighting coefficient: 4.71%, lighting uniformity: 0.541, the average intensity of illumination: 235.39 lx. The simulation results show that the lighting uniformity of this venue is poor, and the average intensity of illumination is not up to standard. According to the figure 13 shows, the illuminance value of north venue is low.

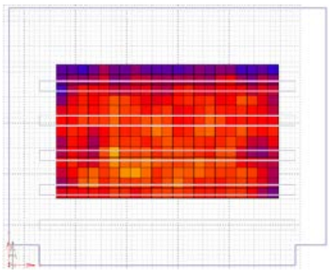

Figure 13 – Simulate Pseudo Color Image

4.2.2 The adjustment of daylight opening

- To increase the area of the skylight:

Increase a skylight of 4 M wide and 50 M long in the north of the original skylight at the height of 2.8 M. The simulation results are as follows: the average intensity of illumination: 6.10%, lighting uniformity: 0.585, the average intensity of illumination: 304.89 lx. Through optimization, the average illuminance of this venue can reach the standard rules, but still can't meet the requirements of lighting uniformity standard.

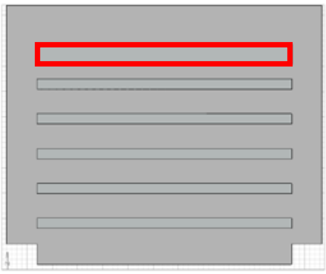

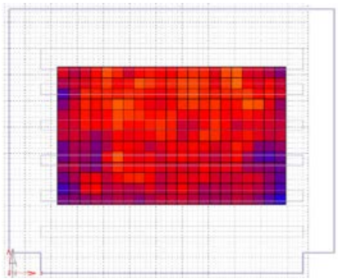

Figure 14 – Increase the Skylight **Figure 15 – Simulate Pseudo Color Image**

- Change the position of daylight opening:

Translate the south skylight to the north side of 2 m , the high and the things on both sides of the side window rearrange (pictured). The simulation results are as follows: the average of lighting coefficient: 6.24%, lighting uniformity: 0.716, the average intensity of illumination: 311.76 lx. We can improve the lighting uniformity of this venue by changing the daylight opening position, greatly meet the design requirements of lighting uniformity standard.

Figure 16 – The Top Surface, East Facade, West Facade

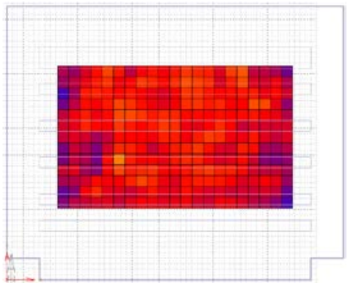

Figure 17 – Simulate Pseudo Color Image

4.2.3 Summary

For existing gymnasiums, it’s difficult to optimize lighting quality from change the construction size. And the only way is to adjust the positions and increase or decrease the area of lighting opening. But, the adjusted lighting opening may not meet the aesthetic design of buildings. Hence, it’s necessary to take lighting design into account when conducting architectural design.

5 Conclusions

Lighting design is a comprehensive process, which needs to take the architecture design, the function and the requirements in usage time into account. However, traditional architectural design in this respect is flawed. Having analyzed the cases that combines actual situation and simulation optimization of the lighting in gymnasiums, this article is aimed to propel lighting and energy-saving consideration in architectural design.

This article only use simulation software to analyze gymnasium lighting conditions in Tianjin area, and it’s insufficient to only adopt CIE standard clear sky in the actual lighting design. Hence, the next step of the study should contrapose regional lighting climate characteristics and take architectural types and function into account. All of these will promote the study and application of lighting design.

References

LIU, J.P. 2000. Architectural Physics (Third Edition). China ConstrucionIndustry Press.

STAOTPROC. 2008, Standardization Administration of The People’s Republic of China. Method of daylighting measurements (GB5699-2008).

STAOTPROC. 2013, Standardization Administration of The People’s Republic of China. Standard for daylighting design of buildings (GB50033-2013).

GUAN, X.F. and ZHAO, H.T. 2010. Measurement and Analysis on Shenzhen University Gymnasium, 2, 31-33.

WANG, A.Y and LI, Z. 2008. Daylighting Features of Falun Palace of Yonghe Lama Temple, 19(3), 22-25.

LI, W.W. WANG, A.Y. and LIAN, Z.Q. Daylighting Strategy of Tianjin Railway Station Waiting Hall, 22(5), 74-78.

PP60

RESEARCH ON ENERGY STANDARD FOR BUILDING LIGHTING

1st Zhao Jianping[1], 2nd Wang Shuxiao[1]
[1] China Academy of Building Research, Beijing, CHINA
wangshuxiao417@163.com

Abstract

As we all known, minimum lighting power density (LPD) is an effective way to reduce lighting energy consumption. In this paper, a brief summary of standards on energy efficient lighting is presented and the shortcomings of these methods are analyzed. Based on the analysis, the mathematic model about the influencing factors on lighting energy efficient is built and presented. And finally, a refined estimated method is introduced, which provides a room index-based adjustment to interior space type LPDs.

Keywords: Lighting, Energy Standard, Lighting Power Density, Room Index

1 Introduction

Lighting is a large and rapidly growing source of energy demand and greenhouse gas emissions. In 2005 grid-based electricity consumption for lighting was 2650 TWh worldwide, which was about 19% of the total global electricity consumption, whereas the electricity consumption for indoor lighting was estimated at 2438 TWh worldwide, which was about 17.5% of the total global electricity consumption, in a document published by the International Energy Agency.

China established the goals of cutting energy consumption intensity by 16%, relative to GDP by 2015, compared with 2010 levels. With the rapid urbanization of China, today the lighting electricity consumption in China account for 13.4% of its 4600 billion kWh electric power production in 2011. So improving the energy efficiency of lighting in China could have a tremendous impact on the overall energy efficiency of buildings. Lighting energy conservation and energy efficiency became an important part of China's government policy from the early 1990s, with the issuance of "Industrial Enterprise Lighting Design Standard" GB50034-92, which first provided recommendation values for indoor lighting energy efficiency, relating the electrical power for lighting to the mean maintained illuminance on a reference plane and to the overall floor area and typically expressed in W/(m^2/100 lx).

In this paper, a brief summary of standards on energy efficient lighting is presented and the shortcomings of these methods are analyzed. Based on the analysis, the mathematic model about the influencing factors on lighting energy efficient is built and presented.

2 Measures for Energy Efficient Lighting

The main idea of energy-efficient lighting is to reduce the amount of electricity used without compromising on the quality of lighting. Savings can be achieved by increasing the efficiency of the lighting system components, and also by using the right amount of light when it is needed and where it is needed. So energy-efficient lighting is a systematic project, which covers effective use of daylight, reasonable choice of energy efficient lighting products, lighting design solutions, control strategies and management schedules. Lighting energy can be reduced by following measures:

Reasonable choice of the most efficient and cost effective lighting technologies

- Using energy efficient lamp;
- Using energy efficient ballast;
- Using high-efficiency luminaire.

Scientific lighting design solutions

- Choice of luminaires with good distribution of luminous intensity according to the room dimensions;
- Optimization of luminaires spacing;
- Selection of reasonable illuminance levels;
- Use of task/ambient lighting.

Effective use of daylight

Rational selection of control strategies and management schedules

- Reduction of switch-on time;
- Occupancy sensors and/or manual/automatic dimming;
- Improvement in maintenance factor.

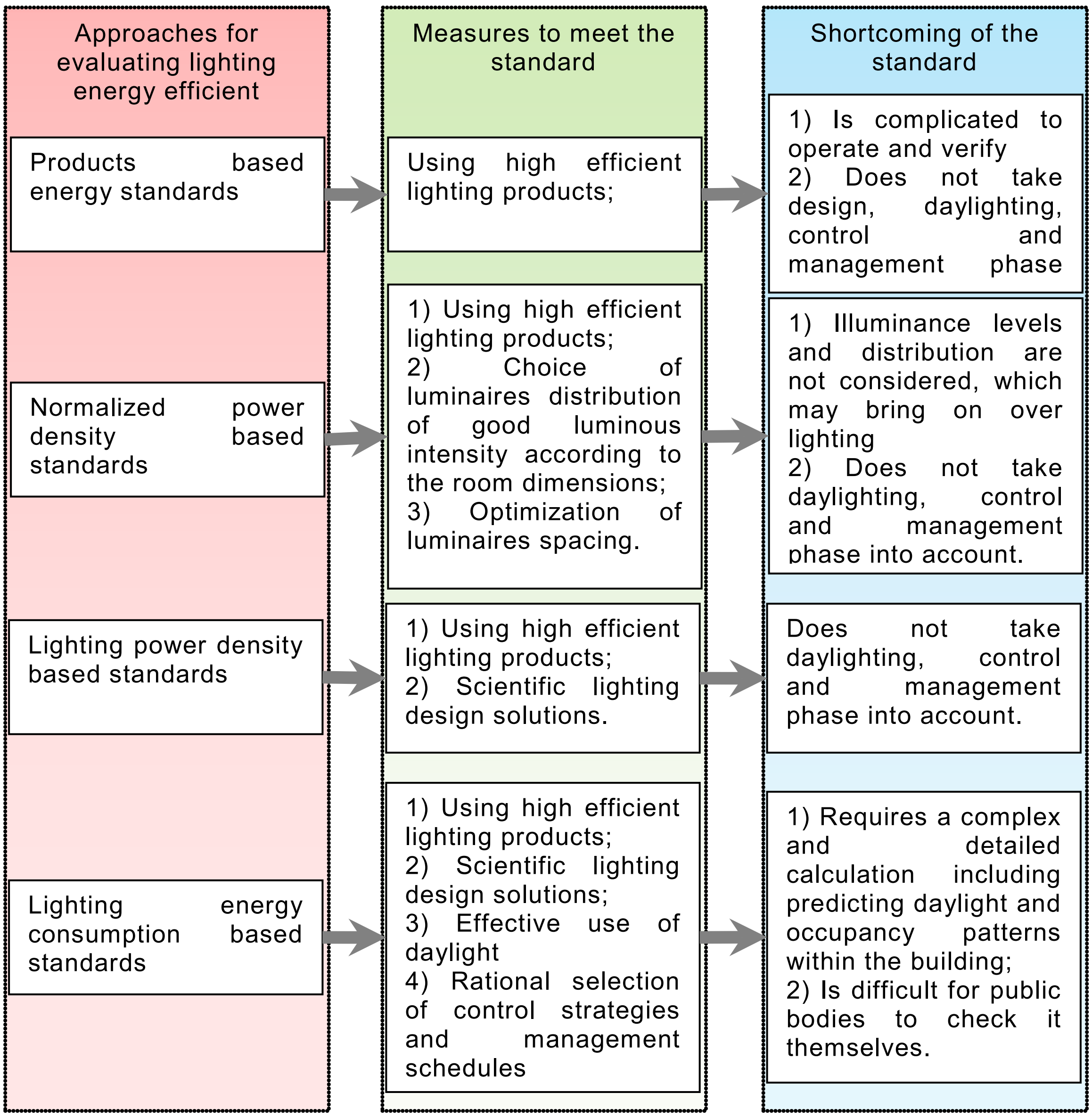

Figure 1 – Comparison of the four lighting energy efficient evaluation approaches

3 Review of Standards on Energy Efficient Lighting

Codes and legislation on energy efficiency have been introduced in different countries to encourage the efficient use of lighting energy, which can be divided into the following categories according to the lighting energy efficient indicators:

- Products based energy standards;
- Normalized power density based standards;
- Lighting power density based standards;
- Lighting energy consumption based standards.

A brief summary of the aforementioned four approaches is presented and their shortcomings of these methods are analyzed in figure 1.

The energy consumption of a lighting installation is strongly dependent on lighting controls (daylight, presence detection, dimming, etc.). From the Figure, we can see that the approach, based on the overall lighting energy consumption of the building including the effect of lighting controls, is set out in EN 15193, which, theoretically speaking, is much more perfect than other approaches. But it would require a much more complex set of criteria because the kWh/m2 figure will depend on hours of use and daylight provision, which is difficult for public bodies to check it themselves.

As the electrical power load of a lighting installation is often a first and significant measure for the energy consumption, thus the simpler method based on installed lighting power density was chosen by many national standards. The next section describes the mathematic modes for lighting power density (LPD) computation.

4 Basis of Lighting Power Density (LPD)

At the core of the LPD methodology is the use of a modified form of the lumen method. The origin of the lumen method date back to 1916,when Harrison and Anderson conducted an experiment that identified the impact of four variable on the average uniform illuminance on an imaginary horizontal plane. The four variables were as follows:

- Room proportions;
- Room-surface reflectance values;
- Luminaire location;
- Luminaire light-distribution type.

In lighting design, the lumen method is a simplified method to calculate the light level in a room. In its simplest form, the lumen method is merely the total number of lumens available in a room divided by the area of the room. In order to perform this calculation, many factors, coefficients, lamp lumen data and other quantities must be gathered. The method is defined as,

$$\overline{E}_{maintained} = \frac{n \cdot m \cdot \eta_{lamp} \cdot \eta_{gear} \cdot UF \cdot MF \cdot P_{sys}}{S} = \frac{n \cdot m \cdot \eta_{lamp} \cdot \eta_{gear} \cdot U \cdot LOR \cdot MF \cdot P_{sys}}{S} \quad (1)$$

where

$\overline{E}_{maintained}$	is the maintained average illuminance on the work plane;
n	is the number of luminaires in the space;
m	is the number of lamps in a luminaire;
η_{lamp}	is the luminous efficiency of the lamp;
η_{gear}	is the efficiency of the gear, which can be defined as,

$$\eta_{gear} = \frac{P_{lamp}}{P_{sys}} \tag{2}$$

P_{sys} is the total power delivered to the lamps and gear ;

P_{lamp} is the total power consumped by the lamp;

UF is the ratio of lumens from a luminaire (fixture) received on the workplane to the lumens emitted by the luminaire’s lamps alone；

LOR is the efficiency of luminaires, which describes the ratio of luminous flux (lumens) emitted by a luminaire to that emitted by the lamp or lamps used therein.

U is the ratio of lumens from a luminaire (fixture) received on the workplane to the lumens emitted by the luminaire；

MF is a factor used to denote the ratio of the illuminance on a given area after a period of time to the initial illuminance on the same area.

S is the area of work plane;

So from the equation 1, we can get,

$$LPD = \frac{n \cdot m \cdot P_{sys}}{S} = \frac{\overline{E}_{maintained}}{\eta_{lamp} \cdot \eta_{gear} \cdot U \cdot LOR \cdot MF} \tag{3}$$

If we carry out lighting design for different-dimension offices with the same high efficiency lighting products, this means that the design has the same maintained average illuminance, efficiency of lighting products, and *MF* value, but not the *U* value. But most active standards all over the world just give one limit for each space type, which, from a practical point of view, reduces the flexibility of lighting design for small spaces, and is also too loose for big spaces, leading lighting energy wastes. So an approach to the solution of this problem is presented in the next section.

5 Adjustment for LPD limit based on room geometrics

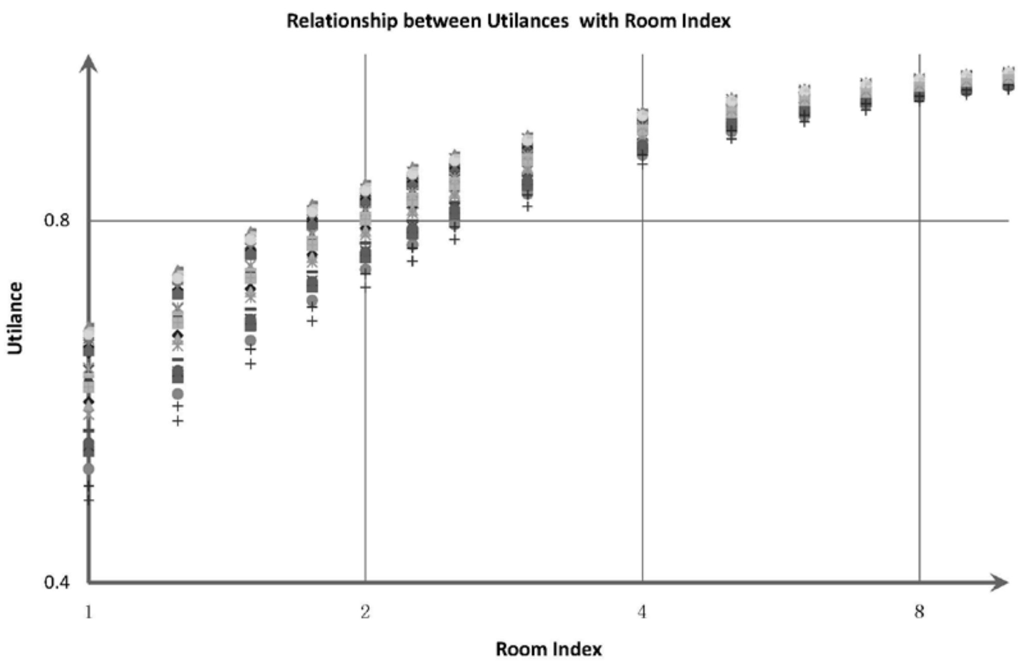

Figure 2 – Relationship between utilances and room index

Actual *U* value is an important part of determining achievable lighting power densities, which gives the fraction of a lumiaire's lumens that reach the workplane, directly from source and from interreflections. It takes into account the impact of the luminaire luminous intensity distribution, room geometry and the room surfaces in its derivation. Thus to determine the method for adjustment for LPD limit based on room geometrics, we should first research the relationship between utilance and room geometry.

For this destination, utilances for different room index of 34 fixtures made by different domestic and international companies were collected and presented in figure 2. From the figure, we can see there are huge differences between U_{10} and $U_{0.3}$, where U_{10} is luminaire's utilance when room index is 10, and $U_{0.3}$ is luminaire's utilance when room index is 0.3. As the figure 3 shown, the biggest value for $U_{10}/U_{0.3}$ is 6.73, and the smallest value is 4.03. It further proves the necessity to make geometric adjustment.

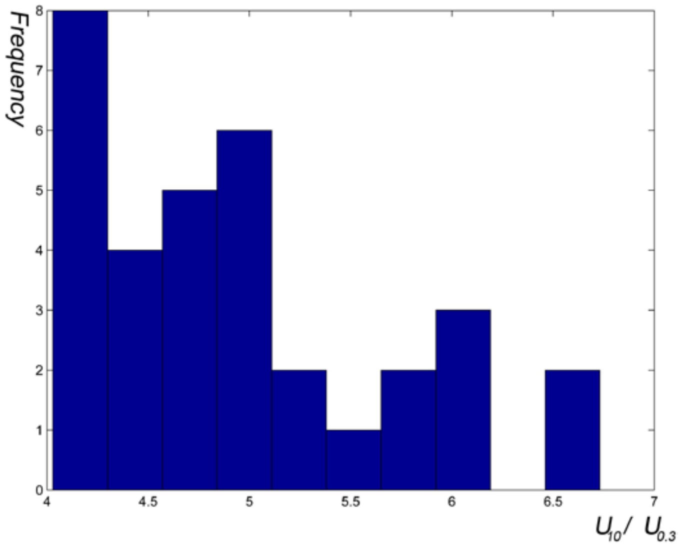

Figure 3 –Histogram of $U_{10}/U_{0.3}$ values

Table 1 – Adjustment factors for LPD limit based on room geometrics

Adjustment Factors		Design Room Index															
		0.4	0.5	0.6	0.7	0.8	0.9	1	1.25	1.5	1.75	2	2.25	2.5	3	4	5
Reference Room Index	1	2.2	1.7	1.5	1.3	1.2	1.1	1.0	0.9	0.8	0.7	0.7	0.7	0.7	0.6	0.6	0.6
	1.5	2.7	2.2	1.9	1.6	1.5	1.4	1.3	1.1	1.0	0.9	0.9	0.9	0.8	0.8	0.7	0.7
	2	3.0	2.4	2.1	1.8	1.7	1.5	1.4	1.2	1.1	1.0	1.0	1.0	0.9	0.9	0.8	0.8
	2.5	3.3	2.7	2.3	2.0	1.8	1.7	1.5	1.4	1.2	1.1	1.1	1.0	1.0	1.0	0.9	0.9

So we got adjustment factors for LPD limits with the use of collected luminaires data as shown in table 1. And the LPD can be adjusted according the room dimensions by:

$$LPD_{design} = LPD_{ref} \cdot AF \qquad (4)$$

where

LPD_{design} is the LPD limits for the designed space;

LPD_{ref} is the reference LPD limits given by the standard;

AF is the adjustment factor got from table 1 according to reference and design room index.

To demonstrate the way how the adjustment factor is used to calculate the LPD for a given lighting space, we will walk through the process using a typical office setting example. As the requirement on office lighting energy efficient of under-drafting China's national standard, "Standard for lighting design of buildings", is shown in table 2.

Table 2 – China's national standard's requirement on office lighting

Indicators	Maintained Illuminance	LPD	Reference Room Index
Standard Value	300 lx	$9 W/m^2$	1.5

The room index of office to be illmuminated is 5, and the reference room index given by standard for office is 1.5, so adjustment factors is 0.7. Finally the design LPD limit can be computed by formula 4.

$$LPD_{design} = 9 \times 0.7 = 6.3 W/m^2 \tag{4}$$

6 Conclusion

This paper presents an alternative approach to obtain an indication of the energy efficiency of an interior space. Taking into account room geometry, the maximum allowable lighting load for a given room for a specific space type can be predicted. This alternative criterion for energy efficient lighting installations is broadly applicable and easy to use as only quite common parameters of the lighting design have to be known.

References

P Hanselaer. C Lootens, WR Ryckaert. 2007. Power density targets for efficient lighting of interior task areas. Lighting Res. Technol. 39,2 (2007) 171–184

Wouter R. Ryckaert, Catherine Lootens. 2010. Criteria for energy efficient lighting in buildings. Energy and Buildings 42 (2010) 341–347

IESNA. 2000. IESNA Lighting Handbook, 9th ed. New York: Publication Department IESNA.

Ministry of Housing and Urban-Rural Development of the People's Republic of China (MOHURD). GB 50034. Standard for lighting design of buildings. Beijing: MOHURD.

Pramod Bhusal. Energy-Efficient Electric Lighting for Buildings in Developed and Developing Countries. Doctor Dissertation. Helsinki University of Technology. 2009.

EN. 2007, European standard: Energy performance of buildings – Energy requirements for lighting. EN 15193.

PP61

HUMBLEBEE – INNOVATIVE LIGHTING SYSTEM AT ENEA - ISPRA

Simonetta Fumagalli[1], Laura Blaso[1], Adriano Antonelli[1],
Giuseppe Leonardi[1], Vito Tarantini[1], Alessandro Costantini[2], Alessandro Cola[3]
[1] ENEA, Ispra, ITALY, [2] Intematix - Italia, Rome, ITALY, [3] NERI, Longiano, ITALY
simonetta.fumagalli@enea.it

Abstract

HumbleBee is an innovative lighting system combining LED - remote phosphors technology (for luminaires) and a customized smart lighting control system (for dimming, switching and changing correlated colour temperature of light) with a wireless network based on ZigBee protocol. The system has been designed at ENEA Ispra and it is realized at ENEA Ispra laboratory. After the installation and the commissioning phase, the operative phase includes a monitoring campaign, aimed to quantify environmental and energy performances (energy consumption, illuminance, state, manual interaction, users presence, malfunctioning, etc.). The monitoring campaign will also calculate the actual energy savings.

The goal of the HumbleBee project is to realize an innovative prototype of lighting system, useful for tertiary sector, able to reduce energy consumption and improve the lighting quality and the visual comfort in work places, through the use of innovative technologies.

Keywords: e.g. Energy Efficiency, Energy Saving, Lighting, Smart Controls, Remote Phosphors, Visual comfort, Light Quality, Indoor Lighting, Tertiary Sector.

1 Introduction

The HumbleBee project has been developed under the national research program "Ricerca di Sistema Elettrico", whose goal is the development of methodologies and instruments aimed at the improvement of high energy efficiency technologies, in order to stimulate the market toward more performing products.

The goal of the HumbleBee project is to realize and test an innovative prototype of lighting system, useful for indoor applications in the tertiary sector, able to reduce energy consumption and improve the lighting quality and the visual comfort in work places, through the use of innovative technologies, user friendly interface and simple cabling (Blaso, 2013).

2 The HumbleBee system

The HumbleBee lighting system has been designed combining two innovative technologies: luminaires with LED + remote phosphors and a smart control system.

The case study is the technology-hall at ENEA Ispra laboratories: people spend many hours every day in these workplaces. It is then important to evolve from the "stereotyped" workplace to the "anthropyzed" workplace. The true challenge is to obtain the correct equilibrium among different key elements, as shown in the following figure.

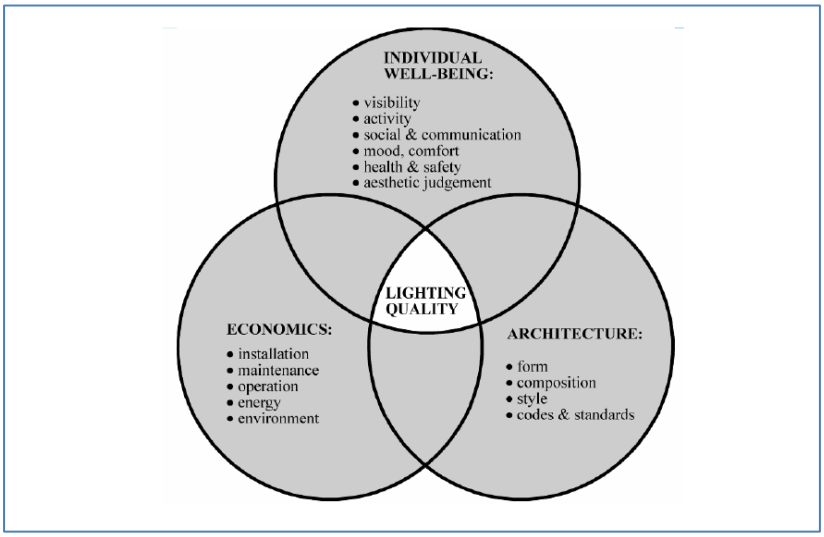

Figure 1 – Elements of light quality (from (Rossi, 2013))

The choice of a remote phosphors LED luminaire comes from the intention to perform field test on one of the most advanced technologies for white light emission.

NOTE: a very complete report on white light generation and on remote phosphors, together with comparison and pro / contra of different technologies can be found – in Italian – in (Rossi, 2013).

The choice of a smart control system comes from the intention to realize a dimmable and optimized lighting system, in order to reduce energy consumption while ensuring and improving light visual comfort on the task areas according to the user's actual needs. Latest technologies have been selected (sensors, web apps, manual and automatic control possibilities, scene settings…), in a wireless transmission framework, able to guarantee robustness, reliability and flexibility. Another advantage of wireless technology is the reduced need of physical cabling: the devices communicate each other trough a central controller and actuators (via cable or wireless). This flexibility allows also easy installation and maintenance, identification / addressing of the components and programming the whole system.

2.1 The case study

Case study is the technology-hall at ENEA Ispra, where two laboratories related to research activities on energy efficiency are active. They are called ICELAB (for household cold appliances) and FIRELAB (for household electric ovens) and they are sharing a number of infrastructures (e.g. climatic chambers). The hall is an industrial-like room, 8.00 x 9.40 m, 7.00 m high.

Task zones for researchers and technicians are 3 climatic chambers and 2 workstations (desks, about 1 m high) where part of the experimental setup is done.

The old lighting system is based on traditional high bay luminaires with high pressure mercury vapour, installed at 7 m height.

In the following figure some views and the planimetry of the hall are given, together with views of the old lighting system and details of a luminaire.

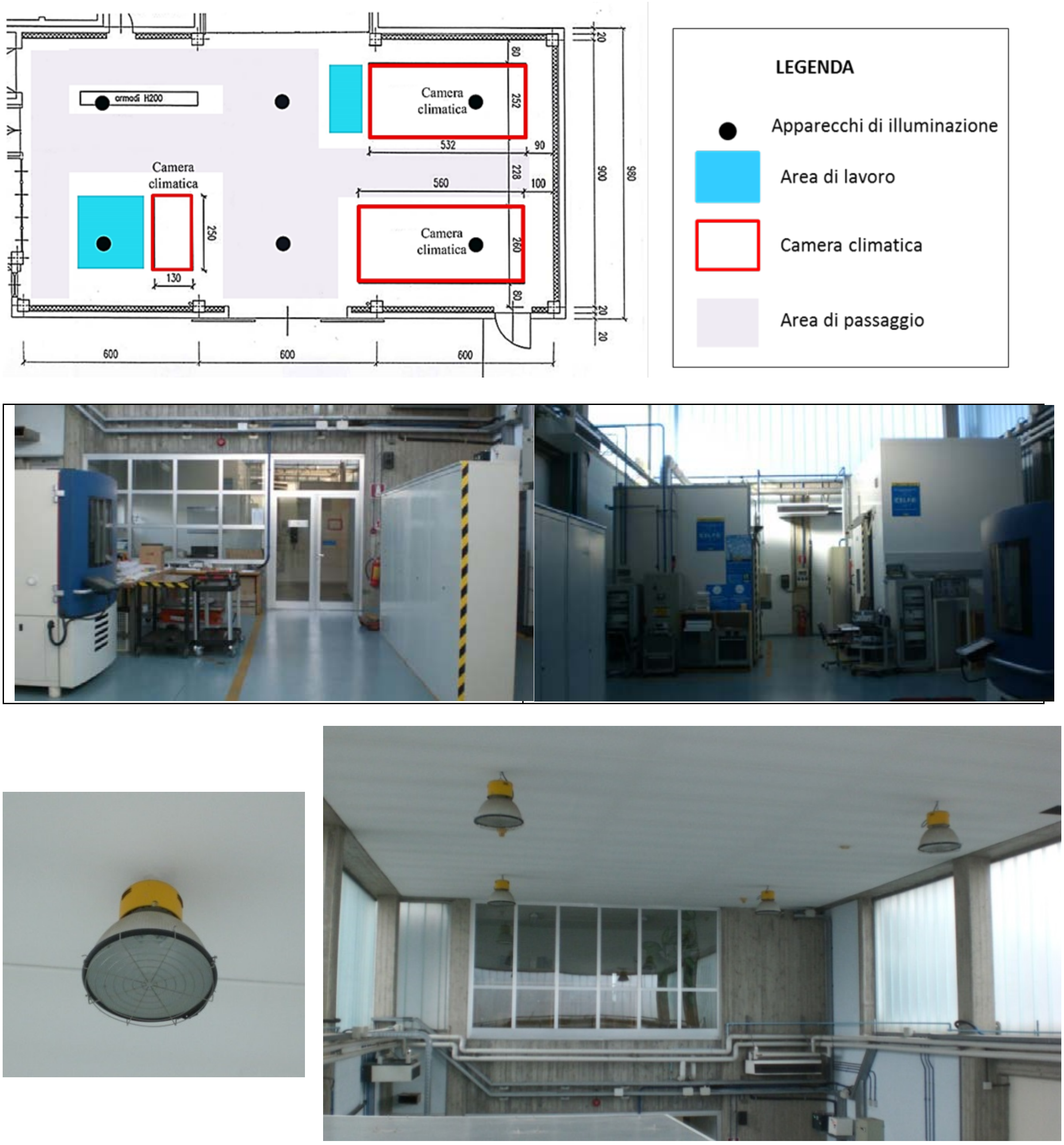

Figure 2 – Planimetry and views of the Technology Hall, with the old lighting system

2.1 The lighting design

Task areas have been identified, reflectances of surfaces (workplanes, walls…) and other relevant parameters have been determined. Then a 3D model of the hall has been realized.

Lighting requirements have been set according to EN 12464-1:2012 standard: main values are E_m = 300 lx and U_{o} = 0.60. A common free software has been used for simulations.

The position and number of the new luminaires result very similar to the old ones, as in the following figure. Photometry of the luminaires are also shown.

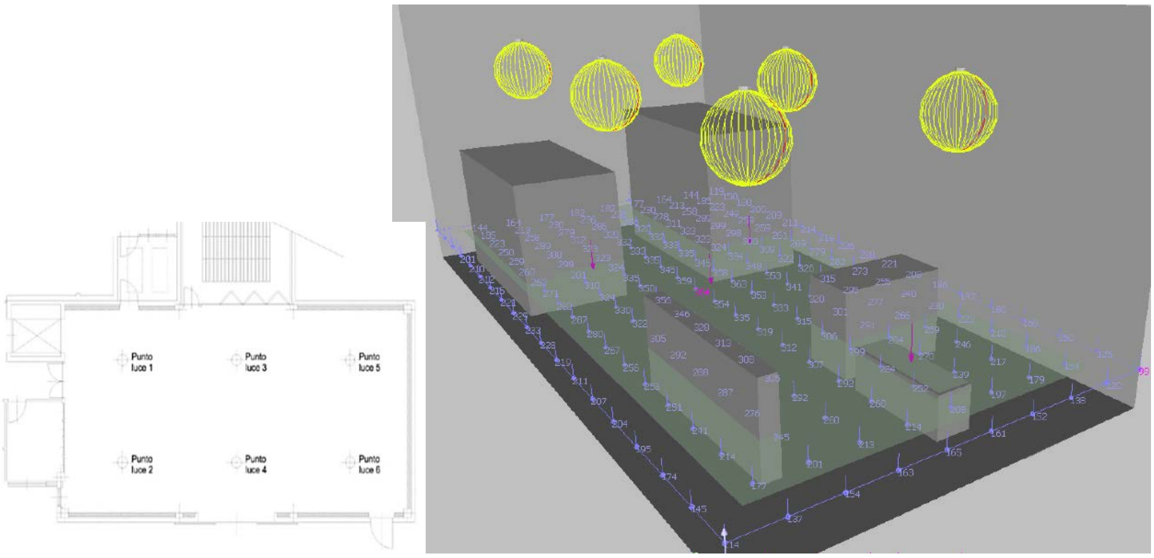

Figure 3 – The new lighting system: simulation

According to the future user needs, there is the possibility to remove luminaire "1" and shift luminaire "2" just in the middle of the corridor between the two bigger climatic chambers. In this case the remaining luminaire will be dedicated to further development of the research project, to enhance the performance of the system. This is possible because the system is not closed.

2.2 The new lighting system

The new lighting system is composed of:

- 6 luminaires with LED + remote phosphors, installed at 7 m height ca. with roto-symmectric emission (almost lambertian, with opening angle of 115° from the remote phosphors surface). At the moment there are no additional optics to modify the light distribution.

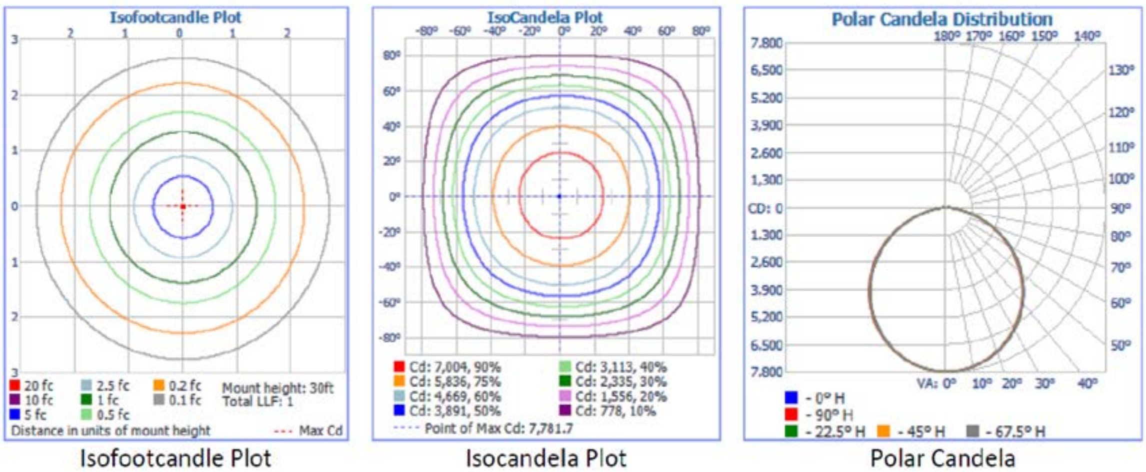

Figure 4 – Photometry of a luminaire

Heat removal occurs through an heat sink shaped as “heat pipe” with fins. Electronics components are inside the central part of the luminaire. Every luminaire has a maximum flux of about 22 klm and a luminous efficacy (ballast excluded) of 110 lm/W.

The luminaires are designed and realized ad hoc, and incorporate electronic devices for wireless communication and antenna.

Presence sensors, originally thought to be inside the luminaires themselves, have been realized as standalone devices, to allow more investigations on user habits while moving sensors through the room.

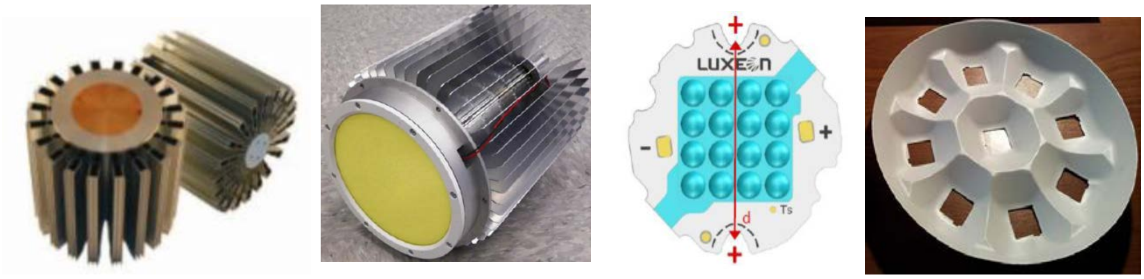

Figure 5 – Heat sink, blue LEDs and mixing chamber

- the dedicated smart control system, for the whole management of the individual luminaires. Wireless ZigBee protocol is used for the communication between all the devices: luminaires, photosensors, actuators, presence sensors, manual control devices, automatic control devices (tablets and touch screen have been selected for the case study, among other possibilities including smartphones). A central controller collects the data from the mesh net and overlooks all the manual and automatic controls.

  The internet browser calls a fix I address of the system server (ENEA server), where the main and additional software run. The main software in its turn calls the software – user interface. This configuration allows remote control and access to data from authorized PCs everywhere. Memory is allocated for the monitoring and data storage of a number of parameters like energy consumption, malfunctioning, lighting levels, presence states, manual interactions…. to allow short and long term assessment of the system;
- there are no traditional wall switches.

Luminaires have been provided by the Italian manufacturer NERI, with Intematix components.

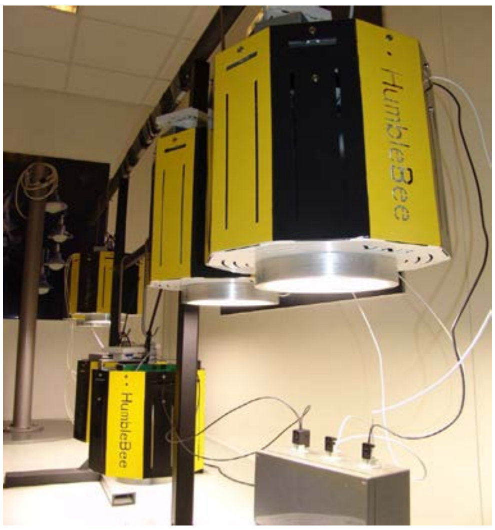

Figure 6 – The luminaires ready for the installation

2.3 The logic of the controls

- Manual controls logic: on /off of the luminaires, dimming, CCT modulation:
  - users can interact with the system on individual luminaires or on all luminaires together.
  - CCT modulation: available LED matrices are at 2500K, 4000K and 6000K. Default setting is 4000K. Independently from the selected CCT, the same illuminance level is maintained.
- Automatic controls logic: on /off of the luminaires through presence sensors, dimming, through photosensor:
  - when one of the presence sensors detects a presence, then luminaires are switched on, with a default setting of 300 lx in the whole hall. Manual controls can modify this settings. In case of strong daylight, illuminance may reach higher values: there are no specific provision for this, like automatic sreens, because the natural light enters the hall trough frosted glazing at more that 3 m height, avoiding any danger of glare or other negative consequences.
  - when all the presence sensors detect no more people in the hall, after a suitable delay time (10 minutes, delay considered suitable for industrial environment) the system is switched off.
  - it is always possible to interact in manual mode with the system, on one or more luminaires: the manual mode overrides the automatic one. After 10 minutes without presence, the system reverts to the automatic mode.
  - photosensors distributed in the hall dim the artificial light depending on the daylight contribution, according to the dynamic variations of the latter, by means of a close-loop control. In a long term perspective, photosensors may also compensate for flux depletion during time.
  - in case the daylight amount is adequate and there is presence of people inside the hall, luminaires are not switched on.
- scene setting: a number of scenes may be set, e.g.:
  - daytime scene: 8.00 AM to 8.00 PM, with manual or automatic controls as above described
  - nighttime scene: 8.00PM to 8.00 AM, thought for surveillance or cleaning personnel. In this scene the system is automatically switched on, set to 100 lx illuminance (no dimming), and it is switched off after the delay time of 10 minutes.

Figure 7 – The HumbleBee logo

3 Conclusions

Design of an innovative lighting system has been preformed and a case study has been implemented. The system is now in the commissioning phase. The following monitoring phase will lead to an assessment to the system, including the energy performances and the visual comfort. The system is open, so that future research and enhancement of the system is possible.

References

BLASO, L., LI ROSI, O., FUMAGALLI, S., LEONARDI, G., TARANTINI, V., POLLIDORI, R., RUSCONI, E., FRASCONE, A., ANTONELLI, A. 2013. Metodi sperimentali per la valutazione della qualità della luce, Sviluppo di sistemi a LED. Public report RdS/2013/114.

ROSSI, M., CASCIANI, D., MUSANTE, F.2013. Fosfori remoti per l’illuminazione di interni. Public report RdS/2013/113

PP62

POWER QUALITY ASSESSMENT ON VARIOUS TYPE OF STREET LIGHT IN TNB DISTRIBUTION SYSTEM

Nor Diana Ruszaini Mohd Zin, Khairuddin Abdullah, Sharni Ahamad Sabki
MALAYSIA

Abstract

Malaysian power utility company, Tenaga Nasional Berhad (TNB) has carried a feasibility study to assess and evaluate the deployment of Light Emitting Diode (LED) and Induction street light technology. Presently, the light source used is High Pressure Sodium Vapor (HPSV) and LED and Induction are the emerging lighting technology in the world that has rapidly developed in recent years as an alternative light. In this study, the study evaluates the energy efficiency, power quality and adaptability of new street lights are evaluated and assessed. The study involves installation of the HPSV, LED and Induction street lights at site, measurement of its electrical performance at site and lab testing. The study indicated that LED and Induction street lightings can provide between 20% to 60% energy saving to the utility. Most of the new emerging technology street lights surveyed also are provided with better Ingress Protection (IP) rating and colour rendering index (CRI) compared to HPSV street light.

Keywords: Light Emitting Diode (LED), Street Lighting, Induction, High Pressure Sodium Vapor

1 Introduction

The Government recently has call to move towards green technology. In specific, this study is concerned with the use of natural resources or replaced by higher efficient technologies. Electric energy is an indispensable component to people. Distribution of electric power from generation, transmission and distribution are important to meet requirement of the customer. Unfortunately, still more and more new technologies connected to the electric power supply have nonlinear voltage current characteristics, thus changing and deteriorating the overall power quality. Lower quality of electric power may effect to correct operation thus permanent damage to street lighting. Networks with non linear concentrated load can introduce distortions in the energy wave shape. In this study, it describes an assessment of LED street lighting technology and Induction street lighting technology as an alternative source to the current High Pressure Sodium Vapor (HPSV) street lighting. Their parameters characterizing the electric power quality in lines supplying lighting system is assessed by means of field measurement and lab testing. A technical test of performance and impact over lighting network is assessed.

For this study, LED and Induction street lighting technologies has been considered for its street lighting retrofit program as the emphasis was on long-life, white light products that improve colour rendering and reduce maintenance costs relative to HPSV street lights, the prevailing technology used today in Malaysia. The main benefits of LEDs and Induction technology are their reduced energy consumption, has longer lifetime better Ingress Protection (IP) rating and colour rendering index (CRI) compared to HPSV street light. The energy savings are claimed to have 40% or more and the lifetime is estimated at 50,000 hours with 4 times longer.

2 Methodology and Findings

A. LED Street Lights Field Trial

Four Pilot LED and Induction Street Light Technology from different countries and manufacturers were selected for this study and installed in Malaysia. The rated power consumption of the LED and Induction street lighting technologies ranges from 90 Watts to

120 Watts. The sites were chosen based on few criteria such as sufficient length of straight roadways with easy access for photometric measurement purpose. The sites shall also have minimum environmental interference such as trees and lighting from other sources which may affect the accuracy of photometric measurement results.

Figure 1: LED Street Light before and after installation

Figure 2: Induction Street Light before and after installation

A total of 80 LED and Induction luminaires were installed at selected public roadways in two different state since March 2012. In all types of luminaires, average and uniformity of illuminance and luminance were measured in order to guarantee level requirements recommended by MS825 Part 1 (Code of practice for the design of road lighting - Part 1: Lighting of roads and public amenity areas (Rev 1)).

B. LED and Induction Luminaires Power Quality Assessment

The quality of the white light is excellent, providing better colour definition unlike the High Pressure Sodium Vapor lights. The ability to clearly see people's faces and true colour of environment is enhanced. Efficacy of LEDs is constantly improving. At the time of publication, LED and Induction street lighting technologies has advanced to efficacy approaching to 120lm/W with lower wattage consumption compared to HPSV luminaires. Power, energy and electrical characteristics measurement are carried out to confirm that the luminaires are operating within the manufacturer specifications and comply with certain standards.

The purpose of the measurements is to determine the effect of introducing LED and Induction street lighting technologies that replaced present HPSV street light. Electric power quality analyzer which is Fluke 1750 Power Analyzer was used to perform continuous measurement of numerous quantities, including voltage, current, power, power factor and harmonics.

1) *Power consumption and Energy Saving*

Power measurement is required to determine the actual power consumption of LED and Induction luminaires. Instantaneous power measurement was performed at sites by using a portable power meter. In addition, monthly power consumption of each LED and Induction street lighting technologies were also monitored using the installed energy meter.

Based on the power consumption measurement, it is shown that the lowest energy consumption is 85Watt by the LED street light technologies A. The highest power consumption recorded is 96Watt by the LED street light technology D. The amount of energy saving by the LED street light technologies range from 36% to 43%, compared to the 150 Watt HPSV. For Induction street light, the lowest energy consumption is 105Watt by the Induction street light technologies G. The highest power consumption recorded is 131Watt by the Induction street light technology H. The amount of energy saving by the LED street light technologies range from 13% to 30%, compared to the 150 Watt HPSV. A summary of measured electric power and its saving results from the study are tabulated in Table 1 and 2.

Table 1: Measured power consumption and energy saving of LED street light technologies compare to 150W HPSV

LED Street Light Technology	Declared Energy Consumption (Watt)	Measured Energy Consumption (Watt)	Energy Saving (%)
A	90	85	43
B	90	92	39
C	90	92	39
D	90	96	36

Table 2: Measured power consumption and energy saving of Induction street light technologies compare to 150W HPSV

Induction Street Light Technology	Declared Energy Consumption (Watt)	Measured Energy Consumption (Watt)	Energy Saving (%)
E	120	118	21
F	120	113	25
G	100	105	30
H	120	131	13

2) *Electrical Characteristics*

Electrical characteristics in terms of power quality and power factor of the LED and Induction street light technologies are assessed to ensure they are operating within the specified limits of certain standards. Power quality measurements were performed at laboratory to determine the harmonic current emission level and flicker level produced by LED and Induction luminaires. Results of power quality measurement results are compared to the MS IEC 61000-3-2: 2000 (Limitation of voltage fluctuations and flicker for equipment input current <16A per phase) and MS IEC 61000-3-3:2005 (Limitation of voltage fluctuations and flicker for equipment input current <16A per phase). The power factor of each LED and Induction street light technology is also measured at laboratory to ensure they are complied with TNB requirement which is more than 0.85.

The site measurement results for electrical characteristics are summarized in Table 3 and 4. Power factor recorded indicates that all four LED and Induction street lighting technologies have a power factor of higher than 0.9. It is observed that individual harmonic current emission for all the LED and Induction street lighting technologies tested are within the limits. LED street light technology D has the highest total harmonic distortion current which is 18.09% and Induction street light technology H has the highest total harmonic distortion current which is 11.23%. Flicker measurements indicate that the short time flicker, Pst for all LED and Induction street light technologies are within the limits of 1.0.

Table 3: Electrical characteristic measurement of LED street light technologies

LED street light Technologies	Power factor	THD Current (%)	Short Time Flicker (pst)
A	0.95	9.50	0.261
B	0.96	7.57	0.308
C	0.94	13.1	0.275
D	0.93	18.09	0.288

Table 4: Electrical characteristic measurement of Induction street light technologies

Induction street light Technologies	Power factor	THD Current (%)	Short Time Flicker (pst)
E	0.98	7.15	0.371
F	0.98	7.97	0.475
G	0.98	8.58	0.330
H	0.99	11.23	0.863

Figures 3, 4 and 5 present selected results of measurements carried out at measurement points on the electric power network shown for LED street light technologies C.

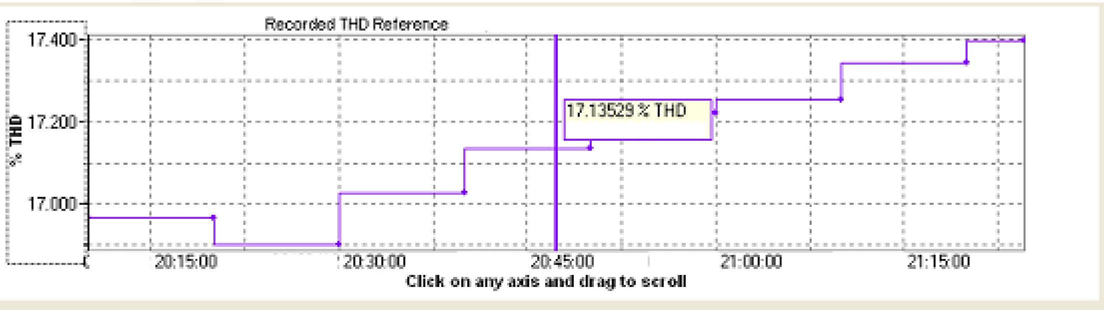

Figure 3: Recorded THD current for LED street light technologies C

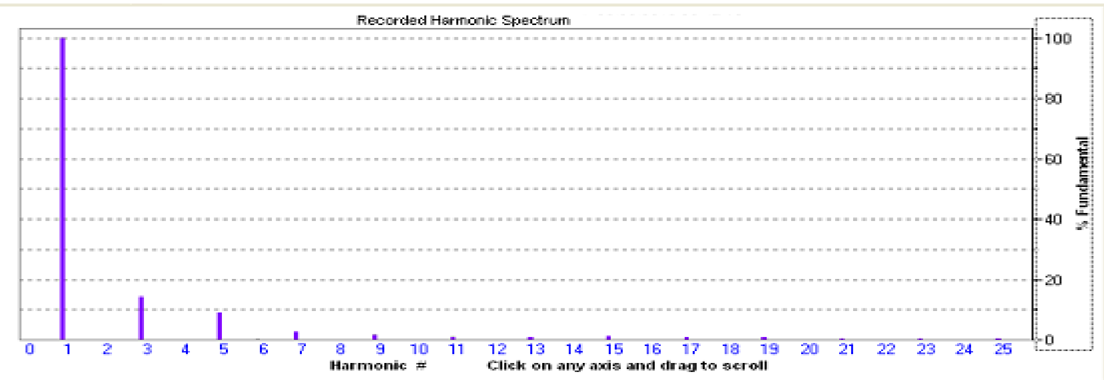

Figure 4: Recorded harmonic spectrum for LED street light technologies C

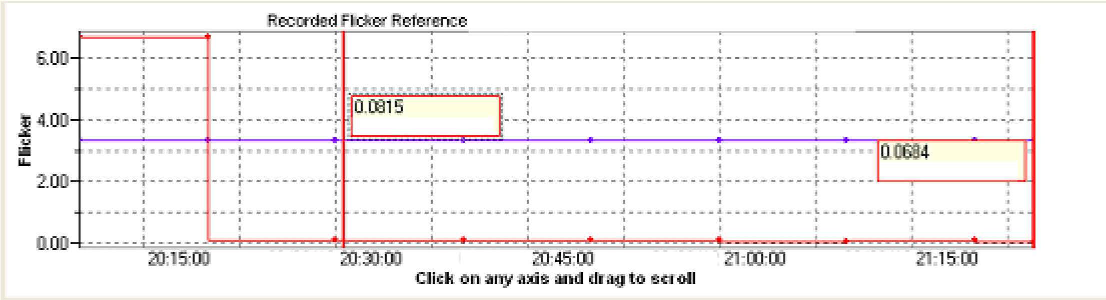

Figure 5: Recorded flicker for LED street light technologies C

3 Conclusion

This paper describes a study of energy saving testing and more efficient luminaires with the concerned the issue of the electric power quality. Field trial and laboratory test were carried on studding the LED and Induction street light technology performance and comparisons were made. The measurements were aimed at determining deployment of LED and Induction street light technologies will result in any significant deterioration of the electric power quality.

Technically, LED and Induction luminaires are possible technologies represent the present world industry best practice solutions as compared to HPSV street light as in terms of energy saving and electrical characteristics. The results provided for power quality, LED and Induction luminaires are not expected to cause any issues since harmonic current emission and flicker generated by LED and Induction luminaires are within the permissible limits. In addition, all LED and Induction street light technologies have recorded more than 0.9 power factor. In terms of energy consumption, the LED and Induction street light technologies have consumed less energy, which is between 13% to 43%, compared to the 150 Watt HPSV. The energy saving obtained is significant and the harmonics are acceptable.

With the viable and continuous improvement of LED street light design and technology, it is expected that it will be beneficial to enable the smooth and timely transition into new technologies to obtain maximum benefit in terms of energy saving, lower maintenance cost and better environmental impact. However, the electric power supply systems affected by the LED and Induction street light technologies should be monitored.

References

[1] Dr. Kurt Schipman, Dr. François Delincé “The Importance of Good Power Quality”

[2] T. Cook, J. Shackelford, M. Johnson, T. Pang, “Demonstration Assessment of Light Emitting Diode (LED) Street Lighting, Phase III Continuation: City of Oakland, California”, Nov. 2008

[3] U. S. Department of Energy, Solid-State Lighting GATEWAY Demonstration Results,

http://www1.eere.energy.gov/buildings/ssl/gatewaydemos_results.html (accessed 9th August 2012)

[4] CEA Technologies Inc, “Power Quality Energy Efficiency Reference Guide”, 2007

[5] Roger C Dugan, Mark F McGranaghan, Surya Santoso, H Wayne Beaty, “Electrical Power System Quality”

PP63

ECONOMICAL IMPACT OF G CLASSES ON LED PHOTOMETRY

Raoul Lorphèvre[1], Laurent Maghe[1], **Jérôme Dehon[1]**
[1] R-TECH SA, Liège, BELGIUM
r.lorphevre@rtech.be

Abstract

LED technology brings many changes to road lighting. The revolution is not only at a technical level but also in the way to make a road design. Some of criteria in current standards are not applicable as such to the LED technology. The purpose of this article is to show that the current state of standards and some changes may decrease the energy advantage of LED technology.

Unfortunately, current and upcoming standards are not equal for absolute photometry compared to relative photometry.

Keywords: Photometry, Exterior applications, Glare

1 Introduction

Many photometric criteria were determined in standards to characterize a light source with or without control of light distribution (reflector, lenses, etc ...). Yet it seems that some of these criteria are not applicable as such to the LED technology. Glare is a part of them. The fact, among other things, to have a point source would affect the perception, the comfort of a user. The purpose of this article is not to prove or seek a physiological solution to glare of LEDs, but to show that the current state of standards and some modifications in upcoming standards may decrease the energy advantage of LED technology.

Several criteria exist to determine and limit the discomfort: Threshold Increment (TI), G classes, D classes (CEN) ... each have their own field of application. G classes are not suitable for LEDs. Indeed, these classes are determined for G matrices in relative photometry, while LM 79-08 recommends that LED lights are measured in absolute photometry. The prEN 13201-2 is trying to correct this problem by proposing another formula to determine G classes for absolute photometry. Unfortunately, this proposal has not the same impact on absolute photometry compared to relative photometry. In general, the same light distribution is one G class lower when it is an absolute photometry than relative photometry.

These criteria are not yet adapted to the LED technology, projects end up with several types of glare requirements. The latest version of the CIE 115-2010 Annex D allows TI requirements for P classes but instead of G classes. A conflict can arises when one imposes a G class on M-class road where TI is applied. G classes are more restrictive than the TI and it has a non-negligible financial impact.

We quantified the impact in terms of energy consumption. Different types of roads, pedestrian areas were compared for several C and P classes equipped with many LED photometries. These photometric distributions have been modified to meet the classes G4 and G6 but also G*4 and G*6 classes for absolute photometry of prEN 13201-2. This standard is the revision draft of the CEN road lighting standard, currently on Enquiry.

2 Glare definition in standards

The G classes are defined in the CIE 115:2010. These are used to control the glare in pedestrian and low speed traffic areas in an alternative way of TI. The Pedestrian and low traffic speed areas (P classes) are now defined with TI values. A G class is calculated with the light distribution in efficiency of a luminaire. The luminous intensities in cd in any direction are divided by the luminous flux of the source; the result is expressed in cd klm^{-1}. Then the G classes is selected based on the table 1.

Luminous Intensity Class	Maximum luminous intensity in cd klm-1			Other requirements
	At 70° and above	At 80° and above	At 90° and above	
G1	---	200	50	None
G2	---	150	30	None
G3	---	100	20	None
G4	500	100	10	Luminous intensities above 95° to less than 1 cd klm-1
G5	350	100	10	
G6	350	100	<1	Luminous intensities above 95° to less than 1 cd klm-1

Table 1: G classes following CIE115:2010

As we see, the G classes are defined with efficiency photometry. But LED luminaires must be measured in absolute photometry. Therefore we must make the observation that these G classes cannot be applied to LED luminaire.

To solve this gap in standards, the prEN 13201-2 defined new G* classes. This project of standard also defined TI values for C and P classes, but these values are not the same as for the CIE 115:2010. The G* classes are recommended when the threshold increment (TI) cannot be calculated and when it’s necessary to restrict glare.

G* class is calculated with the absolute photometry of a luminaire. The luminous intensities in cd in any direction are divided by the luminous flux emitted in directions below the horizontal; the result is expressed in cd klm^{-1}. Then the G* classes is selected based on the table 2.

Class	Maximum proportion between the luminous intensity and the luminous flux emitted in directions below the horizontal in cd/klm			Other requirements
	At 70°	At 80°	At 90°	
G1	---	200	50	None
G2	---	150	30	None
G3	---	100	20	None
G4	500	100	10	Luminous intensities above 95° to be zéro
G5	350	100	10	
G6	350	100	0	Luminous intensities above 95° to be zéro

Table 2: G* classes following prEN 13201-2

This new glare classification allows giving a solution to the glare of LED luminaire and the formula is the same for HID and LED luminaires. The table 1 and 2 are similar, but the formulas to determine it are different. We realize such comparisons with simulations to show the differences.

3 Method

The G and G* classes are advisable for pedestrian and low speed traffic areas. We will carry out a series of photometric comparison of different lighting classes of illumination (C & P). For each new set, two results will be highlighted: the largest spacing and layout that consumes the least.

To perform reliable calculation, we take several very different light distributions. We determine the G and G* classes to show the differences in the two formulas. At the same time, these distributions are modified to match G4 and G6 classes performance (if necessary) and G*4 and G*6 classes according to prEN 13201-2. These new light distributions are compared with the best results obtained with the original distribution.

3.1 G classes *Vs* G*classes

We choose eight light distributions which cover most of the needs for road lighting. They are identified by numbers from 5068 to 5118. For each light distribution, we determine the G and the G* classes.

Light distribution number	Description	Efficiency	G classes	G* classes
5068	Pedestrian Area	81.1%	G1	G*1
5096	EN Road Lighting	84.2%	G2	G*1
5098	Pedestrian Area	84.9%	G4	G*2
5102	EN Road Lighting	85.2%	NC(1)	NC(1)
5103	EN Road Lighting	83.7%	NC(1)	NC(1)
5112	Nam Road Lighting	81.7%	NC(1)	NC(1)
5117	Nam Road Lighting	87.4%	G3	G*2
5118	Nam Road Lighting	87.0%	G3	G*2

(1) Not Classified.

Table 1: G and G* classes of different light distributions.

Most of these light distributions are optimized for road lighting and luminance requirements. In road lighting, the TI is the requirement used to evaluate the glare. These are design to perform good TI not G classes. We observe this in the Table 1. We find also that in general the light distribution loses one class between G and G* classes. Following this result for the same level, G* classes are less glaring. This implies that the glare classes are not the same for CIE and CEN and fixtures that meet the old G classes of CEN are no more compliant.

3.2 New G and G* light distributions

The definition of G classes imposes maximum luminous intensities at certain angle (70°, 80°, 90°) and above. Which means that no luminous intensity can exceed the luminous intensities in cd/klm at the angle given in the table for the class and above. For G* classes, the luminous intensities in cd/klm shall be maximum the value obtained by linear interpolation between the two angles given in the table for the class.

The figure 1 represents an original light distribution, the figure 2 and 3 represent respectively G4 and G*4 classes by simulations. For all our simulations we keep simulations of G* classes following prEN 13201-2 which are more realistic. We kept the same output flux for each new light distribution.

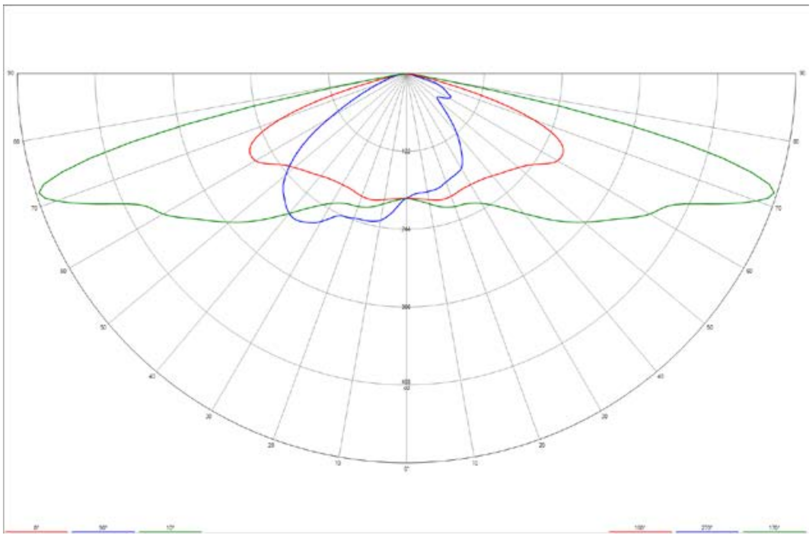

Figure 1: Original light distribution (G2 class).

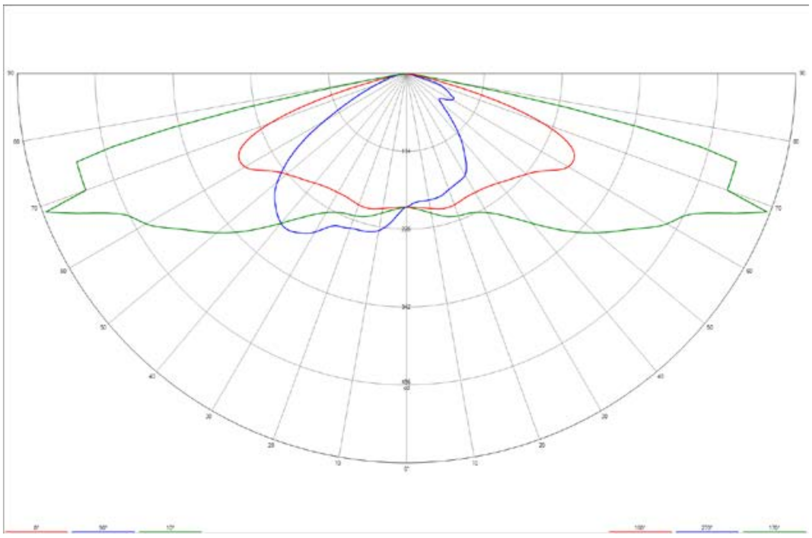

Figure 2: G4 class by simulation following CIE 115:2010.

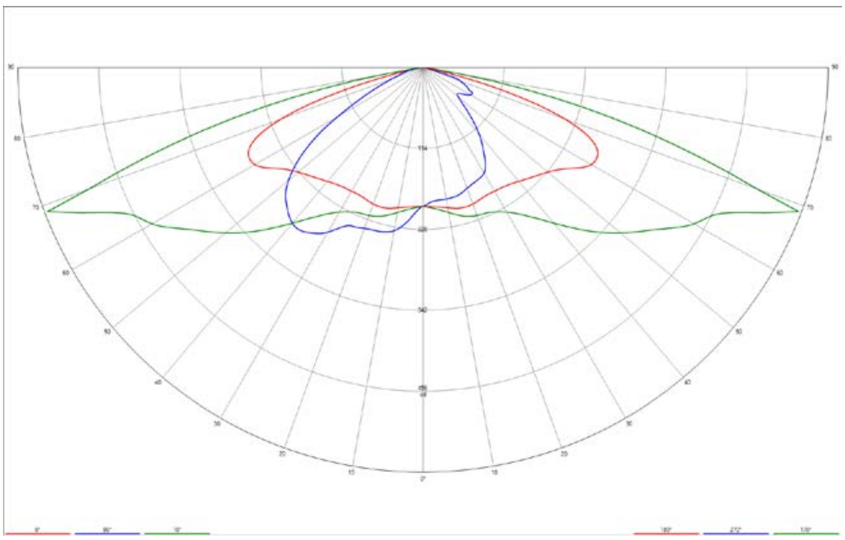

Figure 3: G*4 class by simulation following CEN 13201-2.

4 Simulations

We realize such simulations on P and C classes. We define a pedestrian path 3m wide with pole of 4 and 5 m high one-sided. The conflict areas are made with a road 6.5m wide with pole of 6 and 8 m high one-sided. We used these designs on all classes (Figure 4).

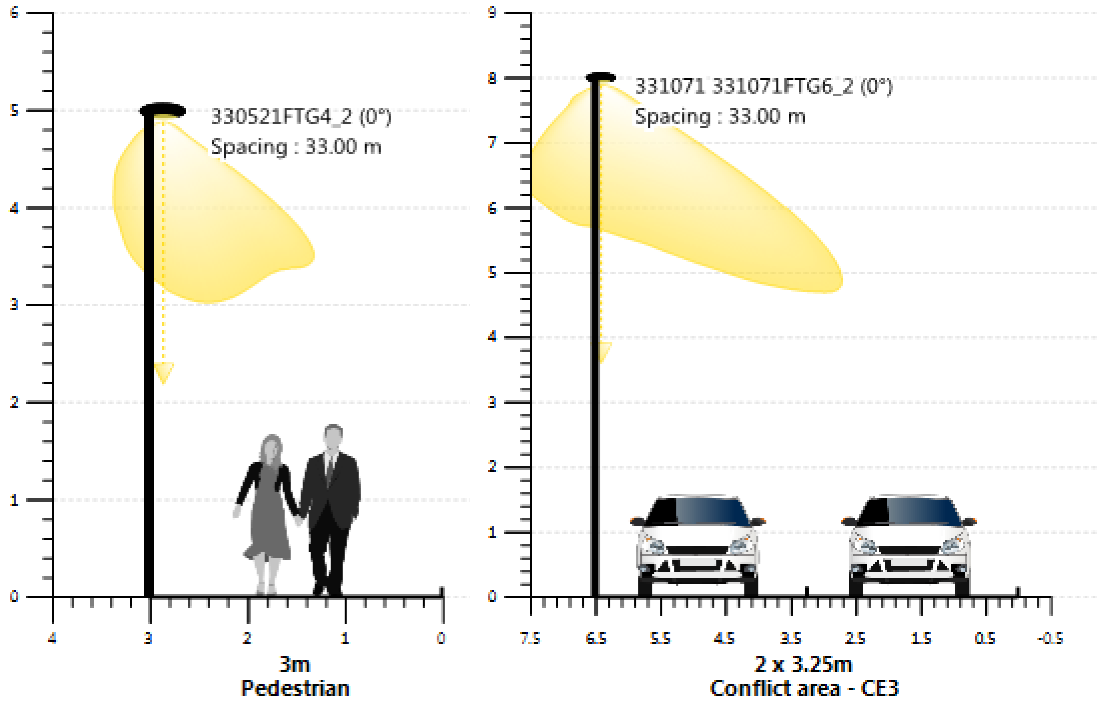

Figure 4: Simulated cross sections.

For each 8 light distributions, we selected the 2 solutions with wider spacing and smallest consumption. These results permit to determine an average installation in terms of power per km. This solution is regarded as benchmark. Then, we perform the same calculations for different G and G* classes (G4, G6, G*4, G*6). The results of the Benchmark and the G and G* classes are compare to bring out increase or decrease of the power following the requirement of G or G* classes.

Class	Height (m)	G4	G6	G*4	G*6
P1	4	2%	20%	3%	15%
	5	6%	14%	9%	16%
P2	4	0%	19%	7%	17%
	5	6%	20%	8%	19%
P3	4	0%	20%	0%	13%
	5	2%	15%	5%	16%
P4	4	14%	28%	15%	26%
	5	2%	14%	2%	8%
P5	4	4%	14%	5%	10%
	5	1%	15%	1%	10%

Table 3: Differences in % between the power of benchmark and G & G* classes for P classes.

We noticed, as expected, that a greater requirement of G and G* classes increases the power per km. In average, when a G4 class is imposed increasing the general power of 3.6% and we reach 5.6% for a G*4 class. With a G6 class the increase may reach 17.8%. The difference is slightly lower for classes G * 6, but reached 15%. Despite the differences in formula to calculate the G and G*classes, the differences are small between the same two levels of classes.

Class	Height (m)	G4	G6	G*4	G*6
C0	6	6%	8%	6%	8%
	8	5%	8%	1%	3%
C1	6	5%	7%	3%	8%
	8	3%	6%	1%	3%
C2	6	0%	6%	-1%	11%
	8	0%	5%	0%	5%
C3	6	2%	7%	6%	12%
	8	0%	4%	2%	4%
C4	6	2%	6%	3%	10%
	8	0%	6%	1%	7%
C5	6	2%	8%	3%	12%
	8	1%	7%	3%	9%

Table 4: Differences in % between the power of benchmark and G & G* classes for C classes.

A first observation from Table 4 is that the influence of the glare class is lower for conflict areas. In fact, the G4 class increases the consumption of 2.2% and for G*4: 2.4%. The effect is the same for G6 class: 6.5% and 7.6% for G*6 class. The differences with the result of P classes can be explained by the height of the luminaires and more over by the requirements of uniformity. Indeed, the overall uniformity of P classes is from 20% to 33% and C classes are always in minimum at 40%. For these two reasons, luminous intensities at high levels in the polar diagram are less important for the results in conflict areas.

The LED Technology allows adjusting the output flux of the luminaire precisely to achieve the requirement. For each simulation, we adjust the flux to decrease the electrical power. Then, we recalculate the differences between the benchmark and the G and G* classes.

P Classes	G4	G6	G*4	G*6
Without Dimming	3.6%	17.8%	5.6%	15.0%
With Dimming	3.5%	16.9%	3.7%	12.4%

Table 5: Differences between benchmark and G&G* classes with and without dimming for P classes.

C Classes	G4	G6	G*4	G*6
Without Dimming	2.2%	6.5%	2.4%	7.6%
With Dimming	2.8%	5.7%	3.1%	4.5%

Table 6: Differences between benchmark and G&G* classes with and without dimming for C classes.

We remark that for level 4 of G and G* classes, the dimming has, in general, a negligible effect to reduce the increase of power consumption. The effect is more important for G6 and G*6 classes but it is not enough to ignore the effect of classes G on power consumption.

5 Discussion

The aim of this paper was to demonstrate that a change in formula to determine a glare class will have an economic impact on the power consumption of new installation. Out the logical power consumption increase when a higher G class is impose, it seems that the proposal of G*classification didn't affect sensibly the power consumption. The differences are negligible. Otherwise, the use of dimming allows reducing the effect of high G class requirements.

Changes in a technology need often an adjustment in the active standards. The LED technology needs a huge standardization work, but should we slightly modify the standards to incorporate new technology or is it just an opportunity to find another way? The adjustment proposal to uniform the glare classification by the prEN13201-2 is a try but not the solution.

The G* class proposal places the HID and LED on the same level but the HID luminaires may not meet certain specifications anymore: Changing G classes to G * classes loses a level all light distributions.

CIE and CEN standards allow today TI for pedestrian and conflict areas. The way to determine TI for CIE and CEN standards is not the same; it explains the different levels for P and C classes. We noticed also that, in general, for CIE 115 the G class is more restrictive than TI. It seems logical to use G class when a lighting project need to have a better glare control. But, in prEN 13201-2, we observe that some G*6 class didn't respond to the TI requirements of the P or C class. This remark needs some further investigation and it seems that the discussion about these values is not yet fixed.

The LED technology allows designing easily a light distribution. Nothing prevents a designer to create a luminaire with a peak of 500cd/klm at 65 °. The light distribution would certainly comply with G*6 class. But it may be more glaring as his classification does not show.

HID sources have, in average, the same light emitting surface for the same output flux. A PCB of LED can have several sizes for the same output flux. The glare will be not same between 1 LED and a PCB of 100 LED (same output flux) but these will have the same glare class. For example, the use of D classes from the prEN13201-2 can be useful. This classification takes only into account the output flux (no matter of efficiency or absolute photometry) and the apparent area of the luminous part at one angle (85°). Can we imagine a general glare classification as a mixt of the G and D classes: A table with maximum luminous intensities in function of apparent area of the luminous part at different angle?

References

CIE 1994. CIE 112:1994 Glare Evaluation System for Use within Outdoor and Area Lighting.

CIE 2002. CIE 146:2002 CIE Equations for Disability Glare.

CIE 2002. CIE 147:2002 Glare for Small, Large and Complex Sources.

CEN 2003. EN 13201 1 to 4 Road Lighting

CIE 2010. CIE 115:2010 Lighting of roads for motor and pedestrian traffic.

CEN 2014. prEN13201-2 Road Lighting Part 2:Performances requirements

PP64

LED TUNNEL LUMINAIRES: WITH OR WITHOUT A PROTECTOR?

Raoul Lorphèvre[1], Laurent Maghe[1], **Jérôme Dehon[1]**
[1] R-TECH SA, Liège, BELGIUM
r.lorphevre@rtech.be

Abstract

Currently, several possibilities exist to protect LED lenses: with or without a protector. To compare these two solutions, we built two identical luminaires, one with flat glass over the lenses and one where the lenses are in direct contact with the atmosphere. To perform the comparison, we installed them in a tunnel, the dirtiest place for a luminaire. Its findings clearly indicate that the presence of a glass protector ensures better safety for users by preserving the luminous flux and the luminance, by reducing maintenance requirements and by contributing to energy efficiency.

Several conclusions can be drawn from this study. The general level of lighting in a tunnel is dangerously reduced in the case of luminaires with unprotected lenses. The precise calculations used to design a tunnel lighting solution that reconciles the required lighting levels with the need for energy efficiency are quickly rendered null and void by the soiling of the lenses that are directly exposed to the atmosphere.

Keywords: Photometry, Exterior applications, Maintenance factor; LED luminaires, Tunnel, Lenses

1 Introduction

Lighting a tunnel for road traffic has the main objective to ensure that visibility conditions enable the vehicles using the tunnel to move about, during the day as well as at night and at a given reference speed, in security, comfort and confidence; these conditions being at least equivalent to those, at the same moment, on the access roads leading to it.

In order to reach that objective, it is essential that the road users have at their disposal inside the tunnel, enough visual information for the geometry of the road section stretching ahead of them, as well as for the presence and motion of potential obstacles, these latter including more specifically, other road users. But it is also essential to maintain these photometric specifications over time.

HID luminaires have always been made the same way: lamp, reflector, protector. Apart from changing the type of lamp, the luminaires did not change. The advent of LED technology has enabled the constitutive elements of a luminaire to be modified. The first one is often the replacement of the reflector by lenses. Some types of lenses allow the protector to be removed from the luminaire. Suppressing this element has a great advantage: it increases the output flux of the luminaire.

However, the atmosphere in a tunnel is aggressive. The soiling of the protector or lenses requires a regular cleaning cycle to maintain the photometrical requirements over time. The deposit of dust on an object depends on its shape. The light emitting surface does not have the same shape with or without a protector. The aim of this paper is to explore if this change is significant or not on the performance of the luminaire over time.

2 Test phase

We created 2 identical luminaires, one with and one without a protector but with the same photometric curve. We chose 3 specific zones in the tunnel (one in the entrance zone and two in the interior zone of each tube).The luminaires were installed overhead for a period of 3 months in the winter. To eliminate all possible influences due to the variation of the output flux in time, the LEDs were turned off during the entire experiment.

2.1 Test site

The test site is Cointe Tunnel, composed of 2 tubes for the 2 different traffic directions (named Cointe and Kinkempois). This tunnel is an urban tunnel in the city of Liège which links two motorways (E25-E40). The average volume of traffic is 70 000 vehicles per day. To ensure the security of this tunnel, maintenance operations are scheduled every 3 months. During this maintenance, the entire tunnel is cleaned. This tunnel was chosen for the traffic density and the frequent cleaning cycle.

2.2 Luminaires

We built 2 identical luminaires. These luminaires are equipped with a linear LED disposition and with an IP 66 protection. One is closed with a flat glass protector, the other with lenses in PMMA (Figure 1). The lenses are disposed to be in contact with the atmosphere. The light distribution is the same in the two luminaires. The two kinds of luminaires are installed near each other in the tube.

Figure 1 – Pictures of the 2 different test luminaires

3 Measurements method

Each luminaire was measured in a goniophotometer. These measurements recorded the lighting distribution of each luminaire before the test. This measurement is considered as a reference (value 100%). The luminaires were measured a second time, just after the test, when they were returned by the contractor who had installed them in the tunnel. And a third time after a manual cleaning.

The luminaires equipped with a protector are just cleaned with a damp cloth. The luminaires without a protector are cleaned lens by lens with a cloth and a soft cleaner.

4 First observations after the test

After twelve weeks in the tunnel, we received the luminaires back from the contractor before the tunnel was cleaned. We visually analysed that the soiling is not the same on the two kind of luminaires. The dirt on the luminaire with a protector is normal and uniform. On the luminaire without a protector, the dirt is non-uniform and asymmetric following the traffic flow direction (Figure 2).

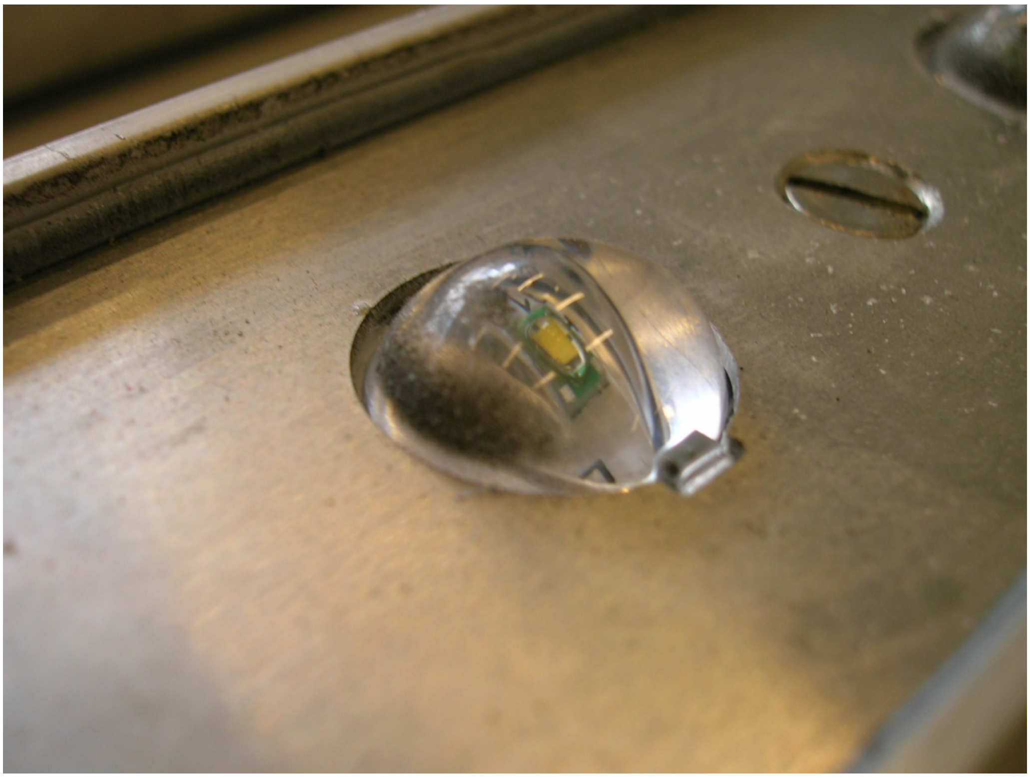

Figure 2 – Lens pictured after the test

5 Results - Change in Efficiency

The results are presented in the two tables below (Table 1 & Table 2) that compare the remaining output flux of the luminaires with or without protector.

Luminaires with protector

Luminaires	Entrance Cointe	Interior Cointe	Interior Kinkempois	Average
New	100	100	100	100
"Dirty" after 3 months	93,3	92	95,9	93,7
Cleaned	100	100	100	100

Table 1 – Results in efficiency for the luminaires with protector

Luminaires without protector

Luminaires	Entrance Cointe	Interior Cointe	Interior Kinkempois	Average
New	100	100	100	100
"Dirty" after 3 months	86,4	81,2	87	84,8
Cleaned	97,9	96,8	97,9	97,5

Table 2 – Results in efficiency for the luminaires without protector

5.1 Analysis

We noticed a "degree of site pollution", a variable depending on the location of the luminaires in the tubes. With or without a protector, the "less polluted" is the interior Kinkempois zone and the "most polluted" is the interior Cointe zone. The difference between the "most polluted" and "less polluted" is 4% for luminaires with a protector and 6.5% without a protector.

Despite carefully cleaning the luminaires without a protector, there is an irreversible loss of efficiency of 2.5% after only 3 months of installation. The average depreciation of luminaires without a protector is 10% higher than that of luminaires with a smooth flat glass.

An examination of photometric surveys (see polar curves) confirmed "asymmetric soiling" observed on devices without protective glass (Figure 3 & Figure 4).

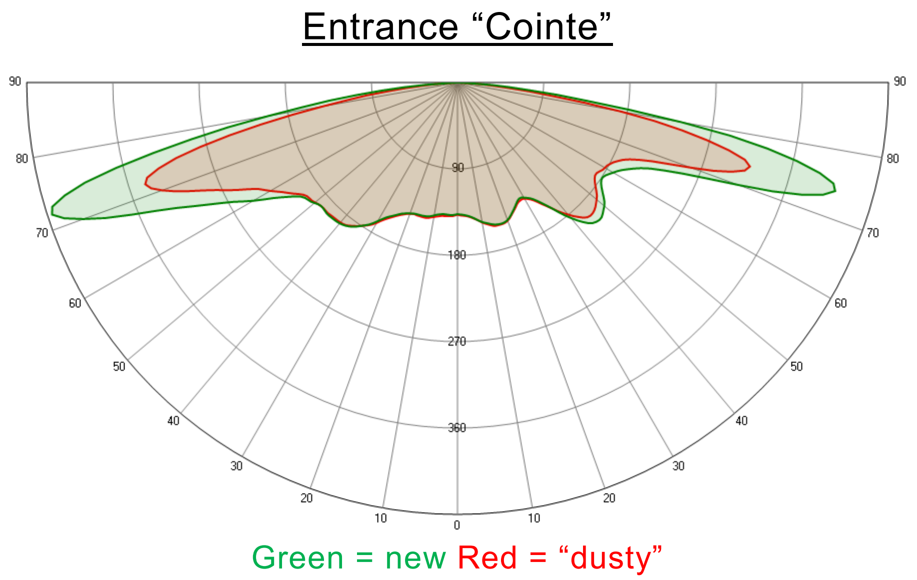

Figure 3 – Photometric curves of luminaires with a protector before and after the test

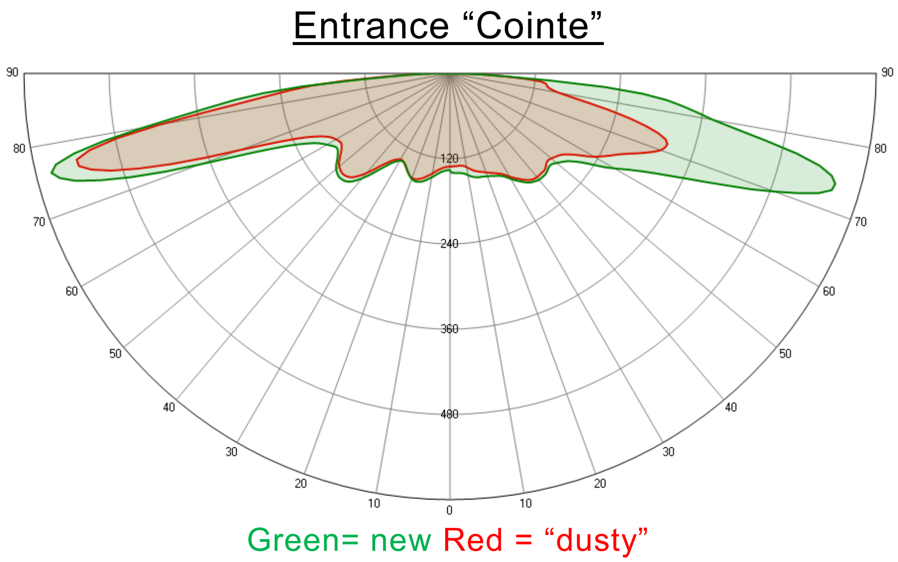

Figure 4 – Photometric curves of luminaires without protector before and after the test

The light distribution became asymmetric type "pro-beam" and changes the results in luminance on the road. We decided to use theses measurement to perform such lighting calculations. The next section gives the luminance level obtained with the "dirty" lighting distribution for three types of road surfaces (R3 - R2 and R1), the level with the new luminaires being considered equal to 100.

6 Results - Change in Luminance

We performed lighting calculations with the photometric curves. The lighting design is the same for each case. The types of road surface have an influence on the level of luminance.

Luminaires with a protector

Luminaires	Entrance Cointe	Interior Cointe	Interior Kinkempois	Average
R3	87,7	85,6	91,3	88,2
R2	89,4	87,7	92,7	89,9
R1	91	89,5	93,7	91,4

Table 3 – Results in luminance for the luminaires with protector

Luminaires without protector

Luminaires	Entrance Cointe	Interior Cointe	Interior Kinkempois	Average
R3	73,2	73,4	58	68,2
R2	78,4	77,7	67,3	74,4
R1	82,7	81,9	76,7	80,4

Table 4 – Results in luminance for the luminaires without protector

The level with new luminaires is considered equal to 100.

6.1 Analysis

Although the average decrease in efficiency of a luminaire with a protector is only 6.3%, the average decrease of the luminance level varies from 8.6 to 11.8% depending on the road surface, and reached in the worst case, 14.4%. The clogged glass protector further reduces the luminous intensities to high angles (> 50 °) which are the most efficient in luminance.

	With protector		Without protector	
	Average flux decrease	Average luminance decrease	Average flux decrease	Average luminance decrease
R3	6.3%	11.8%	15.2%	31.8%
R2	6.3%	10.1%	15.2%	25.6%
R1	6.3%	8.6%	15.2%	19.6%

Table 5: Summary of results

For luminaires without a protector, while the average decrease in efficiency is 15.2%, the average decrease of the luminance level varies from 19.6 to 31.8% depending on the road surface, and reached in the worst case, 42%. These large losses are caused by the large and asymmetric contamination of the lenses. Note that for luminaires without a protector, we still have a loss of 2.5% of flux after intensive cleaning.

7 Conclusions and further development

To estimate the depreciation coefficient based solely on the change in total output is insufficient, especially when it comes to roads made of asphalt. Any luminaire that is not enclosed by a protective smooth glass should be avoided for tunnel lighting.

The next step of this study is currently on-going; we have put new luminaires in the tunnel but will leave them for a longer period to see the effect of the real cleaning system used on the two kinds of luminaires. We also expect to find an effect on the dirt in function of the transversal and longitudinal installation across the tunnel.

References

CIE 2004. CIE 88:2004 2d edition. Guide for the lighting of road tunnels and underpasses. Vienna: CIE.

SPW 1998. SPW Cahier special des charges n°33-1. Tunnel sous Cointe – Equipement électromécanique - Eclairage. Liège: SPW.

Royer, M. 2013. Lumen maintenance and light loss factors: consequence of current design practices for LEDs, LEUKOS: The journal of the illuminating Engineering Society of North America, 10:2, 77-86.

PP65

EMPIRICAL EVIDENCE TOWARDS APPROPRIATE LIGHTING CHARACTERISTICS FOR PEDESTRIANS

Steve Fotios[1], Biao Yang[1], Phil Edwards[2]
[1] School of Architecture, University of Sheffield, UK
[2] London School of Hygiene & Tropical Medicine, UK
steve.fotios@sheffield.ac.uk

Abstract

There is a need for empirical data to review design standards for pedestrian lighting. This paper presents a summary of two ongoing UK research projects, the MERLIN project which is examining lighting for pedestrians' visual tasks, and the LANTERNS project which is examining the effect of lighting on reported crime and accidents associated with pedestrians, discussing research methodology and tentative findings from the MERLIN project.

Keywords: e.g. Road lighting, pedestrians, visual tasks, crime

1 Introduction

In the UK and the EU the target average illuminance levels for subsidiary roads (which includes residential roads) range between 2 lx and 15 lx in six classes [BSI 2003]. However, these illuminance levels do not appear to be based on appropriate empirical evidence and thus are in need of review [Fotios & Goodman, 2012]. A new TC is being established in Division 4 to do this. Two approaches to establishing appropriate light levels are a bottom-up task approach and a top-down cost-benefit approach. The task approach seeks to identify optimum lighting conditions for tasks critical to pedestrian activity: the cost-benefit approach seeks to optimise the cost of lighting provision against the benefits of pedestrian safety. The Technical Committee will also seek to consider users expectations by surveying international standards for pedestrian lighting.

2 Visual tasks

2.1 Critical tasks

One approach to establishing optimum light levels for pedestrians is to identify their critical needs and then investigate how these needs are affected by variations in lighting. These needs are typically assumed to be obstacle detection and recognition of the intent and/or identity of other road users, together with subjective evaluations of reassurance and comfort [Caminada & van Bommel, 1980; Fotios & Goodman, 2012]. Recent work has been carried out to validate these assumptions.

Eye-tracking was used to investigate pedestrians visual fixations, in daytime and after dark, with a concurrent dual task employed to better identify the fixations critical for safe walking from the unconscious (day-dreaming) and non-essential fixations [Fotios et al, in press (a)]. The output of an eye-tracking study is a video of the test participant's field of view upon which is superimposed a crosshair marking the direction of gaze – the visual fixation. A common approach to interpretation of these data is to count the frequency by which certain types of objects are fixated. This approach suffers from erroneous assumption that the object fixated is indeed of importance, and also that the frequency of occurrence of an object in a natural setting (e.g. the number of pedestrians encountered) affects the frequency of fixation – if only few pedestrians are encountered this leads to a low frequency of fixation but that does not imply that fixation on pedestrians is unimportant. The dual task approach was found to provide a good indication of critical fixations by helping to ignore the less-critical fixations and to be robust against the frequency of occurrence.

It was concluded that the near path (<4 m) and distant people (>4 m) are critical targets of visual fixation for pedestrians. Fixation on the near path may be related to identification of obstacles, and this would be aided by enhanced detection at a further distance. Fixation on distant people suggests a desire to evaluate the intentions of others at sufficient distance to take avoiding action if necessary.

2.2 Reassurance

Reassurance is the confidence a pedestrian might gain from road lighting (amongst other factors) to walk along a road, in particular if walking alone after dark, and is used here to encompass the terms perceived safety and fear of crime as used in past studies. A first question is whether there is robust evidence that lighting does indeed affect reassurance. While there is evidence from past studies to suggest that the presence of lighting enhances pedestrian reassurance, it is possible that the procedures used unintentionally led respondents toward responses that suggest a relationship between lighting and fear, for example: (i) Road lighting is presented as one of a limited set of options from which respondents must choose [Bernhoft & Carstensen, 2008]; (ii) Changes in lighting were an obvious difference between evaluated scenes, such as the photographs used by Loewen et al [Loewen et al, 1993]; (iii) Lighting and fear were the focus of rating scales [Hanyu, 1997]. and focussing on an issue encourages respondents to give an opinion about an item they would not otherwise raise [Acuña-Rivera et al, 2011].

The association between lighting and reassurance was explored in a study using a qualitative method [Fotios et al, in press (b)]. Test participants provided photographs of locations where they would, and would not, be confident to walk alone after dark. Discussion during subsequent interviews was used to identify the reasons for the choice of locations. Lighting was associated with reassurance in 62% of the 210 locations evaluated (Figure 1), a more frequent association than physical features associated with prospect and refuge but less frequent than the availability of access to help if needed in an emergency.

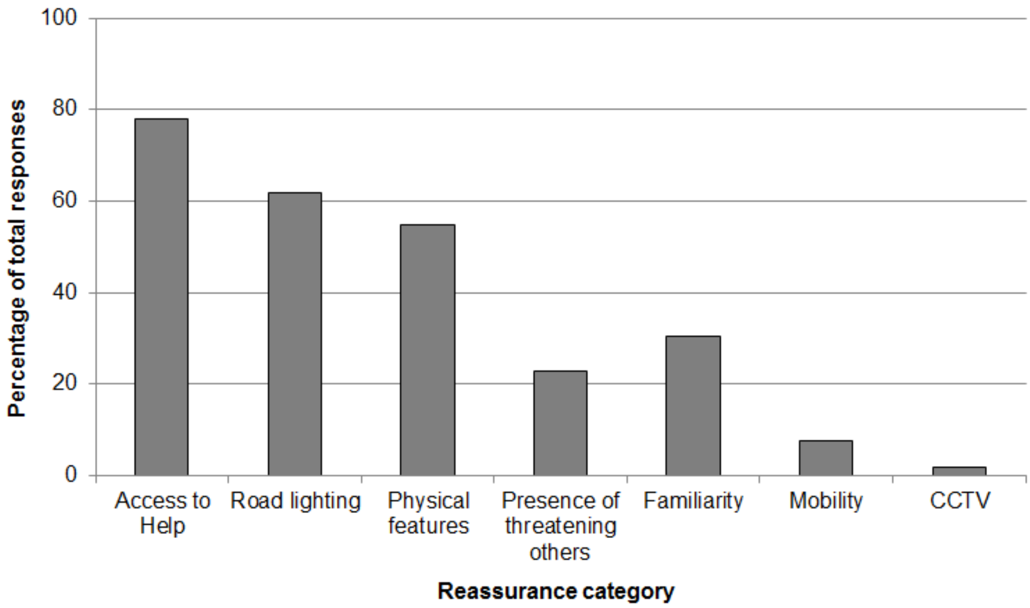

Figure 1 – Frequencies with which reasons were given for feelings of reassurance when walking alone after dark during interview with visual prompts for specific locations.

The evidence from this qualitative approach [Fotios et al, in press (b)] provides support for the findings of studies using quantitative procedures [Loewen et al, 1993; Hanyu, 1997; Bernhoft & Carstensen, 2008] that lighting enhances reassurance after dark. Having drawn this conclusion, further evidence was sought as to how variations in the characteristics of lighting effect reassurance, i.e. variations in illuminance, spatial distribution and spectral power distribution (SPD). This is reviewed in detail elsewhere [Fotios et al, in press (b)].

For illuminance, the results of several studies suggest that higher illuminance enhances reassurance [Vrij & Winkel, 1991] at least for females [Atkins et al, 1991]. This alone is insufficient evidence for setting design a target: rather than ever-higher illuminance, what is needed is evidence of an optimum illuminance. Fortunately there is such evidence from the study of Boyce et al [2000] who examined perceived safety in car parks, at daytime and after dark. Test participants were asked to describe the lighting using ratings of perceived safety. Rather than simply report the ratings, with any effect of lighting being confounded by local environmental factors, Boyce et al examined the *difference* between daytime and after-dark ratings (Figure 2). As illuminances increased, the difference between ratings of perceived safety recorded at daytime and after dark tended to decrease. These data suggest an optimum horizontal illuminance of 10 lux; higher illuminances do not tend to improve reassurance at a particular location relative to the level of reassurance in daytime at that same location. Further data are required to confirm whether these data are valid in the context of for residential roads where light levels are typically lower (2.0 to 15 lux) than the car parks surveyed by Boyce et al (up to 50 lux).

For lamp SPD it is proposed that lighting of higher S/P ratio enhances reassurance. This proposal is derived from evidence that lighting of higher S/P ratio appears brighter [Fotios & Cheal, 2011a] and that a location with brighter lighting is considered to be safer [Blöbaum & Hunecke, 2005]. While the results of three field studies provide some evidence that lighting of higher S/P ratio leads to higher ratings of safety [Akashi et al, 2004; Knight, 2010] it remains to be validated. As to spatial distribution of light, guidance for road lighting design tends to use measures associated with variations of illuminance across the lit surface (uniformity of horizontal illuminances). The effect of uniformity on reassurance has yet to be investigated.

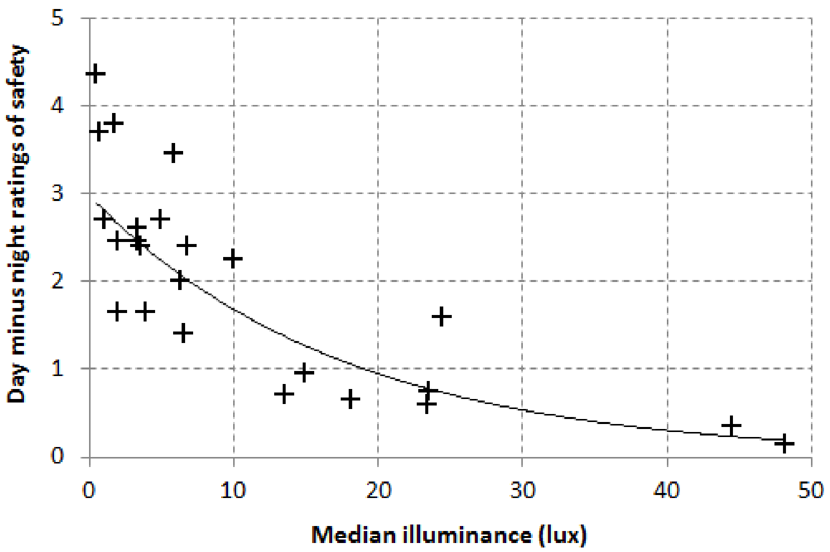

Figure 2 – Difference between daytime and night-time ratings of perceived safety of car parks plotted against median illuminance, after Boyce et al [2000].

2.3 Interpersonal judgements

One contribution of lighting to reassurance is that it should be possible for a pedestrian to recognise whether another person is likely to be friendly, indifferent or aggressive in time to make an appropriate response. Past studies in lighting have tended to investigate one limited aspect of this task, the ability to recognise the faces of others. Three tasks have been used (recognition of the face of a well-known person such as a TV celebrity [Yao et al, 2009], picking the target face from a set of several possible faces [Rea et al, 2009], and ratings of recognisability [Rombauts et al, 1989]), with evaluations using fixed distances [Rombauts et al, 1989] or stop-distances [Yao et al, 2009] of real people and of celebrities. These studies have led to mixed results, in particular regarding the effect of SPD: new research suggests that this is due to methodology: SPD is important when the task is difficult [Lin & Fotios, 2013; Fotios et al, 2013].

Two studies provide some evidence as to light levels for facial recognition. Caminada and van Bommel [1980] used a stop-distance procedure to examine facial recognition and concluded that semi-cylindrical illuminances (ESC) of 0.8 lx and 2.7 lx were needed for recognition at 4 m and 10 m respectively, while Rombauts et al [1989] suggested Esc of 0.4 lx and 3.0 lx for these same distances.

Rather than examine facial recognition, Fotios et al [2013] examined ability to recognise the emotion conveyed by facial expressions and body postures. This decision followed evidence that facial expression and body posture contribute to social judgements that are related to evaluation of threat [Willis et al, 2011], precisely 'approachability', which might be considered the positive end of an approach-avoid dimension of evaluation of threat. This was done under a range of luminances, lamp types and equivalent interpersonal distances using a detection task. Optimum light levels were estimated from the knee in the plateau-escarpment trend displayed by the results (Figure 3). The results suggest a minimum luminance of 0.1 - 1.0 cd/m2 if facial expressions are to be identified accurately at 4 m, but a luminance above 1.0 cd/m2 for identification at 10m. These luminances are equivalent to semi-cylindrical illuminances in the range of 0.7 to 7.0 lux for the 4 m targets and 7.0 lux or greater for the 10 m targets.

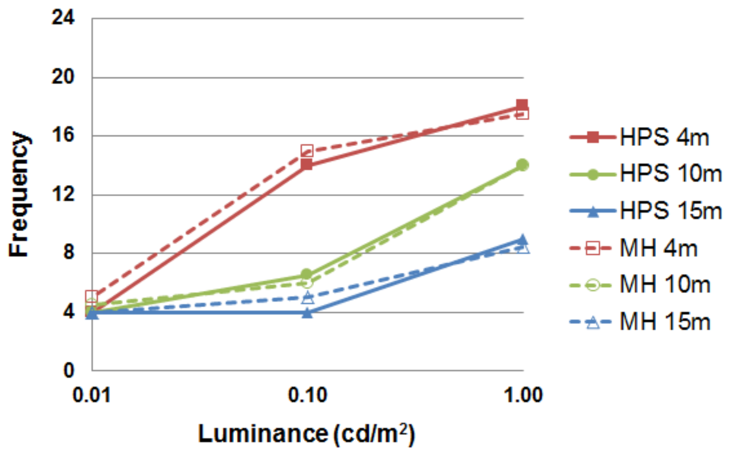

Figure 3 – Results of a facial expression recognition test [Fotios et al, 2013]

These results lead towards identification of an optimum illuminance for interpersonal judgements. To do so, however, requires further understanding of the critical task and the desirable distance at which this task can be done. Townshend [1997] suggests that at distances below 15 m the space in which pedestrians have time to react to avoid an undesirable situation becomes reduced beyond comfortable levels, determined using a field study of pedestrians after dark. Analysis of eye-tracking data [Fotios et al, in press (a)] indicates a tendency to fixate upon other pedestrians in the range of approximately 8 m to 16m, with a mode of approximately 12 m. Thus 15 m is representative of the distance at which interpersonal judgements are desirable. At a distance of 10 m, results of facial recognition trials suggest semi-cylindrical illuminances of approximately 3.0 lux [Caminada & van Bommel, 1980; Rombauts et al, 1989] while results of experiments using the facial expression task suggest a semi-cylindrical illuminance of 7.0 lux at 10 m [Fotios et al, 2013].

There is reason to suspect that SPD can affect facial judgements when the task is difficult [Yip & Sinha, 2002; Lin & Fotios, 2013]. Colour cues facilitate image segmentation (i.e. edge definition) rather than providing precise hue-related diagnostic cues to identity [Yip & Sinha, 2002]. Such segmentation may be enhanced by using light sources which enhance the discrimination between different colours, such as those with a large colour gamut. Judgements of body posture suggest an effect of SPD when task performance was within an apparent escarpment region (135 m at 1.0 cd/m2; 10 m at 0.1 cd/m2; 10 m at 0.01 cd/m2). These three cases were those in the middle of the luminance and distance combinations: when the task was either relatively difficult (i.e. small and low luminance) or easy (i.e. large and high luminance) then lamp type did not affect the task [Fotios et al, 2013]. However, judgements of facial expressions at 10 m (the greatest of the three distances examined) did not suggest a significant effect of SPD [Fotios et al, 2013].

2.4 Obstacle detection

Eye-tracking studies [Fotios et al, in press (a)] suggest that fixations at the near path are important, and one purpose of such fixations is to inspect pavement obstacles in the approaching path. Pavement obstacles include uneven pavement surfaces (e.g. static items such as a raised paving slab or manhole cover) that may cause a pedestrian to trip if it is not detected in sufficient time to plan gait adaptation to go over or around the obstacle. The success rates for implementing strategies for adjusting step length and width is greater than 80% when a visual cue is available one step ahead, while steering (a change in direction to go around an obstacle) has to be planned in the previous step cycle; success rate is near zero when only one step cycle duration is available for changing direction [Patla, 1997]. To carry out these actions requires some visual input: negotiation of an obstacle during gait requires an individual to determine the height and distance to the obstacle an plan appropriate foot placement and limb elevation for successful clearance [Buckley et al, 2011]. Continuous vision of the target is not necessary. Thomson [1980] found that his test participants were able to navigate around obstacles in a 9m travel path (no collisions in 70% of trials) when vision was only available at the start, although this was not the case beyond 9 m, subsequently suggested to indicated cognitive mapping of the path ahead for a period of 8 s.

Peripheral vision of a suddenly appearing obstacle in the travel path is sufficient for successful obstacle avoidance during locomotion: visual fixation is generally not re-directed to either the obstacle or landing area [Marigold et al, 2007]. However the near path appears to be a critical foveal fixation [Fotios et al, in press (a)]. What may be happening is that objects initially detected with peripheral vision are then fixated to feed in to the cognitive map of the approaching terrain, following which peripheral vision provides sufficient on-line information for successful avoidance action. Thus studies of obstacle detection have examined peripheral vision using a detection task, with obstacles of varying height presented at unknown peripheral locations under a range of luminances and lamp types [Fotios & Cheal, 2009, 2013]. These results demonstrate that higher luminances and higher S/P ratios improve detection of peripheral obstacles (Figure 4).

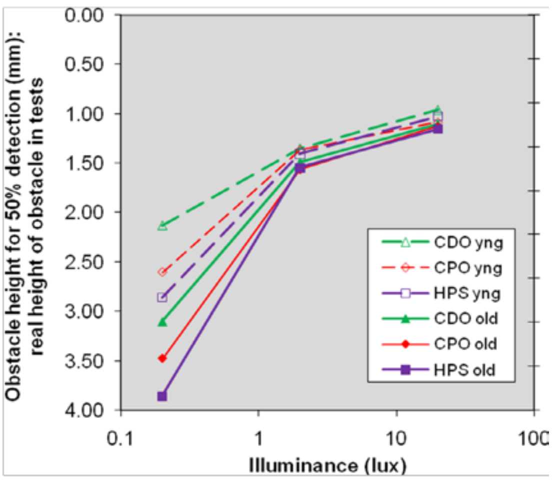

Figure 4 – Mean obstacle height for the 50% detection probability plotted against illuminance to show obstacle detection ability of older and younger observers under different illuminances for three types of lamp.

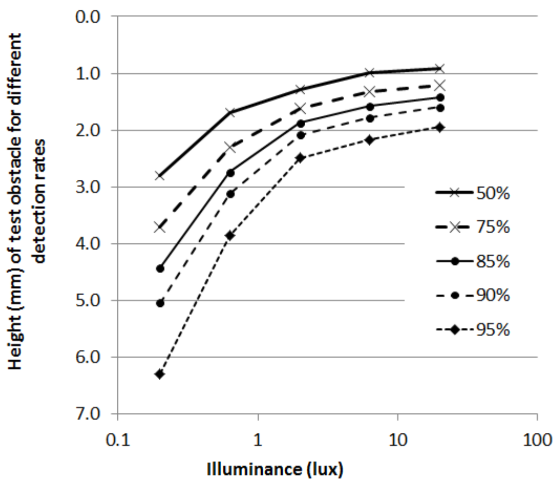

Figure 5 – Mean detection heights of obstacles 1 to 4 for detection probabilities of 50%, 75%, 85%, 90% and 95%.

Two methods have been used to interpret an optimum light level from these data, a performance approach and a legal approach. The first of these employed the apparent plateau-escarpment relationship between obstacle detection ability and illuminance, and assumed that the transition between plateau and escarpment defines an optimum: higher illuminances offer diminishing increase in obstacle detection while lower illuminances lead to rapidly diminishing performance. According to Figure 4 this transition lies at approximately 2.0 lux [Fotios & Cheal 2009]. Clearly, the transition in Figure 4 may be a result of a graph drawn from only 3 data points (luminances) and hence the second study was carried out using 5 luminances to better define the curve [Fotios & Cheal, 2013]. This is shown in Figure 5. In this study the change in curve with detection probability was explored. The ideal probability remains to be confirmed: we assumed 95%. The 95% probability curve suggests a more pronounced plateau-escarpment relationship than does the 50% probability curve, with a knee in the region of 2.0 lux.

The second approach to identifying the optimum illuminance is to ask what size of obstacle lighting is expected to reveal and what probability of detection should be expected, and this was considered from the point of view of a local authority demonstrating that it is taking reasonable steps towards meeting its obligations for pedestrian safety. This might be considered the legal approach because many solicitors are keen to encourage legal action should a pedestrian suffer a trip accident. The critical physical size of obstacle was concluded to be 25 mm (above or below the pavement surface), this determined from local authority guidelines as to when a pavement defect should be rectified and information from solicitors as to the conditions likely to lead to financial compensation for a tripping accident. The visual size of a 25 mm surface irregularity changes with viewing distance. Corrections to gait require that the obstacle is detected at least two steps ahead [Patla, 1997]. Hence detection of the 25 mm obstacle was considered when placed at forward distances of two, four, six, eight and ten paces, with the distance of a pace defined as 600mm. An illuminance of approximately 0.6 lux is required to detect an obstacle of the smallest size (13.5 minutes, i.e. 6 m ahead) and 95% probability of detection [Fotios & Cheal, 2013]. Note that these data are from observations by young people under HPS lighting: lower illuminances would be expected when using lighting of higher S/P ratio such as metal halide lamps, and higher illuminances would be expected when considering older people.

Having drawn these two conclusions, Figure 4 leads to interesting conclusions regarding the effects of lamp SPD and observers age. At 2.0 lux, defined as the transition between plateau and escarpment, effects of age and SPD are not significant: while at 0.6 lux, there are significant effects of age and SPD.

2.5 Summary

Table 1 shows a summary of tentative estimates of optimum design criteria established through consideration of three visual tasks considered to be important for pedestrians: evaluation of reassurance, ability to interpret the intent of other pedestrians, and detection of pavement hazards. For all three tasks there are estimates of optimum illuminance. Current design guidance focusses primarily on horizontal illuminance; while this may be suitable for reassurance and obstacle detection tasks, interpersonal judgements may be better characterised using the illuminance on vertical surfaces, such as semi-cylindrical illuminance.

Table 1 – Tentative estimates of optimum design criteria established through consideration of visual tasks. Note that these require much validation

Visual task	**Illuminance**	**SPD**
Reassurance	10 lux horizontal (tbc for residential roads)	High S/P ratio
Interpersonal judgements	Semi-cylindrical illuminances: • 3 lux for facial recognition at 10 m • 7 lux for facial expression at 10 m	High gamut area
Obstacle detection: i) Legal approach ii) Transition in performance curve	 0.6 lux horizontal illuminance 2.0 lux horizontal illuminance	 High S/P ratio No effect of SPD.

For SPD, it appears that lighting of higher S/P ratio and higher gamut area will be of benefit to pedestrians. Note, however, that whether or not the effect of SPD is significant may depend upon the illuminance used, as has been found in the studies of obstacle detection and interpersonal judgements. Recent guidance developed for the UK [Fotios & Goodman, 2012] proposed to use CIE general colour rendering index (Ra) instead of gamut area, partly because Ra is more widely available lamp property than gamut area and partly because it gives better correlation with judgements of preferred appearance [Fotios & Cheal, 2011b]. Unfortunately there is currently insufficient information regarding uniformity of illuminance – either estimates of an optimum or trade-offs between uniformity and illuminance.

Further work is on-going to improve these estimates, including a repeat of the Boyce et al [2000] study of reassurance but in residential roads rather than car parks and obstacle detection imposing cognitive distraction on the test participants (i.e. walking and a non-static fixation point).

3 Lighting and Crime

The cost-benefit approach of setting light levels requires evidence of street crime and lighting conditions in residential areas. Research is on-going in the UK within the LANTERNS project.

3.1 Background

Several local authorities of England and Wales are considering reducing, or have reduced, some street lighting provision. This is partly to reduce costs, but also to contribute towards climate change mitigation and help reduce environmental light pollution [Royal Commission 2009]. Many proposals to reduce street lighting, particularly in urban areas, have attracted considerable public and media concern. Expressed concerns have centred on crime, public perceptions of safety, and road safety. However, potential positive impacts of reduced lighting have also been noted, in particular for amateur astronomy, and reductions might, in theory, mitigate the negative health impacts some have claimed from ‘light at night’ such as disrupted sleep [Navara, 2007]. To date, there is little robust evidence on which to judge whether these concerns are well-founded [Welsh and Farrington, 2008; Beyer and Ker, 2010; DeFRA, 2011]. There are therefore policy imperatives to generate good quality evidence on whether reductions in street lighting provision are associated with public health effects. The LANTERNS project is analysing data from across England and Wales to make a more reliable assessment of the possible impact of street lighting reductions on two important public health outcomes, road traffic injuries and crime.

3.2 Methods

One aim of the LANTERNS project is to statistically assess evidence for any changes to road traffic injuries (including pedestrians injured in collisions with vehicles) and any changes to crime (including violence against the person) that are associated with switching off street lights at night (e.g. part-night lighting) or with reducing lighting levels (e.g. dimming or trimming). The project also aims to compare the societal costs of lighting adaptation schemes against the societal benefits in a cost-benefit analysis framework, and to explore public opinion on the potential for reducing streetlight at night.

Data sources Every local authority in England and Wales was approached in 2013 with a request for the specific locations of all street light columns where part-night lighting, dimming or trimming has either been implemented or is planned, together with the month and year that changes were introduced. For road traffic injuries, STATS19 data for the period 2000-2012 were obtained – this is the official dataset of personal injury road collisions and casualties that occur on the public highway in the UK. These data include the date, time of day, location, severity (slight injury, serious injury, fatal injury) by type of casualty (pedestrian, cyclist, car occupant, powered two-wheeler) for all road collisions. For crime, data from the police.uk website have been obtained from December 2010. These data include the month, name of roads where incidents occurred, approximate geographic co-ordinates, and type of crime. A disadvantage of this publicly available data set is that time of day is not included, however the project will assess the validity of these results by comparing them with results using samples of detailed crime data (i.e. including exact time and location) from a sample of police forces.

Sample size and power The study's sample size calculations have assumed that street light reduction schemes have been implemented on streets on which only 1% of pre-intervention traffic injuries and crime events occurred. For road traffic injuries, statistical power will be maximised by using data for 10 years before street lighting changes were implemented. If 150 night-time injuries per year are expected on intervention roads this would give 1,500 night-time injuries on intervention roads during 10 years before light reduction schemes were implemented, and 150 injuries one year after, providing 90% power to detect an increase of 32% above pre-intervention injury levels. This magnitude of effect is consistent with that estimated in a Cochrane review [Beyer and Ker, 2010]. For crime, if around 20,000 day and night-time crimes per year are expected on intervention roads, then the study will have 90% power to detect a 5% increase in crimes above pre-intervention levels, and for major crime sub-categories (e.g. violence against the person) it will have 90% power to detect increases of about 10% in crimes. As data have been received from local authorities, it is already apparent that a greater proportion of crime and road injuries occur on intervention streets, which means that these power calculations are conservative.

Analysis Using a Geographical Information System (GIS) we will link data sets to a road segment database that includes the characteristics of all classified and unclassified roads. Each road segment will be classified according to the type of street lighting reduction scheme (e.g. part-night switch-off; 'dimming'; etc.) and by the census 'Lower Super Output Area' within which it is located. GIS will also be used to generate adjacent areas around streets (i.e. streets that are not part of lighting reduction schemes but which are adjacent to streets that are). From the combined dataset, counts of crimes and road traffic injuries for each road segment will be generated by month and by year. The road segments will allow stratification of results by area deprivation (i.e. based on Index of Multiple Deprivation of areas) and whether they are adjacent to streets where lighting has been reduced. As it is difficult to define appropriate population denominators to estimate rates on individual road segments, analyses will be based on change in counts within each road segment.

For optimal control of confounding the proposed analysis will compare change in counts of crimes and traffic injuries in the street before and after lighting is reduced, relative to trends seen on other roads. The estimated effect is therefore specific to roads with decreased lighting compared with other roads.

Conditional fixed effects Poisson models will be used. The number of injuries (or crimes) $Y_{s,t}$ in road segment *s* in year *t* is therefore modelled as follows:

$$Y_{s,t} \sim \text{Poisson}(\mu_{s,t})$$

$$\log(\mu_{s,t}) = \alpha_s + S(t,z_s) + ßx_{s.t}$$

… where α_s is the road segment effect, $S(t,z_s)$ is a function of year to allow for nationwide trends in injuries and crime incidents, dependent on road segment characteristics z_s, $x_{s.t}$ is a vector of indicator (0,1) variables identifying road segments with 'reduced lighting' and (separately) adjacent areas, after the lighting reduction had been implemented, and ß is a vector of coefficients representing the effect of decreased street lighting and adjacent areas on injuries and crime incidents. The α_s nuisance parameters are "conditioned out" in the conditional fixed effects Poisson model, allowing models to be based on annual counts of injuries and crime incidents within each road segment. For transparency, the underlying trends in injuries and crime incidents $S(t,z_s)$ will be fitted with linear terms.

Additional analyses will examine potential biases relating to 'regression to the mean' (arising from the fact that low numbers of traffic injuries and crimes may be factors in the decision to reduce street lighting in some areas). For this, the analyses will be repeated excluding data for periods of one and two years before changes to street lighting were implemented. Evidence for diffusion of crime and displacement of road accidents and crimes from better-lit nearby roads will also be investigated, and evidence for a 'lag' effect of street lighting reduction will be examined by modelling change in effects on events by month since implementation of lighting reduction.

For the cost-benefit analysis the monetary values of street lighting provision (infrastructure cost, maintenance costs, and energy consumption) are being obtained. Data on the monetary values (i.e. economic and societal costs) of road traffic injuries are being assembled, as well as the economic and societal costs of crimes by type of crime using Home Office definitions [Home Office, 2005]. The societal costs of street lighting schemes will be compared against the societal benefits in a cost-benefit analysis framework.

By the end of 2013 data had been received from a total of 42 local authorities of England & Wales. Part-night lighting had been introduced in 14 (33%) of these areas, dimming of lights in 24 (57%) areas, and trimming lighting times in 16 (38%) areas. A national workshop is to be convened at the end of 2014 with local authorities and third sector organisations to learn how our results might be of most use.

Acknowledgement The Sheffield contribution to this work was carried out through support from EPSRC (EP/H050817) as part of the MERLIN project. The LANTERNS project is funded by NIHR Public Health Research Programme. The views and opinions expressed in this article are those of the authors and do not necessarily reflect those of the NIHR PHR Programme or the Department of Health

References

ACUÑA-RIVERA, M., UZZELL, D., BROWN, J. 2011. Perceptions of disorder, risk and safety: The method and framing effects. *Bilingual Journal of Environmental Psychology*, 2; 167-177.

AKASHI, Y., REA, M., MORANTE, P. 2004. Progress Report: Improving acceptance and use of energy-efficient lighting. Unified photometry: An energy-efficient street lighting demonstration in Easthampton, Massachusetts. Lighting Research Center: Troy, USA.

ATKINS, S., HUSAIN, S., STOREY, A. 1991. The Influence of Street Lighting on Crime & Fear of Crime. Crime Prevention Unit, Paper No. 28. London: Home Office.

BERNHOFT, IM., CARSTENSEN, G. 2008. Preferences and behaviour of pedestrians and cyclists by age and gender. *Transportation Research Part F*, 11; 83–95.

BEYER, FR,, KER, K. 2009. Street lighting for preventing road traffic injuries. Cochrane Database of Systematic Reviews. DOI: 10.1002/14651858.CD004728.pub2.

BLÖBAUM, A., HUNECKE, M. 2005. Perceived danger in urban public space. The impacts of physical features and personal factors. *Environment and Behaviour*; 37(4); 465-486.

BOYCE, PR., EKLUND, NH., HAMILTON, BJ., BRUNO, LD. 2000. Perceptions of safety at night in different lighting conditions. *Light. Res. Technol*, 32; 79-91

BSI. 2003. BS EN 13201-2:2003. Road lighting - Part 2: Performance requirements. London: BSI.

BUCKLEY, JG., TIMMIS, MA., SCALLY, AJ., ELLIOT, DB. 2011. When is visual information used to control locomotion when descending a kerb. *PLoS ONE*,; e19079. doi:10.1371/journal.pone.00119079.

CAMINADA, JF., VAN BOMMEL, W. 1980. New lighting considerations for residential areas. *Int. Lighting Rev*, 3; 69-75.

DeFRA. 2011. A review of local authority road lighting initiatives aimed at reducing costs, carbon emissions and light pollution..

FOTIOS, SA., CHEAL, C. 2011a. Predicting Lamp Spectrum Effects At Mesopic Levels. Part 1: Spatial Brightness. *Light. Res. Technol*, 43(2); 143-157

FOTIOS, SA., CHEAL, C. 2011b. Predicting Lamp Spectrum Effects At Mesopic Levels. Part 2: Preferred Appearance and Visual Acuity, *Light. Res. Technol*, 43(2); 159-172.

FOTIOS, S., CHEAL, C. 2013. Using obstacle detection to identify appropriate illuminances for lighting in residential roads. *Light. Res. Technol*, 45(3); 362-376.

FOTIOS, SA., CHEAL, C. 2009. Obstacle detection: A pilot study investigating the effects of lamp type, illuminance and age. *Light. Res. Technol*, 41(4); 321-342.

FOTIOS, S., GOODMAN, T. 2012. Proposed UK guidance for lighting in residential roads. *Light. Res. Technol*, 44(1): 69-83.

FOTIOS, S., UNWIN, J., FARRALL, S. (in press (b)). Road lighting and pedestrian reassurance after dark: A review. *Light. Res. Technol*.

FOTIOS, S., UTTLEY, J., CHEAL, C., HARA, N. (in press (a)). Using Eye-Tracking To Identify Pedestrians' Critical Visual Tasks. Part 1. Dual Task Approach. *Light. Res. Technol*.

FOTIOS, S., YANG, B., CHEAL, C. 2013. Effects of Outdoor Lighting on Judgements of Emotion and Gaze Direction. *Light. Res. Technol*. doi:10.1177/1477153513510311

HANYU, K. 1997. Visual properties & affective appraisals in residential areas after dark. *Journal of Environmental Psychology*, 17; 301–315.

HOME OFFICE. 2005. The economic and social costs of crime against individuals and households 2003/04. Economics & Resource Analysis Research, Development and Statistics.

KNIGHT C. 2010. Field surveys investigating the effect of lamp spectrum on the perception of safety and comfort at night. *Light. Res. Technol*, 42(3); 313-330.

LIN, Y., FOTIOS, S. 2013. Investigating methods for measuring facial recognition under different road lighting conditions. *Light. Res. & Technol*. DOI: 10.1177/1477153513505306

LOEWEN, LJ., STEEL, GD., SUEDFELD, P. 1993. Perceived Safety from Crime in the Urban Environment. *Journal of Environmental Psychology*, 13; 323-331.

MARIGOLD, D S, WEERESTEYN, V, PATLA, A E, DUYSENS, J.2007. Keep looking ahead? Re-direction of visual fixation does not always occur during an unpredictable obstacle avoidance task. *Experimental Brain Research*; 176(1): 32-42.

NAVARA, KJ., NELSON, RJ. 2007. The dark side of light at night: physiological, epidemiological, and ecological consequences. *J. of Pineal Researc,*43(3):215-24.

PATLA AE. 1997. Understanding the roles of vision in the control of human locomotion. *Gait and Posture*, 1997; 5; 54-69.

REA, MS., BULLOUGH, JD., AKASHI, Y. 2009. Several views of metal halide and high-pressure sodium lighting for outdoor applications. *Light. Res. Technol*., 41(4): 297-320.

ROMBAUTS, P., VANDEWYNGAERDE, H., MAGGETTO, G.1989. Minimum semicylindrical illuminance and modelling in residential area lighting. *Light. Res. Technol,* 21: 49-56.

THE ROYAL COMMISSION ON ENVIRONMENTAL POLLUTION. 2009. Artificial Light in the Environment. London: The Stationary Office.

THOMSON, JA. 1980. How do we use visual information to control locomotion? *Trends in NeuroScience*, 3; 247-250.

TOWNSHEND, T. Safer City Centres: The Role of Public Lighting. *Safer City Centres: Reviving the Public Realm*. London: Paul Chapman Publishing Ltd; 1997. p. 119-29.

VRIJ, A., WINKEL, FW. 1991. Characteristics of the built environment and fear of crime: a research note on interventions in unsafe locations. *Deviant Behavior*, 12; 203-215.

WELSH, BC., FARRINGTON, DP. 2008. Effects of improved street lighting on crime. Campbell Systematic Reviews 2008:13. DOI: 10.4073/csr.2008.13

WILLIS, ML., PALERMO, R., BURKE, D. 2011. Judging approachability on the face of it: The influence of face and body expressions on the perception of approachability. *Emotion*, 11(3); 514-523.

YAO, Q., SUN, Y., LIN, Y. 2009. Research on Facial Recognition and Color Identification under CMH and HPS Lamps for Road Lighting. *LEUKOS,* 6(2): 169-178.

YIP AW, SINHA P. 2002. Contribution of color to face recognition. *Perception*, 31; 995-1003.

PP66

ROAD LIGHTING AND PEDESTRIAN REASSURANCE AFTER DARK: A REVIEW OF THE EVIDENCE

Steve Fotios
School of Architecture, The University of Sheffield, UK
steve.fotios@sheffield.ac.uk

Abstract

Road lighting is installed in residential areas is to increase pedestrians' reassurance, their confidence when walking after dark, which in past studies has been expressed as perceived safety or fear of crime. This article reviews past studies of road lighting and pedestrian reassurance to enable better understanding of whether lighting is effective, and of whether variations in illuminance and lamp type, are effective at improving reassurance. This review presents evidence that road lighting increases feelings of reassurance after dark, that higher illuminance increases this reassurance (and that it may be possible to identify a plateau to this effect) and that a higher S/P ratio enhances reassurance.

Keywords: e.g. road lighting, pedestrians, reassurance

1 Introduction

This article concerns the reassurance gained from road lighting in residential areas. In such areas it is normal to provide lighting that focuses more, but not exclusively, on the needs of pedestrians compared to those of drivers [CIE, 2010a]. Following previous use [DoE, 1994; Cozens et al, 2003] the term *reassurance* is used here to indicate confidence when using a road and is used here as an alternative for the perceived safety and fear of crime that have been used in previous studies: higher reassurance implies higher perceived safety and lower fear of crime.

One reason for investigating reassurance is that there is a link with walking decisions: a low level of reassurance can lead to constrained behaviour such as deciding to use an alternative means of transport to walking or to avoid going out at all. Walking is of wider interest because it is a common means by which physical activity can be introduced into people's daily routines in order to encourage good health [Loukaitou-Sideris, 2006]. The link between feelings of risk and fear and high levels of inactivity is particularly strong for women, children and the elderly [Loukaitou-Sideris, 2006]. In the US, estimates of clinical obesity based on clinical measurements indicate that (in 2000) one-third of the adult population are obese [Pucher & Dijkstra, 2003]. An increase in sedentary lifestyles and higher rates of obesity is concurrent with a steady decline in walking [Alfonzo, 2005]. Within North America and Europe, the US has the lowest percentage (7%) of trips in urban areas made by walking and cycling, followed by Canada (12%) and the UK (16%) while in Denmark and the Netherlands it is greater than 40% [Pucher & Dijkstra, 2003].

People's attitudes about walking are determined by beliefs about the likely consequences (e.g. health, injury) weighted by the evaluation of how good or bad these outcomes would be. Two types of risk that are of importance for pedestrians are the risk of being involved in an accident and the risk of being victim of criminal offences, violence or threats: in most cases it is the latter type of risk that is of importance for pedestrians, and which influences their behaviour [Fyhri et al, 2010].

A place will be considered unsafe (i.e. at risk of criminal offences, violence or threats) if it offers refuge to offenders and limited prospect and escape to potential victims [Fisher & Nasar, 1992]. These are physical features or an environment. It is important to perceive a potential danger as soon as possible [Blöbaum & Hunecke, 2005]: prospect is a measure of how well a person can look ahead to anticipate whom or what he/she is likely to encounter.

Good prospect also implies that the pedestrian is visible to others. Escape is the opportunity for exit at various points along the path or in a location. Narrow alleys are considered more dangerous than wide alleys [Herzog and Flynn-Smith, 2001] as they are less likely to suggest good possibilities for escape. Natural and artificial features along a route could provide a place to hide and these have dual possibilities, providing either a place for a potential attacker to wait out of sight (concealment) or a place for a potential victim to hide (refuge).

With regards to lighting and vision the influence of these physical features may considered under the categories of *visibility of others* and *visibility by others* [Luymes & Tamminga, 1995] raising questions such as *how much can I see?* and *how much am I seen?* [Greene & Greene, 2003]. People feel the safest if they have a good overview of the space in which they are moving and if they have the feeling that they are supported by other users [Greene & Greene, 2003]. Visibility of others, associated with prospect, is the ability to see ones surroundings clearly; the ability to appraise and recognise strangers; and the ability to survey visually approach directions and areas in close proximity to one's position. Visibility of others is related with refuge: people feel safer in cities when they are not isolated from contact with the larger urban realm. The ability to be seen allows casual surveillance by others who may defuse or be of assistance in threatening situations [Luymes & Tamminga, 1995].

Fear increases after dark because there are fewer people around, contributing to feelings of isolation from help if needed, and because visibility is reduced, which may provide offenders with more opportunities for concealment and may make it more difficult to identify escape routes should they be necessary [Dravitski et al, 2003]. Functionally, the most obvious and only certain effect better lighting can have is to change how well people can see: increasing the adaptation luminance increases the speed of visual processing, improves the discrimination of detail, makes colour judgements more accurate and increases the distance at which we can see anything suspicious [Boyce & Gutkowski, 1995]. Road lighting enhances vision after dark, thus we expect road lighting to improve the visibility of others and visibility by others, and thus to improve feelings reassurance compared with an unlit or poorly lit space. Thus road lighting has the potential to influence whether people choose to walk or cycle in their neighbourhood.

This paper presents a review of studies investigating the influence of road lighting on reassurance, a step toward establishing criteria for design guidance. The first studies reviewed are those which explore the influence lighting as a single entity and this is followed by investigations of two characteristics of lighting – illuminance and spectral power distribution (SPD).

2 Does lighting affect reassurance?

2.1 Evaluations of photographs

If light has an effect on reassurance, then a large difference in lighting conditions should lead to a large effect. This can be seen in the results from Loewen et al [1993] who compared photographs of scenes in daylight (with light) and at night-time (without light). Loewen et al presented 16 photographs, these being two different outdoor scenes for each of the eight combinations of light, open space, refuge, the items most frequently identified in their pilot study, for which participants were asked to provide ratings of items including safety. The results are shown in Figure 1. In all four situations regarding the presence or absence of open space and refuge, with-light was rated safer than without-light and this effect was larger than that found for differences in open space or refuge.

Hanyu [1997] sought judgements from 28 students regarding locations on their university campus (Ohio, USA), thus being evaluation of a familiar environment, using colour photographs observed in a dark classroom. There were 20 locations, for which photographs were taken at night-time, and were presented on a 6 feet x 5.5 feet (1.8 m x 1.7 m) screen in random order. Twelve items including brightness and uniformity were rated using a 5-point response scale (1 = not at all so; 5 = a great deal). Six emotional items including fear were rated on a 5-point bipolar scale (3 = neutral). The test duration was approximately 25 minutes for whole task and therefore these were rapid judgements. Hanyu's analysis suggested a relationship between safe and well-lit where well-lit included uniform lighting, legibility, complexity and brightness.

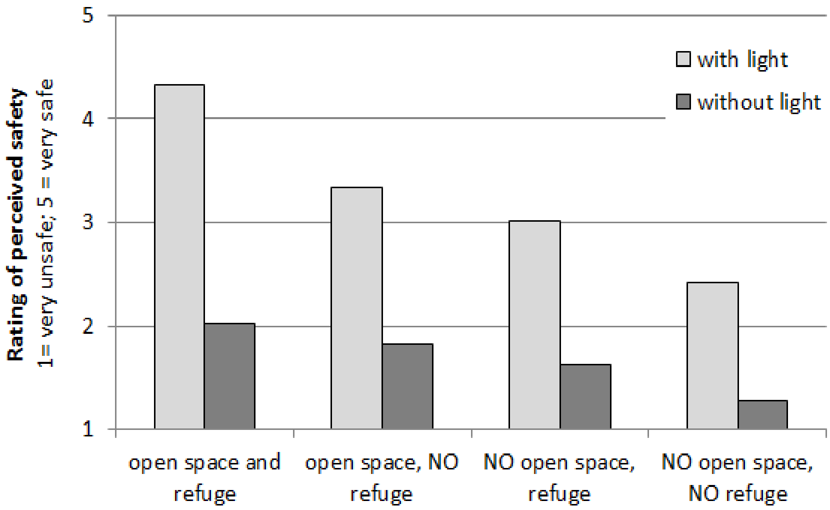

Figure 1 – Mean ratings of perceived safety of images of outdoor scenes as reported by Loewen et al [1993].

2.2 Evaluations of real locations

A potential limitation of the Loewen et al and Hanyu studies is that judgements made from observation of photographs of outdoor scenes do not give the same judgement as when made in the real location [Toet & van Schaik, 2012; Bishop & Rohrmann, 2003]. One approach to overcoming this is to obtain judgements whilst test participants are located in the real outdoor location. Painter [1994] surveyed pedestrians in three locations in London (Edmonton, Tower Hamlets, and Hammersmith and Fulham). In these three roads, the existing LPS lighting was replaced with HPS lamps, these installed to achieve an average of 10 lx (minimum 5 lx) while the original lighting provided less than 3.5 lx. Pedestrians were questioned about their experience within 5 minutes' walk of the location over the past 12 months. It was reported that "over 90% of pedestrians interviewed in all locations thought that fear of crime in the surrounding area had decreased" following installation of the HPS lighting although there is no statistical analysis. This suggests a change of lighting has effect, although it is not possible to determine whether it was the broader spectrum or higher illuminance of the HPS lighting that led to the apparent improvement in reassurance.

Okuda et al [2007] investigated attitudes to safety and security using a survey of local residents (n=249) carried out at night on streets in Hiroshima. A questionnaire sought identification of the roads and road features considered to be the most insecure and their opinion on what affects safety. The factors reported related to issues of lighting, presence of other people and traffic. Of these, dark street lighting and an empty street were the two most frequently mentioned by respondents (36%), followed by narrow street (25%) and no street light (20%). Note that the questionnaire was not presented in the report, and it is possible that it identified lighting as a potential factor, contributing to the frequency of responses identifying lighting as a factor.

Koga et al [2003] asked test participants to rate 32 items (including clean-dirty, light-dark, friendly-unfriendly) when stood in streets in Fukuoka, Japan. It was concluded that feelings of security increase in light and busy streets. Factor analysis derived five common factors from the evaluated items (liveliness, order, openness, intimateness, and unity) and lighting was essential to every factor. Three potential problems with this study are that the full set of questions and their analyses were not clearly reported, conclusions from some of the rated items may be misconstrued through translation, and the time of day at which ratings were made is not reported.

2.3 Evaluations from memory

Two studies surveyed large samples of people about outdoor locations likely to be familiar and reported effects of lighting. These responses were likely gained from residents whilst at home and are therefore founded on their memory of the outdoor environment. Van Cauwenberg et al [2012] report a survey of 48,879 Belgian people aged >65 years old which included a question asking if street lighting was sufficiently present in the neighbourhood (Yes/No) and a series of rating scales to measure feelings of unsafety. The results suggested the presence of street lighting to increase feelings of safety and this was associated more with females than with males. It is not certain however whether judgements of sufficient street lighting relate to the presence/absence of street lighting or to the quantity (such as brightness) of some attribute of the lighting.

Bernhoft and Carstensen [2008] surveyed 1905 people (1017 older people aged >70 years old, 888 people aged 40-49 years old) in two Danish cities. One question asked "*Which of the following conditions are most important for your route choice when walking/cycling in your hometown*?" and respondents were asked to choose a maximum three of the eight given statements including 'Good street lighting'. While this was clearly not a direct question of reassurance, there may be an element of reassurance in decisions to walk and of which route to take [Fyhri et al, 2010] and these data provide insight as to the relative effect of lighting. The results are shown in Figure 2, these being the percentage of people identifying each of the eight statements. Bernhoft and Carstensen [2008] report the results for male and females separately; Figure 2 presents an estimated average of these (in only two case were the difference male and female responses suggested to be significant). Good street lighting was not the most frequent reason for route choice. For the younger age group, getting to the destination quickly and by the most direct route were more important; for the older group, all items were more frequently important than good street lighting. Note however that while it was possible to not pick good street lighting as a criterion for route choice, many did. It is of course possible that the importance of any of these eight issues was inflated simply by being presented as an option.

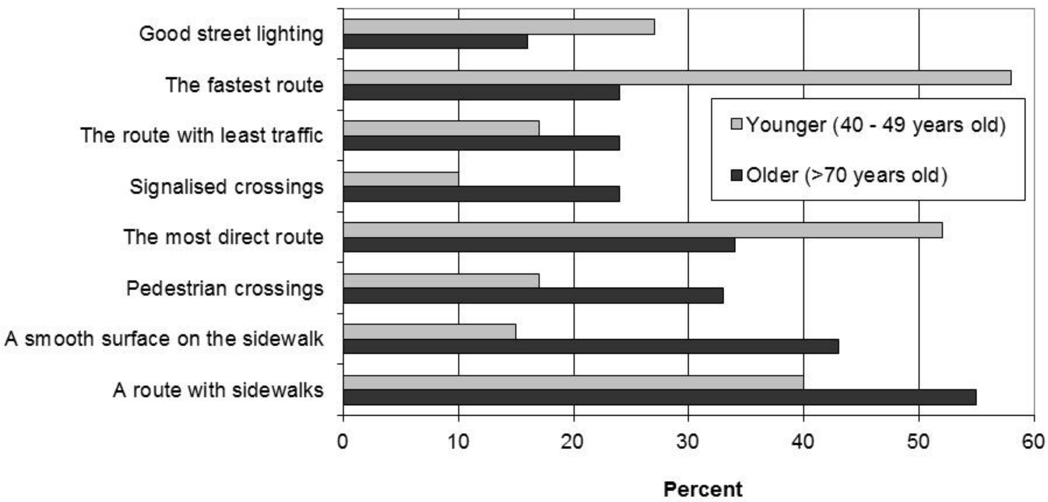

Figure 2 – Conditions of importance for pedestrians route choice, from Bernhoft and Carstensen [2008]. Note: these values are estimated from their Figure 1 and are average values of the male and female responses presented.

2.4 Summary

Results from several studies suggest that lighting enhances, or is associated with, reassurance. While the evidence from any one particular study may be questioned, confidence is drawn from the convergence of conclusions gained by independent research groups using different stimuli and methods. Having drawn this conclusion, what is needed is an understanding as to how particular characteristics of lighting affect reassurance.

3 Illuminance

For a particular location, a higher illuminance will lead to a brighter environment. There is evidence that outdoor locations reported to be brighter will also be considered as safer

[Blöbaum & Hunecke, 2005] and thus higher illuminances are expected to enhance reassurance. This expectation was confirmed in three studies, these using different approaches to change between low and high illuminances. In the study by Matsui [2007], lighting that was normally dimmed to 30% output would increase automatically to 100% when a person approached the area. 82% of local residents reported that the higher illuminances gave them a greater sense of security. Vrij and Winkel [1991] sought ratings of safety from passing pedestrians before and after illuminance was increased by a factor of 5 in the test location (the increases were 0.1 lx to 0.5 lx on the bridge, 0.18 lx to 1.11 lx on the cycleway and 0.24 lx to 1.31 lx on the footpath). Atkins et al [1991] surveyed household before and after relighting in an urban area of the UK, providing a four-fold increase in illuminance (values not reported). It is likely there was a simultaneous change in lamp type but this is not clear. Surveys of local residents were administered before and after the relighting did not reveal a general increase in feelings of safety but did suggest a significant increase in safety amongst females.

Nair et al [1997] also investigated reassurance before and after changes to the lighting in a street in Glasgow, using a change in luminaire optics to increase average illuminance on the footway from 10 lx to 36 lx, but these results are not considered to be credible. One item asked how apprehensive the test participant had been that something unpleasant may have happened to them while walking along the street, and it appears that a 1-10 response scale was used for this item. The reported data imply a significant reduction in apprehensiveness, but there are reasons why this may not be a fair assessment. Responses were categorised as representing fearless, normal or timorous people, these being ratings of 1-2, 3-5 and 6-10 respectively. This uneven distribution of scores to assumed behaviour may not be a fair interpretation (and since the questions were not reported, this cannot be known for certain). It may be that collating ratings of 1-3, 4-7, and 8-10 would better represent fearless, normal and timorous people and may lead to a different interpretation of the data. Secondly, note that the targeted street was one that was generally considered to be unsafe at night-time and attracted unwelcome and unsavoury nocturnal activities, but which was used as it provided a useful short cut. The study also attempted to weight the results of the after survey (n=117) to match the gender profile of the before survey (n=102), and there are no data as to how this was done nor how it affected the results.

These studies suggest that higher illuminance enhances reassurance. A critical question for design is whether more illuminance will always be better or whether there is an optimum illuminance above which the increase in reassurance is negligible. Studies examining only two levels of illuminance provide insufficient evidence. Fortunately, there is one study [Boyce et al, 2000] that does provide evidence of an optimum illuminance, and this arises from the appraisal of several locations of different illuminance and from a novel approach to interpretation of the data.

Boyce et al [2000] carried out field surveys of 24 car parks in urban and suburban areas in New York and Albany in the US to investigate how the amount of light effected the perception of safety at night. Test participants were transported to the sites in four vehicles and these visited the sites in different orders at both daytime and night-time. At each site they were asked to walk around and then describe lighting using a series of semantic differential ratings scales including ratings of perceived safety when walking alone. As illuminances increased, the difference between ratings of perceived safety recorded at daytime and night-time tended to decrease (Figure 3). In other words, higher illuminances increased reassurance after dark towards the level experienced in daytime at that particular location. These data suggest an optimum horizontal illuminance of 10 lux; higher illuminances do not tend to improve reassurance at a particular location relative to the level of reassurance in daytime at that same location. Note, however, that the car parks surveyed had mean horizontal illuminances of up to 50 lux, higher than the 2.0 to 15 lux typically used in residential roads [CIE, 2010a] and thus there is a need to question if these data are appropriate.

In summary, there is evidence that road lighting of higher illuminance improves reassurance and furthermore, evidence that there may be a plateau to the effect [Boyce et al, 2000] thus allowing interpretation of an optimum illuminance.

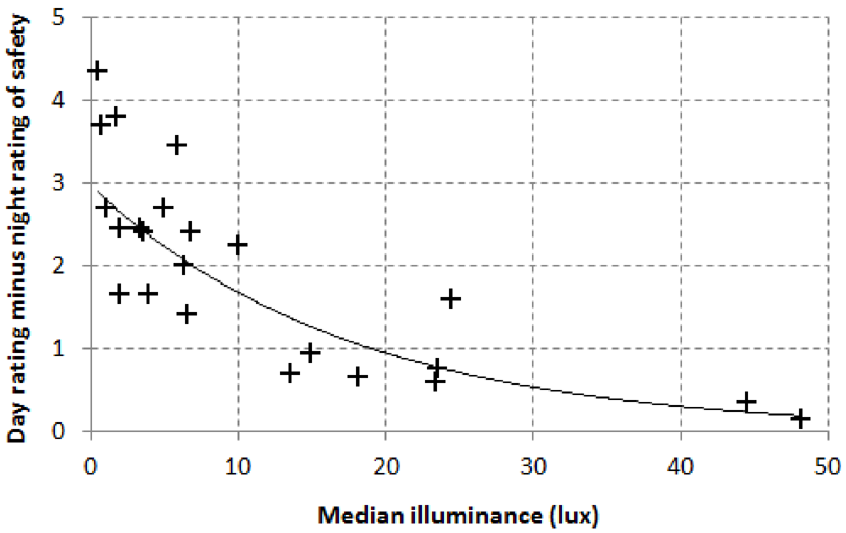

Figure 3 – Difference between daytime and night-time ratings of perceived safety of car parks plotted against median illuminance, after Boyce et al [2000].

4 Lamp spectrum

4.1 Field studies

Following the introduction of light sources such as metal halide (MH) for exterior lighting, informal assessment of trial schemes in the UK led some lighting practitioners to the opinion that these lamps, having broader SPD than traditional low pressure sodium (LPS) and high pressure sodium (HPS) lamps, presented benefits in visual perception and performance [ILE, 2008, Bennett, 2000]. While these trials tend to identify positive effects of improved lighting on reassurance the articles did not sufficiently describe details of the lighting installations, the people who were asked to give their judgements, the method by which judgements were obtained or the numeric data collected. This means the findings cannot be considered as reliable evidence or extrapolated to other situations.

A number of larger scale surveys have been carried out. While it would be expected that these provide more complete data, this is not always the case. Nair et al [1993] carried out before and after surveys following improvements to street lighting in a residential area. First, they fail to report the survey questions and the changes in lighting (lamp type and illuminance). The results include a reduction by 6% in the number of people worried about assault and harassment, although an increase by 9% in the number of people who avoided going out at all and an increase by 9% in the number of people who would avoid certain areas. However, the reported changes in opinions are not statistically analysed and the changes are small (e.g. 6% means two of the 33 respondents changed opinion). The results reported for one question serve to demonstrate the questionable validity of the Nair et al data; in the survey carried out before the lighting improvements had taken place, 17% of respondents reported recent improvement in lighting despite there being no such action (and in the after survey this was only 18%).

Three field studies present evidence that lamp SPD affects reassurance. In these, existing HPS lighting was replaced by lamps of broader spectral distribution and the environment evaluated by pedestrians using rating scales before and after the change. Morante [2008] surveyed two roads; in one, HPS lighting providing an average illuminance of 8.7 lx was replaced by QL lighting providing 2.7 lx; in the second road HPS lighting providing an average illuminance of 3.2 lx was replaced by MH lighting providing 3.1 lx. Akashi et al [2004] compared HPS street lighting with that from a 6500 K fluorescent lamp, these providing average photopic illuminances of 3.4 lx for the HPS lamp and 2.8 lx for the fluorescent lamp. In these two studies the lower photopic illuminances of the after lighting were chosen so that the before and after lighting provided equal unified luminance [Rea & Bullough, 2007]. In the final study, Knight [2010] reported evaluations of the perception of brightness and safety before and after road lighting was changed from HPS to one of two types of MH (2800 K and 4200 K), with average illuminances in the given areas being similar before and after the change of lamp. In all three studies, the new lighting was found to provide higher ratings of safety than did the HPS, these differences being confirmed to be statistically significant in two studies [Akashi et al, 2004; Knight, 2010].

In any before and after study it is possible that respondents are responding to the attention being given to their local area, a Hawthorn-like response, rather than to a purposeful change in lighting characteristics. Alternatively, responses may be inflated by the high initial lumens of new lamps. The existing installation may have been near the end of its useful working life, with the inherent lamp failures, depreciated lumen output, and dirty lanterns, whilst the new installation was clean and benefited from the initial over-lighting included to offset subsequent lumen depreciation. However, if this initial response is the one that residents retain, that may be considered a useful contribution to resident satisfaction. An interesting feature of Knight's [2010] study is that a reverse change was included, in which the MH lighting was replaced with HPS lighting: the results suggest a statistically significant reduction in the perception of safety ($p<0.05$). What this result suggests is that the change in lighting matters. Further such evidence of a negative effect would be interesting.

4.2 Unpublished field studies

Fotios carried out two field studies of reassurance in collaboration with local authorities in the UK, taking advantage of their communications with residents during relighting schemes. One study was carried out in West Sussex and was reported in an ILE report [ILE, 2008]: the second study, carried out in South Tyneside, used the same procedure but was not previously published. Questionnaires were distributed to residents before and after the lighting in their street was changed. These questionnaires sought judgements of brightness, glare, perceived safety when walking alone at night and overall satisfaction. Ten questions required a yes/no response (e.g. it is safe to walk alone here, alone, during the day?; it is safe to walk alone here, alone, at night?) and there were two 10-point rating scales to evaluate brightness and overall satisfaction.

In South Tyneside, the existing low pressure sodium (LPS) lamps were replaced with Cosmopolis metal halide (CPO) lamps. The LPS lighting targeted an average illuminance of 6 lx (2.5 lx minimum; BS5489-3: 1992 category 3/2) and the new CPO lighting targeted 5 lx (1 lx minimum; BS5489-1:2003 class S4). 174 'before' questionnaires and 254 'after' questionnaires were received, of which there were 82 matched pairs as identified by household address and these results are shown in Table 1. Questions 1 to 10 demanded a yes/no response and these were analysed using McNemar's test: questions 11 and 12 asked respondents to rate the brightness of the street and their satisfaction with the lighting on a 1 to 10 scale and these were analysed using the Wilcoxon test. These results suggest that the new CPO lighting was considered to be better than the existing LPS lighting despite that it was designed to provide a lower illuminance: there was an increase in perceived safety at night-time and other attributes including brightness and overall satisfaction.

In West Sussex the 35W LPS lamps in a residential estate were replaced with 55W CFL lamps [ILE, 2008]. The same spacing was used (30m) and column height was increased from 5m to 6m. The LPS lamps gave a mean illuminance of 4.7 lux and an illuminance uniformity (minimum to average) of 0.26: the CFL lamps provided a mean illuminance of 4.9 lux and a uniformity of 0.32 (data provided by the local authority). Thus other than lamp type, differences between the two installations were small. The change in lighting did not affect judgements of safety when walking alone at day or night and did not affect judgements of comfort or glare. What the change in lighting did affect were judgements of visibility, uniformity and colour. Compared to the original LPS lighting the CFL lighting was considered to be significantly brighter, more uniform, better illuminated the whole street and distant people, and revealed colours better. Both brightness and satisfaction were significantly higher under the new CFL lighting.

Table 1 – Results of lighting survey in South Tyneside; results from the 82 matched pairs. For questions 1-10 the reported response is the number of 'yes' responses. For questions 11 & 12, the reported response is the mean rating

Question		Response to Questionnaire			Interpretation
		Before (LPS)	After (CPO)	Statistical difference	
Q1	It is safe to walk here, alone, during the day.	77	80	n.s.	No change in perceived safety at day
Q2	It is safe to walk here, alone, at night.	32	61	$p<0.01$	Better perceived safety with CPO at night
Q3	The lighting is comfortable.	41	71	$p<0.01$	Better comfort with CPO
Q4	The lighting shows up the whole street well.	30	68	$p<0.01$	CPO shows up street better
Q5	The lighting lets me see people at a distance, clearly.	25	65	$p<0.01$	Can see distant people better under CPO
Q6	The lighting is too bright.	3	4	n.s.	No change
Q7	The lighting is too dark.	45	9	$p<0.01$	Increase in brightness
Q8	The lighting is uneven (patchy).	45	19	$p<0.01$	CPO is less uneven
Q9	The lighting is glaring.	6	4	n.s.	No change in glare
Q10	The lighting does show colours properly.	21	61	$p<0.01$	Better colour appearance under CPO
Q11	Now, using a scale of 1 to 10, please rate how bright the street lighting is (1 = very dark, 10 = very bright).	5.5	7.9	$p<0.01$	CPO is brighter
Q12	Now, using a scale of 1 to 10, please rate how satisfied you are with the lighting (1 = very dissatisfied, 10 = very satisfied).	5.4	8.4	$p<0.01$	CPO gives higher satisfaction

4.3 S/P ratio

At mesopic levels of adaptation lighting from lamps of higher S/P ratio tends to appear brighter, for example scenes lit by lamps such as MH and fluorescent appear brighter than when lit by HPS lamps of equal illuminance [Fotios & Cheal, 2007, 2011], and thus lighting of higher S/P ratio may also enhance reassurance. The S/P ratio is an interesting metric for outdoor lighting, providing characterisation of visual performance [CIE 2010b] in addition to spatial brightness [Fotios & Cheal, 2011] and is the basis of new road lighting guidance in the UK [Fotios & Goodman, 2012: ILP, 2012]. There is evidence that higher S/P ratio enhances reassurance in the results of the field studies described above where existing LPS or HPS lighting was replaced by lamps of broader spectral distribution [Akashi et al, 2004; Knight, 2010; Morante, 2008].

5 Conclusion

This review sought to establish evidence of how lighting characteristics may influence pedestrians reassurance when walking after dark. There is some evidence that lighting is associated with reassurance by pedestrians [Painter, 1994, 1996; Okuda et al, 2007; Koga, 2003; Van Cauwenberg et al, 2012, Bernhoft & Carstensen, 2008; Hanyu, 1997]. There is evidence that illuminance [Boyce et al, 2000; Vrij & Winkel, 1991] and SPD [Akashi et al, 2004; Knight, 2010; Morante 2008] matter. Pedestrian reassurance is enhanced by lighting that is brighter. This brightness can be achieved using higher illuminance and/or higher S/P ratio. For illuminance, at least, there is some evidence that there may be a plateau (10 lux) beyond which further increase in illuminance does not lead to significant increase in reassurance [Boyce et al, 2000] but that evidence requires confirmation in the context of residential roads. This article has not addressed the spatial distribution of light: there is insufficient evidence regarding the effect of illuminance uniformity but there is some evidence that lighting the immediate vicinity of a pedestrian and natural objects enhances reassurance [Haans & de Kort, 2012; Nikunen & Korpela, 2012].

Acknowledgement This work was carried out through support from EPSRC (EP/H050817) as part of the MERLIN project.

References

AKASHI, Y., REA, M., MORANTE, P. 2004. Progress Report: Improving acceptance and use of energy-efficient lighting. Unified photometry: An energy-efficient street lighting demonstration in Easthampton, Massachusetts. Lighting Research Center. USA: Troy.

ALFONZO, MA. 2005. To walk or not to walk? The hierarchy of walking needs. *Environment & Behavior*, 37; 808-836.

ATKINS, S., HUSAIN, S., STOREY, A. 1991. The Influence of Street Lighting on Crime & Fear of Crime. Paper 28, Crime Prevention Unit. London.

BENNETT, R. 2000. White light reduces fears. *The Philips Lamp & Gear Magazine*, 3(2); 14-17.

BERNHOFT, I.M., CARSTENSEN, G. 2008. Preferences and behaviour of pedestrians and cyclists by age and gender. *Transportation Research Part F*, 11; 83–95.

BISHOP, ID., ROHRMANN, B. 2003. Subjective responses to simulated and real environments: a comparison. *Landscape and Urban Planning*, 65; 261-277.

BLÖBAUM, A., HUNECKE, M. 2005. Perceived danger in urban public space. The impacts of physical features and personal factors. *Environment and Behaviour*, 37(4); 465-486.

BOYCE, PR., EKLUND, NH., HAMILTON, BJ., BRUNO, LD. 2000. Perceptions of safety at night in different lighting conditions. *Lighting Research & Technology*, 32; 79-91.

BOYCE, PR., GUTKOWSKI, JM. 1995. The if, why and what of street lighting and crime: A review. *Lighting Research and Technology*, 27(2); 103-112.

VAN CAUWENBERG, J., CLARYS, P., DE BOURDEAUDHUIJ, I., VAN HOLLE, V., VERTÉ, D., DE WITTE, N., DE DONDER, L, BUFFEL, T., DURY, S., DEFORCHE, B. 2012. Physical environmental factors related to walking and cycling in older adults: the Belgian ageing studies. *Public Health*, 12; 142.

CIE. 2010a. CIE 115:2010. Lighting of Roads for Motor and Pedestrian Traffic. Vienna: CIE

CIE. 2010b. CIE 191:2010. Recommended system for visual performance based mesopic photometry. Vienna: CIE.

COZENS, PM., NEALE, RH., WHITAKER, J., HILLIER, D., GRAHAM, M. 2003. A critical review of street lighting, crime and fear of crime in the British city. *Crime Prevention & Community Safety: An International Journal*, 5(2); 7-24.

Department of the Environment and Welsh Office. 1994. Planning Out Crime Circular 5/94. Crown Copyright: London.

DRAVITZKI, VK., CLELAND, BS., WALTON, D., LAING, JN. 2003. Measuring commuting pedestrians' concerns for personal safety and the influence of lighting on these concerns. 26th Australasian Transport Research Forum. Wellington, New Zealand. 1-3 October, 2003.

FISHER, BS., NASAR, JL. 1992. Fear of Crime in Relation to Three Exterior Site Features : Prospect, Refuge, and Escape. *Environment and Behavior,* 24(1); 35-65.

FOTIOS, SA., CHEAL, C. 2011. Predicting Lamp Spectrum Effects At Mesopic Levels. Part 1: Spatial Brightness. *Lighting Research & Technology*, 43(2); 143-157.

FOTIOS, SA., CHEAL, C. 2007. Lighting for subsidiary streets: investigation of lamps of different SPD. Part 2 – Brightness. *Lighting Research & Technology*, 39(3); 233-252.

FOTIOS, S., GOODMAN, T. 2012. Proposed UK Guidance for Lighting in Residential Roads. *Lighting Research & Technology*, 44(1); 69-83.

FYHRI, A., HOF, T., SIMONOVA, Z., DE JONG, M. 2010. The influence of perceived safety and security on walking. Walk21; Getting communities back on their feet. Den Haag, Netherlands, 16-19 November 2010. 49-70.

GREENE, M., GREENE, R. 2003. Urban safety in residential areas: Global spatial impact and local self-organising processes. 4th International Space Syntax Symposium London 2003. pp52.1-52.8

HAANS, A., DE KORT, YAW. 2012. Light distribution in dynamic street lighting: Two experimental studies on its effect on perceived safety, prospect, concealment, and escape. *Journal of Environmental Psychology*, 32; 342-352.

HANYU, K. 1997. Visual properties and affective appraisals in residential areas after dark. *Journal of Environmental Psychology*, 17; 301-315.

HERZOG TR AND FLYNN-SMITH JA. 2001. Preference and perceived danger as a function of the perceived curvature, length and width of urban alleys. *Environment and Behavior*, 33; 653-666.

ILE. 2008. TR29: White Light. Rugby: ILE.

ILP. 2012. PLG03:2012. Lighting for Subsidiary Roads: Using white light sources to balance energy efficiency and visual amenity. Rugby; ILP.

KNIGHT, C. 2010. Field surveys investigating the effect of lamp spectrum on the perception of safety and comfort at night. *Lighting Research & Technology*, 42(3); 313-330.

KOGA, Y., TANAKA, R., SHIBATA, D. 2003. Evaluation structure on night streets. A case study in Fukuoka. 25th Session of the CIE. San Diego, 25 June to 2 July 2003. ppD5 82-85

LUYMES DT, TAMMINGA K. Integrating public safety and use into planning urban greenways. Landscape and Urban Planning, 1995; 33; 391-400.

LOEWEN, LJ., STEEL, GD., SUEDFELD, P. 1993. Perceived Safety from Crime in the Urban Environment. *Journal of Environmental Psychology*, 13, 323-331.

LOUKAITOU-SIDERIS, A. 2006. Is it Safe to Walk?1 Neighborhood Safety and Security Considerations and Their Effects on Walking. *Journal of Planning Literature*, 20: 219-232.

MATSUI, T. 2007. A study on a street lighting that makes change illuminance is effective for both reducing fear of crime and saving energy. 26th Session of the CIE, pp D5-112 – D5-115. China: Beijing

MORANTE, P. 2008. Mesopic street lighting demonstration and evaluation. Final Report for Groton Utilities, Groton, Connecticut. Lighting Research Center. USA: Troy.

NAIR, G., MCNAIR, DG., DITTON, J. 1997. Street lighting: Unexpected benefits to young pedestrians from improvement. *Lighting Research & Technology*, 29(3); 143-149.

NAIR, G., DITTON, J., PHILLIPS, S. 1993. Environmental improvements and the fear of crime. *British Journal of Criminology*, 33,4, 555-561.

NIKUNEN, H., KORPELA, KM. 2012. The effects of scene contents and focus of light on perceived restorativeness, fear and preference in nightscapes. *Journal of Environmental Planning and Management*, 55(4); 453-468.

OKUDA, S., ISHII, J., FUKAGAWA, K. 2007. Research on the lighting environment in the street at night. Part 1. Resident’s attitude on the safety and security in the street at night. 26th session of the CIE, Beijing, July 2007.

PAINTER, K. 1994. The impact of street lighting on crime, fear and pedestrian street use. *Security Journal*. 5(3); 116-124.

PUCHER, J., DIJKSTRA, L. 2003. Promoting safe walking and cycling to improve public health: Lessons from the Netherlands and Germany. *American Journal of Public Health*, 93(9); 1509-1516.

TOET, A., VAN SCHAIK, MG. 2012. Effects of signals of disorder on fear of crime in real and virtual environments. *Journal of Environmental Psychology*, 32; 260-276.

VRIJ, A., WINKEL, FW. 1991. Characteristics of the built environment and fear of crime: a research note on interventions in unsafe locations. *Deviant Behavior: An Interdisciplinary Journal*, 12; 203-215.

PP67

RESEARCH ON SIMULATION ANALYSIS OF SAFETY EVALUATION INDEX OF CLOVERLEAF WITH HIGH MAST LIGHTING

1st Pengfei Guo [1], 2nd Lixiong Wang[1], 2nd Yuhong Cheng[1]
[1] Tianjin University, Tianjin, CHINA
13672006710@163.com

Abstract

Through the investigation of overpasses in Beijing and Tianjin, it proves that cloverleaf intersection is the most typical overpass form. According to the research on different parts of cloverleaf (main road, flyover and entrance etc.) and the analysis of the DIAlux simulation results, the more suitable evaluation indexes for disability glare were discussed in the paper.

Keywords: Overpass, High Mast Lighting, Glare Rating (GR), Increment Threshold (TI)

1 Introduction

Overpass is an important node in road network, its negative effect on the traffic network cannot be neglected. The overpass road is classified as fast road, which belongs to the intersection area in the city. Drivers need to identify the traffic signal and signage in rapid movement (Niu, 2007), therefore, compared with ordinary road, overpass need higher quality requirements for lighting. According to these features, most of the overpass roads use high-mast lamps, which require strict limits on disability glare that will cause adverse effects on the drivers. A favourable overpass lighting environment helps decrease the traffic accidents in the city. It is significant to research the lighting environment in overpass road.

2 Evaluation indexes for disability glare

The evaluation indexes for disability glare have not yet been mentioned explicitly in domestic and international standards. Previous studies use increment threshold (TI) index to measure the degree of disability glare (Niu, 2007), however, it is still unclear. In this paper, whether glare rating (*GR*) index can be used for disability glare in overpass road is proved.

2.1 Glare rating GR

Glare rating is subjective psychological parameter of the discomfort in the human eyes, which caused by the lighting devices in outdoor stadium and other outdoor venues. It can be calculated by CIE glare rating equation.

Three conditions are included in the application scope of glare rating. Firstly, observation direction of the observer changes constantly rather than remain statically. Secondly, arrangement of the light sources is not necessarily a linear distribution. Finally, the installation height and the illumination level of lighting devices often beyond the effective range of the concept of ordinary road lighting.

2.2 Increment threshold TI

Standard for Lighting Design of Urban Road (CJJ45-2006) shows the definition of threshold increment (TI): "The measure of disability glare expressed as the percentage increase in contrast required between a standard object and its background (the carriageway) for it to be seen equally well with the source of glare present as with it absent, derived in the specified manner."

CIE Publication 132-1999, Design Methods for Lighting of Roads, which describes the calculation model of TI in detail and then gives specific examples to validate it. On account of the limitation of this paper, the calculation process will not be described.

3 A typical form of overpass

Most of the overpasses were built in heavy traffic areas, and the way of traffic passing through was of great complexity. As a consequence, there is a great variety of overpass forms in the city. In order to make the study more representatively, only the most typical form of overpass will be discussed in this paper.

3.1 Statistic of overpass in Beijing

Since the first overpass built in Beijing (1974), there have been thousands of overpasses were distributed through ring roads and main roads of Beijing in order to solve the problem of traffic congestion.

The overpasses that range from 2nd to 6th ring roads in Beijing have been recorded in this section. The statistics are shown in Table 1.

Table 1 – Summary of Beijing Overpass Forms

Form	Interchange							Separate
	Cloverleaf			Other forms				
	Two layers	Three layers	Four layers	Leaf shape	Annulus	Trumpet	Hybrid	
Item number	11	8	1	1	3	3	0	13
Subtotal	20			7				13
Grand total	40							
Proportion	50%			17.5%				32.5%

Interchange accounted for 67.5% in Beijing overpass investigation. What is more, 50% of the statistics was cloverleaf.

3.2 Statistic of overpass in Tianjin

Although the number of overpasses in Tianjin is not as many as it in Beijing, there are hundreds of overpasses in the city at present. Forty of the most crucial overpasses in Tianjin are studied in the investigation. Moreover, the proportions of several common types are summarized in the following table.

Table 2 – Summary of Tianjin Overpass Forms

Form	Interchange							Separate
	Cloverleaf			Other forms				
	Two layers	Three layers	Four layers	Leaf shape	Annulus	Trumpet	Hybrid	
Item number	0	13	4	1	0	0	4	18
Subtotal	17			5				18
Grand total	40							
Proportion	42.5%			12.5%				45%

Interchange accounted for 55% in Tianjin overpass investigation. Moreover, 42.5% of the statistics was cloverleaf. Thus it can be seen that the cloverleaf interchange was widely used in China’s big cities.

3.3 Summary

On the basis of the investigation in Beijing and Tianjin, several data can be illustrated that the separated overpass accounted for 38.75%, interchange accounted for 61.25%, and the percentage of cloverleaf reached up to 46.25 %.

Table 3 – Summary of Beijing and Tianjin Overpass Forms

Form	Interchange							Separate
	Cloverleaf			Other forms				
	Two layers	Three layers	Four layers	Leaf shape	Annulus	Trumpet	Hybrid	
Item number	11	21	5	2	3	3	4	31
Subtotal	37			12				31
Grand total	80							
Proportion	46.25%			15%				38.75%

According to the statistics of the investigation in Beijing and Tianjin, the conclusions can be drawn that the most typical form of overpass is the cloverleaf interchange.

4 Digital simulation of cloverleaf interchange

4.1 Model construction

Cloverleaf interchange includes four parts: main road, flyover, ramp and entrance. Each part could be designed by the lighting standard of their own. The index of luminance, illuminance and surround ratio on main road area should be accorded with the *Standard for Lighting Design of Urban Road (CJJ45-2006).*The index of ramp, speed change lane and collector-distributor lane should be designed according to the standard of main road or a level below it. Entrance area and triangle area could be designed refer to the lighting standard of road cross area in *CJJ45-2006.*

On the premise of meeting the lighting standard above, parameters for DIALux simulation were set. Luminaire: PHILIPS MVF024 C 1xSON-T1000W SGR MB. There are four 41m high-mast lamps on the centre of the ramps, each lamp panel arranges 15 lamps; Eight 25m high-mast lamps in the triangle area, each lamp panel arranges 11 lamps. Lamp elevation angle is 60°. Location of the high-mast lamps is shown in Figure 1.

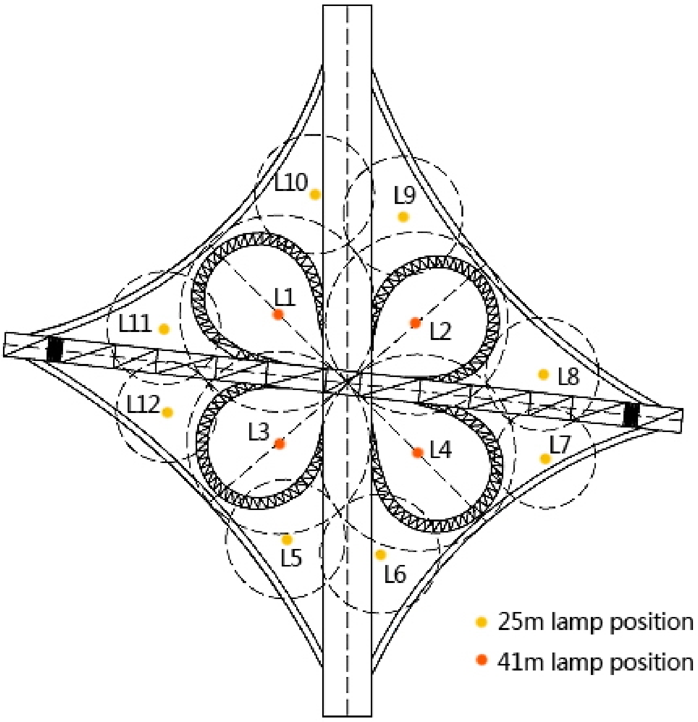

Figure 1 – Lamp Position (Photo Credit: Author's Self-Drawing)

4.2 Calculation of *GR*

As position of the observer chosen follows the most unfavorable principle; it means the observer should be set in the most susceptible to the maximum glare. The location of observer and the observation direction are shown as follows.

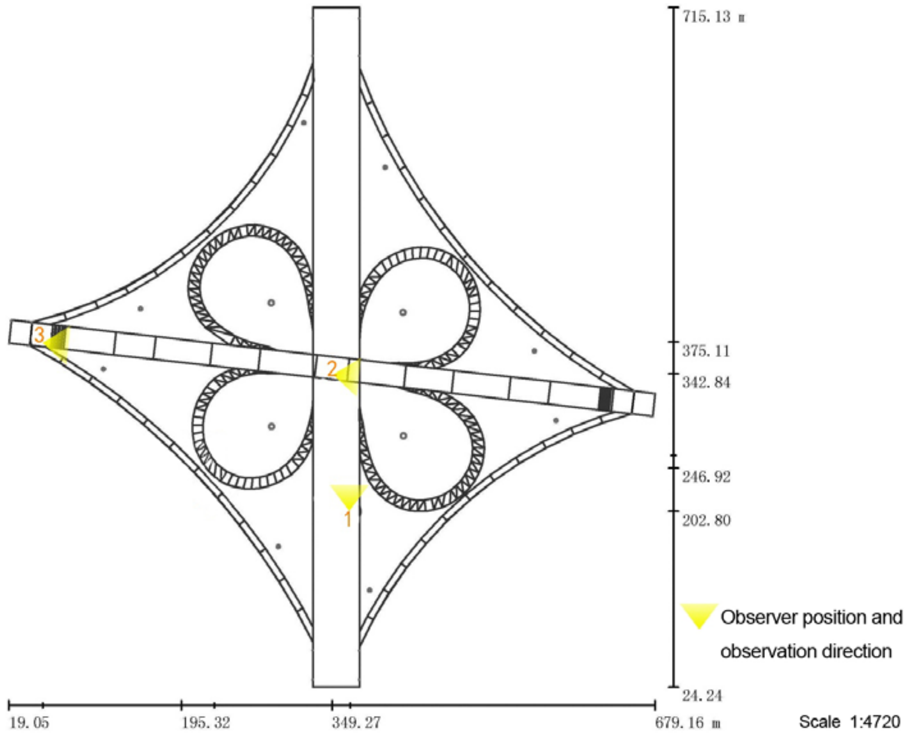

Figure 2 – Observer Position and observation direction (Photo Credit: Author's Self-Drawing)

Table 4 – Parameter of observer

Position		1 Main road	2 Flyover	3 Entrance
Height(m)		1.5	7.5	1.5
Observing angle(°)	Starting angle	0	-90	-90
	Ending angle	180	90	90

The maximum value of GR (GR_{max}) can be got by the calculation of DIAlux lighting simulation (Table 5).

Table 5 – Value of GR_{max}

GR observer position	1 Main road	2 Flyover	3 Entrance
GR	48	35	47

In *Glare Evaluation System for Use Within Outdoor Sport and Area Lighting (CIE 122-1994),* the stipulation of GR_{max} in “normal traffic” is 45. The glare rating results calculated by DIAlux in main road and entrance are more than 45, which go beyond the standard of 4.4%~8.9%. While the GR in flyover are less than 45, which meet the requirements of this standard.

4.3 Calculation of TI

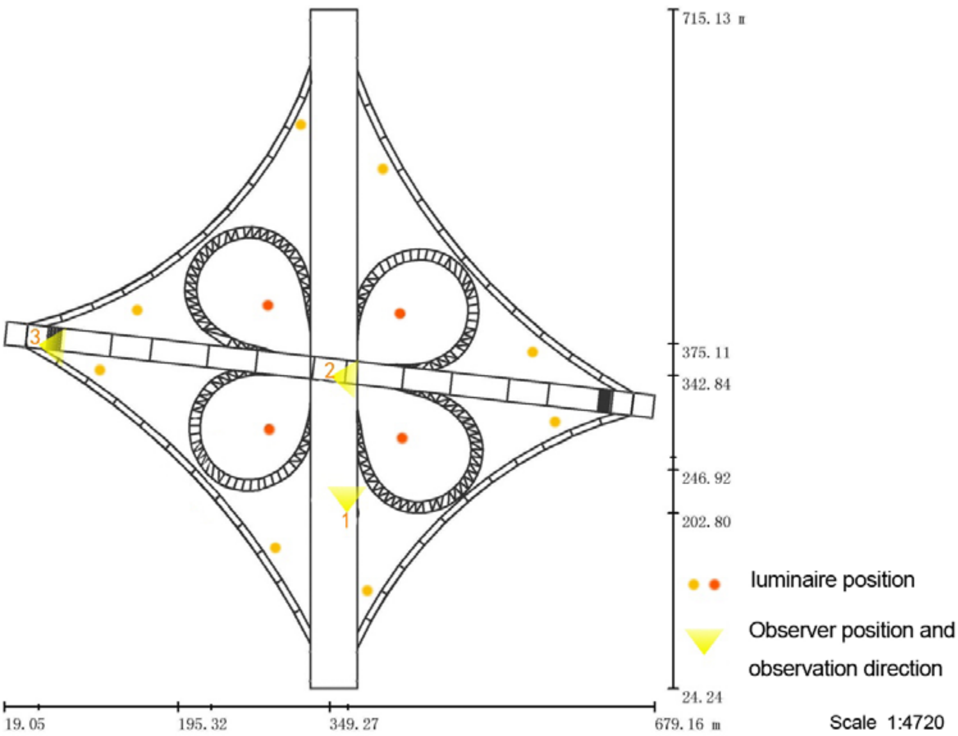

Figure 3 – Observation and Luminaire Position (Photo Credit: Author's Self-Drawing)

In DIAlux, observer position coordinates and luminnaire position coordinates are shown as follows.

Table 6 –Observer Position Coordinate

Number	Observer	Coordinate		
		X_O	Y_O	Z_O
1	Main road---Observer 1	367.625	202.796	1.500
2	Flyover ---Observer 2	349.272	342.844	7.500
3	Entrance---Observer 3	53.726	375.109	1.500

Table 7 –Luminaire Position Coordinate

Lamp number	Coordinate		
	X_O	Y_O	Z_O
L1	287.100	414.885	40.000
L2	421.655	405.307	40.000
L3	287.483	289.222	40.000
L4	422.100	279.737	40.000
L5	294.400	166.986	25.000
L6	387.646	122.644	25.000
L7	578.000	295.300	25.000
L8	555.809	366.033	25.000
L9	403.500	552.700	25.000
L10	320.345	597.928	25.000
L11	153.635	408.849	25.000
L12	115.800	347.598	25.000

TI calculation of Observer 1:

For Observer 1, view field of the human eyes set at 180° in front. Except L5 and L6, the rest of lamps are all included. We need to calculate S angle to clarify whether the other luminaire contribute to TI. The luminaire would not be included in the calculation if it was more than 20°

Table 8 –Value of Luminaire S angle

Lamp number	L1	L2	L3	L4	L7	L8	L9	L10	L11	L12
S°	10.298	10.764	24.011	26.583	14.252	8.192	3.842	3.404	6.506	9.218

L3 and L4 are not included in the calculation as their S angles are more than 20°.

Other equivalent veiling luminance is calculated by:

$$L_v = \frac{\mathrm{K} \times E_{gl}}{\theta^2} \tag{1}$$

where:

L_v is the equivalent veiling luminance in cd/m^2;

K is a constant;

For practical purposes K=10 when θ is expressed in degree or equal to 0.003 when θ is expressed in radian. K is amongst others dependent on the age of the observer.

E_{gl} is the illuminance in lux on the observer's eye in the plane perpendicular to the line of sight, produced by the glare source;

θ is the angle (in degree or radian) between the line through the eye and the centre of the glare source and line of sight.

The illuminance (E_{gl}) of luminaire on observer's eyes is 34lx, it can be learned according to the DIAlux simulation. What is more, the value of P, Q, R and θ can be got by calculating that are shown in Table 9.

Table 9 –Value of Luminaire θ

Lamp number	L1	L2	L7	L8	L9	L10	L11	L12
P	52948.270	45412.196	53366.881	62611.786	124272.075	158916.946	88801.809	84935.700
Q	7387.064	7387.064	7387.064	7387.064	7387.064	7387.064	7387.064	7387.064
R	23999.122	18109.218	44925.793	42013.826	71591.679	98463.219	60845.068	67506.161
θ	23.271	18.737	66.510	49.411	7.582	8.105	46.371	60.306

Put E_{gl}, θ in equation (1), calculation is shown in Table 10.

Table 10 –Value of Luminaire $L_{v,total}$

Lamp number	L1	L2	L7	L8	L9	L10	L11	L12
L_v	0.628	0.969	0.077	0.139	5.915	5.175	0.158	0.093
$L_{v,total}$	13.154							

According to equation (2), TI in Observer 1 is 261.62. (L_{av} is 4.2cd/m^2 by DIAlux simulation.)

$$TI = 65 \cdot \frac{L_{v,\,total}}{L_{av}^{0.8}} \tag{2}$$

where:

TI is the threshold increment in %;

$L_{v,total}$ is the veiling luminance in cd/m^2;

L_v is the average road surface luminance in cd/m^2.

In the same way, the values of TI in Observer 2, 3 are listed in Table 11.

Table 11 –Value of *TI*

Observer location	Main road (Observe 1)	Flyover (Observe 2)	Entrance (Observe 3)
TI	261.62	242.80	250.14

Standard for Lighting Design of Urban Road (CJJ45-2006) defines that *TI* maximum of main road is 10, the software simulation results are considerably larger than the standard.

4.4 Comparison of indexes

The results of *GR* and *TI* of three positions are obtained by the simulation, which are shown in Table 12.

Table 12 –*TI* and *GR*

Observer location	*GR*	*TI*	Sketch (Author's Self-Drawing)
1 Main road	48	261.621	
2 Flyover	35	242.796	
3 Entrance	47	250.144	
Standard	45	10	

In this section, conclusions are summarized by comparing *GR* and *TI* with relevant standards. Simulation results of *TI* are considerably larger than the relevant standard while the results of *GR* fluctuate above and below the standard.

According to the analysis of computational principle of *TI*, the reasons of great differences between the simulation results and the standard values can be summarized in the following points.

- Regular calculation of *TI* rest on two guiding principles: one is the luminaires are arranged in regular, the other one is the viewing direction is 1° downward from the horizontal. But in this simulation, the high-mast lamps are dispersed among the bridge area, rather than ranged along a straight line.

- There are fifteen 1000w lamps in one panel of high-mast lamp, while the ordinary street lamp is 250w, and there are only one or two lights in lamp holder.
- Cloverleaf is an interchange bridge, the flyover has a certain height from the ground. When driving to higher position, the vertical distance from the lamp mast to the driver decreases. High-power lamps are effecting direct light to human eyes, which have a greater impact on safe driving. Therefore, calculated value of TI in flyover area is larger than the standard.

5 Conclusion

This paper selects lighting design software—Dialux to simulate the lighting environment of overpass road. Computer model is established by the lighting standard of each parts of overpass. Calculated by the model, the value of GR and TI of three points (main road, flyover and entrance) which would be the most likely positions for disability glare were got. The GR and TI with relevant standards were compared to make sure whether they could measure disability glare of overpass. Using TI to evaluate the index of glare, the calculated value will be considerably larger than the relevant standard, while GR is more accurate to measure glare in intersections, its value fluctuates above and below the standard.

References

CIE 1994. CIE 122:1994. *Glare Evaluation System for Use within Outdoor Sport and Area Lighting*. Vienna: CIE.

CIE 1999. CIE 132:1999. *Design Methods for Lighting of Road*s. Vienna: CIE.

MOHURD 2006. Ministry of Housing and Urban-Rural Development of the People’s Republic of China. CJJ 45-2006. *Standard for Lighting Design of Urban Road*.

NIU, S.N. 2007. Study on the Obtrusive Light and TI Value of Urban Interchange Illuminating. *China Illuminating Engineering Journal*. 18(2), 25-27.

PP68

STREET LIGHTING APPRECIATED BY PEDESTRIANS: A FIELD STUDY

Romnée, A.[1], Bodart, M.[1]
[1] Architecture & Climat, Université catholique de Louvain, Louvain-la-Neuve, BELGIUM
ambroise.romnee@uclouvain.be

Abstract

Street lighting standards are based on quantitative measurements of various parameters such as luminance, illuminance, glare and lateral light distribution. At the moment, we know that subjective criteria are also important for pedestrians in order to achieve high quality street lighting.

A field study was conducted under LED light and HPS light in order to identify the indicators of a high quality street lighting designed for pedestrians. The survey compares these indicators to the characteristics, enumerated by the participants, for each LED light or HPS light. Finally, the survey measures the feeling of safety, the visual comfort and the perception of lighting atmosphere for pedestrians.

This paper shows that the near visibility, the feeling of safety, the brightness, the illumination uniformity and a non-glare light are cited as the more important indicators of high quality street lighting for pedestrians.

Moreover the paper also shows that the characteristics of LED light, appreciated by pedestrians, are well correlated to the indicators of a high quality street lighting.

Finally this research shows that pedestrians always prefer LED light to HPS light whatever the concept of feeling of safety, the concept of visual comfort or the perceived luminous atmosphere is concerned.

Keywords: Field study; LED street lighting; pedestrians; indicators

1 Introduction

Street lighting standards recommend to provide sufficient amount of light to ensure to cover the street safely with a good visual comfort and an appreciated luminous atmosphere.

Several studies have shown that other criteria, essential for the user and especially for pedestrians, should also be considered in order to achieve high quality street lighting.

The aim of this paper is to reveal these criteria and to discover how the light spectrum may influence their perception.

Several studies have already been carried out to investigate the appreciation of light by pedestrians, under different conditions. Jaatinen (Jaatinen, 2010) found that LED lighting is too bright and causes glare but it is not always considered as a negative feature. He also found that pedestrian walking in streets illuminated by LED luminaires feel safer than in streets illuminated by MH luminaires. Rea and al. (Rea, Bullough, Akashi, 2009) said that at identical lighting level, a street lit by white lamp appears brighter and safer than a street lit by HPS sources. Boyce and Bruno (Boyce, Bruno, 1999) discovered that the higher the photopic illuminance, the more positive the perceptions and the stronger the preference, regardless of lamp spectrum. Knight (Knight, 2010) found that, as same light level, spaces illuminated by white sources are perceived brighter, safer and more comfortable than spaces illuminated by orange sources.

The results of these studies suggest a significant positive effect of LED sources to the appreciation of street lighting.

To go further than these studies, a field study was conducted in two adjacent streets in order to study the pedestrian appreciation of public lighting under LED sources and HPS sources.

The survey firstly aimed to identify which are the indicators of a high quality street lighting designed for pedestrians.

It also aimed to compare these indicators with the positive aspects, enumerated by the participants, of each LED light or HPS light.

The survey finally aimed to measure the feeling of safety, the visual comfort and the perception of lighting atmosphere for pedestrians.

2 Method

2.1 Overview

The experiment took place in a pilot site developed for the GEPPADI project (Romnée et al., 2013).

Forty one subjects experienced two similar streets, each illuminated by different light source installed in the same type of luminaire. The first street, called “reference street”, was illuminated by HPS sources and the second street, called “test street”, was lit by LED sources.

For both streets, each subject was first immersed in the light by walking in the street and then driven to the test location. At each test location, the subject was asked to answer a questionnaire (identical in both streets) about its appreciation of the light.

Through this questionnaire, subjects were asked to give their opinions or their feeling of safety and of visual comfort and their perception of the lighting atmosphere. They were also asked to points out which are, to their opinion, the indicators of a high quality street lighting. They were finally asked to characterize both light sources, according to these indicators.

The subjects, 21 men and 20 women, were grouped by 5. The experiment was conducted during 4 nights in March 2013 with 2 groups per night. In order to investigate the influence of the order of exposition (from LED street to HPS street and vice versa), one group started the survey from LED street and the other group started simultaneously from HPS street.

41 % of subjects were under 30 years. 37 % of subjects were between 30 and 60 years. 22 % of subjects were older than 60 years. The average year of participants was 42.

2.2 Independent and dependent variables

Performing an inquiry request to compare two types of variables: independent and dependent variables. An independent variable is a hypothetical factor affecting the activity studied. A dependent variable that depends on the action of the independent variable is intended to undergo the action of this factor (De Singly, 1992). The independent variables are the elements of the analysis so that the dependent variables are the means used to perform the analysis.

Two independent variables were used in the survey: lamp type (LED or HPS) and profile of participants (the age, the order of exposition).

Twelve dependent variables fell into three concepts were measured during the experiment. These concepts are the feeling of safety, the feeling of visual comfort and the perception of lighting atmosphere. These concepts are abstracts objects of synthetic and intuitive knowledge. In order to be studied, they have to be measured by some dependent variables or indicators (De Singly, 1992). One dependent variable or indicator can measure different concepts.

Table 1 (next page) summarises the relationship between the variables, on base on the following research papers; (Boyce, Bruno,1999; Akashi, Rea, 2001; Raynham, Saksvikronning, 2003; Bacelar,2005; Fotios, Cheal, 2007; Deleuil, 2009; Rea, Bullough, Akashi, 2009; Alferdinck et al, 2010; Jaatinen, 2010; Knight, 2010; Ylinen, Paluolakka, Halonen, 2010; Viikari et al, 2011).

Table 1 - independent and dependent variables

INDEPENDENT VARIABLES	DEPENDENT VARIABLES	
	CONCEPTS	INDICATORS (non-exhaustive)
- **Lamp type** (LED or HPS) - **Profile of participants** (age, gender, order of exposition)	- **Feeling of visual comfort**	- Distance vision / Perspective - Color rendering / Identification of color - Amount of light - Glare - Readability of path / Contrast - Color of light - Vision surroundings - Uniformity of light
	- **Feeling of safety**	- People appearence - Color rendering / Identification of color - Walking alone at night - Socialization - Glare - Readability of path / Contrast - Distance vision / Perspective - Amount of light - Uniformity of light - Identification of people
	- **Perception of luminous atmosphere**	- Uniformity of light - Color rendering / Identification of color - Amount of light - Color of light

2.3 Construction of the questionnaire

In both streets subjects were asked a series of identical questions that addressed the three concepts explained above (see Table 1).

As the investigation pursued different objectives, the questionnaires presented 3 types of questions (see a sample in Figure 1): firstly, subjects were asked to mark their level of agreement with a proposal on a scale of 6 steps; secondly; they were asked to take position between two opposite characteristics of light on a scale of 6 steps and thirdly, they were asked to give their own opinion about what is a high quality street lighting and about some characteristics of each light source.

Each question referred to an indicator (see Table 1) of the studied concept. An indicator could be measured by many questions in order to compare responses. A concept was covered by many questions.

1 - I can see clearly other people in the street.

not agree at all ☐ ☐ ☐ ☐ ☐ ☐ *strongly agree*

2 - I think the light is evenly distributed all along the sidewalk on wich I walk.

not agree at all ☐ ☐ ☐ ☐ ☐ ☐ *strongly agree*

3 - The sidewalk on wich I walk appears dark.

not agree at all ☐ ☐ ☐ ☐ ☐ ☐ *strongly agree*

I think the color of the light is …

13 - *cold (bluish)* ☐ ☐ ☐ ☐ ☐ ☐ *warm*

14 - *unpleasant* ☐ ☐ ☐ ☐ ☐ ☐ *pleasant*

15 - *stressful* ☐ ☐ ☐ ☐ ☐ ☐ *relaxing*

According to you, what are the qualities of a good public lighting (3 or 4 words)

Figure 1 - sample of the questionnaire

2.4 Quantitative analysis of a qualitative appreciation

For each question, the subjects were asked to give their opinion on a scale of 6 steps. So each question was given a score between 1 and 6.

By convention, the score 6 corresponded to the highest score and was related to the answer: “Strongly agree” to the first type of question or to the most positive expression in the second type of question. Conversely, a score of 1, related to a “not agree at all” answer, corresponded to the lowest score.

As each question received a score, we were able to evaluate the appreciation of each indicator. The score of an indicator was the average scores for each question assessing the indicator.

A score was assessed for each indicator, which allowed then to evaluate a score for each concept. Based on the literature (Martin, 2005: Deleuil, 2009) we constructed an index of appreciation in order to evaluate the three concepts (the feeling of safety, the feeling of visual comfort and the perception of luminous atmosphere).

We then calculated the satisfaction index I_a which indicates a level of positive or negative satisfaction, ranging from +100 to -100, for the studied dependent variables (or concept). This satisfaction index I_a is based on the average scores for each indicators assessing the concept (see Table 1).

$$I_a = 200 * \sum_{x=1}^{N} \frac{i_x}{N * 6} - 100 \qquad (1)$$

where

I_a is the satisfaction index of the studied concept
i_x is the score of an indicator assessing the studied concept

N is the number of indicator assessing the studied concept

It is then possible to make a graph (Figure 2, left) whose abscissa is the index of appreciation of the concept studied for the street lit with HPS sources and whose ordinate is the satisfaction index of the concept studied for the street lit with LED sources. Each dot represents a subject.

A graph is then created for each dependent variable and consists in four quadrants whose signification is explained in Figure 2 (right). Moreover, the graph inform about:

1) People who have a very little marked or very low opinion on the analysed concept (subjects for whom $I_a \leq |50|$).
2) People who always prefer LED lighting compared to HPS lighting (subjects located above the 45°-line ($I_a > 45°$)).
3) People who appreciate the LED lighting and depreciate the HPS lighting (subjects located in Q4).

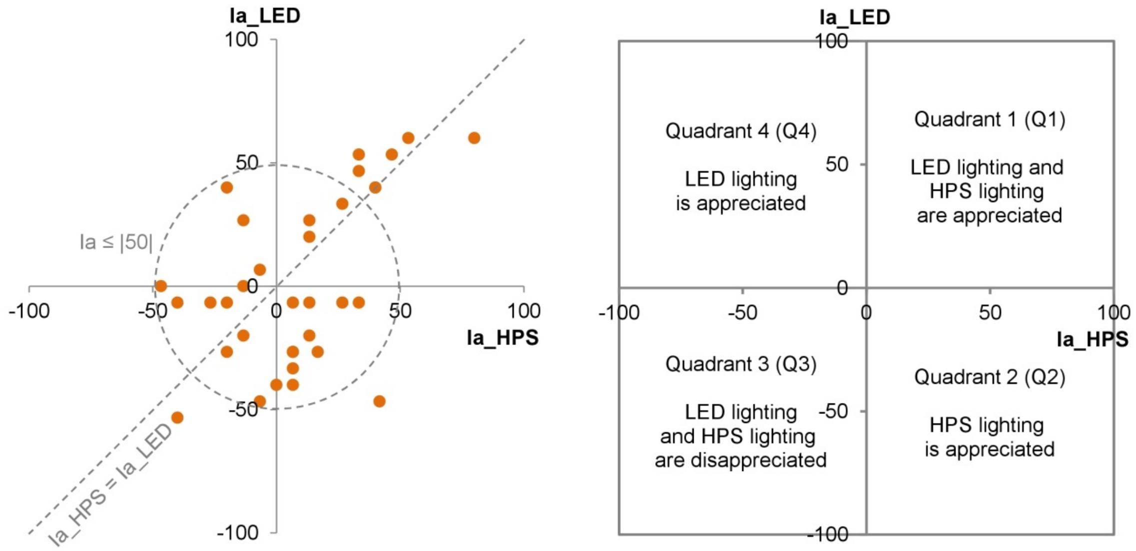

Figure 2 - method of analysis

3 Results

3.1 Indicators of a street lighting of high quality

Data collected with the open question (What are the qualities of a good public lighting?), in each street, were analysed regrouping the opinion of subjects on each topic. These topics are the indicators of a high quality street lighting designed for pedestrians.

We have counted the frequency of citation of each indicator in order to identify which are dominating for pedestrians.

Seventeen indicators of street lighting have been cited by pedestrians for characterising a street lighting of high quality. 15 of these 17 indicators had been used to measure the different dependent variables of the survey.

The two additional indicators relate to the ecological, economic aspect and to the feature to be adapted to the function.

Five indicators are cited by 60 % of the participants (Figure3). They are thus considered as the dominant.

For pedestrians street lighting of high quality is thus a lighting allowing to see closely, providing a feeling of safety, with an enough amount of light, uniform and not glaring.

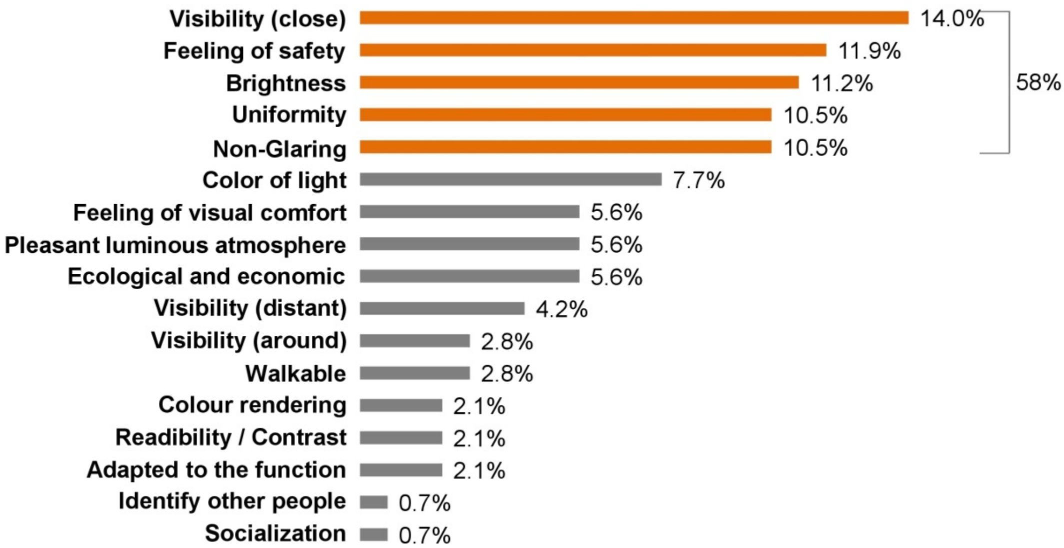

Figure 3 - indicators of a high quality street lighting designed for pedestrians

3.2 Comparison between the indicators of a street lighting of high quality and the encountered light characteristics

In each street, we asked the subjects to indicate some characteristics of the public lighting. These characteristics were then considered as the indicators of a street lighting of high quality, as mentioned above (Figure 3).

According to pedestrians, LED sources are soothing for a late afternoon, modern, nice but dazzling when one stares and a little cold. HPS sources are shabby, dingy, old fashion, sad, scenery of a sufficient place for the sweet horror movie but satisfactory for the season.

Among these characteristics, we have counted the frequency of mentioned qualities that we compared to the frequency of mentioned indicators of quality.

In this way, we can measure the difference of percentage between the frequency of mentioned qualities of LED lighting or HPS lighting and the frequency of citation of the general qualities expected of a public lighting designed for pedestrians (Figure 4).

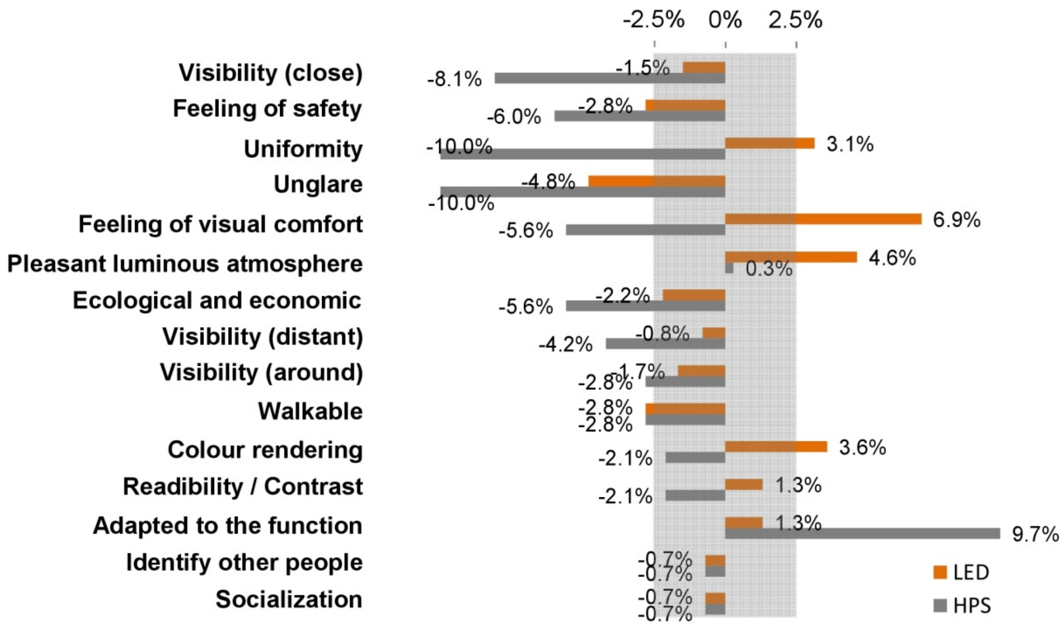

Figure 4 - comparison between a high quality street lighting and LED lighting or HPS lighting

According to Figure 4, 50 % of the characteristics cited as qualities for LED lighting are also indicators for street lighting of high quality, designed for pedestrians (IC 95 - ± 2.5 % around 0 %). Moreover the average difference between the qualities of LED lighting and a street lighting of high quality is 2 % compared to the average difference of 7 % for HPS lighting.

The need for lighting to be adapted to its function for pedestrian street is the only indicator cited more often for warm sources than for LED sources. Moreover this indicator is the only characteristic of warm sources to be recognised by pedestrians as positive. All other indicators are negative for the warm sources.

Some indicators are recognized by pedestrians as positive for LED lighting and negative for HPS lighting. The feeling of visual comfort is more appreciated under cold sources than under warm sources. The colour rendering and the readability/contrast of the pavement are cited as advantage for LED lighting and as disadvantage for HPS lighting. The uniformity appears more relevant under LED lighting than under HPS lighting.

3.3 Analysis of dependent and independent variables

The answers to questions were translated to a score between 1/6 and 6/6 as explained above.

For each subjects, for each light sources, we calculated the satisfaction index of the concept studied (see Table 1 and Equation 1). Results are presented in Figure 5 to 8.

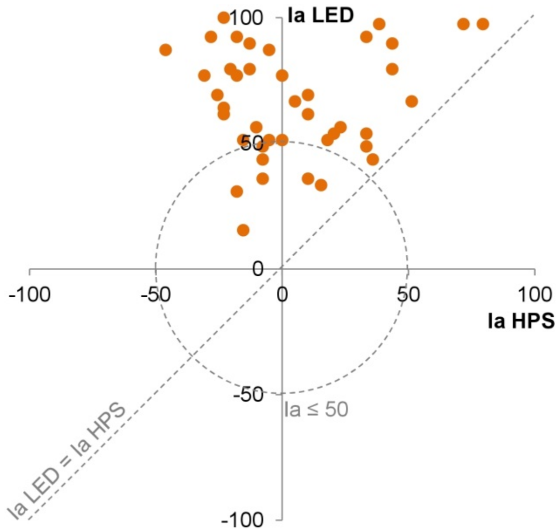

Figure 5 - global appreciation of light

1. $I_a \leq |50|$: 22 %
2. $I_a > 45°$: 100 %
3. Q4 : 51 %

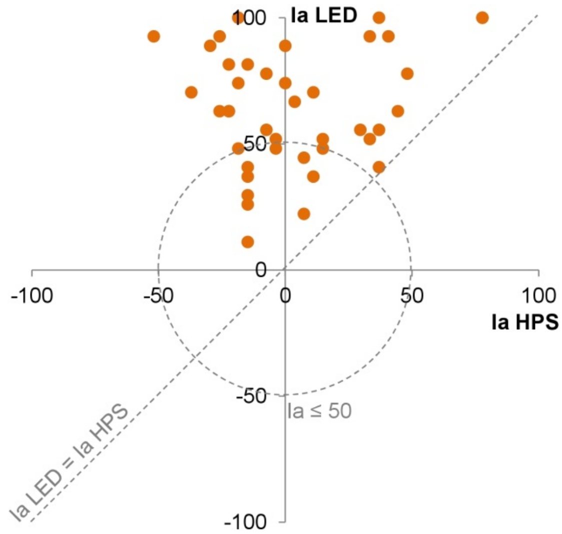

Figure 6 - global feeling of safety

1. $I_a \leq |50|$: 29 %
2. $I_a > 45°$: 100 %
3. Q4 : 51 %

The global appreciation of light (consideration of all questions in the questionnaire, regardless of the notion) and the global feeling of safety depend on the type of light source: in both dependent variables 100 % of people prefer LED lighting to HPS lighting ($I_a > 45°$) for 100% of the subjects.

Moreover, half of people feel safe and enjoys LED lighting while do not feel safe and do not enjoy HPS lighting (analysis of Q4).

Finally, more than 70 % of subjects have a significant opinion for each dependent variable (analysis of $I_a \leq |50|$). This confirms that the type of light source influences the appreciation of light and the feeling of safety.

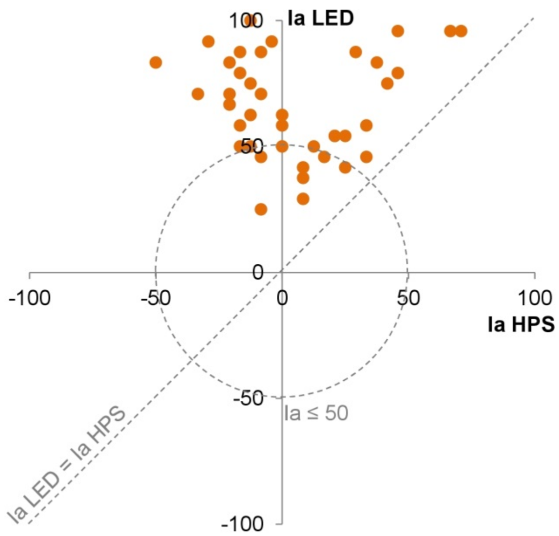

Figure 7 - global feeling of visual comfort

1. $I_a \leq |50|$: 19 %
2. $I_a > 45°$: 100 %
3. Q4 : 49 %

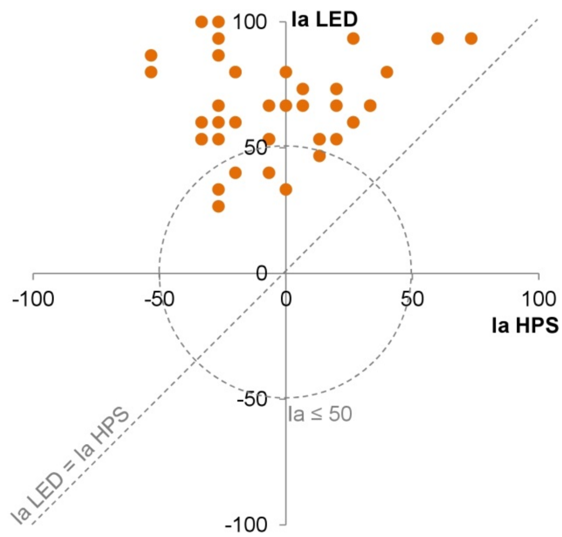

Figure 8 - global perception of luminous atmosphere

1. $I_a \leq |50|$: 15 %
2. $I_a > 45°$: 100 %
3. Q4 : 54 %

The global feeling of visual comfort and the perception of luminous atmosphere depend on the type of light source: in both dependent variables 100 % of people prefer LED lighting to HPS lighting (analysis of $\mathrm{I_a} > 45°$).

Moreover, half of people feels visually comfortable and enjoys the luminous atmosphere of LED lighting while they do not feel visually comfortable and do not perceive a good luminous atmosphere under HPS lighting (analysis of Q4).

Finally, more than 80 % of subjects have a significant opinion for each dependent variable (analysis of $\mathrm{I_a} \leq |50|$). This confirms that the type of light source influences the visual comfort and the perception of luminous atmosphere.

Table 2 provides a cross analysis between the dependent variables and the independent variables.

We don't specifically analyse the criteria $\mathrm{I_a} > 45°$ because we have seen above that whatever the subject and whatever the concept analysed, 100 % of the subjects prefer LED lighting.

Table 2 - analysis of dependent and independent variables

		Appreciation		Safety		Comfort		Atmosphere	
		Ia ≤ |50|	Q4	Ia ≤ |50|	Q4	Ia ≤ |50|	Q4	Ia ≤ |50|	Q4
Direction	**LED -> HPS**	14%	52%	19%	48%	19%	57%	14%	52%
	HPS -> LED	30%	50%	40%	55%	20%	40%	15%	55%
Gender	**Male**	28%	52%	38%	52%	28%	48%	19%	57%
	Female	15%	50%	20%	50%	10%	50%	10%	50%
Age	**< 30 years**	37%	37%	37%	31%	44%	44%	19%	50%
	30 - 60	19%	62%	31%	69%	25%	69%	12%	62%
	≥ 60 years	11%	78%	11%	78%	11%	67%	11%	78%

The order of lamp exposition affects all notions except the perception of luminous atmosphere: seeing first the white light sources LED increase the appreciation of each concept ($\mathrm{I_a} \leq |50|$ under HPS sources is two times higher than $\mathrm{I_a} \leq |50|$ under LED sources while Q4 is relatively equal).

The gender affects all notions: women are more categorical in favour of LED sources ($\mathrm{I_a} \leq |50|$ for male is two times higher than $\mathrm{I_a} \leq |50|$ for female while Q4 is relatively equal). Women, on average, rated more severely HPS sources.

We perceive the two same effects of age on the four notions: firstly, the older you are, the more you appreciate the LED sources and the more you depreciate HPS sources (Q4 becomes higher as we get older), secondly, the older you are, the more categorical you become categorical in our appreciation of notions in favour of LED sources ($\mathrm{I_a} \leq |50|$ becomes lower as we get older).

4 Discussion

The main result of the survey is that the type source influences the feeling of safety, the feeling of visual comfort and the perception of luminous atmosphere. For pedestrians, LED lighting is always preferred to HPS lighting. This agrees with the findings of previous studies assessing that white sources are more appreciated than yellow ones (Morante, 2008) (Deleuil, 2009) (Knight, 2010).

The profile of the subject (gender and age) affects the feeling of safety, the feeling of visual comfort and the perception of luminous atmosphere.

Women are more assertive in their appreciation. This observation confirms a previous study of Deleuil (Deleuil, 2009).

The older you are, the safer you feel, the more visually comfortable you feel. Older people appreciate also more the luminous atmosphere of LED lighting. These results should be confirmed by other studies using the same number of participants per age category. However, the results should be confirmed by another study increasing the number of subjects.

Moreover, in agreement with other studies (Mosser, 2003) (Deleuil, 2009) the characteristics of a quality public lighting should consider quantitative variables and qualitative variables.

Street lighting standards should integrate, in addition to the brightness, the uniformity or the glare, some requirements about the feeling of safety or the close visibility. These five requirements are cited by the population as indicators of a street lighting of a high quality, designed for pedestrians.

This study confirms that it is essential to integrate environmental and economic considerations in current standardisation in order to obtain public lighting of high quality.

Funding

The GEPPADI project (Sustainable and Intelligent Public Lighting Management in Business Parks), funded by the Walloon Region, is organised in partnership with companies of ARTHOS Technics et Ets. E. Ronveaux SA, SPI, the economic development agency for the province of Liège, the Electronics, Microsystems, Measurements and Instrumentation unit (EMMI) at the University of Liège and the Architecture & Climate laboratory of the Catholic University of Louvain.

References

ALFERDINCK, J., HOGERVORST, M., VAN EIJK, A., KUSMIERCZYK, J., 2010, Mesopic vision and public lighting - A literature review and a face recognition experiment. TNO - Ministery of Infrastructure and Environment (I&M).

AKASHI, Y., REA, M., 2001, The effect of oncoming headlight glare on peripheral detection under a mesopic light level. In, 2001. Herbert Utz Verlag, 9.

BACELAR, A., 2005, The Influence of Dimming in Road Lighting on the Visibility of Drivers. *Journal of Light & Visual Environment*, 29, 44-49.

BOYCE, P., BRUNO, L., 1999, An evaluation of high pressure sodium and metal halide light sources for parking lot lighting. *Journal of the Illuminating Engineering Society*, 28, 16-32.

DELEUIL, J.-M. (2009). EVALUM: De l'évaluation de différentes sources lumineuses par les usagers. In. Deleuil J.-M. (éd.) (2009) *Eclairer la ville autrement : Innovations et expérimentations en éclairage public*.Lausanne : Presses Polytechniques et Universitaires Romandes. pp. 36-52

DE SINGLY, F., (1992), *L'enquête et ses méthodes: le questionnaire*, 2nd édition, Paris : Armand Colin éd.

FOTIOS, S., CHEAL, C., 2007, Lighting for subsidiary streets: investigation of lamps of different SPD. Part 2—Brightness. *Lighting Research and Technology,* 39**,** 233.

JAATINEN, S, 2010, The use of LEDs in pedestrian ways, parking areas and parks – A user study. Thesis: Master of Science. Espoo : Aalto University

KNIGHT, C. 2010. Field surveys of the effect of lamp spectrum on the perception of safety and comfort at night. Lighting Research and Technology, 42, 313.

MARTIN, O., (2005), *L'enquête et ses méthodes: l'analyse de données quantitatives*, 2nd édition, Paris : Armand Colin éd.

MOSSER, S., (2003), *Eclairage urbain; enjeux et instruments d'actions*, Thèse de doctorat : Urbanisme, Paris : Université Paris 8 – Vincennes-Saint-Denis

REA, M., BULLOUGH, J., AKASHI, Y. 2009. Several views of metal halide and high-pressure sodium lighting for outdoor applications. *Lighting Research and Technology*, 41, 297.

RAYNHAM, P., SAKSVIKRONNING T., 2003, White light and facial recognition. *The Lighting Journal*, 68, 29-33.

ROMNÉE, A., LEJEUNE, G., BODART, M. *A new real time intelligent management model for street lighting*. CIE Centenary Conference : Towards a New Century of Light (Paris, du 15/04/2013 au 16/04/2013). In: *Proceedings of CIE Centenary Conference : Towards a New Century of Light*, 2013.

VIIKARI, M., PUOLAKKA, M., HALONEN, L. & RANTAKALLIO, A. 2012. Road lighting in change: User advice for designers. *Lighting Research and Technology,* 44**,** 171-185.

YLINEN A., PUOLAKKA M., HALONEN L., *Impact of mesopic design on outdoor lighting energy efficiency*. In: CIE 2010 Lighting Quality and Energy Efficiency, 2010 Vienne.

PP69

DOES LED LITGHING IMPROVE PEDESTRIANS VISUAL PERFORMANCES?

Romnée, A.[1], Bodart, M.[1]
[1] Architecture & Climat, Université catholique de Louvain, Louvain-la-Neuve, BELGIUM
ambroise.romnee@uclouvain.be

Abstract

A field survey was conducted in order to determine whether light spectrum of public lighting influences the ability of pedestrians to perform several visual tasks. This survey aims to compare the visual performance of pedestrian under two kinds of light sources: LED and HPS sources.

Visual performance of 40 people aged between 17 and 78 years have been measured through 4 specific tasks: facial and intent recognition, colour recognition, visual acuity and off-axis detection.

The results show that the spectral distribution of the lamps influences visual performance and that the magnitude of the effect varies according to the task. Depending on the task, people can perform as well under LED sources than under HPS sources,. But for peripheral tasks, people perform better under LED sources than under HPS sources.

This paper confirms that under mesopic light levels, where rods and cones work simultaneously, LED sources are more efficient for pedestrians.

Keywords: Field study; LED street lighting; pedestrians; visual performances

1 Introduction

The objective of public lighting is to allow human activity, walking, for example, to be completed comfortably, safely and in pleasant lighting conditions. Pedestrians, while being attentive to its progress and to guidance information should be able to identify the presence and intent of other pedestrians.

Previous studies, described here below, show that simultaneous tasks of pedestrians are detection of off-axis and foveal obstacles, recognition of people and of their intention, recognition of colours and finally orientation, which is linked to visual acuity.

The main objective of this paper is to study the influence of LED and HPS lighting on the achievement of these four visual tasks by pedestrians.

It has been shown (Eloholma, 2005) (CIE, 2009) that under mesopic vision conditions, lamps with a high S/P-ratio (typically LED sources) are perceived as brighter than lamps with a low S/P-ratio (typically HPS sources). They also improve peripheral perception.

Fotios and Cheal (Fotios, Cheal, 2009) revealed that the lamp type can affect obstacle detection and that the effect is weak when approaching the photopic state.

Colours recognition provides a better sense of safety and visual comfort. Some studies (Boyce, Bruno, 1999) (Fotios, Cheal, 2007) have shown that the type of lamp and the luminance affect the ability to recognize colours: lamps with a high colour rendering index or a high luminance favour a better colour recognition.

Different experiments were conducted to determine if the type of lamp influences the facial recognition. Some of them (Raynham, Saksvikronning, 2003; Yao et al., 2009; Knight, 2010) have concluded that facial recognition was affected by the type of lamp. Other studies (Rea, et al., 2009; Alferdinck et al, 2010) have found that the type of lamp has no significant effects on facial recognition. Recently Lin and Fotios (Lin, Fotios, 2013) found that for a short time of observation there is a significant effect of lamp spectral power distribution (SPD) on facial recognition: MH lamps permit correct identification at greater distances than HPS and LED sources. But for a longer time of observation the data do not suggest a significant effect. More than the facial recognition, the intent recognition provides the most effective means of communication and interaction (Chen, Chen, 2010).

In order to confirm or invalidate results of past studies dealing with the effects of light spectrum on visual performances of pedestrians, a field study was set up in two adjacent streets, lit by LED sources or by HPS sources.

2 Method

2.1 Overview

For both streets, each subject was first immersed in the light by walking in the street then driven to the test location. At each test location, the subject was asked to perform 4 visual tasks, identical in both streets.

Forty one subjects took part into the survey. Twenty one men and twenty women were grouped in groups of 5. The experiment was conducted during 5 nights in March 2013 with 2 groups per night. 41 % of subjects were under 30 years. 37 % of subjects were between 30 and 60 years. 22 % of subjects were older than 60 years. The average year of participants was 42.

2.2 Off-axis and foveal detection

This experiment consisted in rapidly detecting a grey cube of 20 cm side. The light reflectance of the cube is 24 %. The cube was placed randomly at 6 precise locations in the visual field of subjects. The 6 target locations were chosen to have 3 of them in the foveal part of the visual field (0°-target, 10°-target, 15°-target), 2 of them in the peripheral part (40°-target, 50°-target) and 1 of them between the two parts (25°-target).

Subjects were asked to evaluate the visibility of the cube on a 5 steps scale from “The target is not visible at all” to “The target is extremely visible”.

Subjects were located 14 m from the cube and 21,7 m from a cone they must stare during the detection experiment.

Figure 1 - diagram of the off-axis detection experiment

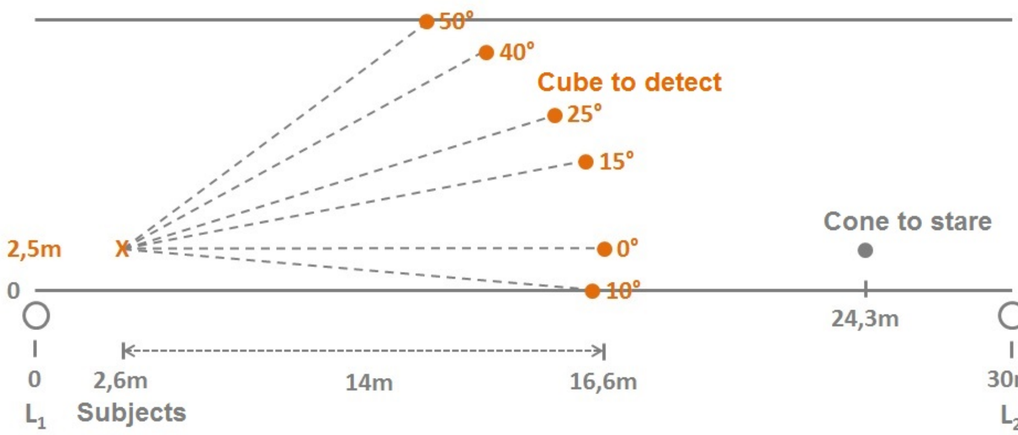

The experiment was conducted in 5 steps:

- First, subjects turned their back to the experiment. The cube was positioned at one of the 6 target locations.

- Then, at the first whistle, subjects rapidly rotated a half turn to face the experiment and stared the cone in front of them.
- Staring the cone, subjects had 2 seconds to detect the cube located somewhere in their visual field.
- After two seconds, a second whistle informed subjects to turn back to their initial position. Then they were asked to rate the visibility of the target they had detected on a 5 steps scale.
- The experiment was repeated 6 times, with the target at different locations in the visual field.

With this visibility evaluation procedure, each target received a score between 1 and 5: 1 corresponding to “The target is not visible at all” and 5 corresponding to “The target is extremely visible”. Beyond 3, we consider that the targets were well seen; below 3, we consider that the target was hardly detected.

2.3 Colour recognition

A 0,7 m × 0,7 m chart with white background and nine 0,2 m × 0,2 m coloured squares was located 16 m ahead the subjects. The centre of chart was 1,6 m above the street level.

The experiment was to transcribe on a paper the colours seen on the chart. The colours except brown were chosen according to the basic colours identified by Boynton and Olson (Boynton, Oslon, 1987).

Subjects have to indicate colour in the same order as presented on the chart. The colours were the same in both streets but the order was different. The evaluation of the experiment was done by counting the number of correctly recognized colours.

Table 1 - colour samples presented to the subjects

Colour name	R	G	B	ρ (%)
Yellow	250	197	80	62
Purple	110	60	89	10
Grey	117	117	106	24
Red	189	78	67	17
Green	85	132	92	16
Blue	64	80	115	12
Brown	106	89	68	11
Orange	213	106	56	25
Pink	182	90	109	19

Figure 2 - diagram of the experiment of colour recognition

2.4 Facial and intent recognition

A target face was located 36 m ahead the subject. The centre of target was 1,6 m above the street level. The target face was a famous well known person in Belgium and changed from one street to another. The targets were King Albert II and the tennis champion Justine Henin (see Figure 4, left and right respectively). The target was a paper reproduction scale 1/1 face of the person to recognize.

Figure 4 - the target faces to recognize were King Albert II and Justine Henin

Figure 3 - diagram of the experiment of facial and intent recognition

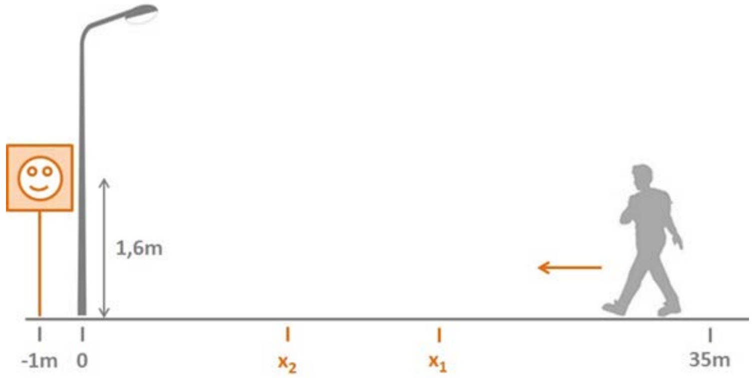

The test procedure required the subjects to walk towards the target in order to either recognize the identity of the person or the intent of the person. The intent of the person is marked either by an open mouth or a closed mouth. An open mouth is an expression of happiness while a closed mouth expresses a neutral intent.

The subject stops walking when he could answer one of these two questions:

- Does the person have an open mouth?
- Who's the person?

For each question, the subject was asked to notice the distance to the target. Once he had answered to one of the two questions, the subject kept walking in order to answer the second question. The evaluation of the experiment was done by the registration and analysis of the distance of face recognition and intent recognition.

2.5 Visual acuity

The visual acuity is tested by a Monoyer chart. The Monoyer chart (Figure 6) is a table composed by 10 rows of capital letters decreasing in size from bottom to up. The aim of this test is to read the smallest letters at a fixed distance from the chart. The visual acuity value is linked to the size of the letters read. The maximum value is 1,0 or 10/10 and the lowest is 0,1 or 1/10.

The realised visual acuity experiment consisted in measuring the distance at which subjects obtained a visual acuity of 10/10.

The centre of the Monoyer chart was1,6 m above the street level. At the beginning of the test, the subject was 11 m ahead the chart. The subject was asked to walk toward the chart until he could read the smallest letters of the chart. This distance was registered and analysed.

Figure 6 - the Monoyer chart

Figure 5 - diagram of the experiment of visual acuity

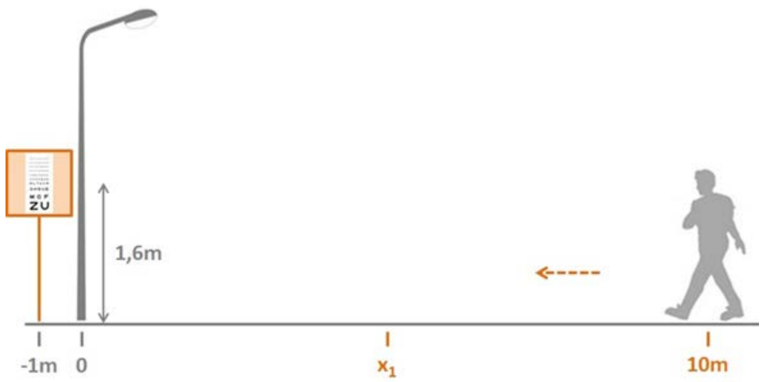

2.6 Photometric measurements

Measurements of target vertical illuminance were performed each night during each experiment. The test conditions were dry. Table 1 shows the mean measurements:

Table 2 - mean vertical illuminance of target under LED and HPS sources

E_V (lux)	LED						HPS						Relative average difference
	Day1	Day2	Day3	Day4	Day5	**Mean**	Day1	Day2	Day3	Day4	Day5	**Mean**	
Obstacle detection	(see below)						(see below)						
Colour recognition	1,0	1,3	1,2	1,4	1,9	**1,4**	2,0	1,8	2,6	2,2	2,6	**2,2**	**36%**
Facial and Intent recognition	1,0	1,2	1,1	1,3	1,9	**1,3**	2,0	1,9	2,4	2,3	2,8	**2,3**	**43%**
Visual Acuity	1,1	1,4	1,2	1,4	2,0	**1,4**	2,0	1,7	2,7	2,2	2,5	**2,2**	**36%**

Despite the low light levels ($E_v < 3\,\mathrm{lux}$) significant relative average difference are pointed out in favour of HPS. This relative difference is due to the targets positioning in both streets not exactly at the same place.

For the obstacle detection experiment, only three days of measurements were made possible. We measured the horizontal illuminance of the cube for each position in the visual field.

Figure 7 here below plot the target horizontal illuminance under LEDs sources against the target horizontal illuminance under HPS lights.

The graph shows that the three illuminance measurements for each target positions, except for the 15° position, are close from each other and mainly equal under LEDs sources and HPS lights.

Indeed, for the 15°-position of the cube, one illuminance measurement is extremely above the others (245 % higher). This measurement may lead to a bias in favour of LEDs sources. For that reason, the 15°-position of the cube will not appear in the analysis.

Figure 7 - targets horizontal illuminance during the obstacle detection experiment

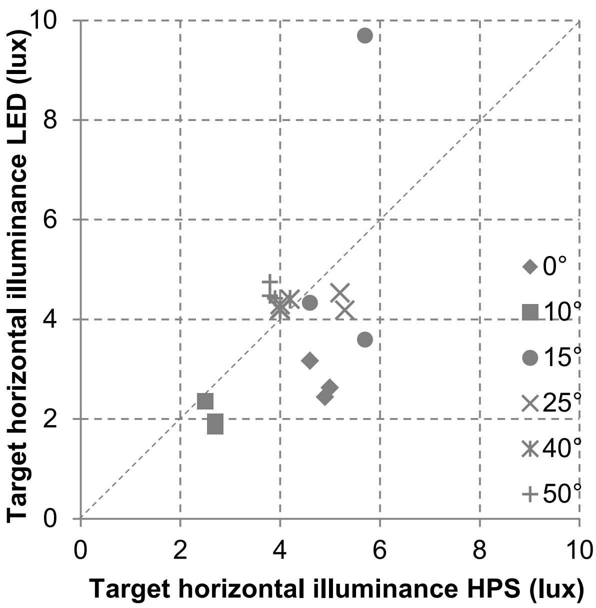

3 Results

3.1 Off-axis and foveal detection

The experiment aims to determine if the foveal targets (0°, 10°, 15°), the intermediate target (25°) and the peripheral targets (40°, 50°) are better detected under LED or under HPS lamps.

The results show some troubles with the 15°-target detection because of excessive vertical illuminance under LED lighting. As explained here above, for that reason, the results for this target are not included in this paper.

Nonetheless, as we can see below (Figure 8), it appears that lamp spectrum influence the target detection.

Figure 8 - mean score visibility plotted against target position in the visual field

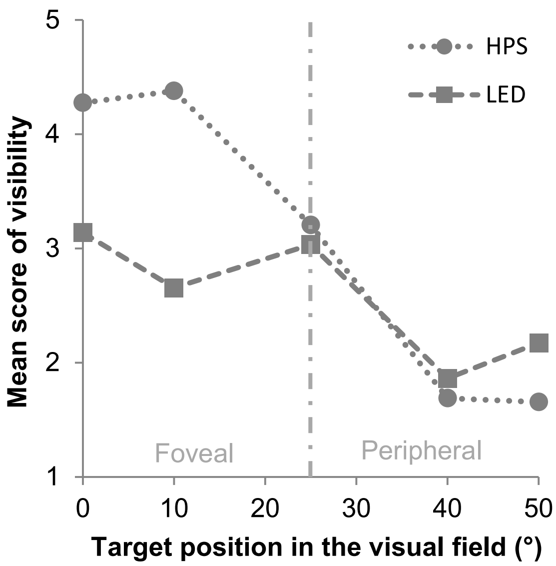

Foveal targets are well seen under both types of lamps: the mean score is above 3. However it is obvious that on-axis detection is better under HPS lamps than under LEDs. This is explained by the fact that in condition of foveal vision, cone photoreceptors are active and their sensitivity corresponds to the wavelength of maximum spectral distribution of HPS lamps.

It is obvious that the intermediate target (25°-target) is well seen under both types of sources.

Peripheral targets are not well detected, whatever the light source under. Nonetheless, we observe that peripheral targets are slightly better detected under LED lighting. This is explained by the fact that peripheral vision is assumed by rods and the rods sensitivity corresponds to the wavelength of maximum spectral distribution of white lamps, e.g. LED.

3.2 Colour recognition

This experiment aimed to determine if the type of lamp would influence the colour recognition.

The Figure 9 expresses the percentage of correct colour recognition under both types of light source.

Figure 9 - percentage of correct colour recognition depending on the type of light source

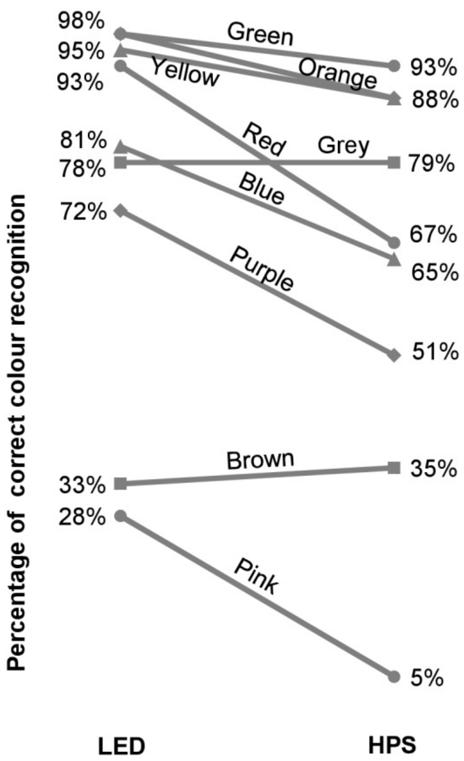

The experiments shows that:

- All colours, except brown and grey are better recognised under LED sources: the percentage of correct colour recognition is always higher for LED sources than for HPS sources.
- Brown and grey are equally recognised under both types of lamps: around 34 % for brown and and 78 % for grey.
- Brown and pink are not well recognised under both types of light source: the percentage of correct colour recognition is below 50 %.
- Two specific colours for road users security are better recognised under LED lamps than under HPS lamps: blue and red. Blue and red are respectively recognized by 81 % and 93 % of the population under LED lamps compared to approximately only two third of the population under HPS lamps.
- Two colours are almost recognised by all the population: green and orange are recognized by 98 % of the population under LED lamps and by approximately 90 % under HPS lamps.

Moreover, despite the low vertical illuminance level of the target (around 2 lux), a significant difference of 36 % of vertical illuminance in favour of HPS lamps has been measured during the experiment.

This difference demonstrates that, even while reducing vertical illuminance by 36%, LED lighting provides better colour recognition than HPS lighting.

Colours are better recognised under LED sources: this is due to the higher colour rendering index for LED light source than HPS light source.

Finally, the experiment shows that both the type of light source and the illuminance influence the colour recognition: the higher the colour rendering index of the source and the higher the illuminance of the target, the better the colour recognition.

3.3 Facial and intent recognition

Figure 10 and Figure 11 plot the distance for facial recognition (Figure 10) and for intent recognition (Figure 11) under LED lamps against the distance for facial recognition and intent recognition under HPS lamps.

On these graphs, a point located on the dotted line means that the subject recognizes the face or intention at equal distance under both types of lamps.

The results show that 56 % of the population (below the dotted line) recognize the face at a higher distance under HPS lamps than under LEDs sources, and that 22 % of the population have a more or less equal facial recognition distance under both types of lamps.

For the intent recognition experiment, the results show that 64 % of the population (below the dotted line) recognize the intent at a higher distance under HPS lamps than under LEDs, and they are 20 % to have a more or less equal facial recognition distance under both types of light source.

However, for both experiments, the linear correlation coefficient r indicates no significant effects of the lamp type on the facial recognition and on the intent recognition: $\mathrm{r} = 0{,}5$ for facial recognition and $\mathrm{r} = 0{,}6$ for intent recognition.

Figure 10 - distance for facial recognition under LED against distance for facial recognition under HPS

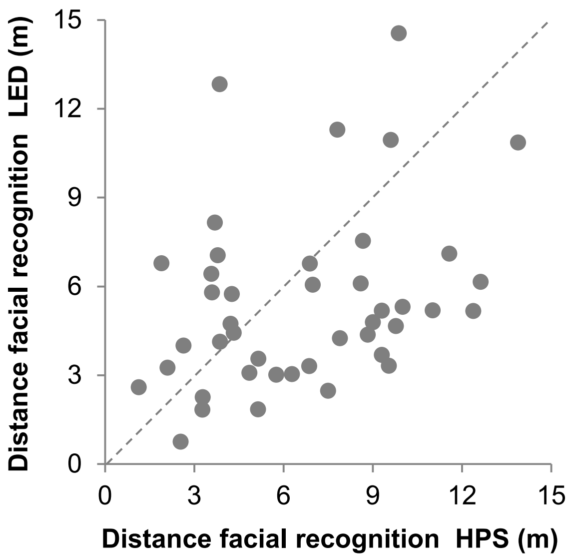

Figure 11 - distance for intent recognition under LED against distance for intent recognition under HPS

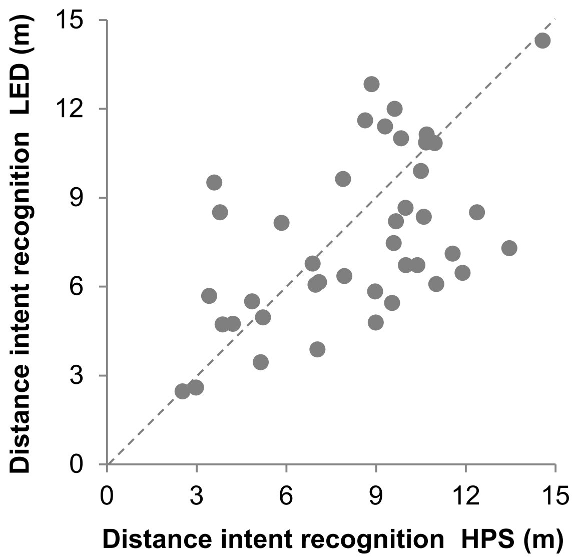

Figure 12 and Figure 13 present the facial recognition distance (Figure 12), and the intent recognition distance (Figure 13), against the target vertical illuminance.

Although the illuminance levels are very low in both streets ($\mathrm{E_v} < 3\,\mathrm{lux}$), there was a relative difference of 43 % vertical illuminance in favour of HPS lamps.

Concerning the average facial recognition distance, the distance is lower by 19% for the LEDs than for the HPS lamps. No conclusion can thus be drawn from this analysis. For intent recognition, the average distance is again lower for LEDs than for HPS, but the difference of 8% is in the confidence interval of 10 % calculated by the statistical JMP software.

It is thus possible that LEDs allow recognizing facial intention the same way than HPS but under lower illuminance conditions.

Figure 12 - facial recognition distance under LED and HPS against vertical target illuminance

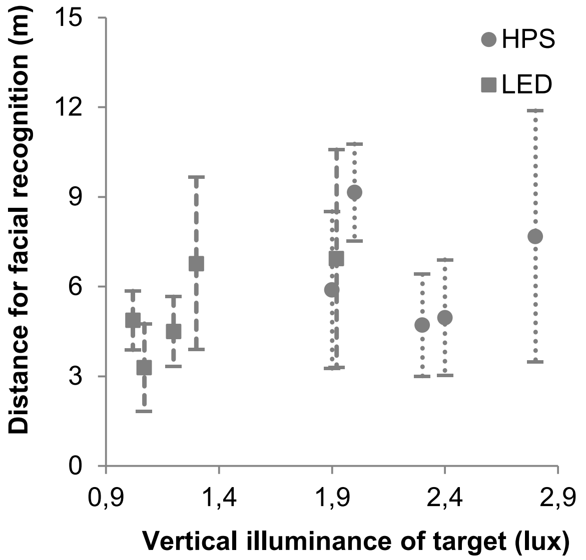

Figure 13 - intent recognition distance under LED and HPS against vertical target illuminance

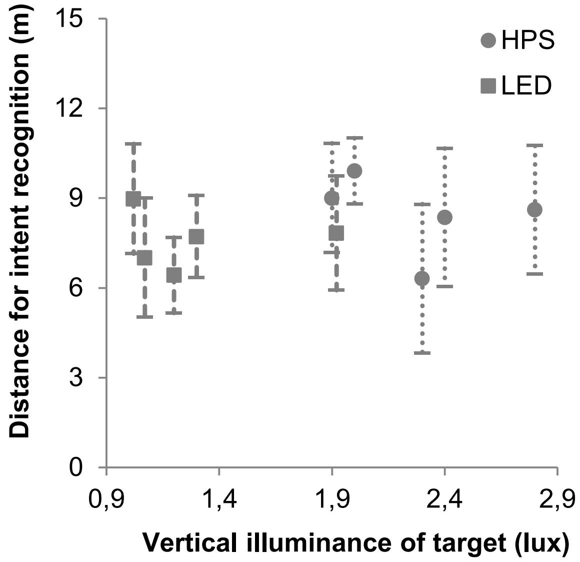

3.4 Visual acuity

A good visual acuity allows perception of details in the public space at a sufficient distance and enhances the visual comfort and the security.

The graph below (Figure 14) expresses the distance required for a perfect visual acuity under LED lighting against the distance required for a perfect visual acuity under HPS lighting. The 45° line represents the locus of points for which the visual acuity is equal, whatever the light source.

It is clear from this graph that 50% of the population obtain a visual acuity of 10/10 at equal distance with both types of light source: 50 % of subjects are located around the 45° line (with a confidence interval of 90 %).

Moreover, the linear correlation coefficient between the distance required under LED lighting and the distance required under HPS lighting is high and close to 1 ($\mathrm{r} = 0{,}8$): the distance required for a perfect visual acuity in LED lighting is highly correlated to the distance required in HPS lighting.

So we conclude from this graph that the lamp type have no effect on the visual acuity, for the two tested light sources.

Nonetheless, although the illuminance levels are very low in both streets ($\mathrm{E_v} < 3\,\mathrm{lux}$), the average illumination of the target in the LED street is 36 % lower than the average illuminance in the HPS street.

The Figure 15 shows that, even with this difference, 50 % of the population obtain a perfect visual acuity (10/10) at equal distance under both types of lamps. Indeed, the average distance for a perfect visual acuity under HPS lamps is only 8 % higher, even with a 36 % higher illuminance level, than the average distance for a perfect visual acuity under LED lamps (the difference of 8% is in the confidence interval of 10 % calculated by the statistical JMP software).

The visual acuity is improved by LED lighting: less illuminance allows an equal visual acuity.

Figure 14 - distance for a perfect visual acuity under LED lamps against distance for a perfect visual acuity under HPS lamps

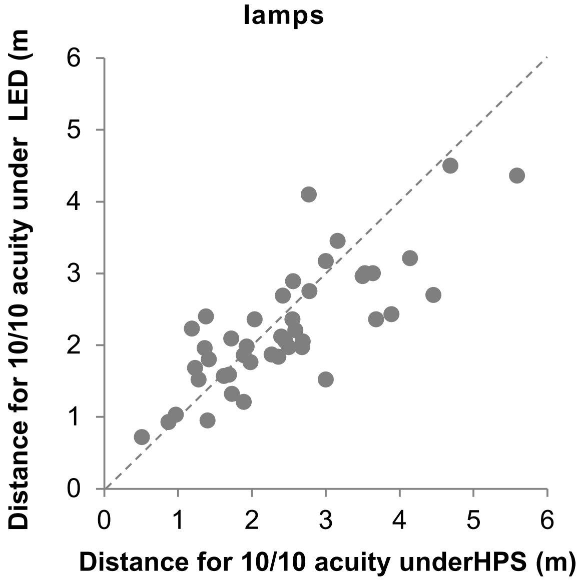

Figure 15 - distance for a perfect visual acuity under LED and HPS lamps against vertical target illuminance

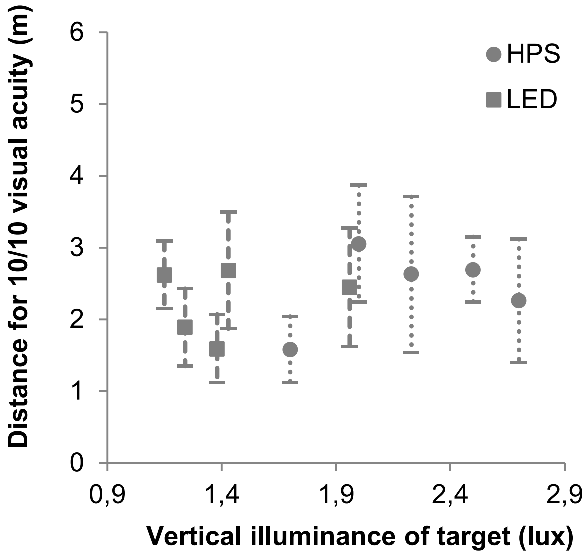

4 Discussion

This work examined the effect of lamp type on the ability to perform some significant visual tasks for pedestrians. The light sources used were HPS on the one hand and LED on the other hand. The illuminance used was around 3 lux covering the range recommended for subsidiary streets and ensuring to operate in mesopic lighting conditions. The visual tasks that were asked to perform by pedestrians consisted in off-axis and foveal obstacles detection, colour recognition, facial and intent recognition and visual acuity.

The main conclusion of this research is that the effect of the lamp type influences visual performances and that the magnitude of the effect varies according to the task.

Moreover, some particular and interesting observations have to be pointed out.

As already demonstrated by previous studies (Fotios, Cheal, 2009; Akashi et al., 2007; Bullogh, Rea, 2000), the lamp type can affect obstacle detection. Warm sources, e.g. HPS, allow to see better foveal obstacles while peripheral obstacles are slightly better detected under white sources, e.g. LED.

Another finding that was already shown by previous studies (Fotios, Cheal, 2007; Boyce, Bruno, 1999), is that colours recognition is improved by the lamp type and the brightness: the higher the colour rendering index of the lamp and the higher the brightness, the better the colour recognition. Moreover, results suggest that the colour rendering index has a more significant effect than the brightness. Finally, results show that orange and the green were always recognised regardless the lamp type and red and the blue were better recognized under LED lamps. This can impact the security considering that the road signs are mainly in blue and red.

About the experiment of facial and intent recognition, the literature presents two opposite conclusions: on the one hand, some researchers suggest that the lamp type affects the recognition; on the other hand, some studies reveal that the facial recognition is not affected by the lamp type.

According to our study, we assume that HPS sources are more efficient than LED sources but LED sources allow us to see details of expression as well as the HPS sources permit. On the opposite, HPS lamps are more efficient when it looking to a face in its entirety.

Finally, it appears that the lamp type has a small effect on the visual acuity: the visual acuity is performed under equal intensity in LED lights than under HPS lamps, even with less illuminance under LED lights.

Funding

The GEPPADI project (Sustainable and Intelligent Public Lighting Management in Business Parks), funded by the Walloon Region, is organised in partnership with companies of ARTHOS Technics et Ets. E. Ronveaux SA, SPI, the economic development agency for the province of Liège, the Electronics, Microsystems, Measurements and Instrumentation unit (EMMI) at the University of Liège and the Architecture & Climate laboratory of the Catholic University of Louvain.

References

ALFERDINCK, J., HOGERVORST, M., VAN EIJK, A., KUSMIERCZYK, J., 2010, Mesopic vision and public lighting - A literature review and a face recognition experiment. TNO - Ministery of Infrastructure and Environment (I&M).

AKASHI, Y., REA, M., BULLOUGH, J. D. 2007. Driver decision making in response to peripheral moving targets under mesopic light levels. *Lighting Research and Technology*, 39, 53-67.

BOYCE, P., BRUNO, L., 1999, An evaluation of high pressure sodium and metal halide light sources for parking lot lighting. *Journal of the Illuminating Engineering Society*, 28, 16-32.

BOYNTON, R., OLSON, C., 1987, Locating basic colors in the OSA space, *Color Research and Application*, 12, 94

BULLOUGH J.D., REA M.S. 2000. Simulated driving performance and peripheral detection at mesopic and low photopic light levels. *Lighting Research and Technology*, 32, 194.

CHEN, M.-Y. & CHEN, C.-C. 2010. The contribution of the upper and lower face in happy and sad facial expression classification. *Vision Research*, 50, 1814-1823.

CIE 2009. Commission Internationale de l'Eclairage. *Recommended system for visual performance based mesopic photometry*. Vienna: CIE

ELOHOLMA, M., (2005), *Development of visual performance based mesopic photometry*. Helsinky University of Technology: Espoo.

FOTIOS, S., CHEAL, C., 2007, Lighting for subsidiary streets: investigation of lamps of different SPD. Part 1—Visual Performance. *Lighting Research and Technology,* 39**,** 233

FOTIOS, S., CHEAL, C., 2009, Obstacle detection: A pilot study investigating the effects of lamp type, illuminance and age, *Lighting Research and Technology,* 41**,** 321

KNIGHT, C. 2010. Field surveys of the effect of lamp spectrum on the perception of safety and comfort at night. Lighting Research and Technology, 42, 313.

REA, M., BULLOUGH, J., AKASHI, Y. 2009. Several views of metal halide and high-pressure sodium lighting for outdoor applications. *Lighting Research and Technology*, 41, 297

RAYNHAM, P., SAKSVIKRONNING T., 2003, White light and facial recognition. *The Lighting Journal*, 68, 29-33.

YAO, Q., SUN, Y. & LIN, Y. 2009. Research on facial recognition and color identification under CMH and HPS lamps for road lighting. *Leukos*, 6, 169-178.

PP70

AN EXPERIMENTAL APPROACH FOR DETERMINING THE EFFECT OF ROAD SURFACE DEPRECIATION ON ROAD LIGHTING DESIGN

Chakraborty , S. [1], Mazumdar , S. [2] , **Mukhopadhyay, S. [3]**
[1]Department of Electrical Engineering, Jadavpur University,Kolkata, INDIA, [2]School of Illumination Science, Engineering & Design, Department of Electrical Engineering, Jadavpur University,Kolkata, INDIA, [3]Philips Lighting Academy, Gurgaon, INDIA,
[1]suddhasatwachakraborty@gmail.com,[2]saswati.mazumdar@gmail.com,
[3]sudeshna.mukhopadhyay@philips.com

Abstract

Road Surface has an essential role in determining the lighting effect on a Road. In this work, few laboratory developed road surface samples made of bituminous and concrete were used for the photometric measurements. The reflection profile of those sample road surfaces were measured initially as Reflection Parameter (R_P) under different Light Sources .Those road surface samples were installed in different real roads of the main campus of Jadavpur University, based upon its different vehicular and pedestrian movement density. The Reflection Parameter (R_P) of those road surface samples were again measured after one year. Finally, it can be inferred that, the depreciation of road Surface materials due to pedestrian and vehicular movement has a significant effect on road lighting. Hence, the selection of the light sources of different spectrums should be considered upon the materials of the Road and its depreciation.

Keywords: e.g. Reflection Parameter, Spectral Power Distribution of light reflected from road surface, depreciation of road surface.

1 Introduction

The task of road lighting design may be best described as intelligent application of input variables to reach as optimized solution for output designed variables like average road surface luminaire, uniformity and glare with quality visual performance and comfort.
The real fact is that the input variables, i.e. the lamp type, luminaire characteristics, road surface type, traffic load, seasonal factors, ambient condition etc. play a predominant role in a visually satisfied optimized road lighting design. So, the assessment of those parameters from real road condition is very important.
In road lighting design, assessment of road surface luminance is very important. The traditional r-table (reduced luminance coefficient) table can be an option of assessment of road surface luminance. Instead of this parameter, a new reflection parameter (R_p) has been proposed here. The (R_p) is basically more realistic as it can directly be measured in the road than r-table, which can be determined by instruments like gonio-reflectometer. This (R_p) value clearly depicts the condition of road surface. This reflection parameter is a ratio of luminance and Illuminance (L/E) (cd/m^2/ lux) at a point on road surface from a fixed observer's position[1].[7][8][10]

The road surface nature changes with time. So, the road surface luminance value also gets depreciated with respect to time. Hence, the designer should take care of this fact while selecting a light source for the design. The road surface property mainly changes with course of time for vehicular and pedestrian movement and also for environmental natural depreciation. The rate of depreciation also differs for different types of road surfaces. As an experimental case study, the metro city Kolkata of India has been chosen, as it is one of the highest populated cities in the world. Kolkata roads are mainly made of Bituminous surface and Concrete surface. The depreciation rate of Bituminous surface and Concrete surface changes with respect to time differentially under the exposure of similar vehicular and pedestrian movement.[][] The experiment was done with different types of light sources of same lumen output but different spectrum. In Fig.1, one Bituminous road at Jadavpur

University campus and in Fig.2. one concrete road at Jadavpur University campus are being shown.

Fig.1. Bituminus Road at Jadavpur University Campus

Fig.2. Concrete Road at Jadavpur University

2 Road Lighting – Road Surface Reflection

The reflection properties of a pavement surface (at a particular point) are defined by the luminance coefficient q, which is the ratio of luminance (L) to the horizontal illuminance (EH) at a specific point on the pavement surface. High q values are associated with brighter (more reflective) surfaces.[4] The luminance coefficient, q, is dependent on numerous variables: position of observer, light source relative to the point of interest on the pavement surface, nature of road surface material,[9][8] etc. Fig. 3 shows α, β, γ, and δ, however, α (the observation angle from the horizontal) has been standardized to 1°. Also, due to the isotropic (independent from the direction of illumination and observation) nature of most pavement surfaces, δ proves to be constant. This leaves q as function of β, γ. Therefore, it follows that: $q(\beta, \gamma) = L / E_H$ ...(1)[1] [5][6][11]

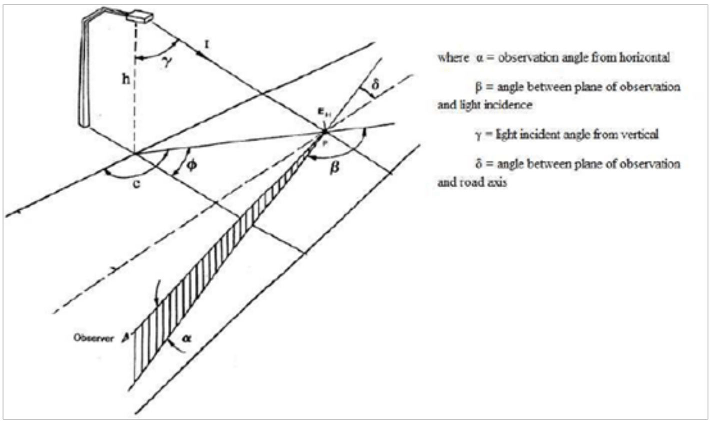

Fig.3.The basic geomerty of Road Lighting Campus

3 Road Lighting & Depreciation

Road lighting design based on luminance calculations has been introduced in many countries. In view of the reflection properties of road surfaces, luminance calculations are based on the average luminance coefficient and on a table of the reduced luminance coefficient (cd/m^2/lux) as mentioned already. The method further assumes that the standard r table represents the individual road surface irrespective of temporal and local variations due to ageing and wears. But in real road, the depreciation of road surface is a very significant subject to be considered of . The depreciation of road surface primarily can be classified like depreciation due to vehicular movement, depreciation due to pedestrian movement & deprecation due to natural wear & tear. Hence, the reflection property of the road surface also changes with respect to time. [2]

Again the reflection rate is also not uniform for all the different types of road surface (i.e. Bituminous & Concrete). So, a designer should take care of these depreciation parameters while selecting the light source also. It is also required to find the behavior of the different surface material under different types of light sources with different types of spectrum.

4 Experimental Setup

Experiment on different Laboratory developed (bituminous & concrete type) Road lighting samples mounted in different roads can easily be assessed with the help of illuminance meter & luminance meter. Here the road surface depreciation has been simulated in the completely dark photometry laboratory.
These three (03) bituminous road surface samples of size 10 cm diameter and three(03) concrete samples of the same size have been prepared in the Civil Engineering Department of Jadavpur University, Road Surface Laboratory . After preparing, the samples were kept immersed in the water for one month to make uniform surface strain & stress. Then samples were then placed under a 4.5 meter high adjustable street light pole in Photometry Laboratory. In this pole, a 70 Watt High Pressure Sodium Vapour lamp (HPSV) based road lighting luminaire was mounted. Under this pole , with a γ angle of 30^0 & β angle of 85^0, all the two types of new samples of concrete & bituminous were placed.Observer's position was fixed up in such a way that ,the effect of δ & α can be ignored. Under this circumstance, illuminace over the road surface (E) in lux & Road surface Luminance from the observer's position (L) in cd/m^2 has been measured.
The ratio of L & E gives the value of (R_p) i.e the reflection parameter , which is basically q value taken at a particular β, γ. [1][9]

The experiment with those six samples was repeated similarly under 70 W MH & 45 W LED based system. All the lighting system have the same lumen output but different types of spectrum.The first measured R_p values were designated as conditions 0^{th} order of depreciation .The samples were mounted in the University campus Roads as shown in Fig.4 and Fig.5.

Fig.4.Laboratory developed New Bituminous Samples are placed in University Road

Fig.5.Laboratory developed New Concrete Samples are placed in University Road

University roads are basically classified like roads with comparatively high Vehicular movement (300 Average daily traffic) (category-I), roads with comparatively more pedestrian Movement, (category-II) and roads with very less vehicle & pedestrian movement (Category-III) [3] .
The samples were kept on those mentioned Roads for 6 months and allowed for its normal use. After 6 months, the samples were taken out again in the dark Photometry Laboratory and the previous experiment was repeated as 1^{st} order of depreciation. After experimentation,

samples have been placed in its previous location again for 6 months. After 6 months over, the samples were taken out again to repeat the experiment under 70 Watt HPSV,70 Watt MH & 45 Watt LED based lighting system in Photometry Laboratory.
The values of Reflection Parameters (R_p) are recorded as 2^{nd} order of depreciation .The same experiment was also conducted for different γ and β angle ranges .The trend of depreciation of R_p parameter for those samples depicts almost similar results for different ranges of γ, β. Hence at a particular γ& β angle, the R_p values are reported in this paper.[11]
The luminous intensity values of the used luminaires & their Luminous flux values have been measured in Photometry Laboratory .by using Mirror Distribution Photometer (5 feet diameter of the mirror) & Integrating Sphere (of diameter 8 feet 3.5 inch). During the experiment the input power for all the lighting equipments are fed from Constant Voltage, Constant frequency Power Supply. Fig.6 and Fig.7 clearly depict the experimental setup for R_P value measurement.

Fig 6.The experimental setup for Reflection Parameter (R_P) data

Fig 7. Road surface samples are being placed during measurement

The experiment also includes the measurement of Spectral Power Distribution of reflected Light from different road surfaces mounted in different categories of road under 70W HPSV lamp ,70W MH lamp & 45W LED based lighting system. The Spectroradiometer (Specbos 1200) ,JETI make, was placed in the observer’s position and was aimed towards the road surface to measure the Spectral power distribution of reflected lights only. The experiment was repeated similarly for different road samples.
Fig.8 depicts the measurement of Spectral Power Distribution (SPD) data by using JETI make Spectroradiometer (Specbos 1200)

Fig 8. Measurement of SPD of reflected light from different sources

.

The details of Luminaires used for the experimentation, with 70W HPSV, 70 W MH & 45 W LED based system have been tabulated in Table:1

Table.1 - The details of Luminaires used for the experimentation

<table>
<tr><td>Parameter</td><td colspan="3">Luminaires Used</td></tr>
<tr><td>Luminaire Type</td><td>Road lighting luminaire suitable for use with High Pressure Sodium Vapour –T 70W</td><td>Compact and sturdy low wattage street lighting luminaire used with 70 W Metal Halide lamps.</td><td>LED luminaire using 24 High Power LEDs with unique peanut lens which ensure uniform distribution desired for street lighting. Green line Consuming 45W (including driver) .</td></tr>
<tr><td>Figure</td><td>
</td><td></td><td></td></tr>
<tr><td>Lumen value</td><td>5992</td><td>5688</td><td>5568</td></tr>
<tr><td>Polar plot</td><td>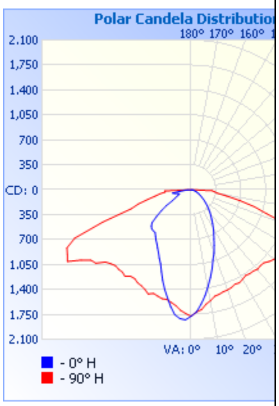
</td><td>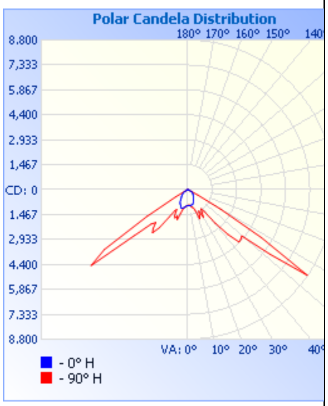
</td><td>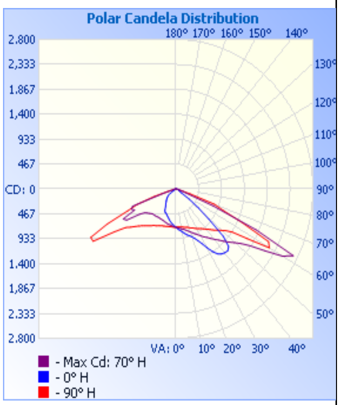
</td></tr>
</table>

5 Experimental Results

The Reflection Parameter (R_P) values have been measured for Bituminous & Concrete Samples with initial condition (0^{th} order depreciation) , after 6 months (1^{st} order depreciation) & after 12 months (2^{nd} order depreciation) under three types of Lighting system. The sample - 1 was placed at category-I road, the sample-2 was placed at category –II road & the sample-3 was placed at category-III road for Bituminous as well as Concrete samples..The values are tabulated below in Table 2. & Table 3. depicting the R_P values in cd/m^2/lux.

Table 2 - Effects of Road Surface & Environmental Depreciation on Reflection Parameter (R_P) for Bituminous Samples

Surface	Bituminous Sample								
Sample	1(at category-I road)			2(at category-II road)			3(at category-III road)		
Month	0	6	12	0	6	12	0	6	12
70W HPSV	0,01337	0,013111	0,013	0,01337	0,01321	0,01305	0,01337	0,01334	0,01326
70W MH	0,0124	0,01015	0,01002	0,0124	0,01238	0,01101	0,0124	0,01223	0,01185
45 W LED	0,01016	0,00965	0,00766	0,01016	0,01005	0,01	0,01016	0,01004	0,0098

Table 3 - Effects of Road Surface & Environmental Depreciation on Reflection Parameter (R_P) for Concrete Samples

Surface	Concrete Sample								
Sample	1(at category-I road)			2(at category-II road)			3(at category-III road)		
Month	0	6	12	0	6	12	0	6	12
70W HPSV	0,020444	0,018692	0,017561	0,020444	0,01964	0,018505	0,020444	0,01993	0,01893
70W MH	0,021785	0,01965	0,01895	0,021785	0,020749	0,01986	0,021785	0,021026	0,02006
45W LED	0,030921	0,030172	0,028261	0,030921	0,030319	0,02887	0,030921	0,030499	0,029135

The graphical representation of all the measured data clearly depicts the trends of depreciation for Bituminous as well as Concrete road samples placed under category-I,II & III types of roads under 70W HPSV lamp, 70W MH lamp ,45W LED based lighting system.

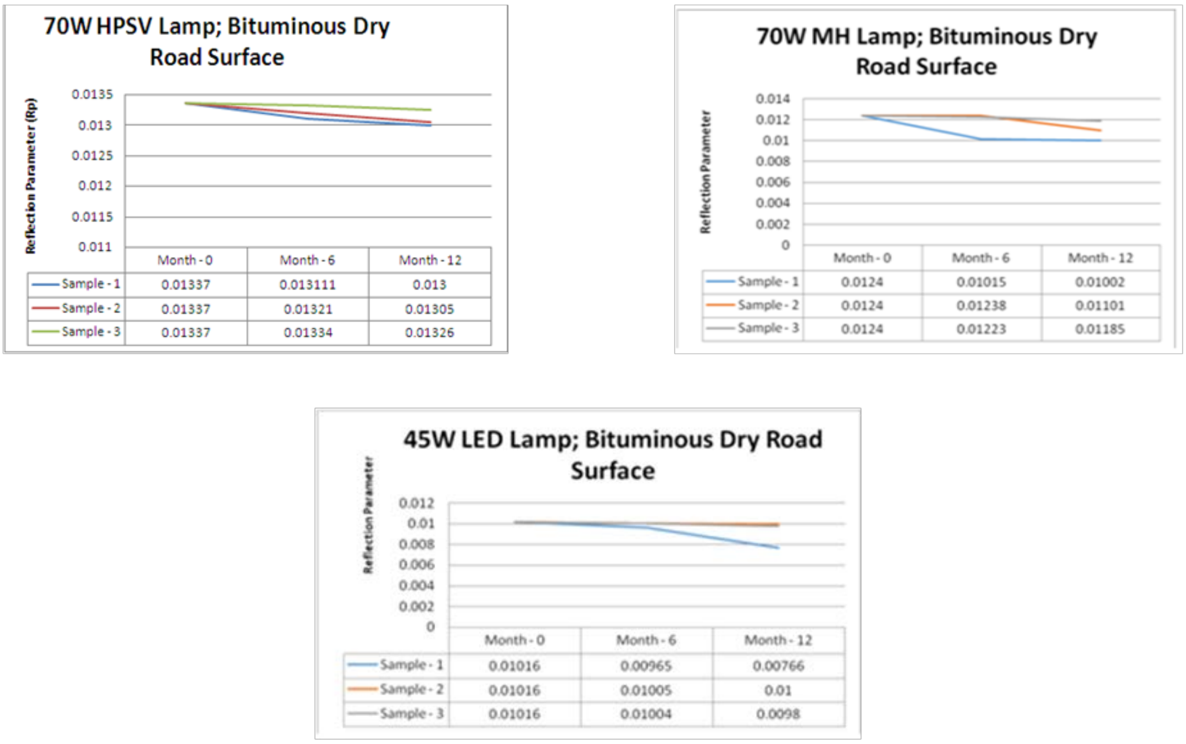

Fig.9.Trends of R_P values under 70 W HPSV & 70 W MH lamp& 45 W LED for Bituminous surface

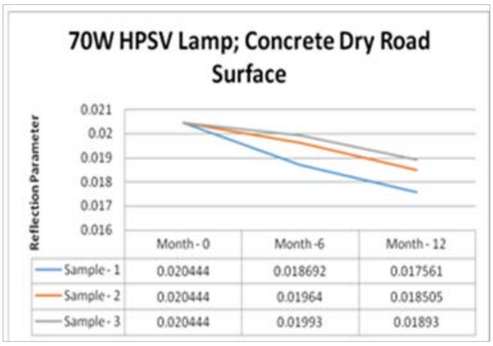

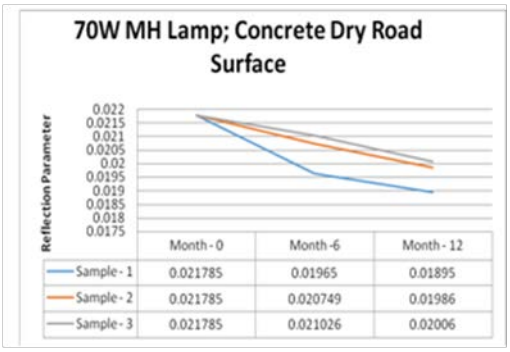

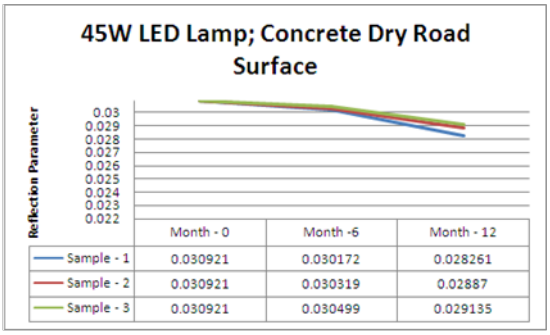

Fig.10.Trends of R_P values under 70 W HPSV & 70 W MH lamp& 45 W LED for Concrete surface

It can be inferred from Fig.9 and Fig.10 that, in category-I road R_P values are decreasing with higher rate than category-II and category-III types road under all types of light source.
The category-II and category-III are not discussed here, as the change of R_P values in those roads are not that significant in comparison with category-I.
In Fig.9, it is clear that, the initial R_P value of the Bituminous sample under 70W HPSV lamp is at much higher than the others, which is always preferred in road lighting. Also the percentage change of R_P value in 1 year for that Bituminous sample placed in category-I road, is only 2.76739 % for 70W HPSV lamp , whereas the change is 19.19355 % for 70W MH lamp and 24.6063 % for 45W LED system.
Hence, it can further be concluded that, as the change of R_P values for Bituminous roads, under 70W HPSV lamp is minimum, it will be the best option in Bituminous type of road.
In Fig.10 , it has been found that, the initial R_P value of the Concrete sample under 45 W LED is at much higher than the others, which is again always preferred in road lighting design. The percentage change of R_P value in 1 year for that Concrete sample placed in category-I road, is only 8.60 % for 45W LED system , but it is 13.0138 % for 70W MH lamp and 14.1094 % for 70W HPSV lamp.
As the change of R_P values for Concrete roads, under 45W LED system is minimum, it will be the best option in Concrete type of road.
The Spectral Power Distribution (SPD) of reflected Light from different road surfaces are measured with Spectroradiometer (Specbos 1200), JETI make.

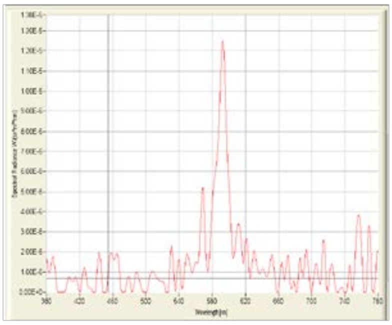

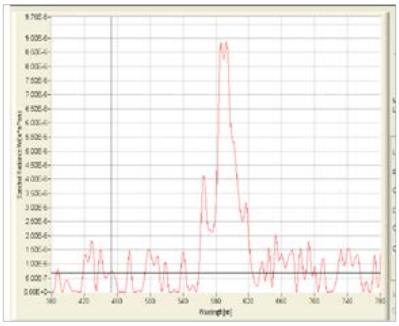

Fig. 11.Measured Spectral Power Distribution of reflected light from new & depreciated Bituminous sample under 70W HPSV lamp

Table 4 - The comparison of measured CRI & CCT values of reflected light from new & depreciated Bituminous & Concrete sample of category-I road.

Surface	Bituminous Sample				Concrete Sample			
Month	0		12		0		12	
Parameters	CCT (K)	CRI	CCT (K)	CRI	CCT (K)	CRI	CCT (K)	CRI
70W HPSV	2389	19,87	2256	15,6	2156	16,49	1767	11,01
70W MH	3285	68,44	3055	51,67	3944	70,02	3359	62,17
45 W LED	4008	67,6	3712	54,78	4041	70,05	4013	66,8

The measured CCT & CRI values of reflected light from new and depreciated dry Bituminous & Concrete samples placed under 70 W HPSV lamp, 70 W MH lamp & 45W LED based system have been tabulated in Table-4. From this Table, it is clear that, for Bituminous sample, under 70W HPSV lamp, change of CCT & CRI values of surface reflected light in 1 year is less than 70W MH & 45W LED based system , whereas for Concrete sample, under 45 W LED based system, change of CCT & CRI values of surface reflected light in 1 year is less than 70W MH & 70 W MH lamp.

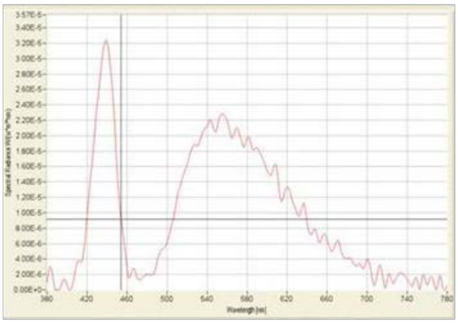

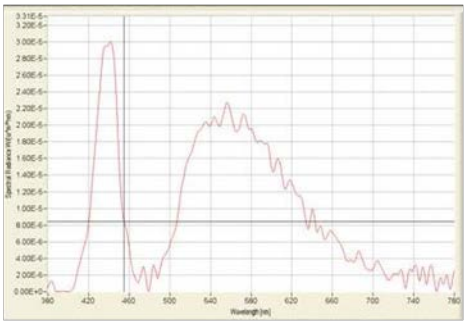

Fig. 12.Measured Spectral Power Distribution of reflected light from new & depreciated Concrete sample under 45 W LED system

Fig.11. shows the measured SPD depicting the trend of depreciation of Bituminous road sample placed in category-I road under 70W HPSV lamp and Fig.12. shows the measured SPD depicting the trend of depreciation of Concrete road sample placed in category-I road under 45W LED system.

6 Conclusion

Indian roads are mostly made by Concrete and Bituminous materials. The roads in city like Kolkata, are highly congested with varieties of heavy, medium and small vehicles and so, the average longevity of the road surface is not impressive. Almost within 5 years, the surface condition of all the Indian roads, change including its reflection profile.

The lighting designer first selects a light source while doing the road lighting design by using a lighting design software. In this entire process, the role of change of Reflection Parameter (R_p) and change of color properties (CCT & CRI) ,Spectral Power Distribution (SPD) of reflected light from the road surface must be taken care with urgent consideration.

The natural & forced depreciation (depreciation due to Vehicular & Pedestrian movement) affect the road surface in years. Hence, the pattern of Rp parameters as well as the color property of reflected light change during this time.

This paper clearly reveals that while selecting a light source, a designer should give the importance to the change of R_p parameters as well as change of Spectral Power Distribution (SPD) & color properties of different types of roads.

In this experimental study, it has been noticed that the surface deprecation really affects the Rp parameters & color properties (CCT & CRI) within 1 year. From there, it can easily be inferred that in long run i.e. in within 5 years, the roads will be depreciated severely, and the R_p values & color properties of reflected light will also be changed accordingly.

As described here ,it has been proved that, for a road made with Bituminous, the minimum change of R_p and minimum change of color properties of reflected light within 1 year are found when 70W HPSV system is used. Hence, assuming that in next four or five years, the depreciation rate being higher enough, 70 W HPSV lamp will be more preferable than 70W MH & 45W LED based system for Bituminous roads.

Again for dry concrete road, 45W LED system is more preferable from rate of deprecation of reflection parameter and color properties point of view. The rate of change of those values are very crucial parameter in this regard.

This should be carried out with higher wattage (250 W or 400 W) HPSV and MH lighting system and equivalent LED system in different major roads of the city for further validation of this experimental approach. The future designer will consider the rate of depreciation of Rp parameters of the road surface as well as shift of color properties by adopting this experimental approach.

The categorization of different roads of Kolkata as per Indian Standard [3] of road lighting is being done. This experiment has been conducted in University roads, but, this depreciation assessment experiment should be verified in different categories of real roads of Kolkata and other cities of India.

References

[1] VAN BOMMEL, W.J.M. DE BOER, J.B. 1980. Road Lighting.United Kingdom. The Macmillan Press Ltd.

[2] BODMANN, H.W.1989. Road surface reflection and road lighting: Field investigations. Lighting Research Technology .4. 159-170.

[3] IS 1970. IS 1944(Parts I and II):1970. Reaffirmed 2003. Code of practice for lighting of public thoroughfare".1981-10.

[4] BOYCE, P. 2008 *Lighting for Driving: Roads, Vehicles, Signs, and Signals*. Boca Ranton, USA. CRC Press.

[5] CIE 1976. CIE 30 :1976. Calculation and measurement of luminance and illuminance in road lighting.

[6] CIE 1982. CIE 30-2 :1982. Calculation and measurement of luminance and illuminance in road lighting.

[7] FREDERIKSEN,E. SORENSEN, K.1976. *Reflection classification of dry and wet road surfaces. Lighting Research and Technology.* 8. 175- 186.

[8] CIE/PIARC 1984 : CIE 066:1984. Road Surfaces and Lighting.

[9] FOTIOS,S .BOYCE, P.ELLIS,C 2005 *The Effect of Pavement Material on Road Lighting Performance*. UK. CRC Press.

[10] MOON, P. HUNT, R.M.. 1938, Reflection characteristics of road surfaces, Journal of the Franklin Institute, 225, 1-21.

[11] RANGE, H.D. 1972. A simplified method for the characterisation of road surfaces for lighting, Lichttechnik, 24, 608.

PP71

THE INFLUENCE OF LED LUMINOUS FLUX MAINTENANCE FACTOR ON THE DETERMINATION OF MAINTENANCE FACTOR

1st Wang Shuxiao[1]，2nd Zhao Jianping[1]
[1] China Academy of Building Research, Beijing, CHINA
wangshuxiao417@163.com

Abstract

One of the main inputs into the design of a street lighting system is the establishment of the maintenance factor (MF) for the lighting system. This factor is the product of three separate factors, the luminaire maintenance factor (LMF) , the lamp survival factor(LSF) and the lamp luminous flux maintenance factor (LLFMF), and is applied during the design process to ensure that the level of illumination never falls below that recommended for the type of road in related standard.In recent years, with rapid development of LED technology, the number of LED streetlight installations has been steadily climbing. But compared to the traditional lighting products, the LED lamp has a different luminous flux depreciation characteristic, so is the maintenance factor of LED products. In this paper we will focus on the topic that how can me determine the maintenance factor when we use LED products in lighting design.

Keywords: Maintenance Factor, Light Emitting Diode, Lighting Design, Street Lighting

1 Introduction

One of the main inputs into the design of a street lighting system is the establishment of the maintenance factor (MF) for the lighting system. This factor is the product of three separate factors, the lamp survival factor(LSF), the luminaire maintenance factor (LMF) and the lamp luminous flux maintenance factor (LLFMF), and is applied during the design process to ensure that the level of illumination never falls below that recommended for the type of road in related standard. For traditional lighting products, CIE 154:2003 offered us a systematic method to determine the value of this indicator, which has a profound meaning for lighting energy saving.

In recent years, with rapid development of LED technology, the number of LED streetlight installations has been steadily climbing. So one problem we need to consider is how to determine the maintenance factor when we use LED products in lighting design. Comparing to the traditional lighting products, the LED lamp has a different luminous flux depreciation characteristic, so is the maintenance factor of LED products. This article discusses the complications related to LLD and LEDs, compares the performance of some conventional and LED products, and tries to establish an approach for determining LLDs for LED products.

2 Definition of MF by CIE 154:2003

CIE 154 is a comprehensive report into maintenance of outdoor lighting systems. In the introduction it takes the definition of “Maintenance Factor” as “Ratio of the average luminance / illuminance on the working plane after a certain period of use of a lighting installation to the average luminance / illuminance obtained under the same conditions for the installation considered conventionally as new.

The document also gives a computation method for MF value, as followed:

$$MF = LLMF \times LSF \times LMF \qquad (1)$$

where

LLMF is the output of all lamps decreases during use. The exact rate, however, depends on the lamp type and ballasting system.

LMF is a number (positive and less than 1) to correct for the depreciation in light output from a luminaire due to the build-up of dirt in the periods between cleaning. It can be expressed as the ratio of the light output ratio of a luminaire at a given time in its life to the initial light output ratio. Dirt accumulation on reflecting surfaces can be minimised by sealing the lamp compartment against entry of dust and moisture. Significant benefits can be obtained with the luminaire optical compartment sealed to at least IP5 – protection. The value of LMF can be determined according to table 1.

Table 1 Luminaire Maintenance Factors（LMF）

Optical Compartment IP Rating	Pollution Category	Exposure time（years）				
		1.0	1.5	2.0	2.5	3.0
IP5X	High	0.89	0.87	0.84	0.80	0.76
	Medium	0.90	0.88	0.86	0.84	0.82
	Low	0.92	0.91	0.90	0.89	0.88
IP6X	High	0.91	0.90	0.88	0.85	0.83
	Medium	0.92	0.91	0.89	0.88	0.87
	Low	0.93	0.92	0.91	0.90	0.90

LSM is the probability of lamps continuing to operate for a given time. The survival rate depends on lamp type and particularly, in the case of discharge lamps, the wattage, frequency of switching and the ballasting system. Failed lamps cause reduction in illuminance and uniformity, but the effect can be minimized by spot replacement of lamps. Compared to traditional lighting products, there is still little data about the LED products. In China, we adopt the spot replacement to keep the roadway lighting systems have a high rate of normal running, for major and express road the LSM should not less than 98% and for the collector road should not less than 96%, so the LSM value can determined as 0.98 and 0.96 respectively.

From the formula 1, the main factor differentiating the MF value between LED and traditional lighting products is the LLMF value, which is the main theme of this paper.

3 Lamp lumen maintenance comparison

In almost all lighting standards, the recommended values are maintained values, which is the minimum value in the service period as figure 1 shown. The minimum value is always happened at the ending of lighting products service life. So to make comparison of the two products and computation for MF values, we need make the analysis of the lamp lumen maintenance performance on the basis of their service life.

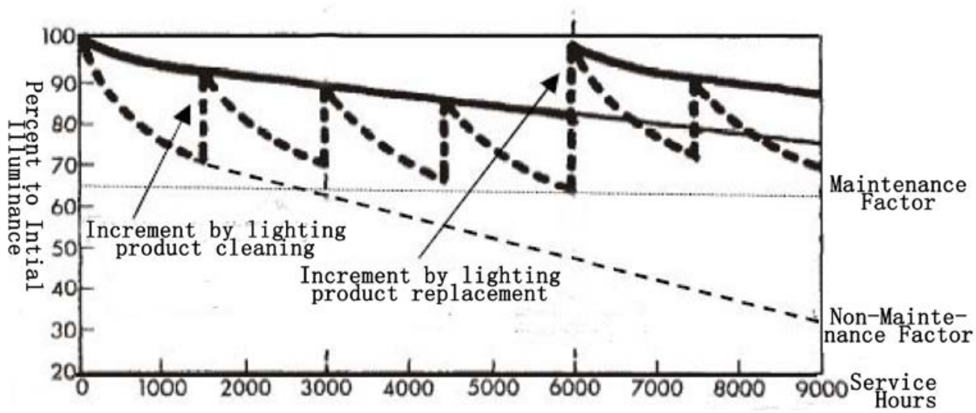

Figure 1 Illustration for Maintain Service

3.1 Traditional lighting products

The lumen maintenance performance of typical lamps used in street lighting application is shown in table 2.

Table 2 Lamp Lumen Maintenance Characterization of Typical Products

Lamp Type	Operation Time （Hours）				
	4000	8000	12000	16000	20000
High Pressure Sodium	0.95	0.93	0.93	0.92	0.91
Quartz Metal Halide	0.89	0.85	0.81	0.80	-

For the traditional lighting products, their life time is defined by median operation life, which means the time when 50% of tested products failed. And when come to the lighting application, the service life of lighting products is defined as 70% of their life time. So the LLMF values for these lighting products can be determined as table 3 shown.

Table 3 Typical Values of LLMF for Street Lighting

Lamp Type	Average Life	Service Life	LLMF
High Pressure Sodium	25000	17500	0.92
Quartz Metal Halide	18000	12600	0.81

3.2 LED products

Until now, the true reliability and lifetime of light-emitting diode (LED) lighting systems is generally not known. So most of standards concerning the lifetime of an LED luminaires (or lamps) give a definition only in terms of lumen output and are specified as the time when half the product population has fallen below 70 percent of average initial light output for any reason.

IES TM21 (Projecting Long Term Lumen Maintenance of LED Light Sources) defines a exponential method for interpreting and projecting lumen maintenance for operating hours past the data collected, as followed:

$$\Phi(t) = B \cdot \exp(-\alpha \cdot t) \tag{2}$$

Where:

t is the operating time in hours;

$\Phi(t)$ is averaged normalized luminous flux output at time t;

B is projected initial constant derived by the least squares curve-fit;

α is decay rate constant derived by the least squares curve-fit.

On the basis of formula 2, we can compute the lumen maintenance performance of typical LED lighting products, with a expected life 25000 hours and 35000 hours, as shown in table 3.

Table 3 Lamp Lumen Maintenance Characterization of LED Products

Operation Time （Hours）	Expected L70 Life	
	25000	35000
3000	95.8%	97.0%
6000	91.8%	94.1%
9000	87.9%	91.2%
12000	84.3%	88.5%
15000	80.7%	85.8%
17500	77.9%	83.4%
18000	77.4%	83.2%
20000	74.1%	81.6%
22500	72.5%	77.9%
25000	70.0%	77.5%
30000	—	73.7%
35000	—	70.0%

If we take the expected L_{70} life asLED products' service life, so the LLMF value can be specified 0.7.

4 MF comparison between traditional and LED products

According to the previous mentioned content and formulas, we can make the computation about the MF of lighting products, as shown in table 4:

Table 4 MF value comparison

Cleaning Interval （years）	High Pressure Sodium			Quartz Metal Halide			LED Products		
	High Pollution	Medium Pollution	Low Pollution	High Pollution	Medium Pollution	Low Pollution	High Pollution	Medium Pollution	Low Pollution
1.0	0.80	0.81	0.82	0.71	0.72	0.72	0.61	0.62	0.62
1.5	0.79	0.80	0.81	0.70	0.71	0.72	0.60	0.61	0.62
2.0	0.78	0.79	0.80	0.68	0.69	0.71	0.59	0.60	0.61
1 LMF values are determined on the consumption that the IP code number of lamp housing is IP6X； 2 LSF value is 0.96.									

5 Adjustment for LPD limit based on room geometrics

From the table 4, we can see that the MF value of LED products is 25% and 14% lower than luminaires with high pressure sodium and quartz metal halide respectively on the basis taking LED L_{70} life as its service life. It means that when we want to achieve the goal of same energy consumption with LED products in lighting application, we need to select a LED product with efficacy 30% and 16% higher than luminaires with HPS and Quartz MH lamps respectively. This simple problem may be a big obstacle for the popularization and application of LED technology. To better push and guide the development of LED industry, some issues should be dealt with in the following area:

1) As the low MF value means that the initial illuminance is much higher than the maintained value, so to reduce the energy consumption cost with the constant illuminance control method, which means that at start of life the lighting systems are dimmed, as the installation ages the dimming is gradually reduced to keep illuminance value be constant on the task surfaces.

2) If we reduce the service life of LED products, of course the MF can got high value. For example, the service life is 70% of L_{70} life, and the MF value should be 0.7, 14% higher than the L_{70} life method. With the installation and energy consumption cost decreased, the cost for replacement of luminaires will increased correspondingly. So we need find a balance point for the service life of LED products. CIE 115:2010 document offer us a comprehensive method for analysis the life cycle costs, one parameter of the formula is

the life time of lamps, so we need make a optimization analysis based on the current technology status, to find a optimum value for LED products.

3) Further improve the reliability and life of LED products of course is the fundamental method to improve the MF value by extending the service life with a high LMF value.

References

CIE S 017/E:2011: ILV: International Lighting Vocabulary

CIE 154:2003, The Maintenance of Outdoor Lighting Systems.

CIE 115-2010 Lighting of Roads for Motor and Pedestrian Traffic

IESNA. 2000. IESNA Lighting Handbook, 9th ed. New York: Publication Department IESNA.

A Sanders, Review of luminaire maintenance factors, 2008

IES TM21, Projecting Long Term Lumen Maintenance of LED Light Sources

PP72

IMPLEMENTATION OF HIGH S/P RATIO LIGHT SOURCES TO EXPRESSWAY LIGHTING MAY ENHANCE PURKINJE PHENOMENON

Kenji Ueda[1], Masaya Iihoshi [2], Yukio Akashi [2], Yoshinori Karasawa [3]
[1] Central Nippon Expressway Company Limited, Nagoya, Aichi prefecture, JAPAN.
[2] University of Fukui, Fukui, Fukui prefecture, JAPAN.
[3] Panasonic Corporation, Kadoma, Osaka prefecture, JAPAN.
k.ueda.ab@c-nexco.co.jp

Abstract

Under mesopic light level experienced when driving a vehicle at night, sensitivity of human eyes toward short wavelength radiation is higher than that under photopic light level. This is because rods with higher sensitivity toward short wavelength radiation than cones work simultaneously with cones which work under photopic light level[1) - 4)]. This is called Purkinje phenomenon. Since density of rods is high in peripheral vision, visual task performance in peripheral vision is improved under mesopic light level, under light sources containing much short wavelength radiation.

Keywords: mesopic vision, purkinje phenomenon, expressway, driver's view, foveal task load

1 Application of Purkinje phenomenon based on visual task load on expressway

When driving on expressway at night, it is necessary to perform simultaneously visual tasks of (1) recognition of traffic lanes, road markings, road signs, obstacles, etc. of front road in the central vision and (2) detection of vehicles and small animals in peripheral vision. Under dual task (or multiple task) conditions imposing visual tasks on both central and peripheral visions, it was already made clear that interference in visual task performance will occur between tasks (*e.g. Pashler: 1994). Visual task load on drivers is especially high on expressways because of high traveling speed. Further, increase of traveling speed narrows drivers' effective visual field and reduces drivers' capability of detecting potential risks in peripheral vision. Therefore, application of Purkinje phenomenon is expectable to improve visibility in peripheral vision during high speed traveling. Therefore, for example, mesopic illuminance of visual targets such as visual target on roads under lighting of light sources rich in short wavelength radiation needs to be estimated higher than that shown by the mesopic vision photometric system. This may also mean that experimental conditions used when mesopic vision photometric system is established influence coefficients of model formula which is the core of the photometric system. Since foveal task load during driving a vehicle is generally non-negligible, influences of the load on visual task performance of peripheral vision and on Purkinje phenomenon need to be clarified. Therefore, we performed experiments aiming at investigating how visual task performance in peripheral vision change among different spectral distributions under mesopic vision environment, using a visual task apparatus capable of controlling visual task load on central vision in addition to visual target of peripheral vision.

2 Outline of experiments

2.1 Installations for the experiment

A high-pressure sodium lamp and three kinds of LED, that are frequently used for road lighting, were used for the experiment. Among the three kinds of LED, one kind had color temperature of 5000 K and two kinds had color temperature of 8000 K. Ratios of scotopic luminance against photopic luminance of the lamps (S/P ratio, hereinafter) were 0,6 (high pressure sodium), 1,7 (5000 K), 2,1 (8000 K) and 2,5 (8000 K), respectively. These light sources [NH, LED (1,7), LED (2,1) and LED (2,5), hereinafter] were lit in a lighting apparatus created for the experiment. Fig. 3 shows spectral distributions of the light sources.

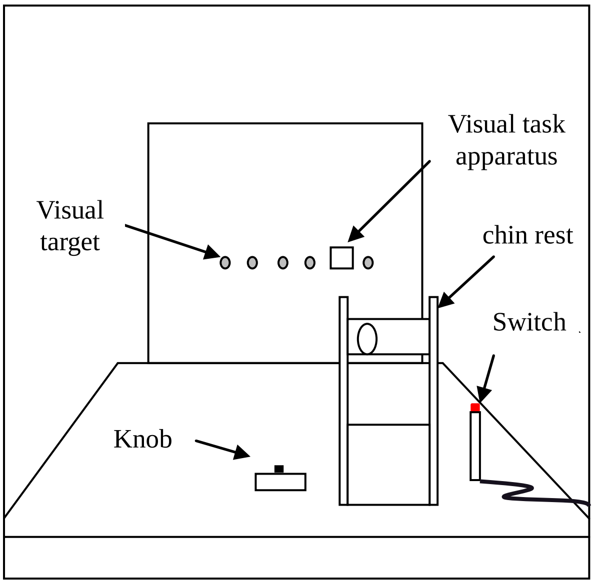

Figure 1 – Experimental apparatus

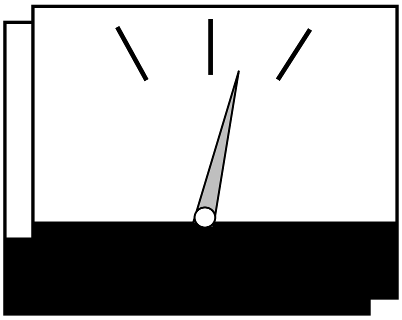

Figure 2 – Visual task apparatus

2.2 Experimental method

Experiments were performed in a dark room where light from outside was cut off with blackout curtains. The visual target presentation apparatus used for the experiments was a black partition having five visual targets and a visual task apparatus which were built in. The visual targets were discs of 13,4 mm in diameter with white front side and black rear side. The visual targets were presented by switching them from black to white instantaneously. The visual task apparatus was an ammeter connected to a computer through an interface. The needle of the ammeter was programmed to move in random directions at 0,1 second intervals. Visibility of the ammeter needle was reduced by reducing contrast between the needle and background to increase load. Contrast between the needle and background was 0,94 for light load condition and 0,5 for heavy load condition. Subjects operated the apparatus by rotating the knob to control the needle to be at the center of vision. This central vision task corresponds to steering wheel operation for controlling a vehicle one is driving to prevent it from deviating from traffic lane. As experimental conditions, four levels of kinds of light source, namely high pressure sodium lamp (NH) and three LEDs (S/P ratio: 1,7, 2,1 and 2,5), as independent variables, two levels of visual target illuminance of 0,3 lx and 1,5 lx, five levels in total of visual target positions of 5 degrees to the right and up to 30 degrees to the left from the central vision, and two levels, heavy or light, of foveal task load were adopted. The S/P ratios in the table represent ratios of scotopic luminance against photopic luminance of the lamps. Higher values mean higher visual task performances of the light sources under dark visual environment. As the experimental procedure, first, each of five visual targets was presented 8 times (40 times in total) in random order under each visual target illuminance condition. The experimenter recorded as reaction time the time until when the subject pushed the switch as soon as he or she discovered the visual target with central vision by operating the needle. Since experiments were performed using left eye only, a black polystyrene board with a hole in it was fixed on the jaw table, and the subjects observed the targets through this hole. Right eye was blindfolded. (Fig. 1) Procedure was repeated for the remaining three conditions. Procedures and were repeated for remaining three lamp conditions, and the experiments were finished. The subjects were 15 students of University of Fukui (11 males and 4 females) aged 22 on average.

Table 1 – Experimental conditions

Independent variable	Level
lamp (S/P ratio)	NH (0,6), LED (1,7) LED (2,1), LED (2,5)
Visual target illuminance [lx]	0,3, 1,5
Visual target position (angle of eccentricity) [degree]	-30, -20, -10, -5,5
Visual task load	Heavy, light

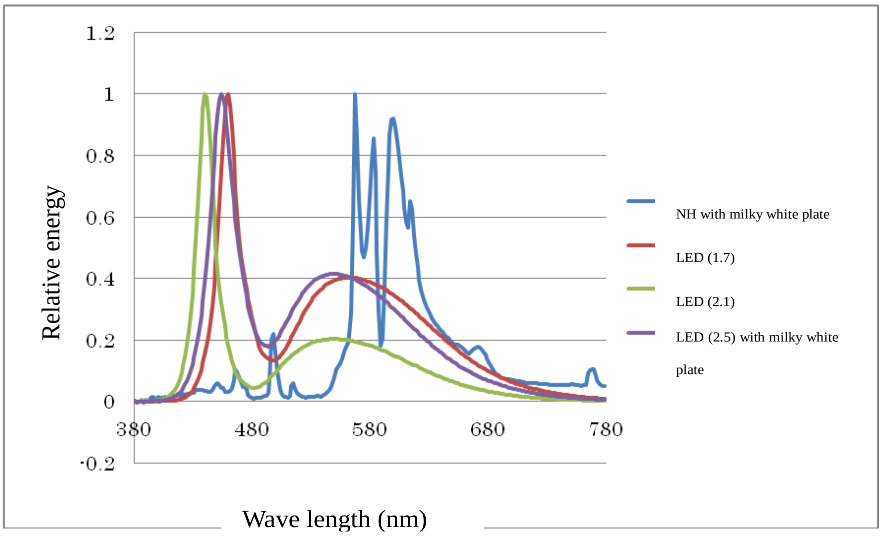

Figure 3 – Spectral distribution of light sources

3 Experimental results

Data for total of 13 subjects were used for the following analyses, eliminating data for 2 male subjects out of 15 subjects with whom experiment was conducted. Average values for each of light sources, visual target illuminances, angles of eccentricity and task load were obtained from the data of measured reaction time. Also, variance analysis against reaction time was conducted for each experimental condition.

3.1 Lighting conditions

Fig. 4-1 and 4-2 show experimental results concerning spectral distribution and illuminance of light sources. Fig. 4-1 shows relation between average reaction time and illuminance of visual target. It is understood that reaction time is shorter at conditions of higher visual target illuminance. (p<0,01**) Fig. 4-2 shows average reaction times among different light sources for each illuminance. By comparison among different spectral distributions, it is understood that reaction time becomes longer as S/P ratio becomes higher in sequence from NH for either illuminance condition. Significant differences were found among NH and three LEDs under the illuminance condition of 1,5 lx. Under illuminance condition of 0,3 lx, significant differences were found among light sources except for between LED (2,1) and LED (2,5). (p<0,01**)

These results show that reaction time becomes shorter under light sources containing more short wavelength radiation. They also show that difference of reaction time among different light sources increases as visual target illuminance reduces.

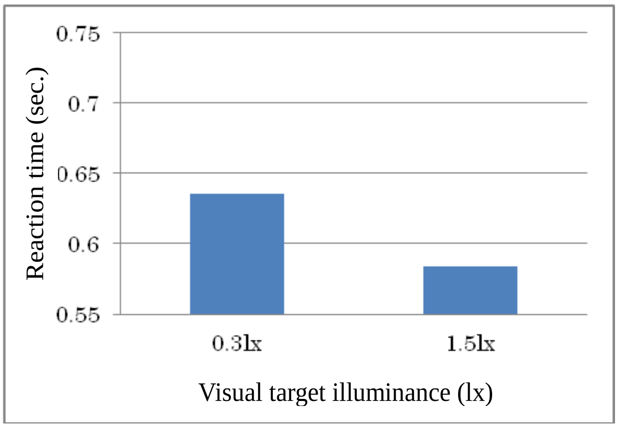

Figure 4.1 – Main effect of visual target illuminance

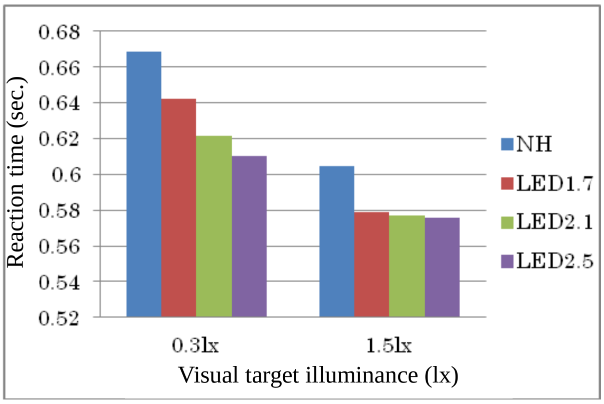

Figure 4.2 – Average values of reaction time (by illuminance, light source)

3.2 Position of visual target

Fig. 4-3 and 4-4 show average values of reaction time for each position of visual target. Fig. 4-3 represents average values of reaction time for each angle of eccentricity under each illuminance condition. Reaction time becomes shortest at angle of eccentricity of around 10° and becomes longer near periphery of visual field. This is considered to be because ratio of distribution of rods becomes maximum near 10° and reduces as angle of eccentricity increases.

Fig. 4-4 represents average values of reaction time for each angle of eccentricity for each light source under illuminance of 0,3 lx. Reaction time is shorter under light source with higher S/P ratio for any angle of eccentricity.

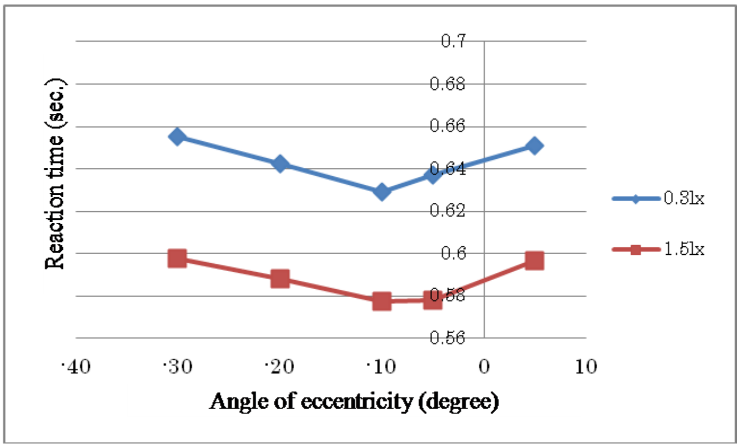

Figure 4.3 – Average values of reaction time for each angle of eccentricity

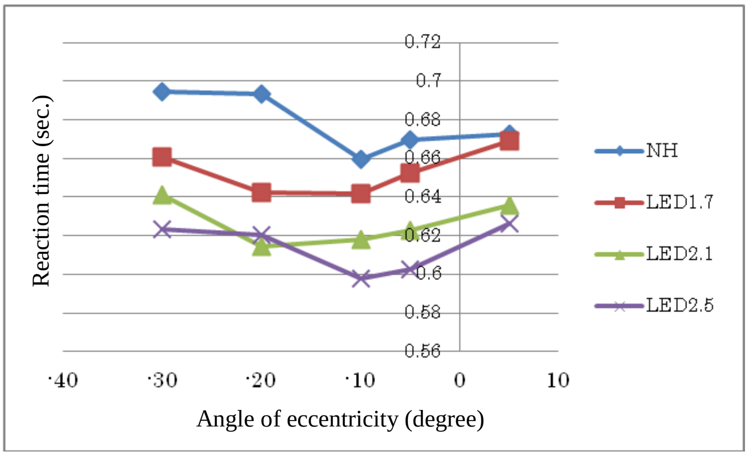

Figure 4.4 – Average values of reaction time for each angle of eccentricity (for each light source, 0,3 lx)

3.3 Foveal task load

Fig. 4-5 shows average values of reaction time for each task load. Average values of reaction time were obtained here irrespective of illuminance, spectral distribution of light sources and angles of eccentricity. From Fig. 4-5, reaction time is found to be longer under heavier load. As the result of variance analysis, main effect was found to exist because significant differences were shown among different task load. ($p<0,01$**)

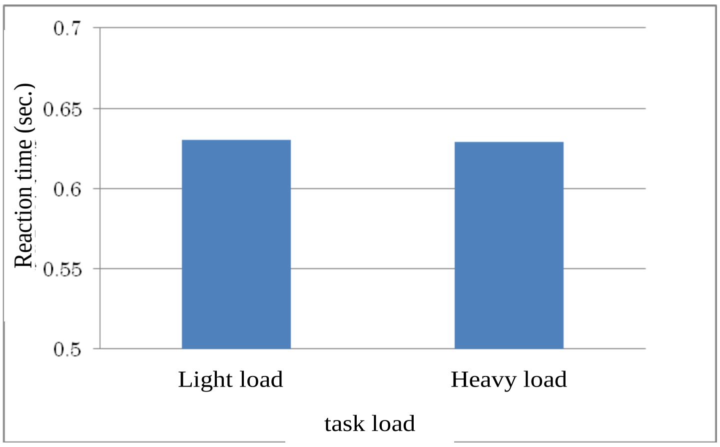

Figure 4.5 – Main effect of visual task load

Fig. 4-6 through 4-9 show average values of reaction time for each light source by each illuminance and load. Average values of reaction time for each angle of eccentricity for light source under 1,5 lx and light load are shown in Fig. 4-6, and the same under 1.5 lx and heavy load are shown in Fig. 4-7.

Dependence of change of difference of reaction time among light sources on central vision load was studied. As the result of statistical analysis, main effects were recognized with spectral distribution of light sources ($p<0{,}001$***), angle of eccentricity ($p<0{,}001$***) and visual target illuminance ($p<0{,}001$***). First, from Fig. 4-2, reaction time was long for NH with low S/P ratio and became shorter as S/P ratio rose from 1,7 to 2,1 and 2,5. Next, from Fig. 4-3, reaction time was shortest at angle of eccentricity of -10° and became longer as angle of eccentricity became smaller or larger. From Fig. 4-1, reaction time also became longer as visual target illuminance decreased.

Further, interaction was found between light sources and illuminance. ($p<0{,}05$) This can be said from Fig. 4-2 because reaction time gradually decreased from a light source to another when illuminance was low, while there was no difference of reaction time among light sources with S/P ratios of 1,7, 2,1 and 2.5 when illuminance was high. This shows that 1,5 lx was not mesopic light level. From Fig. 4-6, under 1,5 lx and condition of light central vision load, significant difference ($p<0{,}05$*) was found between NH and LED (2,5) but no significant difference was found between NH and LED (1,7) or LED (2,1). Under 1,5 lx and condition of heavy load in Fig. 4-7, significant difference was found between NH and three LEDs ($p<0{,}01$** for all). When compared with same light sources, significant difference ($p<0{,}01$**) was found with NH among different load conditions (No significant difference was found with three LEDs even when load was changed.). Therefore, it was confirmed that increase of central vision load enlarged difference of reaction time between NH and three LEDs, namely, increased degree of Purkinje phenomenon.

Fig. 4-8 is under 0,3 lx and condition of light central vision load and Fig. 4-9 is under 0,3 lx and heavy central vision load. Comparison of them shows significant difference ($p<0.01$) with LED (1,7) under conditions of different loads but no significant difference with other light sources. Increase of load resulted in delay of reaction time under condition of LED (1,7) alone, so that relation between central vision load and increase of Purkinje phenomenon could not be confirmed here.

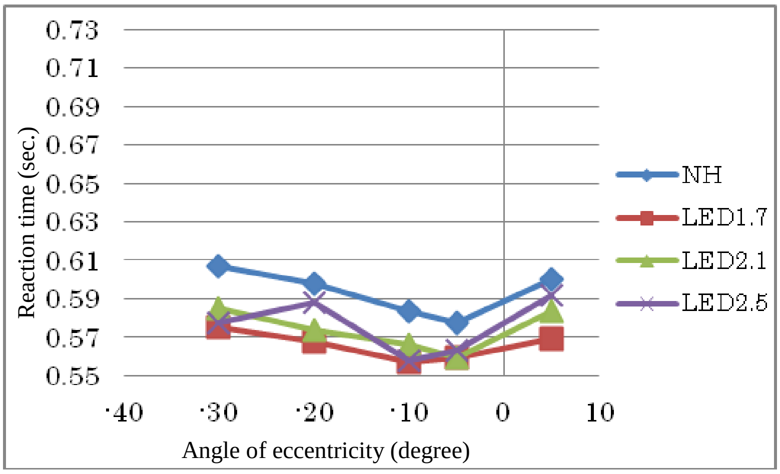

Figure 4.6 – Average values of reaction time for each angle of eccentricity for each light source (1,5 lx, light load)

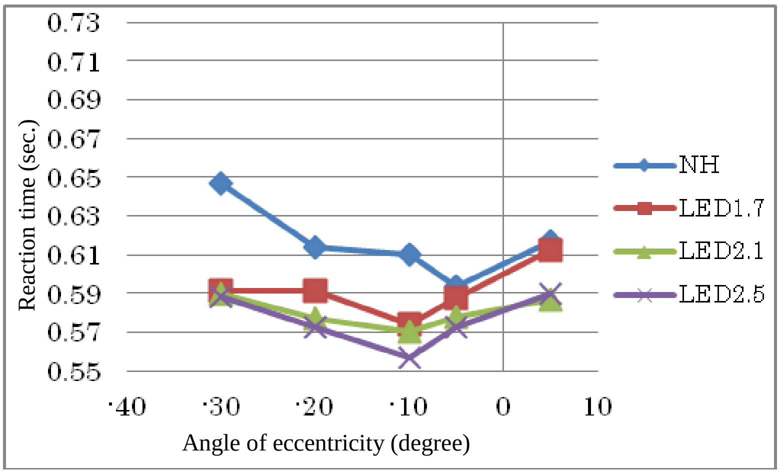

Figure 4.7 – Average values of reaction time for each angle of eccentricity for each light source (1,5 lx, heavy load)

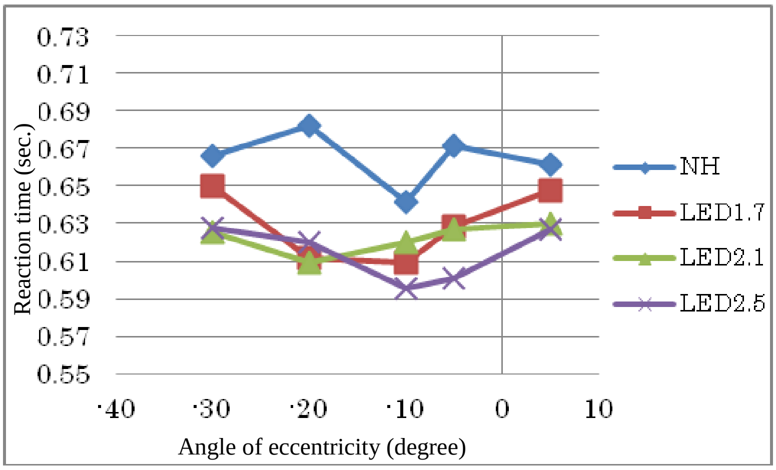

Figure 4.8 – Average values of reaction time for each angle of eccentricity for each light source (0,3 lx, light load)

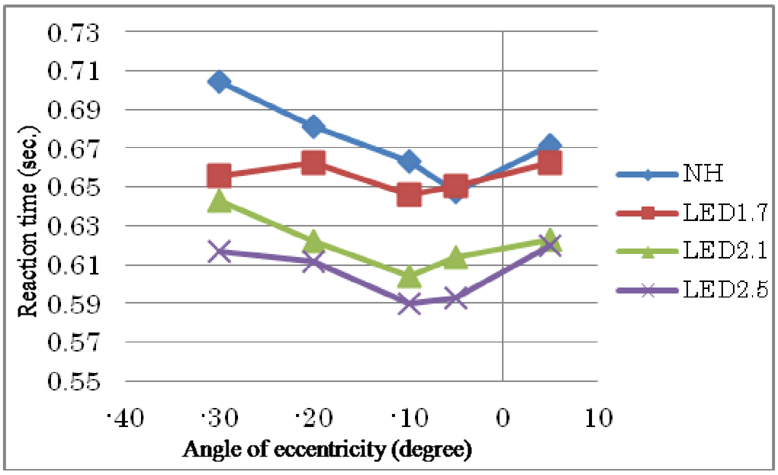

Figure 4.9 – Average values of reaction time for each angle of eccentricity for each light source (0,3 lx, heavy load)

4 Conclusion

Experiments were performed to investigate how visual task performance in peripheral vision change among different spectral distributions by changing visual task load on central vision under mesopic light level. As the result, it was clarified that Purkinje phenomenon tends to seem to increase by increasing foveal task load. Therefore, application of lighting of light sources rich in short wavelength radiation in practical environment of mesopic light level such as road at night is considered to provide higher visual task performance than that predicted from mesopic luminance calculated based upon mesopic vision photometric system, and to be able to improve safety on roads.

In expressways, where speed is high and task load is heavy, light sources in which Purkinje phenomenon is taken in consideration can be expected to help improvement of safety.

References

1) Rea, MS., Bullough, MS., Freyssinier-Nova JP, Bierman A: A proposed unified system of photometry, Lighting Research & Technology, 36, 2, 85-111(2004).

2) CIE 191: Recommended System for Mesopic Photometry Based on Visual Performance, Vienna: CIE (2010).

3) Kimitaka Shirakura, Yukio Akashi, Takashi Saito: Journal of the Illuminating Engineering Institute of Japan, 96, 5, 259-271 (2012).

4) Keiko Nakagawa, Yukio Akashi: Journal of the Illuminating Engineering Institute of Japan, 96, 5, 298-302 (2012).

PP73

MEASUREMENT OF LUMINANCE DISTRIBUTION OF STREET LIGHT UNDER DIFFERENT WEATHER CONDITIONS

Dubnicka Roman, Janiga Peter, Gasparovsky Dionyz, Barcik Michal
Slovak University of Technology, Faculty of Electrical Engineering and Information Technology, Bratislava, SLOVAKIA
Contact e-mail address: roman.dubnicka@stuba.sk

Abstract

Street lighting has undoubtedly big potential for electricity energy consumption. At present approximately 85% of street lighting networks are unregulated. Till now regulation is based on change of usage of road and then reclassification on other class according to standard. Regulation of roads influenced by weather currently is considered only minimally. Paper concerns about results of field measurements of luminance distribution by means of image photometry which can serve as future proposal on methodics of regulation street lighting based on change of road surface. Measurements were performed under various weather conditions. It analyses changes of road surfaces of different classes when surface was covered by snow or water. Results were also analysed with standard dry condition of roads surfaces which is defined also for computations of photometric parameters according to standard CIE140:2000. Evaluated were standard roads with different street luminaires (HPS, HID, LED). Results showed some interest findings which can influence luminance distribution on the road surfaces. At the end of paper are shown potential topics which shall be solved in the future.

Keywords: street light, luminance distribution, energy saving, weather conditions

1 Introduction

The priority now is saving energy resources and in the context of the conservation funds. To this is using various tools for example, energy labeling. Main task is to enable operators and users to decide for technology in energy intensity. The same trend can be observed also in lighting.

Significant potential savings are hidden in the operation of public lighting networks. It is possible to apply the newer and more efficient technology reducing energy consumption but also can achieve significant savings with management. For designing the control and regulation is required to comply with the requirements and the proposal should be implemented by experts in the field.

Unauthorized intervention in order to save funds, can lead to inappropriate solutions such as switching off every other lamp or the entire system after midnight. Voltage regulation without observance the minimum luminance and illumination intensity is also unacceptably. These and similar solutions are to the detriment of road safety and people.

The most of cities of Slovakia has upgraded street lighting and therefore is focused for solutions to optimize the management. Possible solutions for rational savings without changing the lighting system is the regulation of old lighting system. Current technology are allowed secure control of two basic ways. Central control and individual control in the lamp. Each method has some advantages and disadvantages. Voltage regulation respectively regulation luminous flux is based on the requirements imposed by the user. Exact values are defined in the enacting legislation. For public lighting is mainly about standard EN 13 201th. During the running time of public lighting can occur the regulation, which takes into account the change in external conditions. In order to most effectively use the controller, we proposed several methodologies, which have reduced energy consumption. It was also about regulating, which reflected maintenance factor.

At present, the data for a methodology of management control are collected, which taking into account the road surface. It means, that lighting controller would get the information about weather impact (snow at the road, wet road…) and based on the proposed algorithm would occurred regulation of voltage and luminous flux too. The proposal of such a methodology need mapping the current situation and impact. That is why the measurements on selected roads were made and results of measurements are described in details. The report is the backround for another analysis and also regulation according to the status of the road. In particular the proposal there is necessary to account a huge amount of factors, which influence last application such as the luminance of the backround, colour of the light and so on.

2 Measurement of luminance on the roads

Measurements of the luminance on the roads under different weather conditions have begun in 2013. Measurements are divided into several groups, because it isn´t possible all weather conditions on the same road. In paper are describes only some measurements and other results are analyzed at the present. All analyzed roads are in cities and towns in Slovakia. Measuring was realized luminance analyzers TechnoTeam:

- LMK 98-4 color
- Canon E350D

Measurements was realized in accordance with the document CIE 140, where is described measurement methodology. All evaluated routes have one lane for one traffic direction and unilateral lighting system. Analyzer (observer) was located 60 m from measured field. in the middle of driving lane and 1,5 m over roadway.

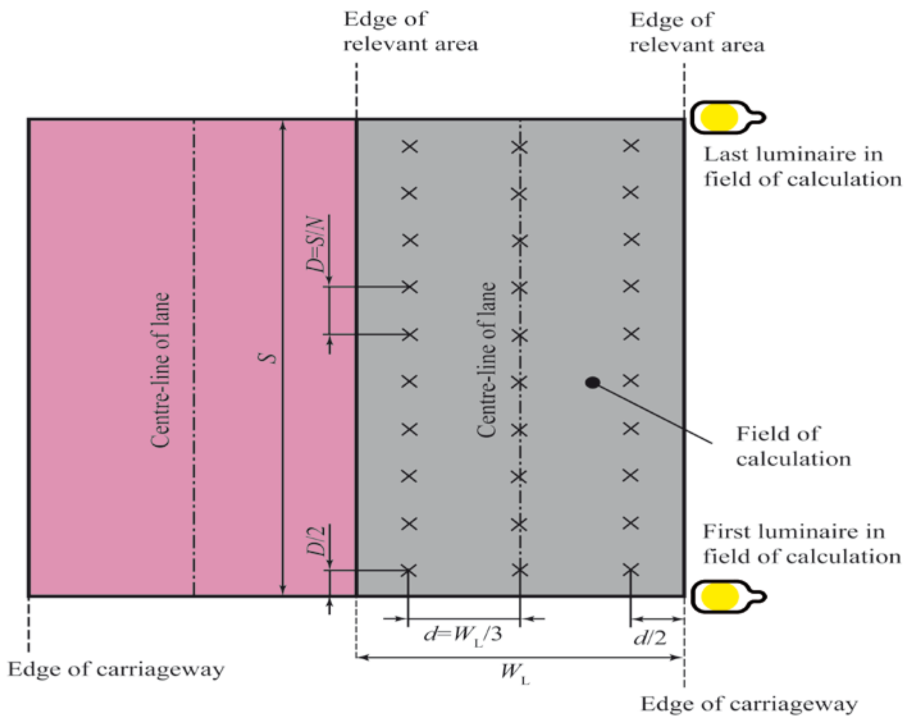

Figure 1 – Layout of measuring points in the analyzed field

Analyzed roads belongs to ME6 class. Characteristics and light requirements for ME/MEW classes results from standard EN 13 201-2. For purpose of study was chosen roads with low traffic.

Impact of traffic density is reflected in the standard EN 13201-1, which describes the methodology of public lighting. Interconnection between traffic density, weather conditions and possibility of regulating public lighting haven´t been analyzed yet. Traffic density influences on quality of snowy surface, quantity of water on carriageway and so on. Analyze of these effects aren´t the subject of this paper.

Table 1 – Parameters of roads

Street parameters	Streets							
	Žiškova			Hviezdna			M. Braxatorisa	
Width $2W_L$ [m]	4,8			6			6	
Distance between two poles S [m]	30			30			20	
Luminaire mounting height H [m]	6			6			5	
Overhang [m]	0,7			2,6			0,3	
Lamp parameters								
Producer	Siteco			Philips			OMS	
Type							Forstreet Sirius	
Lamp wattage (W)	70						72	
Type of lamp	High pressure sodium lamp			LED			LED	
Network parameters	Dry	Wet	Snowy	Dry	Wet	Snowy	Dry	Wet
Voltage U [V]	227	227	227	242	241	241	238	239
Date and time of measurement	12.6. 13, 22:40	11.10. 13, 22:00	11.12. 12, 18:20	26.2.14 23:40	16.2.14, 23:40	14.1.14 , 00:20	1.2.14, 23:20	25.1.14 , 22:40
Temperature [°C]	21	12	-1	3	5	-2	5	3

Ziskova street is located on the estate among residential houses with low speed of cars, where the cyclists and pedestrians move. Hvezdná street is located in a small town Malinovo near the capital city Bratislava in new district with a lot of houses. It is driveway for new district. M. Braxatorisa street is located in Senica in district with houses and is intented for cars with low speed, cyclists with increased movement of people.

3 Impact influence on the values of luminance

Distribution of luminance influence many factors on the road. These factors can influence differently.

3.1 Snowy surface

Valuation to luminance of snowy surface is very difficult. If the carriageway is continuously overlay with snow it is possible to notice the increase of luminance on the road and surroundings. This effect can be rate like positive. It is possible to assume, that decrease the level of luminous flux of luminaries ensure the needed illumination on the road and along with lower power consumption.

For exactly definition increase of values of luminance on the road is needed to consider the conditions on the carriageway. That is mean:

- new or slick snow
- continous layer or running out lines
- uniformity and quantity of snow

These effect are difficult to quantify and measure.

3.2 Wet surface

Wet surface are among the most common impact, that can be occur on the road. Rain have negative impact to luminance on the road. During rain increases risk of glare from the oncoming cars and public lighting, surrounding lighting and so on. Main impacts influenced the luminance on the wet carriageway are:

- water in running out lines
- water fog from other cars
- water pool

The worst negative impact on wet carriageway is alternation bright and dark places. The human eye can´t be adapt on the fast changes and then can´t be discern details on the road.

3.3 Impact surrounding buildings and objects

The surrounding objects affecting to level of illumination on the roads. This effect is often variable during daytime hours. The increase of the luminous flux from the surrounding buildings and objects is in the evening. This phenomenon may be positive but also negative.

Illumination from the surrounding buildings can be used to illuminate on the surrounding roads such as sidewalks. It can cause This may cause nonuniformity of the illumination. It can be caused by show-window illumination or illumination of the building facades.

The above-described effects of buildings and objects are positive but the surrounding objects can also increase the risk of glare. It is necessary to increase the background illuminance in this case. such as public lighting. Increase the background illumination is provided by using public lighting.

The most important effects of surrounding buildings are:

- -building illumination,
- -billboards,
- -show-window illumination,
- -seasonal decorations illumination,
- -floodlighting

Just as in the evaluation the impact of wet and snowy road is the most effective way of determining the impact of measurement in real operation.

3.4 Impact of trees and greenery

This is the impact that does not contribute by luminous flux but affecting to illumination of the road.

Impact of greenery was visible on the measurement results during the measurements . In the surroundings of roads and communications are leafy trees and density of the leaves is changed during the year. Transmittance of light through the trees is better during the winter months when the leaves are fallen. Full tree crowns seems like aperture in the summer and autumn.

4 Measurement results

The measured values show an increase of luminance in snowy conditions. Differences may arise from inequalities of snowy conditions. Snow was parted out but were there slight ripple. Another effect, that is complicate to evaluate in measurement is luminance of surrounding building and from public lightning. Even though was choosen roads with consideration to eliminate effect of surrounding lightning and luminance from surrounding objects, was impossible completely eliminate this impact. One of the reason is that public lighting was measured in town and next reason is that public lighting is not located separated but is part of public lighting nets.

Measured values show big diferences between measured points, which is caused by reflection from other luminaires, roughness of carriageway, quantity of water and so on.

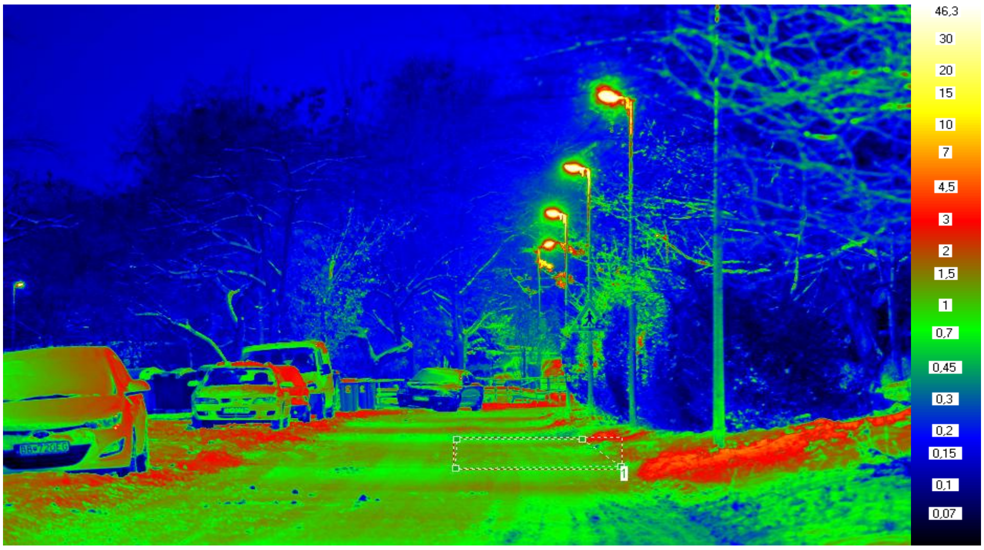

Figure 2 – Situation in measurement of luminance

a,

b,

c,

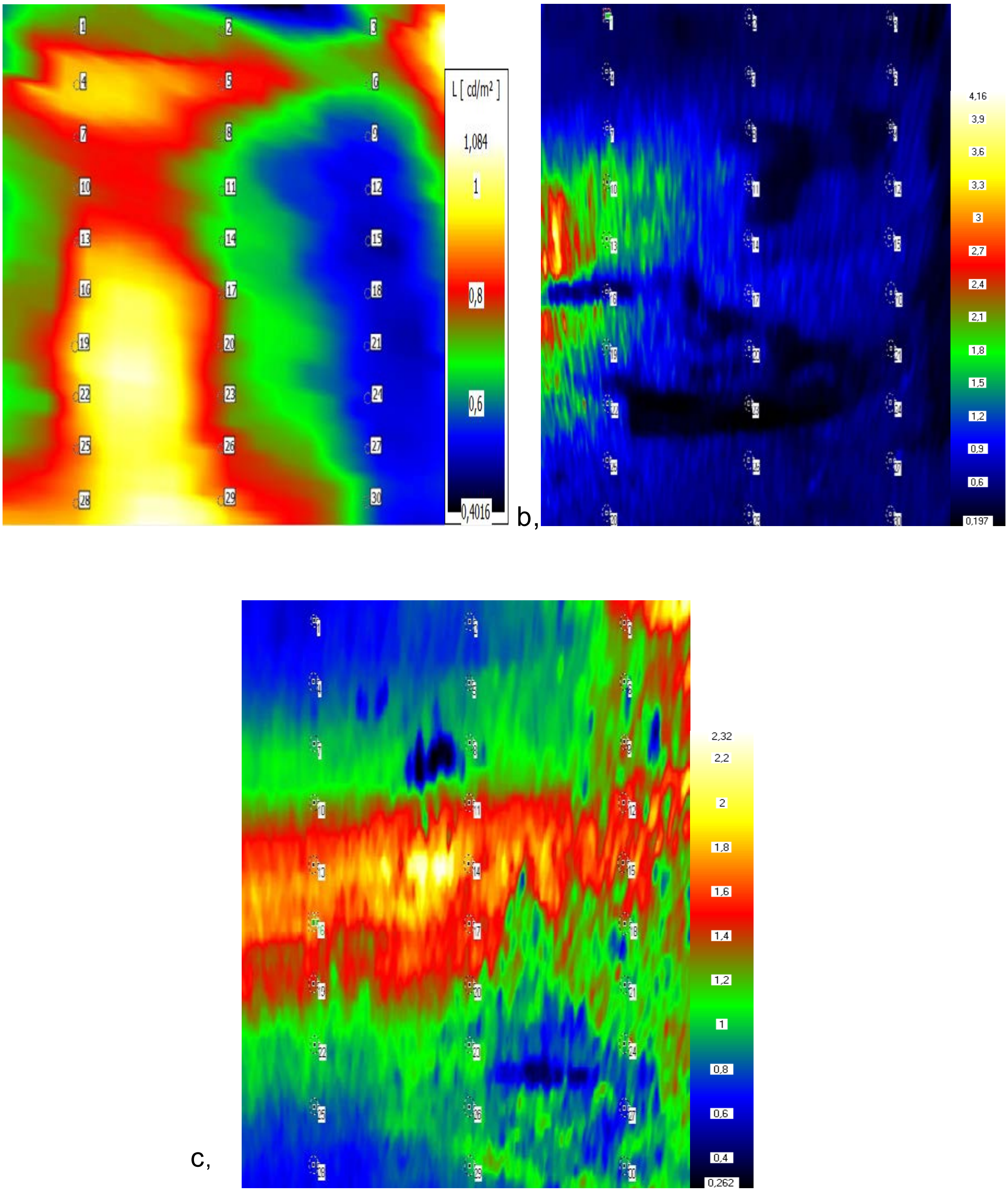

Figure 3 – Comparisom one of the driving lane for a, dry surface b, wet surface c, snowy surface (Žižkova)

Table 2 – Measured values

Street	Žižkova						M.Braxatorisa	
	Road line 1			Road line 2			Road line 1	
Measured point	Luminance L [cd/m2]	Luminance L [cd/m2]	Luminance L [cd/m2]	Luminance L [cd/m2]	Luminance L [cd/m2]	Luminance L [cd/m2]	Luminance L [cd/m2]	Luminance L [cd/m2]
	Dry	Wet	Snow	Dry	Wet	Snow	Dry	Wet
1	1,081	0,8163	0,807	0,5322	0,5343	0,634	1,462	1,171
2	0,7528	0,8737	0,6751	1,29	0,487	0,7802	1,328	0,9237
3	0,9118	7,854	0,771	0,4077	0,4587	1,409	1,138	0,8605
4	1,167	0,8381	0,9699	0,7654	0,5234	0,744	1,524	1,183
5	0,7308	5,671	0,859	1,33	0,5455	0,9007	1,267	1,005
6	0,9547	3,994	1,141	0,4959	0,5429	1,184	1,102	0,8579
7	1,219	1,021	1,258	0,9878	0,9634	0,974	1,534	1,307
8	0,8029	3,856	1,167	1,402	0,5298	1,007	1,266	1,101
9	0,9525	7,618	1,509	0,7025	0,4659	1,339	1,084	0,8549
10	1,176	1,489	1,326	1,281	1,927	1,248	1,53	1,464
11	0,7799	1,469	1,204	1,395	0,7813	1,405	1,295	1,176
12	1,034	3,678	1,252	0,8158	0,6536	1,528	1,075	0,8519
13	1,071	2,355	1,261	1,377	1,841	1,686	1,468	1,54
14	0,8564	1,557	1,133	1,452	0,8772	1,756	1,308	1,195
15	1,002	2,524	0,8984	0,9496	0,7119	1,428	1,074	0,8205
16	1,028	1,476	1,254	1,282	0,6597	1,743	1,359	1,476
17	1,079	9,799	1,161	1,31	0,9685	1,575	1,259	1,045
18	1,106	2,066	0,793	0,8632	0,6414	1,256	1,074	0,7571
19	0,9793	0,6123	1,243	1,149	1,397	1,431	1,229	1,277
20	1,046	3,232	1,132	1,173	0,6999	1,352	1,174	0,9355
21	1,142	1,434	0,9914	0,8079	0,3906	1,01	1,102	0,7223
22	0,8964	0,9359	1,29	1,072	1,109	1,062	1,178	1,165
23	0,7302	2,426	1,145	1,095	0,3103	0,9931	1,139	0,8869
24	1,079	3,564	1,17	0,9226	0,5991	1,063	1,14	0,6852
25	0,8263	1,206	1,17	1,023	0,7899	0,8679	1,174	1,072
26	0,6656	1,459	1,085	1,006	0,6174	0,9271	1,137	0,8335
27	0,9914	1,524	1,225	0,8157	0,5603	0,7268	1,195	0,6533
28	0,8366	1,035	1,065	0,9634	0,6744	0,7044	1,223	0,9703
29	0,6766	8,69	0,8973	0,9946	0,5645	0,9657	1,127	0,8176
30	0,7478	3,2	0,9814	0,7268	0,5478	0,8849	1,212	0,6147

Table 3 – Measured values

Street	M.Braxatorisa		Hvezdná					
	Road line 2		Road line 1			Road line 2		
Measured point	Luminance L [cd/m2]	Luminance L [cd/m2]	Luminance L [cd/m2]	Luminance L [cd/m2]	Luminance L [cd/m2]	Luminance L [cd/m2]	Luminance L [cd/m2]	Luminance L [cd/m2]
	Dry	Wet	Dry	Wet	Snow	Dry	Wet	Snow
1	1,373	1,351	0,9234	0,3702	1,872	0,3268	0,1095	0,5613
2	1,354	1,874	1,103	0,4649	1,936	0,278	0,1153	0,5694
3	1,393	1,211	0,9085	0,3975	1,72	0,1801	0,06917	0,3759
4	1,375	1,346	0,8757	0,3651	1,943	0,3125	0,0993	0,5604
5	1,437	1,615	1,089	0,4536	2,116	0,2629	0,09652	0,5694
6	1,396	1,267	1,072	0,4218	1,886	0,175	0,06687	0,3705
7	1,37	1,377	0,7815	0,3373	1,912	0,3121	0,09766	0,557
8	1,474	1,617	0,9512	0,422	2,124	0,261	0,09414	0,5677
9	1,414	1,322	1,075	0,4021	1,98	0,1739	0,06725	0,3763
10	1,349	1,577	0,7166	0,3014	1,854	0,3429	0,1013	0,5598
11	1,489	1,668	0,8273	0,3842	2,07	0,2787	0,09658	0,5432
12	1,442	1,369	0,972	0,3561	2,013	0,1825	0,07276	0,3922
13	1,322	1,645	0,6936	0,282	1,775	0,3938	0,1187	0,6405
14	1,487	1,87	0,7811	0,3561	1,996	0,3405	0,1128	0,5911
15	1,489	1,457	0,8393	0,2868	1,984	0,2133	0,08679	0,428
16	1,319	1,636	0,6986	0,283	1,64	0,4422	0,129	0,7269
17	1,472	1,888	0,7794	0,3593	1,898	0,4074	0,1425	0,7137
18	1,502	1,483	0,7269	0,2751	1,701	0,2535	0,09783	0,4789
19	1,327	1,57	0,7176	0,2766	1,447	0,5009	0,1512	0,7956
20	1,396	1,698	0,8462	0,3782	1,795	0,4614	0,1651	0,8564
21	1,523	1,475	0,6933	0,2584	1,564	0,2849	0,1038	0,4907
22	1,364	1,482	0,7897	0,2777	1,341	0,5363	0,1597	0,8224
23	1,382	1,414	1,011	0,3755	1,707	0,4686	0,1619	0,8015
24	1,53	1,469	0,6892	0,2484	1,508	0,2777	0,09607	0,443
25	1,449	1,386	0,8539	0,2823	1,367	0,5209	0,1527	0,7599
26	1,405	1,389	1,153	0,3758	1,62	0,4204	0,1261	0,6797
27	1,531	1,43	0,8553	0,2621	1,473	0,2121	0,0871	0,3874
28	1,484	1,286	0,8802	0,2952	1,422	0,4776	0,1428	0,6523
29	1,422	1,34	1,233	0,3943	1,729	0,328	0,1015	0,5336
30	1,525	1,347	1,034	0,3047	1,613	0,1872	0,07943	0,3516

5 Conclusion

The contribution describes the impact of snowy and wet road to change luminance. Impact is shown by measurements that was made on chosen roads. There is no attempt to quantify change luminance but to show how conditions change when you change the properties of roads. Precise quantification would require deeper analysis and comprehensive consideration of numerous factors such as the background luminance, temperature, etc. The measurements serve as a basis for further analysis and public lighting control options, depending on external factors.

Acknowledgement

This publication is the result of the project implementation:
Research centre of light and lighting technology, ITMS 26220220150,
supported by the Research & Development Operational Programme funded by ERDF.

Operačný program VÝSKUM a VÝVOJ

Agentúra
Ministerstva školstva, vedy, výskumu a športu SR
pre štrukturálne fondy EÚ

Podporujeme výskumné aktivity na Slovensku/
Projekt je spolufinancovaný zo zdrojov EÚ

Európska únia
Európsky fond regionálneho rozvoja

.

References

SOKANSKY, K.; NOVAK, T. 2008. Energy savings in public lighting, Przegląd Elektrotechniczny, 84 (2008), nr 8, 72-74.

SKODA, J., BAXANT, P. 2011. Effect of directional reflectance in lighting. Przeglad Elektrotechniczny. 87(4). p. 38 - 40. ISSN0033-2097.

PAVELKA, T., BAXANT, P., KRBAL, M., SKODA, J., DOSTAL, L. 2011. Parameters of classic bulbs under extreme conditions. In Proceedings of the 12th International Scientific Conference Electric Power Engineering 2011. First edition. Ostrava, Czech Republic, VSB - Technical University of Ostrava. p. 1 - 4. ISBN 978-80-248-2393-5.

ONAYGIL, S., GULER, Ö., ERKIN, E. 2012. Cost analyses of LED luminaires in road lighting. Light and Engineering, 20 (2012) nr 2, 39-45.

SOKANSKY, K.; NOVAK, T. 2008. Power Saving Potential of Public Lighting in the Czech Republic, 9th International Scientific Conference on Electric Power, Brno Univ Technol, Published: 2008, Pages: 401-403.

SKODA, J., BAXANT, P. 2009. The reduction in electricity consumption through proper lighting. In EPE - Electric Power Engineering 2009. p. 1 - 5. ISBN 978-80-248-1947-1.

CIE 140:2000. Road lighting calculations.

PP74

MEASUREMENT PROCEDURE FOR MESOPIC IN-FIELD CHARACTERIZATION OF SSL ROAD LIGHTING INSTALLATIONS

G. Rossi[1], P. Iacomussi[1], M. Radis
[1] INRIM, Torino, ITALY
g.rossi@inrim.it

Abstract

Considering CIE TR 115 (CIE 2010) and the current European standards (EN 2004), the characterization of road lighting installations requires the measurements of luminance or illuminance using photonic quantities, even if the recommended lighting levels are those typical of the mesopic vision. In the past, this strange situation was not a real problem because the selection of lamps for road lighting was very limited (mainly high-pressure sodium vapour lamps or mercury vapour lamps) and the standard requirements (lighting classes) agreed after heuristic subjective experiments and worldwide experience (CIE 1992). The correct link between vision conditions for safety and lighting level was correctly obtained but specified using the wrong photonic quantities.

With the introduction in the market of luminaires with sources like LED or metal halide lamps that have a completely different spectral distribution, the above mentioned link breaks and requirements and verification measurement should be done using mesopic quantities.

This work describes the method developed at INRIM for the characterization of road lighting installations in the mesopic range. The procedure uses traditional instruments, calibrated in photonic quantities, and spectral measurement of the observed radiation to obtain the correct values of luminance or illuminance in mesopic units.

Keywords: road lighting installation measurements, mesopic vision, spectral measurement systems.

1 Introduction

The photometric characteristics and performances of luminaires are usually specified given the emitted luminous flux, the luminous intensity distribution and the luminous efficacy, as in the European standard EN 13032 (EN 2004). Some standards require other parameters that can be gathered knowing the luminous intensity distribution, like the luminous flux emitted in peculiar solid angles (e.g. the upward light output ratio R_{ULO}). Generally, these quantities are measured considering photopic photometry. However, in specific applications, as road lighting, the lighting levels are typical of the mesopic range; traditionally, also in these cases photopic quantities are used to specify standard requirements, as in the European standard EN 13201-2 (EN 2004), to design installations (EN 13201-3, EN 2004) or to characterize their performances (EN 13201-4, EN 2004).

For road lighting applications, the use of mesopic quantities for normative requirements could optimize the lighting level considering the real vision conditions and could permit an important energy saving without reducing road safety. According to the spectral luminous efficiency at the actual mesopic vision conditions, an optimization of the spectral distribution of the light emitted by luminaires could reduce the installed luminous flux and the artificial sky radiance.

The EN 13201 set of CEN standards considers exclusively photopic quantities (EN 2004). The revision of these standard has started in 2010, but unfortunately one of the first decisions has been to maintain this approach also in the next edition, scheduled for the middle of 2015. The reasons of this choice are:

- the lack of experience in the use of mesopic quantities;

- the fact that the luminaires characterization does not give information to correctly calculate mesopic quantities;
- the absence of proposal for algorithms aimed at calculating road lighting installation using mesopic quantities;
- difficulties in the measurements of quality parameters using mesopic quantities.

For these reasons, some national standards try to adopt simplified approaches partially following guidelines written in CIE TR 206 (CIE 2014).

For example the Italian standard for the selection of lighting classes (UNI 2012) requires a risk analysis to find the best sources for a given road situation. When the optimal lighting class is selected, if the peripheral vision is important and if the light sources have a colour rendering index R_a greater then 60, the designer can select the first class with less performance requirements. This approach simplifies the scientific problems without considering the CIE model for mesopic vision, described in CIE TR 191 (CIE 2010).

While mathematically the CIE recommended system (CIE 2010) is completely defined, several conditions for the correct evaluation of the mesopic values of lighting parameters (average luminance, uniformities, etc.) are not completely described and are topics of research activities, as for example the adaptation luminance that should be chosen in road lighting or the influence of glare sources (luminaires, headlamps of incoming cars, etc.).

For this reason the measuring method developed at INRIM (the Italian National Institute for Metrological Research) for the in-field characterization of road lighting installations tries to obtain as much photometric information as possible from the lighted environment. In this way it is possible to estimate the sensitivity of the evaluated parameters to the spectral distribution of the seen radiation, to glare sources (luminaires or other light sources) and the adaptation luminance considering different angular extensions and conditions.

The method measures the road surface luminance, the horizontal illuminance and the luminance of environment surfaces. At the same time the spectral horizontal irradiance and the average spectral radiance of the road surface is measured. In this way the traditional parameters are obtained and the mesopic road surface luminance or horizontal illuminance can be calculated using a conventional value of the photopic luminance of the visual adaptation field and the measured values of the S/P ratio of the incident radiation on the road surface or observed radiation from the road surface.

The method can be used for static or dynamic measurements. In the past INRIM developed several dynamic measurement systems (i.e IACOMUSSI 2005). Only the solutions for the spectral measurements are described here.

2 The spectroradiometric measurement system for horizontal irradiance

The INRIM dynamic system for the measurement of horizontal illuminance uses the split detector principle (CIE 2011), but for economical reasons only one detector measures the spectral irradiance. In road lighting this is not a great limitation because practically all installations have luminaires with a symmetrical luminous intensity distribution. In tunnel lighting, where counter beam luminaires are often adopted, the irradiance from the hemisphere with the greater light contribution is measured.

A calibrated silicon cell with a picoammeter is used as illuminance detector. For the spectral irradiance measurement the schematic showed in Figure 1 is adopted.

The luminaires lights the detector of the calibrated illuminance meter. The lighted surface of the detector reflects a fraction of this light that is captured by a lens and measured by a spectrometer, connected through an optical fibre.

The system is realized using a shaped aluminium tube with a screen to stop the radiation from the unwanted hemisphere and a baffle to reduce the influence of inter-reflections between internal tube wall and the detector. The lens focuses the detector surface on the optical fibres input. At the optical fibres output a CCD array spectrometer acquires the spectral signal. The readings of the two detectors are synchronized and with the same integration time: this assures to measure the radiation in the same point, even if the detector is moving during the measurements.

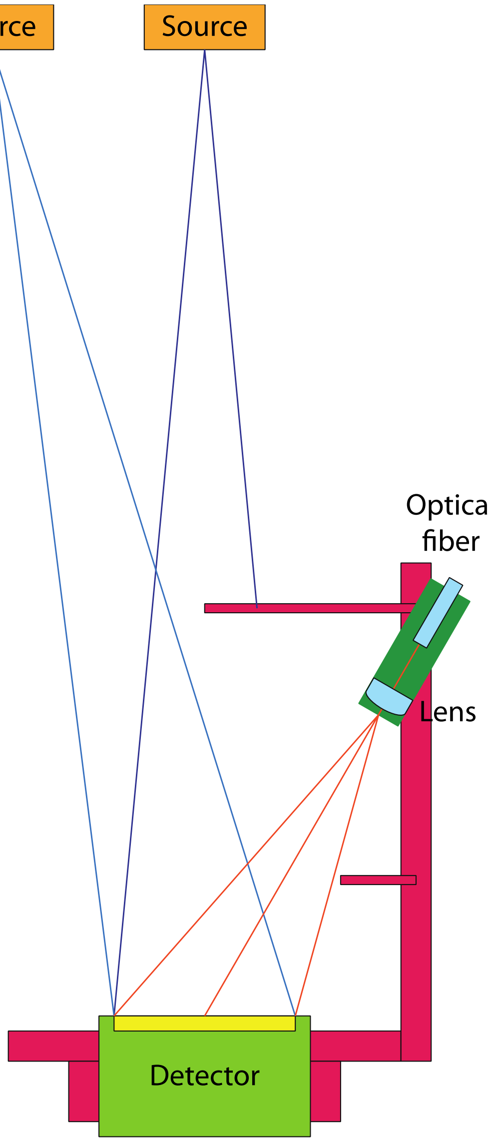

Figure 1 – The schematic of the measurement system for spectral irradiance.

The path of the optical radiation is show in figure 2. If $\Phi(\lambda)$ is the radiant flux incident on the detector surface, the spectrometer lens capture a fraction of the reflected flux $\Phi_{r(}\lambda)$:

$$\Phi_c(\lambda) = f(\lambda)\, \Phi_r(\lambda) = f(\lambda)\, \Phi(\lambda)\, \rho_g(\lambda) \tag{1}$$

where:

- $\Phi(\lambda)$ is the radiant flux incident on the detector surface, in watt.
- $\Phi_r(\lambda)$ is the radiant flux reflected by the detector surface, in watt.
- $\Phi_c(\lambda)$ is the radiant flux the lens of the spectrometer captures, in watt.
- $f(\lambda)$ is the ratio between the reflected radiant flux $\Phi_c(\lambda)$ the lens captures and the reflected radiant flux $\Phi_r(\lambda)$. Dimension 1.
- $\rho_g(\lambda)$ is the spectral reflectance of the detector opaline glass measured at normal incidence and at the spectrometer lens observation angle. Dimension 1.

The output signal Y_s (λ) of the spectrometer, in counts and for an observed radiation of a given wavelength λ, is:

$$Y_s(\lambda) = \Phi_c(\lambda)\,\tau_s(\lambda)\,\tau_o(\lambda)\,s_s(\lambda) \tag{2}$$

where:

$\tau_s(\lambda)$ is the spectral transmittance of the lens of the spectrometer. Dimension 1.

$\tau_o(\lambda)$ is the spectral transmittance of the fibre optics of the spectrometer. Dimension 1.

$s_s(\lambda)$ is the spectral responsivity of the spectrometer in count per watt.

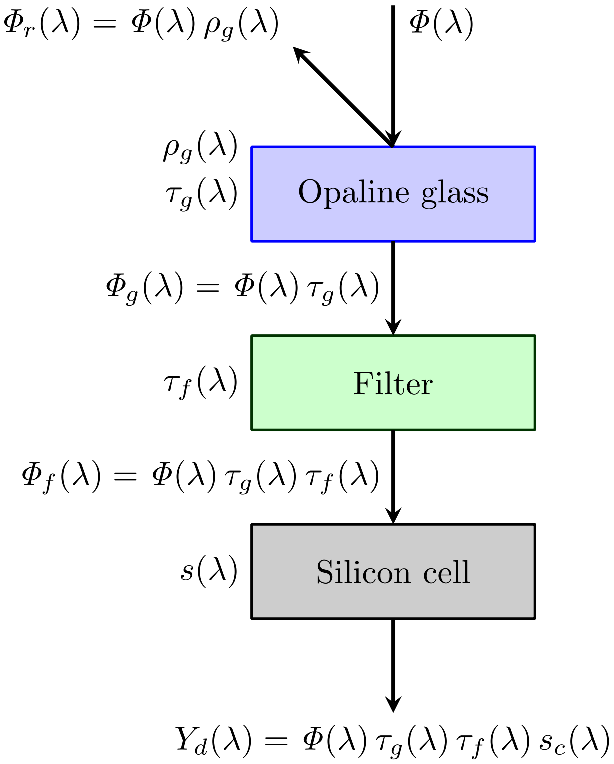

Figure 2 – The paths of the optical radiation.

The illuminance detector is a LMT photometer head AP 30 SCT with a very fine *V*(*λ*) approximation (f'_1 < 1 %) calibrated using an illuminant A source. The reflectance (figure 3) of the opaline glass was measured considering an angle of incidence of 0° and a reflection angle of 30° corresponding to the mechanical layout of the optical system. The measurement has been carried out considering the opaline glass alone or installed in the detector. The ratio of the two functions has a maximum value of about 1,49 near 640 nm.

The instrument part used for the spectral measurement is composed by:

- a lens that sees the acceptance area of the detector at a 30 ° angle respect to the surface normal;
- an optical fibre, 0.5 m long;
- an Ocean Optics CCD spectrometer (model USB2000) with a grating working from 350 nm to 850 nm and a resolution of 1,4 nm.

The spectrometer lens captures a fraction of the radiant flux reflected by the detector filter. The correct evaluation of this fraction is not easy because depends mainly from:

- the fixed visual angle of the lens;
- the uniformity of the illuminance on the detector acceptance surface;
- the position, respect to the vertical axis of photometric detector, of the spectral detector;
- the rotation, respect to the vertical axis of the measurement system, of the photometric detector;
- the light incidence direction.

Considering the typical measurements situations:

- The uniformity of the illuminance on the detector acceptance surface is usually very high.
- The maximum angle of incidence respect to the detector surface normal is near 90°. The specular reflected component of the incident light at higher angle can't be measured, but the luminaires involved are very far from the detector and therefore their contribution is very low. The influence of the radiation not measured is considered in the measurement uncertainty evaluation and was obtain simulating typical road lightning installation layout.
- For its calibration, the photometric detector is removed from the measurement system and the repeatability of its angular positioning in its holder is better then 1°. The influence of this rotation is reduced during the calibration of the spectral part of the device and it is considered in the measurement uncertainty evaluation.

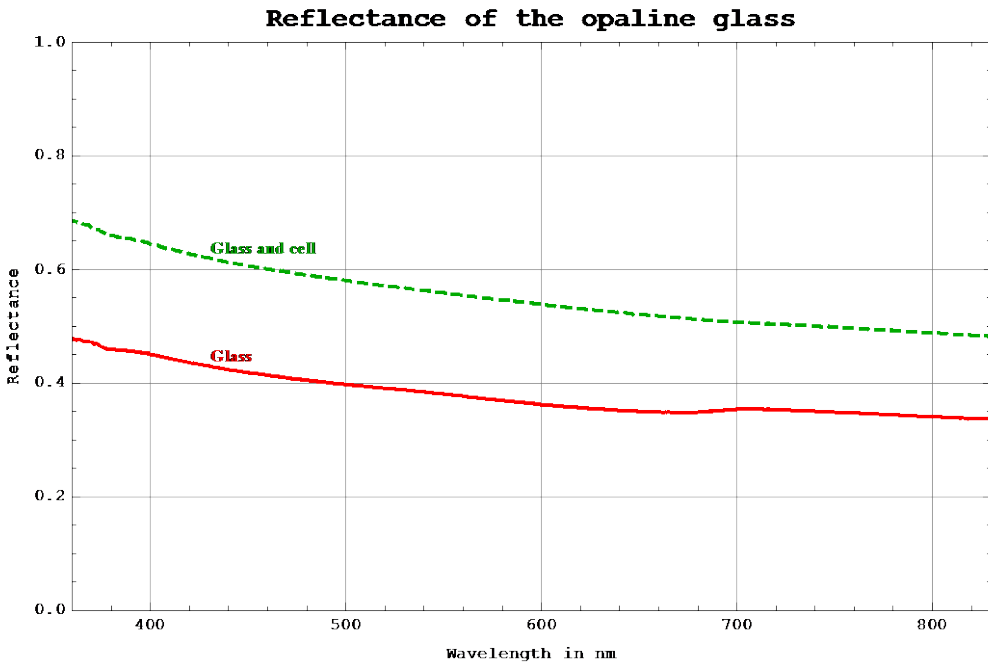

Figure 3 The spectral reflectance of the opaline glass in the direction of observation of the spectrometer and with normal incidence.

The focal length of the lens has been selected to create an image of the detector surface at the optical fibre input. To improve the quality of this image and to maximize framed acceptance areas of the detector avoiding to frame part of the detector holder, the acceptance surface plane, the lens plane and the image plane (i.e. the plane of the input surface of the fibre optics) are inclined with angles that are a compromise between the Scheimpflug condition, the minimization of perspective distortion and mechanical constrains. This inclination is not shown in the schematic draw of figure 1.

The lens has a diameter of 30 mm and an aperture angle of about 12 ° respect to the centre of the detector surface.

The calibration of the photometric detector is extremely important for the uncertainty budget and it is carried out on the detector with the same electronic equipment used for reading the detector photocurrent. According to (CIE 2011) the calibration is carried out with the detector surface rotated of 45° respect to the incident light beam.

The calibration of the spectro-radiometric part is done considering the entire system and a spectral calibrated lamp.

If $S_{cal}(\lambda)$ is the relative spectral distribution of the calibration source given by the calibration certificate, the following equation can be used for calculate the calibration coefficient $k_{cal}(\lambda)$ of the measurement system:

$$S_{cal}(\lambda) = k_{cal}(\lambda)\left(Y_{s,cal}(\lambda) - Y_{s,dark}(\lambda)\right) \tag{3}$$

where:

$k_{cal}(\lambda)$	is the calibration coefficient of the measurement system for relative spectral distribution measurements. Dimension inverse of count.
$Y_{s,cal}(\lambda)$	is the output signal of the spectrometer during calibration for an observed radiation at a given wavelength λ, in counts.
$Y_{s,dark}(\lambda)$	is the output signal of the spectrometer at a given wavelength λ in the absence of observed radiation, in counts.

The absolute calibration of the spectroradiometers is obtain comparing the measured photopic illuminance with the relative spectral distribution measured:

$$E_{\mathrm{v}} = k_{cal,\mathrm{v}} \int_0^{\infty} \left(Y_{s,cal}(\lambda) - Y_{s,dark}(\lambda)\right) k_{cal}(\lambda)\, V(\lambda)\, \mathrm{d}(\lambda) \tag{4}$$

where:

E_{v}	is the photopic illuminance measured with the illuminance detector, in lux.
$k_{cal,\mathrm{v}}$	is the calibration coefficient of the measurement system for relative spectral distribution measurements. Dimension lux count^{-1}.
$k_{cal}(\lambda)$	is the calibration coefficient of the measurement system for relative spectral distribution measurements. Dimension inverse of count.
$Y_{s,mea}(\lambda)$	is the output signal of the spectrometer during measurement for an observed radiation at a given wavelength λ, in counts.
$Y_{s,dark}(\lambda)$	is the output signal of the spectrometer at a given wavelength λ in the absence of observed radiation, in counts.

The wavelength calibration of the spectrometer is independent from the optical system of the instrument and it is carried out using a mercury argon calibration source with optical fibre connector.

3 The spectroradiometric measurement system for spectral radiance

For the measurement of the spectral radiance of the road surface a similar approach has been adopted. A lens frames part of a lane of the carriage on the optical fibre input of the spectroradiometer. This lens is mechanically in-built to the lens of the ILMD (Image Luminance Measurement Device). At the measuring distance, the portion of the road surface measured by the spectroradiometer is compared with the luminance of the same part measured by the ILMD.

The relative spectral calibration of the spectroradiometer with its lens and optical fibre is carried out using the light of spectral calibrated lamp reflected by a calibrated white diffusing surface.

4 Examples of measurement results

In figure 3, the relative spectral distribution of the road horizontal irradiance is shown, considering different points along the central line of the standard calculation grid of a experimental installation with only one luminaire. The effect of the different spectral emission with the angle of the luminaire is clearly visible.

Considering an experimental installation with only two luminaires, in figure 4 the relative spectral distribution of the road radiance in a point (first standard grid point along the central line) is shown. In this case different observation angles are considered to highlight the small influence of the observation angle in the spectral distribution of the reflected radiation, at least for the road surface of this experimental setup.

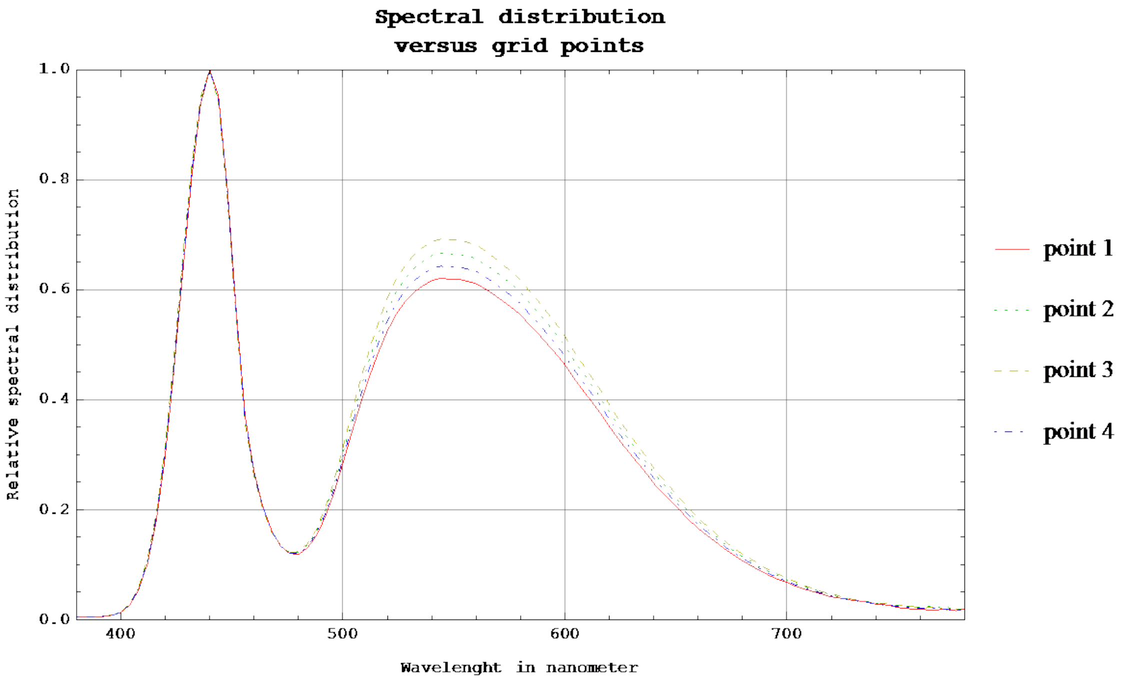

Figure 3 – Example of relative spectral distribution of the horizontal irradiance.

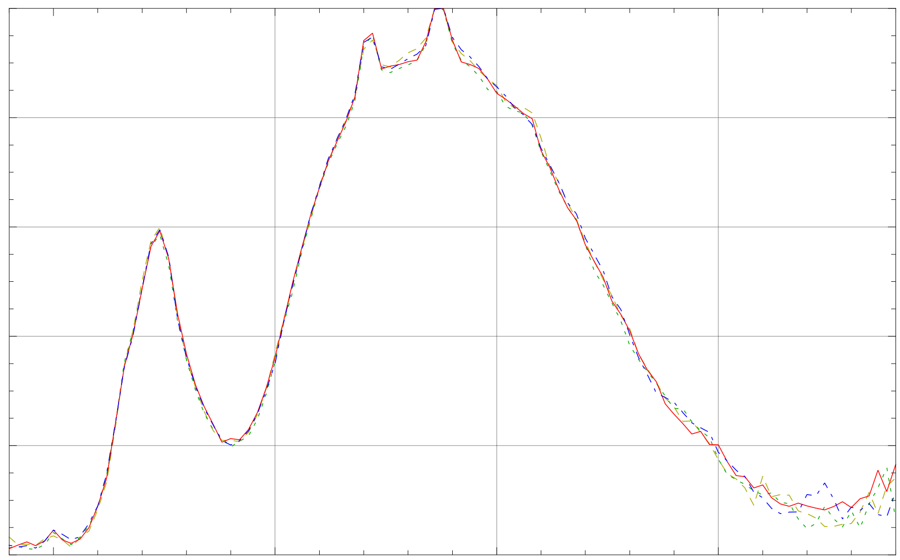

Figure 4 – Exampel of tthe relative spectral distribution oft he road radiance at different observation angles.

5 Conclusions

The measurement of mesopic parameters requires the knowledge of the spectral distribution of the observed light.

For the design of road lighting installations this information can be obtained from luminaires data, but for the installation characterization the spectral radiance or irradiance should be measured due to the optical properties of the luminaires, the influence of the spectral reflectance of the road surfaces and the possible presence of other light sources.

The solution adopted at INRIM considers the photopic quantities obtained using calibrated illuminance meters and luminance meter known as Image Luminance Measurement Device (ILMD). The spectral data are obtained with two different spectroradiometric systems that require a simplified calibration procedure.

The measurement uncertainty at low speed of the dynamic system is generally lower then 5% and is mainly determined by the photopic calibration of the detectors and by the measurement conditions in the field.

Acknowledgments

This work has received funding from the European Union on the basis of Decision No 912/2009/EC in the In the EMRP Joint Research Project (JRP) “Metrology for Solid State Lighting”.

References

CIE 1992. CIE 093:1992: Road Lighting as an Accident Countermeasure

CIE 2010. CIE 115:2010 (2nd edition): Lighting of Roads for Motor and Pedestrian Traffic, Vienna CIE

CIE 2010. CIE 191:2010: Recommended System for Mesopic Photometry based on Visual Performance

CIE 2011. CIE194:2011: On Site Measurement of the Photometric Properties of Road and Tunnel Lighting

CIE 2014. CIE 206:2014: The Effect of Spectral Power Distribution on Lighting for Urban and Pedestrian Areas

EN 2004. EN 13201-2:2004, Light and lighting - Road lighting - Part 2: Performance requirements.

EN 2004. EN 13201-4:2004, Light and lighting – Road Lighting Part 4: Methods of measuring lighting performance

EN 2004. EN 13032:2004, Light and lighting - Measurement and presentation of photometric data of lamps and luminaires - Part 1: Measurement and file format

IACOMUSSI, P. 2005. The development of a new mobile photometric laboratory *Congress Leon 2005*, Leon (Spain), May 2005.

UNI 2012. UNI 11248:2012, Light and Lighting - Road Lighting, Selection of Lighting Classes, (in Italian)

PP77

GLARE OF LED LIGHTING IN OUTDOOR ENVIRONMENT

Kohko, S[1], Ayama, M[2], Mori, T[3], Iwata, M[4], Itsuki, H[5], Kyoto, N[6], Inoue, Y[7], Mochizuki, E[8], Toyota, T[9], Hattori, H[10], Kimura, T[11], Kodaira, Y[12]
[1] Iwasaki Electric Co., Ltd., Tokyo, JAPAN
[2] Utsunomiya University, Tochigi, JAPAN
[3] Panasonic Corporation, Sapporo, JAPAN
[4] Setsunan University, Osaka, JAPAN
[5] Inaba Electric Work Co.,Ltd. Osaka, JAPAN
[6] GS Yuasa Corporation, Kyoto, JAPAN
[7] Nara Women's University, Nara, JAPAN
[8] Chiba Institute of Technology, Chiba, JAPAN
[9] Industrial Research Institute of Shizuoka Prefecture, JAPAN
[10] Seiwa Electric MFG.Co.,Ltd., Tokyo, JAPAN
[11] Stanley Electric Co.,Ltd., Kanagawa,JAPAN
[12] Koito Electric Industries,Ltd. Kanagawa, JAPAN
kouko-shunsuke@eye.co.jp

Abstract

With the price of high-output white LED light sources becoming practical, the LED lighting has been increasingly used in many outdoor environments such as parks, squares, streets, roads, tunnels and exterior of buildings. LED lighting is advantageous in design flexibility and compactness, but said to have greater discomfort glare than the conventional light sources, depending on the viewing direction. Accordingly, this study was conducted aiming at establishing a glare evaluation method in the outdoor lighting environment, which is available for the conventional and LED light sources without distinction.

Keywords: Outdoor Lighting, Discomfort Glare, White LED

1 Study Background

Along with development of higher-output, longer-life and lower-price LED light sources, and promoted by an energy conservation policy, the LED light sources have been prevailing at a dramatic rate these days.

With the price of high-output white LED light sources becoming practical, the LED lighting has been increasingly used in many outdoor environments such as parks, squares, streets, roads, tunnels and exterior of buildings. LED lighting is advantageous in design flexibility and compactness, but said to have greater discomfort glare than the conventional light sources, depending on the viewing direction.

Glare criteria in the outdoor environment includes the GR, TI and luminance limitations of light-emitting parts. These criteria, however, have been decided, targeting the lighting fixtures whose luminance of the light-emitting part is almost even, such as electric bulbs, fluorescent lamps and HID; they are not always appropriate for the minute high-luminance LED lighting with uneven light-emitting parts. In addition, glare may not only give discomfort to pedestrians, but lower visibility and inhibit safety.

Accordingly, this study was conducted aiming at establishing a glare evaluation method in the outdoor lighting environment, which is available for the conventional and LED light sources without distinction.

2 Experimental Method

An experimental field modeled on a 5 m-wide residential road was set up in a factory site in Nara Prefecture to conduct a subjective evaluation experiment on discomfort glare on Oct. 16 to 19, 2012.

Used as lighting equipment (hereinafter, referred to as evaluation objects) were two kinds of conventional light sources and 5 kinds of white LEDs listed in Table 1. It is pointed out that glare evaluation of the LED lighting has an effect on the pebbly texture of modules. For this reason, lens diffusion plates with different diffusion angle characteristics (hereinafter, referred to as the 20° and 80° diffusion plates) were attached to the outside of Light-5 and added to evaluation objects as Light-3 and Light-4 so that the luminance distribution of the light-emitting surface will be relatively even.

Table 1 – Types of conventional street lighting fixtures

No.	Evaluating stimuli
Light-1	HF100X HID mercury lamp
Light-2	FHT57W fluorescent lamp
Light-3	LED lamp (2000lm) with 20-degree lens diffusion plate
Light-4	LED lamp (2000lm) with 80-degree lens diffusion plate
Light-5	LED lamp (2000lm)
Light-6	LED lamp (3000lm)
Light-7	LED lamp (1000lm)

This experiment mainly considers the effects of changing luminance, solid angle and elevation angle on glare. An adaptation level was fixed at 5 lx on the assumption that the experimental road was a residential road where pedestrians in the residential area and cars coexist. Glare was evaluated at 6 spots of A to F shown in Fig. 1, thus giving changes to the apparent size of the evaluation objects (solid angle: 0.000057 sr to 0.0015 sr) and an elongation from the center of the visual field (elevation angle: 5° to 40°) presented to observers. The experiment employed 21 observers listed in Table 2, who have a binocular vision of 0.7 or higher (based on Japanese measurement) (corrected vision acceptable)

Using an evaluation scale shown in Fig. 2, the observers evaluated glare in order of observation positions A to F. When this was done, the observers were given a task to evaluate visibility of a visual target (human face) installed before them in order to control their eye direction.

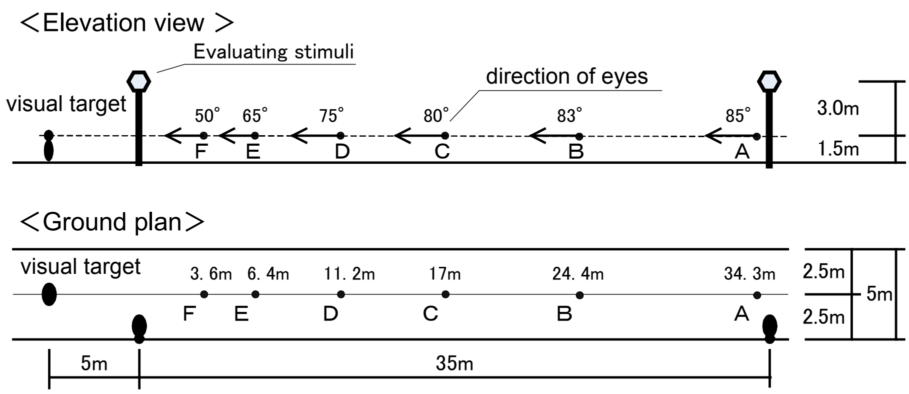

Figure 1 – Observation points

Table 2 – Observers

	20's	30's	40's	50's	60's	total
Males	5	3	3	-	1	12
Females	6	1	-	2	-	9

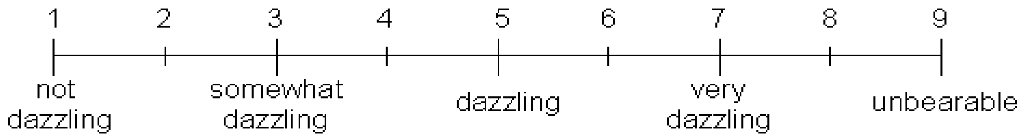

Figure 2 – Evaluation scale of glare

3 Experimental Results

Fig. 3 shows the relations between the glare evaluation and the observation distance. From the observation positions A to E, glare increases as you get closer to the evaluation object. Glare at the observation position F is lower than that at the observation position E, but this results from the deviation of the evaluation object, a glare source, from the field of vision.

A degree of glare differs from one evaluation object to another. Light-5 and -6 were evaluated particularly dazzling, followed by Light-2. Light-1, -3, -4 and -7 had relatively low glare. Based on these results, the differences in glare evaluation among the evaluation objects were verified by t-testing. Consequently, it was found out that the evaluation objects were largely sorted into two groups; those with relatively even luminance distribution of the light-emitting surface (Light-1, -3, -4 and -7) and those allowing you to see the LED module beyond the globe and with uneven luminance distribution of the light-emitting surface (Light-2, -5 and -6), at the 1% significance level, respectively. There was an evaluation difference of approx. 1.5 between the both groups on the 9-step glare evaluation scale shown in Fig. 2. In this document, the respective groups are referred to as evaluation objects with even luminance distribution and evaluation objects with uneven luminance distribution.

Next, Fig. 4 shows the relations between the standard deviation of evaluation scores and the observation distances. You can see from the figure that the evaluation objects with uneven luminance distribution are evaluated more variably than the evaluation objects with even luminance distribution.

To see a glare evaluation tendency by age bracket, the observers were divided into two groups, one for those in their 20s and the other for those aged 30 to 60, as shown in Fig. 5 and 6. It was confirmed that those in the 20s were relatively less sensitive to glare.

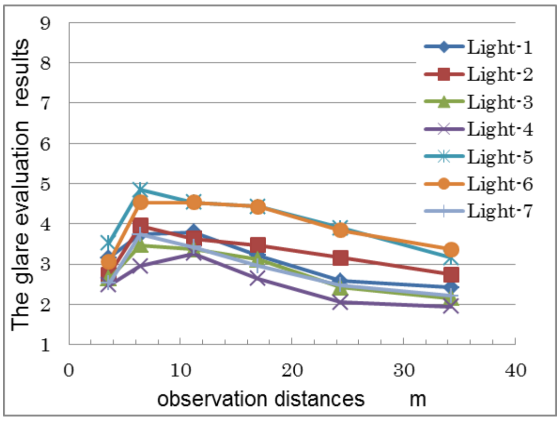

Figure 3 – The relationship between the glare evaluation results and observation distances

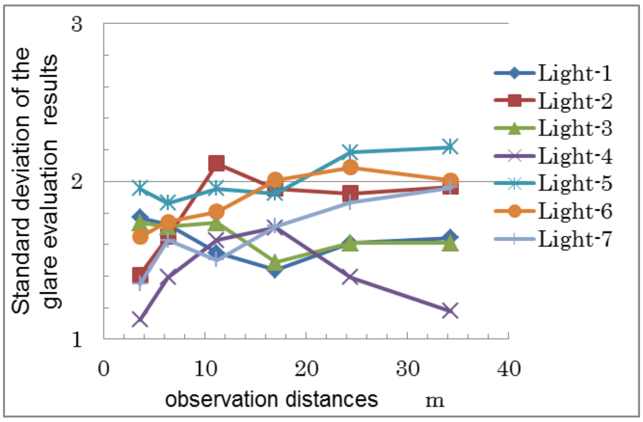

Figure 4 – Trend of evaluation error

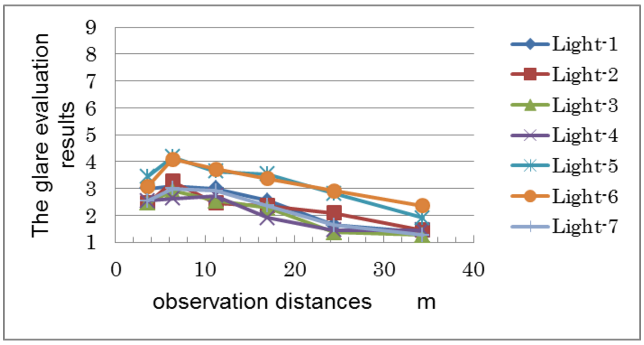

Figure 5 – Trend of the evaluation of 20s

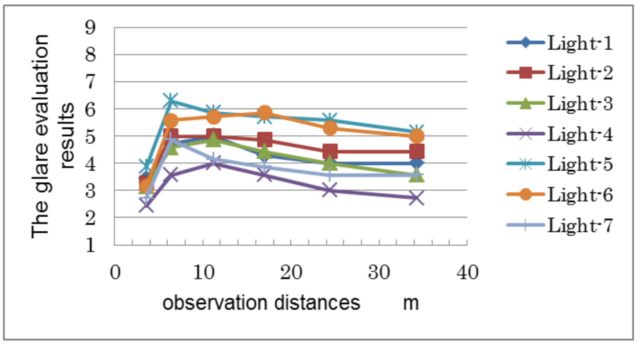

Figure 6 – Trend of the evaluation of 30 to 60

4 Consideration

The following considers the relations between the glare evaluations of the evaluation objects with even luminance distribution and evaluation objects with uneven luminance distribution, and the optical measurement values (Table 3).

Table 3 – The optical measurement values

Leq	equivalent veiling luminance cd/m²
Lvl	the veiling luminance produced by the luminaires cd/m²
Ev	the illuminance on the observer's eye lx
Lmax	the maximum luminance cd/m²
Lave100	Average luminance of the light-emitting part of the lighting fixtures (part having 1/100 or more of the maximum luminance) cd/m²

Consideration uses the evaluation data at the observation positions A to E except those at the observation position F. This is because glare evaluation at the observation position F was low as previously pointed out because it is believed that the evaluation object went out of the field of vision.

The equivalent veiling luminance and average luminance listed in Table 3 were calculated based on the luminance distribution data measured by photographic photometry[1)].

The following lists the measuring conditions for photographic photometry.

Camera: Digital single-lens reflex camera
Lens: 10 mm
Image size: 3,072 x 3,072
Resolution: 1.03 minutes/pixel
Luminance measurable range: 0.005 cd/m^2 to 3,490,000 cd/m^2

Fig. 7 shows the relations between the glare evaluation and the vertical illuminance at the observer's eye level (Ev). A determination coefficient R^2 for the evaluation objects with even luminance distribution was as high as 0.71, but the one for the evaluation objects with uneven luminance distribution was 0.53, slightly lower. The determination coefficient R^2 by all the data was further down to 0.40. Based on these results, it is said that the vertical illuminance at the observer's eye level is not appropriate as a glare evaluation index, because the vertical illuminance at the observer's eye level requires you to consider the evaluation objects with even luminance distribution and evaluation objects with uneven luminance distribution separately from each other in explaining glare evaluation results; they cannot be singly handled. This point is consistent with the experimental data of Ayama et al. reporting the importance of luminance distribution of the light-emitting surface[2].

In equivalent veiling luminance (Lvl) by glare evaluation and glare light as well, the experimental results indicated that the evaluation objects with even luminance distribution and evaluation objects with uneven luminance distribution cannot be singly handled, as with the vertical illuminance at the observer's eye level. That is, the GR, which is the glare evaluation index of outdoor floodlighting calculated with the equivalent veiling luminance by glare light, also shows a trend similar to the vertical illuminance at the observer's eye level as shown in Fig. 8. Accordingly, there are still some problems in using the GR, the current criteria, as the glare evaluation index of the LED light sources.

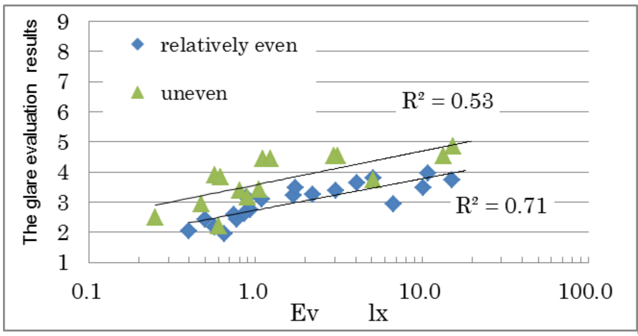

Figure 7 – The relationship between the glare evaluation results and Ev

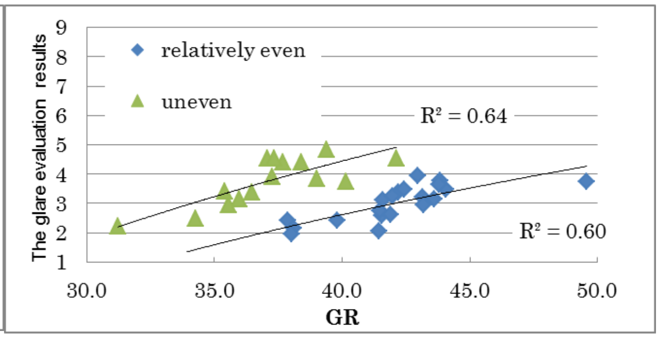

Figure 8 – The relationship between the glare evaluation results and GR

Considered next was the relations between the glare evaluation and the luminance value of the evaluation objects. As shown in Fig. 9, the maximum luminance (Lmax) of the evaluation objects had strong correlations (R^2 = 0.74) with the glare evaluation without having to distinguish the evaluation objects with even luminance distribution from the evaluation objects with uneven luminance distribution.

Strong correlations (R^2 = 0.73) were also confirmed between the average luminance (Lave100) of the evaluation objects and the glare evaluation as shown in Fig. 10 without having to distinguish the evaluation objects with even luminance distribution from the evaluation objects with uneven luminance distribution.

The apparent area of the light-emitting part of the lighting fixtures was calculated from the part having 1/100 or more of the maximum luminance[3].

The above considerations indicates that by using the maximum and average luminance values of the evaluation objects, the glare evaluation can be explained without having to distinguish the evaluation objects with even luminance distribution from the evaluation objects with uneven luminance distribution.

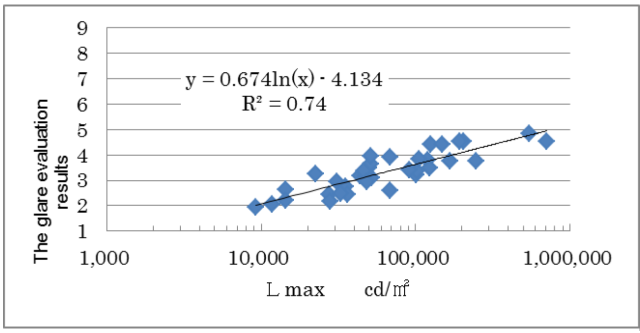

Figure 9 – The relationship between the glare evaluation results and Lmax

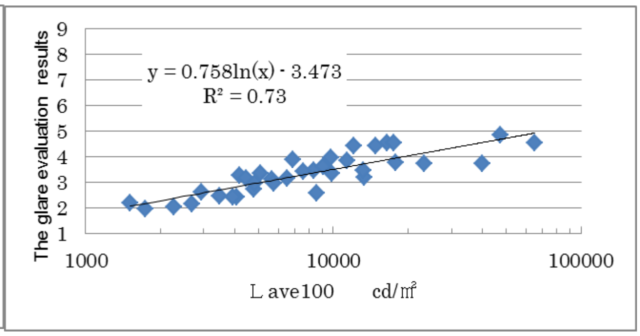

Figure 10 – The relationship between the glare evaluation results and Lave100

5 Conclusion

As noted above, the following findings were obtained from the peripheral vision experiment.

1) Compared with the evaluation objects with even luminance distribution, the glare evaluation of the evaluation objects with uneven luminance distribution varies widely from one observer to another.

2) The relations between the glare evaluation and the vertical illuminance at the observer's eye level or the equivalent veiling luminance depend on the luminance distribution of the light-emitting part of the evaluation objects.

3) The evaluation objects with uneven luminance distribution are felt more dazzling than the evaluation objects with even luminance distribution. Their difference is approx. 1.5 on the 9-step glare evaluation scale.

4) By using the maximum and average luminance values of the evaluation objects, the glare evaluation can be explained without depending on the luminance distribution of the light-emitting part of the evaluation objects.

From now on, I would like to further analyze the experimental results such as an effect of the solid angle on the glare evaluation and develop a high-precision glare evaluation method.

6 Acknowledgements

This research was conducted by the the "Research & Investigation Committee on Glare of LED Lighting Fixtures in Outdoor Lighting Environments" of the Illuminating Engineering Institute of Japan under entrustment of JLEDS. We hereby express our sincere gratitude to the JLEDS, the Committee, and all concerned.

References

[1] T.Yamada, S,Kohko: Glare evaluation system using imaging photometry, Proceedings of CIE Centenary Conference "Towards a New Century of Light," pp.627-630,Paris (2013).

[2] M.Ayama, T.Tashiro, S.Kawanobe, T.Kimura-Minoda, S.Kohko, T.Ishikawa:Discomfort glare of white LED source of different spatial arrangements. Proceedings of CIE Centenary Conference "Towards a New Century of Light," pp.119-122, Paris (2013).

[3] Glare And Uniformity in Road Lighting Installations, CIE31 （1976）

PP78

A NEW LUMINAIRE CLASSIFICATION METHOD FOR KOREAN CITY AREA LIGHTING

Jongsung Han[1*], Minwook Lee[1], Jungsu Gil[1], Janghyeon Lim[1], Seongsik Yoo[1], Inkyu Kim[2], Hoon Kim[1]
[1] Department of Electrical and Electronic Engineering, Kangwon National University, Chuncheon, SOUTH KOREA, [2] Korea Environment Corporation, Incheon, SOUTH KOREA
jshan@kangwon.ac.kr

Abstract

It is not unusual that outdoor lighting, however well designed, negative affect its installed spot and surroundings. When planning an outdoor lighting, therefore, we need to take from the initial stage full consideration not only of its primary function to provide light, but its side effect, light pollution.

Since February, 2013 Korea has enforced the Light Pollution Control Act, according to which the local governments must evaluate the effects of light pollution more than once every three years and report its result to the Minister of Environment. The Act regulates that various effects that can be caused by light pollution must be controlled by such aspects as illumination and luminance. However, it has an institutional limit that the degrees of pollution are measured and evaluated only after lighting installment, with a problem that it is not easy to measure and evaluate the effects after lighting installation.

Accordingly, it is necessary to lay out a scheme to evaluate before lighting installation the possible light pollution of the luminaires and to select those suitable for the installation surroundings, for which a kind of luminaire classification system can be one of the desirable alternatives.

To know the lighting installation conditions and the affected surroundings by area lighting represented by security lights and park lights, this study investigates the actual conditions of area lighting and analyzes the causes of light pollution by it. On the basis of the research data was suggested a new luminaire classification method that fits the Light Pollution Control Act now in force in Korea.

Keywords: Light Pollution, Area Lighting, Luminaire Classification, Light Trespass

1 Introduction

Since February, 2013 Korea has enforced the Light Pollution Control Act. The Act regulates that various effects that can be caused by light pollution must be controlled by such aspects as illumination and luminance. However, it has an institutional limit that the degrees of pollution are measured and evaluated only after lighting installment, with a problem that it is not easy to measure and evaluate the effects after lighting installation.

Accordingly, it is necessary to lay out a scheme to evaluate before lighting installation the possible light pollution of the luminaires and to select those suitable for the installation surroundings, for which a kind of luminaire classification system can be one of the desirable alternatives.

This study proposed the requirements of simulation to calculate the illuminance on the vertical plane of the residence area. The calculating of illumination according to the requirements can make it possible to evaluate light trespass by the luminaires. The study suggests a method to classify in terms of the installating conditions the luminaires that satisfy illuminance requirements of the vertical plane.

2 Determining the requirements of simulation for calculating the illuminance on the vertical plane of the residence area

The permissible limits of light emission by the Light Pollution Control Act regulate that the maximum illuminance on the windows in the residence area near the lighting installments shall be less than the luminance set up according to the lighting environmental zones.

The maximum illuminance on the windows of the residence area can be checked by menas of simulation or by calculating the illuminance on the vertical plane in the area where the windows are placed in the vicinity of a luminaire. However, other surrounding objects than the road are not considered in the course of outdoor lighting calculation or lighting simulation, and it is almost impossible to specify the position of the individual windows in a wide lighting area.

This study suggests an evaluation standard to check, in the stage of lighting design, the illuminance distribution of the vertical plane in the residence area where security lighting is provided, on the basis of the investigation results of (a) the environmental conditions of lighting installation, (b) actual conditions of light trespass, and (c) the results from simulation about the causes of light trespass.

2.1 Difficulties in simulation for calculating illuminance on a vertical plane in the residence area

The actual investigation of the security lights in the metropolitan area of Korea showed that except for a few places, many of the luminaires were affixed to the utility(telephone, power) poles by the roads, not to separate poles exclusive for lighting. Due to the wires and other objects on the utility poles the luminaires are installed at different heights(5,0~7,5 m). Most of the forward horizontal distances of the luminaires vary depending on the width of the roads while their backward distances are very short (1~2 m) since houses and buildings are located near the roadside.

As the height of each luminaire and the position of each window are different, it is virtually impossible to calculate luminance and perform a simulation in a condition that a vertical plane on which illuminance of each point is calculated (‘the plane calculated’ hereafter) should be placed at the actual height of the luminaire, at the actual position of the window, and on the actual road condition.

2.2 Conditions of simulation for estimating light trespass

The affect of light trespass from a security light can be estimated in the stage of design by putting as variables the factors that can vary in the course of factors (horizontal distance between the nadir and the window plane, the height of calculated plane). (Figure 1)

① Height of luminaire (MH): The actual height of the luminaire installed are to apply including all of those expected to vary within the installation area.

② Window positions: The plane calculated can be placed at the same position with that of the window when the position of the window can be fixed; otherwise the whole affected area is to be assumed as the window position.

③ Nadir - window plane distance: Since most roads structures have been fixed, the horizontal distance between the road border and the plane calculated is to be taken as the nadir - window plane distance.

④ Left and right scope of the plane calculated (L): The security lighting of Gauss type affects the area of 10 meters right and left from the luminaire, but the affected area can vary to the light distribution and height of luminaire. The scopes must be determined in consideration of the KS C 7658[1] which applies to calculation of a horizontal plane, giving a maximum scope of 8 m for both right and left.

⑤ Height of the plane calculated (H): The affection by backward light of a luminaire usually reaches the peak when measured at the height of the luminaire, and as its height increases, the affection decreases drastically. The height of the luminaire plus 1 m is to apply as the height where illuminance is calculated.

⑥ Maintenance factor: Since light trespass is likely to be the greatest when the lighting is first installed, the maintenance factor is determined to be 1.

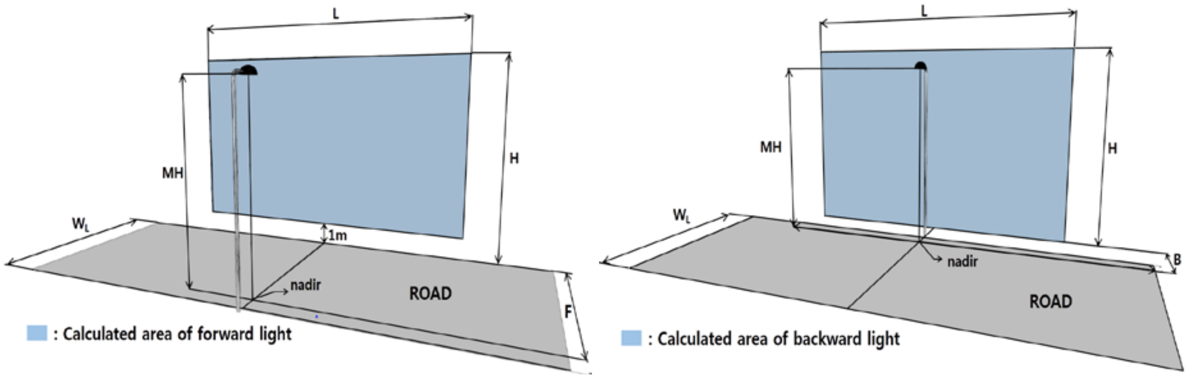

Figure 1 – Calculated Areas of the Forward Light and the Backward Light

3 Classification codes of luminaires (in terms of light pollution)

3.1 Assigning luminaire classification codes

Created was a method by which luminaires can be classified according to the illuminance on the vertical plane by evaluating their light trespass.

Table 1 - Classification of Luminaires for Evaluating Their Light Trespass

Factors	Codes	
Height of luminaire (m)	H	Road lighting luminaire: 8, 10, 12
Height of luminaire (m)	H	Security lighting luminaire: 4, 5, 6
Installation area (A)	RA, CA	
Forward distance free of light trespass (m)	F	1, 2, 3, 4...
Backward distance free of light trespass (m)	B	1, 2, 3, 4...
Upward light rating (U rating)	U	0, 1, 2, 3, 4, 5
Glare rating (G)	FC, C, SC, NC	

The codes mean:

① H: The height of the luminaire installed. The heights in the table are the regular ones determined by Korean Industrial Standards(KS)[1], which can be applied in the simulation.

② RA, CA: Lighting installation area. RA is 'Residential Area' and RA is 'Commercial Area'.

③ F: The minimum forward distance from the luminaire to the point on the forward plane calculated, where occurs no light trespass (less than 10 lx in residence area and 25 lx in commercial area - the maximum illuminance regulated by 'the standards of illuminance on the vertical plane')

④ B: The minimum backward distance from the luminaire to the point on the forward plane calculated, where occurs no light trespass (less than 10 lx in residence area and 25 lx in commercial area - the maximum illuminance regulated by 'the standards of illuminance on the vertical plane')

⑤ U: Upward light rating.

⑥ G: Glare rating. The existing Cutoff classification is applied: FC(Full cutoff), C(Cutoff), SC(Semi-cutoff), and NC(Non-cutoff)

The classification codes of luminaire which does not exceed the limit of light trespass in the commercial area to the forward distance 8 m and backward distance 4 m at the height of 10 m are expressed as follows:

H	-	A	-	F	-	B	-	U	-	G
H10	-	CA	-	F8	-	B4	-	U0	-	C

The standards for attestation of luminaires follow the calculation requirements suggested herewith, and each luminaire is given classification codes according to its light measurement.

3.2 Examples of application of the luminaire classification codes

On the basis of the data from the simulation of light pollution, classification codes were applied to the sample luminaires of the road lighting and the security lighting applicable in the commercial area and residence area after evaluating their light pollution such as scattered light and light trespass.

The optical specifications of the sample luminaires are shown in Table 2. Table 3 shows the results of the simulation to evaluate light pollution, together with upward light rating and cutoff rating.

Table 2 - The Specifications of the Sample Luminaires

	Light source	Lamp power consumption	Luminaire power consumption	Luminous flux	Efficiency	BUG Ratings			Type		Cutoff
						B	U	G			
Road lighting	HIE	150W		10500lm	73%	1	2	2	Ⅱ	Short	Cutoff
Security lighting	LED		60W	3800lm	100%	1	0	1	Ⅱ	Short	Semi

Table 3 - The Results of the Simulation to Evaluate Light Pollution

	Road lighting	Security lighting
Luminaire	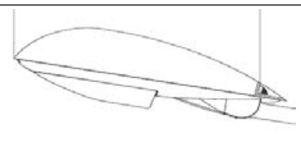	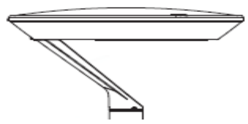
Light distribution curve	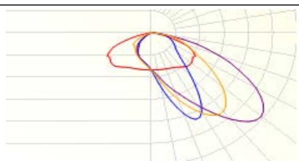	
Height of luminaire	10m	7m
Place applied	Road in commercial area	Road in residence area
Min. forward distance for non trespass light	5m	6m
Min. backward distance for non trespass light	3m	4m
Upward light rating	U2	U0
Cutoff rating	Cutoff	Semi-Cutoff

The classification codes for light pollution resulted from the data of the simulation and the upward light rating and cutoff rating are as follows:

Classification codes of the road lighting: H10 - CA - F5 - B3 - U2 - C

Classification codes of the security lighting: H7 - RA - F6 - B4 - U0 - SC

4 Conclusion

The above example classification codes for light pollution present that for the road lighting in the commercial area, when the luminaire is installed 10 m high, the window plane placed at the horizontal distance of 5 m forward and 3 m backward from the center of the luminaire(light source) can meet the illuminance standards that 'the Light Pollution Control Act' requires of the commercial area (lighting environmental zone 4). In addition, the upward light ratings and cutoff rating make it possible to predict the degree of sky glow and glare.

The minimum forward and backward distances for preventing light trespass is a distance that do not cause illuminance over the required limit by law. The road lighting described above, when installed 10 m high, satisfies the lighting requirements for the vertical planes that are placed farther than 5 m forward and 3 m backward from the luminaire.

References

1. Korean Agency for Technology and Standards(KATS). 2013. KS C 7658:2013: LED Luminaires for Road and Street Lighting. Gwacheon-Si: KATS.

PP80

MEASURE THE BRIGHTNESS OF THE SURROUNDING TREE-LINED OUTDOOR LIGHTING COMPARED

Jong Min Lim[1], Hyo Joo Kong[1], Young Mok Yi[1]
[1] Korea Institute of Lighting Technology, Bucheon, SOUTH KOREA
ljm4097@kilt.re.kr

Abstract

In this paper, tree-lined area by measuring the brightness of outdoor lighting installation were compared by type and location. In this study, outdoor light source in a horizontal position and within 1m of height by measuring the brightness of the part of the blade fixtures by type, by location, were compared using the equipment surface luminance meter was used. Measure around the wetland areas were selected measurement time after sunset 9:00 p.m. to 12:00 p.m. measured on. This measure light pollution to analyze the risk of ecological survey was conducted to advance. Measured by a tree-lined street near each type of light source to measure the brightness of light pollution, ecological risk assessment was conducted for the pre-survey. This measure light pollution nowadays emerging avenue for Ecological Risk Assessment reckless outdoor lighting installed around any impact on the surrounding environment, to analyze the basic data and the results of these measurements will be used in future ecological risk assessment.

Keywords: Light pollution, Luminance, Street light, Park light

1 Introduction

Light pollution is deadly to humans many adverse effect, but also adversely affect animal and plants. A pleasant and ecological environment in order to reduce the light pollution is essential. For the good lighting environment, ‘Light Pollution Prevention Act’ was enforced from 2 February 2013 in Korea [1, 2]. Light pollution in South Korea enacted a law to have as many issues. Accordingly, It has been studied and a number of policies. Previous research analysed light pollution on human health [3, 4]. Also, light pollution of ecosystem has been analyzed by many researcher [5]. However, light pollution in ecosystem environment has not been widely applied to park, street and wetland in Korea. Thus, this paper aims to analyzed and compared the light pollution in park, street and wetland area. For the purpose, park, street and wetland area was selected. The equipment surface luminance meter was used.

2 Methodology

In order to measure light pollution of the plant, near the wetland area and street trees was selected as the measurement point. Measurement factor include plant surface of the luminance was measured. The measurements were carried out on 18 November 2013. Measurement time was from 21:00 to 24:00. This time the vehicle is less time to light effects. The light pollution was measured under clear sky condition. The three environment conditions were located in Seoul, South Korea. Figure 1 shows the environment conditions of wetland, street trees and park. Fist, the wetland area is around the apartment complex and hill. The street trees environment is eight-lane road and skyscraper. Movement of the vehicle, and the park environment is limited and there are a lot of people’s movement.

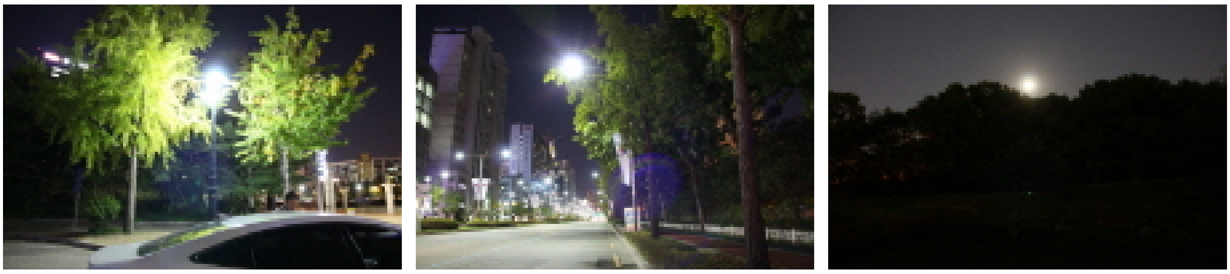

Figure 1 – Environment conditions of park, street trees and park

Park's lighting source is installed two MH100 W. Installation height is 5 m. Wetland area's lighting source is installed two NH100 W. Installation height is 5 m. Street's lighting source is installed two MH100 W. Installation height is 10 m.

Table 1 – Lighting Environment of park, street trees and park

	Lighting source	Height	Amount
Park	MH100 W	5 m	2
Wetland area	NH100 W	5 m	2
Street	MH100 W	10 m	2

Figure 2 – Light pollution measurement equipment

The measurement equipment was used the LMK Mobile Advanced, CS-110 luminance meter, and digital cameras. Figure 2 shows the measurement equipment. Compare to the light pollution prevention act in Korea. However, a criterial of the plant has not been proposed. Thus all were compared light pollution act standard. Table 2~5 shows the light pollution prevention act in Korea [1, 2].

Table 2 – Classification of Zones in the Act in Korea [1, 2]

Zone rating	Description	Land use purpose
E1	Zones where the light might adversely affect the natural environment	Natural environment conservation areas, green conservation areas and natural green areas
E2	Zones where the light might adversely affect agriculture or distrub the character of the area. The vision of human residents and users is adapted to low light levels.	Agriculture and forestry areas, productive green areas and conservation/productive/planning and management areas
E3	Zones where the vision of human residents and users is adapted to moderate light levels. The lighting is generally desired for safety, security and convenience.	Residential and semi-residential areas, as well as industrial and semi-industrial areas
E4	Zones where the vision of human residents and user is adapted to high light levels. The lighting is generally desired for various convenience and commercial activities.	Commercial and exclusive industrial areas

Table 3 – Standards of maximum permissible vertical illuminance on windowns in Korea [1, 2]

Environmental zones	E1	E2	E3	E4
Limitation (lx) (maximum illuminance)	10	10	10	25

Table 4 – Standards of maximum permissible luminance on the light emitting or reflecting surfaces of decorative lighting in Korea [1, 2]

Environmental zones	E1	E2	E3	E4
Limitation (cd/m^2) (maximum luminance)	20	60	180	300
Limitation (cd/m^2) (average luminance)	5	5	15	25

Table 5 – Standards of maximum permissible luminance on the light emitting or reflecting surfaces of advertisement lighting in Korea [1, 2]

Environmental zones	E1	E2	E3	E4
Limitation (cd/m^2) (maximum illuminance)	50	400	800	1000

3 Results

To analyze the risk of ecological and light pollution of street lighting, wetland lighting, park lighting, luminance of plants was evaluated. The total of measuring points was eight point. There were taken from location, 1 meters distanced from the plants of each area. The measuring points for each plant are leaves.

Table 6 – Results of the measurements

Category	Night Scene	Luminance distribution	Maximum Luminance
Park's lighting 1	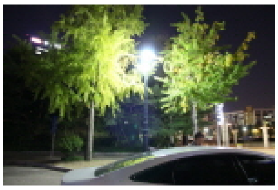	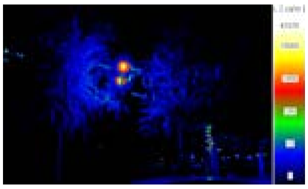	2,641.00
Park's lighting 2	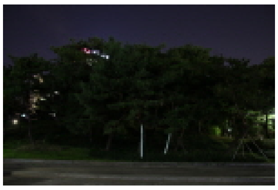		1.88
Park's lighting 3	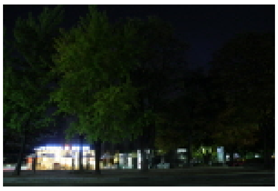	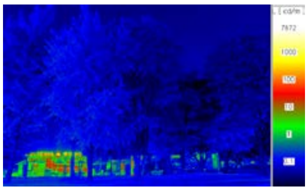	0.60
Street's lighting 1	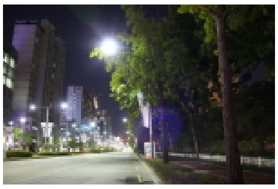		40.63
Street's lighting 2	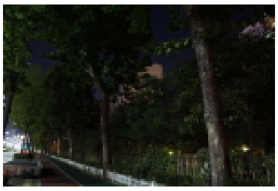	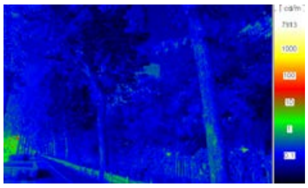	1.84
Street's lighting 3	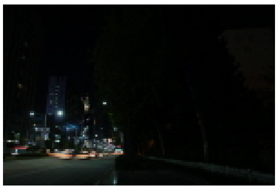		1.86
Wetland's lighting 1	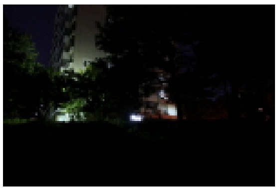	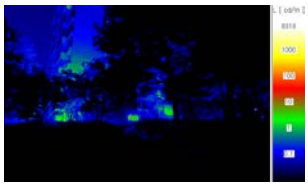	2.56
Wetland's lighting 2			0.07

Light pollution prevention act classifies environment areas into four classes to evaluate light pollution and suggest the luminance of decorative and advertisement lighting and illuminance levels on window according to each class [1, 2]. The park, wetland area is as E1 class, according to the light pollution prevention act in Korea. The street lighting area is as E4 class, according to the light pollution prevention act in Korea. A short summary of the results of the measurements in Table 6.

The maximum luminance on plant leaf in park's lighting 1 was 2,641.00 cd/m^2. It was 2.5 times hight than that with standard of maximum permissible luminance on the light emitting or reflecting surfaces of advertisement lighting. In other words, this is going to change the color of leaves near the lighting, it will be affect in ecological systems. On the contrary, the maximum luminance in the park's lighting 2, 3 was 1.88 cd/m^2, 0.60 cd/m^2. However, the human eye cannot feel even a little change of light plant germination, stem and leaf growth, flowering, fruit growth can be affected [5]. Therefore, plants receiving at least as light.

The maximum luminance on plant for a street's lighting 1 was 40.63 cd/m^2. It was over 25 cd/m^2 of standards of average permissible luminance on the light emitting or reflecting surfaces of decorative lighting in Korea. The maximum luminance of street lighting 2 and 3 was 1.84 cd/m^2 and 1.86 cd/m^2. The previous research found that the exposure to artificial light, and the trees are deferent trees do not have leaves in the fall when the life has been delayed [5]. Therefore, the proper lighting design in street is needed.

As for wetland area, the maximum luminance on plant was 2.56 cd/m^2 and 0.07 cd/m^2. Compared to standard light pollution has been shown satisfactory. However, It can effect on the ecological system. The amount of light was perceived by the street light. However, Korea has not yet provided proper guidelines for the control of light pollution, it is necessary to take appropriate measure for it.

4 Conclusion

This study analyzed the luminance of plant on the park, wetland and street. Finally, the light pollution prevention act and previous research was compared. The results of the measurement can be summarized as follows:

As park's lighting, the maximum luminance on leaves was 2,641.00 cd/m^2. Compare to the light pollution prevention act in Korea the level the luminance of leaves were about 2.5 times higher. Also, the human eye cannot feel even a little change of light plant germination, stem and leaf growth, flowering, fruit growth can be affected [5]. This measure light pollution nowadays emerging avenue for Ecological Risk Assessment reckless outdoor lighting installed around any impact on the surrounding environment, to analyze the basic data and the results of these measurements will be used in future ecological risk assessment

References

[1] Ministry of Environment. 2013. Light Pollution Prevention Act in Korea

[2] Cha, J. S., Lee, J. W., Jung, J. W., Lee, K.M. Han, J. S., Gu, J. H. 2014. Policy and status of light pollution management in Korea. Lighting Res. Technol., 46, 78-88.

[3] Falchi, F., Cinzano, P., Elvidge, C. D., Keith, D. M., Haim A. 2011. Limiting the impact of light pollution on human health, environment and stellar visibility. Journal of Environmental Management, 92, 2714-2722.

[4] Kerenyi, N. A., Pandula, E., Feuer, G. 1990. Why the incidence of cancer is increasing: the role of light pollution. Medical hypotheses, 33, 75-78.

[5] Gallaway, T., Olsen, R. N., Mitchell, D. M. 2010. The economics of global light pollution. Ecological Economics, 69, 658–665.

PP83

BEYOND THE LABORATORY – THE DYNAMICS OF LIGHT EXPOSURE IN THE MELANOPSIN AGE

Price, L.L.A.
Public Health England, Centre for Radiation, Chemical and Environmental Hazards, Didcot, OX11 0RQ, UK
Luke.Price@phe.gov.uk

Abstract

During work to collect and analyse light exposures for circadian health studies, it became apparent that to use the light exposure time series data being collected it would be necessary to define the meaning and requirements of light exposures in the context of the 24-hour day as well as for the individual's subjective circadian timeframe.

Laboratory studies can measure photoperiod, phase and amplitude of lighting easily, as they are controlled simply by turning on and off the lights and designed into the experimental protocols which also control the subjective time of the subjects. When studying light exposures in everyday life, the edges become blurred to the extent that these definitions lose their meaning. Laboratory conditions are more closely defined and controlled even than the light conditions in the architectural models used by lighting designers.

This paper presents a technique to overcome this hurdle using a simple but powerful smoothing method – exponential moving average (EMA). The method allows complex patterns of light exposure to be compared using their bulk circadian properties through the circadian metrics it makes possible. Measures for duration (photoperiod), timing (phase) and magnitude (amplitude) of 24-hour light exposures are provided. By studying the conditions at fixed locations in buildings, it is hoped that these measures can help guide lighting design that supports circadian entrainment.

The EMA of the light exposure also provides an analogy to the light drive used in mathematical circadian models. Mathematically simpler than many of these models, this is the first light drive model to allow for persistency, which is a characteristic feature of non-visual photoreception and responses mediated by retinal ganglion cells expressing melanopsin. In the future, such models can either aim for simplification or for a finer more accurate description of the physiology of photoreception and downstream entrainment processes; in either case persistency is likely to be seen as a desirable feature.

Keywords: Circadian dosimetry, Light drive, Light and health

1 Methods and Mathematics

The methods of the original circadian health studies involved collecting time series of personal light exposure, measurements at fixed locations inside building and outside or collecting both types of data. These were collected using the Actiwatch Spectrum (Philips Respironics, USA) which combine actigraphy and dosimetry. The use of these devices for this purpose has been studied previously (Price, 2012).

The commonly used optical dosimetry assumption of reciprocity is substituted by equating the smoothed value of recent light exposure measurements to a dynamic exposure dose variable, D:

$$\mathrm{d}D = \beta \cdot (E - D) \cdot \mathrm{d}t \tag{1}$$

where

E is the spectrally weighted circadian irradiance; and

β is a rate constant governing smoothing time-horizon.

The EMA method has been used before for related fields (Griess, 1981) and Table 1 exploits actuarial compound interest results (i.e. annuities and present values) for calculations.

For mathematical models of circadian physiology, D would be a direct replacement for the feed-forward light drive variable (Kronauer, 1999). In constant irradiance E, $D \rightarrow E$:

$$D = E - (E - D_0) \cdot e^{-\beta t} \tag{2}$$

Table 1 – Actuarial results apply in dosimetry where Equation (1) is valid. The results are useful starting points for aggregating repetitive exposures or other doses.

Actuarial (discounting)	**Dosimetry** (decaying)
Future events	Past events
n years	t seconds apart
Interest rate, i	Decay ratio, r
$1+i = e^{\delta}$ $v = e^{-\delta}$	$r = e^{-\beta}$
Continuous payment	Constant exposure
$\bar{a}_{\overline{n}\rceil} = \dfrac{1-v^n}{\delta}$	$\dfrac{1-r^t}{\beta}$
£1 annuity in advance	Repeated unit doses
$\ddot{a}_{\overline{n}\rceil} = \dfrac{1-v^n}{1-v}$	$\dfrac{1-r^t}{1-r}$

2 Visualisation

The following charts, Figures 1 to 8, illustrate how exponential smoothing relates to time series of light exposures at fixed positions in buildings, to experimental data on light exposure durations and melatonin suppression, circadian rhythm metrics, photoperiod estimation parameters and mathematical representations of the human circadian oscillator.

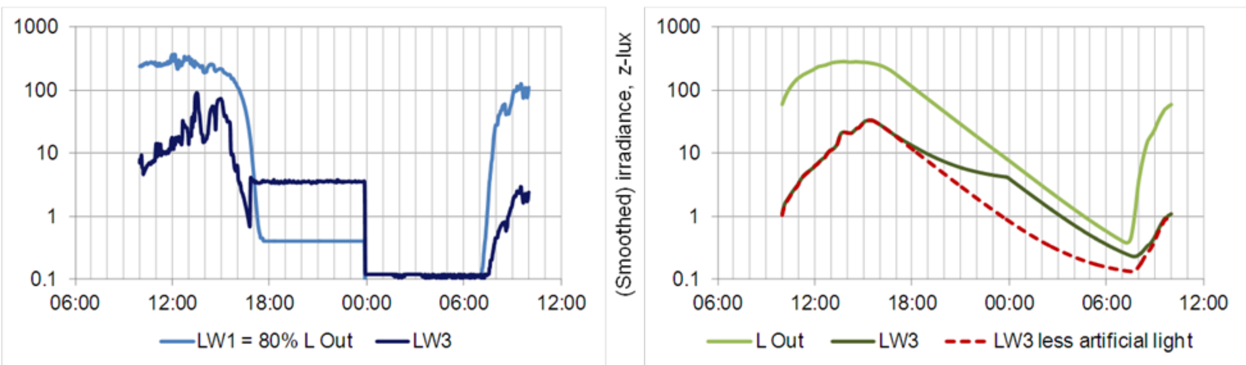

Figures 1 and 2 – 1. Circadian weighted irradiance from living area of private dwelling in South England, (31 January). Actiwatch LW1 placed on patio door facing NNE; LW3 facing ESE, 3.3 m from LW1. 2. Exponentially smoothing (EMA) applied to Figure 1 data, $t_{0.5}$ = 90 minutes.

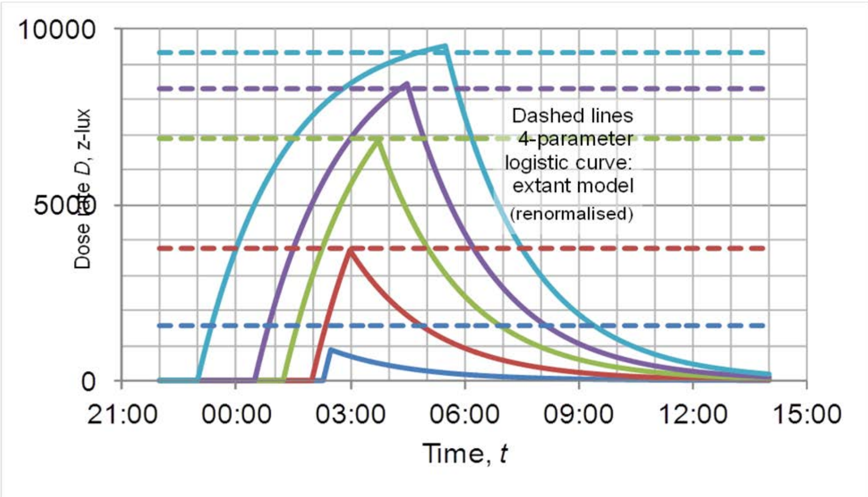

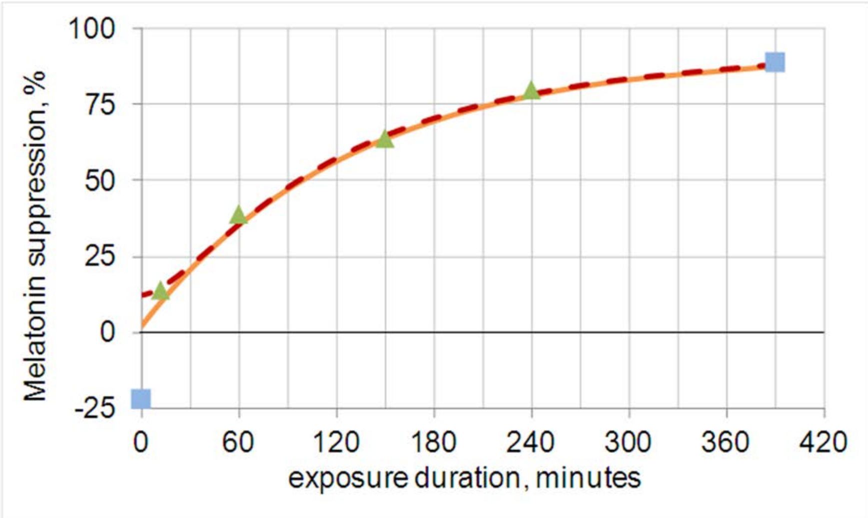

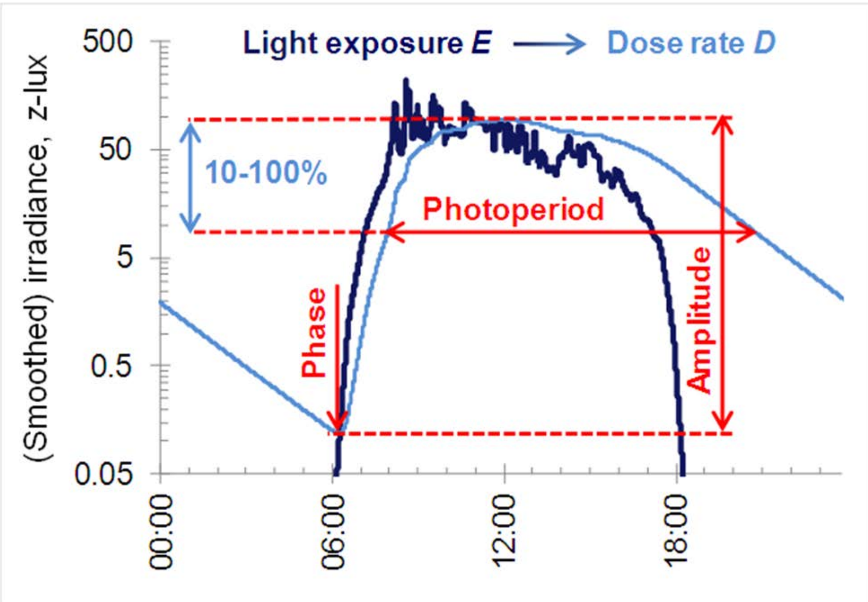

Figures 3 to 5 – 3. Comparing predictions from a recent model (dotted lines, Chang, 2012) and the time evolution of EMA model (curved lines) is included to show the persistency of the dose rate. 4. The 4-parameter logistic model (red dashed, Chang, 2012) as fitted to data (green triangles, blue points not fitted) versus EMA model (orange solid line, $t_{0.5}$ = 90 min). 5. Metrics based on exponential smoothing (or EMA) for quantifying photoperiods, phase and amplitude of complex light exposures.

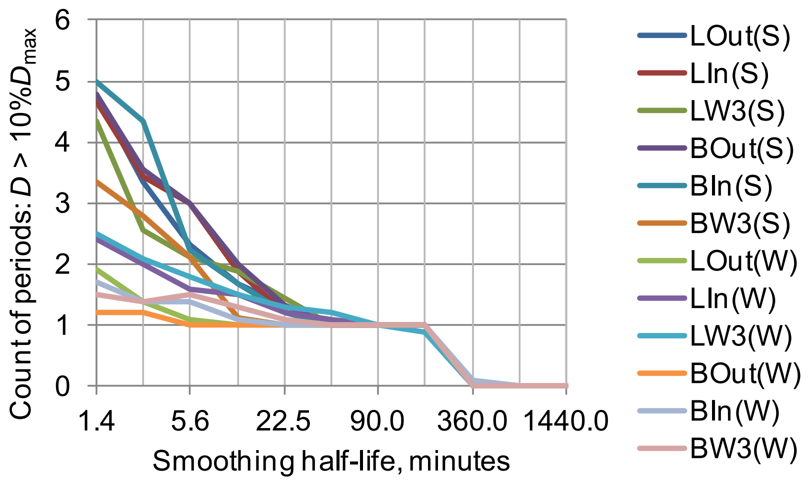

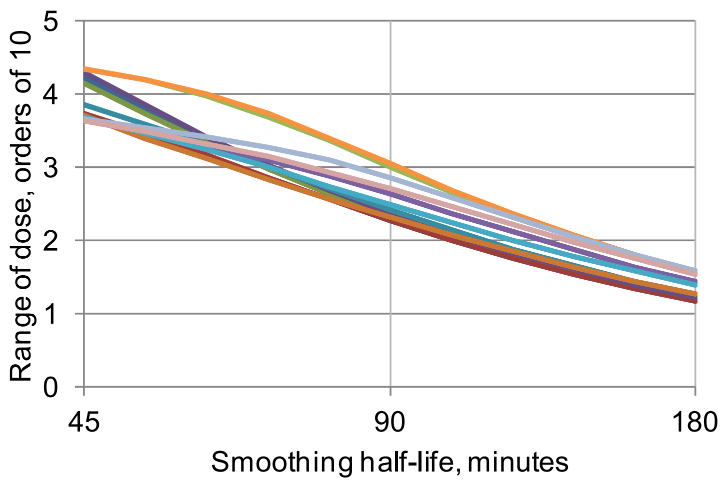

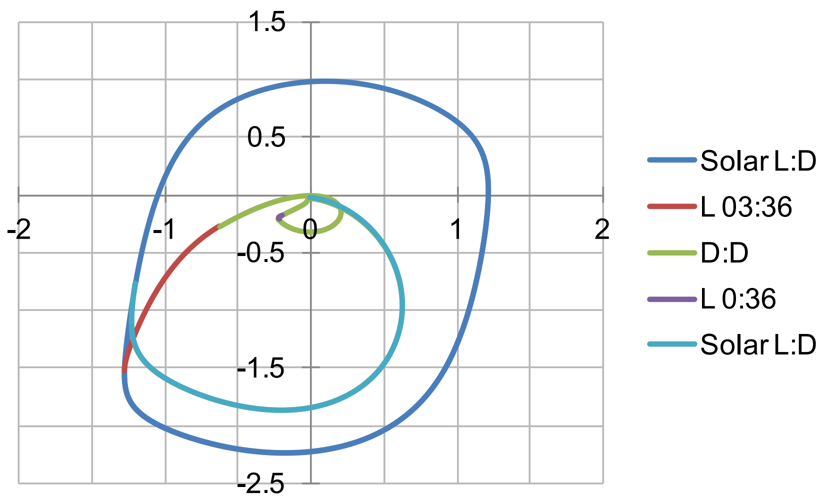

Figures 6 to 8 – 6-7. Choosing the metric parameters. Fig.4 shows that $t_{0.5}$ = 90 min provides a good fit to long duration constant exposures. Fig.6 shows that with dissimilar values of $t_{0.5}$ there are often multiple photoperiod measures per day using a range of measurement positions and seasons, at circa 51°N. Fig.7 shows that the percentage parameter must be greater than 1% or the metric may not be well defined at 90 minutes (e.g. see Fig 6. > 360 minutes). 8. Phase space diagram (e.g. core body temperature vs serum cortisol rhythm; the persistent light drive D drives the oscillator qualitatively as required in a variety of conditions.

3 Discussion and Conclusions

Scientists wishing to predict the effects of complex light exposures would probably refer to the mathematical models of physiological state variables that were initially suggested by A. T. Winfree (Winfree, 2001), and which are still being developed in ever finer detail today. To date, these models lack the persistence of melanopsin signalling (and of the retinal cells expressing melanopsin) and the signal ceases as soon as the lights go off; this is contradicted by experiment (Lucas, 2014).

- Applied and basic scientists have different objectives; one group seeks predictions of outcomes, the other details of mechanisms.
- There is a similar conflict between predicting outcomes for one individual with precisely known initial conditions and predicting the effects of exposures for people in a range of initial states.
- Time-of-day should act as a proxy for their initial state variables, and in fact it must do, where the goal is to support entrainment (i.e. everyday life), rather than to adjust it (e.g. treatment).

When considering the circadian impact of lifestyle advice, lighting and building design, a number of factors will be relevant. People should be transported from their likely entry state to a desired exit state (both based on time-of-day):

- what time period does the space use or activity cover?
- what other exposures might they get in the same day?
- should the exposure work with or against the natural light cycle?
- are there conflicting needs for different people?
- how to adjust for season, latitude and time zone anomalies?

All the above goals involve mimicking biology and converting volatile environmental light patterns into information about time-of-day. This is why they all benefit from smoothing techniques.

The EMA method put forward is purposely the simplest possible smoothing technique, and one which is achievable at little cost:

- There is no need to store and repeatedly process lengthy prior light histories, only the prevailing value of D; an adaptive trait which appears to be built-in to non-visual photoreception.
- Other smoothing mechanisms are possible, but it is hoped that this simple model is a good first order approximation.
- It is not complete, however, without a clock mechanism; here matching Winfree's model structure(s) to the bio-physical genetic mechanisms in the SCN is what is required.
- This has been completed before, but should be repeated based on the true retinal signalling dynamics, including persistency.

Acknowledgement

This paper is work commissioned by the National Institute for Health Research, UK. The views expressed in this paper are those of the author and not necessarily those of the NHS, the National Institute for Health Research or the Department of Health. I would like to thank the home-owners and Dr John O'Hagan and Marina Khazova who all provided helpful support throughout this work.

References

CHANG, A.M., SANTHI N., ST HILAIRE M., GRONFIER C., BRADSTREET, D.S., DUFFY, J.F., LOCKLEY, S.W., KRONAUER, R.E. and CZEISLER, C.A. 2012. Human responses to bright light of different durations. J Physiol., 590:3103-3112.

GRIESS, G.A., and BLANKENSTEIN, M.F. 1981. Additivity and repair of actinic retinal lesions. Investigative Ophthalm & Vis Sci., 20(6):803-807.

KRONAUER, R.E., FORGER, D.B., and JEWETT, M.E. 1999. Quantifying human circadian pacemaker response to brief, extended, and repeated light stimuli over the phototopic range. J Biol Rhythms., 14(6):501-516.

LUCAS, R.J., PEIRSON, S.N., BERSON D.M., BROWN, T.M., COOPER, H.M., CZEISLER, C.A., FIGUEIRO, M.G., GAMLIN, P.D., LOCKLEY, S.W., O'HAGAN, J.B., PRICE, L.L.A., PROVENCIO, I., SKENE, D.J., and BRAINARD, G.C. 2014. Measuring and using light in the melanopsin age, Trends in neurosci., 37(1):1-9.

PRICE, L.L.A., KHAZOVA, M., and O'HAGAN J.B. 2012. Performance assessment of commercial circadian personal exposure devices. Lighting Res and Technol., 44(1):17-26.

WINFREE, A.T. 2001. The geometry of biological time, Vol. 12. Springer.

PP84

MEASUREMENTS OF IN-FLIGHT UV EXPOSURES OF PILOTS

Price, L.L.A.[1], Baczynska, K.[1], Chorley, A.C.[2], Higlett, M.P.[1], Hunter, R.[3], and Khazova, M.[1]
[1] Public Health England, Centre for Radiation, Chemical and Environmental Hazards, Didcot, OX11 0RQ, UK
[2] UK Civil Aviation Authority, Aviation House, Gatwick Airport South, Sussex, RH6 0YR, UK
[3] BALPA, BALPA House, 5 Heathrow Boulevard, 278 Bath Road, West Drayton, UB7 0DQ, UK
Luke.Price@phe.gov.uk or Michael.Higlett@phe.gov.uk

Abstract

Population and animal studies indicate that long-term exposure to short-wavelength visible light and ultraviolet radiation (UVR) increases the risks relating to certain ocular pathologies such as cataracts and maculopathy (Chorley, 2011).

Levels of UVR at cruise altitude, around 10 km for commercial aircraft, may be 2 to 3 times greater than at ground level (Blumthaler, 1997).

Research investigating civilian pilot exposure to UVR and Blue Light hazard is limited (Diffey, 1990; Roscoe, 1994).

An improved understanding of UV exposures could pave the way to reducing the risk of developing skin cancers and sun-related eye disorders; information on the levels of solar UV exposures collected at altitude is essential for the assessment of occupational risk from UVR to pilots.

Keywords: Automated acquisition, Pilots, UV exposure

1 Objectives

To carry out detailed assessments of the UV exposures of commercial pilots, whilst in flight and on the ground, and provide recommendations relating to managing occupational exposures.

To develop and implement automated measurement protocols for acquiring solar UVR and visible radiation exposure data inside aircraft cockpits, by combining synchronised broadband and spectral measurements.

Figure 1 – Researcher positioning input optics

2 Methods

Measurements were carried out using a broadband illuminance meter in different directions near the pilot's face. These directions were selected to represent typical tasks during flight, and were time synchronized with automated measurements of spectral irradiance in the cockpit just behind the front aircraft windscreen.

The spectral irradiance was measured over the range of 300 nm to 1100 nm with a miniature CCD array spectroradiometer.

Within each scheduled acquisition, three spectral regions were chosen to optimise the dynamic performance of the spectrometer over the full spectral range, by automating integration time selection, based on prevailing conditions. An automated external shutter was used to provide contemporaneous dark measurements (i.e. carried out immediately after each light acquisition).

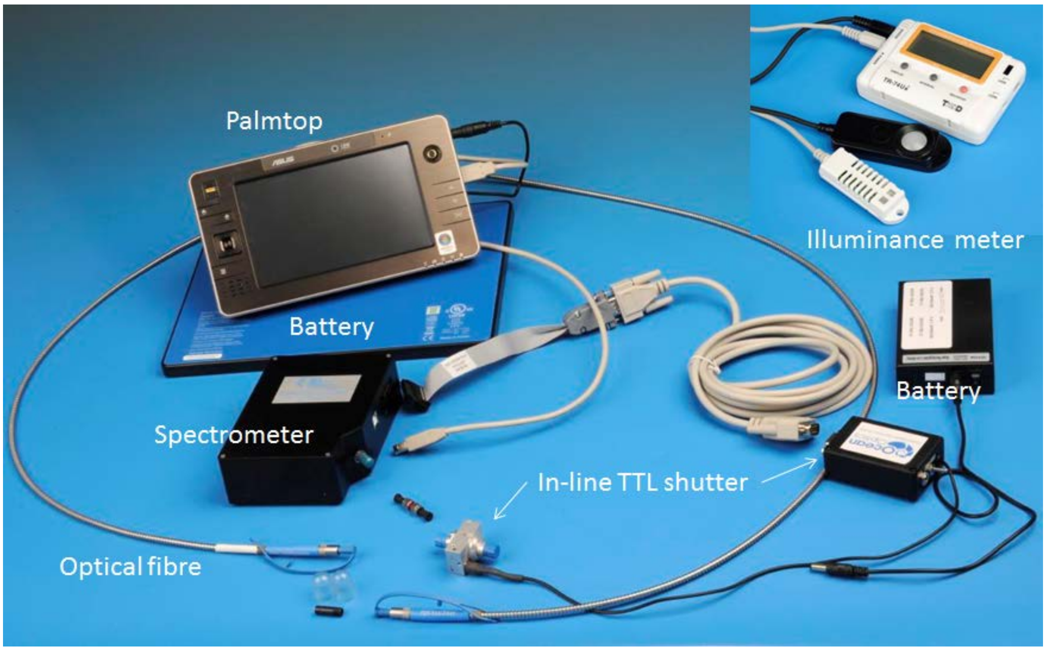

Figure 2 – Measurement equipment including: T&D Corporation TR-74Ui illuminance and UV recorder, and Ocean Optics HR4000 array spectroradiometer, optical fibre and in-line TTL shutter

The combined broadband illuminance data and spectral irradiance were used to determine UV-A, erythema and Blue Light weighted irradiance estimates based on applying hazard ratios, calculated as weighted irradiance / illuminance, to the broadband data.

3 Results and Discussion

The automated measurement system was deployed during a number of aeroplane and helicopter flights during 2012-13. The sample data presented were taken from a flight on 1 March 2013 from London Gatwick (LGW), UK, 51.61°N to Alicante (ALC), Spain, 38.29°N on an Airbus A321.

The UV-A exposure for the duration of this flight measured at the aircraft windscreen exceeded 97 $kJ.m^{-2}$. UV-A exposure varied between approximately 40 $kJ.m^{-2}$ (at the eye, looking down) and 52 $kJ.m^{-2}$ (looking ahead).

The ocular exposure measured during this 2 hour flight could easily cause the maximum exposure over an 8 hour period under the ICNIRP guidance (10 $kJ.m^{-2}$ UV-A exposure) (ICNIRP, 2004) to be exceeded unless appropriate eye protection was used.

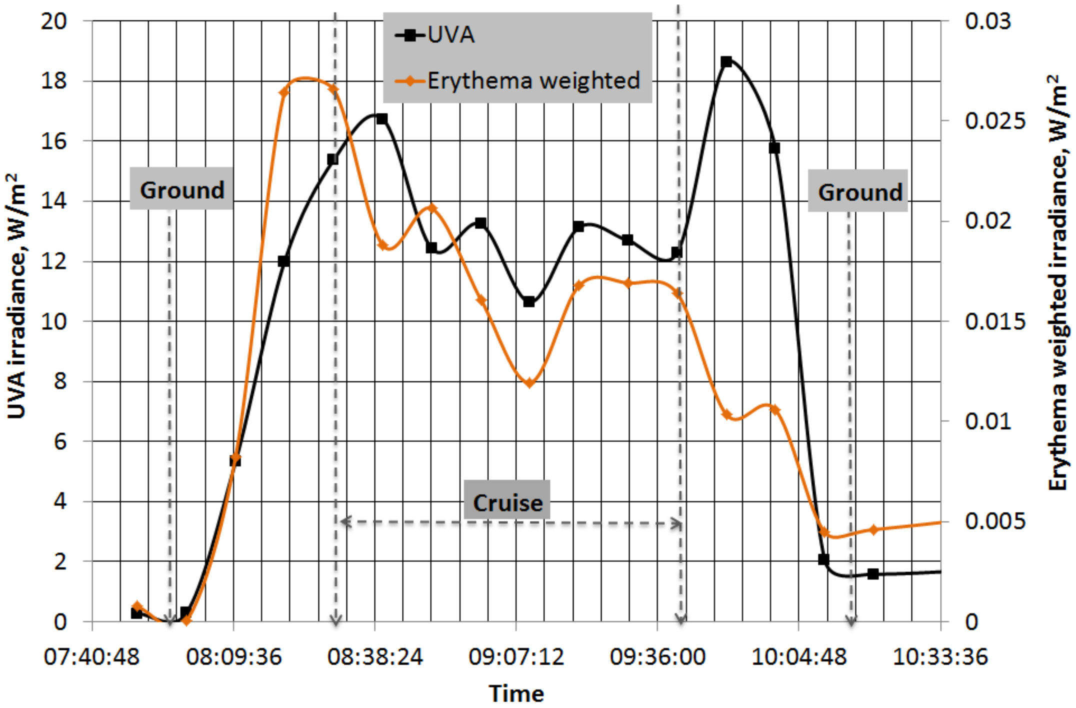

Figure 3 – Variations of UV-A and erythema weighted irradiance during flight

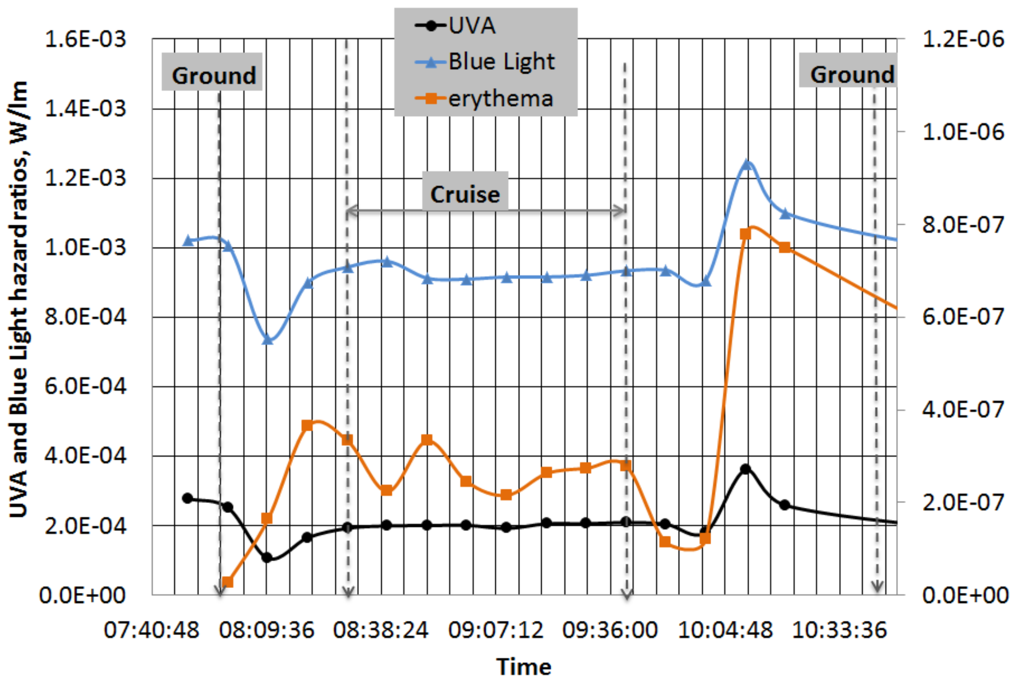

Figure 4 – Variation of hazard ratios during flight

The erythema weighted exposure during this flight reached 1.4 SED in less than 2 hours. (1 SED = 100 J.m^{-2})

At cruise altitude, UV-A irradiance measured behind the aircraft windscreen increased by a factor of almost 50 compared with LGW in the morning, and by a factor of up to 7 compared with ALC in the early afternoon.

Hazard ratios were relatively stable at cruise altitude and were very similar at LGW and ALC.

References

BLUMTHALER, M, AMBACH W, ELLINGER, R. 1997. Increase in solar UV radiation with altitude. Journal of Photochemistry and Photobiology B: Biology, 39:130-144.

CHORLEY, A, EVANS, B, BENWELL, M. 2011. Civilian Pilot Exposure to Ultraviolet and Blue Light and Pilot Use of Sunglasses. Aviation, Space, and Environmental Medicine, 82(9):895-900.

DIFFEY, BL, ROSCOE, AH. 1990. Exposure to solar ultraviolet radiation in flight. Aviation, Space, and Environmental Medicine, 61:1032-1035.

ICNIRP 2004. Guidelines on Limits of Exposure to Ultraviolet Radiation of Wavelengths between 180 nm and 400 nm (Incoherent Optical Radiation). Health Physics, 87(2):171-186.

ROSCOE, AH, DIFFEY, BL. 1994. A preliminary study of blue light on an aircraft flight deck. Health Physics, 66:565-567.

PP85

TEMPERATURE DEPENDENCE OF ARRAY SPECTRORADIOMETERS AND IMPLICATIONS FOR PHOTOBIOLOGISTS

Price, L.L.A., Hooke, R.J., Khazova, M.
Public Health England, Centre for Radiation, Chemical and Environmental Hazards, Didcot, OX11 0RQ, UK
Luke.Price@phe.gov.uk

Abstract

Miniature CCD array spectroradiometers are increasingly used by photobiologists in a range of applications where rapidly changing spectral information is required to be captured at specified times, such as in medical applications (Coleman, 2008), solar monitoring (Seckmeyer, 2010) or measurements of sunbed emissions (Ylianttila, 2005). Although CCD array spectroradiometers offer many advantages, amongst their limitations, some of their characteristics are influenced by ambient temperature (Blumthaler, 2013).

The performance of some of these devices had been previously investigated in laboratory conditions; however, there remained a need for systematic study of temperature dependence to determine the conditions under which they can be expected to function accurately outside of a temperature-controlled environment.

The initial results from analysing the performance of six spectroradiometers are presented, including two thermo-electrically cooled models with in-built fans. The following characteristics were investigated:

- Thermal stability and relaxation to changing ambient temperatures
- Dark signal as a function of both ambient temperature and integration time
- Changes in sensitivity with ambient temperature
- Relative wavelength shifts due to ambient temperature changes

Each spectroradiometer had different thermal relaxation properties and took a different length of time to stabilise after a change in ambient temperature. Signal-to-noise ratios became unmanageable for combinations of high ambient temperatures and long integration times for non-TE-cooled instruments, as the dark signal standard deviations grew to a substantial proportion of well depth. Whilst TE-cooling was effective in improving noise management, it did not substantially mitigate changes of sensitivity with ambient temperature.

Keywords: CCD Array Spectrometers, Temperature Dependence, Photobiology

1 Methods

The spectroradiometers (Table 1) were placed inside a sealed Contour Delta environmental chamber (S/N A3278, Design Environmental, UK); the input optics (Ocean Optics, USA) and a CL6 tungsten-halogen lamp (Bentham Instruments, UK) were placed outside (Figure 1).

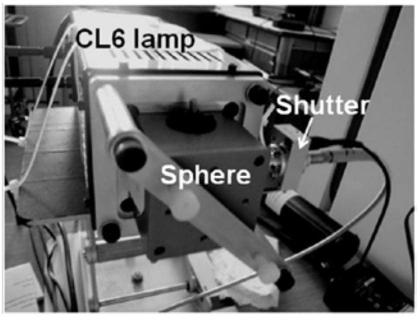

Figure 1 – CL6 lamp with attached sphere and in-line shutter (from Coleman, 2008)

Table 1 – The spectroradiometers tested

Model	Range, nm	Cooling	Make
USB2000+	340 to 1000	No	1.
HR4000	200 to 1100	No	1.
QE65000	230 to 410	3 settings: TEC=-20°C TEC=-10°C TEC off	1.
Glacier X	200 to 422	1 setting: TEC=-15°C	2.
Quest U	200 to 850	No	2.
Exemplar LS	170 to 915	No	2.
1. Ocean Optics Inc, Dunedin, Florida, USA			
2. B&W Tek Inc, Newark, New Jersey, USA			

For each spectroradiometer the protocol outlined in Scheme 1 was followed.

Scheme 1 – Outline of the measurement protocol

Step 1 Stabilise the equipment for 1 hour at 22°C
1.1 Measure Hg lines
1.2 Measure dark signal for all integration times
1.3 Measure calibration lamp (CL6) and dark signal

Step 2 Change ambient temperature to 30°C
2.1 Repeat 1.3 every 5 to10 minutes until sensitivity, dark signal and all temperatures are stable
2.2 Repeat 1.3 again three times (with pauses of 5 to10 minutes in between)
2.3 Repeat all Step 1 measurements

Step 3 Change ambient temperature to 35°C
3.1 Repeat all Step 2 measurements

Step 4 Change ambient temperature to 40°C
4.1 Repeat all Step 2 measurements

Step 5 Change ambient temperature to 22°C
5.1 Repeat all Step 2 measurements

Repeat the entire protocol for low temperatures
22°C→15°C→10°C→5°C→15°C→22°C

2 Results

The results are split into the four following sections, accompanied by figures to show examples of the performance characteristics with changing ambient temperatures:

- Thermal stability and relaxation
- Dark signal
- Changes in sensitivity
- Relative wavelength shifts

2.1 Thermal stability and relaxation

Where available, the board temperature stabilisation data can be modelled using the assumption that the rate of change of board temperature, T_B, is linearly related to the difference between board and ambient temperature, T_A, as follows:

$$\mathrm{d}T_B \approx (\beta \cdot (T_B - T_A) + c) \cdot \mathrm{d}t \qquad (1)$$

where

c is an intercept constant to allow for the electrically generated waste heat; and

β is a rate constant governing the pace of relaxation.

This model follows the data remarkably closely, as illustrated in the examples in Figure 2. Fitted rate constants are given in Table 2.

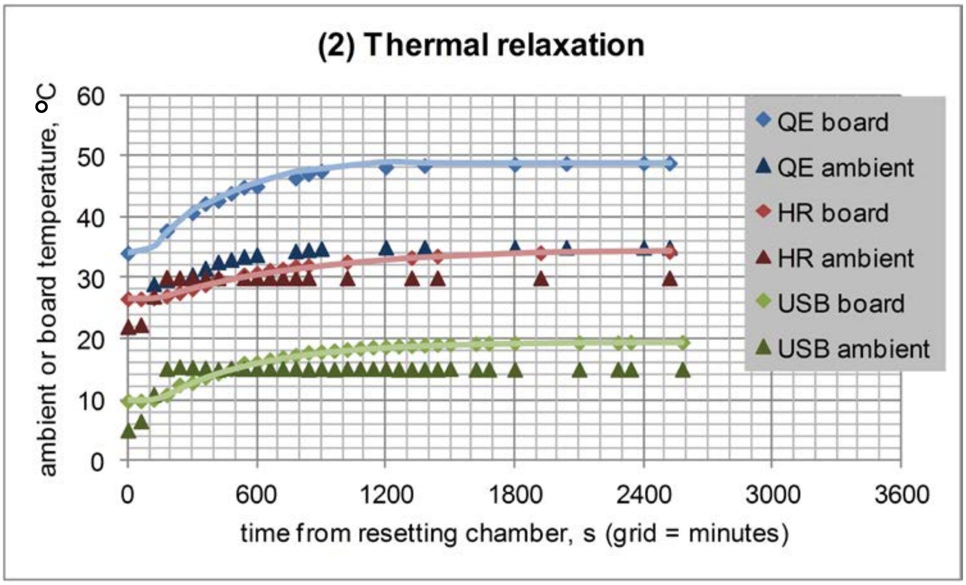

Figure 2 – Model of thermal stabilisation for the uncooled QE65000 (fan on), HR4000 and USB2000+.

Table 2 – Fitted rate constants and estimated relaxation times to within 0,5°C and 0,1°C of stabilised board temperature, following a 5°C change of ambient temperature.

Model	β, min^{-1}	Relaxation time, min	
		within 0,5°C	within 0,1°C
USB2000+	0,12	19	33
HR4000	0,084	27	46
QE65000 (TEC off)	0,30 (fan on)	8	13

2.2 Dark signal

The mean and standard deviation of the counts in the dark signals, μ_{ds} and σ_{ds}, increased linearly with integration time, t_{int}. Both these effects can reduce the available signal-to-noise ratio for any given measurement.

- σ_{ds} increased as a proportion of well depth for longer t_{int} and/or higher T_A values (Fig.3)
- TE-cooling eliminated this effect for integration times shorter than ~ 100 s (not shown)
- μ_{ds} decreased with increasing temperature, for the USB2000+, and became effectively negative above 30°C (e.g. lower purple line)
- The HR4000 dark signal was not spectrally flat for shorter t_{int} and/or lower T_A values, and also dipped around t_{int} = 0.7 s.

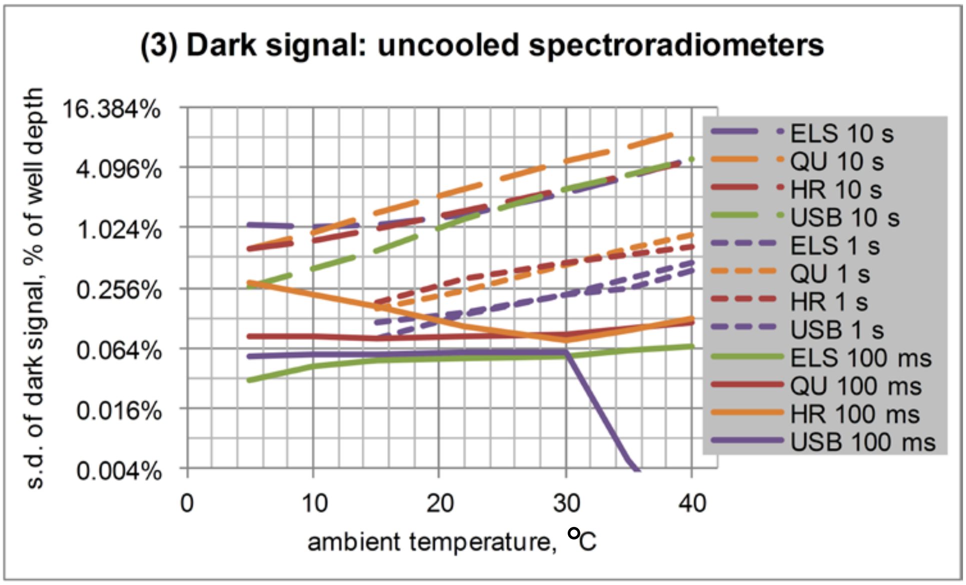

Figure 3 – Uncooled spectroradiometers' dark signal s.d. versus ambient temperatures.

2.3 Sensitivity

Sufficiently high throughput at the array was only available at longer wavelengths to demonstrate the changes in spectroradiometers' sensitivities to ambient temperatures. Between around 15°C and 30°C ambient, the differences in sensitivity relative to 22°C were small for all the spectrometers.

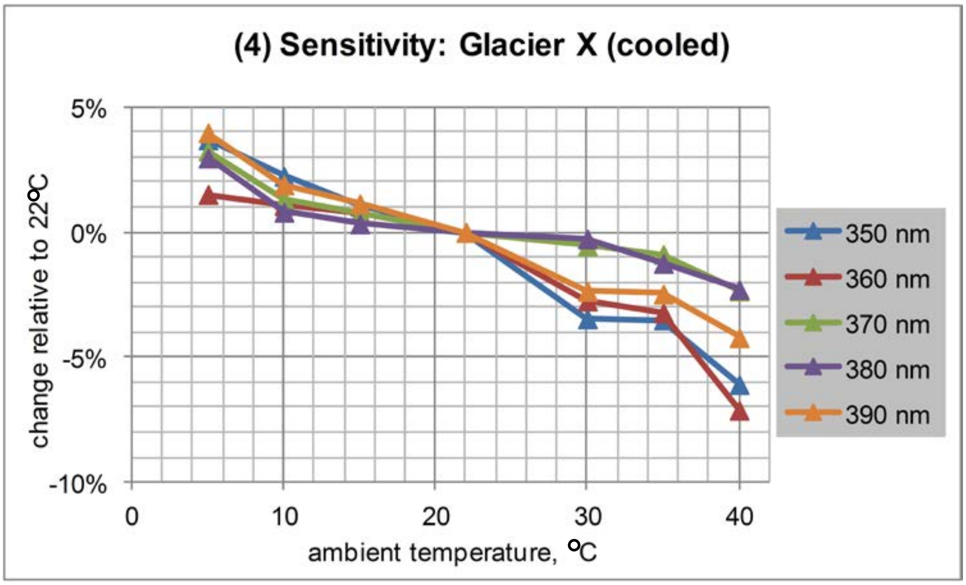

Figure 4 – Glacier X sensitivity compared to 22°C for a sample of representative, high throughput pixels.

- For the Quest U, Exemplar LS and USB2000+ the differences changed sign depending on wavelength; relative sensitivity was positively correlated to ambient temperatures for longer wavelengths and negatively correlated for shorter wavelengths.
- Figure 4 shows negative correlation for the Glacier X between 350 nm and 390 nm.
- There was a broadly positive correlation for the QE65000 from 280 nm to 390 nm.
- The sensitivity of the HR4000 was maximal (i.e. independent of T_A) at around 22°C, at least in the range 420 nm to 700 nm.

2.4 Wavelength shifts

Both the QE65000 and HR4000 distorted the Hg lines at low T_A values (Figure 5). Glacier X, Quest U and Exemplar LS shifts were within a single pixel; like the USB2000+, no distortion of the peaks was observed. Figure 6 shows wavelength shifts for selected instruments.

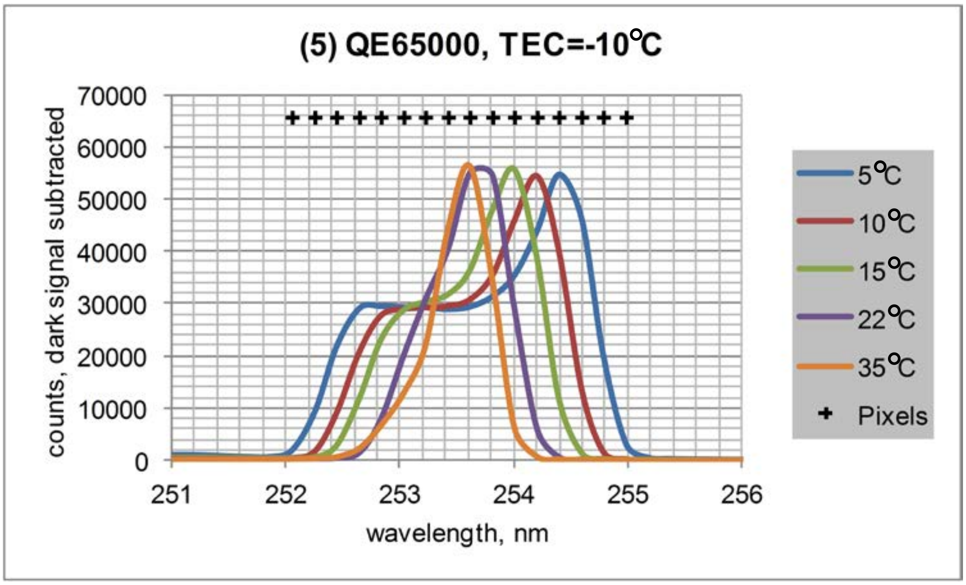

Figure 5 – QE65000 TEC=-10°C 253.65 nm Hg line, showing wavelength shift and slit function distortion.

3 Discussion and Conclusions

Spectrometers which are widely used by photobiologists may perform differently as ambient temperatures change. The results above would be difficult to anticipate without this systematic approach to characterisation.

The various temperature effects combine to increase measurement uncertainties outside of a temperature controlled environment, although to a lesser extent for TE-cooled spectroradiometers:

- Even at stable temperatures, outside the range of between 15°C and 30°C, the performance of the instruments may be unmanageable
- These considerations become particularly relevant when using an instrument for measurements with long integration times
- At long integration times and/or high ambient temperatures, difficulties with noise can dominate other sources of uncertainty

Noise management may be critical for high values of T_A and/or t_{int}:

- The standard deviation of the dark signal counts can grow to a substantial proportion of well depth
- Due to the long integration times often involved, this is important for measurements of environmental UVR in particular.

TE-cooling is effective in improving many aspects of performance:

- It largely eliminates the increase in noise for integration times below around 100 seconds
- However, changes of sensitivity due to ambient temperature are not reduced substantially

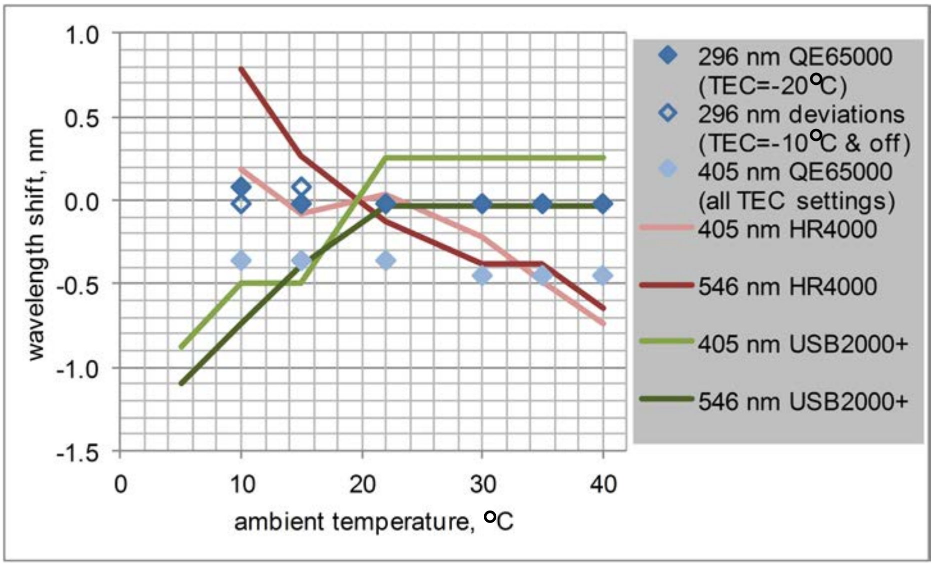

Figure 6 – Wavelength shifts due to ambient temperature for the Ocean Optics instruments.

Different CCD array spectrometers take different lengths of time to stabilise after a change in ambient temperature. There may be advantages to both fast and slow relaxation times:

- Slow relaxation times reduce the sensitivity to changes in the ambient temperature
- Fast relaxation times allow stability to be reached more quickly

Understanding the thermal relaxation properties is also important when constructing field measurement protocols:

- Relaxation times can be accurately predicted

- The data rigorously establish the case for contemporaneous dark measurements
- The data also establish an exception for at least one of the TE-cooled instruments studied – as the dark signals were indistinguishable for a wide range of measurement conditions.

Acknowledgements

This study was funded by a Researcher Excellence Grant within EMRP ENV03 “Traceability for surface spectral solar ultraviolet radiation”. The EMRP is jointly funded by the EMRP participating countries and the European Union.

The authors would like to thank Dr John O’Hagan for continuing support and valuable advice and Andy Pearson for the assistance with measurements.

References

BLUMTHALER, M, GRÖBNER, J, EGLI, L, NEVAS, S. 2013. A guide to measuring solar UV spectra using array spectroradiometers. AIP Conf. Proc. 1531:805.

COLEMAN, A, SARKANY, R, WALKER, S. 2008. Clinical ultraviolet dosimetry with a CCD monochromator array spectroradiometer. Phys Med Biol., 53(18):5239-5255.

SECKMEYER, G, BAIS, A, BERNHARD, G ET AL. 2010. Instruments to measure solar ultraviolet radiation Part 4: Array Spectroradiometers, WMO/GAW No.191, World Meteorological Organization, Geneva.

YLIANTTILA, L, VISURI, R, HUURTO, L, JOKELA, K. 2005. Evaluation of a single-monochromator diode array spectroradiometer for sunbed UV-radiation measurements. Photochem Photobiol. 81(2):333-341.

PP86

WINDOW EFFECTS ON RELAXATION AND CIRCADIAN REGULATION

Mochizuki, E.[1], Ishii, C.[2], Murae, Y.[3], Mori, K.[3], Niwa, H.[4], Yagishita, K.[5]
[1] Chiba Institute of Technology, Chiba, JAPAN,
[2] Graduate School of Chiba Institute of Technology, Chiba, JAPAN,
[3] Toda Corporation, Tokyo, JAPAN, [4] Murata Manufacturing Co., Ltd., Kyoto, JAPAN,
[5] Ushio Lighting, INC., Tokyo, JAPAN
etsuko.mochizuki@p.chibakouadai.jp

Abstract

The purpose of this study is to identify the optimum light exposure pattern through a day with considerations of the effects of window from the viewpoints of the occupants' comfort and circadian regulation. In this paper, the results of subjective experiment conducted in a real scale model assuming a hospital room are reported. Six cases considering the window size and light exposure pattern during the daytime were examined. The results showed that the subjects could have better sleep (i.e. higher sleeping efficiency and shorter delayed time before sleep) in the cases when they spent the daytime in the room with windows than in the cases in the room without windows. It was also identified that supplementing artificial light in the morning besides the daylight from window had much impact on increasing sleeping efficiency.

Keywords: Window, Circadian rhythm, Dimming control, Hospital room

1 Introduction

It is well known that the change in light over time of a day have a good influence for stabilizing the sleep/wake rhythm (Wojtysiak, A. and Lang, D. 2013). Daylight through windows or outdoors can be a good source of short-wavelength and bright daytime light exposure to regulate circadian rhythms. For the occupants who cannot be exposed to much sunlight in the daytime, such as patients in hospital, shift workers and etc., it is recommended to supplement artificial light in their living space in line with the outer environment for their health and comfort. However, the optimal pattern of light exposure to entrain circadian rhythms has not been yet clearly established (Veitch, J.A. et. al, 2013). In addition, it is not sure whether daylight from window is alternative to artificial light or not.

The purpose of this study is to identify the optimum light exposure pattern through a day with considerations of the effects of window from the viewpoints of the occupants' comfort and circadian regulation. In this paper, the results of subjective experiment conducted in a real scale model supposing a hospital room, where it is required to create non-stressful environment for the occupants who lead monotonous life by following the fixed schedule, are presented.

2 Method

2.1 Experimental conditions

A pair of experimental chamber assuming a hospital room as shown in Figure 1 was used for the subjective experiment. The size of the room was 4,775 mm in width, 6,500 mm in depth and 2,800 mm in height. Two beds and two desks were set in each room. Six LED luminaires of 600 mm square were mounted uniformly on the ceiling. The luminaire was consisted of white LEDs and amber LEDs, 320 of each. The illuminance and the correlated colour temperature (hereafter CCT) were set combining the output of white LEDs and that of amber LEDs both with the steps of 255 by radio control. The size of the window facing south was set at three levels by covering with movable partition walls, large (W: 3,860*H: 1,130), small (W: 1,922*H: 1,130) and no window.

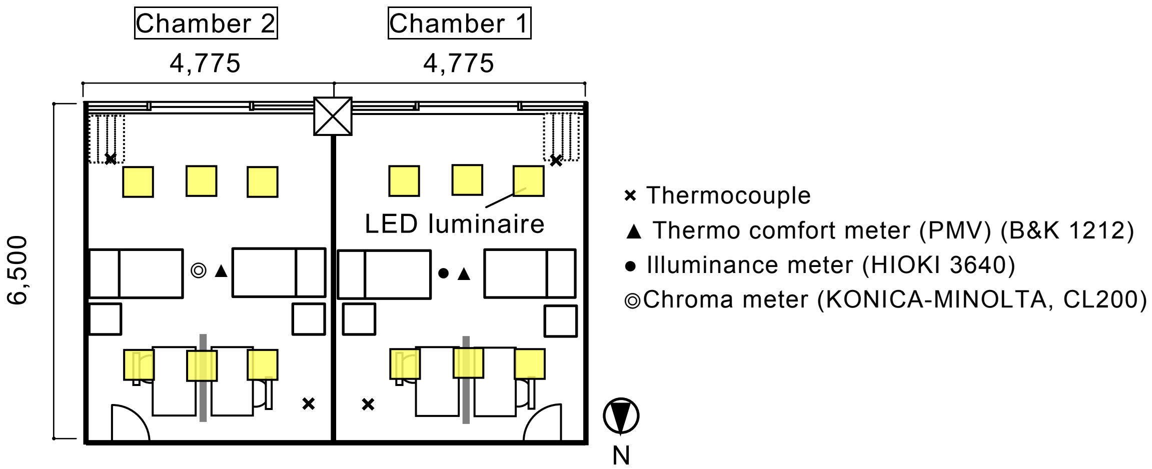

Figure 1 – Plan of the experimental chambers

All 6 experimental cases combined with the pattern of the light exposure during the daytime and the size of the window as shown in Table 1 were experimented. In the case of change for luminous setting, the setting was changed in 60sec for the subjects not to sense the change of lighting condition.

Table 1 – Experimental conditions

Case	Window	Illuminance	Correlated colour temperature
1	Large 	As daylight from window	
2	Small 		
3	Large 	7:00-11:00 1,200 lx 11:00-13:00 1,000 lx 13:00-16:00 600 lx 16:00-18:00 300 lx	7:00-11:00 4,600 K 11:00-13:00 4,000 K 13:00-16:00 4,000 K 16:00-18:00 3,000 K
4	No window 		
5		630 lx constant	
6		630 lx constant	4,600 K constant

The total amount of the light exposure through a day with the cases of 3, 4, 5 and 6 was controlled almost the same. For variable illuminance conditions, the cases 3 and 4, horizontal illuminance at the centre of the chamber (800 mm from the floor) was set 1,200 lx from 7 a.m. till 11 a.m., 1,000 lx from 11 a.m. till 1 p.m., 600 lx from 1 p.m. till 4 p.m., and 300 lx from 4 p.m. till 6 p.m. For the variable luminous colour conditions, the cases 3, 4 and 5, the CCT was set 4,600 K from 7 a.m. till 11 a.m., 4,000 K from 11 a.m. till 4 p.m., and 3,000 K from 4 p.m. till 6 p.m.

2.2 Experimental procedure and evaluation items

Subjective experiment was conducted for 6 days from 20th August till 28th August, 2013. Four healthy male, aged from 21 to 23 years old, participated in the experiment as the subjects. He was asked to wear clothing ensembles (the total clo value was 0,37), cotton short-sleeve shirt (0,08 clo), trousers (0,22 clo), underwear (0,04 clo) and slippers (0,03 clo) during the experiment. The activity level of the subjects during the experiment was assumed 1,1 met. The air temperature and the relative humidity in the experimental chamber was set 27°C and 40-60%rh respectively to set PMV (Predicted Mean Vote) as -1,0-+1,0.

Figure 2 shows the experimental procedure and experimental scenes. The subjects were divided into two groups. Each condition was set for two days. Two subjects at a time entered in one side of the experimental chamber and they were exposed to each condition. He stayed in the experimental chamber from 7 a.m. till 6 p.m. He was asked to stay in the chamber as they liked, reading books, playing cards, playing games and etc. After the daytime experiment, the subjects moved to the lodging attached to the building where the experimental chamber was placed. Then he had dinner, took a bath and went to bed before 9 p.m. The subjects stayed in the bedroom alone. Each subject adjusted the air temperature in the bedroom for him to feel comfortable using air-conditioner. On the next day, the subjects woke up at 6 a.m. and moved to the experimental chamber at 7 a.m., and then he was exposed to another experimental condition.

The subjects were asked to measure his body temperature under his arm (CT422, CITIZEN), blood pressure and pulse (HEM-6022, OMRON) and take saliva to evaluate salivary α-amylase activity (NIPRO) every one hour from 6 p.m. till 9 p.m. He was also asked to fill out the sheets of questionnaire to evaluate the thermal and lighting environment in the experimental chamber and to measure sense of time to evaluate how he was relaxed every one hour from 8 a.m. till 6 p.m. Additionally, he was asked to do some visual tasks, puzzle, maze and number placing puzzle game, every two hours from 9 a.m. till 5 p.m. to test his vitality. The subjects had breakfast after the evaluation at 7 a.m. and had lunch after the evaluation at 0 p.m. in the experimental chamber.

The subjects were asked to wear Actiwatch (Philips respironics) to evaluate his sleeping efficiency and heart rate sensor (WHS-1, UNION TOOL Co.) throughout the experiment. The subjects answered the OSA sleep inventory MA version just after they woke up in the morning for everyday. Moreover, the subjects did number learning task for 1 minute, mistake-searching game for 3 minutes, and arithmetic operation of two-digit numbers for 5 minutes three times each at 6 a.m., 7 a.m. and 8 a.m. to test their wakefulness level in the morning.

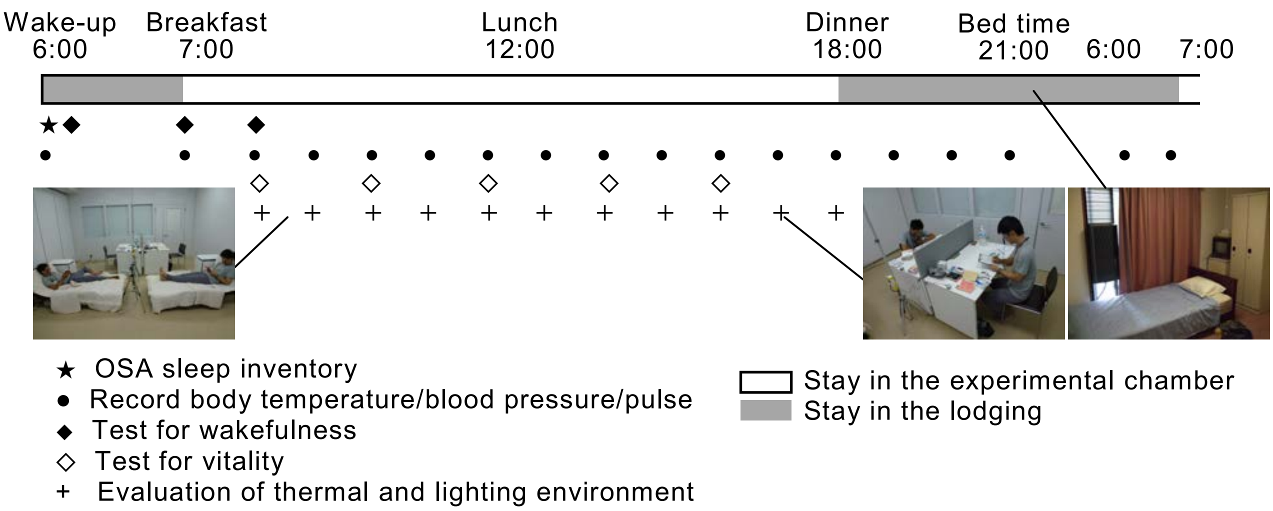

Figure 2 – Experimental procedure and experimental scenes

2.3 Measurement items

During the experiment, horizontal illuminance was recorded in the centre of the chamber (800 mm from the floor) at intervals of 30 seconds (HIOKI 3640 LUX LOGGER) and the CCT was monitored in the centre of each chamber (CL-200, KONICA-MINOLTA). The air temperature and relative humidity were recorded at five different levels in two points continuously at intervals of 30 seconds (TR-701NW, T&D Corporation). PMV was measured at intervals of 30 seconds under supposition of 1,1 Met of the activity level and 0,37 clo of the clothing (B&K 1212).

3 Results

3.1 Thermal environment and subjects' thermal sensation

Figure 3 shows an example of the air temperature measured at 10 different points (5 different levels x 2 places) in each chamber on August 22, 2013. It can be seen that the difference in the air temperature depending on the measurement points was rather small in each chamber. In the chamber 1, the air temperature was kept nearly constant during the experiment, although the air temperature fluctuated continuously in the chamber 2. Experiments with each case were conducted for two days, the difference in PMV was smaller than 1,0 category

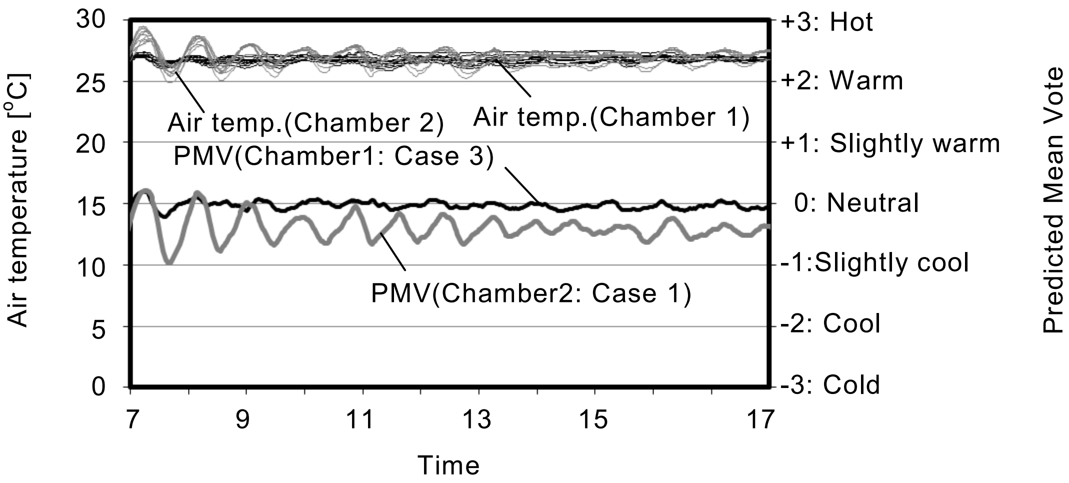

Figure 3 – Air temperature and PMV in each chamber (Aug 22, 2013)

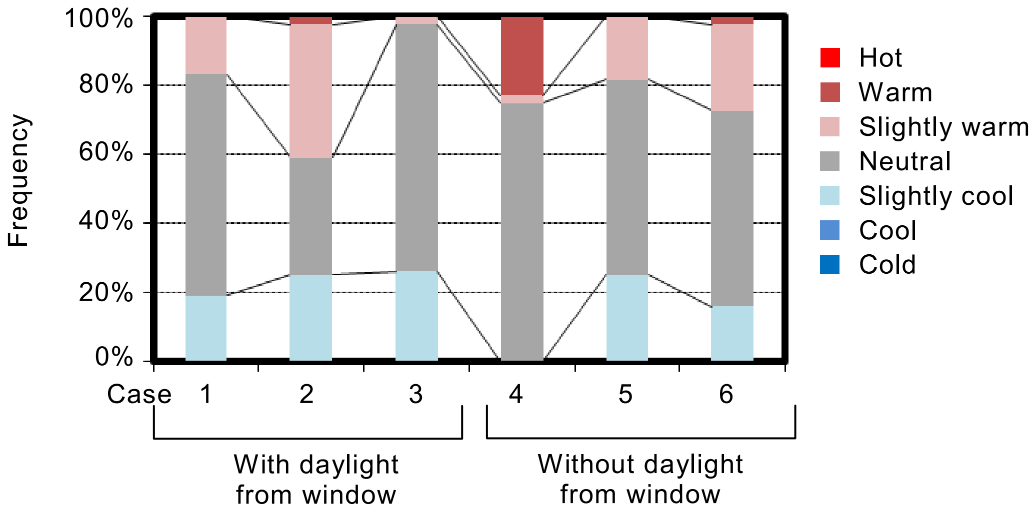

Figure 4 – Subjective evaluation of the thermal environment

between the two days.

Figure 4 shows the percentage of the subjects' thermal sensation vote in the chamber with each case. The subjects evaluated the thermal environment with each case every one hour from 8 a.m. to 6 p.m. Therefore the total number of the vote was 44 (4 subjects x 11 times) for each case. It can be seen that almost all of the subjects evaluated the thermal environment in the chamber 'Slightly cool', 'Neutral' or 'Slightly warm', except for the case 4. It was certified that the subjects did not feel the thermal environment with windows warmer than that without windows. Although some subjects evaluated the thermal environment 'warm' in some cases, none of the subjects judged the thermal environment uncomfortable.

3.2 Lighting environment and subjects' brightness

Figure 5 shows the horizontal illuminance and the CCT measured at the height of 800 mm from the floor in the centre of the chamber with each case. The experiments with each case were conducted for two days, it was certified that all of the subjects were exposed to almost the same lighting environment in each case, except for 9:40-10:30 in the case 1.

Figure 6 shows the percentage of the subjects' evaluation of the brightness in the chamber with the case 3 and that with the case 4 as examples. The illuminance in both cases was set nearly the same and it was reduced gradually from morning to evening. The subjective evaluation of brightness became lower as the time passed. It can be seen that the subjects evaluated the lighting environment with the case 4 was much brighter than that with the case 3, however they judged the lighting environment with the case 3, that was lit with both daylight from windows and LEDs, was more comfortable than that with the case 4, that was lit only by

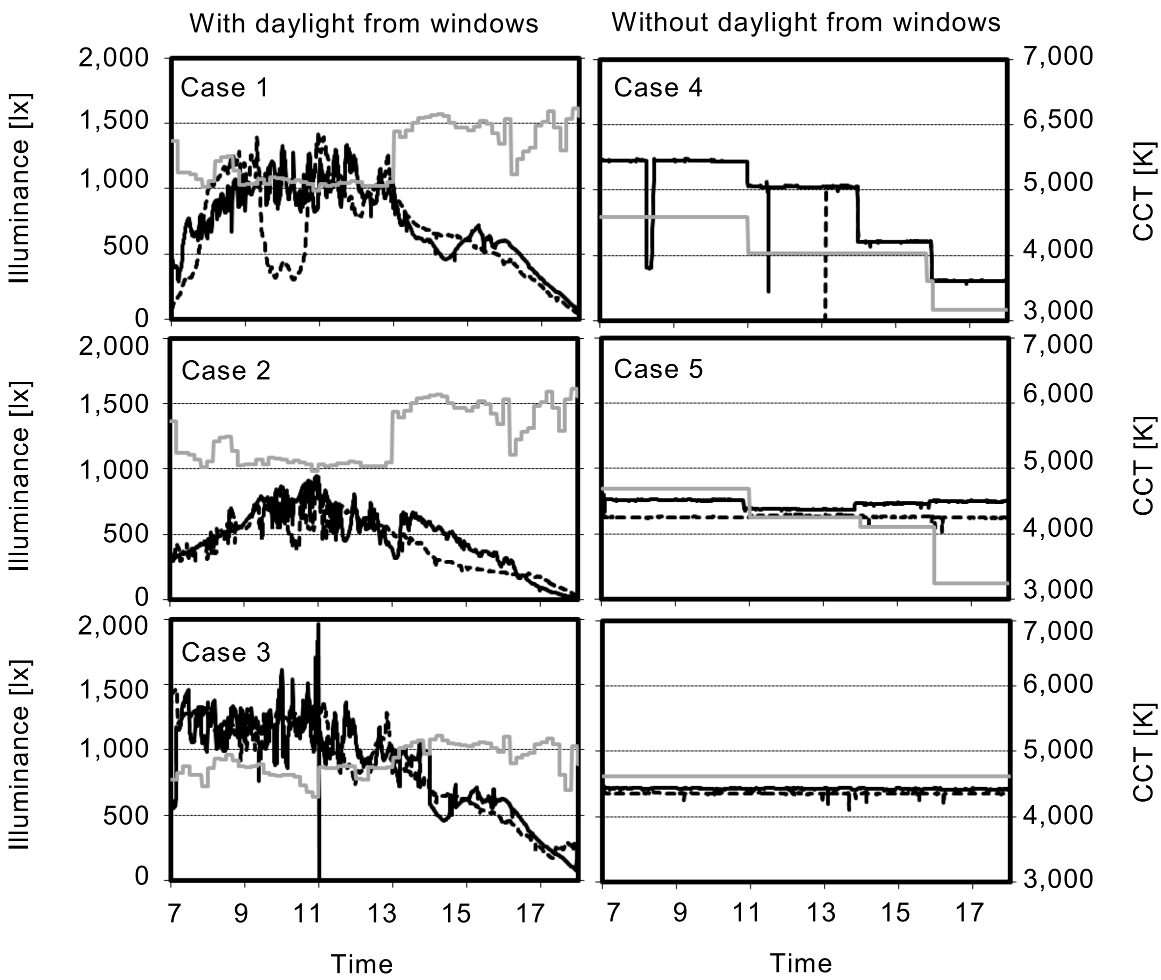

Figure 5 – Illuminance and CCT in each case

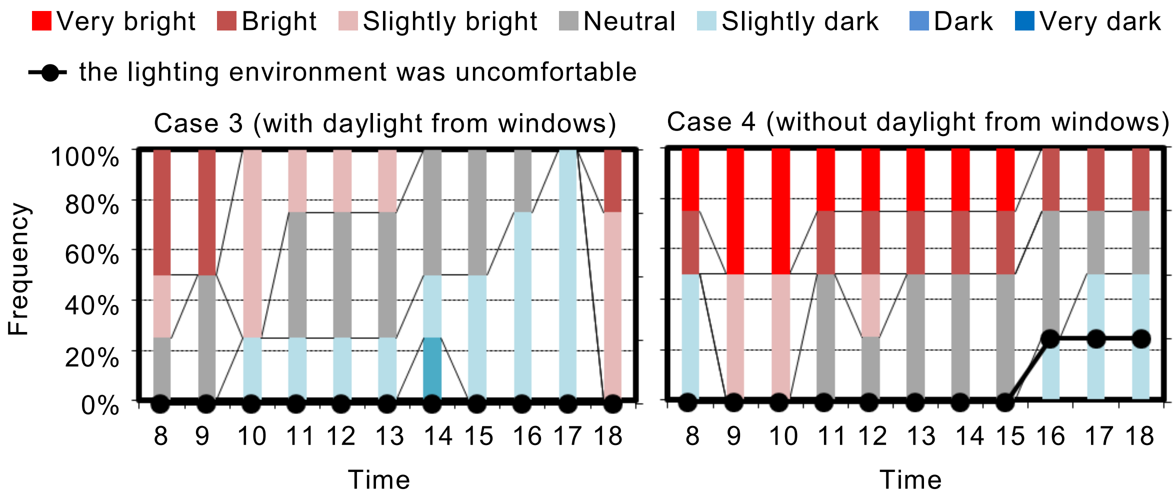

Figure 6 – Subjective evaluation of brightness

LEDs, in the evening.

3.3 Variation in body temperature and heart rate

Figure 7 shows the variation in the body temperature and Figure 8 shows that in the heart rate of the subject S as an example. The higher body temperature or the higher heart rate means more active or wakeful. On the other hand, the lower body temperature or the lower heart rate means sleepy or relaxed. In the cases 1 and 2, those were when the chamber was lit only by daylight, the body temperature in the morning was rather higher than that in the other cases. It can be seen that the variation in the body temperature in the cases when he spent the daytime in the chamber without windows, the cases 4, 5 and 6, was smaller than that in the cases when he spent in the chamber with windows.

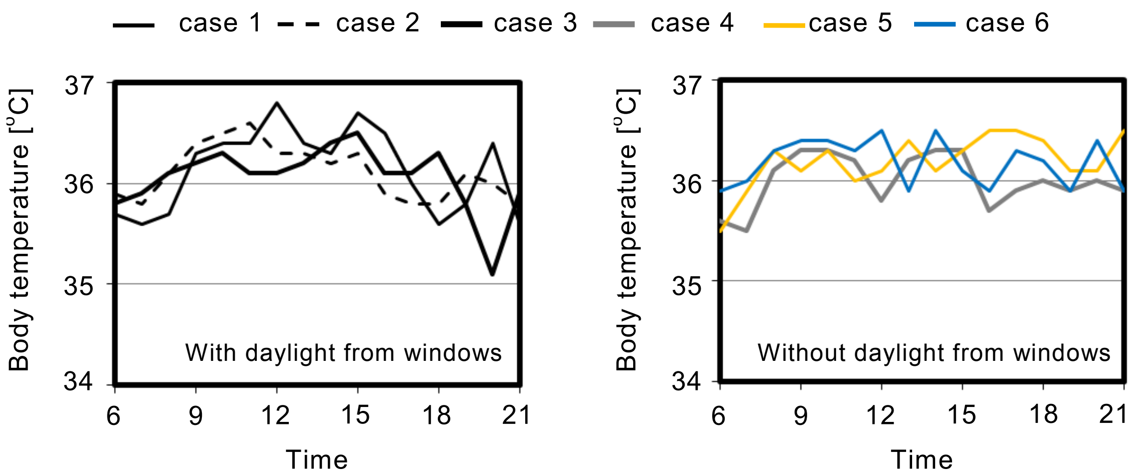

Figure 7 – Variation in body temperature (Subject S)

As shown in Figure 8, the heart rate was clearly lower during the sleep hours than during the awake hours. Especially in the cases 2 and 3, those were when he stayed in the chamber with the large size windows, the heart rate during the bed time was quite lower than the other cases. Figure 9 shows the ratio of the heart rate during the bedtime (median value during 9 p.m. and next 6 a.m.) to that during the awake time (median value during 6 a.m. and 9 p.m.). The lower the ratio the more the subjects relaxed in the bed time or the more the subjects were activated during the daytime. It can be seen that the ratio in the case 1 was lower than

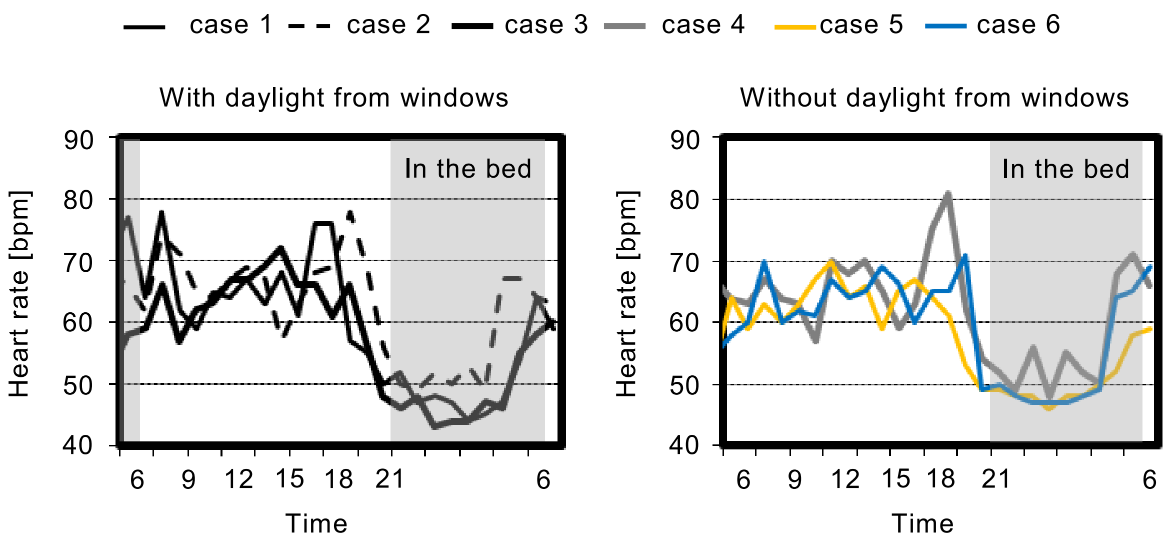

Figure 8 – Variation in heart rate (Subject S)

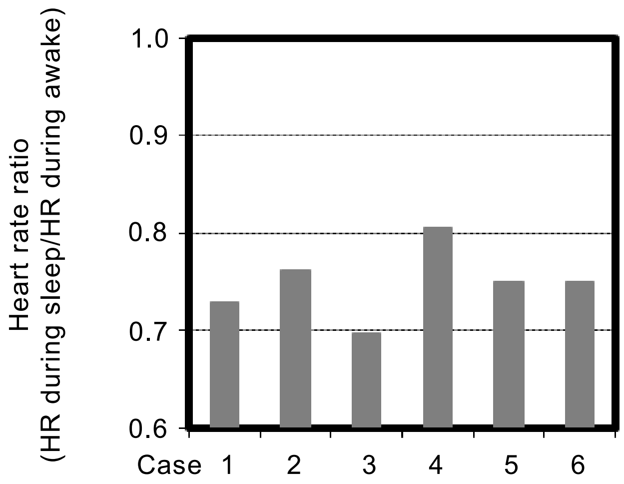

Figure 9 – Ratio of heart rate during sleep to awake (Subject S)

that in the case 2, the ratio in the case 3 was lower than that in the case 1. Moreover, the ratio in the case 3 was much lower than that in the case 4. It can be supposed that the larger window and the larger amount of light exposure in the morning activated the subject during he was awake and calmed him during sleep.

3.4 Sleeping efficiency and sleep evaluation

Figure 10 shows the sleeping efficiency and the delayed time before sleep of each subject. Comparing the results in the case 1 and those in the case 3, the size of the window was the same in both cases, 3 of 4 subjects showed higher sleeping efficiency in the case 3 than in the case 1. Comparing the results in the case 3 and those in the case 4, the illuminance was set nearly the same in both cases, every subject showed higher sleeping efficiency in the case 3 than in the case 4, and the delayed time before sleep was shorter in the case 3 than in the case 4 for the subjects N, S and M. It can be concluded that supplementing illuminance in the morning in addition to introducing daylight from window had good influences on sleep.

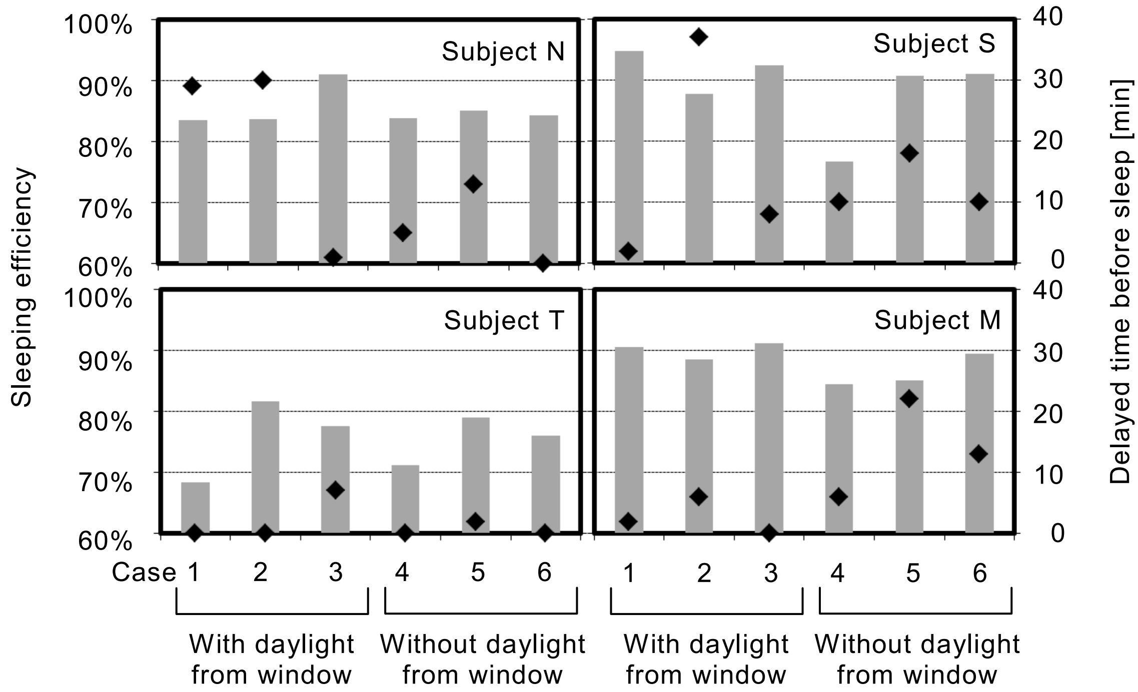

Figure 10 – Sleeping efficiency and delayed time before sleep in each case

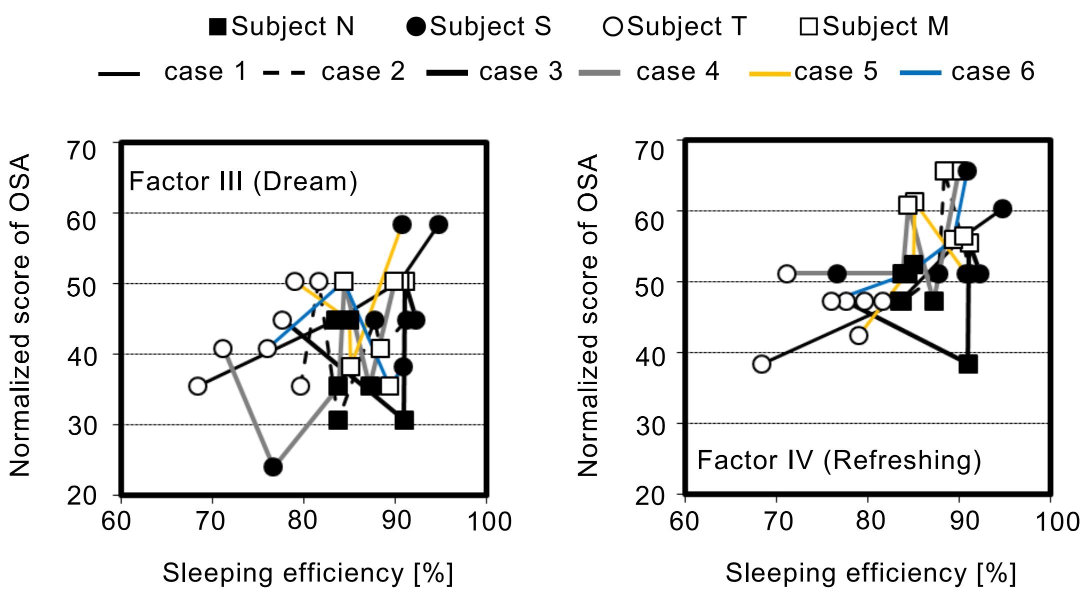

Figure 11 – Sleeping efficiency and sleep evaluation

Figure 11 shows the relationship between the sleeping efficiency and the normalized OSA scores for dream and those for refreshing. The OSA scores were obtained by summing up the score for 16 questions about sleep. There could be seen a slight tendency that the higher the sleeping efficiency the higher the score of OSA for dream for the subject T. However, clear relationship between the sleeping efficiency and the sleep evaluation common to each subject could not be found.

Figure 12 shows the relationship between sleeping efficiency and the number of numerals that the subject could memorize just after he woke up in the morning. The larger the number of numerals means that the wakefulness level was higher. The number of the numerals that the subjects could memorize was smaller in the case 3, although the sleeping efficiency was

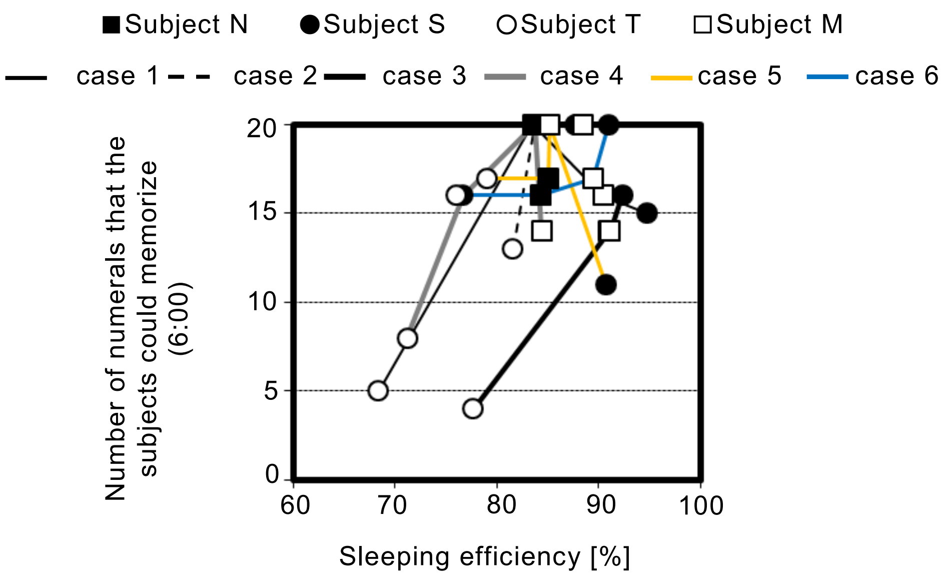

Figure 12 – Sleeping efficiency and wakefulness level

rather higher than in the other cases. On the other hand in the case 4, the light exposure pattern during the daytime was almost the same with the case 3, the number of numerals that the subjects could memorize was much higher than that in the case 3. Detailed analysis with considerations of the experimental order to eliminate the effects of practice or the subjects' fatigue is necessary.

4 Discussion

The results of the subjective experiment identifying the physiological effects of the light exposure pattern during the daytime with considerations of daylight from windows are presented. The results indicated that windows had good effects on body temperature, heart rate and also on sleeping efficiency, which can be robust indices for circadian rhythm.

In this study, the experiment was conducted in the summer and only one type of the view from windows was evaluated. Psychological and physiological effects of various types of the view from windows should be examined in the future work. Moreover, seasonal difference of the effects of light exposure pattern on circadian regulation should be identified and that may conclude the annually ideal lighting environment which can contribute for human circadian rhythm.

5 Conclusion

Subjective experiment was conducted to identify the effects of light exposure pattern thorough a day on the occupants' visual comfort and circadian regulation, especially on sleep. In the experiment, the combined effects of daylight from windows and light from LED luminaires whose luminous flux and luminous colour were controlled to be variable in line with daylight from windows were examined. The results showed that the subjects could have better sleep (i.e. higher sleeping efficiency and shorter delayed time before sleep) in the cases when they spent their time during the daytime in the room with windows than in the cases without windows nevertheless the exposed illuminance and correlated colour temperature were almost the same. It was also identified that supplementing artificial light in the morning besides the daylight from window was effective for increasing sleeping efficiency.

Acknowledgements

The authors would like to show special thanks to Mr. S. Yoshioka, Ms. A. Saito and Mr. T. Yoneyama who contributed to the subjective experiment.

References

Wojtysiak, A. and Lang, D. 2013 Application studies on non-visual effects of light with traditional and solid state light source, Proceedings of CIE centenary conference, 91-94

Veitch, J.A., Christoffersen, J. and Galasiu, A.D. 2013 What we know about windows and well-being, and what we need to know, Proceedings of CIE centenary conference, 169-177

PP86

POTENTIAL HAZARD OF LED SOURCES TO CAUSE BLH IN SPECIFIC POPULATION

Esther de Prado, **Alicia Pons**, José Luis Velázquez, Joaquín Campos, Alejandro Ferrero, Maria Luisa Hernanz
Departamento de Imágenes, Visión e Instrumentación Óptica, Instituto de Óptica, CSIC, C/Serrano, 121 c. p. 28006, Madrid, SPAIN.
alicia.pons@csic.es

Abstract

Starting from the spectral transmittance values of various models of commercial intraocular lenses (IOLs), modifications of the action spectrum for the Blue-Light Hazard photo biological effect are proposed for each type of IOL. Then, using the corrected action spectra, the potential hazard of different types of LED sources on subjects implanted with those IOLs, as compared to the potential hazard of the same sources for a person whose crystalline lens has not been removed, has been calculated.

Keywords: e.g. BLH, intraocular lenses, LED sources.

1 Introduction

Light-emitting diode based SSL products are becoming a replacement of choice for conventional lamps (e.g., incandescent and fluorescent lamps) due to its unique advantages. The exposure limits (ELs) of European/International standards/directive (EN 62471, IEC 62471, CIE S009, AORD) for retinal damage are experimentally defined considering irreversible damage of the eyes caused by the light of a single source but do not consider more realistic situations where persons work in SSL lighted rooms or offices for several hours and with several types of light sources. The underlying concept is that the BLH (Photochemical Retinal Hazard) exposure limits should account for long-term exposure and several light sources of different types (directional, diffuse, point-like sources, panels) in the FOV of specific occupational activities. Not considered in IEC and EN standards, these aspects are very important in applications when worker’s health is of primary concern (very long exposure to artificial light, night workers).

The BLH is characterized by its action spectrum (CIE, 2000), which represents the relative weight of each wavelength in terms of the potential damage it can cause to the retina. This permits a direct comparison of different radiation sources to determine the relative effectiveness or the potential hazard that each one can cause. The global BLH for a given source depends, not only on the total radiant power emitted by the source, but also on its relative spectral distribution.

In addition to the function B(λ) for the normal eye an additional function A(λ) was later developed based on studies of Ham in rhesus monkeys with the crystalline lens surgically removed (Ham, 1982). The function A(λ) (the aphake hazard function) should then be applied for persons whose crystalline lens has been removed through a chirurgical procedure or do not have an intraocular lens which absorbs ultraviolet radiant energy in the UV-A spectral region. Figure 1 shows the two different action spectra for BLH: B(λ), which represents the action spectrum for a standard (phakic) eye; and A(λ) (aphakic eye) as recommended by CIE.

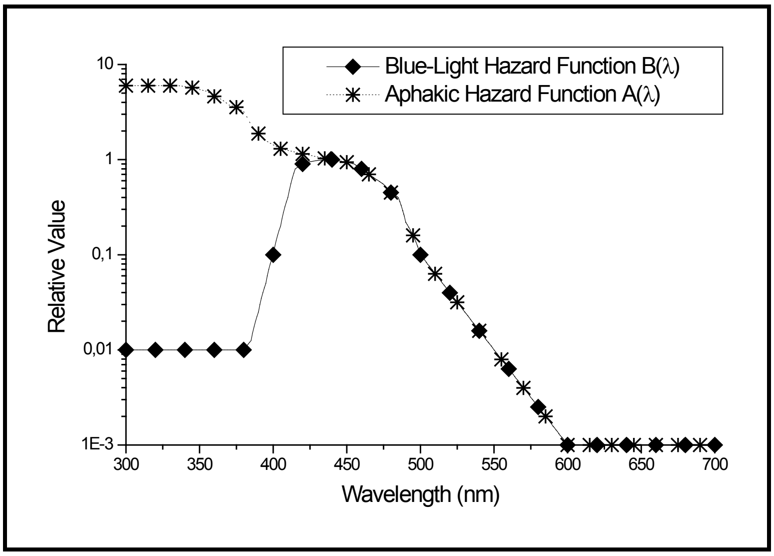

Figure 1 – Spectral weighting functions for retinal hazards A(λ) (aphakic eye) and B(λ) (normal eye)

Nowadays there are very few occurrences of aphakic eyes since usually during cataract surgery the removed crystalline lens is replaced by an intraocular lens (IOL). Although IOLs available today are provided with optical filtering (UV and blue blocking), generally they transmit much more violet and blue light than the crystalline lens at any age, yielding to an increased potential hazard for retinal photochemical injury.

The action spectrum for the BLH plays the role of spectral weighting function, which has to be included in the calculations of the threshold limit values (TLVs). Based on these values one can then evaluate the potential hazard to cause BLH or the recommended maximum exposure times for a given radiation source. The relative hazard of a given radiation source is defined as follows:

$$X_{blue} = \sum_{305}^{700} X_{\lambda} B(\lambda)\Delta\lambda \qquad (1)$$

where X_{λ} is the spectral radiance or spectral irradiance of the optical radiation source, B(λ) is the BLH function which represents the relative spectral effectiveness for the BLH, and Δλ is a wavelength interval at the center of which B(λ) is defined and over which spectral irradiance or spectral radiance is measured.

The aim of this work is to assess the impact upon the action spectrum for the BLH derived from the use of intraocular lenses (IOLs) and to evaluate the potential hazard to cause BLH by white LEDs sources on subjects whose crystalline lenses have been removed through a chirurgical procedure to implant intraocular lenses. The spectral transmittance of various models of intraocular lenses (IOLs) currently available in the market, which was measured by us and published in a previous work (Pons, 2007) has been used.

2 Intraocular lenses

Four models of commercial intraocular lenses from different manufacturers were used. Table 1 shows the main features of each IOL. As can be seen, all four IOLs are provided with a UV-filter, and one of them (the one named Acrysof Natural) incorporates a blue filter as well.

Table 1 – Intraocular Lenses (IOLs) Characteristics.

Manufacturer	Material	Filter	Name of lens
Alcon	Acrylic	UV+blue	Acrysof Natural
Bausch & Lomb	Hydrogel/PMMA	UV	Hidroview
Bausch & Lomb	Silicone elastomer/hydrophilic acrylic copolymer	UV	Akreos
LCA	Hydrophilic acrylic copolymer	UV	Istacryl

Figure 2 shows the normalized spectral transmittance curves for every intraocular lens, in comparison with ideal transmittance of crystalline lens (calculated as expressed in section 2.1). Significant differences among the various IOLs, mostly regarding the cut-off wavelength, can be seen. They all show a complete absorption of UVC (200 nm - 280 nm) and UVB (280 nm - 320 nm); however their behavior inside the UVA range (320 nm - 400 nm) differs considerably. Only Acrysof Natural completely absorbs UVA radiation, while the rest of the IOLs under analysis show different values for the cut-off wavelength, ranging from 350 nm (Akreos) to 370 nm or 380 nm (Istacryl and Hidroview respectively).

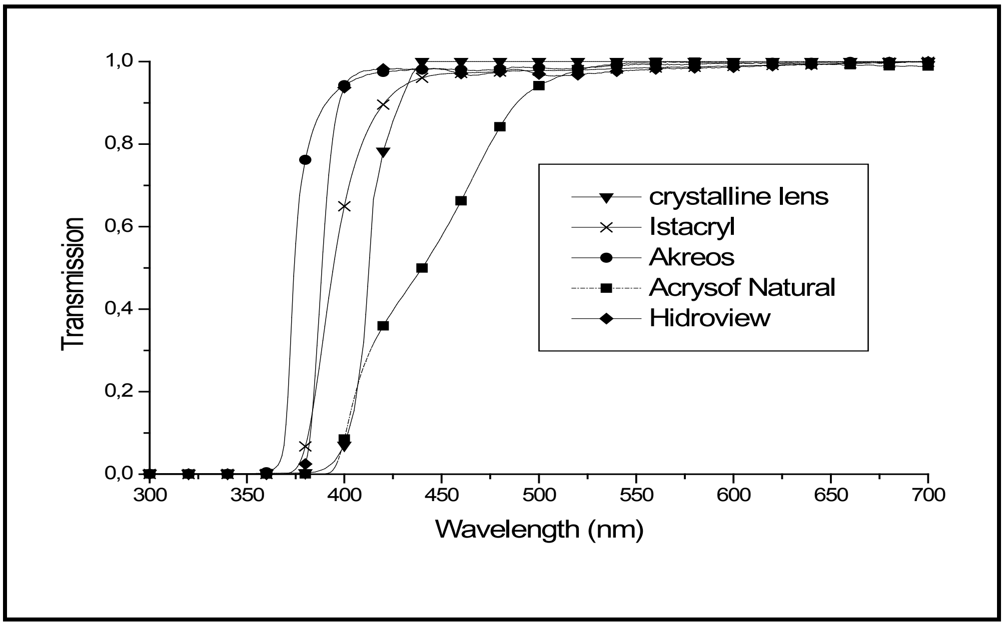

Figure 2 –Transmittance curves (normalized) of the intraocular lenses under study in comparison with the ideal transmittance of crystalline lens.

2.1 Impact upon the action spectrum for the BLH

Considering that the discrepancy between the two action spectra for the BLH discussed here ($A(\lambda)$ for aphakic eyes and $B(\lambda)$ for standard, phakic eyes) is only due to the effect of the crystalline lens, it means that crystalline's ideal spectral transmittance can be inferred by means of the $B(\lambda)/A(\lambda)$ ratio; that is:

$$B(\lambda) = \tau_{crystalline}(\lambda) \cdot A(\lambda) \tag{2}$$

Then, and just by reversing the above reasoning, it will be possible to calculate the corrected action spectrum function for eyes implanted with IOLs if its spectral transmittance is known. Thus, applying equation (2) to every of the IOLs under study yields:

$$B_{IOL}(\lambda) = \tau_{IOL}(\lambda) \cdot A(\lambda) \tag{3}$$

Figure 3 shows the resulting curves $B_{IOL}(\lambda)$ for each IOL after applying equation (3) to the spectral transmittances that had been measured.

The differences in transmittance among the different IOLs and with respect to the crystalline lens, especially regarding the cut-off wavelength, imply significant modifications of the corresponding action spectrum in the UVA region. For longer wavelengths, the alterations to the action spectrum are either very small or even non-existent. As for the Acrysof Natural IOL, one can notice that its action spectrum for the blue range is significantly lower than the standard one, due to the IOL being provided with a blue filter, as described in table 1.

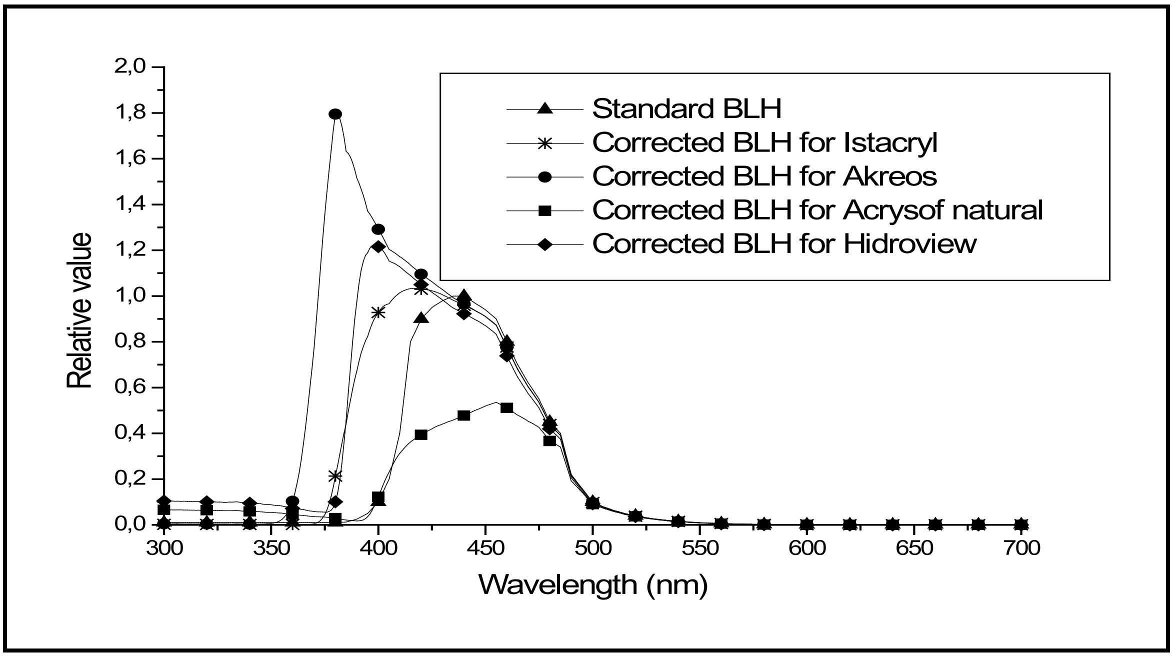

Figure 3 – Standard action spectrum for BLH and corrected action spectra computed for each IOL

3 Assessment of the potential hazard for LED sources

Replacing in equation (1) the corrected $B(\lambda)$ function (the ones shown in figure 3) and including the corresponding relative irradiance curve for the radiation sources under analysis (white LED sources in this work), it is possible to calculate the potential hazard that each source presents to wearers of the different IOLs as compared to the potential hazard of the sources for a person whose crystalline lens has not been extracted.

The LED sources of choice for the present study were the following ones:

Single high power LEDs: Blue, Warm white, White, Cool white and Neutral white manufactured by Cree XR-C

LED lamps: Master LED bulb E27 (2700 K) manufactured by Philips; PAR16 20 CW 20° (5000 K) manufactured by OSRAM and SMD Clear Tube 120 cm length 6000K 140° manufactured by RetroFix

Relative spectral irradiances of LED sources were measured in our laboratory by means of a UV-VIS spectroradiometer (Corredera, 1991).

Table 2 shows the the $X_{blue(IOL)}/X_{blue(BLH\ standard)}$ ratio obtained for each radiation source under study and for each IOL (i.e., for each corrected action spectrum).

Table 2 – Relative hazard factor $X_{blue(IOL)}/X_{blue(BLH\ standard)}$

LED source	Istacryl	Akreos	Acrysof Natural	Hidroview
Blue	0,97	0,98	0,67	0,98
Warm white	0,98	1,02	0,66	0,98
White	0,98	1,03	0,58	1,01
Cool white	0,98	1,02	0,58	1,01
Neutral white	0,98	1,01	0,67	0,98
Master LED bulb E27	0,92	1,03	0,67	1,01
PAR16 20 CW 20°	1,02	1,09	0,54	1,06
SMD Clear tube 120 cm Length 6000K 140°	0,98	1,01	0,64	0,99

According to these values, non-significant increase of the hazard factor with respect to a standard eye can be suggested. Only to mention the fact that for the Akreos IOL, the associated hazard factor increases about 10% with respect to the standard one for the PAR 16 LED lamp.

The authors have no interests in the development or marketing of any product mentioned in this study.

References

CIE 2000 CIE 138:2000. CIE Collection In Photobiology and Photochemistry. Vienna:CIE.

CORREDERA, P. 1991 et al. Realization of an absolute spectroradiometer. *Appl Opt*, 30, 1279-1284

HAM, W.T.1982 et al. Action spectrum for retinal injury from near-ultraviolet radiation in the aphakic monkey. *Am J Ophthalmol*, 299-306.

PONS, A. 2007. Determination of the action spectrum of the blue-light hazard for different intraocular lenses. *J. Opt.Soc.Am.A*,24(6), 1545-1550.